ESTRO School

DOSE MODELLING AND VERIFICATION FOR EXTERNAL BEAM RADIOTHERAPY

Course Directors
Tommy Knöös (SE)
Brendan McClean (IE)

Faculty
Anders Ahnesjö, (SE)
Maria Mania Aspradakis (CH)
Núria Jornet I Sala, (ES)
Bram van Asselen, (NL)

Local Organiser
Bram van Asselen, (NL)

Utrecht, the Netherlands
6 -10 March 2016

ACKNOWLEDGEMENTS

ESTRO
the European Society for Radiotherapy and Oncology
wishes to thank the local organiser:

Bram van Asselen
Medical Physicist
UMC Utrecht
The Netherlands

For his hospitality and for having gracefully accepted to take care of the local organisation of this course.

NOTE TO THE PARTICIPANTS OF THE ESTRO TEACHING COURSE ON

DOSE MODELLING AND VERIFICATION FOR EXTERNAL BEAM RADIOTHERAPY

The present texts and slides are provided to you as a basis for taking notes during the course. In as many instances as practically possible, we have tried to indicate from which author these slides have been borrowed to illustrate this course.

It should be realised that the present text can only be considered as notes for a teaching course and should not in any way be copied or circulated. They are only for personal use. Please be very strict in this as it is the only condition under which such services can be provided to the participants of the course.

Disclaimer

This course is accredited **CPD points** submitted to the European Federation of Organisations for Medical Physics (EFOMP), as a CPD event for Medical Physicists. Information on the status of the applications can be obtained from the ESTRO office.

Course Directors
Tommy Knöös (SE)
Brendan McClean (IE)

Faculty
Anders Ahnesjö, (SE)
Maria Mania Aspradakis (CH)
Núria Jornet I Sala, (ES)
Bram van Asselen, (NL)

Local Organiser
Bram van Asselen, (NL)

ESTRO School

SCIENTIFIC PROGRAMME

Teaching Course on

Dose Modelling and Verification for External Beam Radiotherapy

Day 1	**Sunday 6 March**	
	Introduction	
09:00 – 09:30	Introduction to course and faculty + Participant Survey	TK/BMcC
09:30 - 10:30	Basic concepts, definitions, convolution, superposition **ray trace, fluence and the Boltzmann transport equation** etc	BMcC
10 :30 –11:00	Coffee	
	Input Data	
11:00 – 12:00	Linac head design	TK
12:00 - 12:45	Dose measurements: Part 1 Relative dose away from reference conditions	NJ
12:45 – 13:45	Lunch	
13:45 – 14:30	Patient characterisation	BMcC
14:30 – 15:00	Phantoms	MMA
15:00 – 15:30	Coffee	
	Verification 1	
15:30 - 16:15	Dose measurements; Part 2 The best detector for different jobs – point detectors.	NJ

Day 2	**Monday 7 March**	
	Modelling 1	
9:00 – 9:30	Pencil kernels	MMA
9:30 – 10:00	Out of field dose modelling	BMcC
10:00 - 10:30	Coffee	
10:30 – 11:15	Multisource models	AA
11:15 – 12:00	Electron Modelling	TK
12:00 – 12:45	Point Kernels	AA
12.45 -13.45	Lunch	
13:45 - 14:15	Grid Based approaches	AA
14:15 – 15:00	Small fields: Measurement	MMA
15:00- 15:30	Coffee	
15:30 – 16:00	Small fields: Modelling	MMA

Day 3	**Tuesday 8 March**	
	Modelling 2 (continued)	
09:00 – 09:45	MU calculations – factor-based? models	MMA/AA
09:45 – 10:15	MU calculations – How are MU calculated in TPS	MMA/AA
10:15 -10:45	Coffee	
10:45 – 11:15	The MR-Linac concept	Bram van Asselen
11:15 – 12:00	Measurement and calculation challenges	Bram van Asselen
12:00 – 13:00	Independent MU Calculation Workshop	MMA
14:00 - 16:00	MR Linac - Site visit	

Day 4	**Wednesday 9 March**	
	Verification 2	
09:00 – 09:45	*Dose measurements; Part 3 The best detector for different jobs - 2D/3D detectors*	NJ
9:45 - 10:45	Methods for Data Comparison	TK
10:45 -11:15	Coffee	
11.15 – 12:15	Commissioning, performance and periodic TPS tests	NJ
12:15 – 12:45	DVH and dose based metrics	BMcC
12:45 – 13:15	Preparation for Modelling exercises	AA/MMA
13:15 -14.15	Lunch	
	Modelling 3	
14:15 -15:15	Practical on Modelling 1	AA/MMA
15:15 -15:45	Coffee	
15:45 – 16:45	Practical on Modelling 2	AA/MMA

Day 5	**Thursday 10 March**	
09:00 – 09:45	In-vivo dosimetry	NJ
09:45 – 10:15	Probabilistic planning and margins	AA
10:15 -10:45	Coffee	
10:45 – 11:30	Action level lecture:	NJ
11:30 – 13:00	Questions and answers session	All

TEACHING STAFF

Course Directors

Tommy Knöös
Physicist
Lund University Hospital (SE)
Email : Tommy.Knoos@med.lu.se

Brendan McClean
Physicist
St. Luke's Hospital
Dublin (IE)
Email : Brendan.McClean@slh.ie

Faculty

Anders Ahnesjö
Physicist
Uppsala University (SE)
Email : anders.ahnesjo@igp.uu.se

Maria Mania Aspradakis
Physicist
Canton Hospital of Lucerne (CH)
Email : mania.aspradakis@physics.org

Núria Jornet I Sala
Physicist
Hospital de la Santa Creu i Sant Pau, Barcelona (ES)
Email : NJornet@santpau.cat

Bram Van Asselen
Physicist
UMC Utrecht (NL)
Email : B.vanAsselen@umcutrecht.nl

Dose Calculation and Verification in External Beam Therapy – 2016 – Utrecht

ESTRO School

Looking back

- 1st Teaching course dedicated to Physicists ONLY
  - initiated by H. Svensson and A. Dutreix after an ESTRO workshop on "MU calculation and verification for therapy machines" in 1995 in Gardone Riviera (Italy) during the 3rd ESTRO biennial physics

- The first courses held between '98-'01
  - Mainly on "Monitor Unit Calculations" which mainly covered factor based models for dose calculation (ESTRO booklet #3 and #6)
  - Since 2002 a much broader physics ("dose determination and verification") content was aimed for photon and electron beam physics, beam modeling and dose calculation algorithms, …

- From 1998 to 2015, the course was held 17 times and about 1500 physicists have participated so far.

Faculty history

- Andrée Dutreix France
- Hans Svensson Sweden
- Gerald Kutcher U.S.A.
- André Bridier France
- Dietmar Georg Austria
- Ben Mijnheer The Netherlands
- Joanna Izewska Austria (IAEA)
- Jörgen Olofsson Sweden
- Günther Hartmann Germany
- **Anders Ahnesjö Sweden**
- **Maria Aspradakis Greece**
- **Brendan McClean Ireland**
- **Tommy Knöös Sweden**
- **Nuria Jornet Spain**

- **Gabriella Axelsson Course Coordinator ESTRO**

Locations

1 : Santorini (GR) 26-30 April 1998
2 : Santorini (GR) 07-11 May 2000
3 : Coimbra (P) 20-24 May 2001
4 : Perugia (I) 21-25 April 2002
5 : Barcelona (E) 06-10 May 2003
6 : Nice (F) 02-06 May 2004
7 : Poznan (PL) 24 -28 April 2005
8 : Izmir (TU) 7 - 11 May 2006
9: Budapest (H) 29 April – 3 May 2007
10: Dublin (IRE) 19 April – 24 April 2008
11: Munich (D) 15 March-19 March 2009
12: Sevilla (ESP) 14 -18 March, 2010
13: Athens (GR) 27-31 March 2011
14:Izmir (TU) 11-15 March 2012
15: Firenze (IT) 10-14 March 2013
16: Prague (Cz) 9-13 March 2014
17: Barcelona (E) 15-19 March 2015
18: Utrecht (NL) 6-10 March 2016

Participants

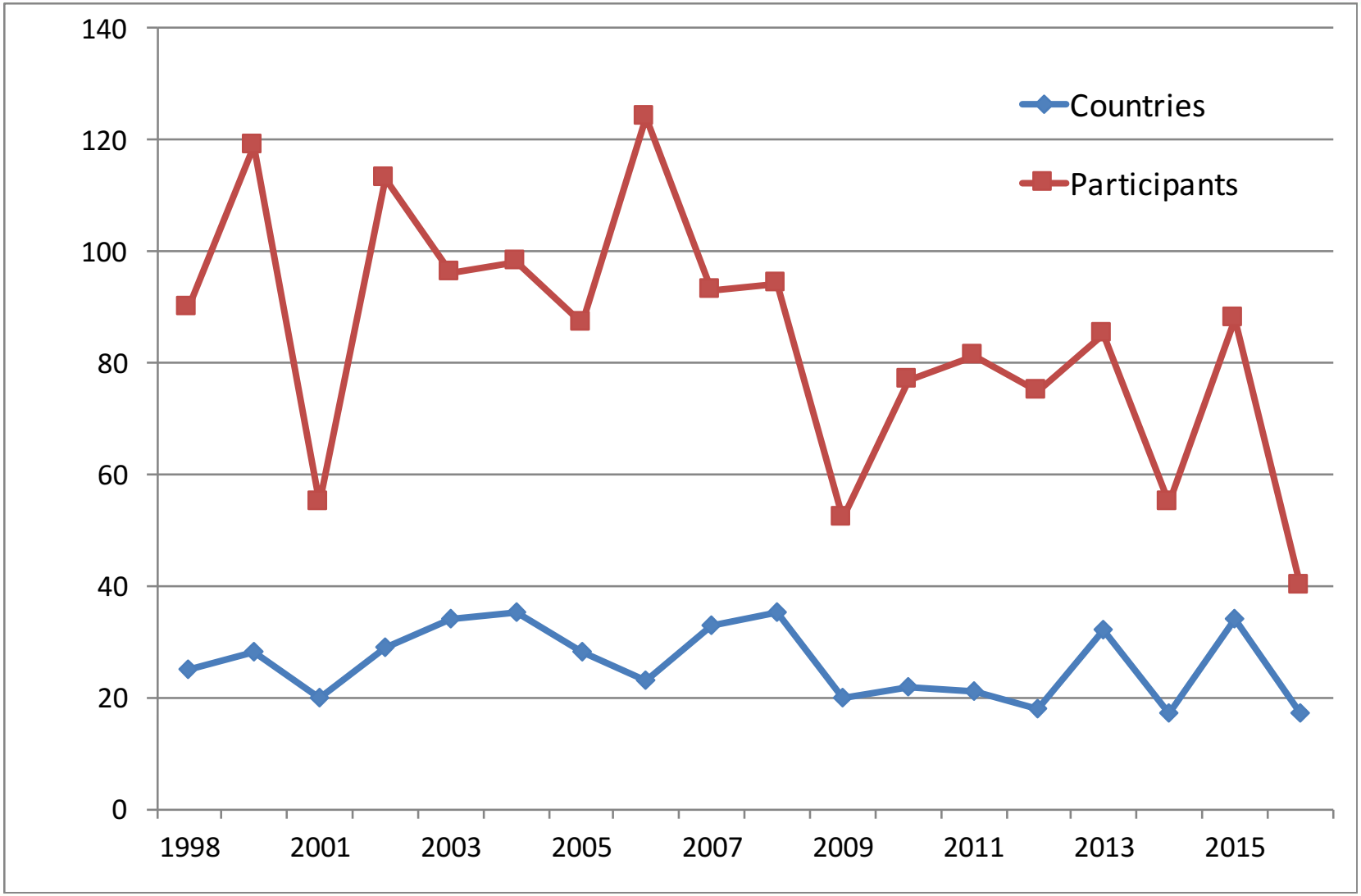

ESTRO School

Why this course?

Utrecht 2016

ESTRO School

What do we know about our systems and safety?

There are recurring themes in reported incidents and accidents

Skills and Rules (Training)
'cookbook' QC is still required

Important to do this with **alertness**, **attention** to detail, **Vigilence**

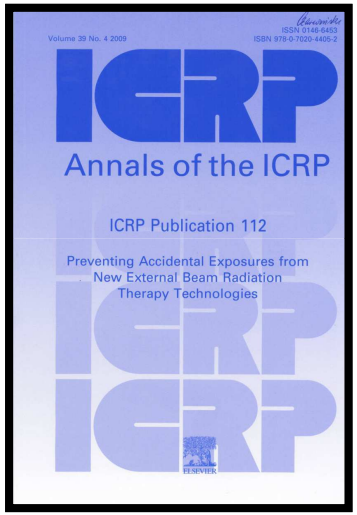

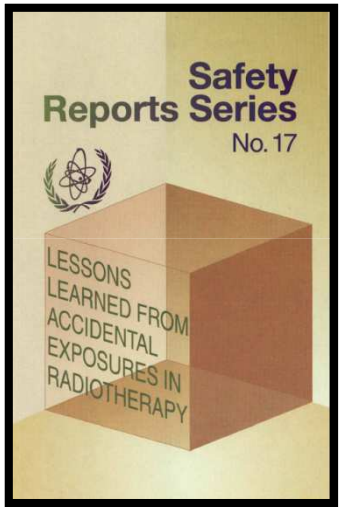

Most (80%?) of what we do falls into these two categories
Need vendor input (applications training)

What do we know about our systems and safety?

There are recurring themes in reported incidents and accidents

Knowledge (Education)
Need to **analyse**, **interpret**, **apply** to new approaches (**critical thinking**)
Real life situations are 'Tangled', dynamically changing – how do you 'train' for that?
Understanding (TP dose calc, optimisation, clinical objectives etc)

Objective of this course!

Commissioning

Inappropriate commissioning

- Reported 2007 at Hôpital de Rangueil in Toulouse, France
- In April 2006, the physicist in the clinic commissioned the new BrainLAB Novalis stereotactic unit
  - Possible to use small fields (6x6mm)
  - "…an ionisation chamber of inappropriate dimensions…" for calibrating the smallest microbeams was used (Farmer chamber was used)
  - The incorrect data was entered into the TPS
  - 145 patients affected

Calibration of TPS - Australia

The incident was discovered in 2006 when an independent measure of machine output, external to the linear accelerator quality assurance process, was performed to implement some new quality assurance software.

These measurements highlighted that there was an under-dosing of 5% when they used data from one of the linacs.

Further investigation at the time of the detection of this anomaly was able to trace back to the TPS beam calibration ratio as the likely cause of the consistent 5% dose discrepancy.

It involved 869 patients between 2004 and 2006.

CT calibration

- Transfer of CT# or HU# to density (physical or electron density depending on TPS)
- Usually performed by scanning

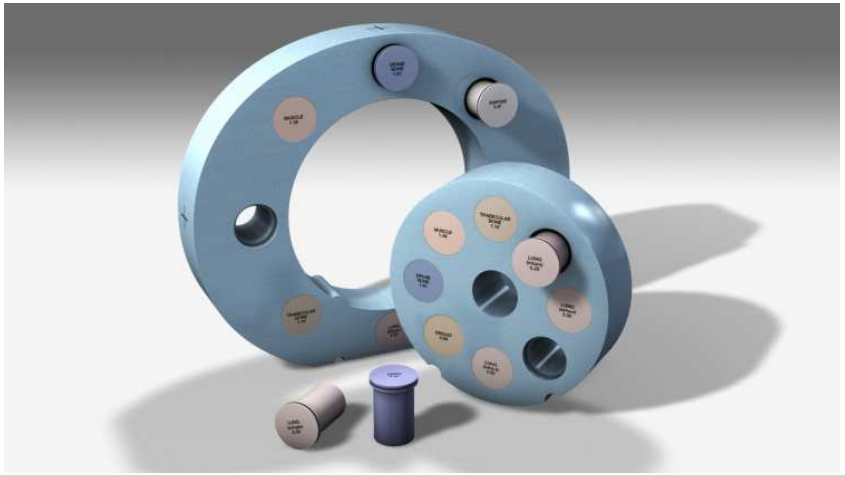

Density vs Hounsfield Number

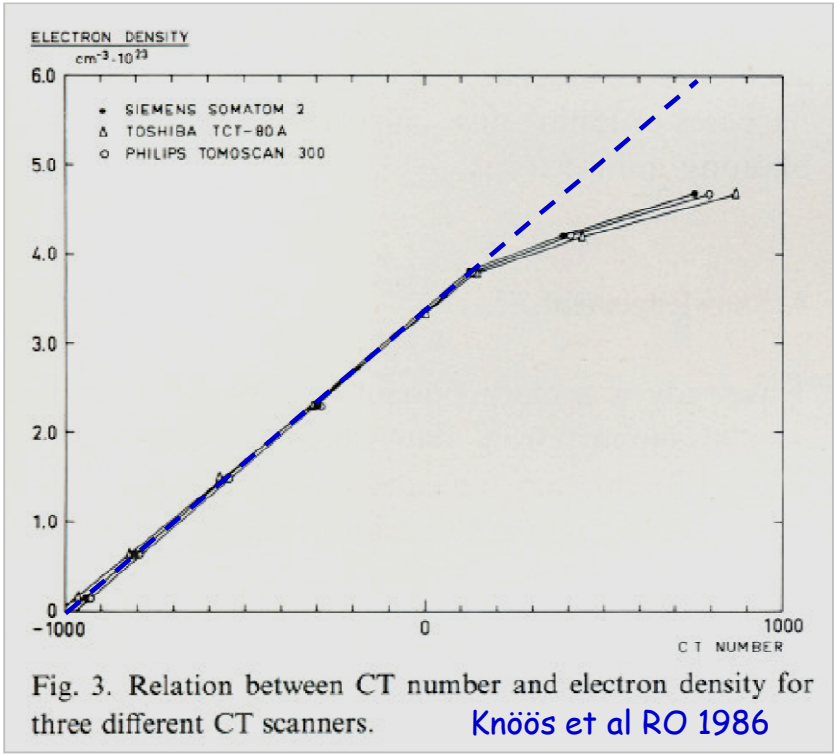

Fig. 3. Relation between CT number and electron density for three different CT scanners. Knöös et al RO 1986

- Lost the dependence of high Z for bone
- Medium not dense enough
- Too low dose
- Most significant for phantoms i.e. IMRT QA
  - -5%

Found during audit

Lessons learned from Epinal

- Potential errors
  - Wrong use of TPS due to lack of training + unsafe screen display #1
  - Dose due to verification imaging (MV portal) not taken into account #2
  - Calculation error due to in-house software, not tested, not qualified #3
  - Sole physicist
- Prevention
  - Time and organisation for continuous training
  - Team of physicists (at least 2)
  - QA for software
  - Software with safe human-computer interaction
  - In vivo dosimetry and second independent calculation

S. Derreumaux, B. Aubert and P. Gourmelon

Institut de Radioprotection et de Sûreté Nucléaire

Radiation Oncologists and physicist in JAIL

- A French court on Wednesday sentenced two doctors and a radiophysicist to 18 months in prison for their role in radiation overdoses given to nearly 450 cancer patients.
- At least 12 people have died as a result of the overdoses administered to patients at the Jean Monnet hospital in Epinal in northeastern France between 2001 and 2006.
- Dozens more are seriously ill as a result of calibration errors that produced the most serious radiation overdose incident France has known.
- The doctors and the radiophysicist had been charged with manslaughter, failure to help people in danger and destroying evidence.

From
The Sunday Times

Aim of this course I

- To review external therapy beam physics and beam modelling
- To understand the concepts behind dose algorithms and modelling in state-of-the-art TPS (today's system)
- To understand the process of commissioning of TP systems

Aim of this course II

- To review dosimetry methods of importance for commissioning and verification
- To review dose verification methods and to offer an overview of available technologies and evaluation methods
- To enable practical implementation of concepts for dose verification in advanced external beam therapy including SRT and IMRT

Programme structure

- Introduction
  - Basic concepts
  - Convolution/superposition
- Input data
  - Linac head design
  - Multisource models
  - Patient characterisation and phantoms
- Modelling 1
  - Point kernels and pencil kernels
  - Grid based approaches
  - Relative dose away from reference conditions
- Verification 1
  - Detectors for measurement; The best detector for different jobs.
  - Uncertainties in our measurements

Programme structure

- Modelling 2
  - How is collected data used in the Beam Model?
  - Small fields
  - Electrons modelling
  - Factor based MU calculations
- MU Calculation Workshop
- Verification 2
  - Methods for data comparison
  - Commissioning, performance and periodic TPS tests
- Modelling 3
  - DVH and dose based metrics
  - Out of field dose modelling
- Practical on Modelling

Programme structure

- In-vivo dosimetry
- Margins in dose calculation
- Guest lecture – MR linac specific issues
- Site visit - UMC Utrecht Center for Image Sciences
- Interactive MCQ

Scheduled activities

- 09.00-17.00 appr.
  - Coffee break x 2
  - Lunch
- Welcome reception/dinner
  - Lobby 7.00pm or in restaurant 7.30pm
- Free Afternoon (Tour? Contact Gabriella)
- For those interested; visit to the Radiation Oncology and Medical Physics Department
- For those interested; visit to the old hospital.
- Other points:
  - Lectures will be (a bit) different from those sent out
  - All faculty are available for questions
  - **Evaluations!**

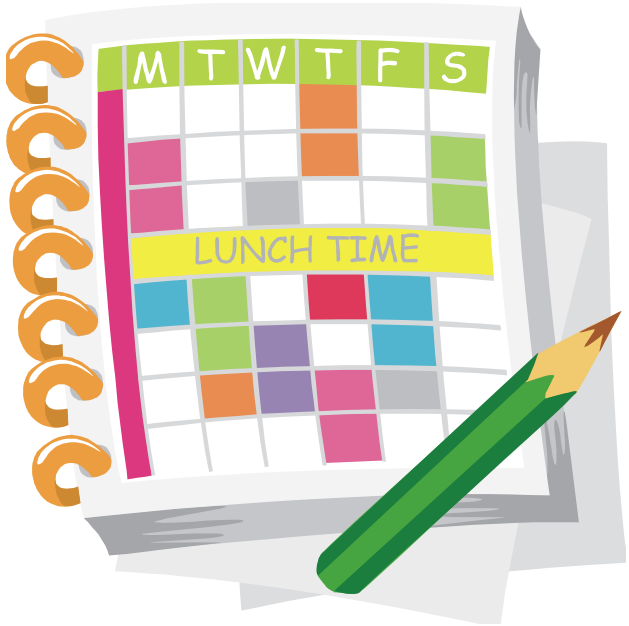

ESTRO School

Hard working people deserve…

ESTRO School

Hard working people deserve…

and

But we hope it doesn't lead to this…….

Enjoy the course!!

ESTRO School

Dose Modelling and Verification for External Beam Radiotherapy

06 - 10 March 2016, Utrecht

Basic concepts: Fluence, Ray trace, Boltzmann Transport Equations

Brendan McClean

St Luke‘s Radiation Oncology Network, Dublin, Ireland

ESTRO School

Content and Learning Objectives:

1) Review the quantities **absorbed dose** and **fluence**
2) Track lengths of a **ray** within voxels (ray tracing)
3) Track lengths of an **individual particle** within voxels (particle tracking)
4) Understand the components and derivation of the particle transport equation

Definition of the quantity absorbed dose

By far the most important “dose” quantity is the quantity of

absorbed dose.

Definition as taken from the ICRU Report 60 (now 85a):

> The **absorbed dose**, D, is the quotient of $\mathrm{d}\bar{\epsilon}$ by $\mathrm{d}m$, where $\mathrm{d}\bar{\epsilon}$ is the mean energy imparted to matter of mass $\mathrm{d}m$, thus
>
> $$D = \frac{\mathrm{d}\bar{\epsilon}}{\mathrm{d}m} .$$
>
> Unit: $\mathrm{J\,kg^{-1}}$
>
> The special name for the unit of absorbed dose is gray (Gy).

$$D = \frac{d\bar{\varepsilon}}{dm}$$

In the following let‘s assume that a specific **voxel** of a 3D patient model can serve as a representative of d*m*

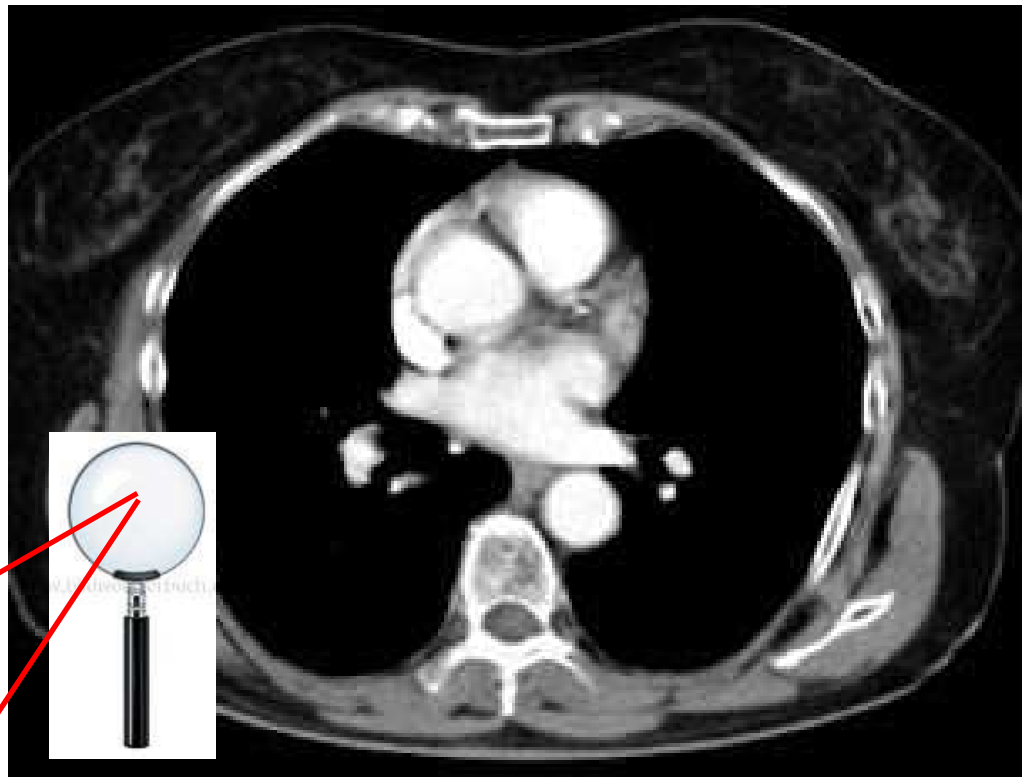

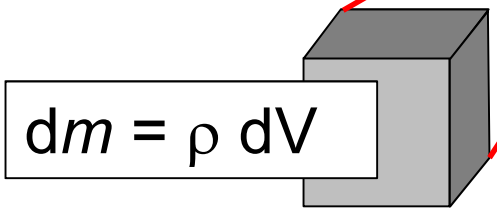

$$D = \frac{\mathrm{d}\bar{\varepsilon}}{\mathrm{d}m}$$ ⟸ mean energy imparted

The term “energy imparted” refers to a balance of radiation energy entering and leaving a volume of mass:

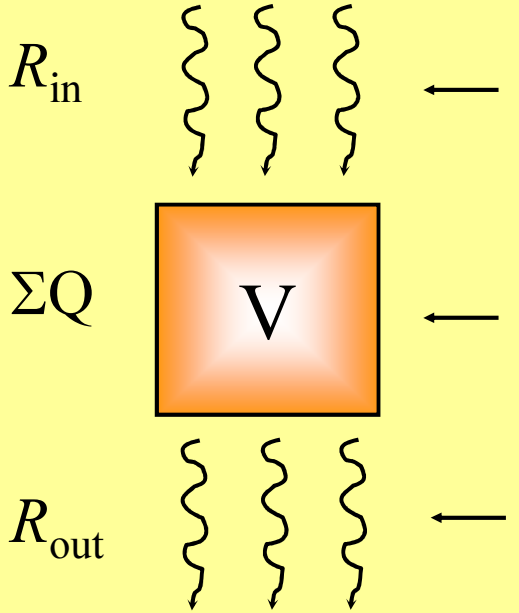

Radiation energy entering a volume (electrons, photons)

In the volume there are:
- many interactions
- ΣQ is the change of rest energies of all particles involved in the interactions

Radiation energy leaving the volume

Energy imparted: $\varepsilon = R_{in} - R_{out} + \Sigma Q$

Absorbed dose

$$D = \int_E \Phi_E \cdot \left(\frac{S_c}{\rho} \right) \cdot dE$$

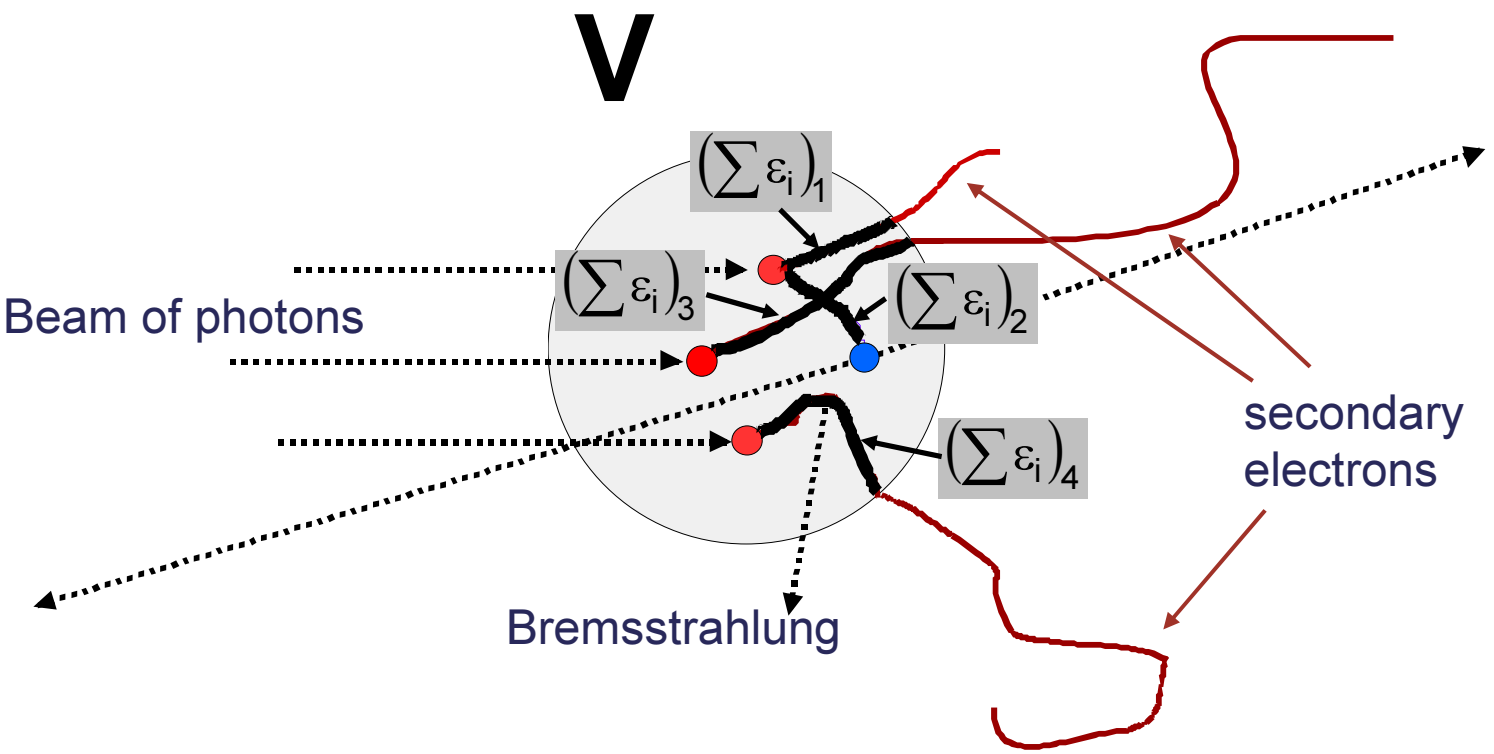

Energy absorbed in volume V = $\left(\sum \varepsilon_i\right)_1 + \left(\sum \varepsilon_i\right)_2 + \left(\sum \varepsilon_i\right)_3 + \left(\sum \varepsilon_i\right)_4$

where $\left(\sum \varepsilon_i\right)$ is the sum of energy lost by collisions along the track of the secondary particles within volume V.

Calculation vs measurement of absorbed dose

- Measurement (of ionization) only at time of delivery of dose
- For retrospective or planned dose need theoretical description
- Calculation requires description of radiation fields in terms of sources of particles, their interactions and a description of receptors
  - Allows calculation of flow in and out of a volume of interest
- Deterministic
  - Particles subject to transport equations so can calculate values at any point in time
- Monte Carlo approaches (stochastic)
  - Track individual particles

Calculation vs measurement of absorbed dose

- Measurement (of ionization) only at time of delivery of dose
- For retrospective or planned dose need theoretical description
- Calculation requires description of radiation fields in terms of sources of particles, their interactions and a description of receptors
  - Allows calculation of flow in and out of a volume of interest
- Deterministic
  - Particles subject to transport equations so can calculate values at any point in time

Requires appropriate definition of 'number of particles'

- Monte Carlo approaches (stochastic)
  - Track individual particles

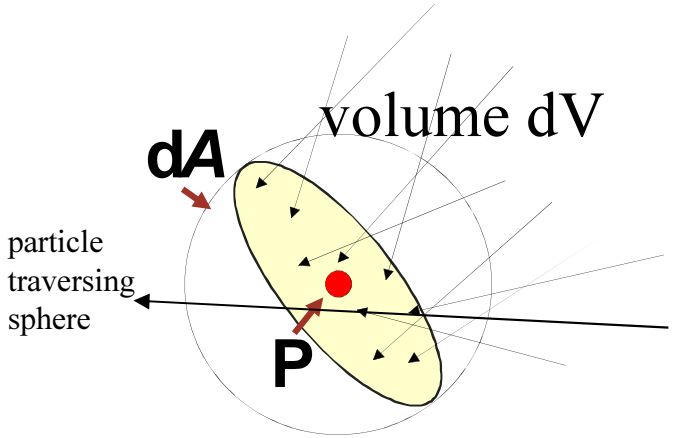
volume dV
dA
particle
traversing
sphere
P

Particle Fluence

N the expectation value of the number of particles striking a finite sphere surrounding point P

$$\Phi = \frac{dN}{dA} \quad \left[m^{-2}\right]$$

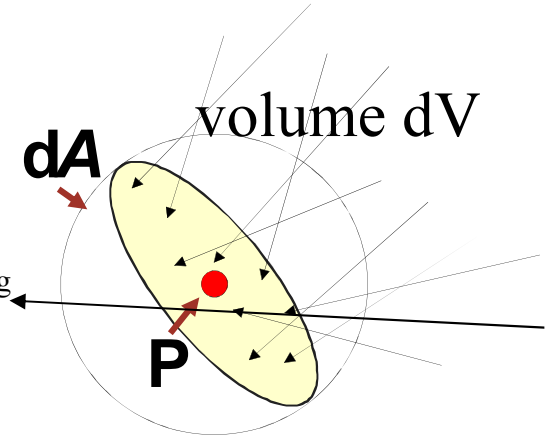

dN is the number of particles incident on a infinitesimal sphere surrounding P of cross sectional area dA

Particle Fluence

N the expectation value of the number of particles striking a finite sphere surrounding point P

$$\Phi = \frac{dN}{dA} \quad \left[m^{-2}\right]$$

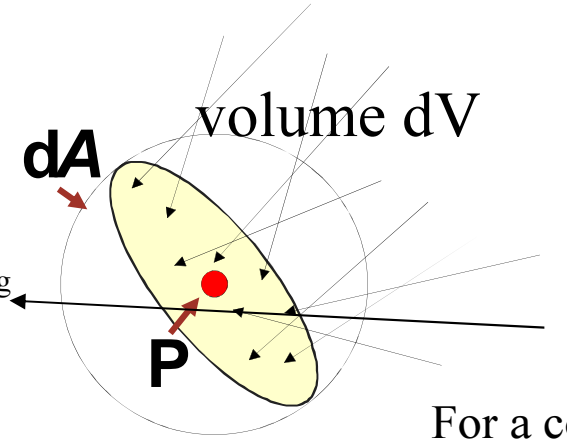

dN is the number of particles incident on a infinitesimal sphere surrounding P of cross sectional area dA

Energy Fluence

The amount of energy 'striking' the sphere

For a monoenergetic beam:

$$\Psi = \frac{dR}{dA} = E\frac{dN}{dA} = E\Phi$$

For a component of a polyenergetic beam:

$$\Psi_E = \frac{d\Psi}{dE} = E\,\Phi_E$$

With R being the expectation value of the total energy (excluding rest mass energy) or Radiant energy carried by all particles N, energy fluence in the quotient of this energy to the cross sectional area dA

X-ray spectrum

Fluence differential in energy
or particle fluence spectrum

$$\Phi_E = \frac{d}{dE}\left(\frac{dN}{dA}\right) = \frac{d\Phi}{dE}$$

Differential energy fluence
or energy fluence spectrum

$$\Psi_E = \frac{d\Psi}{dE} = E\frac{d\Phi}{dE} = E\,\Phi_E$$

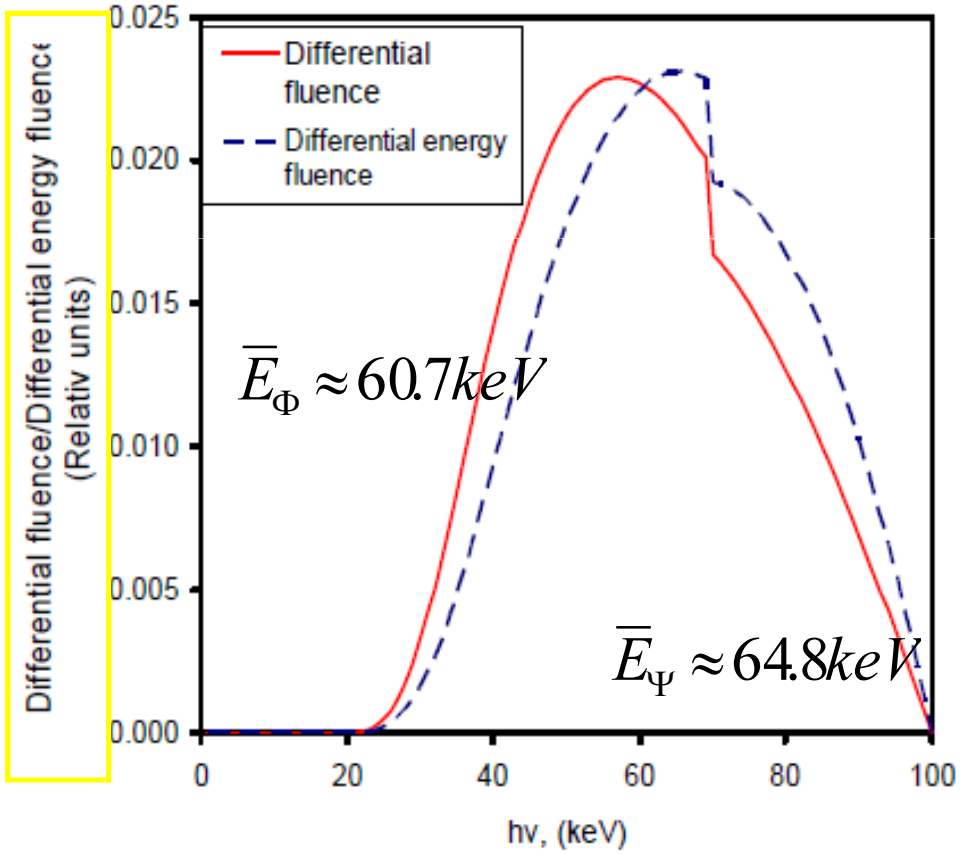

Required quantities: Particle number

- More general, in a time **independent** situation the number ***N*** may be described within a six dimensional **phase space** (x;Ω;E) in which:

  x = (x1; x2; x3) is the spatial coordinate,

  Ω is the particle direction which is a point on a unit sphere S with the angles coordinates φ and θ

  E is the energy variable.

$$N = N(\mathrm{x}, \mathrm{y}, \mathrm{z}, \varphi, \theta, \mathrm{E})$$

Required quantities: Alternative definition of fluence

The fluence can also be defined by the

track-length density (= track-length per volume)

of particles at a point in space within a small volume:

$$\Phi(\vec{r}) = \frac{dL(\vec{r})}{dV}$$

The fluence at a point P is numerically equal to the expectation value of the sum of the particle track lengths (assumed to be straight) that occur in an infinitesimal volume dV at P divided by dV

Chilton 1978, Health Physics *34*, 715

Chilton, Health Physics, 34, 715-716, 1978

Definition 1:

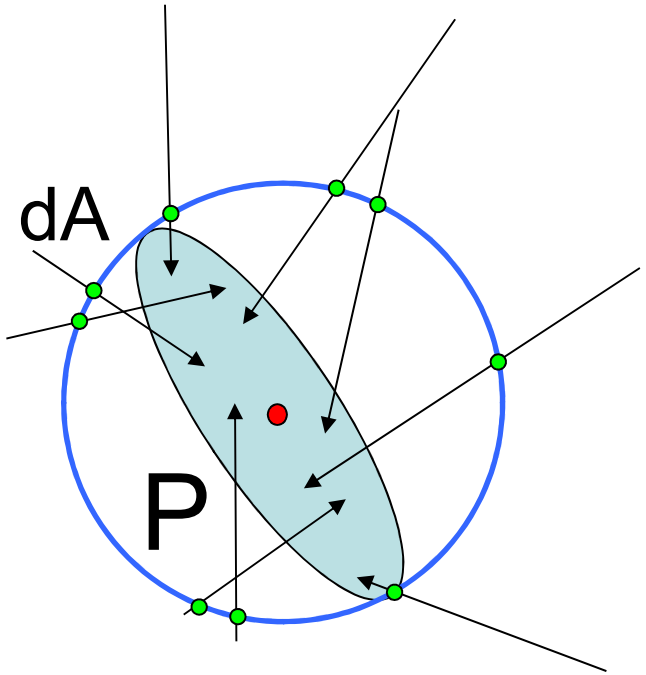

$$\Phi(\vec{r}) = \frac{dN}{dA}$$

Definition 2:

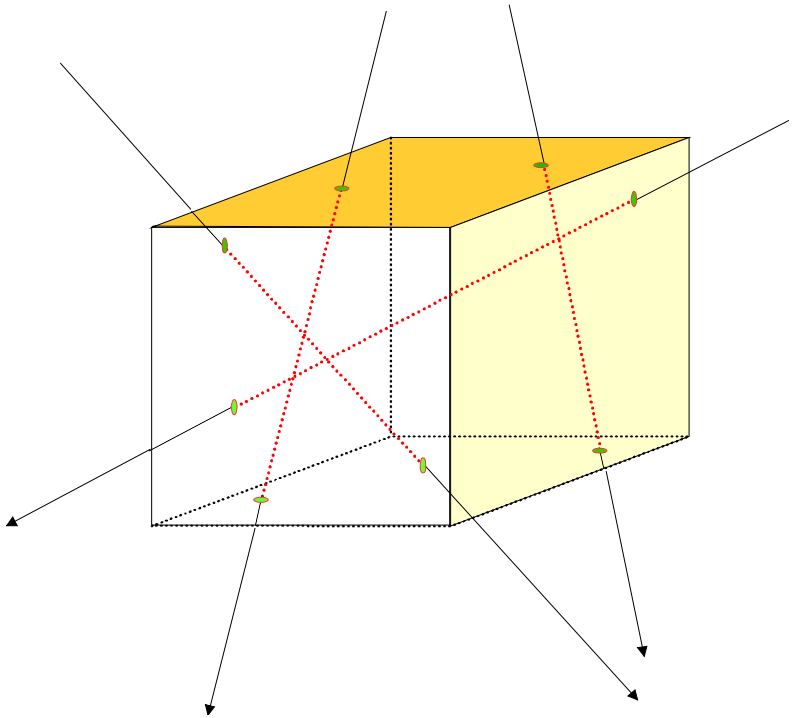

$$\Phi(\vec{r}) = \frac{dL(\vec{r})}{dV}$$

Possible Methods of dose calculation

Dosimetrical quantity	Principle of calculation	Required methods & ingredients
Absorbed dose in a medium	factor based	factors such as: $e^{-\mu d}$ (PDD, TPR), OF, etc
	within a 2D/3D matrix	ray tracing algorithm through a matrix
	Advanced methods: • solution of the Boltzmann Transport Equation, • Monte Carlo simulation	Boltzmann Transport Equation Monte Carlo code (particle tracking)
Other dosimetrical quantities such as **KERMA** or **TERMA**	fluence based: combination with interaction coefficients	fluence, Integration of interaction coefficients times fluence over all energies
	Superposition method	Superposition/convolution algorithms

Kerma, collision kerma

Kerma is the expectation value of the energy transferred by photons to the medium per unit mass

$$K = \frac{d\bar{\varepsilon}_{tr}}{dm} \quad [Gy]$$

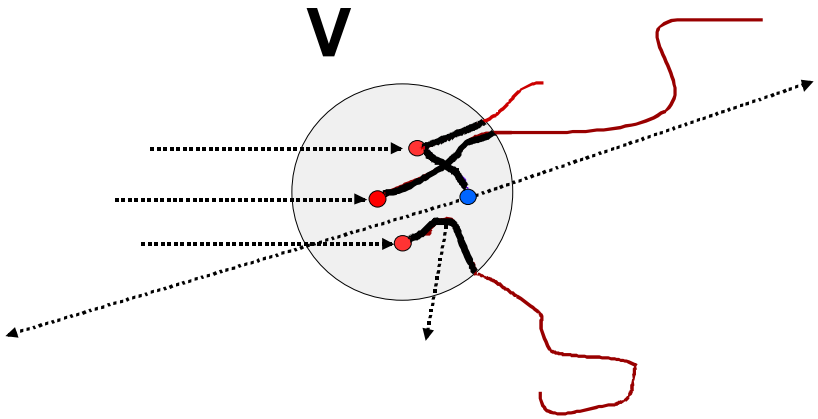

Monoenergetic photon beam

$$K = \Phi E \left(\frac{\mu_{tr}}{\rho} \right) = \Psi \left(\frac{\mu_{tr}}{\rho} \right)$$

$$K = K_{col} + K_{rad}$$

K includes all energy transferred to collision and radiation losses

$$K_{col} = K(1-g)$$

Collision Kerma: energy transferred to charged particles

$$K_{col} = K \frac{\left(\frac{\mu_{en}}{\rho} \right)}{\left(\frac{\mu_{tr}}{\rho} \right)} = \Psi \left(\frac{\mu_{en}}{\rho} \right)$$

Total Energy Released per unit Mass

TERMA

refers to the total energy removed from the primary beam (energy of secondary electrons + scattered photons)

$$T = \Psi \left(\frac{\mu}{\rho} \right) \quad [Gy]$$

$$Note: \quad \frac{\mu_{tr}}{\rho} = \left(\frac{\mu}{\rho} \right) \frac{\overline{E}_{tr}}{E}$$

$$K = \Psi \left(\frac{\mu_{tr}}{\rho} \right)$$

TERMA always greater than Kerma by $\frac{\mu}{\mu_{tr}}$

Basic dosimetric quantities

$$\frac{radiation\ energy\ (transferred\ or\ absorbed)}{mass}\left[\frac{J}{kg}\right]$$

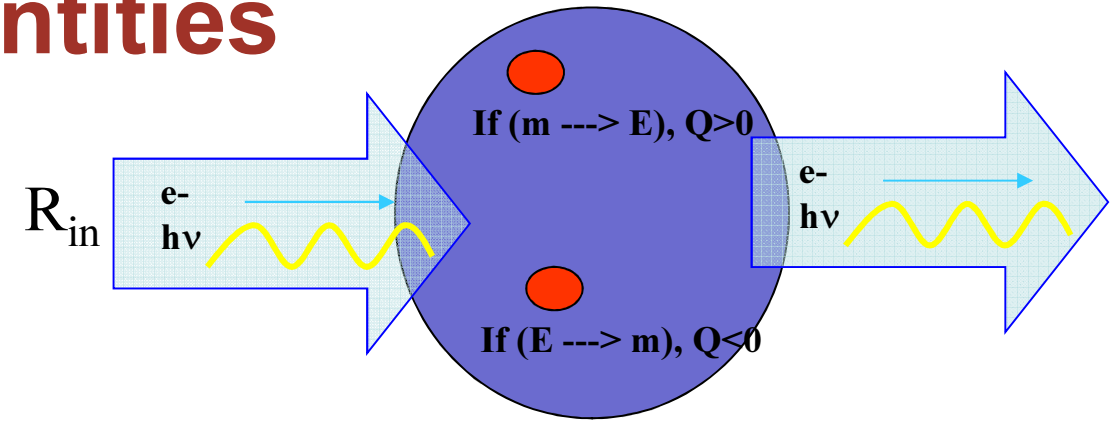

R_{in} R_{out}

Q: changes in rest mass

energy transferred

↳ kerma

$$\varepsilon_{tr} = (R_{in})_u - (R_{out})_u^{nonr} + \sum Q$$

net energy transferred

↳ collision kerma

$$\varepsilon_{tr}^{n} = \varepsilon_{tr} - R_u^r$$

energy imparted (absorbed)

↳ absorbed dose

$$\varepsilon = (R_{in})_u - (R_{out})_u + (R_{in})_c - (R_{out})_c + \sum Q$$

radiant energy of ALL uncharged particles leaving the volume

(Attix 1986)

Absorbed dose

$$D \overset{\text{CPE}}{=} K_{col}$$

$$K_{col} = \int E \cdot \Phi_E \cdot \left(\frac{\mu_{en}}{\rho} \right) dE$$

in terms of interaction coefficients

$$D \overset{\text{CPE}}{=} \left(\frac{\mu_{en}}{\rho} \right) E \, \Phi$$

mono-energetic beam

$$D \overset{\text{CPE}}{=} \int_0^{E_{max}} E \, \Phi_E \left(\frac{\mu_{en}(E)}{\rho} \right) dE$$

poly-energetic beam

Possible Methods of dose calculation

Dosimetrical quantity	Principle of calculation	Required methods & ingredients
Absorbed dose in a medium	factor based	factors such as: $e^{-\mu d}$ (PDD, TPR), OF, etc
	within a 2D/3D matrix	ray tracing algorithm through a matrix
	Advanced methods: • solution of the Boltzmann Transport Equation, • Monte Carlo simulation	Boltzmann Transport Equation Monte Carlo code (particle tracking)
Other dosimetrical quantities such as **KERMA** or **TERMA**	fluence based: combination with interaction coefficients	fluence, Integration of interaction coefficients times fluence over all energies
	Superposition method	Superposition/convolution algorithms

Ray tracing

The term “Ray tracing” is frequently used to determine the radiological path length through a voxel array (with densities ρ_{11}, ρ_{12}, ρ_{13}, …).

$$\Phi = \Phi_0 e^{-r_{radiol} \cdot \mu}$$

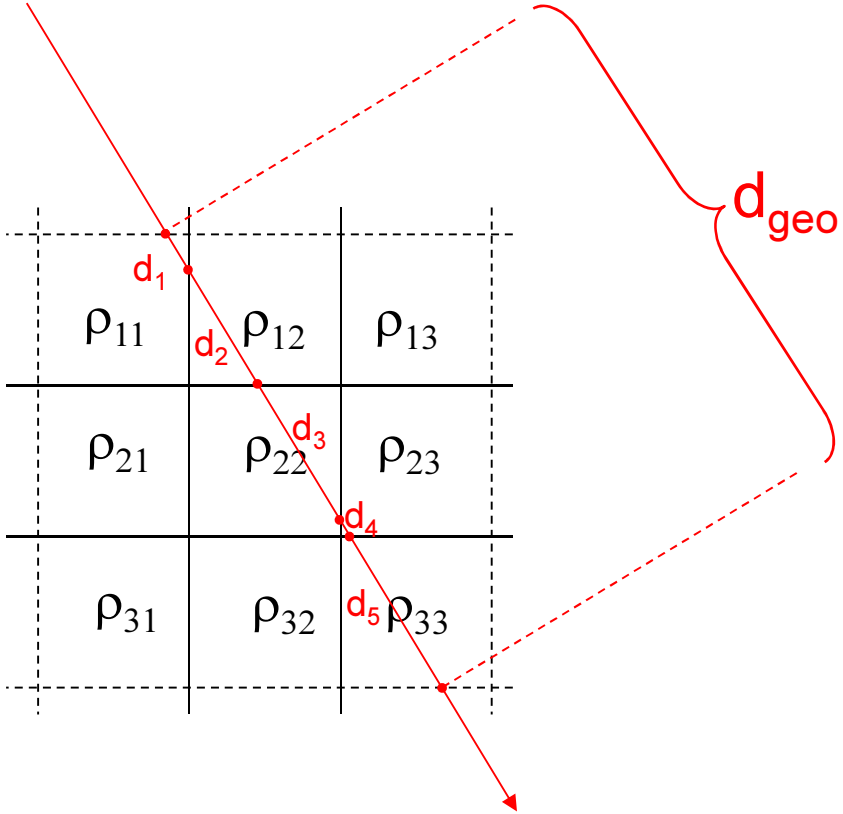

d_{geo} is the geometrical path within the patient:

d_{radiol} is the radiological path within the patient (simplified):

$$d_{radiol} = \frac{1}{\rho} \cdot \sum_{i=1}^{N} d_i \rho_i$$

Ray Tracing

In order to determine the radiological path d_{radiol} through the patient, one has to determine – voxel by voxel – the segments d_1, d_2, .. in each single voxel.

voxel with index i,j,k

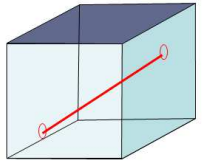

segment $d_{i,j,k}$

In a general formulation, the radiological path d_{radiol} is:

For photons:

$$d_{radiol} = \frac{1}{\mu} \sum_i \sum_j \sum_k d_{i,j,k} \cdot \mu_{i,j,k}$$

The evaluation of this equation scales with the number of voxels = $N_i \cdot N_j \cdot N_k$

(for instance: 256 x 256 x 64 = 4 x10^6 iterations)

Ray Tracing

However, there are algorithms of ray tracing which are **much** faster:

Fast calculation of the exact radiological path for a three-dimensional CT

Robert L. Siddon

Med. Phys. 12 (2), Mar/Apr 1985

Ray Tracing: Siddon's algorithm (illustrated in 2D)

Consider the intersection points:

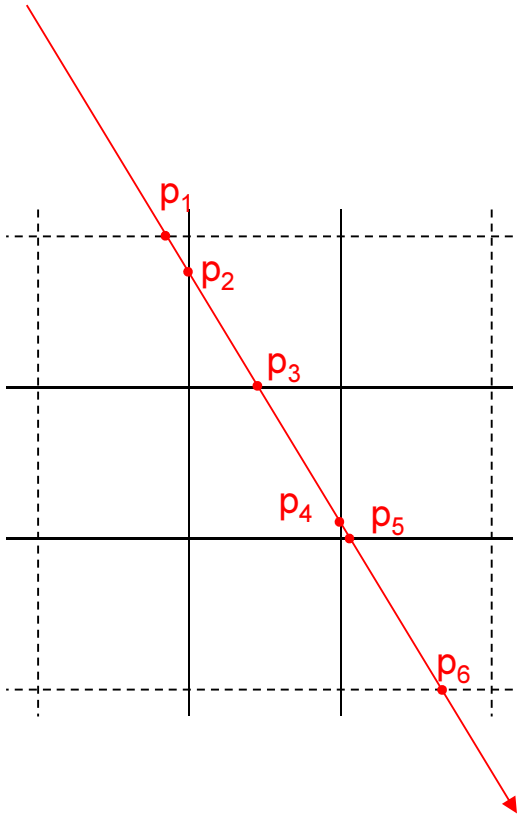

Ray Tracing: Siddon's algorithm (illustrated in 2D)

…… as being intersections p_i with the equally spaced vertical and horizontal lines (by a) in blue and green

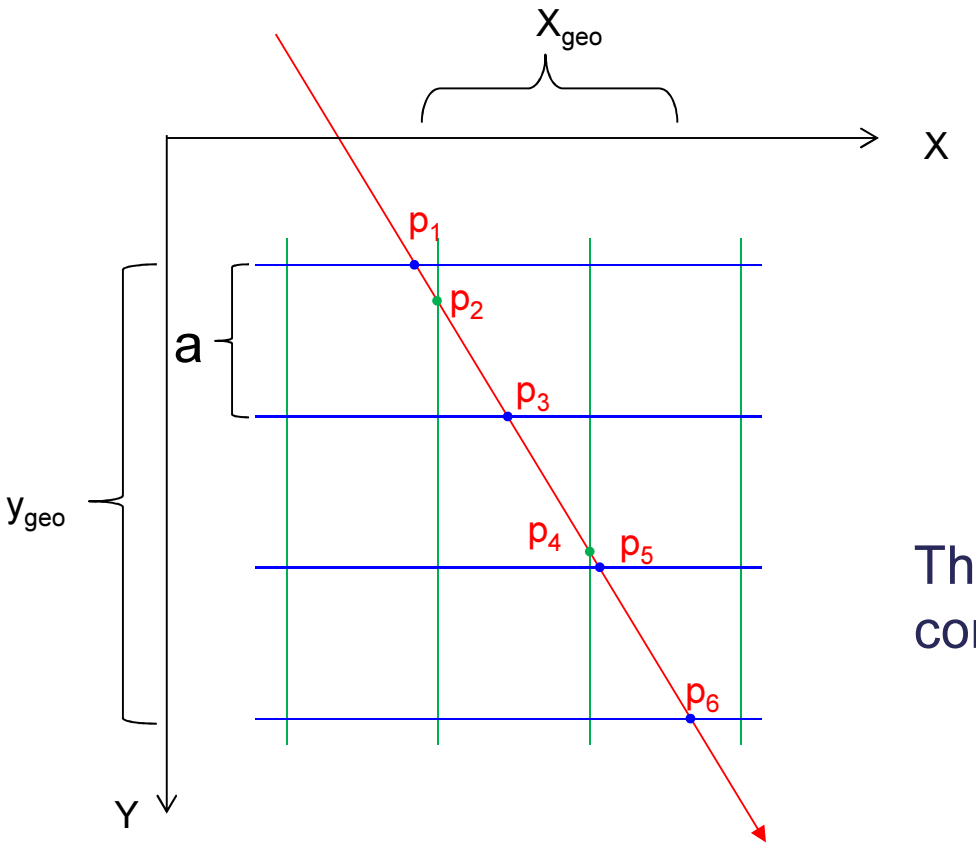

X coordinates of the intersection points (green):

$$x_{i=2,4} = x_1 + \alpha_{x,i} \cdot x_{\text{geo}}$$

$$\alpha_{x,i} = (x_i - x_1) / x_{\text{geo}}$$

Y coordinates of the intersection points (blue):

$$y_{i=1,3,5,6} = y_1 + \alpha_{y,i} \cdot y_{\text{geo}}$$

$$\alpha_{y,i} = (y_i - y_1) / y_{\text{geo}}$$

The $\alpha_{x,i}$ and $\alpha_{y,i}$ can be merged into a common series of **increasing values**:

$$\{\alpha\} = \{merge[\alpha_{x,i}, \alpha_{y,i}]\}$$

$$\{\alpha_1, ..., \alpha_m, ..., \alpha_6\}$$

Ray Tracing: Siddon's algorithm

An individual distance d_1 , d_2 , ..d_m .. d_M can be calculated as:

$$d_m = d_{\text{geo}} \cdot [\alpha_m - \alpha_{m-1}] \qquad \text{with} \qquad d_{\text{geo}} = \sqrt{x_{\text{geo}}^2 + y_{\text{geo}}^2}$$

Finally, one obtains the radiological path as:

$$d_{\text{radiol}} = d_{\text{geo}} \cdot \sum_m [\alpha_m - \alpha_{m-1}] \cdot \mu_{i(m),j(m),k(m)}$$

This approach does not scale with the number of **voxels** N_i x N_j x N_k but with number of **planes** $(N_i+1)+(N_j+1)+(N_k+1)$.

For instance in the same voxel array:
Instead of 256 x 256 x 64 = 4 million iterations we need only (256+1)+(256+1)+(64+1) = 579 iterations

Possible Methods of dose calculation

Dosimetrical quantity	Principle of calculation	Required methods & ingredients
Absorbed dose in a medium	factor based	factors such as: $e^{-\mu d}$ (PDD, TPR), OF, etc
	within a 2D/3D matrix	ray tracing algorithm through a matrix
	Advanced methods: • solution of the Boltzmann Transport Equation, • Monte Carlo simulation	Boltzmann Transport Equation Monte Carlo code (particle tracking)
Other dosimetrical quantities such as **KERMA** or **TERMA**	fluence based: combination with interaction coefficients	fluence, Integration of interaction coefficients times fluence over all energies
	Superposition method	Superposition/convolution algorithms

Establishing a "transport formula"

A model equation for the fluence of the electrons and positrons within a volume of interest can be derived from the particle transportation and conservation within a small volume element ΔV.

The following is simply a book keeping process of particles in the phase space*.

Particles refer to:

1) photons
2) electrons
3) positrons

*) E BOMAN, Thesis, University of Kuopio, Finland, 2007

Establishing a "transport formula"

Due to particle conservation, the number of particles within a small volume element ΔV can be obtained from 4 processes:

Note: The index j refers to a particular type of particle

$$dN_j = -dN_{j,\text{in-out}} - dN_{j,\text{att}} + dN_{j,\text{secondaries}} + dN_{j,\text{source}}$$

$dN_{j,\text{in-out}}$ the net number of particles j flowing in and out of the volume ΔV

$-dN_{j,\text{att}}$ the number of particles j that are attenuated in ΔV

$+dN_{j,\text{secondaries}}$ the number of particles j that are born by interactions with medium atoms in ΔV

$+dN_{j,\text{source}}$ the number of particles j produced by the sources inside the volume ΔV

Looking at the 4 terms in more detail

(1) The net number of particles j flowing out of the volume ΔV :

$$dN_j = \Phi_{j,E,\Omega}\, d\Omega dE$$

at the surface element dA:

$$dN_{j,\text{in-out}} = \vec{\Omega}\,\Phi_{j,E,\Omega}\, d\vec{A}\, d\Omega dE$$

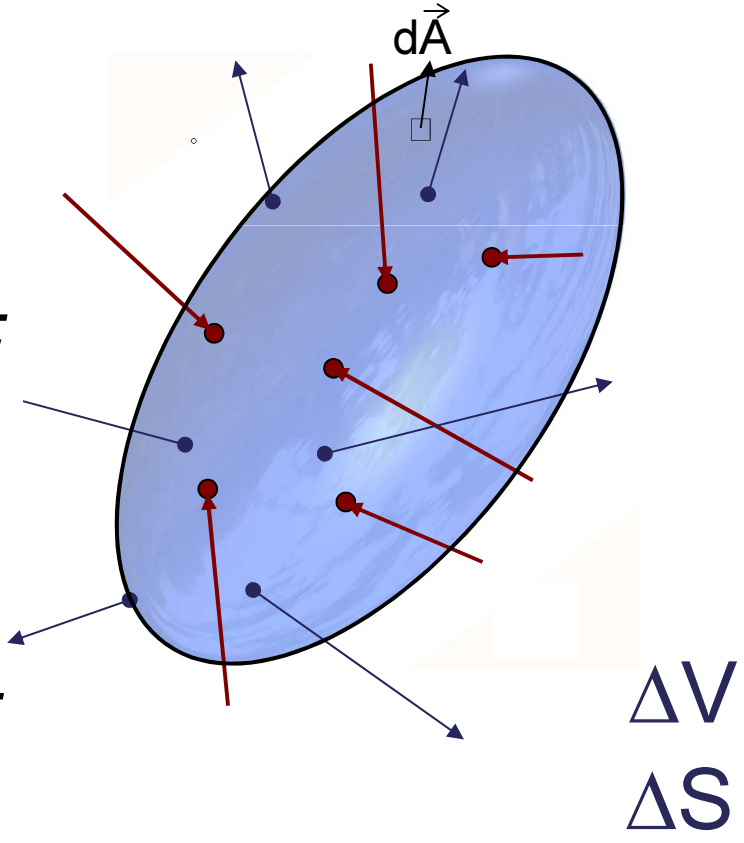

over the entire surface:

$$dN_{j,\text{in-out}} = \int_{dS} \vec{\Omega}\,\Phi_{j,E,\Omega}\, d\vec{A}\, d\Omega dE$$

Establishing a "transport formula"

- There is a famous mathematical theorem on a surface integral well known as Gauss's theorem:

$$\int_{dS} G(\vec{r})\, d\vec{A} = \int_{dV} \nabla G(x,y,z)\, dV$$

Establishing a "transport formula"

(1) The net number of particles j flowing out of the volume ΔV :

$$dN_{j,\text{in-out}} = \int_{dS} \vec{\Omega}\,\Phi_{j,E,\Omega}\; d\vec{A}\, d\Omega dE$$

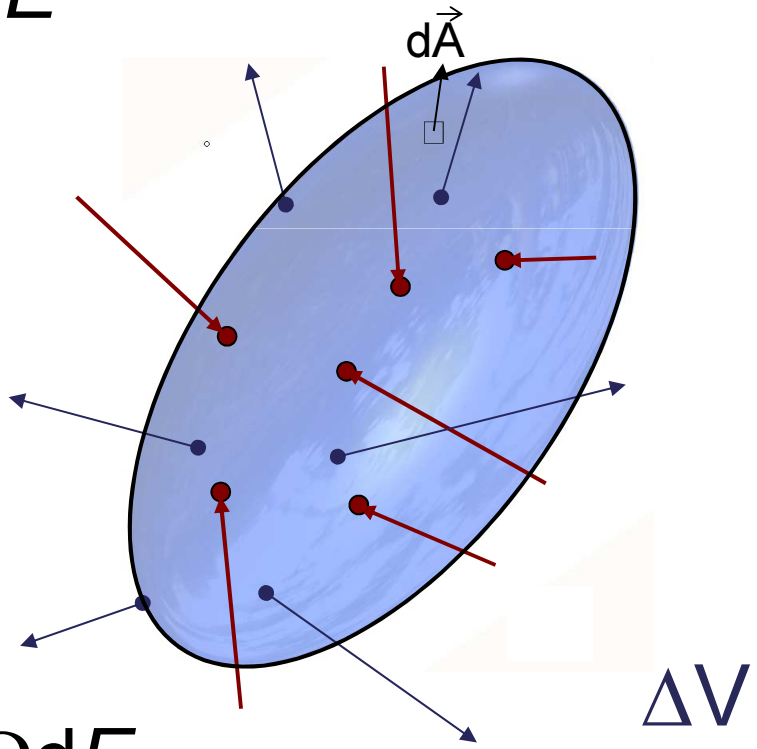

therefore the surface integral can be written as a volume integral:

$$dN_{j,\text{in-out}} = \int_{dv} \vec{\Omega}\,\nabla\,\Phi_{j,E,\Omega}\; dV d\Omega dE$$

Establishing a "transport formula"

(2) The number of particles j that are attenuated in ΔV:

Introducing $\sigma_{j,att}$ as the probability per **unit path length** for particle j of energy E and direction Ω to attenuate, we have:

$$\Phi = dL/dV$$

$$dL = \Phi \cdot dV$$

$$dN_{j,att} = \int_{dv} \sigma_{j,att} \cdot d\Omega\, dL$$

$$= \int_{dV} \sigma_{j,att} \cdot \Phi_j \, d\Omega dE dV$$

Establishing a "transport formula"

(3) The number of particles j that are born in the scattering interactions with medium atoms in ΔV :

Introducing $\sigma_{j'\to j}$ as the probability per unit path length that a particle j' with energy E' and direction Ω' will produce a secondary particle j with energy E and direction Ω, we have:

$$\mathrm{d}N_{\mathrm{j,secondaries}} = \int_{\mathrm{d}V}\int_{\Omega}\int_{E}\sum_{j'=1}^{3}\sigma_{j'\to j}\cdot \mathrm{d}L_{j'}\mathrm{d}\Omega'\mathrm{d}E'$$

$$= \int_{\mathrm{d}V}\int_{\Omega}\int_{E}\sum_{j'=1}^{3}\sigma_{j'\to j}\cdot \Phi_{j'}\,\mathrm{d}\Omega'\mathrm{d}E'\mathrm{d}\Omega\mathrm{d}E\mathrm{d}V$$

Establishing a "transport formula"

(4) The number of particles j produced by the sources inside the volume ΔV :

Introducing $Q_j(x,\Omega,E)$ as the source term for particle j inside the volume V, we have:

$$\mathrm{d}N_{\mathrm{j,source}} = \int_{\mathrm{d}V} Q_j \mathrm{d}V\mathrm{d}\Omega\mathrm{d}E$$

Establishing a "transport formula"

- Now we can combine these four terms:

$$\mathrm{d}N_{\mathrm{j}} = -\mathrm{d}N_{\mathrm{j,in\text{-}out}} - \mathrm{d}N_{\mathrm{j,att}} + \mathrm{d}N_{\mathrm{j,secondaries}} + \mathrm{d}N_{\mathrm{j,source}}$$

$$\mathrm{d}N_{\mathrm{j,in\text{-}out}} = \int_{\mathrm{d}V} \vec{\Omega} \nabla \Phi_{\mathrm{j,E,\Omega}} \, \mathrm{d}V\mathrm{d}\Omega\mathrm{d}E$$

$$\mathrm{d}N_{\mathrm{j,att}} = \int_{\mathrm{d}V} \sigma_{j,att} \cdot \Phi_j \, \mathrm{d}\Omega\mathrm{d}E\mathrm{d}V$$

$$\mathrm{d}N_{\mathrm{j,secondaries}} = \int_{\mathrm{d}V} \int_{\Omega} \int_{E} \sum_{j'=1}^{3} \sigma_{j' \to j} \cdot \Phi_{j'} \, \mathrm{d}\Omega' \mathrm{d}E' \mathrm{d}\Omega\mathrm{d}E\mathrm{d}V$$

$$\mathrm{d}N_{\mathrm{j,source}} = \int_{\mathrm{d}V} Q_j \mathrm{d}V\mathrm{d}\Omega\mathrm{d}E$$

Establishing a "transport formula"

… which yields:

$$dN_j = d\Omega dE \int_{dV} \Big[\underbrace{-\vec{\Omega} \nabla \Phi_{j,E,\Omega}}_{\text{net number through surface}} \underbrace{- \sigma_{j,att} \cdot \Phi_j}_{\text{attenuation term}} + \underbrace{\int_{\Omega} \int_{E} \sum_{j'=1}^{3} \sigma_{j' \to j} \cdot \Phi_{j'} \, dE' d\Omega'}_{\text{secondary particle production}} + \underbrace{Q_j}_{\text{source term}} \Big] dV$$

Establishing a "transport formula"

After having exposed the volume of interest, no particle will remain. This means, the integrand must be zero:

$$\mathrm{d}N_{\mathrm{j}} = \mathrm{d}\Omega\mathrm{d}E\int_{\mathrm{d}V}\Big[-\vec{\Omega}\nabla\Phi_{\mathrm{j,E,\Omega}} - \sigma_{j,att}\cdot\Phi_{j} + \int_{\Omega}\int_{E}\sum_{j'=1}^{3}\sigma_{j'\to j}\cdot\Phi_{j'}\,\mathrm{d}E'\,\mathrm{d}\Omega' + Q_{j}\Big]\mathrm{d}V$$

The entire integrand must be zero

Establishing a "transport formula"

The entire integrand must be zero

$$-\vec{\Omega}\nabla\Phi_{\mathrm{j,E,\Omega}} - \sigma_{j,att}\cdot\Phi_j + \int_{\Omega}\int_{E}\sum_{j'=1}^{3}\sigma_{j'\to j}\cdot\Phi_{j'}\,\mathrm{d}E'\mathrm{d}\Omega' + Q_j = 0$$

We finally obtain three sets of equation, where the

“j=1" refers to photons,

“j=2" refers to electrons, and

“j=3" refers to positrons

Establishing a "transport formula"

$$\vec{\Omega}\nabla\Phi_{1,E,\Omega} + \sigma_{1,att}\cdot\Phi_1 - \iint_{\Omega E}\sum_{j'=1}^{3}\sigma_{j'\to 1}\cdot\Phi_{j'}\,dE'd\Phi' = Q_1$$

$$\vec{\Omega}\nabla\Phi_{2,E,\Omega} + \sigma_{2,att}\cdot\Phi_2 - \iint_{\Omega E}\sum_{j'=1}^{3}\sigma_{j'\to 2}\cdot\Phi_{j'}\,dE'd\Phi' = Q_2$$

$$\vec{\Omega}\nabla\Phi_{3,E,\Omega} + \sigma_{3,att}\cdot\Phi_3 - \iint_{\Omega E}\sum_{j'=1}^{3}\sigma_{j'\to 3}\cdot\Phi_{j'}\,dE'd\Phi' = Q_3$$

These set of equation are well known as

Boltzmann transport equation

which are based on the conservation of particles in space.

Establishing a "transport formula"

The Boltzmann transport equation represent a coupled integro-differential system of stationary linear equations for external radiation therapy.

By solving these equation system, one can obtain the fluence of electrons and positrons and hence the absorbed dose effected by these particles.

Linear Boltzman Equation

- Describes the transport of particles through a medium (incl photons)
- The **linear** equation means particles only interact with medium not with each other i.e. cross section do not depend on fluence
  - No magnetic field is present
- A **closed** form or **analytical** solution would give the exact solution of the dose distribution in a irradiated medium e.g. a patient – this is not possible
  - Only possible in very restricted problems
- An **open** form must be used i.e. a **numerical** solution
- Can use **Monte Carlo** which indirectly can provide an approximate solution
- Or – use **Deterministic** approaches (Grid Based Boltzmann Solvers GBSS)

  - Directly solve BTE
  - Inhomogeneities easily handled
  - Free of statistical noise

Monte Carlo simulations of particle transport processes are a faithful simulation of physical reality because:

- particles are “born” according to distributions describing the **source**,
- they **travel certain distances:**
  a) to the next point of interaction, or
- b) going through the entire voxel without an interaction
- **scatter into another energy and/or direction** according to the corresponding differential cross section, **possibly producing new particles** that have to be transported as well.

This methods requires a tracking of each individual particle through a certain geometry, and the summation over a large number of particles.

Individual particle tracking within the Monte Carlo method

The **path length** within a volume of interest and thus the fluence can be determined by the following procedure:

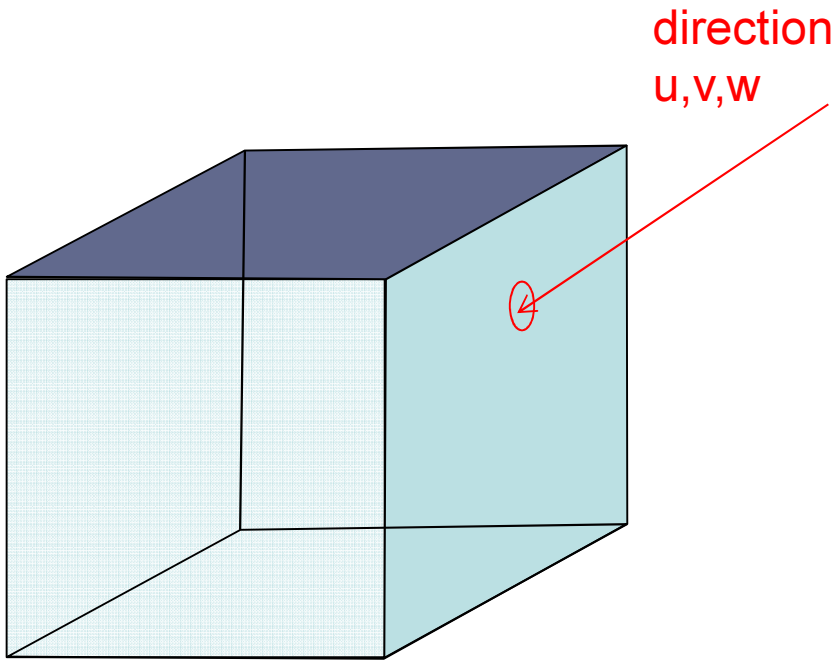

We start with a photon which has a direction according to the 3 directional cosines

u in direction x,
v in direction y,
w in direction z

and which is entering a volume (voxel) at x_0, y_0, z_0.

Individual particle tracking within the Monte Carlo method

Step 1: The track length d to the next interaction of an individual photon – starting from the entry point – can be anywhere.
For an individual photon it must be taken from a **distribution** determined by the
mean free path length d_{mfp}

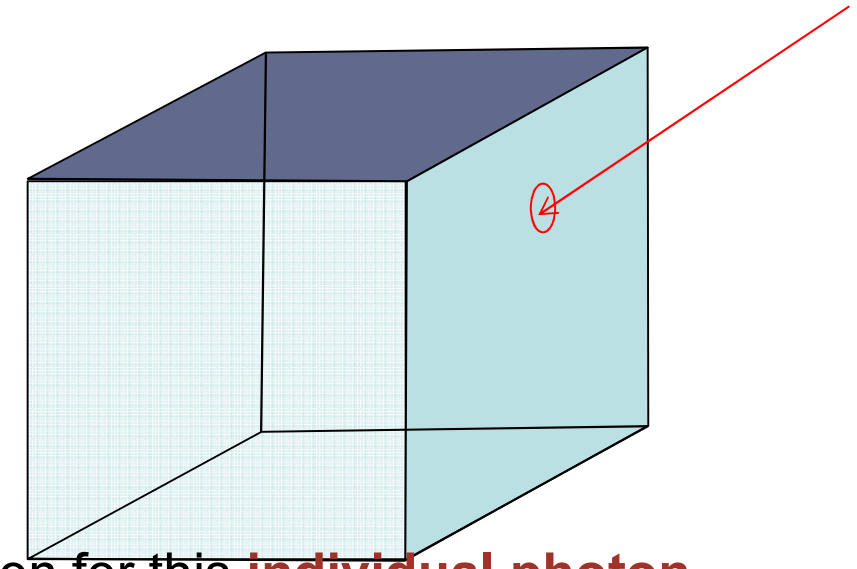

This is accomplished by a very simple method:

$$d_{sample} = -d_{mfp} \cdot \ln(r)$$

d_{sample} distance to the next interaction for this **individual photon**
d_{mfp} distance to the next interaction **on average**
r a random number out of the interval {0,1}

Individual particle tracking within the Monte Carlo method

Step 2:
Also calculate the geometrical path length d_{geo} within V

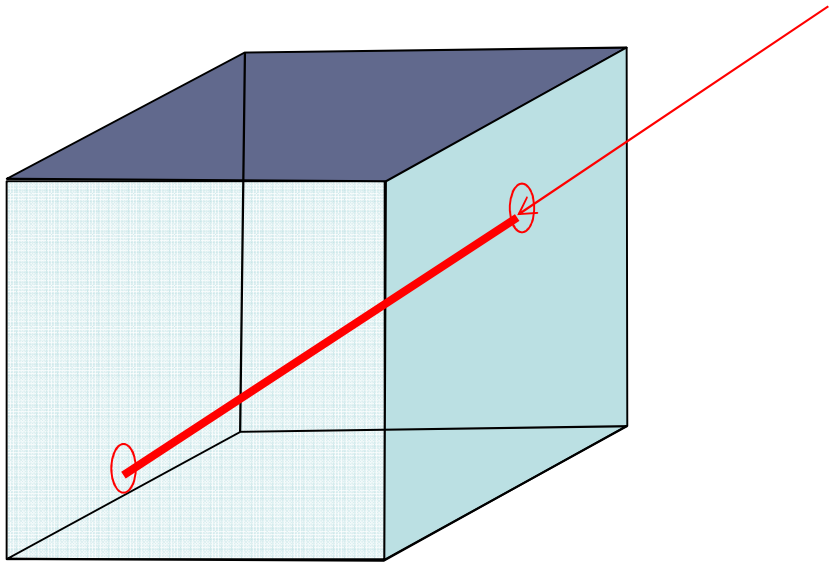

Step 3: Make a differentiation between

Case 1: $d_{sample} < d_{geo}$

The interaction occurred within the voxel.
Take d_{sample} for the track length

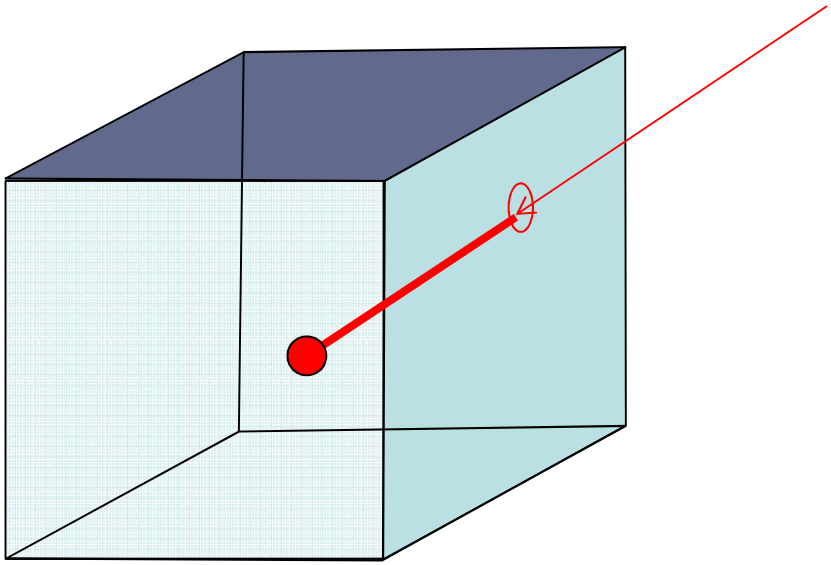

Case 2: $d_{sample} > d_{geo}$

No interaction within the voxel.

Take d_{geo} for the track length

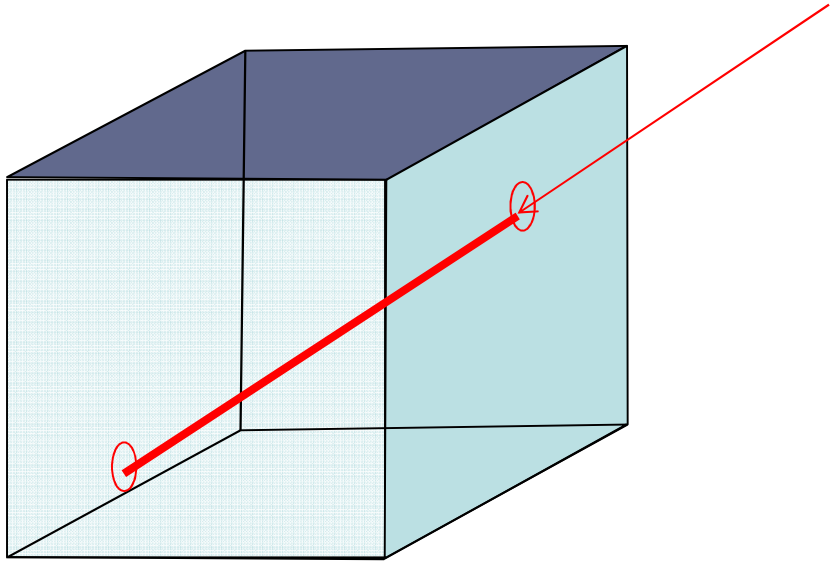

Individual particle tracking within the Monte Carlo method

Step 4 in case that an interaction occured:

Determine energy and direction of the new photon (if produced) and continue tracking, now starting at the point of interaction

Step 4 in case that no interaction occured:

Go to adjacent voxel and determine the next $d_{sample,next}$ as:

$$d_{sample,next} = d_{sample} - d_{geo}$$

Step 5:
Repeat everything for any voxel and any new photon

Tracking in Monte Carlo Codes

More generally speaking, the term **tracking** can be used to describe the procedure of subsequently determining the trajectories in the **six dimensional phase space** between each two interactions.

The six dimensions are $(x;\Omega;E)$
where:

- $x = (x_1; x_2; x_3)$ are the spatial coordinate variable,
- Ω is the particle direction which is a point on a unit sphere S with the angles coordinates φ and θ
- E is the energy variable.

Summary

$$D = \frac{d\bar{\varepsilon}}{dm}$$

1) Definition of absorbed dose:
2) Important radiation field quantities are:
   - particle fluence $\Phi = \frac{dN}{dA}$
   - alternative definition $\Phi = \frac{dL}{dV}$
   - particle fluence differential in energy

$$\Phi_E(E) = \frac{d\Phi}{dE} = \frac{d^2N}{dAdE} \left[\frac{1}{m^2 J}\right]$$

Summary

3) A radiation transport formula can be derived from bookkeeping process of particles in the phase space:

$$\mathrm{d}N_j = \mathrm{d}\Omega\mathrm{d}E\int_{\mathrm{d}V}\Big[\underbrace{-\vec{\Omega}\nabla\Phi_{j,E,\Omega}}_{\text{net number through surface}} \underbrace{-\sigma_{j,att}\cdot\Phi_j}_{\text{attenuation term}} + \underbrace{\int_{\Omega}\int_{E}\sum_{j'=1}^{3}\sigma_{j'\to j}\cdot\Phi_{j'}\,\mathrm{d}E'\mathrm{d}\Omega'}_{\text{secondary particle production}} + \underbrace{Q_j}_{\text{source term}}\Big]\mathrm{d}V$$

Summary

… leading to the Boltzmann Transport equations:

$$\vec{\Omega}\nabla\Phi_{1,E,\Omega} + \sigma_{1,att}\cdot\Phi_1 - \iint_{\Omega E}\sum_{j'=1}^{3}\sigma_{j'\to 1}\cdot\Phi_{j'}\,dE'd\Phi' = Q_1$$

$$\vec{\Omega}\nabla\Phi_{2,E,\Omega} + \sigma_{2,att}\cdot\Phi_2 - \iint_{\Omega E}\sum_{j'=1}^{3}\sigma_{j'\to 2}\cdot\Phi_{j'}\,dE'd\Phi' = Q_2$$

$$\vec{\Omega}\nabla\Phi_{3,E,\Omega} + \sigma_{3,att}\cdot\Phi_3 - \iint_{\Omega E}\sum_{j'=1}^{3}\sigma_{j'\to 3}\cdot\Phi_{j'}\,dE'd\Phi' = Q_3$$

Summary

4) The Monte Carlo method is the most popular method to solve the Boltzman Transport Equations

5) " **Tracking** “ describes the procedure of subsequently determining the trajectories in the **six dimensional phase space** between each two interactions.

6) "**Ray tracing**" is a procedure to determine the individual segments d_1, d_2, .. through a voxel array which are required to calculate the **radiological path length**.

for photons: $$d_{radiol} = \sum_i \sum_j \sum_k d_{i,j,k} \cdot \mu_{i,j,k}$$

Appendix: Alternative definition of fluence

We follow a proof given by A. B. Chilton in 1977 (Health Physics 34, 1978)

- Consider the small irregular volume of interest ΔV.
- Assume a radiation field with particles of any **arbitrary directional distribution** .
- However, **initially** consider only those particles going in the direction Ω.

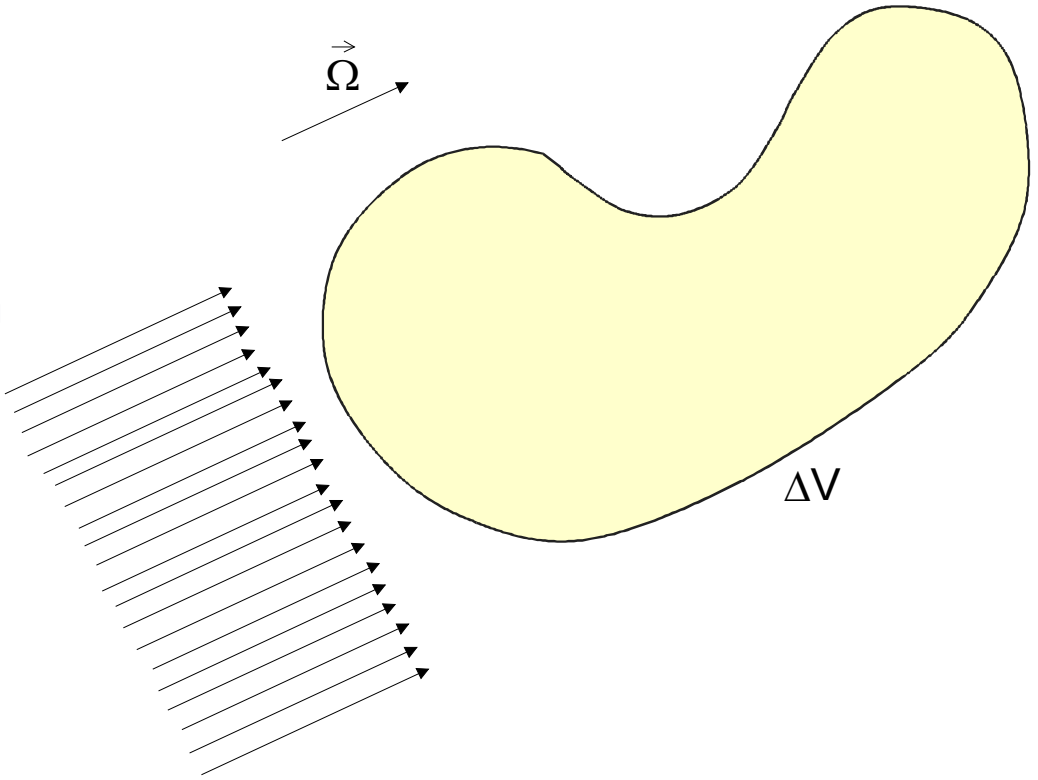

- Establish "tubes" within the volume of differential cross section **da** and differential length **$h_i(x,y)$**
- The differential number of particles N with direction Ω is

$$dN(\vec{\Omega}) = \Phi_{\Omega}(\vec{\Omega}) \cdot d\Omega da$$

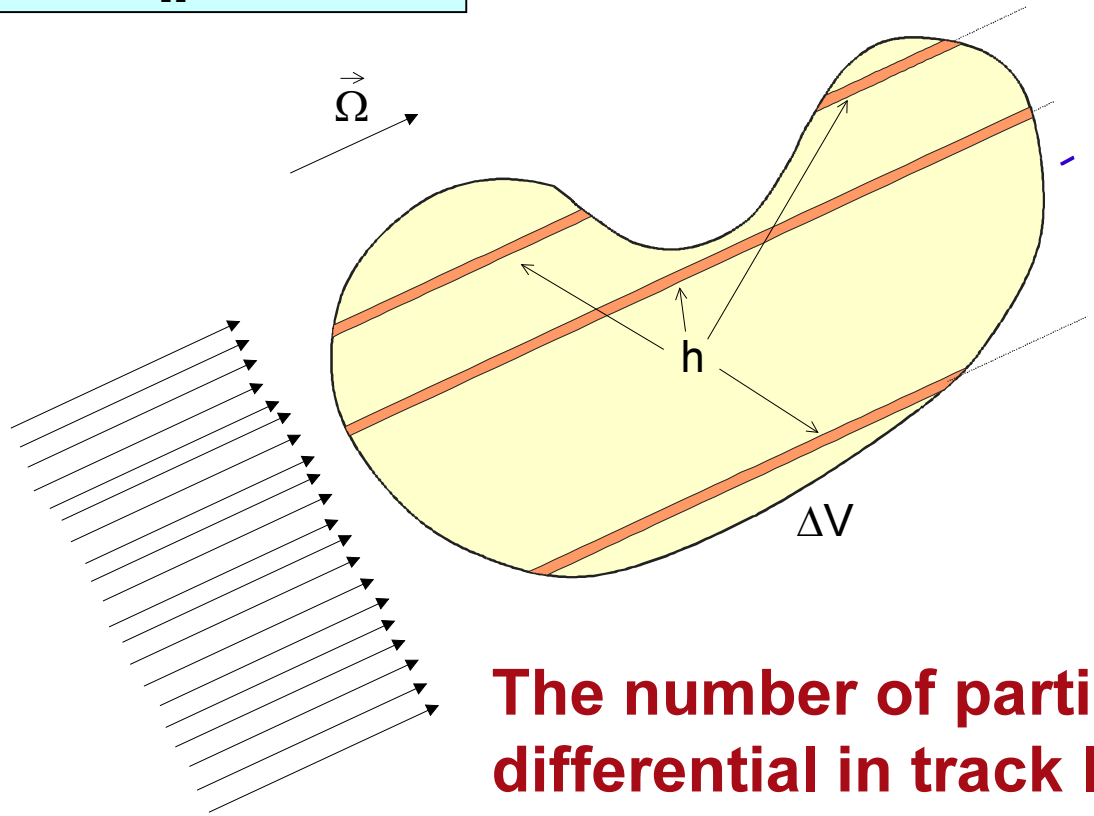

The number of particles differential in track length dL is

$$dL(\vec{\Omega}) = dN(\vec{\Omega}) \cdot h(x,y) = \Phi_{\Omega}(\vec{\Omega})\, d\Omega da \cdot h(x,y)$$

- We continue with the number of particles differential in track length dL

  The number of particle differential in track length dL in one direction Ω was

$$\mathrm{d}L(\vec{\Omega}) \quad = \quad \Phi_{\Omega}(\vec{\Omega})\,\mathrm{d}\Omega\mathrm{d}a \cdot \mathrm{h}(\mathrm{x},\mathrm{y})$$

- We need the differential track length over all directions.

⇒ **Requires integration over all directions**: $\int_{4\pi} \left[\mathrm{d}L(\vec{\Omega}) \right] d\Omega$

- and yields the total number differential in track length:

$$dL \quad = \quad \int_{4\pi} \left[\Phi_{\Omega}(\vec{\Omega})\, d\Omega da \cdot h(x,y) \right] d\Omega$$

- The integral $$dL = \int_{4\pi} \left[\Phi_{\Omega}(\vec{\Omega})\, d\Omega da \cdot h(x,y) \right] d\Omega$$

can be further modified, knowing, that $h(x,y) \cdot da = dV$

$$\Rightarrow \quad dL = \int_{4\pi} \left[\Phi_{\Omega}(\vec{\Omega})\, d\Omega \cdot dV \right] d\Omega$$

- Since $$\int_{4\pi} \left[\Phi_{\Omega}(\vec{\Omega})\, d\Omega \right] d\Omega = \Phi$$

we obtain $$dL = \Phi \cdot dV$$ or $$\Phi = \frac{dL}{dV}$$

Linac head designs: Photon and electron beams

Tommy Knöös

Sweden

ESTRO School

Learning objectives

- To know how a clinical high-energy photon beam is produced through an X-ray target and (most often) a flattening filter.
- To learn about basic photon beam characteristics, such as beam quality and lateral distributions.
- To understand how the photon beam is shaped and modulated in collimators and wedges.
- To understand how the “raw” electron beam is converted into a flat and clinically useable electron beam through scattering foils.
- To learn about electron beam collimation.
- To understand the basic characteristics of a clinical electron beam.

A typical linac of today

Varian Clinac®
Engineered for Clinical Benefits

1 Gridded Electron Gun
Controls dose rate rapidly and accurately. Permits precise beam control for dynamic treatments, since gun can be gated. Removable for cost-effective replacement.

2 Energy Switch
Patented switch provides energies within the full therapeutic range, at consistently high, stable dose rates, even with low energy x-ray beams. Ensures optimum performance and spectral purity at both energies.

3 Wave Guide
High efficiency, side coupled standing wave accelerator guide with demountable electron gun and energy switch.

4 Achromatic 3-Field Bending Magnet
Unique design with fixed ± 3 % energy slits ensures exact replication of the input beam for every treatment. The 270° bending system, coupled with Varian's 3-dimensional servo system, provides for a 2 mm circular focal spot size for optimal portal imaging.

5 Real-Time Beam Control Steering System
Radial and transverse steering coils and a real-time feedback system ensure that beam symmetry is within ± 2 % at all gantry angles.

6 Focal Spot Size
Even at maximum dose rate – and any gantry angle – the circular focal spot remains less than 2 mm, held constant by a focus solenoid. Assures optimum image quality for portal imaging.

7 10-Port Carousel
New electron scattering foils provide homogeneous electron beams at therapeutic depths. Extra ports allow for future development of specialized beams.

8 Ion Chamber
Dual sealed ion chambers with 8 sectors for rigourous beam control provide two independent channels, impervious to changes in temperature and pressure. Beam dosimetry is monitored to be within ± 2 % for longterm consistency and stability.

9 Asymmetric Jaws
Four independent collimators provide flexible beam definition of symmetric and asymmetric fields.

10 Millennium™ Multi-Leaf Collimator
Dynamic full field high resolution 120 leaf MLC with dual redundant safety readout for most accurate conformal beam shaping and IMRT treatments.

11 Electronic Portal Imager
High-resolution PortalVision™ aS1000 Megavoltage imager mounted on a robotic arm for efficient patient setup verification and IMRT plan QA.

12 On-Board Imager®
kV X-ray source (12a) and high-speed, high-resolution X-ray detector (12b) mounted on two robotic arms orthogonal to the treatment beam for Image Guided Radio Therapy (IGRT). The unique system provides kV imaging at treatment and includes radiographic, fluoroscopic and Cone Beam CT image acquisition and patient repositioning applications.

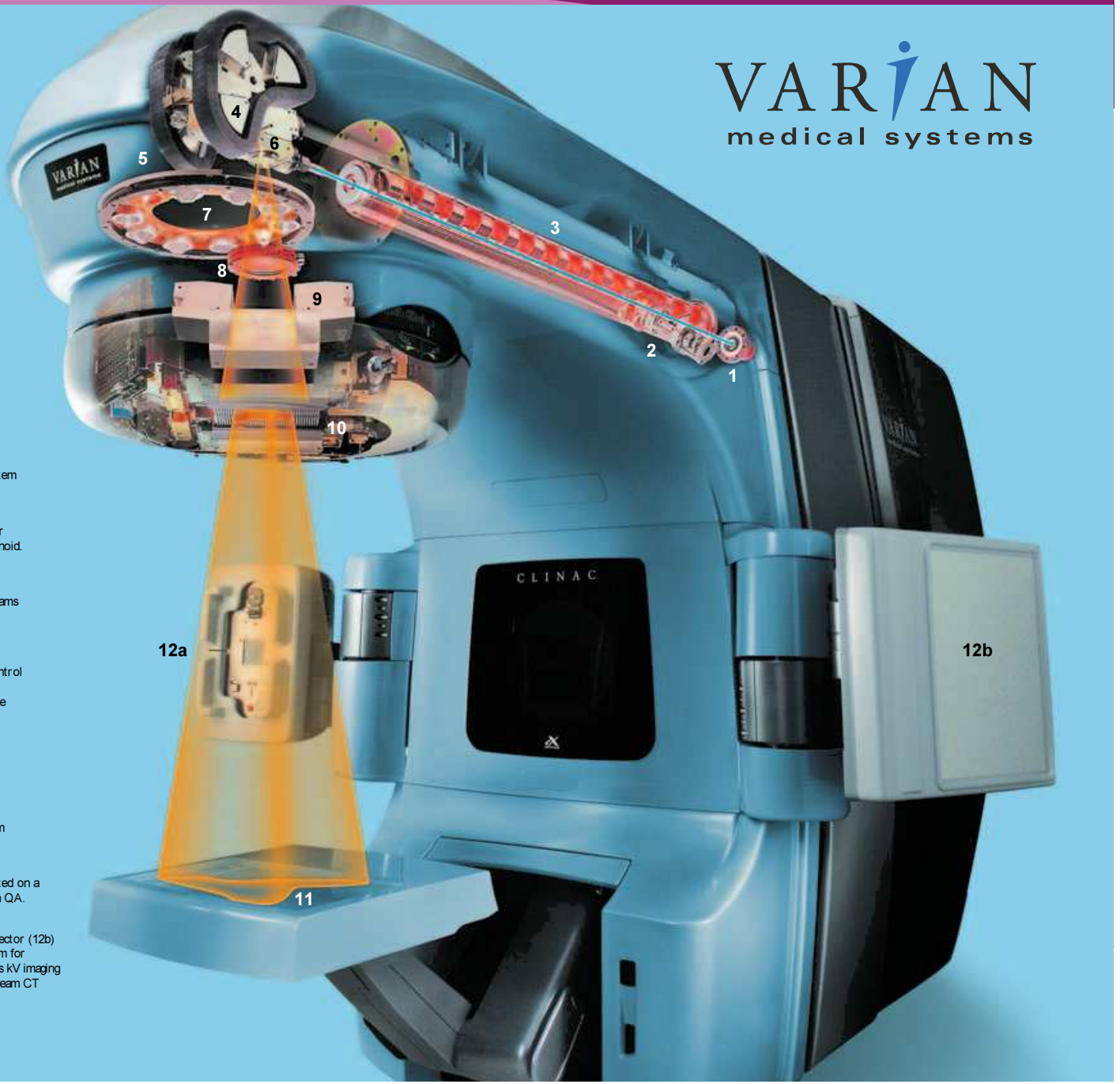

A typical linac of today

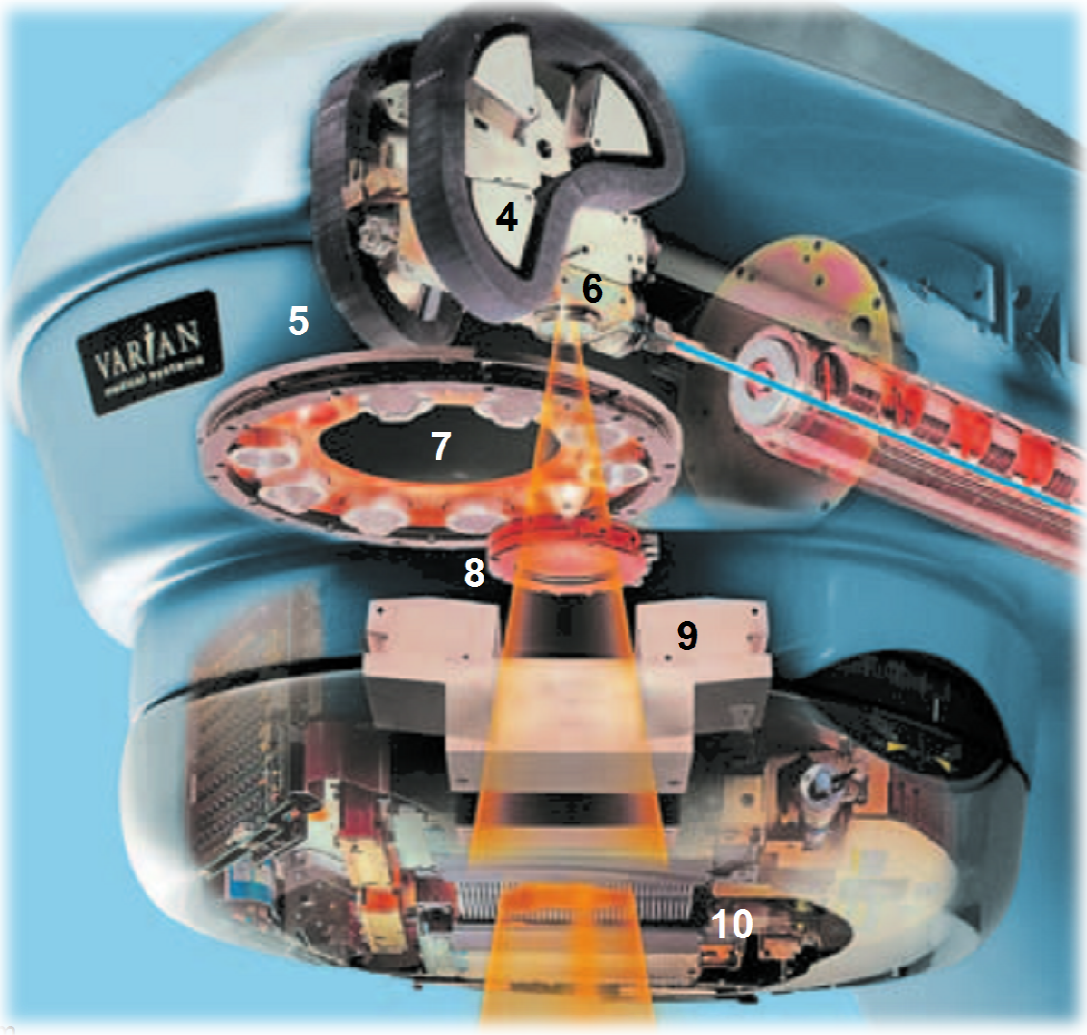

Bending magnets

Critical component as it controls the electron beam energy.
Why not use a simple 90° bending magnet?

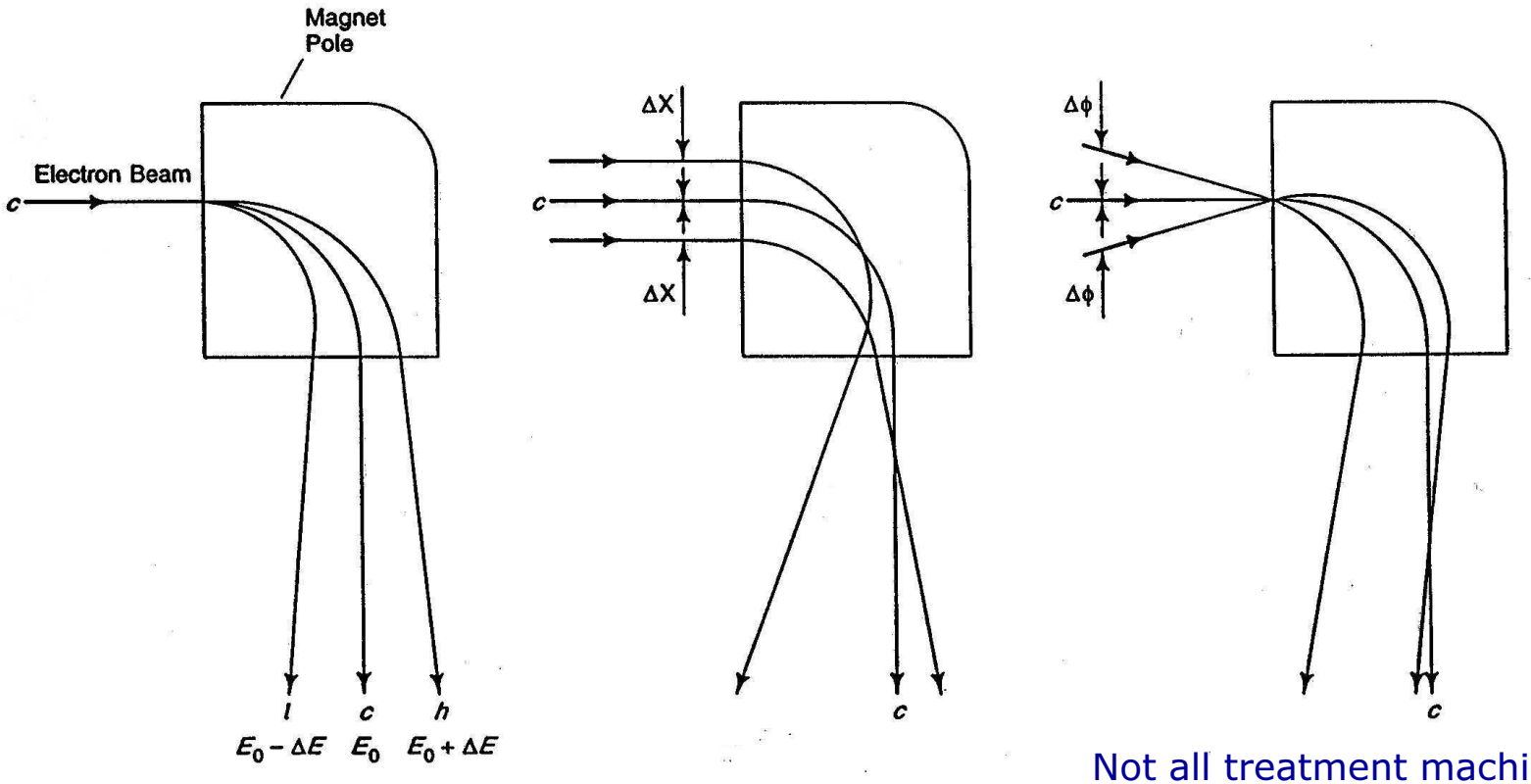

Not all treatment machines have a bending magnet.

Karzmark *et al* [1]

ESTRO School

Achromatic bending magnets

3×90° (Varian Clinac, high energy)

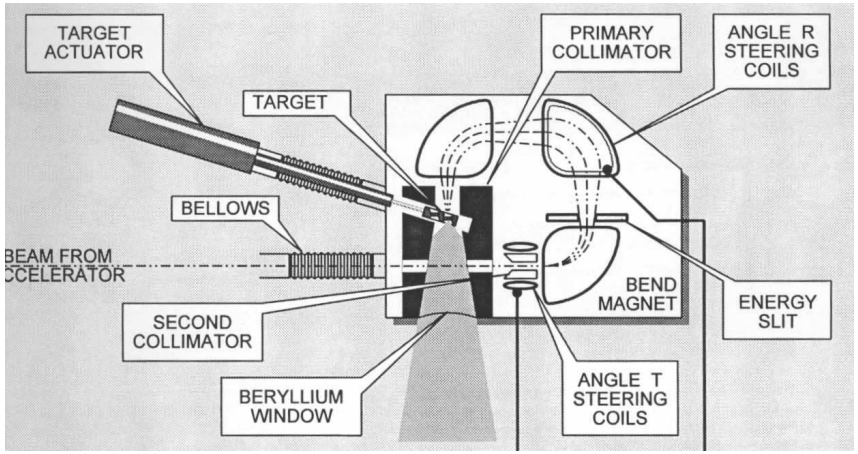

270° (Siemens Primus)

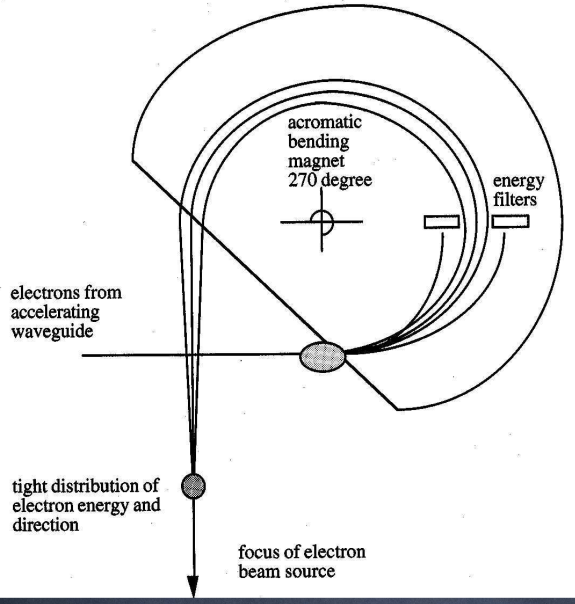

112° Slalom (Elekta)

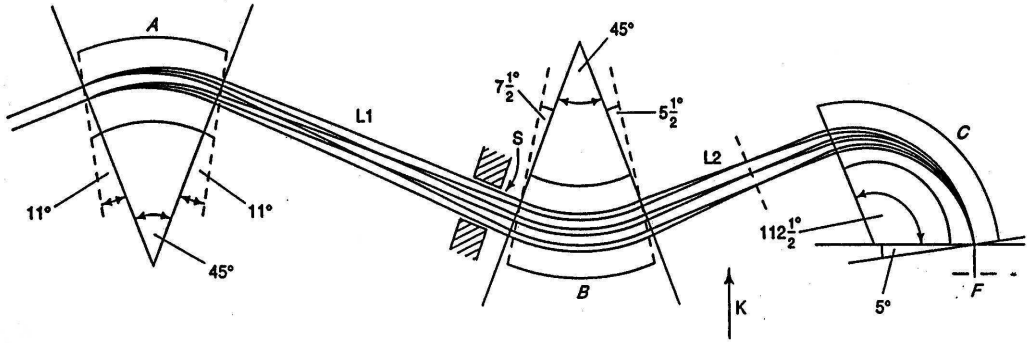

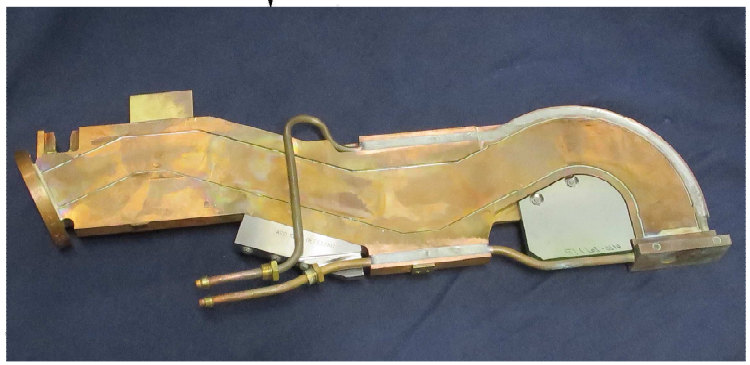

Karzmark *et al* [1]

ESTRO School

Other designs exist without bending magnet

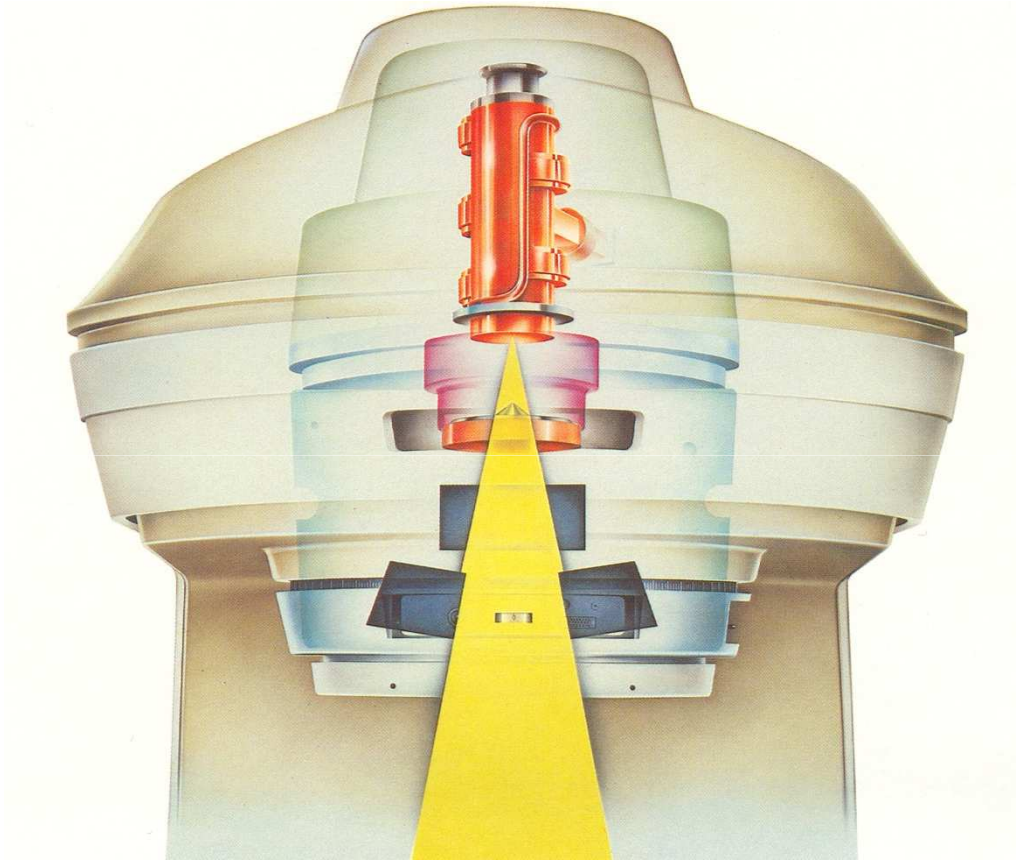

Example – Varian low energy machine 4/6 MV

Target materials

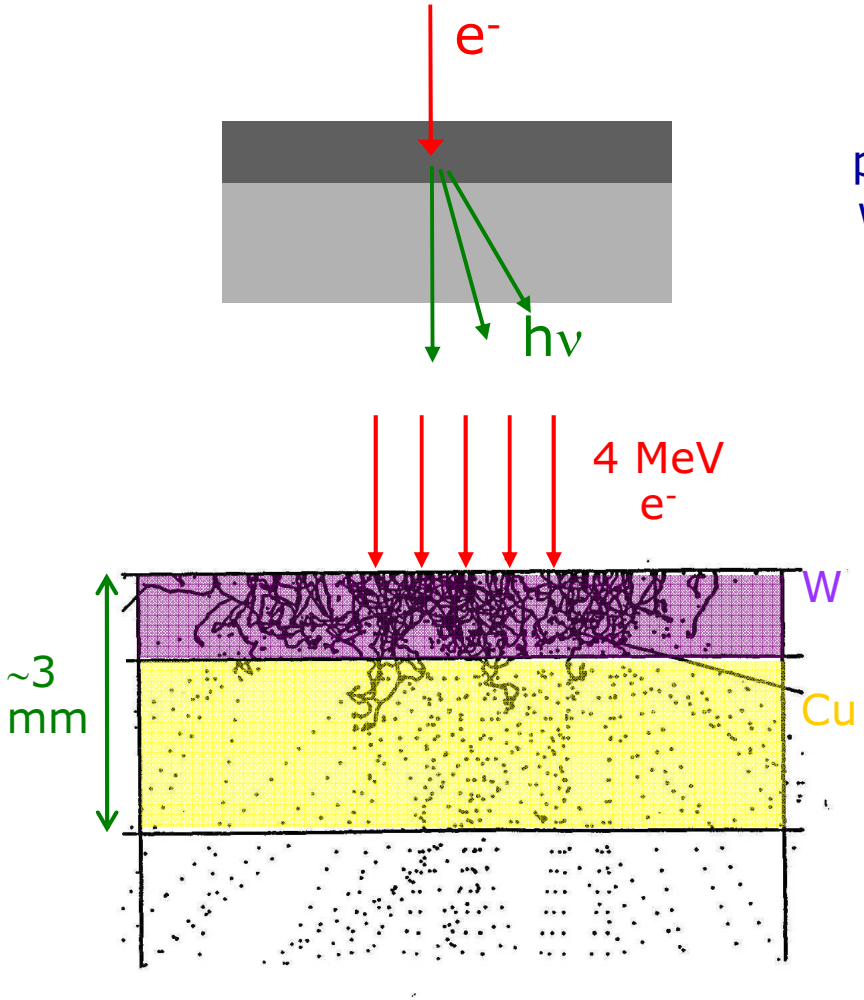

X-ray targets can be constructed in two layers; one high-*Z* (W, Au) for photon production and a second layer with lower *Z* (Cu, Al) to fully stop the electrons and harden the photon spectrum. (and providing cooling)

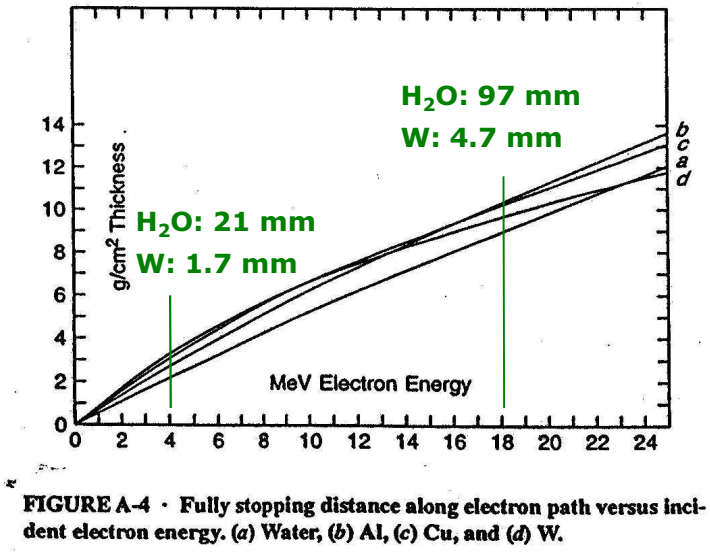

FIGURE A-4 · Fully stopping distance along electron path versus incident electron energy. (*a*) Water, (*b*) Al, (*c*) Cu, and (*d*) W.

Karzmark *et al* [1]

ESTRO School

The Focal source spot

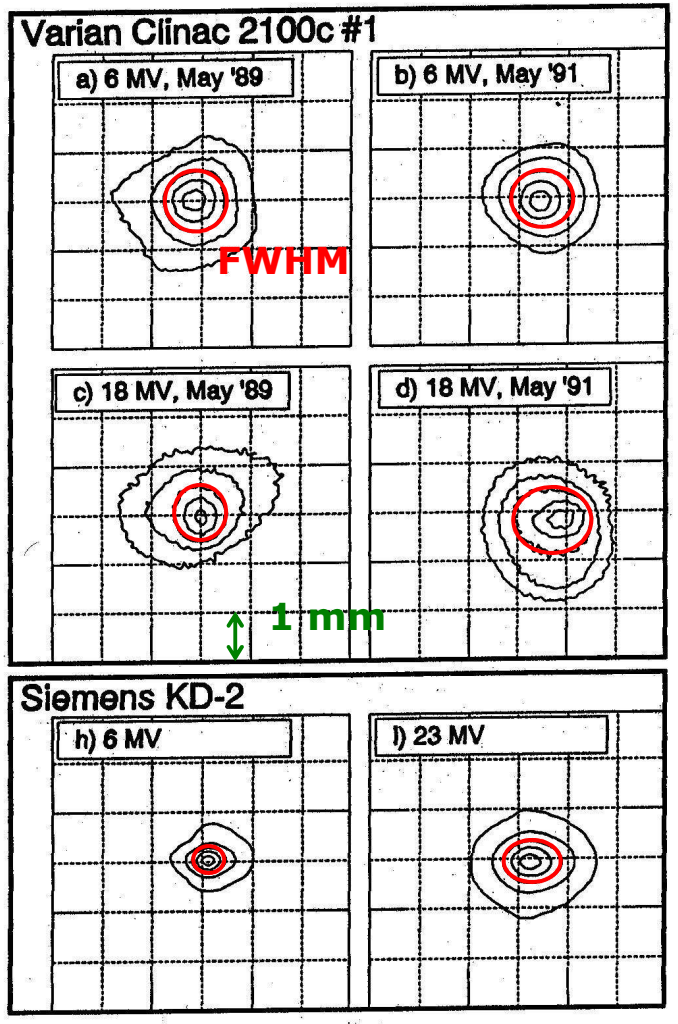

Approximately Gaussian source distributions, in some cases elliptical. Typical FWHM is 1-2 mm.

(Measured using a rotated slit camera and a diode.)

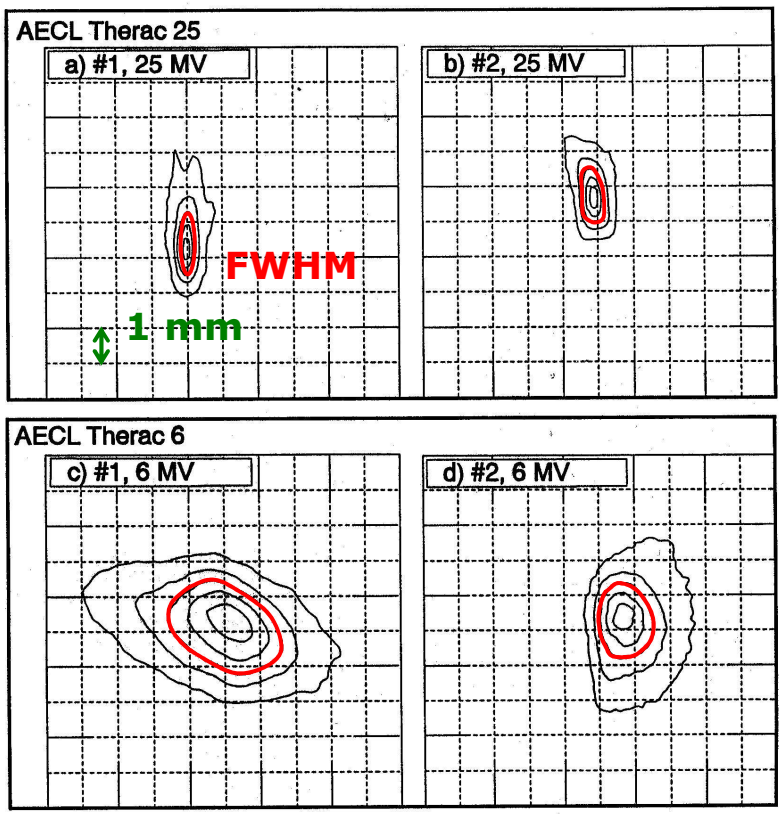

Jaffray *et al* [2]

ESTRO School

Geometric penumbra

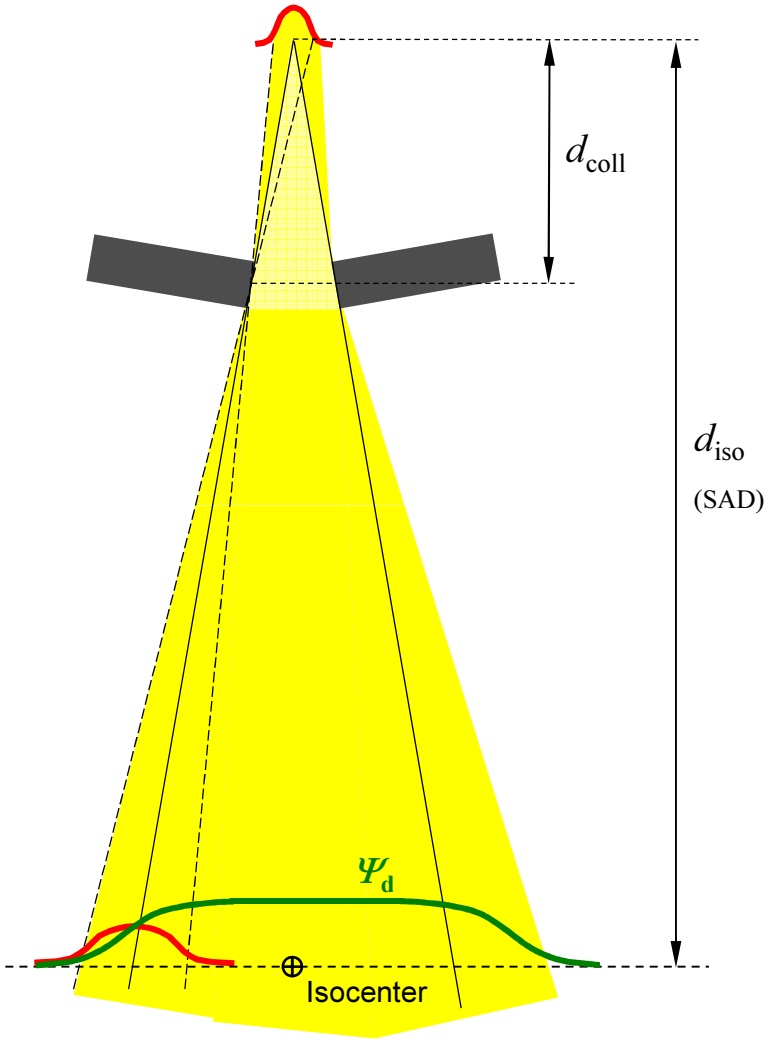

The source related *geometric penumbra* (10-90%) typically has a width of 3-5 mm at isocenter level, but can in more extreme cases extend up to about 10 mm.

Particularly important for small beams and IMRT.

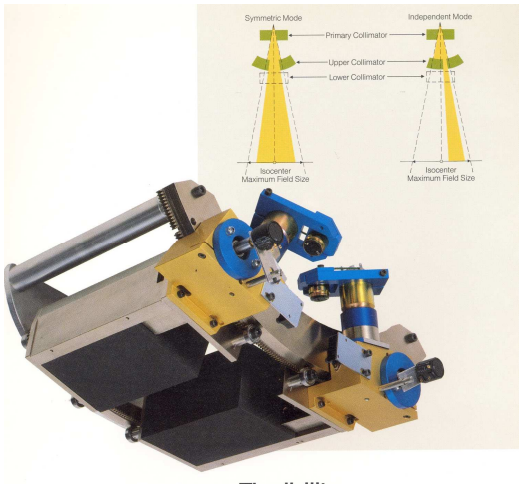

Focal/direct fluence characteristics

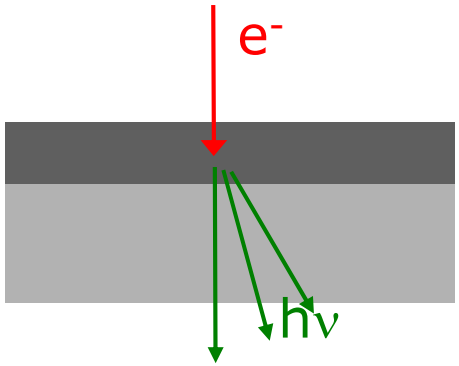

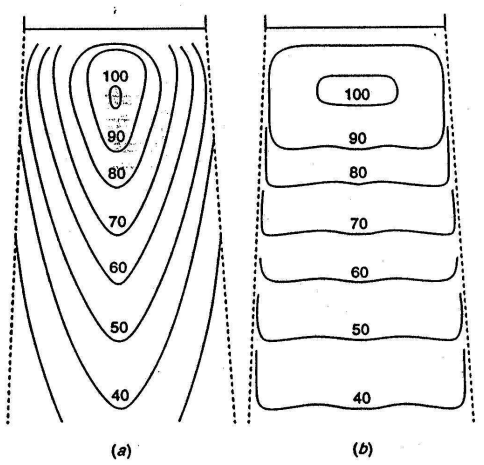

FIGURE 8-7 · Isodose curves for 20-MV x-ray beams; (*a*) without and (*b*) with a beam flattening filter. (Courtesy of W. J. Meredith and J. B. Massey.)

Lateral fluence distribution

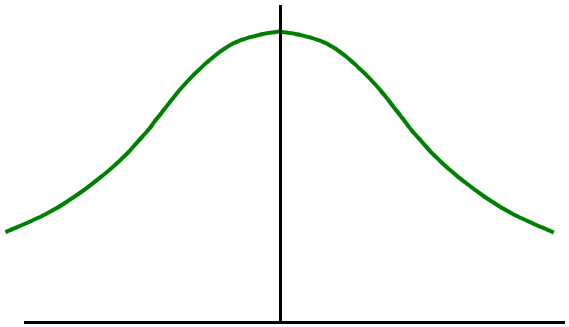

Mean energy - lateral variation
(Off-axis softening)

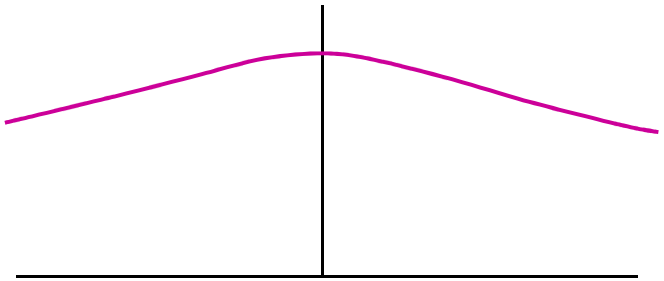

Karzmark *et al* [1]

ESTRO School

Flattening of the direct photon beam

The conical *flattening filter* absorbs 50-90% of the direct photons on the central axis.
In addition, it works as a scatter source located 7-15 cm downstream from the target, adding 5-10% at isocenter.

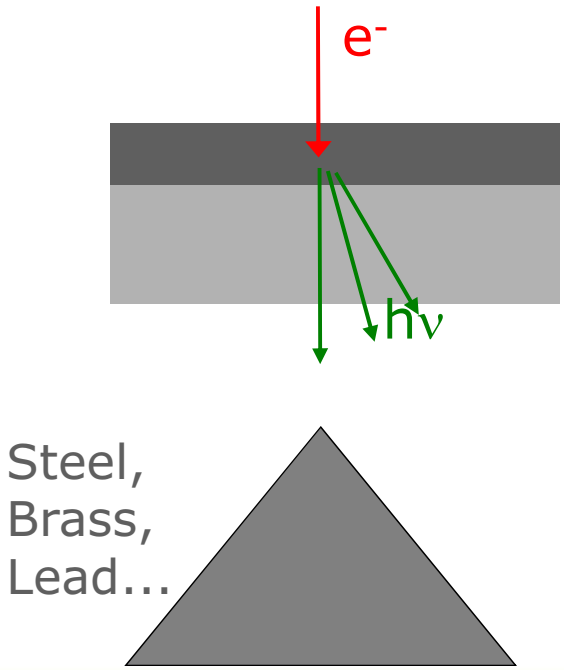

Lateral fluence distribution

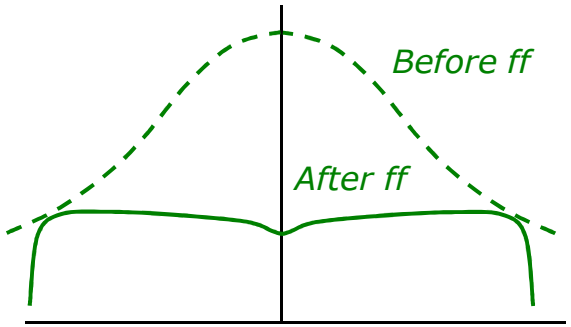

Consequences of a flattening filter

Head scatter

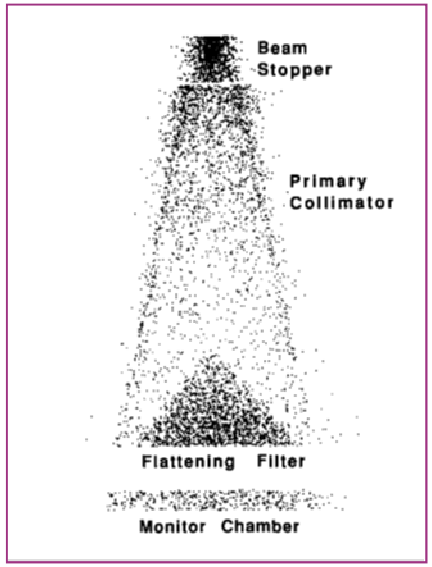

From Chaney 1994

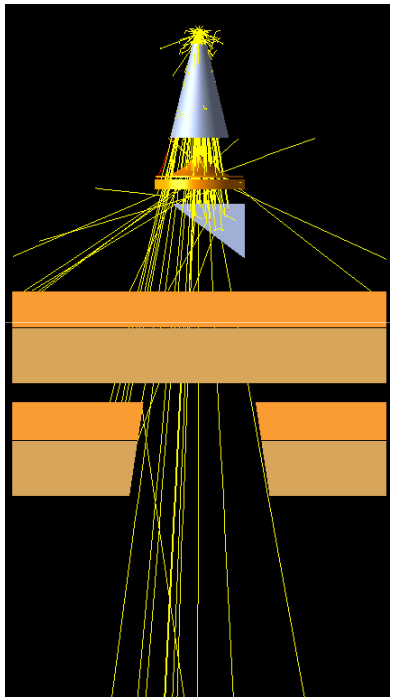

Energy variations off-axis

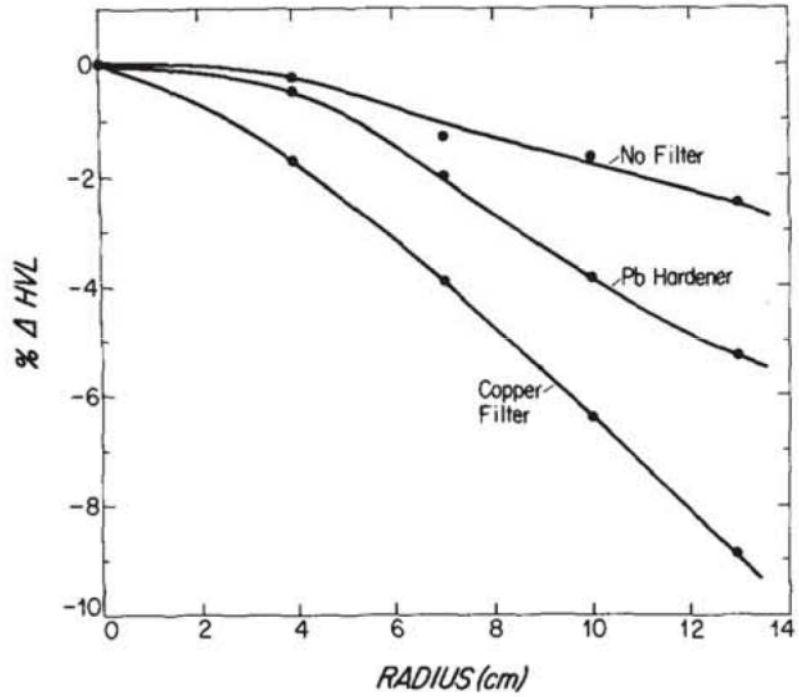

FIG. 4. Percentage changes in HVL, measured in brass, but with each curve normalized to its value on the central axis.

From Lutz and Larsen 1984

Flattening filters

Elekta

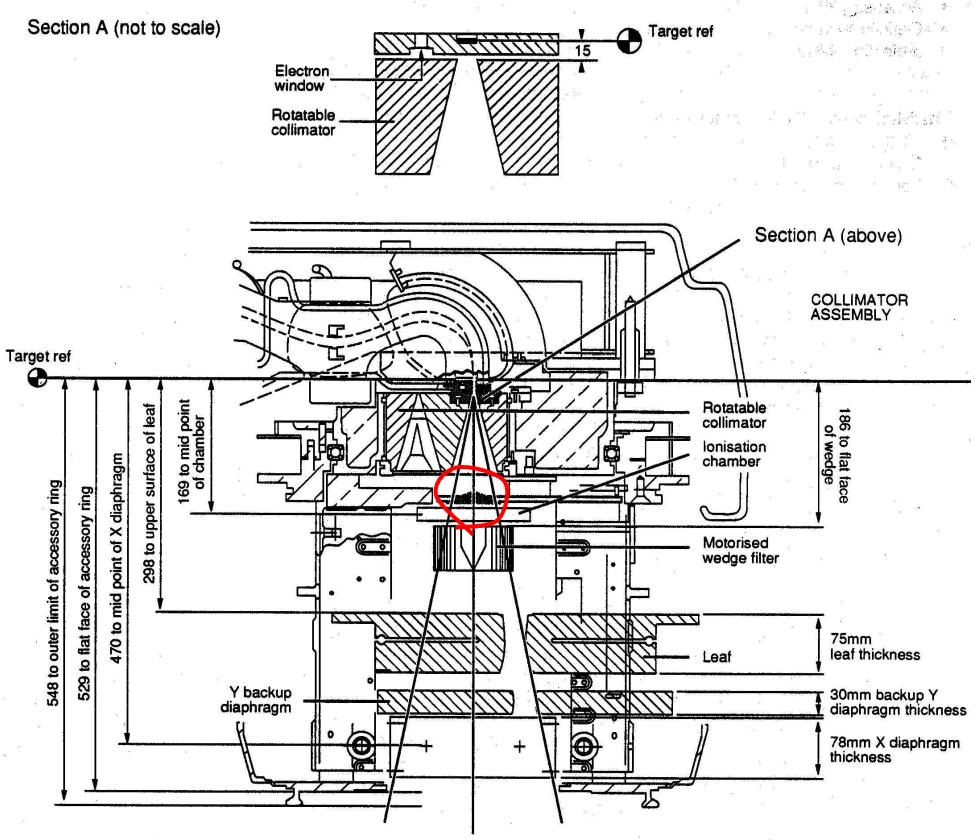

Varian (Clinac, high energy)

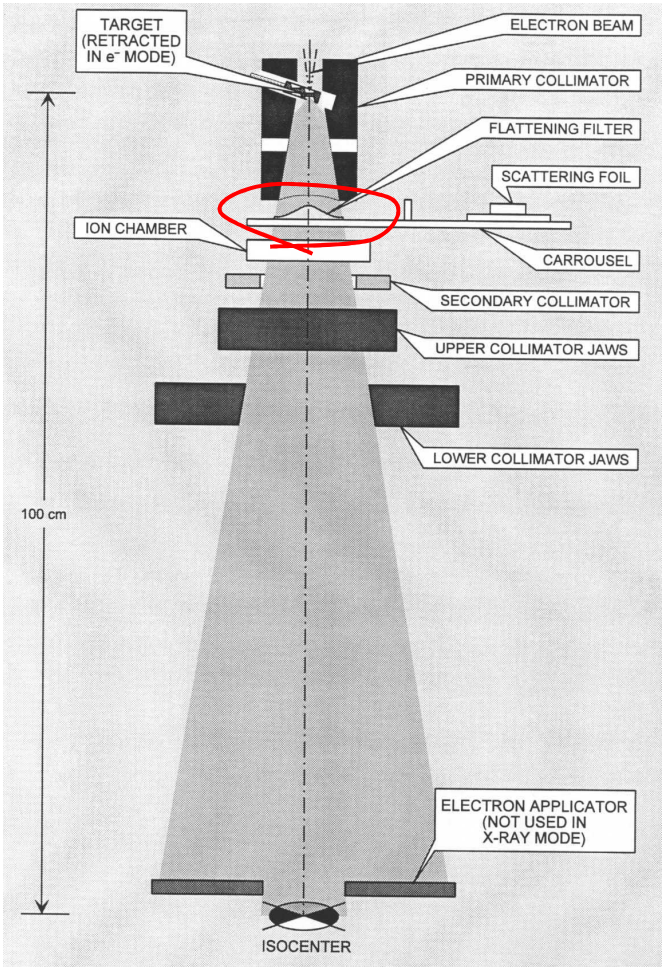

ESTRO School

Carousel from Elekta Precise

TrueBeam carousel

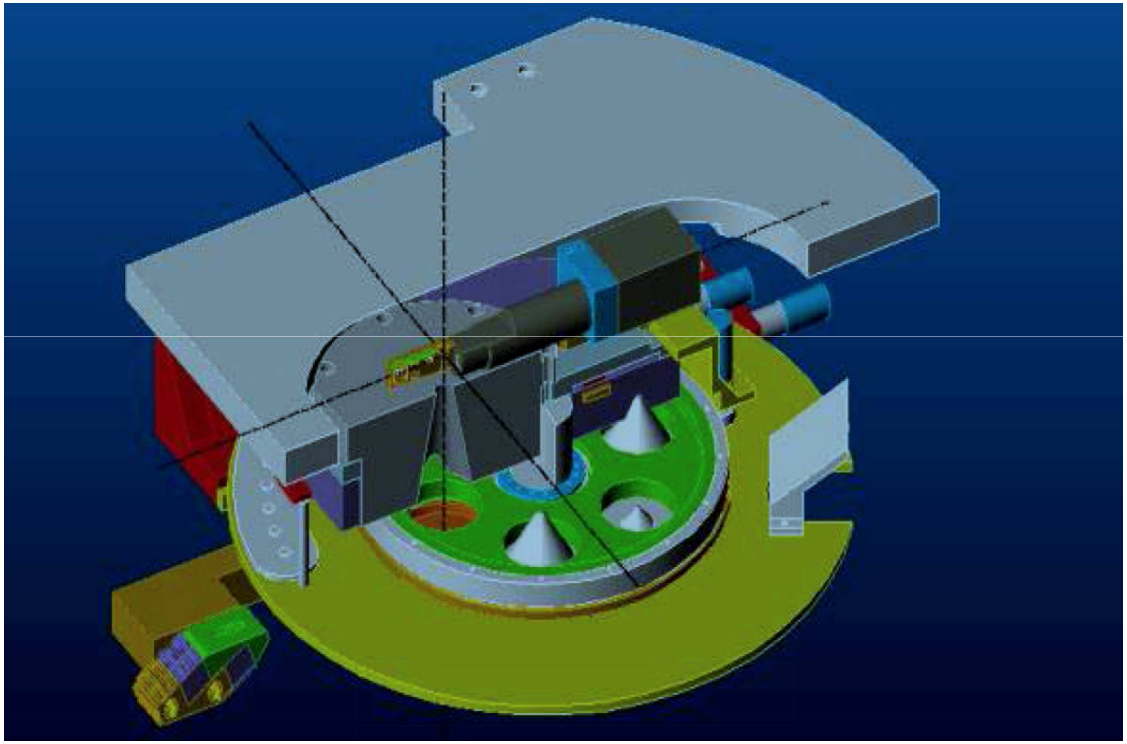

Resulting photon spectra at isocenter

Average photon energies (in MeV):

≤10MV: ~ MV/3

>10MV: ~ MV/3.5-4

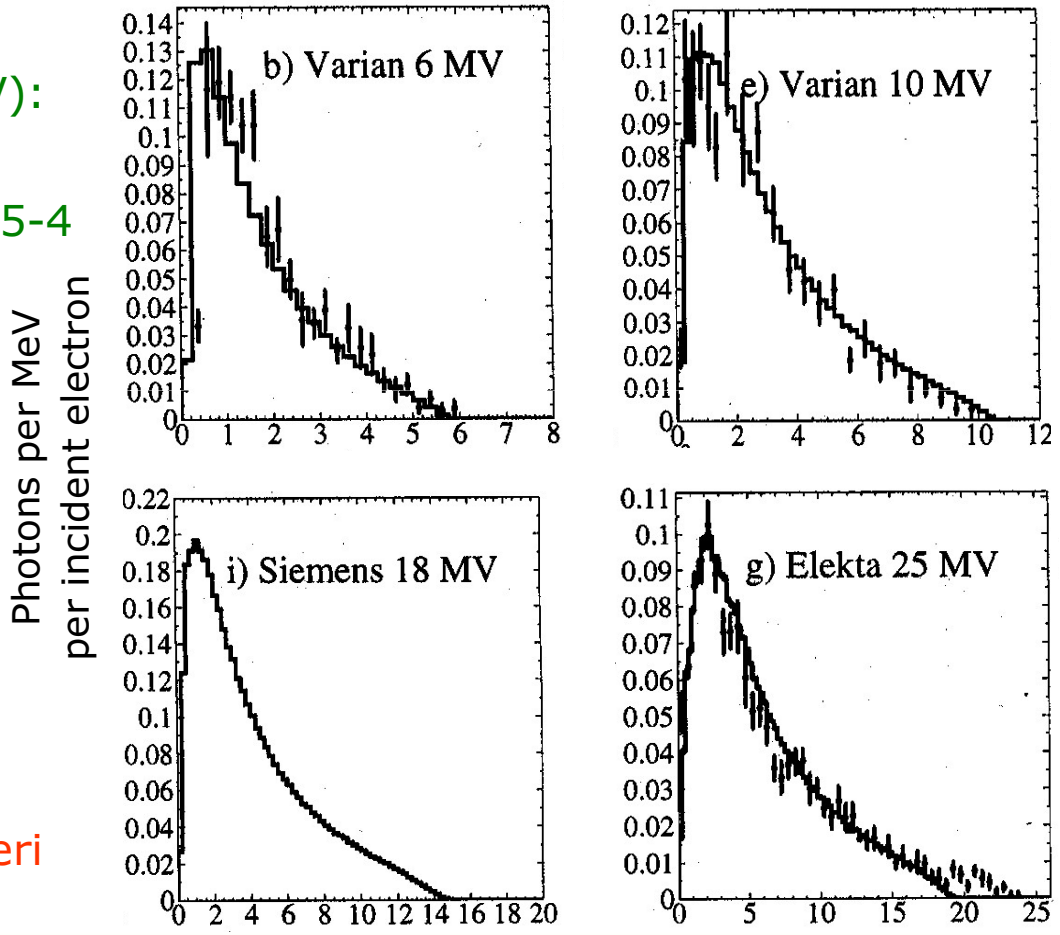

Sheikh-Bagheri *et al* [4]

Resulting energy fluence spectra at isocenter (in log scale)

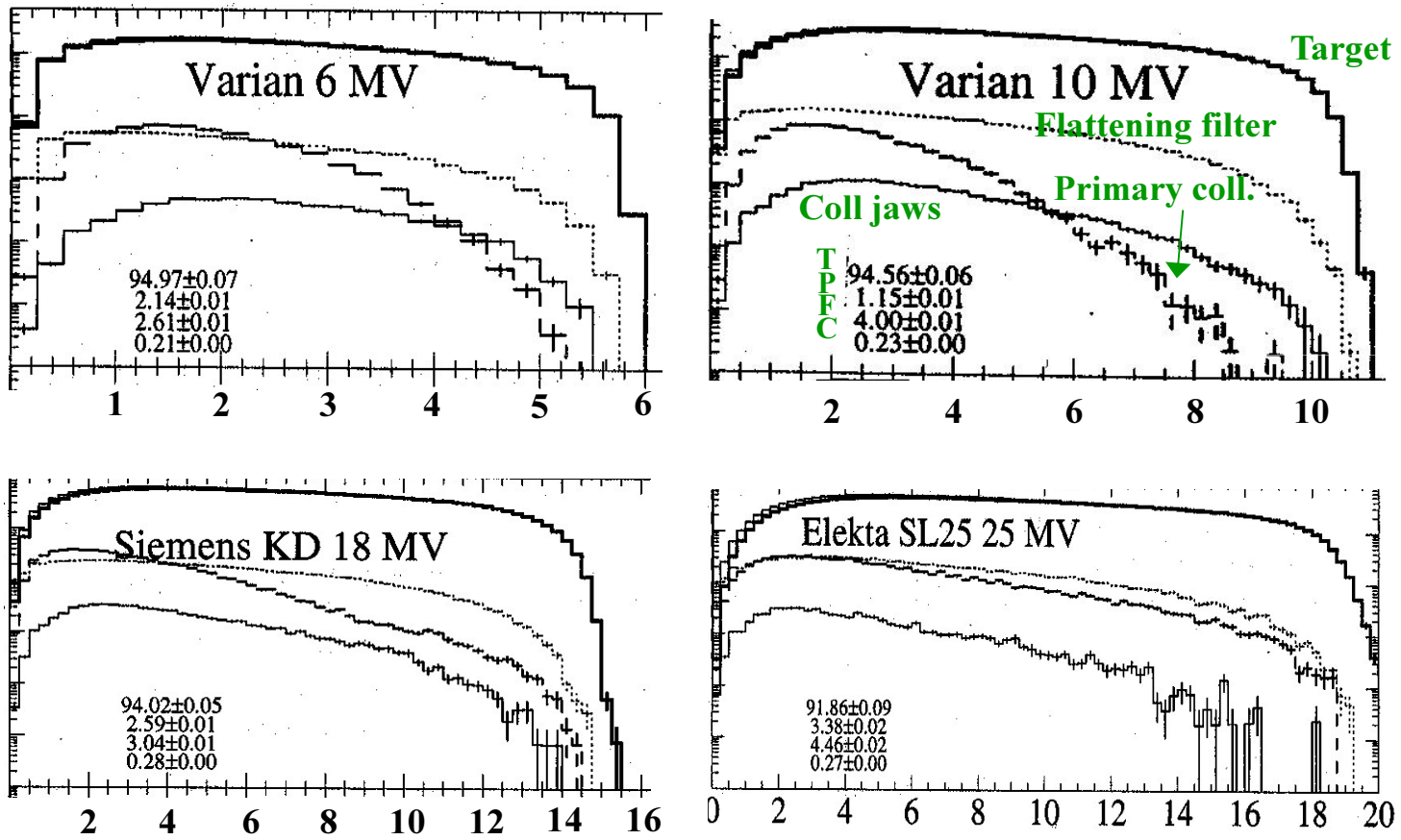

Sheikh-Bagheri *et al* [4]

Photon fluence w/wo FF

Flattened

Unflattened

6 MV

10 MV

Courtesy Mårten Dalaryd

Beam quality variations off axis

6 MV

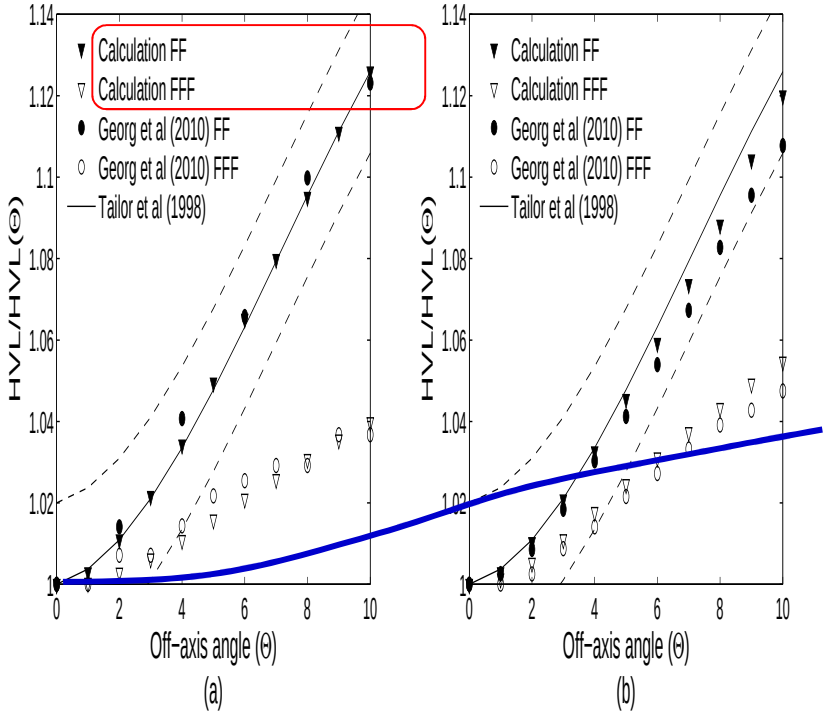

10 MV

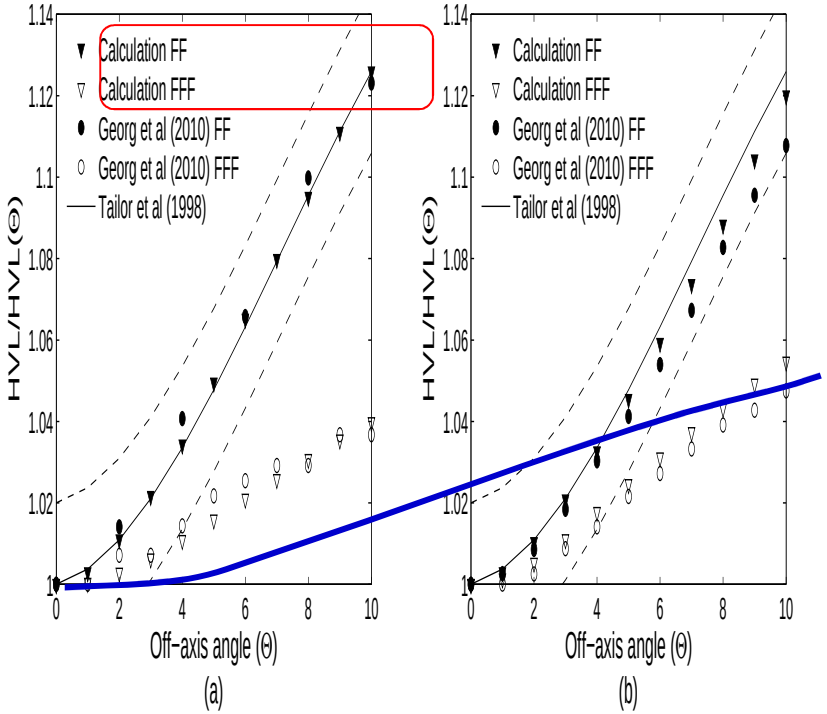

Courtesy Mårten Dalaryd

ESTRO School

Significance of off-axis softening

MC simulation of a clinical 4 MV photon beam, dose reconstruction at 10 cm depth.

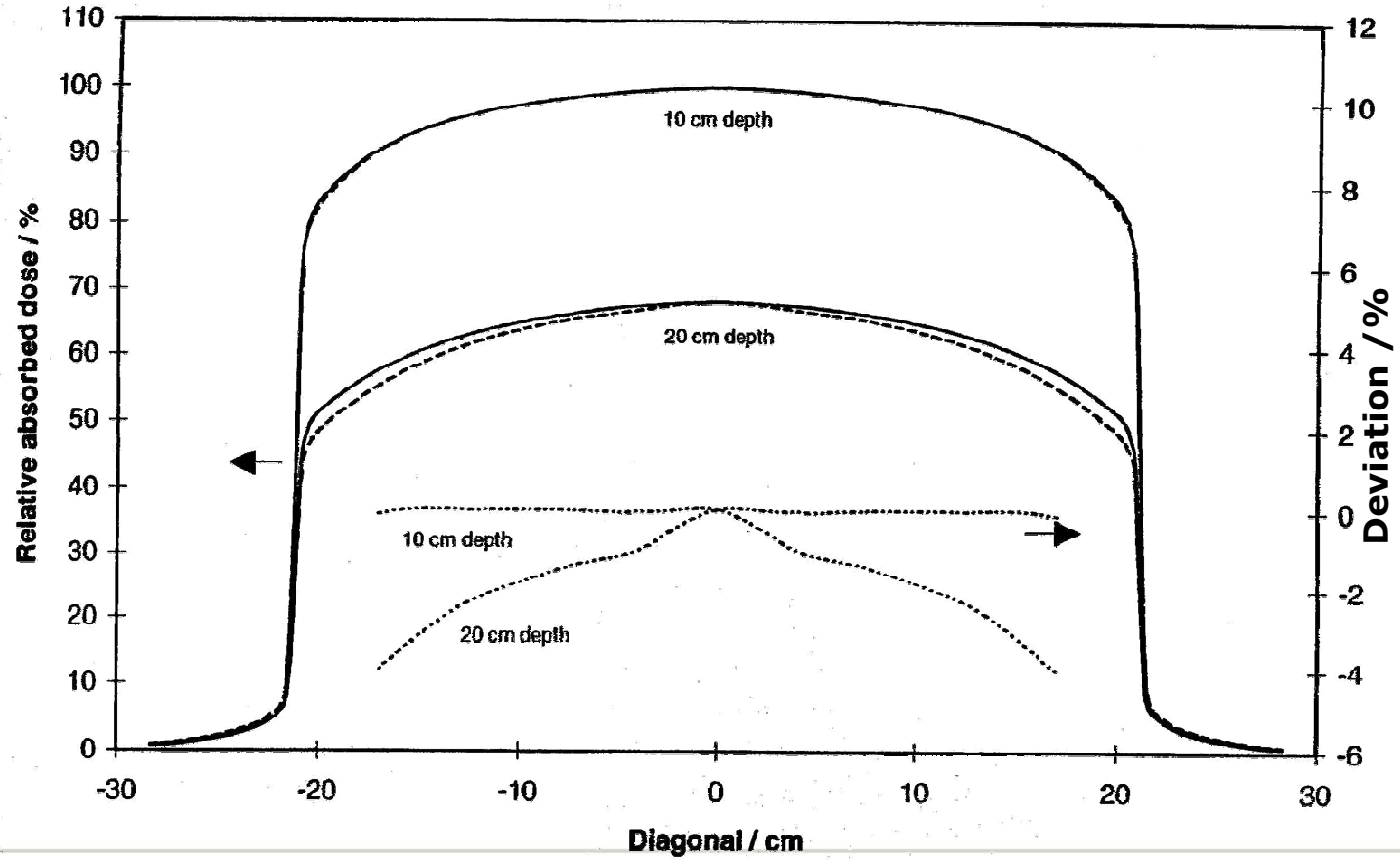

Sätherberg *et al* [3]

ESTRO School

Flattening filter free megavoltage photon beams
Lateral dose profile – 10 MV

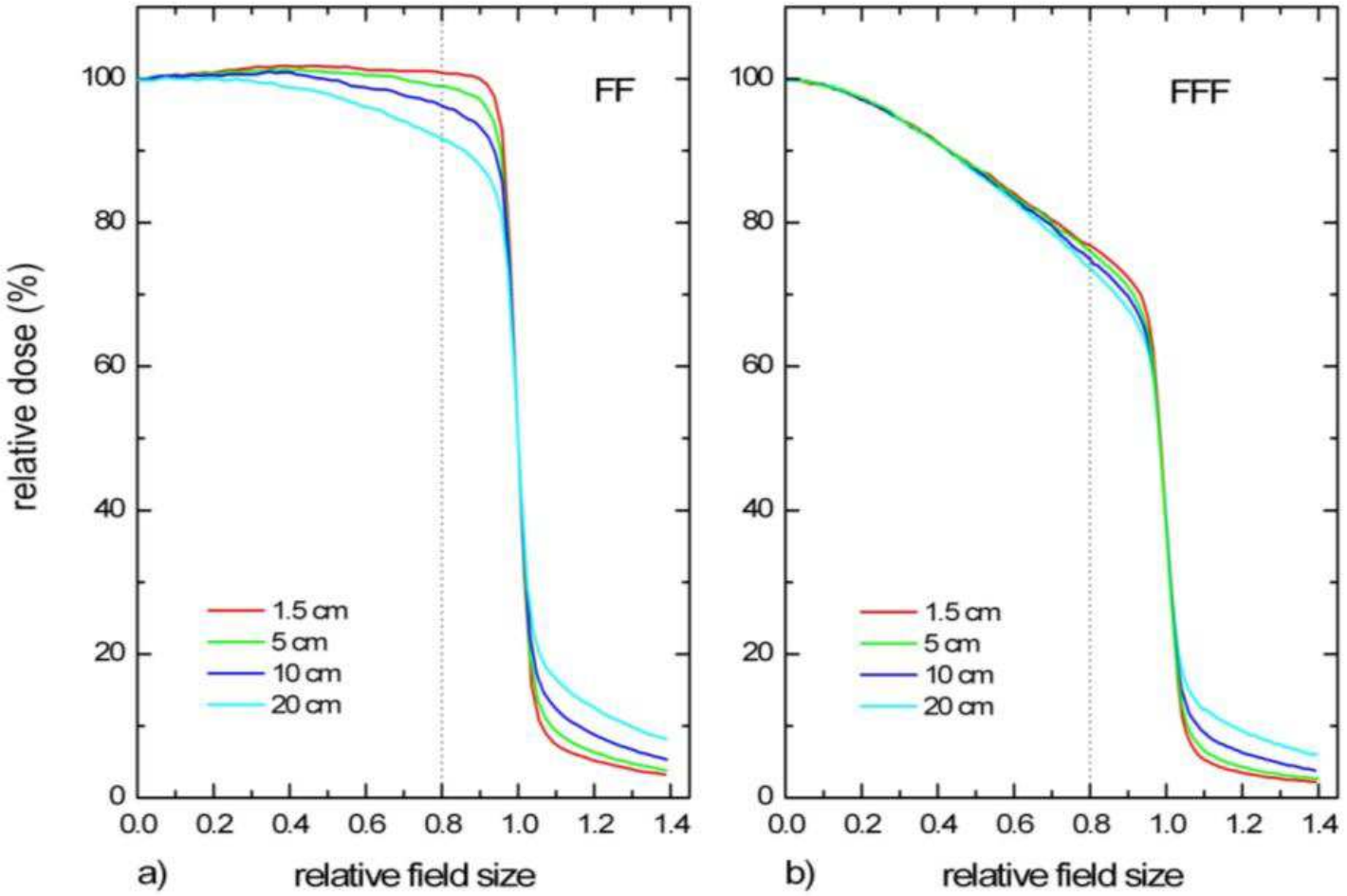

Kragl *et al* [10]

ESTRO School

The TomoTherapy treatment unit

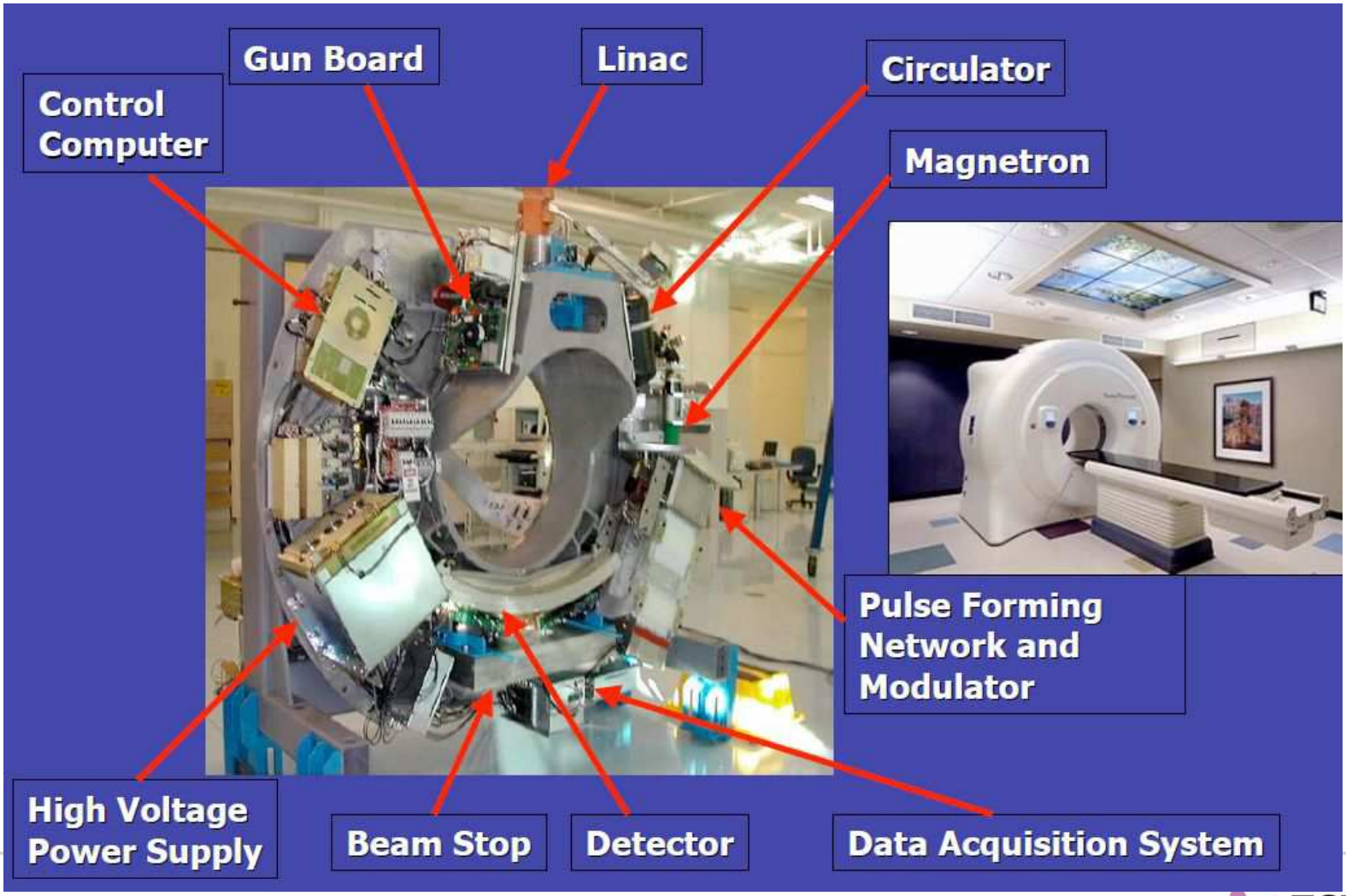

The TomoTherapy treatment head

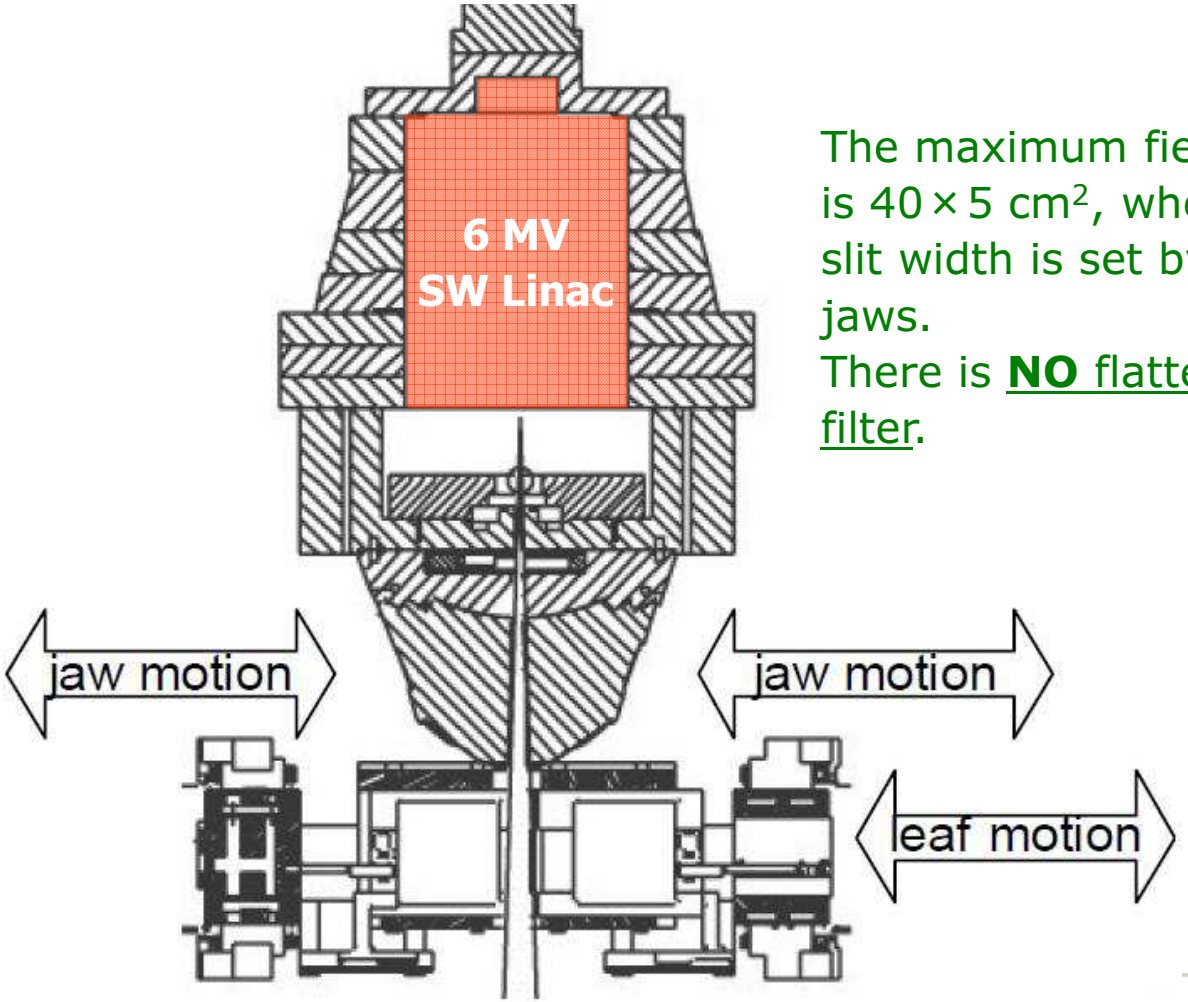

The maximum field size is 40×5 cm^2, where the slit width is set by the jaws.
There is **NO** flattening filter.

TomoTherapy treatment beam

40 cm long slits on film (1, 2.5, and 5 cm wide).

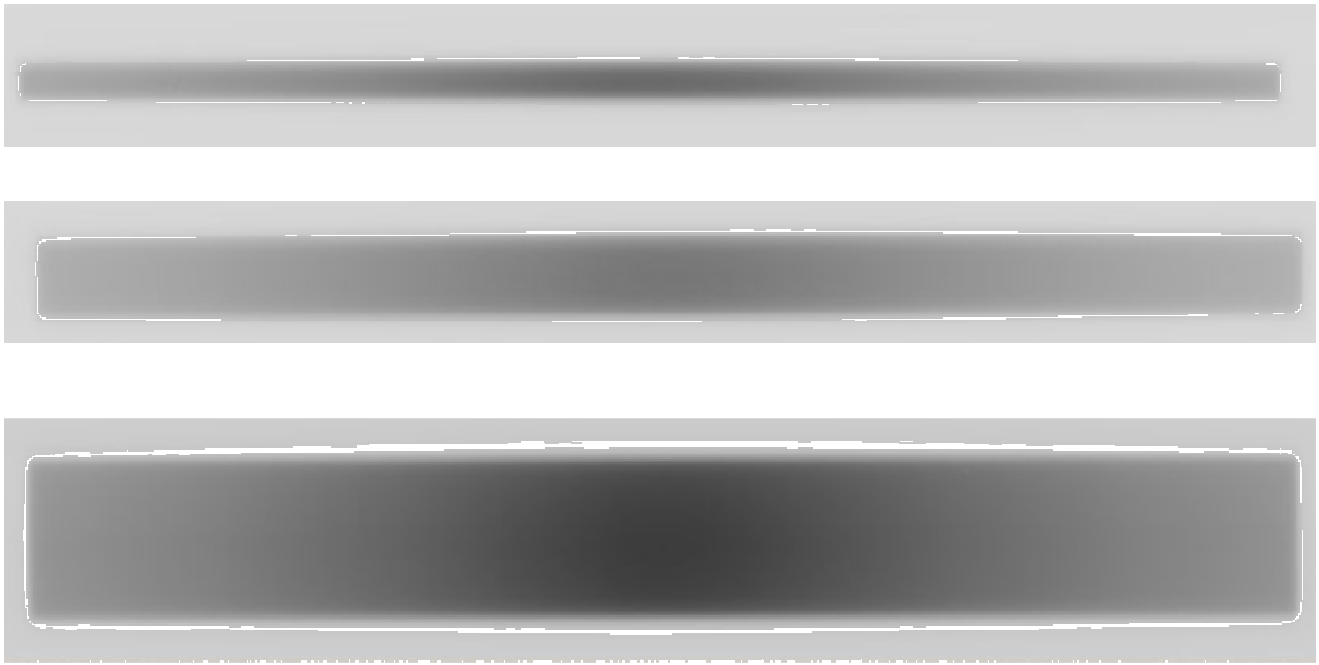

TomoTherapy dose profiles

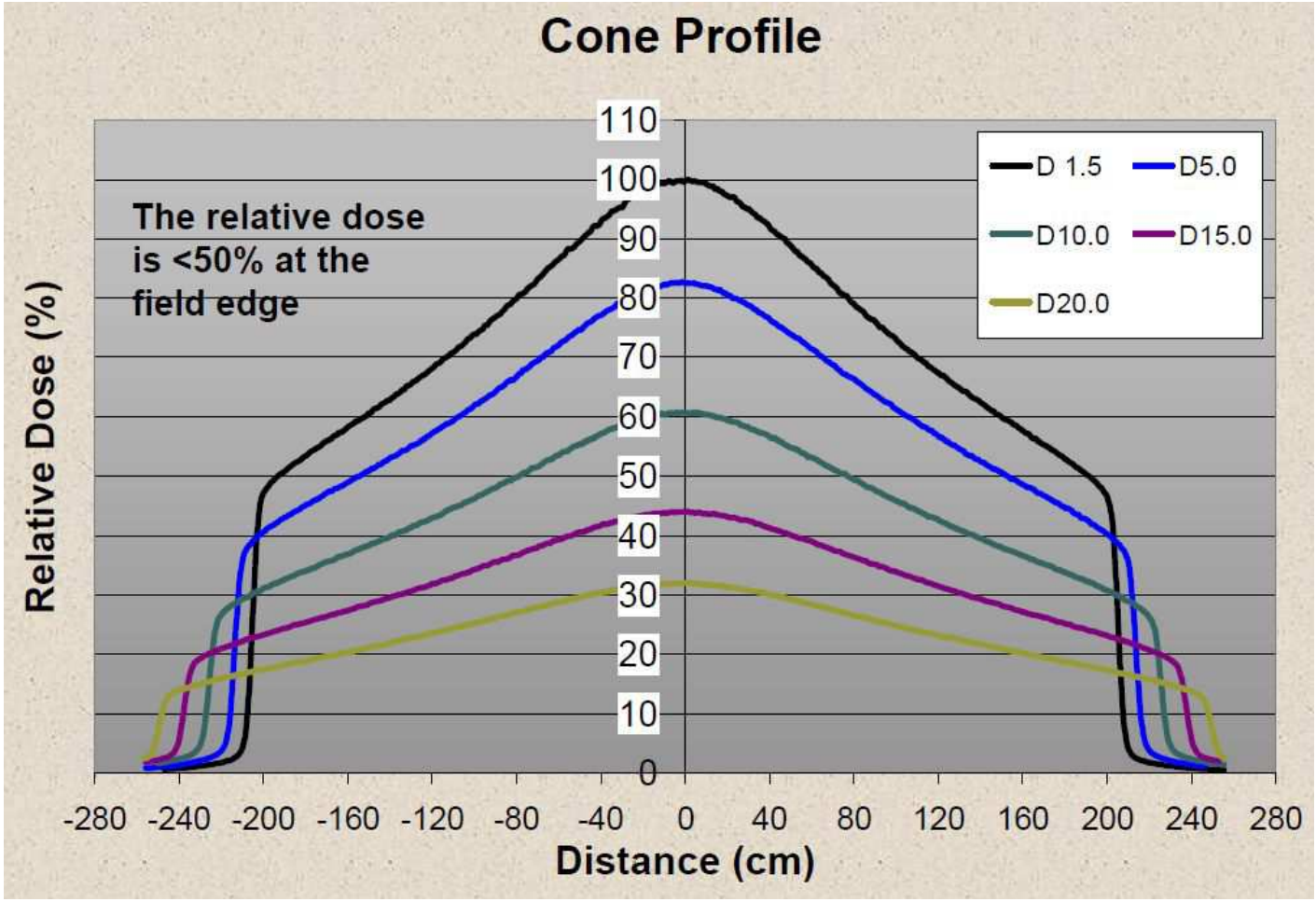

ESTRO School

Beam alignment on flattening filter

Perfect alignment **Angle error** **Position error**

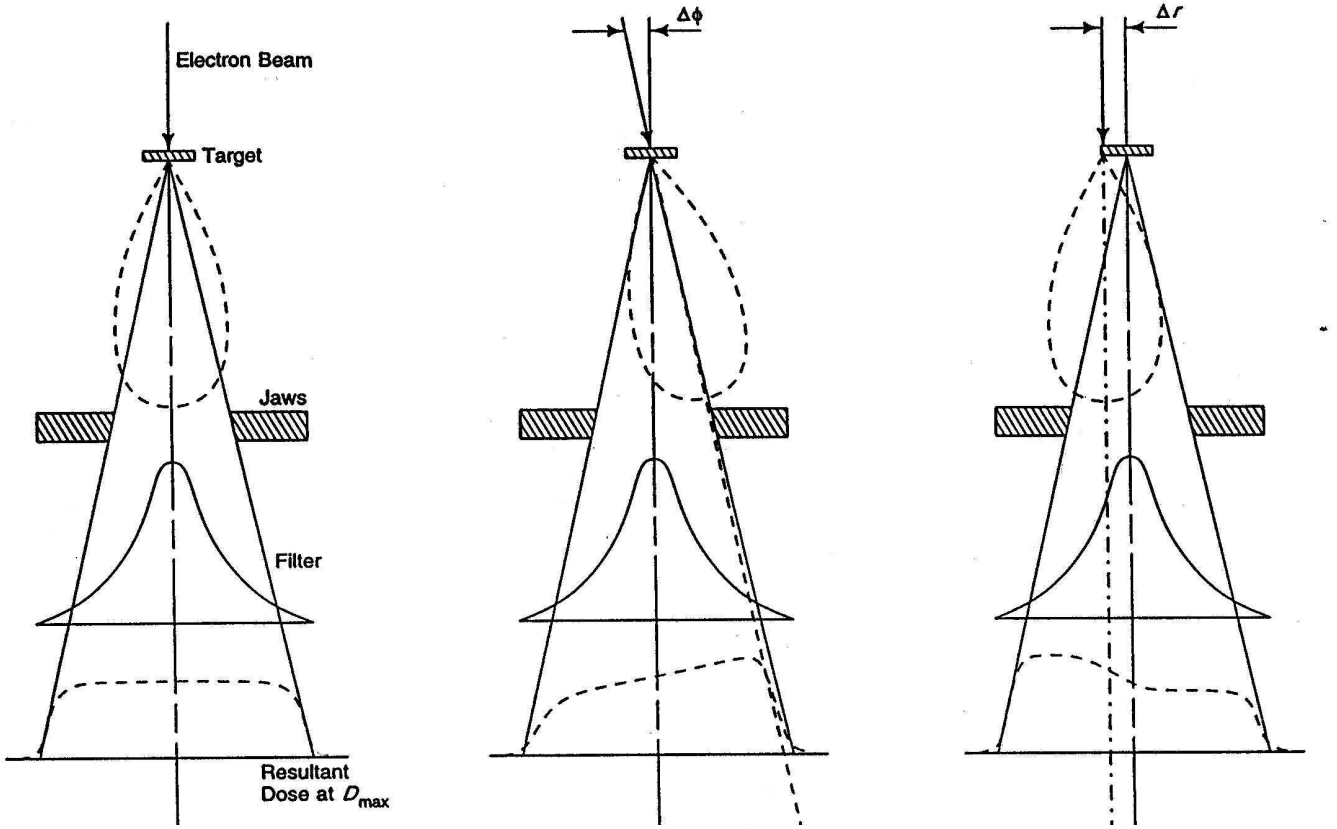

Karzmark *et al* [1]

ESTRO School

Lateral dose distributions

max field size at d_{max} and 10 cm depth

Beam flatness is normally optimized at 10 cm depth, which means that there will be "horns" at d_{max}.

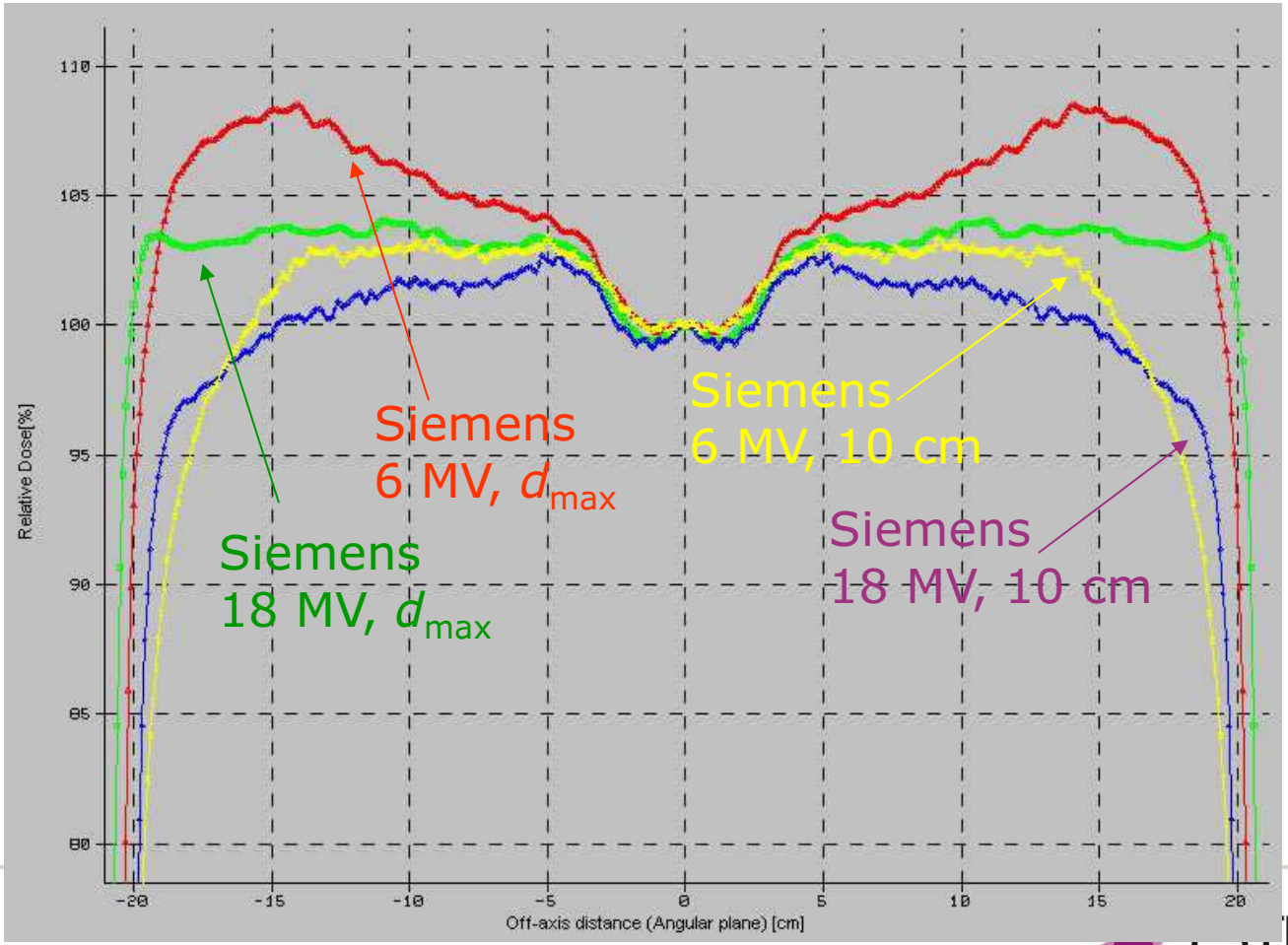

Lateral dose distributions

10x10 cm² at d_{max} and 10 cm depth

In smaller fields the "horns" contributes to the dose close to the field edges, yielding better beam flatness.

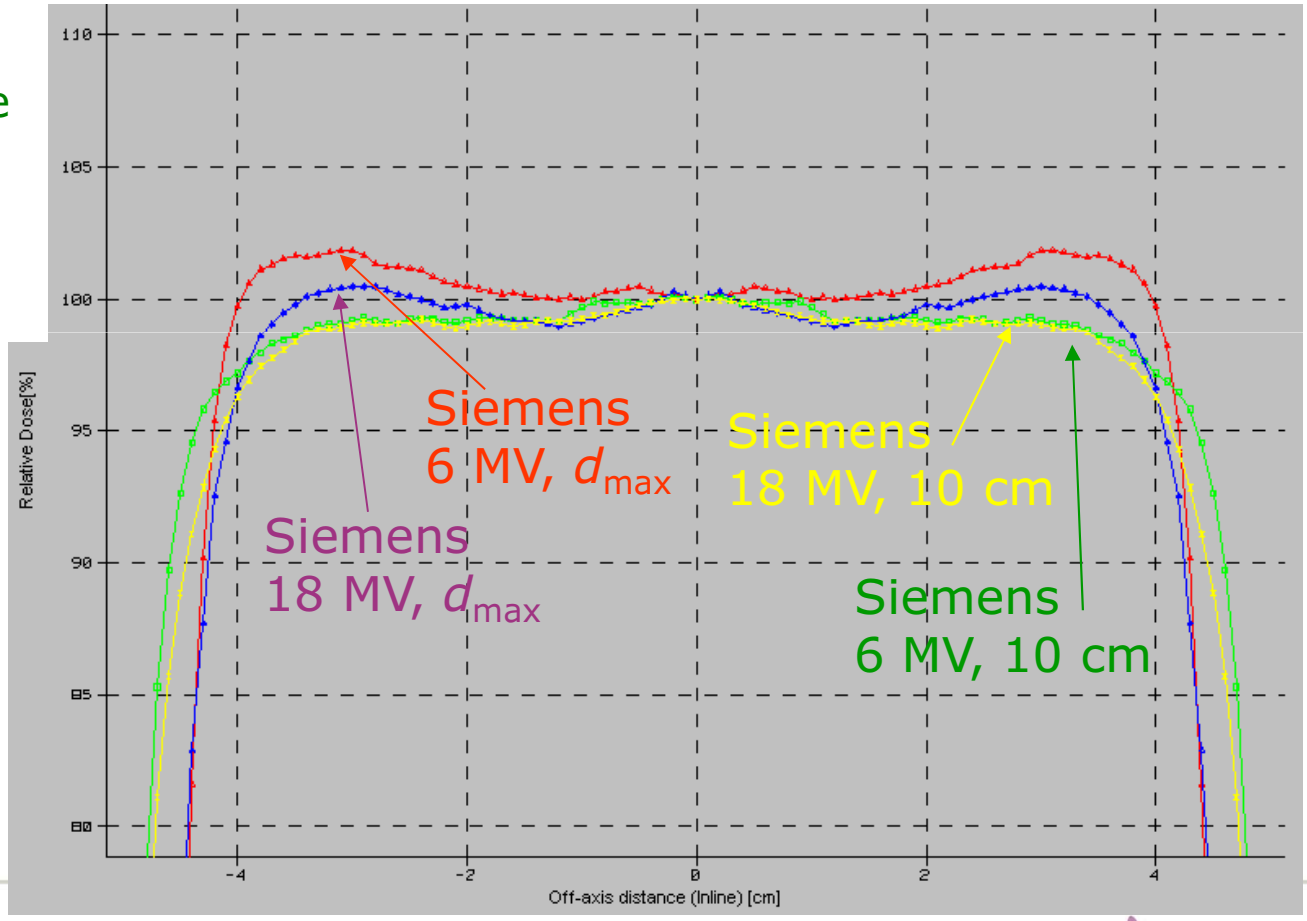

ESTRO School

Dose monitor chamber

Transmission ionization chamber that monitors and controls delivered dose (MU), dose rate, beam symmetry and flatness.

Varian

Elekta

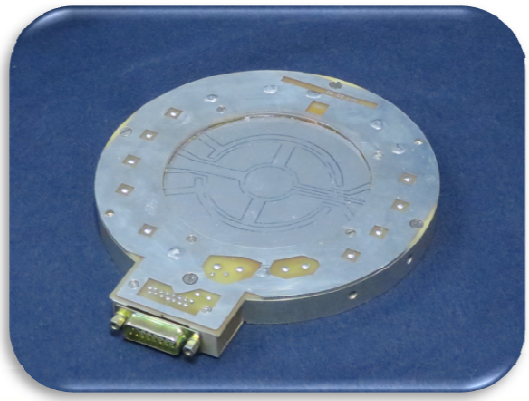

The dosimetry system must contain two independent channels.

Sealed or open compensated chambers ⇒ no dosimetric influence from ambient air pressure or temperature.

The E-field (bias voltage) should be high (~ 500 V/mm) in order to minimize recombination/dose rate dependence.

Commonly layered through thin and strong foils with condensed Au or Cu. Total thickness ~ 0.2 mm.

Dose monitor chamber

Transmission ionization chamber that monitors and controls delivered dose (MU), dose rate, beam symmetry and flatness.

Varian True beam

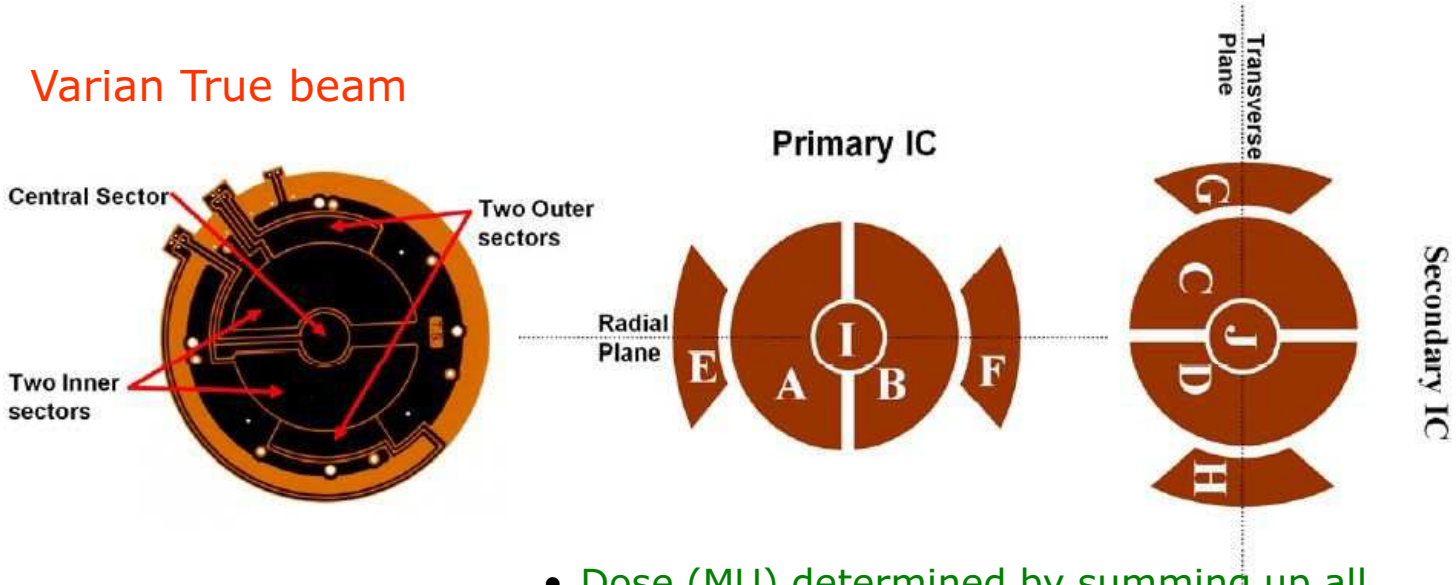

- Dose (MU) determined by summing up all sectors, divided into two independent channels.
- Symmetry determined through comparisons between left/upper and right/lower side.
- Flatness (new on True Beam) is determined by comparing ratios between (A+B) and I or (C+D) and J.

Monitor feedback/Beam symmetry servo

The monitor signal can be used as feedback to the electron beam transport, i.e. steering magnets, to optimize beam symmetry.

Varian
(*Clinac HE*)

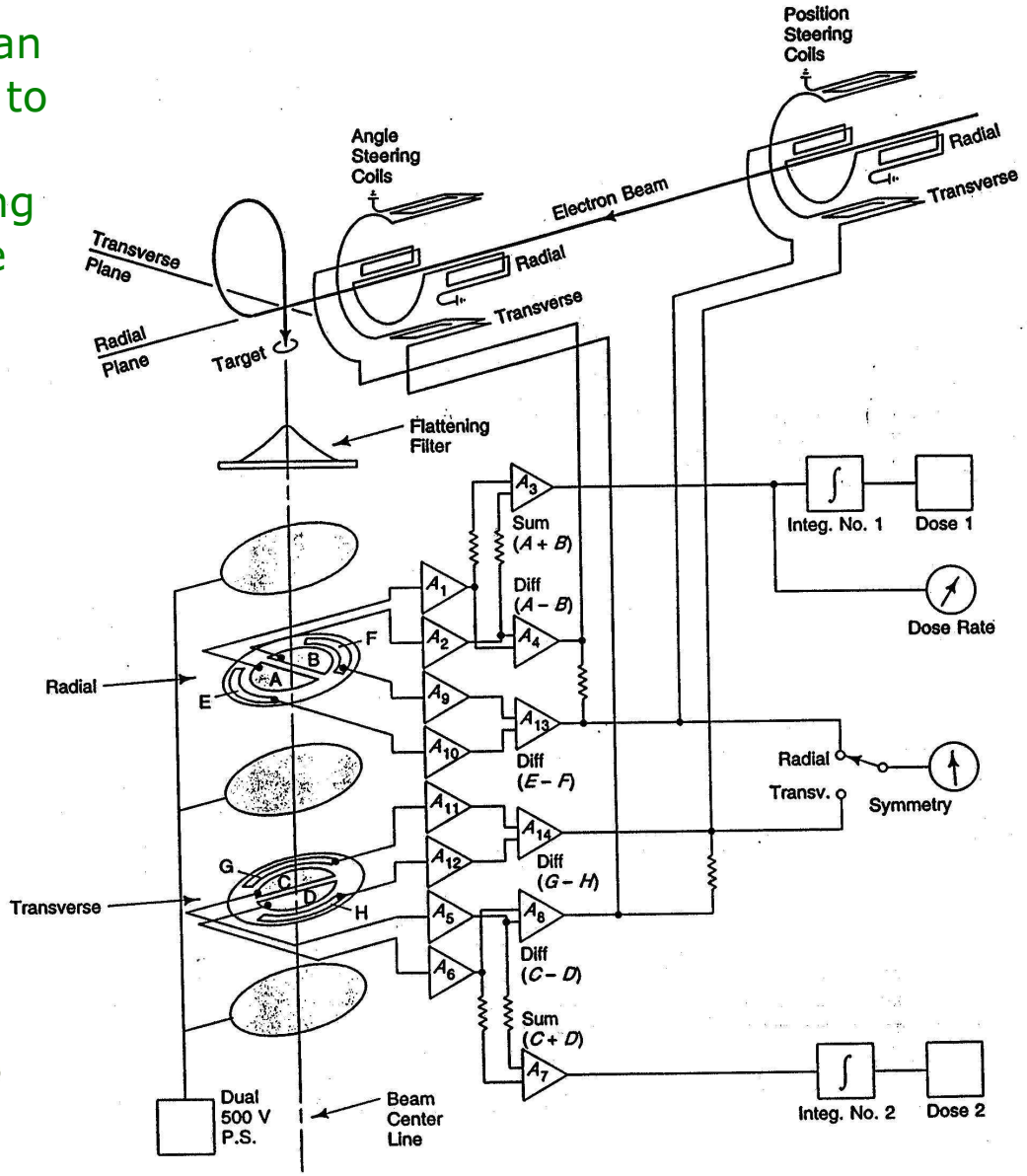

ESTRO School

Monitor feedback/Beam energy servo

An increase in beam energy causes a rise in the dose rate in the center of the field, and vice versa.
The X-ray gun servo system of an Elekta linac uses this property to detect energy changes by using the two hump plates.
The difference between the two hump plates is used to produce an error signal, which gives a correction to the nominal level of gun current set by the operator.

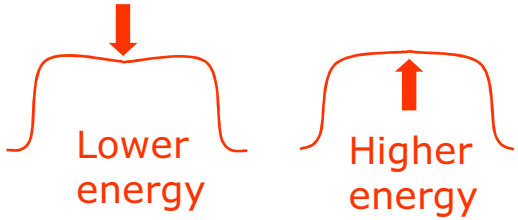

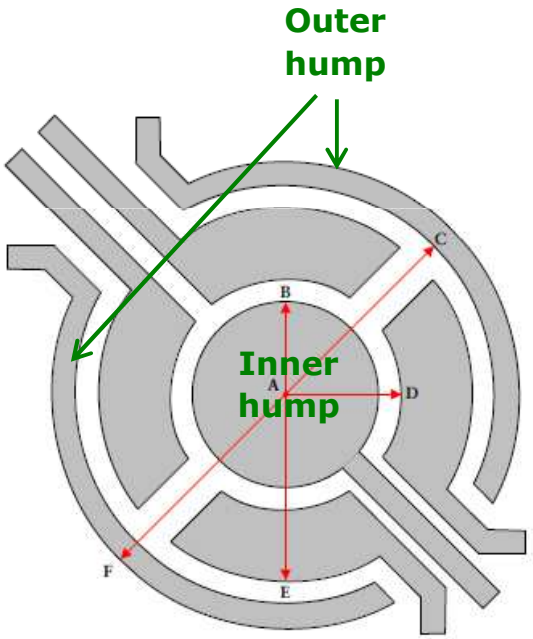

Elekta Dosimetry System

A→B = 5.8 cm
A→C = 16.5 cm
A→D = 7.3 cm
A→E = 15.3 cm
A→F = 18.2 cm

Figure 3.4 *Servo plate coverage at the isocenter*

MLC design – I – Lower jaw replacement

EXAMPLES:

(*Siemens*)

(*GE*)

(*Scanditronix*)

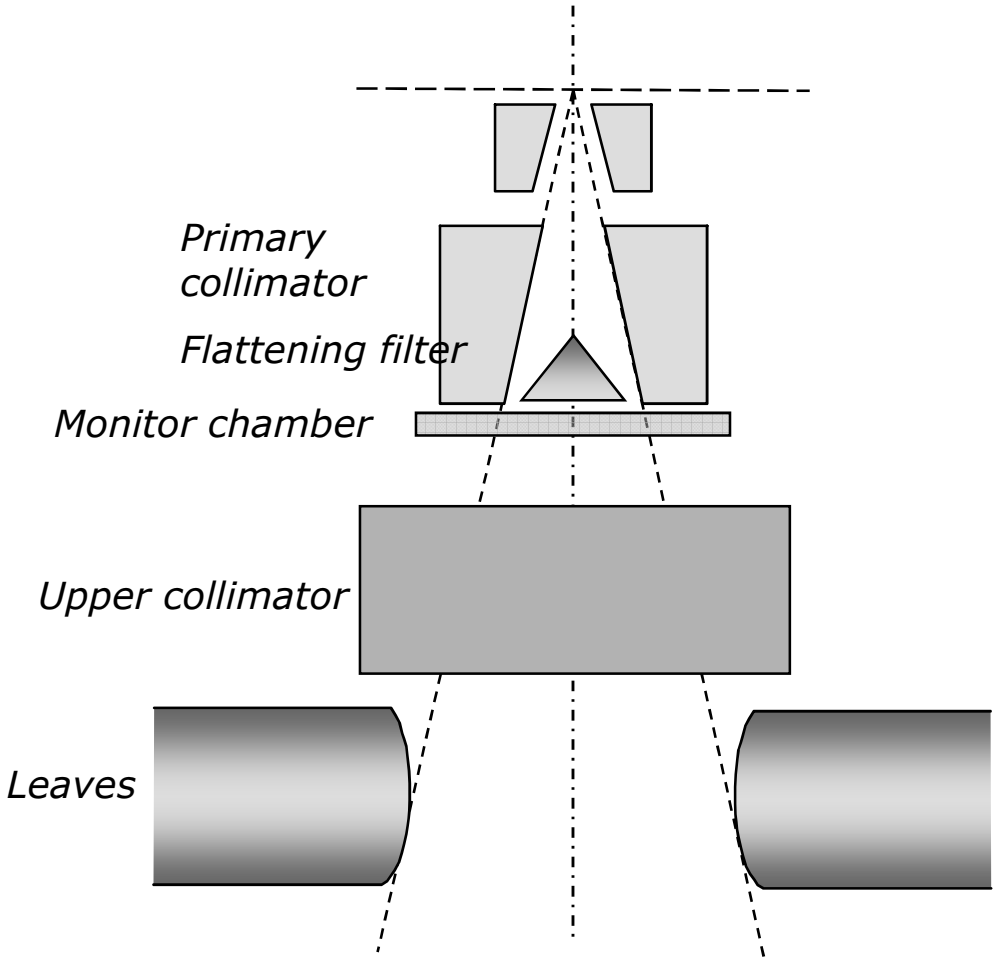

MLC design – II – Upper jaw replacement

EXAMPLE:

ELEKTA

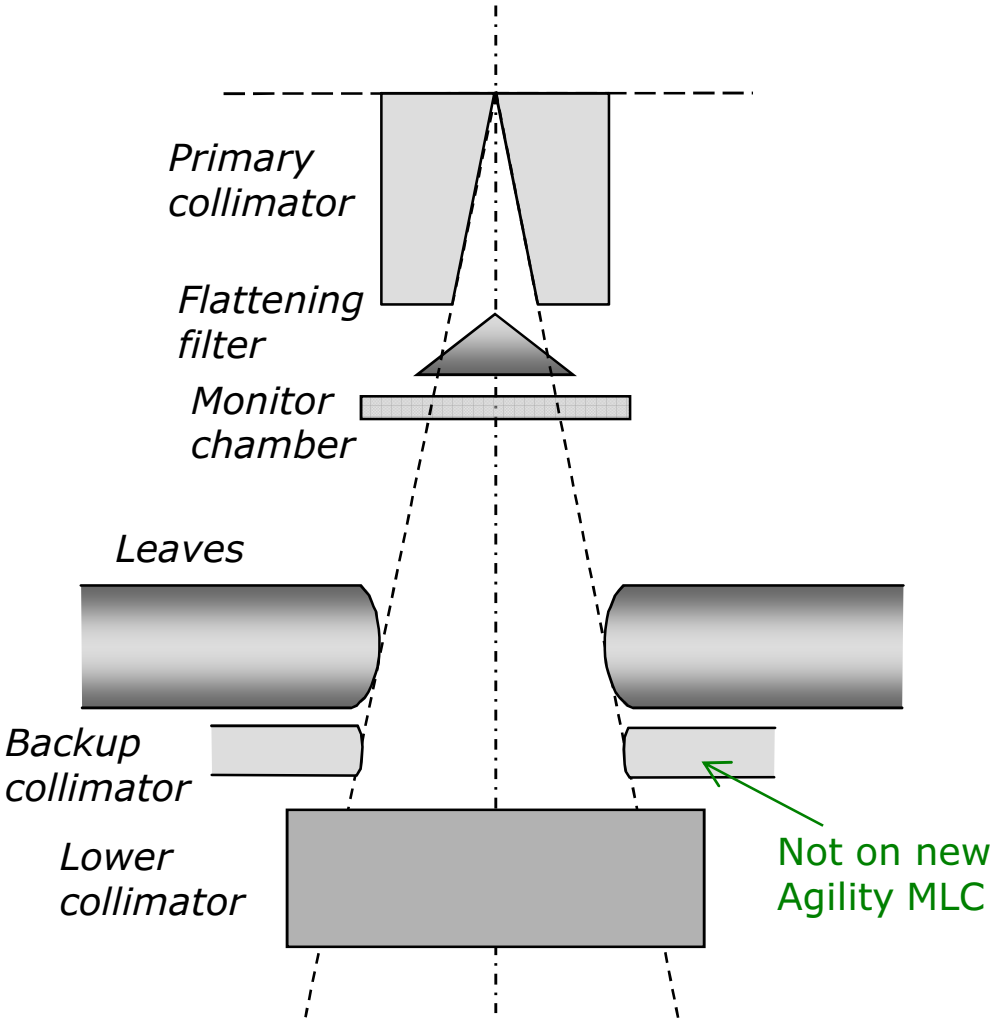

MLC design – III – Third level configuration

EXAMPLES:

VARIAN medical systems

μMLCs

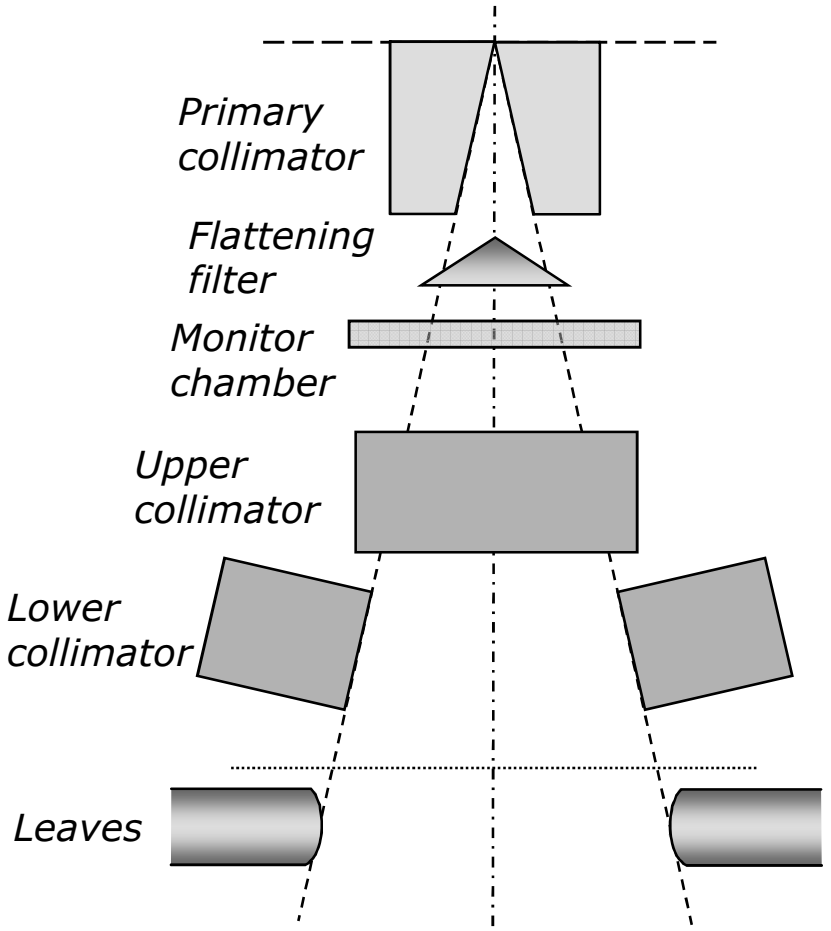

ESTRO School

Collimator alignment

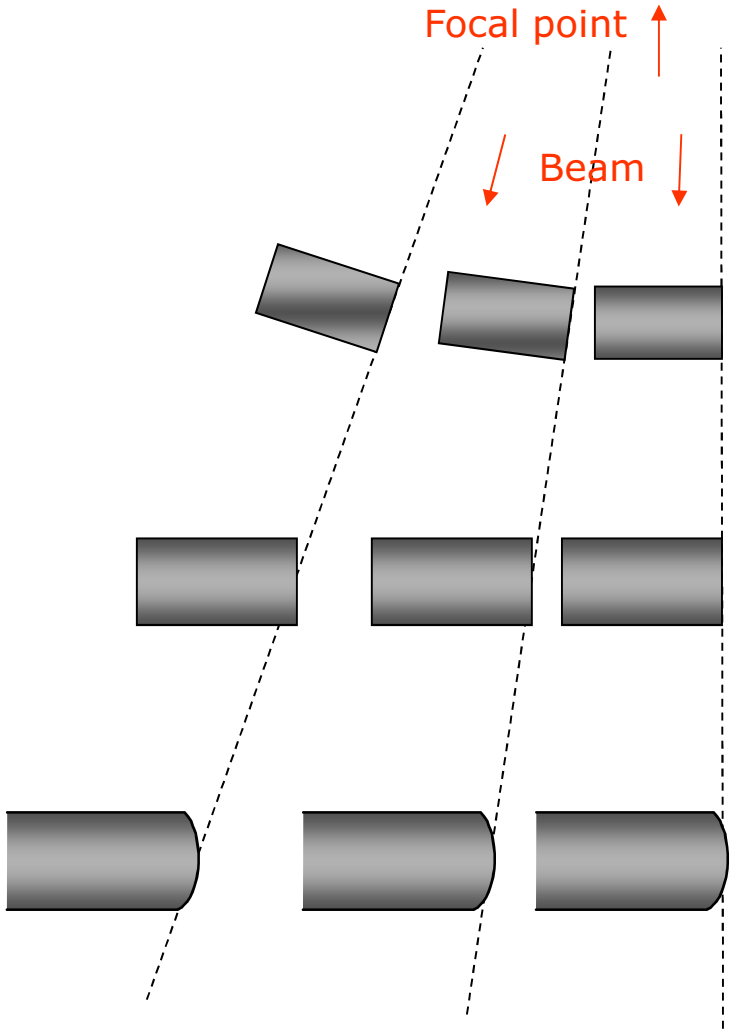

Collimator alignment	Geometric penumbra
Focused leaf edge *advanced mechanics*	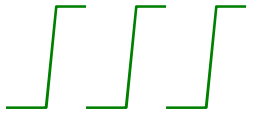
Straight leaf edge *Not used for large fields*	
Rounded leaf edge *Most common solution for MLC*	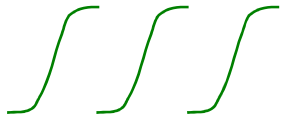

Positioning rounded collimator edges

Important for dose calculations in small fields and IMRT.

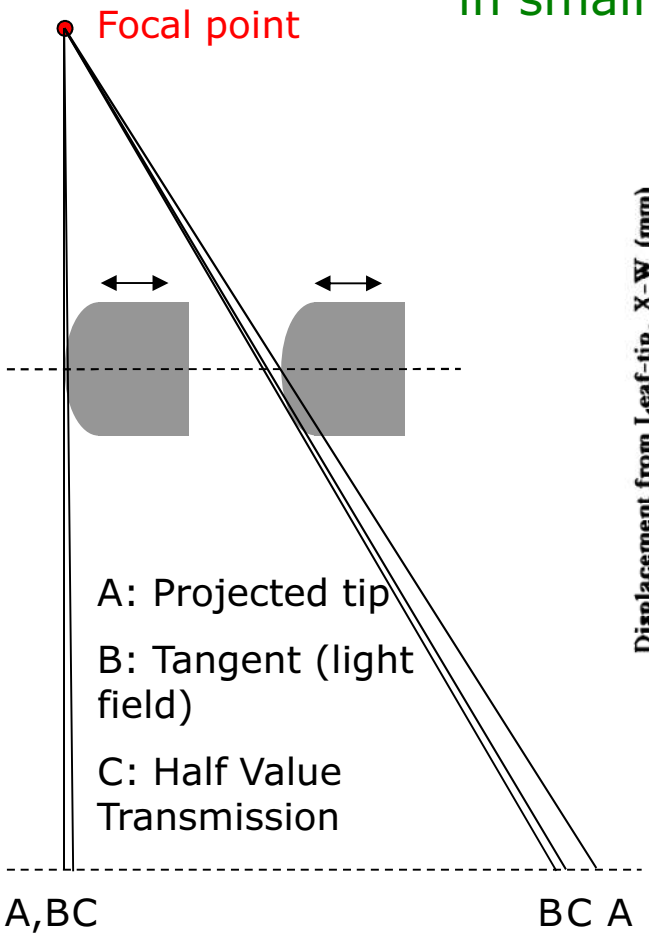

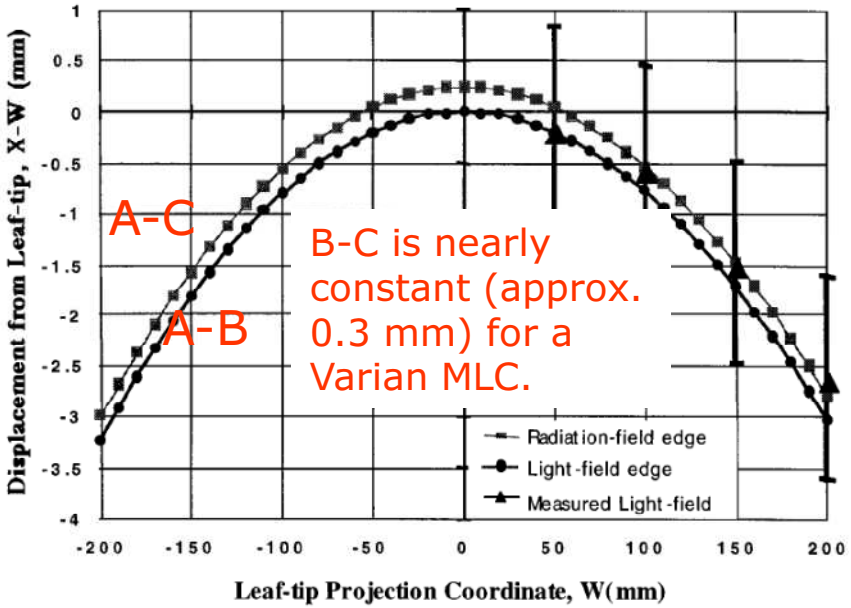

Boyer and Li [6]

Rounded collimator edges

The design of the rounded edge can vary, depending on the geometry (thickness, location and maximum over-travel).

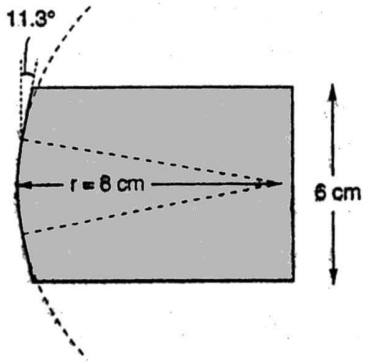

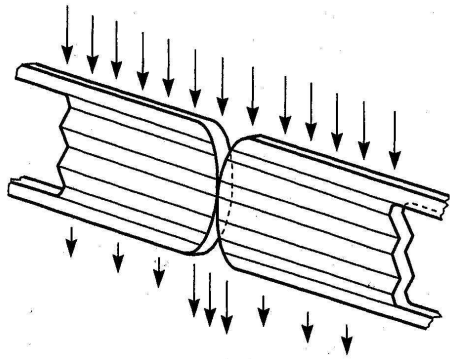

Increased leakage if no backup collimator is present

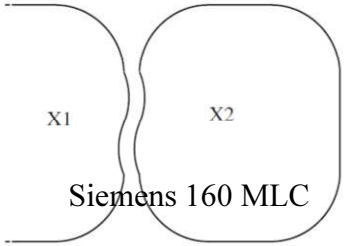

Tacke *et al* [11]

Penumbra widening due to rounded leaf edges

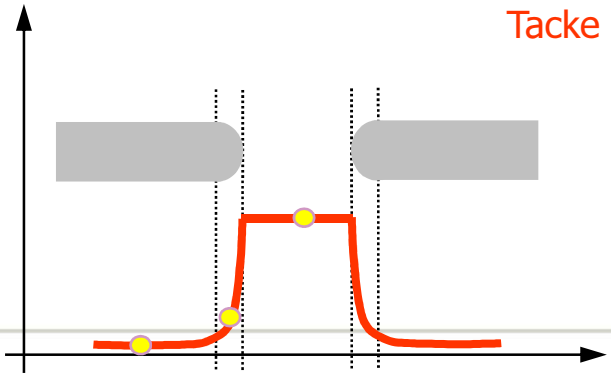

MLC penumbras (motion direction)

The resulting penumbra is not only dependent on the leaf edges, but also on the location of the MLC in the treatment head.

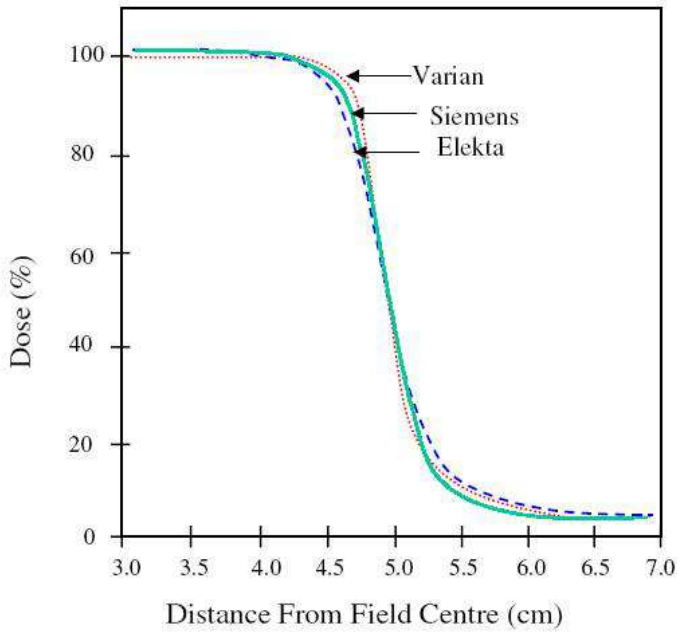

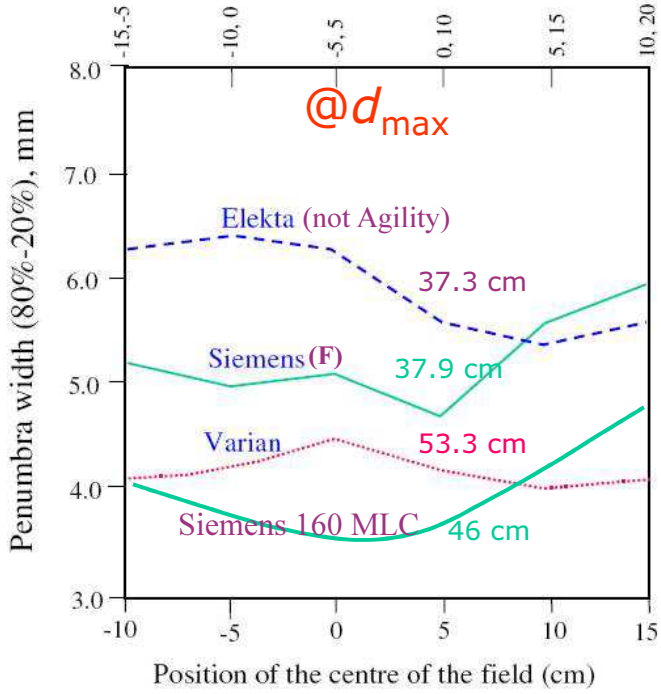

Numbers equal SCD (outer edge)

Huq *et al* [5]

Leaf design in the width direction

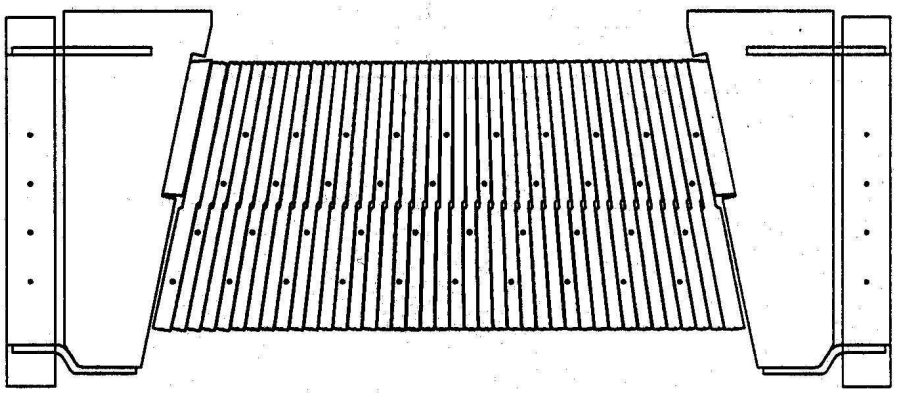

The leaves are thicker at the base in order to follow the divergence of the beam.

Inter-leaf leakage is minimized through "tongues" and "grooves".

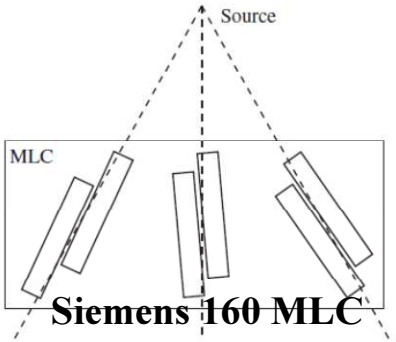

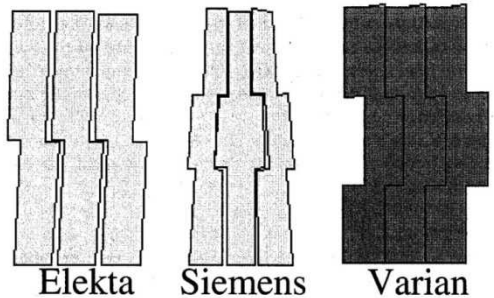

No backup collimators in place!

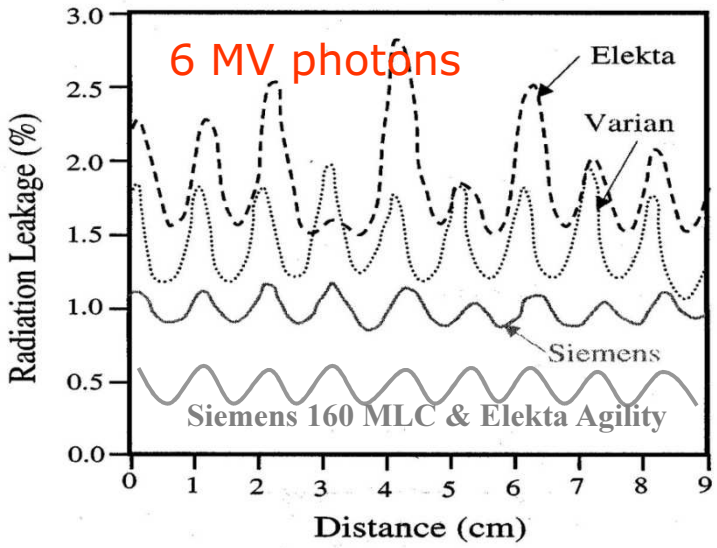

Huq *et al* [5]

ESTRO School

Tongue and groove effect

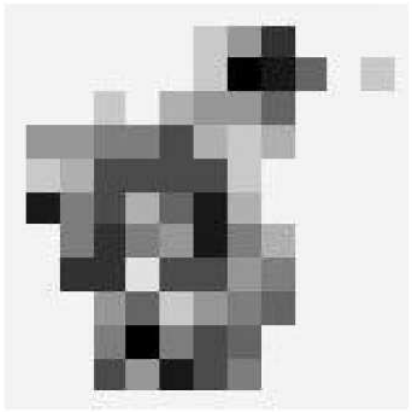

(a)

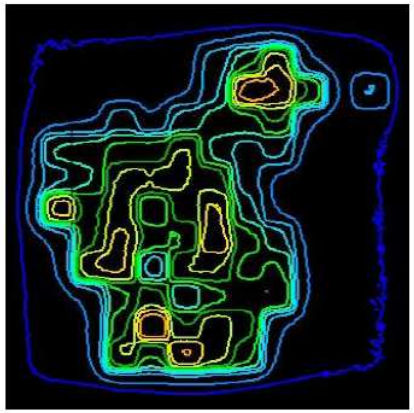

(b)

W/o T/G

MC calculations

MLC

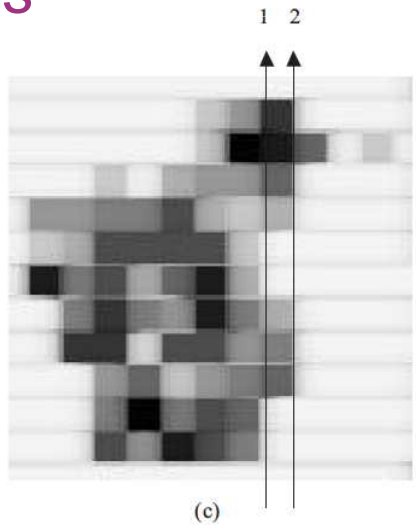

(c)

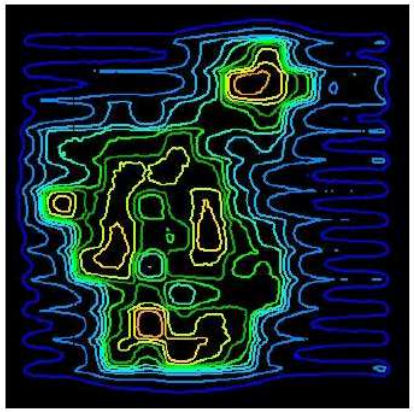

(d)

With T/G

Deng et al [15]

MLC design – IV – TomoTherapy MLC

Pneumatic "binary" MLC, opening/closing in 20 ms.

The 64 Tungsten leaves are 10 cm thick and 0.625 cm wide (at isocenter distance =85 cm), <0.5% transmission.

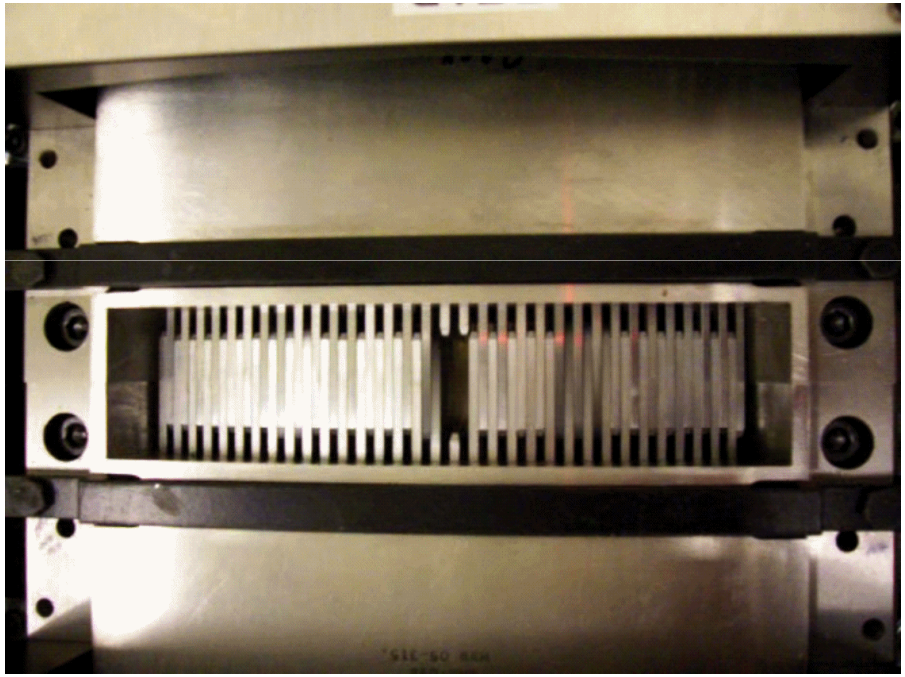

Different methods for creating wedged dose distributions

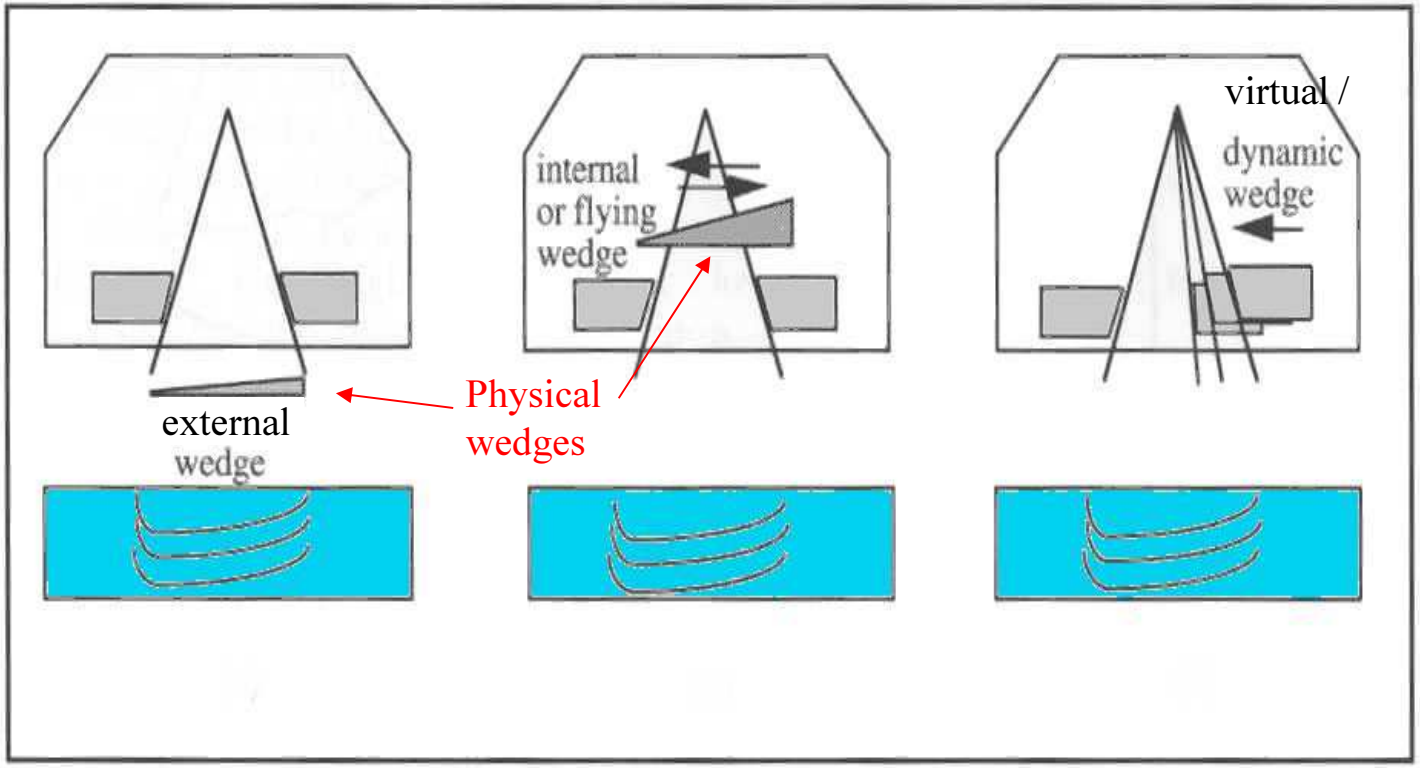

Wedge induced beam quality shifts

Physical wedges filter the beam, yielding beam hardening. Although, above approx. 15 MV the pair production process will balance the hardening, resulting in unaffected (or even softer) beam quality.

Zhu *et al* [9]

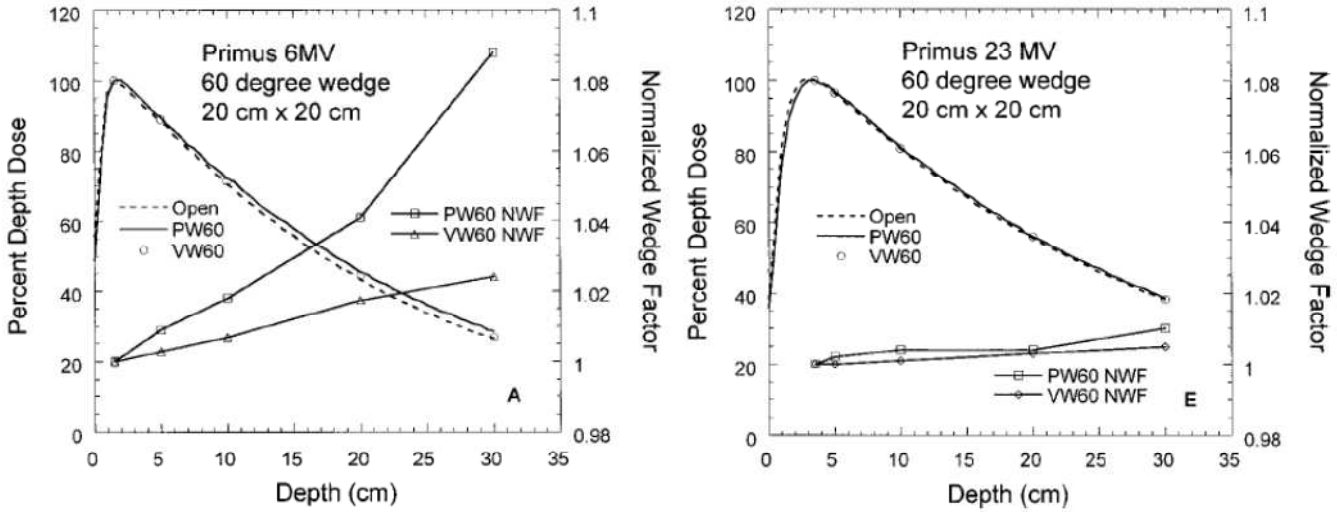

Knöös and Wittgren [16]

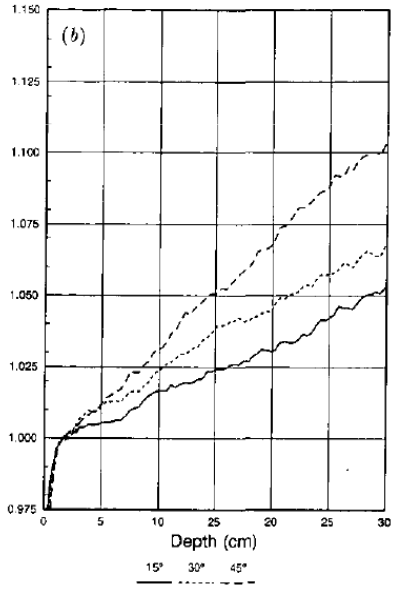

PW60=60 deg Physical wedge
VW60=60 deg Virtual wedge

ESTRO School

Wedge induced head scatter

A physical wedge acts as a scatter source. For external wedges, i.e. located below the collimators, the wedge scatter will result in increased doses outside the beam edges.

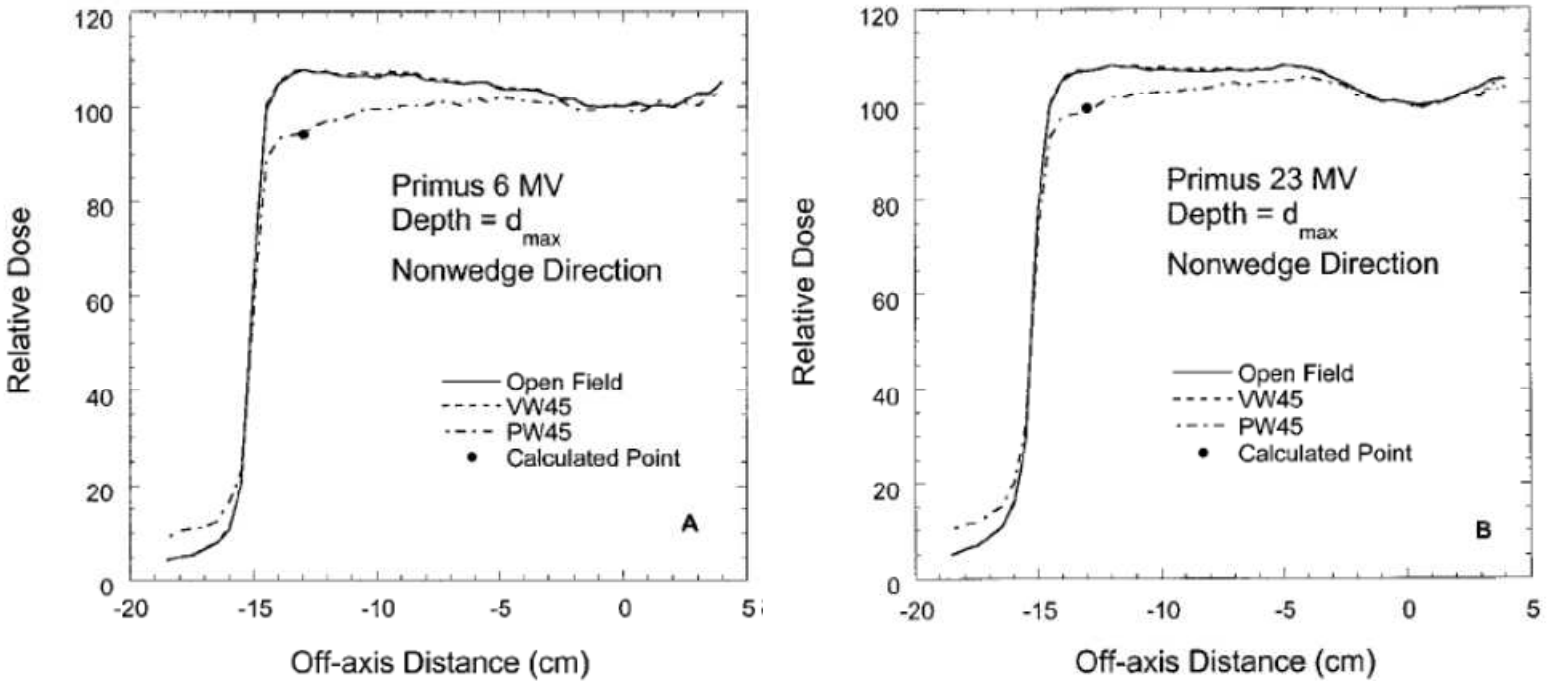

VW45=45 deg Virtual wedge
PW45=45 deg Physical wedge

Zhu *et al* [9]

Hard wedges

Manual mounted - Varian

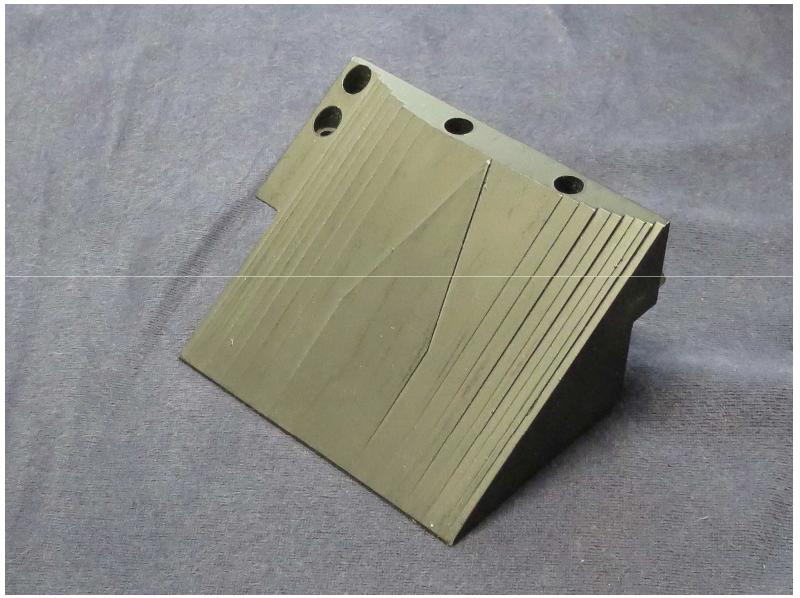

Remote controlled - Elekta

Resuming an interrupted wedge treatment

The time varying fluence distribution means that an interrupted treatment can not be resumed without information about the delivered fraction (not necessary for physical wedges).

Hence, both delivered and remaining/given MUs must be known by the accelerator control software.

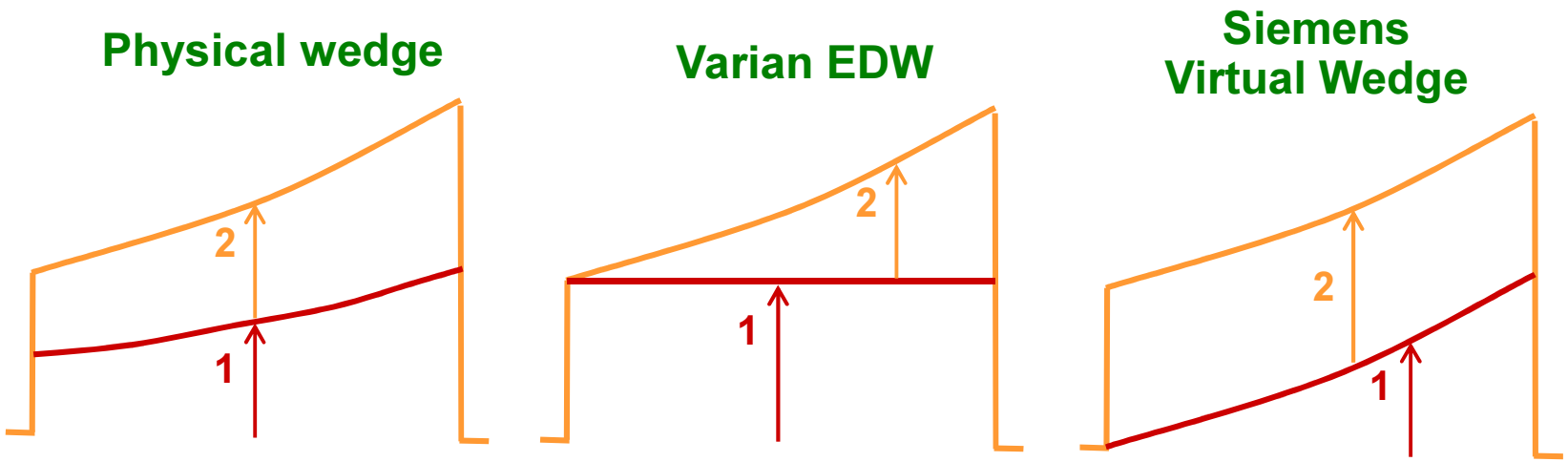

Note: Impossible to deliver few MUs using dynamic/virtual wedge!

Electron treatment heads

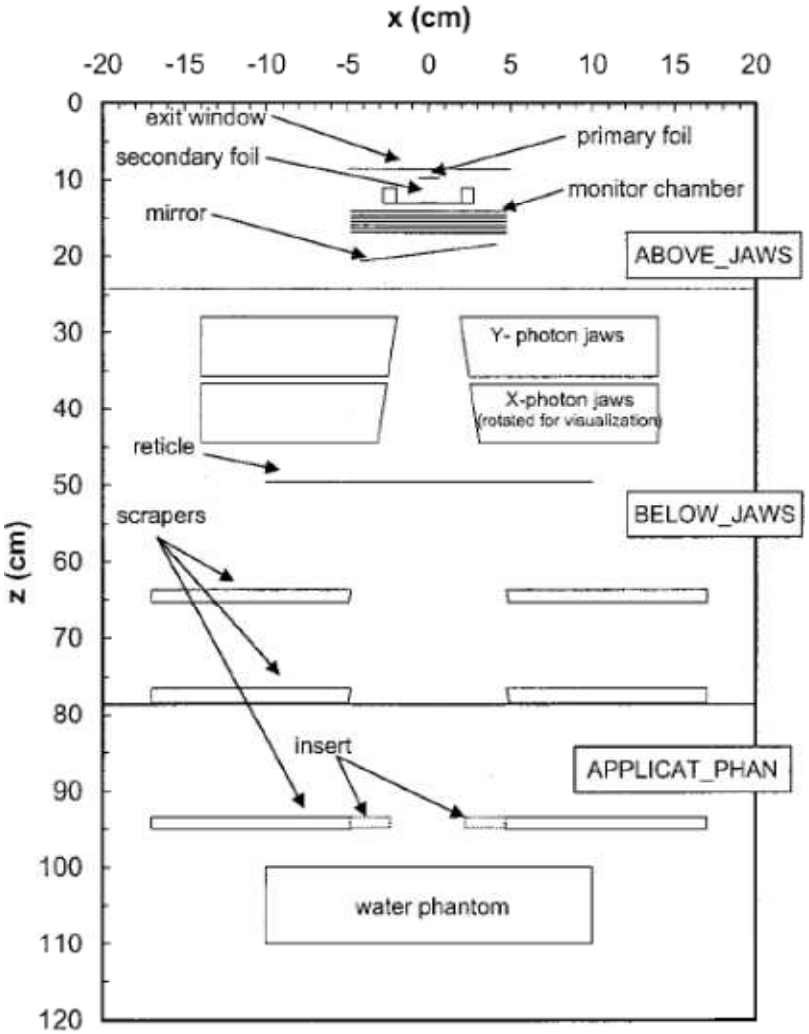

Bieda *et al* [12]

Electrons are much more influenced by scattering and energy loss interactions than photons.

The shape of the electron dose distribution depends therefore more on treatment head design parameters than it does for photons.

Creating a clinically useable electron beam

Traditionally a single foil technique was used ⇒

To get a broad enough beam the single foil has to be quite thick ⇒

Significant energy loss and spread.

The introduction of a secondary foil downstream reduces these problems since the total foil thickness can be reduced considerably.

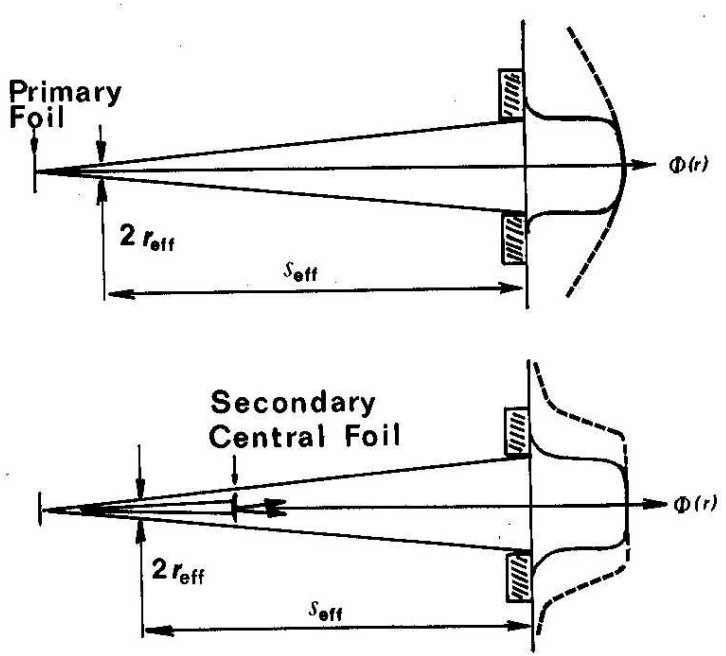

ICRU 35 [8]

Design of scattering foils

Primary foil: High *Z*-mtrl, e.g. Au or Ta, gives the highest linear scattering power vs. collision stopping power, i.e. the most effective scattering. Thickness (t) ≈ 0.05-0.4 mm (energy dependent).

Secondary foil: Lower *Z*-mtrl, e.g. Al, often used in order to reduce bremsstrahlung production. Thickness (h) $\lesssim$ 3 mm.

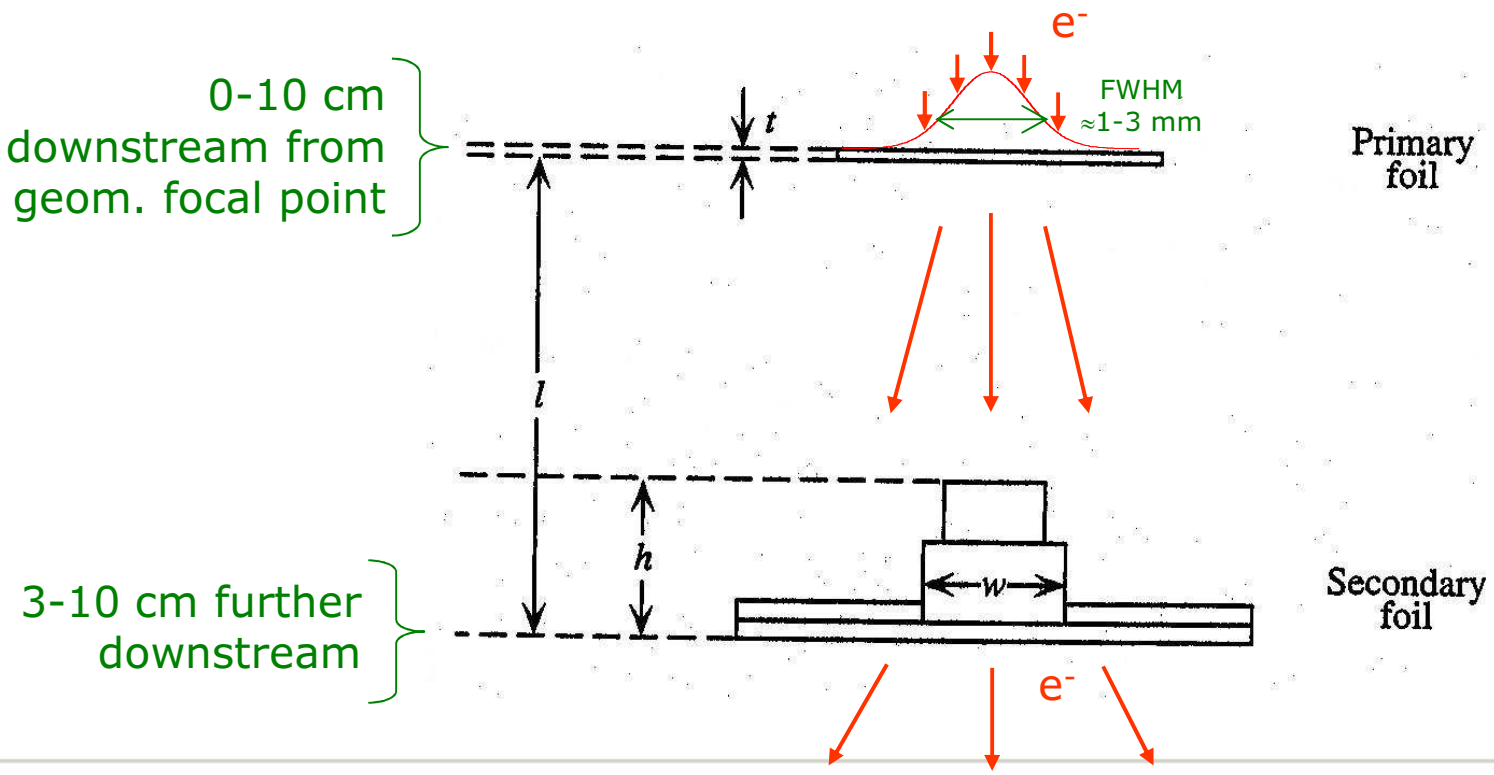

Bieda *et al* [12]

ESTRO School

Filter assembly for a Varian Clinac

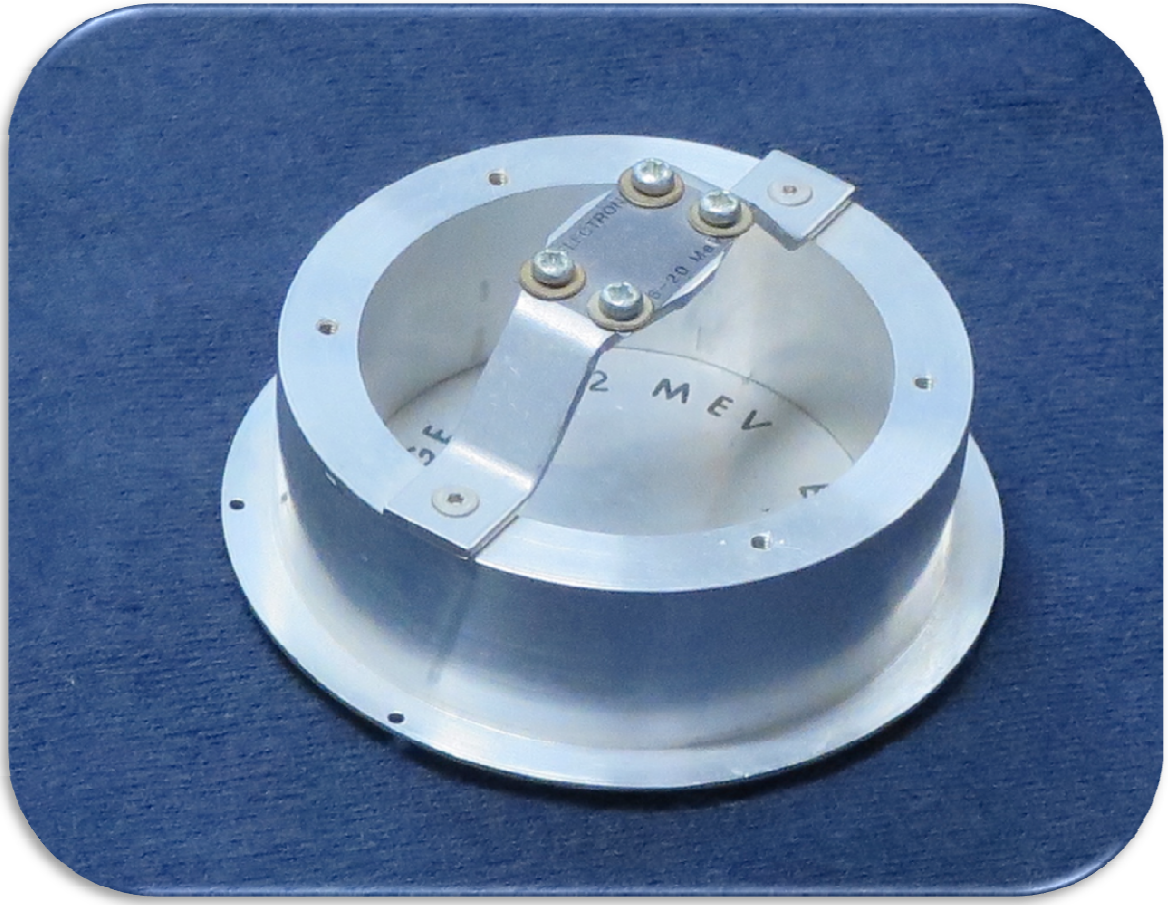

Secondary scattering foils

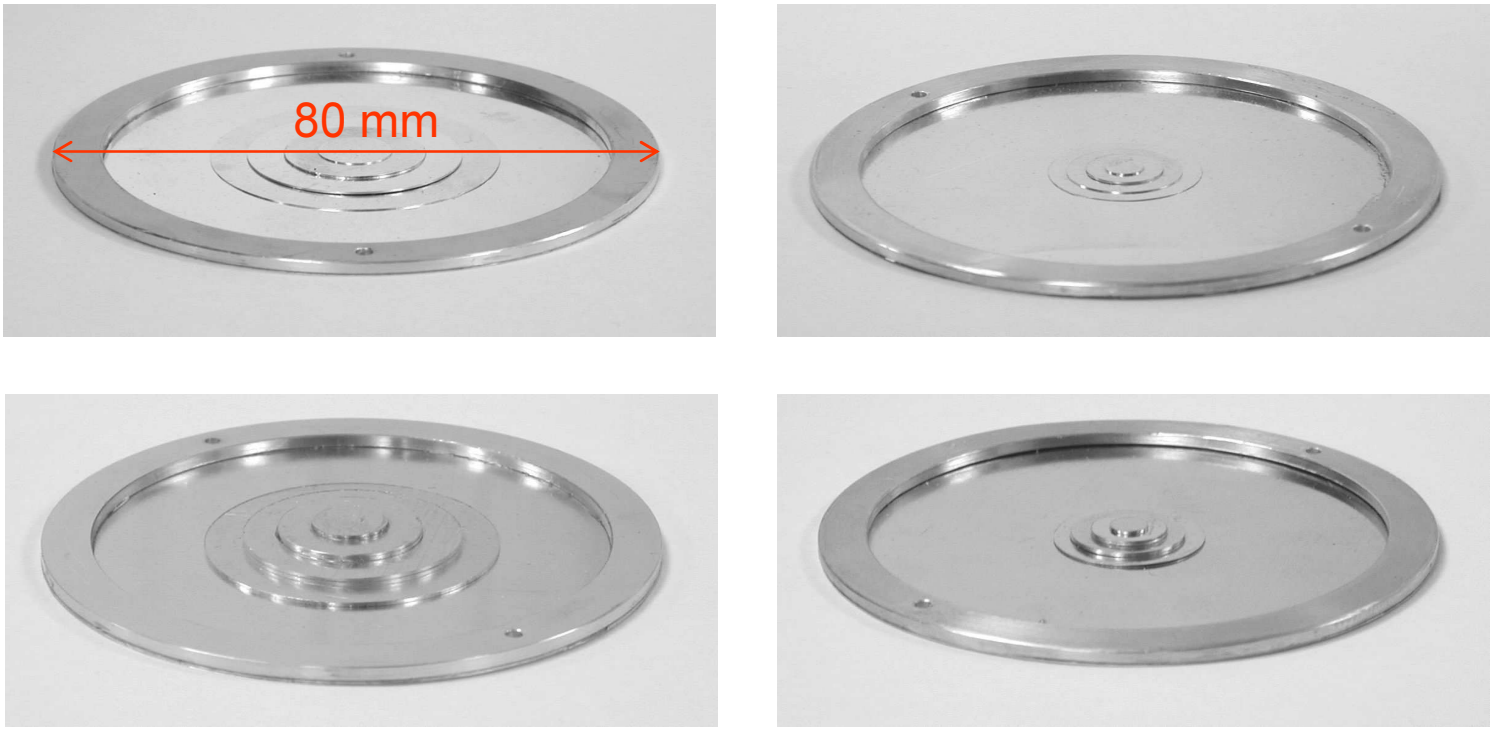

Scattering foils from research work by Magnus G Karlsson (Umeå)

Different electron collimators

Cone/tube collimator

Modified tube collimator

Diaphragm collimator

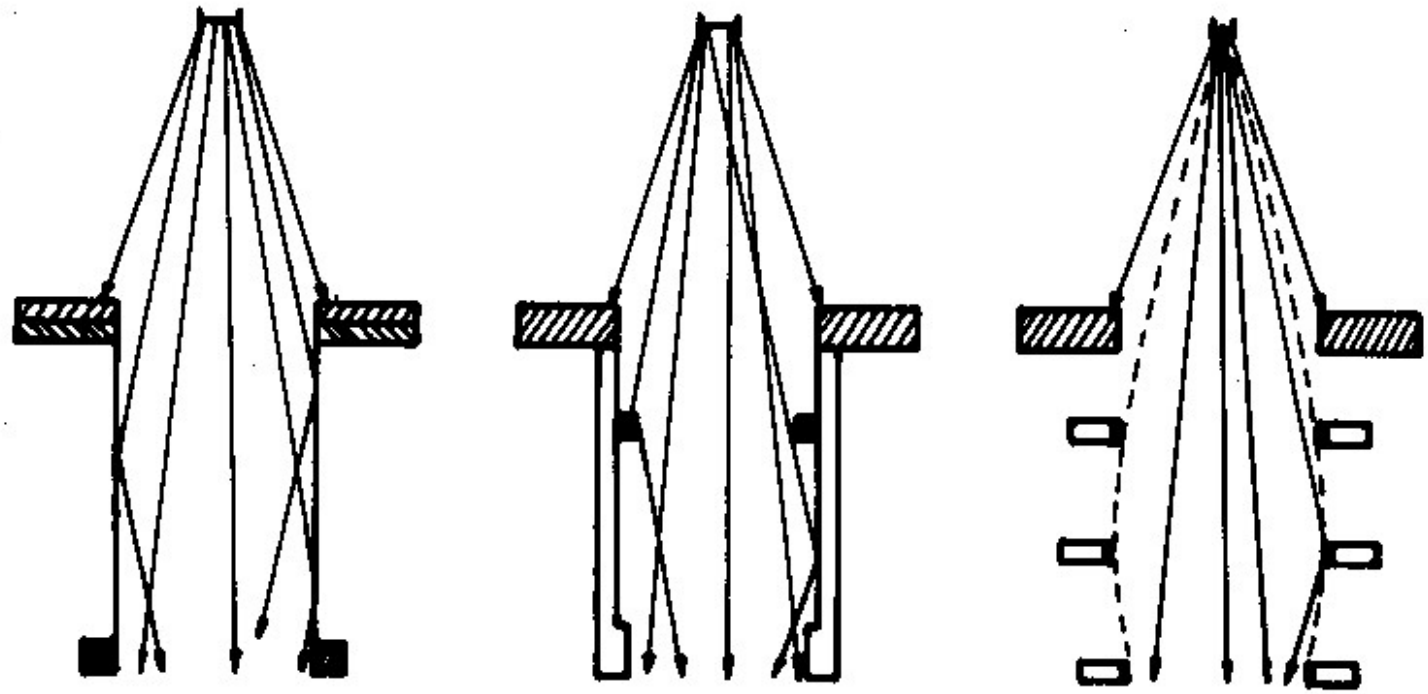

ICRU 35 [8]

← More scattered electrons ←

Actual electron collimators

Siemens

Varian

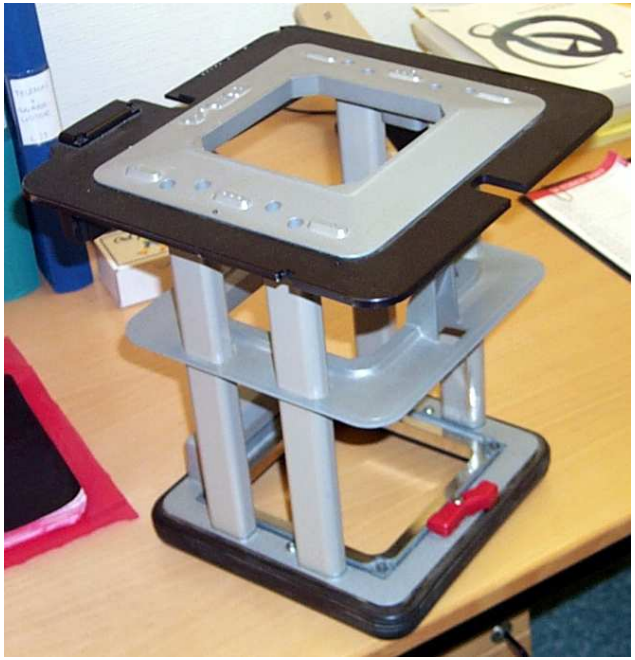

Elekta

Typical insert

20 MeV electron w/wo applicator

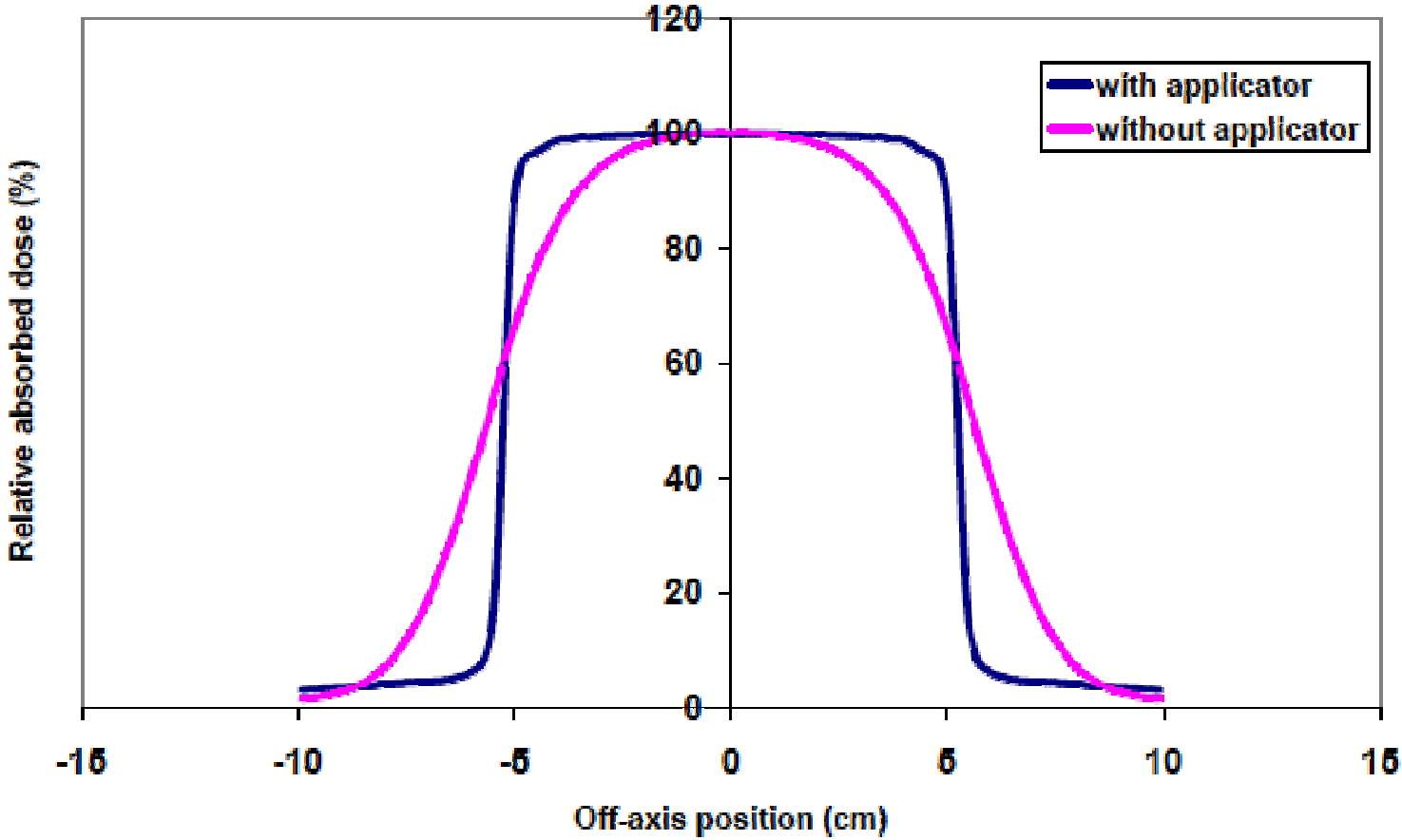

Figure 1. Absorbed dose profiles with and without an electron applicator for an Elekta SLi Plus machine. The applicator size is 10×10 cm^2 and the nominal energy is 20 MeV. The measurements were performed with a diode detector at 1 cm depth in a water phantom. SSD= 100 cm.

Olsson 2003 [17]

Summary

- The focal spot size (FWHM typically 1-2 mm) influences the photon beam penumbra width.
- Lateral photon beam flattening through a conical flattening filter also creates additional scatter and increases the off-axis softening effect.
- Mean photon energy [MeV] at isocenter roughly equals MV/3, somewhat lower for high-energy beams.
- The geometrical beam alignment is not trivial for rounded leaf edges. It may vary between accelerator vendors and should be better known among users and TPS vendors.
- Electron beams are strongly influenced by scattering and energy loss interactions inside the treatment head and depends therefore more on treatment head design than photons.

References I

1. Karzmark CJ, Nunan CS, and Tanabe E (1993) Medical Electron Accelerators. McGraw-Hill, Inc. ISBN 0-07-105410-3.
2. Jaffray DA and Battista JJ (1993) X-ray sources of medical linear accelerators: Focal and extra-focal radiation. Med Phys 20, 1417-27.
3. Sätherberg A, Karlsson MG, and Karlsson M (1996) Theoretical and experimental determination of phantom scatter factors for photon fields with different radial energy variation. Phys Med Biol 41, 2687-94.
4. Sheikh-Bagheri D and Rogers DW (2002) Monte Carlo calculation of nine megavoltage photon beam spectra using the BEAM code. Med Phys 29, 391-402.
5. Huq MS, Das IJ, Steinberg T, and Galvin JM (2002) A dosimetric comparison of various multileaf collimators. Phys Med Biol 47, N159-70.
6. Boyer AL and Li S (1997) Geometric analysis of light-field position of a multileaf collimator with curved ends. Med Phys 24, 757-62.
7. Vassiliev ON, Titt U, Pönisch F, Kry SF, Mohan R, and Gillin MT (2006) Dosimetric properties of photon beams from a flattening filter free clinical accelerator. Phys Med Biol 51, 1907-17.
8. ICRU Report 35 (1984) Radiation Dosimetry: Electron Beams with Energies Between 1 and 50 MeV. ISBN 0-913394-29-7.

References II

9. Zhu XR, Gillin MT, Jursinic PA, Lopez F, Grimm DF, and Rownd JJ (2000) Comparison of dosimetric characteristics of Siemens virtual and physical wedges. Med Phys 27, 2267-77.
10. Kragl G, af Wetterstedt S, Knäusl B, Lind M, McCavana P, Knöös T, McClean B, and Georg D (2009) Dosimetric characteristics of 6 and 10 MV unflattened photon beams. Radiother Oncol 93, 141-6.
11. Tacke MB, Nill S, Häring P, and Oelfke U (2008) 6 MV dosimetric characterization of the 160 MLCTM, the new Siemens multileaf collimator. Med Phys 35, 1634-42.
12. Bieda MR, Antolak JA, Hogstrom KR (2001) The effect of scattering foil parameters on electron-beam Monte Carlo calculations. Med Phys 28, 2527-34.
13. Brahme A, Svensson H (1979) Radiation beam characteristics of a 22 MeV microtron. Acta Radiol Oncol Radiat Phys Biol 18, 244-72.
14. van Battum LJ, van der Zee W, Huizenga H (2003) Scattered radiation from applicators in clinical electron beams. Phys Med Biol 48, 2493-507.
15. Deng J, Pawlicki T, Chen Y et al, The MLC tongue-and-groove effect on IMRT dose distributions, Phys Med Biol 46 (2001) 1039-1060.
16. Knöös T and Wittgren L, Which depth dose data should be used for dose planning with wedge filters? Phys Med Biol 36 (1991) 255-267.
17. Olsson M-L, Monte Carlo simulations of the Elekta Sli Plus electron applicator system – A base for a new applicator design to reduce radiation leakage, MSc Thesis, Lund University, 2003.

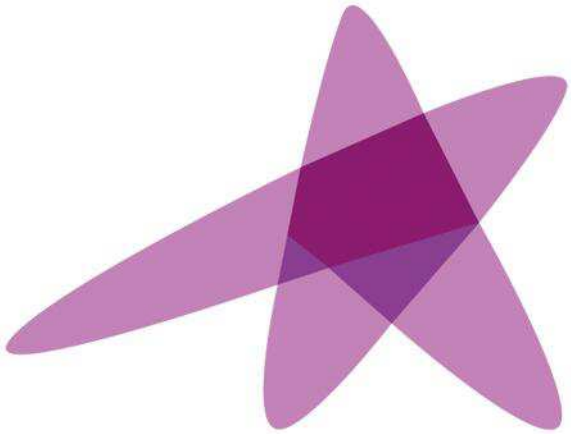

ESTRO School

WWW.ESTRO.ORG/SCHOOL

Absorbed dose determination:

Part 1: Measurements away from reference conditions

Núria Jornet

Servei de Radiofísica
Hospital Sant Pau, Barcelona

Lecture Content

1. Absorbed dose determination: Differences between reference and non reference conditions (standard and non-standard radiation beams)

   Going back to some fundamentals of dosimetry to understand the validity of the factors and corrections applied to detectors readings in different irradiation conditions.

2. Specific problems associated with relative dose measurements (scans/output).

   Importance of how data are measured phantom and detector.

3. Summary.

Learning objectives

1. Review the fundamentals of absorbed dose measurements (back to the cavity theory).
2. Define reference dosimetry, relative dosimetry, standard and non standard beams.
3. Understand how the changes in beam fluence outside reference conditions may modify the calculation of the absorbed dose in water from the detector's reading.

Q1: What is the quantity of interest to calibrate radiotherapy beams?

1. The absorbed dose in the detector.
2. The absorbed dose at a point in water.
3. The detector reading in water
4. The absorbed dose at a point in tissue.

To determine the absorbed dose at a point in water we need a dose detector

1. The dose detector will have a **finite sensitive volume.**
2. The signal collected from this detector will depend on the dose absorbed in it.
3. The detector will **not** be **constituted of water**.

Q2: **Being D_w the dose absorbed at a point in water and D_{det} the averaged absorbed dose in the detector placed at that point . What of the following equalities is true?**

1. $D_{det}(P) = D_w(P)$
2. $D_{det}(P) \times f(Q) = D_w(P)$
3. $D_{det}(P) \times CF = D_w(P)$
4. $D_{det}(P) = D_w(P')$

Where f(Q) is the cavity factor and depends on the quality of the beam

Where CF is a calibration coefficient that is independent of the beam quality

ESTRO School

How to go from detector reading to dose to media?

f_Q is determined using MC alone or MC combined with experimental measurements

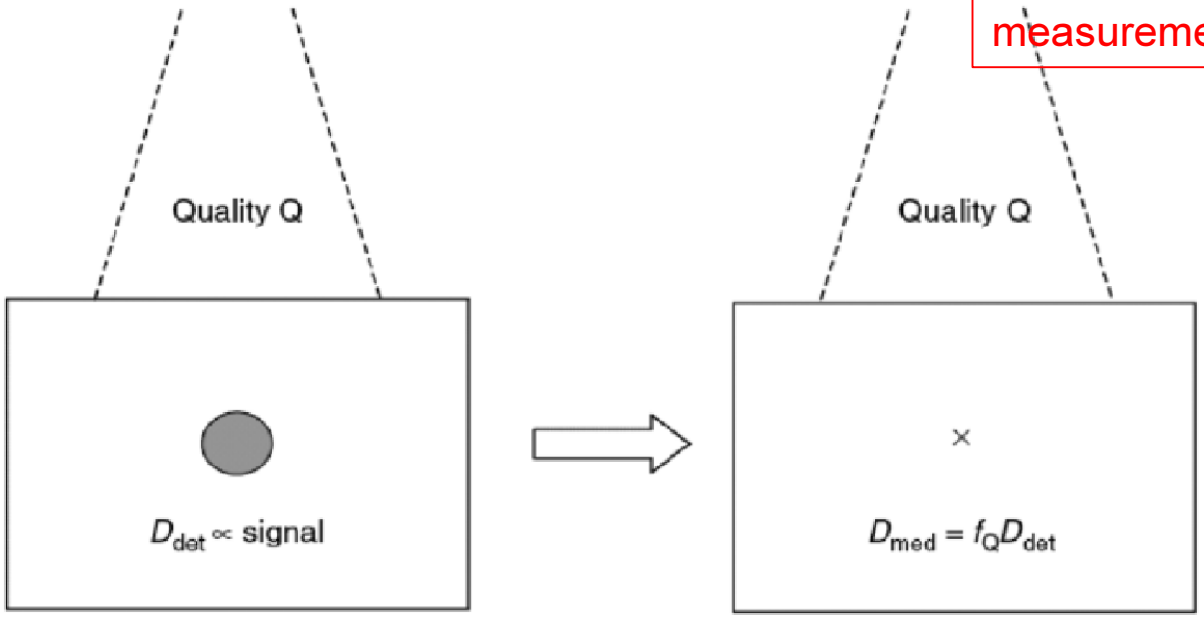

$$D_w = M \cdot \alpha \cdot k_l \cdot f_Q$$

$$M = M^* \cdot k_{env} \cdot k_{dr}$$

α factor to convert R to D_{det} (for a given dose)

Ki ("linearity factor")

Bragg Gray Cavity [electron sensor, range of electrons>cavity] $f_Q \approx S_{w,det}$

If it isn't a Bragg Gray Cavity $f_Q \approx [\mu_{en}/\rho]_{w,\,det}$

ESTRO School

α is the calibration coefficient (Ddet/M, determined for one dose). There are detectors (such as TLDs) which show a non-linear behaviour, and therefore k_l must be taken into account.

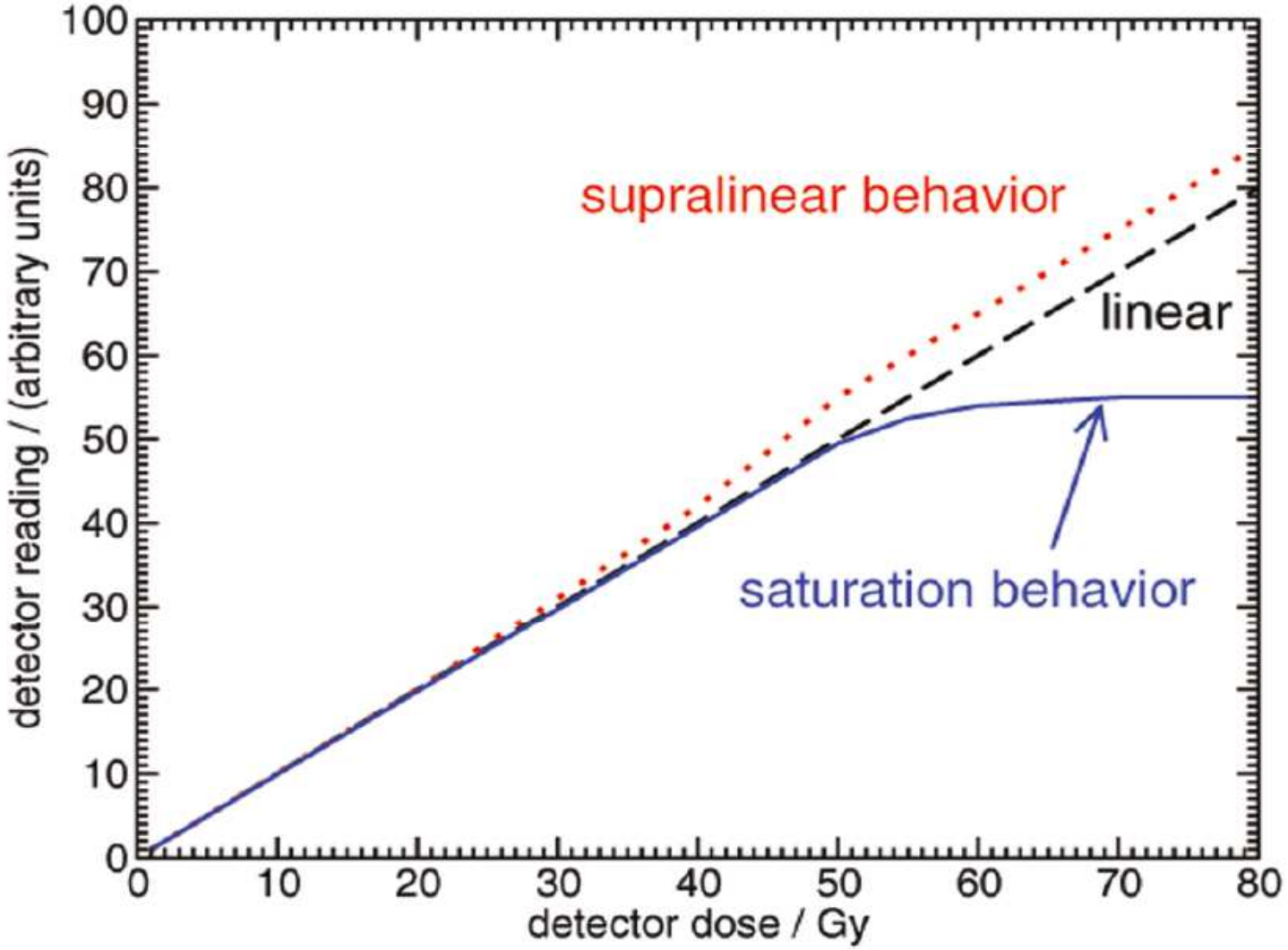

ESTRO School

Q3: Semiconductor detectors in a 6MV X-ray beam behave as:

1. A Bragg Gray Cavity
2. Burlin cavity
3. A photon detector

Q4: **Semiconductor detectors in a 6MV X-ray; beam energy deposition mainly due to:**

1. A Bragg Gray Cavity (electron's interactions)
2. Burlin cavity (photon's and electron's interactions)
3. A photon detector (photon's interactions)

How to go from detector reading to dose to media

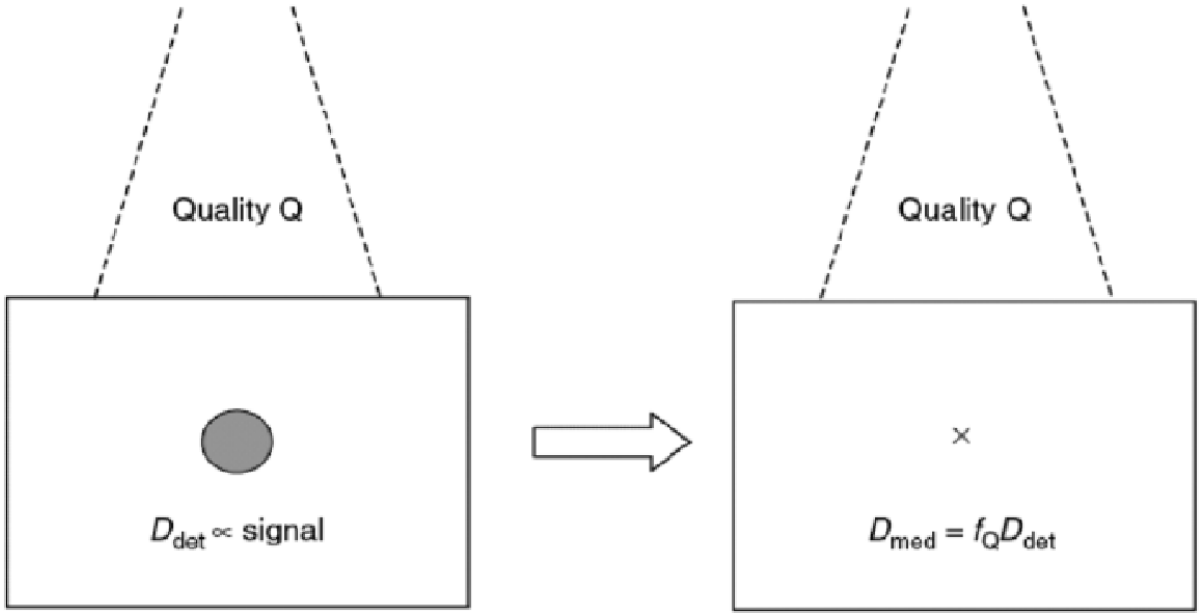

$$D_w = M \cdot \alpha \cdot k_i \cdot f_Q$$

Burlin cavity theory:

$$f_Q = d \cdot S_{w,det} + (1-d) \cdot [\mu_{en}/\rho]_{w,det}$$

Bragg Gray cavity: Ionisation chambers in High Energy X-ray Beams

Burling cavity: High density detectors such as diodes, MOSFET, diamonds for High Energy X-ray beams

ESTRO School

Q5 Is CPE or TCPE needed to determine absorbed dose from measurements?

1. Yes
2. No

CPE was useful for classical cavity theories

1. Estimation of electron fluence semi-analytically. [needed to calculate stopping power ratios, Spencer-Attix theory]
2. Assuring that the presence of the detector does not perturb the fluence crossing it (Fano's theorem) [detectors will always perturbate the electron fluence]

Pertubation effects

1. Density perturbation effects.
2. Atomic composition perturbation properties
3. Extra-cameral effects (wall/central electrode)

The cavity theory is not enough to describe the detector response

$$D_w = M \cdot \alpha \cdot k_l \cdot f_Q$$

Burlin cavity theory:

$$f_Q = d \cdot S_{w,det} + (1-d) \cdot [\mu_{en}/\rho]_{w,det}$$

$f_{Q,\ ideal}$

Need of correcting cavity breakdown by applying **PERTURBATION FACTORS** P_Q

P_Q should be determined using MC and as single perturbation factor.

P_Q : Wall, central electrode CF
Fluence and gradient perturbation factors

ESTRO School

How to go from detector reading to dose to media

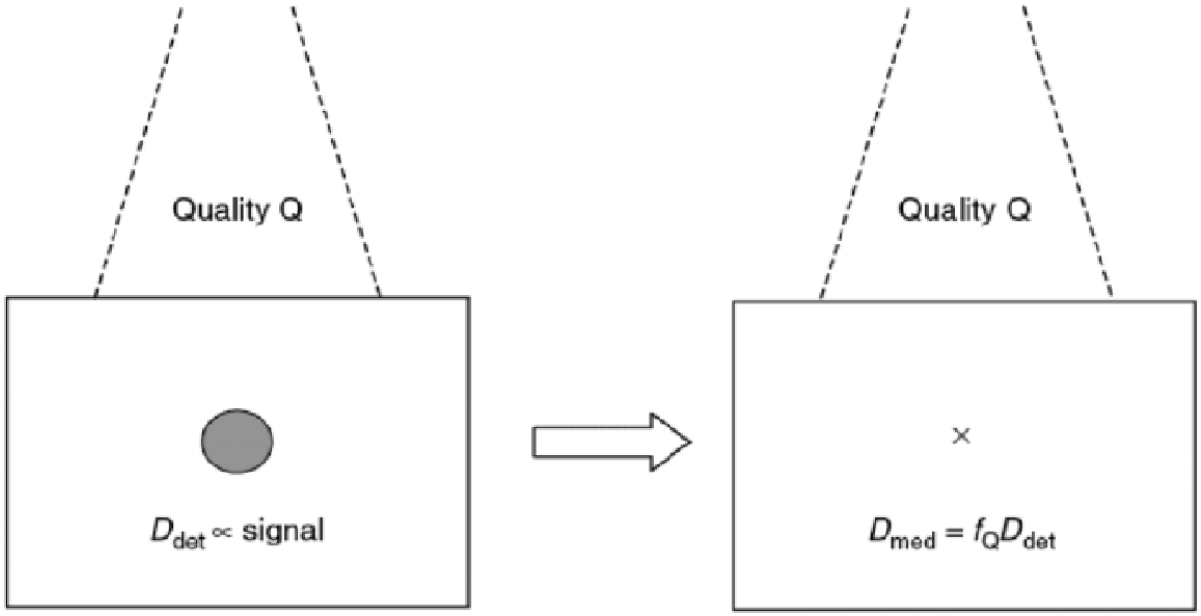

$$D_{med} = M \cdot \alpha \cdot k_i \cdot f_{Q,ideal} \cdot P_Q$$

Burlin cavity theory:

$$f_Q = d \cdot S_{w,med} + (1-d) \cdot [\mu_{en}/\rho]_{w,med}$$

d=1 $f_{Q,ideal} \approx S_{w,med}$ Ionisation chambers in High Energy X-ray Beams

d=0 $f_{Q,ideal} \approx [\mu_{en}/\rho]_{w,med}$ High density detectors such as diodes, MOSFET, diamonds for High Energy X-ray beams

ESTRO School

Reference condition described in dosimetry CoP

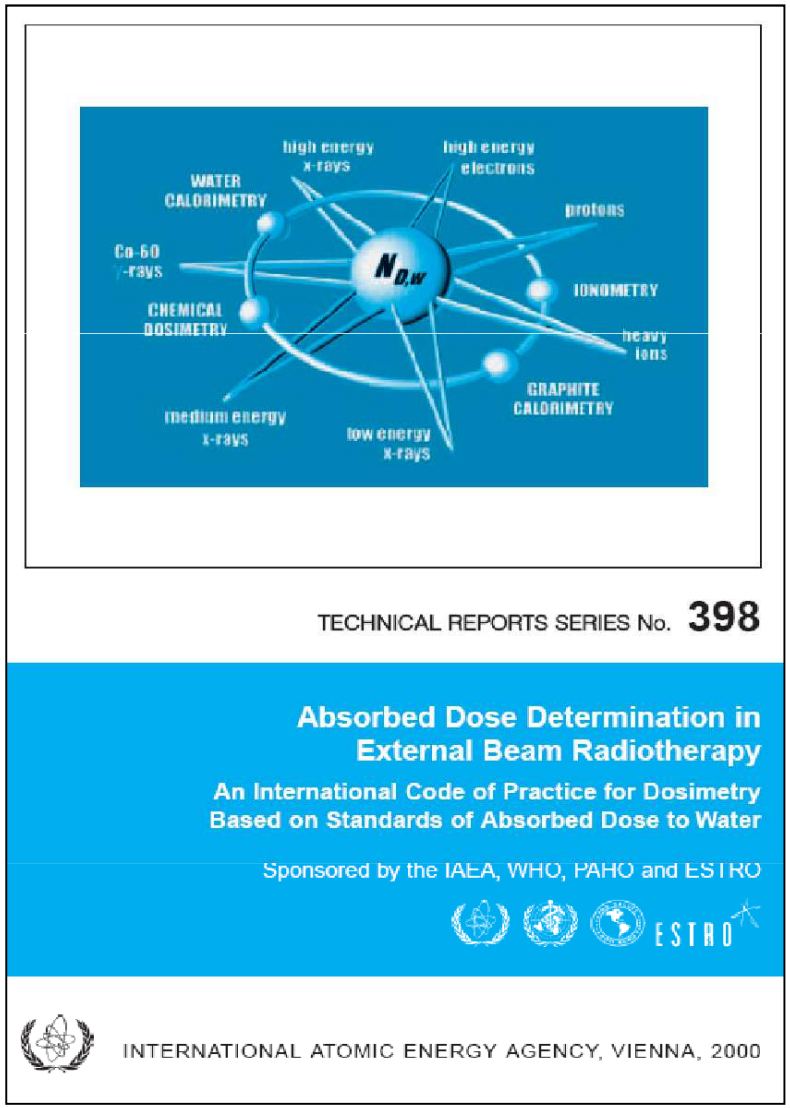

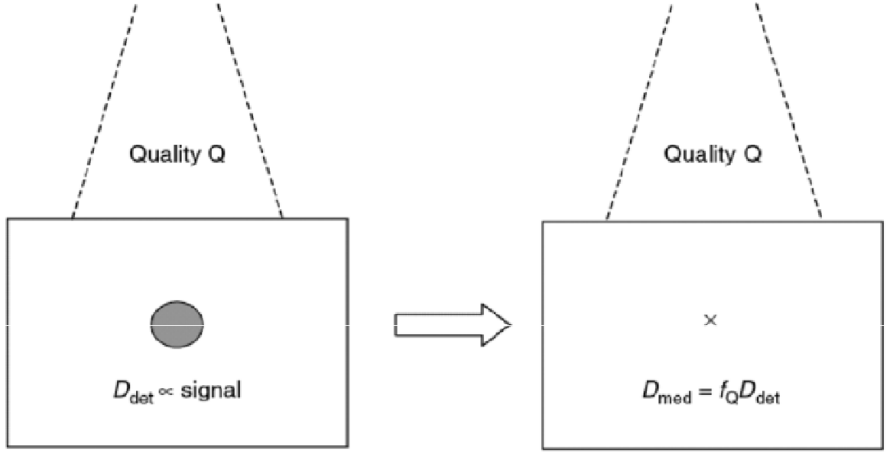

Detector: air (ionisation chamber)

Med: Water

For reference irradiation conditions:

Fixed field size

Fixed depth

Fixed SSD

$$D_{w,Q} = M^* \cdot k_i \cdot N_{D,w}$$

$$N_{D,w} = \alpha \cdot k_l \cdot f_{Q,ideal} \cdot P_Q$$

Calibrated in terms of water absorbed dose in ^{60}Co-radiation in units of Gray per Coulomb

ESTRO School

Reference Conditions: Example for Photons

TABLE 13. REFERENCE CONDITIONS FOR THE DETERMINATION OF ABSORBED DOSE TO WATER IN HIGH ENERGY PHOTON BEAMS

Influence quantity	Reference value or reference characteristics
Phantom material	Water
Chamber type	Cylindrical
Measurement depth z_{ref}	For $TPR_{20,10} < 0.7$, 10 g/cm^2 (or 5 g/cm^2)[a] For $TPR_{20,10} \geq 0.7$, 10 g/cm^2
Reference point of the chamber	On the central axis at the centre of the cavity volume
Position of the reference point of the chamber	At the measurement depth z_{ref}
SSD/SCD	100 cm[b]
Field size	10 cm × 10 cm[c]

ESTRO School

Q6 Which of the following is a reference condition

1. Measuring at a point at the equivalent reference depth , field size 10x10cm^2, SSD=100 cm, in a plastic water equivalent phantom
2. Measuring at a point at the reference depth, field size 20x20cm^2
3. Measuring in a lung equivalent phantom
4. Out axis measures
5. Small field measures
6. None of the above are reference conditions

Determination of Relative Dose Away from Reference Conditions may refer to:

- Data acquisition for a TPS
  - PDD
  - profiles (off-axis measurements)
  - output factors
- Small field dosimetry
- Dose verification
  - IMRT verification
  - measurements in a medium different from water

Relative dose measurements compare the dose measured under non-reference conditions to the reference dose

Challenges: reference versus relative dosimetry

Reference conditions

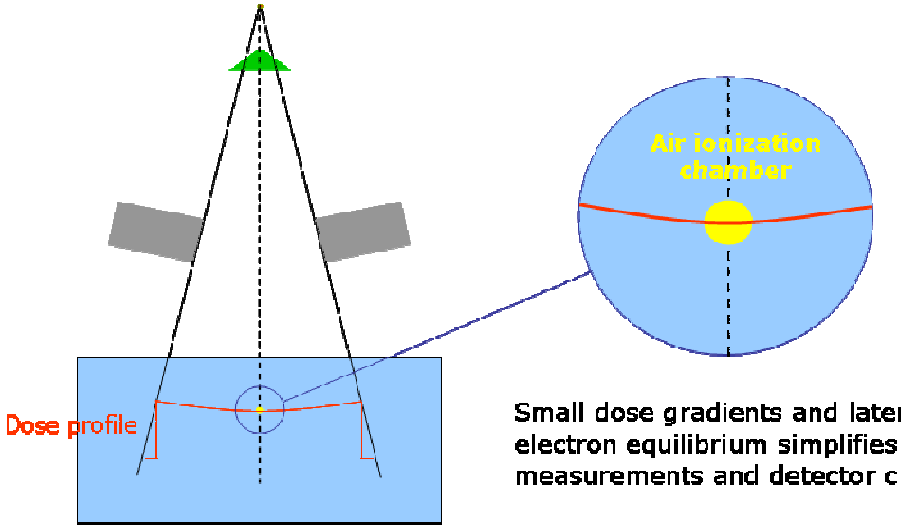

- Uniform electron fluence distribution over the detector.
- Beam spectra at the reference point in ref. conditions known.
- Detector of choice: **Ion Chambers**

Non reference conditions: *Relative dosimetry*

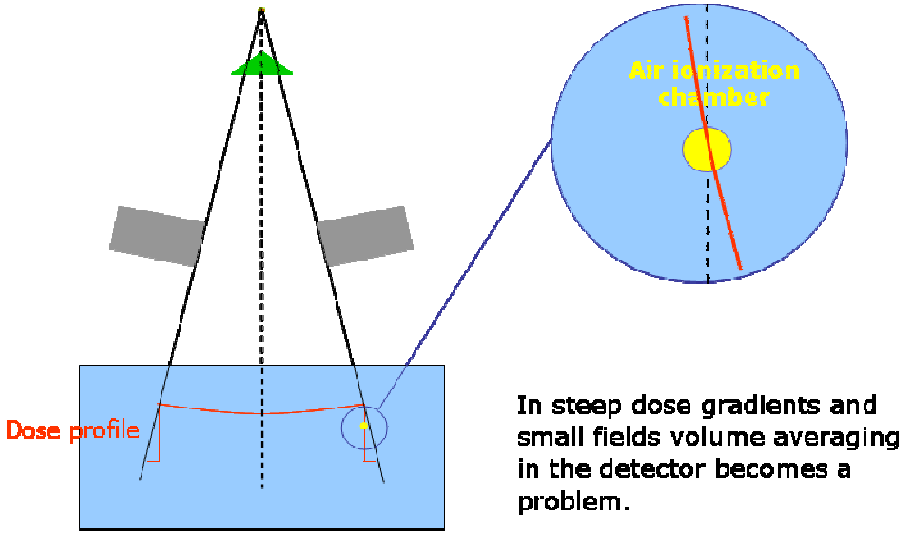

- Non-Uniform electron fluence distribution over the detector. **VOLUME AVERAGING**
- Beam spectra at the reference point may differ from beam spectra at the measuring point. **ENERGY DEPENDENCE; PERTURBATION FACTORS**
- Detector of choice: **???**

ESTRO School

Challenges: reference versus relative dosimetry

Reference conditions

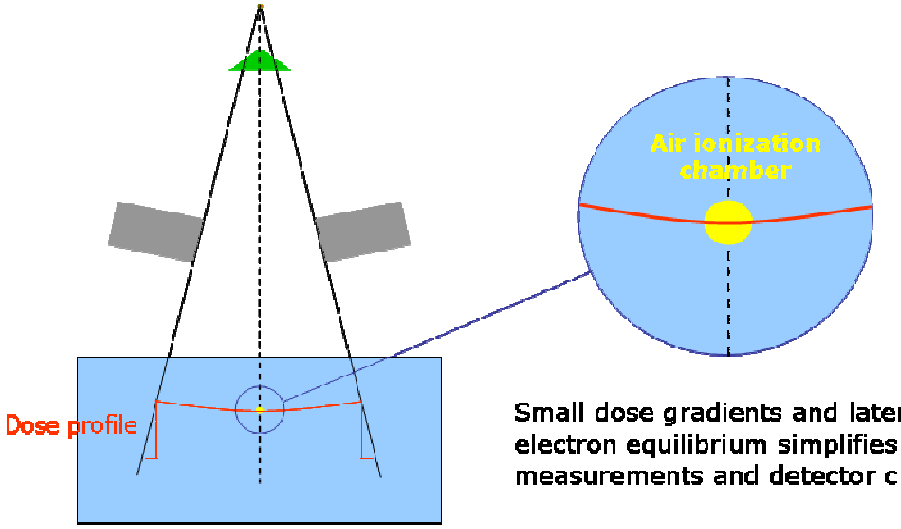

- Uniform electron fluence distribution over the detector.
- Beam spectra at the reference point in ref. conditions known.
- Detector of choice: **Ion Chambers**

Non reference conditions: *Relative dosimetry*

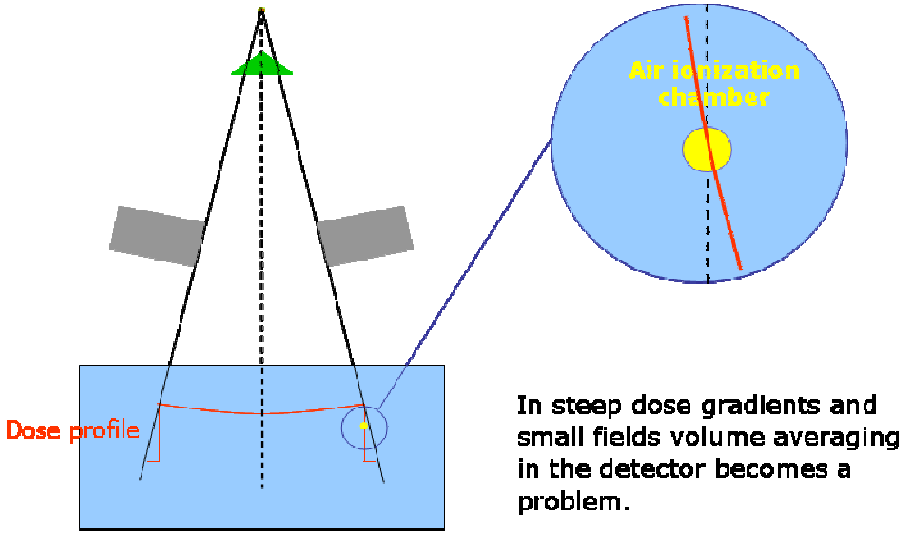

- Non-Uniform electron fluence distribution over the detector. **VOLUME AVERAGING**
- Beam spectra at the reference point may differ from beam spectra at the measuring point. **ENERGY DEPENDENCE; PERTURBATION FACTORS**
- Detector of choice: **???**

ESTRO School

Scenario in which the detector will work

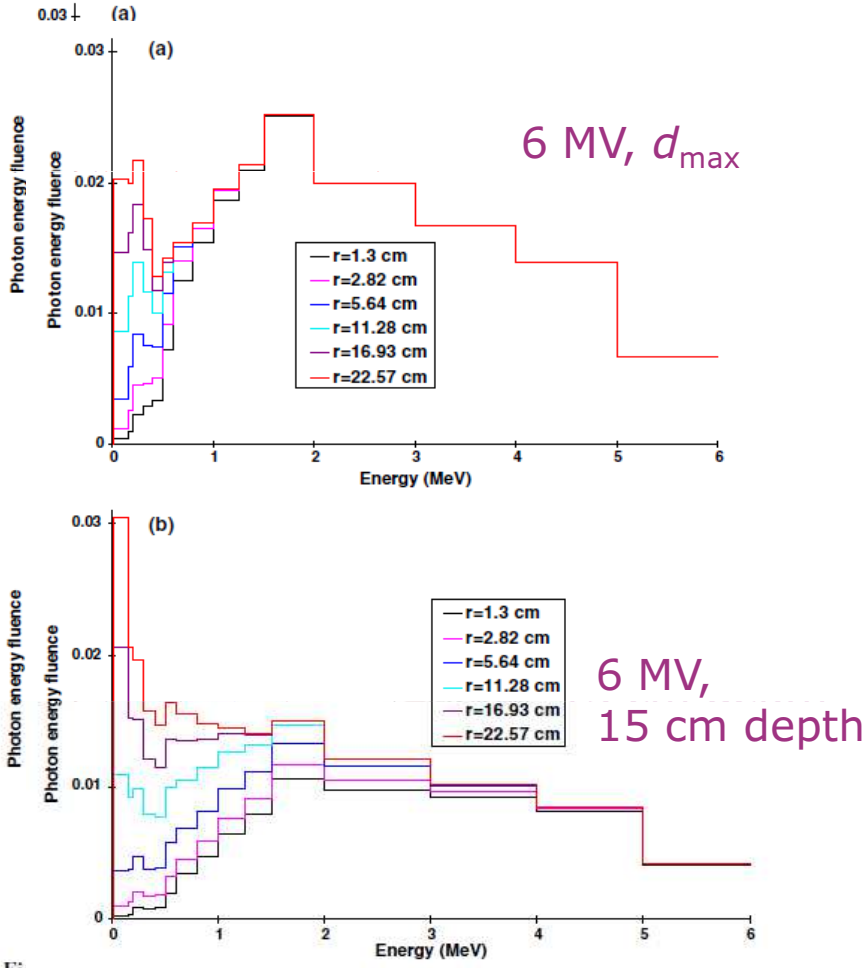

Figure 1. Total 6 MV photon energy fluence calculated using Monte Carlo FLURZnrc (EGSnrc) code as a monotonically increasing function of field size at (a) peak and (b) 15 cm depth of water.

Yin *et al* [1]

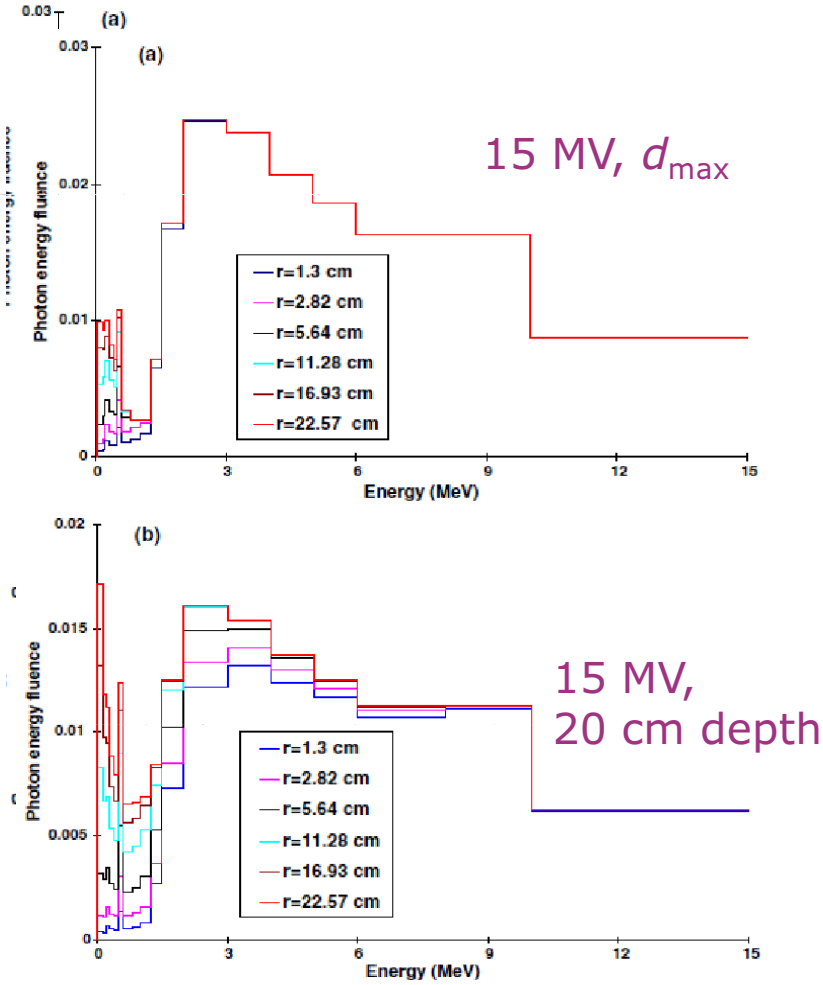

Figure 2. Total 15 MV photon energy fluence calculated using Monte Carlo FLURZnrc (EGSnrc) code as a monotonically increasing function of field size at (a) peak and (b) 20 cm depth of water.

Back to μ_{en}

ESTRO School

Mean energies in a 6 MV beam depending on field size and depth

Two counteracting effects as depth increases: Beam hardening of primary fluence and increasing amount of scattered photons.

photons

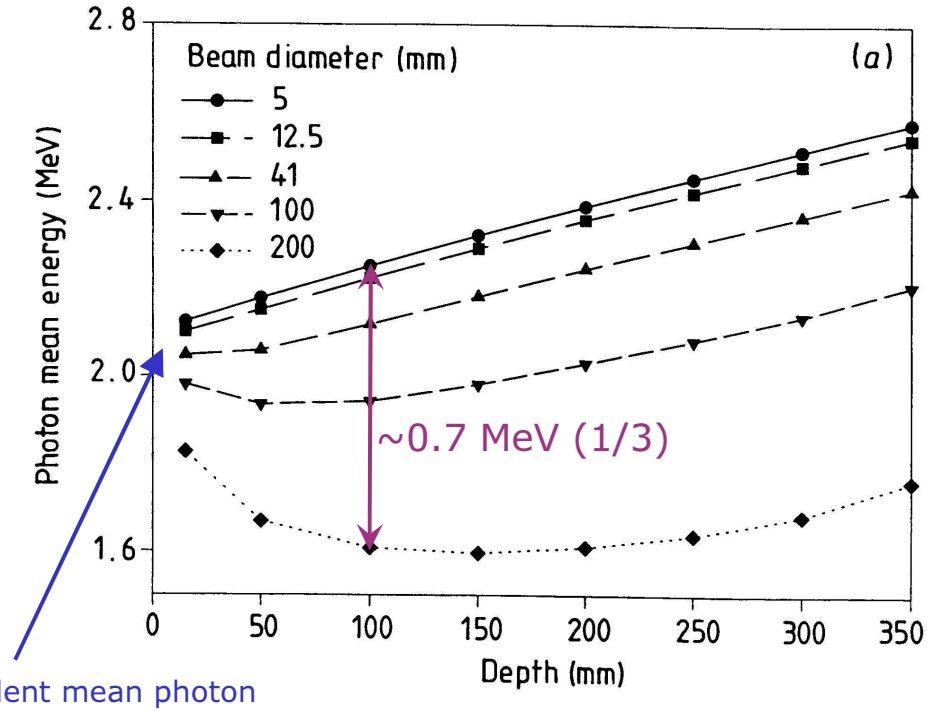

Incident mean photon energy = 2.11 MeV

electrons

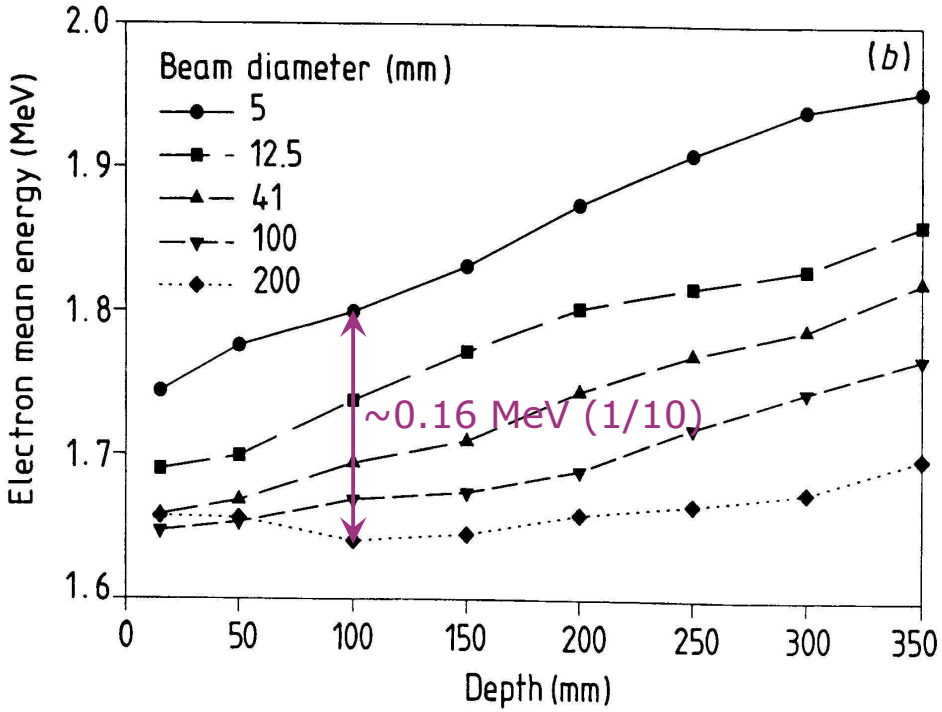

Heydarian *et al* [2]

Back to Stopping-power ratios

Variation of $s_{water,air}$ for ion chamber measurements

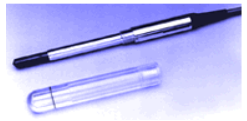

10^7 photons

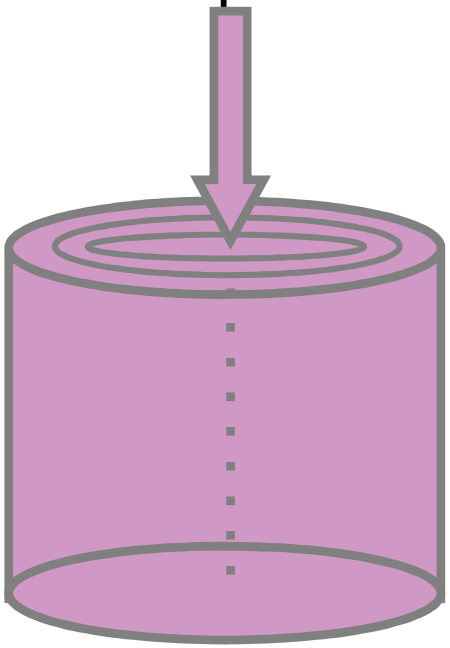

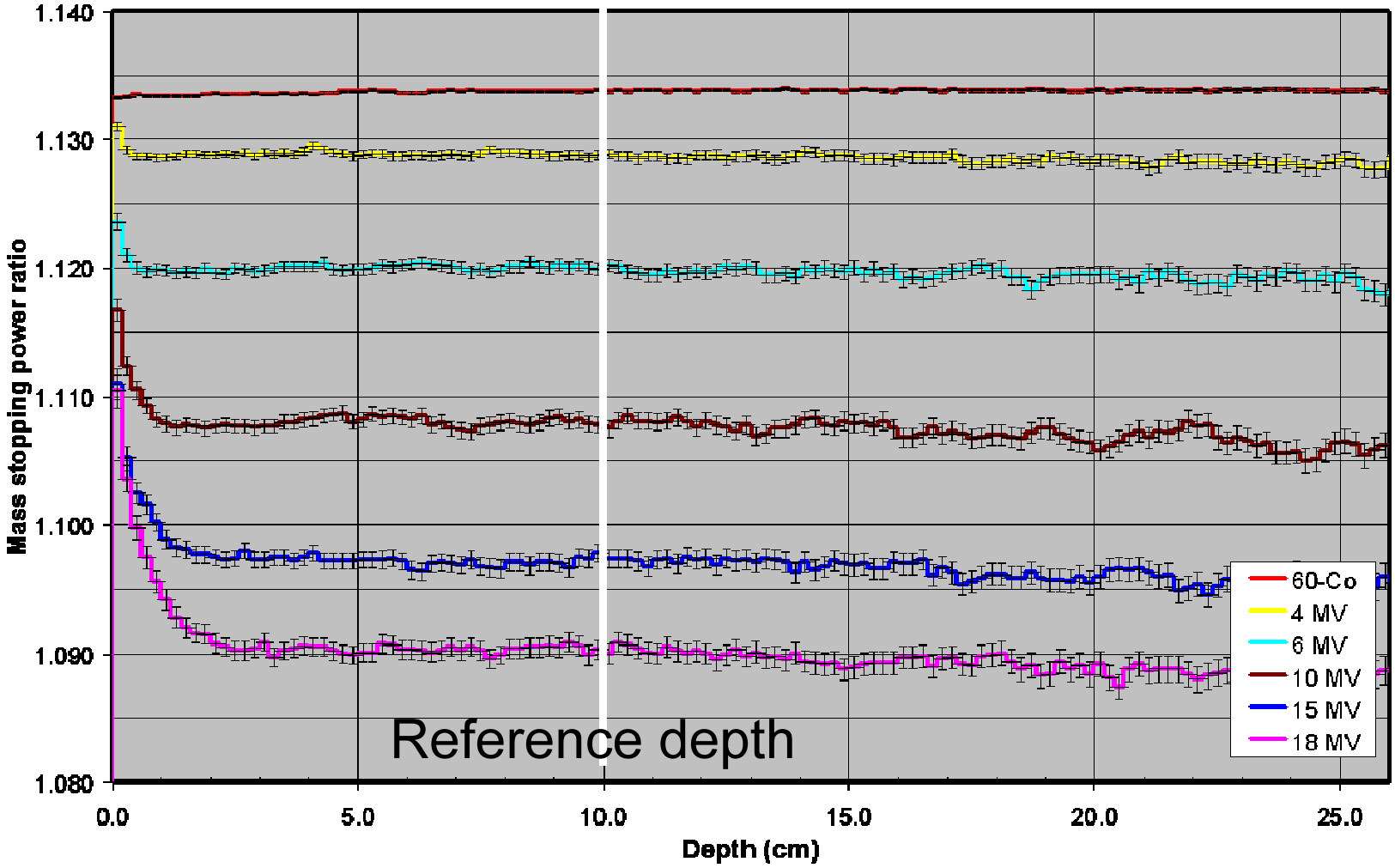

Calculations performed with SPRrznrc

Variation of $s_{water,air}$ for ion chamber measurements

10^7 photons

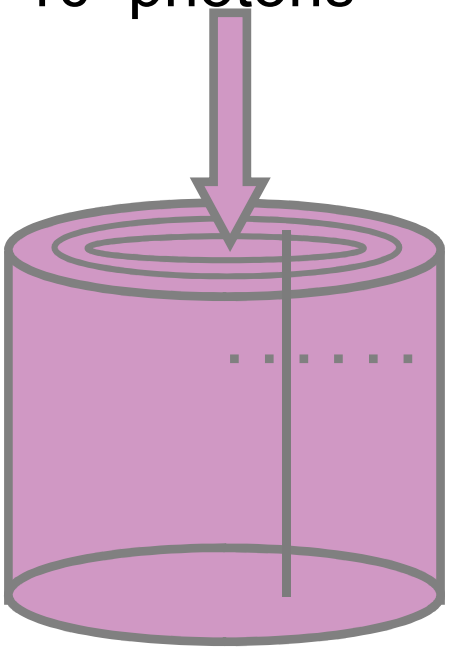

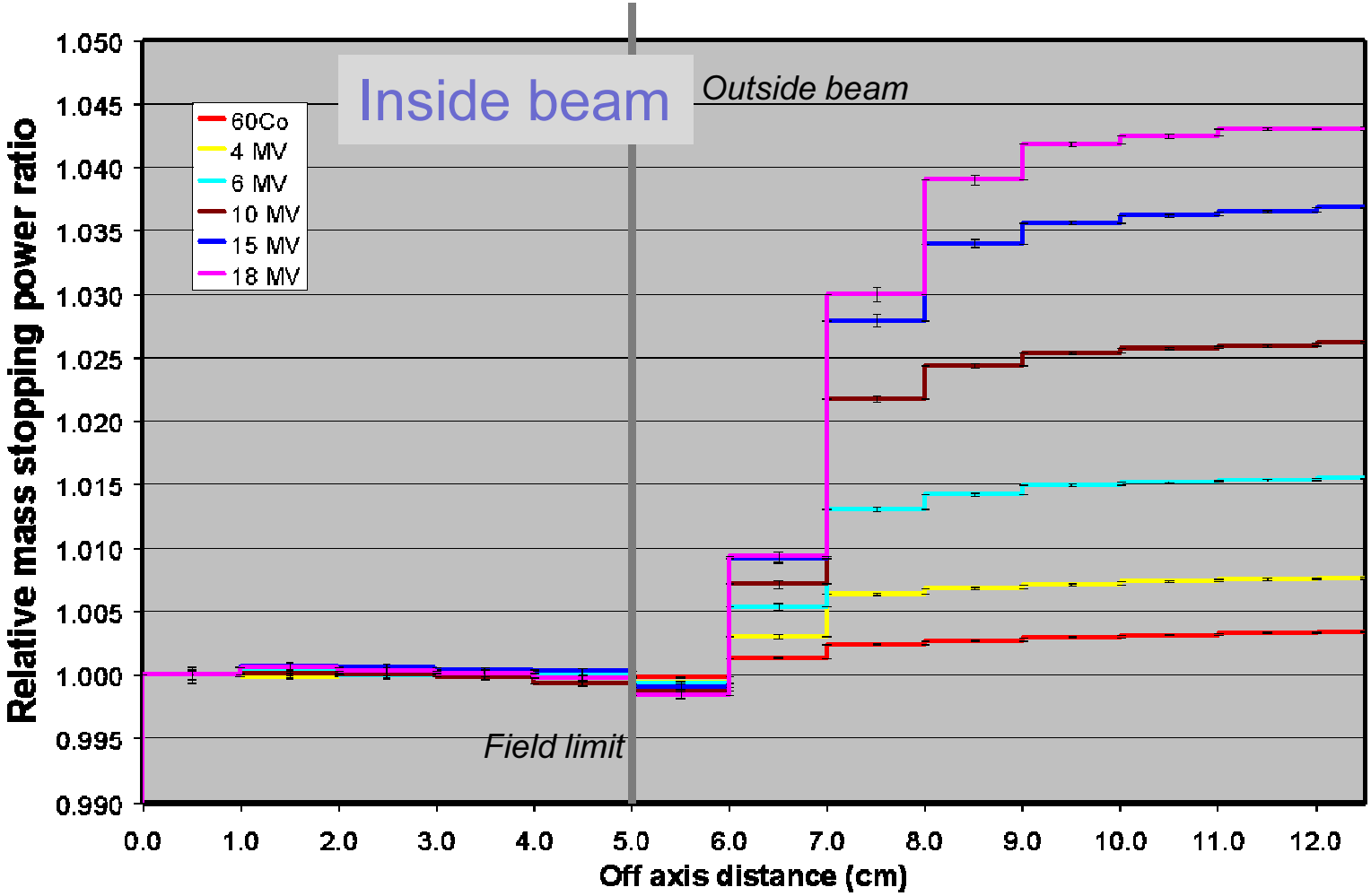

Calculations performed with sprrznrc

Constant spectra over the field

Stopping power ratios along a radii at 10 cm depth in water

Q8 We are measuring a depth dose curve in a 15MV X-ray beam. At point r

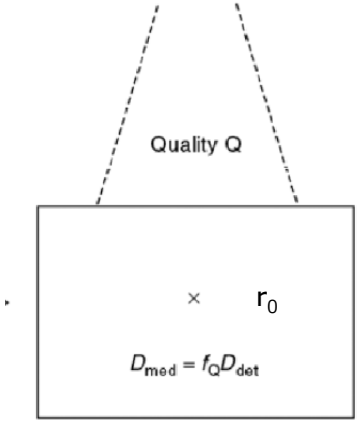

$D_{med}(r_0) = D_{det}(r_0) \cdot p(r_0) \cdot f_Q(r_0) \cdot$

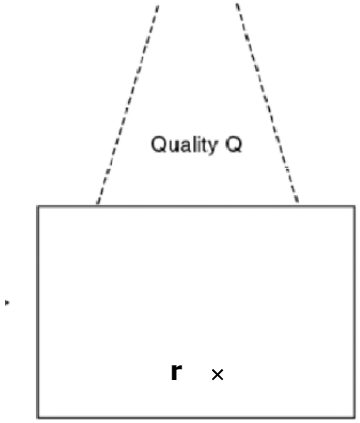

$D_{med}(r) = D_{det}(r) \cdot p(r) \cdot f_Q(r) \cdot$

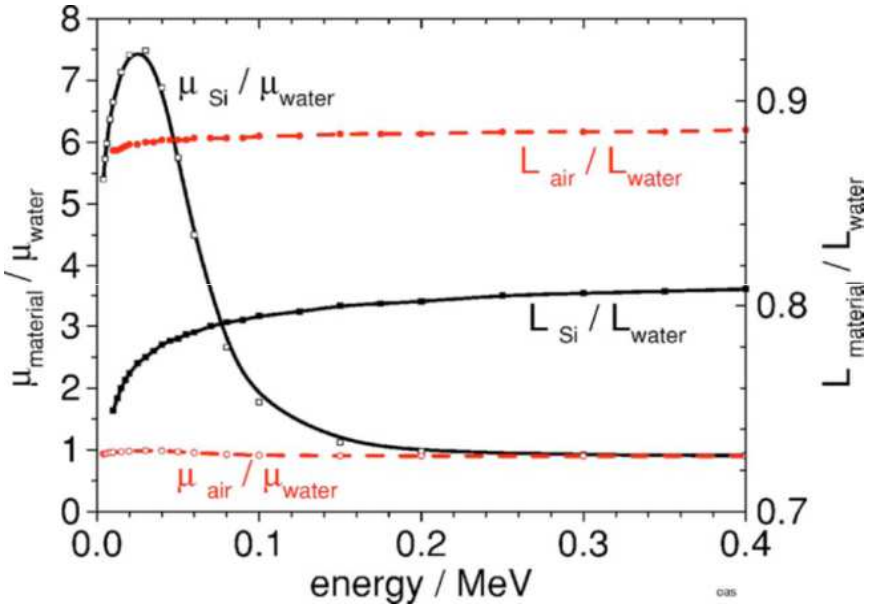

Sauer & Wilbert MP **34**, 2007, 1983-1988

1. A silicon diode will overestimate the dose to water
2. A silicon diode will underestimate the dose to water
3. An air ionisation chamber will underestimate dose to water
4. An air ionisation chamber will overestimate dose to water

ESTRO School

Conceptual frame

$$\frac{D_{non\,ref}}{D_{ref}} = \frac{M_{non\,ref}}{M_{ref}}$$

$$\frac{D_{non\,ref}}{D_{ref}} = \frac{M_{non\,ref}}{M_{ref}} \cdot \frac{f_{Q,non\,ref}}{f_{Q,ref}} \cdot \frac{P_{Q,non\,ref}}{P_{Q,ref}}$$

Look for detectors that make this factors equal to 1 for the non reference conditions of interest

ESTRO School

Measurements under non-reference conditions: Output factors

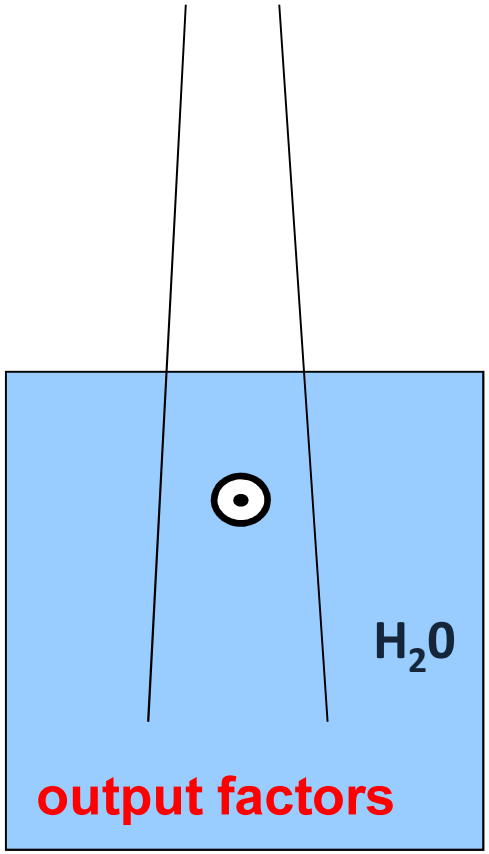

Q8 For large fields:

For which detector the ratio of readings is not the output factor :

1. 0.6 cc air vented ionisation chamber
2. Diode
3. 0.125 cc air vented ionisation chamber

ESTRO School

Measurements under non-reference conditions: Output factors

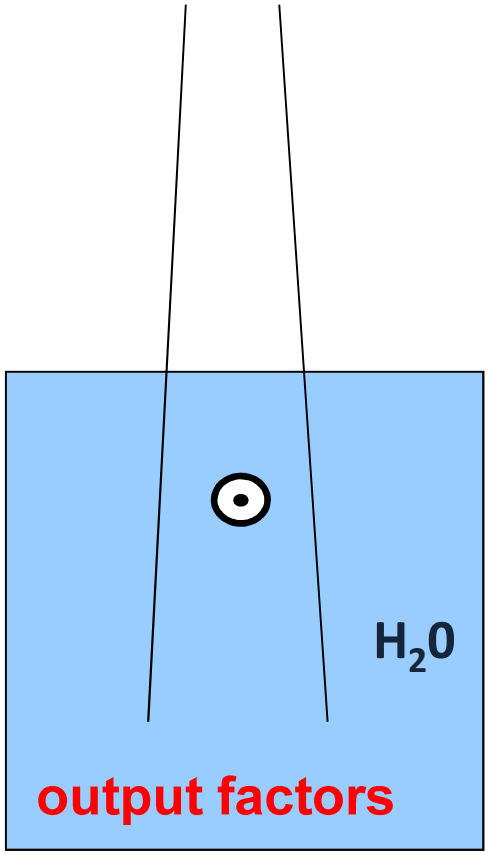

Large fields:

Changes in photon fluence in the beam axis.

More low energy photons.

Air vented ion chamber: $f_Q(A_{ref}) = f_Q(A) = S_{w,air}$

Diode: Burlin cavity theory:

$f_Q = d \cdot S_{w,med} + (1-d) \cdot [\mu_{en}/\rho]_{w,silicon}$

$[\mu_{en}/\rho]_{w,silicon}$ for A and A ref differ

ESTRO School

Energy dependency detectors

What is meant by "Energy dependence"?
A varying relation between the detector signal and the investigated dose (water), caused by spectral changes of the beam.

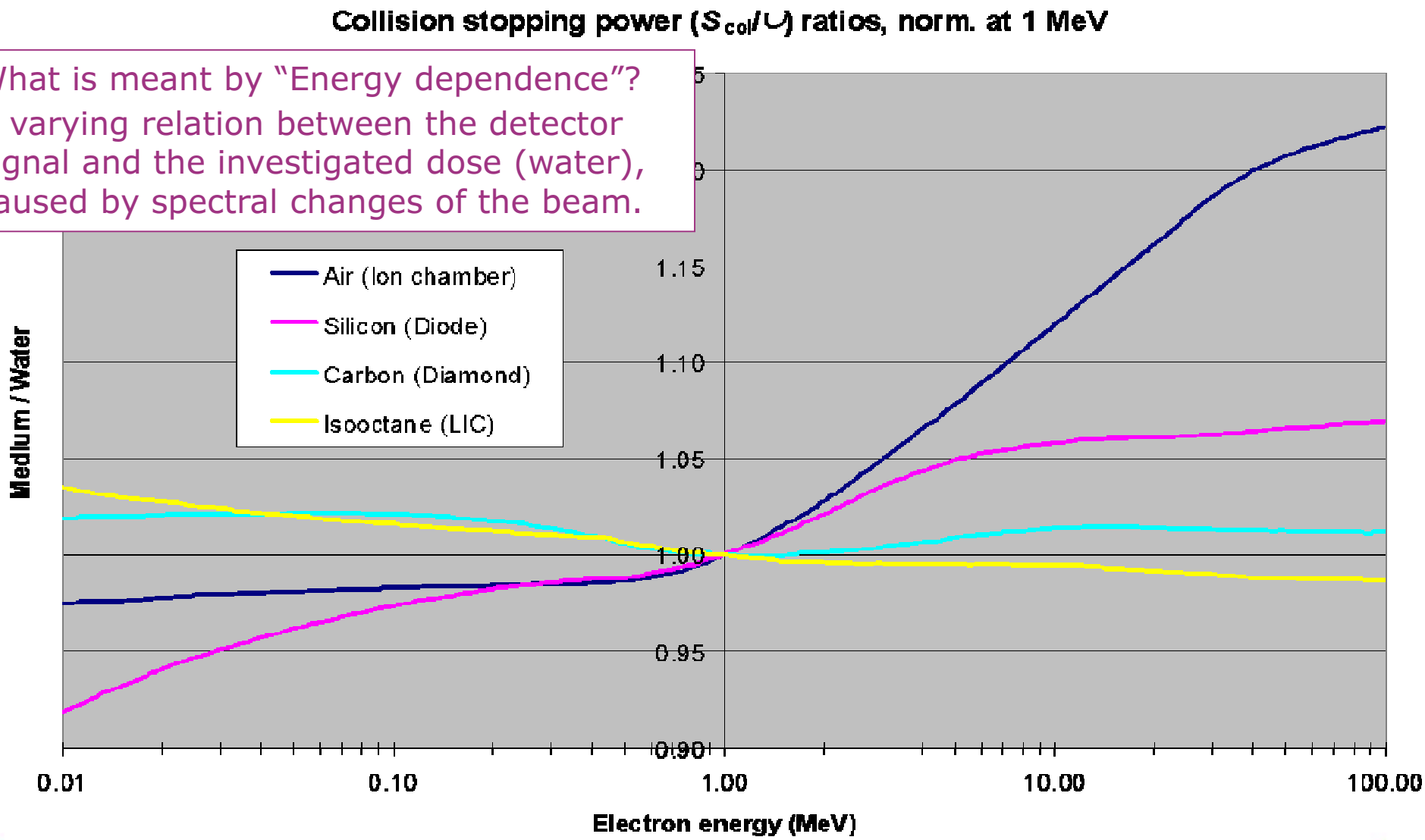

ESTRO School

Energy dependence detectors

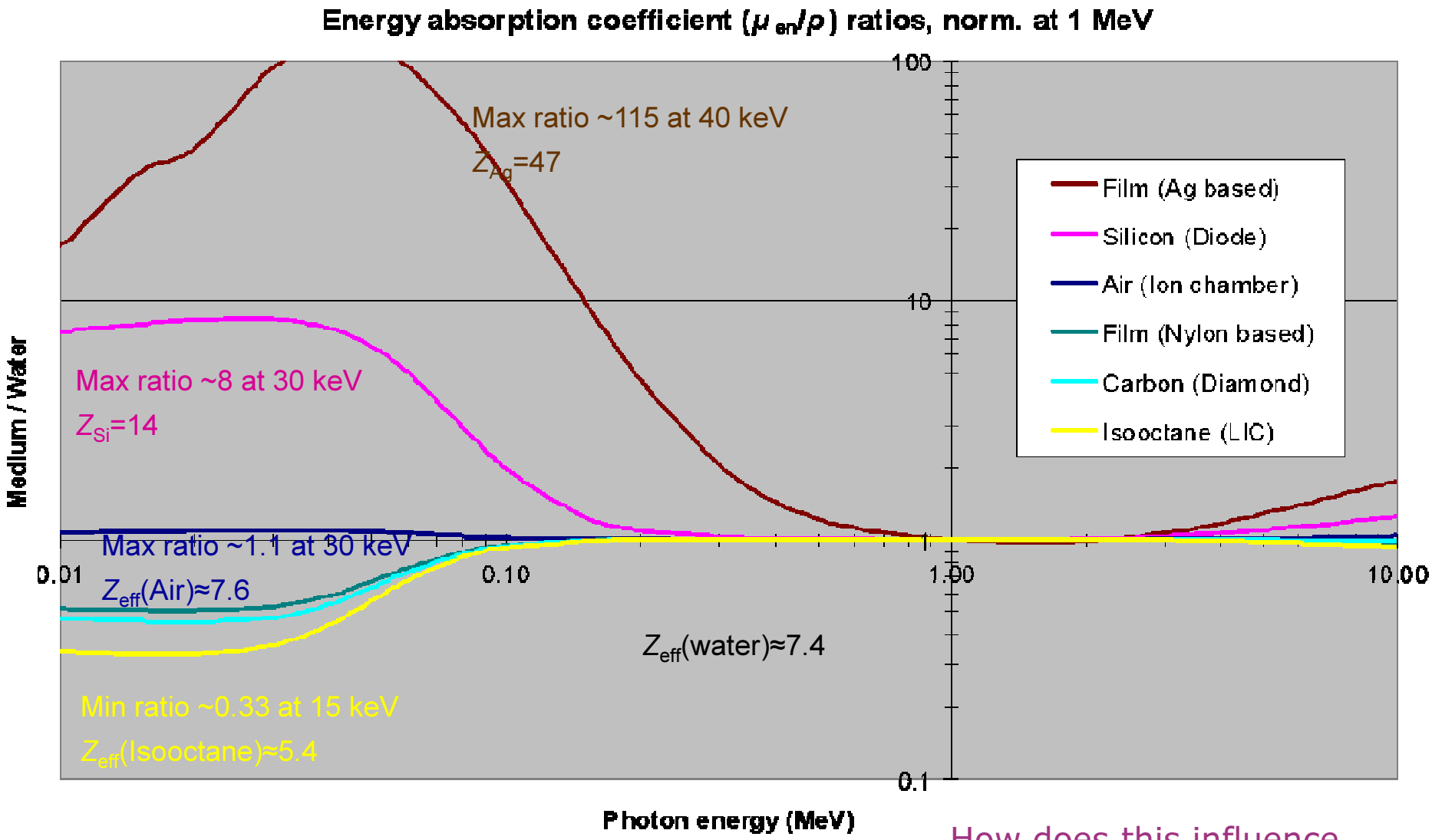

How does this influence measurements in high-energy (MV) beams?

ESTRO School

Measurements under non-reference conditions: Percentage depth doses- electrons

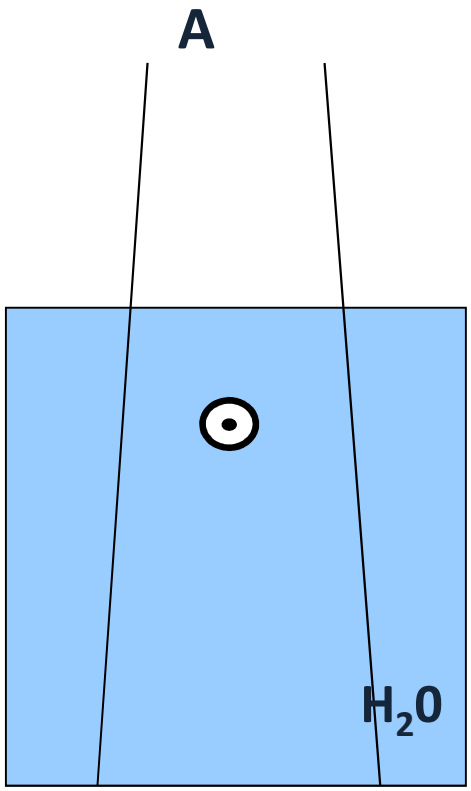

PDD;
lateral profiles

Q9 We are measuring PDD on a 20 MeV electron beam:
For which detector the ratio of readings is not the percentage depth dose:

1. Plane parallel ionisation chamber
2. Diode
3. Diamond

ESTRO School

Measuring PDD in an electron beam

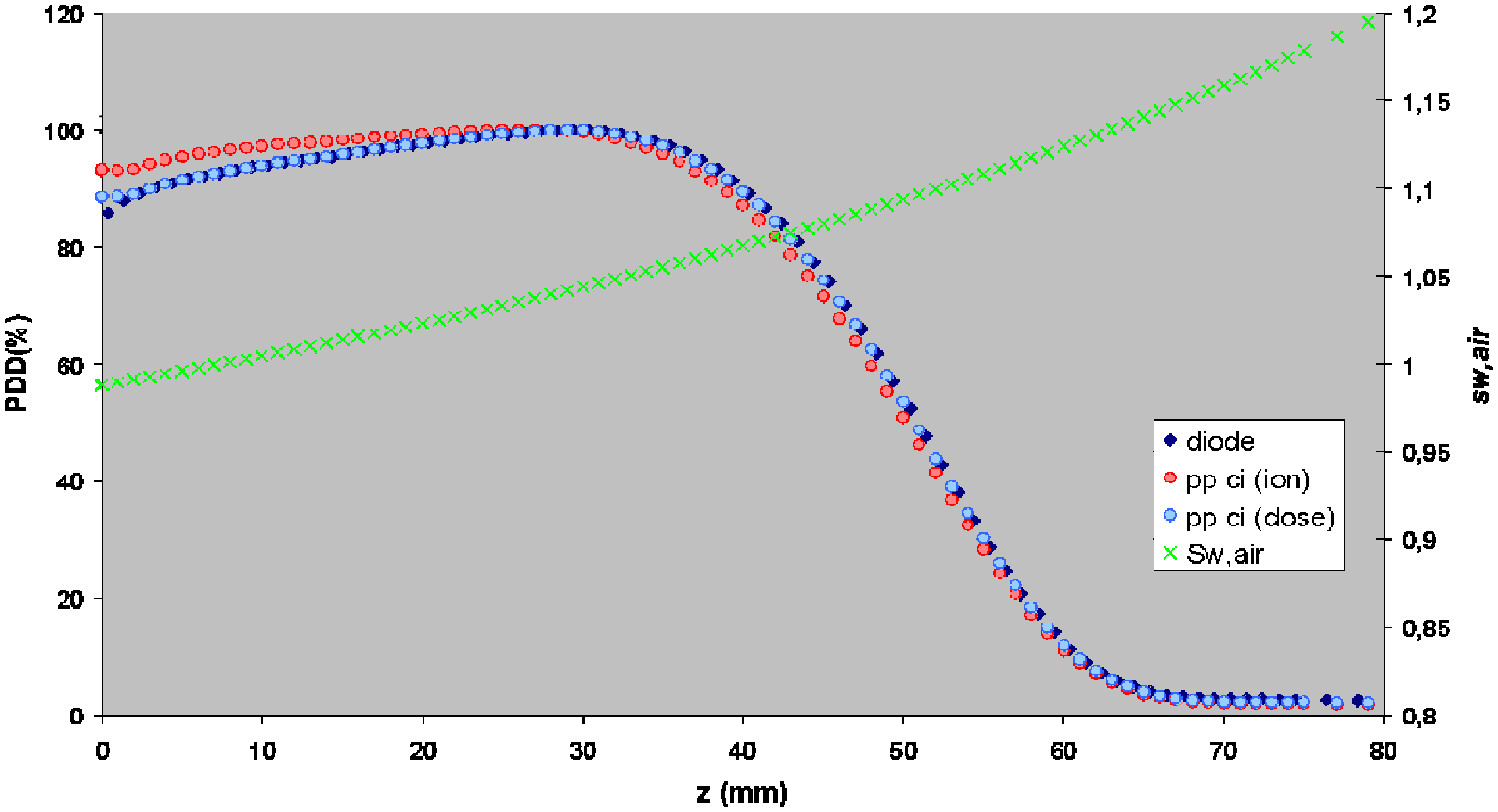

Energy dependence in electron beams

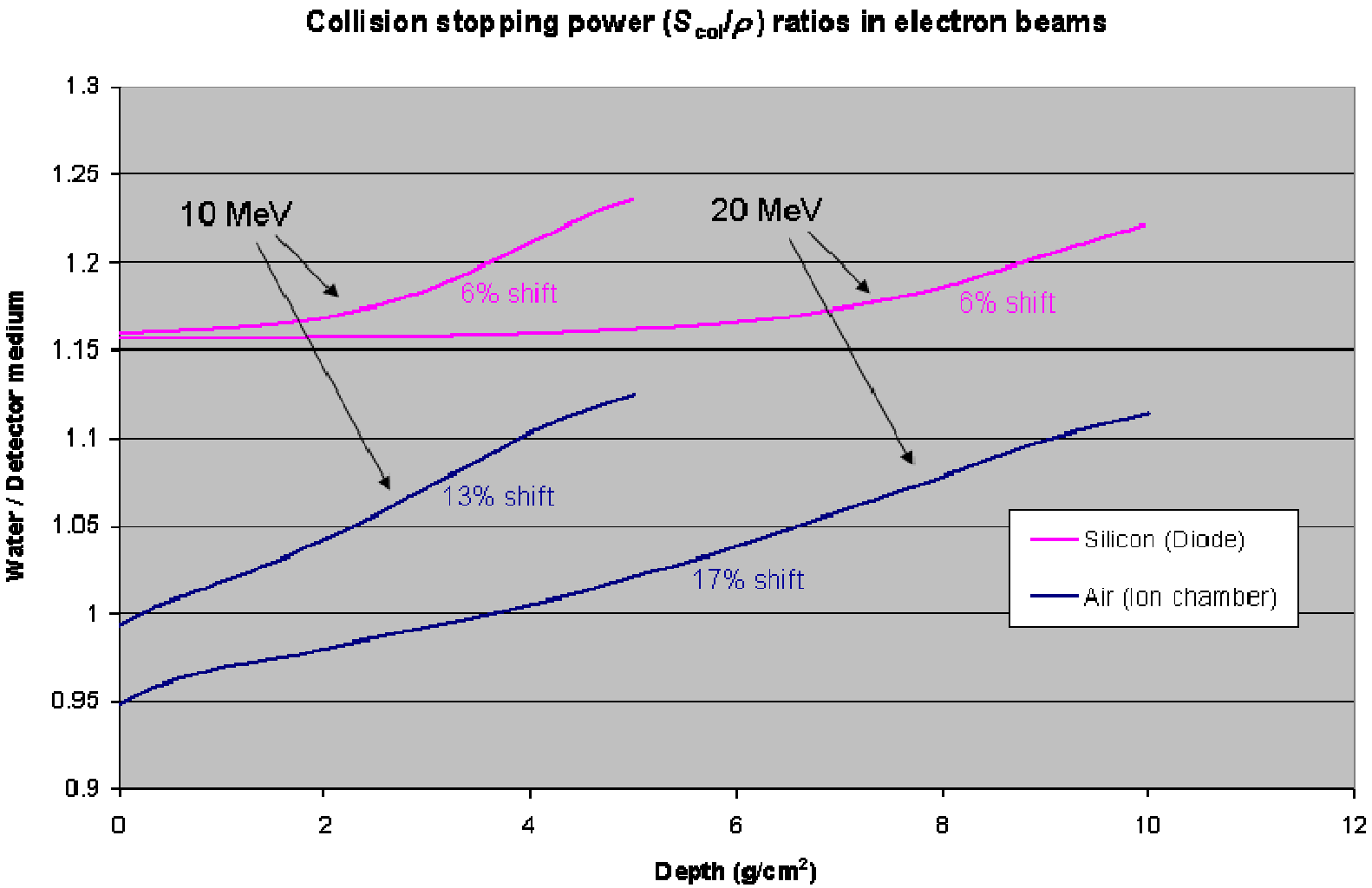

ESTRO School

Energy dependence due to changing Stopping-power ratios

(dose deposition due to electrons)

What is meant by "Energy dependence"?

A varying relation between the detector signal and the investigated dose (water), caused by spectral changes of the beam.

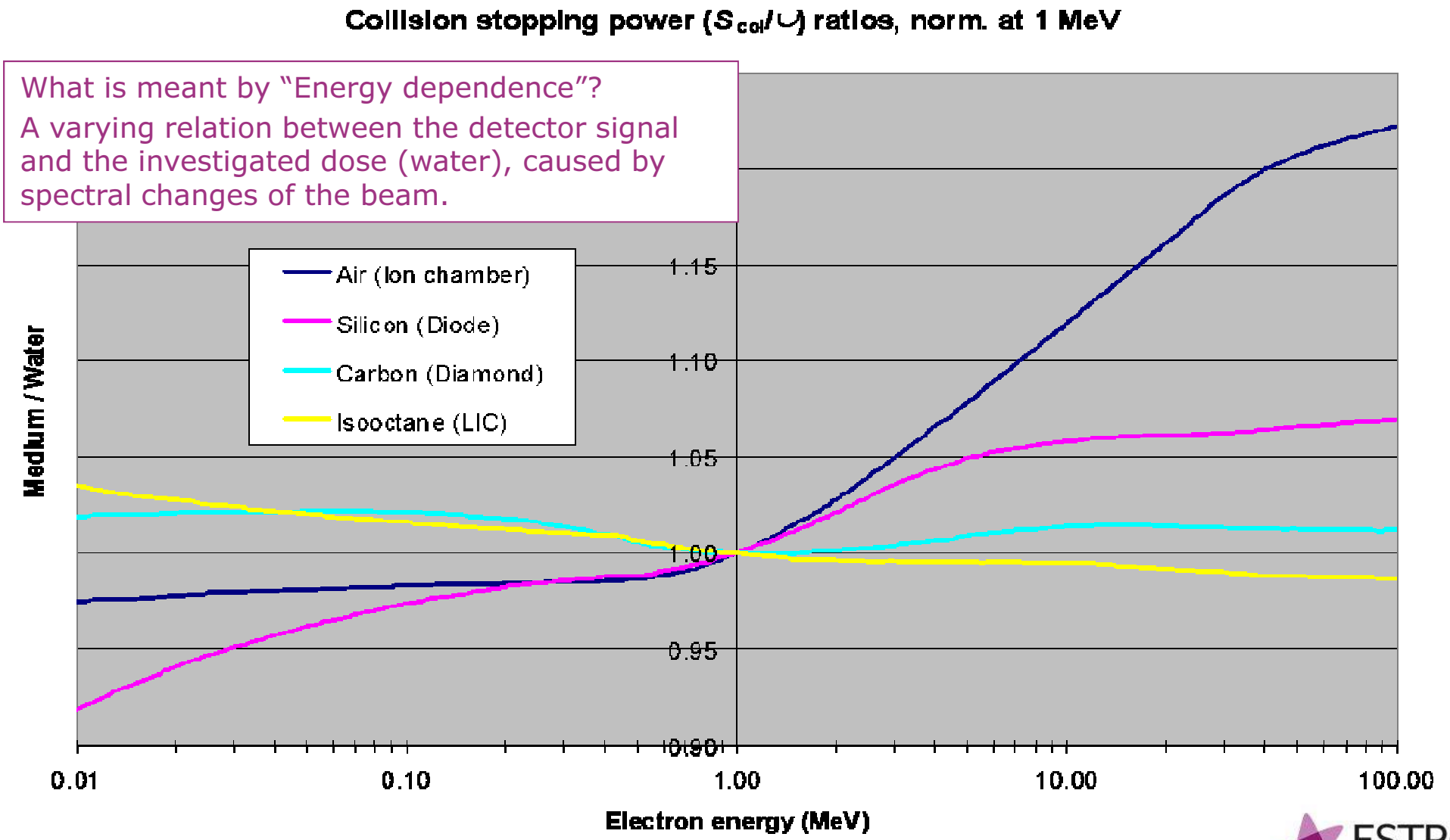

ESTRO School

Challenges: reference versus relative dosimetry

Reference conditions

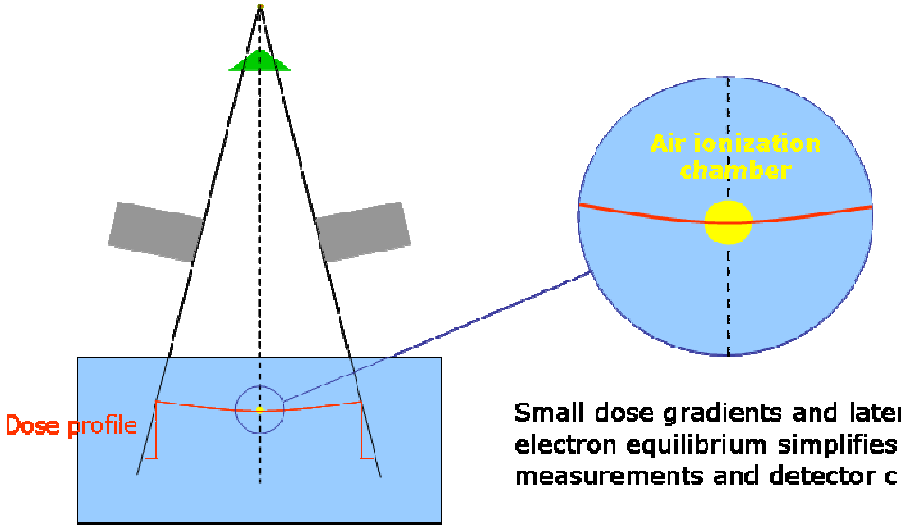

- Uniform electron fluence distribution over the detector.
- Beam spectra at the reference point in ref. conditions known.
- Detector of choice: **Ion Chambers**

Non reference conditions: *Relative dosimetry*

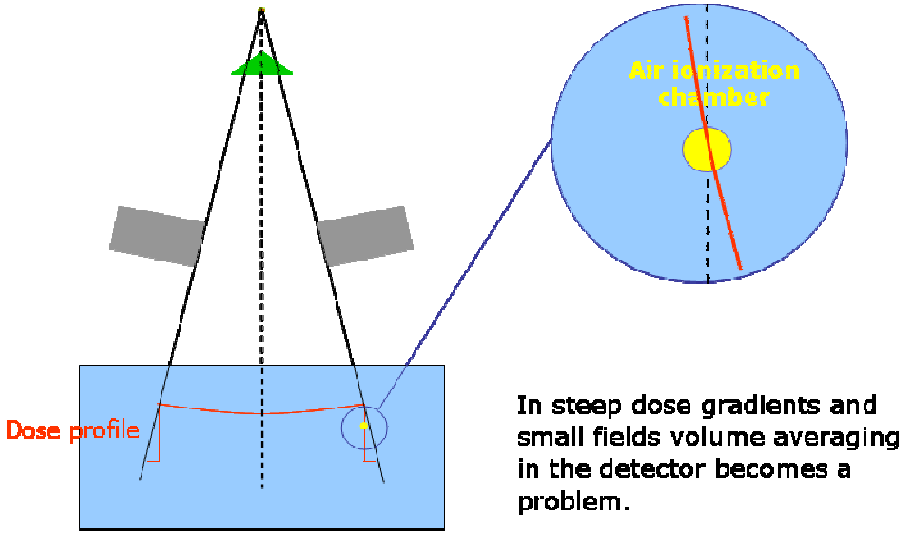

- Non-Uniform electron fluence distribution over the detector. **VOLUME AVERAGING**
- Beam spectra at the reference point may differ from beam spectra at the measuring point. **ENERGY DEPENDENCE; PERTURBATION FACTORS**
- Detector of choice: **???**

ESTRO School

Dose measurements in standard photon beams

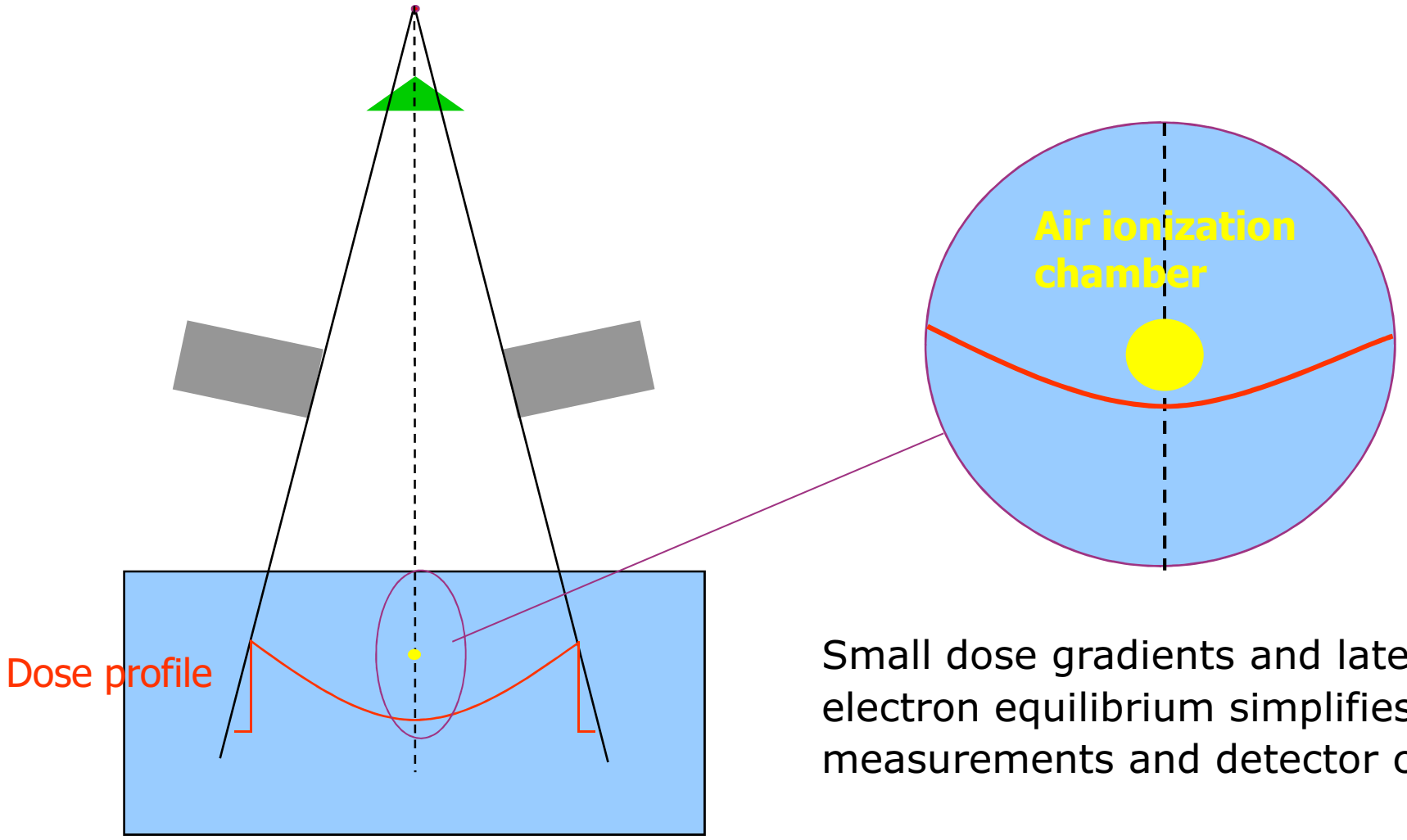

Small dose gradients and lateral electron equilibrium simplifies measurements and detector choice.

ESTRO School

Dose measurements in non-standard photon beams

Modulated fluence

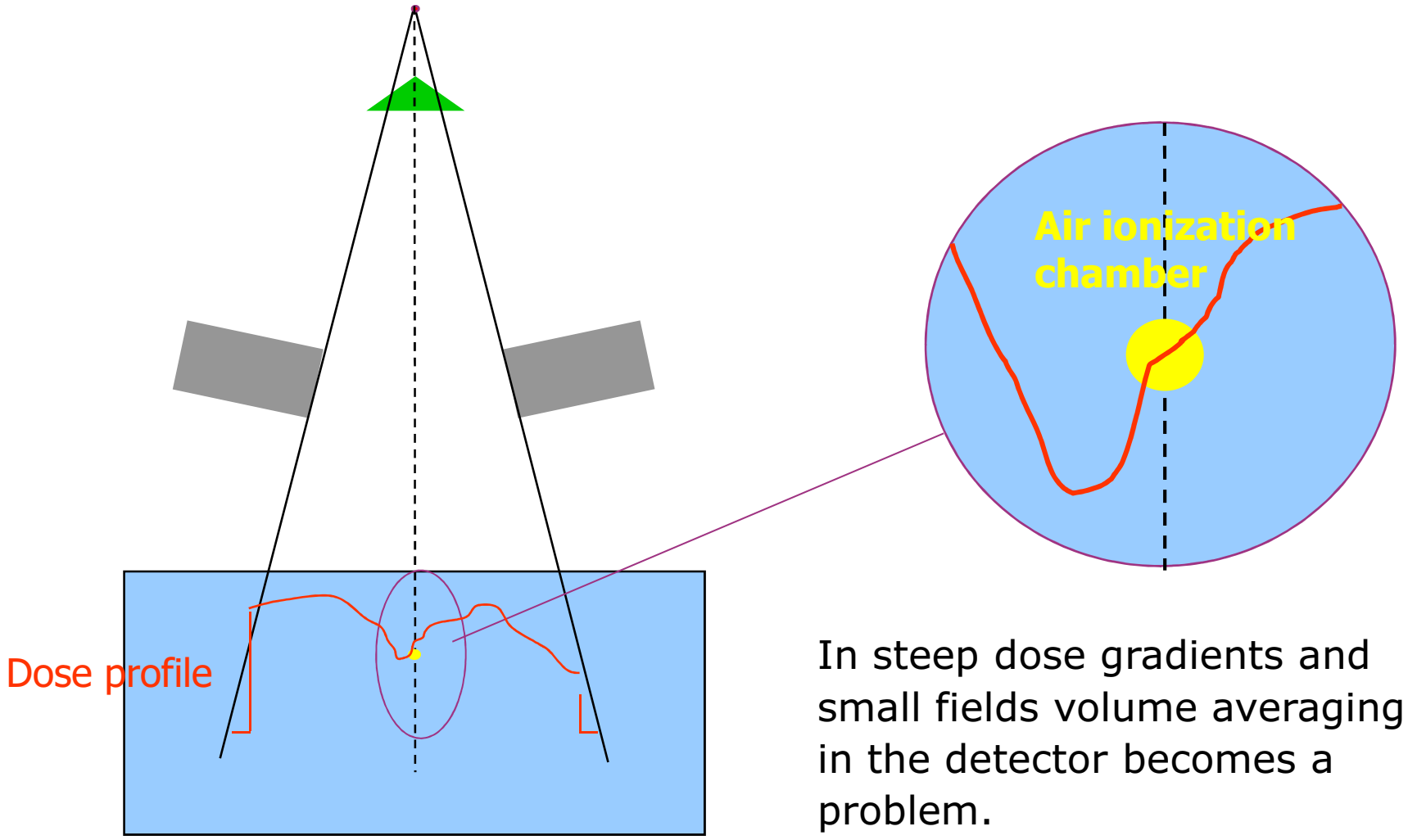

In steep dose gradients and small fields volume averaging in the detector becomes a problem.

ESTRO School

Dose measurements in IMRT photon beams

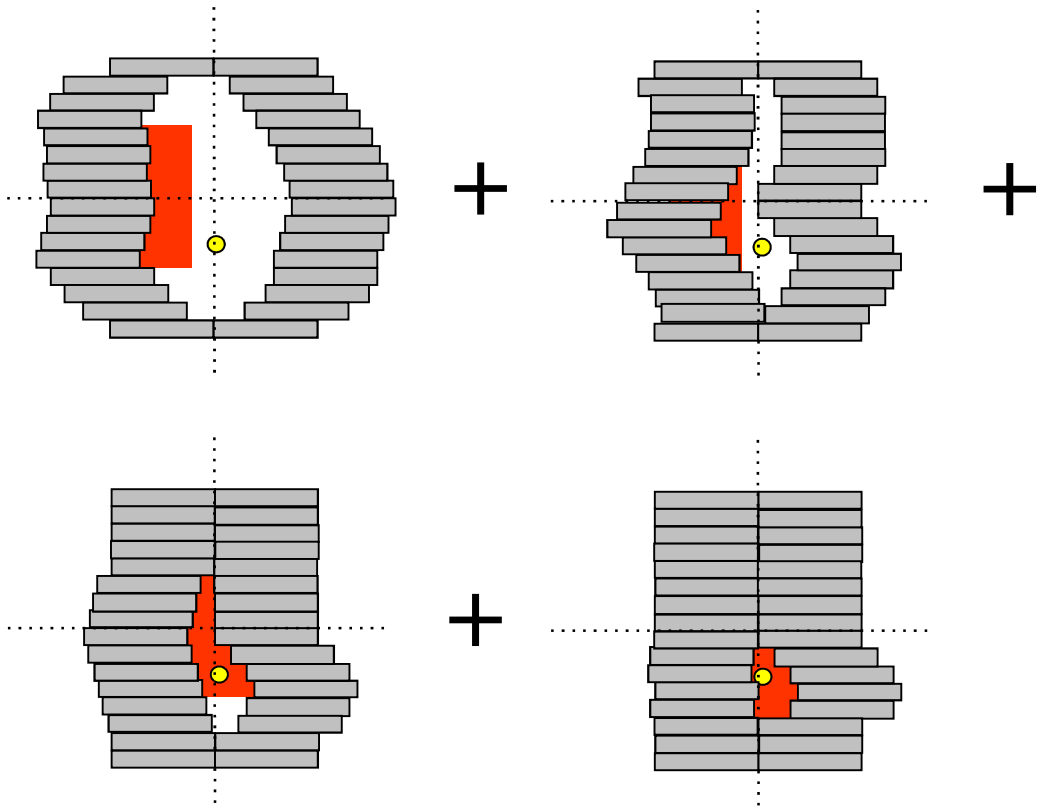

IMRT-fields are often made up by both large and small subfields. Some may be too small to supply lateral electron equilibrium, i.e. similarities to measurements in stereotactic radiosurgery.

Does the dose measured by the detector correspond to the absorbed dose to the depth were the detector center is?

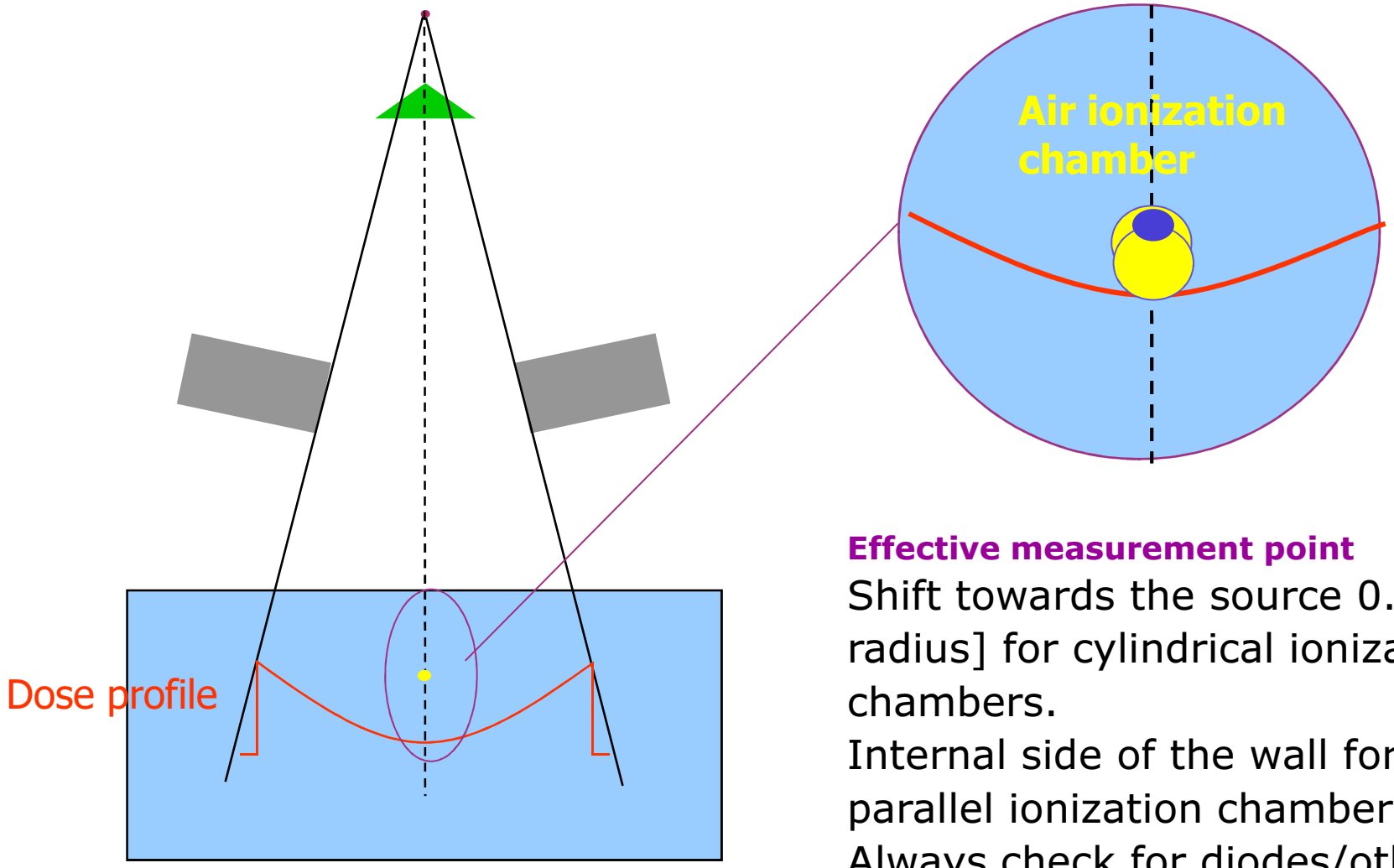

Effective measurement point

Shift towards the source 0.6 r [inner radius] for cylindrical ionization chambers.

Internal side of the wall for plane-parallel ionization chambers

Always check for diodes/other detectors

ESTRO School

How to place the detector in the water tank so that collected data are assigned to the right depth?

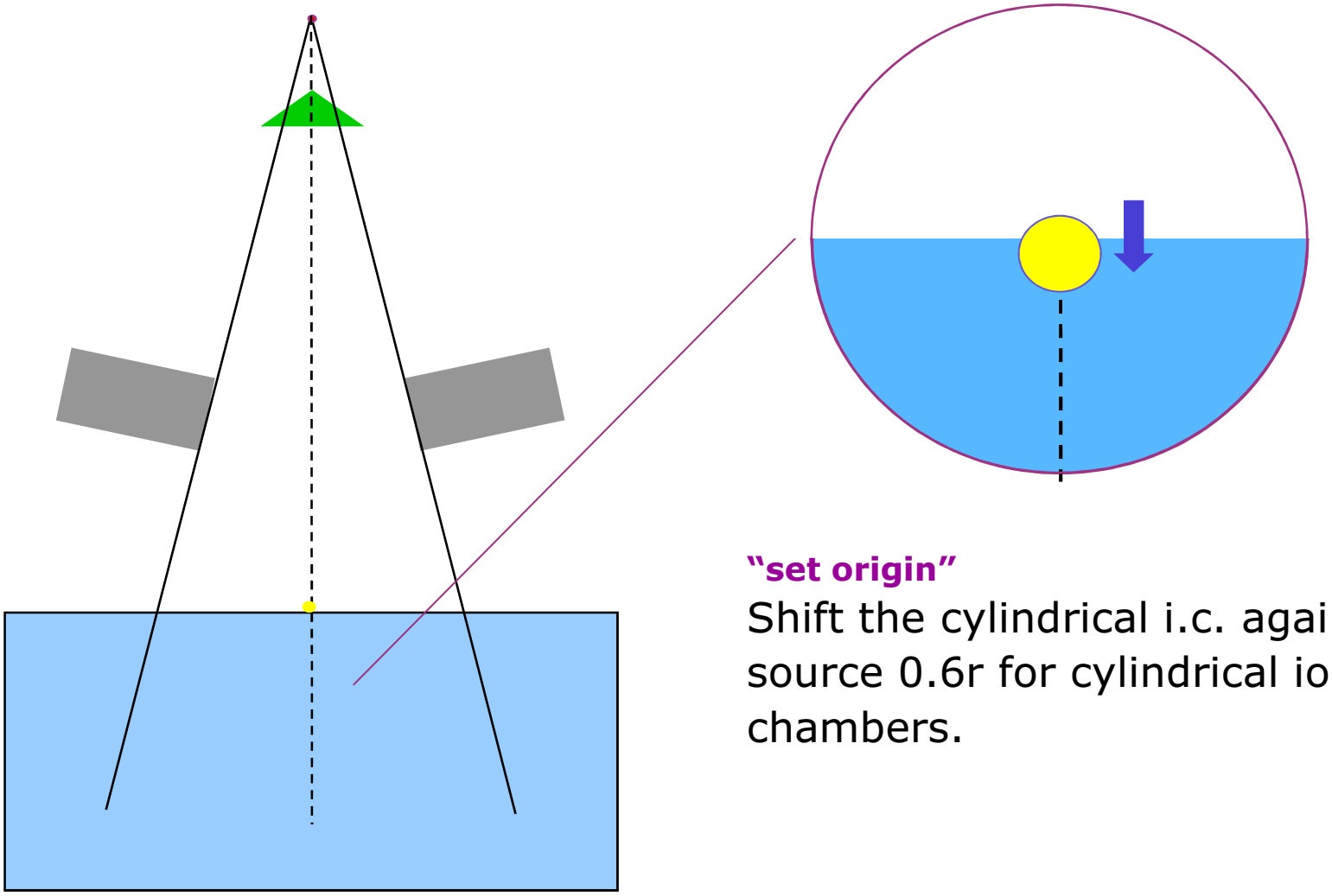

"set origin"

Shift the cylindrical i.c. against the source 0.6r for cylindrical ionization chambers.

How to place the detector in the water tank so that collected data are assigned to the right depth?

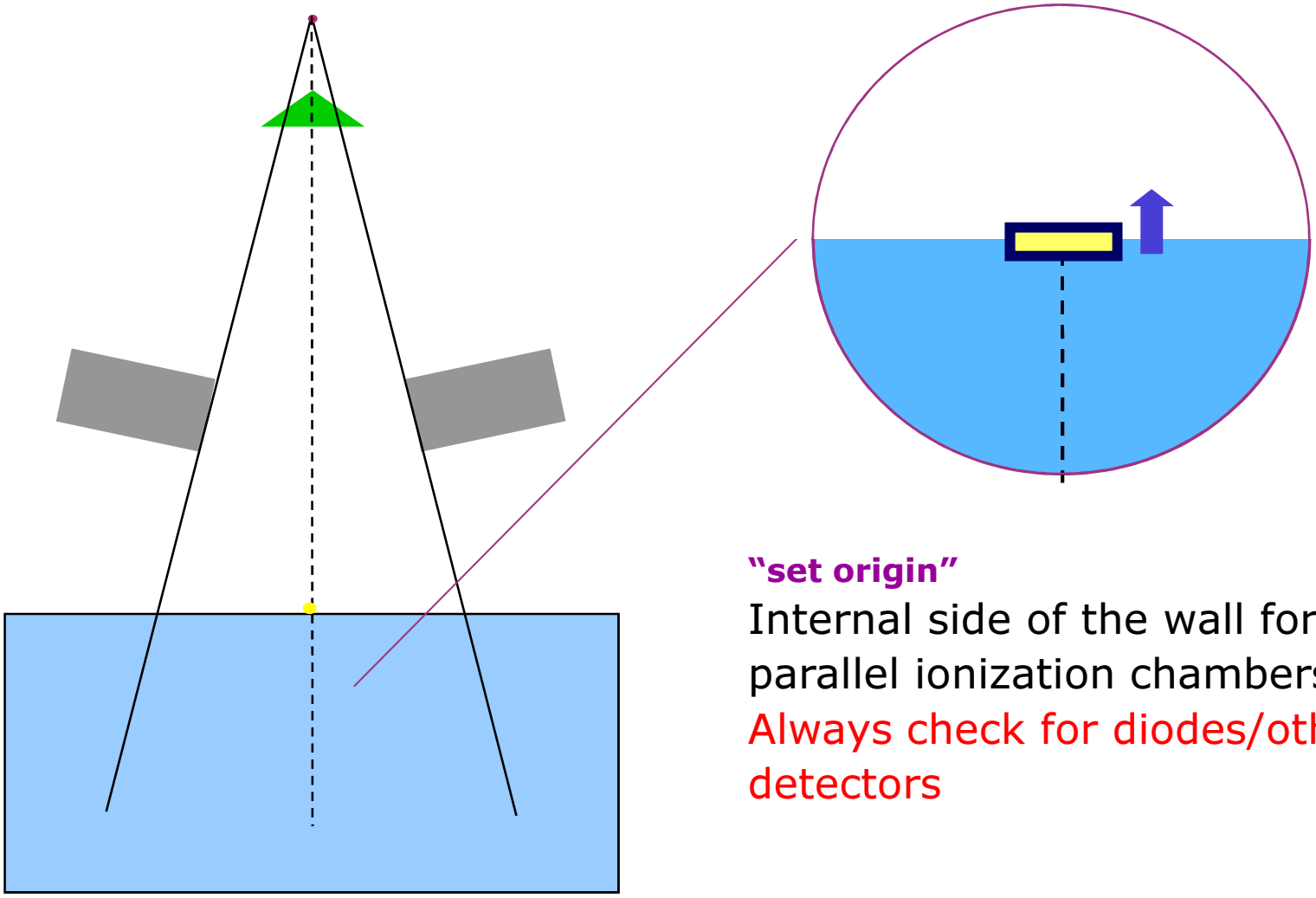

"set origin"

Internal side of the wall for plane-parallel ionization chambers

Always check for diodes/other detectors

ESTRO School

Does size matter?
Profiles

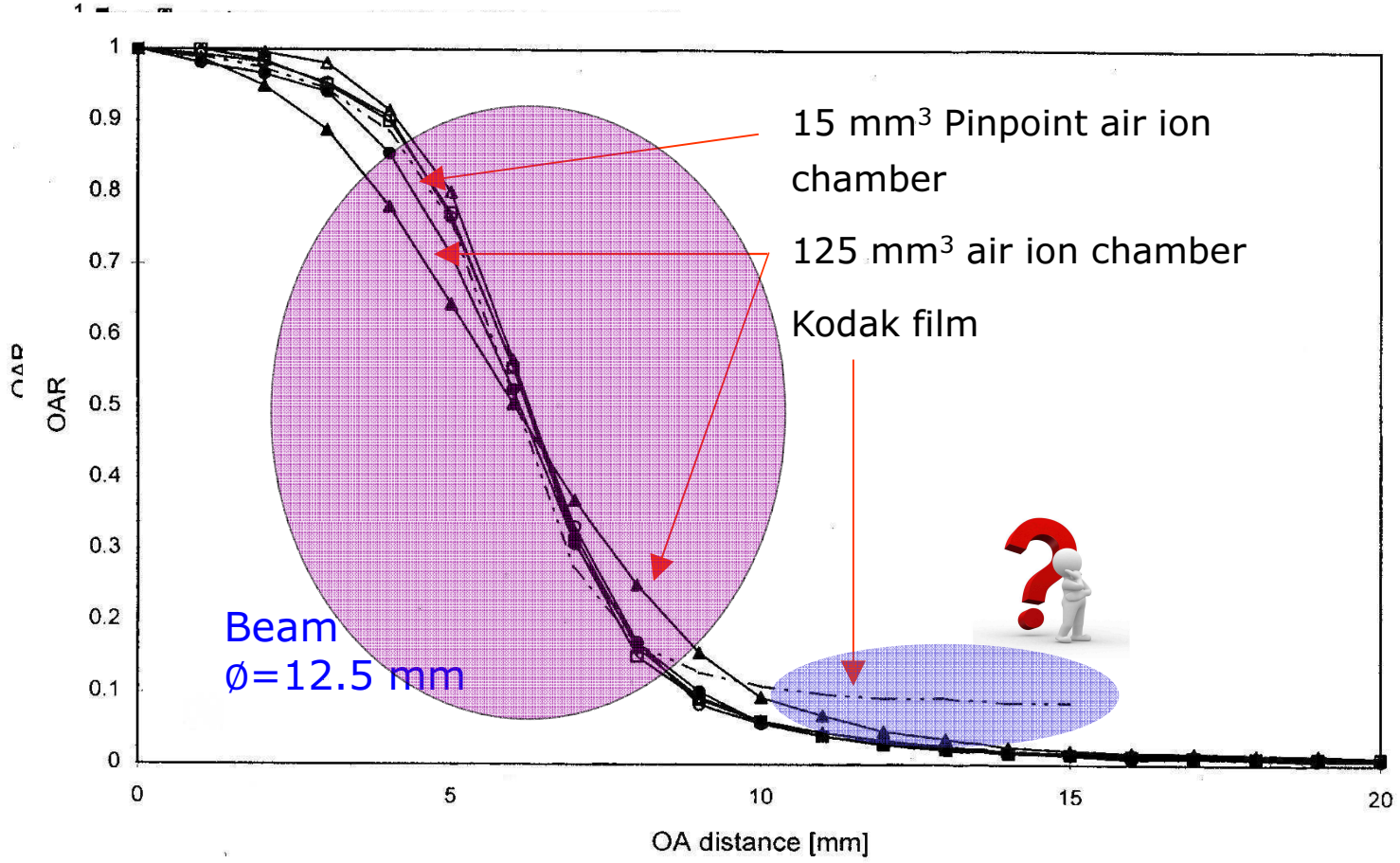

Film gold standard (resolution)
Film gold standard (resolution)

ESTRO School

Measurements under non-reference conditions: Dose profiles

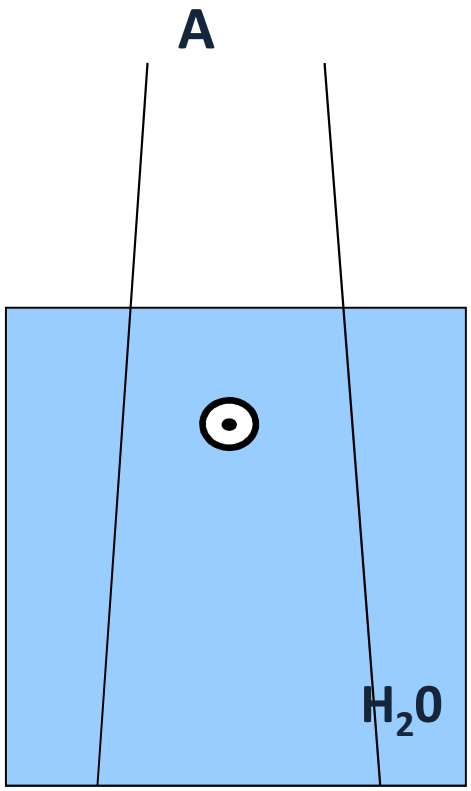

lateral profiles

Volume averaging in the penumbra region

Low energy photon scatter in outside the field edges

Dose measurements in a tissue equivalent phantom

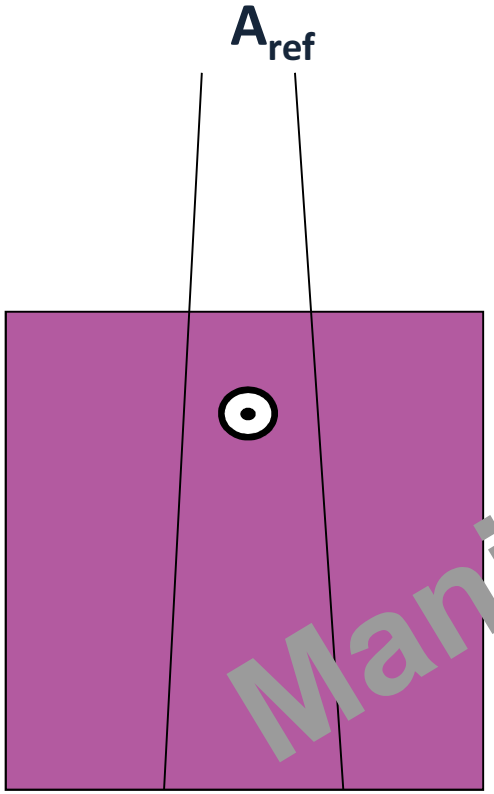

$$D_{med} = M \times ND \times f_{Q,ideal} \times P_Q$$

Measurements under non-reference conditions: Output factors

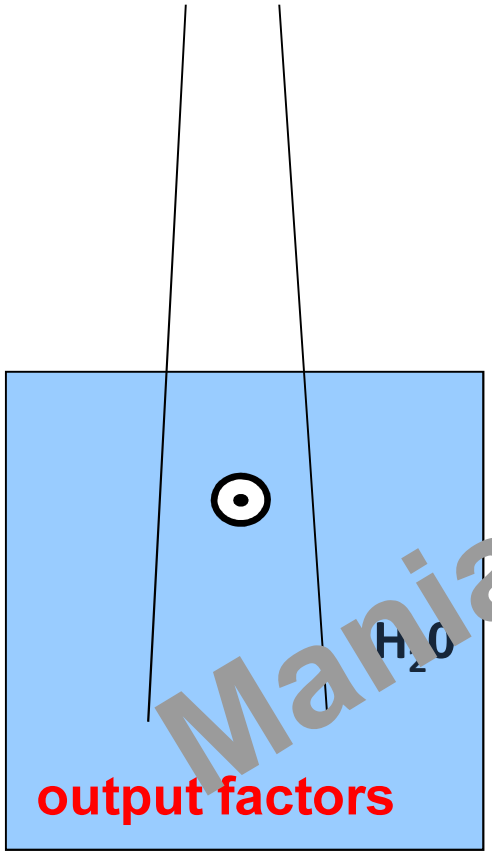

Small fields:

Changes in photon fluence in the beam axis.

Perturbation caused by the detector.

Volume averaging.

Summary

1. We are interested in dose to a point in water
2. We need to know the energy fluency at that point to calculate dose to water to dose to detector.
3. There is no need of CPE or TCPE to estimate dose from detector's readings.
4. When moving from reference conditions in a standard beam to non-reference conditions or/and non standard fields, the dose ratio may not be equal to the detector's reading ratio.

Tissue Characterisation for Radiotherapy

Brendan McClean

Feidhmeannacht na Seirbhíse Sláinte
Health Service Executive

Saint Luke's
Radiation Oncology
Network

Objectives and aims

- To understand how patients are represented in a typical TPS
- To examine the implications of different ways of representation
- To distinguish between dose to water and dose to tissue calculations and the consequences of using either

Outline

- Methods of Calibration of CT images for radiotherapy
- Limitations of CT data
- Dose to water/Dose to tissue
- Dosimetric impact of assumptions for:
  - MV
  - keV
  - Protons
- Developments

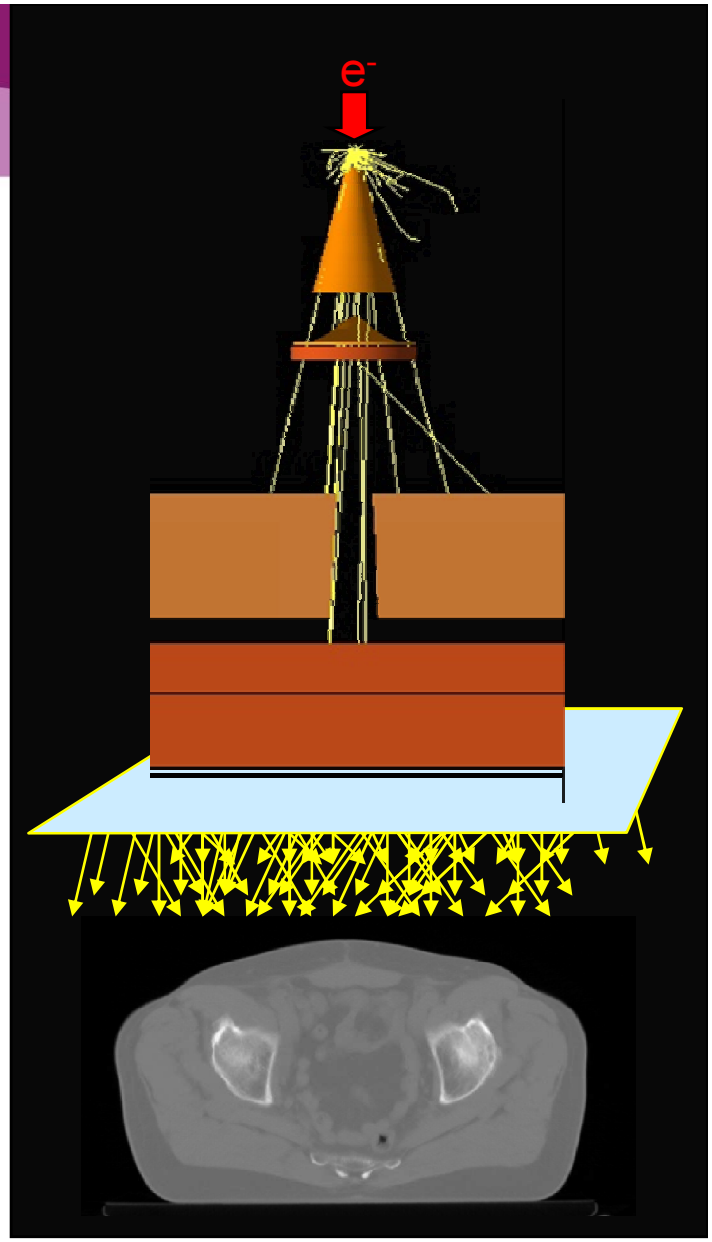

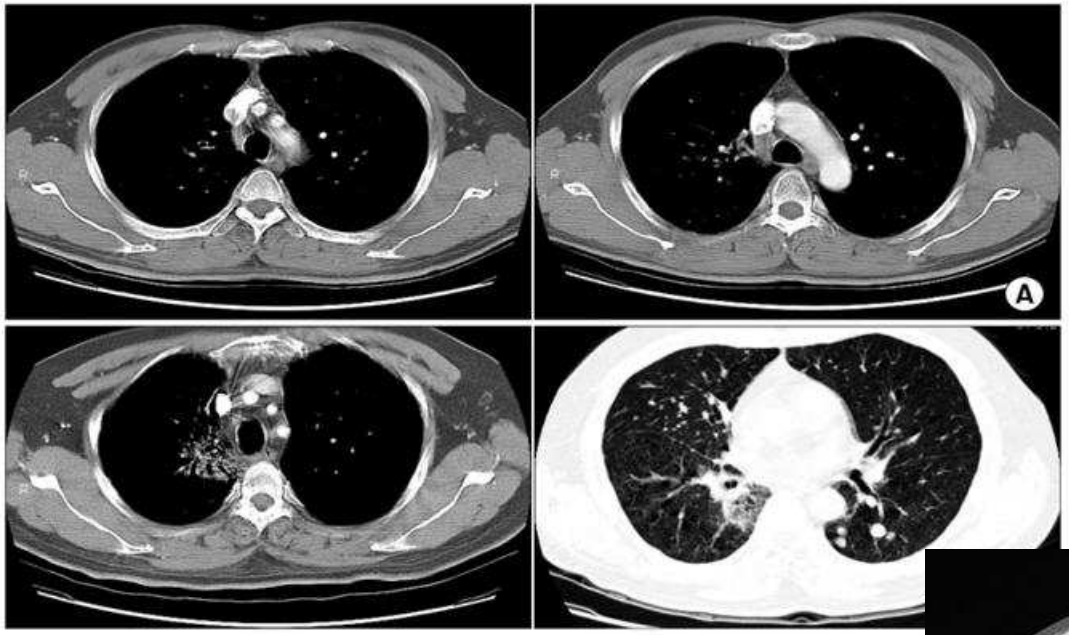

CT

- **Accurate reconstruction of patient's anatomy**
  - **Exact anatomical location of inhomogeneities**
- **CT numbers contain quantitative information on radiological properties of different materials**

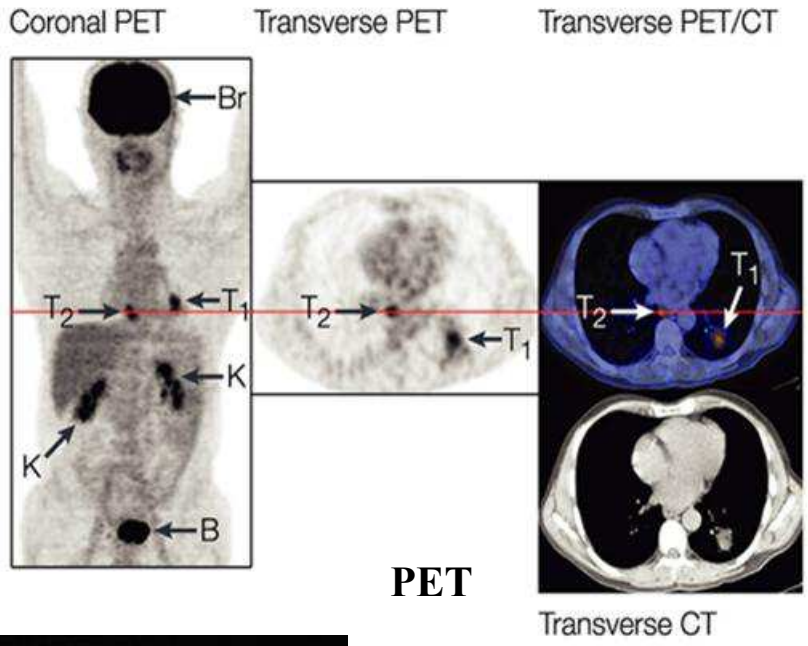

PET

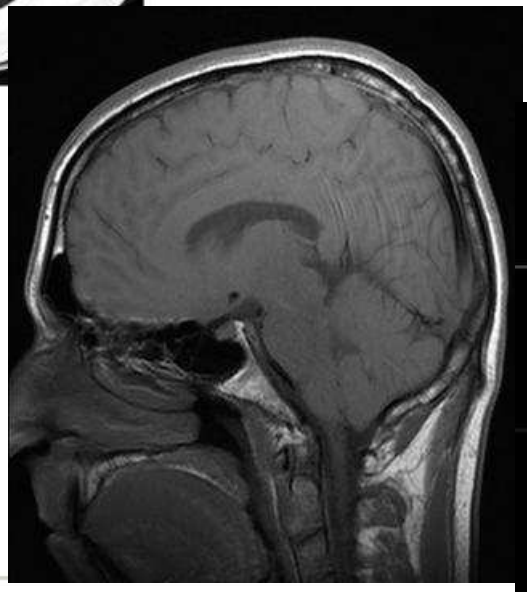

MRI

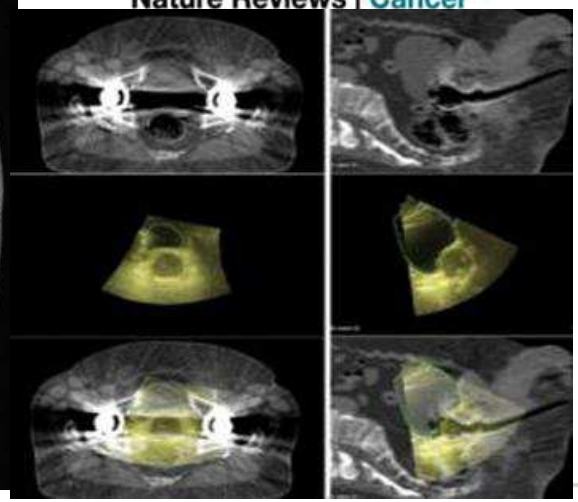

Ultrasound

ESTRO School

What the user sees….

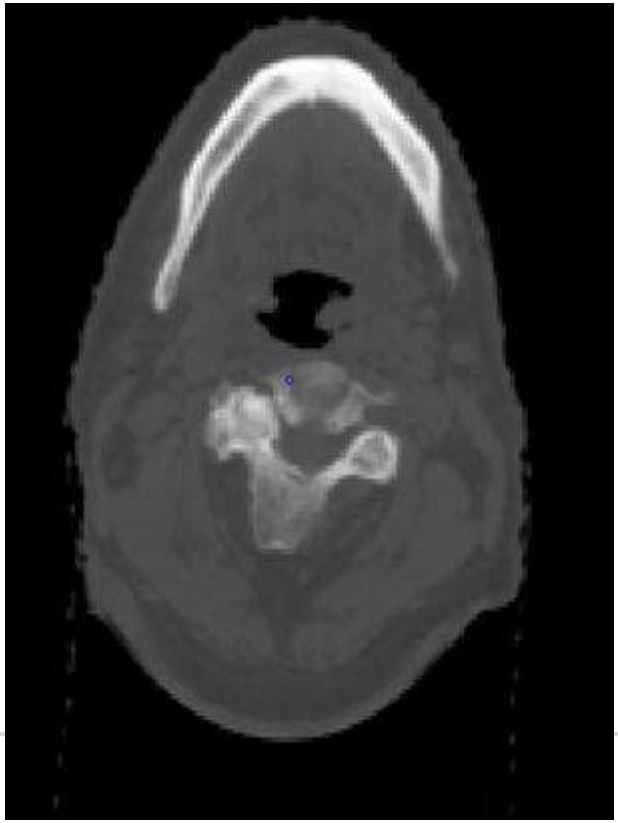

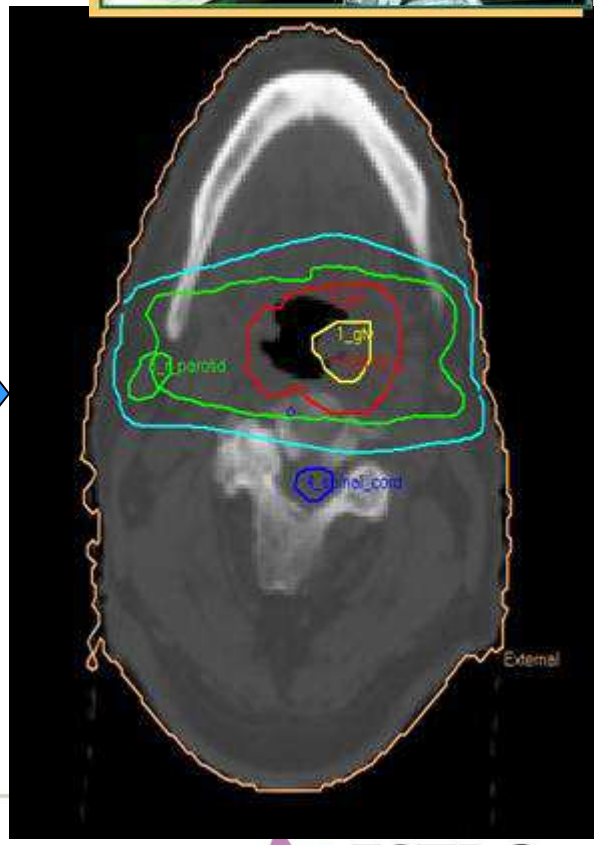

What does the TPS ‘see’? What impact does this have on dose calculation?

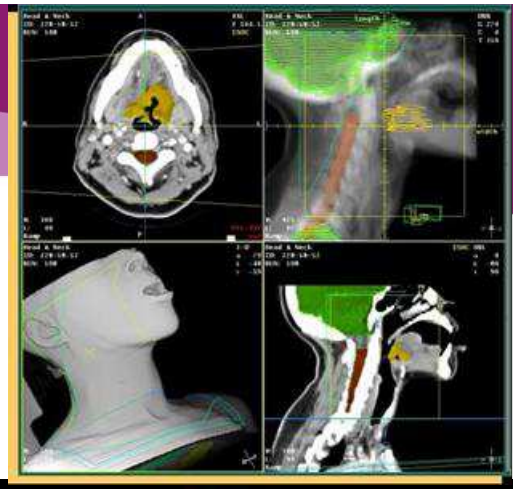

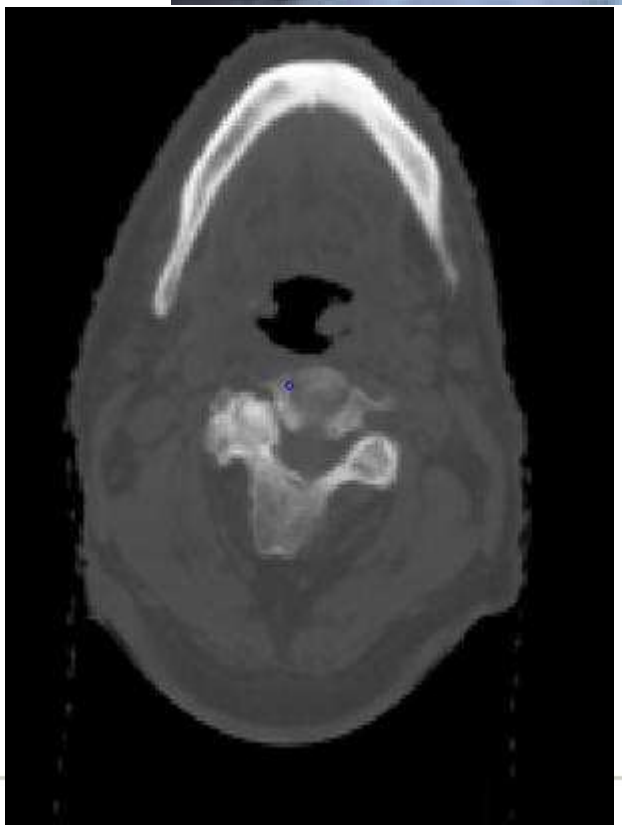

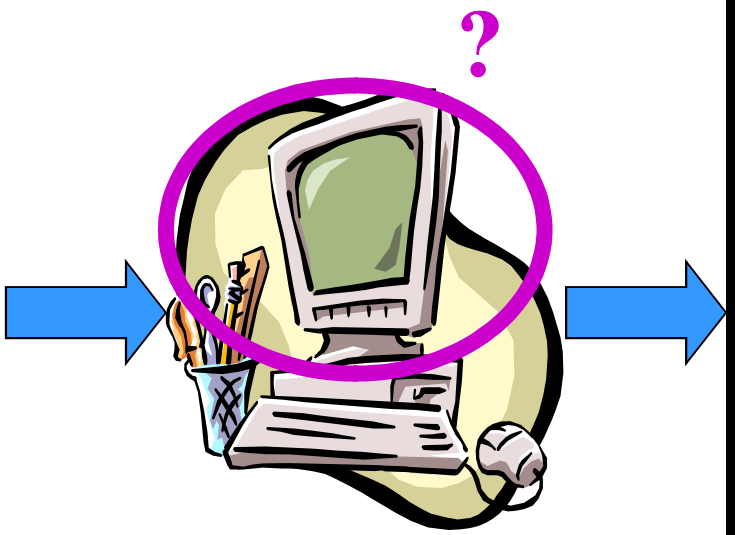

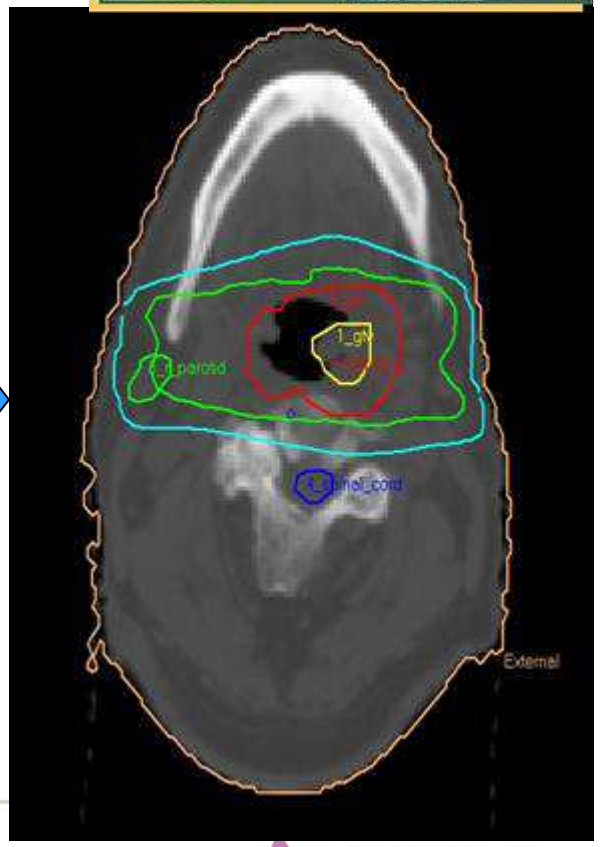

ESTRO School

Principle of CT operation

$$\Phi_{E,0}(E)$$

$$\Phi_E(E) = \Phi_{E,0}(E)\exp\left(-\int_0^s \mu(E,t)dt\right)$$

$$\mu(E) = \rho N_A \sum_i^N \left(\frac{w_i}{A_i}\sigma_i(E)\right)$$

$$\lambda = \ln\left(\frac{\Phi_0}{\Phi}\right) = \int_0^s \mu(E,t)dt$$

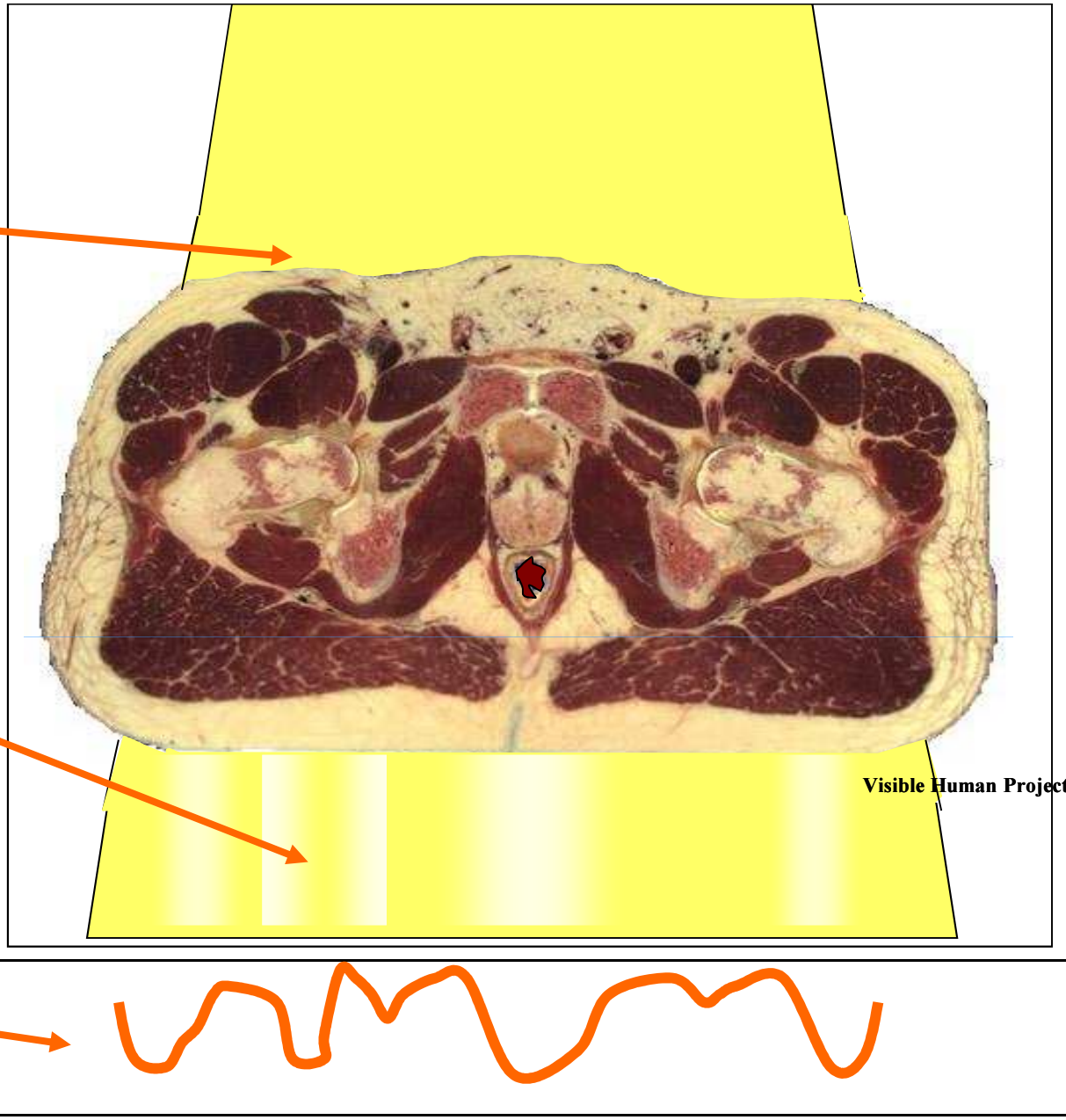

μ(E) depends on ρ_e (linear) and Z_{eff}^{x} (x=3-4)

The End Point…

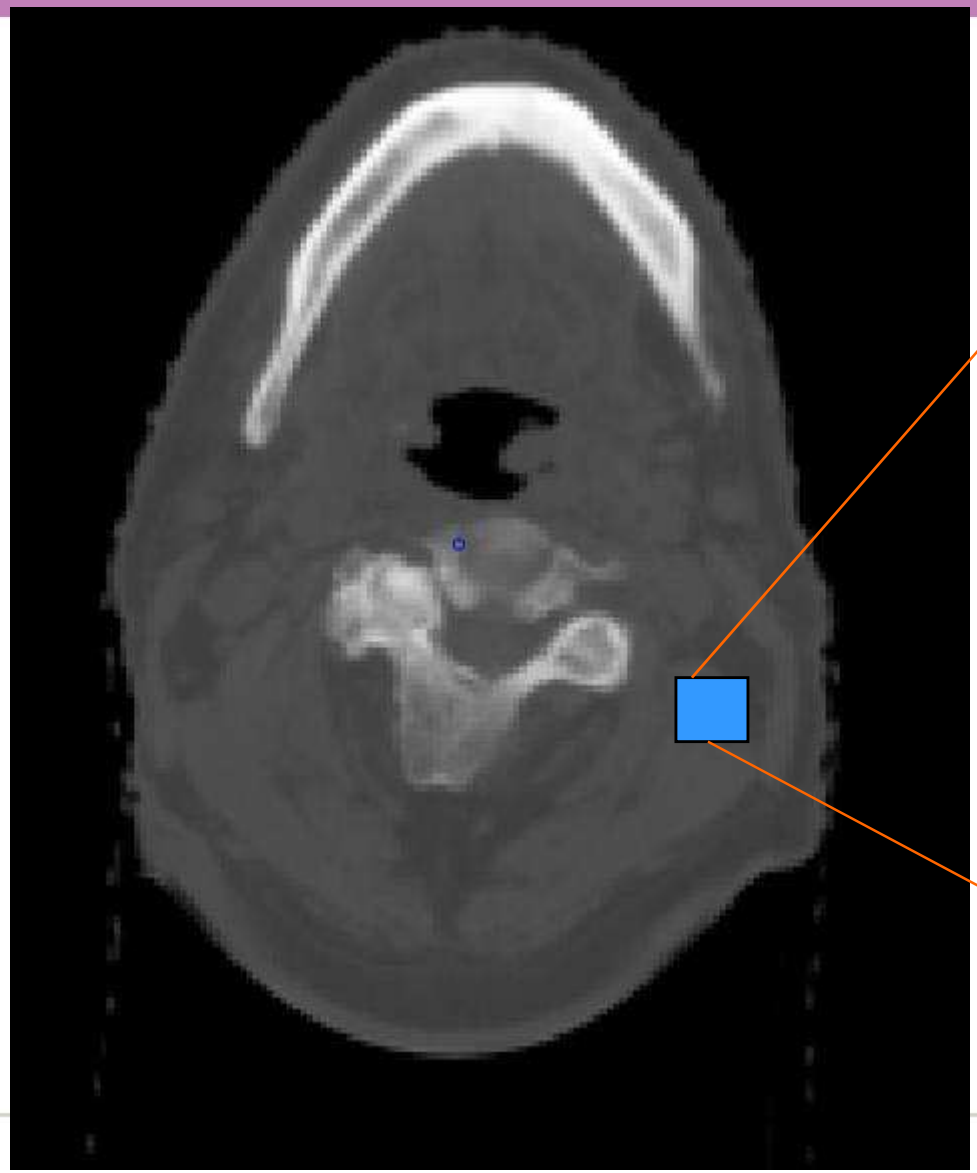

20	40	17	20	37	17	52	31
40	31	40	20	25	17	20	25
17	52	22	37	22	25	37	22
25	20	25	31	25	17	20	17
17	25	40	20	31	40	40	40
37	22	37	17	40	40	22	22
37	22	37	20	31	17	25	22
37	37	17	22	31	31	22	52

$$N_{CT} = \frac{\mu_m - \mu_w}{\mu_w} x\,1000$$

ESTRO School

Now: Patient represented by large number of voxels each with a Hounsfield number

For non-water and direct simulation of radiation transport need:
- Electron Density
- Mass Density
- Chemical composition

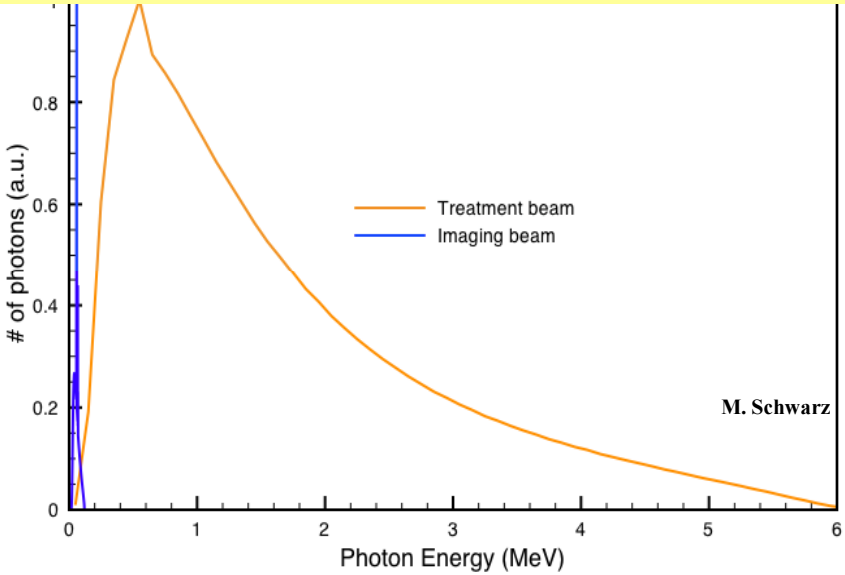

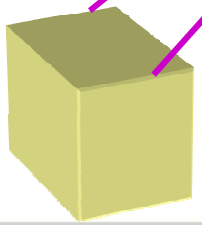

Each voxel assumed to have single atomic composition and density

Assigned by a calibration curve

However CT is at kV energies → Radiological properties relevant to MV are not directly available

ESTRO School

CT Calibration

Electron Density CT Phantom
Gammex 467

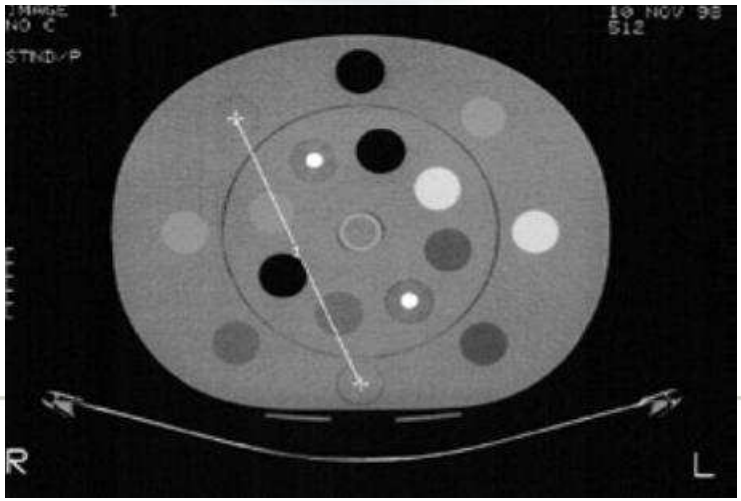

Rod Material	Electron Density Relative to Water	Physical Density g/cm³
Lung (LN-300)	0.28	0.30
Lung (LN-450)	0.40	0.45
Adipose (AP6)	0.90	0.92
Breast	0.96	0.99
CT Solid Water	0.99	1.02
Brain	1.05	1.05
Liver (LV1)	1.07	1.08
Inner Bone	1.09	1.12
Bone (B200)	1.11	1.15
Bone (CB2-30% Mineral)	1.28	1.34
Bone (CB2-50% Mineral)	1.47	1.56
Cortical Bone (SB3)	1.69	1.82
True Water	1.00	1.00

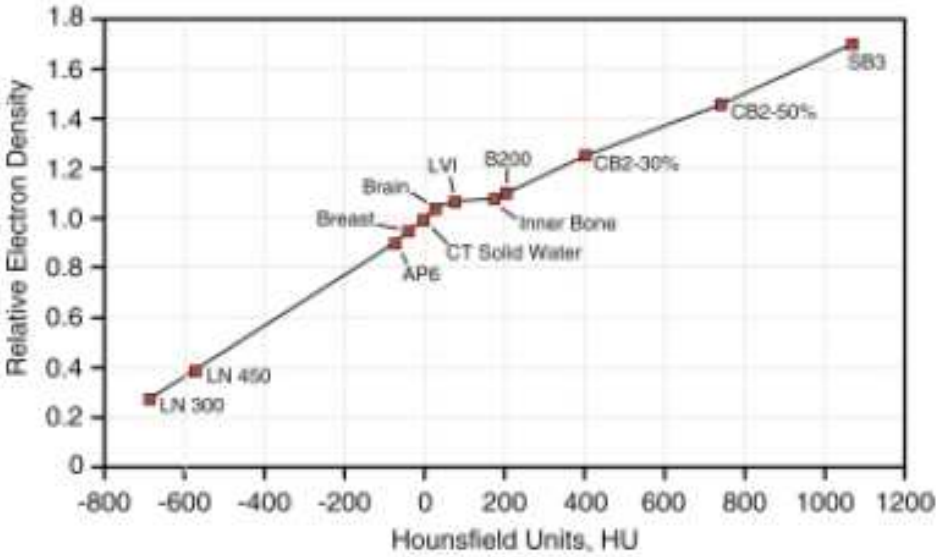

Relationship between the relative electron density and CT number (in Hounsfield Units, HU) of materials in the Electron Density CT Phantom as measured by a GE CT/i scanner.

CONVERTING CT NUMBERS TO DENSITY

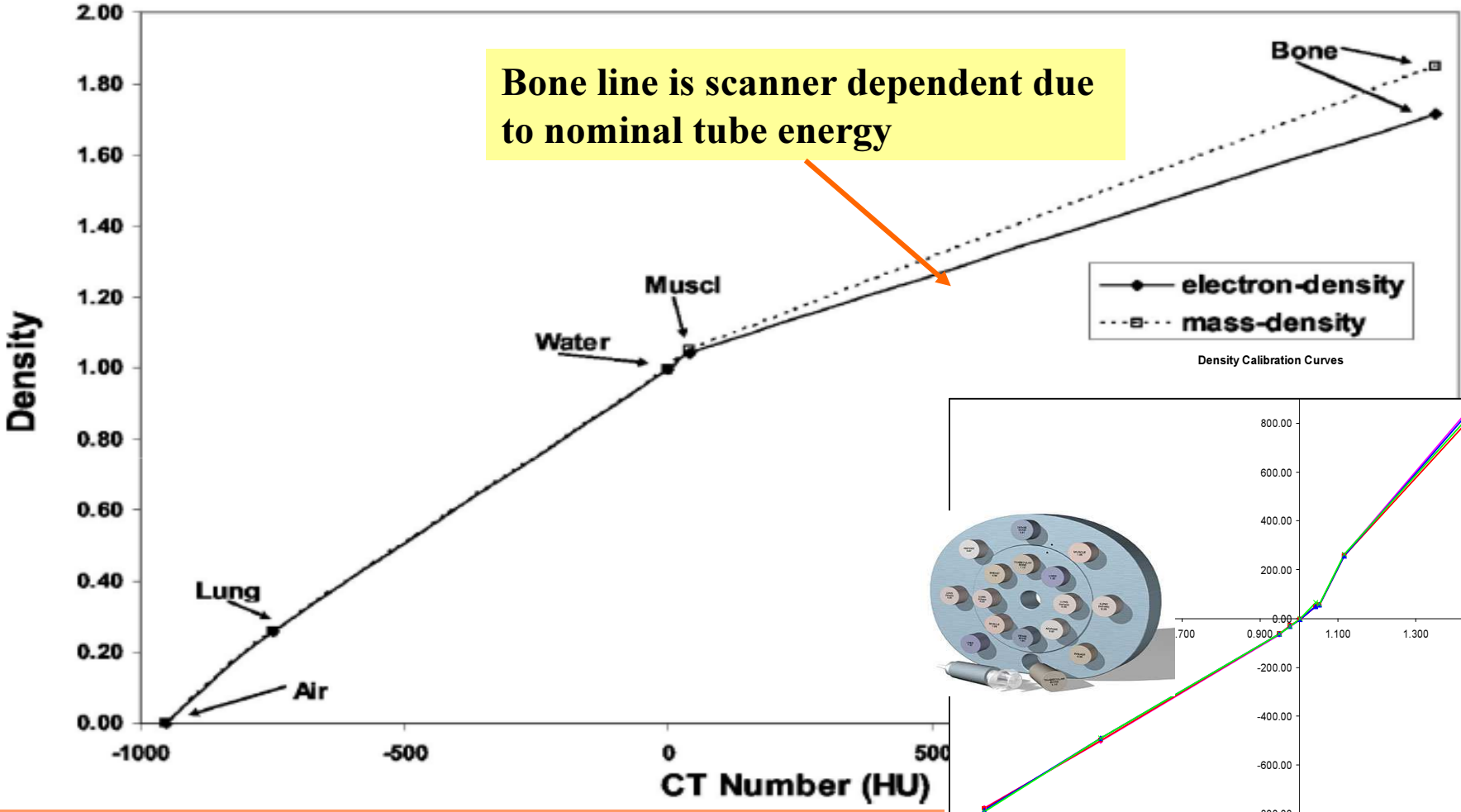

Note only one calibration per CT unit regardless of patient size

N_{CT} α electron density ρ^e_t

$$\rho_t^e = \rho_t N_A \sum_i w_i \frac{Z_i}{A_i}$$

ESTRO School

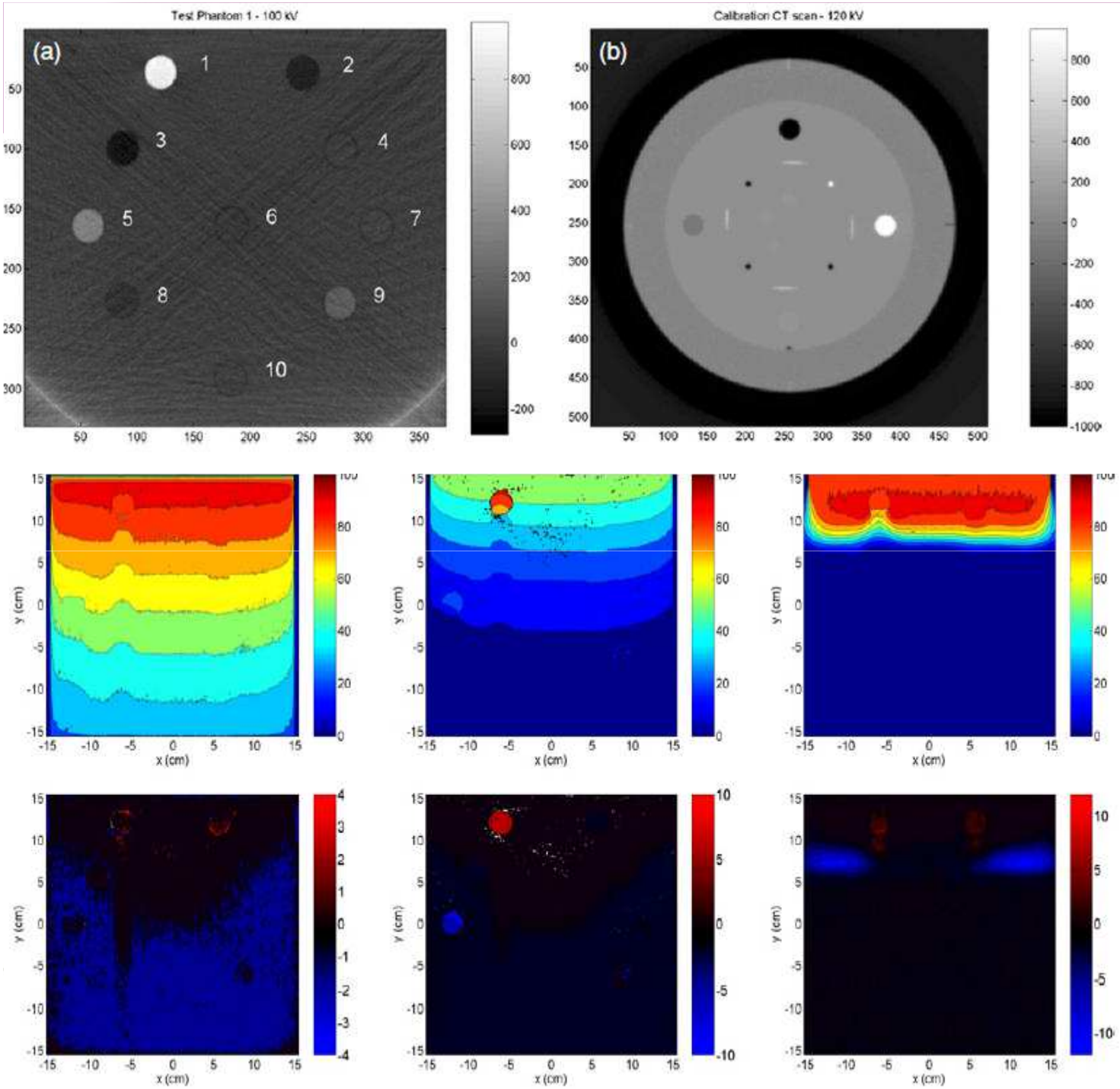

$$\frac{D_{exact} - D_{default}}{D_{default}}$$

10% 6MV and 15MV
30% 18MeV
40% kV

Verhaegen and Devic, PMB 2005

ESTRO School

Common misunderstandings in published literature:

Dose calculation engines on TPS (referred to as 'conventional' excluding Monte Carlo models):

- use CT number calibration tables in terms of relative electron density
- calculate dose to water

Not always the case!

Dose calculation models on TPS differ in implementation

Tissue and Phantom Material Characterization

-as used in Oncentra MP-

Composition	$\frac{\rho_{mass}}{\rho_{mass,H_2O}}$	$\frac{\rho_{elec}}{\rho_{elec,H_2O}}$	H	H_{DCM}
Air (outside patient)	0.00121	0.00109	-992	-128
Air (inside patient)	0.00121	0.00109	-976	-127
Lung (ICRU 44)	0.50	0.50	-480	-96
Adipose (ICRU 44)	0.95	0.95	-96	-72
Muscle (ICRU 44)	1.05	1.04	48	-63
Cartilage (ICRP 23)	1.10	1.08	128	-58
2/3 Cartilage, 1/3 Bone	1.35	1.29	528	-33
1/3 Cartilage, 2/3 Bone	1.60	1.52	976	-5
Bone (ICRP 23)	1.85	1.72	1488	27
Bone (ICRP 23)	2.10	1.95	1824	48
½ Bone, ½ Aluminum	2.40	2.15	2224	73
Aluminum	2.70	2.34	2640	99
Aluminum	2.83	2.46	2832	111
Iron	7.87	6.60	>2832	112
Water	1.00	1.00	-	“127”

Note: Water is not part of an anatomical scale

The scale will interpret a water CT-image as a mixture of adipose and muscle

Plastics are not part of the scale either

ESTRO School

Why do some TPSs require CT calibration tables in terms of relative mass density

e.g. in point kernel dose calculation engines it is TERMA and point kernels that are scaled

$$T(r) \approx \frac{\bar{\mu}}{\rho}(MV, r, medium(r))\ \Psi_o\ e^{-\int_0^r \frac{\bar{\mu}}{\rho}(MV, r', medium(r'))\, r' dr'}$$

Effective (spectrum averaged) mass attenuation coefficient at radiological distance r for the medium with certain density

Primary energy fluence at the surface

- **Mass attenuation coefficients usually pre-stored as weighted averages for an energy spectrum and for media with different composition and mass density**
- **$N_{CT} \Rightarrow$ relative mass density and material composition**
- **$\Rightarrow$ mass attenuation coefficient and linear attenuation coefficient**

e.g. in Pinnacle, TomoTherapy PS

Tissue and Phantom Material Characterization

-as used in Oncentra MP-

Composition	$\frac{\rho_{mass}}{\rho_{mass,H_2O}}$	$\frac{\rho_{elec}}{\rho_{elec,H_2O}}$	H	H_{DCM}
Air				-128
Air				-127
Lun				-96
Adi				-72
Mus				-63
Car				-58
2/3				-33
1/3 Cartilage, 2/3 Bone	1.60	1.52	976	-5
Bone (ICRP 23)	1.85	1.72	1488	27
Bone (ICRP 23)	2.10	1.95	1824	48
½ Bone, ½ Aluminum	2.40	2.15	2224	73
Aluminum	2.70	2.34	2640	99
Aluminum	2.83	2.46	2832	111
Iron	7.87	6.60	>2832	112
Water	1.00	1.00	-	“127”

- how many linear segments should be used?
- which tissue-equivalent materials are suitable for calibration?
- where should the boundaries between tissue types be set?

.....

Quality of conversion affects dose calculation

- one of the weakest links in the calculation chain!

ESTRO School

ICRP PUBLICATION 23: REFERENCE MAN: ANATOMICAL, PHYSIOLOGICAL AND METABOLIC CHARACTERISTICS, 23

International Commission on Radiation Units & Measurements

Tissue Substitutes in Radiation Dosimetry and Measurement (Report 44)

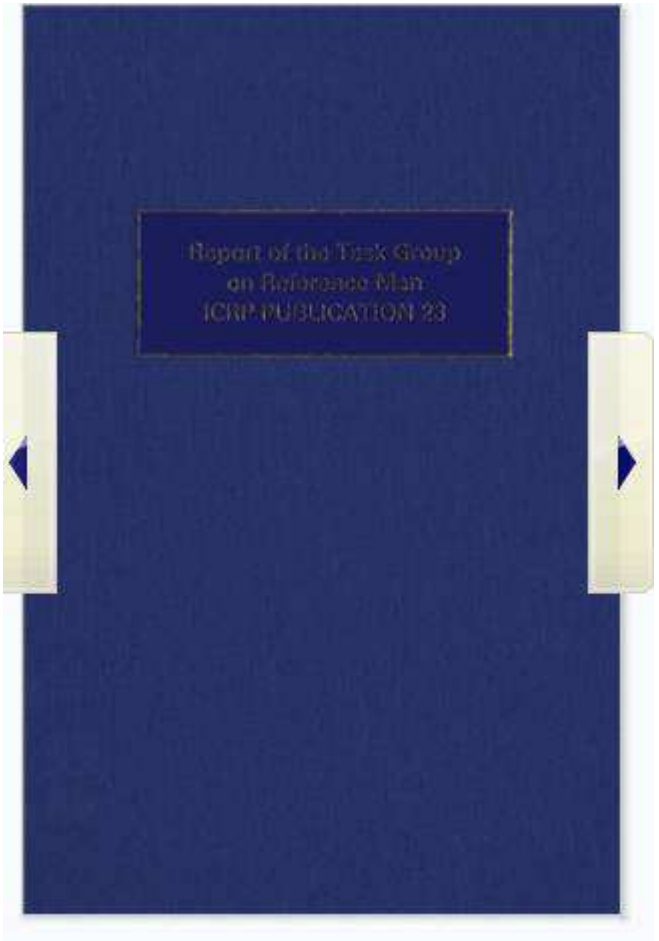

Note: implicit assumption that elemental composition, weights and density values correspond to 'standard' compositions as in ICRU 44 and ICRP23

This ignores patient to patient variation (~15%)

' body tissue compositions should not be given the standing of physical constants'

Gender? Ethnicity? Number of samples?

ESTRO School

Tissue composition

- How accurate are published 'reference' tissues?
- Variability over population?
- Variability with age (breast)
- The myth of the 50-50 breast (Yaffe et at MP 2009)

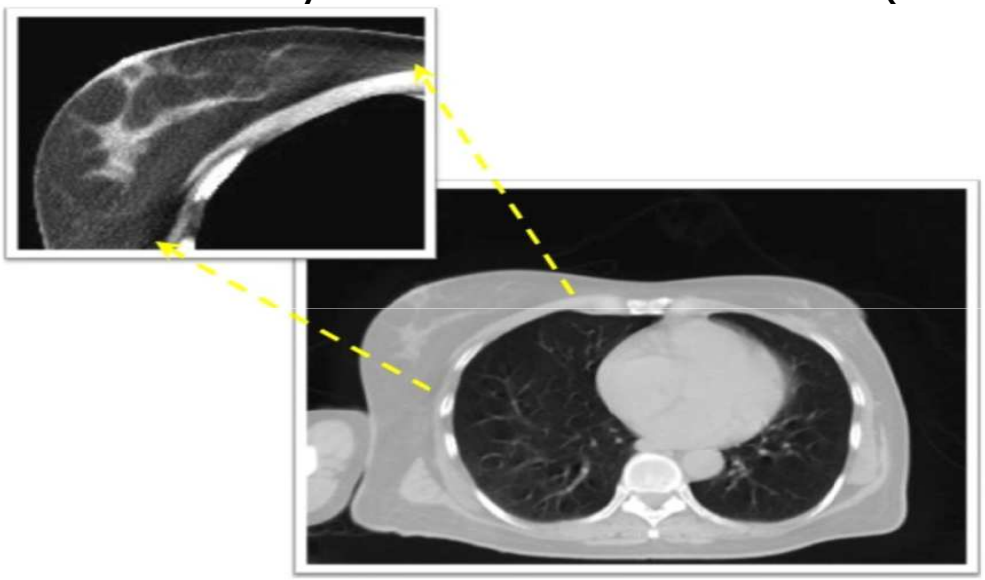

Afsharpour et al PMB 2011

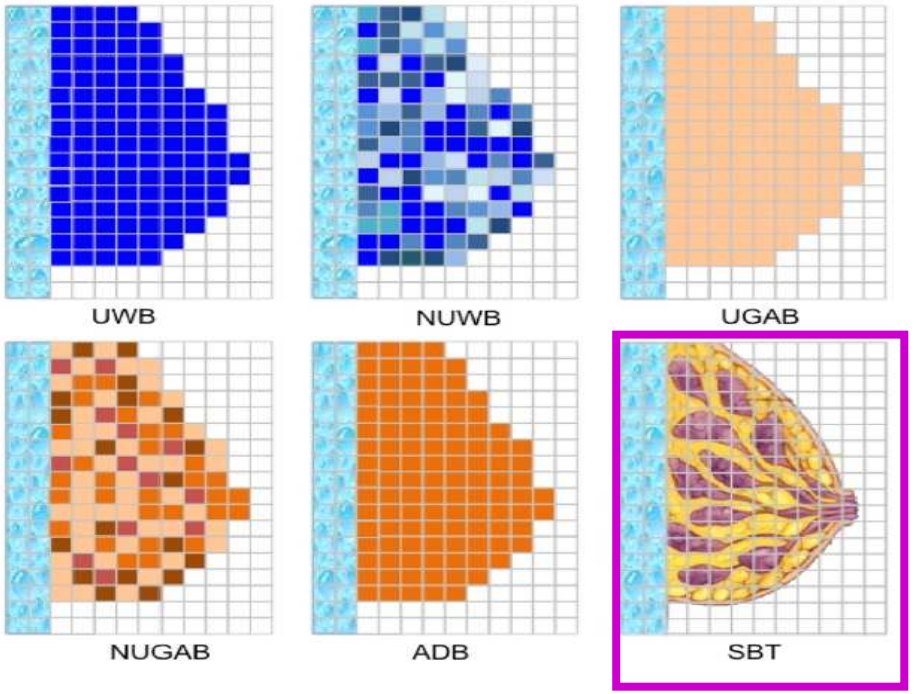

Breast was long assumed: 50% adipose, 50% gland (brighter above)

Reality: mean composition is much closer to 80% A / 20% G

ESTRO School

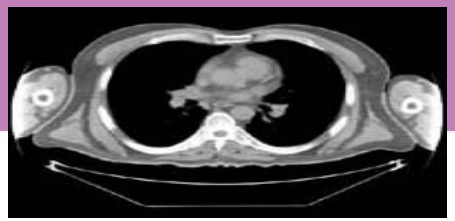

Voxelization based on dose grid resolution

Adapted from van Dyk

CTCREATE process

Read CT Data

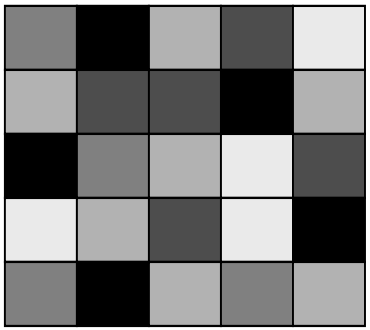

Apply Transport grid

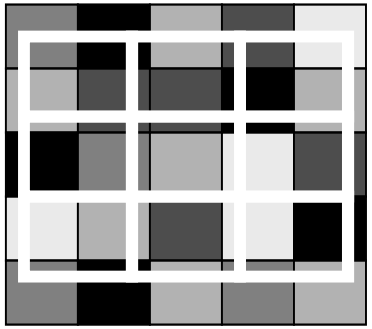

Resample CT

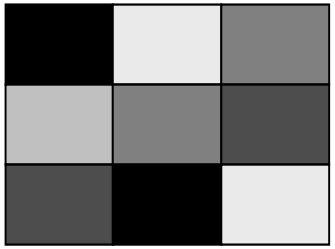

Convert to Densities

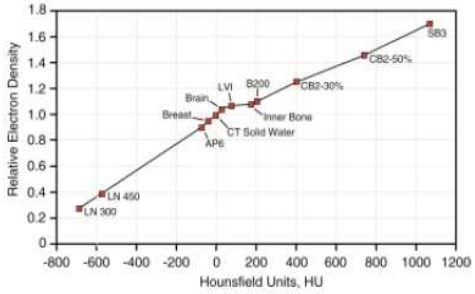

Relationship between the relative electron density and CT number (in Hounsfield Units, HU) of materials in the Electron Density CT Phantom as measured by a GE CT/i scanner.

Convert to materials

Rod Material	Electron Density Relative to Water	Physical Density g/cm³
Lung (LN-300)	0.28	0.30
Lung (LN-450)	0.40	0.45
Adipose (AP6)	0.90	0.92
Breast	0.96	0.99
CT Solid Water	0.99	1.02
Brain	1.05	1.05
Liver (LV1)	1.07	1.08
Inner Bone	1.09	1.12
Bone (B200)	1.11	1.15
Bone (CB2-30% Mineral)	1.28	1.34
Bone (CB2-50% Mineral)	1.47	1.56
Cortical Bone (SB3)	1.69	1.82
True Water	1.00	1.00

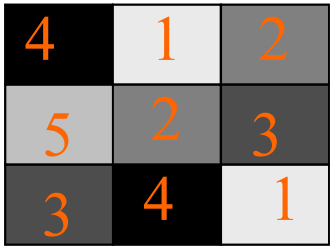

How accurate are CT numbers…?

- HU of homogeneous material can vary by 1-2%
- Depends on location (beam hardening) – up to 3%
- Variation across scanners for high density (>5% in cases)
- Electron Density of Tissue Substitutes
- Tissue substitutes=tissues?

- Tissue Assignment (ICRU and ICRP)?

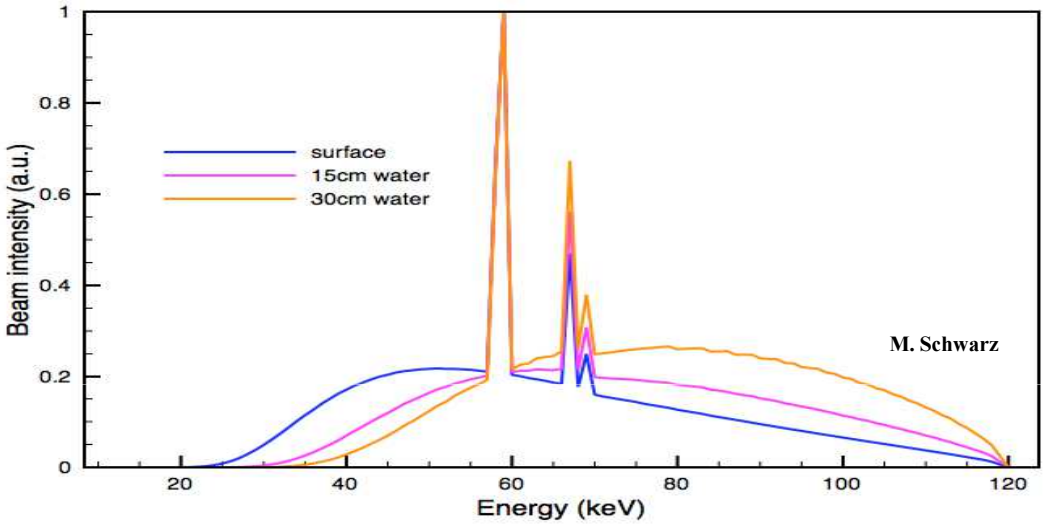

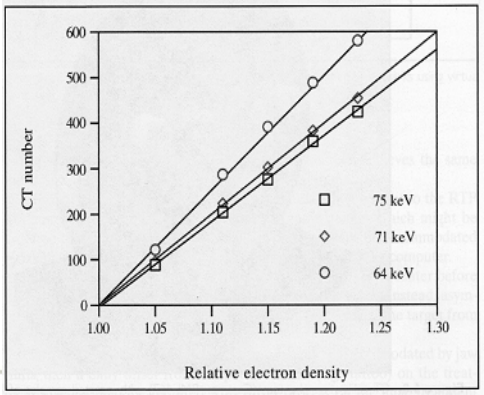

ESTRO School

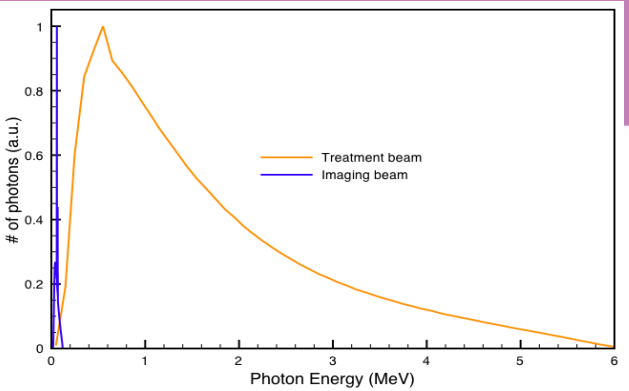

CT number is determined not only by electron density.

→ two media of identical ρ_e but different Z_{eff} will have different HU

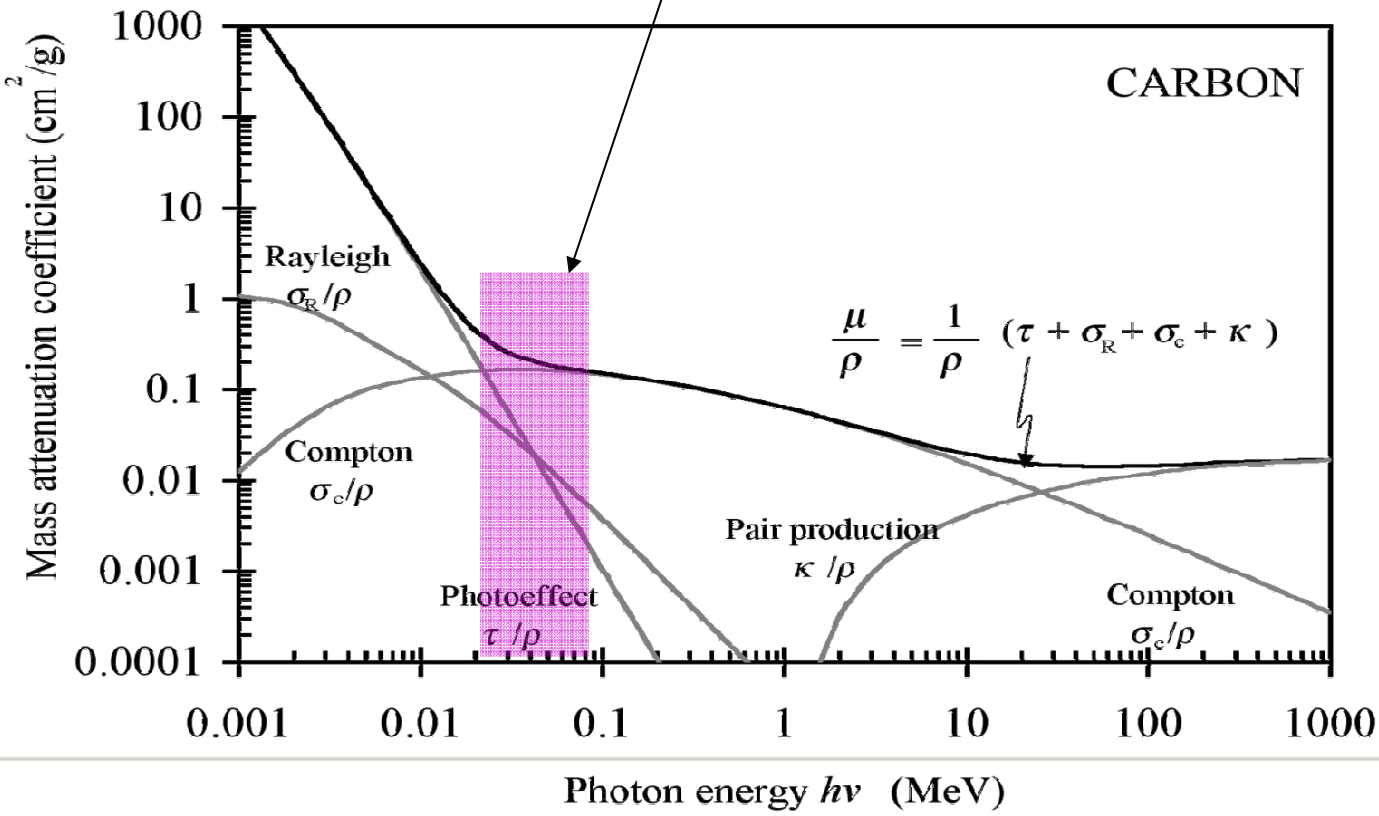

Adapted from Schwarz

Tissues with different Mass density and elemental weights can have same HN

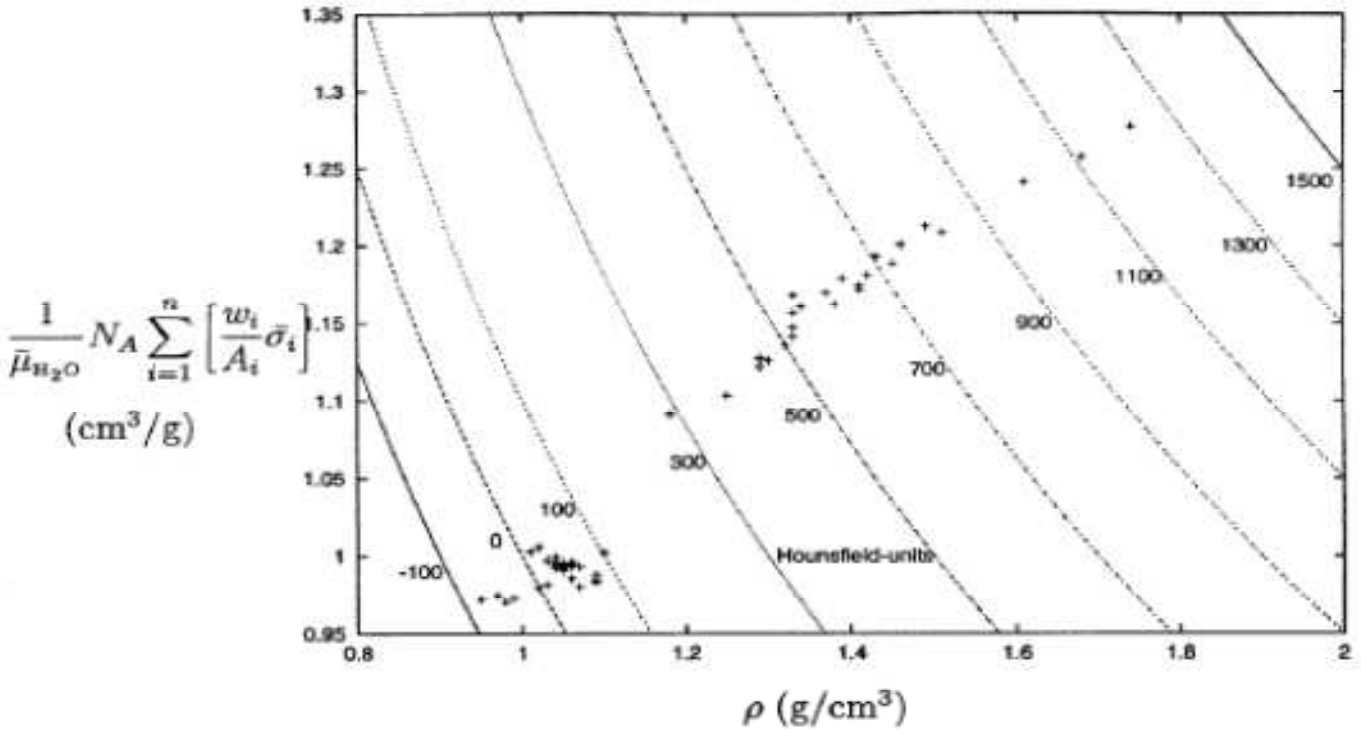

Figure 3. Projection of the space of tissue parameters (ρ, w_i). The data points are corresponding to the 71 human tissues. Along the hyperbolas, the CT number is constant.

W. Schneider et al PMB 45 2000

Tissues with different Mass density and elemental weights can have same HN

Where do we define boundaries between ρe of media?
How many media?

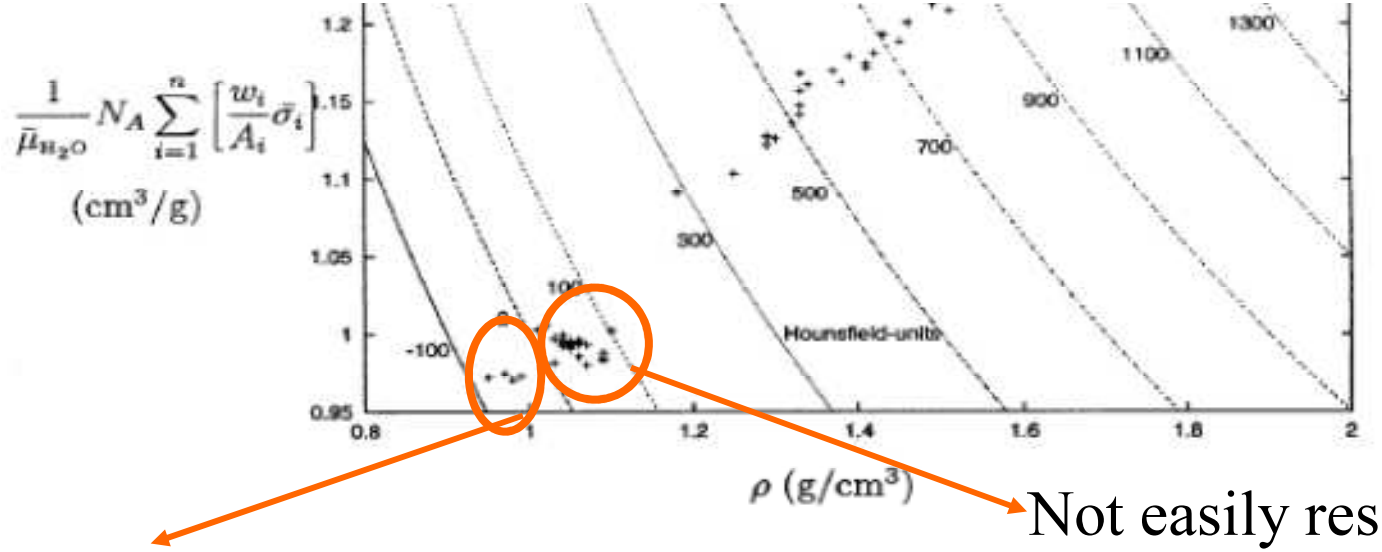

Resolved

Not easily resolved!

Figure 3. Projection of the space of tissue parameters (ρ, w_i). The data points are corresponding to the 71 human tissues. Along the hyperbolas, the CT number is constant.

W. Schneider et al PMB 45 2000

Uncertainties on CT calibration

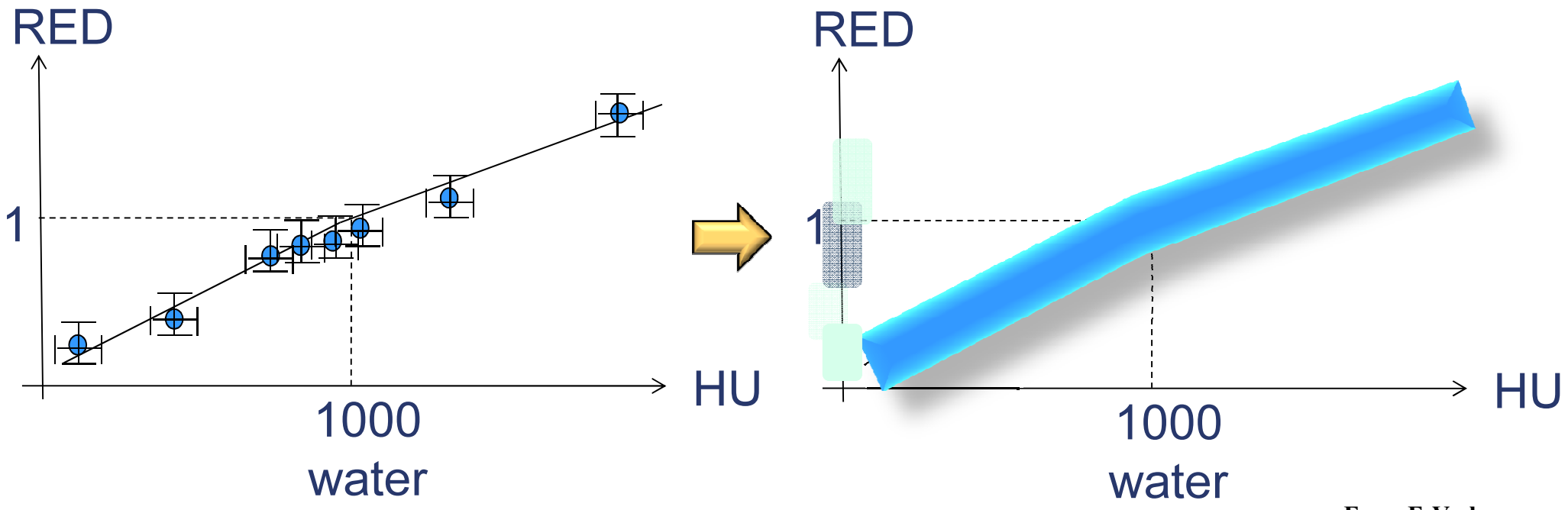

From F. Verhaegen

-uncertainty on (e-) density

-uncertainty on material assignment

ESTRO School

Stoichiometric calibration: An improved approach

U. Schneider et al PMB 1996

Calculate Relative Electron Density:

$$\rho_e = \frac{\rho N_g}{\rho^{water} N_g^{water}}$$

Using chemical composition:

$$N_g = \sum N_g^i = N_A \sum \frac{w_i Z_i}{A_i}$$

$$H = 1000 \frac{\mu}{\mu_w}$$

Relative proton stopping power

$$\rho_s = \rho_e \frac{\log\left[2m_e c^2 \beta^2 / I_m \left(1-\beta^2\right)\right] - \beta^2}{\log\left[2m_e c^2 \beta^2 / I_w \left(1-\beta^2\right)\right] - \beta^2} = \rho_e K$$

Rutherford et al 1976

$$\mu = \rho N_g(Z,A)\left\{K^{ph}\tilde{Z}^{3.62} + K^{coh}\hat{Z}^{1.86} + K^{KN}\right\}$$

By making measurements of H for different tissue substitutes of known composition one can get a fit of data to derive values for $K^{ph/coh/KN}$ which characterize the CT scanner

From this can plot a curve to predict H for range of tissues substitutes and real tissue

ESTRO School

Stoichiometric calibration: An improved approach

U. Schneider et al PMB 1996

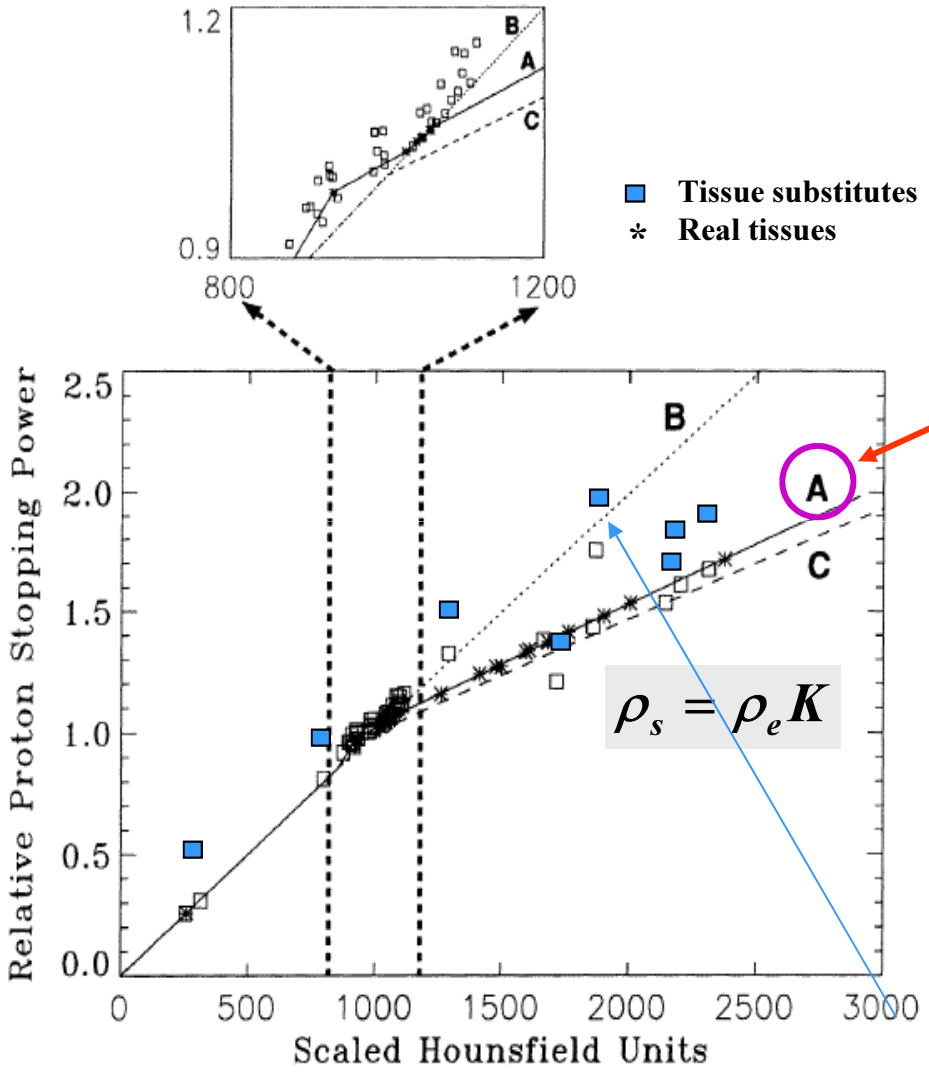

Verified for proton stopping power by measurements in a sheep head

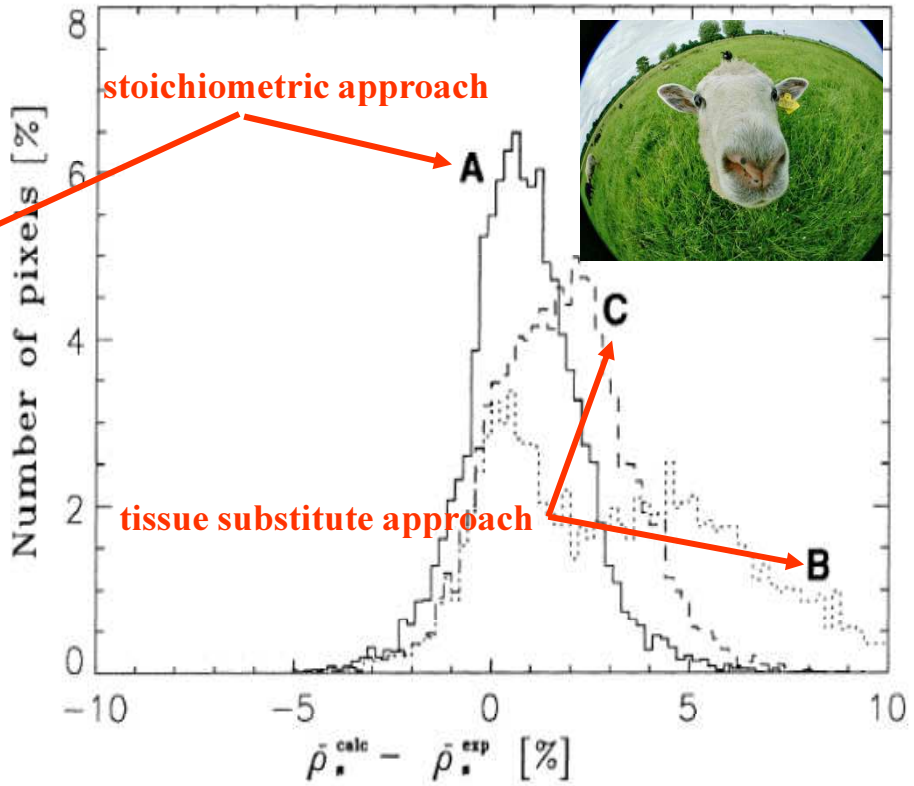

Calibration based on tissue substitutes only is very sensitive to material chosen. Different substitutes give different calibration curves

ESTRO School

How many materials are needed?

- Du Plessis et al (MP 25(7) 1998)
  - Combined 16 human tissues into 7 dosimetrically equivalent subsets with constant elemental composition to give dose accuracy of <1%.
  - Needed further subdivision in bone and lung (57) by varying density only
- W.Schneider (stoichiometric) calibrating H with mass density and elemental weights
  - Extended to 71 tissues
  - Grouped into 24 bins
  - Simplified using interpolation functions for 4 sections of calibration curve+
- 'Ctcreate' from BEAMnrc
  - 4 major tissue types (air, lung, soft tissue, bone)
  - ICRU tissue composition used and mass density from linear interpolation

D_w or D_m?

Now we have the patient tissue represented (in some way), do we report *Dose to Water* or *Dose to Tissue*?

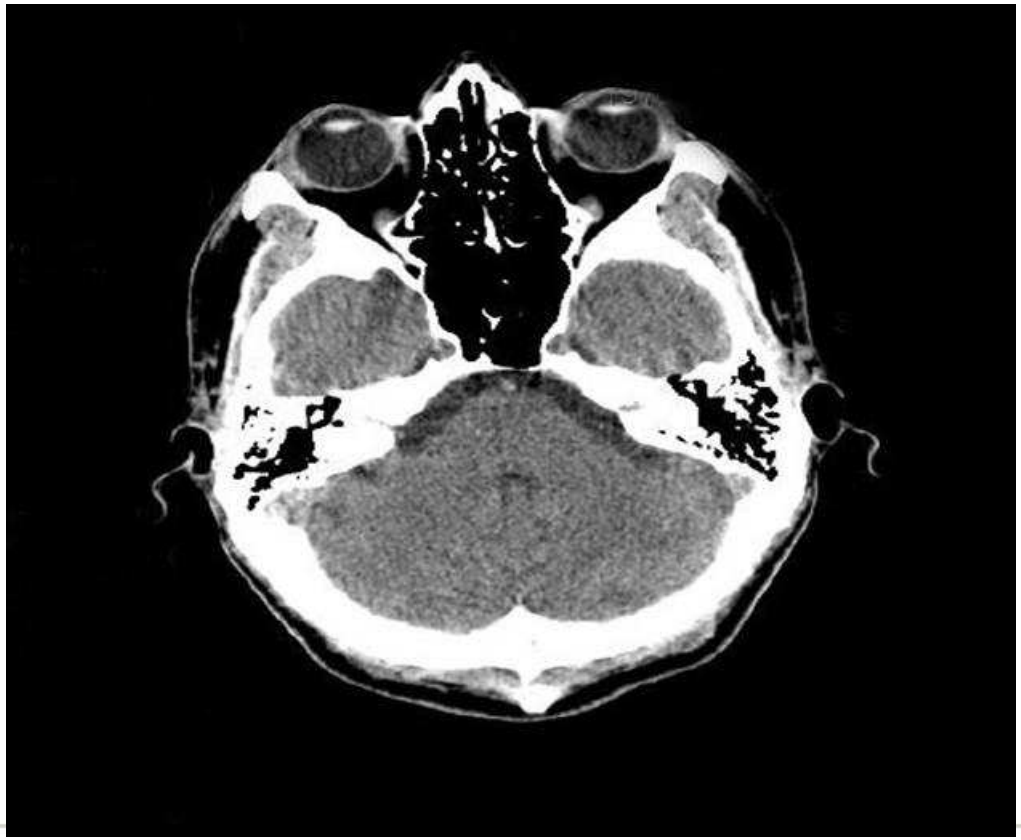

Dose to Water or Dose to Tissue?

- $D_{w,W} \cong \frac{\mu_{en,w}}{\rho} \Psi_o e^{-\mu_w z}$

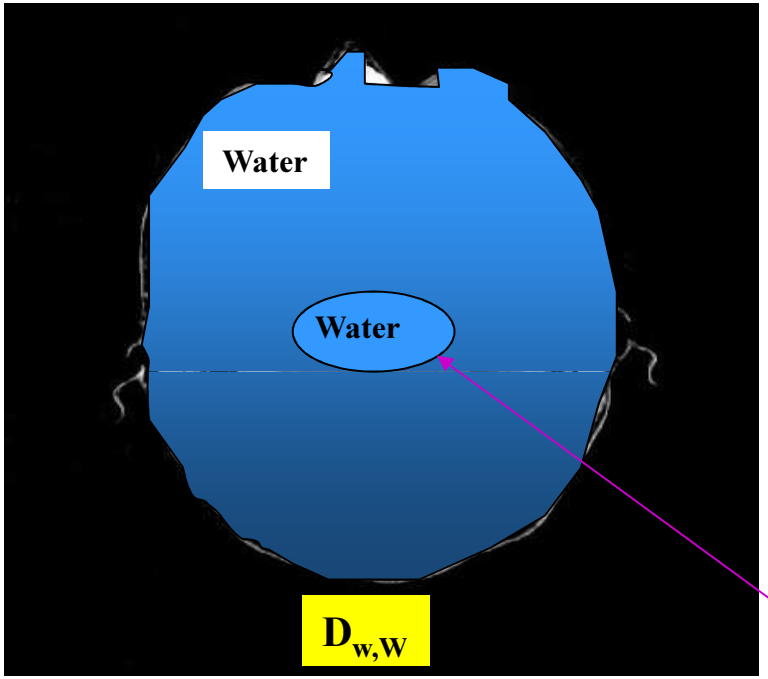

Scoring Volume

from Anders Ahnesjö

ESTRO School

Dose to Water or Dose to Tissue?

$$D_{w,W} \cong \frac{\mu_{en,w}}{\rho} \Psi_o e^{-\mu_w z}$$

$$D_{w,M} \cong \frac{\mu_{en,m}}{\rho} \Psi_o e^{-\mu_m z} \left(\frac{\bar{S}}{\rho} \right)_m^w$$

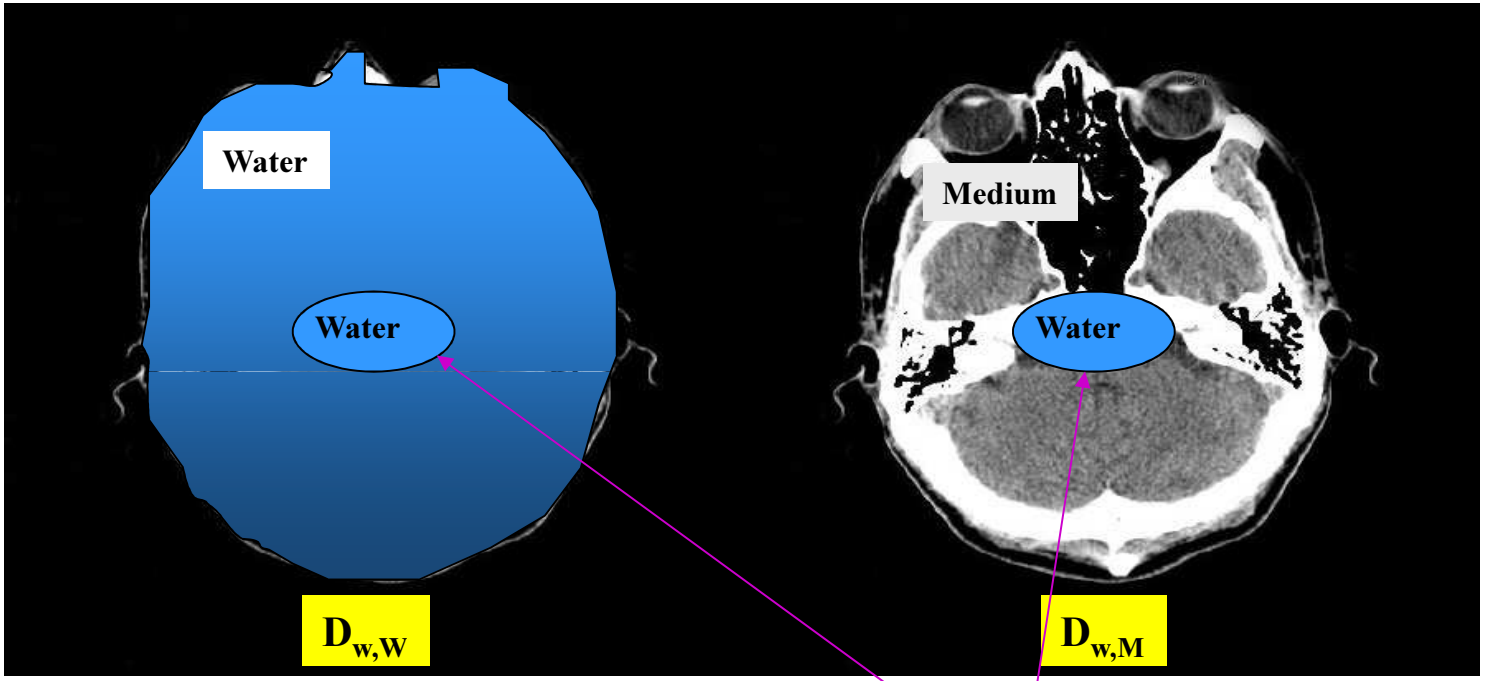

Scoring Volume

from Anders Ahnesjö

ESTRO School

Dose to Water or Dose to Tissue?

○ $D_{w,W} \cong \frac{\mu_{en,w}}{\rho} \Psi_o e^{-\mu_w z}$ ● $D_{w,M} \cong \frac{\mu_{en,m}}{\rho} \Psi_o e^{-\mu_m z} \left(\frac{\bar{S}}{\rho}\right)_m^w$ ○ $D_{m,M} \cong \frac{\mu_{en,m}}{\rho} \Psi_o e^{-\mu_m z}$

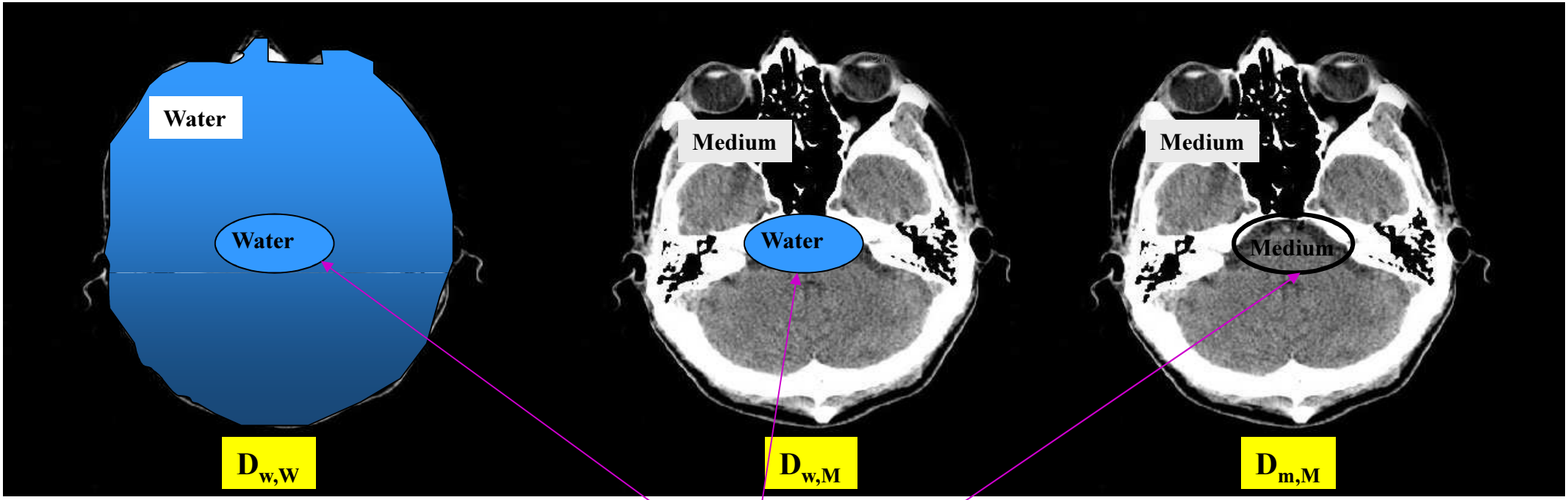

Scoring Volume

$\Rightarrow$ conversion of dose to medium to dose to water $D_{w,M} = D_{m,M} \left(\frac{\bar{S}}{\rho}\right)_m^w$

from Anders Ahnesjö

ESTRO School

Stopping power ratios

$$D_{w,M} = D_{m,M}\left(\frac{\bar{S}}{\rho}\right)^{w}_{m}$$

TABLE I. Water-to-material mass-stopping-power ratios along the central axis and off-axis in 6 MV and 18 MV photon beams with a 10×10 cm^2 open field.

Beam energy	Material	SPR at CAX			SPR at OAX[c]
		This study	Siebers *et al.*[a]	SPRRZnrc[b]	This study
6 MV	Air	1.119	1.117	1.121	1.129
	Soft Bone	1.031	1.035	1.030	1.033
	Cortical Bone	1.126	1.116	1.125	1.128
	ICRU Tissue	1.010	1.010	1.008	1.010
	Lung	0.998	0.999	0.996	1.004
18 MV	Air	1.086	1.085	1.086	1.100
	Soft Bone	1.027	1.035	1.027	1.026
	Cortical Bone	1.123	1.110	1.123	1.125
	ICRU Tissue	1.010	1.010	1.009	1.010
	Lung	0.984	0.985	0.980	0.982

[a]Results were from Siebers *et al.* (Ref. 9).
[b]Results from SPRRZnrc calculations that included track-end effect for electrons below cutoff energy (10 keV).
[c]Results were obtained at 2 cm outside beam edge and 1.5 cm depth.

Differences between Dw and Dm in soft tissue is ~1
In cortical bone it is ~10%

Jaing et al Med. Phys., V34, 2007, pp 1388-97

ESTRO School

Clinical Significance – MV energies

Compact Bone Tissue

$S_{w,med}$
= 0.98 for low density lung
=1.01 for soft tissue
=1.03 for soft bone
=1.12 for hard bone

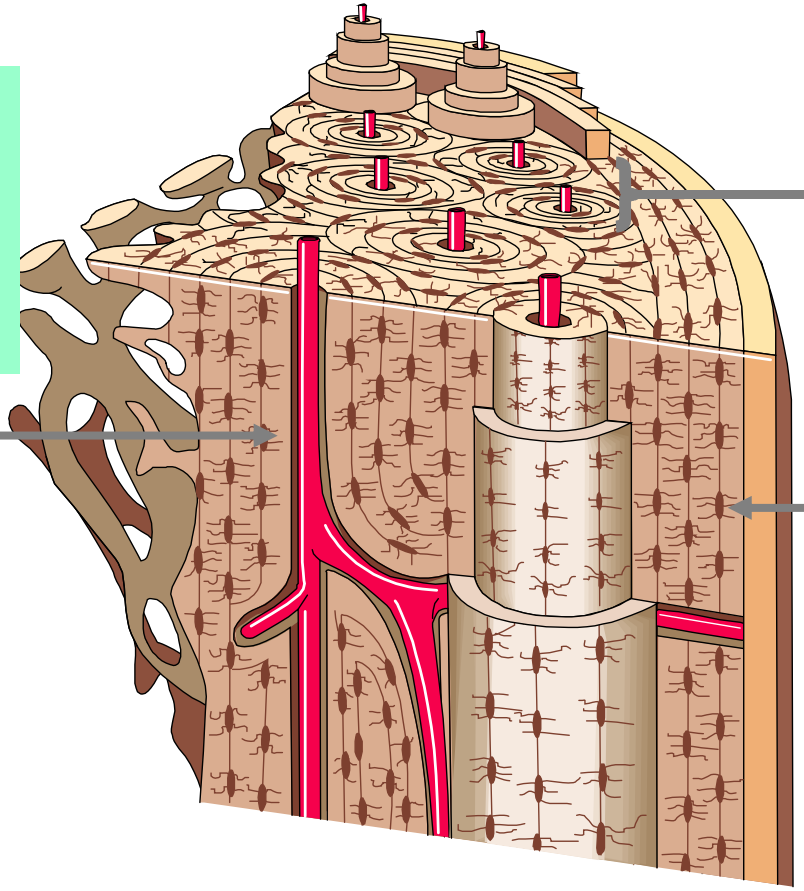

LifeART. *Super Anatomy Collection*, Baltimore, MD: Williams & Wilkins

Given importance of DNA damage, it is reasonable to assume that the biologically most relevant dose target is the cell nucleus, and that it is best treated as a water cavity. **Enger et al PMB 2012**

ESTRO School

Dose calculations with the **Monte Carlo method**

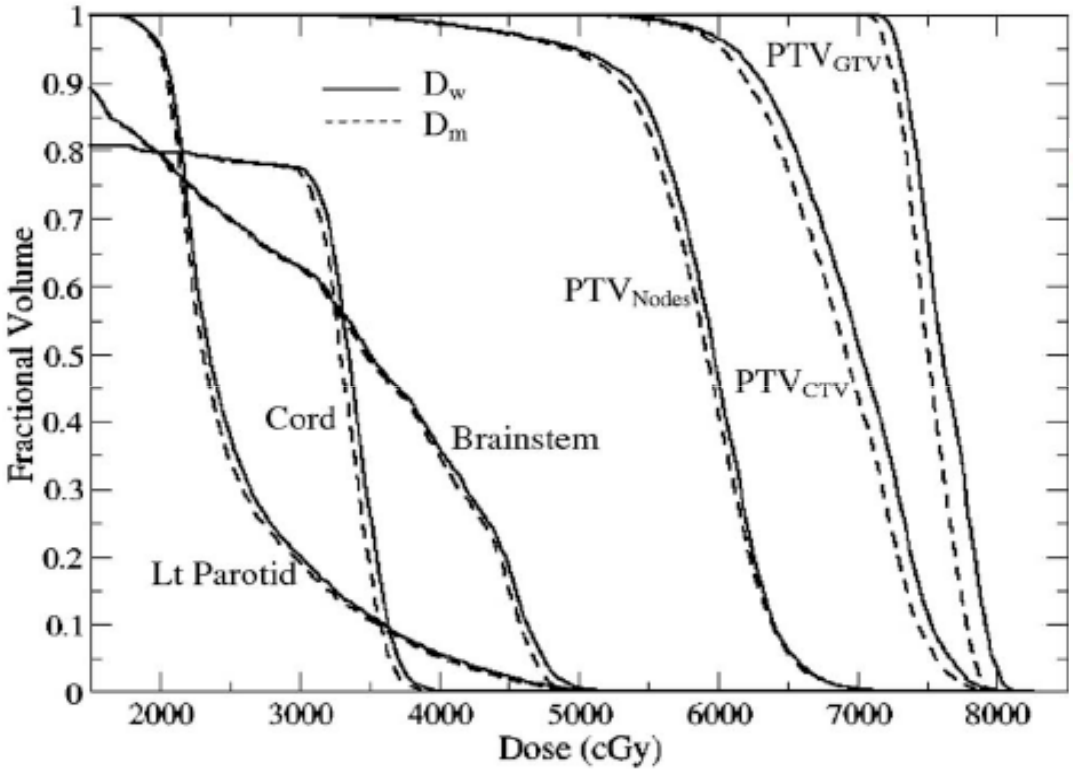

D_{tissue} D_{water}

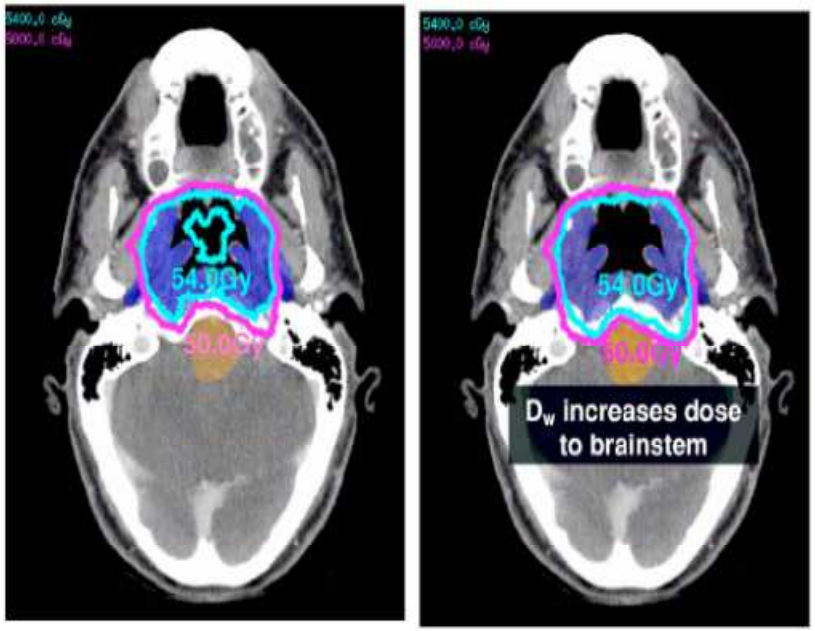

Dogan at al, Phys Med Biol, 51,4967, 2006

Converting Dm to Dw leads to systematic errors of up to 5.8% in PTV and 2.7% for OAR

ESTRO School

Clinical Significance – MV energies

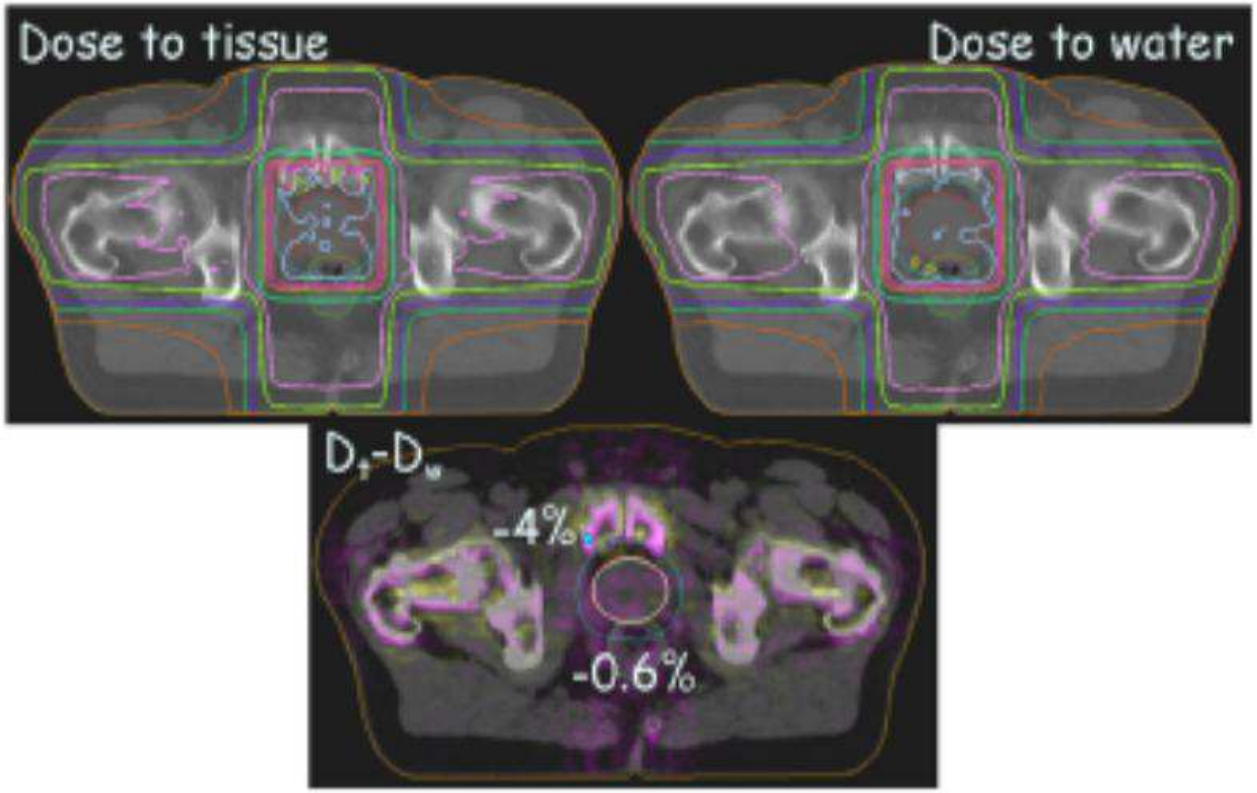

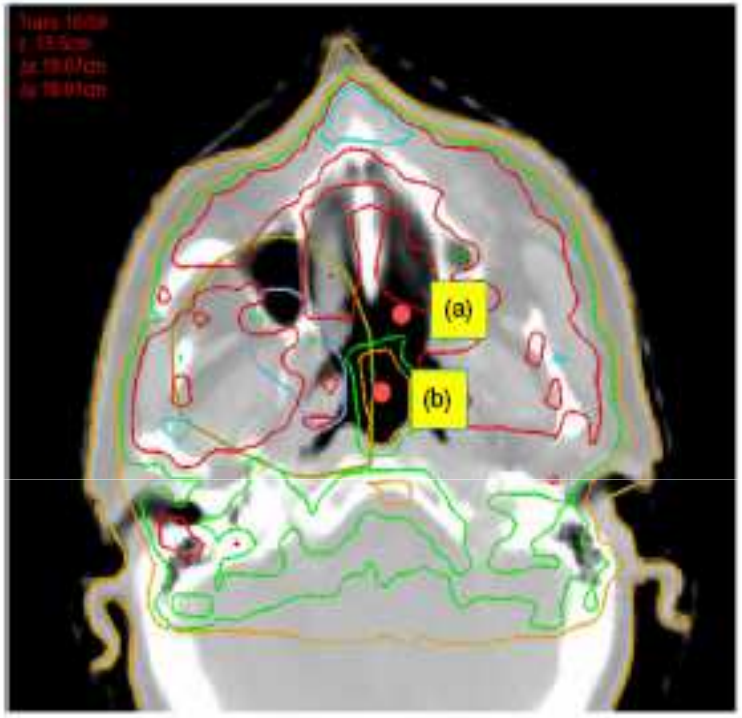

Figure 4. Dose distribution for the MC benchmark set for 6 MV in the head and neck region. The cross section is positioned at 6 cm cranial of the isocentre. The absorbed dose at point (a) is 100% and at (b) 87%. The displayed isodose lines are 90, 95, 100 and 105%.

$$D_{\mathrm{w,M}} = D_{\mathrm{m,M}} \left(\frac{\bar{S}}{\rho} \right)_m^w$$

Knöös et al PMB 51 2006

ESTRO School

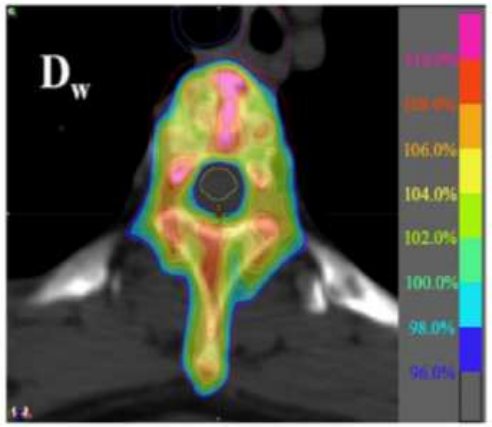

(a)

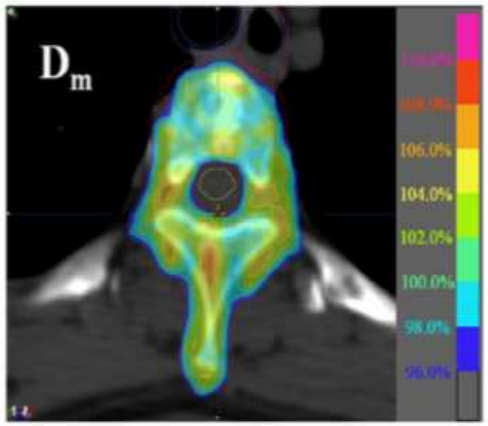

(b)

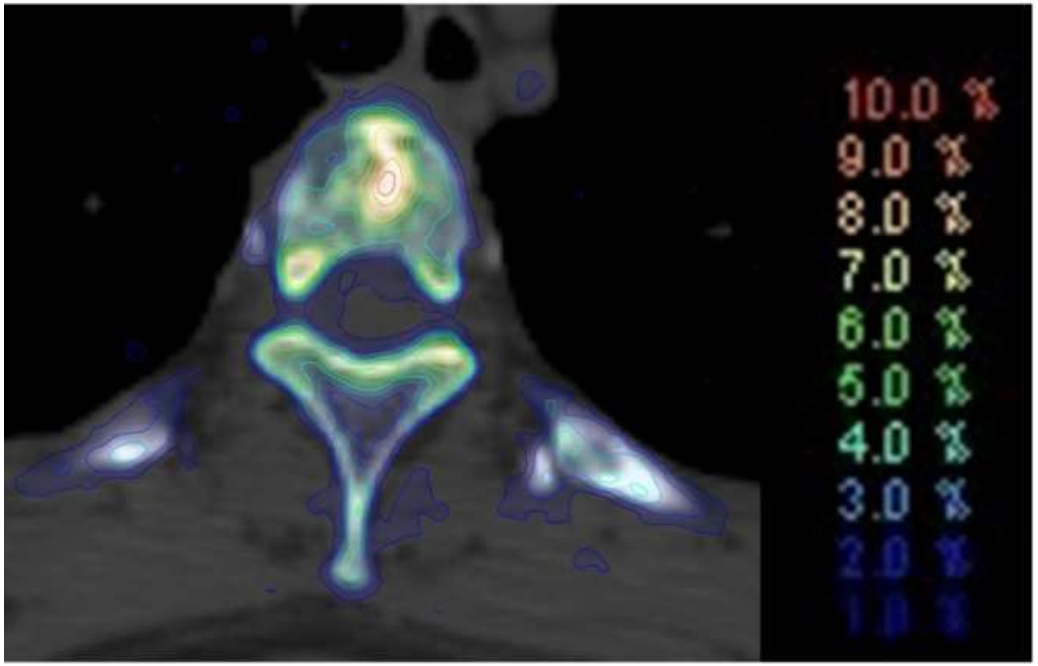

(a)

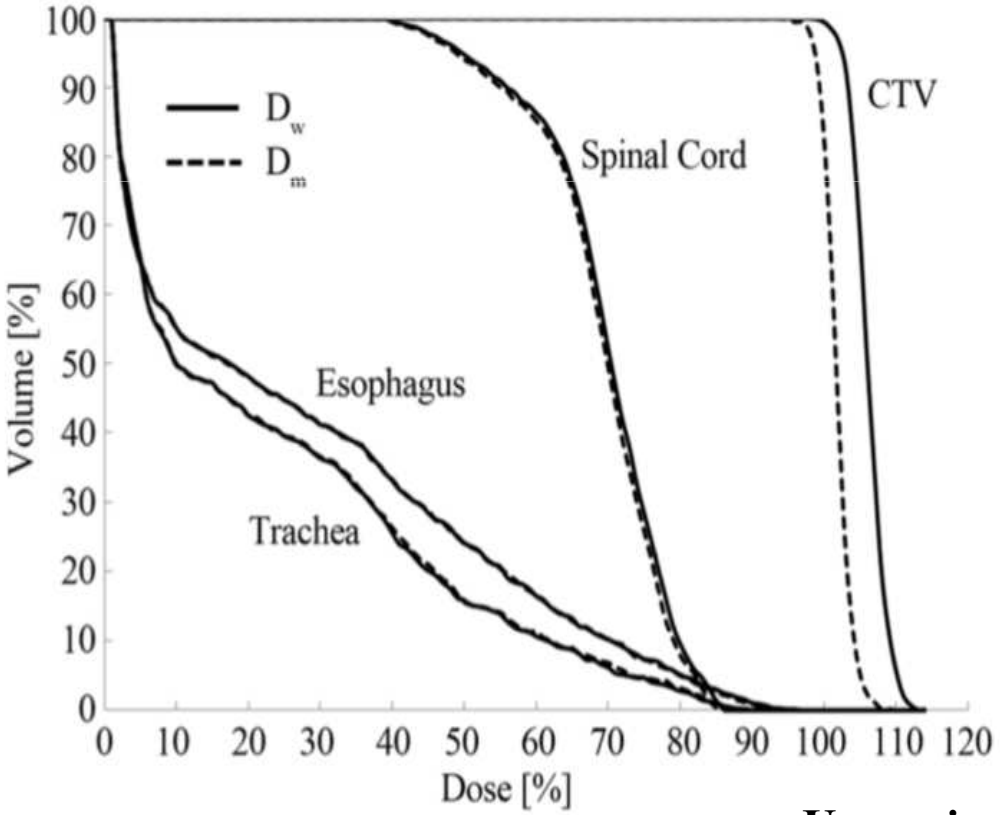

(c)

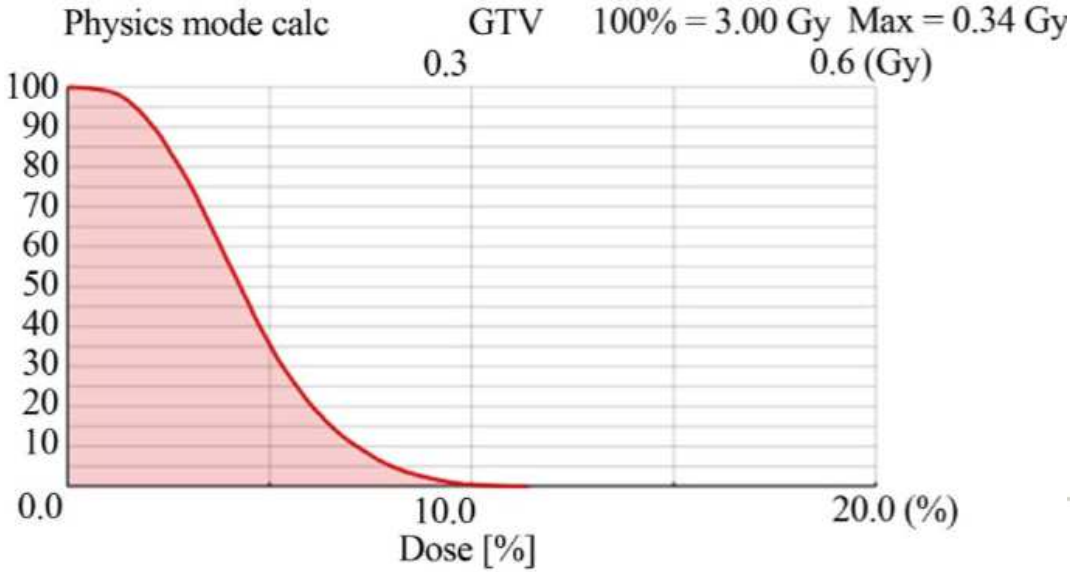

Usmani et al IJMPCERO 2014

(b)

Dose calculations with the **Monte Carlo method**

Ma & Li , Phys Med Biol, 2011, 56, 3073-

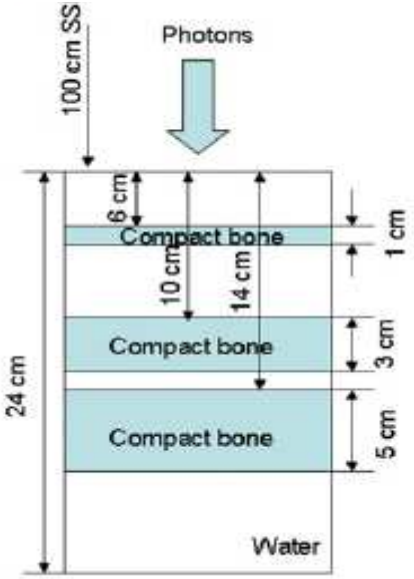

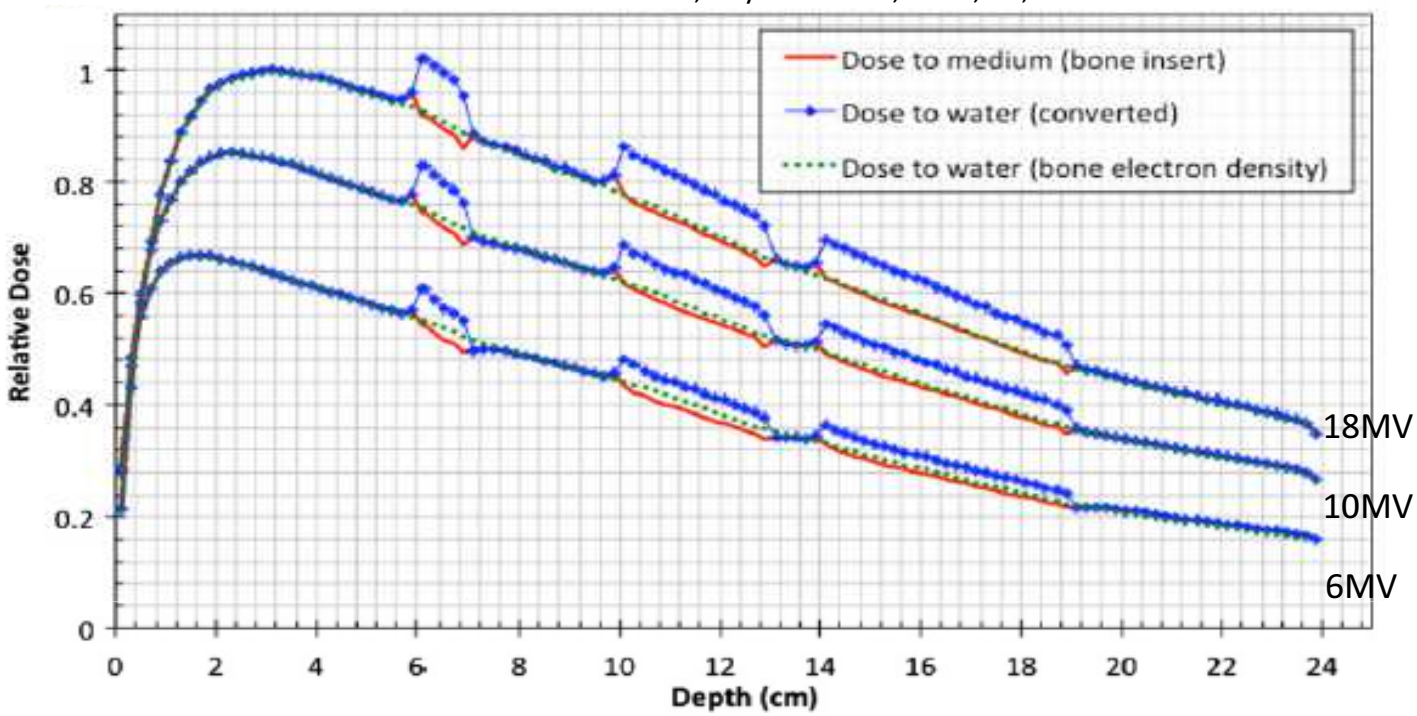

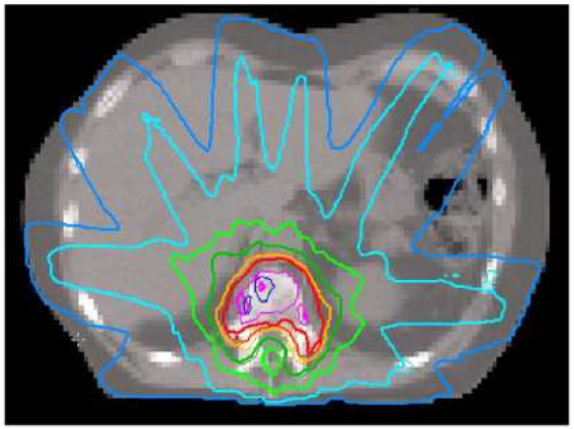

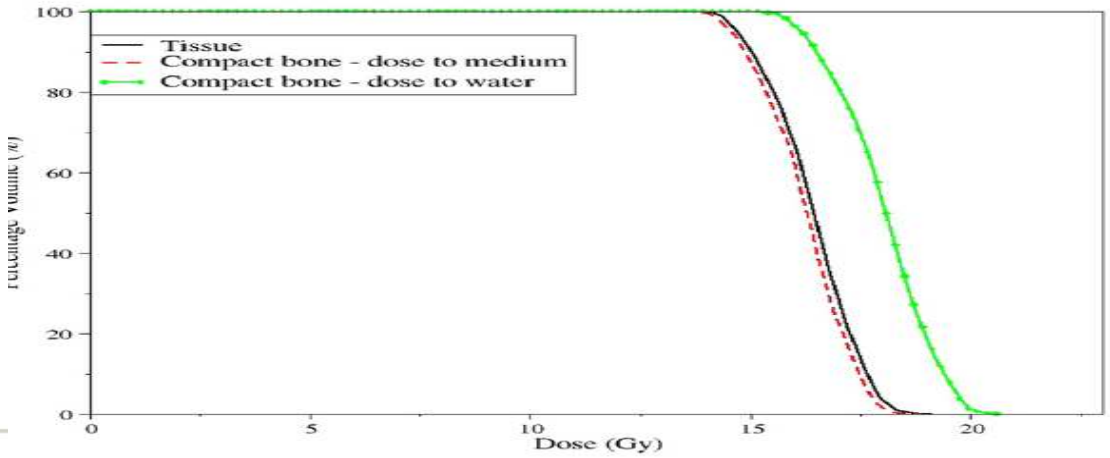

Ma et al: **Recommend using Dm reporting for MC to be consistent with previous RT experience**
Walters et al PMB 2010 **– Use Dw for dose to red bone marrow where high trabecular volume**

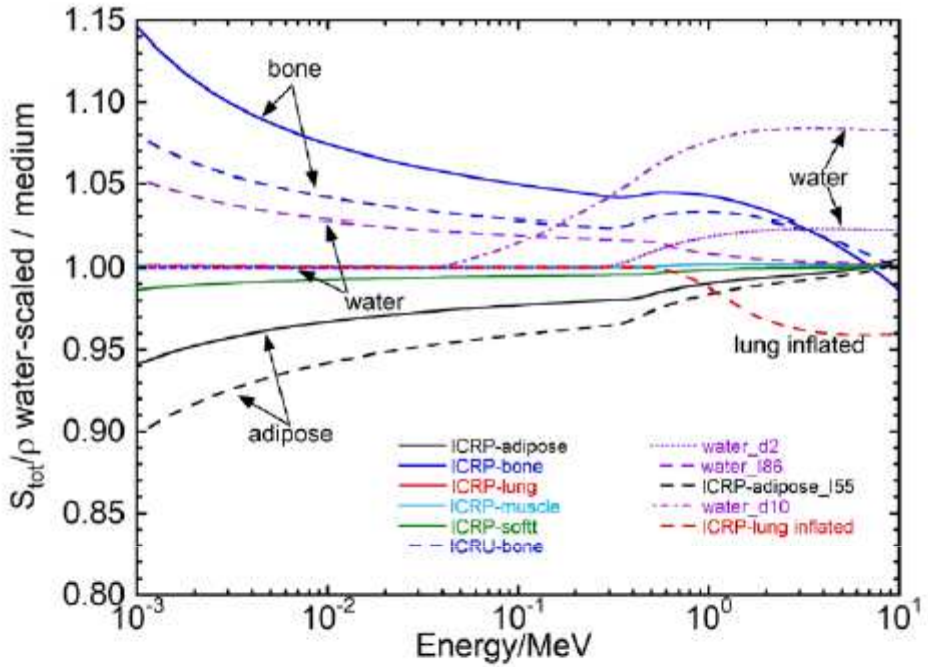

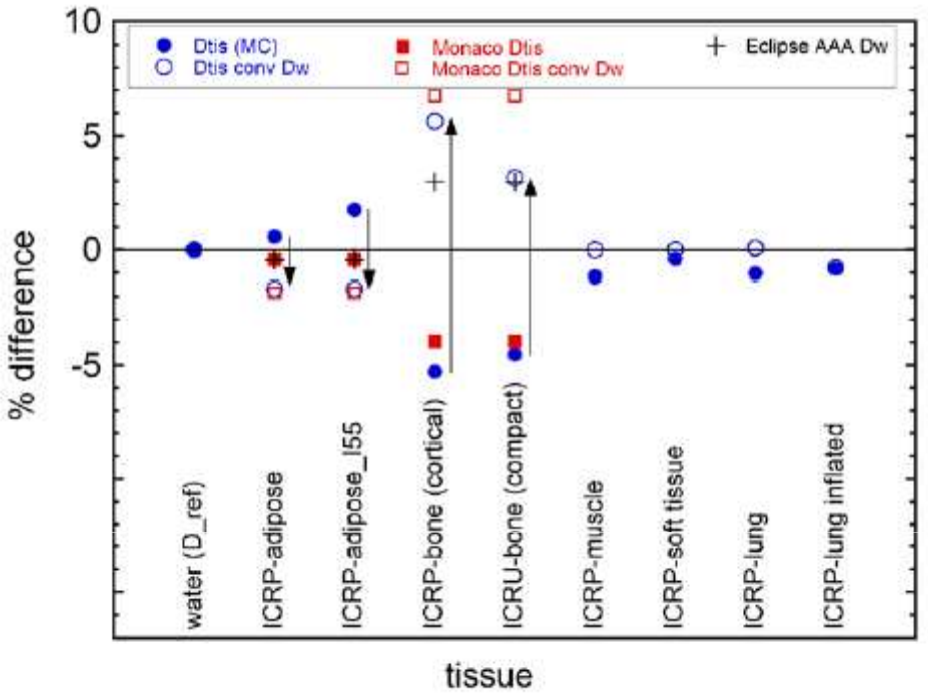

Electron density scaled S_{tot} can be quite different from true stopping powers
- This approach is used in some of the previous MCTP comparisons

Conclude use D_{tis} as conversion can lead to even worse agreement

Pedro Andreo, PMB 2015

ESTRO School

Clinical Significance – Protons

• H only reflects attenuation coefficient of tissue to diagnostic x-ray energies

• Electron density insufficient for protons

Need RSP and Z

Proton interactions:

- Electronic
  - ionization
  - excitation
- Nuclear
  - Multiple Coulomb scattering, small θ
  - Elastic nuclear collision, large θ
  - Nonelastic nuclear interaction

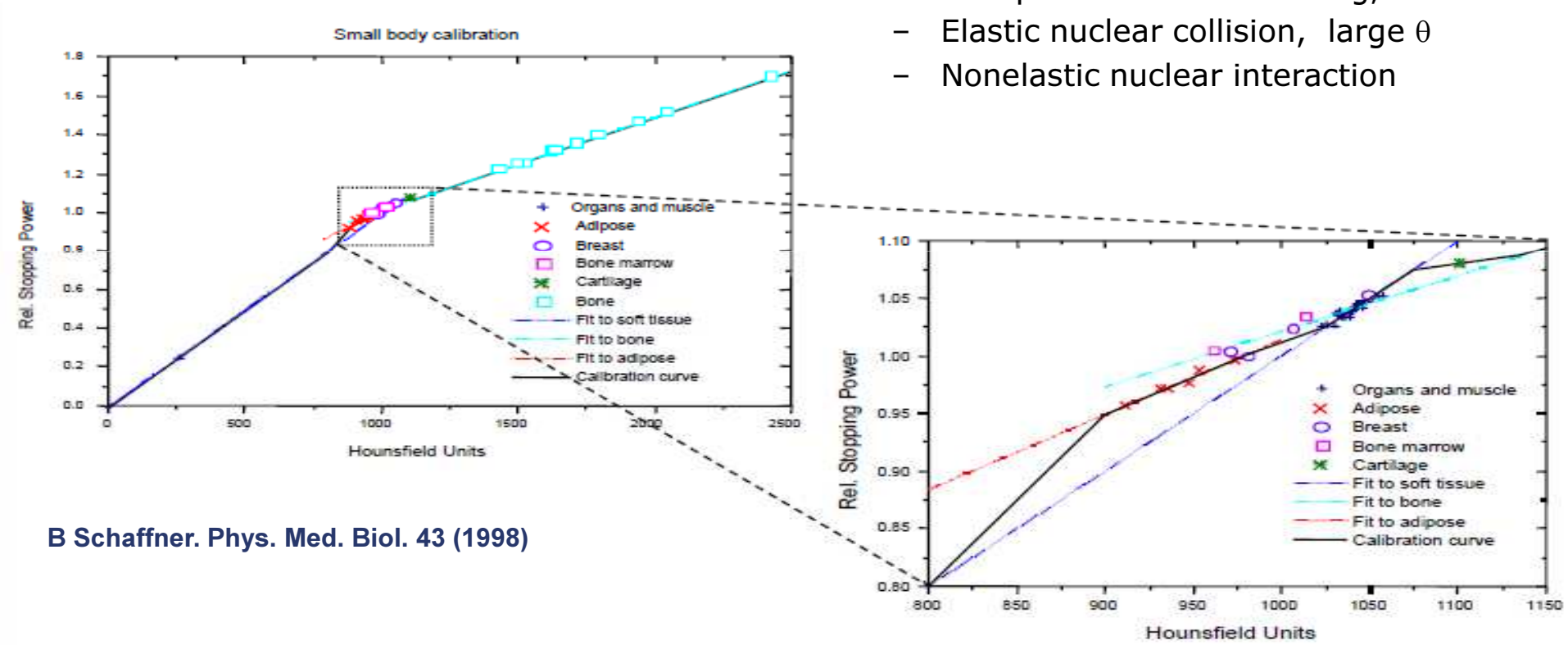

B Schaffner. Phys. Med. Biol. 43 (1998)

Matsufuji (2003) looked at extending stoiciometric for multiple scattering

And found up to 10% errors but minimum effect on patient distributions

ESTRO School

Range Uncertainty

- Range accuracy is the 'Achilles Heel' of proton treatments
- Small errors in segmentation can result in significant changes in range if they accumulate over the beam path
- Accurate CT calibration curves more important in proton than photon
- Few % error in CT calibration causes few % shift in range - due to the high distal gradient of the dose, this may lead to 100% difference in dose

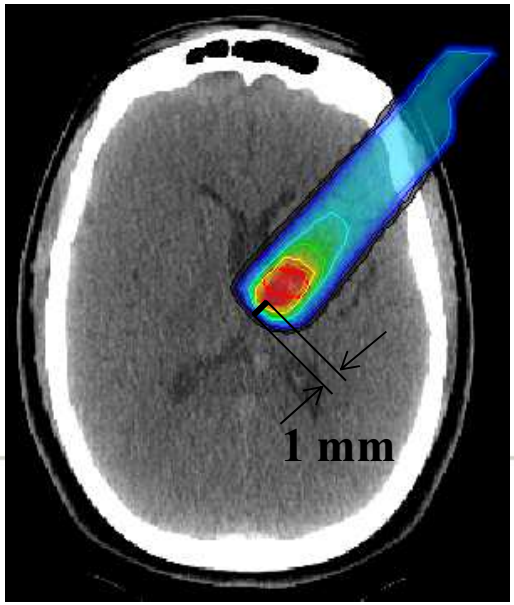

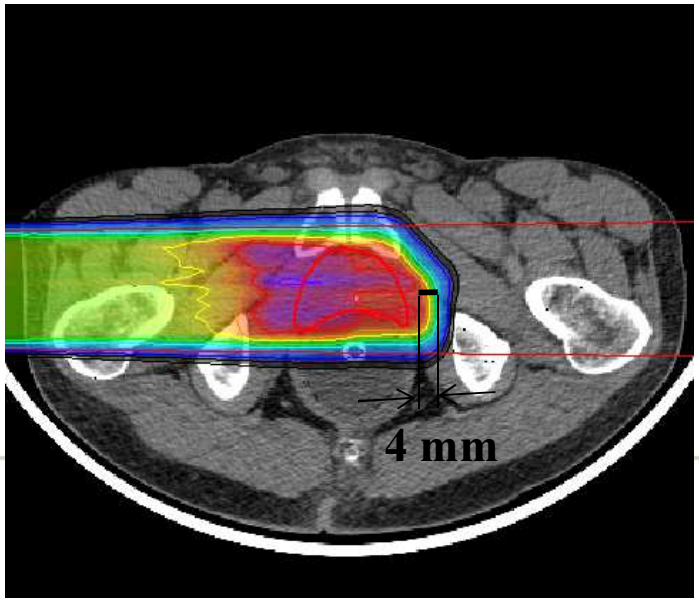

Reinhard W. Schulte
Loma Linda

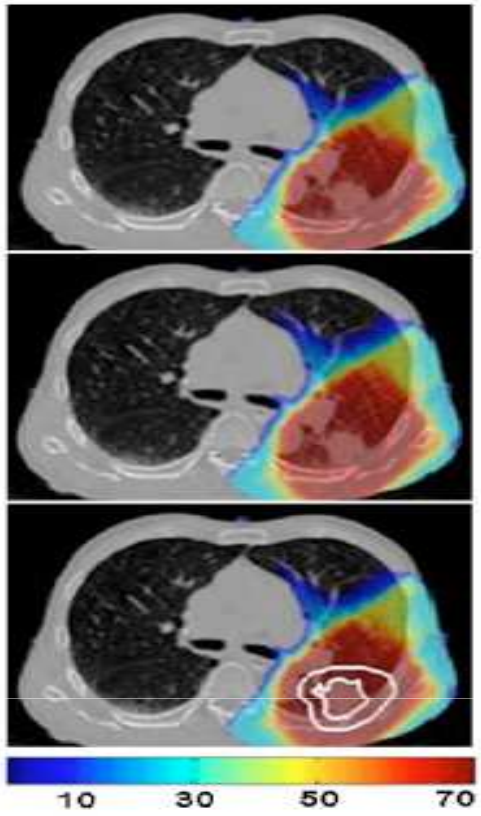

Schneider

BEAM

Dm

Water

Dw

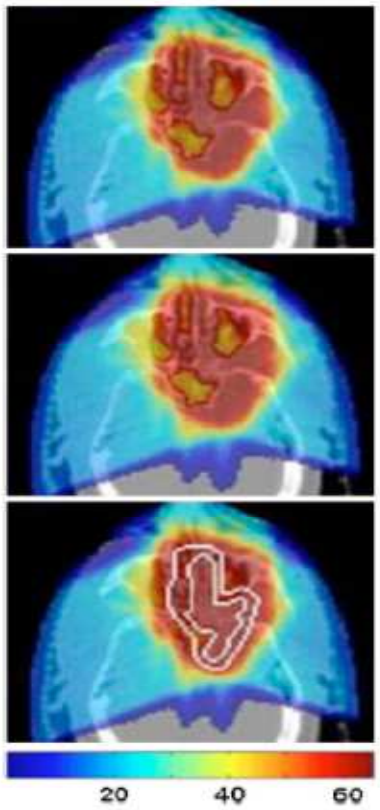

Jiang et al MP 2007

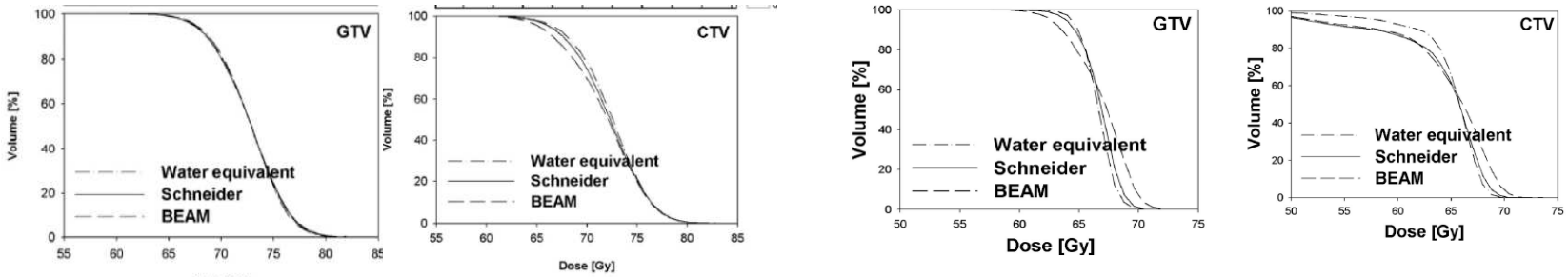

- **Method chosen to assign tissue materials (mass density and elemental composition) affects dose distribution**
- **More important in OAR (distal ranges)**
- **Ranges calculated using Dw and Dm for protons stopping in bone can differ by 2-3mm (Paganetti 2009)**

ESTRO School

Clinical Significance – keV energies

At keV energies….
(AAPM TG 186 for model based calculation)

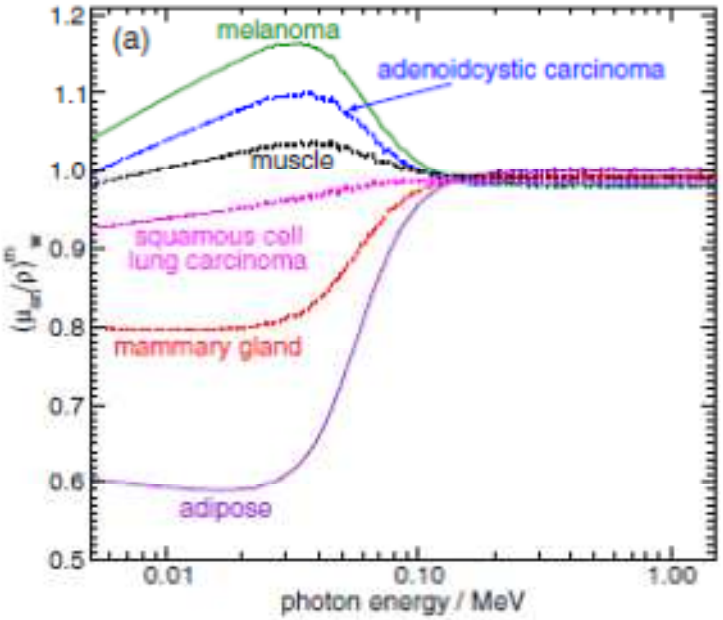

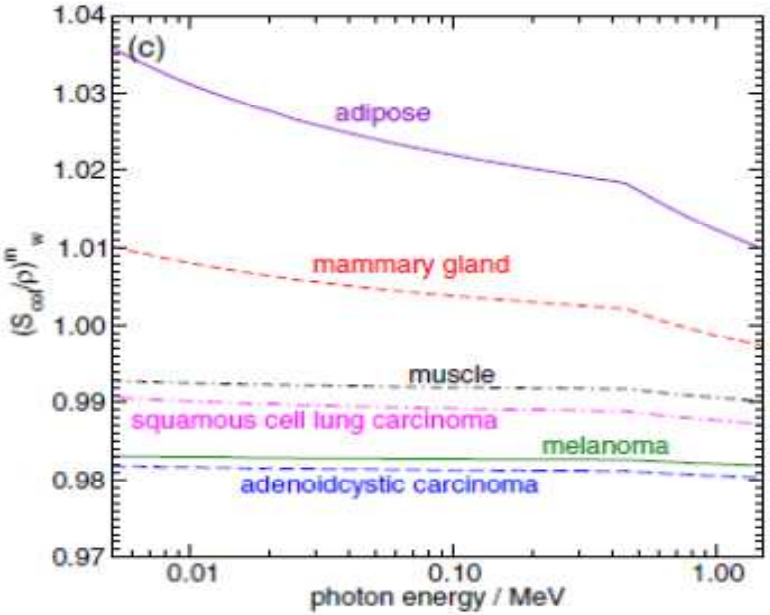

- **Deviations from water based dose calculations (TG43) at low energies**
- **Cells are not radiologically equivalent to either water or bulk tissue**
- **Dose from low energy photons is very sensitive to medium composition**

Thomson et al PMB 2013

ESTRO School

Enger et al PMB 2012/Thomson et al PMB 2013

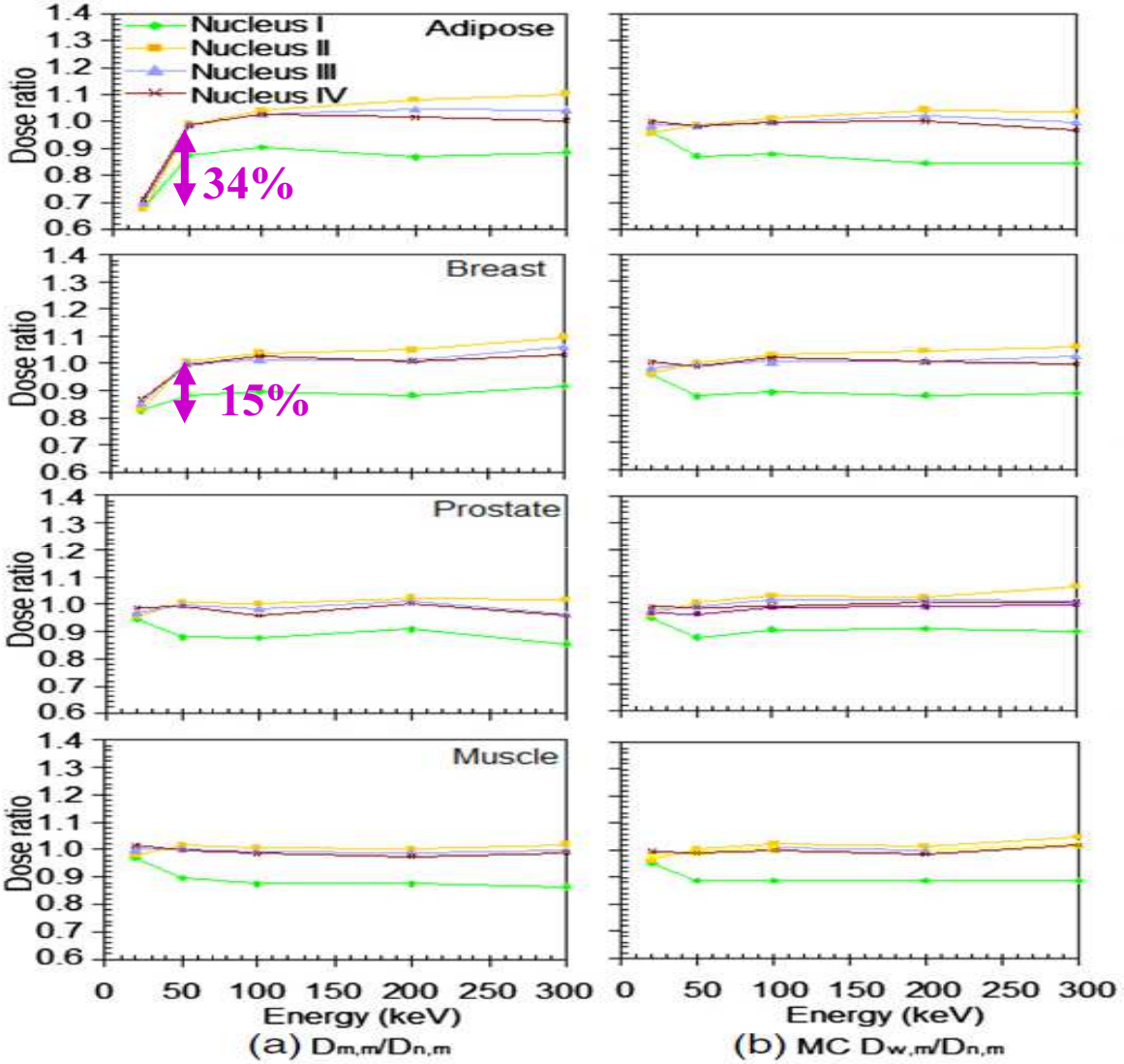

Assuming relevant target is cells nucleus:

Does $D_{m,m}$ or $D_{w,m}$ best reflect $D_{n,m}$?

4 Nuclear compositions in 4 different tissue types

Enger conclude: **$D_{w,m}$ is a good surrogate for $D_{n,m}$ for all energies and compositions studied**

Thomson conclude: **Neither track nuclear dose although error decreases if use $D_{w,m}$. Nuclear material not representative**

Both: **Need more accurate data on composition of tumour and healthy cells**

ESTRO School

Pre-clinical studies (keV)

Bazalova and Graves. MP 38 June 2011

120kV, 225kV, 320kV and Ir-195 on centrally located lung tumour in small animal

Conclude: Tissue segmentation based on mass density leads to Errors of up to 27% for 120kV

Need tissue segmentation based on effective atomic number and 39 tissues to get below 2%

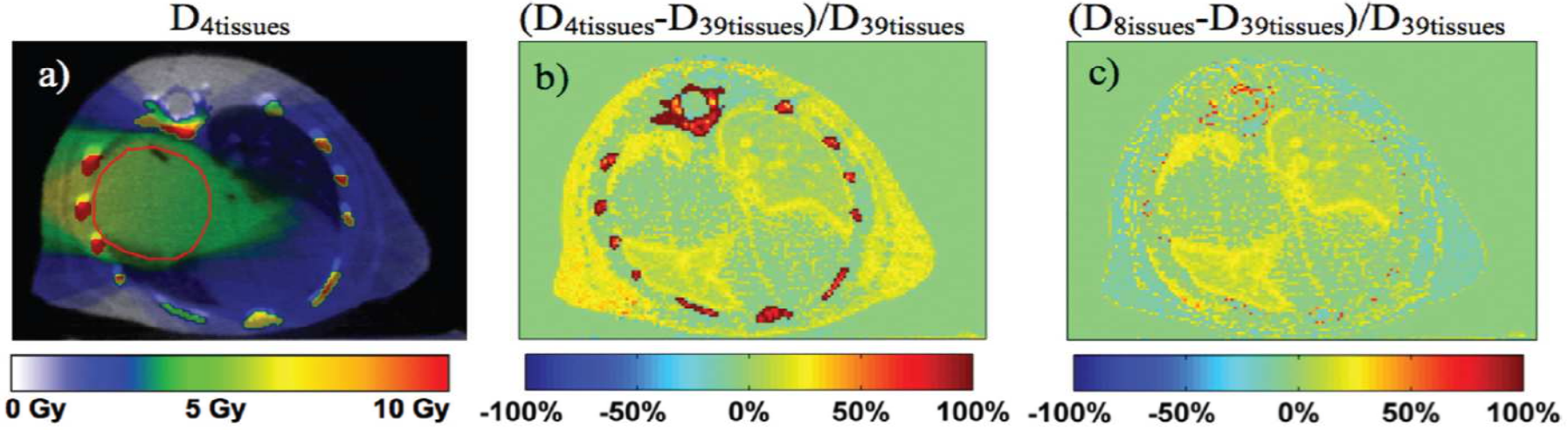

FIG. 10. Monte Carlo dose distribution for an orthotopic lung tumor with the standard 4-tissue segmentation scheme (a) for a 120 kVp plan. The percentage difference maps $(D_{4tissues}-D_{39tissues})/D_{39tissues}$ and $(D_{8tissues}-D_{39tissues})/D_{39tissues}$ are shown in (b) and (c), respectively. The PTV is delineated in red.

ESTRO School

Dose to tissue?

External Beam

For

- $D_{m,m}$ is the 'natural' quantity from MC
- To report D_w then if convert back to water – uncertainty in $s_{w,m}$
- Makes little difference for soft tissues
- CT numbers converted using ICRU or ICRP but who is 'standard?

Against

- D_w clinical experience (Ma et al?)
- Dosimetry protocols
- NTCP, TCP reported in dose to water
- Uncertainties lower
- Target is a 'water' cell in bone
- Report both?

Brachytherapy

- Mass energy absorption coeffs quite different between tissue types and water
- $D_{m,m}$ and $D_{w,m}$ can be very different
- Accurate dosimetry requires atomic composition
- MC-$D_{w,m}$ good substitute for MC-$D_{n,m}$ for all energies and tissue types studied **(Enger et al PMB 2012)**

Some developments: DECT

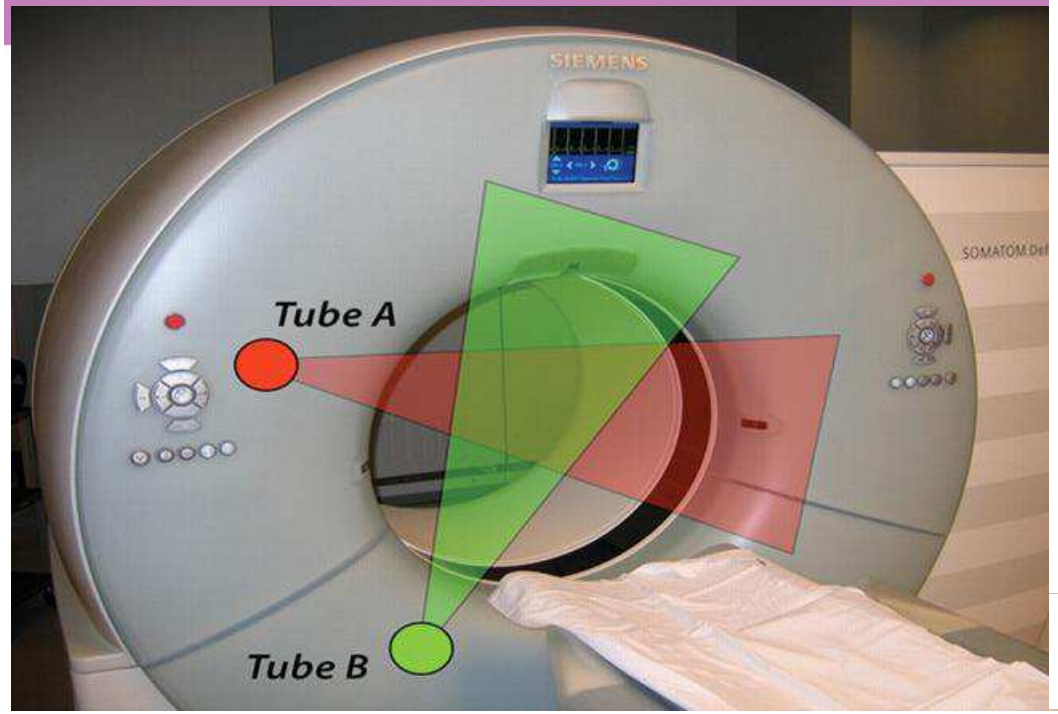

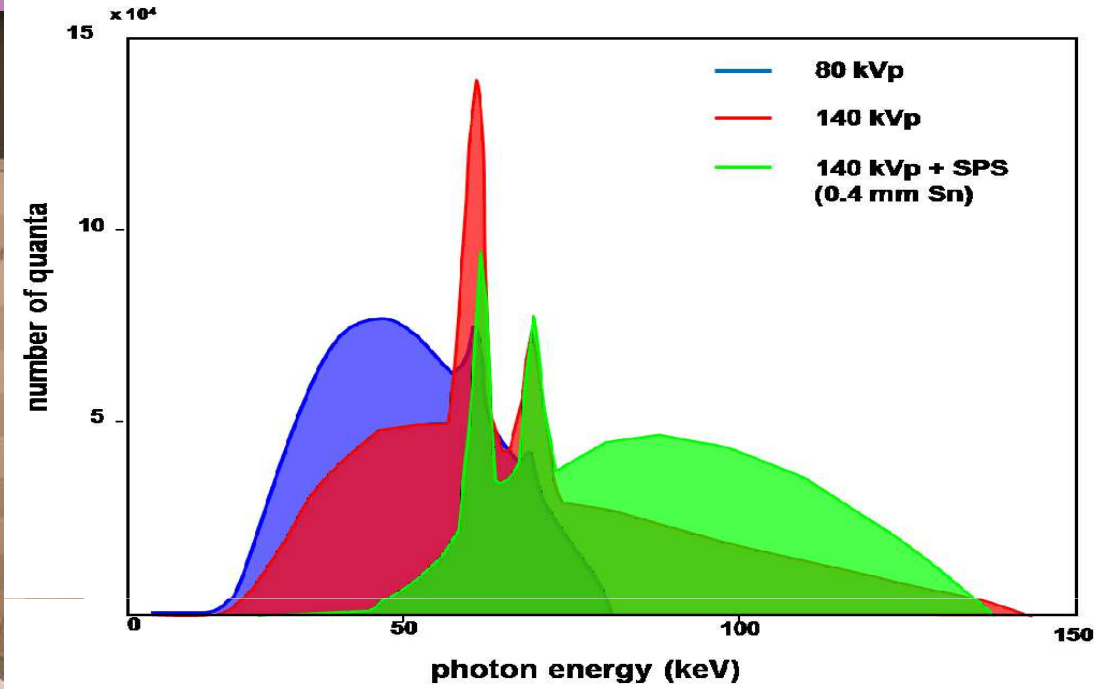

Attenuation is function of medium density and elemental composition
Several materials same HU but different densities and elemental compositions

DECT exploits energy and compositional dependence of μ at keV energies

$\mu(E) = \rho(af_{compton}(E) + bf_{PE}(E))$

a and b depend only on composition of material

Scan at 2 energies to give Z_{eff} and electron or mass density via simultaneous equations

ESTRO School

Dose uncertainties in MC MV photon dose calculations

- **Bazalova PMB 2008, *Dual-energy CT-based material extraction for tissue segmentation in Monte Carlo dose calculations***

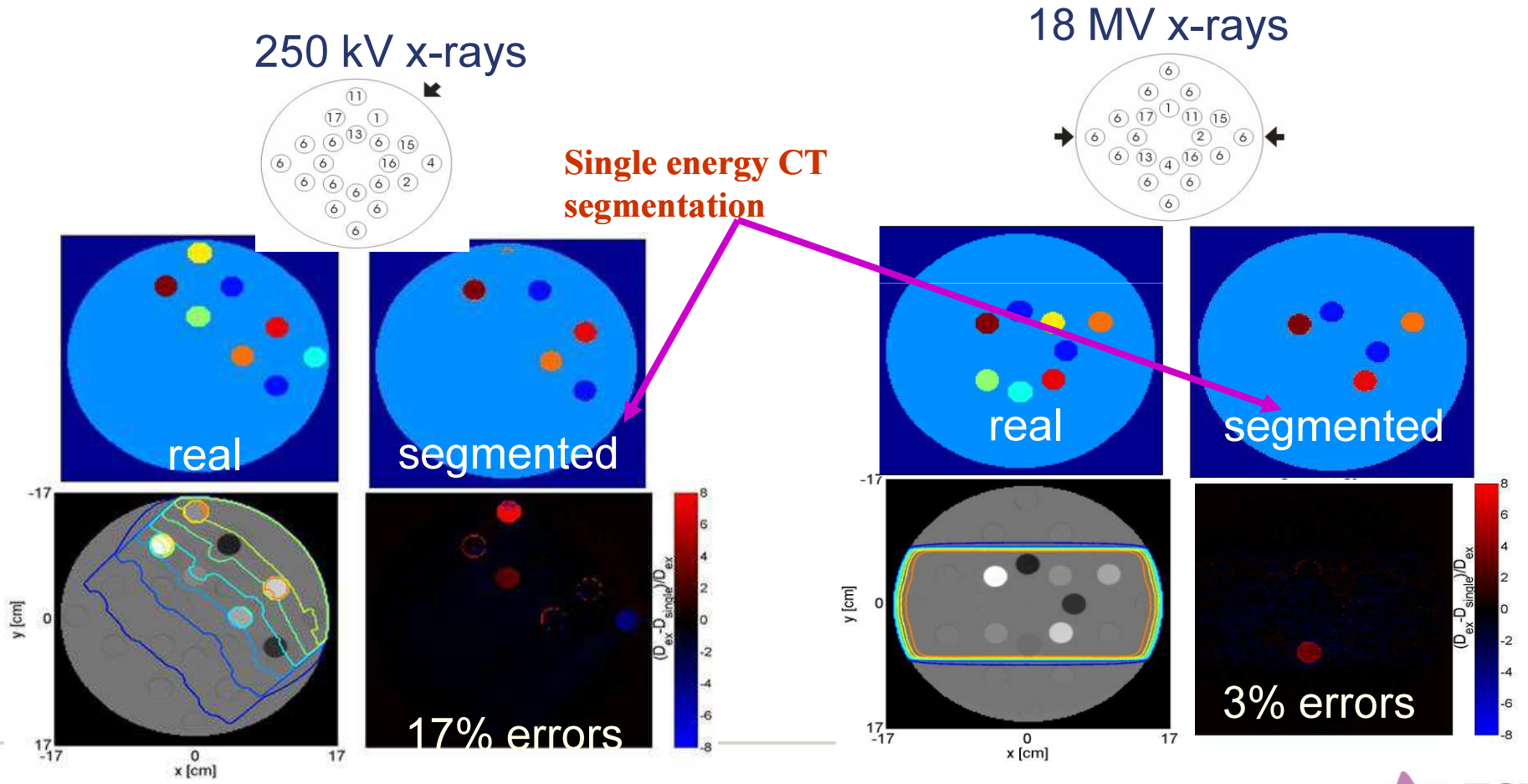

From F Verhaegen

But <1% when dual energy used

ESTRO School

Menten et al Medical Physics 2015

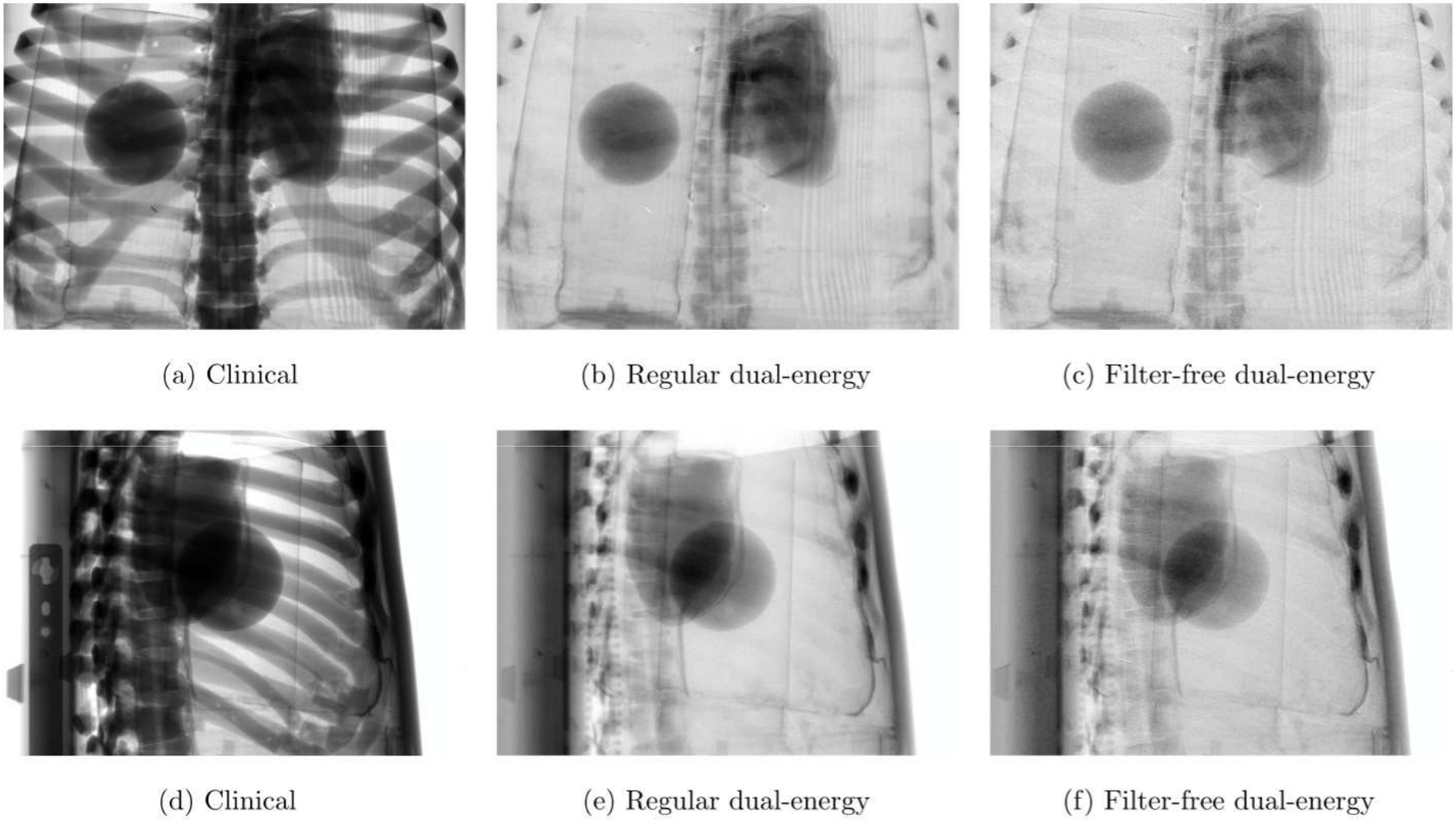

(a) Clinical (b) Regular dual-energy (c) Filter-free dual-energy

(d) Clinical (e) Regular dual-energy (f) Filter-free dual-energy

FIG. 4. Experimentally acquired radiographs of the Lucy phantom in [(a)–(c)] AP imaging direction and [(d)–(f)] LR imaging direction. The windowing settings in all images were set based on the minimum and maximum intensity in the lung.

ESTRO School

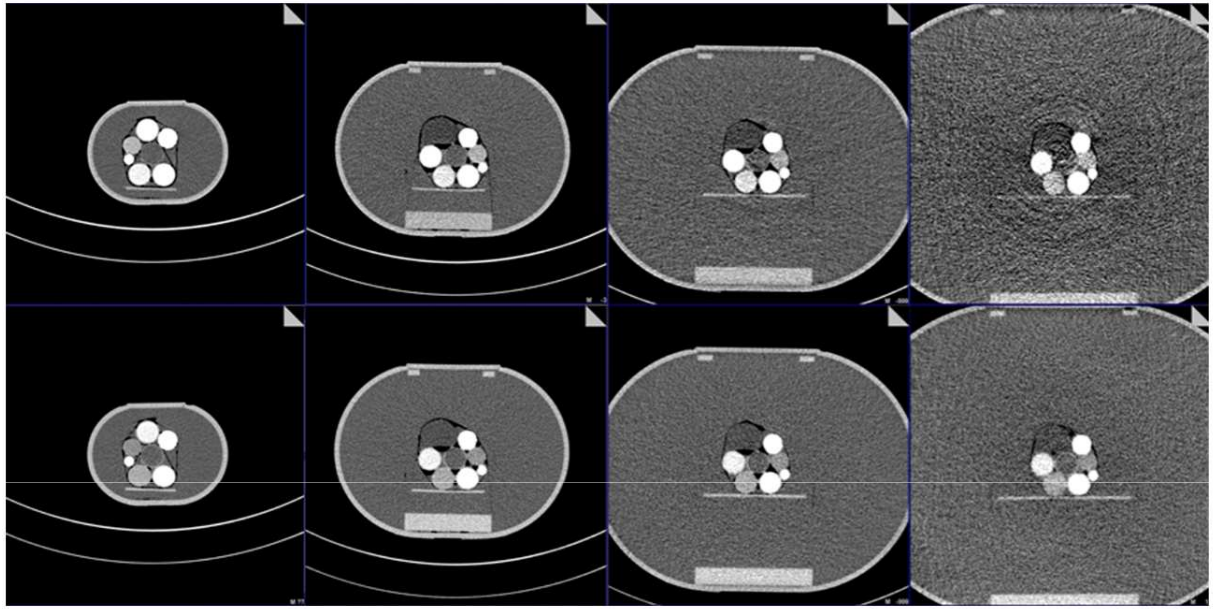

Michalak et al Medical Physics 2016

FIG. 3. Example images using a SE technique of 70 kV (top) and DE technique of 90/150Sn kV (bottom). The phantom sizes were, from left to right, 15, 25, 35, and 45 cm lateral width.

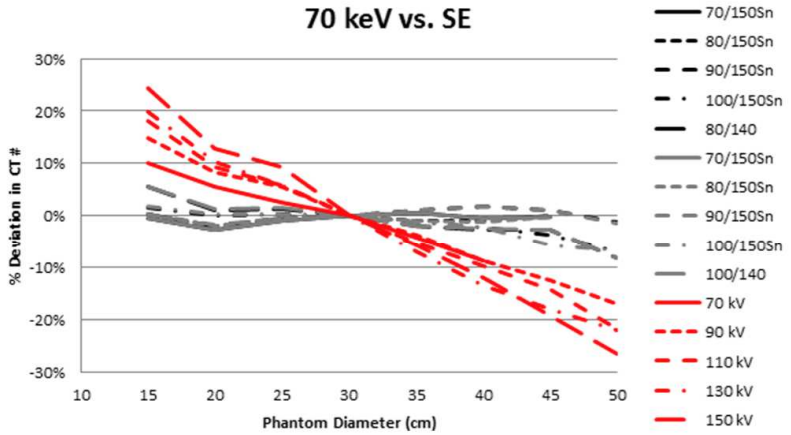

FIG. 5. Percent deviation in CT number relative to the 30 cm phantom with respect to phantom size. DE data are shown in black (mono) and gray (mono+) while SE data are shown in red. The virtual monoenergetic energy shown for the DE images is 70 keV.

ESTRO School

Other image possibilities

Cone beam CT images?

- Image quality of CBCT images << CT images
  - $HU_{CT} \neq HU_{CBCT}$
  - Needs separate calibration
  - CBCT sensitive to motion artifacts
- Hatton PMB 54 (2007): 20% dose errors for MV photons based on CBCT

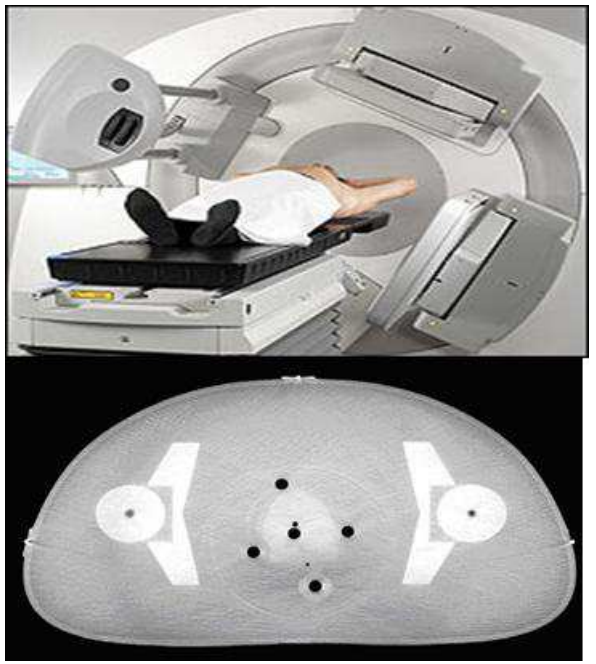

MRI images?

- Dowling IJROBP 83 (2012). Prostate
- Atlas-based electron density mapping method
- PseudoCT and planning CT dose differences<2%.
- Planning CT and pseudoCT distributions equivalent
- Full examination of uncertainties needed

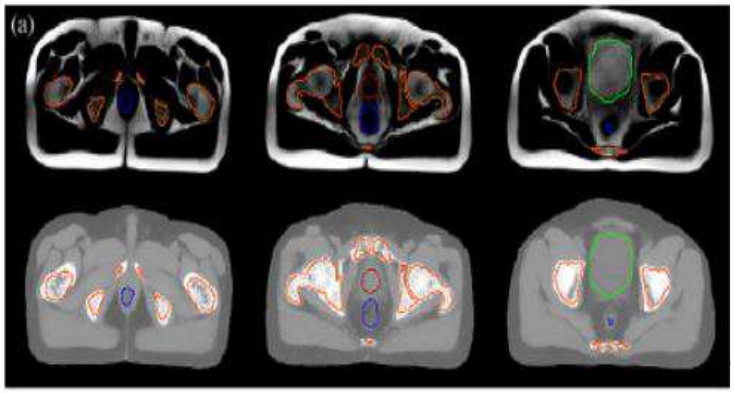

ESTRO School

Conclusions

Numerous approximations whose impact on the final dose accuracy should not be ignored!

- CT remains the preferred image modality
- CT calibration curves and tissue segmentation key to accurate dose calculation
  - More important for Protons and keV (and Brachytherapy)
  - Some common practices to establish tissue characterisatoin can introduce systematic errors into dose planning
- Dw and Dm debate continues but important to specify medium in literature
  - We're talking about cell composition!
  - Verification of Dm calculations?

Thank you!

Thanks to **F. Verhaegan**
H Nystrom
M. Schwarz
T. Knoos
Anders Ahnesjö
M Aspradakis **for slide material**

ESTRO School

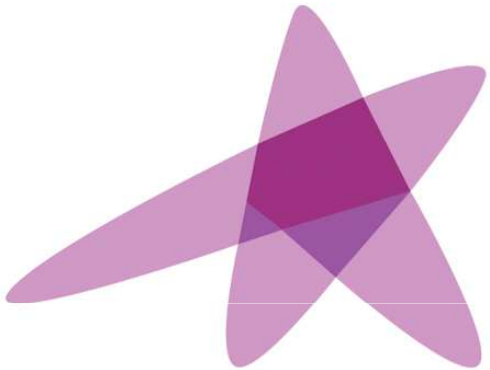

ESTRO School

WWW.ESTRO.ORG/SCHOOL

Phantoms

Mania Aspradakis
maria.aspradakis@luks.ch

Acknowledgement: Prof. Anders Ahnesjö & Dr Nuria Jornet

Learning Objectives

- Learn when a solid plastic phantom is water equivalent
- Understand the formalism that relates measurements in solid phantom to dose to water in water
- Appreciate how measurements in solid phantoms relate to treatment planning system (TPS) calculations in such phantoms

Outline

- Why use water and water-equivalent phantoms for radiotherapy dosimetry?
- What defines water-equivalence of a solid plastic phantom?
- Derivation of the formalism to convert chamber ionisation readings in a water-equivalent solid phantom to dose to water.
- Checking water-equivalence of solid plastics in the clinic
- The use of solid plastic phantoms for treatment plan verification

Why water or water-equivalent phantoms

Need to determine absorbed dose in the different tissues in human body

- Water is a good soft tissue equivalent material for high energy photon and electron beams.

Dosimetry for beam characterisation & TPS verification:

- Reference dosimetry: most dosimetry Codes of Practice (CoP) use water as reference medium
- Relative dosimetry: relative depth functions (PDD, TPR), beam profiles, output factors etc. are measured in water

Phantoms for beam characterization: liquid water

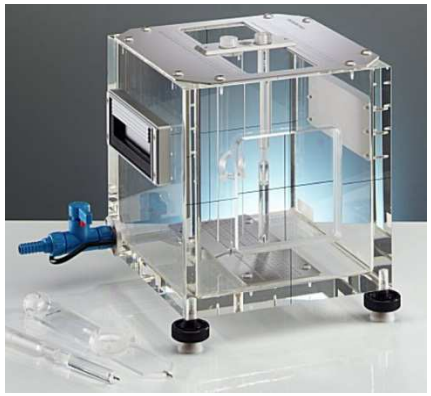

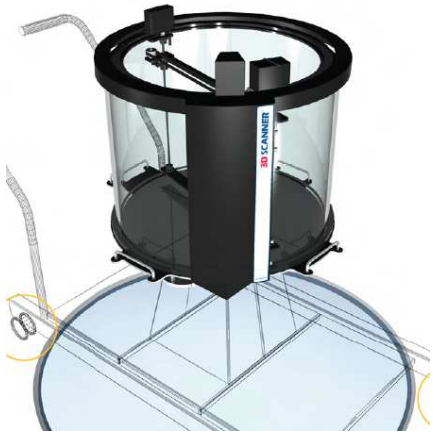

Advantages

- Widely used and available
- Known composition
- Detectors can be placed at any point inside the phantom
- Large enough to characterize the beam under full scatter conditions

Disadvantages

- Not all detectors are waterproof
- Not quick and easy to set up
- Too large to simulate the dimensions of a real patient and be used for the dosimetric verification of a treatment plan

Phantoms for beam characterization: solid plastics

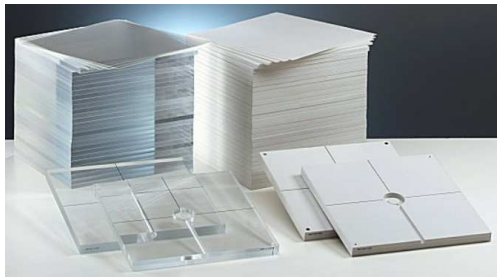

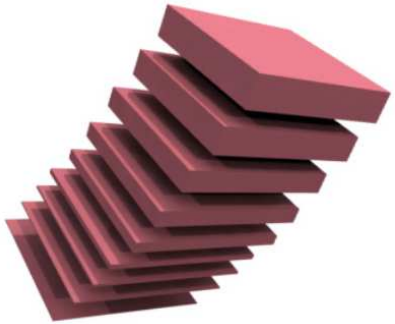

Advantages

- Robust
- Allow easy, quick and reproduceable setup
- Can be used with non water-proof detectors
- Easier to use with films

Disadvantages

- Water-equivalence depends on modality and energy (MV, kV, MeV)
- Expensive if manufactured to be water-equivalent
- Different samples of same type of plastic could vary in composition and from manufacturer specification
- Possible degradation with time
- Possible charge storage effects

Phantoms for beam characterization: solid plastics

The elemental compositions, physical densities, electron densities and relative electron densities for solid phantoms.[2,5–7)]

Elements	Water	WT1	457-CTG	RW3	MixDP	WE211	WE211R	Plastic Water	Plastic Water DT	Virtual Water	Polystyrene	PMMA	ABS [a]
H	0.1119	0.0810	0.0810	0.0759	0.1277	0.0821	0.0838	0.0779	0.0740	0.0770	0.0774	0.0805	0.0810
B									0.0226				
C		0.6720	0.6720	0.9041	0.7682	0.6633	0.6738	0.5982	0.4670	0.6874	0.9226	0.5998	0.8490
N		0.0240	0.0240			0.0221	0.0219	0.0178	0.0156	0.0227			0.0700
O	0.8881	0.1990	0.1990	0.0080	0.0511	0.2065	0.1953	0.2357	0.3352	0.1886		0.3196	
Mg					0.0386				0.0688				
Al									0.0140				
Cl		0.0010	0.0010			0.0040	0.0024	0.0023	0.0024	0.0013			
Ca		0.0230	0.0230			0.0220	0.0228	0.0676		0.0231			
Ti				0.0120	0.0144								
ρ [g cm^{-3}]	0.998 [b]	1.020	1.043	1.045	1.000	1.018	1.018	1.030	1.039	1.030	1.060	1.190	1.050
ρ_e [$\times 10^{23}$ g^{-1}]	3.343	3.249	3.249	3.231	3.382	3.252	3.257	3.238	3.218	3.237	3.238	3.248	3.249
$(\rho_e)_{pl,w}$		0.972	0.972	0.966	1.012	0.973	0.974	0.969	0.963	0.968	0.969	0.972	0.972
Z_{eff} [c]	7.22	6.35	6.35	5.83	6.38	6.34	7.07	6.83	6.83	6.35	5.61	6.24	5.67

Fujita, Y. et al (2010). J Radiat Res **51**(6): 707-713.

ESTRO School

Phantoms for plan QA

- Simple geometric

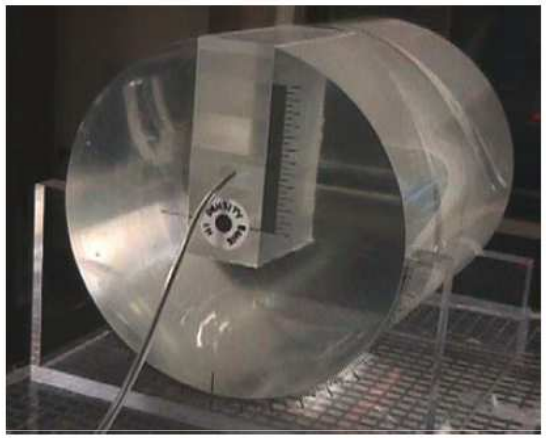

- Anthropomorphic

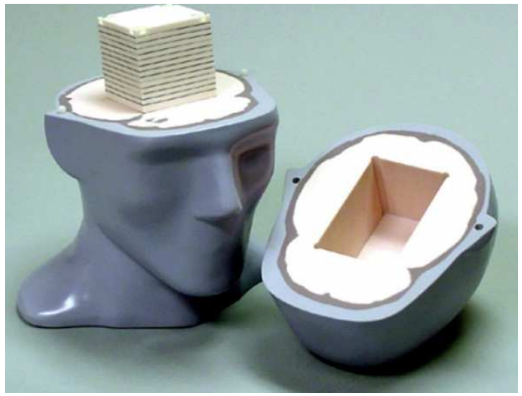

Water-equivalence of solid phantom materials

A phantom material is water-equivalent for dosimetry when it mimics water in all relevant physical and dosimetric properties in the particular radiation modality

This means, the material should have:

Same attenuation, scatter and absorption properties as that of water

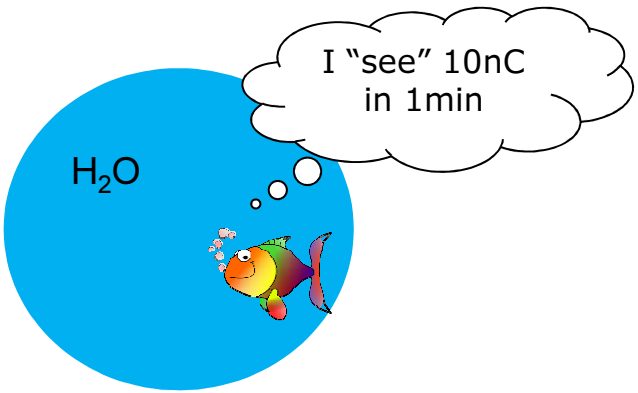

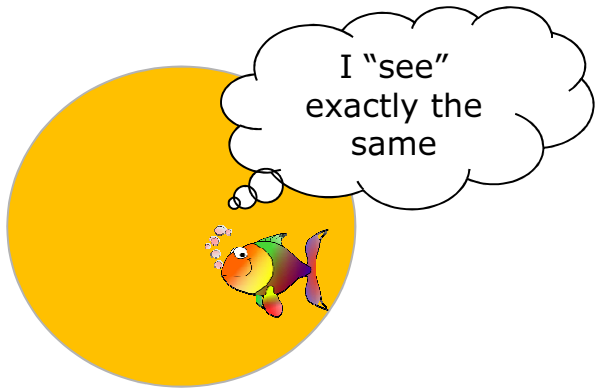

Could there be a material that water-equivalent for the whole range of beam modalities used for radiation therapy?

Formalism to convert ionisation in plastic to dose to water

Ionization chamber measurements in a plastic phantom: what is being measured?

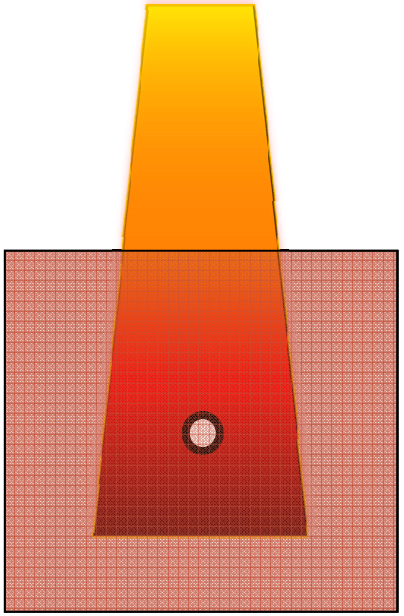

1. Ionizations (charge) in air embedded in a phantom
2. Ionizations (charge) in water
3. Dose in air in a water phantom
4. Dose in water

Formalism to convert ionisation in plastic to dose to water

Ionization chamber measurements in a plastic phantom: what is being measured?

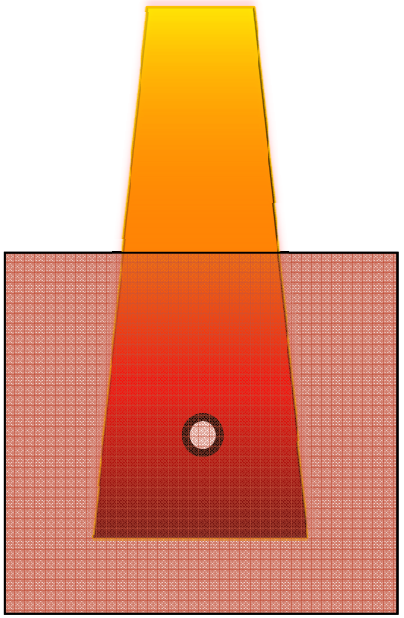

1. Ionizations (charge) in air embedded in a phantom
2. Ionizations (charge) in water
3. Dose in air in a water phantom
4. Dose in water

Formalism to convert ionisation in plastic to dose to water

Ionization chamber measurements in a plastic phantom: what is being measured?

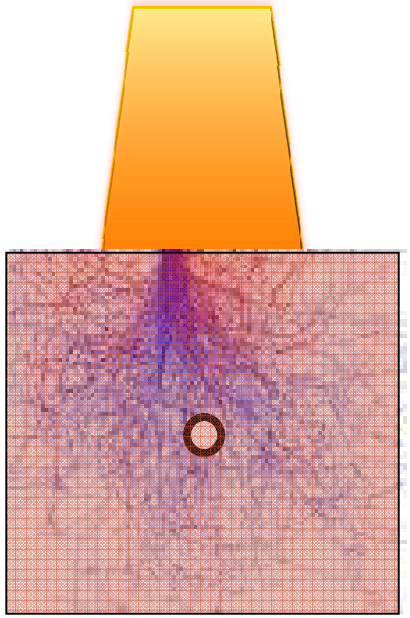

Ionizations (charge) in air embedded in a phantom

$$M_{air}\,[nC]$$

- Number of electrons at the chamber position → Electron fluence
- Energy of these electrons at the chamber position → Electron energy spectra

Formalism to convert ionisation in plastic to dose to water

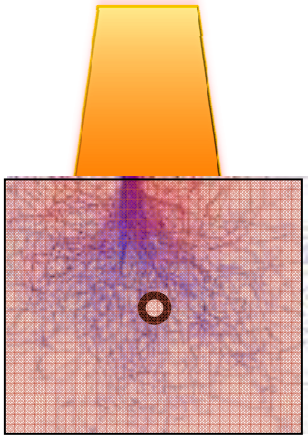

Formalism in Dosimetry Code of Practice
for dose to water from a measurement in plastic

$$D_{w,Q}(z_{ref}) = M_{s,Q}(z_{eq})\, N_{D,w,Q_o}\, k_{Q,Q_o}\, k^{Q}_{w,s}$$

from dose to water formalism

Dose at a point in water from an MV photon beam

Photon energy fluence: Ψ

Dose: $D_{w,Q}(z_{ref}) = \Psi(z_{ref}) \left[\frac{\mu_{en}}{\rho}\right]_w \beta_w$

collision kerma (K_c)

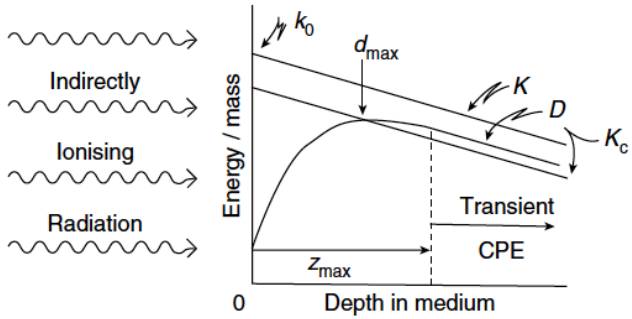

β_w CPE =1
TCPE scaling factor for high x-ray energies

ESTRO School

Derivation of formalism to convert ionisation in plastic to dose to water Equivalent Depth

In water at a reference depth

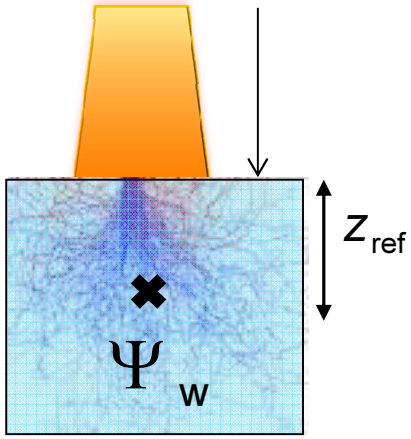

Phantoms irradiated with the same MV photon beam

In solid plastic at an equivalent depth

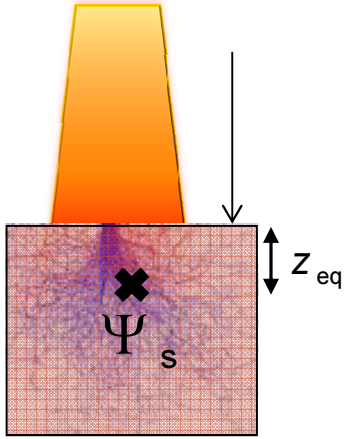

The energy fluences at corresponding depths in the two media can be related using O'Connor's density scaling theorem

According to this theorem energy fluences can be related through the inverse square law, once all distances in irradiation geometry (*SSD, field size and depth*) are scaled with the inverse ratio of relative electron densities of the two media

$$\frac{z_{s,eq}}{z_{w,ref}} = \frac{r_{s,eq}}{r_{w,ref}} = \frac{\rho_{e,w}}{\rho_{e,s}}$$

electron density in terms of electrons/g

Field size (radius)

O'Connor, J. E, PMB 1, 352-369, 1957

ESTRO School

Derivation of formalism to convert ionisation in plastic to dose to water
Scaling photon energy fluence

In water at a reference depth

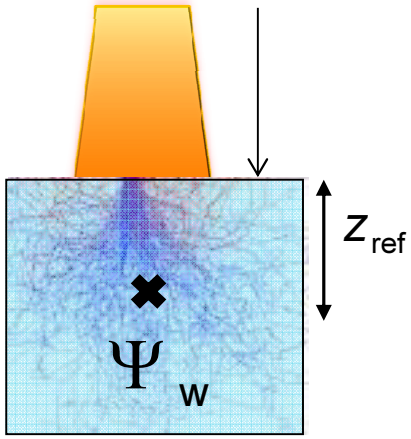

Phantoms irradiated with the same MV photon beam

In solid plastic at an equivalent depth

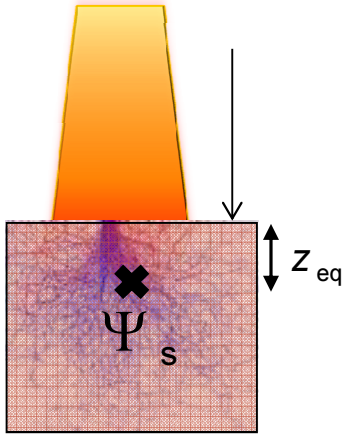

The energy fluences at corresponding depths in the two media can be related using O'Connor's density scaling theorem

According to this theorem energy fluences can be related through the inverse square law, once all distances in irradiation geometry (*SSD, field size and depth*) are scaled with the inverse ratio of relative electron densities of the two media

$$\frac{\Psi_w(z_{ref}, r_{ref})}{\Psi_s(z_{eq}, r_{eq})} = \left(\frac{SSD_{eq} + z_{eq}}{SSD_{ref} + z_{ref}}\right)^2$$

r : *field size*
(ref: in water)

O'Connor, J. E, PMB 1, 352-369, 1957

Derivation of formalism to convert ionisation in plastic to dose to water
Scaling photon energy fluence

In water at a reference depth

In solid plastic at an equivalent depth

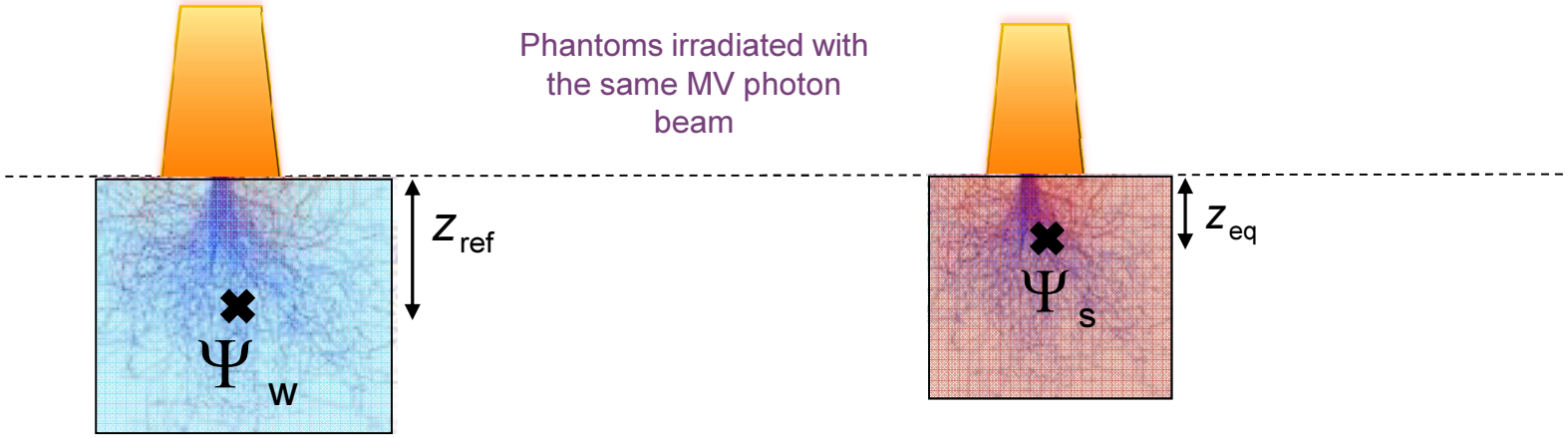

Simplification: by keeping SSD and field size (r) the same for the irradiation in solid phantom:

$$\frac{\Psi_w(z_{ref}, r_{ref})}{\Psi_s(z_{eq}, r_{ref})} = \left(\frac{SSD_{ref} + z_{eq}}{SSD_{ref} + z_{ref}}\right)^2 \frac{S_{p,s}(r_{eq})}{S_{p,s}(r_{ref})}$$

← Phantom scatter factors in solid phantom

Seuntjens et al, 2005, Med.Phys. 32 pp2945-

ESTRO School

Derivation of formalism to convert ionisation in plastic to dose to water
Converting dose in plastic to dose in water

In water at a reference depth

Phantoms irradiated with the same MV photon beam

In solid plastic at an equivalent depth

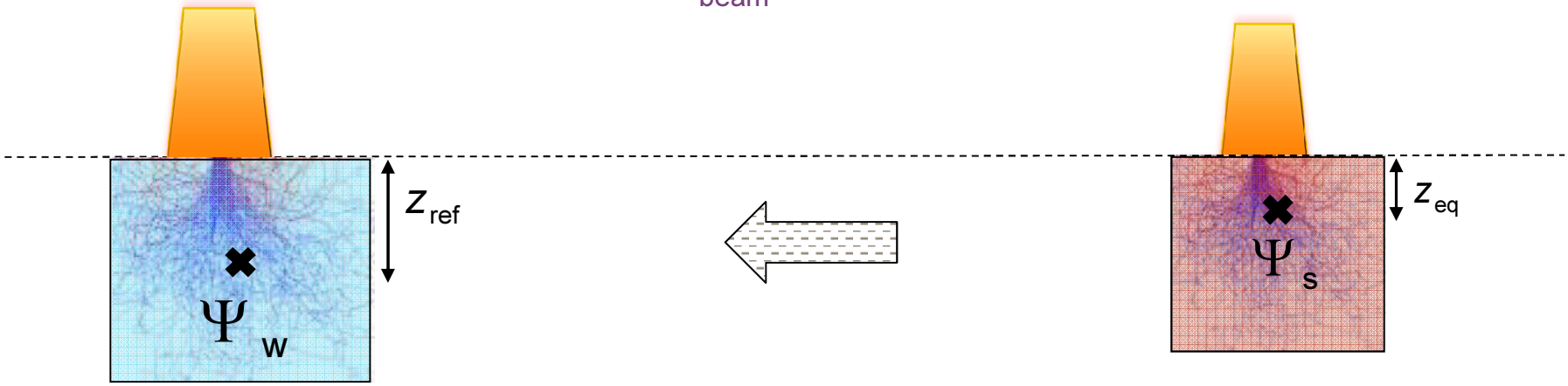

$$D_{w,Q}(z_{ref}) = \Psi_w(z_{ref}) \left[\frac{\mu_{en}}{\rho}\right]_w \beta_w$$

$$D_{s,Q}(z_{eq}) = \Psi_s(z_{eq}) \left[\frac{\mu_{en}}{\rho}\right]_s \beta_s$$

$$D_{w,Q}(z_{ref}, r_{ref}) = D_{s,Q}(z_{eq}, r_{ref}) \left(\frac{SSD_{ref} + z_{eq}}{SSD_{ref} + z_{ref}}\right)^2 \frac{S_{p,s}(r_{eq})}{S_{p,s}(r_{ref})} \left(\frac{\overline{\mu}_{en}}{\rho}\right)_s^w \beta_s^w$$

ESTRO School

Derivation of formalism to convert ionisation in plastic to dose to water
Converting ionisation measurement in plastic to dose in water

In water at a reference depth

Phantoms irradiated with the same MV photon beam

In solid plastic at an equivalent depth

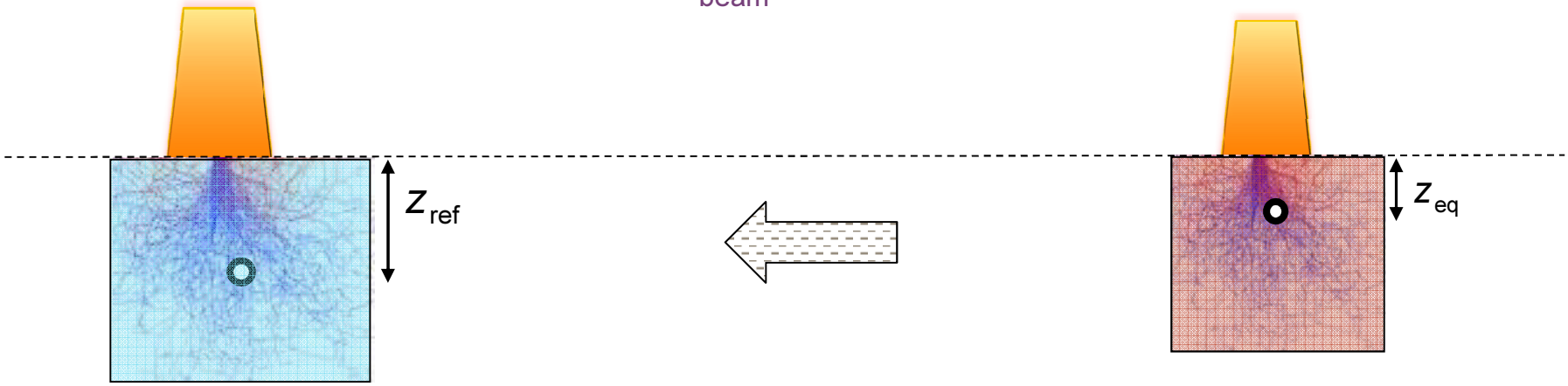

$$D_{w,Q}(z_{ref}, r_{ref}) = D_{s,Q}(z_{eq}, r_{ref}) \left(\frac{SSD_{ref} + z_{eq}}{SSD_{ref} + z_{ref}} \right)^2 \frac{S_{p,s}(r_{eq})}{S_{p,s}(r_{ref})} \left(\frac{\bar{\mu}_{en}}{\rho} \right)_s^w \beta_s^w$$

$$D_{s,Q}(z_{eq}) = M_{s,Q}(z_{eq}) N_{air} \left(\frac{\bar{S}}{\rho}(z_{eq}) \right)_{air}^s p_s$$

$$D_{s,Q}(z_{eq}) = M_{s,Q}(z_{eq}) N_{D,w,Qo} \cdot k_{Q,Q_0} \cdot \frac{\left[\bar{S}/\rho \right]_{air}^s \cdot p_{Q,s}}{\left[\bar{S}/\rho \right]_{air}^w \cdot p_{Q,w}}$$

ESTRO School

Derivation of formalism to convert ionisation in plastic to dose to water
Converting ionisation measurement in plastic to dose in water

In water at a reference depth

Phantoms irradiated with the same MV photon beam

In solid plastic at an equivalent depth

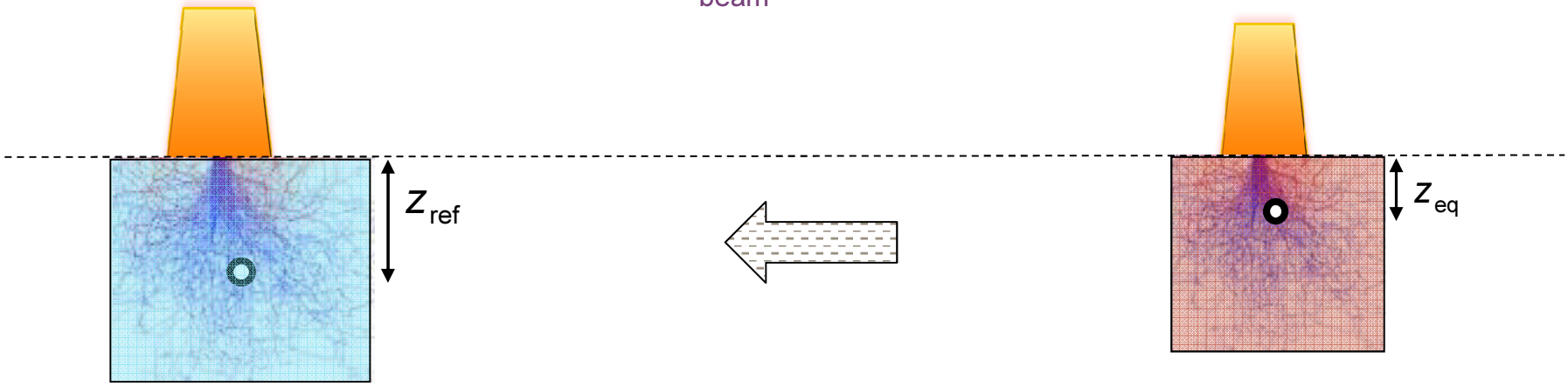

$$D_{w,Q}(z_{ref}, r_{ref}) = M_{s,Q}(z_{eq}, r_{ref})\, N_{D,w,Q_o} \cdot k_{Q,Q_o} \cdot \frac{\left[\bar{S}/\rho\right]_{air}^{s} \cdot p_{Q,s}}{\left[\bar{S}/\rho\right]_{air}^{w} \cdot p_{Q,w}} \cdot \left(\frac{SSD_{ref} + z_{eq}}{SSD_{ref} + z_{ref}}\right)^2 \cdot \left(\frac{S_{p,s}(r_{eq})}{S_{p,s}(r_{ref})}\right) \cdot \left.\frac{\overline{\mu_{en}}}{\rho}\right|_{s}^{w} \cdot \beta_s^w$$

Phantom dose conversion factor for the ionisation chamber

$$D_{w,Q}(z_{ref}) = M_{s,Q}(z_{eq})\, N_{D,w,Q_o}\, k_{Q,Q_o}\, k_{s,w,Q}$$

Seuntjens et al, 2005, Med.Phys. 32 pp2945-

ESTRO School

Derivation of formalism to convert ionisation in plastic to dose to water
Converting ionisation measurement in plastic to dose in water

In water at a reference depth

Phantoms irradiated with the same MV photon beam

In solid plastic at an equivalent depth

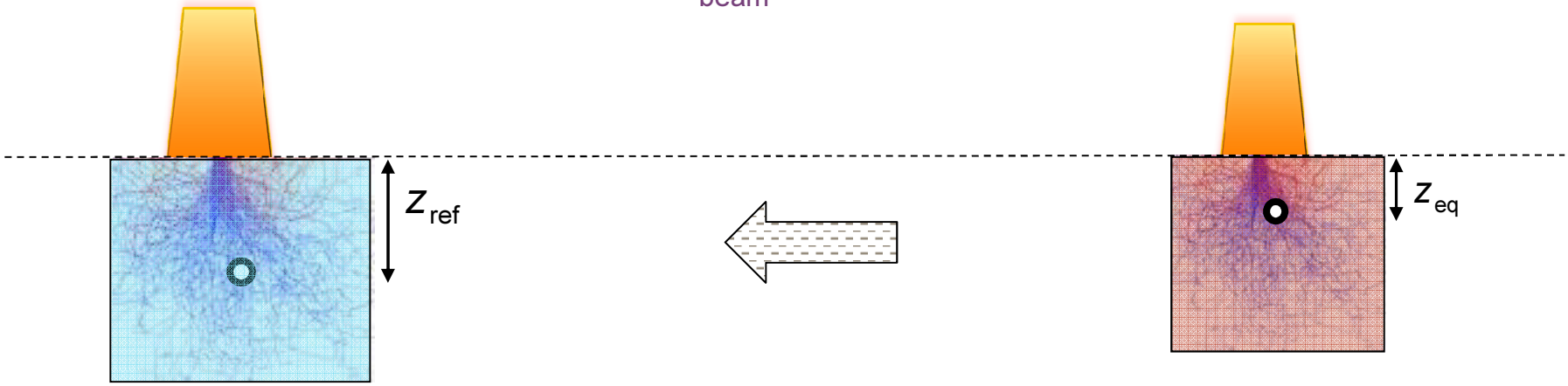

$$D_{w,Q}(z_{ref}) = M_{s,Q}(z_{eq})\, N_{D,w,Q_o}\, k_{Q,Q_o}\, k_{s,w,Q}$$

How does one determine:

equivalent depths
and
phantom dose conversion factors?

ESTRO School

Derivation of formalism to convert ionisation in plastic to dose to water
Derivation of depth scaling factor

Depth scaling, from exponential attenuation law,
for a monoenergetic photon beam and when Compton interactions dominates:

in water $\Phi_w = \Phi_o e^{-(\mu/\rho)_w z_w}$

in solid phantom $\Phi_s = \Phi_o e^{-(\mu/\rho)_s z_s}$

$$z_w = z_s \frac{\mu_s}{\mu_w} = z_s \mu_w^s \propto z_s (\rho_e)_w^s \qquad (z \quad in \ cm)$$

$$z_w = z_s \frac{(\mu/\rho)_s}{(\mu/\rho)_w} = z_s \left(\frac{\mu}{\rho}\right)_w^s \propto z_s (\rho_e)_w^s \qquad (z \quad in \ g/cm^2)$$

depth scaling factor

ESTRO School

Distance scaling (range-scaling factor)

Field size (radius)

depth [cm]

$$\frac{z_{s,eq}}{z_{w,ref}} = \frac{r_{s,eq}}{r_{w,ref}} = \frac{\rho_{e,w}}{\rho_{e,s}}$$

electron density in terms of electrons/g

Valid when mass attenuation coefficient proportional to electron density. i.e mono-energetic beams and low energy MV beams

Formalism to convert dose to phantom to dose to water

Compton & pair production attenuation coefficients μ/ρ

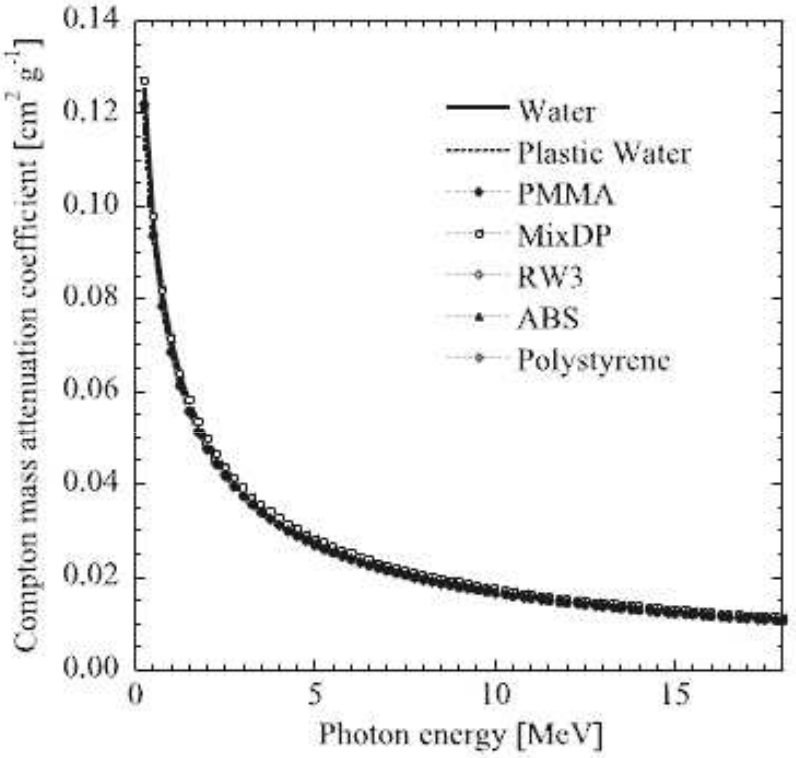

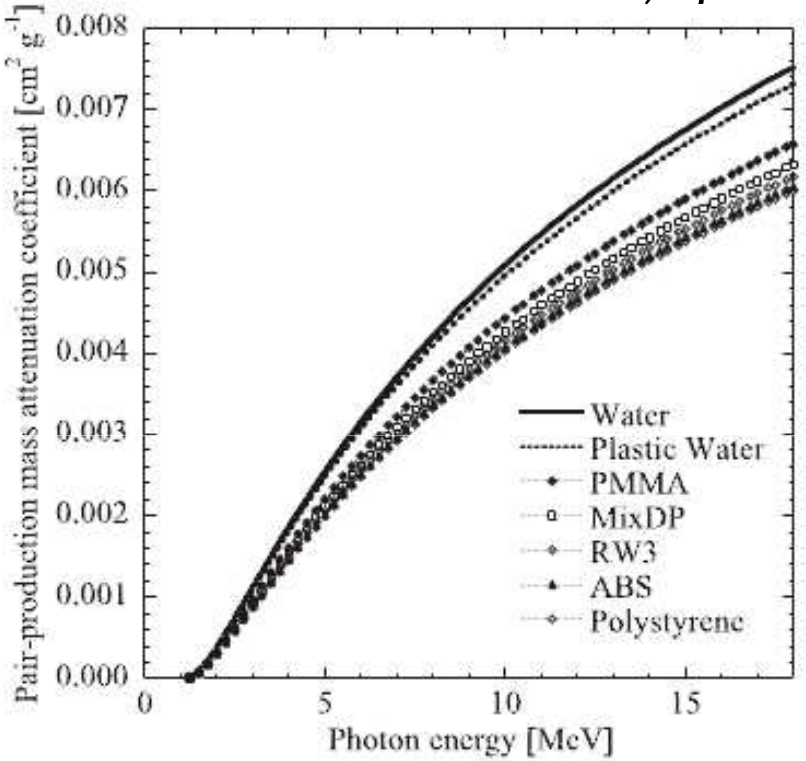

Elements	Water	WT1	457-CTG	RW3	MixDP	WE211	WE211R	Plastic Water	Plastic Water DT	Virtual Water	Polystyrene	PMMA	ABS [a]
Z_{eff} [c]	7.22	6.35	6.35	5.83	6.38	6.34	7.07	6.83	6.83	6.35	5.61	6.24	5.67

Fujita etal 2010 Radiat. Res. 51 707-

ESTRO School

Derivation of formalism to convert ionisation in plastic to dose to water
Derivation of depth (distance) scaling factor

$$(\rho_e)_w^s \quad vs \quad \left(\frac{\bar{\mu}}{\rho}\right)_w^s$$

Table 2. Depth scaling factors for the open and blocked field and relative electron densities of commercially available solid phantoms. The depth scaling factors are determined from photon energy spectra at 10 cm depth for 10 cm × 10 cm open and blocked field, respectively.

Phantom	$(\rho_e)_{pl,w}$	Nominal photon energy [MV]							
		4		6		10		15	
		Open	*MBF	Open	MBF	Open	MBF	Open	MBF
WT1	0.972	0.971	0.970	0.970	0.969	0.967	0.966	0.964	0.965
457-CTG	0.972	0.971	0.970	0.970	0.969	0.967	0.966	0.964	0.965
RW3	0.966	0.965	0.964	0.964	0.962	0.958	0.957	0.953	0.954
MixDP	1.012	1.010	1.009	1.008	1.006	1.001	1.000	0.996	0.997
WE211	0.973	0.972	0.972	0.971	0.970	0.968	0.967	0.965	0.966
WE211R	0.974	0.974	0.973	0.973	0.972	0.969	0.969	0.966	0.967
Plastic Water	0.969	0.970	0.970	0.970	0.970	0.970	0.970	0.970	0.970
Plastic Water DT	0.963	0.963	0.963	0.962	0.962	0.962	0.962	0.961	0.961
Virtual Water	0.968	0.968	0.967	0.967	0.966	0.963	0.963	0.961	0.961
Polystyrene	0.969	0.967	0.966	0.965	0.963	0.958	0.957	0.953	0.954
PMMA	0.972	0.970	0.970	0.969	0.968	0.965	0.965	0.963	0.963
ABS	0.972	0.970	0.969	0.968	0.966	0.961	0.960	0.956	0.957

*MBF : MLC blocked field

$$\bar{\mu}/\rho = \frac{\int_{E_{min}}^{E_{max}} \Psi(E)[\mu(E)/\rho]\,dE}{\int_{E_{min}}^{E_{max}} \Psi(E)\,dE}$$

Ratio of electron densities good approximation for 4MV.

For some materials energy dependence up to 4%

For the clinical x-ray beams scaling by the electron density ratio is not a good approximation.

Fujita etal 2010 Radiat. Res. 51 707-

ESTRO School

Derivation of formalism to convert ionisation in plastic to dose to water
Distance scaling in a clinical beam

depth scaling, polyenergetic photon beam:

$$\frac{z_{s,eq}}{z_{w,ref}} = \frac{(\bar{\mu}/\rho)_w}{(\bar{\mu}/\rho)_s}$$

effective mass attenuation coefficients

$$TPR(z, A) \approx e^{-\left(\frac{\bar{\mu}}{\rho}\right)(z - z_{ref})}$$

depth

field size

Depths in (g/cm^2)
z_{ref} where TPR is normalised

Depth scaling factor for the clinical beam:

$$c_s = \frac{\left(\bar{\mu}/\rho\right)_s}{\left(\bar{\mu}/\rho\right)_w} \approx \frac{z_w}{z_s} \Rightarrow z_{s,eq} = \frac{z_{w,ref}}{c_s}$$

ESTRO School

Derivation of formalism to convert ionisation in plastic to dose to water
Distance scaling in a clinical beam

Example: distance scaling for Plastic Water DT (PWDT)

$$c_{\mathrm{PWDT}} = \frac{\left(\bar{\mu}/\rho\right)_{\mathrm{PWDT}}}{\left(\bar{\mu}/\rho\right)_{\mathrm{w}}} \approx \frac{z_{\mathrm{w}}}{z_{\mathrm{PWDT}}} \Rightarrow z_{s,eq} = \frac{z_{\mathrm{w,ref}}}{c_{\mathrm{PWDT}}}$$

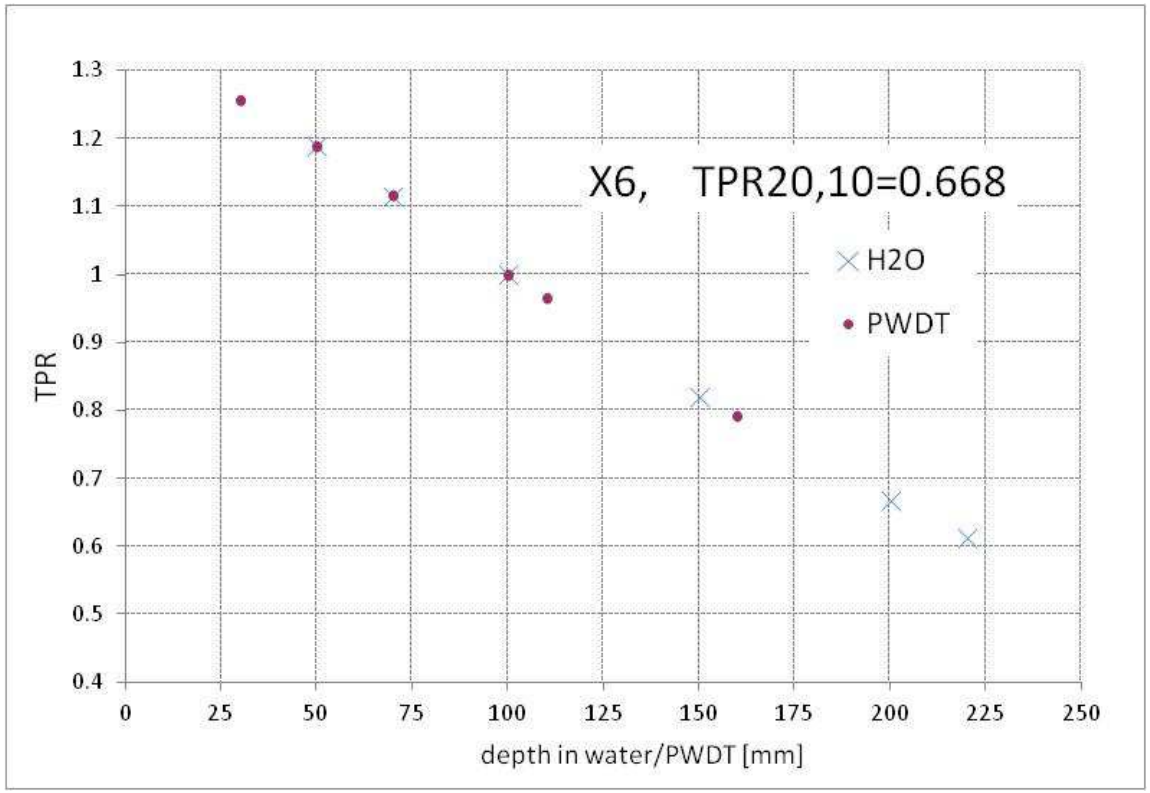

At the depth of 5cm:

$$c_{\mathrm{PWDT}} = 0.983$$

and NOT:

The water equivalent distance of 5cm PWDT is 4.92cm

ESTRO School

Derivation of formalism to convert ionisation in plastic to dose to water
Phantom dose conversion factor

$k_{s,w,Q}$

- Calculated; using basic (tabulated) interaction coefficient data; and: stopping power ratio data and chamber perturbation factors generated by Monte Carlo methods
- Directly measured

$$k_{s,w,Q} = \left. \frac{M_{w,Q}(z_{ref})}{M_{s,Q}(z_{eq})} \right|_{\text{equal MUs}}$$

Example: at 5cm PWDT, 6MV (TPR20,10=0.668), PTW30013 cylindrical chamber

$$c_{\text{PWDT}} = 0.983$$

$$k_{\text{PWDT},w,Q} = \left. \frac{M_{w,Q}(5,\text{SSD})}{M_{\text{PWDT},Q}(5.09,\text{SSD})} \right|_{\text{equal MUs}} = 1.004$$

ESTRO School

Derivation of formalism to convert ionisation in plastic to dose to water
Phantom dose conversion factor

Water equivalence for: Solid water (RMI-457) and Lucite (PMMA)

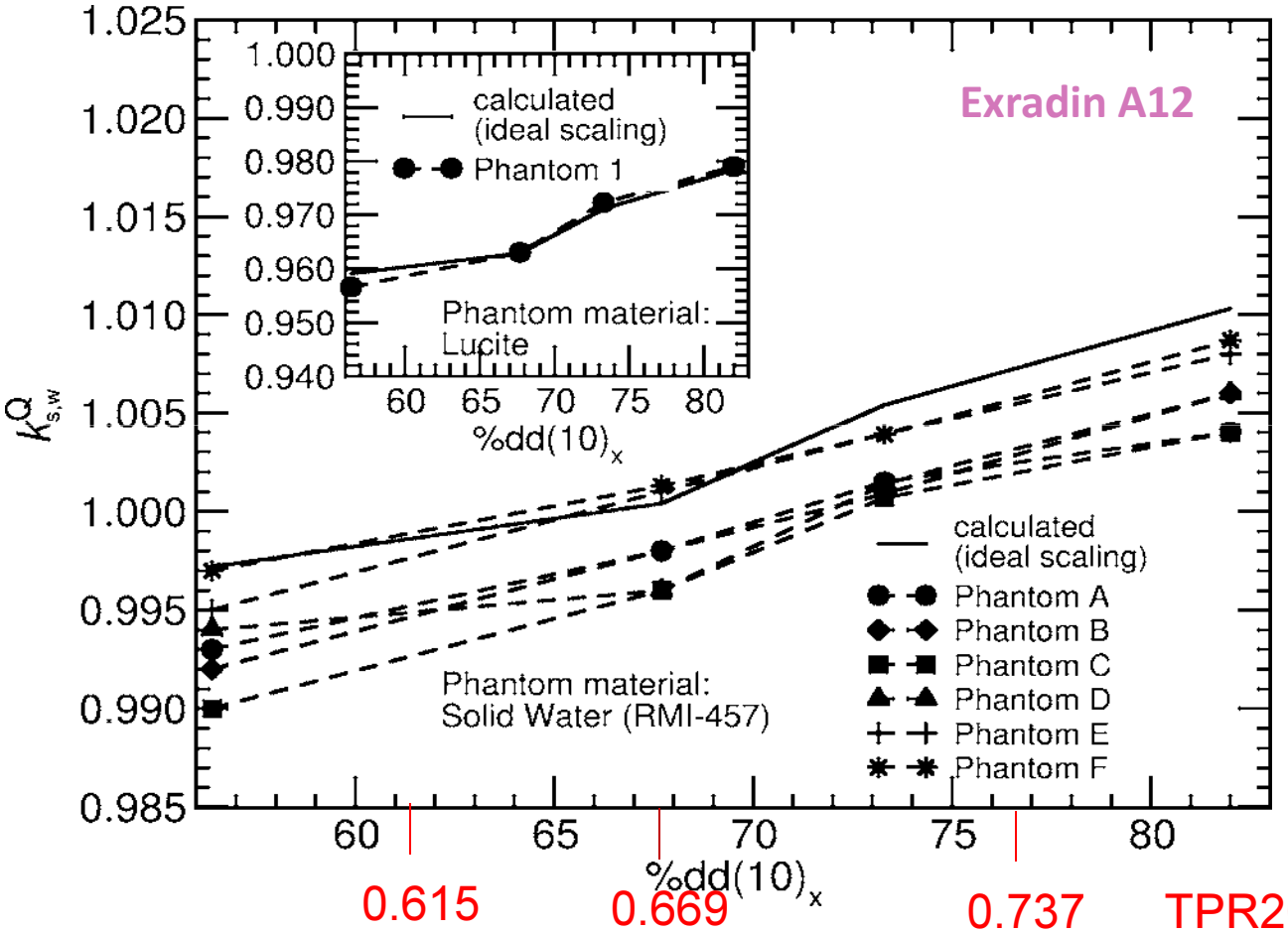

RMI-457
6 & 18MV: ~+/-0.5%

PMMA
6MV ~-4%
18MV ~-2%

0.615 0.669 0.737 TPR2010

Jan Seuntjens etal, 2005, Med.Phys. 32 pp2945-

ESTRO School

Derivation of formalism to convert ionisation in plastic to dose to water
Phantom dose conversion factor

Water equivalence for: Plastic water (PW) and Plastic Water DT (PWDT) by CIRS

	TPR_{10}^{20}	0.615	0.669	0.737	0.779
Chamber	$\%dd(10)_x$	61.8	66.3	73.3	80.9
		PW			
PTW 30001		0.996	0.997	0.998	1.000
PTW 30013		0.997	0.998	0.999	1.001
PTW 30002 and 30004		0.997	0.998	0.998	1.000
Exradin A12		0.998	0.998	0.999	1.001
		PWDT			
PTW 30001		0.995	0.997	0.999	0.999
PTW 30013		0.996	0.998	1.000	1.001
PTW 30002 and 30004		0.996	0.998	0.999	1.000
Exradin A12		0.996	0.998	1.000	1.001

$k_{s,w,Q}$

0.995 -1.001

=1 within 0.5%

(0.6% - 0.7%, 1σ)

PTW 30001 Farmer type chamber

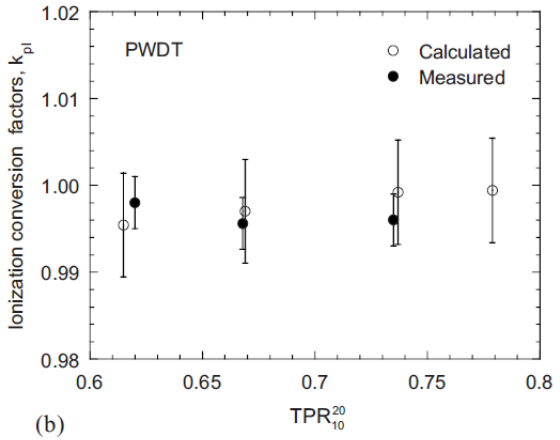

Araki et al, 2009, Med.Phys. 36 (7) pp2992-

ESTRO School

Derivation of formalism to convert ionisation in plastic to dose to water
Phantom dose conversion factor

Water equivalence: dose ratios solid/water

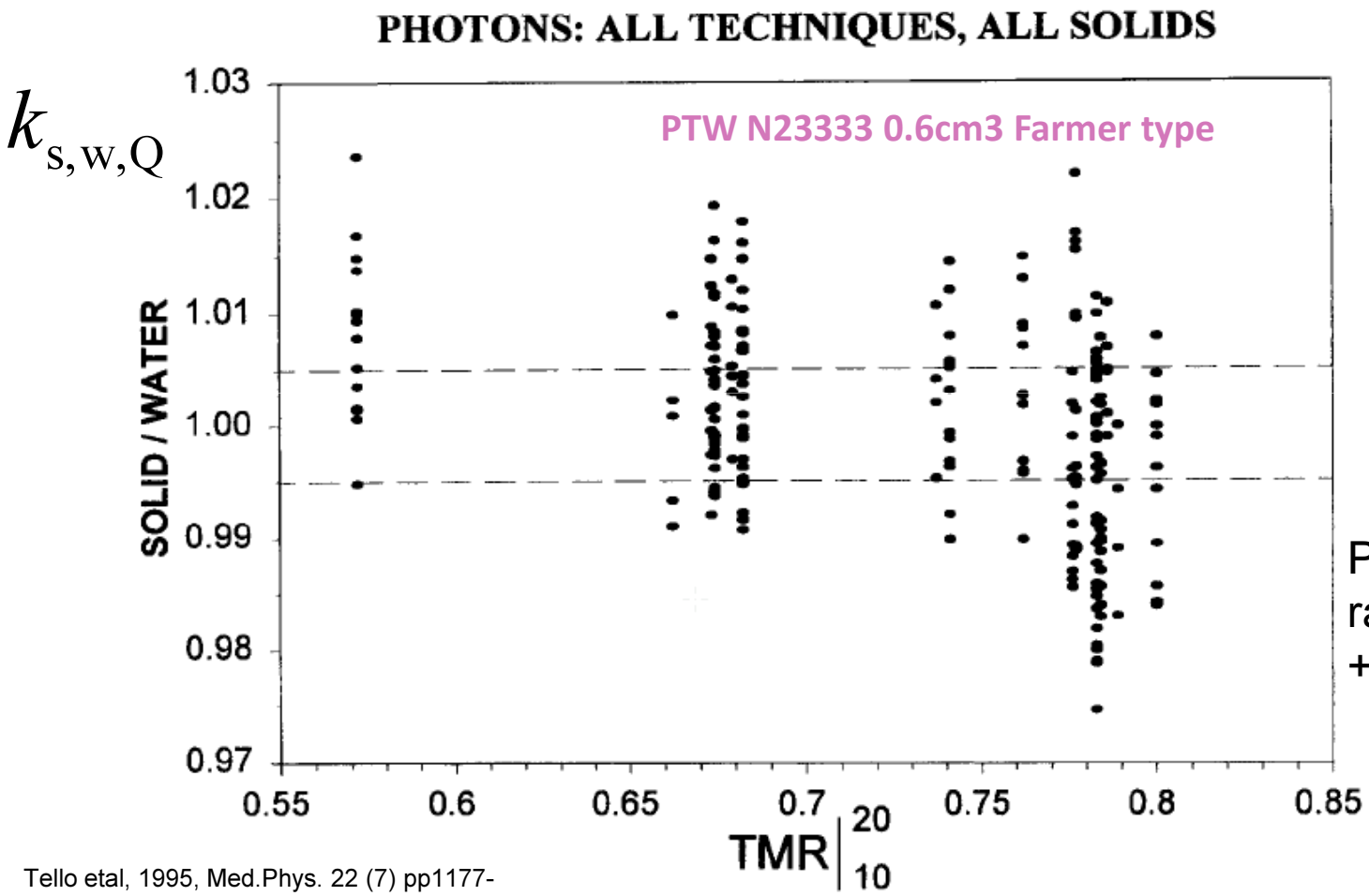

Plastic Water (PW) ratios within +/-1%

Tello etal, 1995, Med.Phys. 22 (7) pp1177-

ESTRO School

Dose to phantom to dose to water in water

The formalism to convert ionisation measured in a phantom to dose in water requires:

- Data on phantom material (available)
- Chamber perturbation factors (not widely available)
- Phantom conversion factor can be determined experimentally
- **Epoxy resin based solid phantoms** shown to be equivalent to within 1% to water

To choose a suitable water- equivalent solid phantom for dosimetry:

•the **depth scaling factor** needs to be close to unity; namely the material needs to have effective mass attenuation coefficient close to that of water

•the **phantom dose conversion factor (fluence scaling factor)** to be close to unity

When can a plastic phantom be considered water-equivalent?

In MV photon beams

(where energy deposition is mainly due to Compton interactions → O'Connor scaling theorem is applicable)

- Depth scaling proportional to **the ratio of mass attenuation coefficients.**
- Measurements in **polystyrene** can show differences from water of up to **3%** (Christ 1995), depending on photon beam quality and depth.T
- The agreement in dosimetric quantities (depth doses, TPR, TMR, OF) between the **epoxy-resin phantom materials** and water are generally within 1% (energy range between Co-60 and 18 MV X-rays)

Jan Seuntjens etal, 2005, Med.Phys. 32 pp2945-

Araki etal, 2009, Med.Phys. 36 (7) pp2992-

When can a plastic phantom be considered water-equivalent?

In kV photon beams

•Energy deposition is mainly due to photo-electric effect and although one would expect that solid plastics with Z_{eff} close to that of water would be water equivalent, recent research has shown otherwise.

•Departure from water equivalence worsens at low kV beams.

•It is thus important to check equivalence with water also in kV beams (comparison of relative dose data, and back scatter factors)

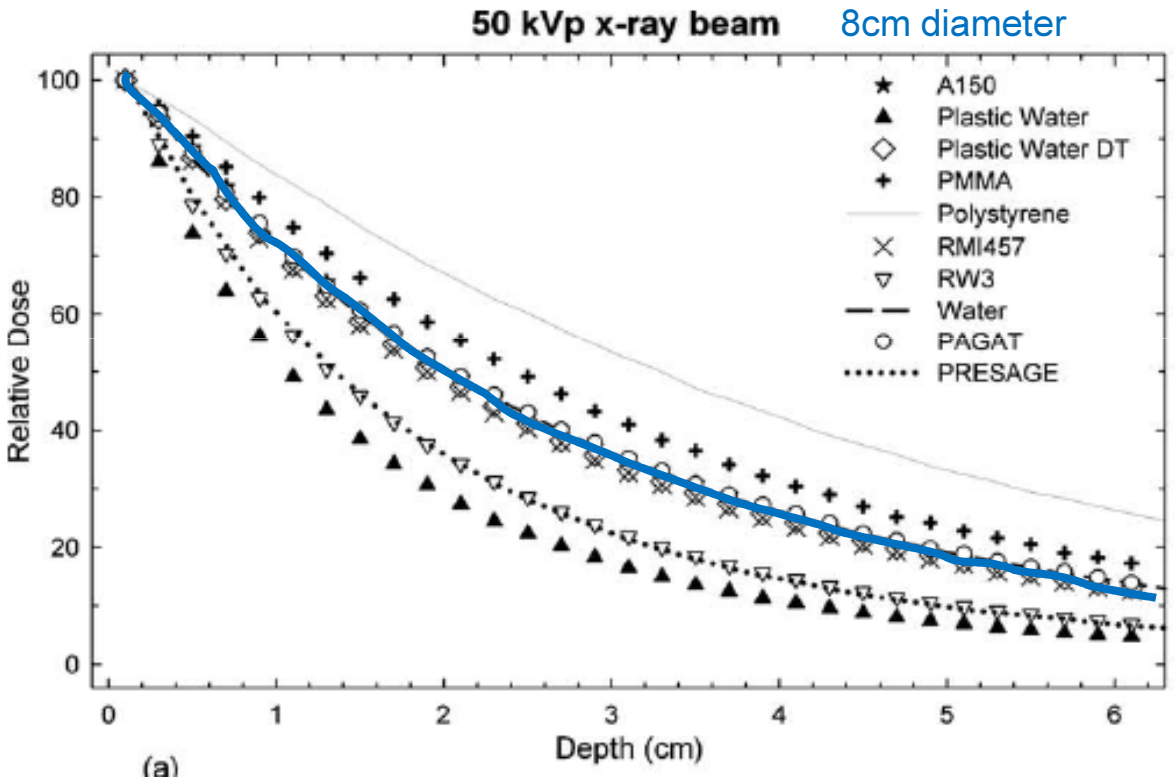

Hill et al, Med Phys, 37 (8), 2010 p4355-

ESTRO School

When can a plastic phantom be considered water-equivalent?

In MeV beams

Depths have to be scaled so that the spectra at the measuring point are similar, the same Sw,air is applicable.

Measuring at a scaled depths, electron fluences differ between two materials, due to different scattering powers.

→ Need of a fluence correction factor h_m (may vary with depth)

Phantoms that are electrical insulators: Charge storage effects, which modify the electron fluence incident on the ion chamber; cylindrical chambers more affected than plane parallel chambers

Recommended to use thin slabs (<2 cm thick) of plastic

McEwen, Med Phys 33(4), 2006, p876-

Classification of solid phantoms for dosimetry

Material	Advantages	Disadvantages
Graphite	Used in standards laboratories for many years, closely matches the scattering properties of water. Burns *et al.*[7] imply that no fluence correction is required.	Large range scaling factor of around 1.14. Handling issues in the clinic. Ding *et al.*[8] showed that the assumption of a zero fluence correction might not be correct.
Generic plastics (polystyrene, PMMA)	Easy to obtain, cheap. Close to water equivalent.	Cannot match both scattering and stopping powers due to carbon content. Charge storage can affect chamber measurement (Galbraith *et al.*[9]).
Epoxy-resin materials	Specifically designed to be water equivalent (i.e. $h_m = C_{pl} = 1$) No reported charge-storage effects.	Limited data in the literature on the differences with water for individual materials.

C_{pl} is spatial scaling factor

h_m is fluence scaling factor

McEwen, Med Phys 33(4), 2006, p876-

Phantom for plan QA: measurement vs calculation

Example: Check dose from treatment plan with measurement in a PMMA phantom

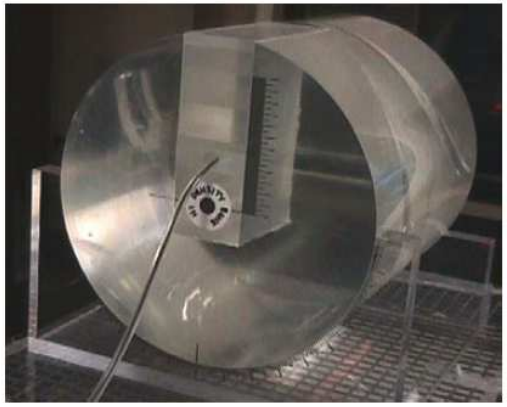

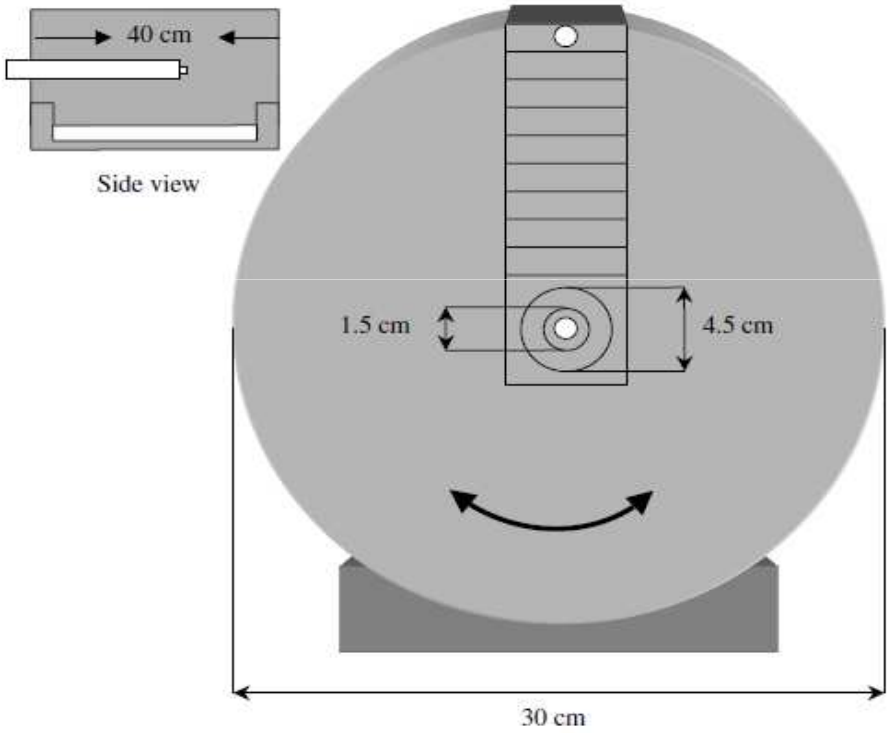

Ma et al, PMB 48 (2003) 561-572

Phantom for plan QA: measurement vs calculation

Dose determination in phantom

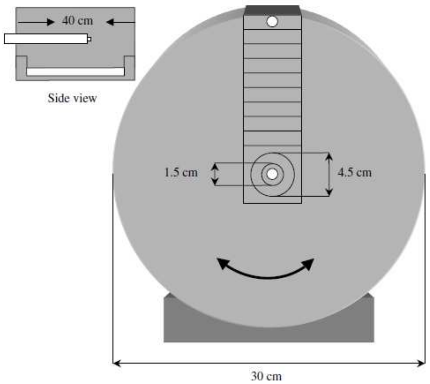

Formalism to derive dose to water from from ionisation measurements in PMMA

$$D_{w}^{clin} = D_{PMMA}^{clin}\left[\left(\frac{\overline{\mu}_{en}}{\rho}\right)_{PMMA}^{w}\right]_{cal}\left[CF_{PMMA\rightarrow w}^{scat}\right]_{cal}$$

$$D_{PMMA}^{clin} = M_{PMMA}^{clin}\ k_{ion}\left[N_{air}\left(\frac{\overline{S}}{\rho}\right)_{air}^{PMMA}\ p_{repl}\,p_{wall}\right]_{cal}$$

Chamber and medium specific perturbation factors are for the calibration geometry and not the clinical field

Ma et al, PMB 48 (2003) 561-572

Calculations of dose in phantom

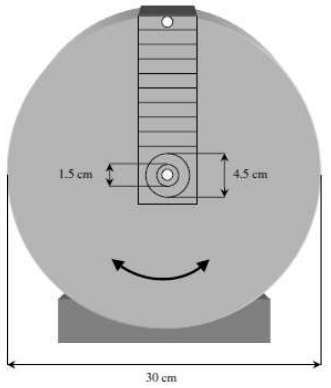

How accurate are the HU-density conversions for plastic phantoms?

Would it be better to create a virtual phantom with the density of PMMA?

How does the TPSs handle materials different from water?

Does the TPS calculates dose to PMMA in PMMA or dose to water in PMMA?

These questions we need to ask ourselves!

ESTRO School

Note on TPS dose reporting (MV beams)

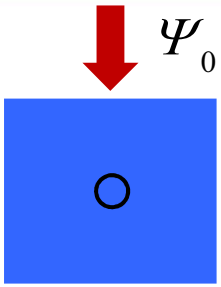

approx. equations:

Reference dosimetry: dose to a small water element *w* embedded at depth *z* in a large water phantom:

$$D_{w,W} \cong \frac{\mu_{en,w}}{\rho} \Psi_o \, e^{-\mu_w z}$$

Assuming that cell nuclei is water (ICRU 83)

i.e. dose to a small water element w embedded in a phantom of medium M:

$$D_{w,M} \cong \frac{\mu_{en,m}}{\rho} \Psi_o \, e^{-\mu_m z} \left(\frac{\bar{S}}{\rho} \right)_m^w$$

Conv. TPS calculate and report this!

Dose to the medium in the medium:

$$D_{m,M} \cong \frac{\mu_{en,m}}{\rho} \Psi_o \, e^{-\mu_m z}$$

MC and some implementations of kernel based alg. calculate and report this

$\Rightarrow$ conversion of dose to medium to dose to water

$$D_{w,M} = D_{m,M} \left(\frac{\bar{S}}{\rho} \right)_m^w$$

Conclusions: measurement in solid phantoms

•Liquid water the recommended medium for **reference dosimetry**.

•Formalism exists to convert dose to solid phantom to dose to water;

- Epoxy resin-based solid phantoms could be used for both reference and relative dosimetry (to within 1%), BUT one needs to check these first for water equivalence.
- Formalism can be used both for dose-to-water and dose-to medium dose verification

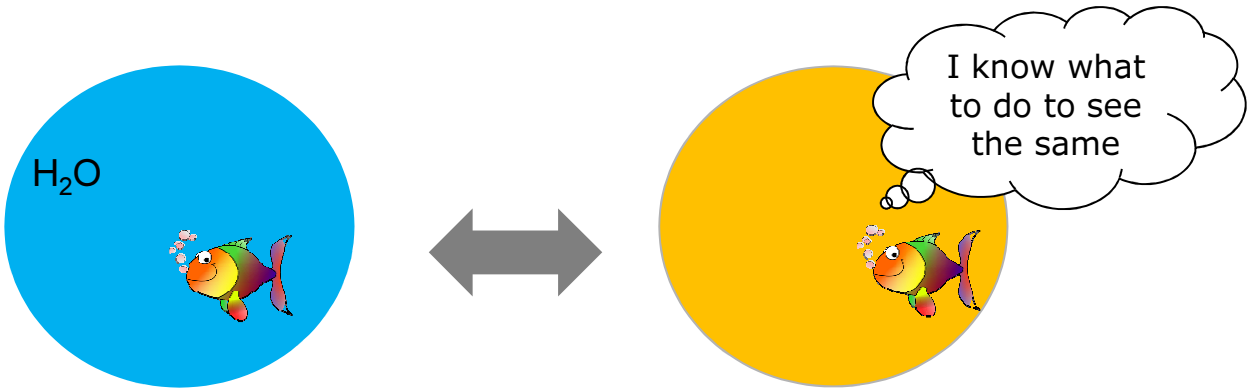

Conclusions: measurement vs calculation in solid phantoms

•It is important to understand how the TPS handles different materials and reports dose.

•We have been working on the assumption that homogeneous solid phantoms which are shown to be water-equivalent for reference dosimetry and relevant dosimetry using an ionization chamber are also water-equivalent under a multiple beam arrangements (for the verification of treatment plans).

•The water-equivalence of complex phantoms with embedded detector systems (not necessarily ionization chambers) and their comparison TPS calculations in these phantoms is an area where more investigations are needed.

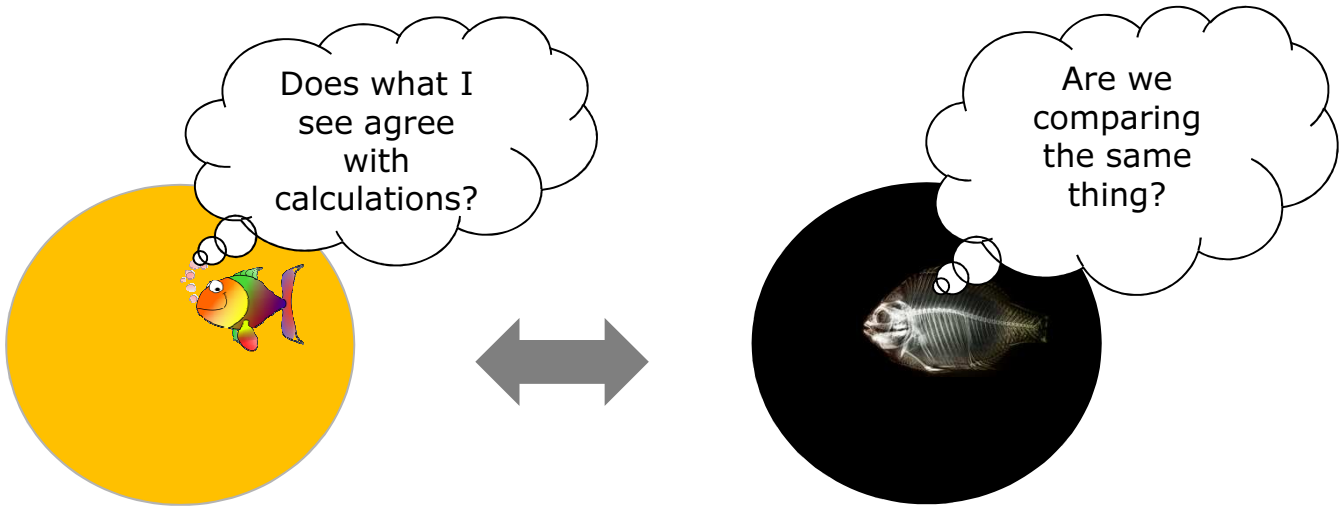

Relevant references

Allahverdi, M., A. Nisbet, et al. (1999). "An evaluation of epoxy resin phantom materials for megavoltage photon dosimetry." Phys Med Biol **44**(5): 1125-1132.

Araki, F., Y. Hanyu, et al. (2009). "Monte Carlo calculations of correction factors for plastic phantoms in clinical photon and electron beam dosimetry." Med Phys **36**(7): 2992-3001.

Fujita, Y., N. Tohyama, et al. (2010). "Depth scaling of solid phantom for intensity modulated radiotherapy beams." J Radiat Res **51**(6): 707-713.

Hill, R., Z. Kuncic, et al. (2010). "The water equivalence of solid phantoms for low energy photon beams." Med Phys **37**(8): 4355-4363.

Ma, C. M., S. B. Jiang, et al. (2003). "A quality assurance phantom for IMRT dose verification." Phys Med Biol **48**(5): 561-572.

Ma, C. M. and J. Li (2011). "Dose specification for radiation therapy: dose to water or dose to medium?" Phys Med Biol **56**(10): 3073-3089.

McEwen, M. R. and D. Niven (2006). "Characterization of the phantom material virtual water in high-energy photon and electron beams." Med Phys **33**(4): 876-887.

Ramaseshan, R., K. Kohli, et al. (2008). "Dosimetric evaluation of Plastic Water Diagnostic-Therapy." J Appl Clin Med Phys **9**(2): 2761.

Seuntjens, J., M. Olivares, et al. (2005). "Absorbed dose to water reference dosimetry using solid phantoms in the context of absorbed-dose protocols." Med Phys **32**(9): 2945-2953.

Tello, V. M., R. C. Tailor, et al. (1995). "How water equivalent are water-equivalent solid materials for output calibration of photon and electron beams?" Med Phys **22**(7): 1177-1189.

ESTRO School

WWW.ESTRO.ORG/SCHOOL

Detectors for measurement; best detector for different jobs

Part 1: Point detectors

Núria Jornet

Servei de Radiofísica
Hospital Sant Pau, Barcelona

Lecture Content

1. Absorbed dose determination: Differences between reference and non reference conditions (standard and non-standard radiation beams)

   Going back to some fundamentals of dosimetry to understand the validity of the factors and corrections applied to detectors readings in different irradiation conditions.

2. Specific problems associated with relative dose measurements (scans/output).

   Importance of how data are measured phantom and detector.

3. Summary.

ESTRO School

I will focus mainly on MV x-rays

I will mainly discuss the use of detectors for relative dose measurements.
I will compare detectors widely used to new kids on the market

Things that I will/won't cover

I won't talk about detectors to be used in proton/ion dose measurements

I won't cover TLD/OSL

Raiders of the perfect detector

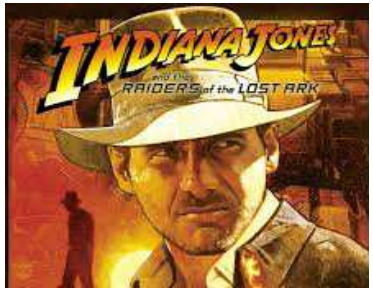

- High Repeatability
- High Reproducibility [no variation of response with i.e. accumulated dose]
- High Accuracy and precision
- High Sensitivity
- Adequate dose range and lineality of the response with dose
- Energy independence
- Insensitivity of the response to influence quantities (dose rate, temperature, pressure, direction…)
- Small dimensions

Precision: Statistical reproducibility of measurements+resolution of measuring system
Accuracy how closely the measurement value agrees with the true value.

Principle of absorbed dose measurements

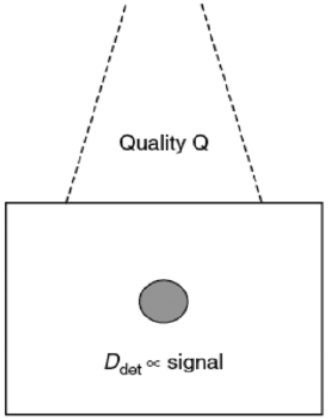

Ionisation chamber	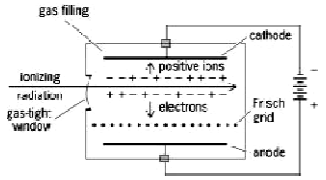	Charge
Diode	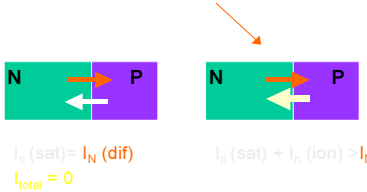	Charge
Diamond	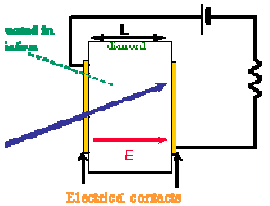	Charge
Scintillator	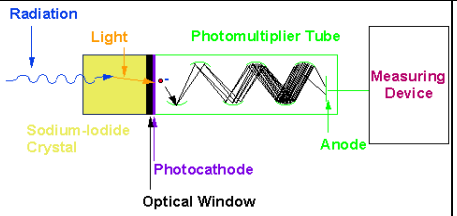	Light
Film	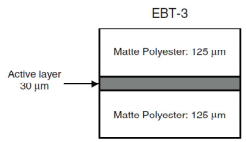	Chemical reaction changes opaqueness. Optical Density

Challenges: reference versus relative dosimetry

Reference conditions

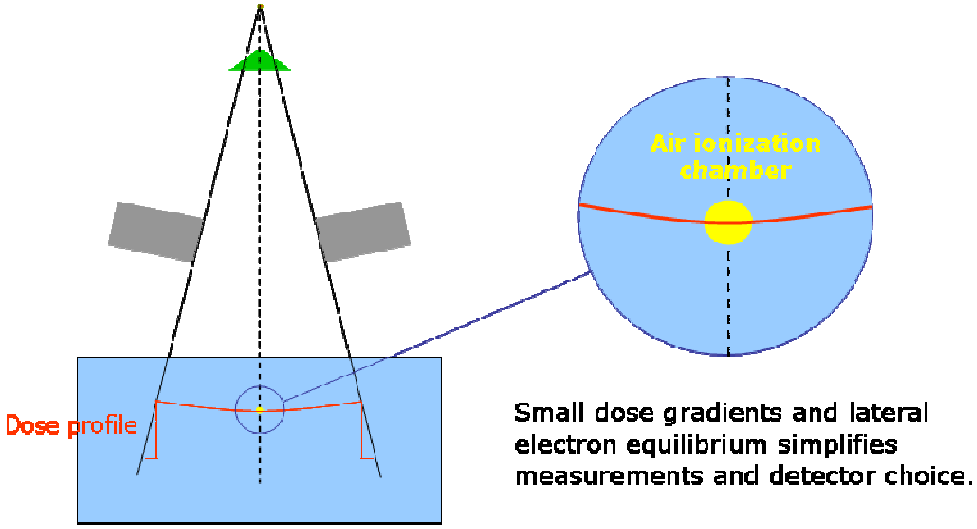

- Uniform electron fluence distribution over the detector.
- Beam spectra at the reference point in ref. conditions known.
- Detector of choice: **Ion Chambers**

Non reference conditions: *Relative dosimetry*

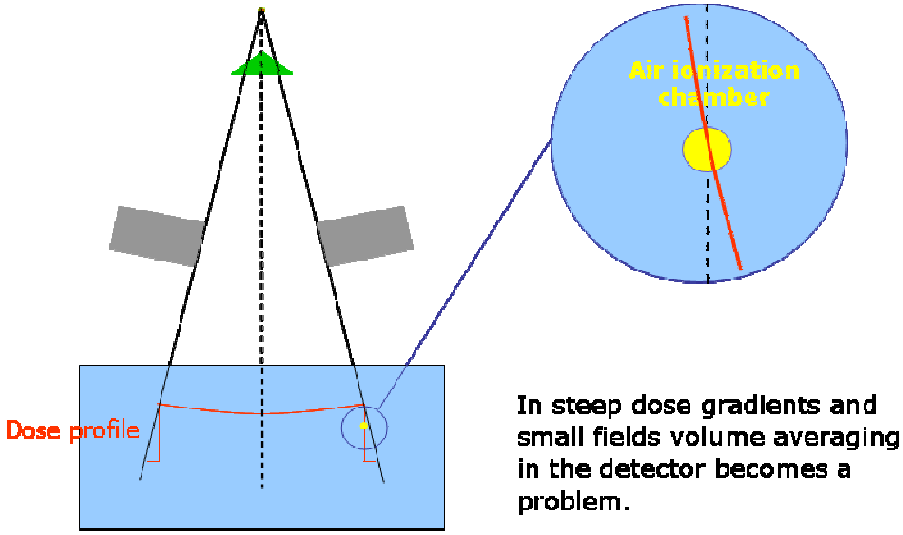

- Non-Uniform electron fluence distribution over the detector. **VOLUME AVERAGING**
- Beam spectra at the reference point may differ from beam spectra at the measuring point. **ENERGY DEPENDENCE; PERTURBATION FACTORS**
- Detector of choice: **???**

ESTRO School

Does the detector used matter?

Accelerator beam data commissioning equipment and procedures: Report of the TG-106 of the Therapy Physics Committee of the AAPM

Indra J. Das[a)]
Department of Radiation Oncology, University of Pennsylvania, Philadelphia, Pennsylvania 19104

Chee-Wai Cheng
Department of Radiation Oncology, Morristown Memorial Hospital, Morristown, New Jersey 07962

Ronald J. Watts
International Medical Physics Services, San Antonio, Texas 78232

Anders Ahnesjö
Uppsala University and Nucletron Scandinavia AB, 751 47 Uppsala, Sweden

John Gibbons
Department of Radiation Oncology, Mary Bird Perkins Cancer Center, Baton Rouge, Louisiana 70809

X. Allen Li
Department of Radiation Oncology, Medical College of Wisconsin, Milwaukee, Wisconsin 53226

Jessica Lowenstein
Radiological Physics Center, MD Anderson Cancer Center, Houston, Texas 77030

Raj K. Mitra
Department of Radiation Oncology, Ochsner Clinic, New Orleans, Louisiana 70121

William E. Simon
Sun Nuclear Corporation, Melbourne, Florida 32940

Timothy C. Zhu
Department of Radiation Oncology, University of Pennsylvania, Philadelphia, Pennsylvania 19104

(Received 4 February 2008; revised 18 July 2008; accepted for publication 18 July 2008; published 22 August 2008)

ESTRO School

Does the detector used matter?

"Since commissioning beam data are treated as a reference and ultimately used by treatment planning systems, it is **vitally important that the collected data are of the highest quality to avoid dosimetric and patient treatment errors** that may subsequently lead to a poor radiation outcome. Beam data commissioning should be performed with appropriate knowl- edge and **proper tools** and should be independent of the person collecting the data."

Detector characteristics

- **Volume effects: Size of sensitive volume**
- Energy dependence: Interactions in detector material
- Cable/stem leakage, polarity effect
- Dose rate dependence: Recombination, bias voltage
- Temperature dependence
- Long term stability/irradiation effects

Does size matter? Output factors

Volume effect detector dimension>1/4 field size

Incident beam direction

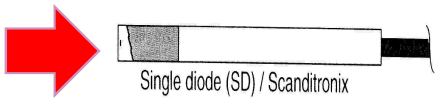

Detector			Φ (mm)	Length (mm)	Minimum field size (mm)
Pinpoint (PTW)	Air i.c.		2	5	8
RK (IBA)	Air i.c.	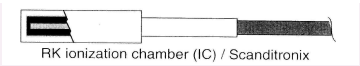	4	10	16
MicroLion (PTW)	Liquid i.c.	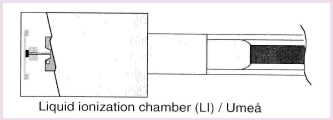	2.5	0.35	10
Diamond (PTW)	Diamond	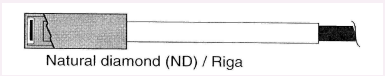	variable	0.3	
MicroDiamond (PTW)	Syntethic Diamond	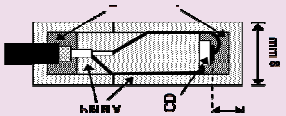	1.1	0.001	4.5
EDE diode (IBA)	Diode	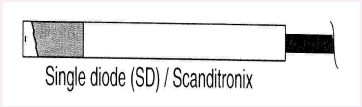	0.6	0.06	2.4
SFD diode (IBA)	Diode	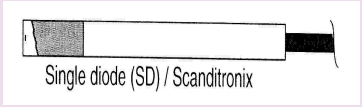	2	0.06	8
W1 (Standard Imaging)	Scintillator		2.8	3	12

Does size matter? Output factors

Volume effect detector dimension>1/4 field size

Incident beam direction

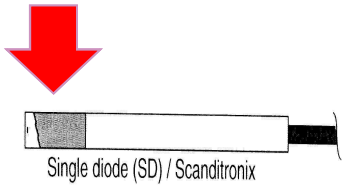

Detector			Φ (mm)	Length (mm)	Minimum field size (mm)
Pinpoint (PTW)	Air i.c.		2	5	20
RK (IBA)	Air i.c.	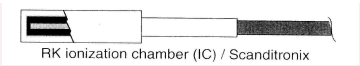	4	10	40
MicroLion (PTW)	Liquid i.c.	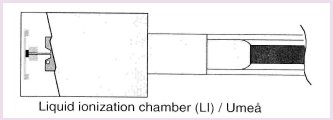	2.5	0.35	1.4
Diamond (PTW)	Diamond	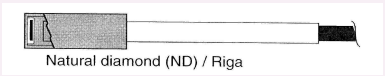	variable	0.3	1.2
MicroDiamond (PTW)	Syntethic Diamond		1.1	0.001	0.004
EDE diode (IBA)	Diode	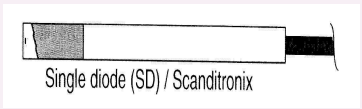	0.6	0.06	0.24
SFD diode (IBA)	Diode	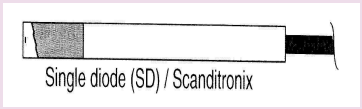	2	0.06	0.24
W1 (Standard Imaging)	Scintillator		2.8	3	12

Does size matter?
Profiles

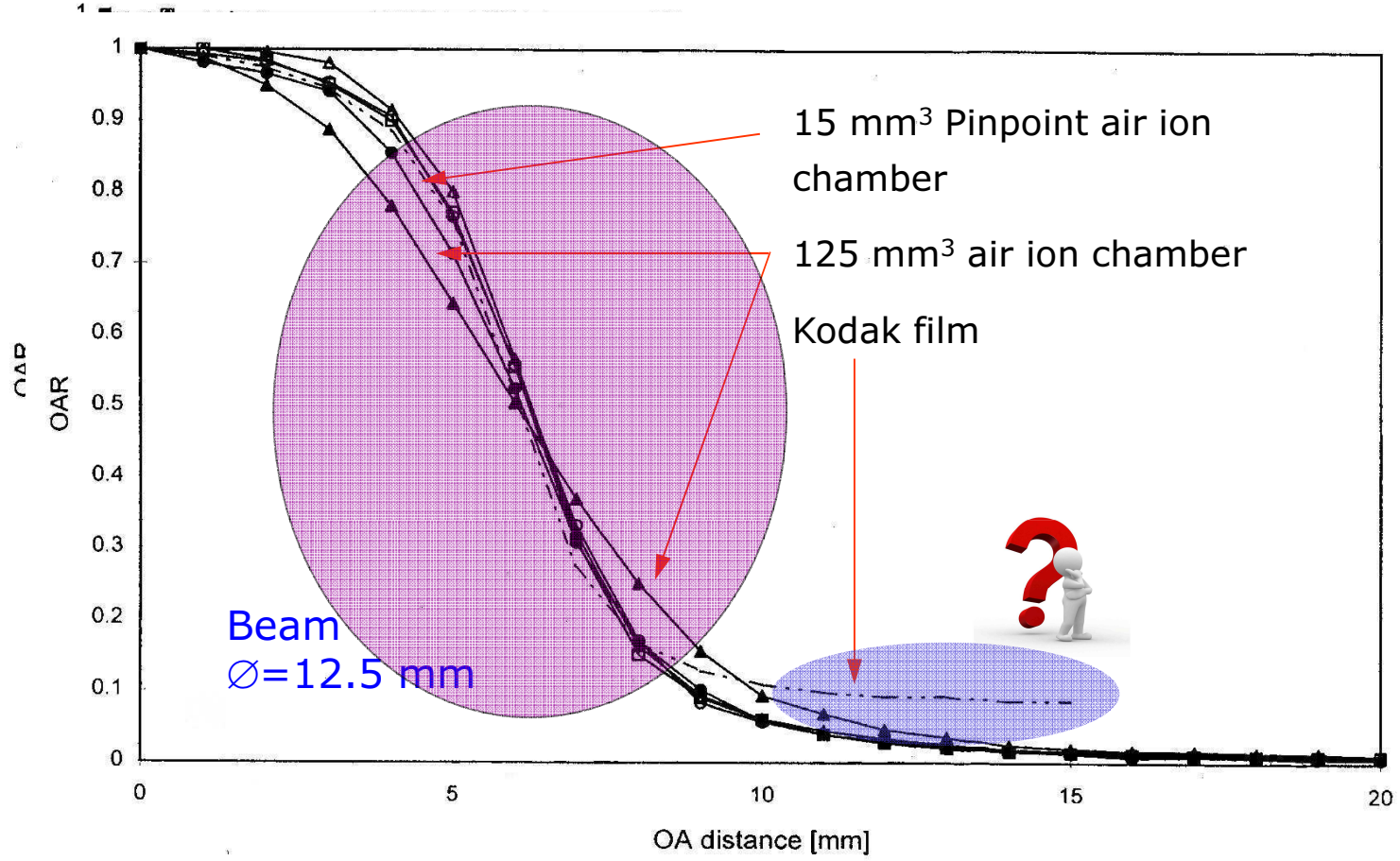

Film gold standard (resolution)
Film gold standard (resolution)

ESTRO School

Beam Profiles: Penumbra measurements using detectors of different sizes
The volume effect

6 MV, d_{max} (1.4 cm depth)

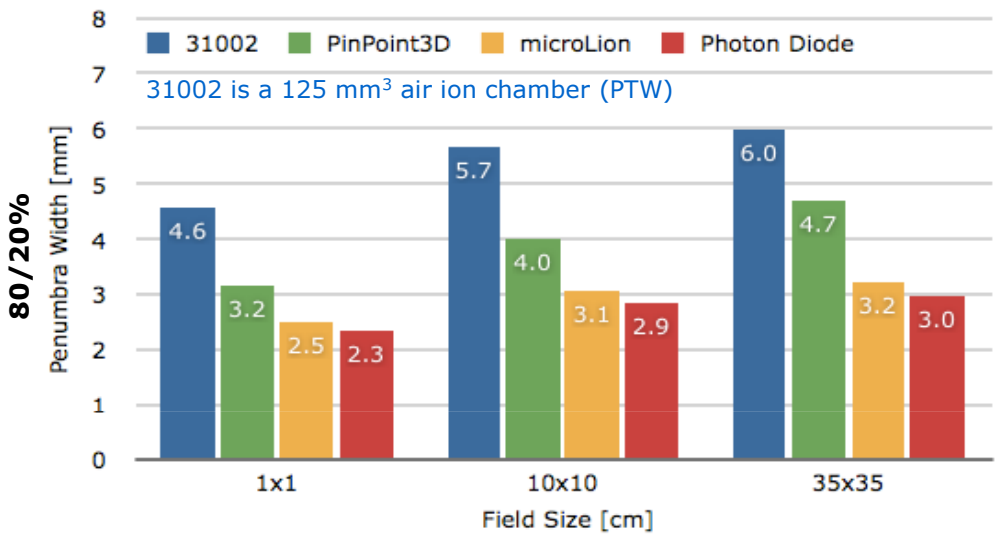

Krauss [20]

6 MV, 30 cm depth

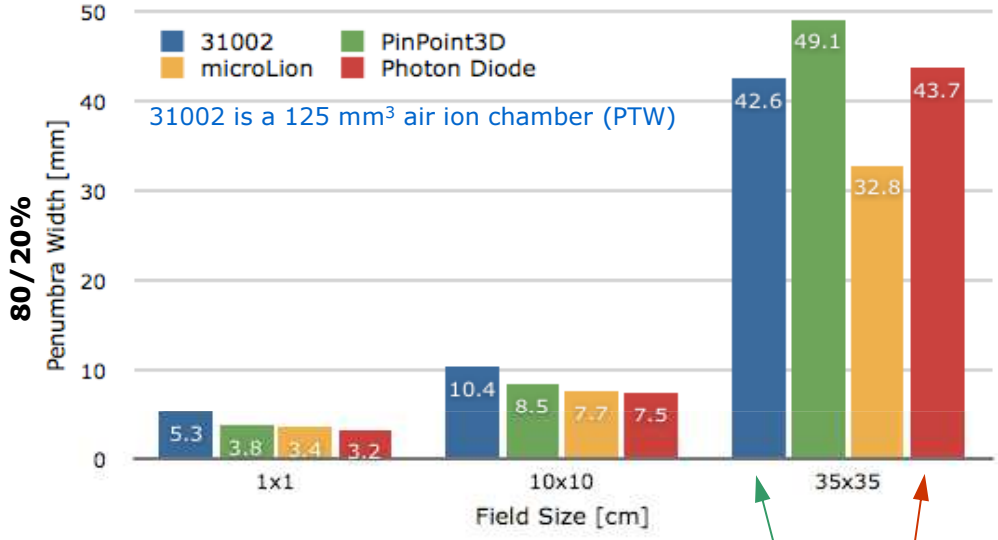

Penumbra widening due to overestimated beam tails (scattered radiation outside beam – energy dependence)

ESTRO School

Beam Profiles: Penumbra measurements using detectors of different sizes
The volume effect

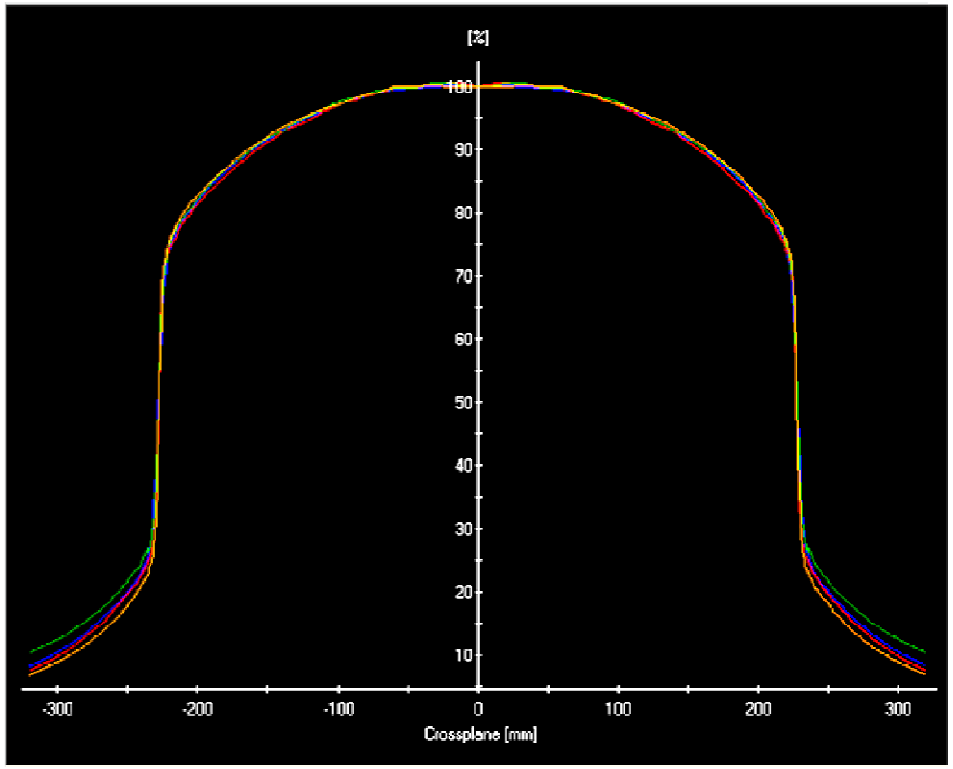

Krauss [20]

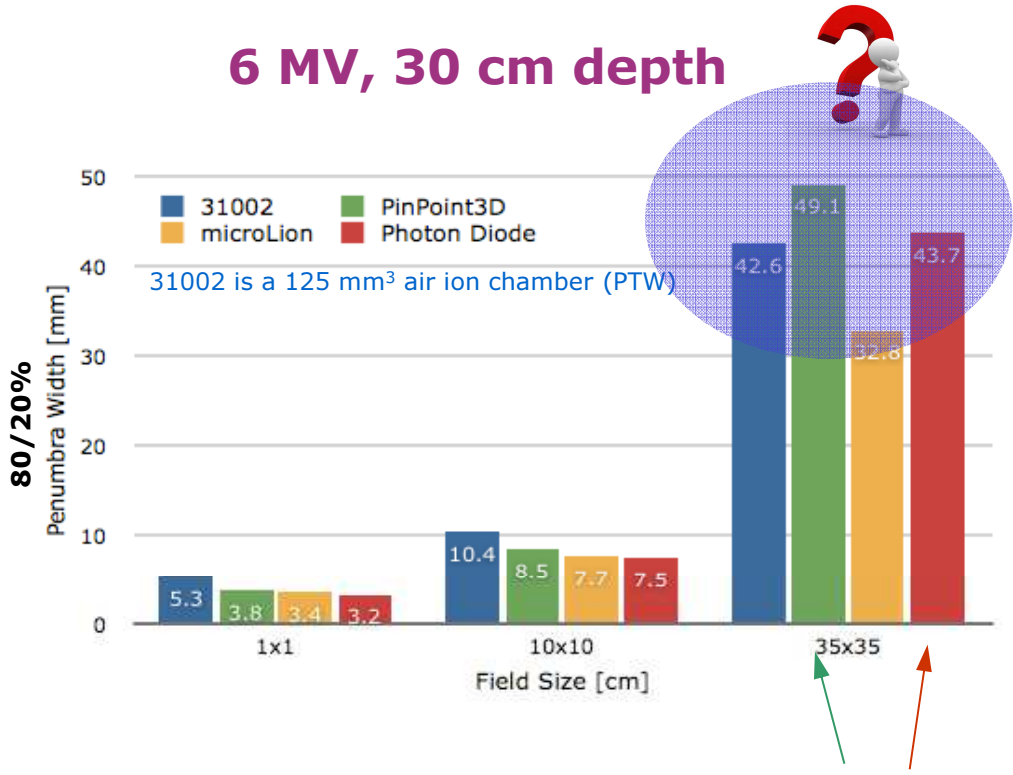

Penumbra widening due to overestimated beam tails (scattered radiation outside beam – energy dependence)

ESTRO School

Output factors: detectors of different sizes
The volume effect

(NACP is a plane parallel
air ion chamber, ∅=20 mm)

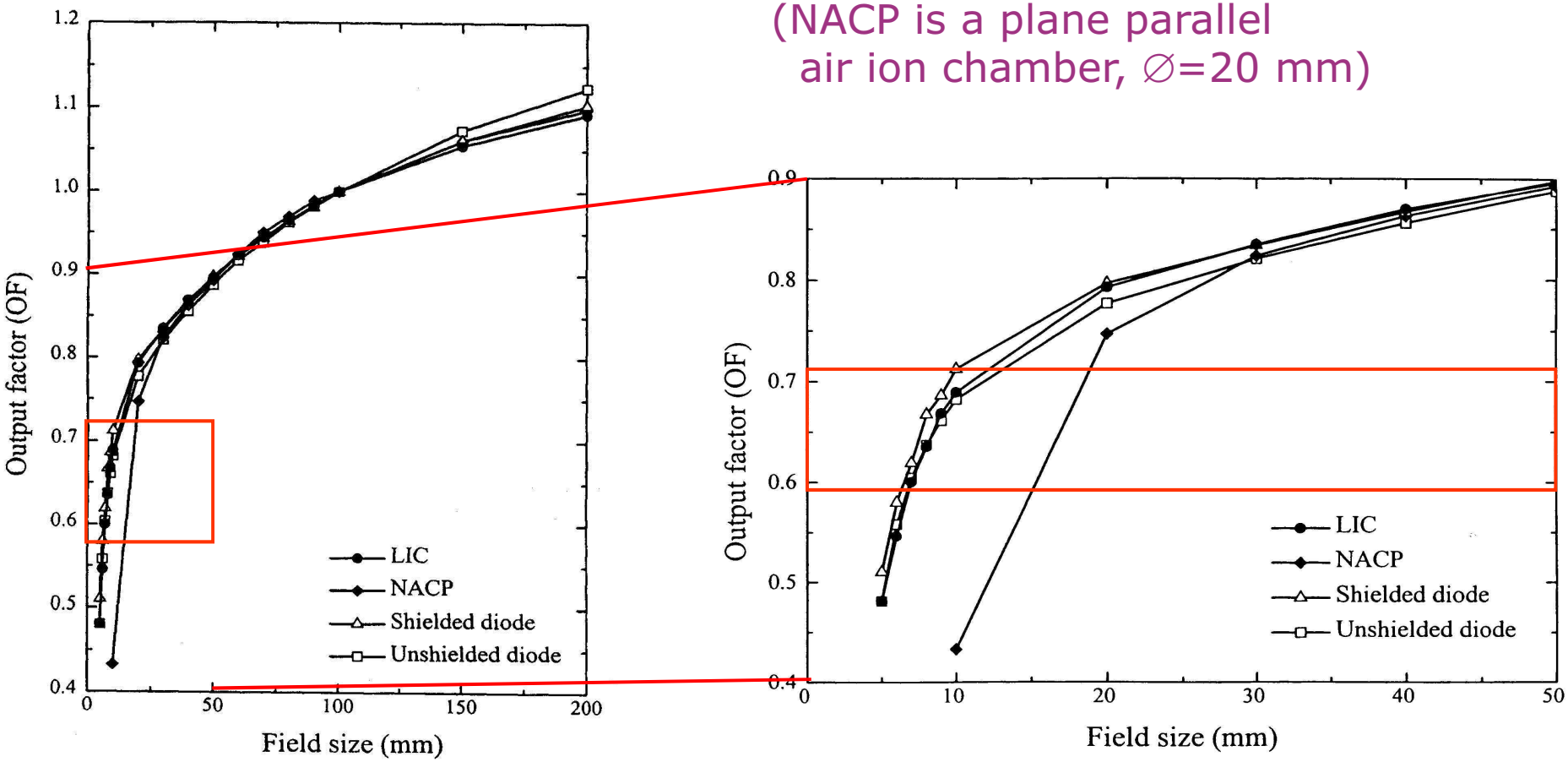

Dasu *et al* [5]

Pushing volume to the lower limit

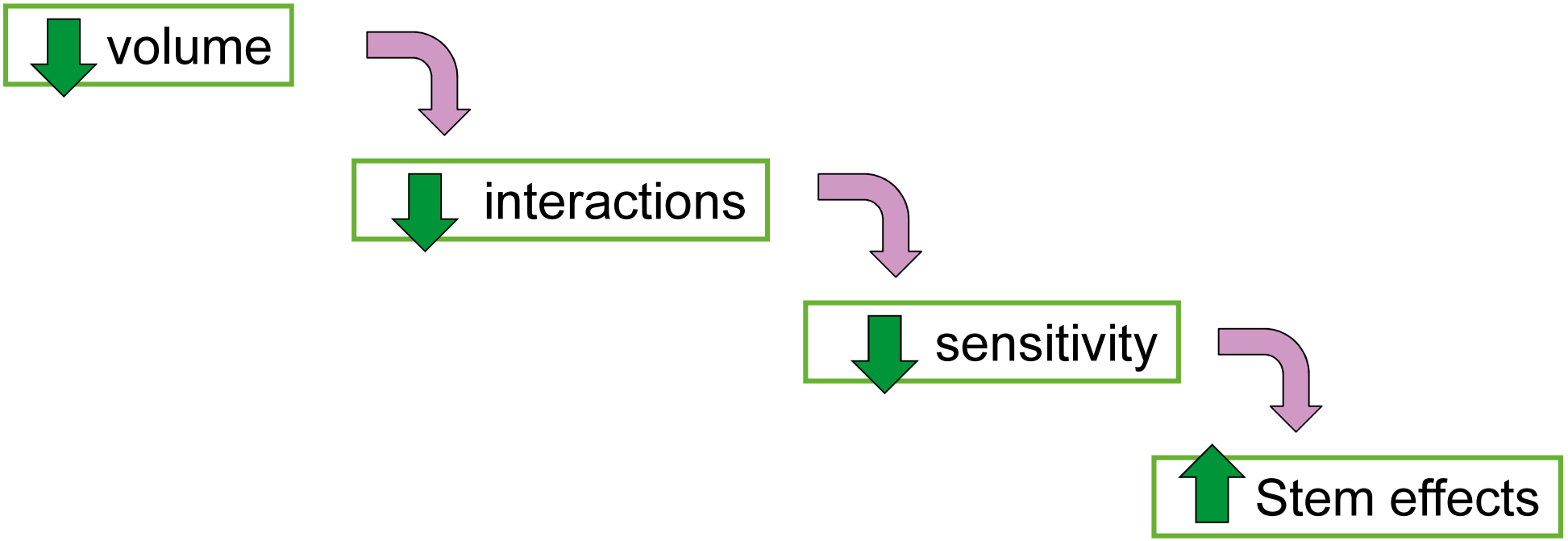

Pushing volume to the lower limit

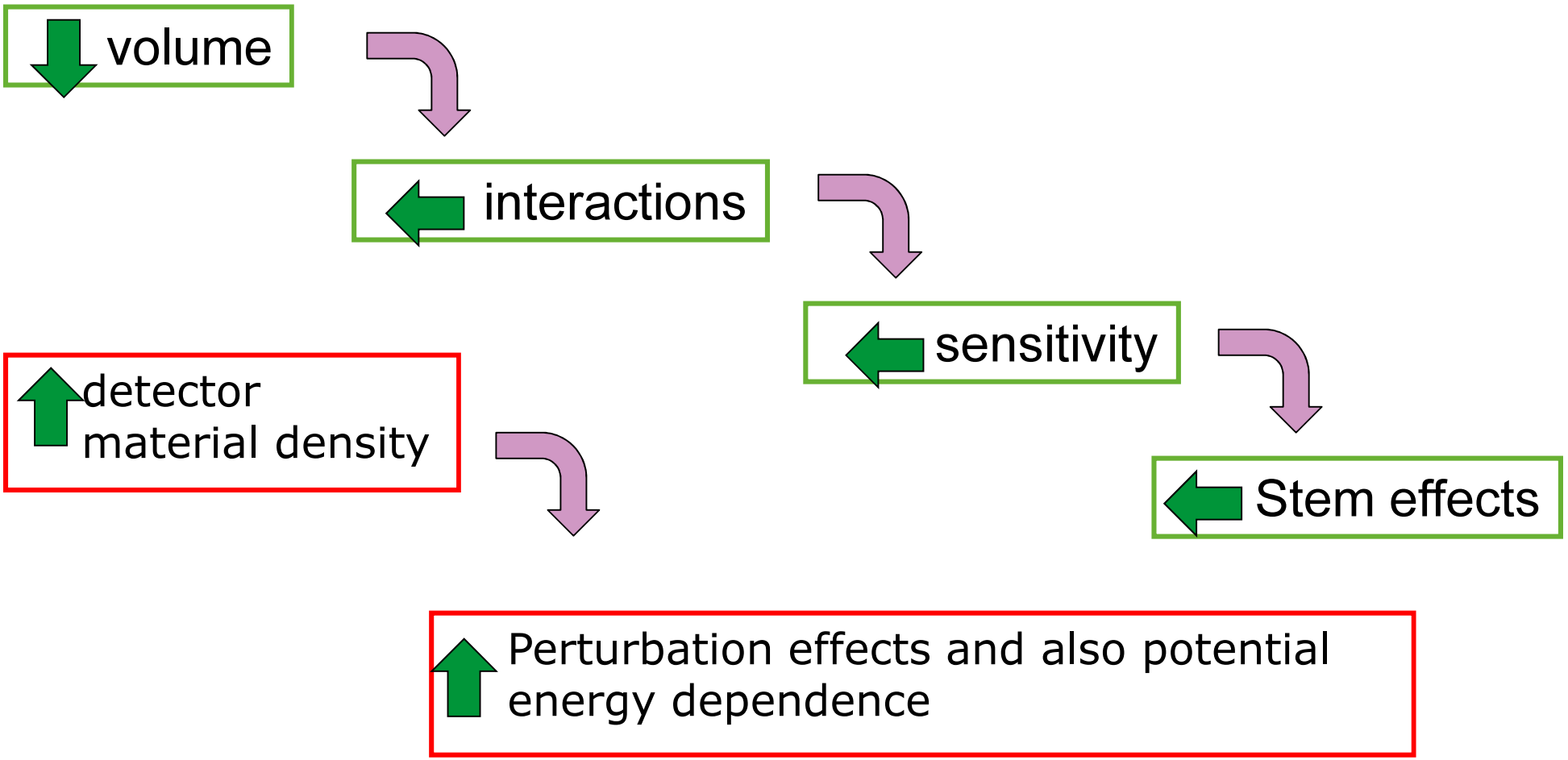

Detector characteristics

✓ Volume effects: Size of sensitive volume

- **Energy dependence: Interactions in detector material**
- Cable/stem leakage, polarity effect
- Dose rate dependence: Recombination, bias voltage
- Temperature dependence
- Long term stability/irradiation effects

ESTRO School

Output factors: Large fields

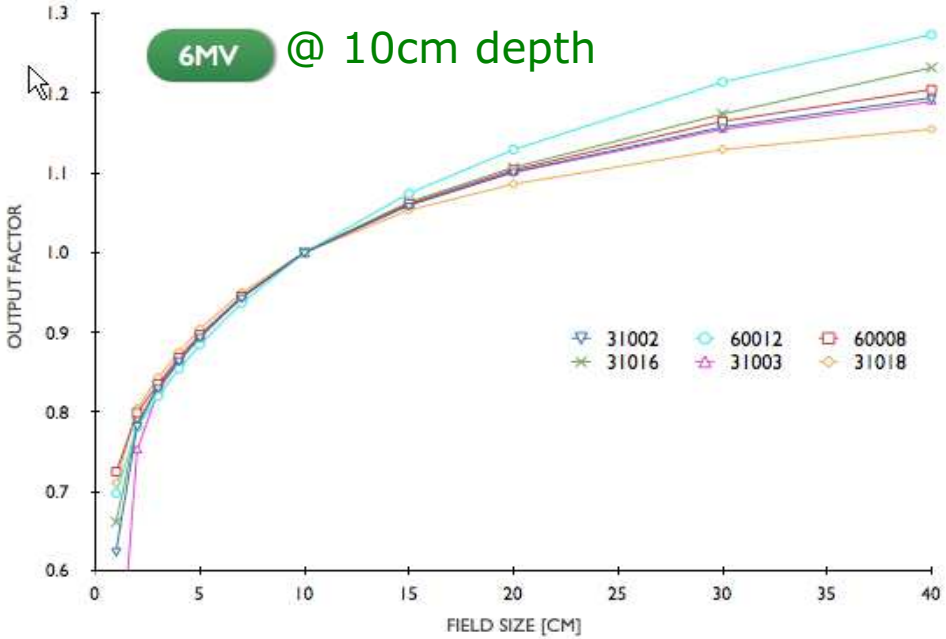

Unshielded Diode

0.125cc i.c.

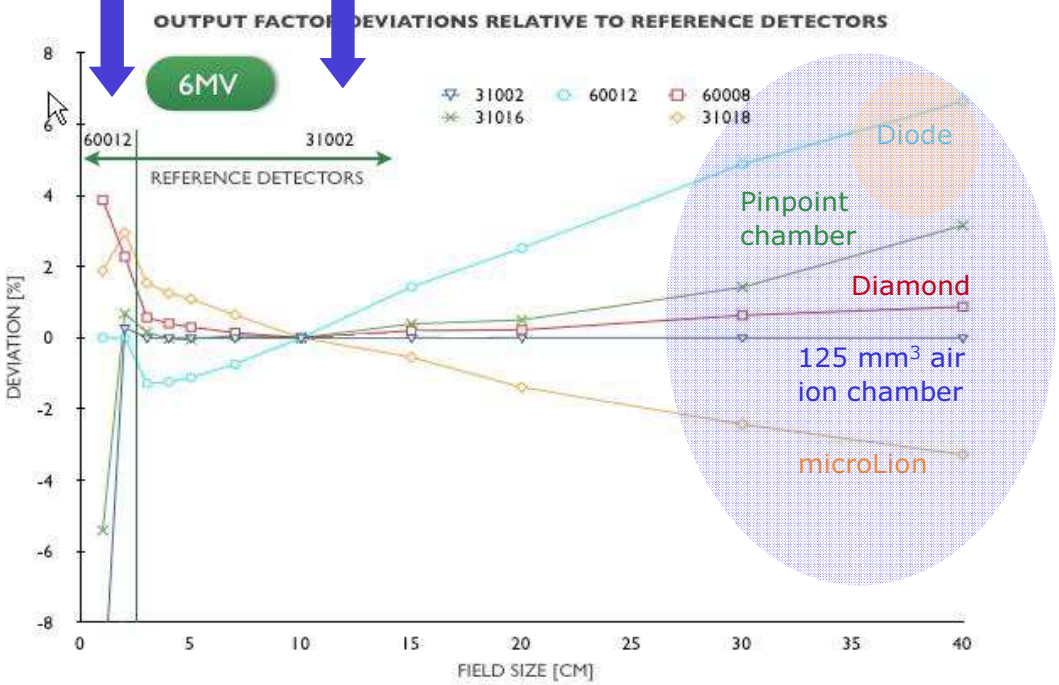

Krauss et al.

www.wienkav.at/kav/kfj/91033454/physik/PTW/liquid.htm

ESTRO School

Energy dependence due to changing Stopping-power ratios

6 MV photon beam

n=narrow beam (∅=0.5 cm)

b=broad beam (∅=10 cm)

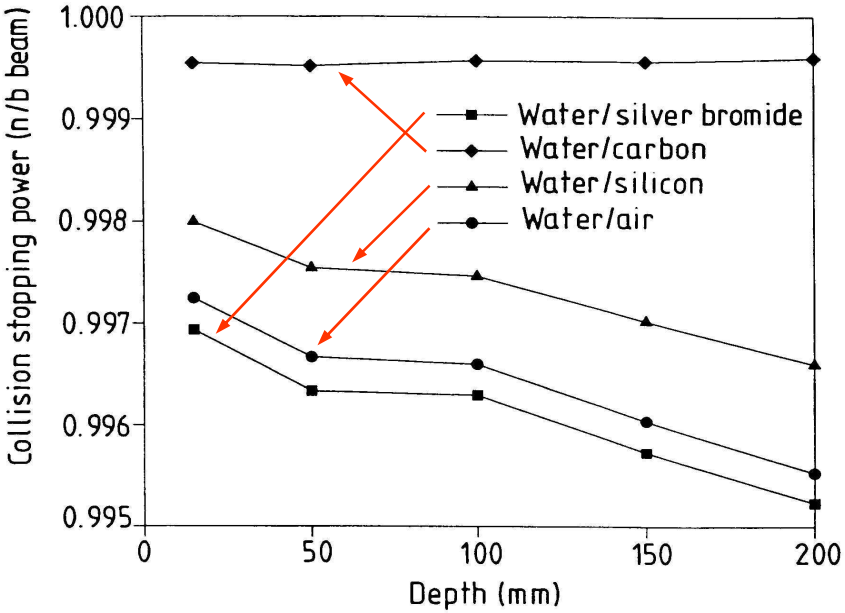

Heydarian *et al*

Cylindrical air ion chambers can be used without correction for energy variations in high energy photon beams, incl. Co-60 (IAEA TRS-398).

The secondary electron energy spectrum is not changing with depth.

Ratio narrow/large field depth dependence
Difference <0.5%

ESTRO School

Energy dependence at low photon energies (photon interactions in the detector medium)

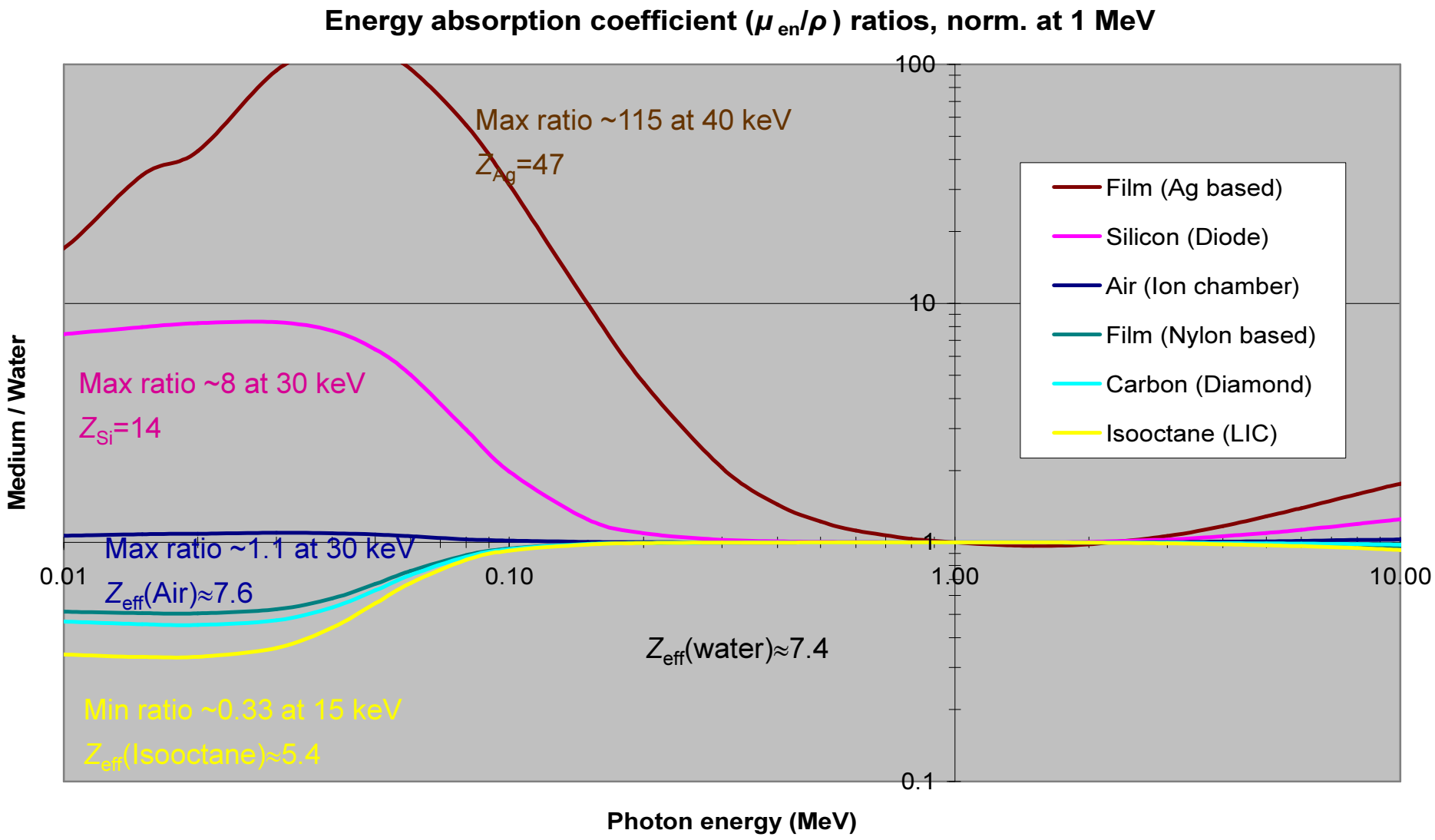

Output factors for large fields using diodes

Shielded Si diodes for compensation of photon energy dependence.

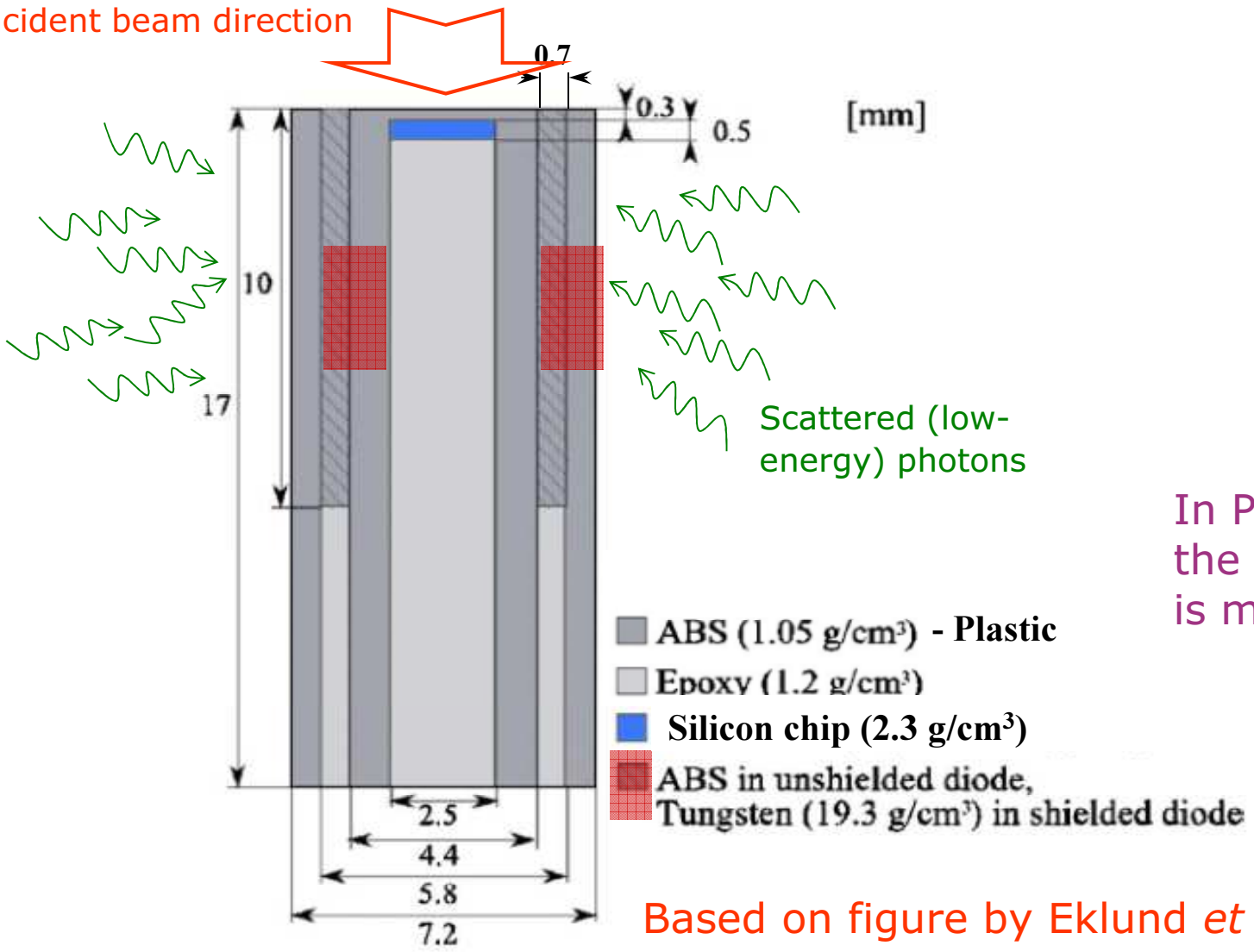

In PTW photon diodes the backscatter shield is made of steel instead.

Based on figure by Eklund *et al* [6] describing IBA Dosimetry diodes (EFD/PFD)

ESTRO School

Scanning results in a 5 MV X-ray beam using p-Si diodes.

Low energy in combination with large beams (here 5 MV and 40x40 cm^2) displays the largest deviations for Si diodes.

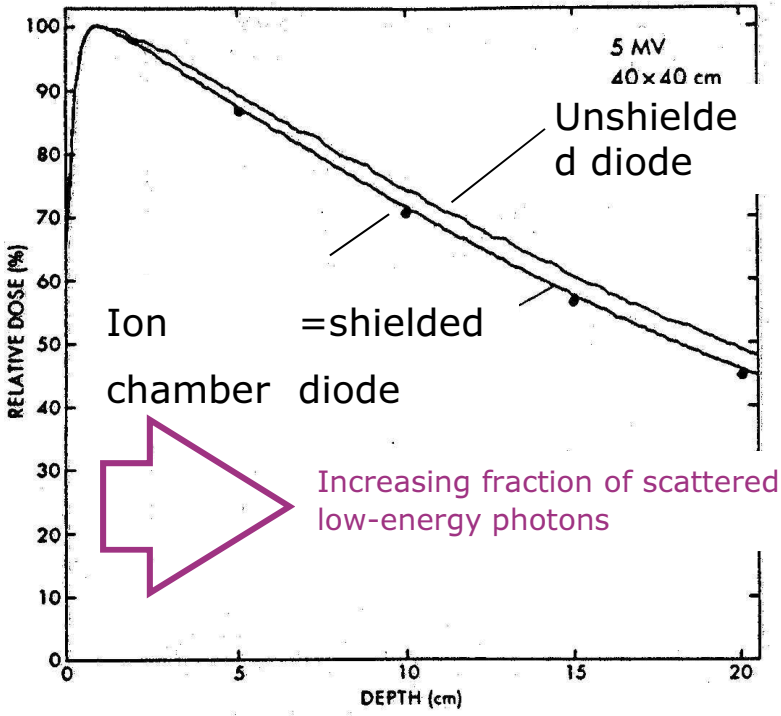

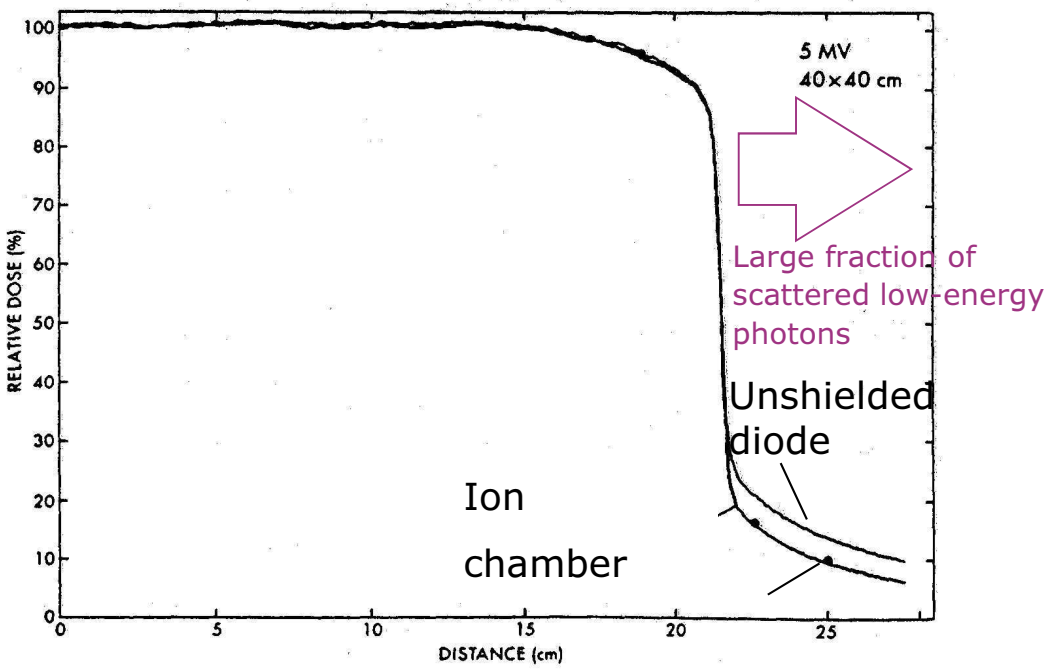

Data from Scanditronix

ESTRO School

OF measurements, incl. corrections, in a 6 MV X-ray beam using p-Si diodes

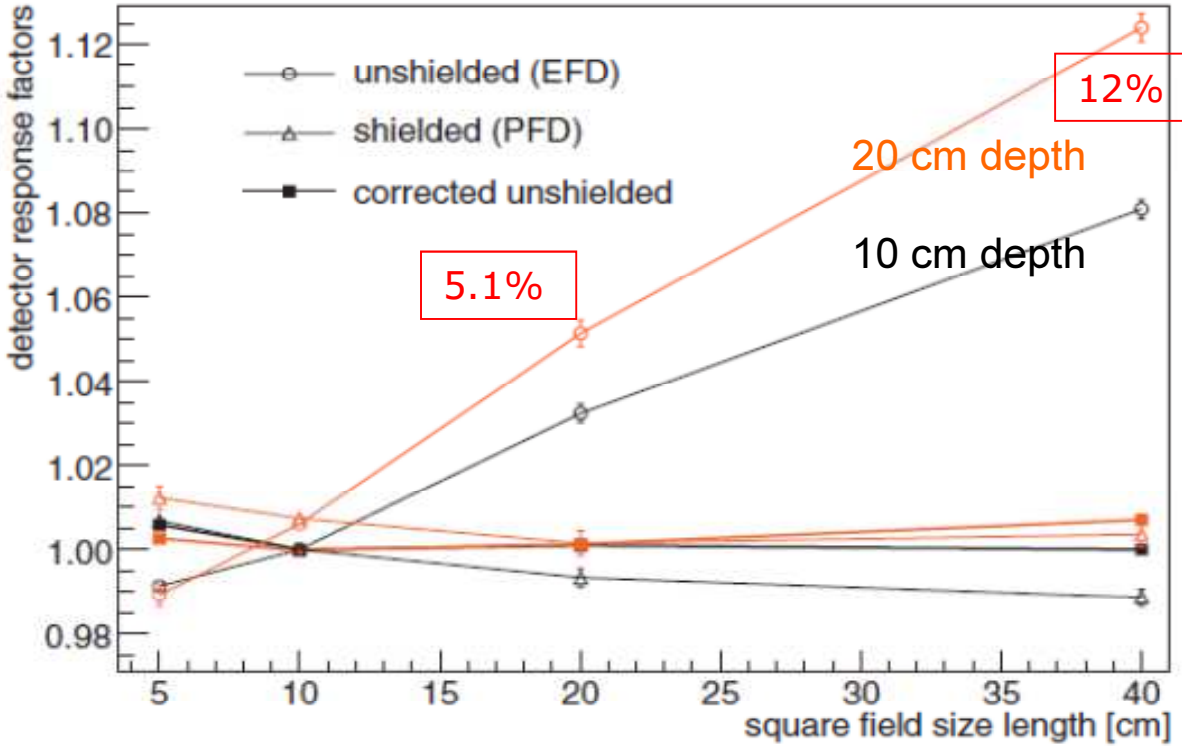

Eklund *et al* [6]

Use shielded diodes for x-ray dosimetry

Exception: Small fields (the shielding would perturbate the field)

ESTRO School

Output factor measurements using detectors of different materials.

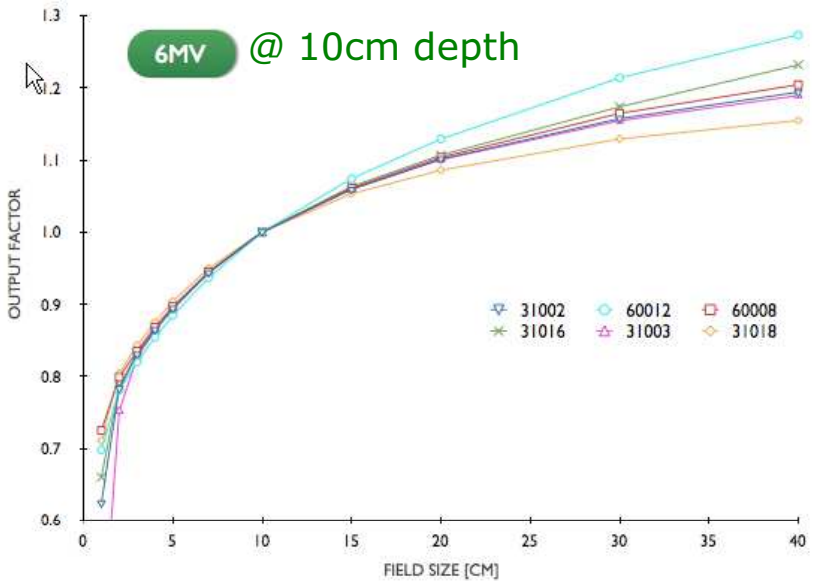

Krauss [20]

Aluminium central electrode

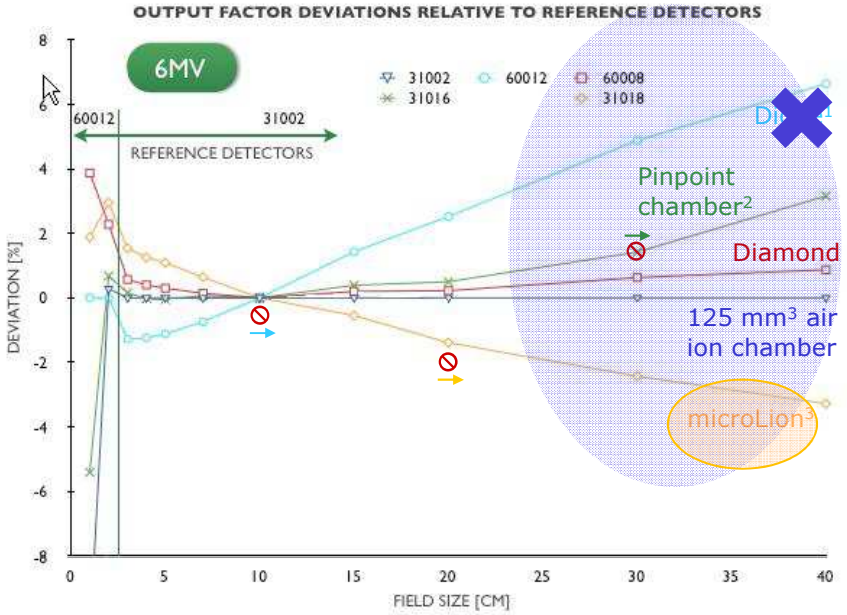

[1]PTW recommends max photon field size: 10x10 cm²

[2]PTW recommends max photon field size: 30x30 cm²

[3]PTW recommends max photon field size: 20x20 cm²

ESTRO School

Energy dependence at low photon energies (photon interactions in the detector medium)

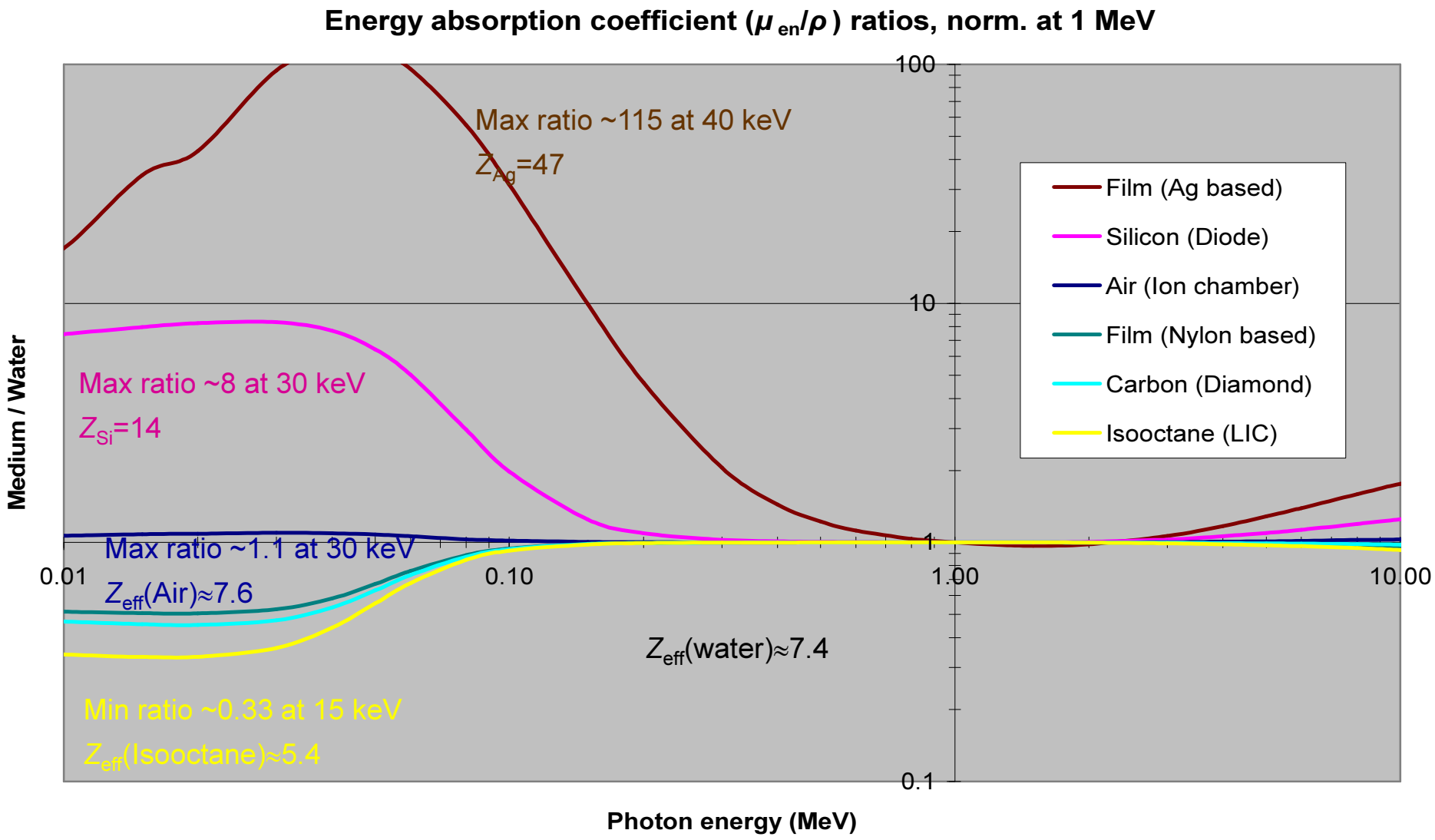

Detector characteristics

✓ Volume effects: Size of sensitive volume

✓ Energy dependence: Interactions in detector material

- **Cable/stem leakage, polarity effect**
- Dose rate dependence: Recombination, bias voltage
- Temperature dependence
- Long term stability/irradiation effects

ESTRO School

Output factor measurements using detectors of different materials.

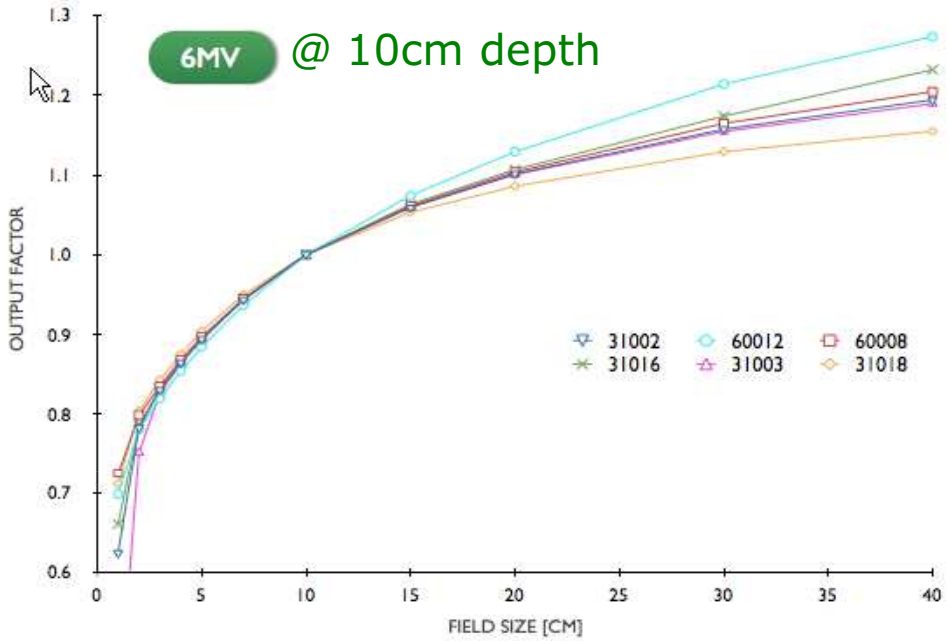

Krauss [20]

Aluminium central electrode

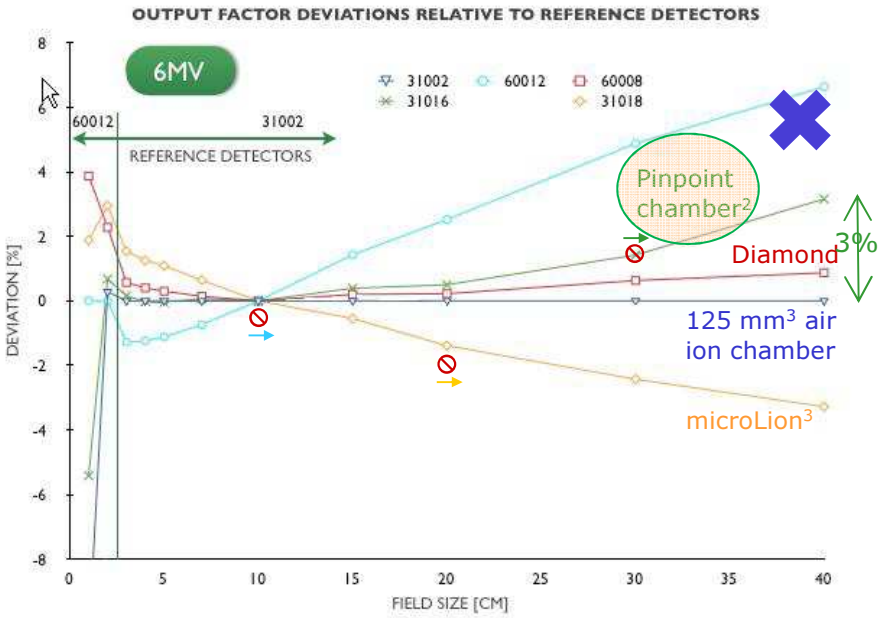

[1]PTW recommends max photon field size: 10x10 cm²

[2]PTW recommends max photon field size: 30x30 cm²

[3]PTW recommends max photon field size: 20x20 cm²

ESTRO School

OF measurements in a 6 MV beam using Pinpoint ion chamber (15 mm3).

Energy dependence (non water equivalence central electrode)

Old PTW chamber 31006 with a central electrode of steel causing similar behaviour as an Si diode.

New PTW pinpoint chambers 31014-6 have aluminium central electrodes.

Measured OF rel. 125 mm³ ion chamber

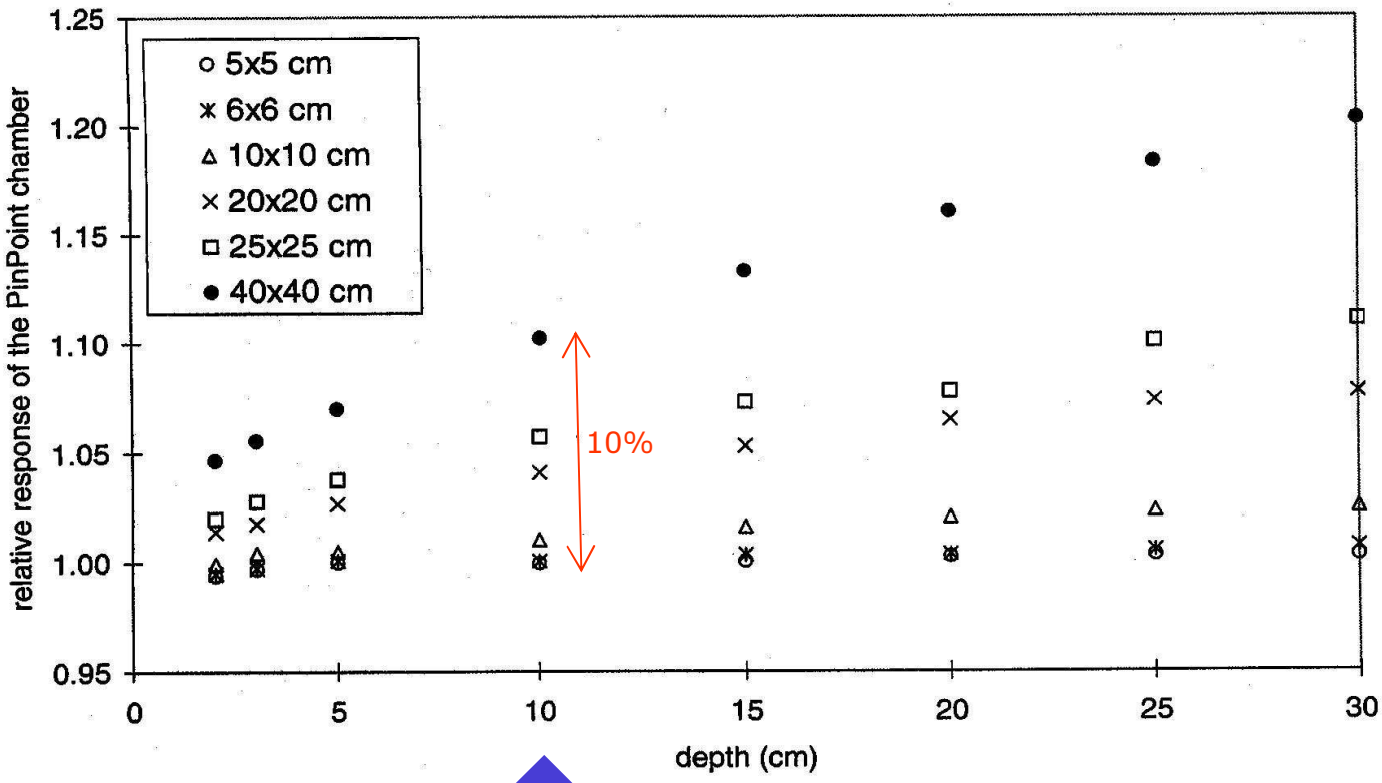

Martens *et al* [12]

OF measurements
Pinpoint ion chamber (aluminium central electrode; 15 mm3)

Measured OF rel. 125 mm³ ion chamber

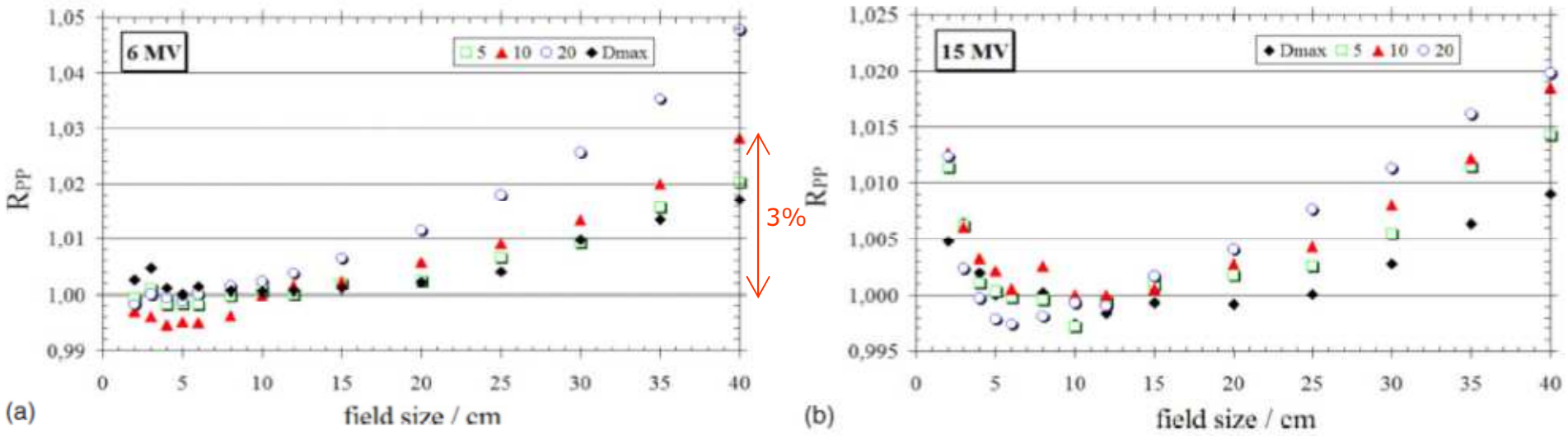

FIG. 5. Uncorrected relative response of type 31014 PinPoint chamber for 6 and 15 MV beams as a function of depth (D_{max} and 5, 10, and 20 cm) and field size.

Agostinelli *et al* [21]

Cable leakage in a PinPoint chamber

Normally, the signal from stem and cable irradiation is small enough (< 1 pC/(Gy·cm)) to be neglected, but the small air volume yields a low detector signal level…

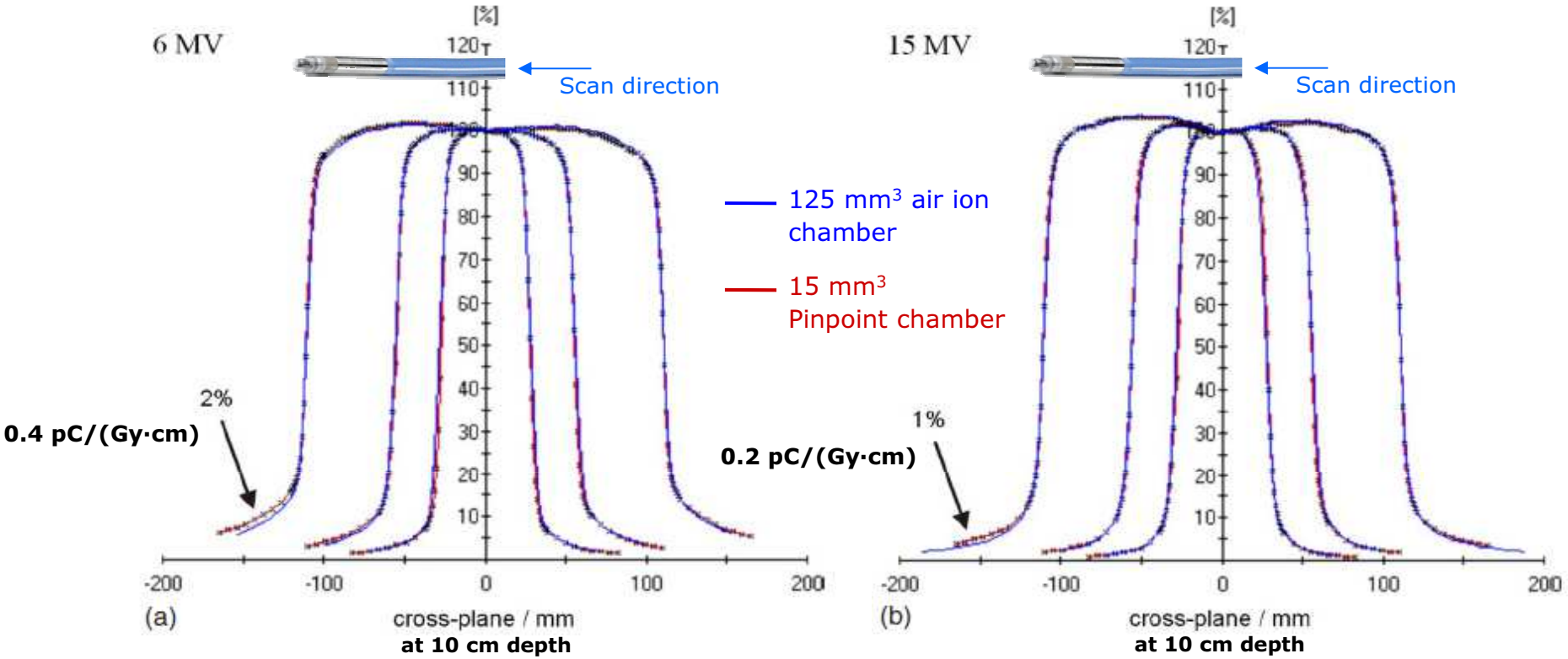

Agostinelli *et al* [21]

OF measurements using a Pinpoint ion chamber (15 mm³)

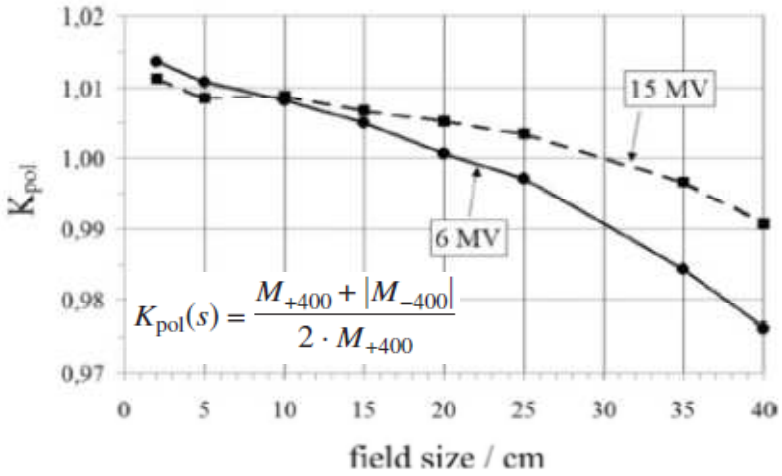

FIG. 3. Polarity correction factor K_{pol} at a 10 cm depth as a function of field size for type 31014 PinPoint chamber. 6 MV (circle solid line), 15 MV (square dashed line).

Agostinelli *et al* [21]

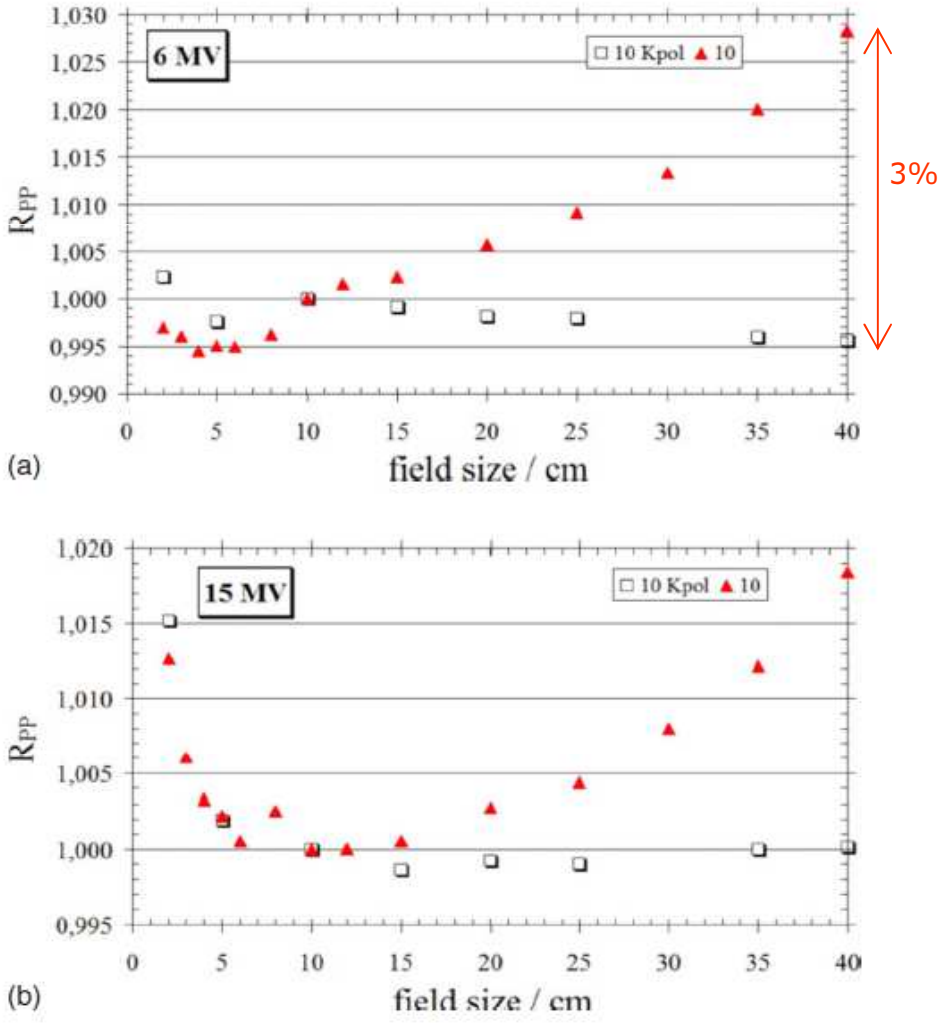

FIG. 4. Polarity-corrected (□) vs. uncorrected (▲) relative response of type 31014 PinPoint chamber for the 6 and 15 MV beams at a 10 cm depth.

ESTRO School

PDD measurements and the polarity effects
X rays

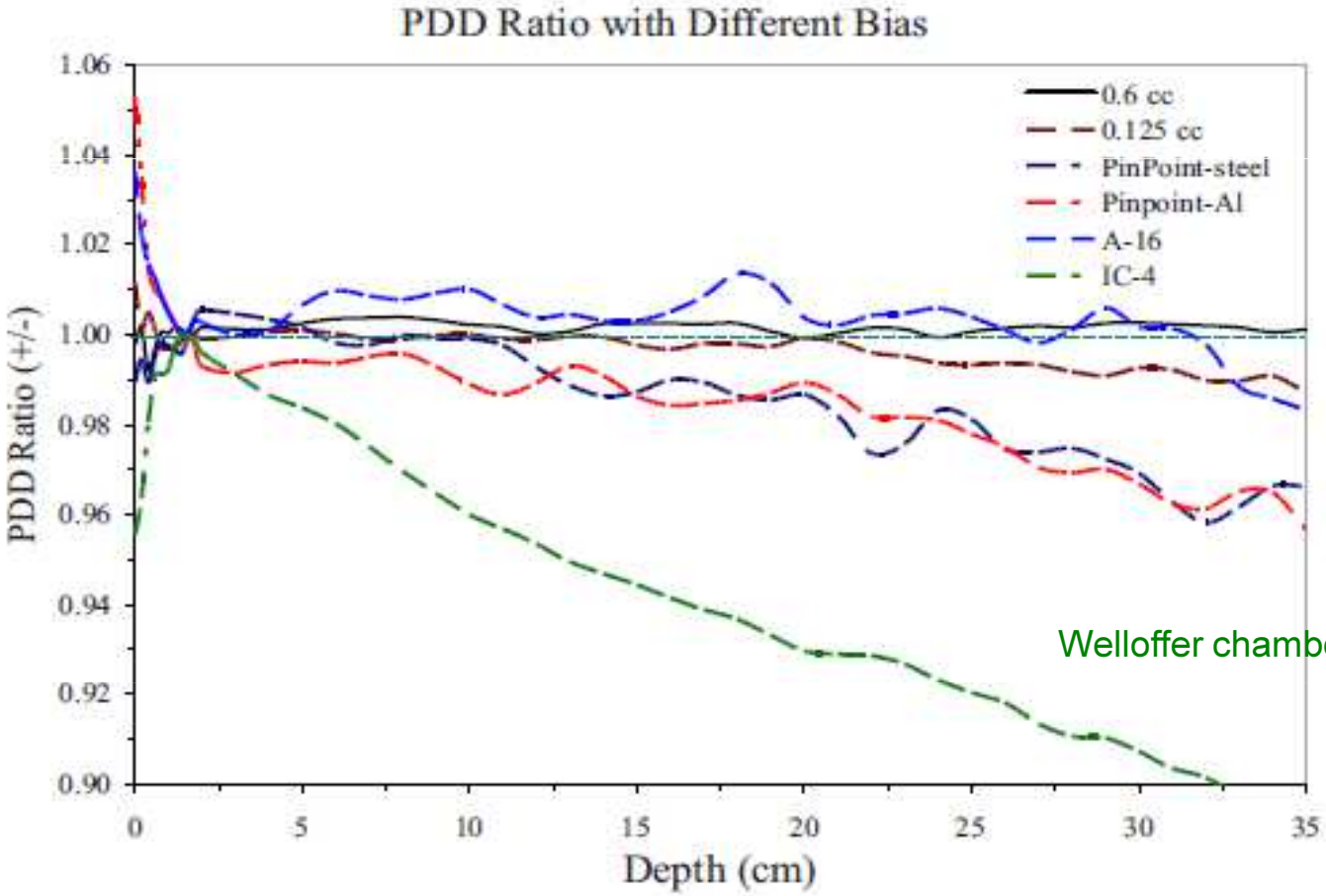

Welloffer chamber 0.04cc

- TG106 AAPM (2008)
- **6MV x-rays – cylindrical i.c.**

ESTRO School

PDD build up region
Plane parallel chamber

Effective point of measurement well defined
Good resolution in depth

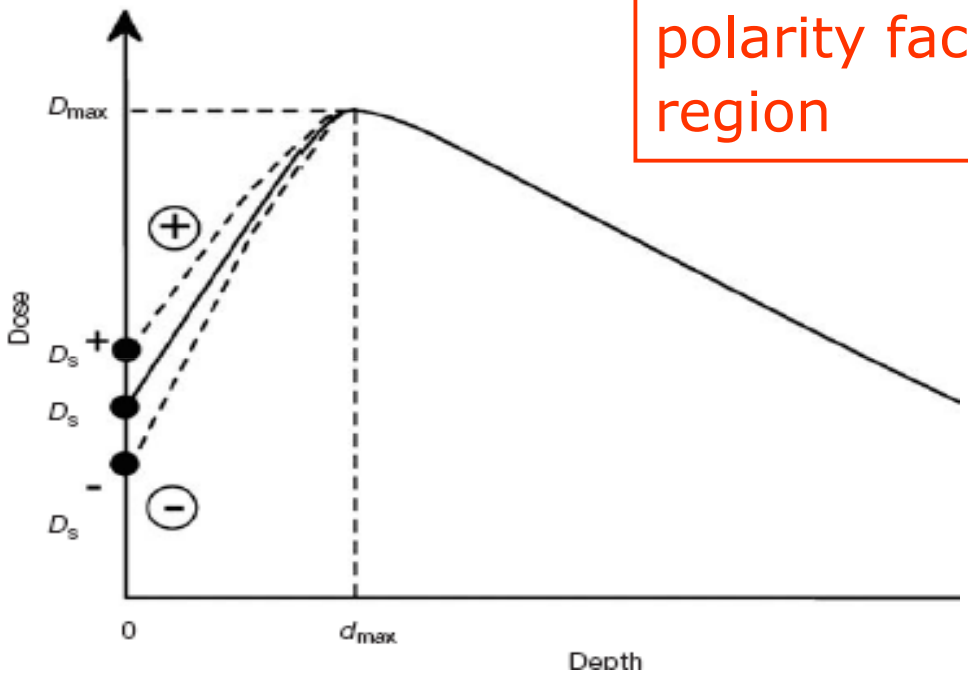

Need of correcting by the polarity factor on the build up region

Detector characteristics

- ✓ Volume effects: Size of sensitive volume
- ✓ Energy dependence: Interactions in detector material
- ✓ Cable/stem leakage, polarity effect
- **Dose rate dependence: Recombination, bias voltage**
- Temperature dependence
- Long term stability/irradiation effects

ESTRO School

Ion-recombination ionization measurements.

- **Initial recombination**: Recombination within one created ion cluster. Depends on material, temperature and bias voltage, not dose rate.
- **Columnar recombination**: Recombination within one particle track. Depends on ionization density of the radiation and bias voltage, not dose rate.
- **General recombination**: Recombination when ions in different particle tracks interact. Depends on bias voltage and dose rate.

Applied bias voltages for different detectors.

- Air ion chamber: 200-500 V
- Liquid ion chamber: 800 V (microLion)
- Diamond detector: 100 V
- p-Si diode: -

Perhaps obvious, but...

It is a good idea to always use the same bias voltage for a given detector to minimize differences when comparing measurement results.

ESTRO School

Dose rate dependence in photon beams
Diodes.

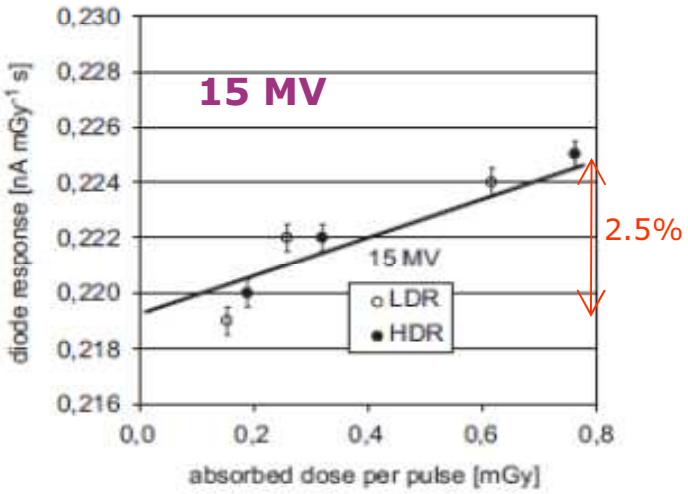

Djouguela *et al* [7]

This positive dose rate dependence is often referred to as *supralinear*.

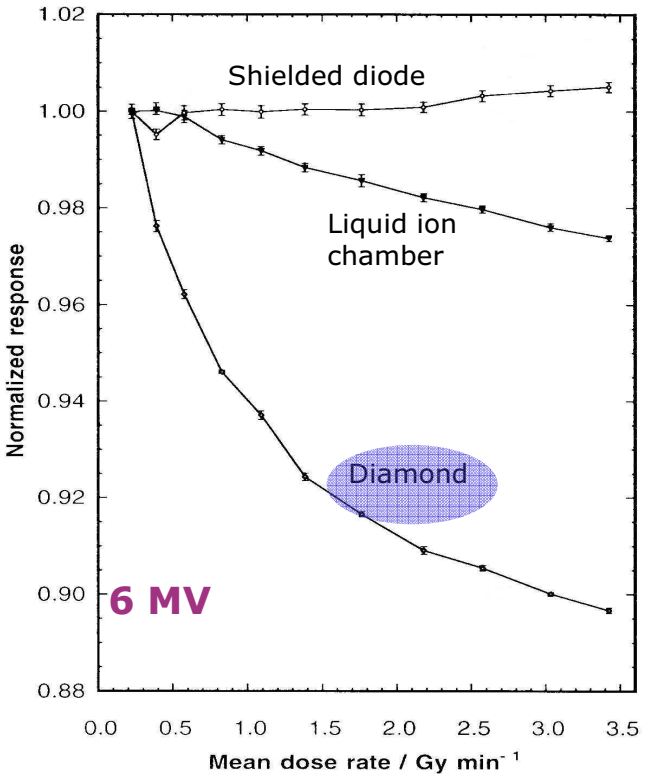

Dose per 4.5 μs pulse (150 Hz) between 0.03 and 0.38 mGy.

Westermark *et al* [3]

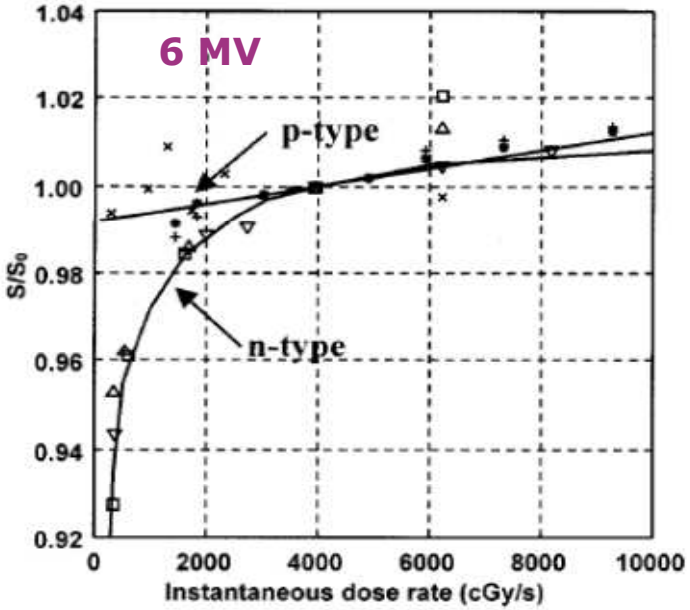

Dose per 3 μs pulse between 0 and 0.3 mGy.

Saini *et al* [8]

0.3 mGy per pulse corresponds to approximately 3-4 Gy/min on a regular medical accelerator.

ESTRO School

Dose rate dependence in photon beams Diamond

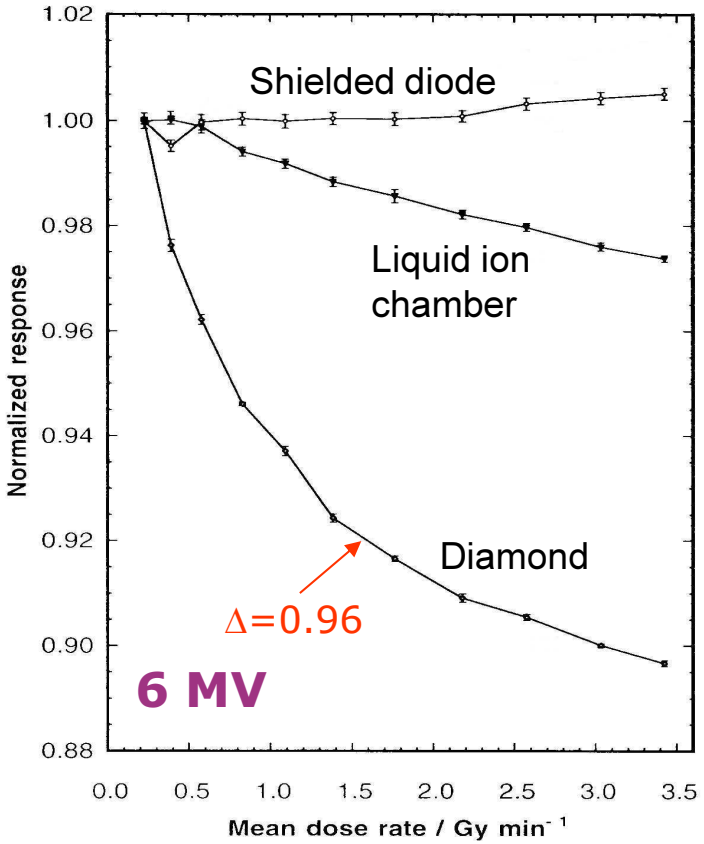

Westermark *et al* [3]

$I = I_{dark} + k \cdot D^{\Delta}$

where k and Δ should be fitted for each individual diamond detector. Typical values of Δ range from 0.90 to 0.99.

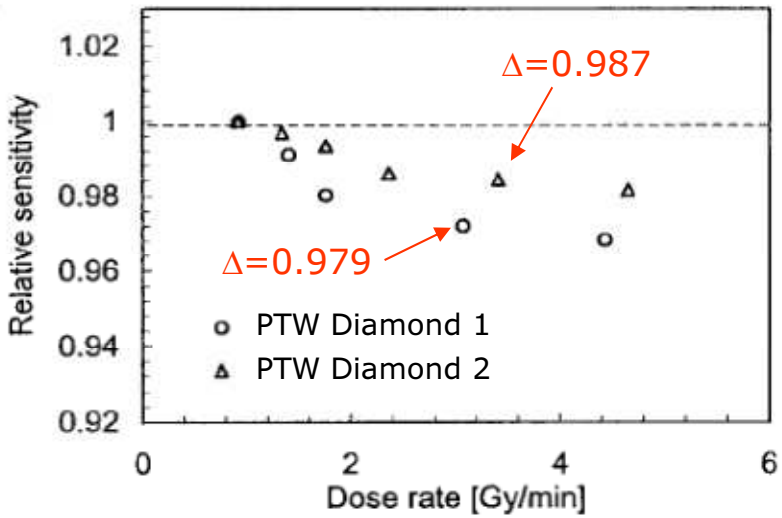

De Angelis *et al* [15]

ESTRO School

Effects from dose rate dependence 6 MV X-ray beams

10x10 cm^2

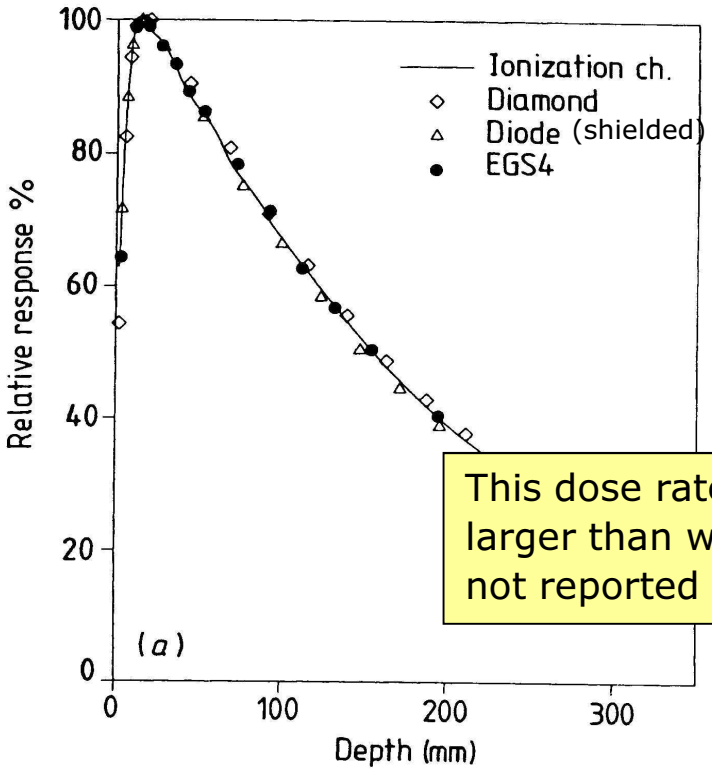

3x3 cm^2

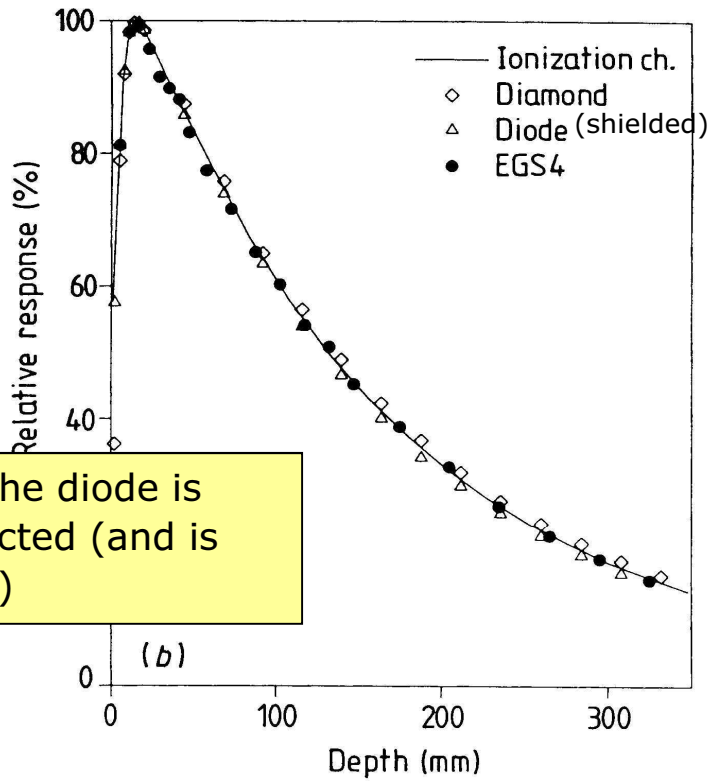

This dose rate effect of the diode is larger than what is expected (and is not reported elsewhere?)

Heydarian *et al* [2]

ESTRO School

Detector characteristics

- ✓ Volume effects: Size of sensitive volume
- ✓ Energy dependence: Interactions in detector material
- ✓ Cable/stem leakage, polarity effect
- ✓ Dose rate dependence: Recombination, bias voltage
- **Temperature dependence**
- Long term stability/irradiation effects

ESTRO School

Temperature effects

TABLE III. Temperature coefficients for *n*- and *p*-type diodes. All measurement were made at depth of 5 cm, 10×10 cm^2, SSD=100 cm.

Diode type	Temperature coefficient 6 MV (%/°C)	15 or 20 MV (%/°C)	Co-60 (%/°C)
Isorad Gold 1, unirradiated	0.06	0.05 (20 MV)	0.45 (T1000)
Isorad Gold 2, unirradiated	0.08	0.10 (20 MV)	0.16 (T1000)
Isorad Red	0.22	0.21 (20 MV)	0.37 (T1000)
QED unirradiated	0.27	0.25 (15 MV)	0.34 (TPhoenix)
QED Blue Diode	0.30	0.31 (15 MV)	0.30 (T780)
QED Red Diode	0.29	0.29 (15 MV)	0.29 (T780)
Scanditronix EDP 10	0.38	0.33 (20 MV)	0.36 (T1000)
Scanditronix EDP 30	0.36	0.34 (20 MV)	0.39 (T1000)

Min Max

Average (pre-irradiated only): 0.31 0.30 0.34

Saini *et al* [8]

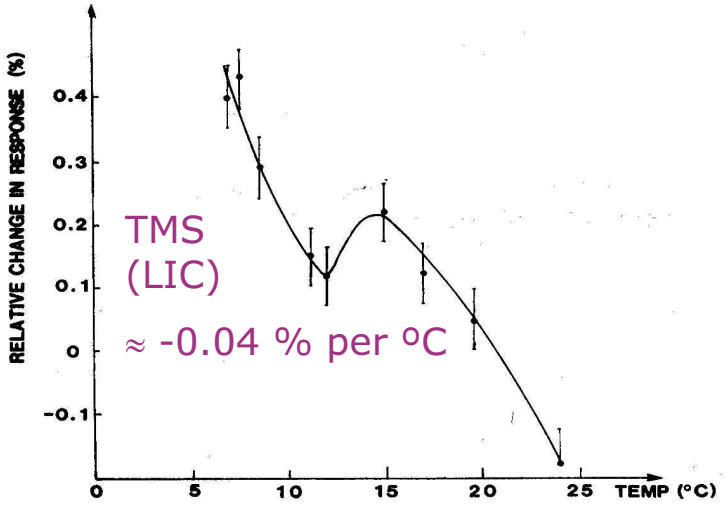

Figure 5. The relative response in TMS at different temperatures.

Wickman *et al* [9]

- PTW diamond detector 60003 has a temperature dependence of approx. 0.1% per °C (De Angelis *et al* [15])
- Open air ion chamber: 1/293 = -0.34 % per °C

In relative dosimetry during one single measurement session the effects caused by temperature variations can normally be neglected. However, *in vivo* dosimetry…

ESTRO School

Detector characteristics

- ✓ Volume effects: Size of sensitive volume
- ✓ Energy dependence: Interactions in detector material
- ✓ Cable/stem leakage, polarity effect
- ✓ Dose rate dependence: Recombination, bias voltage
- ✓ Temperature dependence
- **Long term stability/irradiation effects**

Effects from dose accumulation in old p-Si diodes.

Sensitivity (8-10 kGy typically pre-irradiated on commercial diodes).

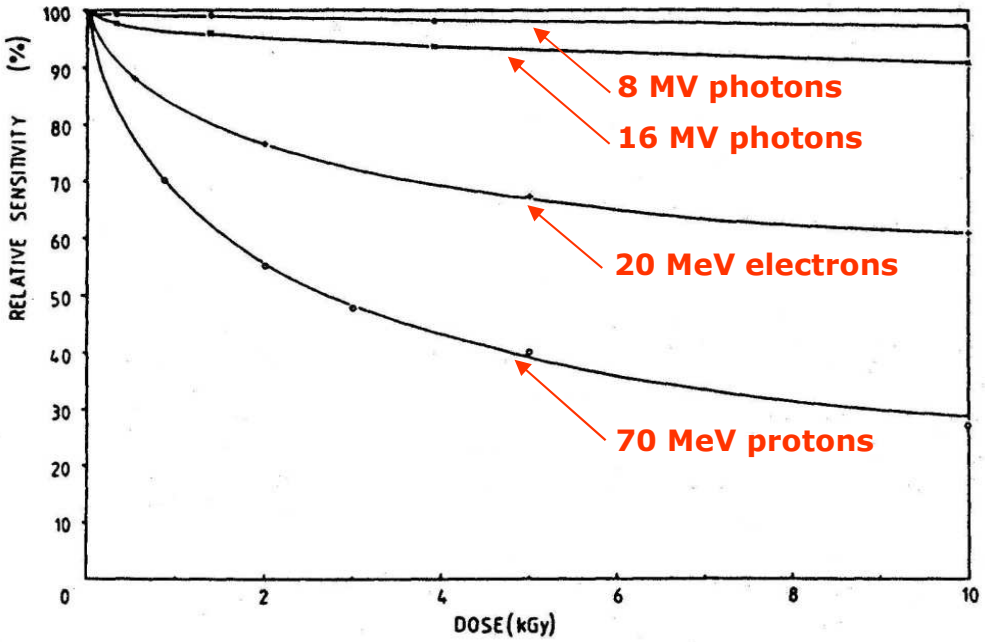

Rikner [10]

PTW states sensitivity losses of <0.1% per kGy for Co-60 and <10% per kGy for 23 MV photons

Temperature dependence.

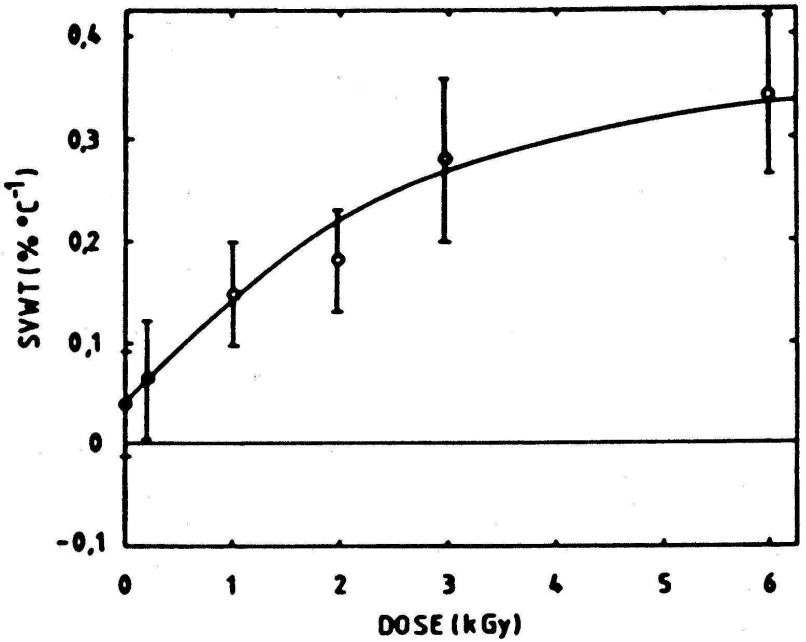

Rikner [10]

ESTRO School

Pre-irradiation effects in PTW diamond detectors (Type 60003)

PTW recommends 10 Gy of pre-irradiation. Mandatory if bias voltage has been turned off.

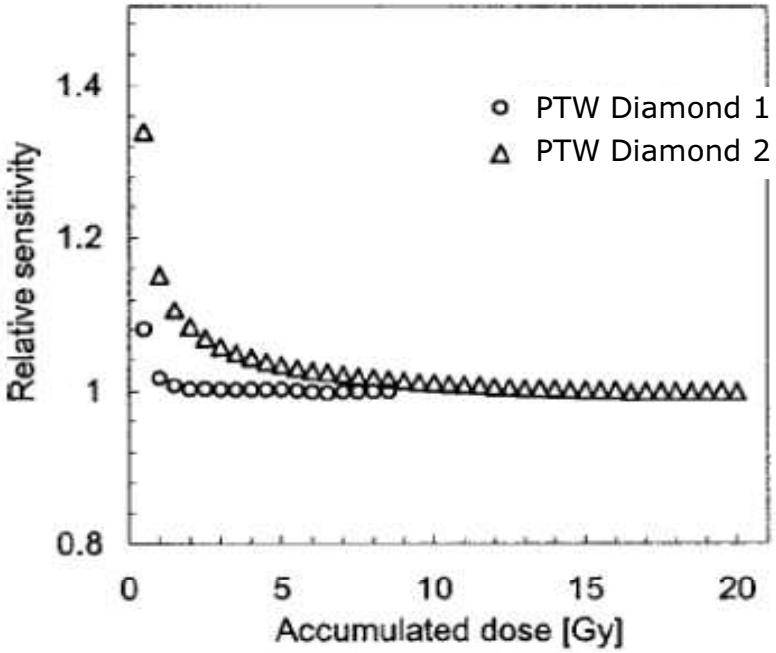

De Angelis *et al* [15]

Dark current after irradiation in a 6 MV beam. Initial level ≈0.4% rel. measurement signal.

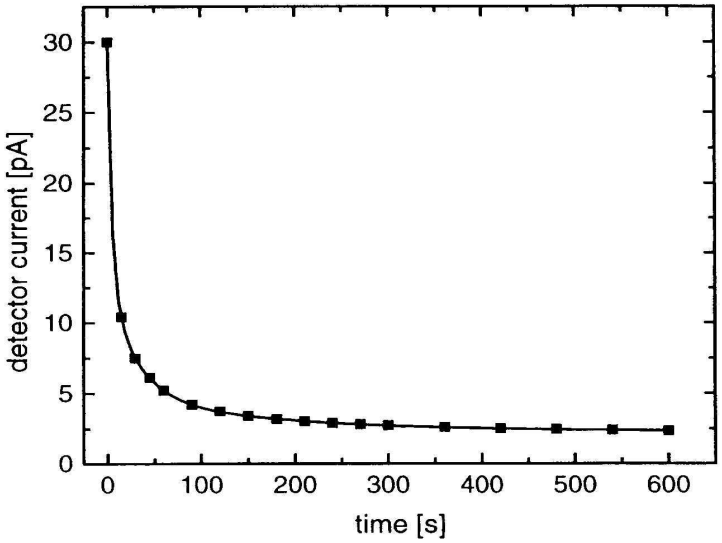

Laub *et al* [11]

ESTRO School

Natural diamond ➡ MicroDiamond

- Good water equivalence of Carbon for high energy photon and electron beams
- High sensitivity: 0.5uC/Gy (dimensions can be reduced)
- Low temperature dependence < 1%/K
- Stable response with accumulated dose (< 0.05% per kGy)

Natural Diamond (60003-PTW)	MicroDiamond (60019-PTW)
Polarization needed (100 V)	No Polarization (Schottky diode conf.)
High response variability between detectors	Reproducible production
Need of 5 Gy pre-irradiation before each set of measurements (response drop 19%)	No need of pre-irradiation
High dark current	Dark current negligible
Dose rate dependence	Low dose rate dependence

OF measurements using a microDiamond detector

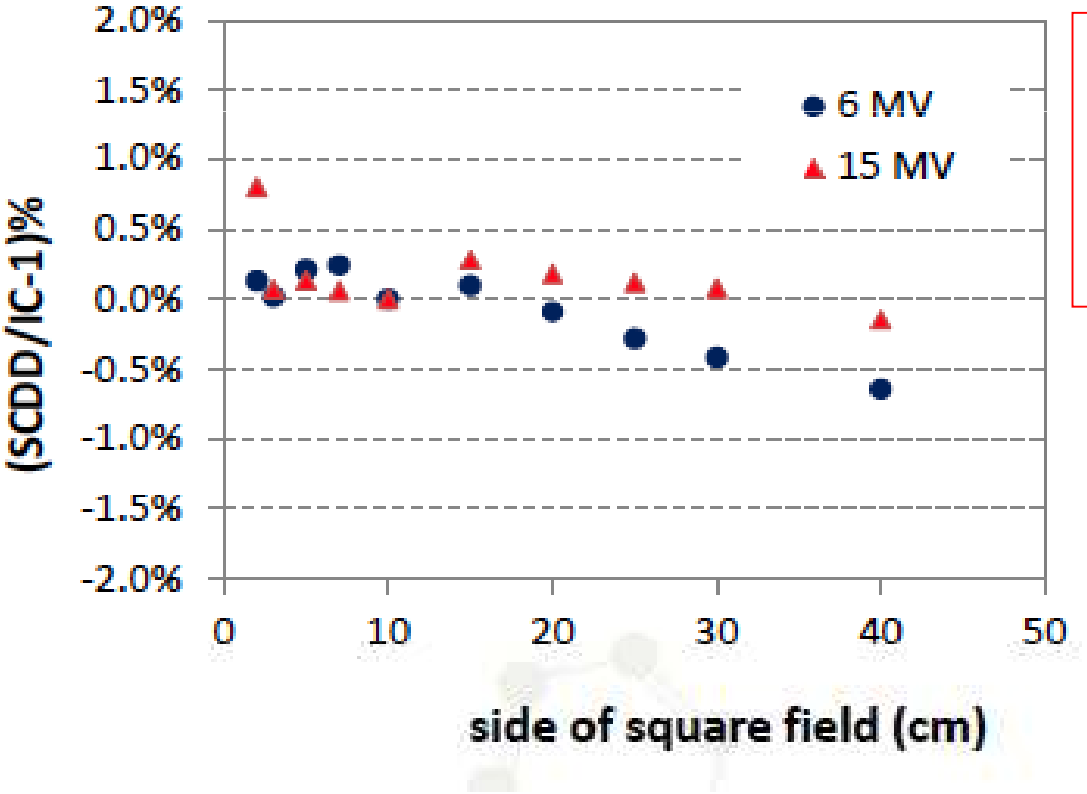

Reference dosimeter:

Field size 5-40 cm side: 0.6 cc cyl ion chamber

Field size <5 cm side: Pinpoint ion chamber

Differences < 1%

From Pimpinella, ESTRO33, Advances in synthetic diamond detector dosimetry

ESTRO School

Organic scintillator
(W1 Standard Imaging)

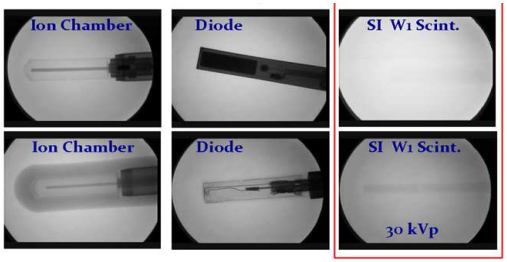

- Good water equivalence for high energy photon and electron beams

Test	Result	Uncertainty
Short-term repeatability (@0.75 Gy)	σ = 0.10%	0.07%
Short-term repeatability (@0.15 Gy)	σ = 0.25%	0.05%
Dose-response linearity	RMS = 0.61 %	0.20%
Angular dependence	RMS = 0.21 %	0.07%
Temperature dependence	-0.225 %·$^{0}C^{-1}$	0.008%·$^{0}C^{-1}$
Time to reach thermal equilibrium*	1 min 40 s	16 s
Repetition rate dependence	RMS = 0.53 %	0.06%
Deviation from ISL	RMS = 0.38 %	0.26%
Loss of sensitivity with accumulated dose	-0.28%·kGy^{-1} [0-15 kGy] -0.032%·kGy^{-1}[15-127 kGy]	0.06%·kGy^{-1} 0.018%·kGy^{-1}

ESTRO School

Organic scintillator
(W1 Standard Imaging)

Energy Dependence; reference conditions

(uncertainty k=1)

Modality	Nominal energy	Difference (%)
High-energy X-rays	6 MV	-
	15 MV	-0.2±0.6
Electrons	6 MeV	-0.5±0.7
	9 MeV	-1.2±0.6
	12 MeV	0.5±0.6
	16 MeV	-0.4±0.6
	20 MeV	-0.2±0.6

ESTRO School

Organic scintillator
(W1 Standard Imaging)

Irradiation produces luminiscence

Light is guided through optical fiber to a photomultiplier

The signal is proportional to absorbed dose

BUT

When we irradiate optical fiber Cerenkov light is produced

Cerenkov light depends on the length of fiber irradiated, not proportional to dose

Cerenkov light and luminiscence have different wave lenghts

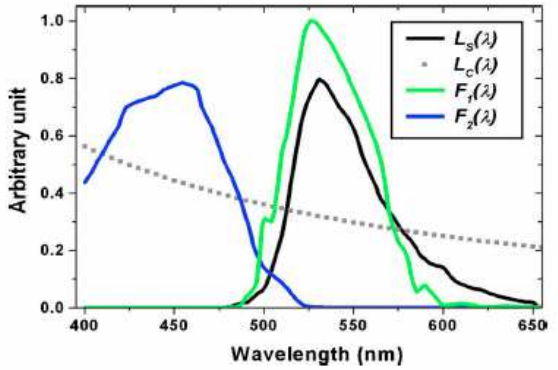

Spectral discrimination method

ESTRO School

Organic scintillator
(W1 Standard Imaging)

Cerenkov light and luminiscence have different wave lenghts

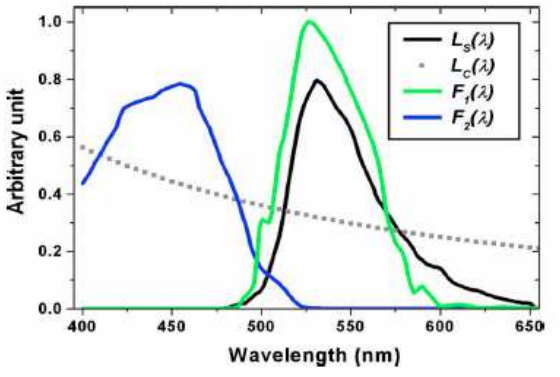

Spectral discrimination method

$CLR = (R_{1\_max\_f1} - R_{1\_min\_f1}) / (R_{2\_max\_f1} - R_{2\_min\_f1})$

$Gain = Dose_{f2} / (R_{1\_min\_f2} - R_{2\_min\_f2} * CLR)$

$Dose = Gain \cdot (R_1 - R_2 \cdot CLR)$

$R_{i\_j\_k}$ where:
R refers to the reading
i refers to channel
j to the fiber configuration (maximum or minimum)
k to the side (cm) of the square radiation field

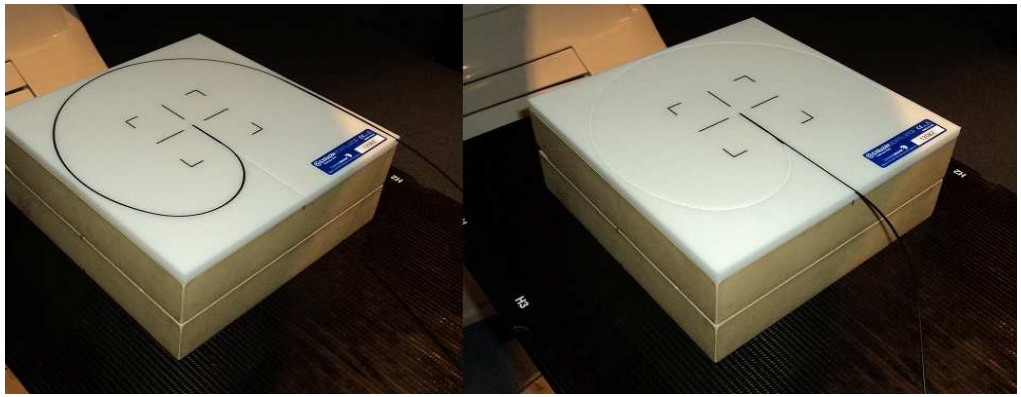

ESTRO School

Organic scintillator
(W1 Standard Imaging)

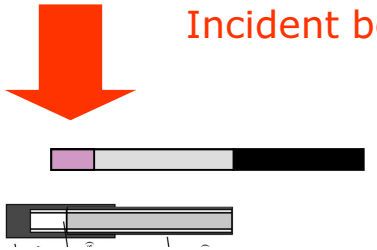

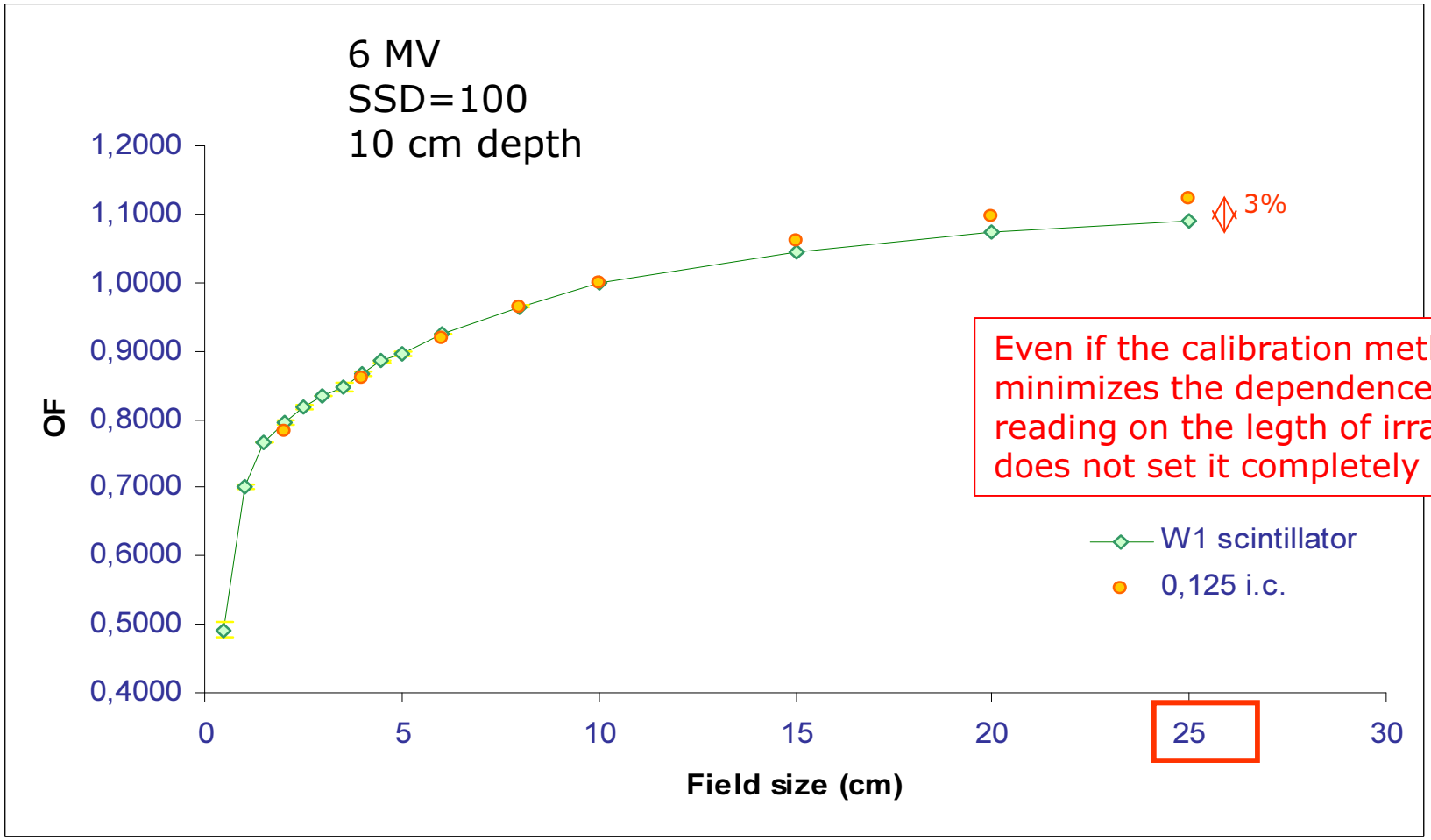

Even if the calibration methodology minimizes the dependence of the detector reading on the legth of irradiated fiber it does not set it completely independent

Organic scintillator
(W1 Standard Imaging)

OF: small fields

Perpendicular to beam axis

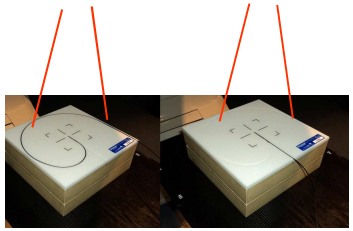

Parallel to beam axis

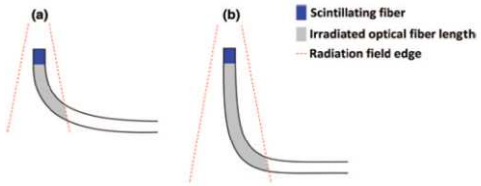

Calibration name	Detector orientation	Phantom	Depth (cm)	SSD (cm)	Field size CRL (f1) cm^2	Field size gain (f2) cm^2
"Standard" (A)	Perpendicular to beam axis	Calibration plate + Plastic water	10	100	40 x 40	10 x10
Small fields (B)	Parallel to beam axis	MP3 water	10	100	10 x 10	10 x 10
Small fields (C)	Parallel to beam axis	MP3 water	10	100	5 x 5	5 x 5

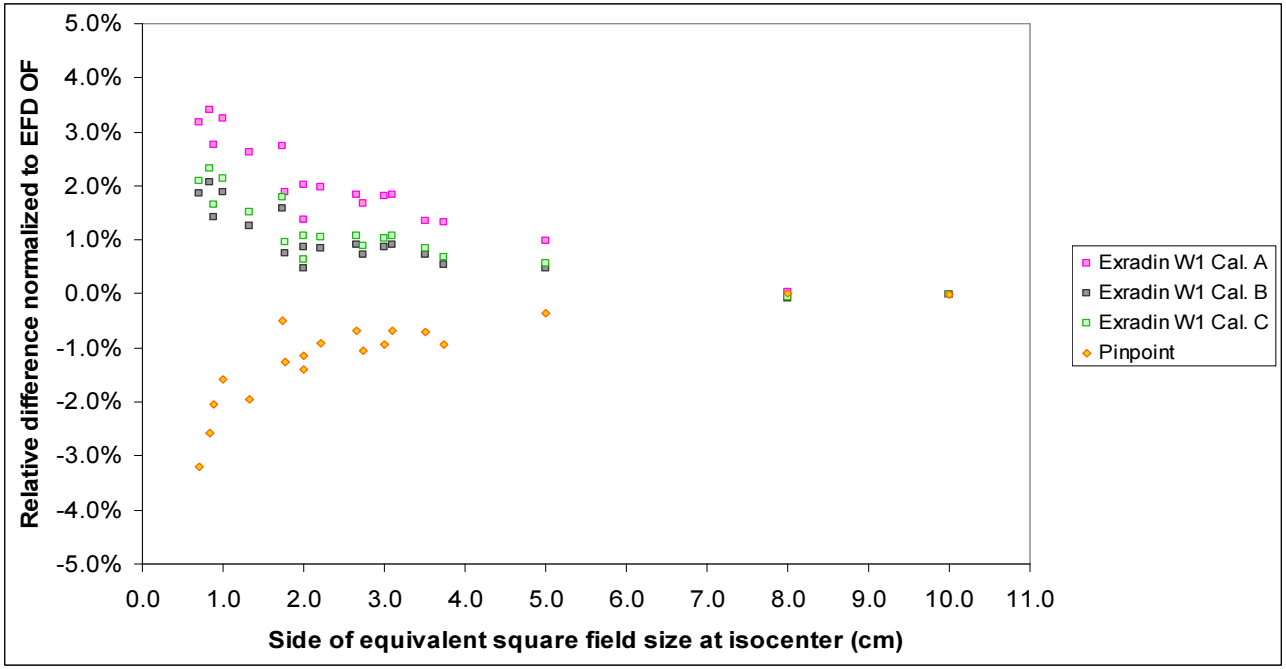

The calibration methodology proposed by the manufacturer is not appropriate for measuring output factors for small fields. Calibration using smaller fields and the detector axis parallel to beam axis should be used.

These results show that the CRL and gain depend on field size and orientation of the scintillator.

Relative differences of OF normalized to EFD-3G OF.

OF are referred to a 10 x 10 cm^2 field size.

ESTRO School

Organic scintillator
(W1 Standard Imaging)

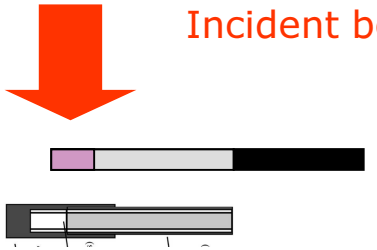

6 MV
SSD=90
10 cm depth

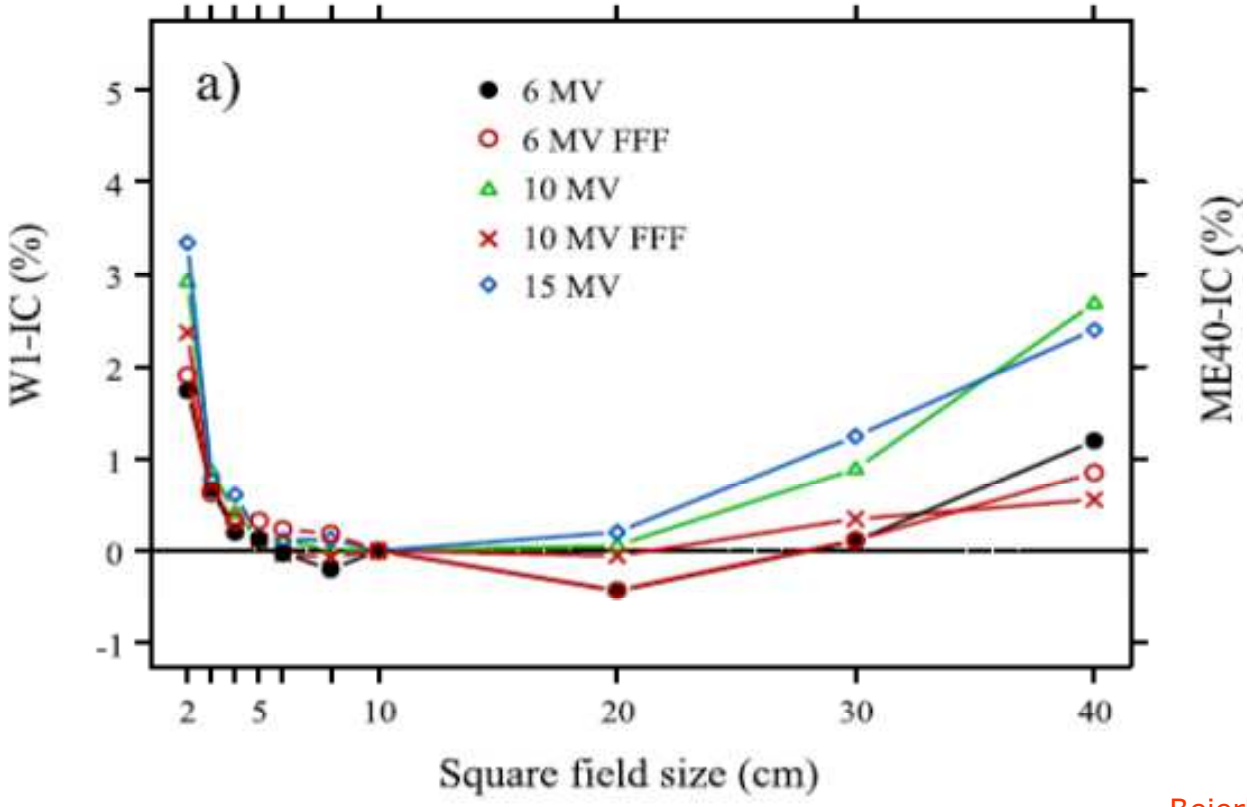

Beierholm, radiat. Measurements,2014

ESTRO School

Detector	Appropiate for	Be careful
Ionization chambers	❑ For x-ray depth dose measurements ❑ Plane-parallel chamber for build-up region ❑ Output factors large fields ❑ Output factors for small fields (micro-chambers)	❑ Check polarity effect for both photon and electron beams ❑ Always measure with the same nominal V ❑ For micro-chambers the stem signal can be an issue ❑ Correct by Sw,air for electron depth dose measurements. ❑ Use small volume detectors for scanning ❑ Effective point of measurement ❑ Check stability temperature during measurements

Diodes	❑ Depth dose measurements and profiles
	  ❑ Shielded detector for x-rays
	  ❑ Non-shielded for electron beams
	❑ Output factors
	  ❑ Shielded detector standard/large fields
	  ❑ Non-shielded for small fields
		❑ Energy dependence
		❑ Sensitivity variation with accumulated dose
		❑ May present sensitivity variation with dose rate
		❑ Check stability temperature during measurements

Detector	Appropiate for	Be careful
Diamond	❑ **Output factors small fields** ❑ **Profiles**	❑ Dose rate dependence ❑ Huge production spread ❑ Not really small > 3mm
Synthetic diamond	❑ **Output factors small fields** ❑ **Profiles**	❑ No dose rate dependence ❑ Production reproducible ❑ Small: 2.2 mm diameter
Organic scintillators	❑ **Depth dose measurements and profiles** ❑ **Output factors** ❑ **Profiles**	❑ Cerenkov radiation response contamination ❑ Commercial solution Standard Imaging

Which detector would you chose to measure…??:

1. PDD in a large 18MV X-ray field:
2. PDD in a 1x1 cm^2 X-ray field:
3. Profile in a 10x10 cm^2 X-ray field:
4. Output factor 2x2 cm^2 X-ray field:
5. PDD 10x10 cm^2 electron field:
6. Output factors electron beam:
7. Reference dose X-ray beam:

Summary

- No detector is (obviously) optimal for all situations ⇒ Understanding strong and weak sides of the experimental setup, including the phantom, is vital.
- Be critical of your measurement results. Try to verify important data, such as TPS input, with independent measurements or calculations.

References 1

1. Yin Z, Hugtenburg RP, Beddoe AH (2004) Response corrections for solid-state detectors in megavoltage photon dosimetry. Phys Med Biol 49, 3691–702.
2. Heydarian M, Hoban PW, Beddoe AH (1996) A comparison of dosimetry techniques in stereotactic radiosurgery. Phys Med Biol 41, 93-110.
3. Westermark M, Arndt J, Nilsson B, Brahme A (2000) Comparative dosimetry in narrow high-energy photon beams.
Phys Med Biol 45, 685-702.
4. McKerracher C, Thwaites DI (1999) Assessment of new small-field detectors against standard-field detectors for practical stereotactic beam data acquisition. Phys Med Biol 44, 2143-60.
5. Dasu A, Löfroth PO, Wickman G (1998) Liquid ionization chamber measurements of dose distributions in small 6 MV photon beams. Phys Med Biol 43, 21-36.
6. Eklund A, Ahnesjö A (2010) Spectral perturbations from silicon diode detector encapsulation and shielding in photon fields. Med Phys 37, 6055-60.
7. Djouguela A, Griessbach I, Harder D, Kollhoff R, Chofor N, Rühmann A, Willborn K, Poppe B (2008) Dosimetric characteristics of an unshielded p-type Si diode: linearity, photon energy dependence and spatial resolution. Z Med Phys 18, 301-6
8. Saini AS, Zhu TC (2002) Temperature dependence of commercially available diode detectors. Med Phys 29, 622-30.

ESTRO School

References 2

9. Wickman G, Nyström H (1992) The use of liquids in ionization chambers for high precision radiotherapy dosimetry. Phys Med Biol 37, 1789-1812.
10. Rikner G (Year?) Symposium on Semiconductor Detectors. Inst. of Oncology, Dept. of Hospital Physics, Uppsala, Sweden
11. Laub WU, Kaulich TW, Nusslin F (1999) A diamond detector in the dosimetry of high-energy electron and photon beams.
Phys Med Biol 44, 2183-92.
12. Martens C, De Wagter C, De Neve W (2000) The value of the PinPoint ion chamber for characterization of small field segments used in intensity-modulated radiotherapy. Phys Med Biol 45, 2519-30.
13. IAEA (2000) Absorbed dose determination in external beam radiotherapy: An international code of practice for dosimetry based on standards of absorbed dose to water. IAEA Technical Report Series Report No. 398, International Atomic Energy Agency (Vienna)
14. Galbraith DM, Rawlinson JA, Munro P (1984) Dose errors due to charge storage in electron irradiated plastic phantoms. Med Phys 11, 197-203
15. De Angelis C, Onori S, Pacilio M, Cirrone GAP, Cuttone G, Raffaele L, Bucciolini M, Mazzocchi S (2002) An investigation of the operating characteristics of two PTW diamond detectors in photon and electron beams. Med Phys 29, 248-54

References 3

16. Zhu TC, Ahnesjö A, Lam KL, Li XA, Ma CM, Palta JR, Sharpe MB, Thomadsen B, Tailor RC (2009) Report of AAPM Therapy Physics Committee Task Group 74: in-air output ratio, Sc, for megavoltage photon beams. Med Phys 36, 5261-91
17. Jursinic PA (2006) Measurement of head scatter factors of linear accelerators with columnar miniphantoms. Med Phys 33, 1720-8
18. Frye DM, Paliwal BR, Thomadsen BR, Jursinic PA (1995) Intercomparison of normalized head-scatter factor measurement techniques. Med Phys 22, 249-53
19. Weber L, Nilsson P, Ahnesjö A (1997) Build-up cap materials for measurement of photon head-scatter factors. Phys Med Biol 42, 1875-86.
20. Krauss H (Institute for Radiooncology, Kaiser Franz Josef Hospital, Vienna, Austria) www.wienkav.at/kav/kfj/91033454/physik/PTW/liquid.htm
21. Agostinelli S, Garelli S, Piergentili M, Foppiano F (2008) Response to high-energy photons of PTW31014 PinPoint ion chamber with a central aluminum electrode. Med Phys 35, 3293-301
22. Aget H, Rosenwald JC (1991) Polarity effect for various ionization chambers with multiple irradiation conditions in electron beams. Med Phys 18, 67-72.

ESTRO School

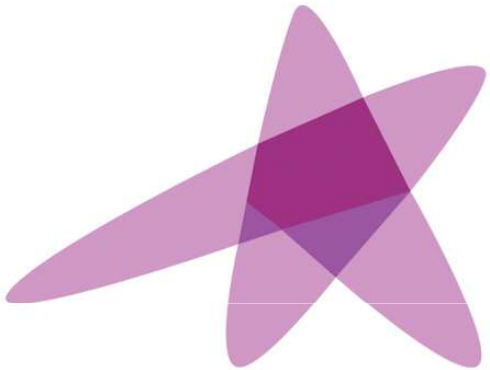

ESTRO School

WWW.ESTRO.ORG/SCHOOL

Pencil kernel models for photon dose calculations

Mania Aspradakis
maria.aspradakis@luks.ch

Acknowledgement
This presentation is based at large on material by **Dr Jörgen Olofsson**, who gave this lecture in this course in previous years

Learning objectives

- To understand the basic concept of pencil kernel based dose calculations.
- To know how photon pencil kernels can be characterized for a given photon beam.
- To learn about different ways to parameterize and summarize/integrate pencil kernels in order to enable efficient dose calculations.
- To understand the most important approximations and limitations that are associated with pencil kernel dose calculations.

Energy deposition kernels

Describe the spatial distribution of summarized energy deposition events caused by specific group of particles interacting at a given point, line, or surface in a given medium (normally water).

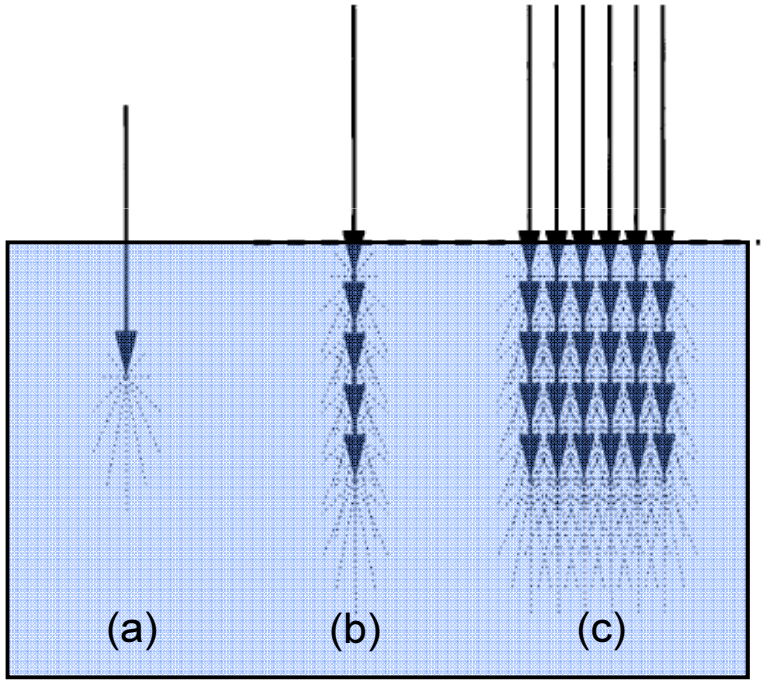

a) Point kernel
b) Pencil kernel
c) Slit kernel

Ostapiak, et al (1997) *Med Phys 24*, 743-50.

Dose through kernel integration

$$D(x,y,z) = \iint_{\text{Field}} \Psi(x',y') \cdot \frac{p}{\rho}(x-x',y-y',z)\,\mathrm{d}x'\,\mathrm{d}y'$$

K and k are other common notations

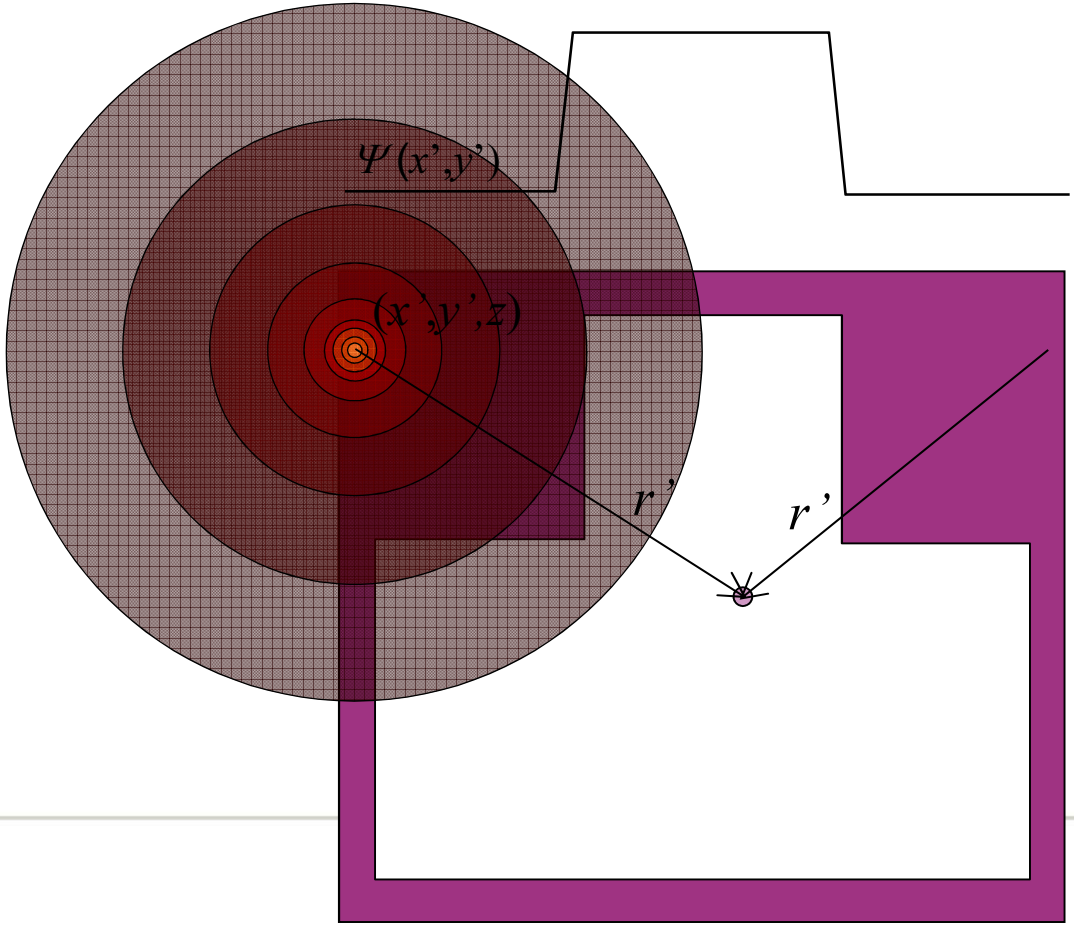

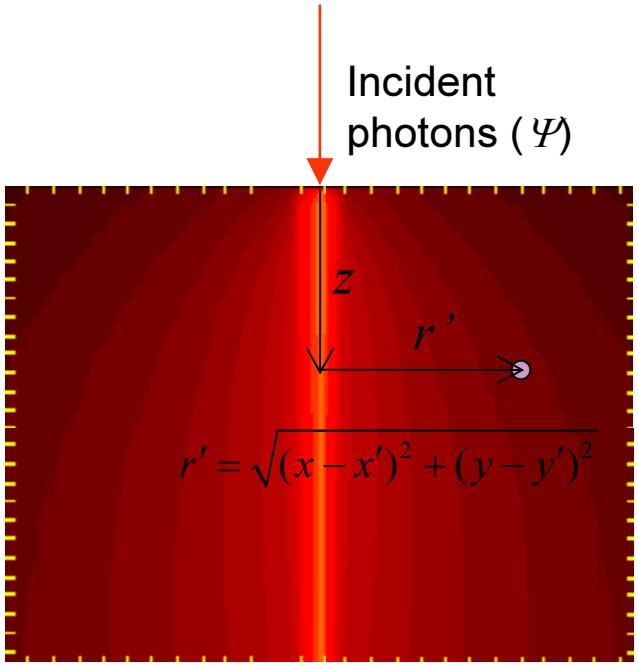

$$\frac{p}{\rho}(x-x',y-y',z)$$

Dose through kernel integration

$$D(x,y,z) = \iint_{\text{Field}} \Psi(x',y') \cdot \frac{p}{\rho}(x-x',y-y',z)\,\mathrm{d}x'\,\mathrm{d}y'$$

K and k are other common notations

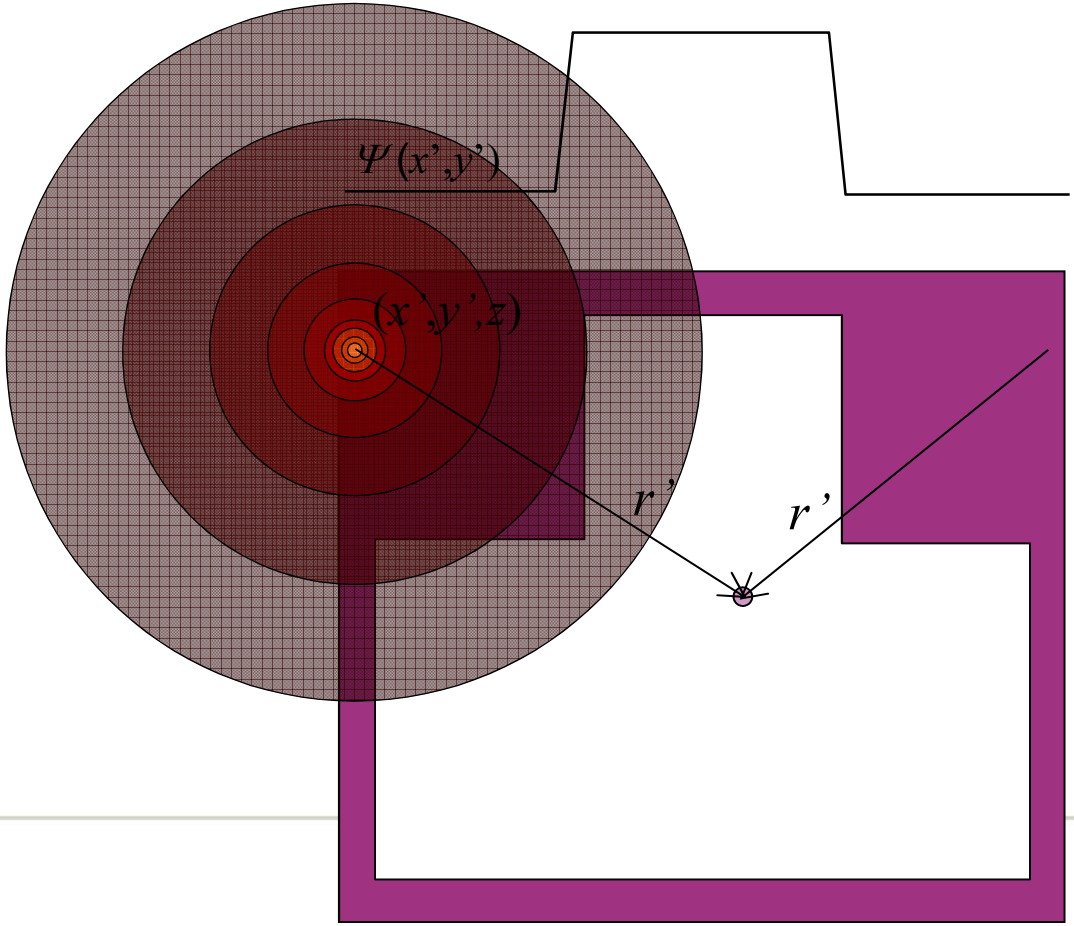

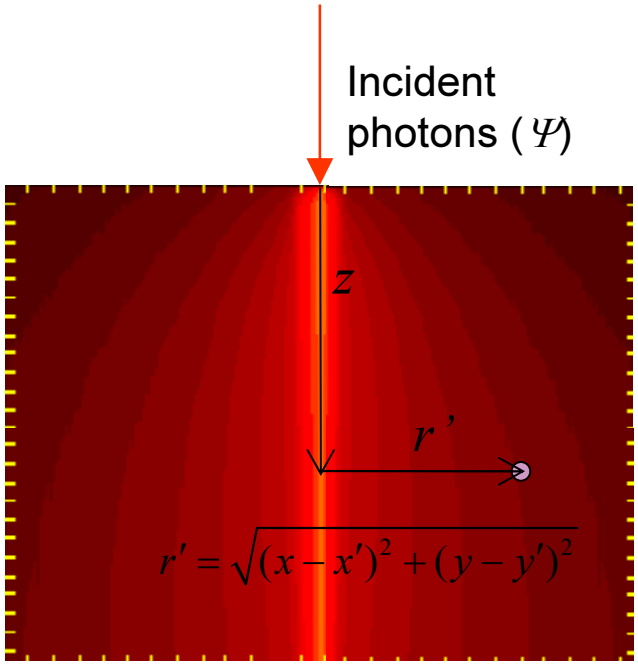

$$\frac{p}{\rho}(x-x',y-y',z)$$

Dimensions of a pencil kernel

Basic equation

$$D(x,y,z) = \iint_{\text{Field}} \Psi(x',y') \cdot \frac{p}{\rho}(x-x', y-y', z)\,\mathrm{d}x'\,\mathrm{d}y'$$

Dimensional analysis

$$\frac{E}{m} \quad \Leftrightarrow \quad \mathrm{E} \quad \cdot \quad \frac{1}{m}$$

Hence, the dimension is:

“One over mass”

Finite sized pencil beams (FSPB or beamlets)

Pre-integrated over a finite beam area. Reduces time for super-position, but requires constant energy fluence over beamlet area.

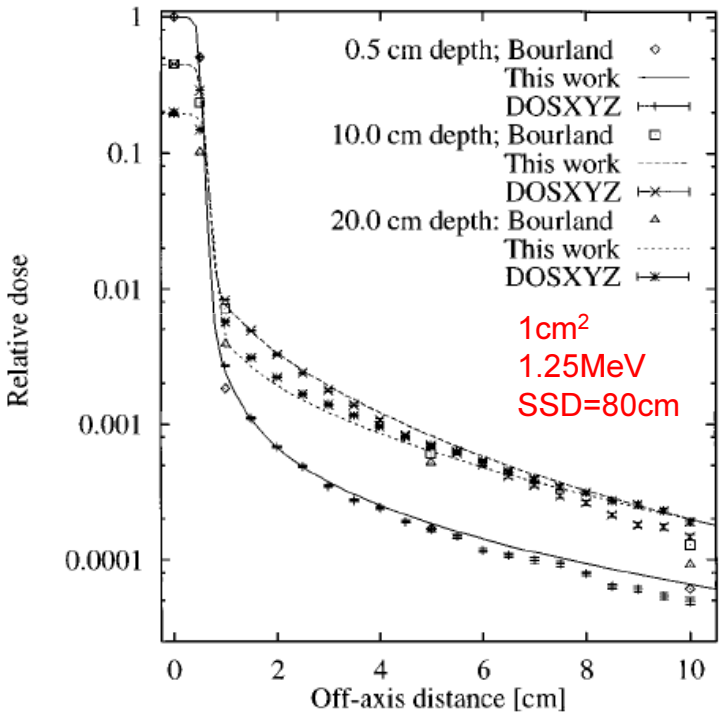

Ostapiak, et al (1997) *Med Phys 24*, 743-50.

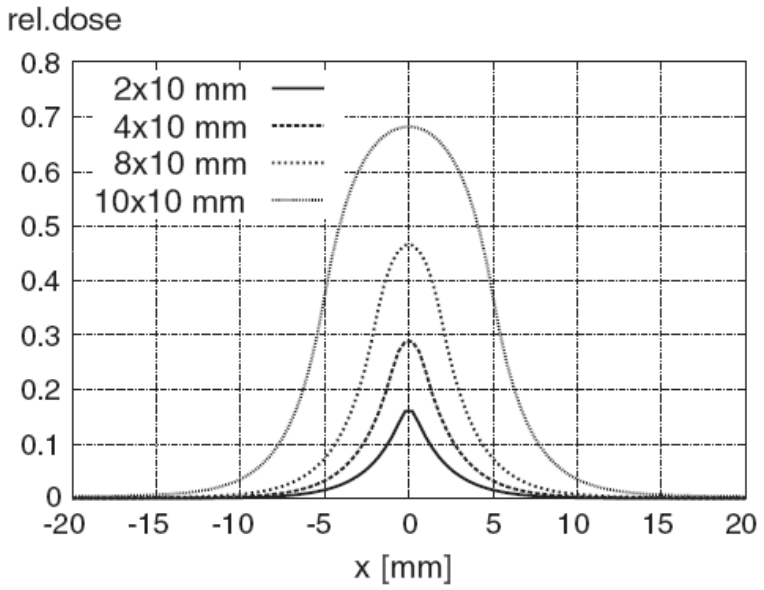

U Jelen, et al (2005) *Phys Med Biol 50*, 1747-66.

Mainly for fast calculations in IMRT optimization. However, the width of a beamlet can not be larger than the resolution of the grid used for fluence optimization.

ESTRO School

Pencil kernel characterization

I. Radial differentiation of relative dose on CAX (using quantities describing broad beam dosimetric data).

$$d(r,z) = \frac{1}{2\pi\, r\, dr} D_{\text{rel,meas}}(r,z)$$

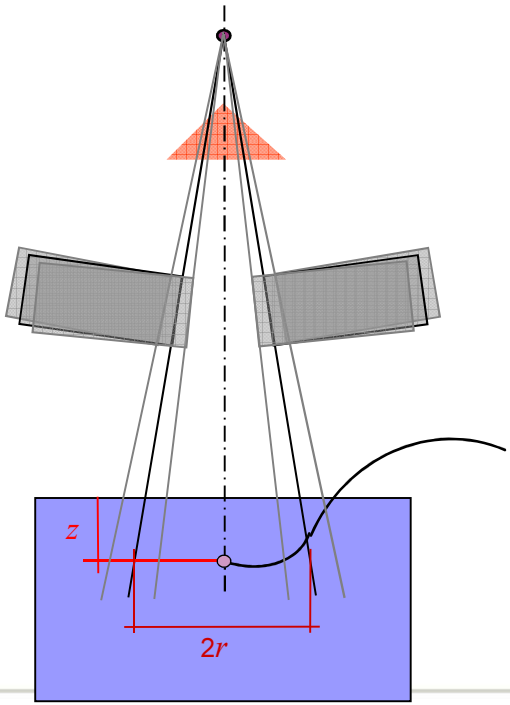

Ignored:

- Beam divergence
- Off-axis changes in fluence
- Off-axis softening

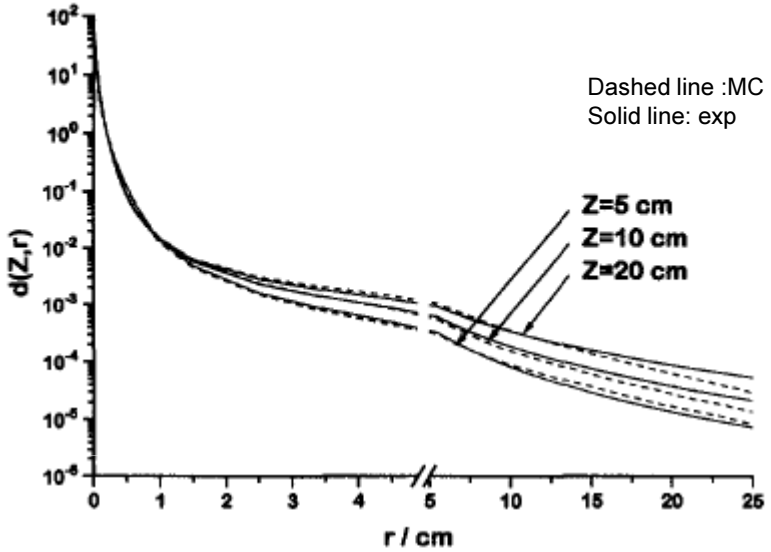

6 MV

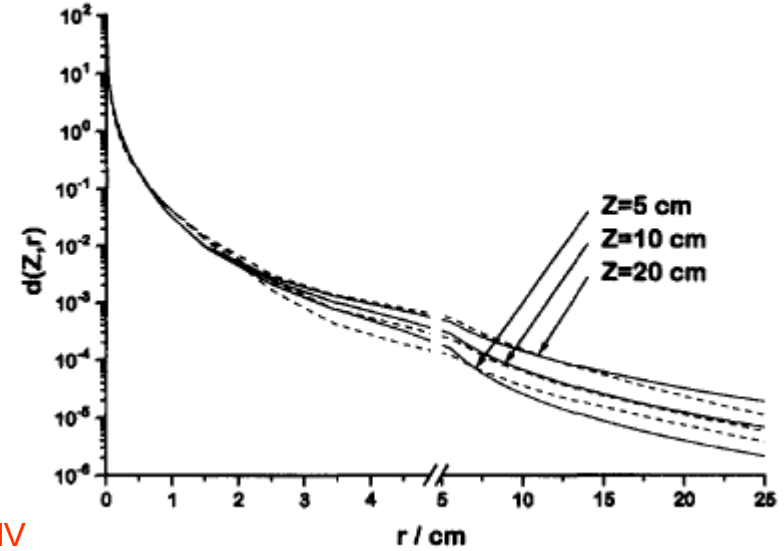

25 MV

CP Ceberg, et al (1996) *Med Phys 23*, 505-11.

Pencil kernel characterization

I. Radial differentiation using quantities describing broad beam dosimetric data.

$$D(Z,R) = M \cdot \left(\frac{D}{M}\right)_{ref} O_0(R) \cdot A(Z) \cdot \int_0^R d(Z,r) 2\pi r \, dr$$

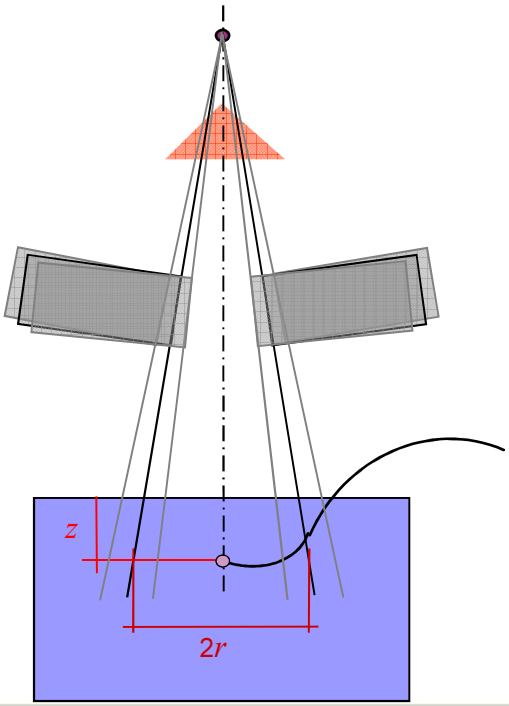

Effects from laterally varying energy fluence etc were ignored in this approach . These should be considered.

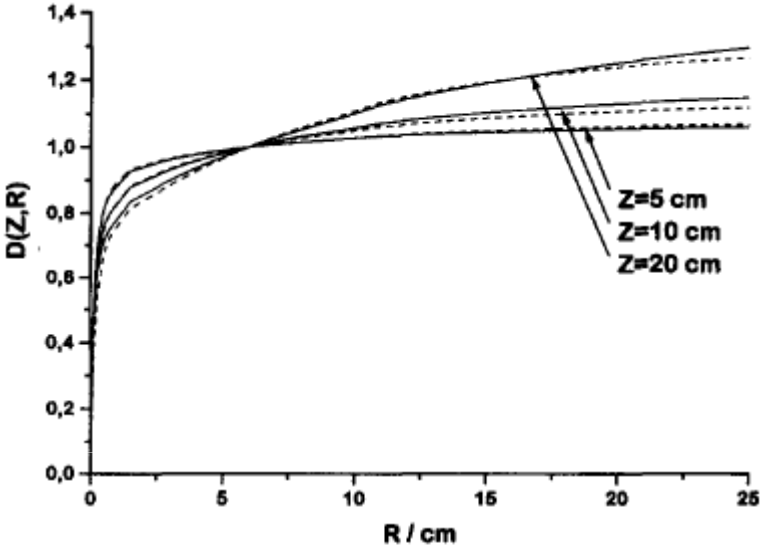

6 MV

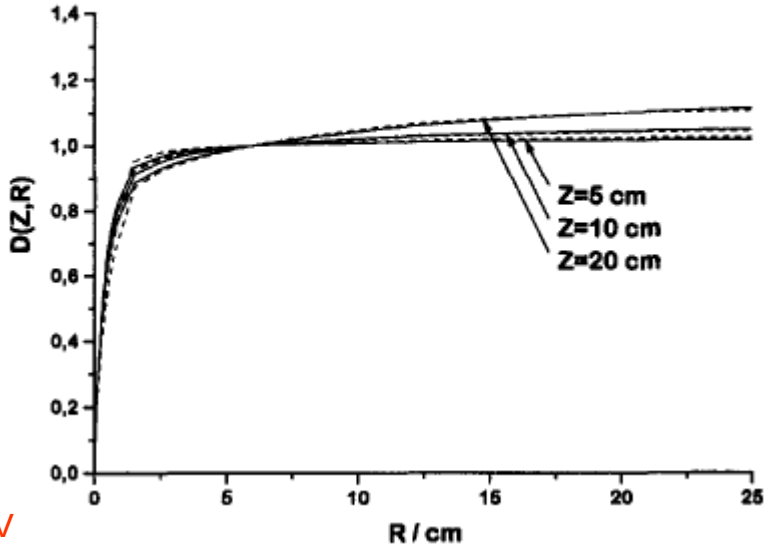

25 MV

CP Ceberg, et al (1996) *Med Phys 23*, 505-11.

Pencil kernel characterization

I. Radial scatter differentiation (measured data)

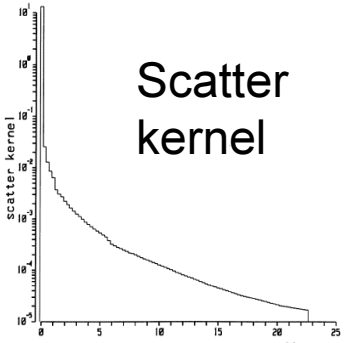

Scatter kernel

Off axis distance [cm]

6MV, 20cm x 20cm

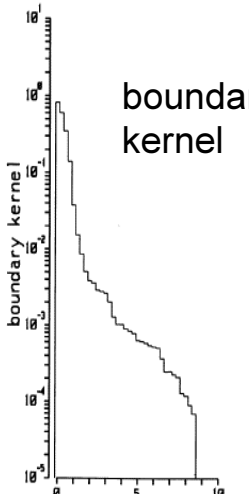

boundary kernel

Off axis distance [cm]

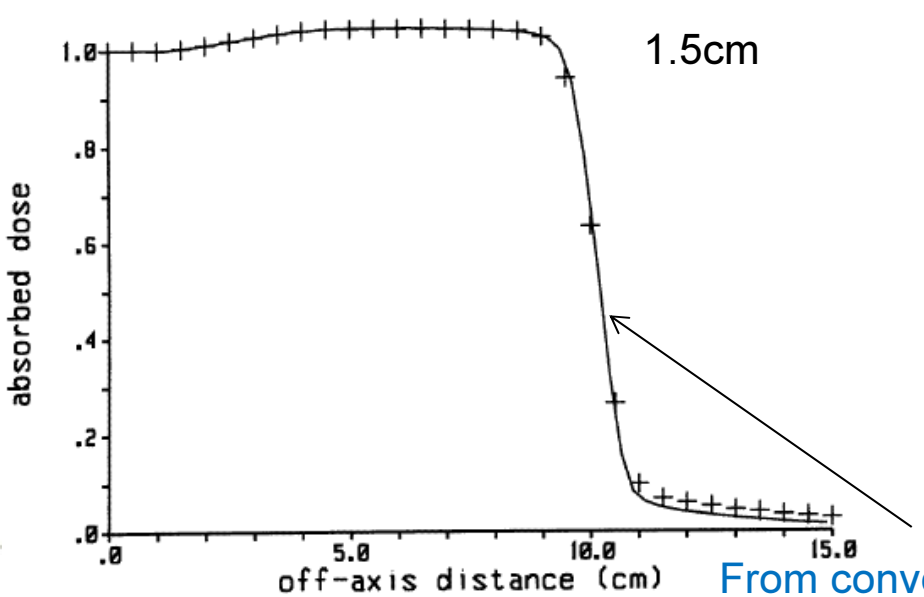

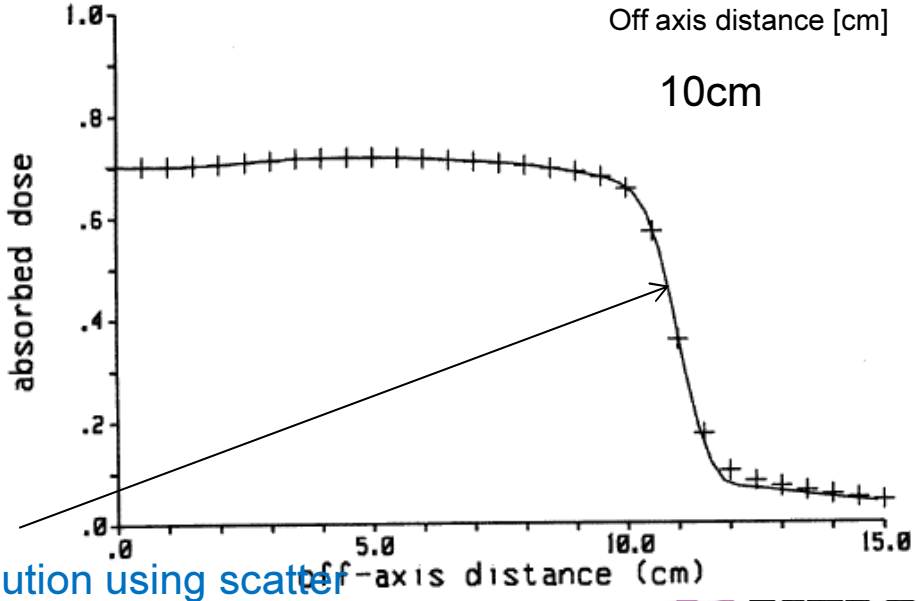

From convolution using scatter and boundary kernels

Storchi, et al (1996) PMB *41*, 637-656.

ESTRO School

Pencil kernel characterization

II. Optimisation of kernel shape - with the aid of a test pattern fluence

Ideal fluence pattern

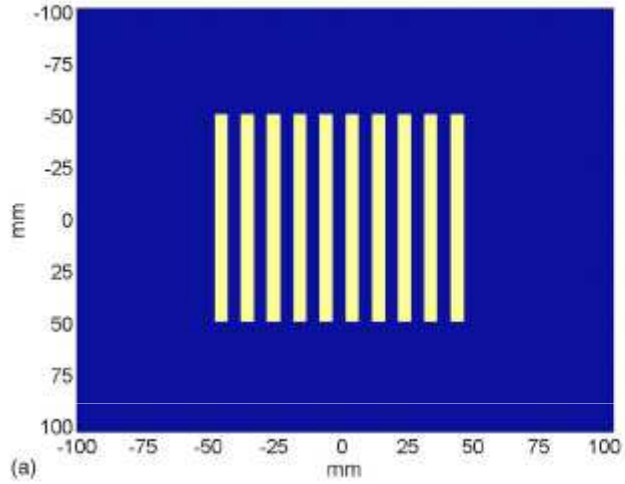

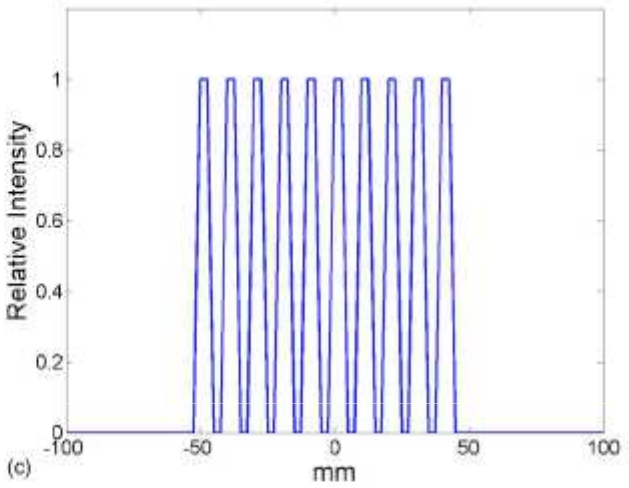

Ideal fluence profile

Actual fluence pattern

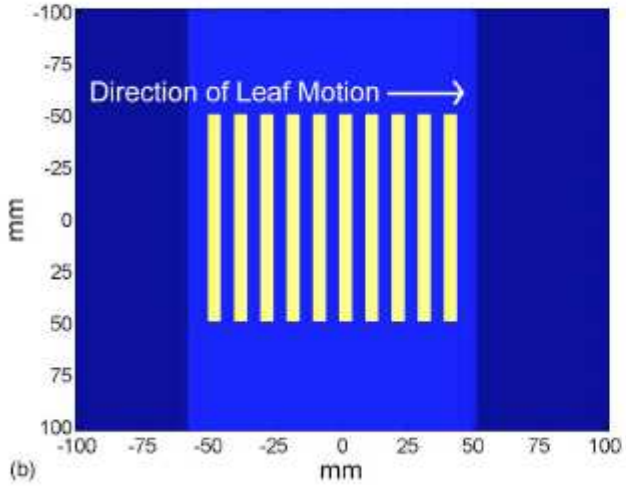

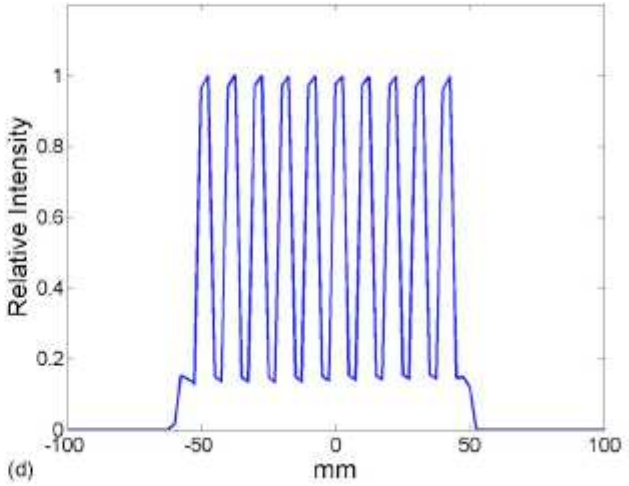

Actual fluence profile

Sensitive to radial pencil kernel properties, but **imperfections in the fluence modelling will yield errors in the resulting pencil kernel.**

Bergman et al (2004) *Med Phys 31*, 3279-87

ESTRO School

Pencil kernel characterization

II. Iterative optimisation of kernel shape

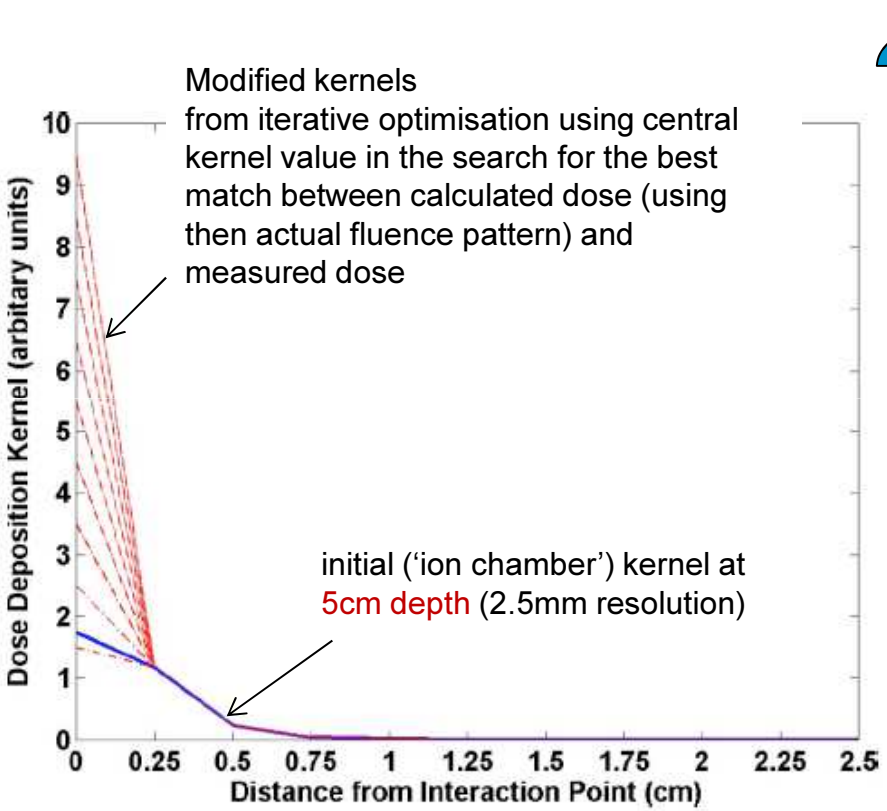

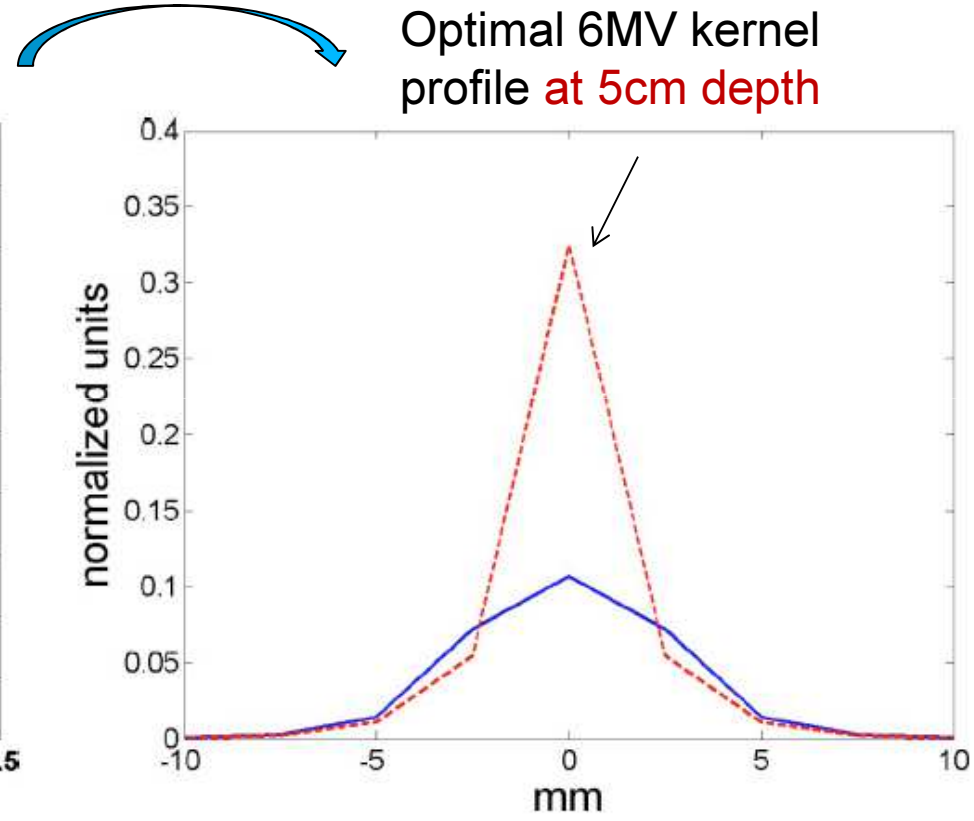

6MV (Varian 21EX), Pencil kernels optimisation on Eclipse TPS (PBC model)

Bergman et al (2004) *Med Phys 31*, 3279-87

ESTRO School

Pencil kernel characterization

II. Optimisation of kernel shape

Calculated dose profile using PBK reconstructed from experimental data measured with an ionisation chamber (IC-10)

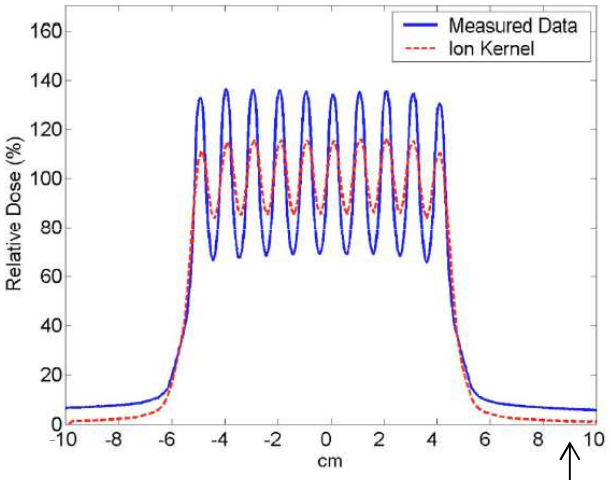

Calculated dose profile using PBK reconstructed from experimental data measured with film

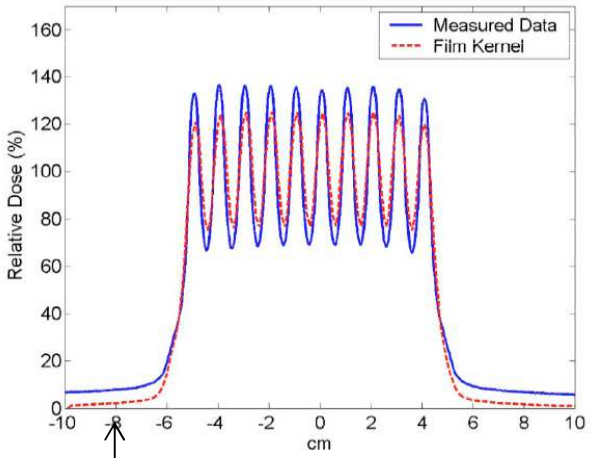

Calculated dose profile using iteratively optimised PBK s

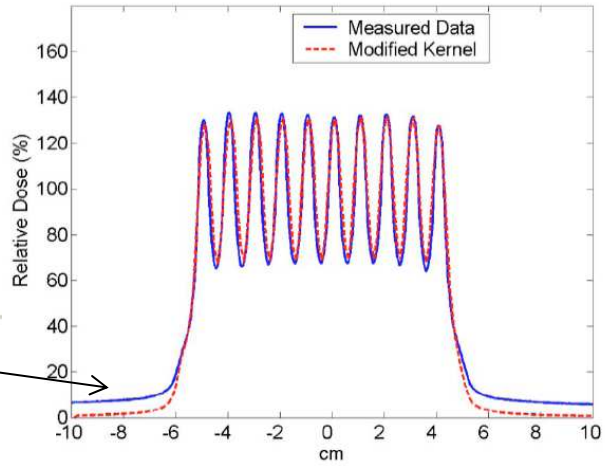

Inaccurate modelling of extra-focal scatter

Bergman et al (2004) *Med Phys 31*, 3279-87

Pencil kernel characterization

II. Optimisation of kernel shape

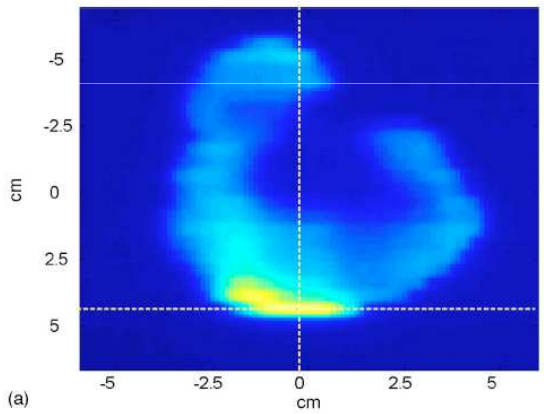

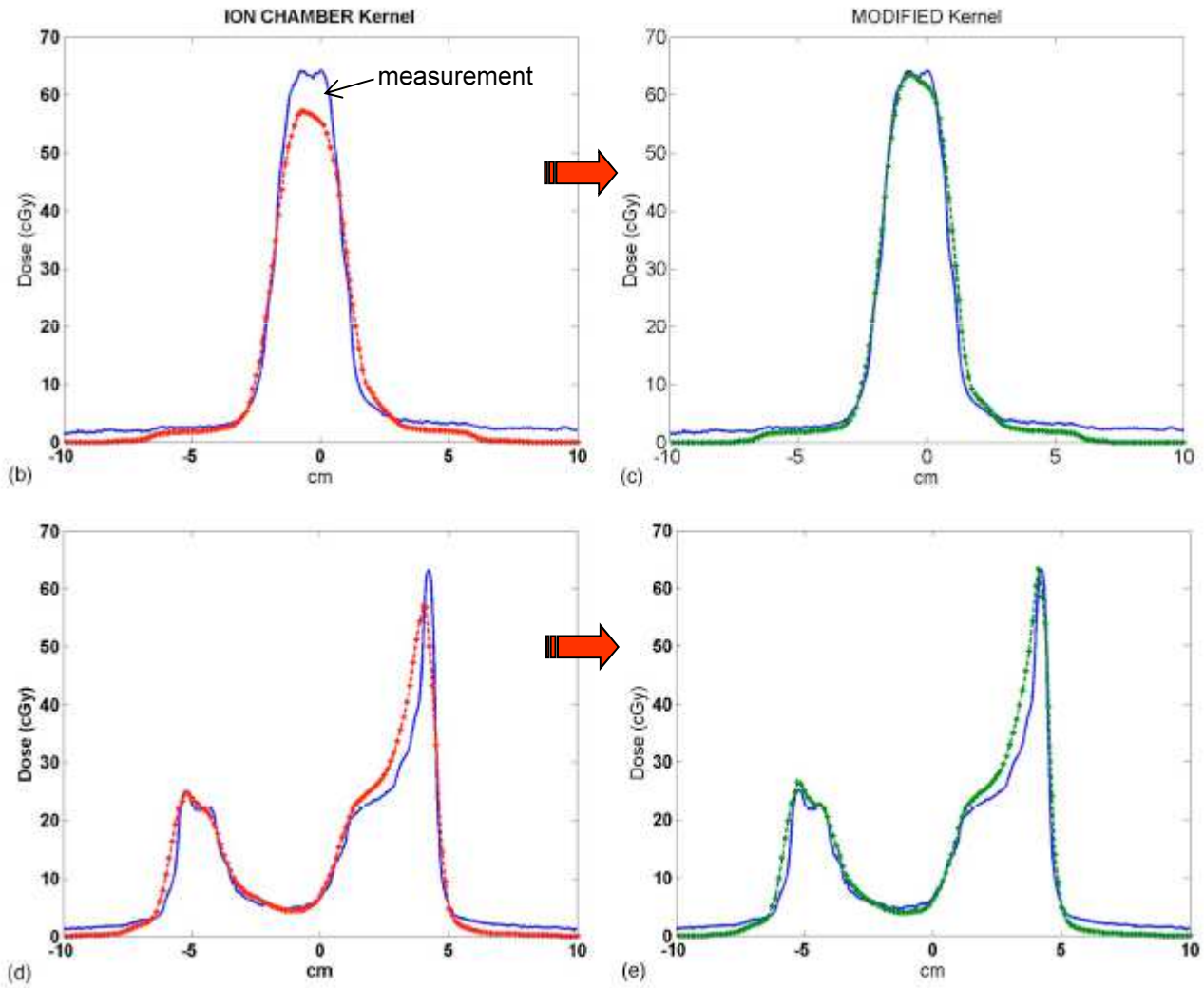

Bergman et al (2004) *Med Phys 31*, 3279-87

Pencil kernel characterization

III. Monte Carlo simulations

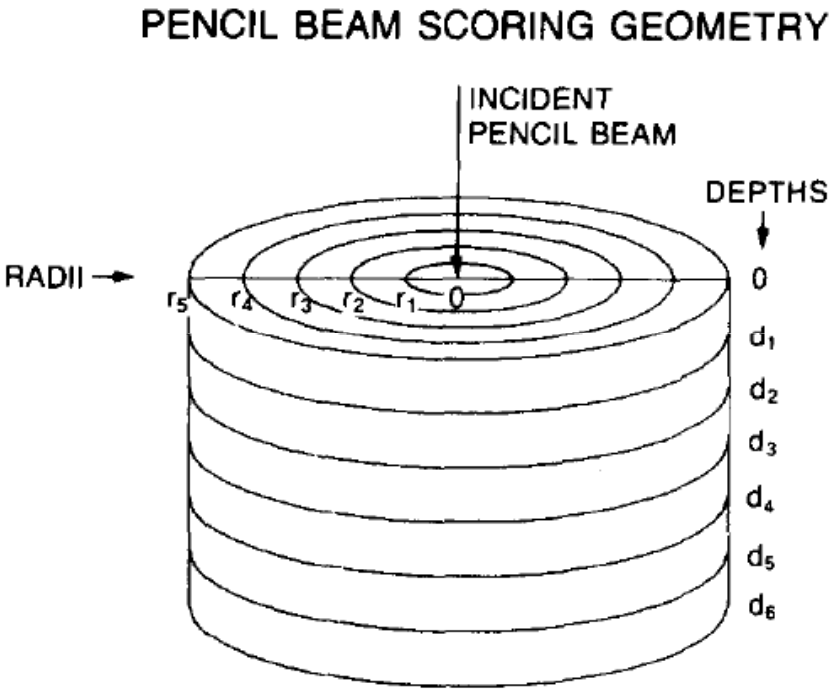

Beam characteristics included in MC simulations (poly-energetic kernels)

Source size modeled but transport through treatment head?

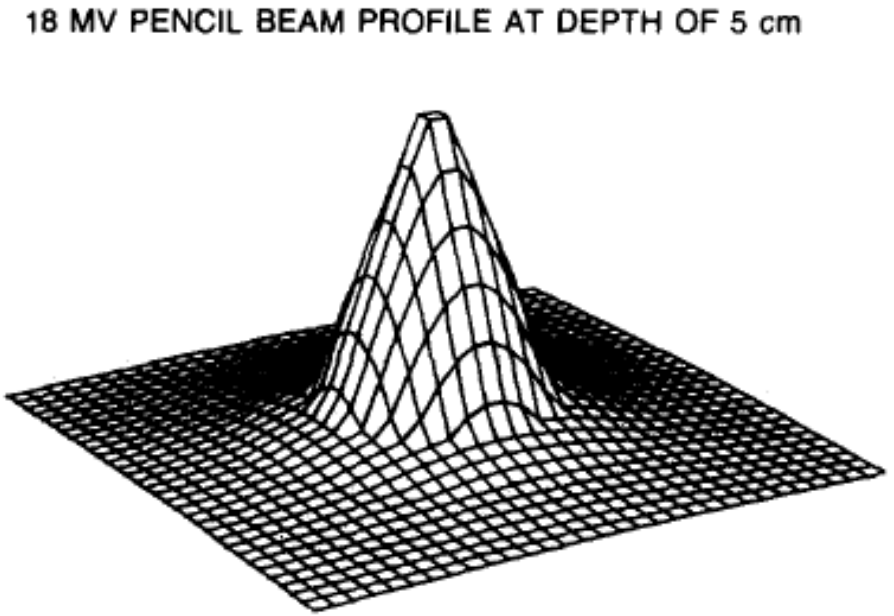

R Mohan and CS Chui (1987) *Med Phys 14*, 70-7

Pencil kernel characterization

IV. Combined MC-simulated mono-energetic pencil beam kernels using clinical beam spectra generated from measured depth doses

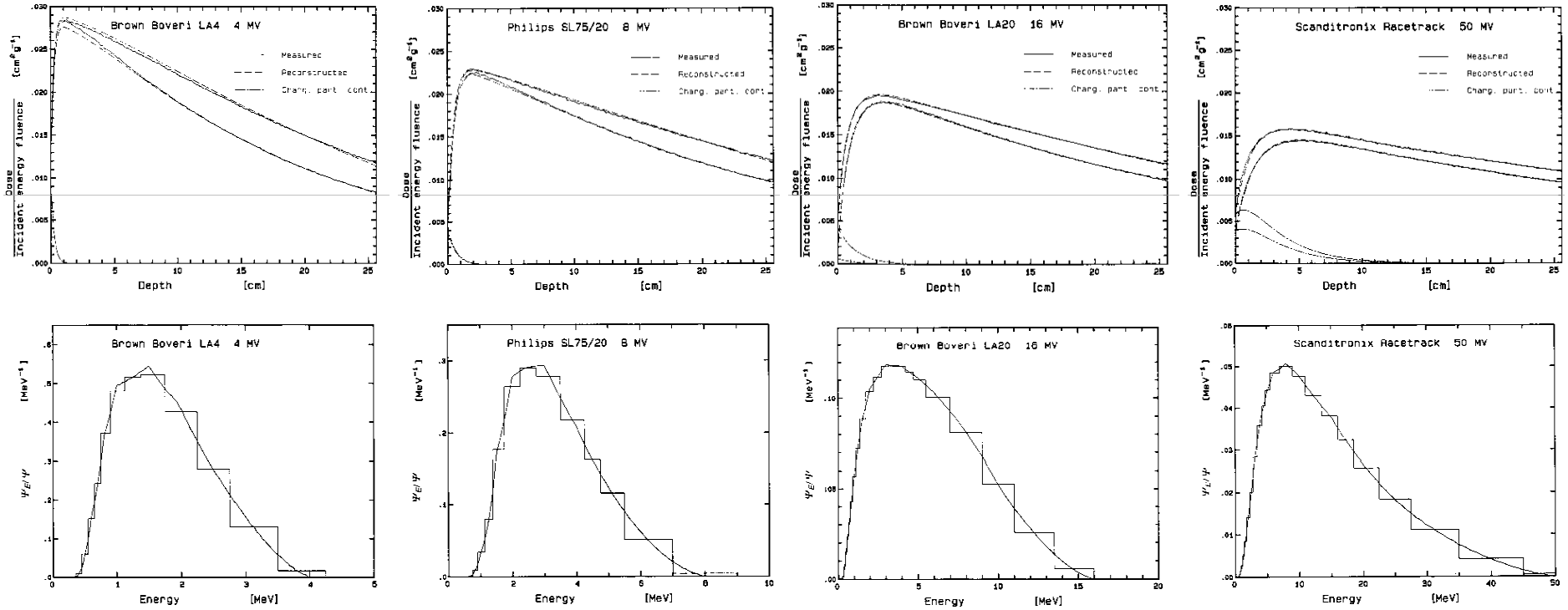

A Ahnesjö and P Andreo (1989) *Phys Med Biol 34*, 1451-64.

A Ahnesjö et al (1992) *Med Phys* 19, 263-273

ESTRO School

Pencil kernel characterization

V. Beam quality index as single parameter to determine pencil beam kernels

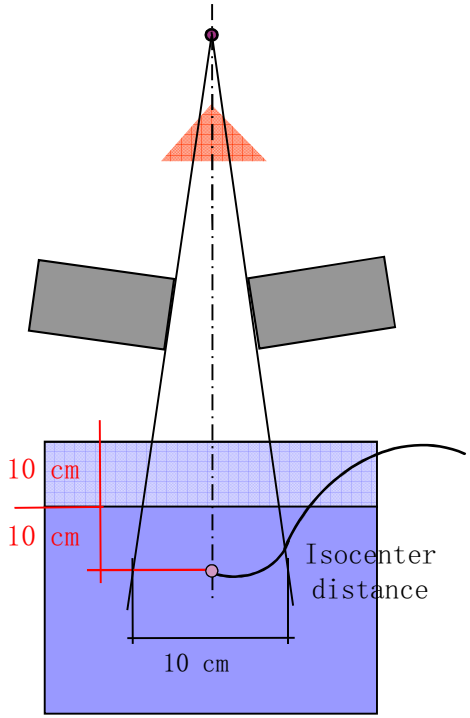

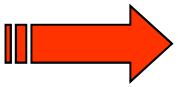

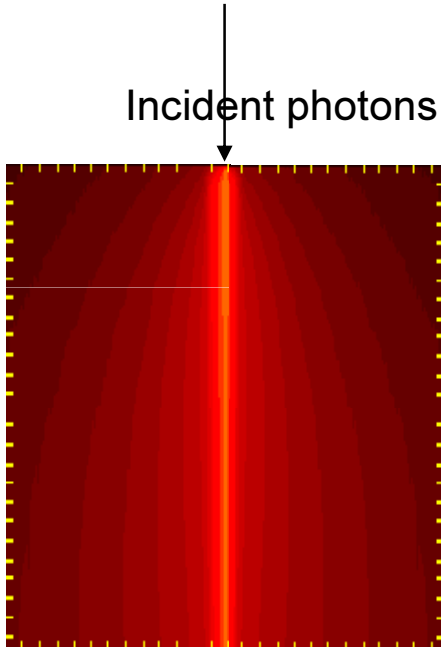

$$TPR_{20/10} = \frac{D(10\times10, z = 20\,cm)}{D(10\times10, z = 10\,cm)}$$

T Nyholm, et al (2006) *Radiother Oncol 78*, 347-51.

ESTRO School

Energy fluence matrix

Sampling approaches

Kernel oriented fluence sampling points

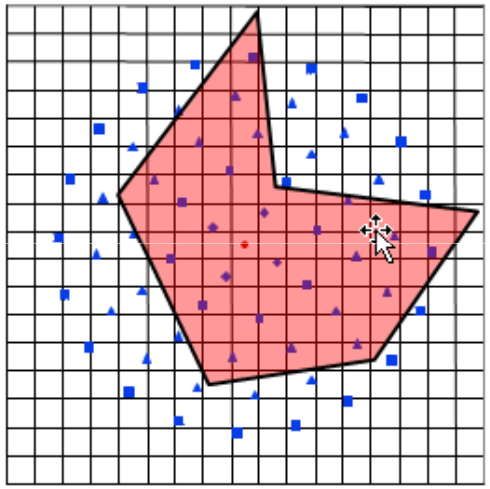

Most effective for
- single point calculations
- kernels of laterally limited range (i.e. primary dose, electron contamination)

Fluence matrix oriented fluence sampling points

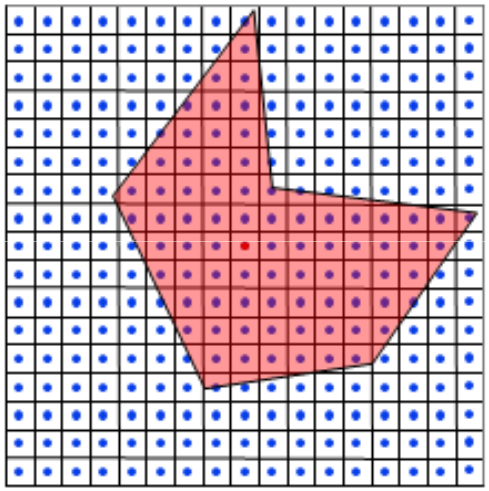

Raw implementation very time consuming. Much faster (per point) by means of fast convolution techniques (yields all points in a lateral plane calculated at once)

Analytical integration over discrete beam segments

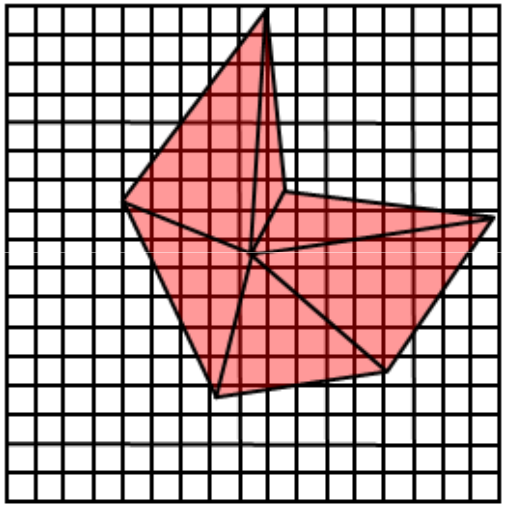

Assumes constant fluence per segment, uses sampling to calculate effective fluence:

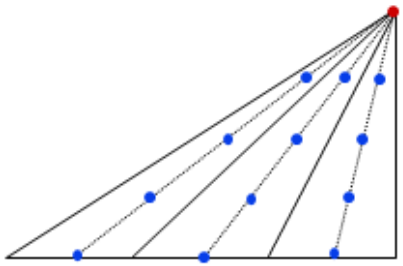

Figures from Anders Ahnesjö

Convolution integral

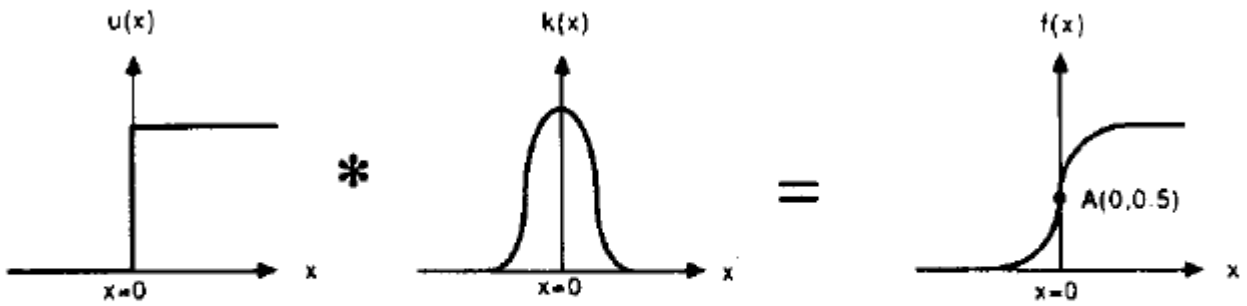

A convolution is an integral that expresses **the amount of overlap of one function as it is shifted over another function**.

C-S Chui and R Mohan, Med Phy 15(2), 1988

$u(x) = 0, \quad \text{if } x<0,$

$= 1/2, \quad \text{if } x=0,$

$= 1, \quad \text{if } x>0.$

step function

$k(x) = k(-x)$

$k(x) \geq 0$

$\int_{-\infty}^{+\infty} k(x)\,dx = 1$

1D kernel function

$f(x) = \int_{-\infty}^{+\infty} u(x')k(x-x')dx' = \int_{0}^{+\infty} k(x-x')dx'$

The steps to convolve these two functions are:

1. Folding
2. Displacement
3. Multiplication
4. Integration

2D definition

$$[f \otimes g](x,y) = \int_{-\infty}^{\infty}\int_{-\infty}^{\infty} f(x',y')g(x-x',y-y')dx'dy'$$

ESTRO School

Convolution theorem

The convolution theorem states that the Fourier of a convolution is the point wise product of Fourier transforms.

$\mathcal{F}$ denotes Fourier transform operator

$$\mathcal{F}\{f\} = \int_{\mathbb{R}^n} f(x) e^{-2\pi i x \cdot \nu}\,\mathrm{d}x$$

$$\mathcal{F}\{g\} = \int_{\mathbb{R}^n} g(x) e^{-2\pi i x \cdot \nu}\,\mathrm{d}x$$

Pointwise multiplication

$$\mathcal{F}\{f * g\} = \mathcal{F}\{f\} \cdot \mathcal{F}\{g\}$$

or

$$\mathcal{F}\{f \cdot g\} = \mathcal{F}\{f\} * \mathcal{F}\{g\}$$

Applying the inverse Fourier transform, $\mathcal{F}^{-1}$

$$f * g = \mathcal{F}^{-1}\{\mathcal{F}\{f\} \cdot \mathcal{F}\{g\}\}$$

Standard (discrete) Fourier convolution for N points has a complexity of: 2 N^2
e.g . For a 256 x 256 matrix, calculation time is proportional to 2 x 65 536

ESTRO School

Fast Fourier Transform (FFT) convolution

FFT is a way to compute the same result more quickly: operations proportional to 2 N ln(N) instead $\Rightarrow$ increase in speed of the order of N/ln(N)

e.g. For a 256 x 256 matrix, complexity in computation of 2 x 617 $\Rightarrow$ increase in speed by **a factor of 106.**

Calculation recipe for the lateral dose distribution at a given depth through FFT convolution.

1. Perform a 2D FFT on the pencil kernel (preferably pre-stored!).
2. Perform a 2D FFT on the lateral energy fluence distribution.
3. Mulitply the two transformed distributions.
4. Perform an inverse 2D FFT (FFT^{-1}) on the resulting product.
5. Convolution (i.e. dose calculation) completed.

R Mohan and CS Chui (1987) *Med Phys 14*, 70-7

Kernels that are laterally invariant enable FFF convolution

ESTRO School

Pencil beam kernel parameterization - 1

PB kernel represented as double exponential, tabulated over depth

$$\frac{p}{\rho}(r,z) = \frac{A_z e^{-a_z r}}{r} + \frac{B_z e^{-b_z r}}{r}; \qquad a_z > b_z$$

"primary" dose — "scatter" dose

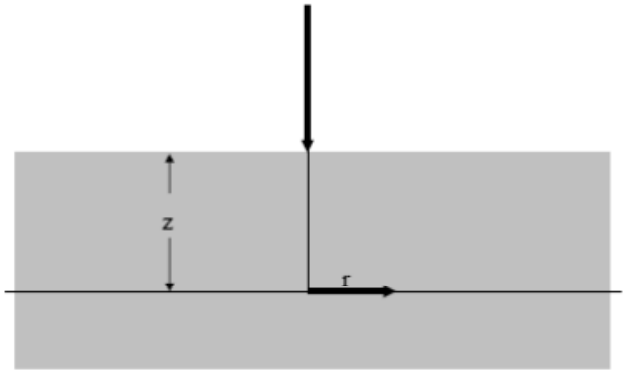

4 parameters required at each depth (z) for a given photon beam

	5 MV				8 MV				18 MV			
z [cm]	A_z [cm g^{-1}]	a_z [cm^{-1}]	B_z [cm g^{-1}]	b_z [cm^{-1}]	A_z [cm g^{-1}]	a_z [cm^{-1}]	B_z [cm g^{-1}]	b_z [cm^{-1}]	A_z [cm g^{-1}]	a_z [cm^{-1}]	B_z [cm g^{-1}]	b_z [cm^{-1}]
2	0.269E-1	6.95	0.506E-4	0.116	0.157E-1	4.59	0.344E-4	0.125	0.827	3.59	0.256	0.167
5	0.221E-1	6.59	0.112E-3	0.159	0.132E-1	4.29	0.754E-4	0.168	0.660	2.62	0.707	0.243
10	0.169E-1	6.64	0.163E-3	0.158	0.105E-1	4.24	0.122E-3	0.173	0.548	2.49	0.919	0.219
15	0.132E-1	6.75	0.162E-3	0.137	0.848E-2	4.26	0.130E-3	0.154	0.460	2.44	0.963	0.193
20	0.103E-1	6.80	0.142E-3	0.119	0.688E-2	4.26	0.121E-3	0.137	0.391	2.41	0.934	0.173

This is the PB kernel parameterization in Oncentra TPS (formely Helax-TMS)

A Ahnesjö et al (1992) *Med Phys* 19, 263-273

Dose through kernel integration - 1

Double exponential, tabulated over depth

The dose to the central axis from a circular field with radius R (and laterally uniform energy fluence) can be calculated as

$$D = 2\pi \int_0^R \frac{A_z e^{-a_z r} + B_z e^{-b_z r}}{r} r\,dr$$

$$= 2\pi \left[\frac{A_z}{a_z}(1 - e^{-a_z R}) + \frac{B_z}{b_z}(1 - e^{-b_z R}) \right]$$

In the same way, the dose to the central axis from a square field, with side s, can be calculated by employing the equivalent circle with $R = 0.561 \cdot s$.

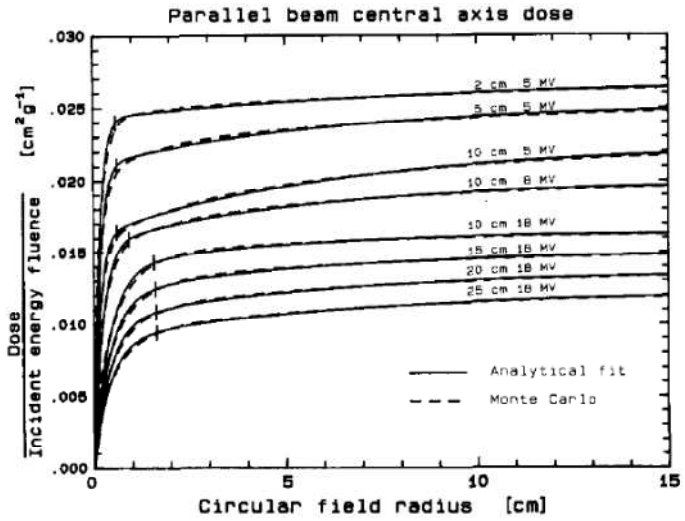

FIG. 4. Comparisons at various depths and beam energies between central axis dose for circular fields calculated directly with Monte Carlo pencil beam kernels (dashed lines) and analytical kernels (solid lines). The vertical bar on each curve marks the field radius for which lateral charged particle equilibrium is established, defined as the radius where the integral of the first term of Eq. (1) equals 98% of its value at infinite radius.

A Ahnesjö et al (1992) *Med Phys* 19, 263-273

This is the PB dose calculation in Oncentra TPS (formely Helax-TMS)

Dose through kernel integration - 1

Triangular surface integrals for double exponential pencil kernel

$$D_z(x,y) = \sum_i \psi_i \kappa_i \int_0^{\theta_i} \int_0^{(L_i/\cos\theta)} \frac{p}{\rho}(r,z)\, r\, dr\, d$$

$$\frac{p}{\rho}(r,z) = \frac{A_z e^{-a_z r}}{r} + \frac{B_z e^{-b_z r}}{r}$$

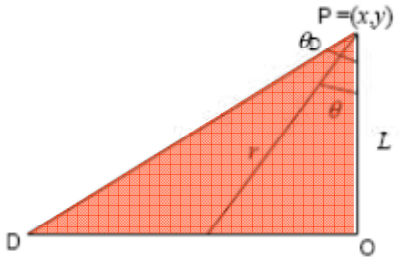

$$\iint_{\Delta POD} \frac{p}{\rho} dA = \int_0^{\theta_D L/\cos\theta} \int_0^{} \frac{p}{\rho} \cdot r\, dr\, d\theta$$

This integral is evaluated in terms of Sievert integrals S_1

Exponential kernel (scatter and second term in primary)

$$\int_0^{\theta_D L/\cos\theta} \int_0^{} \frac{e^{-ar}}{r} \cdot r\, dr\, d\theta = \frac{1}{a} \int_0^{\theta_D} \left(1 - e^{-aL/\cos\theta}\right) d\theta = \frac{1}{a} \cdot S_1(aL, \theta_D)$$

M Saxner (1999) Lecture: Pencil kernel dose engine.

Physics course for Helax TMS users in Uppsala, Sweden.

ESTRO School

Dose through kernel integration - 1

Triangular decomposition of arbitrary polygons (field shapes)

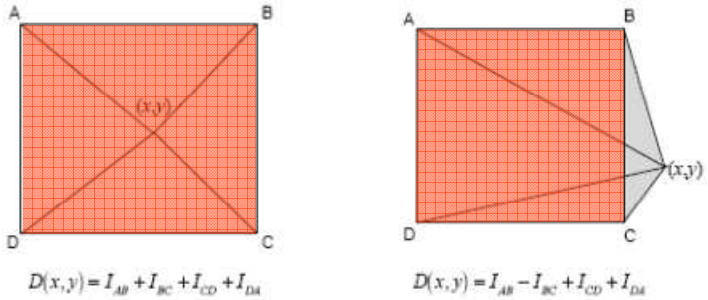

Fluence must be sampled over entire triangle:

Weighted mean over triangle:

$$\overline{\Psi}_{\Delta POD} = \frac{\sum_j e^{-br_j} \cdot \Psi(\mathbf{r}_j)}{\sum_j e^{-br_j}}$$

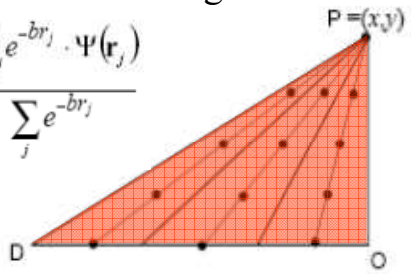

M Saxner (1999) Lecture: Pencil kernel dose engine.

Physics course for Helax TMS users in Uppsala, Sweden.

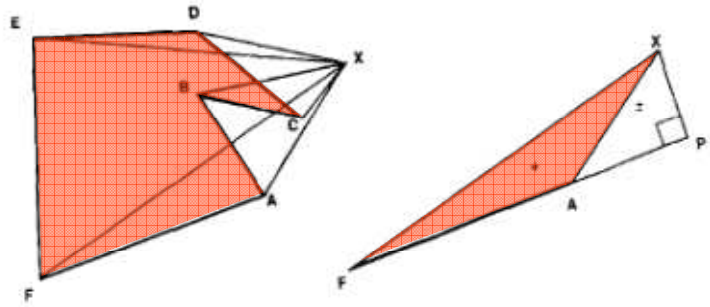

FIG. 2. A field shape given by the polygon chain ABCDEF (left) may, from the calculation point X, be decomposed into triangles XAB, XBC, etc. In this example, dose contributions from XAB and XCD have negative signs while the other contributions have positive signs. Each triangle is further decomposed into two right triangles as shown to the right, where the triangle XAF is decomposed into XPF with positive sign and XPA with negative sign.

A Ahnesjö et al (1992) *Med Phys* 19, 263-273

ESTRO School

Pencil beam kernel parameterisation - 2

Double exponential, incl. depth parameterization, solely based on $TPR_{20,10}$ (extracted from photon beam database)

Dose at the centre of a circular field with laterally constant energy fluence in a parallel beam:

$$D(R,d) = 2\pi\Psi\left[\frac{A}{a}(d)[1-\exp[-a(d)R]] + \frac{B}{b}(d)[1-\exp[-b(d)R]]\right]$$

d: depth in cm

$$\frac{A}{a}(A_{1-5};d) = A_1\left[1-\exp\left[A_2\sqrt{d^2+A_5^2}\right]\right]\exp[A_3 d + A_4 d^2]$$

$$\frac{B}{b}(B_{1-5};d) = B_1\left[1-\exp\left[B_2\sqrt{d^2+B_5^2}\right]\right]\exp[B_3 d + B_4 d^2]$$

$$a(a_{1-2};d) = a_1 + a_2 d$$

$$b(b_{1-5};d) = b_1\left[1-\exp\left[b_2\sqrt{d^2+b_5^2}\right]\right]\exp[b_3 d + b_4 d^2]$$

Kernel parameters can be partly interpreted physically

$$A_1 = \sum_{i=0}^{5} c_{i,A_1}(\mathrm{TPR}_{20/10})^i$$

The pencil kernel is completely defined through 17 parameters that can be calculated using $TPR_{20,10}$ (utilizing 6×17=102 coefficients).

This parameterization is valid and covers $TPR_{20,10}$ from 0.6 up to 0.81 at depths down to 50 cm.

$$\frac{D(x,d:A)}{M(A)} = \frac{1}{M(A)}\int \Psi(p;A)\frac{p}{\rho}[|x-p|,d,QI(p)]d^2p$$

T Nyholm, et al (2006) *Radiother Oncol 78*, 347-51.

This is the PB kernel parameterization in ESTRO MUV model
http://estro-education.org/publications/Documents/EstroBooklet10bw.pdf

ESTRO School

Pencil beam kernel parameterisation - 2

Double exponential, incl. depth parameterization, solely based on $TPR_{20,10}$ (extracted from photon beam database)

$$A_1 = \sum_{i=0}^{5} c_{i,A_1} (TPR_{20/10})^i$$

Table 1
Coefficients used for to calculate pencil beam parameters as a function of $TPR_{20/10}$

	C_0	C_1	C_2	C_3	C_4	C_5
A_1 ($cm^2\ g^{-1}$)	0.0128018	−0.0577391	0.1790839	−0.2467955	0.1328192	−0.0194684
A_2 (cm^{-1})	16.7815028	−279.4672663	839.0016549	−978.4915013	470.5317337	−69.2485573
A_3 (cm^{-1})	−0.0889669	−0.2587584	0.7069203	−0.3654033	0.0029760	−0.0003786
A_4 (cm^{-2})	0.0017089	−0.0169150	0.0514650	−0.0639530	0.0324490	−0.0049121
A_5 (cm)	0.1431447	−0.2134626	0.5825546	−0.2969273	−0.0011436	0.0002219
B_1 ($cm^2\ g^{-1}$)	−42.7607523	264.3424720	−633.4540368	731.5311577	−402.5280374	82.4936551
B_2 (cm^{-1})	0.2428359	−2.5029336	7.6128101	−9.5273454	4.8249840	−0.7097852
B_3 (cm^{-1})	−0.0910420	−0.2621605	0.7157244	−0.3664126	0.0000930	−0.0000232
B_4 (cm^{-2})	0.0017284	−0.0172146	0.0522109	−0.0643946	0.0322177	−0.0047015
B_5 (cm)	−30.4609625	354.2866078	−1073.2952368	1315.2670101	−656.3702845	96.5983711
a_1 (cm^{-1})	−0.0065985	0.0242136	−0.0647001	0.0265272	0.0072169	−0.0020479
a_2 (cm^{-2})	−26.3337419	435.6865552	−1359.8342546	1724.6602381	−972.7565415	200.3468023
b_1 (cm^{-1})	−80.7027159	668.1710175	−2173.2445309	3494.2393490	−2784.4670834	881.2276510
b_2 (cm^{-1})	3.4685991	−41.2468479	124.9729952	−153.2610078	76.5242757	−11.2624113
b_3 (cm^{-1})	−39.6550497	277.7202038	−777.0749505	1081.5724508	−747.1056558	204.5432666
b_4 (cm^{-2})	0.6514859	−4.7179961	13.6742202	−19.7521659	14.1873606	−4.0478845
b_5 (cm)	0.4695047	−3.6644336	10.0039321	−5.1195905	−0.0007387	0.0002360

The numerical values are given with a very high precision. Not because we claim this precision in the determination of specific parameters, but because of the bad conditioning of the problem, where just slight differences in the parameters can make large difference in the end.

T Nyholm, et al (2006) *Radiother Oncol 78*, 347-51.

This is the PB kernel parameterization in ESTRO MUV model
http://estro-education.org/publications/Documents/EstroBooklet10bw.pdf

ESTRO School

Pencil beam kernel parameterization - 2

Double exponential, incl. depth parameterization, solely based on $TPR_{20,10}$ (extracted from photon beam database)

T Nyholm, et al (2006) *Radiother Oncol 78*, 347-51.

$$D(R,d) = 2\pi\Psi\left[\frac{A}{a}(d)[1-\exp[-a(d)R]] + \frac{B}{b}(d)[1-\exp[-b(d)R]]\right]$$

6 MV

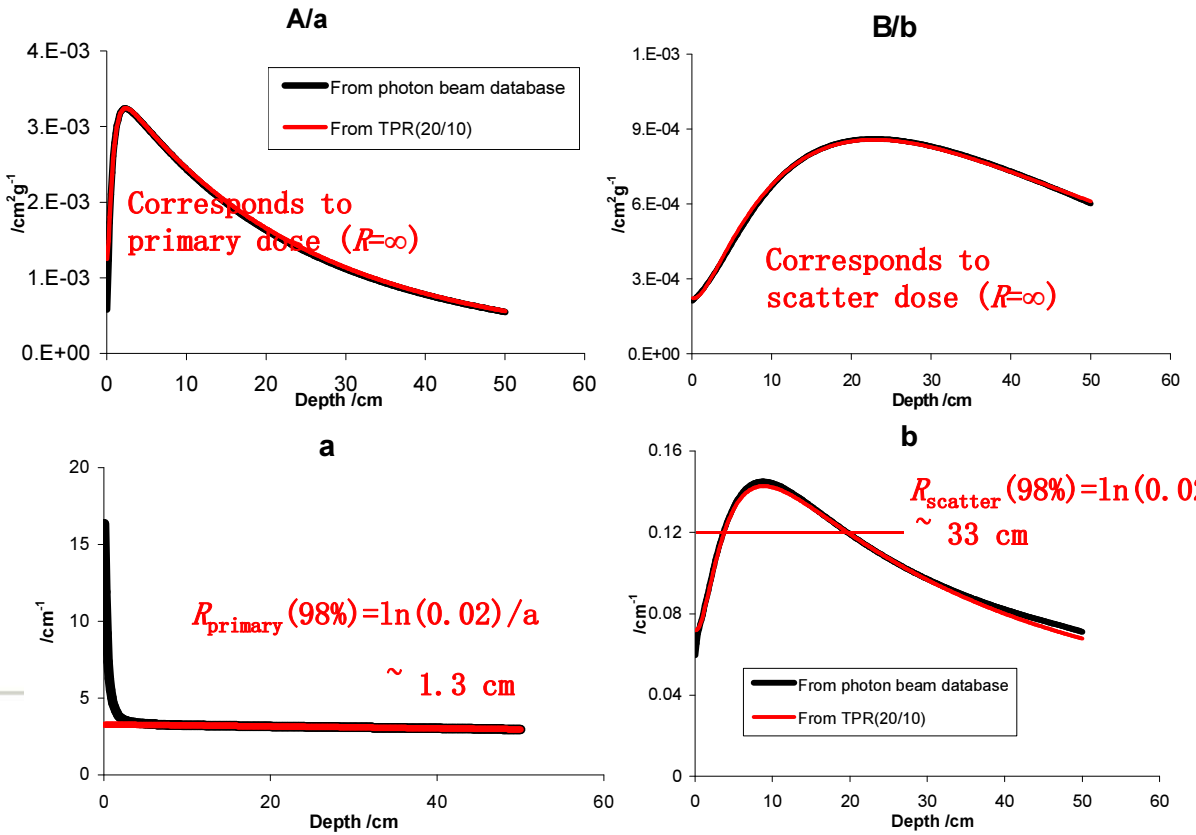

If one assumes that lateral equilibrium is established when one gets 98% of the total dose on axis from a field with infinite field size

ESTRO School

Dose through kernel integration - 2

Double exponential, incl. depth parameterization, solely based on $TPR_{20,10}$ (extracted from photon beam database)

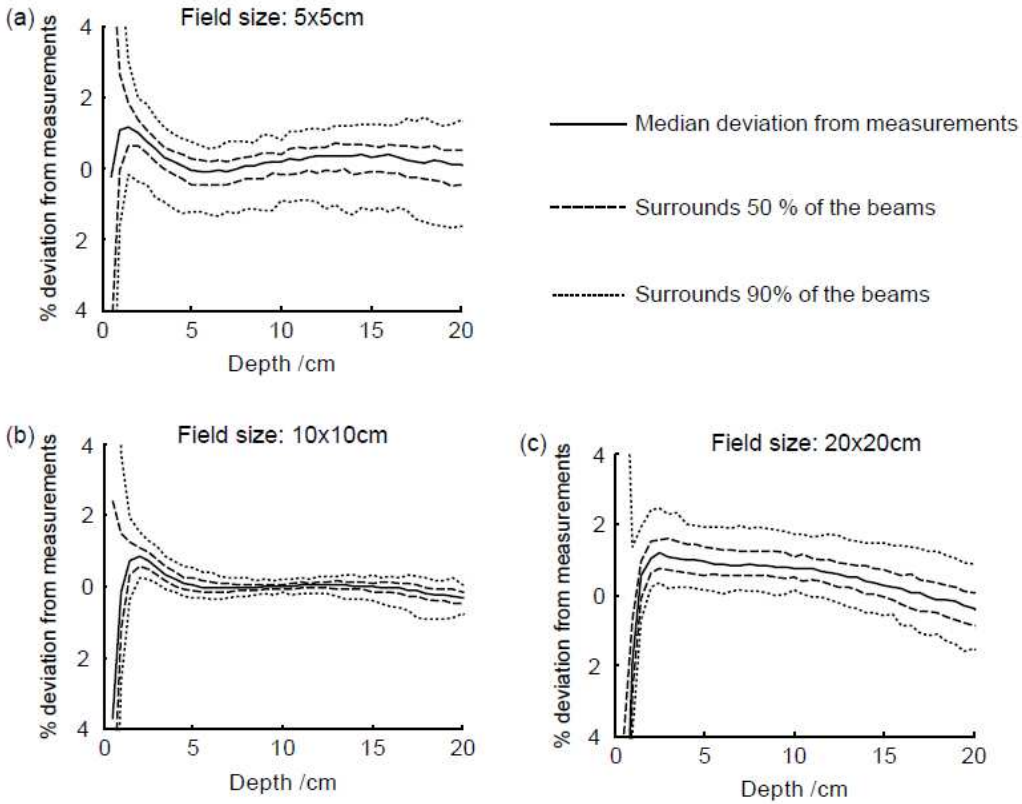

Error plots for beams with TPR20/10 in the interval between 0.645 and 0.682 (210 beams), mostly 5 and 6 MV beams. The errors are normalized in a small interval around 10 cm in the 10 × 10 cm field.

T Nyholm, et al (2006) *Radiother Oncol 78*, 347-51.

ESTRO School

Lateral variation of beam quality

Double exponential, incl. depth parameterization and lateral beam quality variations (“off-axis softening”) for flattened beams

$$\frac{D(x,d:A)}{M(A)} = \frac{1}{M(A)} \int \Psi(p;A) \frac{p}{\rho}[|x-p|,d,QI(p)]d^2p$$

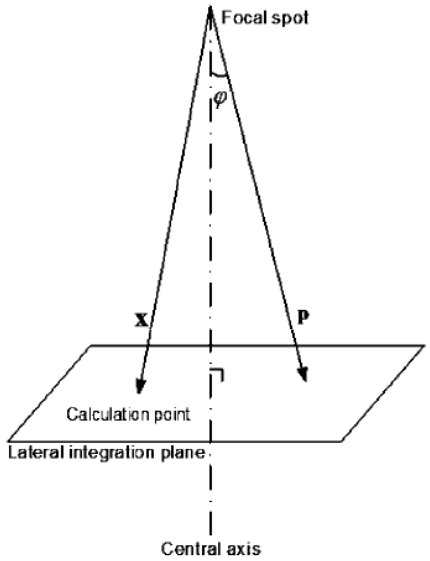

Need to express PB kernel as a function of a parameter that relates to the change of beam quality with the position off axis

T Nyholm, et al (2006) *Phys. Med. Biol. 51 4111-4118*

ESTRO School

Lateral variation of beam quality

$$\mathrm{HVL}(\phi) = \frac{\mathrm{HVL}(0)}{1 + d_1\varphi + d_2\varphi^2 + d_3\varphi^3}$$

$$d_1 = 0.00181 rad^{-1}, d_2 = 0.00202 rad^{-2}, d_3 = -0.0000942 rad^{-3}$$

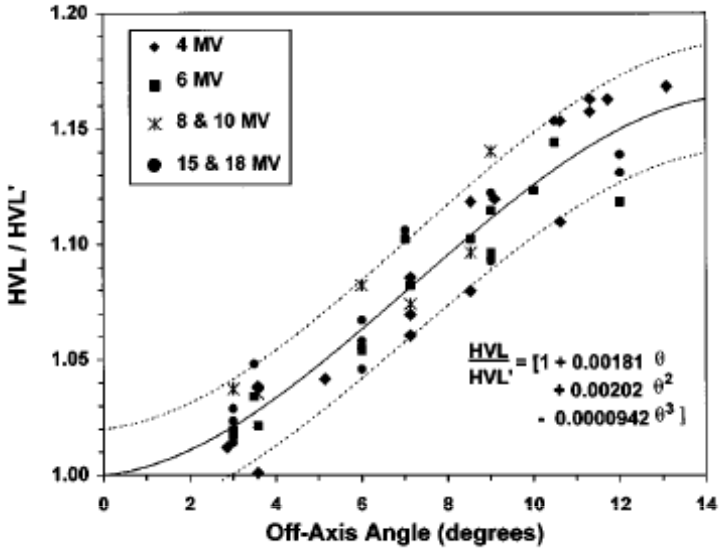

$$\mathrm{HVL} = a_1 + a_2\mathrm{TPR}_{20/10} + a_3\mathrm{TPR}^2_{20/10}$$

or the inverse

$$\mathrm{TPR}_{20/10} = -\frac{a_2}{2a_3} \quad \underset{(-)}{+} \quad \sqrt{\left(\frac{a_2}{2a_3}\right)^2 - \frac{a_1 - \mathrm{HVL}}{a_3}}$$

$$a_1 = 56cm, a_2 = -185.4cm, a_3 = 185.7cm$$

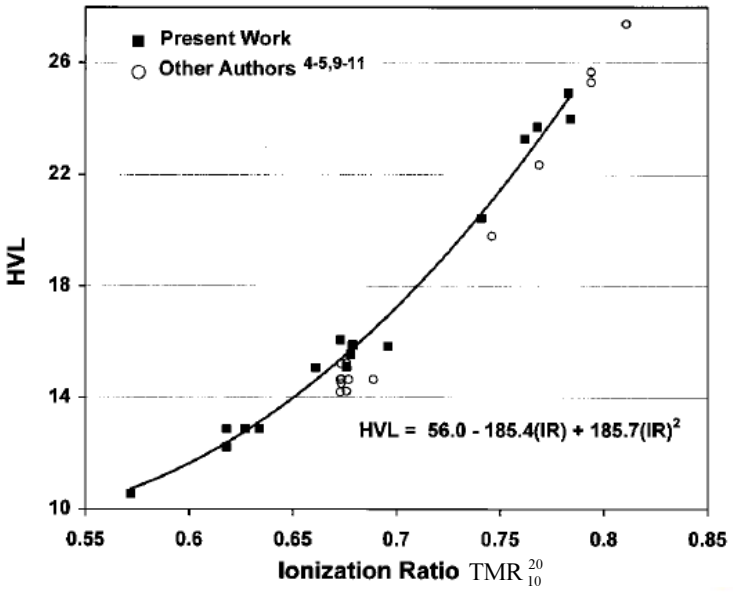

Tailor et al (1998) *Med Phys 25*, 662-7.

ESTRO School

Lateral variation of beam quality

Double exponential, incl. depth parameterization and lateral beam quality variations ("off-axis softening") for flattened beams

Laterally constant kernel:

$$\frac{D(\mathbf{x},d;A)}{M(A)} \approx \frac{1}{M(A)} \sum_{i=1}^{I} \overline{\Psi}_{i;A} \cdot \int_{r_{\text{in},i}}^{r_{\text{out},i}} \frac{p}{\rho}\left(r,d,\text{HVL}_{\text{CAX}}\right) 2\pi r\, dr \Big|_{x}$$

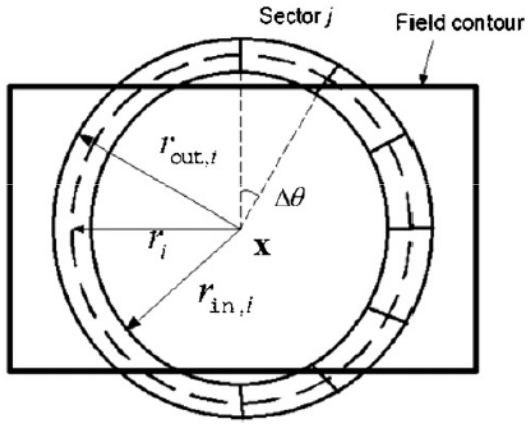

Including lateral beam quality shift:

$$\frac{D(\mathbf{x},d;A)}{M(A)} \approx \frac{1}{M(A)} \sum_{i=1}^{I} \sum_{j=1}^{J} \frac{\overline{\Psi}_{i,j;A}}{J} \cdot \int_{r_{\text{in},i}}^{r_{\text{out},i}} \frac{p}{\rho}\left(r,d,\overline{\text{HVL}_{i,j}}\right) 2\pi r\, dr \Big|_{x}$$

T Nyholm, et al (2006) *Phys. Med. Biol. 51 4111-4118*

Olofsson et al (2006) *Med Phys 33*, 3418-25

ESTRO School

Lateral variation of beam quality

Modelling “off-axis softening” for flattened beams

$$OF_{total}(x,d;A) = \frac{D(x,d;A)/M(A)}{D(x_{ref},d_{ref};A_{ref})/M(A_{ref})}$$

% diff (meas-calc)

Laterally constant kerne

Including lateral beam quality shift:

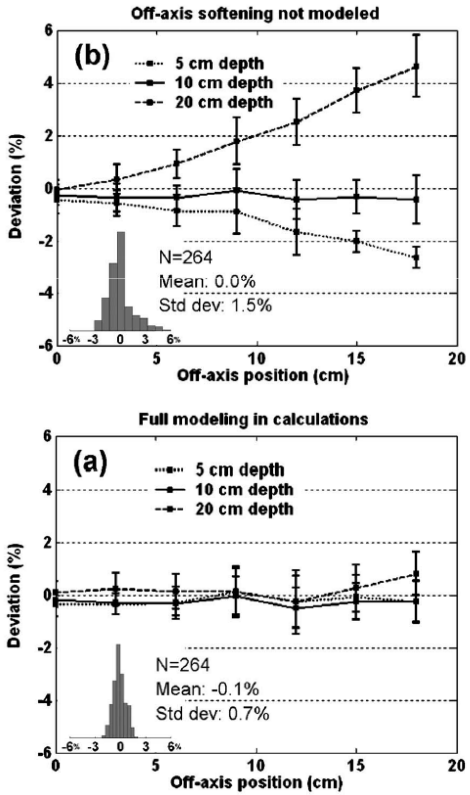

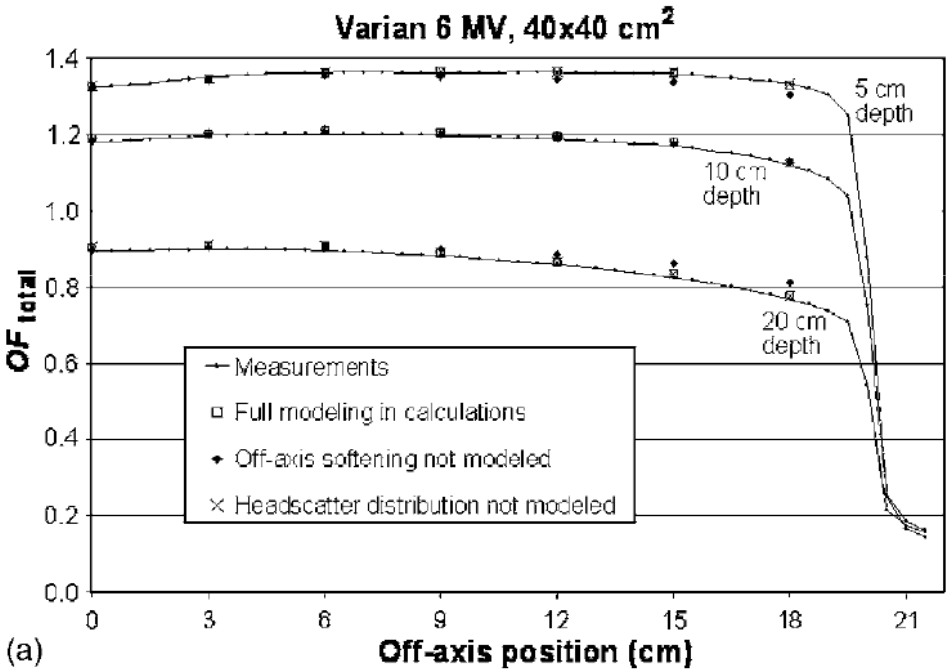

Much smaller effect in FFF beams!

Olofsson et al (2006) *Med Phys 33*, 3418-25

ESTRO School

Modelling geometric penumbra

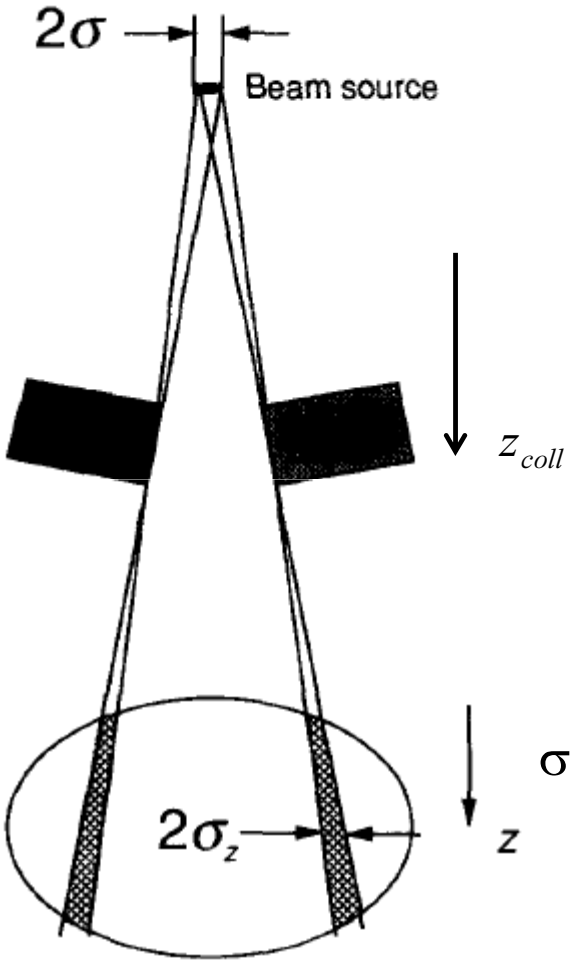

$$\frac{p}{\rho}(r,z) = \frac{A_z e^{-a_z r}}{r} + \frac{B_z e^{-b_z r}}{r}$$

$$\frac{p_{p_{eff}}}{\rho}(r,z) = \frac{1}{\pi\sigma_z^2} e^{-r^2/\sigma_z^2} \otimes \frac{A_z e^{-a_z r}}{r}$$

Gaussian source distribution

$$\sigma_z = \sigma \cdot \frac{z - z_{coll}}{z_{coll}}$$

As z_{coll} varies for different collimators the additional part of the kernel, describing the geometric penumbra, should vary between different calculation points ⇒ Problems for fast convolutions.

A Ahnesjö et al (1992) *Med Phys* 19, 263-273

ESTRO School

Modelling charged particle contamination

Needed when pencil beams kernels are derived from MC simulations

Charged particle contamination kernel

$$\frac{p_{c_\pm}}{\rho}(r,z) = \alpha\, e^{-\beta z} e^{-\gamma r^2}$$

The parameters α, β, and γ can be determined through fitting to the difference between measurements and calculated photon dose.

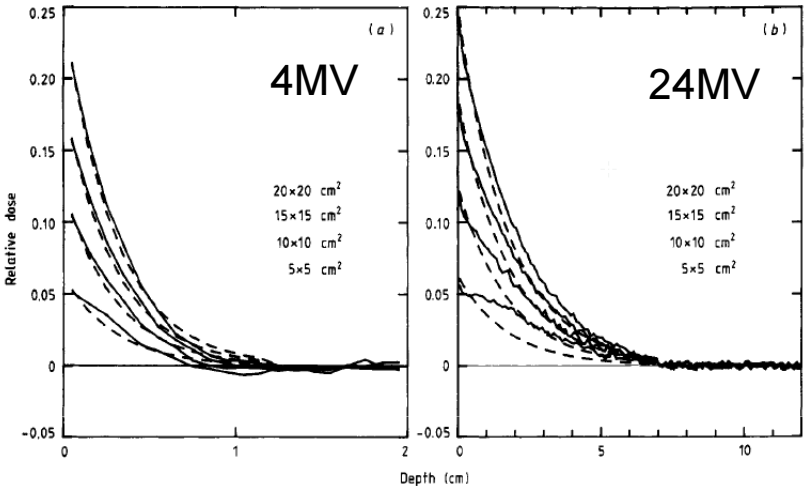

A Ahnesjö and P Andreo (1989) *Phys Med Biol 34*, 1451-64.

Contaminant dose per incident primary photon fluence at depth z

$$\frac{D_{c_\pm}(z,f)}{\psi} = \alpha e^{-\beta z} \int_{-f/2}^{f/2}\int_{-f/2}^{f/2} e^{-\gamma(x^2+y^2)}\,dx\,dy$$

$$= \alpha e^{-\beta z}\frac{\pi}{\gamma}\,\mathrm{erf}^2\left(\sqrt{\gamma}\frac{f}{2}\right),$$

where the error function is defined as

$$\mathrm{erf}(x) = \frac{2}{\sqrt{\pi}}\int_0^x e^{-t^2}\,dt.$$

A Ahnesjö et al (1992) *Med Phys* 19, 263-273

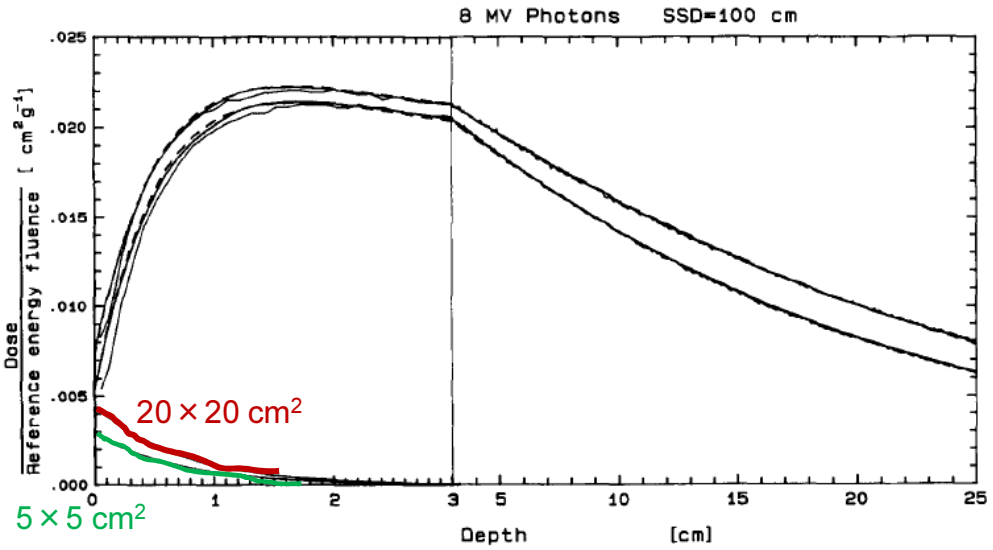

Approximations in dose calculation

Infinite slab approximation: doses at phantom boundaries

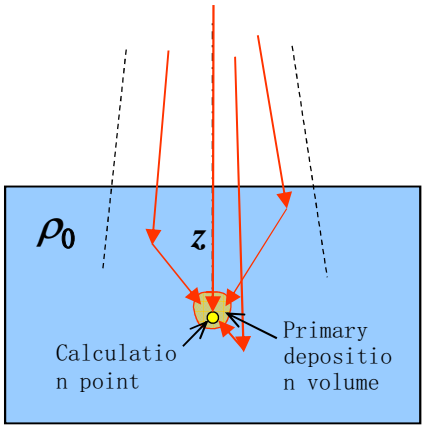

Ideal case

The depth (z) is generally assumed to be constant within the lateral integration plane during calculation of the scatter dose to a point.

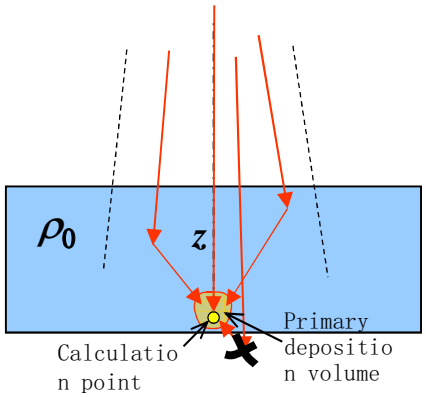

Backscatter overestimated

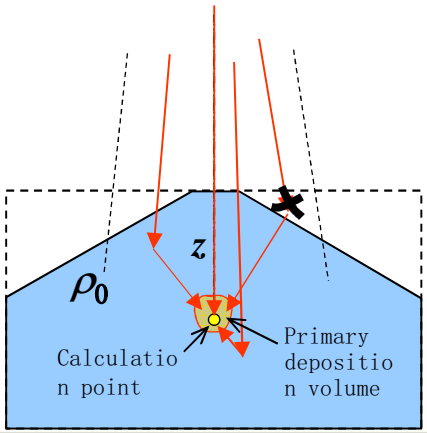

Scatter overestimated

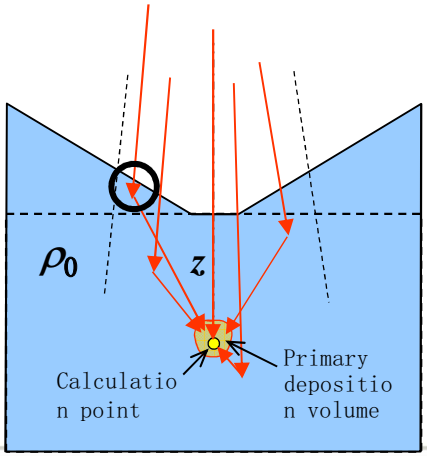

Scatter underestimated

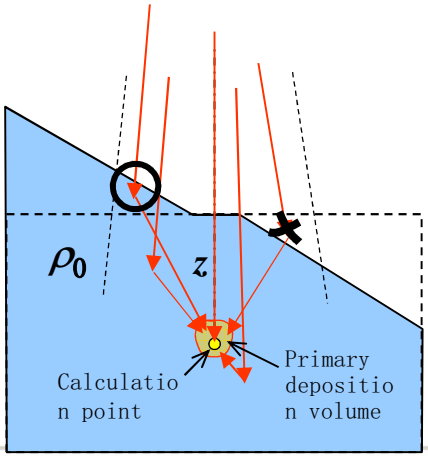

Errors cancel (roughly)

ESTRO School

Approximations in dose calculation

Non water-like media: kernel scaling

Standard Pencil beam

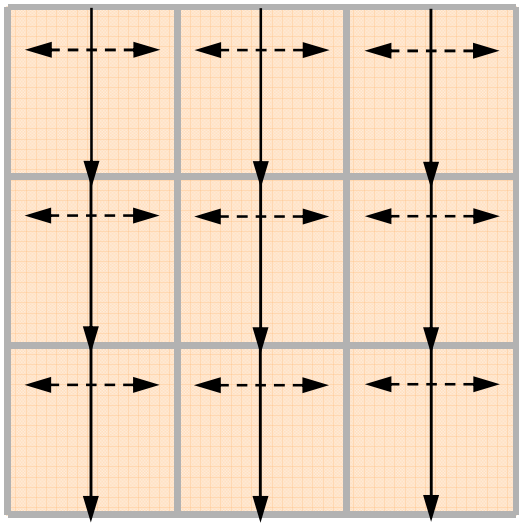

Energy transport: Along rayline and laterally.

Kernel scaling by radiological pathlengths: Only along rayline.

Varian AAA
(Anisotropic Analytical Algorithm)

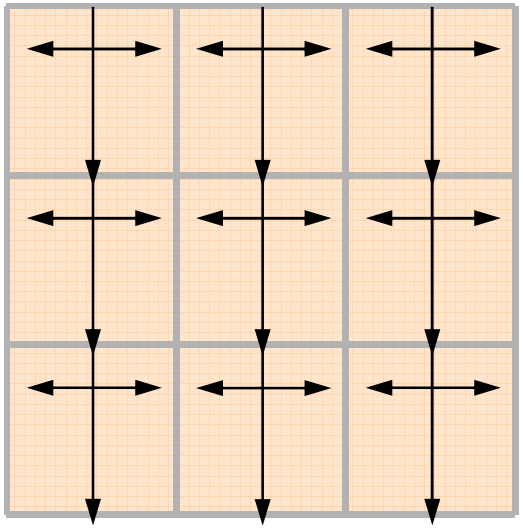

Energy transport: Along rayline and laterally (16 directions).

Kernel scaling by radiological pathlengths: In all (17) directions.

Convolution superposition/ Collapsed cone

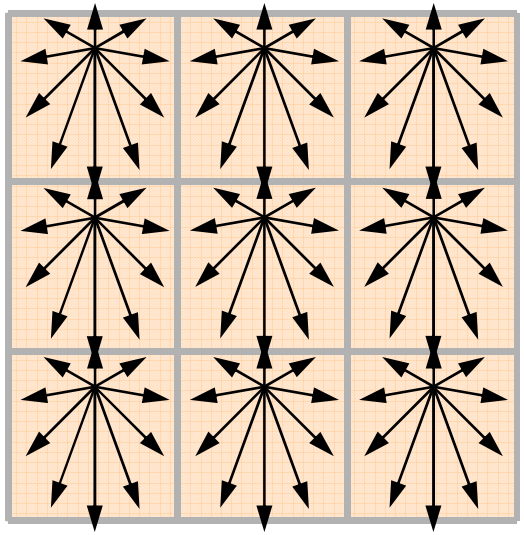

Energy transport: Along approx. 100 directions.

Kernel scaling by radiological pathlengths: In all directions.

ESTRO School

Approximations in dose calculation

Heterogeneous media: kernel scaling

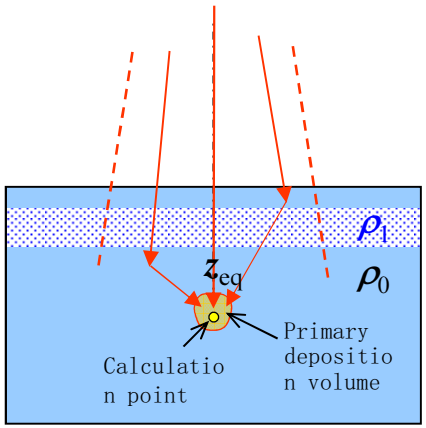

Heterogeneous slab phantom

ρ_1 illustrates a low density region, e.g. lung tissue.

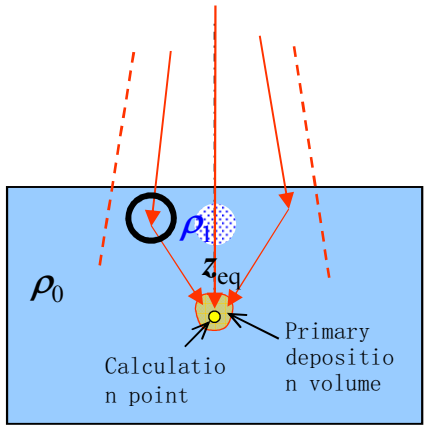

Scatter underestimated

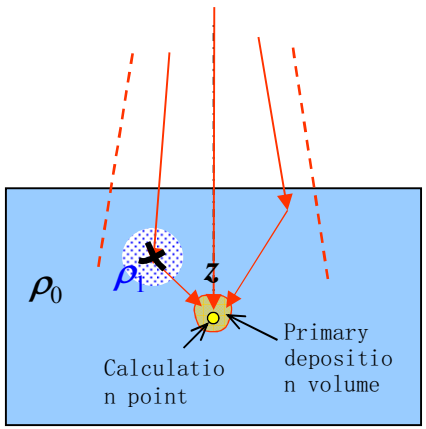

Scatter overestimated

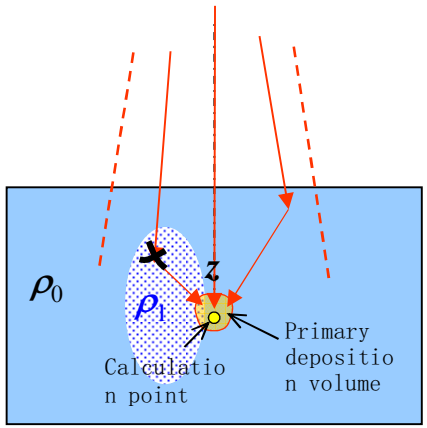

Scatter and primary overestimated

ESTRO School

Approximations in dose calculation

Heterogeneous media: kernel scaling in Eclipse AAA

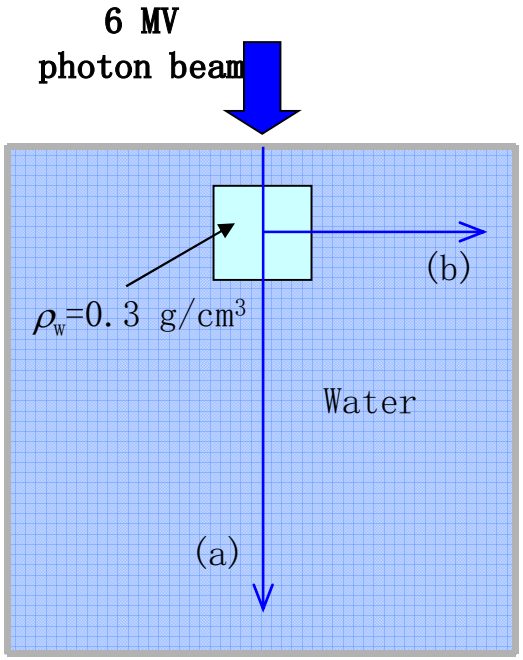

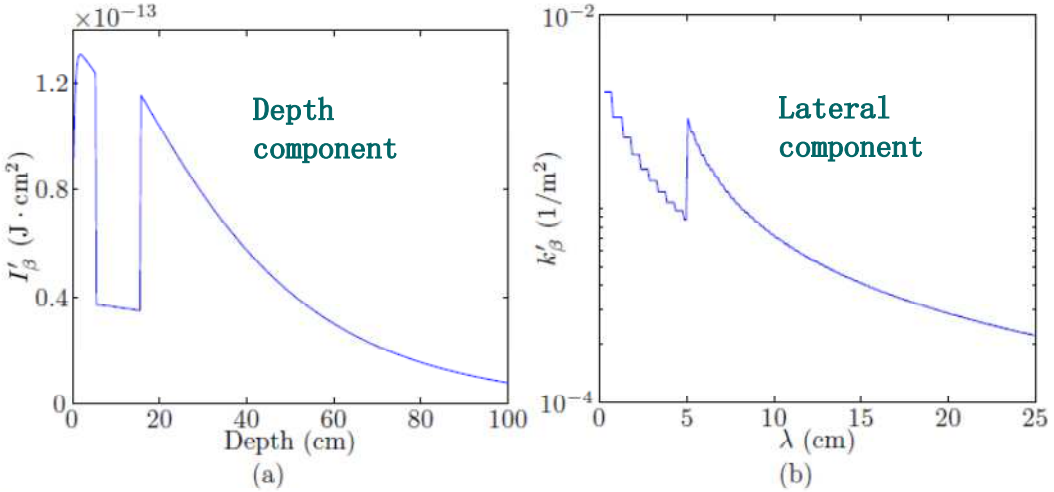

Fig. 10: The effect of a cylindrical insert of density $\rho_w = 0.3$ with a radius of 5 cm and length of 10 cm, located at 5-cm-depth in water, on the individual pencil-beam components. The beamlet going through the center of the cylinder for a 6 MV beam is examined. (a) The heterogeneity corrected depth-directed component $I'_\beta(p_z)$, and (b) the heterogeneity corrected lateral component $k'_\beta(\theta, \lambda, p_z)$ as a function of λ at 10-cm-depth for an angular sector $\theta = [0, \ldots, \pi/8]$.

L Korhonen (2009) m *PhD thesis*, Department of Biomedical Engineering and Computational Science, Helsinki University of Technology

ESTRO School

Approximations in dose calculation

Kernel scaling in Eclipse AAA, build-up/down correction

Doses will change too fast at material/tissue interfaces when just applying an effective depth correction. To model gradual changes at material interfaces, a correction is introduced based on a convolution using a build-up kernel along the depth direction.

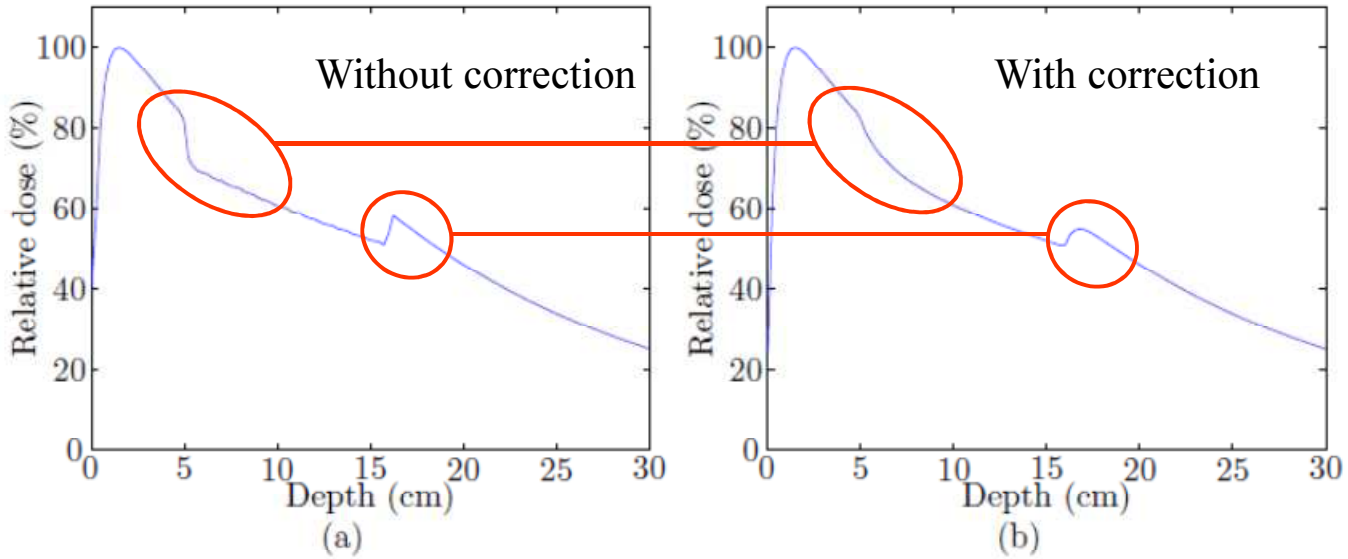

Fig. 11: The calculated dose for a 3×3 cm^2 field for a 6 MV beam incident on a water phantom with lung insert ($\rho_w = 0.3$) from $z = 5, \ldots, 15$ cm (a) without the build-up/build-down correction, and (b) with the correction turned on.

L Korhonen (2009) m *PhD thesis*, Department of Biomedical Engineering and Computational Science, Helsinki University of Technology

ESTRO School

Approximations in dose calculation

Comparison of methods (pencil kernel, AAA, point kernel, MC)

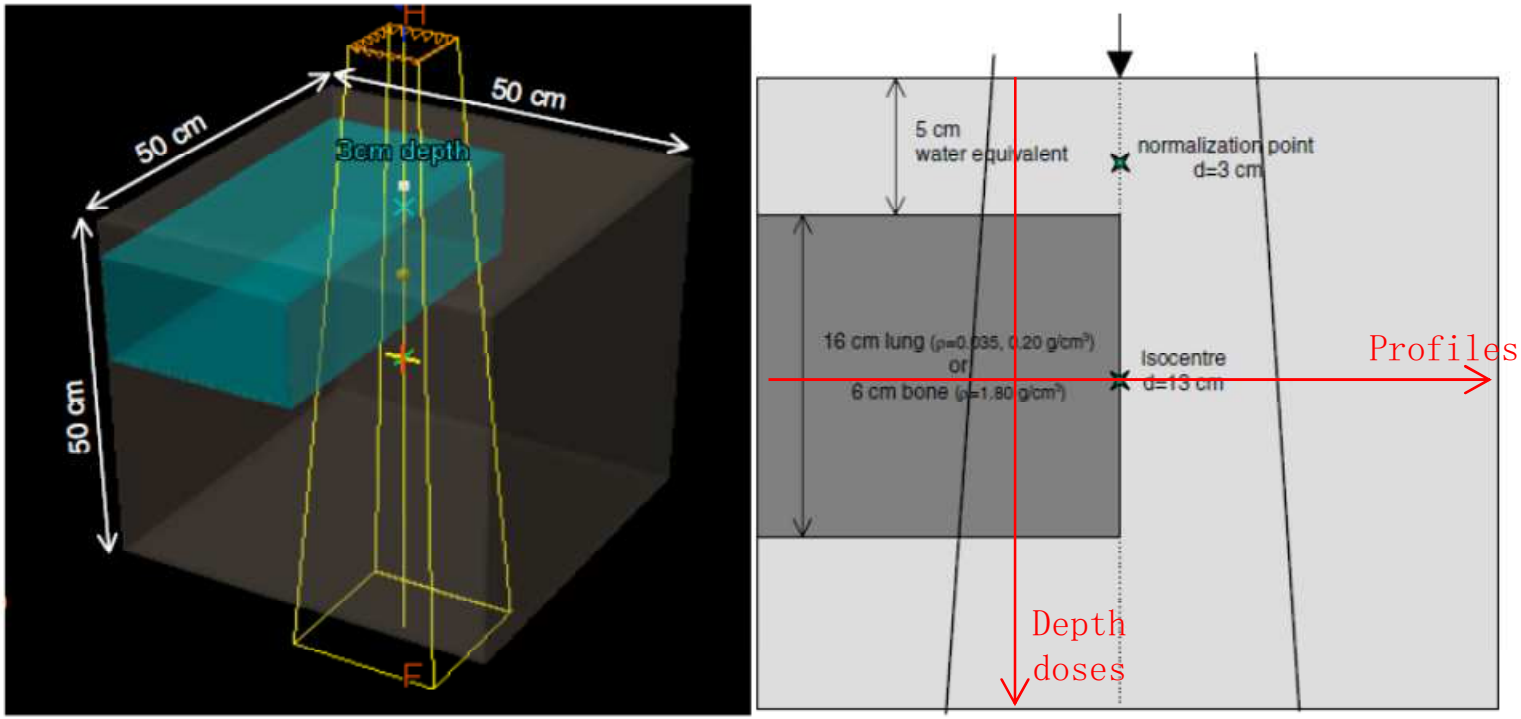

Fogliata A et al (2007) Phys Med Biol 52, 1363-85.

ESTRO School

Approximations in dose calculation

Comparison of methods (pencil kernel, AAA, point kernel, MC)

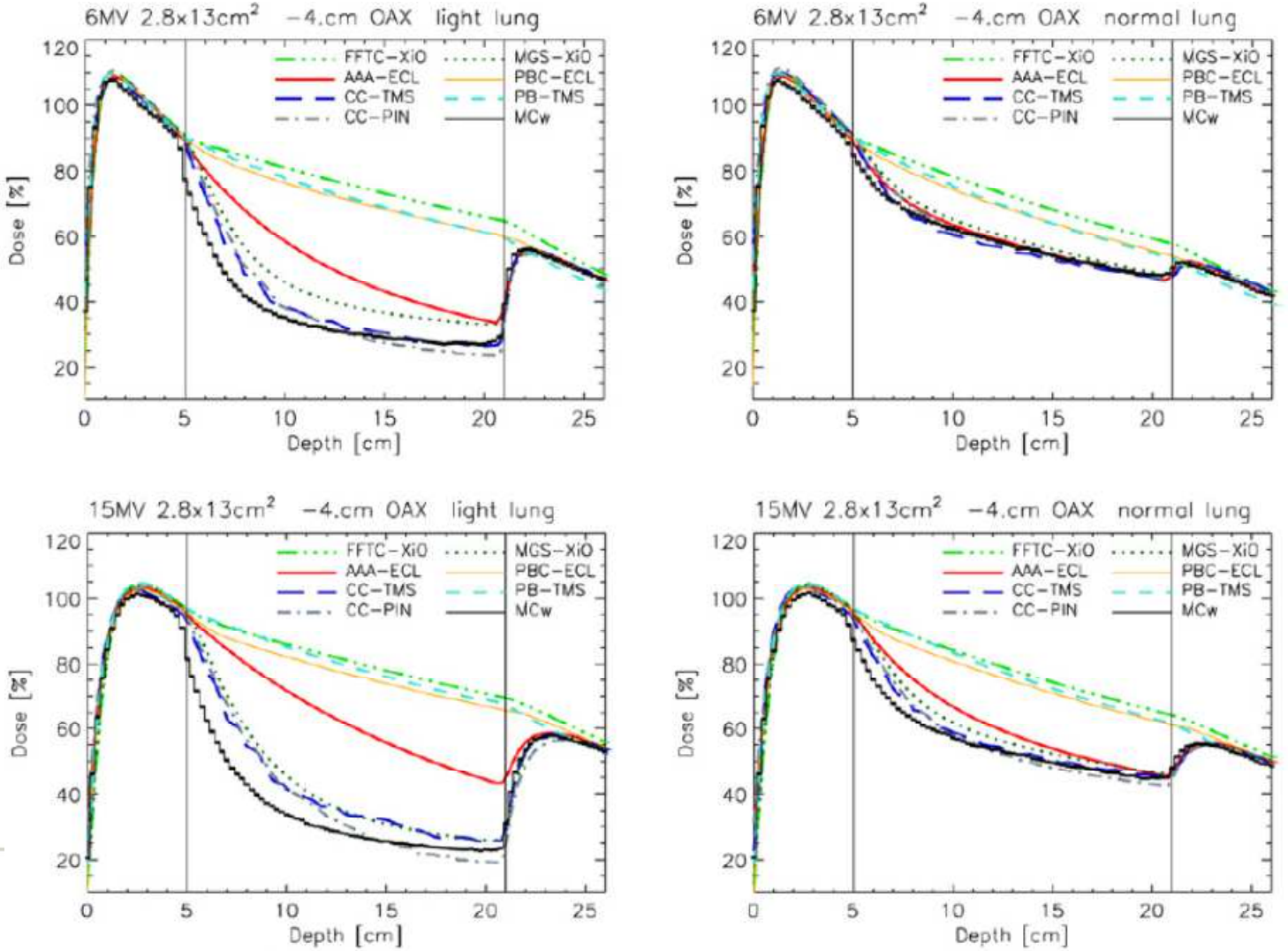

Fogliata A et al (2007) Phys Med Biol 52, 1363-85.

ESTRO School

Approximations in dose calculation

Comparison of methods (pencil kernel, AAA, point kernel, MC)

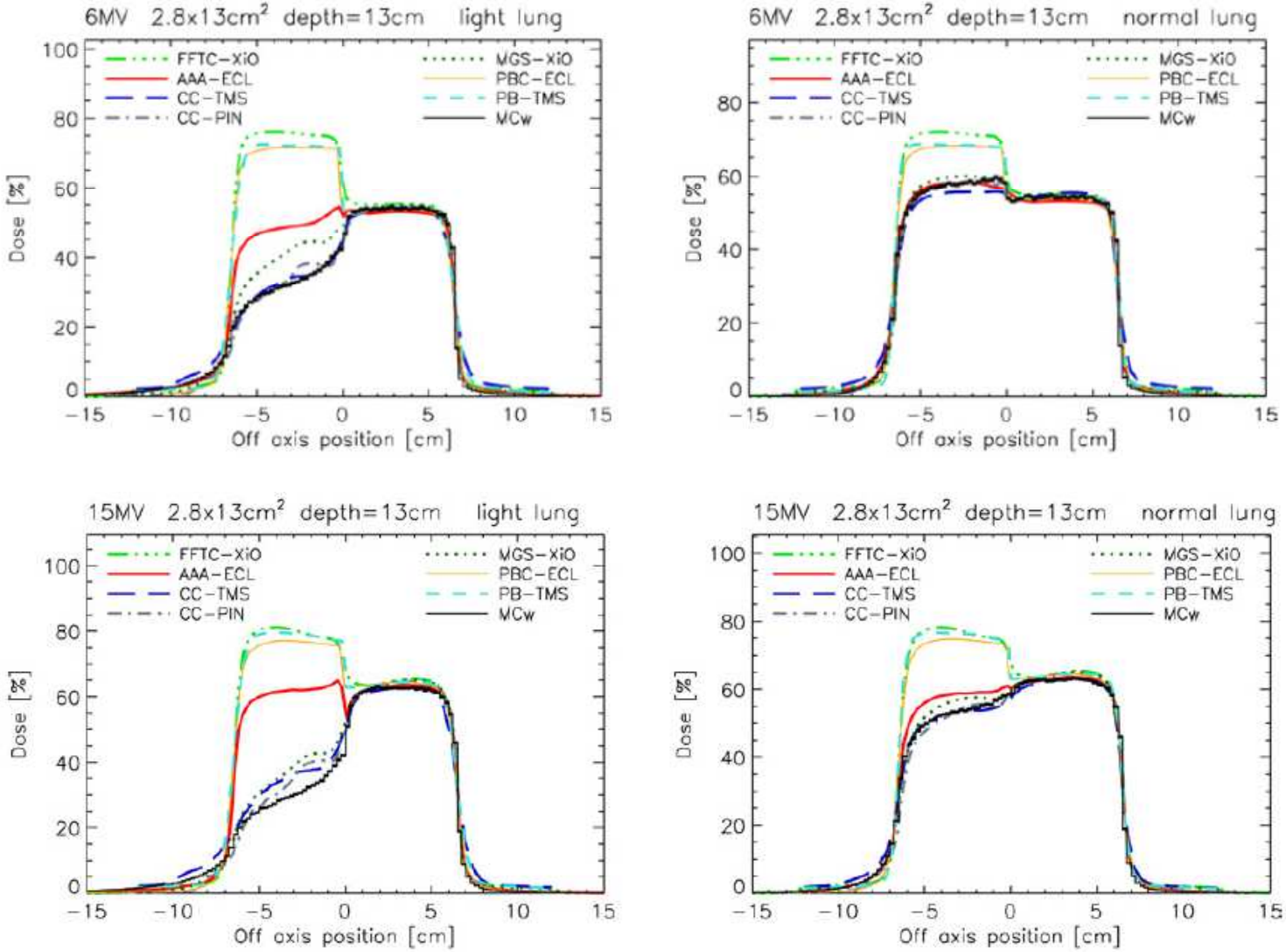

Fogliata A et al (2007) Phys Med Biol 52, 1363-85.

ESTRO School

Approximations in dose calculation

Comparison of methods (pencil kernel, AAA, point kernel, MC)

15 MV photons

(Dose contr. normalization)

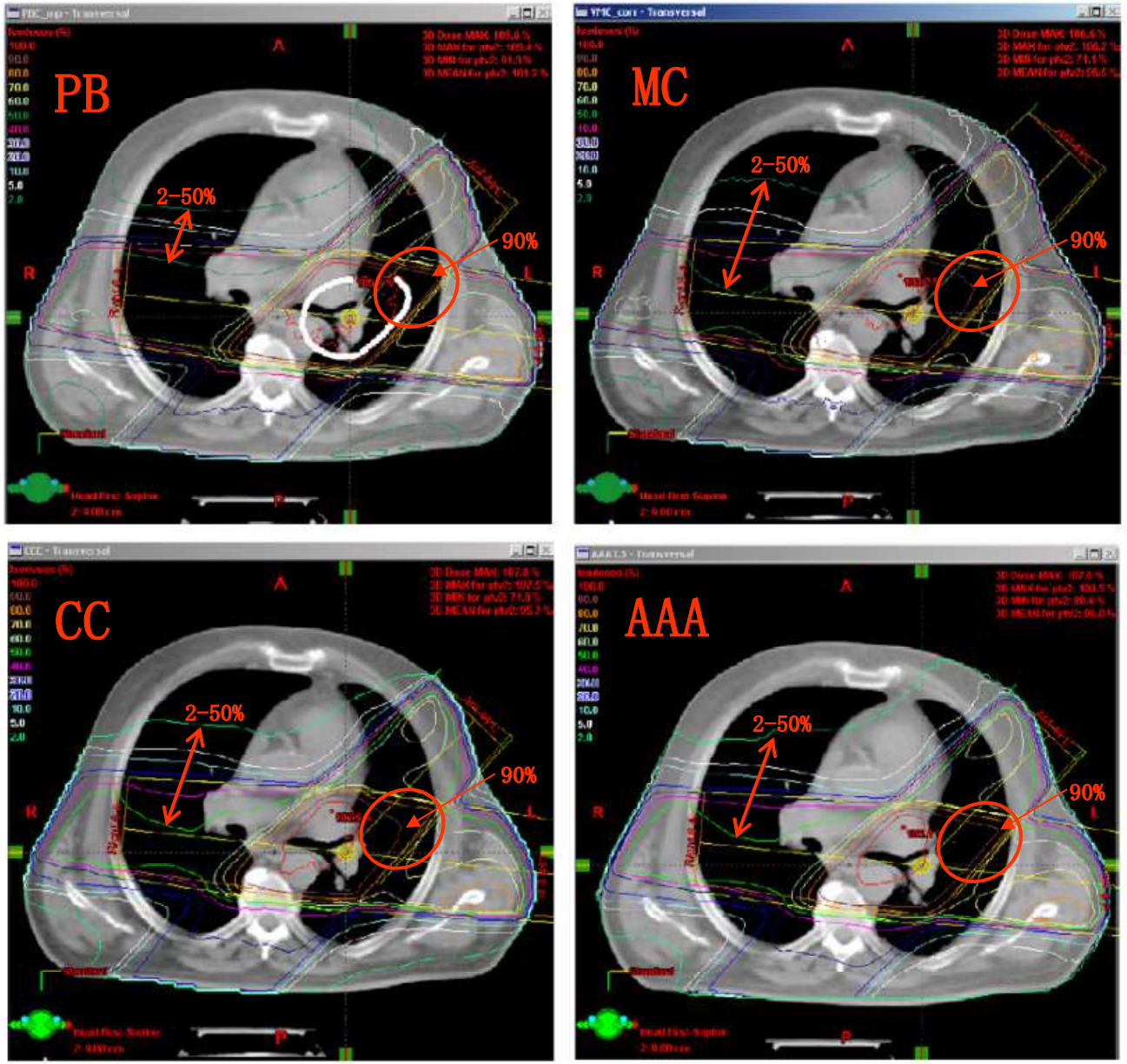

Hasenbalg F (2007) *Phys Med Biol. 52*, 3679-91

Approximations in dose calculation

Comparison of methods (pencil kernel, AAA, point kernel, MC)

Cumulative DVH for PTV and left lung (case from previous page)

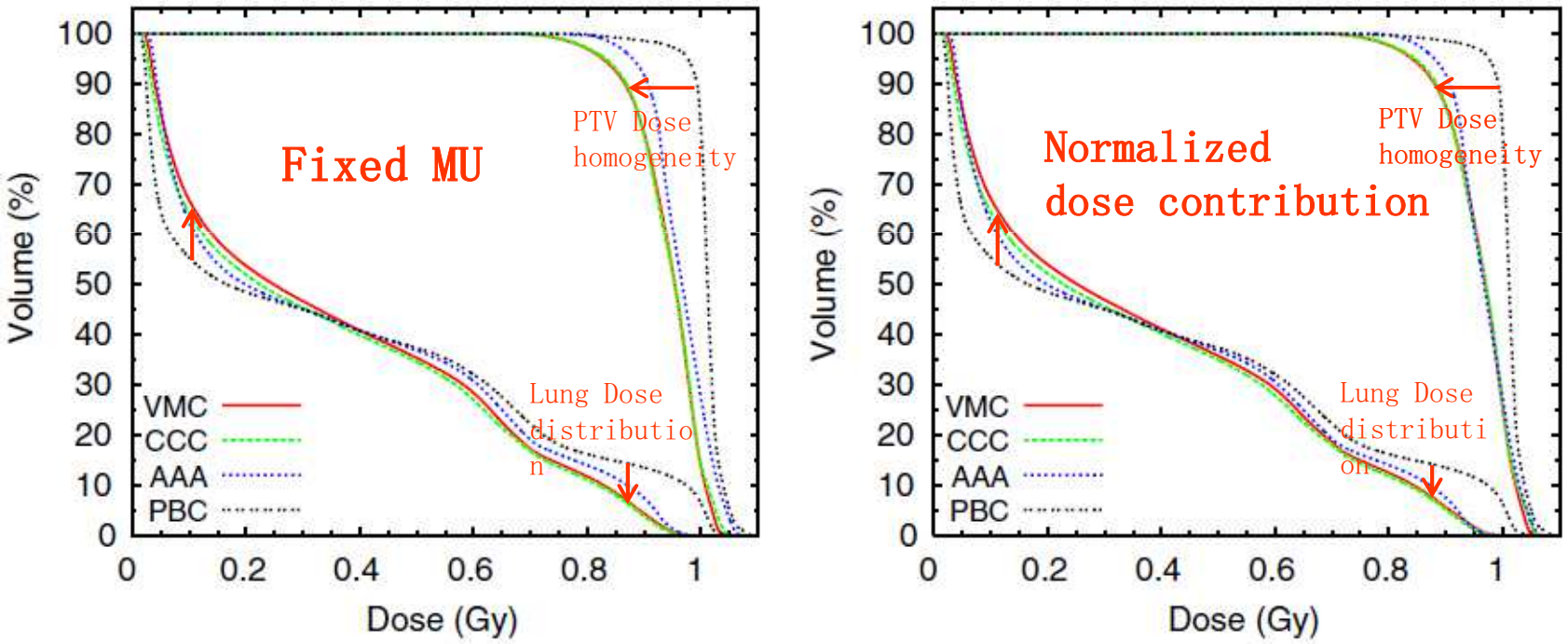

Hasenbalg F (2007) *Phys Med Biol. 52*, 3679-91

ESTRO School

Approximations in dose calculation

Comparison of methods (pencil kernel, AAA, point kernel, MC)

6 MV photons

(Dose contr. normalization)

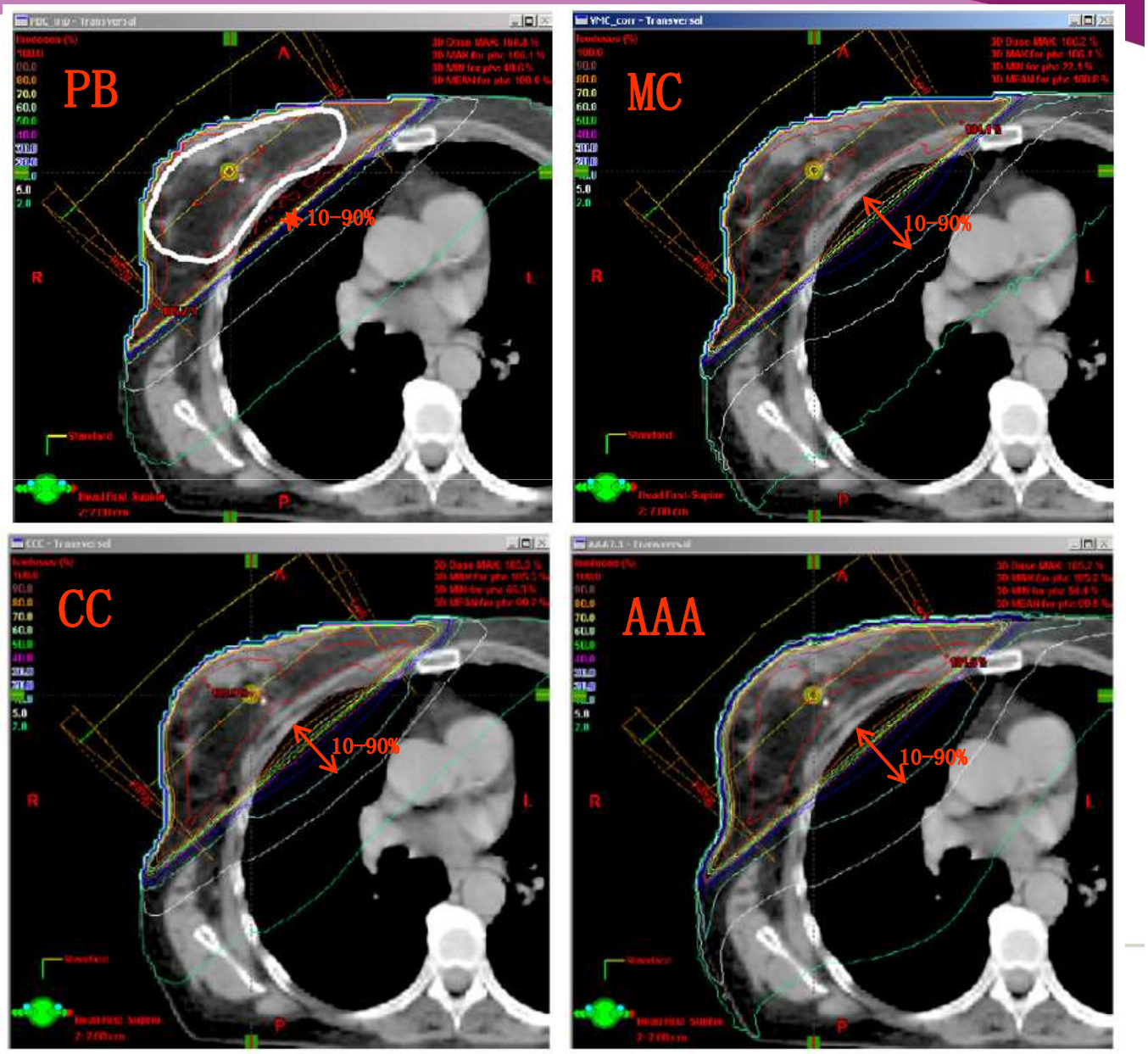

Hasenbalg F (2007) *Phys Med Biol. 52*, 3679-91

Conclusion

•Several different methods are available when characterizing, parameterizing and integrating pencil kernels.

•Generally, the pencil kernel implementation is associated with a number of approximations and limitations, related to the actual photon beam or the dose calculation object.
Some of these errors can be minimized through more advanced modelling while other errors, mainly related to tissue heterogeneities, require algorithms employing explicit 3D-modelling.

•Pencil kernel algorithms are widely used in clinical treatment planning systems for photon dose calculations. Their popularity is related to the fact that they offer a good **compromise** between flexibility, accuracy and speed. For this reason they are the dose engine of choice used in plan optimisation calculations.


Out of field dose modeling and measurement in radiotherapy treatments
Brendan McClean
ESTRO Utrecht 2016
Saint Luke's
Radiation Oncology
Network

Learning Objectives

- Explain why we are interested in out of field dose (OFD)
- Understand the origin of OFD
- Investigate the effects of OFD
- Examine the accuracy of calculation of OFD with TPS
- Discuss the measurement of OFD

Why are we interested in out of field dose?

- Success of RT means longer survival of patients (Second Primary)
- New treatment techniques (VMAT)
- Improved optimisation based on DVC's
- Peripheral doses to IED's
- Differences in TPS?

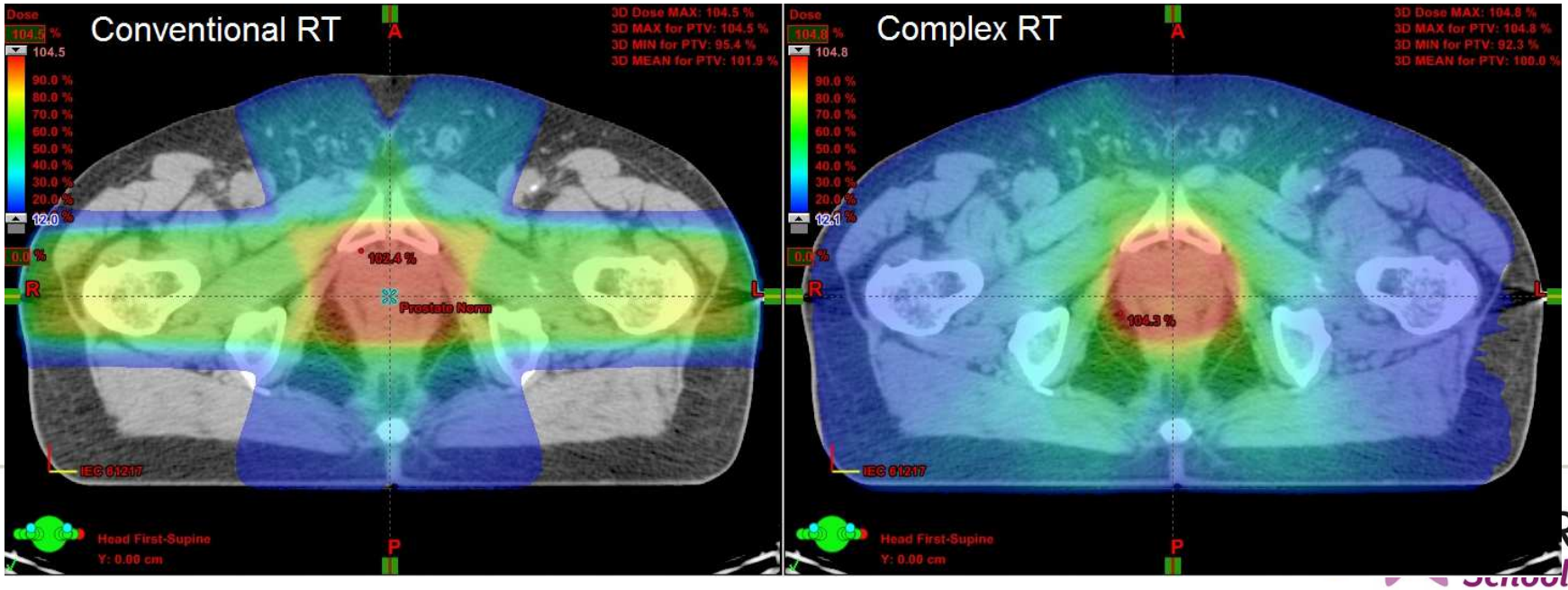

Origin of peripheral dose contributions

Anders A.

Patient scatter

- Unavoidable
- Decrease from target essentially as: $\frac{e^{-\mu \cdot r}}{r^n}$ n=1 column shaped scatter source
  n=2 " aped scatter source

Head scatter

- Sources are all irradiated parts of the treatment head, main source the flattening filter
- Limited by the collimating devices
- Machine design dependent (FFF machines have less!)

Leakage, including scatter leakage

- Depends on collimator and shield thicknesses and material (density)
- Collimator design dependent
- **Treatment technique dependent**

Neutrons

- Mainly a high Z phenomena at photon energies above photonuclear threshold values
- Avoidable by lower beam energy

Only one factor user controllable on a daily basis, all other once per decade (replacement)!

Patient scatter example: Dose determination to pregnant patient

Without shield

With shield

Treatment Site:	Right Oral Cavity
Technique:	6-field IMRT, 6 MV
Prescribed Dose:	66 Gy
Total Fractions:	33
Fractions Treated:	20

	Full Plan MU All Gantry Angles No Lead	Full Plan MU Gantry = 0° No Lead	Full Plan MU Gantry = 0° Under Lead	
1RPO	42.0 pC	35.5 pC	8.0 pC	
1RLO	21.0 pC	22.0 pC	5.5 pC	
1RLAT	33.5 pC	38.5 pC	25.5 pC	
1RAO	76.5 pC	82.0 pC	25.0 pC	
1LAO	66.5 pC	70.0 pC	20.0 pC	Effect of Shielding
1LPO	37.0 pC	27.0 pC	8.0 pC	
TOTAL	276.5 pC	275.0 pC	92.0 pC	-67%

Estimated dose to foetus:						
From full plan, unmodified:	0.017	Gy from	33	fractions	0.026%	
From treated fractions:	0.010	Gy from	20	fractions		
From remainder + lead:	0.003	Gy from	13	fractions		
From full plan, modified:	0.013	Gy from	33	fractions	-24% best case: difficult to shield obliques	

Or similar: Pregnant breast cancer patient
0.015Gy over 25 fractions (50Gy)

ESTRO School

Head scatter

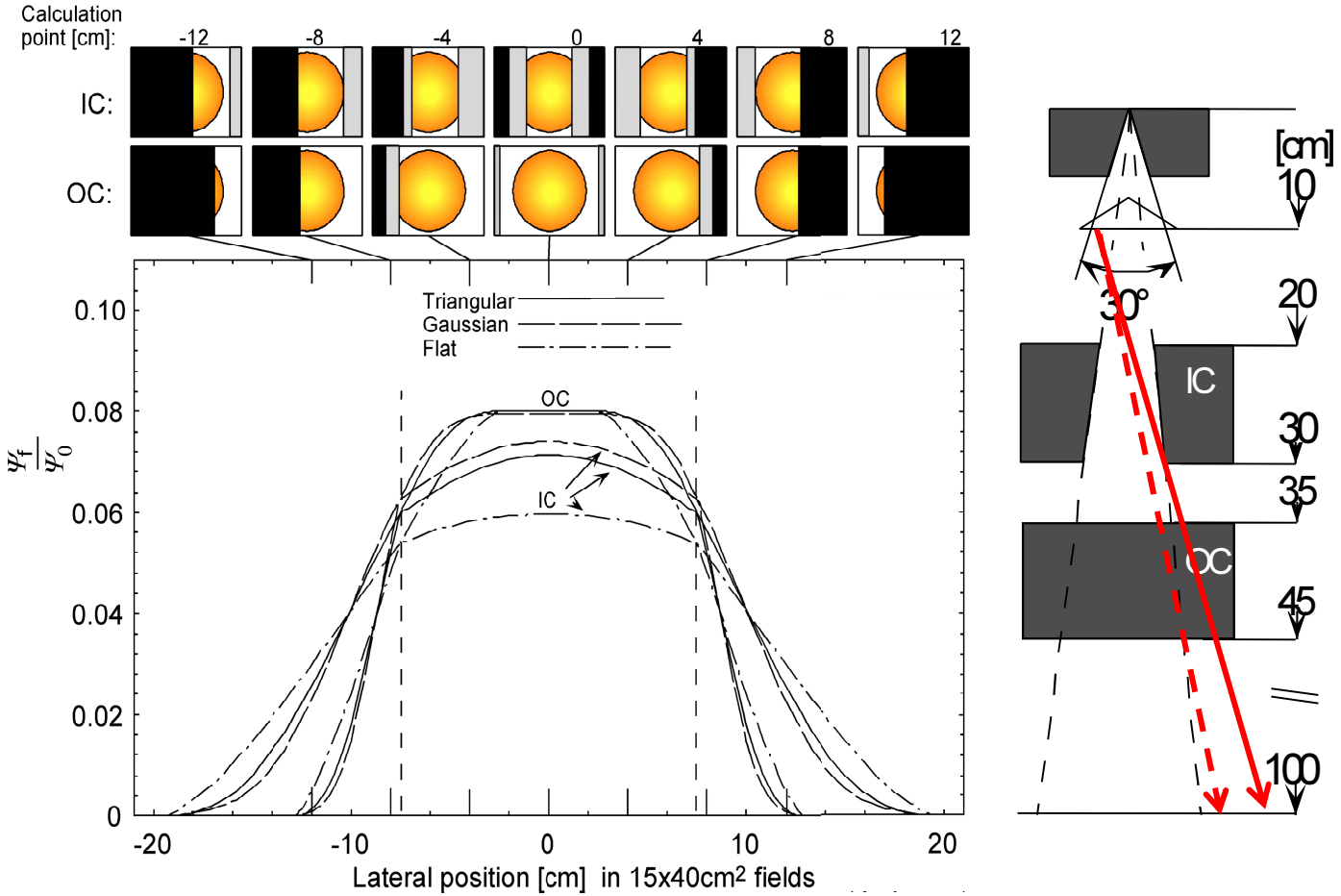

Ahnesjö 1994 Med. Phys. **21** 1227-35

Flattening filter or not? MLC or jaws?

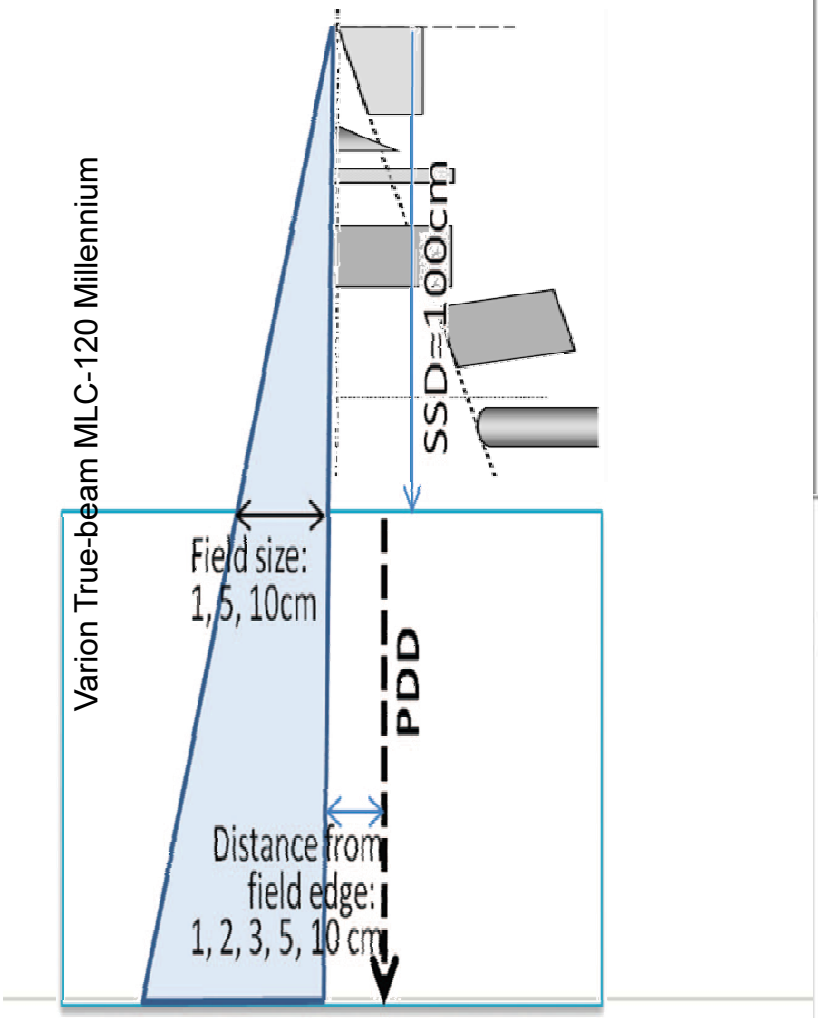

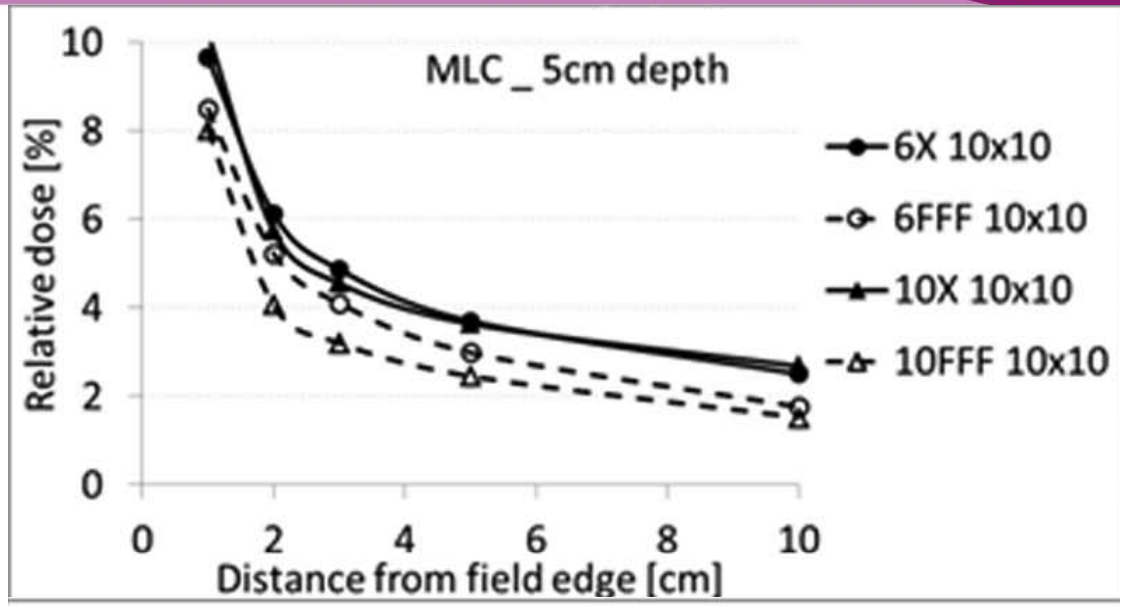

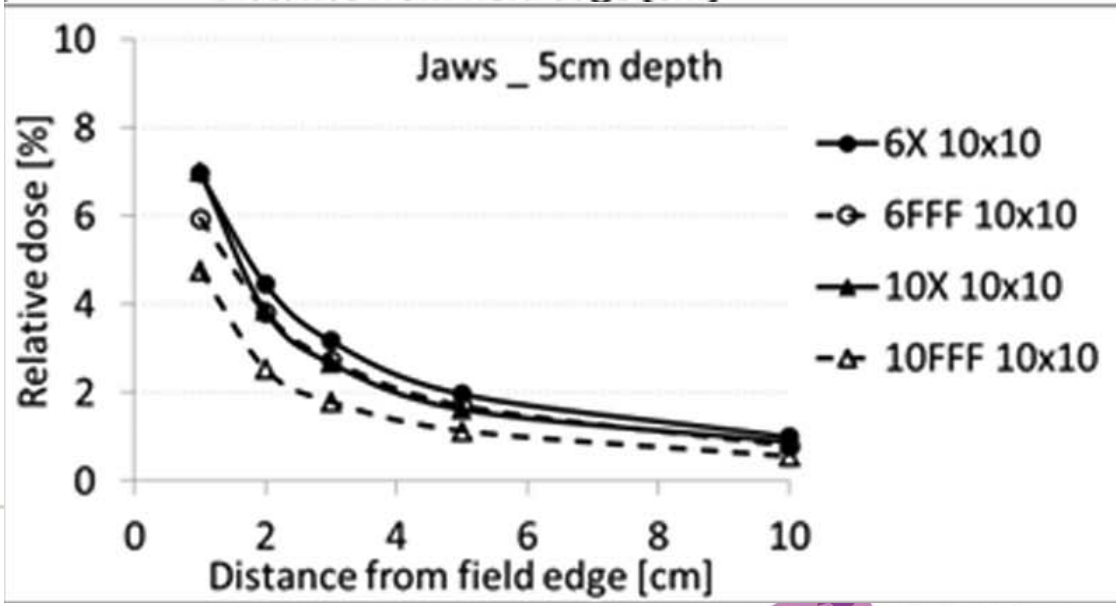

Fogliata etal 2013 MedPhys 40(10) p101706-1

Collimator leakage - intraleaf and interleaf

Two effects:

- Diffused dose from spiky interleaf fluence leakage
- *Intraleaf* attenuation

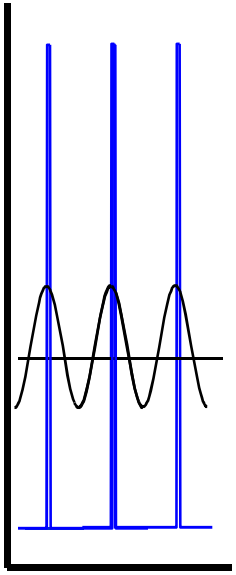

Intraleaf leakage very small:

$$e^{-\frac{\mu}{\rho}\rho \cdot t} \xrightarrow[\text{8 cm tungsten at 3 MeV}]{} e^{-0.0408 \times 18.0 \times 8.0} = 0.28\%$$

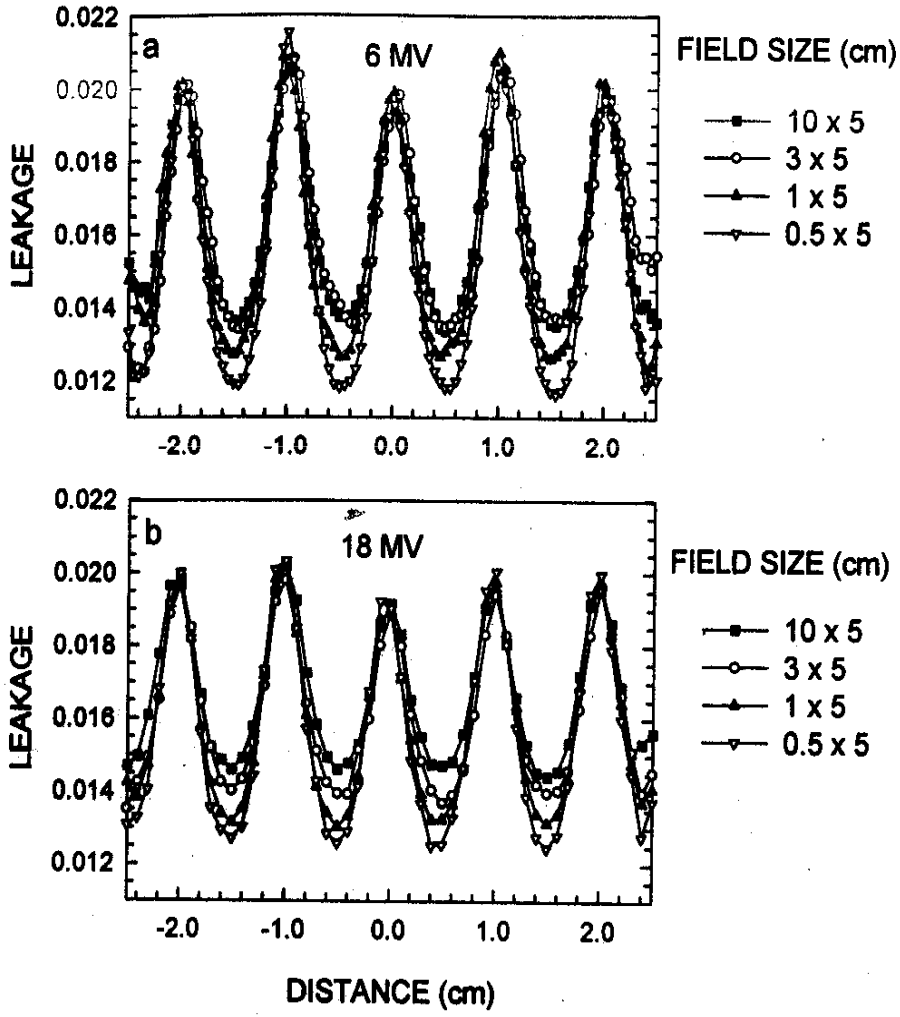

Measuements from Arnfield *et al*, 2000 Med. Phys. **27**

Interleaf leakage

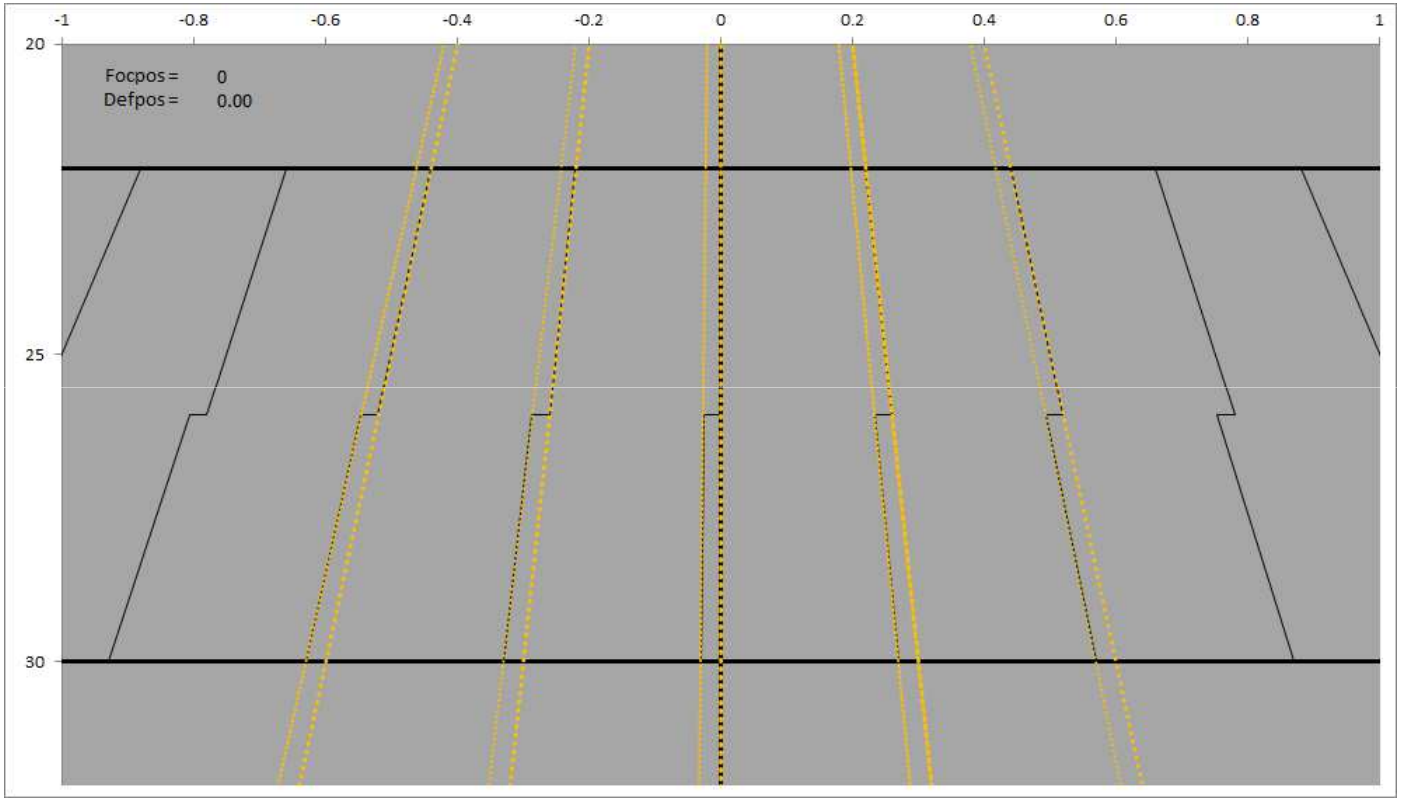

ESTRO School

Interleaf leakage

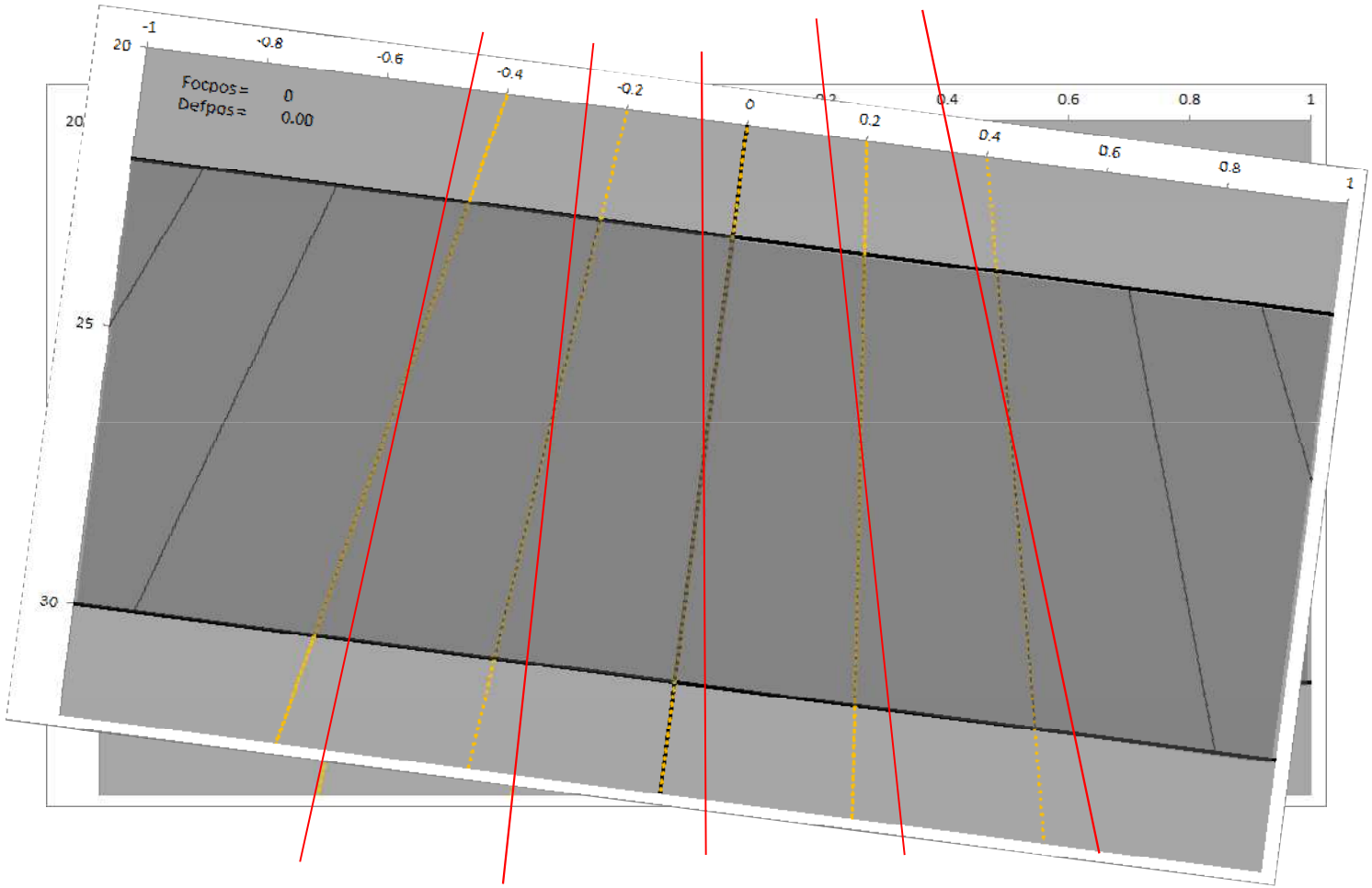

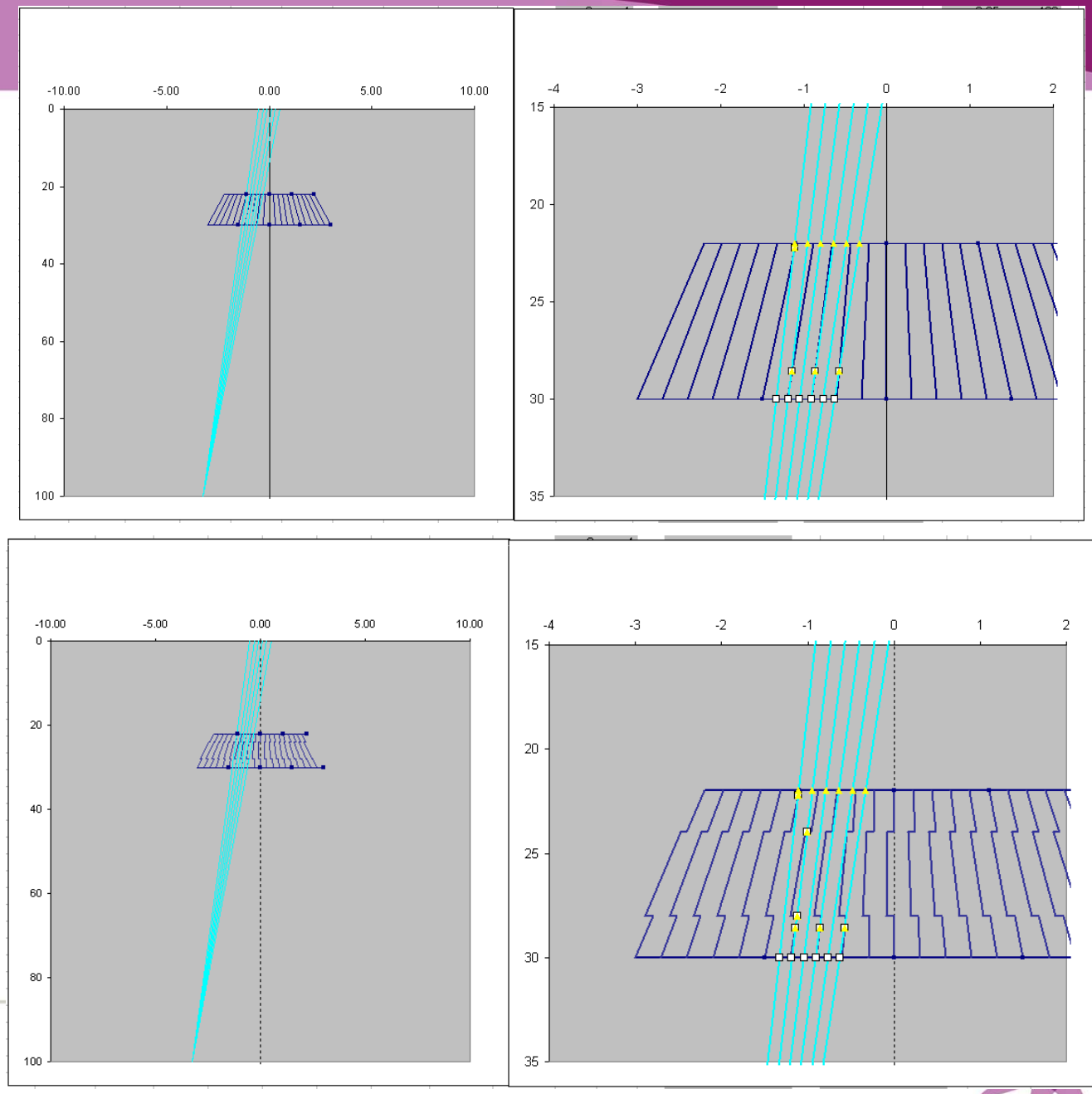

From Oncentra Physics Manual, Elekta

Peripheral dose components

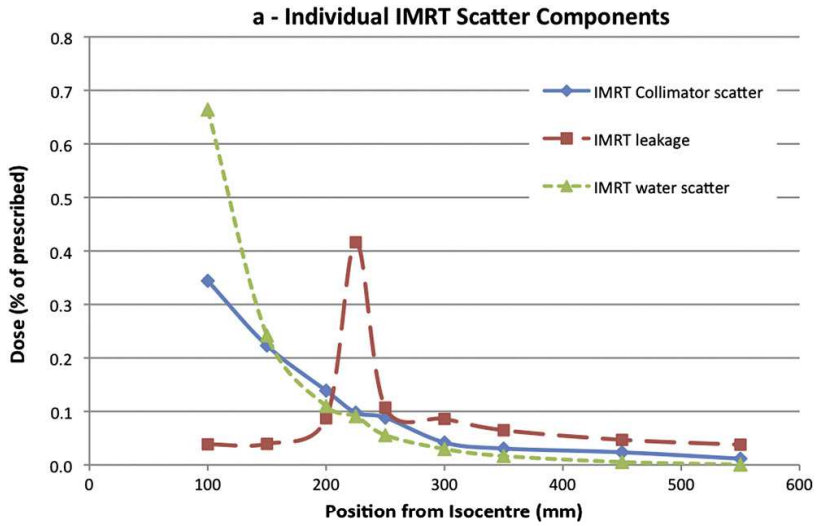

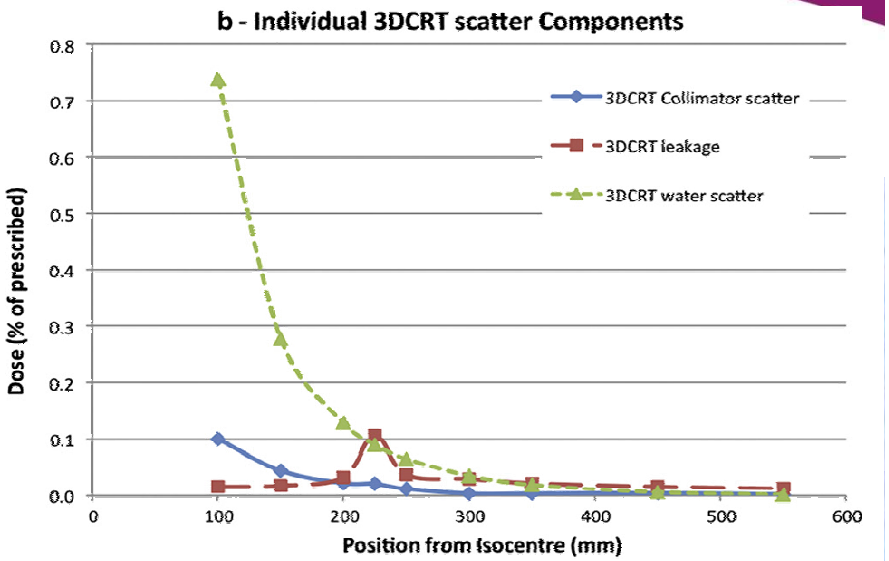

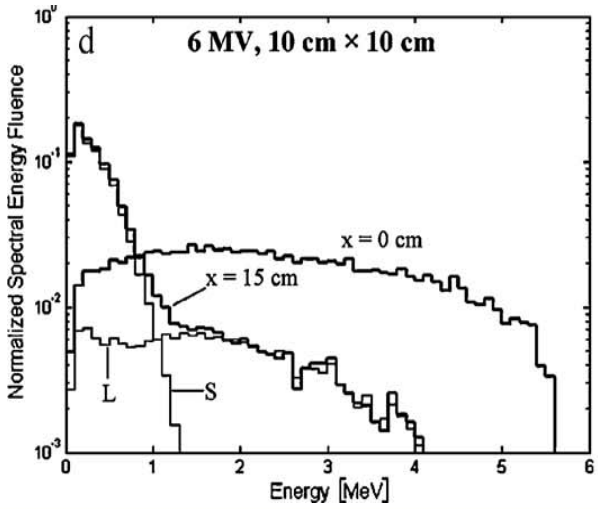

L - head leakage
S - phantom scatter

Ruben etal, IJROBP, Vol. 81, No. 5, pp. 1458–1464, 2011

Chofor etal, Z. Med. Phys. 21 (2011)

ESTRO School

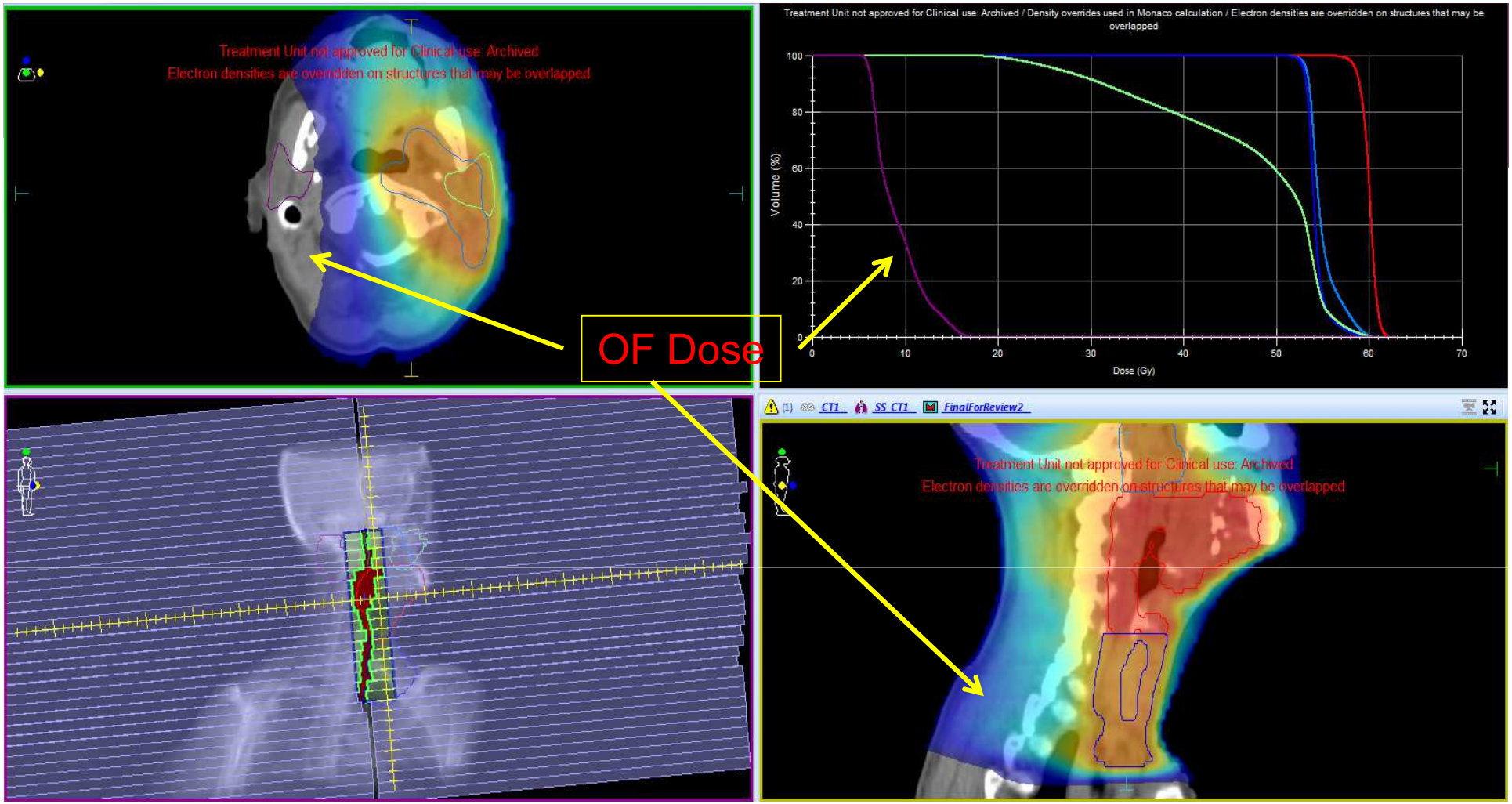

- **Effect of out of field doses?**
- **How accurate is the calculation of out of field dose?**
- **How do we measure it?**

Effect: Fluence optimization

Structure	Cost Function	Enabled	Status	Manual	Weight	Reference Dose (Gy)	Multicriterial	Isoconstraint	Isoeffect	Relative Impact
evalptv60	Target Penalty	☑	On	☐	1.00			60.000	0.000	
	Quadratic Overdose	☑	On	☐	2.05	61.500		0.500	0.000	
evalptv54_sup	Target Penalty	☑	On	☐	1.00			54.000	0.000	
	Quadratic Overdose	☑	On	☐	2.27	55.500		0.500	0.000	
	Quadratic Overdose	☑	On	☐	0.01	58.000		0.500	0.000	
evaptv54_inf	Target Penalty	☑	On	☐	1.00			54.000	0.000	
	Quadratic Overdose	☑	On	☐	3.62	55.300		0.500	0.000	
	Quadratic Overdose	☑	On	☐	0.01	58.000		0.500	0.000	
parotid_right	Parallel	☑	On	☐	3.46	10.000	☐	40.00	0.00	
spinal_cord_5mm	Serial	☑	On	☐	23.79		☐	36.000	0.000	
brainstem_3mm	Serial	☑	On	☐	0.01		☐	39.000	0.000	
External	Quadratic Overdose	☑	On	☐	4.10	53.000	☐	0.500	0.000	
	Quadratic Overdose	☑	On	☐	0.01	35.000	☐	1.500	0.000	

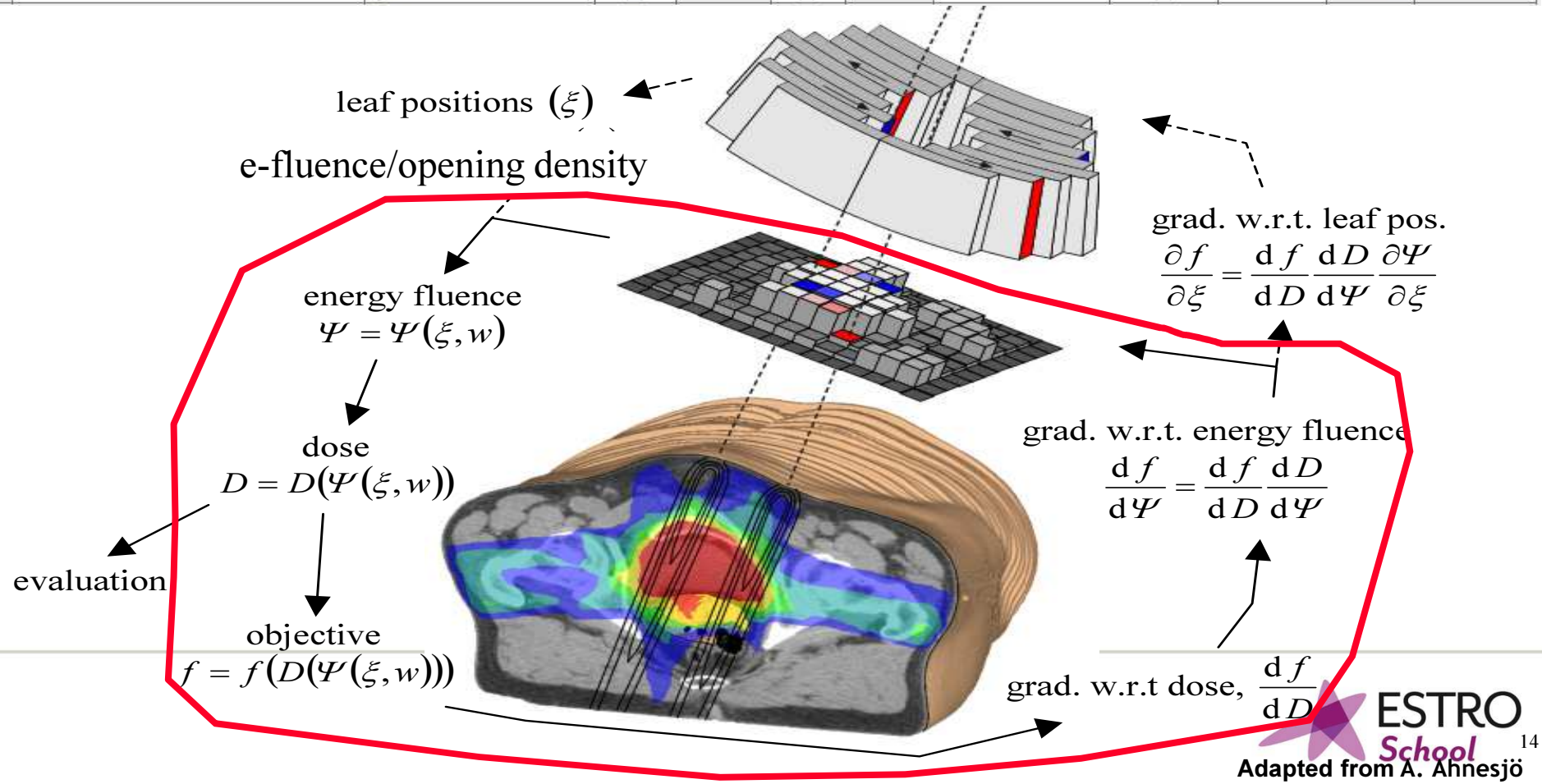

Adapted from A. Ahnesjö

Effect: Second Primary Malignancies (SPM)

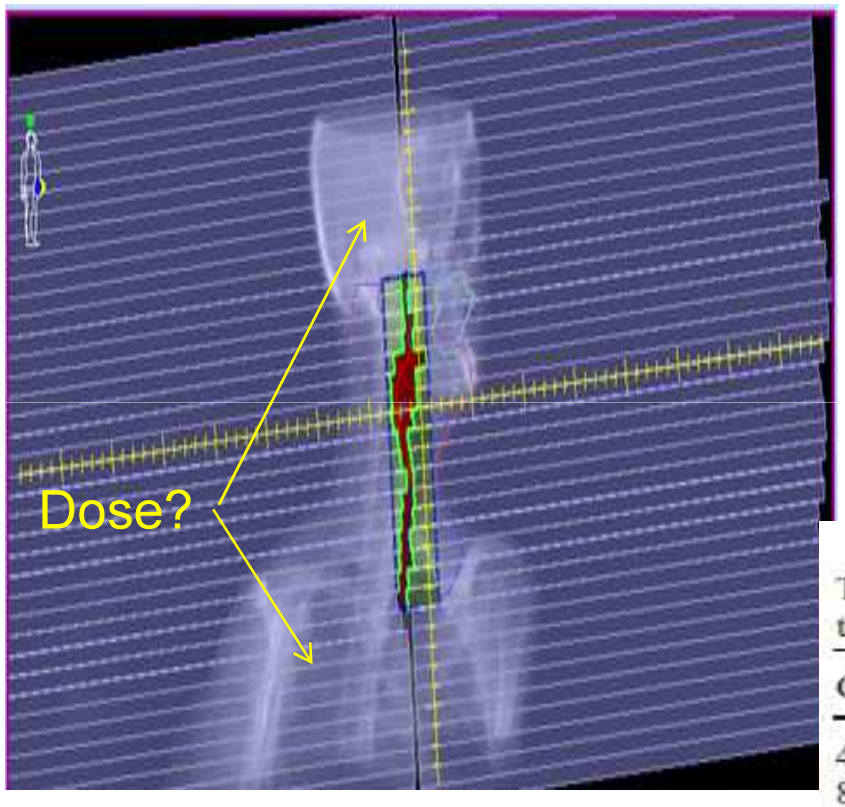

Implantable devices etc too…

- SPM's mostly in tissues >2Gy (fractionated)
  - Thresholds of 0.6Gy (adult) and 0.1Gy (children)
- Practical guidelines: aim for reducing volume <3.5Gy **Tubiana, R&O 2009**
- SPM incidence has reduced due to better conformality of dose (heart, lung, breast) **Tubiana, R&O 2009**
- Somewhat controversial but ***clear need for organ specific doses and distributions*** **K.Trott R&O 2009** (patient specific?)

Table 3. Fatal cancer risk for various organs in terms of a 70-Gy tumor dose[a] **Mesbahi etal, Jpn J Radiol 2010 28:398-403**

Cobalt-60	6 MV	9 MV	Organ
4.53E-06	5.31E-06	5.10E-06	Bladder
8.25E-03	8.50E-03	9.00E-03	Bone marrow
5.25E-05	6.60E-05	7.44E-05	Liver
3.82E-04	4.87E-04	5.55E-04	Lung
1.04E-02	1.11E-02	1.22E-02	Skin
5.53E-04	6.89E-04	7.25E-04	Stomach
5.22E-02	6.32E-02	7.34E-02	Thyroid

[a]Estimated using the MC calculated organ dose and coefficients in Table 2 for conventional radiation therapy of the nasopharynx

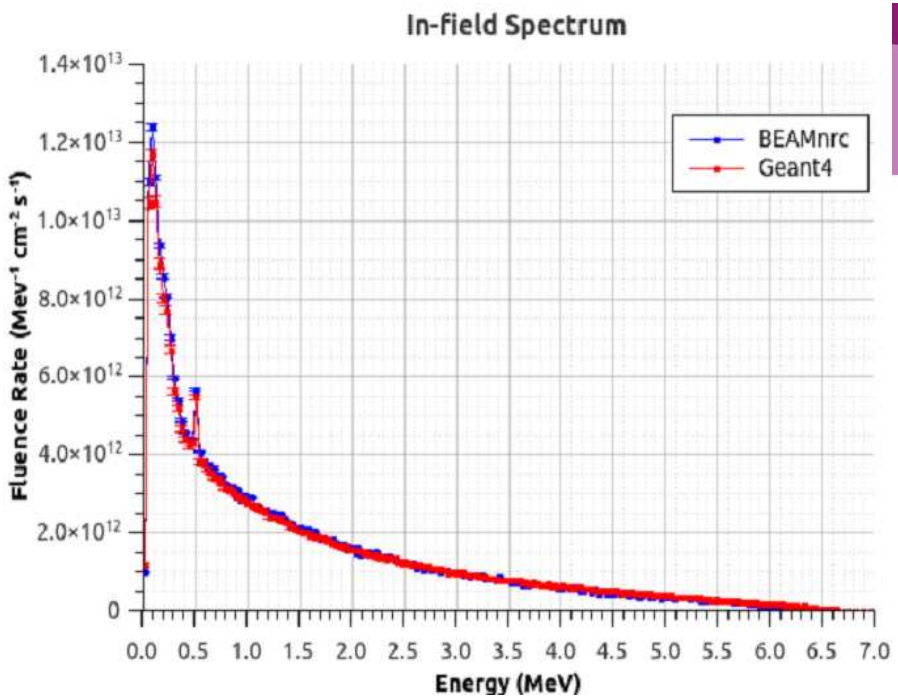

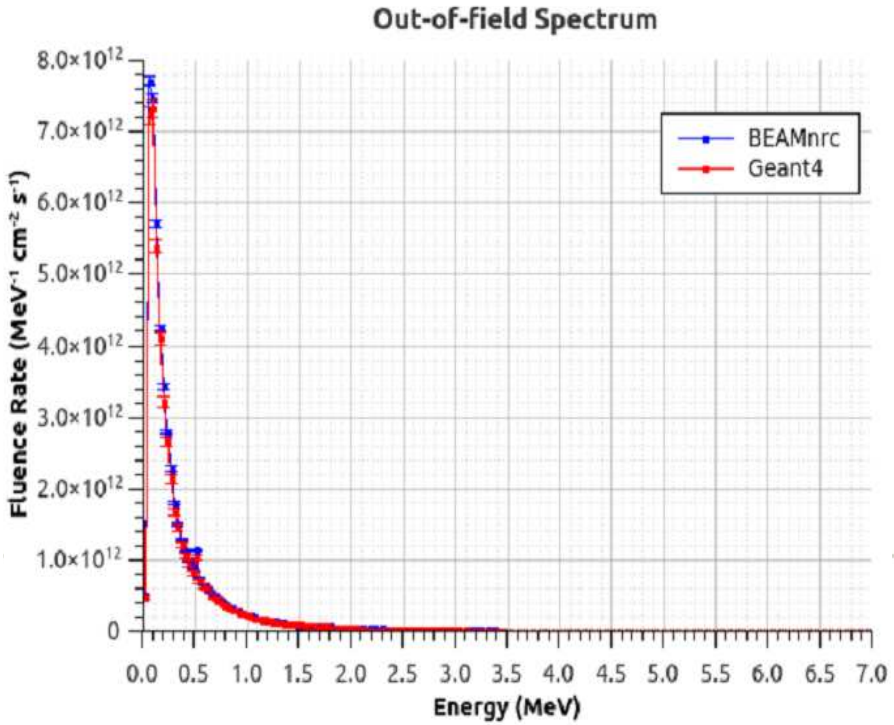

Energy spectrum out of field

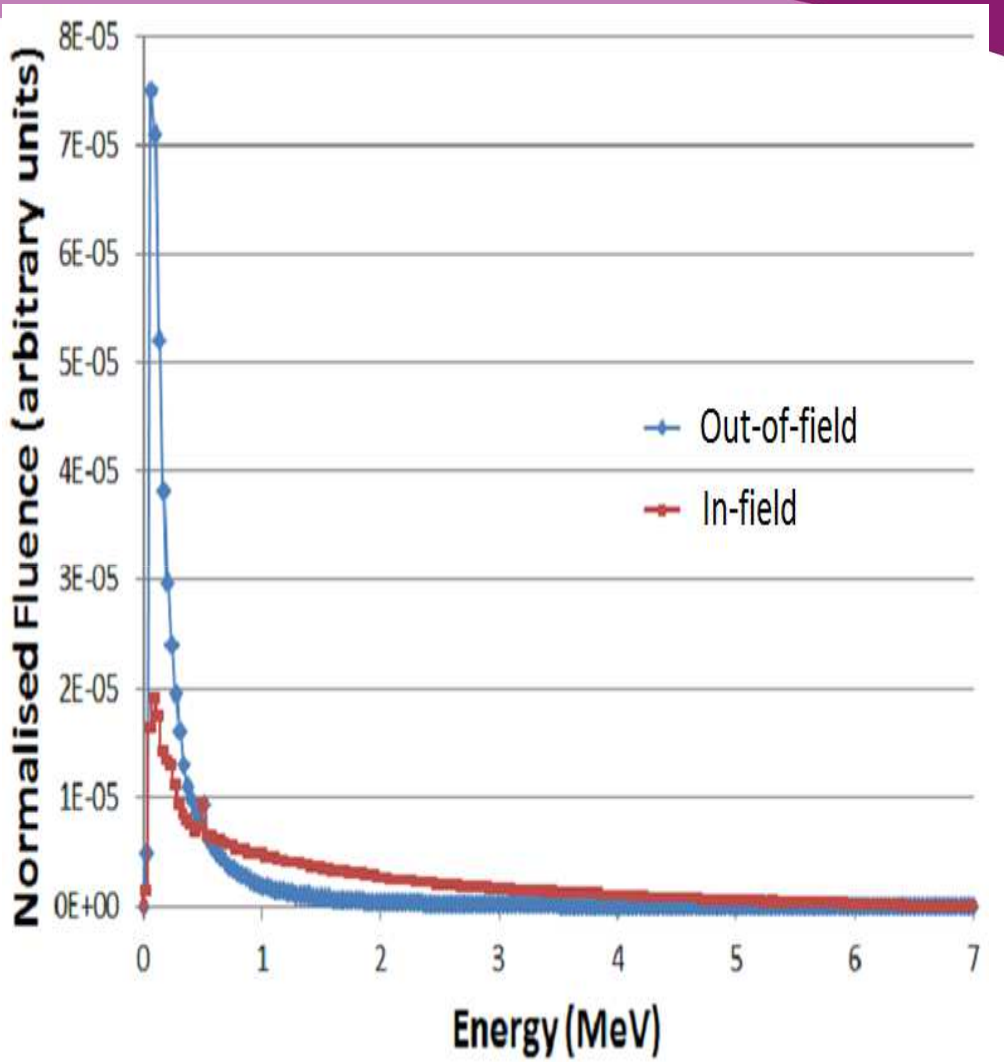

ESTRO School

Scattered radiation - lower energy - different RBE?

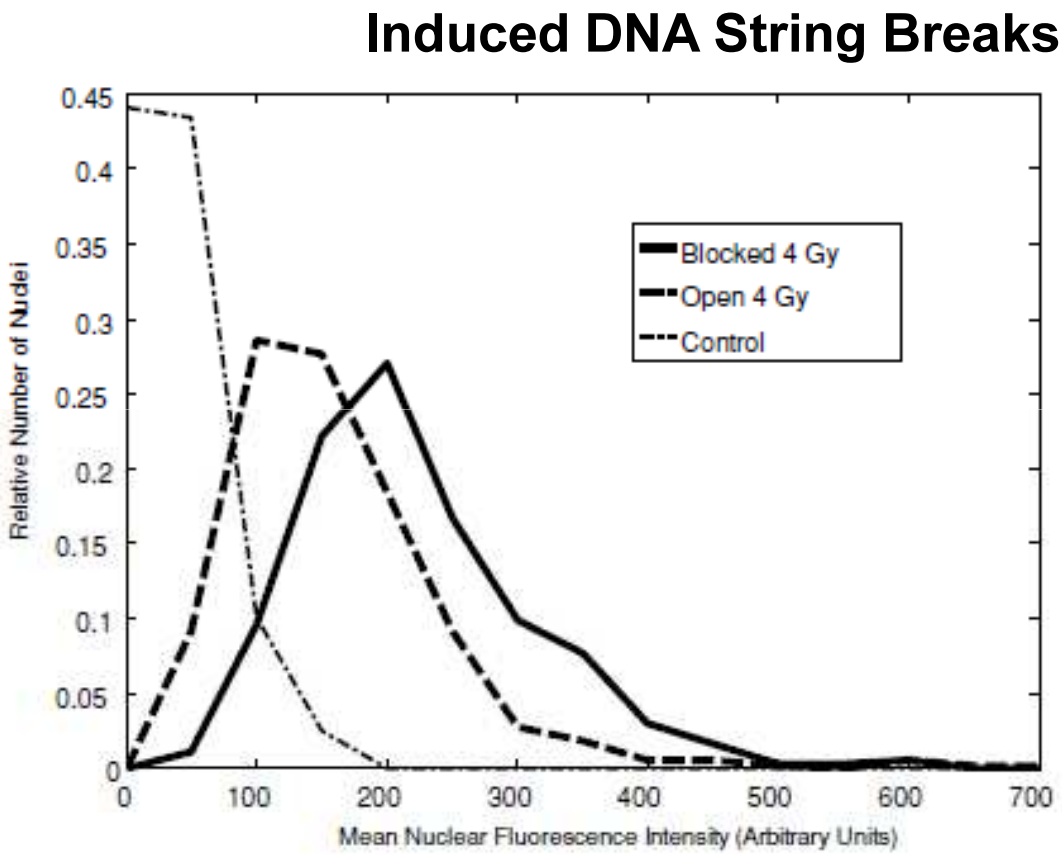

Figure 5. Distributions of mean nuclear fluorescence intensity for control cells and cells irradiated in the blocked and open geometries. The separation between the blocked and open geometries is more apparent in the 4 Gy data but an increase in mean nuclear fluorescence intensity is evident at 2 Gy as well.

Syme etal, PMB 54 (2009) p6623-6633

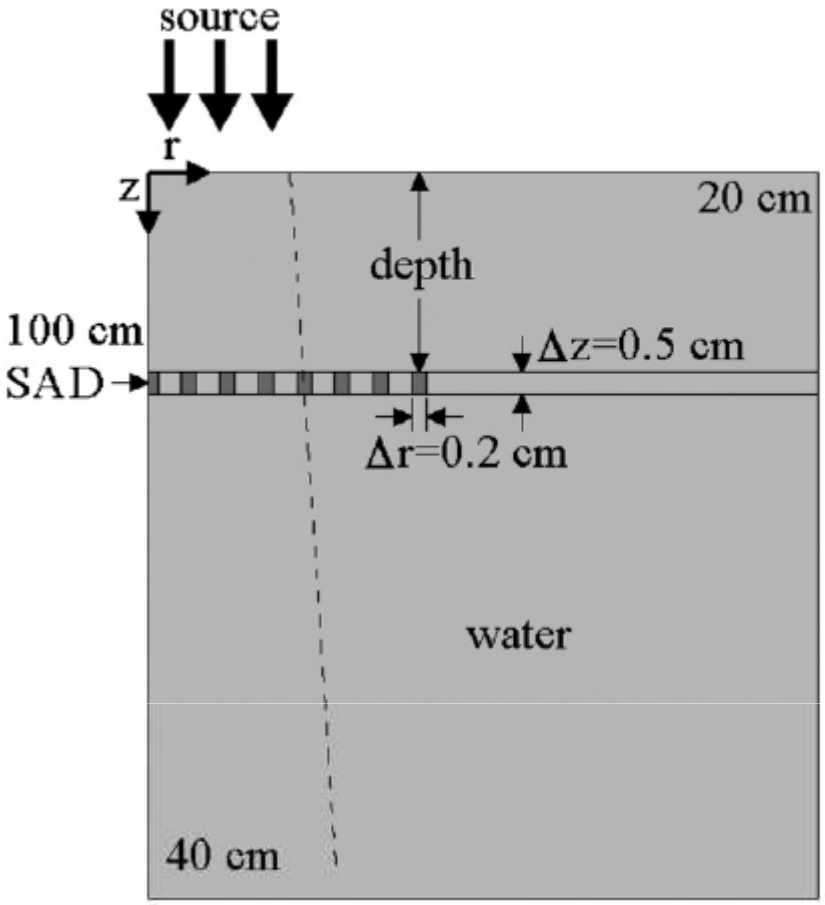

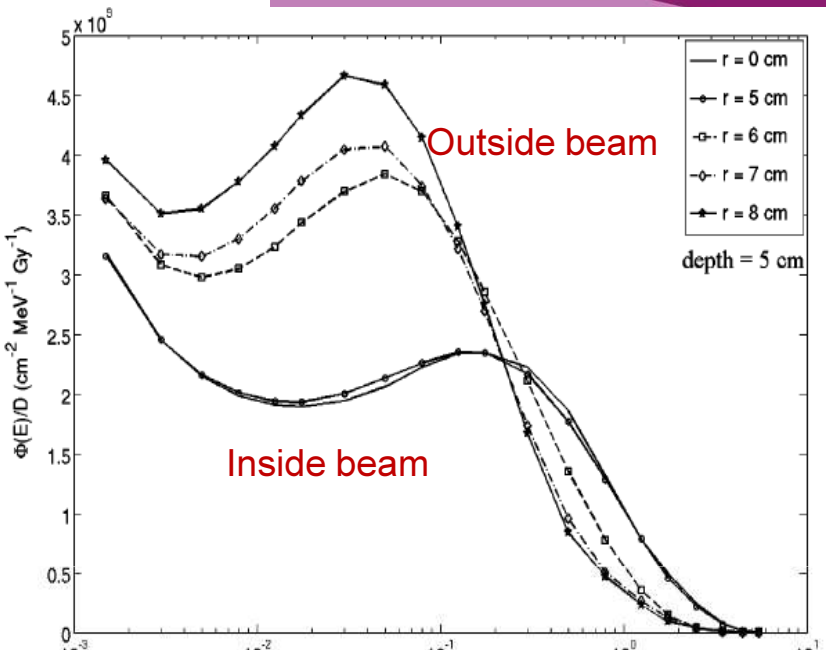

5cm radius 6MV beam

Increase of 25% in RBE 2cm from field edge

Kirkby et al PMB 2007

ESTRO School

Non-Target Culture Flask: Normal Prostate Cells (PNT1A)

Target Culture Flask: Prostate Cancer Cells (LNCap)

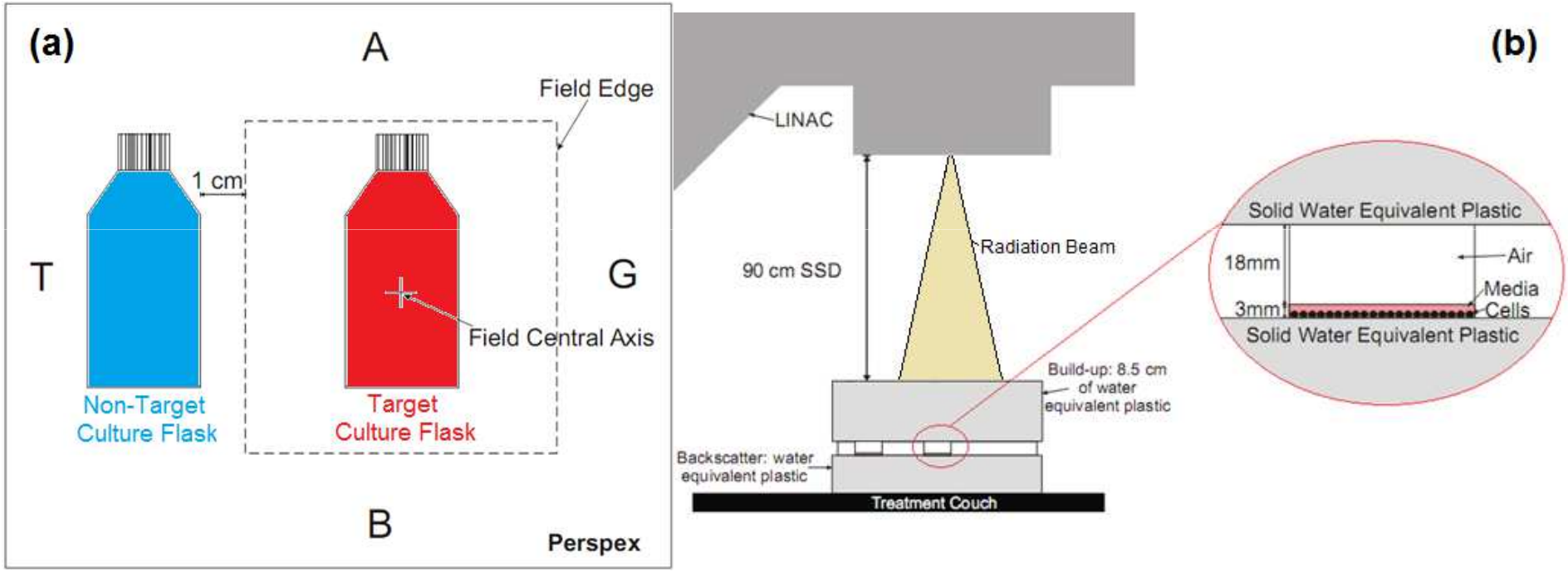

Flask	Average Dose (cGy) ± SD
Target	199.4 ± 3.3
Non-Target	10.8 ± 4.2

ESTRO School

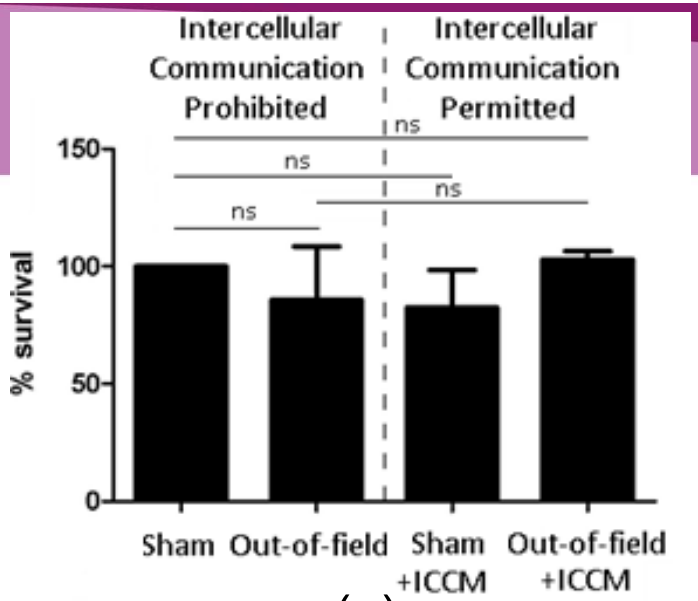

(a)

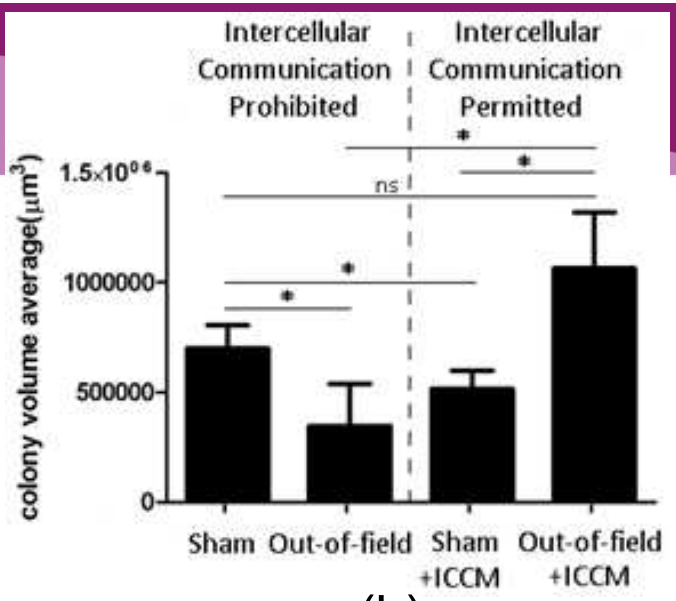

(b)

Shields et al. RADIATION RESEARCH 182, 499–506 (2014)

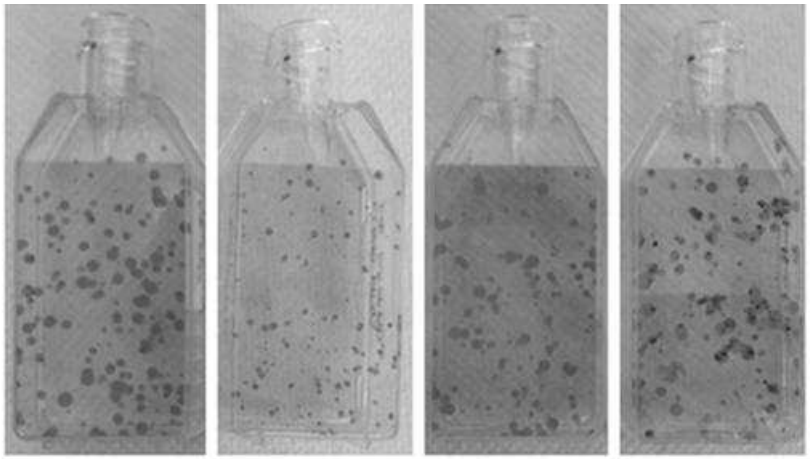

(c)

Figure 3(a) Percentage survival, (b) Average Colony Volume and (c) Photograph of clonogenic assay flasks of the sham and out-of-field cells both with and without ICCM transfer after irradiation of 2 Gy in-field.

Results: Energy Spectrum changes

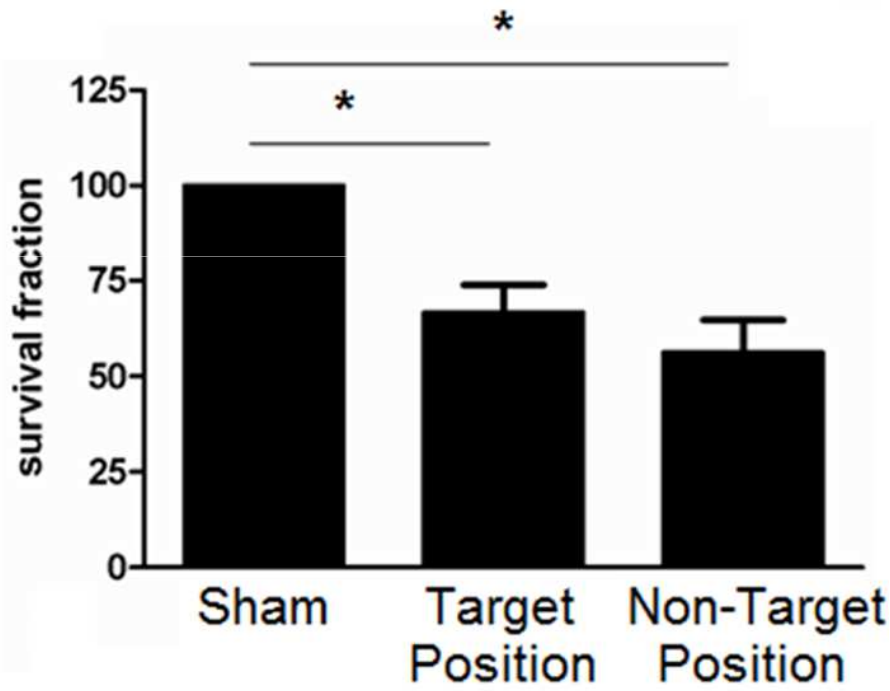

- It is unclear whether or not the non-target energy spectrum is more radiobiologically effective than the target energy spectrum

Pilot study

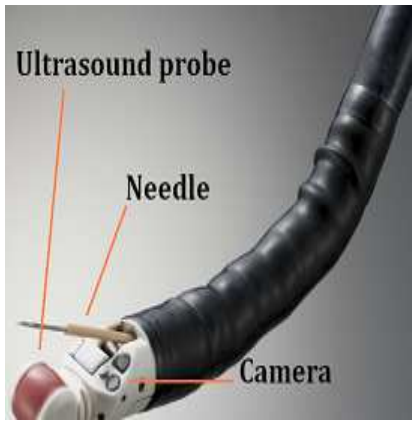

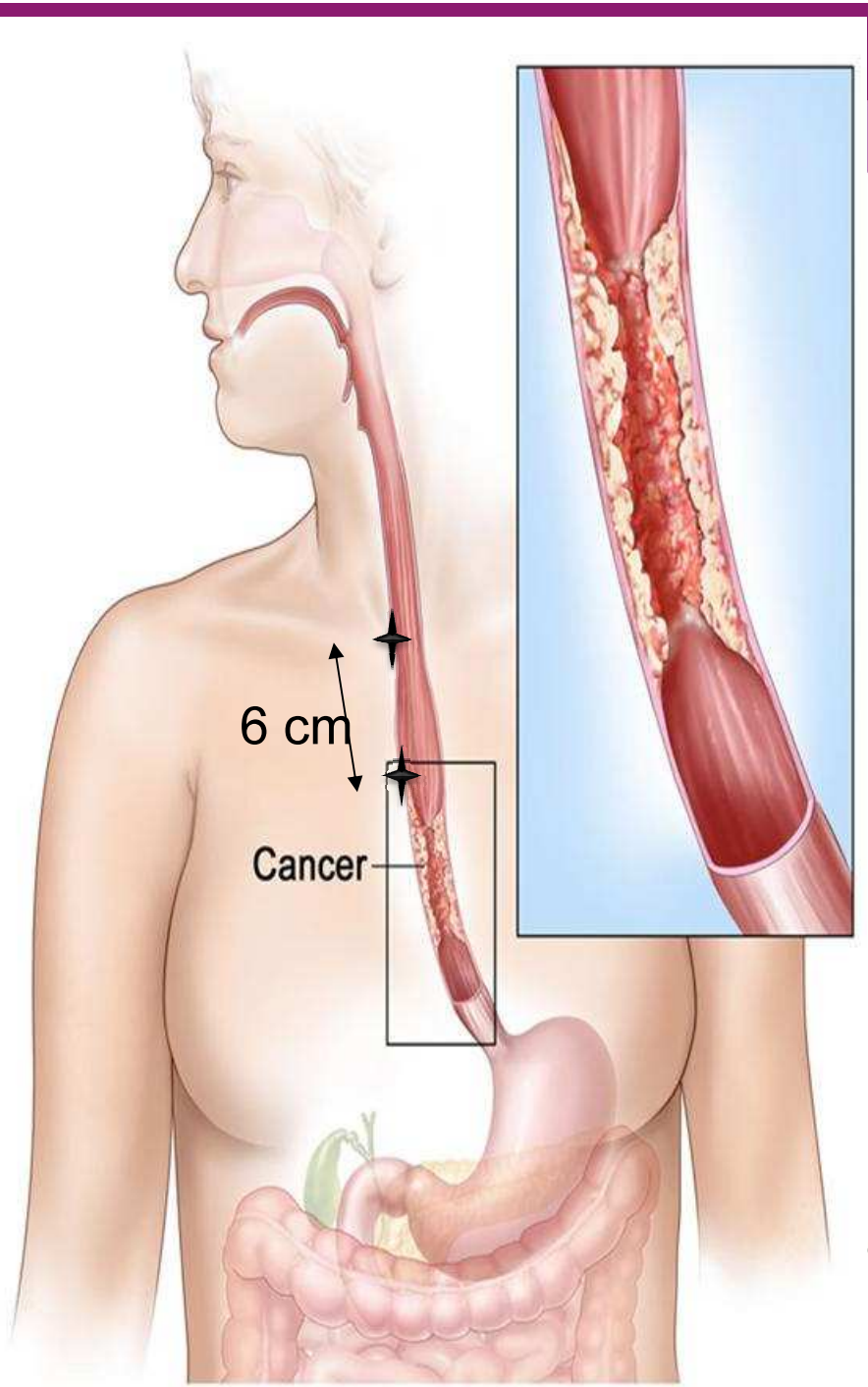

Energy Deposition (ED) and Cluster analysis

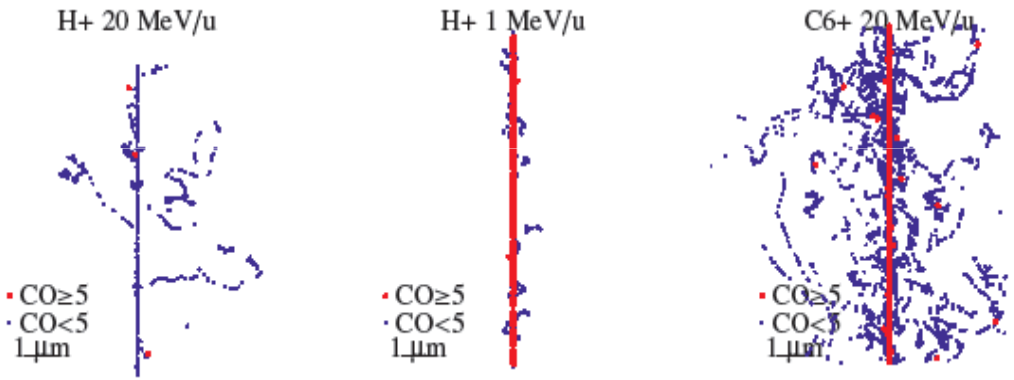

Track structure MC code used to simulate spatial patterns of ED's at nanometer scale

Clustering was examined using distance to nearest neighbour

Used to explore semi-mechanistic model of RBE

UPPSALA UNIVERSITET

Digital Comprehensive Summaries of Uppsala Dissertations from the Faculty of Medicine 930

Protons, other Light Ions, and ^{60}Co Photons: Study of Energy Deposit Clustering via Track Structure Simulations

GLORIA BÄCKSTRÖM

ACTA UNIVERSITATIS UPSALIENSIS UPPSALA 2013

ISSN 1651-6206
ISBN 978-91-554-8736-2

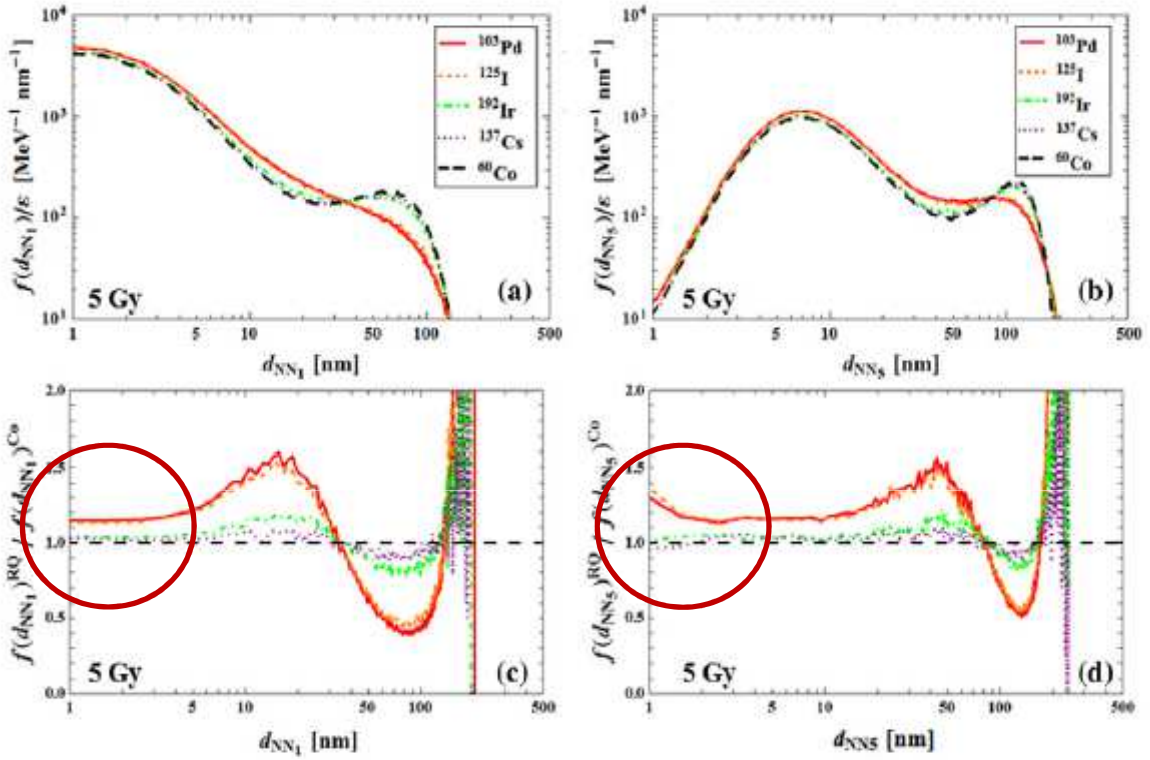

Figure 1. Frequency distributions of (*a*) the first $f(d_{NN_1})$ and (*b*) the fifth $f(d_{NN_5})$ nearest neighbour normalized per deposited energy ε, for the investigated sources. The density of scored EDs corresponds to a dose of 5 Gy using the multi-track approach. In the lower panel graphs, the ratios of the frequency distributions of the different radiation qualities (RQ) with respect to ^{60}Co are shown for the first (*c*) and the fifth (*d*) neighbouring EDs, demonstrating the presence of more dense ionizations for the low energy sources ^{103}Pd and ^{125}I.

Cluster pattern analysis of energy deposition sites for the brachytherapy sources 103Pd, 125I, 192Ir, 137Cs, and 60Co

ESTRO School

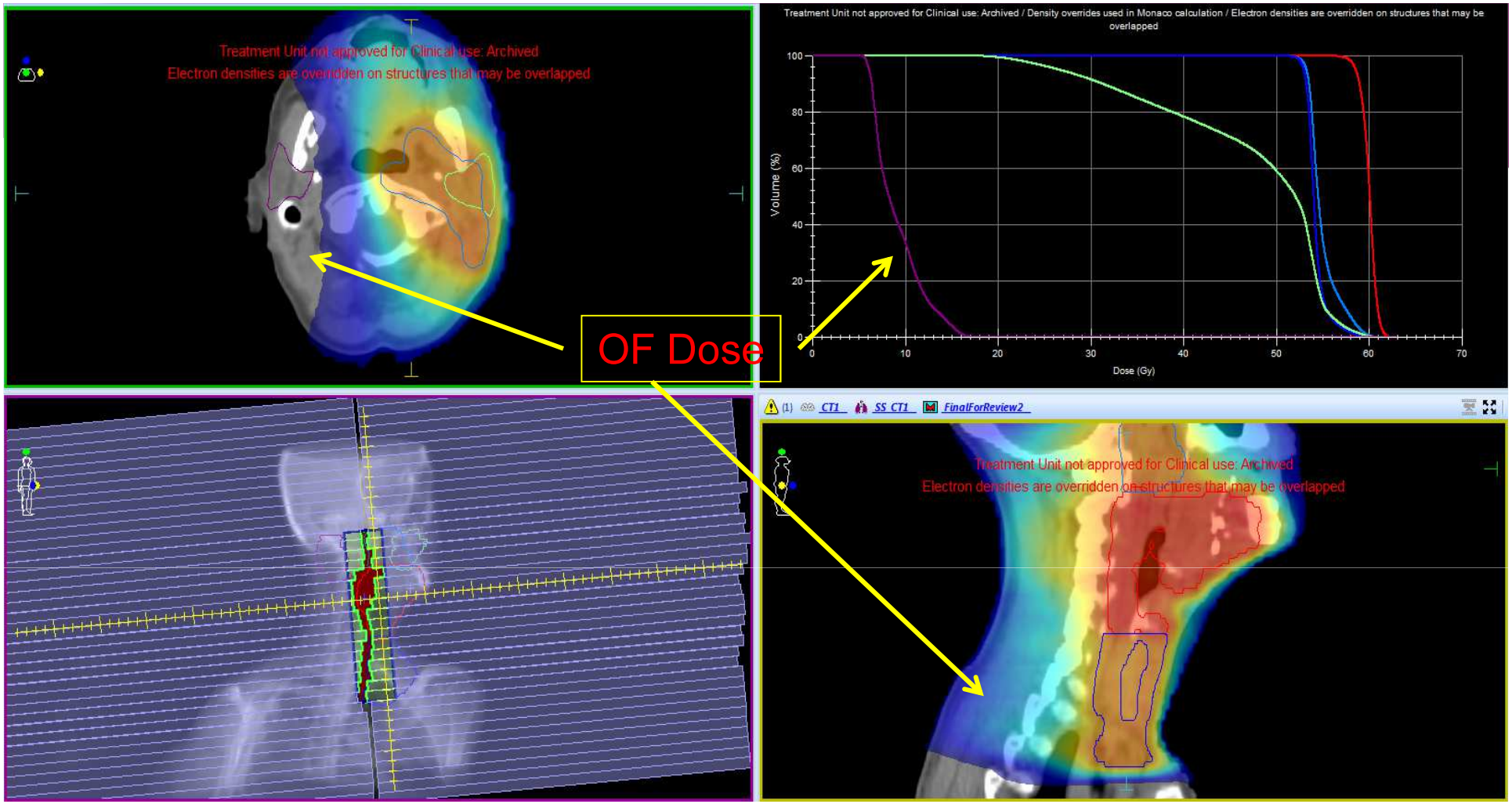

- **Effect of out of field doses?**
- **How accurate is the calculation of OFD?**
- **How do we measure it?**

TPS, general limitations Anders A

Dose calculations bound to grids (fluence map/phase space & dose voxel matrix)

- lack of beam data to drive dose calculations outside the largest field

Main TPS concern is planning dose to target (and saving nearby risk organ)

- Dose in the beam channel and penumbras modeled correctly…
- …scatter usually OK but…
- …less focus on accurate leakage outside of penumbra, far away scatter & neutrons

Peripheral dose considered as a radiation protection issue

- radiation protection management have a population/class solution oriented context
- TPS designed for individual patient contexts

Geometrical models in TPS

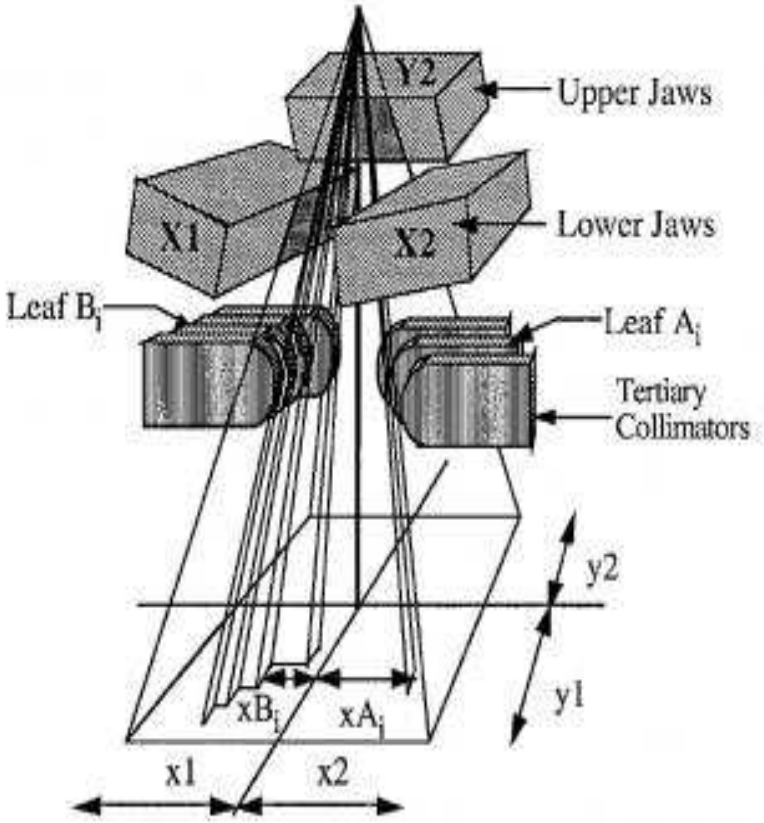

Geometrical models in Monte Carlo

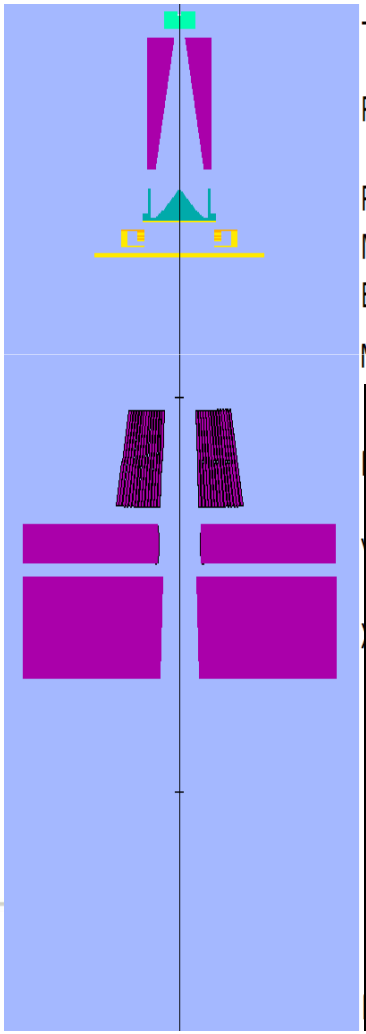

Target (Surrounded with Copper)

Primary Collimator

Flattening Filter

Monitor Chamber (some features missing in reconstruction)

Backscatter Plate

Mylar Mirror (asbent from view)

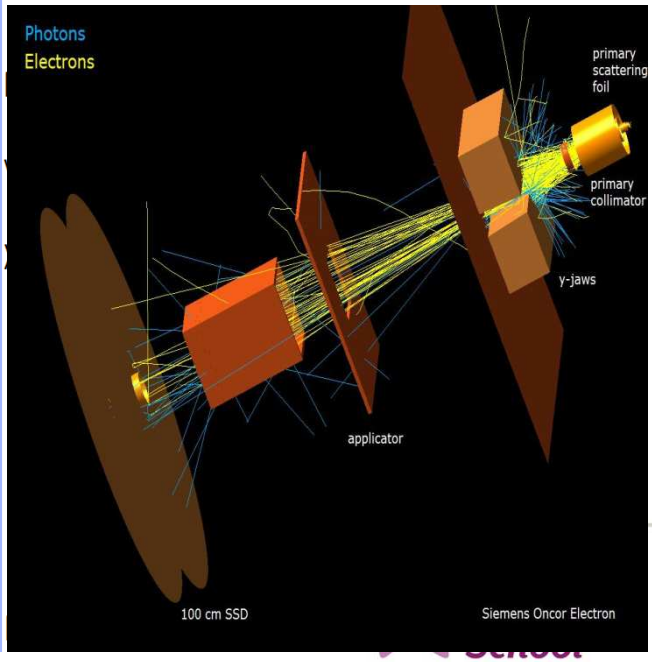

Reality!

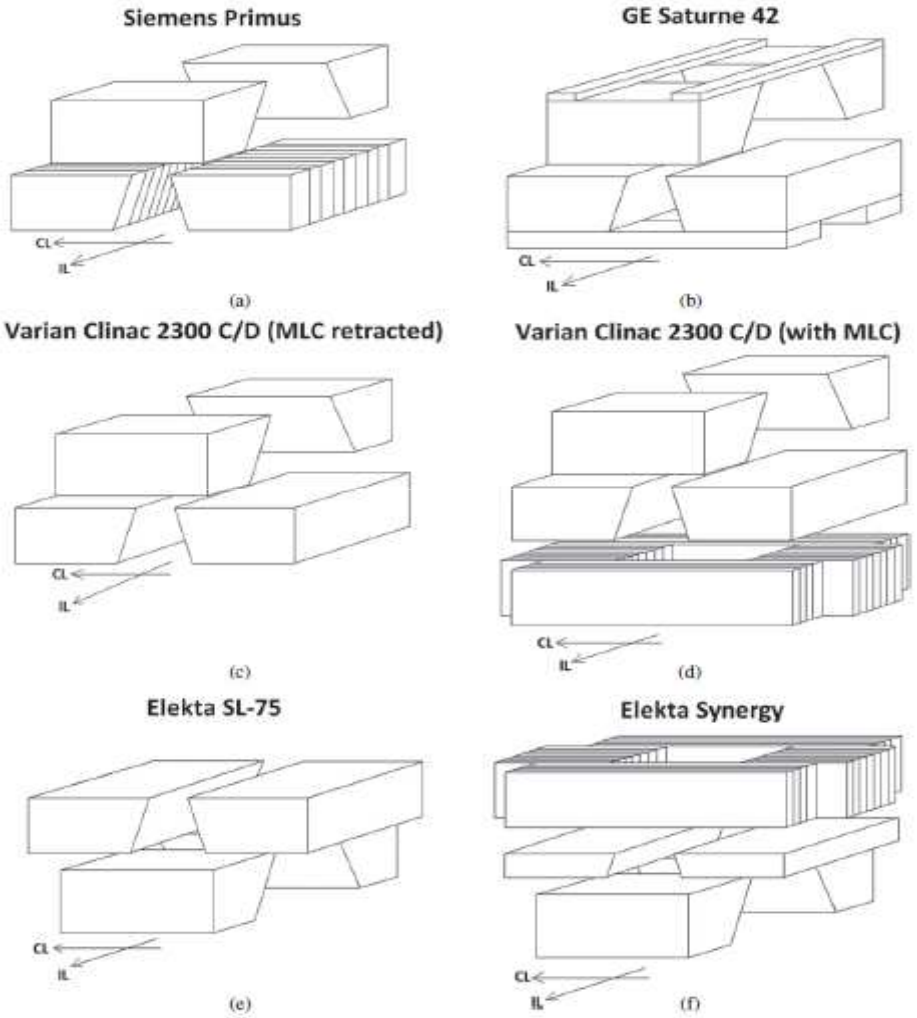

ESTRO School

TPS modelling/tests

Varian Eclipse: ”Physical jaws are assumed to have zero transmission, except for Elekta virtual wedge calculation,for which jaw transmission needs to be defined in Beam Configuration” 2-3 papers claim the system underestimates peripheral dose due to neglecting leakage

Oncentra: very detailed approach - ”…direct fluence is obtained by modulating the open beam fluence with the attenuation from the different elements of the treatment head…. ray trace is performed from each beam source grid point down through the treatment head to the “dose” point” but there are no published tests.

Xio: one paper states ”too simple beam model”

Other systems: ?

TPS test

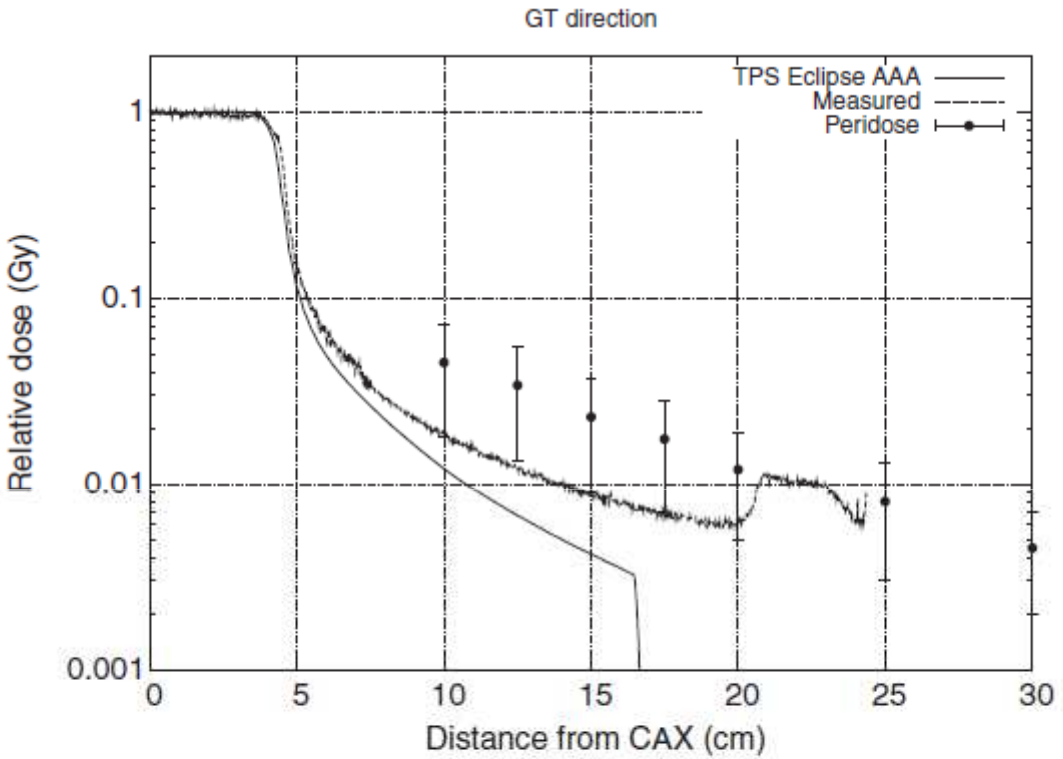

Fig. 2. The out-of-field dose of an IMRT treatment is shown. Note the increase between 20 and 22 cm distance. This represents a gap in the additional shielding provided by the MLC, which acts as a tertiary collimator in a Varian accelerator. The Peridose software predicts the shape as well as the correct dose at the gap.

Van den Heuvel, Rad Onc 105 (2012) 127–132

ESTRO School

TPS Calculation of out-of-field doses PMB 2011

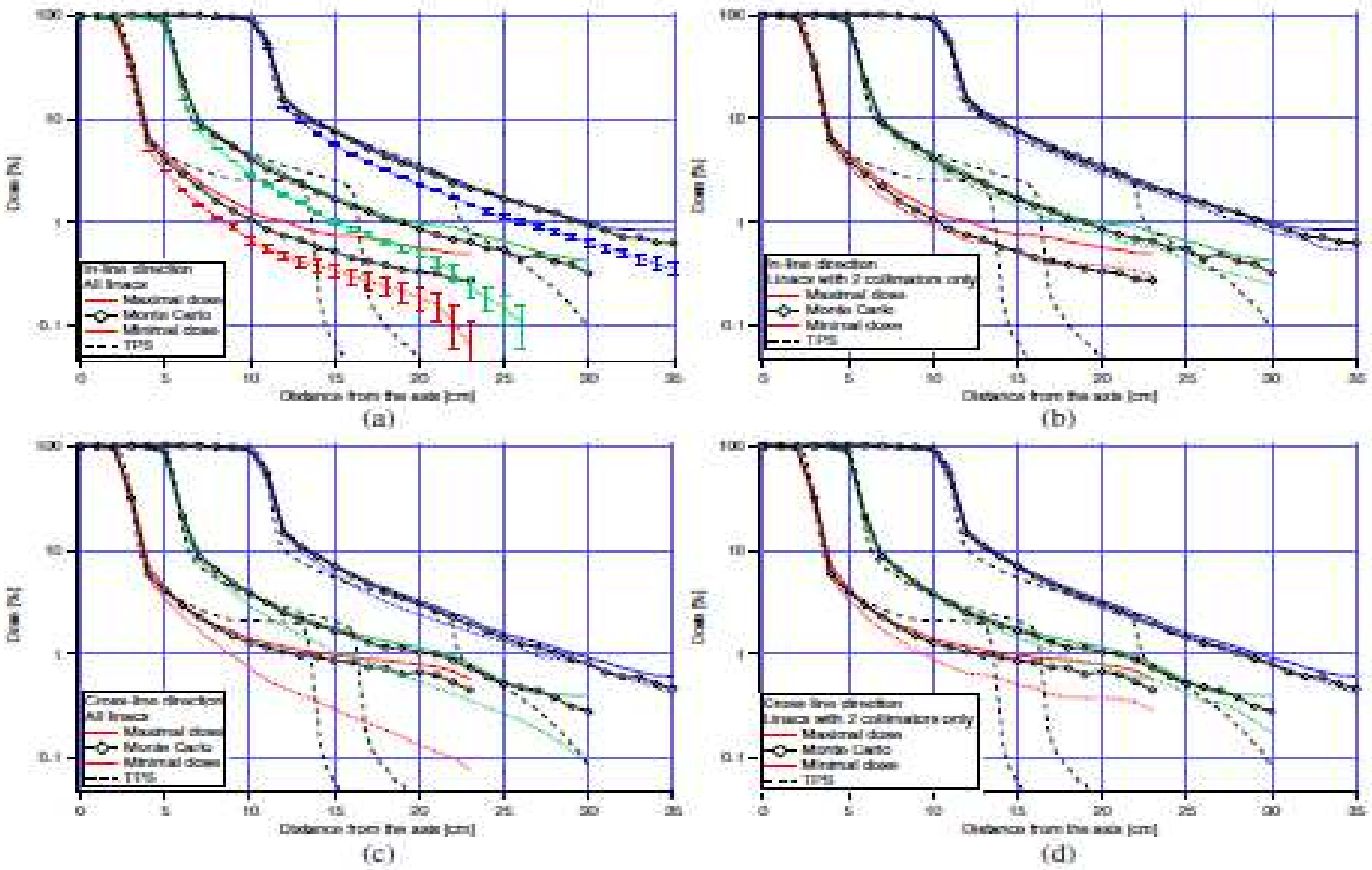

Figure 7. MC, the TPS and the 'envelope' of measured linacs for the 5 × 5 (red line), 10 × 10 (green line) and 20 × 20 cm^2 (blue line) fields at 6 MV and 10 cm depth for: (a) IL direction and all linacs, (b) IL direction and linacs with two collimators only, (c) CL direction and all linacs and (d) CL direction and linacs with two collimators only. For readability, the error bars are plotted only in (a); they correspond to an uncertainty of 0.05% of the normalized dose.

Patient scatter

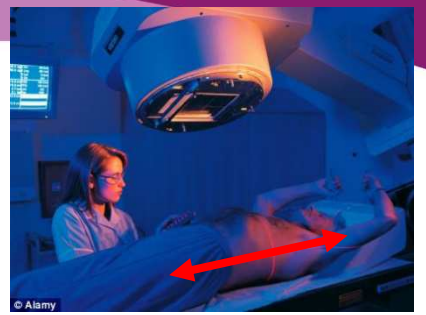

Pencil kernel models * ***Best in class!***

- Heterogeneity scaling lacking (water patient)

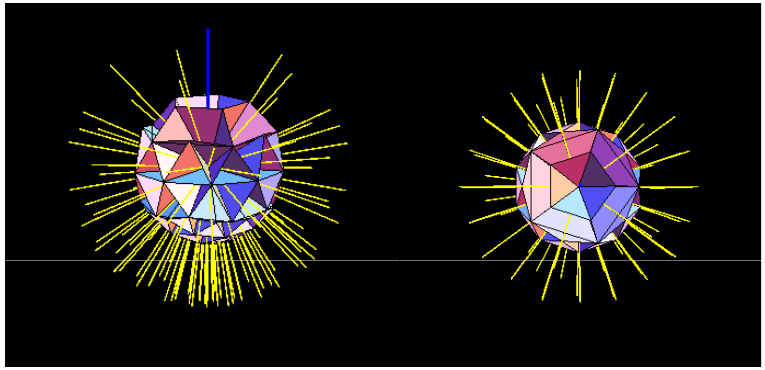

Point kernel

- Heterogeneity scaling typically included
- Collapsed Cone yield angular discretization effects at far away distances

Grid solvers

- Angular discretization effects?

Monte Carlo

- Low doses far away from field is extremely computer time demanding to achieve statistics

Howell et al PMB 2010
Average 40% difference

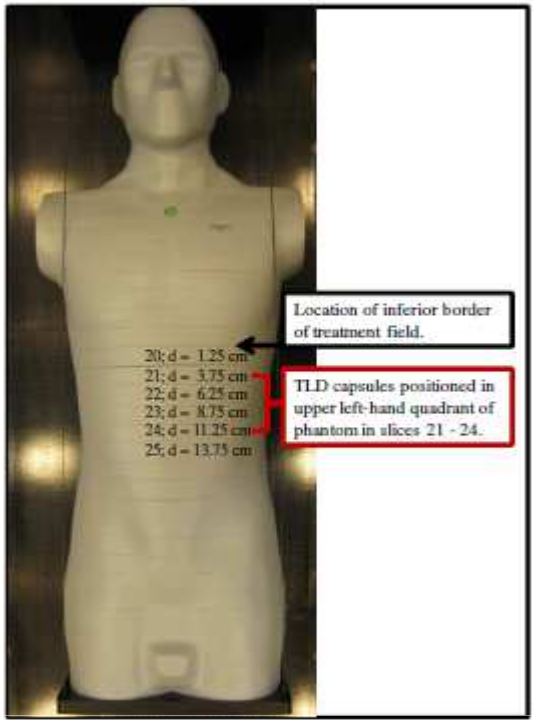

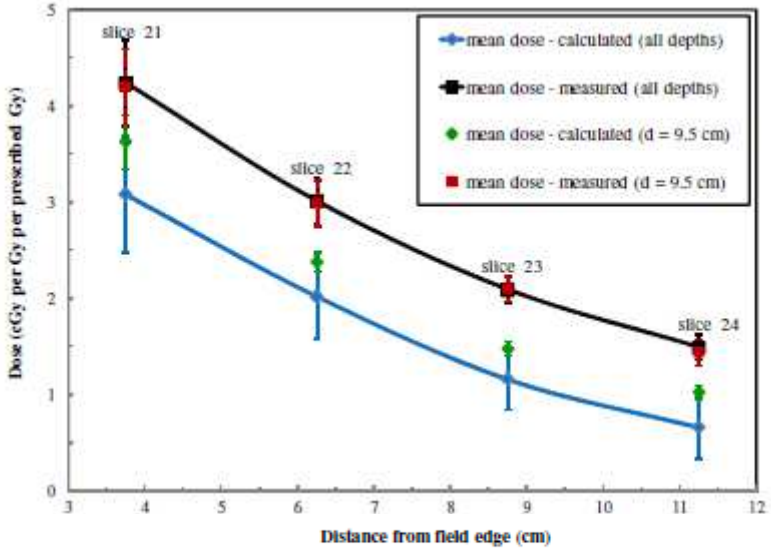

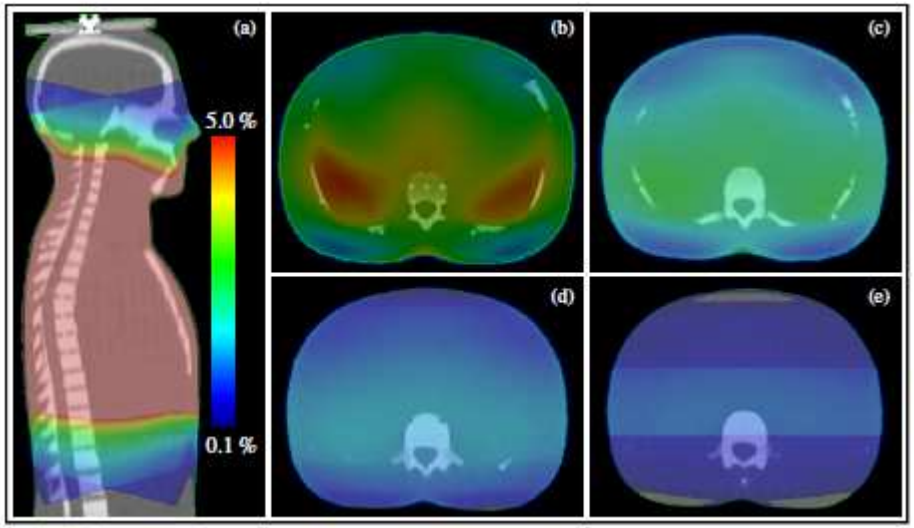

Also: Huang et al J. Appl Clin Med Phys 2013
Average 50% difference

Input data dependant? Detector dependant?

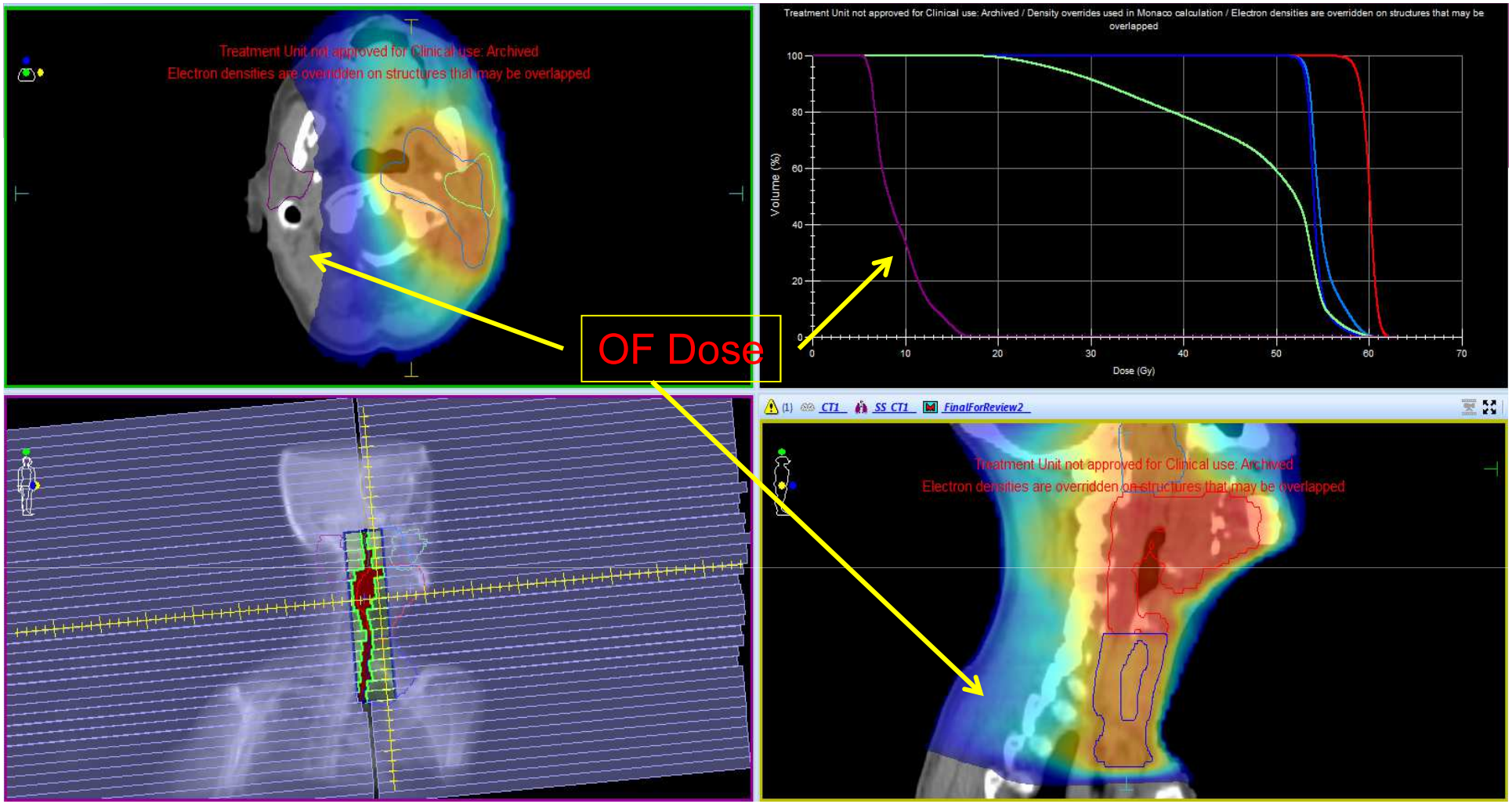

SLH H&N plan VMAT 2015. Marion Quinn

- **Effect of out of field doses?**
- **How accurate is the calculation of out of field dose?**
- **How do we measure it?**

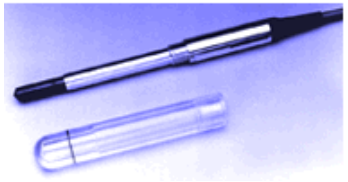

Variation of $s_{water,air}$ for ion chamber measurements

10^7 photons

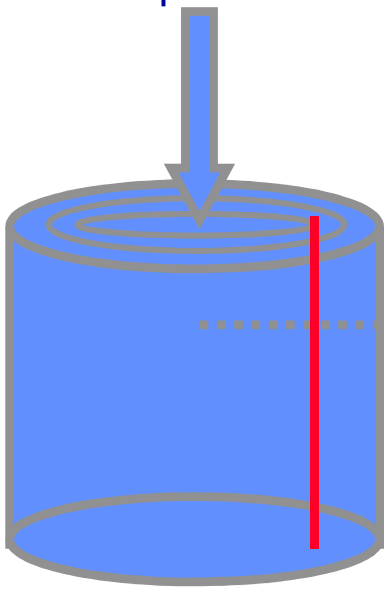

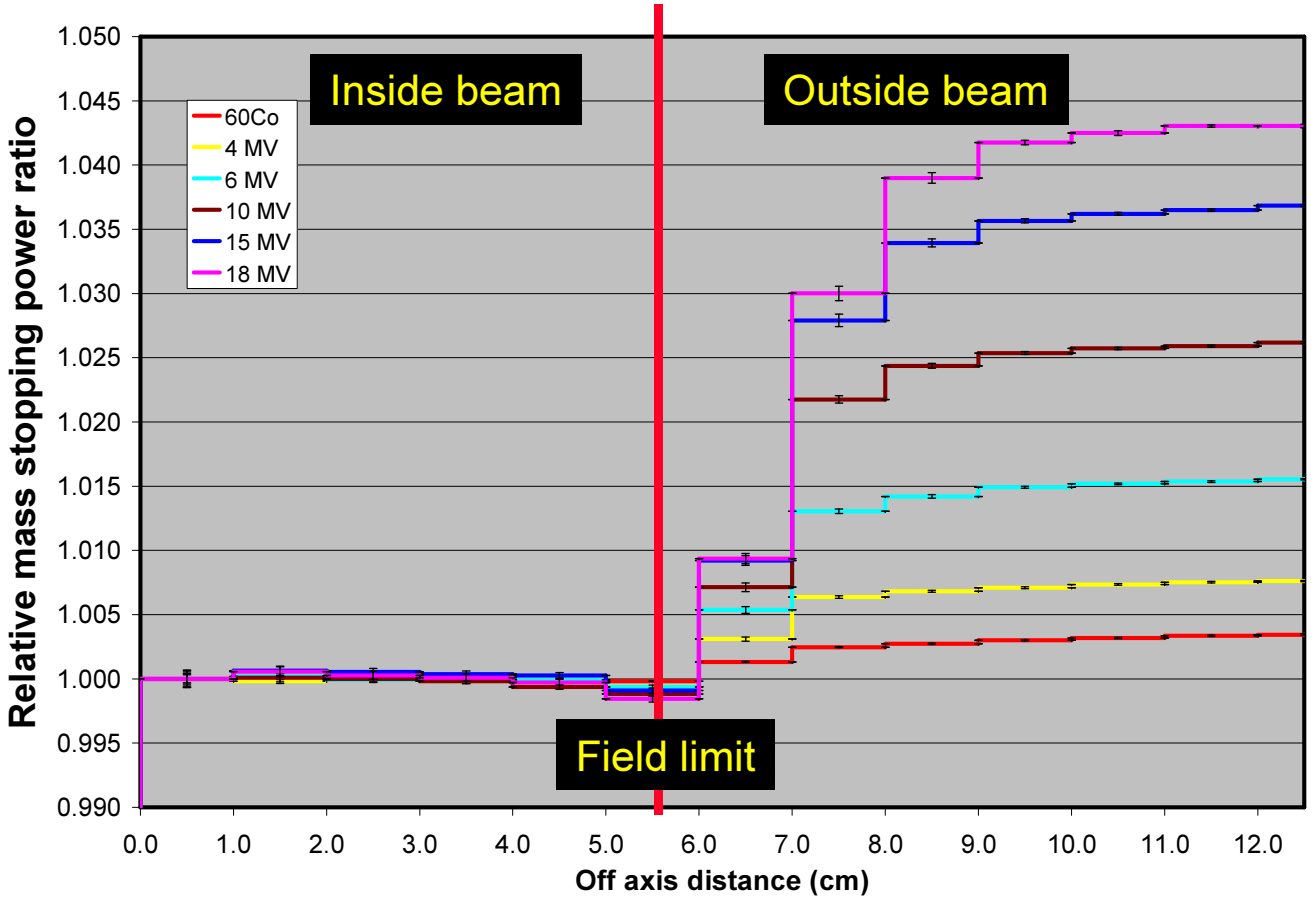

Calculations performed with sprrznrc

Constant spectra over the field

From T. Knöos

Stopping power ratios along a radii at 10 cm depth in water

ESTRO School

Experimental Set-up

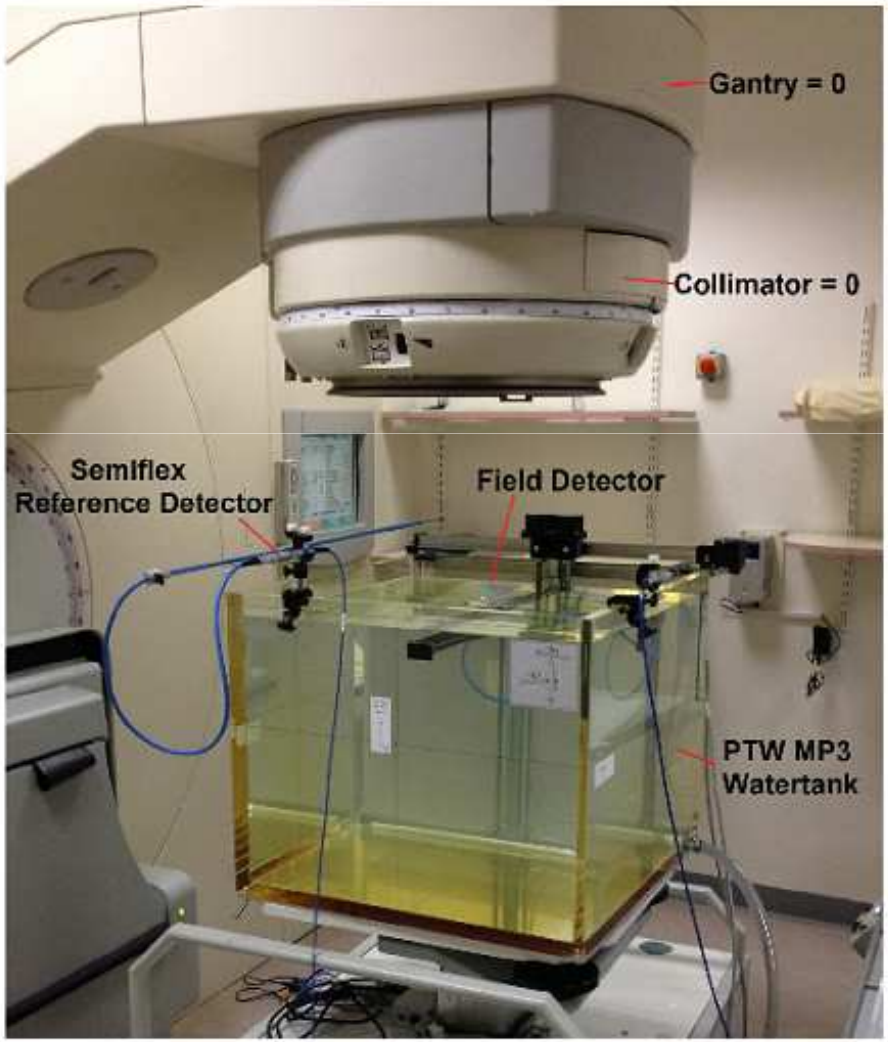

- Detector centred at each depth
- All profiles were shifted with respect to the electron diode so that all field edges aligned
- All profiles normalised to the field edge

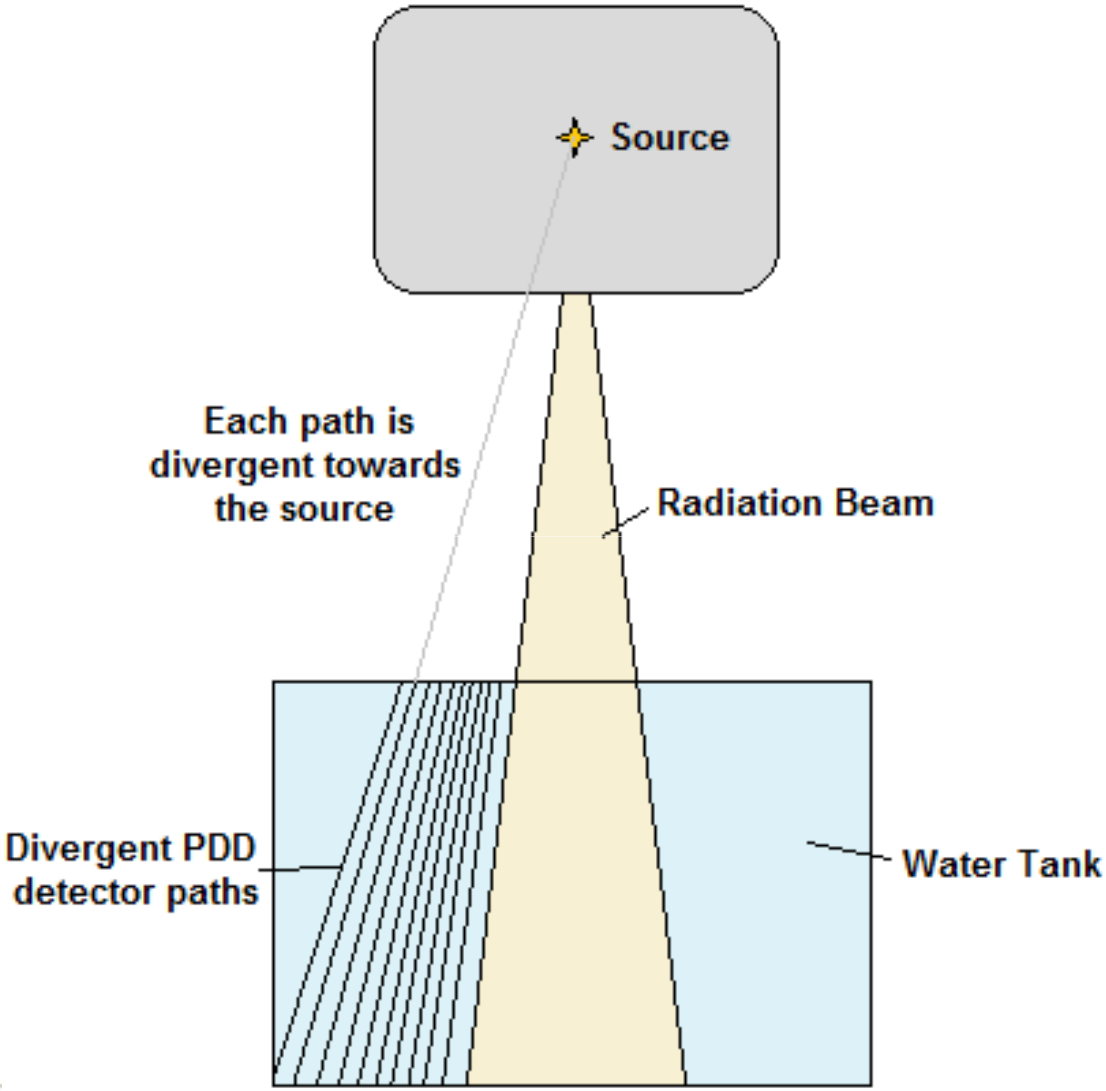

What does a divergent, out of field PDD look like??

Divergent PDD measurement set-up

Summary

- Out of field doses in radiotherapy can be relatively high
- Modern treatment techniques can deliver low doses to larger volumes
- Need improved methods to track dose delivered out of field
  - Deformable models
- Need improved dose models and measurements to assess:
  - radiobiological impact – effects on cell types
  - clinical impact – improved optimisation and clinical DVC's
  - Cancer induction risks
- Further work on suitability of detectors for out of field measurements
- Guidelines for commissioning TPS for out of field doses?

Multi-source beam modeling and TPS data commissioning for photons

Anders Ahnesjö
Uppsala University
Sweden

ESTRO

UPPSALA UNIVERSITY

Learning objectives

To understand:

1. the different roles in a modern TPS of fluence engines versus dose engines

2. how a multisource fluence engine for photons can be designed

3. the role of measured data in beam modelling

Model based dose calculations

Energy fluence engine, multisource models

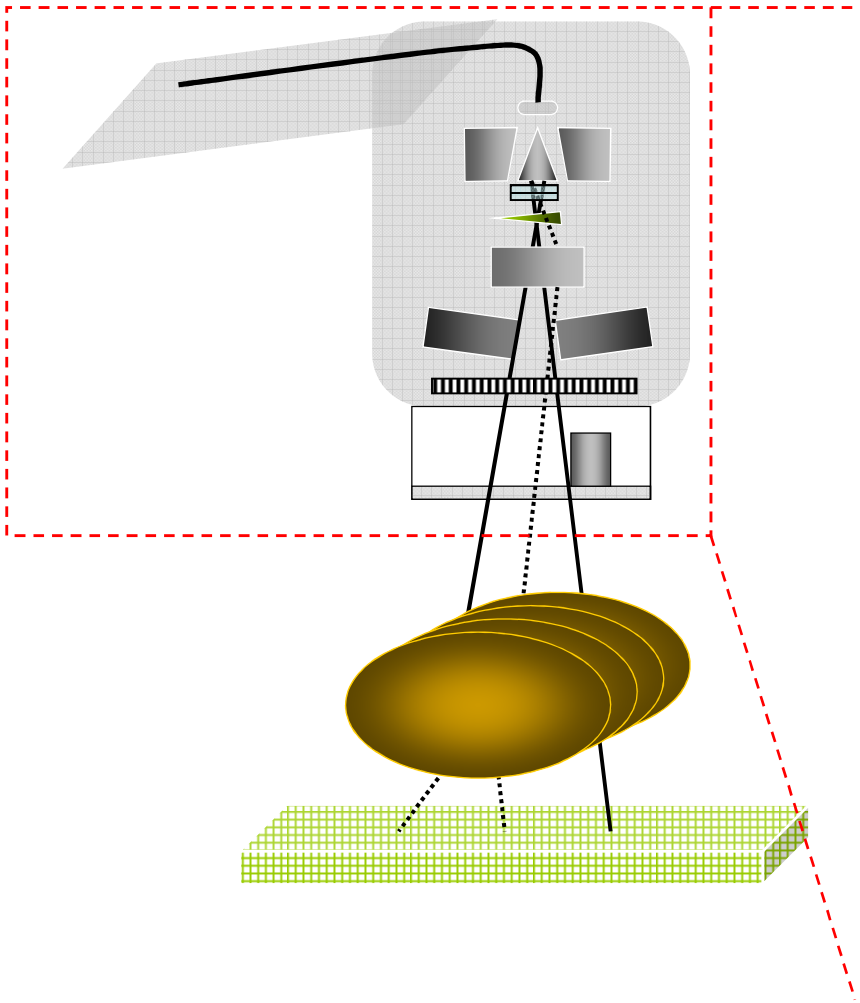

- Finite photon source size
- Open fluence distribution
- Fluence modulation
  - Step&shot
  - Dynamic
  - Wedges
- Head scatter sources
  - flattening filter
  - collimators
  - wedges
- Monitor back scatter
- Collimator leakage, including
  - MLC interleaf leakage
  - shape of MLC leaf ends
- Beam spectra
- Spectral changes
- Electron contamination

Processes to include

What algorithms can different beam data sets support?

Beam data objects	***Fluence/Dose engines***
Dose profiles & Output factors	•No explicit treatment head modelling •Dose calculations based on correction factors from geometrical scaling and attenuation
Description of individual particles	•Explicit treatment head modelling yielding *phase space* of individual particles
Description of multiple sources	•Explicit treatment head modelling yielding fluence distributions •Dose calculations from fluence using kernel superpositions OR explicit transport calculations
Mixed approaches also possible!	

A feasible energy fluence engine should

- **be simple enough to understand the behaviour of the model**
- **have only a small number of free parameters**
- **the model parameters should be determined by measurements that are not too complicated and time consuming i.e. output factors, profiles or depth dose curves in water and air**
- **be complex enough to confirm all measurements in agreement with the accuracy demands**
- **fast in sampling the particle properties (if used for Monte Carlo dose engines)**

(Fippel *et al.* MedPhys(30)2003: 301-311):

Alt 1: Using Dose profiles & Output factors

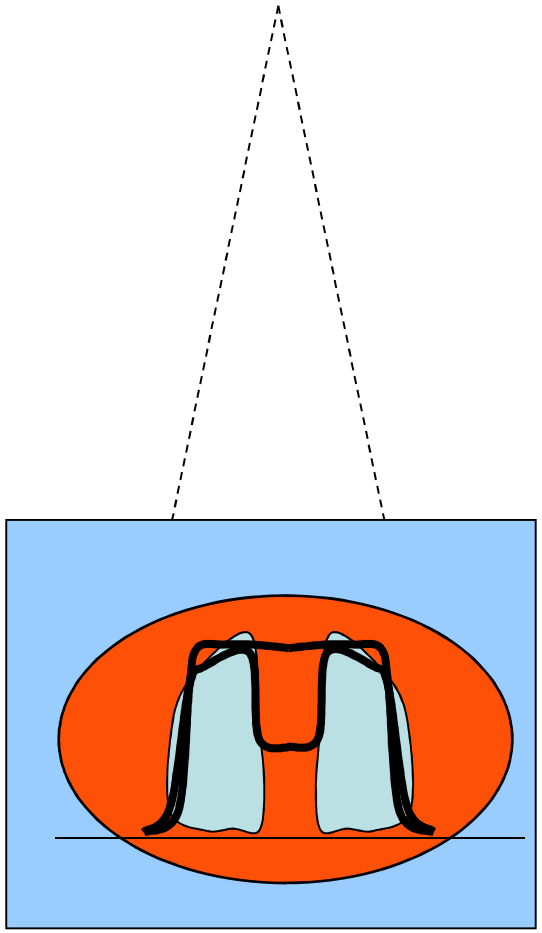

- Dose profiles reshaped using factors deduced from first order, point source fluence changes
- Workhorse in old time “2D” TPS and current Monitor Unit Check programs
- OK for a limited set of field geometries at non-violated equilibrium conditions, e.g. stereotactical treatments
- **Breaks down for general CRT/IMRT/VMAT conditions!**

Alt 2: Describing individual particles – Phase Space

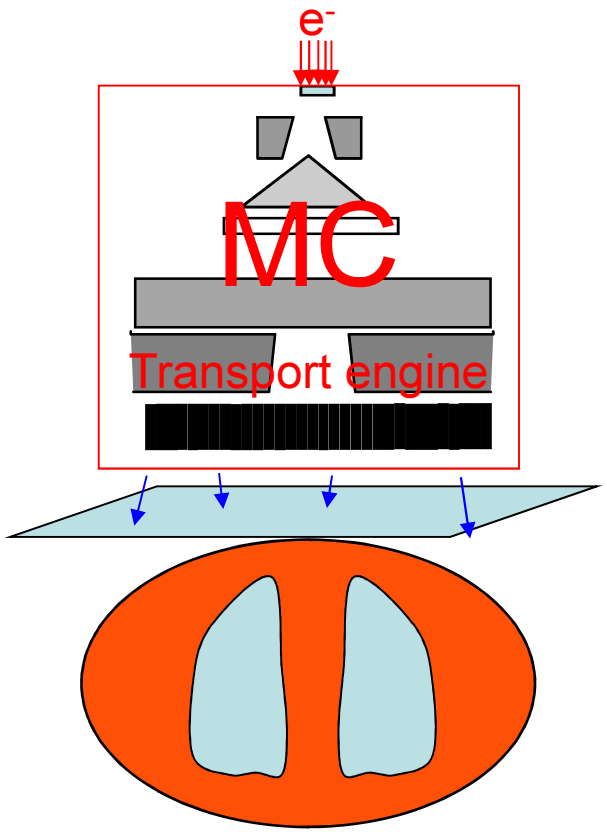

- Monte Carlo transport engine used to yield long list (millions…) of output particles at an exit interface
- Each output particle specified to type, energy, lateral position and direction
- Electron source onto target tweaked to match the output to dose measured in water
- Excellent research tool, **less practical for routine work**

Energy fluence engine based on Multi-Source models

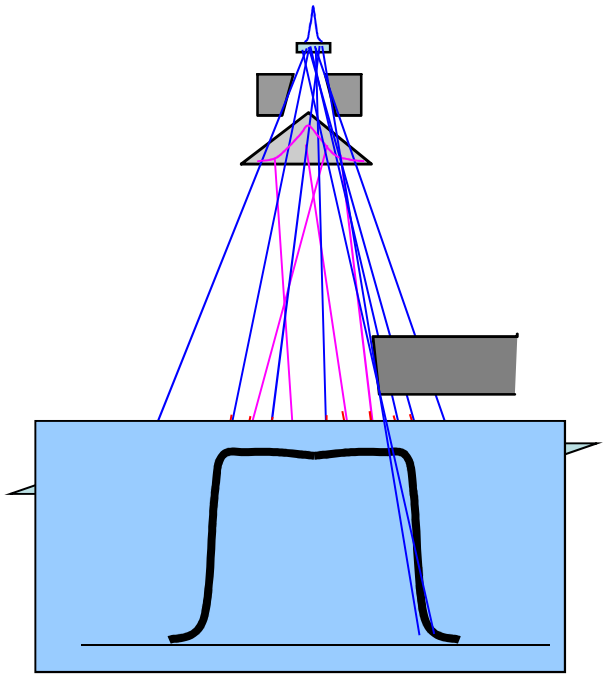

- Back trace the particles of a Monte Carlo generated phase space to their sites of last interaction (i.e. particle source positions)
- Group dense locations of last interaction sites into sources, calculate emission characteristics of each source

OR

- **Use *a priori* information about the sources and fit parameterized models versus measurements**

- **Measurements can be specialized for explicit source data OR standard dose and output data**

Multi-Source model implementation concept

Multi-source modelling give energy fluence maps for the direct beam and the head scattered beam. Particle characteristics to feed the dose engine are then deduced through:

- **Number of particles** – matrix element value (which has to consider partial source blocking while being computed!)
- **Position** – matrix element location
- **Direction** – as if the particles were coming directly from respective source to the matrix element, angular spread can be included
- **Energy** – given by a beam spectrum, off axis variations may be included
- **Extended sources** to model partial blocking

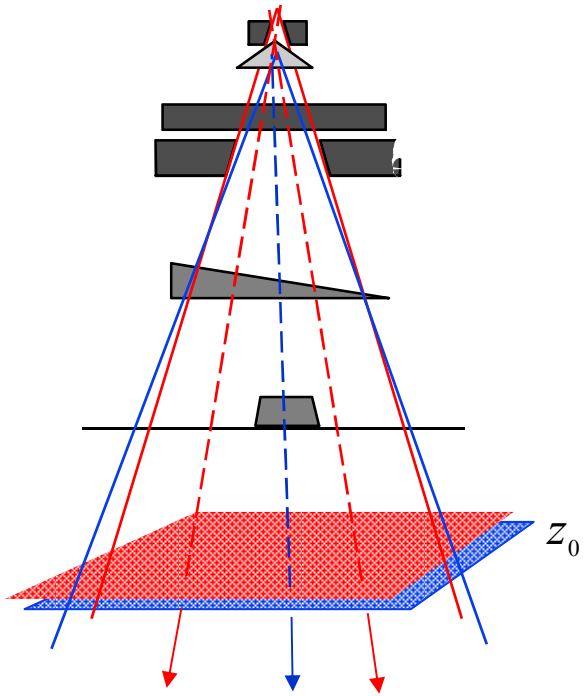

Calculate the value of a fluence matrix element

The width, shape and other radiative properties of the source

Collimators can be raytraced, or approximated as ideal beam blockers

IMPLEMENTATIONS MAY DIFFER WIDELY!

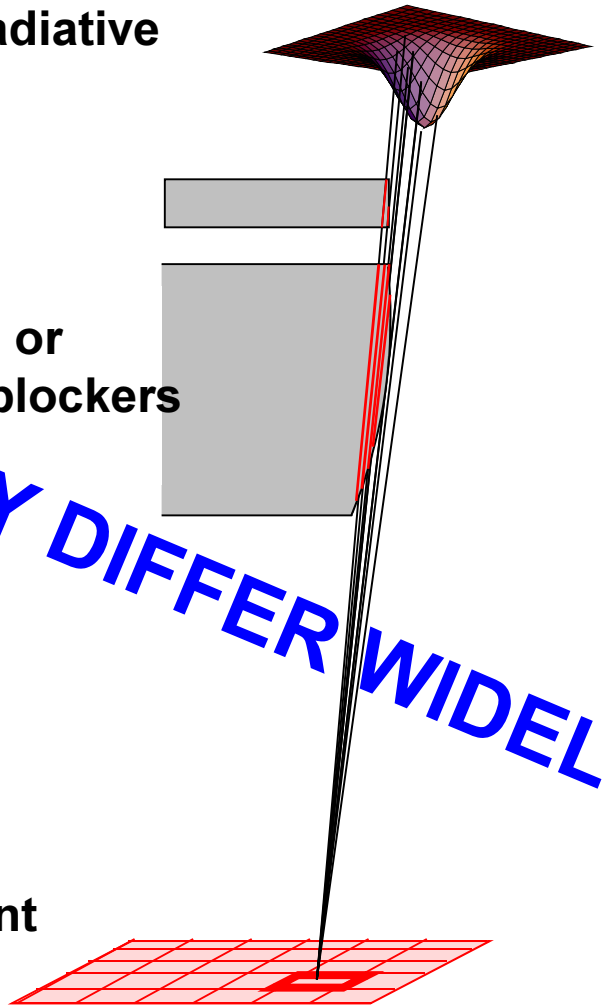

For each element, find the contributions from the relevant sources

Properties of the direct beam source

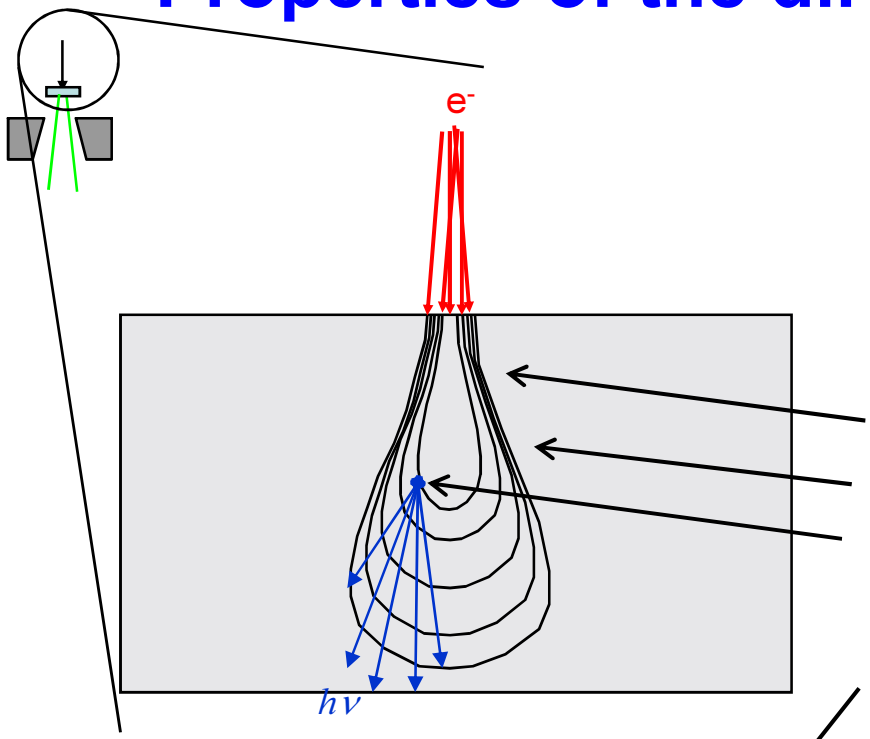

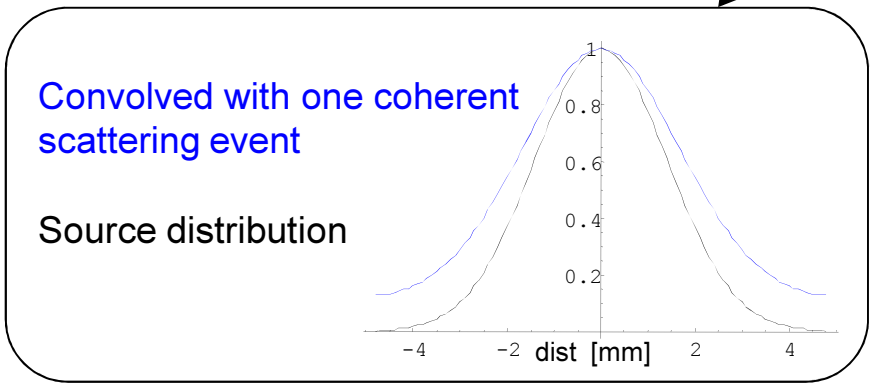

Four blurring steps:

1. **Electron beam distribution**
2. **Electron scattering in target**
3. **Brems X-section angular distribution**
4. **Coherent scatter in flattening filter (affecting the view of the source from downstream)**

Beam source size

reconstruction using beam-spot camera

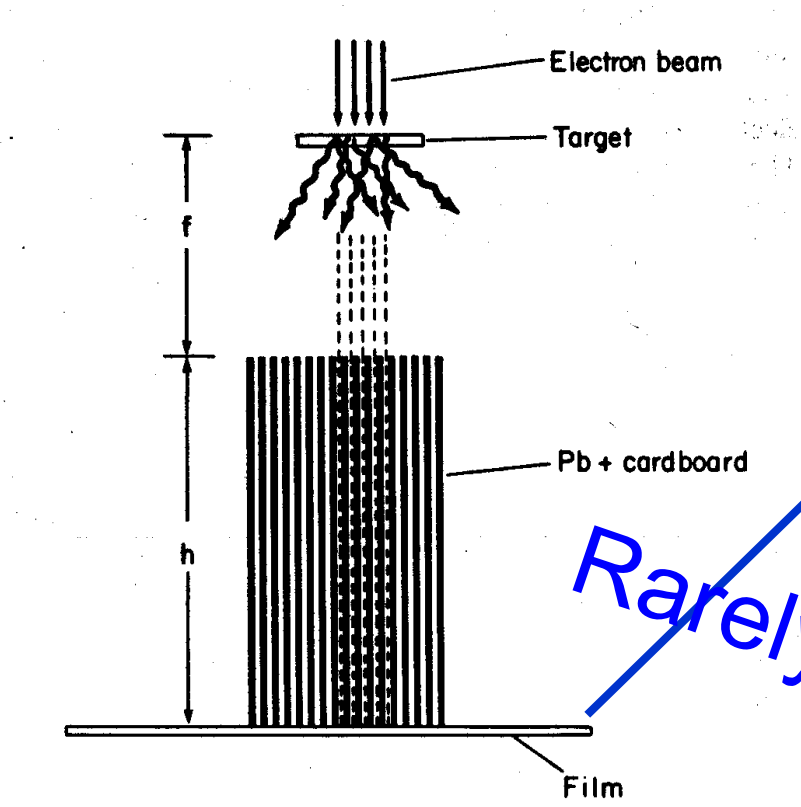

FIG. 1. Diagram illustrating the principle and function of the beam-spot camera.

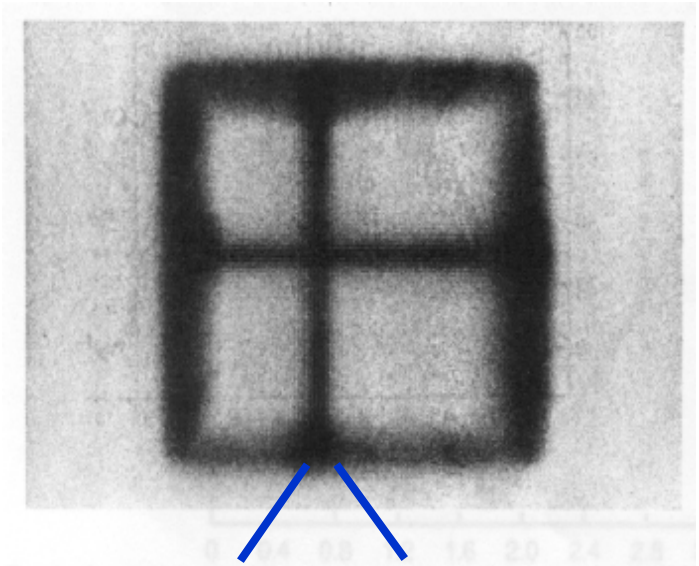

FIG. 2. Magnified image of the x-ray source of a linear accelerator producing 8-MV x rays. The camera was turned 90° between the two exposures. The actual distance between adjacent parallel dark lines is 0.47 mm.

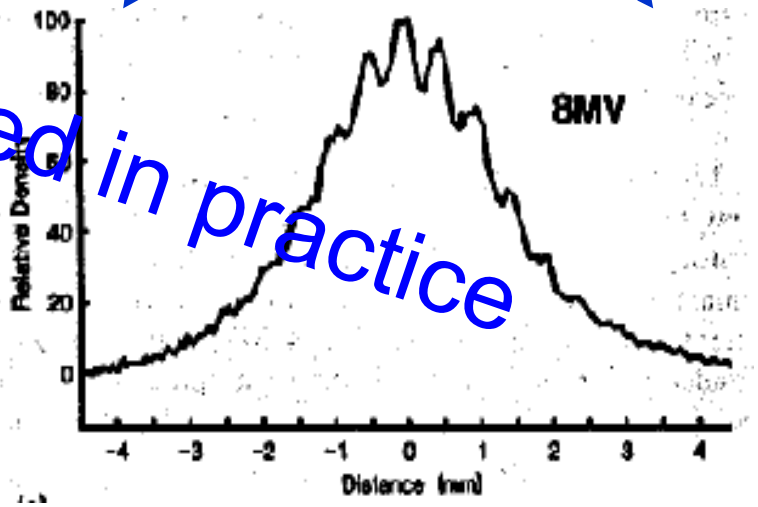

Rarely used in practice

from Lutz, Maleki & Bjärngard, Med.Phys. **15**, p 614-617

Beam source size

reconstruction from slit images

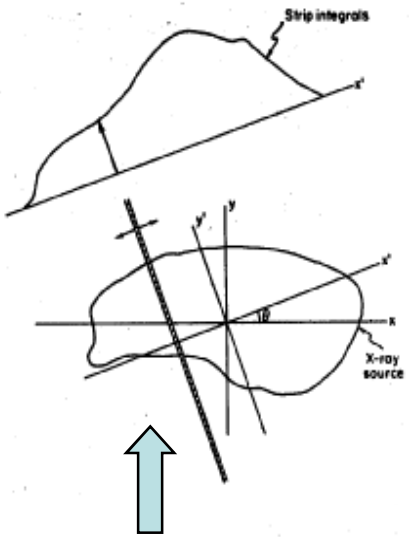

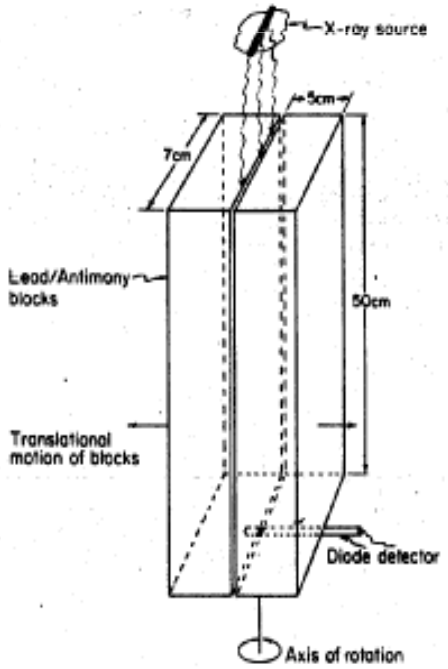

CT algorithms

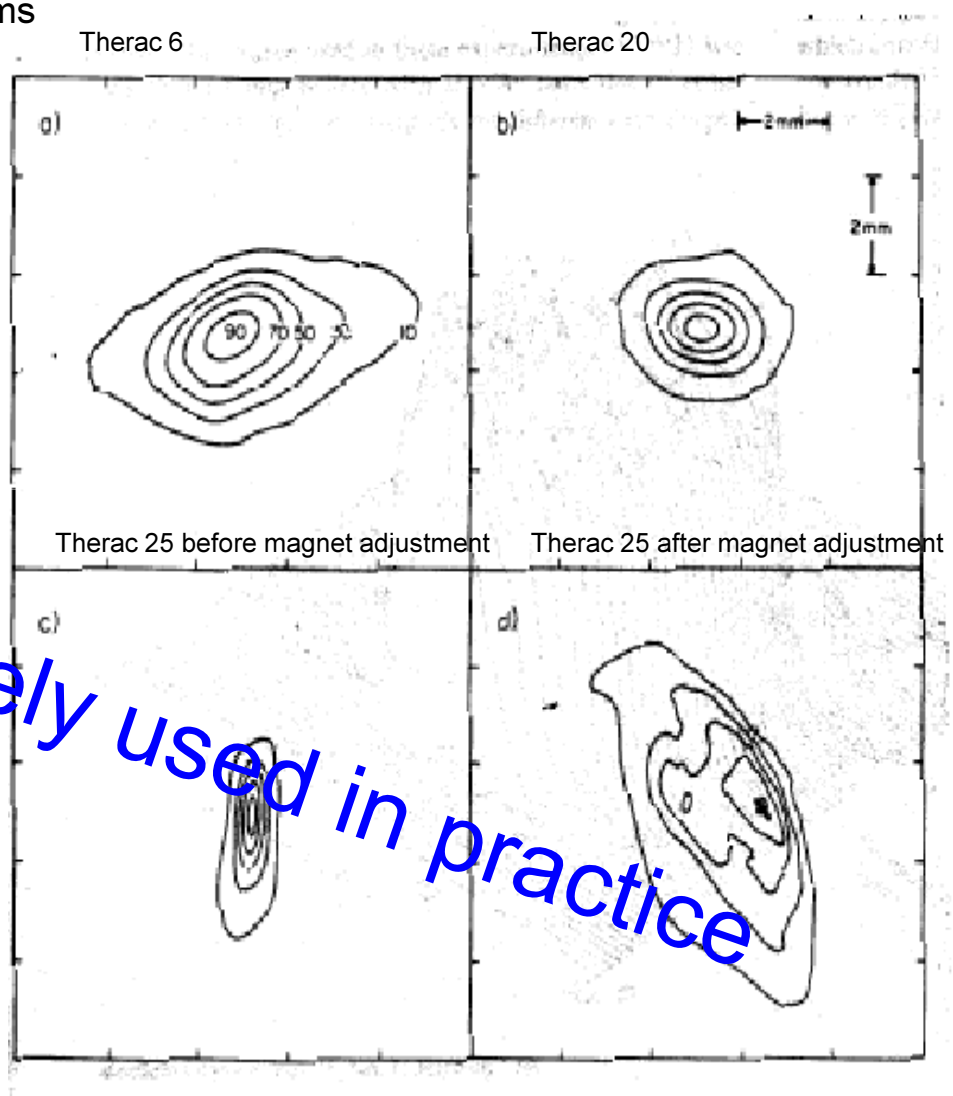

Rarely used in practice

from Munro & Rawlinson, Med. Phys. **15**,1988, p517-524

Beam source size

by fitting calculated profiles to measured profiles by varying the source size

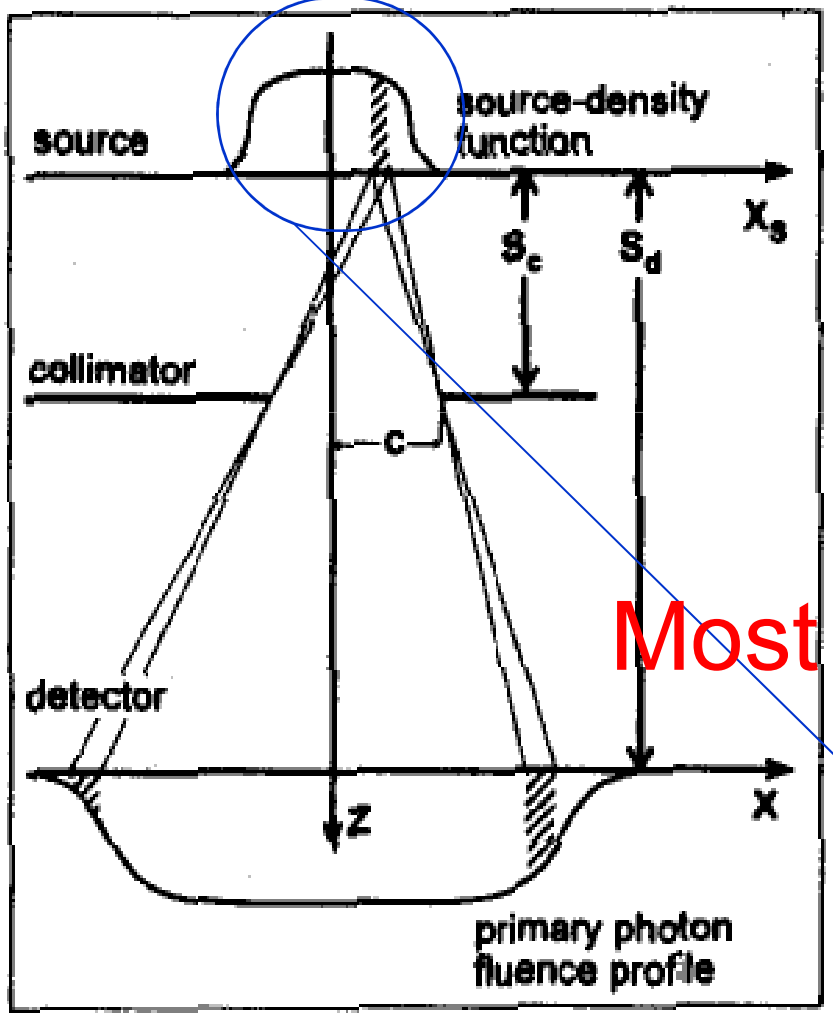

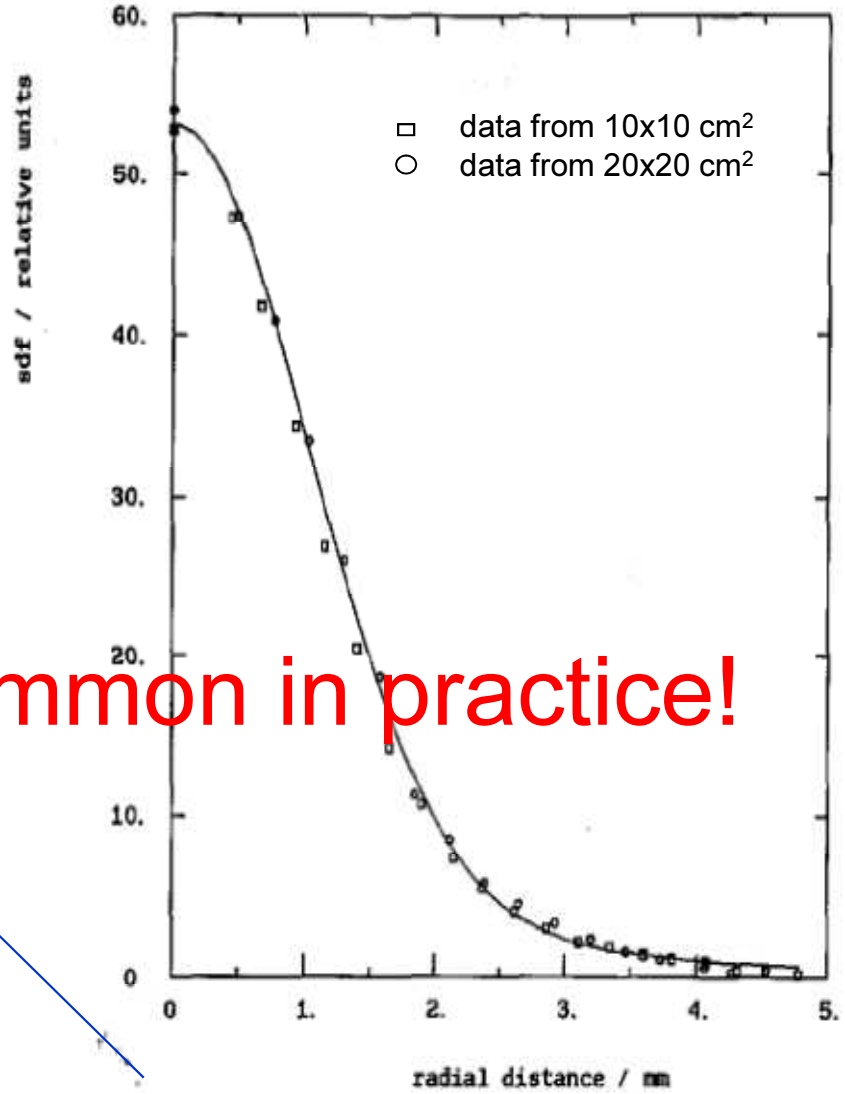

Most common in practice!

from Treuer *et al*, Mediz. Physik,1987, p375-80

Source size determination by fitting calculated dose profiles to measured profiles for 10x10 cm^2 fields.

Results from 59 clinical Siemens machines in Nucletrons customer database

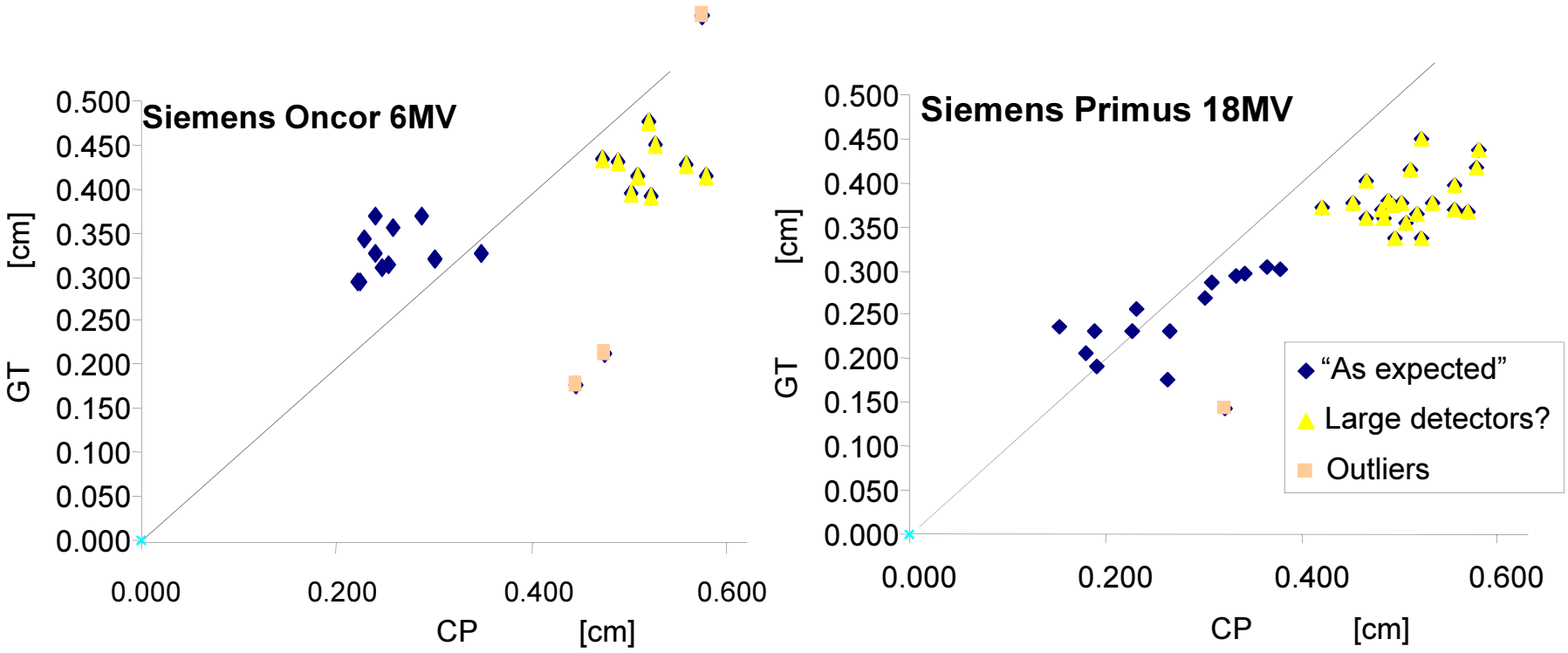

Source size effects, focused leafs

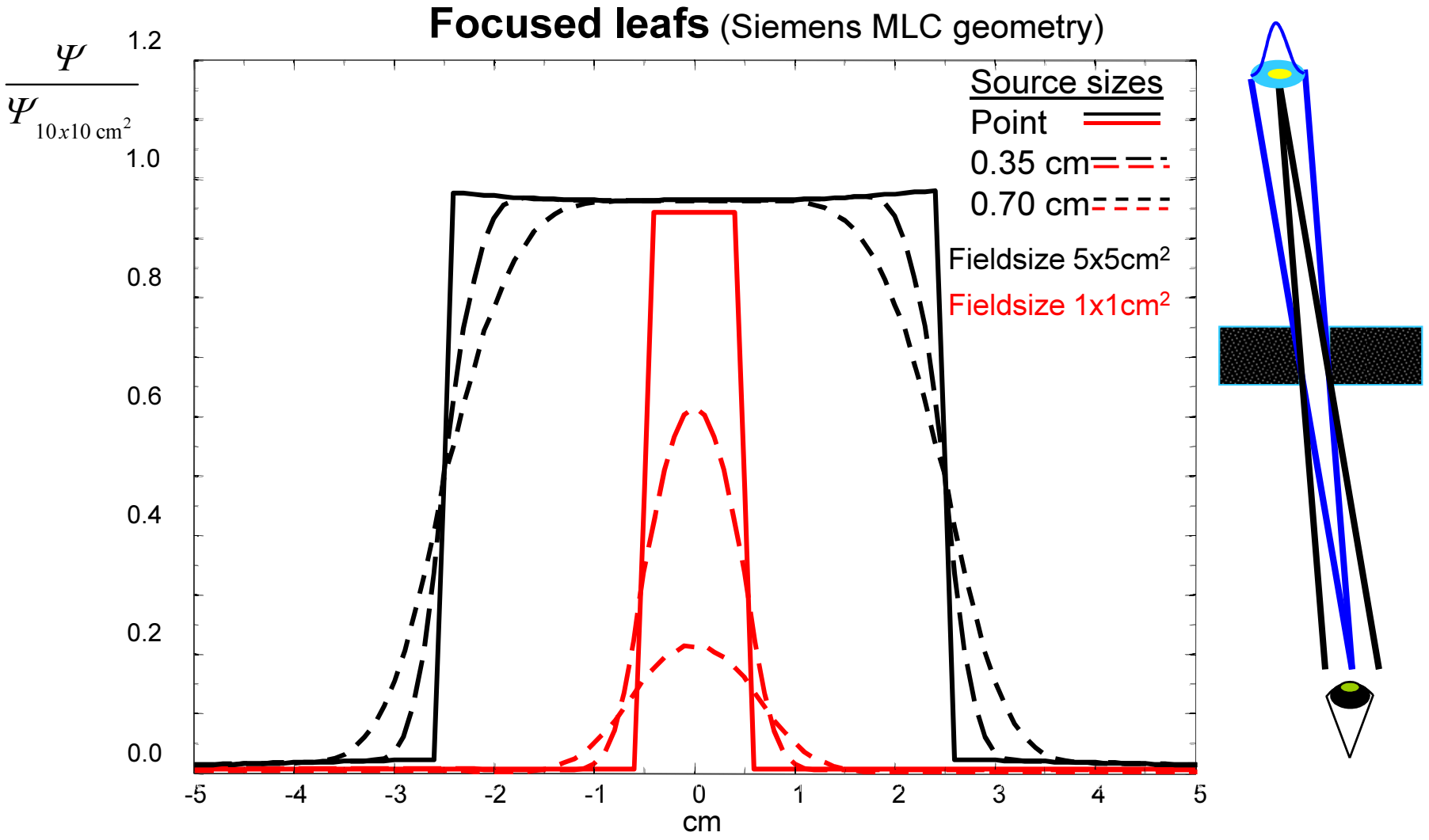

When the source "fills" the "inverse" view we get dramatic decrease in fluence output with increasing source size!

Upper and lower penumbra parts have different slopes

Focused leafs (Siemens MLC geometry)

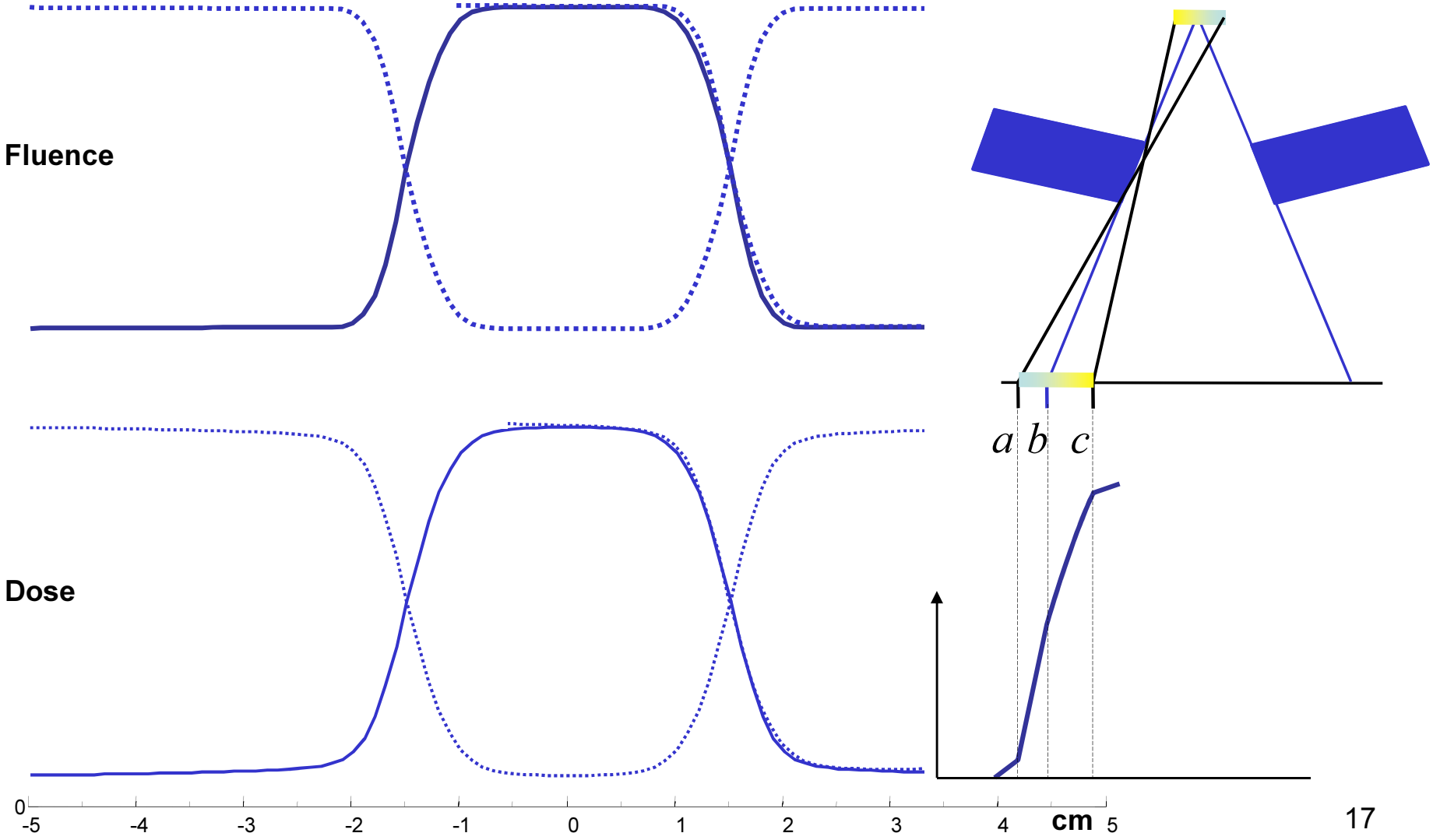

Alignement of multiple collimators – potential issue for delivery robustness & calculation consistency

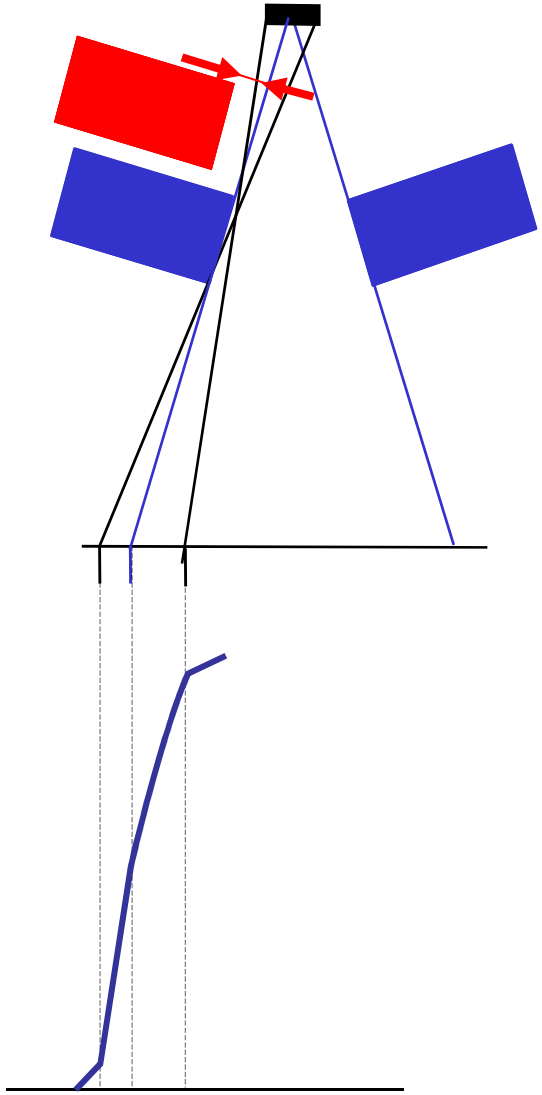

A margin for setting additional jaws make penumbra conditions more robust!

Direct beam source
- open beam fluence distribution

The joint effect of

- **angular variations of the direct beam source radiance**
- **flattening filter absorption/modulation**

commonly expressed as an open beam fluence matrix

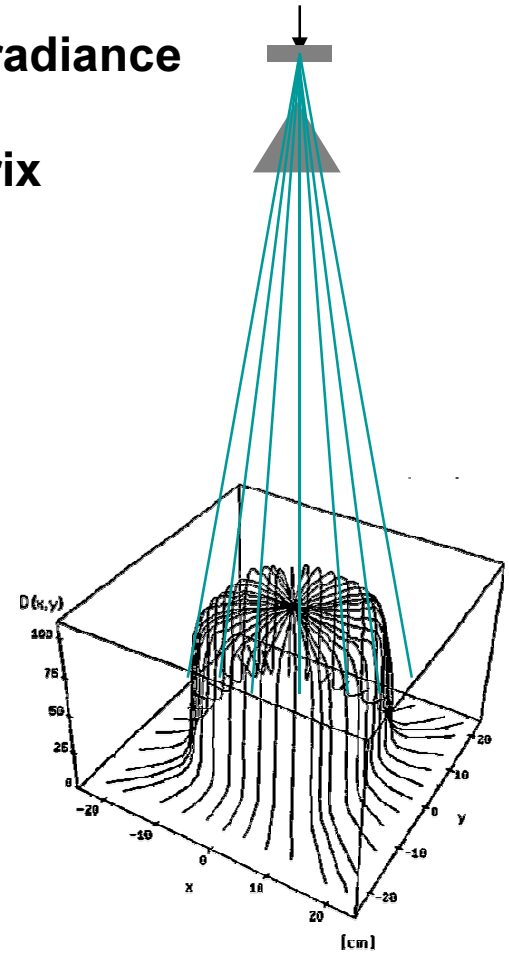

Can be acquired through a variaty of means:

- **diagonal water phantom dose profile**
- **”in air” scanning**
- **”star” dose measurements and subsequent deconvolution/fluence fitting**

In air scanning of lateral profiles

The signal scored by a scanned detector is directly proportional to the energy fluence only if the spectrum is constant!

Signal is proportional to $s_{\mathrm{m}}^{\mathrm{a}}(x,y)\cdot\frac{\mu_{\mathrm{en}}}{\rho}(x,y)\cdot\Psi(x,y)$

The energy absorption coefficient μ_{en} of the buildup material varies with lateral spectral shifts.

Since primary dose for CPE is very close to $(\mu_{\mathrm{en}}/\rho)\cdot\Psi$, scanning in air yield results that decribes how the primary dose will vary laterally!

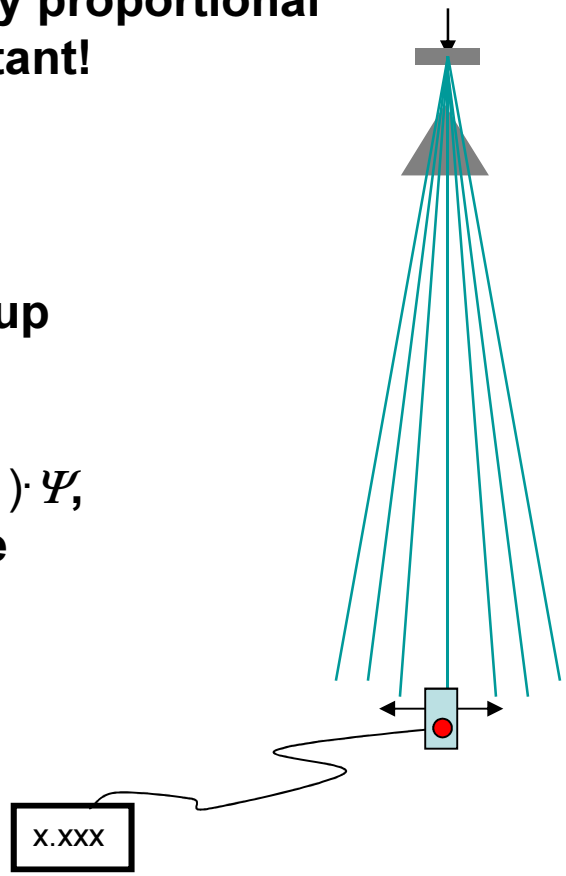

Star dose measurements – machine variability

58 of Varian Clinac 2100 6 MV

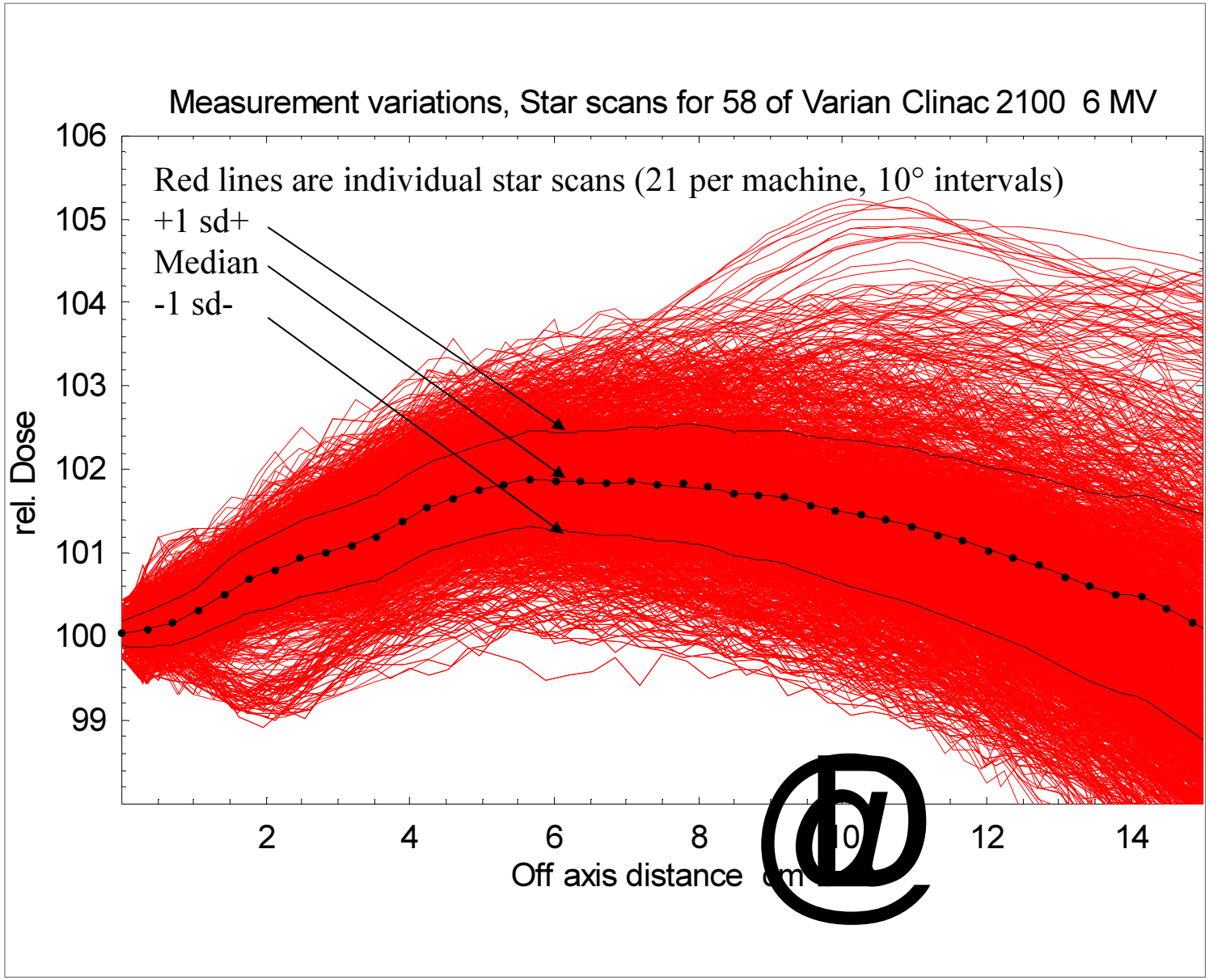

Star dose measurements – machine variability

12 Siemens Primus 10 MV

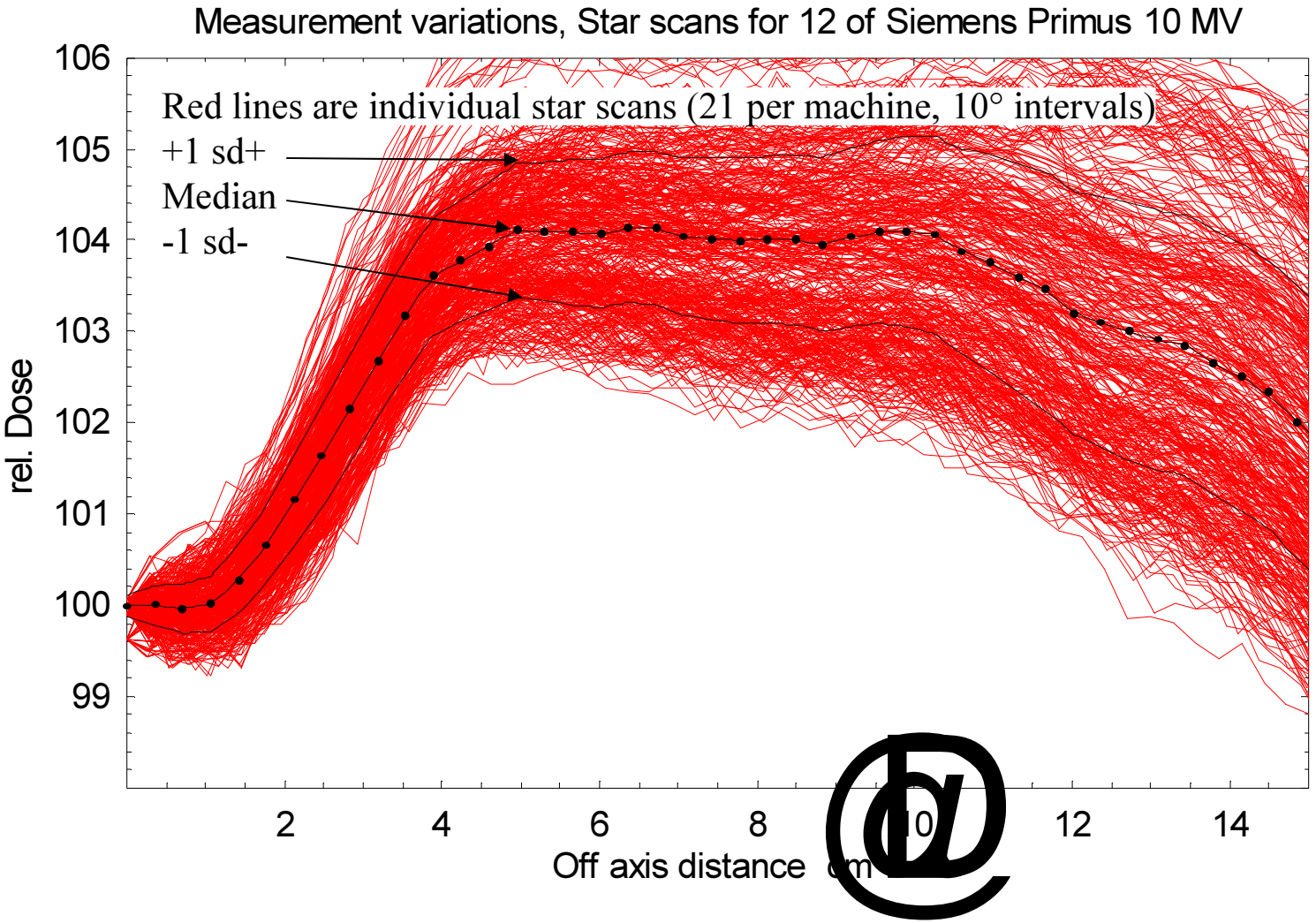

Beam energy spectra
- spectral filtering by the flattening filter

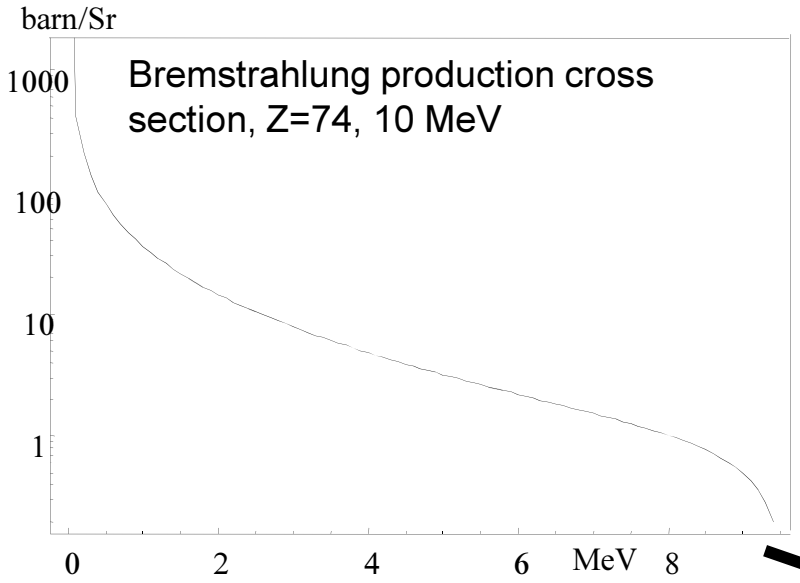

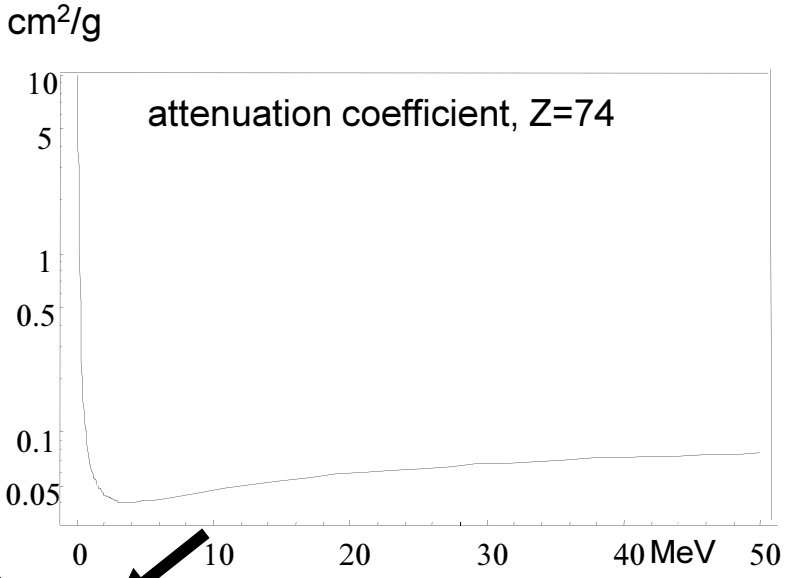

Direct beam spectrum, principal shape.
Spectrum distorted offaxis towards lower energies due to less filtration & decreasing energy with increasing brem angle

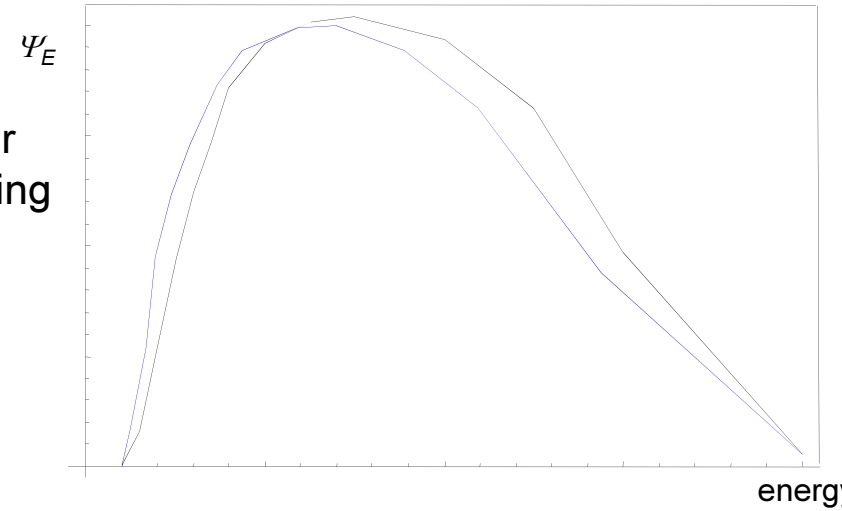

Beam energy spectra
- methods to determine spectra for clinical beams

require trimming of the resulting spectrum so that measured dose matches calculated dose

Measurements
- Low beam current and/or Compton scatter methods
- Not practical for clinical use

Monte Carlo methods
- Mohan et al MedPhys 12 p 592 1985 widely used for testing
- BEAM (EGS4/nrc) standard tool
- Other codes also used, PENELOPE, GEANT, etc.
- Still not practical for routine use
- MC data to be standard part of linac purchase procedure?

Analytical modelling from cross sections
- Target designs requires use of 'thick target theory', i.e. must model the electron transport prior to bremsstrahlung interactions

Unfolding from transmission through attenuators
- Based on 'in air' measurements
- Requires good control of attenuator purity
- Most methods use some support of spectral shape constrains

Unfolding from depth dose distributions in water
- **Requires access to monoenergetic depth dose data (Monte Carlo)**
- **Unfolding methods needs spectral shape constrains**

Beam energy spectra
Measurements – Compton spectroscopy

Reduce the fluence to a countable level by Compton scattering. Spectrum derived by correcting for energy loss during scattering. Setup complexity makes it unpractical for clinical use.

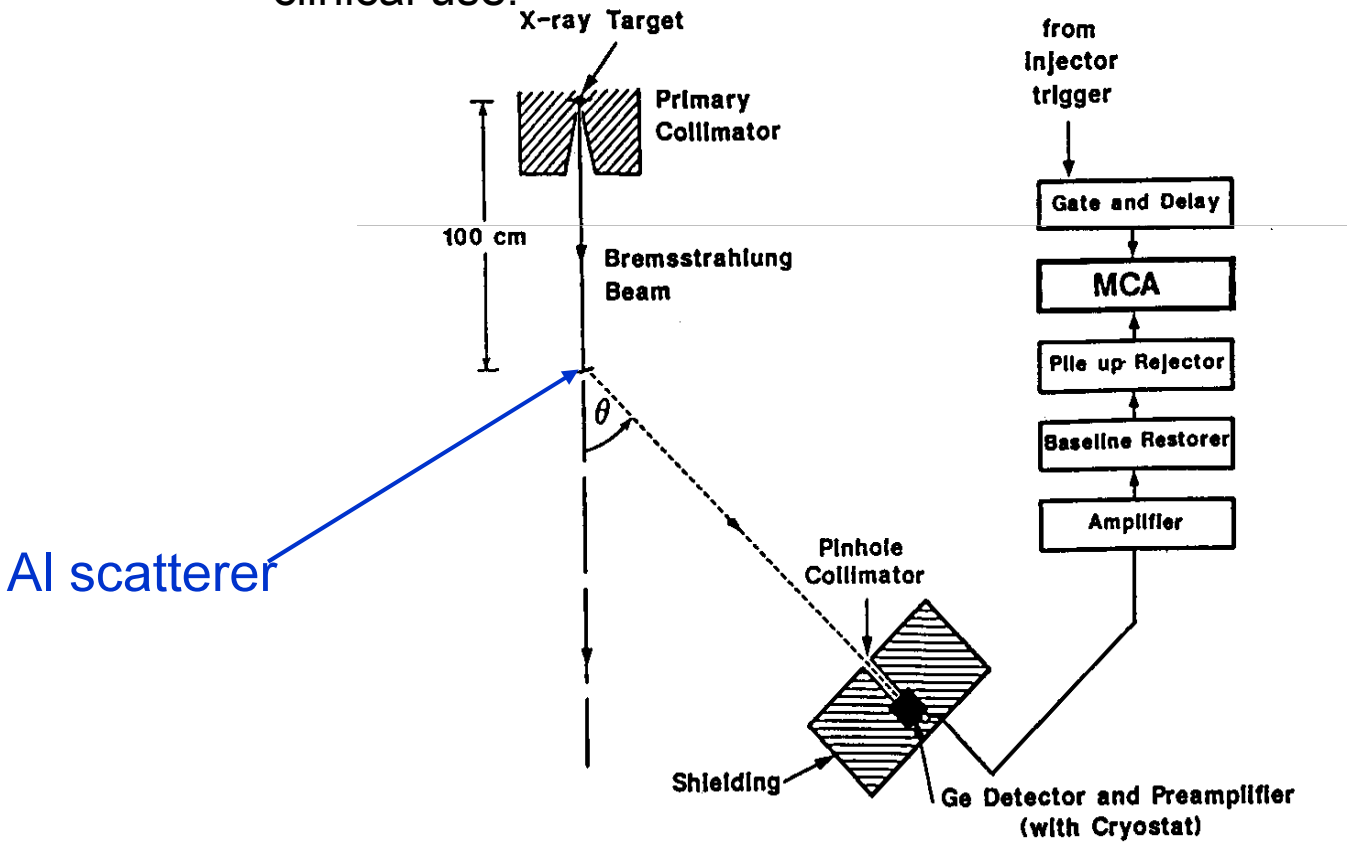

from Landry and Anderson, MedPhys 18, 1991, p 527

Beam energy spectra analytical modeling

Numerical integration of X-sections and attenuation data, results similar to Monte Carlo

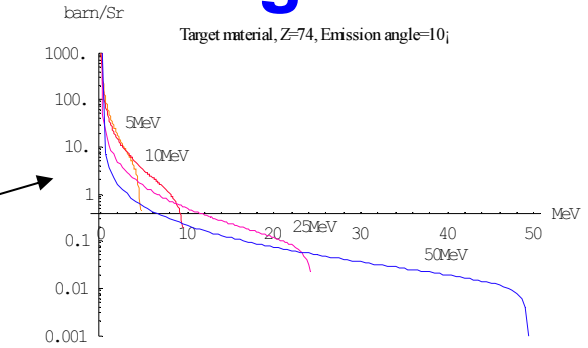

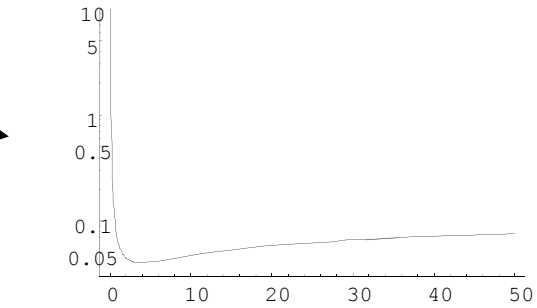

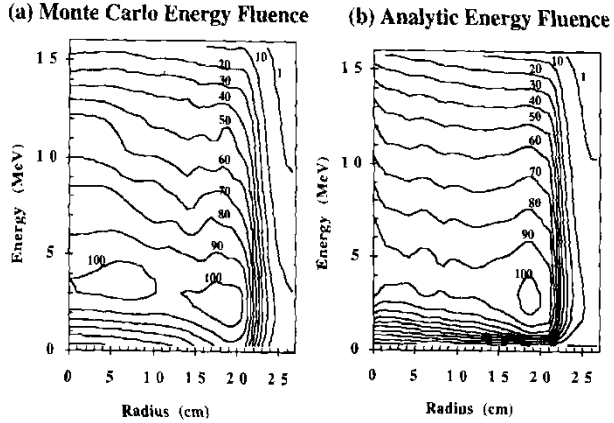

Simple models, parametric control of spectral shape $\Psi_E = \Psi_E(p_1, p_2, p_3)$

from Desobry & Boyer, MedPhys 21, 1994, p 1943

Beam energy spectra
Unfolding measured transmission data

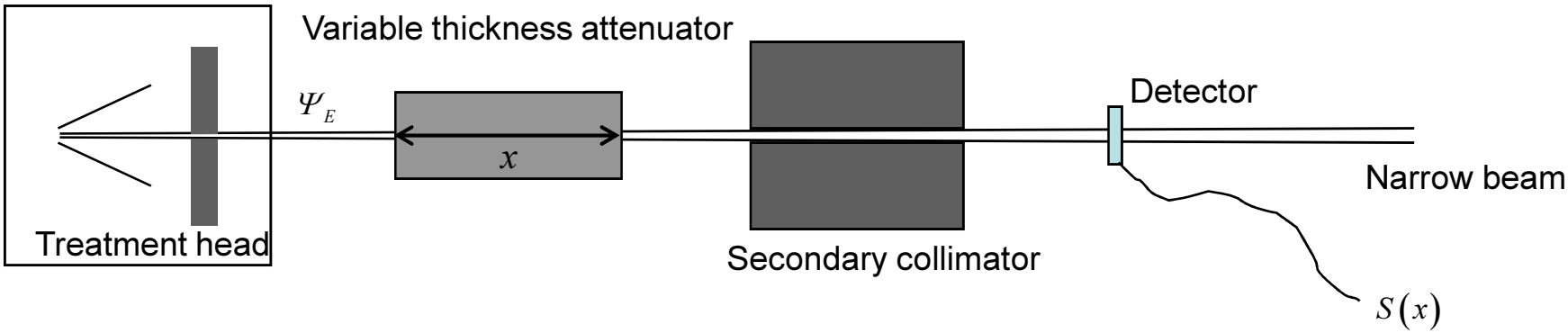

General:

$$\frac{S(x)}{S(0)} = \frac{\int_0^{E_{\max}} R(E)\Psi_E \, e^{-\mu(E)\cdot x} \, dE}{\int_0^{E_{\max}} R(E)\Psi_E dE}$$

$R(E)$ Detector response

Ψ_E Energy fluence spectrum

Simple approach:
(neglects energy response variations)

$$S(x_j) = \sum_i \Psi_{E_i} \, e^{-\mu(E_i)\cdot x_j} \, \Delta E_i \quad \Leftrightarrow \quad \underbrace{S_j = \sum_i \Psi_i A_{i,j}}_{\text{to be solved by numerical methods (linear algebra)}}$$

Beam energy spectra

Constrained unfolding of spectra from depth dose measured in water

Recipe:

Minimize the difference between measured depth dose and spectral weighted monoenergetic Monte Carlo calculated depth dose. Explicitly consider electron contamination depth dose in the buildup region (or exclude the buildup zone from depth doses!):

$$\delta\left(s_1, s_2 \ldots, e_1, e_2 \ldots\right) = \sum_{\text{fsize}} \sum_{\text{depth}} \left| c_{\text{fsize}} D_{\text{depth, fsize}} - \left(\left(\sum_{\text{ebin}} \Psi_{\text{ebin}}\left(s_1, s_2 \ldots\right) \cdot d_{\text{depth, fsize, ebin}} \right) + d_{\text{depth}}^{\text{electron cont}}\left(e_1, e_2 \ldots\right) \right) \right|$$

Measured depth dose, phantom scatter normalized

MC calc depth doses for monoenergetic photons

Error norm to minimize by varying parameters

Spectrum model, constrained to a "physical" shape

Electron contamination model

Ahnesjö & Andreo, 1989 PMB 34, p 1451-64

Beam energy spectra
- results from constrained unfolding

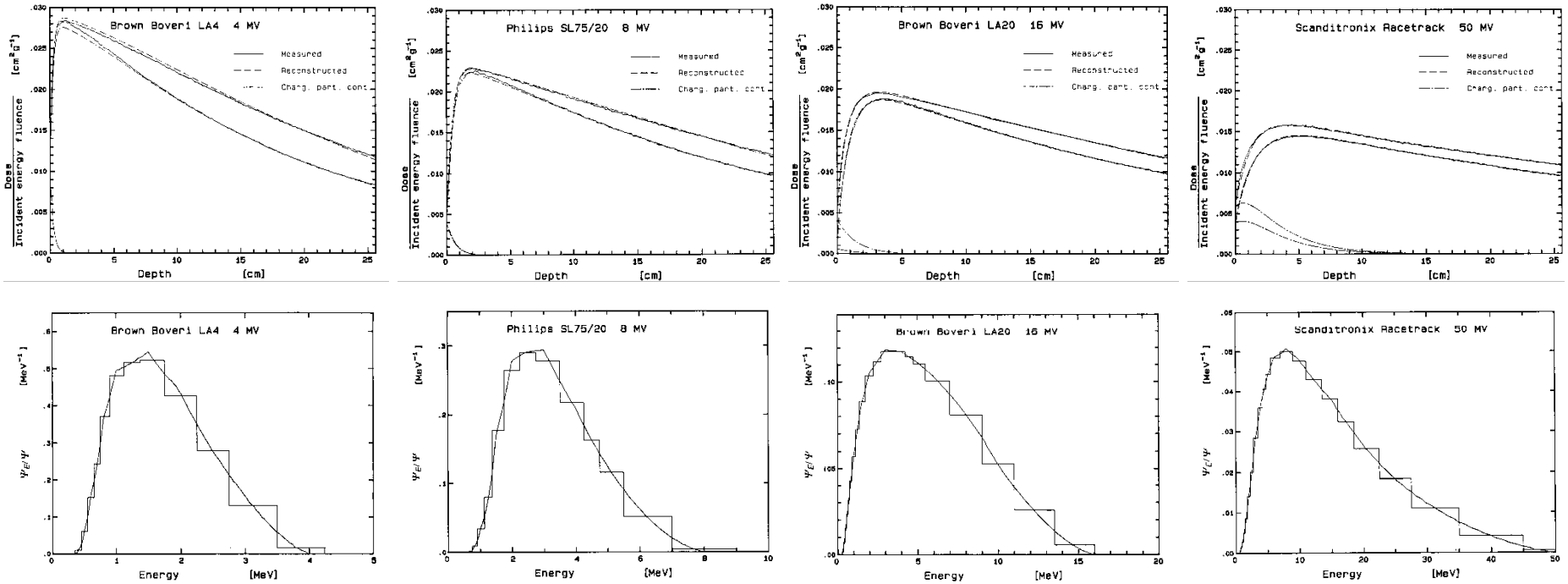

Ahnesjö & Andreo, 1989 PMB 34, p 1451-64

Spectral changes from off axis filtration

Lateral variation of the spectrum, such as off axis softening can be modelled by varying coefficients of attenuation and energy release.

Off axis HVL values can therefore be modelled without explicit knowledge of the spectrum change causing it!

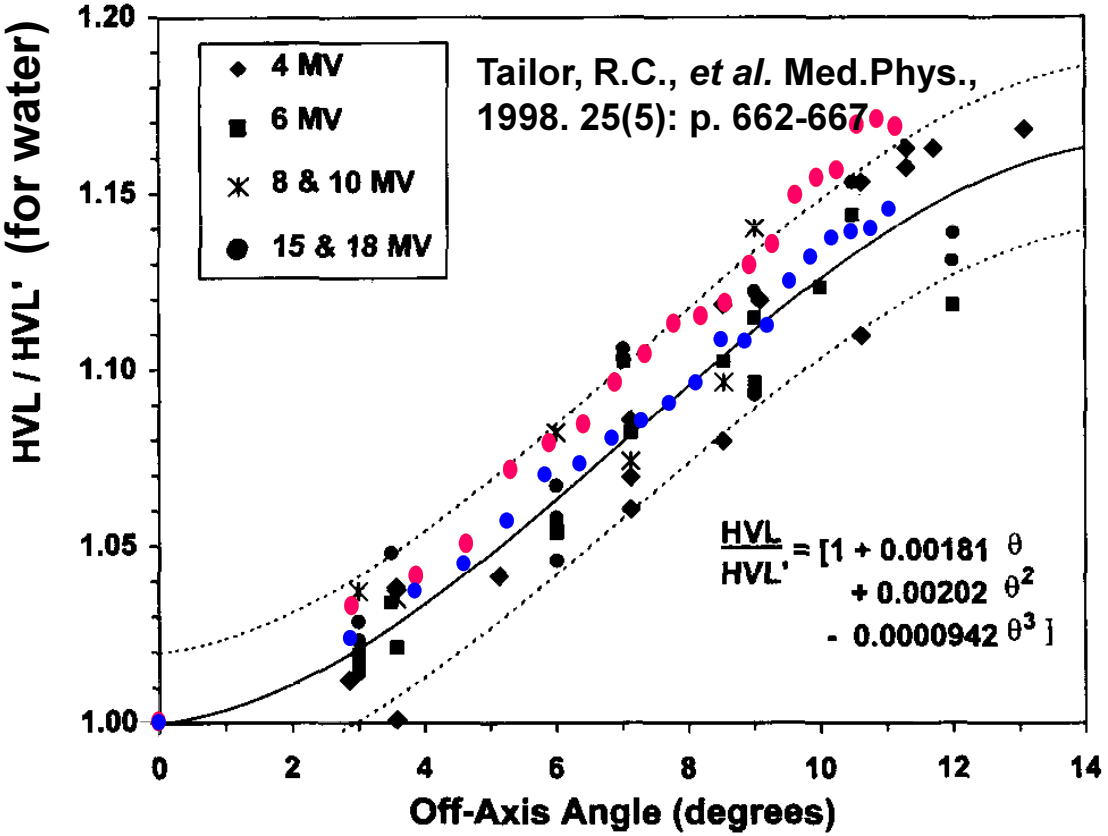

$$\mu(\text{direct beam}) \approx \frac{\ln 2}{\text{HVL}}$$

Monte Carlo data
Sheikh-Bagheri priv. com.

BEAM (EGS4) Elekta SL 25, 25 MV

BEAM (EGS4) Elekta SL 25, 6 MV

Depth dose – machine variability

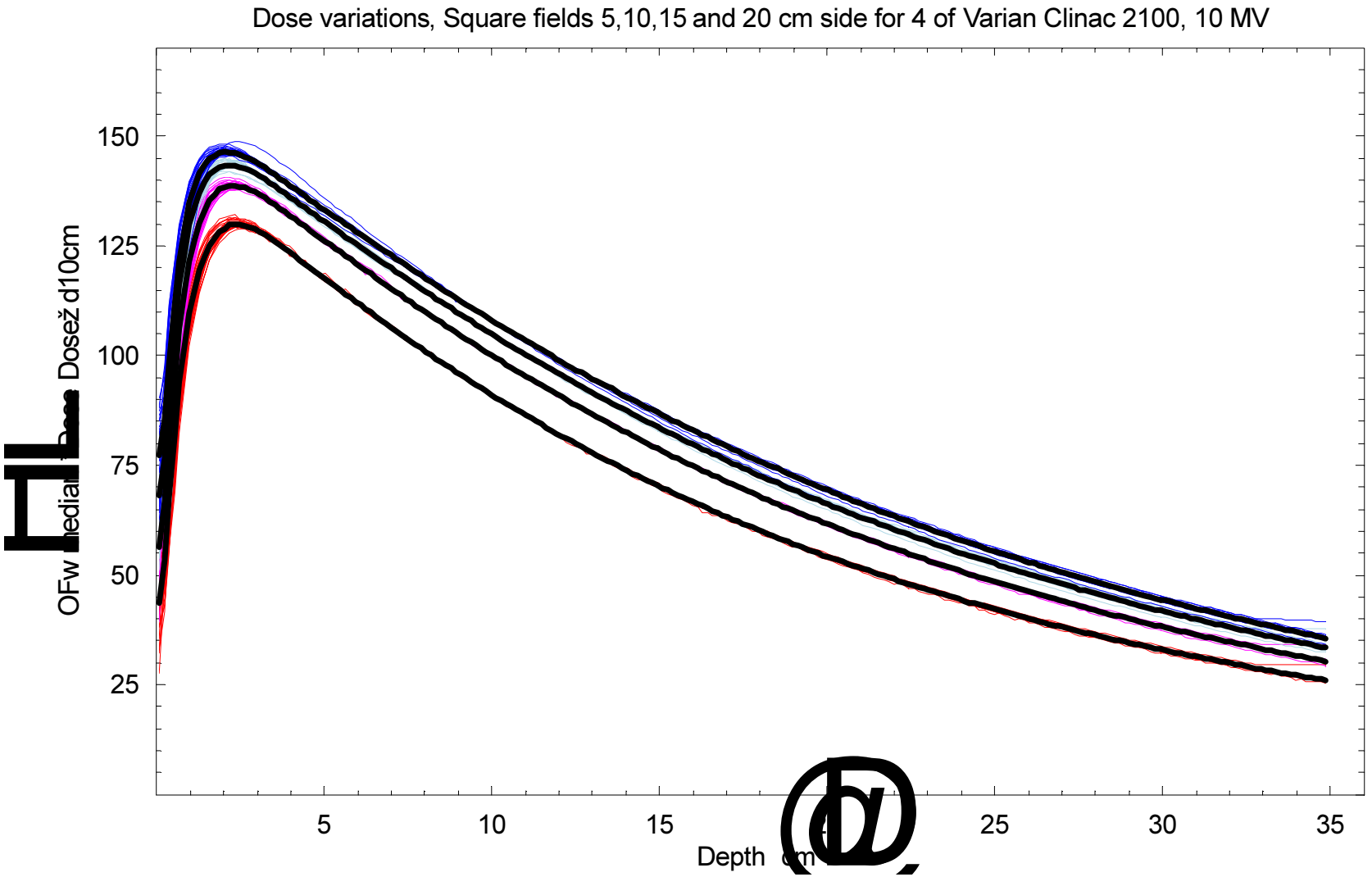

Electron contamination

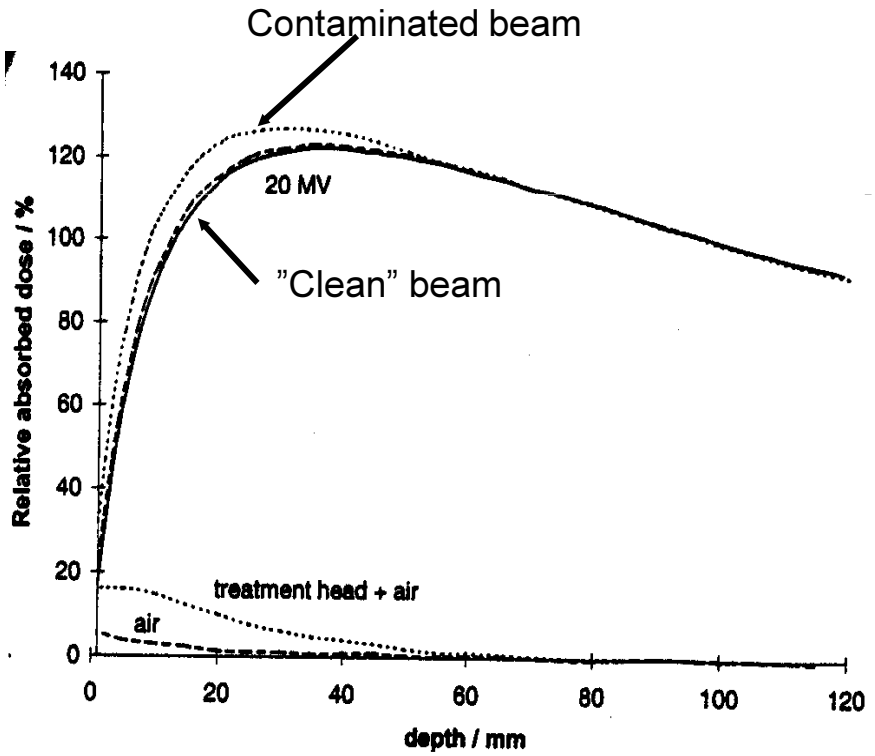

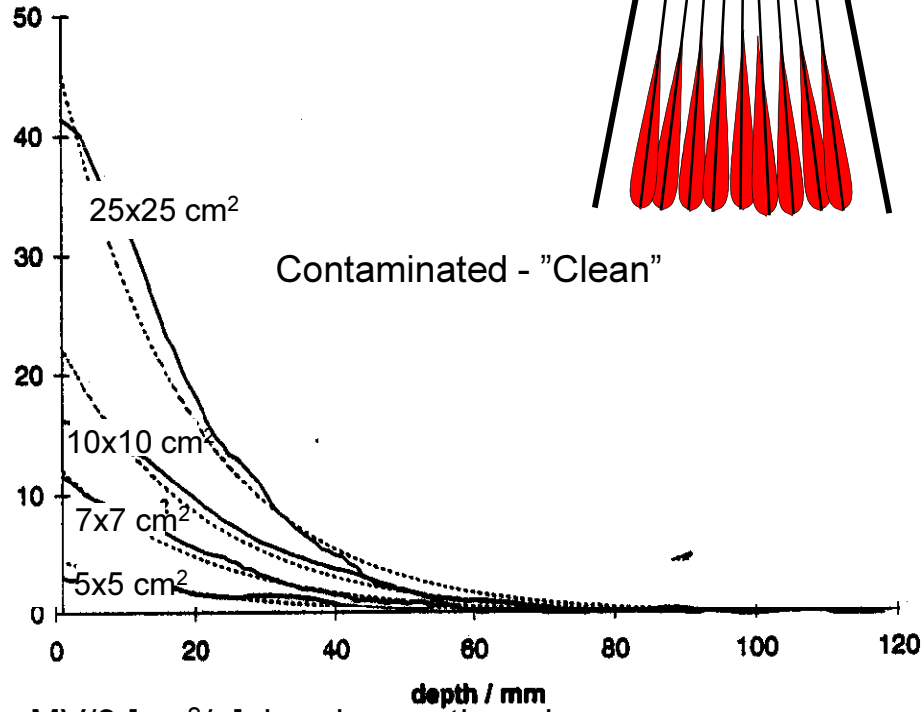

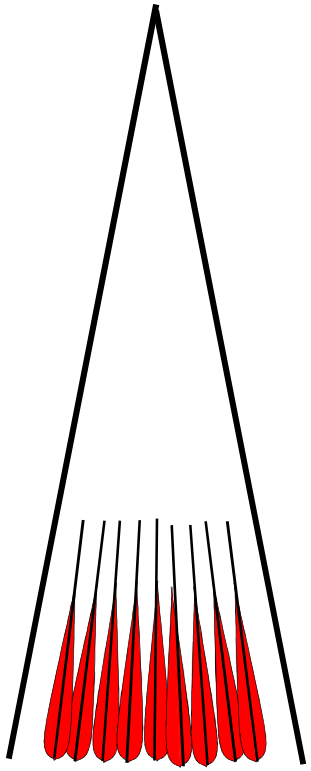

Contaminated - "Clean"

Maximum penetration depth appr. MV/3 [cm^2/g], i.e. deeper than d_{max}....

Field size most important factor for magnitude, no impact on penetration depth.

Sjögren & Karlsson, Med. Phys. **23** 1996 p 1873-1881

Electron contamination, cont…

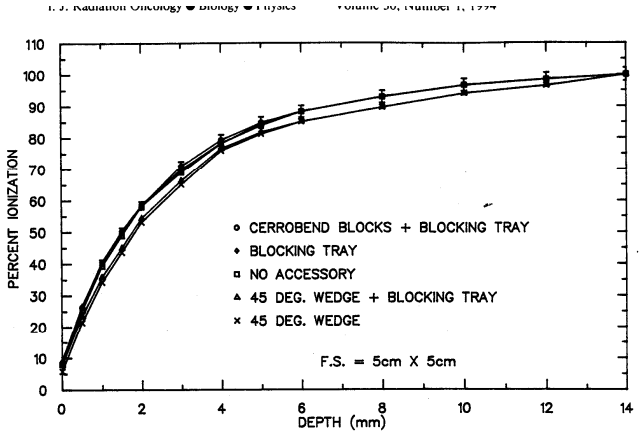

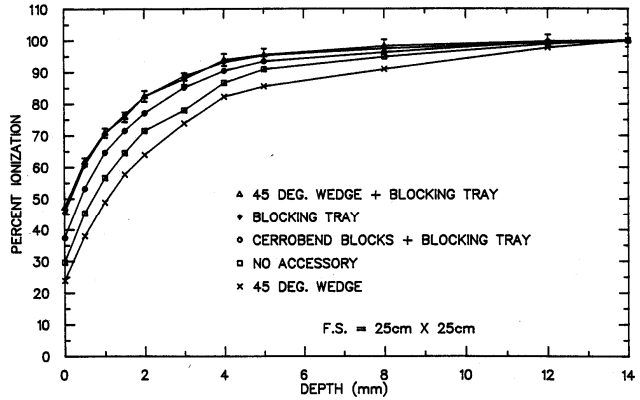

Fig. 2. Comparison of accessory effects on build-up for 6 MV photons; field sizes: 5 × 5 cm and 25 × 25 cm.

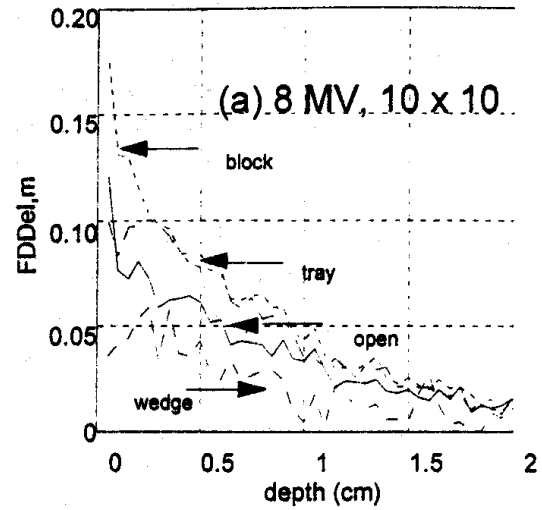

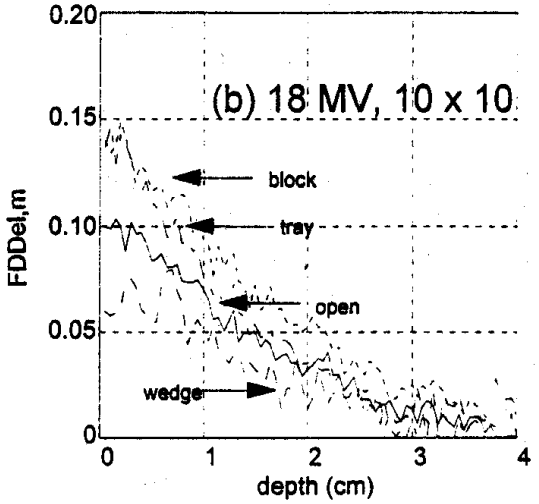

Everything in the beam path has an impact, still field size is most important single factor!

Fontenla *et al* IJROBP. 1994 **30** p 211-219

Zhu & Palta, 1998 Med. Phys. **25** p 12-19

Flattening filter scatter the major extrafocal contribution *Monte Carlo proof:*

Mevatron & EGS4

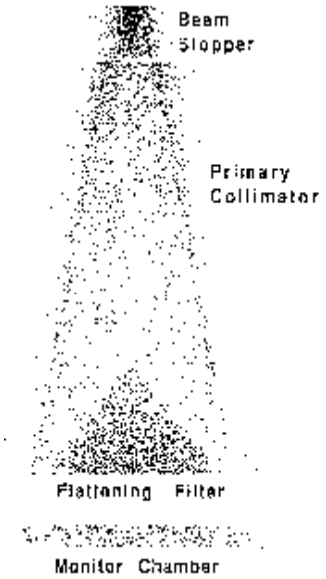

Distribution of origin site. Note clouds at beam stopper, primary collimator and flattening filter

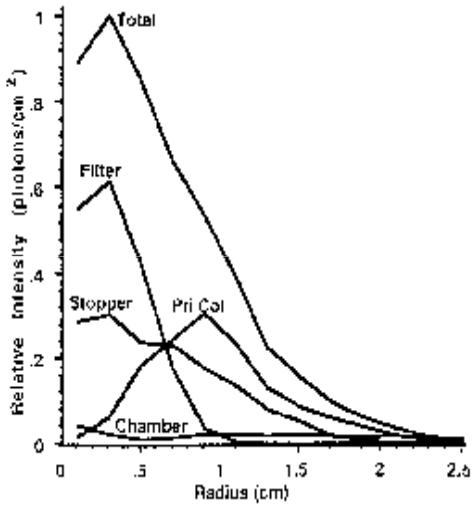

Lateral distribution of origin sites, projected to a common distance from the target.

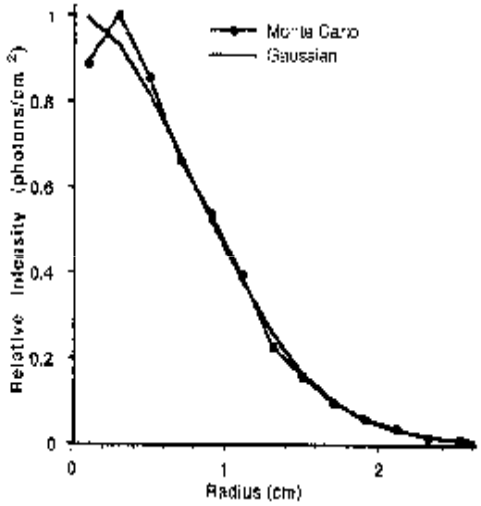

All scatter sources merged to an effective source distribution.

Chaney E L *et al* 1994 A Monte Carlo study of accelerator head scatter *Med. Phys.* **21** 1383-9

Flattening filter scatter, semi-analytical approach

$$\frac{\Psi_f}{\Psi_0} = \iint_{\substack{\text{area as viewed backward through the aperture}}} \underbrace{k_\sigma(\phi)\,k_C(\phi)}\,\frac{(c_0 - c_1\theta)}{\underbrace{(z_{calc} - z_{filt})^2}}\,\mathrm{d}A$$

Assumptions (Med. Phys. 21 p 1227-1235):

- Predominantly first order scatter
- Triangular source distribution over the *visible* filter area
  - Fit parameters c_0 and c_1 from measured output factors.
- Correction factors for:
  - Energy loss in Compton scattering.
  - Klein-Nishina cross section angular variation.
- Modulate the resultant fluence if modulators are present

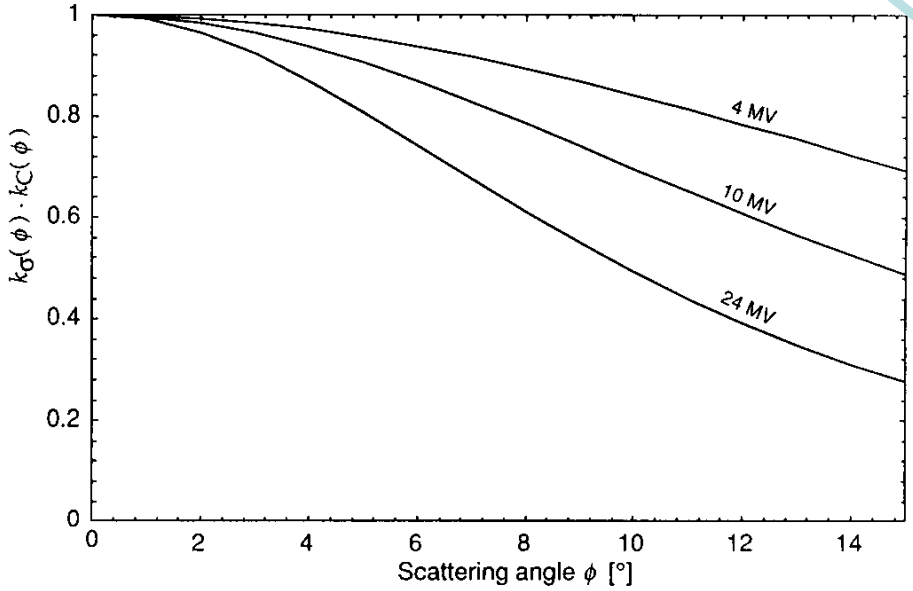

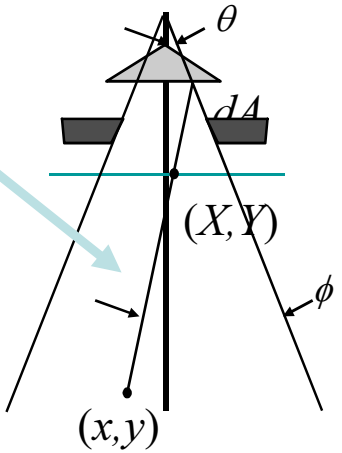

$$\eta = \prod_i \eta_i(X_i, Y_i)$$

Head scatter fluence calculation
- integration over extended sources

Main steps in the OOPS (Object Oriented Pixel Shadowing) back projection algorithm for head scatter geometry integrations:

I. **Cover scattering surface by a pixel matrix.**
II. **Set all pixels as scattering.**
III. **Illuminate the matrix by a light source place in the calculation point.**
IV. **Construct the shadow cast on the matrix from each collimating element (collimator, MLC, block,…).**
V. **Combine all shadows (reset shadowed pixels).**

Only visible pixels remains set !

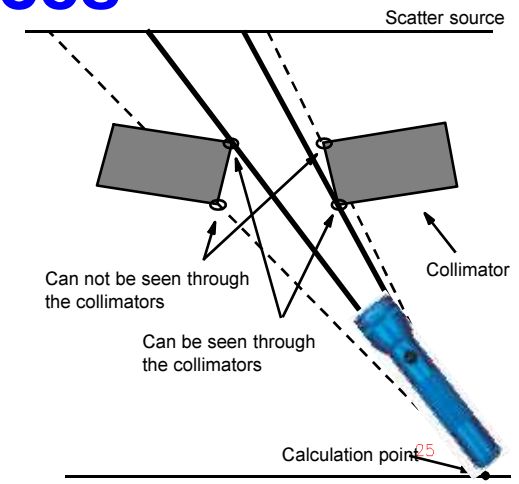

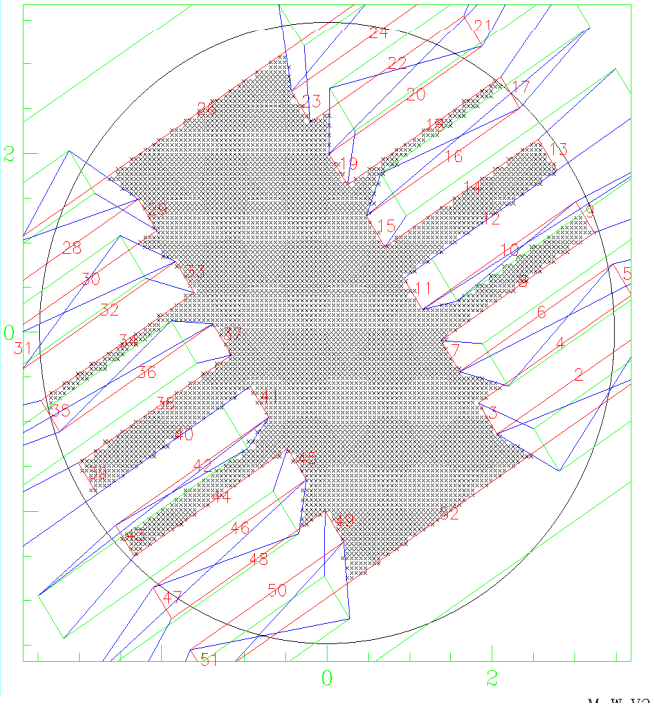

Flattening filter scatter cause variation of S_c - used for source data acquisition!

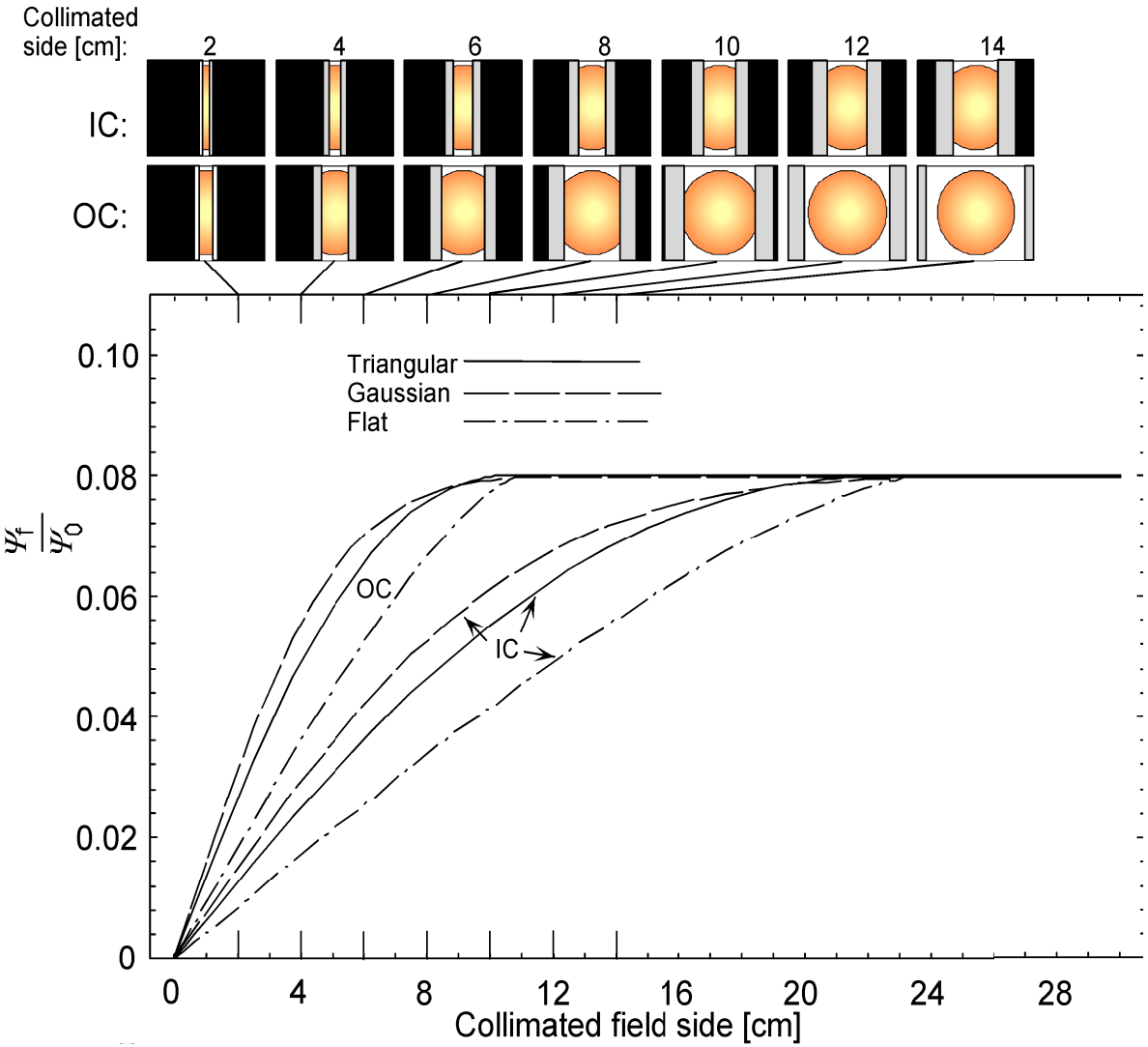

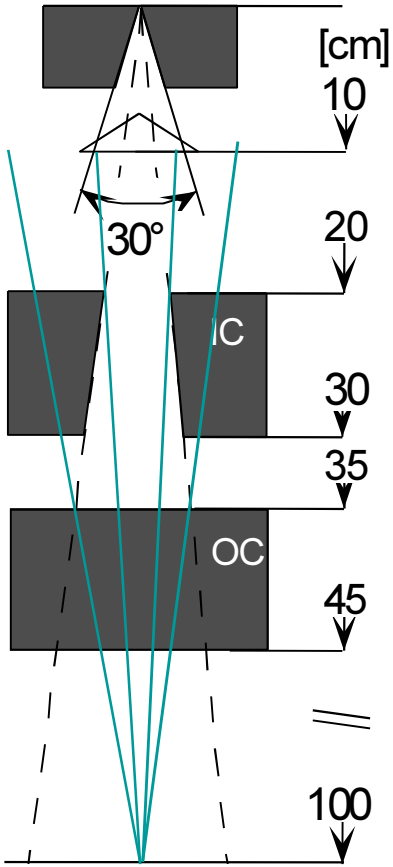

Ahnesjö 1994 Med. Phys. **21** 1227-35

Flattening filter scatter varies laterally !

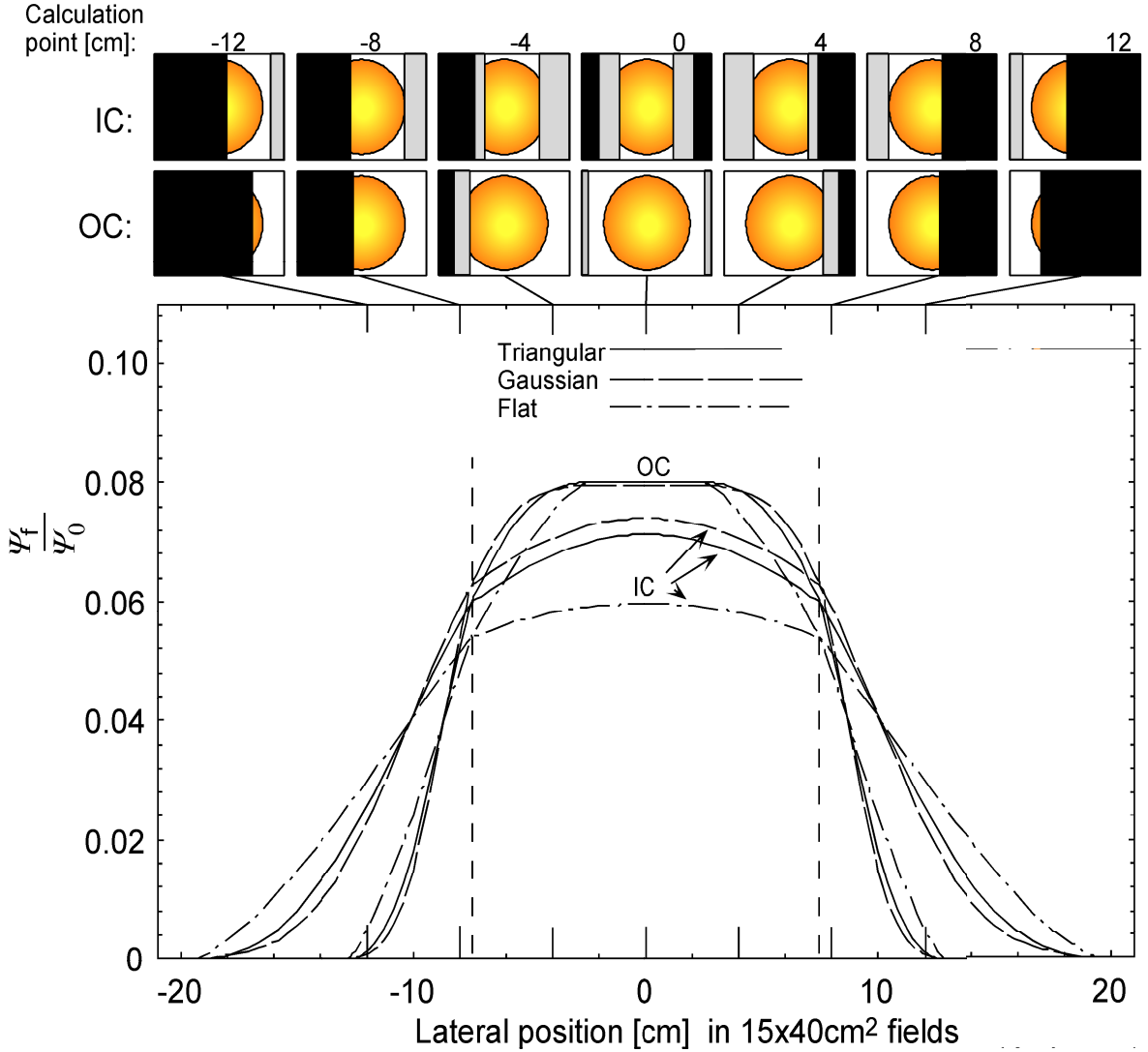

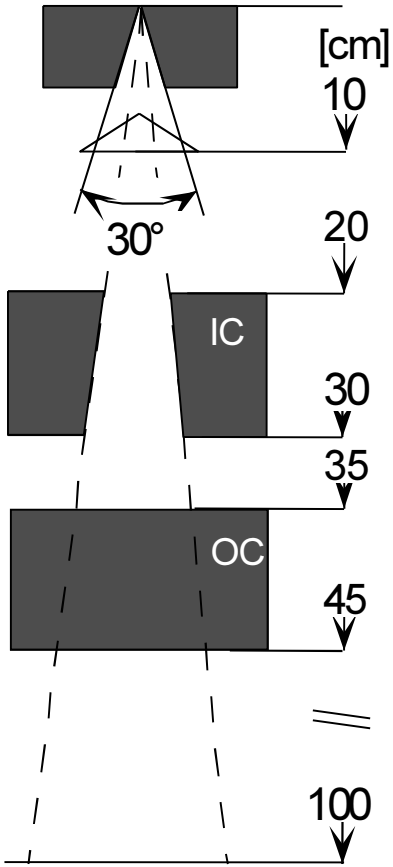

Ahnesjö 1994 Med. Phys. **21** 1227-35

Head scatter machine (man?) variability

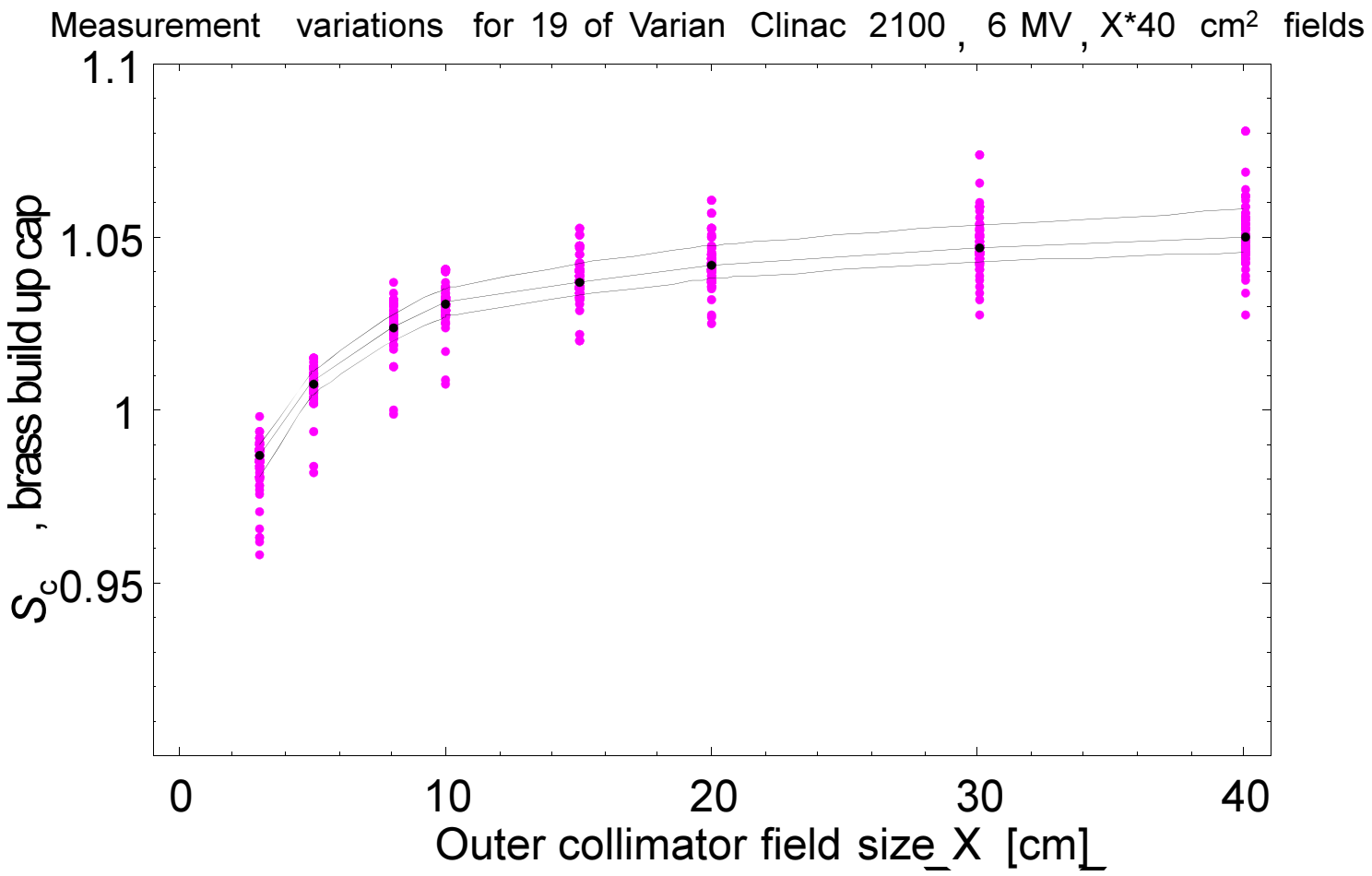

Collimator scatter

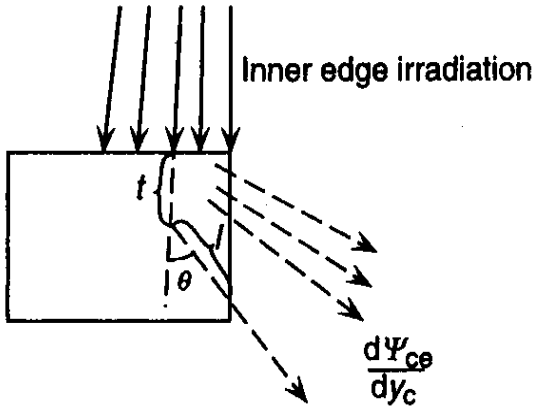

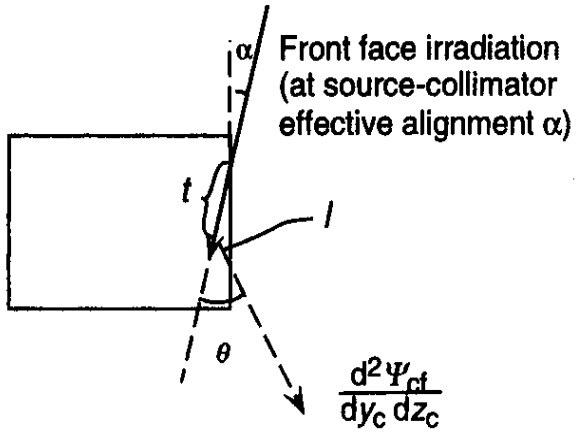

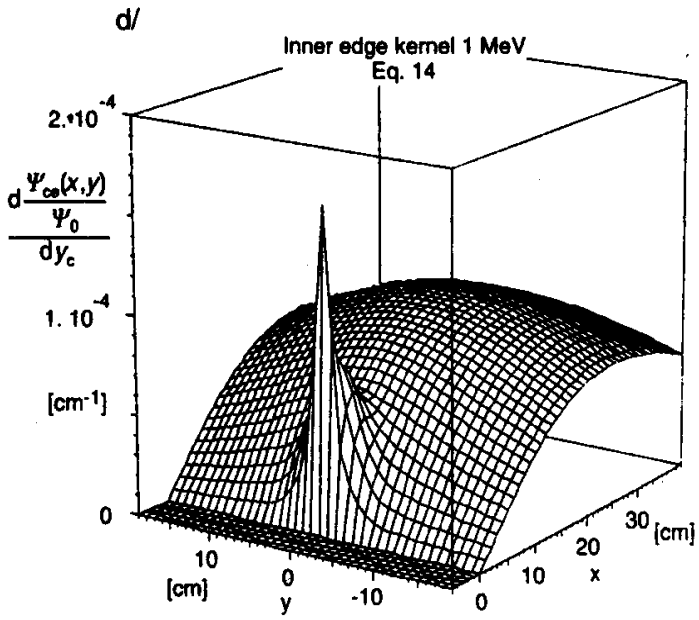

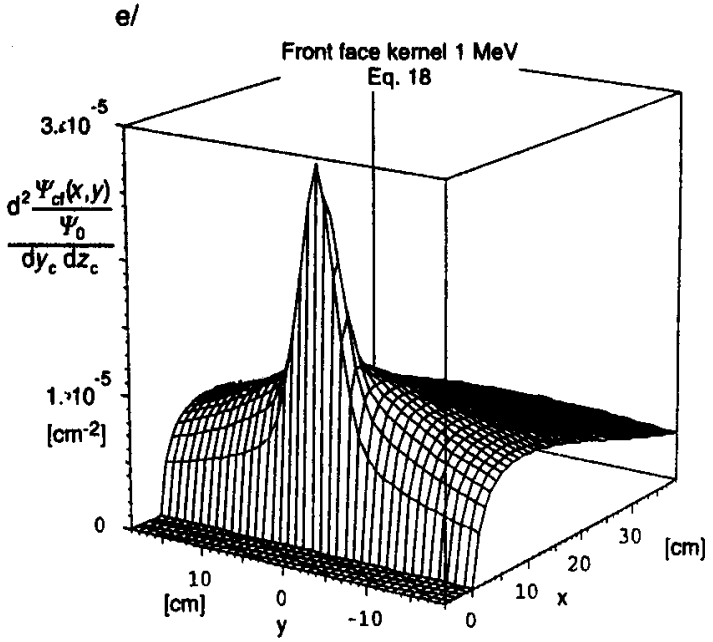

Ahnesjö, Med. Phys. **22** p 267-278

Collimator scatter, cont…

- minor influence

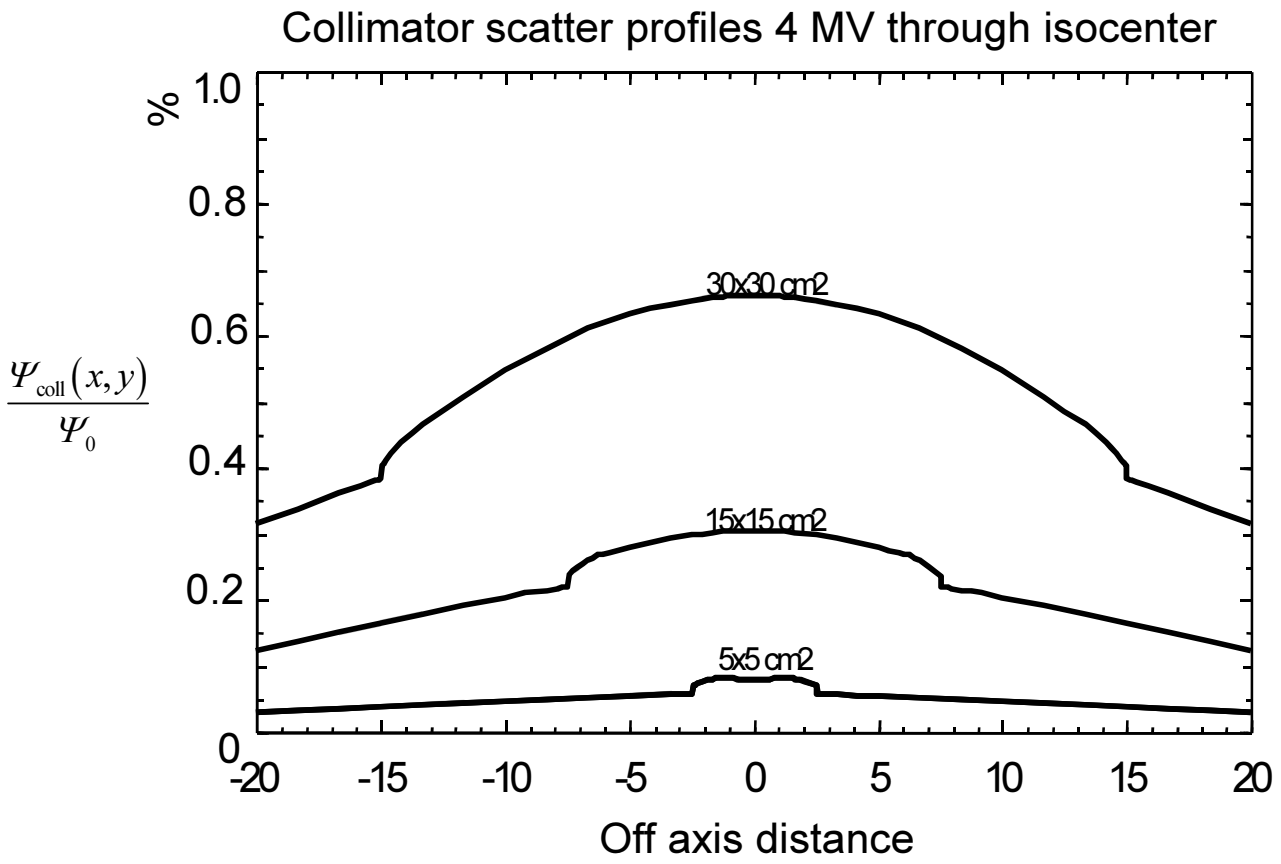

Ahnesjö, Med. Phys. **22** p 267-278

Monitor back scatter

$$\frac{\Psi_0}{M} = \frac{\Psi_0}{M_0 + M_b(A)} = \frac{\Psi_0}{M_0}\left[\frac{1}{1+b(A)}\right]$$

- Usually a very small effect
- Dominated by low energy charged particles, can be stopped by a protection sheet.
- Can be modelled by a monitor's-eye-view of the collimators:
  - Distance source to monitor and collimator.
  - Shape of visible collimator surface.
  - Empirical constant, 0.3 to 0.4.

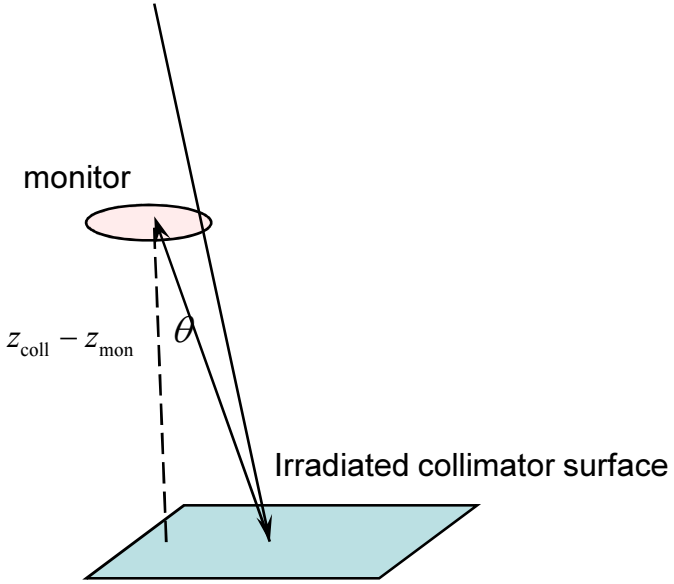

$$b(A) = k_{back} F \frac{z_{mon}^2}{z_{coll}^2}$$

$$F = \iint_{\substack{\text{Irradiated} \\ \text{collimator} \\ \text{area}}} \frac{\cos^3\theta}{\pi\left(z_{coll} - z_{mon}\right)^2} \, \mathrm{d}A$$

PMB 44 p R99-R155

Monitor back scatter

Table 2. Relative BSR-related output changes for the indicated ranges of jaw-defined field sizes measured by the pulse-counting method.

Photon beam energy, linear accelerator	Square fields from 5 × 5 cm^2 to 40 × 40 cm^2 (%)	Rectangular fields, $x = 40$ cm, y from 5–40 cm (%)	Rectangular fields, $y = 40$ cm, x from 5–40 cm (%)
6 MV, Clinac 600C	−0.1 ± 0.4	0.0 ± 0.4	0.0 ± 0.4
6 MV, Clinac 2100C (No 1)	1.6 ± 0.4	1.2 ± 0.4	0.7 ± 0.4
18 MV, Clinac 2100C (No 1)	2.4 ± 0.4	1.7 ± 0.4	1.2 ± 0.4
6 MV, Clinac 2100C (No 2)	1.7 ± 0.4	1.4 ± 0.4	0.6 ± 0.4
18 MV, Clinac 2100C (No 2)	2.1 ± 0.3	2.0 ± 0.3	1.1 ± 0.3
6 MV, Clinac 2300CD	1.2 ± 0.3	1.0 ± 0.3	0.5 ± 0.3
15 MV, Clinac 2300CD	1.8 ± 0.3	1.6 ± 0.3	0.5 ± 0.3
6 MV, Clinac 2300CD (MLC)	—	—	−0.2 ± 0.3[a]

[a] MLC-defined field width varied from 5–25 cm with X jaws retracted and Y jaws defining a fixed length of 25 cm.

Yu *et al* 1996 *PMB* **41** 1107-1117

Head scatter model parameterization example

Scatter component	Model	Model parameters
Flattening filter scatter	Triangular source distribution	c_0 and c_1
Collimator scatter	Scatter kernel integration around the field edge	None
Backscatter to monitor	Monitor's eye view factors of irradiated block areas	Backscatter coefficient k_b
		Σ 3 *parameters*

The parameters are determined by fitting measured S_c (OF_{air}) to calculations!

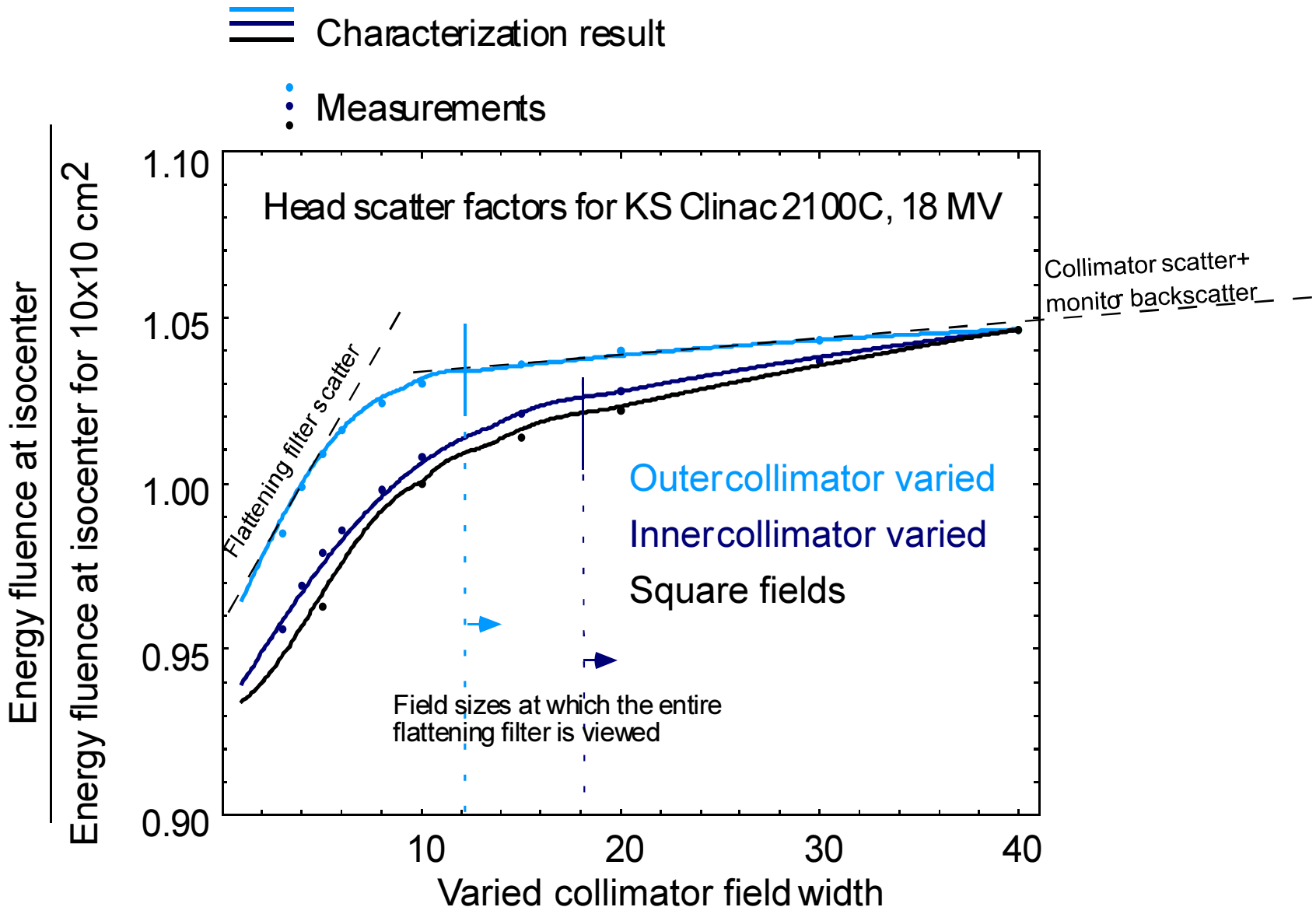
Characterization result
Measurements
Head scatter factors for KS Clinac 2100C, 18 MV
Energy fluence at isocenter
Energy fluence at isocenter for 10x10 cm2
1.10
1.05
1.00
0.95
0.90
10
20
30
40
Varied collimator field width
Flattening filter scatter
Collimator scatter+
monitor backscatter
Outercollimator varied
Innercollimator varied
Square fields
Field sizes at which the entire
flattening filter is viewed

Collimator leakage

MLC intraleaf and interleaf

Two effects:

- Diffused dose from spiky interleaf fluence leakage
- *Intraleaf* attenuation

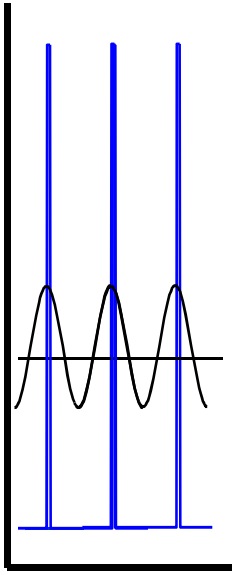

Intraleaf leakage very small:

$$e^{-\frac{\mu}{\rho}\rho \cdot t} \xrightarrow[\text{8 cm tungsten at 3 MeV}]{} e^{-0.0408\times 18.0\times 8.0} = 0.28\%$$

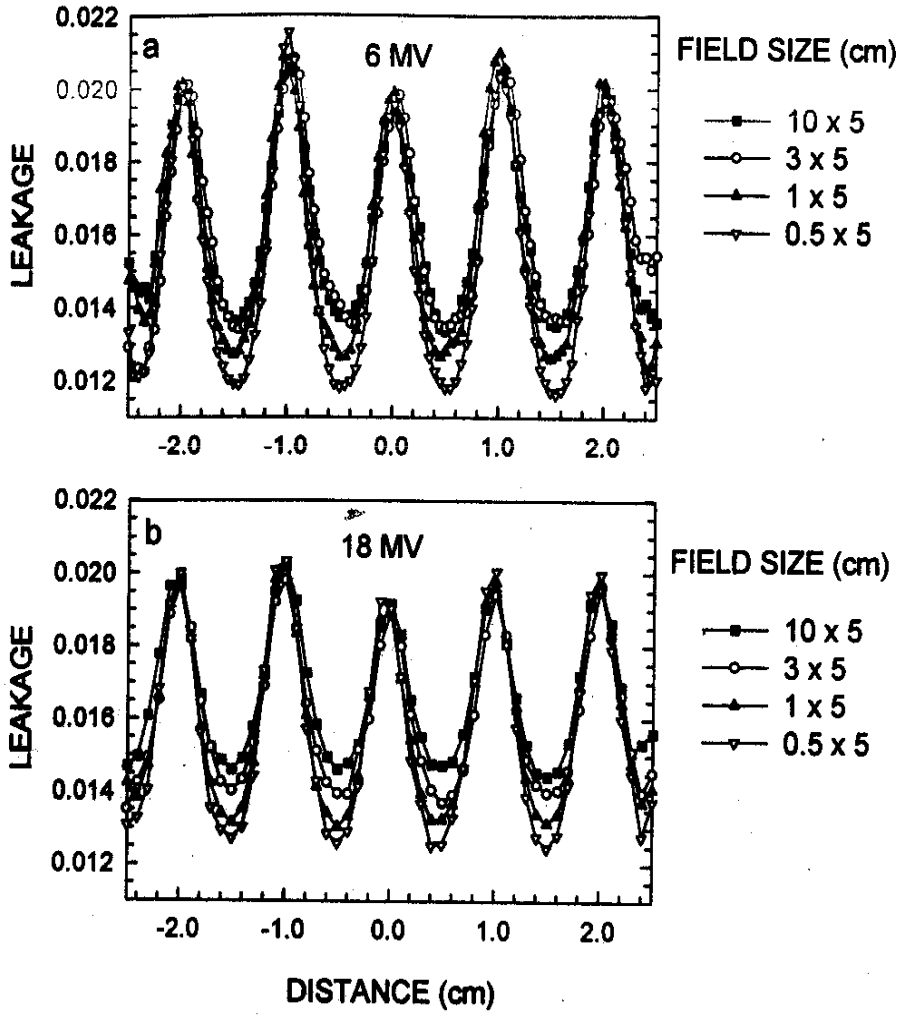

Measuements from
Arnfield *et al*, 2000 Med. Phys. **27** p 2231-2241

Some practical considerations in beam data commissioning

1. Understand the use/purpose of **all** your data items!
   - Checked TPS vendor information?
   - How are the data driving the dose calculations?
   - Used to verify a resulting source parameterization?
   - Error propagation analysis?

2. Be critical to your beam data!
   - Best practice used?
   - Are they qualatively correct?
   - ”Common” errors checked?
   - Compared with similar data?
   - Reviewed by somebody else?

3. Be critical to your TPS!
   - What are the approximations?
   - What are your acceptance levels?
   - How to handle exceded levels?

Understanding the purpose... *Oncentra*

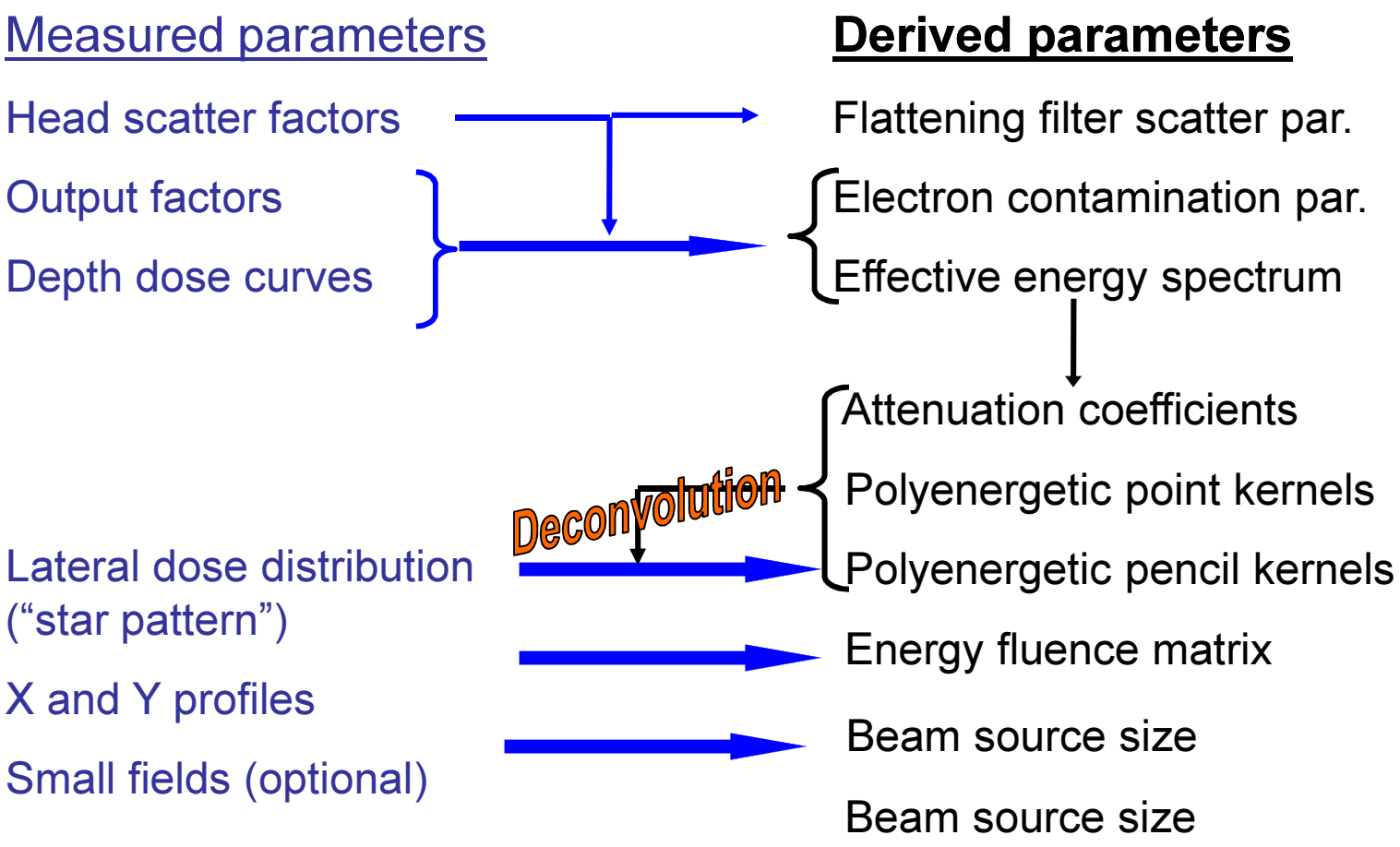

Ahnesjö *etal*, 2005 MedPhys 32 pp 1722-37

Be critical to your data – best practice used?

Report of AAPM Therapy Physics Committee Task Group 74: In-air output ratio, S_c, for megavoltage photon beams

The **in-air output ratio**, S_c is now defined as the ratio of primary collision water kerma in free-space, K_p, per monitor unit between an arbitrary collimator setting, c, and the reference collimator setting, c_{ref}, at the same location on the central axis,

$$S_c(c) \equiv \frac{K_p(c;z_{ref})/\mathrm{MU}}{K_p(c_{ref};z_{ref})/\mathrm{MU}}, \qquad (3)$$

where z_{ref} is the reference source-to-detector distance (usu-

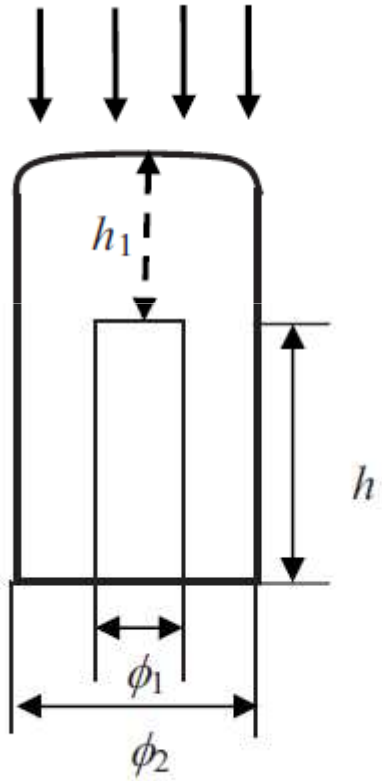

FIG. 10. Schematics of a brass miniphantom recommended for measurements of S_c for square fields larger than 1.5×1.5 cm^2 and photon energy less than 25 MV.

What to expect from your TPS ... *Oncentra*

Mean error±1.s.d. for appr. 1000 linacs

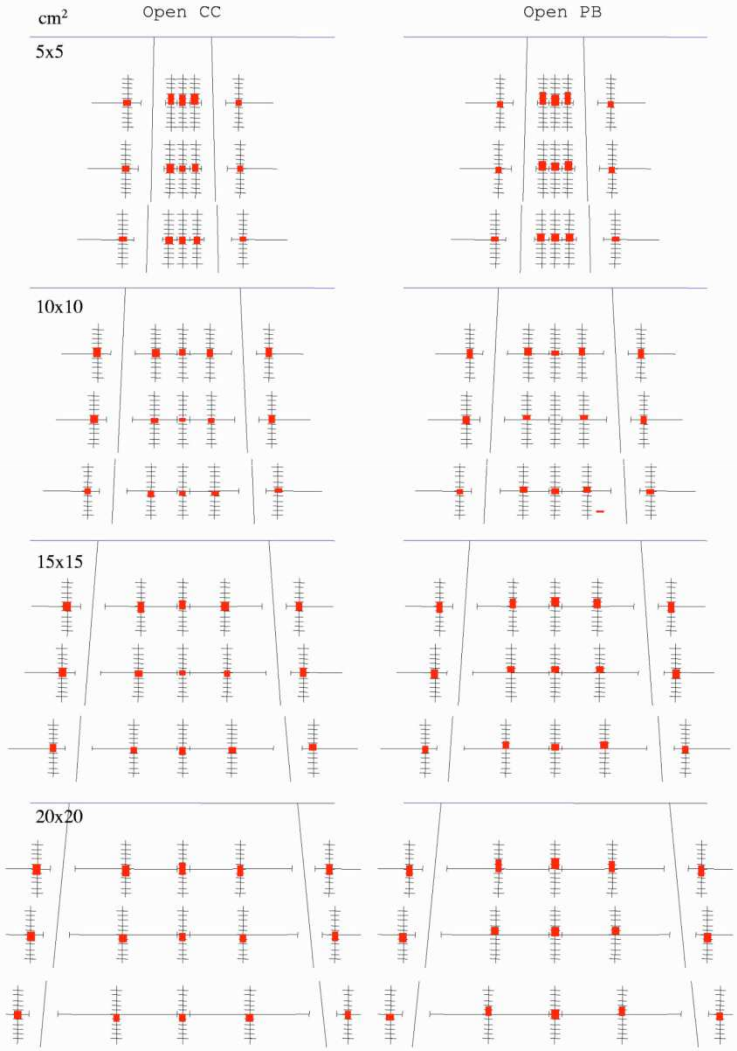

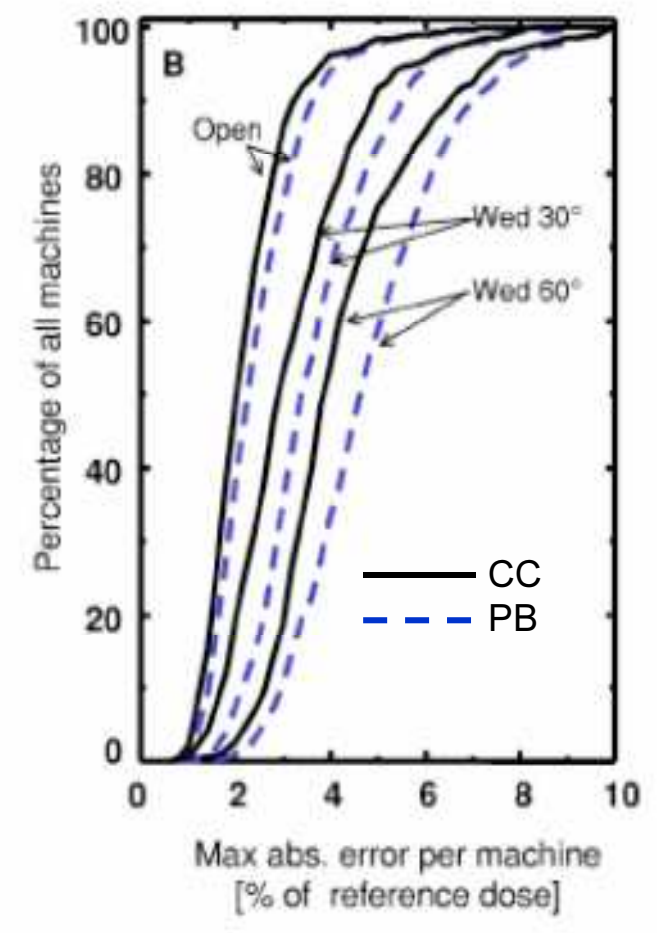

Ahnesjö *et al,* 2005 Med. Phys., Vol. 32, pp1722-37

Summary

Multisource beam representations

- developed for several beam modalities
- allow modelling of individual machines by parameter settings
- actual implementations may vary with great impact on e.g. narrow beam and IMRT performance
- automated methods exist for parameter setting from measured data
- parameters can also be readily derived from Monte Carlo phase space data

Be critical to your data!

For new, well controlled and standardized machines one may consider using a standard set of data!

Understanding the purpose... *Pinnacle*

Gaussian height	An increase in the value of this parameter decreases the sharpness of the transition between the low-dose gradient region outside the radiation field and the high-dose gradient region.	The accuracy of monitor unit calculations for elongated fields decreases with an increase in the value of this parameter of around 0.05. The value of this parameter increases with field size.
Gaussian width	This parameter has a similar effect on the off-axis profile as the Gaussian height parameter.	Because of the low value of the Gaussian height parameter required for accurate monitor unit calculations, this parameter has little effect on off-axis profile.
Jaw transmission	An increase in the value of this parameter increases the value of the off-axis profile in the low-dose gradient region outside the radiation field.	Changes in this parameter of 0.005 have a noticeable effect on the off-axis profile in the low-dose gradient region outside the radiation field. The value of this parameter typically increases with field size.
Modifiers		
Modifier Scatter Factor	This parameter affects off-axis profiles for wedged fields. An increase in the value of this parameter decreases the value of the off-axis ratio in the region of the thin end of the wedge and increases the off-axis ratio in the region of the thick end of the wedge.	Changes in this parameter of 0.1 are needed to have a noticeable effect on the off-axis profile. The value of this parameter typically increases with field size.
Electron Contamination		
Maximum Depth (cm)	The value of this parameter is determined by the energy of the radiation beam and is typically set to be approximately $2 \times d_{max}$.	The exact value of this parameter is not too critical. It is independent of field size.
Surface dose (Dose/Fluence)	Increasing the value of this parameter increases the dose at very shallow depths to the region of electron	The exact value of this parameter is not critical, as the tolerance of the accuracy of the model near the surface is significantly looser than elsewhere.

Starkschall *et al.*: Beam-commissioning methodology . . .

Journal of Applied Clinical Medical Physics, Vol. 1, No. 1, Winter 2000

Understanding the purpose... *Pinnacle – ABMOS*

(automated beam model optimization system)
Létourneau *etal* Med. Phys. 37 „5, 2010, pp2110

TABLE I. Description of the beam model parameters a

Available for optimization	
Description	Abbre
- MLC transmission	%
- Jaw transmission	$\%T_{X\text{-jaws}}$
- MLC interleaf leakage	L_{height} and
- Orthogonal source size	S_X a
- Extrafocal scatter source	G_{height} and
- Geometric correction for rounded leaf MLC leaf-end	Pc

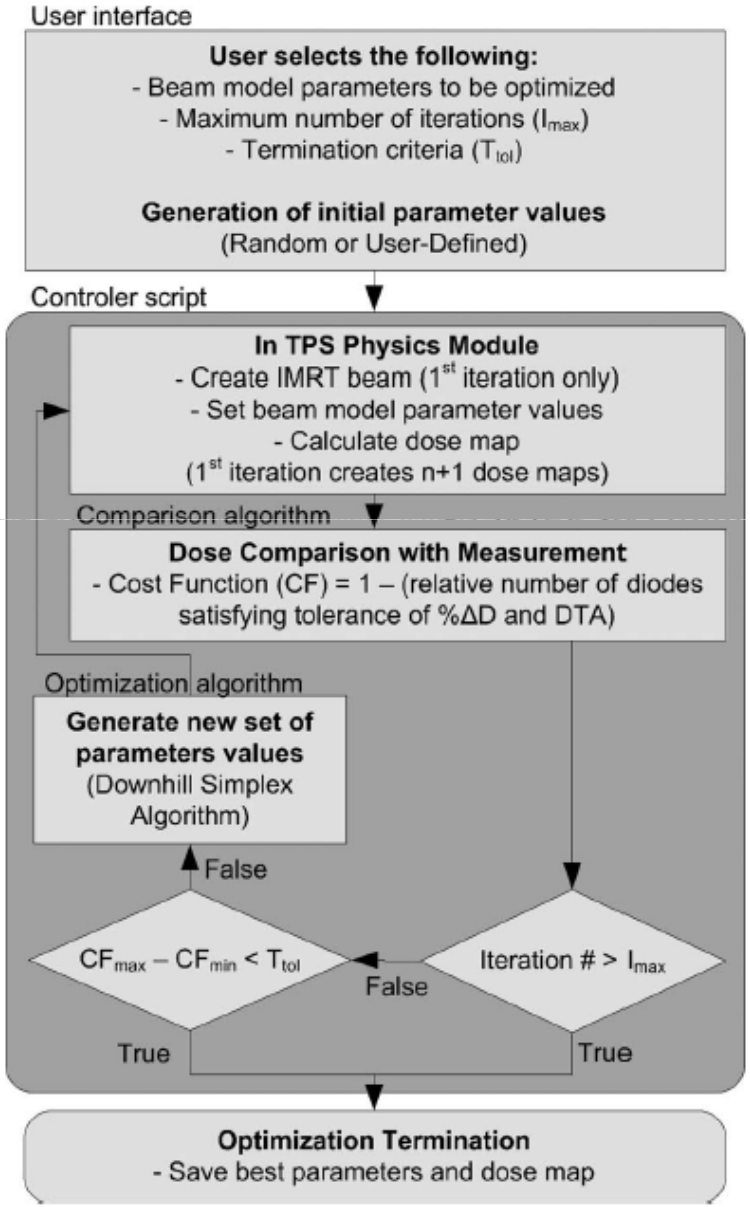

Understanding the purpose... *Eclipse*

2.3. The optimization procedure for parameter derivation

The proposed automatic optimization procedure is based on the minimization of an objective function measuring the deviation between dose calculations and measurements. To obtain acceptable calculation times, a fast point dose calculation method ($M_{\text{p.d.}}$) presented in section 2.2.2 is used during the optimization instead of the volumetric calculation method ($M_{\text{v.d.}}$) presented in section 2.2.1. Since $M_{\text{p.d.}}$ is only capable of calculating the photon dose, $M_{\text{v.d.}}$ is still used to derive the electron contamination parameters. The procedure consists of the following phases:

(i) Resampling, adjustment and scaling of the measured beam data.
(ii) Initial optimization of photon parameters $\bar{E}(r), I(r), \sigma_{\text{ef}}, w_{\text{ef}}$ and $\bar{E}_{\text{ef}}$ using Powell's direction search method. The measurements in the build-up region are ignored in this phase.
(iii) Optimization of the electron contamination parameters $\sigma_{\text{e},1}, \sigma_{\text{e},2}, c$, and the weights $w_{\text{e},i}$ $(i = 1, \ldots, 6)$ for $c_{\text{e}}(z)$ based on the differences between the measured PDDs and calculated PDDs without electron contamination.
(iv) To allow the use of $M_{\text{p.d.}}$ also in the build-up region, the differences between $M_{\text{p.d.}}$ and $M_{\text{v.d.}}$ are evaluated at the current parameter values. The differences are mostly due to the inability of $M_{\text{p.d.}}$ to calculate the electron dose. The measured beam data, which are used as an optimization target, are replaced by the original measurements subtracted by the differences.
(v) Refining the optimization based on the modified measurement data to take the measurements in the build-up region into account.

The optimization process is not sensitive to the initial parameter values used in step (ii), which is demonstrated with an example case in section 3.1. In the following sections the above steps are described in more detail.

Tillikainen *etal*, 2007 PhysMedBiol 52 pp 1441-67

Possible errors and expected consequences
Oncentra examples

- Build-up blurring from finite sized ion chambers
  => *bad electron contamination fit*
- Penumbra blurring due to ion chamber long axis along beam edge
  => *bad effective source size fit =>bad small field D/MU*
- Partly blocked ion chambers for small fields OFair
  => *bad effective source size fit =>bad small field D/MU*
- Depth offset
  => *bad effective spectrum fit, wrong depth doses (but not as measured!)*
- Noisy data
  => *error analysis difficult*
- Too thin or too low density of build-up cap for S_c meas.
  =>*bad values of flat.filt.scat. parameters=>overestimated output variation*

Be critical to your data – compare with others...

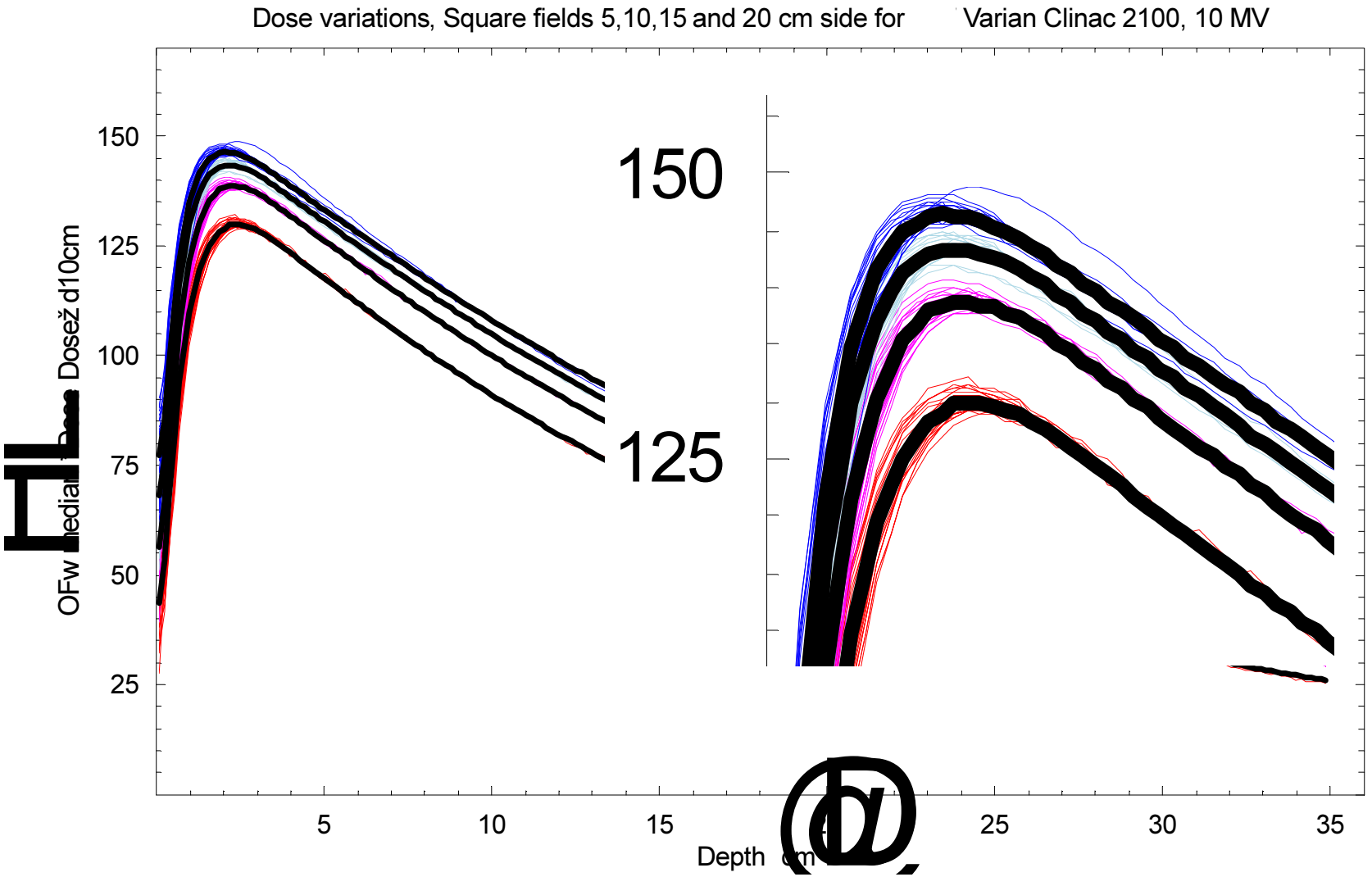

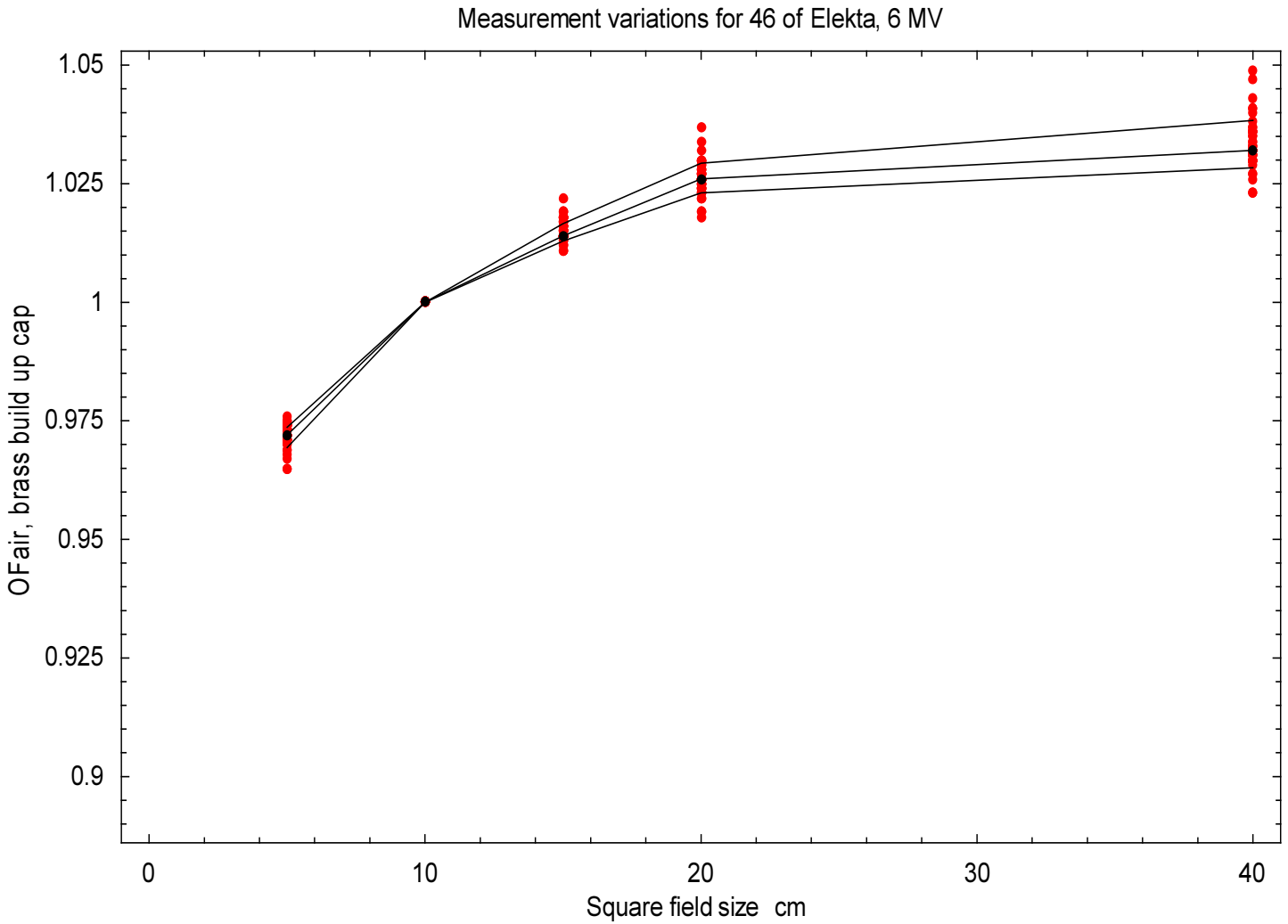
Measurement variations for 46 of Elekta, 6 MV
OFair, brass build up cap
1.05
1.025
1
0.975
0.95
0.925
0.9
0
10
20
30
40
Square field size cm

Be critical to your data – best practice used?

Report of AAPM Therapy Physics Committee Task Group 74: In-air output ratio, S_c, for megavoltage photon beams

The **in-air output ratio**, S_c is now defined as the ratio of primary collision water kerma in free-space, K_p, per monitor unit between an arbitrary collimator setting, c, and the reference collimator setting, c_{ref}, at the same location on the central axis,

$$S_c(c) \equiv \frac{K_p(c;z_{ref})/\mathrm{MU}}{K_p(c_{ref};z_{ref})/\mathrm{MU}}, \qquad (3)$$

where z_{ref} is the reference source-to-detector distance (usu-

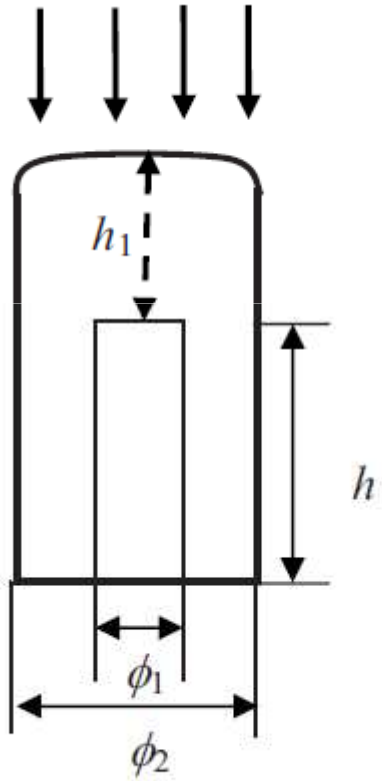

FIG. 10. Schematics of a brass miniphantom recommended for measurements of S_c for square fields larger than 1.5×1.5 cm^2 and photon energy less than 25 MV.

Be critical to your data – best practice used?

Accelerator beam data commissioning equipment and procedures: Report of the TG-106 of the Therapy Physics Committee of the AAPM

IPEM Report: Small Field MV Photon Dosimetry

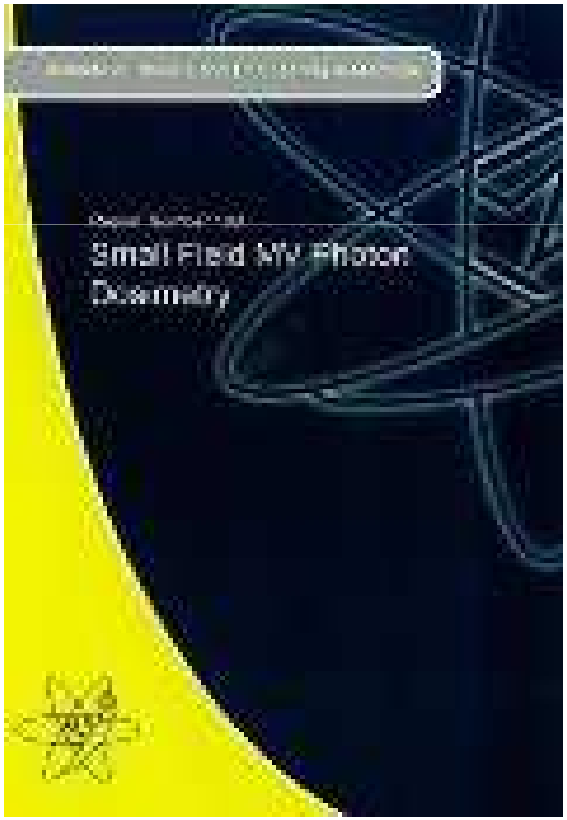

What to expect from your TPS ... *Oncentra*

Mean error±1.s.d. for appr. 1000 linacs

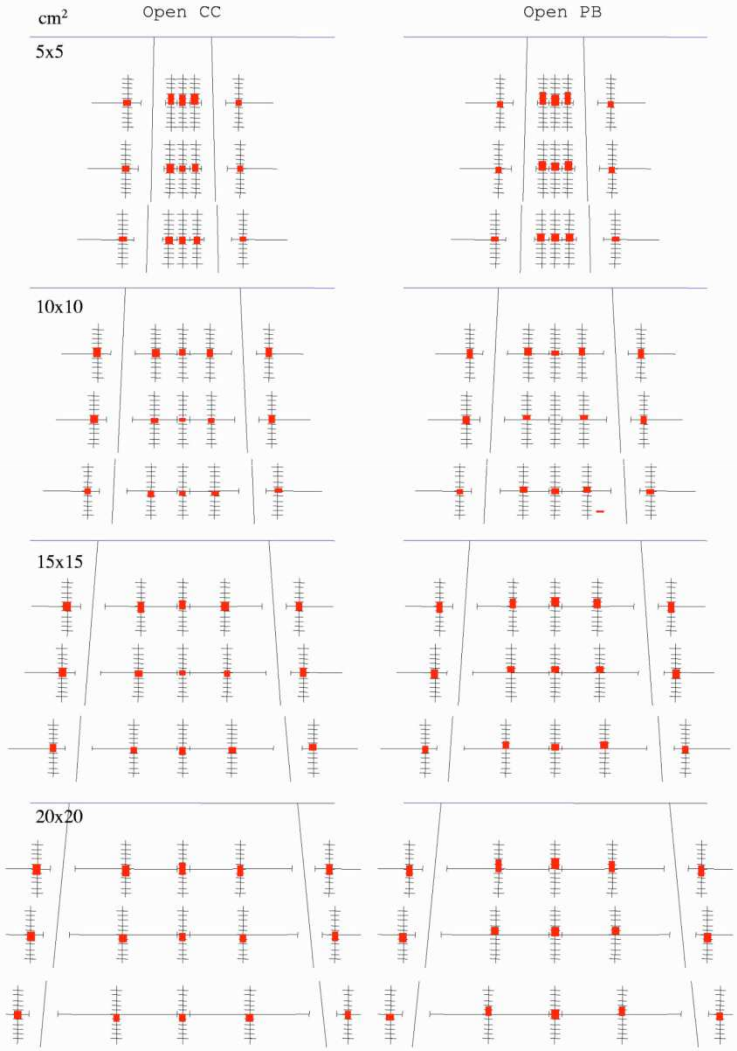

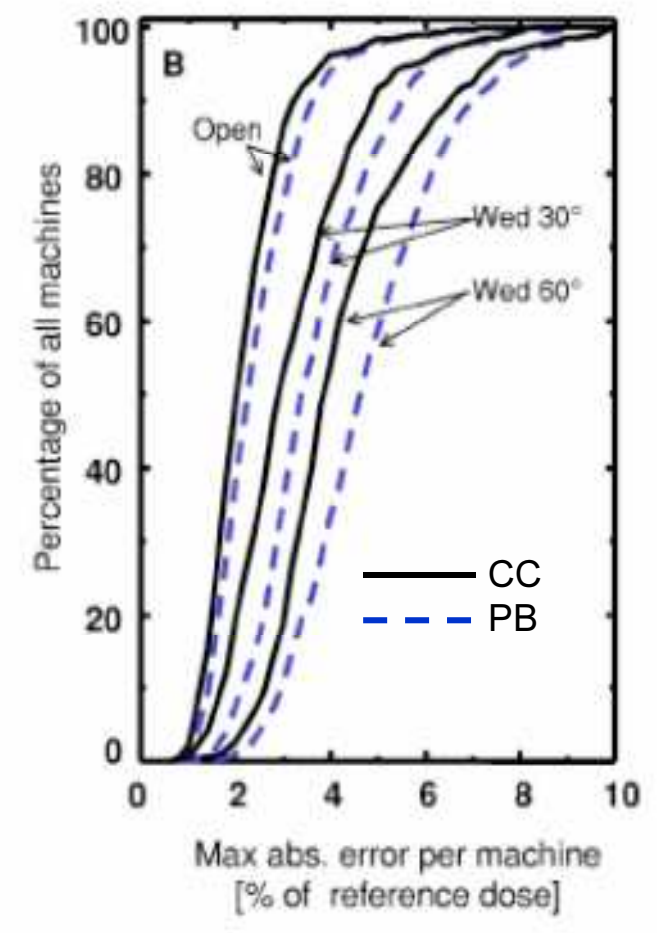

Ahnesjö *et al,* 2005 Med. Phys., Vol. 32, pp1722-37

The most practical item is a good theory!

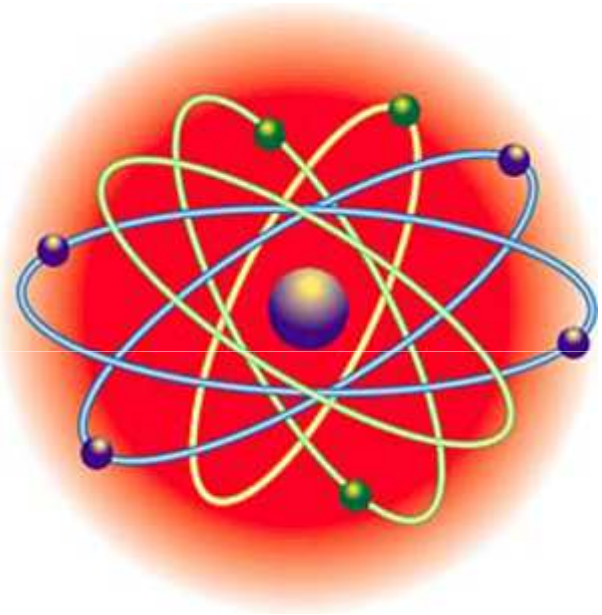

T Knöös

With some help from the faculty

ESTRO School

Learning objectives

- To understand what beam models and dose engines we are using for treatment planning of electrons
  - Pencil Beams
  - Monte Carlo
- Comparison and Performance

Patient dose calculation

PENCIL BEAM METHODS…

Pencil beam dose kernels in water – MC generated

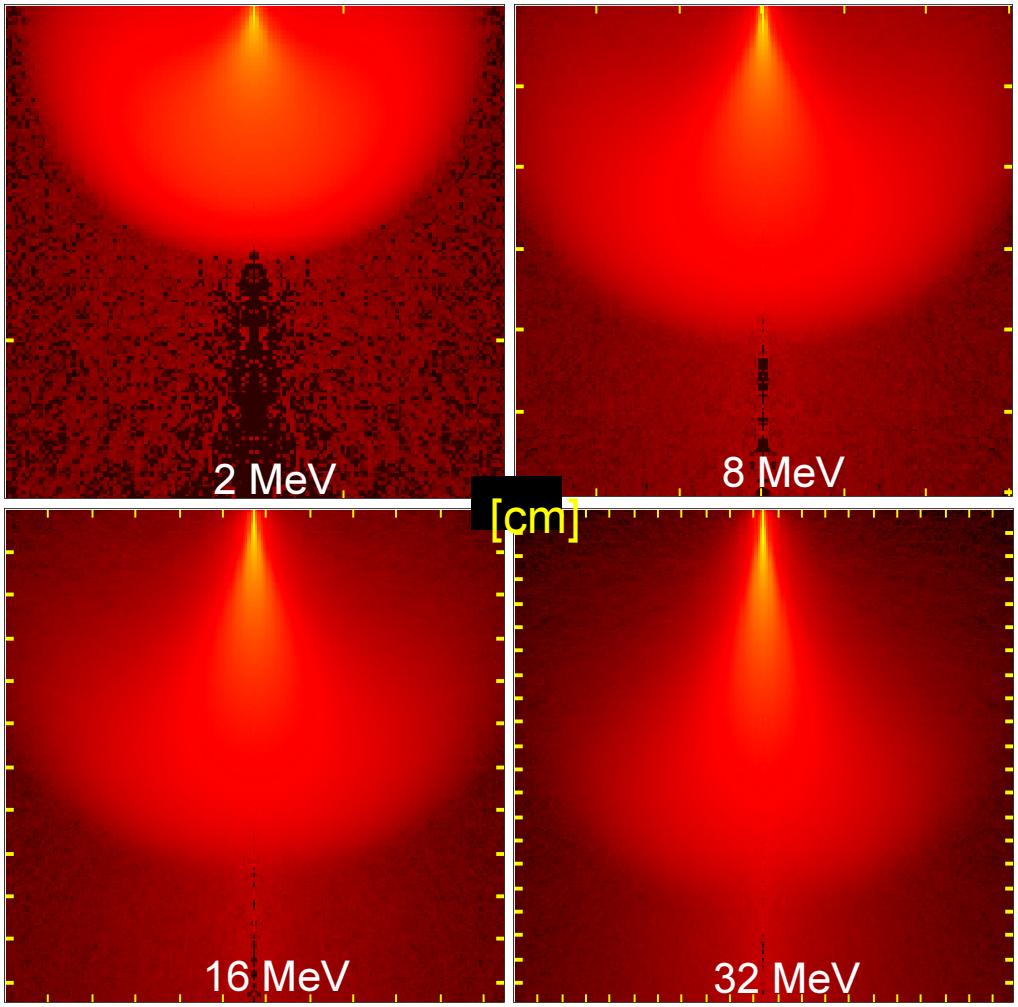

Length scale not the same

From A Ahnesjö

ESTRO School

Fermi-Eyges theory for pencil beam propagation in slab media

Fermi-Eyges theory describes the broadening of a pencil beam due to multiple scattering along its path. The result is Gaussian distributions of the electrons characterized by:

- Mean square of scattering angle: $\overline{\theta^2}$
- Mean radius-angle covariance: $\overline{r\theta}$
- Mean square of radius: $\overline{r^2}$

In a stack of slabs one gets, after slab *i*:

$$\overline{\theta_i^2} = \overline{\theta_{i-1}^2} + h_i T_i \left(\Sigma_{i-1} + k h_i S_i / 2 \right)$$

$$\overline{r\theta}_i = \overline{r\theta}_{i-1} + h_i \left[\overline{\theta_{i-1}^2} + \frac{1}{2} h_i T_i \left(\Sigma_{i-1} + k h_i S_i / 3 \right) \right]$$

$$\overline{r_i^2} = \overline{r_{i-1}^2} + h_i \left\{ 2\overline{r\theta}_{i-1} + h_i \left[\overline{\theta_{i-1}^2} + \frac{1}{3} h_i T_i \left(\Sigma_{i-1} + k h_i S_i / 4 \right) \right] \right\}$$

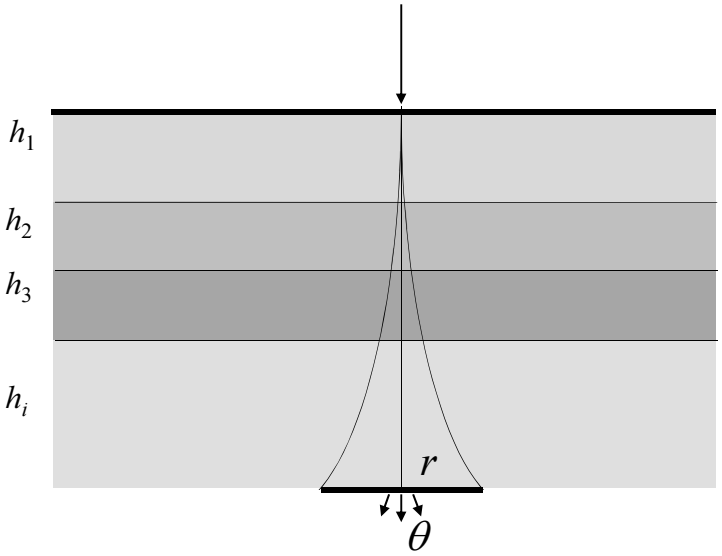

where

h_i thickness of stack i

T_i scattering power of stack i

S_i stopping power of stack i

$\Sigma_{i-1} = \Sigma_i + k h_i S_i$

k a scaling constant to increase T with depth (Brahme-Lax)

Mix of Hogstrom and Brahme/Lax papers

Pictorial description of pencil beam modeling

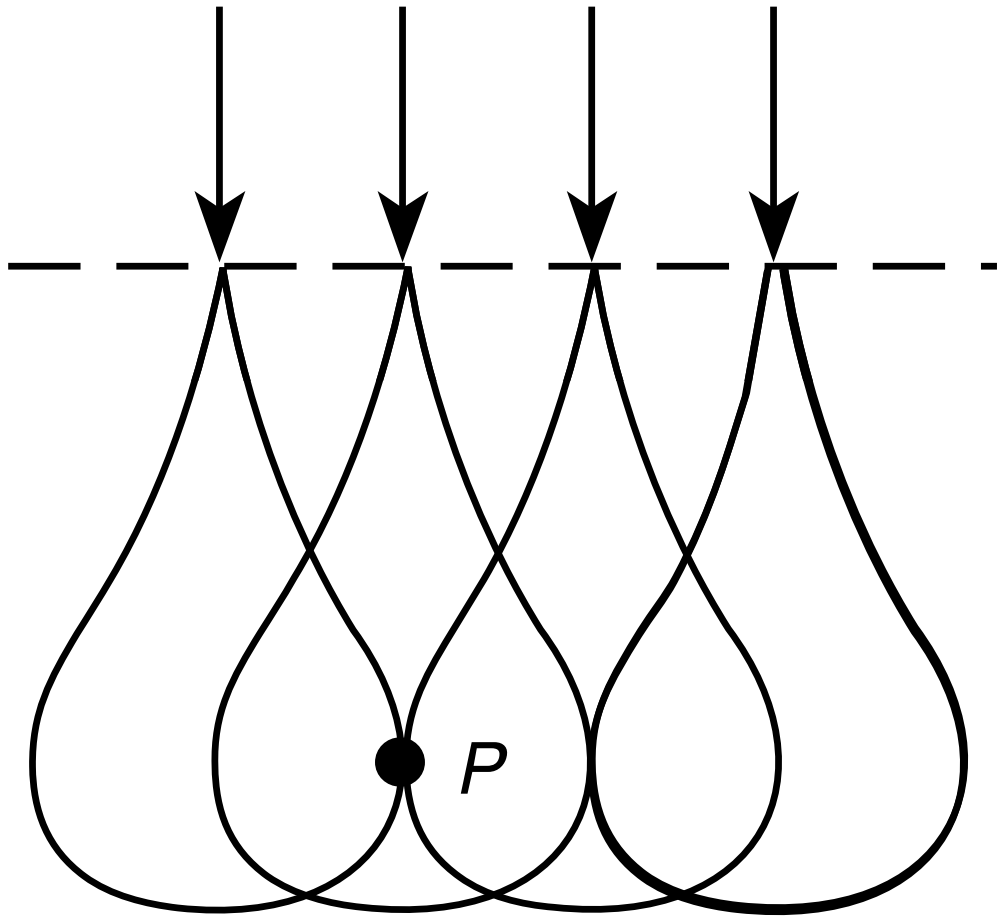

From Handbook of Radiotherapy Physics
Ed Mayles, Nahum and Rosenwald

Fermi-Eyges for electrons

- Referring to a Cartesian coordinate system (x,y,z) and an electron, incident perpendicularly on a medium at (0,0,0) in the z direction, the Fermi–Eyges expression for the probability of finding the electron at depth z with displacement between x and $x+dx$, y and $y+dy$ is

$$p(x,y,z)\mathrm{d}x\,\mathrm{d}y = \frac{1}{2\pi\sigma^2_{\mathrm{MCS}}}\exp\left[-\frac{x^2+y^2}{2\sigma^2_{\mathrm{MCS}}}\right]\mathrm{d}x\,\mathrm{d}y$$

- Where

$$\sigma^2_{\mathrm{MCS}} = \frac{1}{2}\int_0^z (z-u)^2 T(u)\mathrm{d}u$$

- $T(u)$ is the linear scattering power of the medium at depth u

From Handbook of Radiotherapy Physics
Ed Mayles, Nahum and Rosenwald

Fermi-Eyges for electrons

- Can be divided as $p(x,y,z)=p(x,z)\,p(x,y)$ where both are given as

$$p(x,z)\mathrm{d}x = \frac{1}{\sqrt{2\pi}\sigma}\exp\frac{-x^2}{2\sigma^2}\mathrm{d}x$$

- This is a Gaussian, or normal distribution, and s can be identified as the standard deviation , which is a measure of the width of the distribution. As the depth increases, σ_{MCS} increases and the pencil spreads out.
- Integration of a Gaussian is written with the erf function

$$\mathrm{erf}(x) \equiv \frac{2}{\sqrt{\pi}}\int_0^x \mathrm{e}^{-t^2}\mathrm{d}t$$

From Handbook of Radiotherapy Physics
Ed Mayles, Nahum and Rosenwald

Fermi-Eyges for electrons

- After some algebra you get

$$N(x,y,z) = \frac{1}{4}\left[\mathrm{erf}\left(\frac{A-x}{\sqrt{2}\sigma_{\mathrm{MCS}}}\right) + \mathrm{erf}\left(\frac{A+x}{\sqrt{2}\sigma_{\mathrm{MCS}}}\right)\right]\left[\mathrm{erf}\left(\frac{B-y}{\sqrt{2}\sigma_{\mathrm{MCS}}}\right) + \mathrm{erf}\left(\frac{B+y}{\sqrt{2}\sigma_{\mathrm{MCS}}}\right)\right]$$

- Recalling that erf(x) is very close to unity for x>2, it can be seen that N(x,y,z)=1 if both x and y are more than about 3 times the σ_{MCS} from the field edges, i.e. the dose profile is flat away from the edges of a broad beam, exactly as one would expect.
- The above result also implies that N (x,y,z) is constant with depth, i.e. the build-up due to scattering is not predicted.
- The Fermi–Eyges theory do not account for electron loss.
  - An empirical correction factor is necessary in order to reproduce measured depth–dose curves.

From Handbook of Radiotherapy Physics
Ed Mayles, Nahum and Rosenwald

How to get the dose distribution?

- To get a depth dose curve one has to correct the planar fluence of electrons

$$d(x,y,z) = p(x,y,z)\, g(z)$$

- The weighting factor g (z) is determined such that the dose as a function of depth on the central axis for a given field size exactly equals the measured central axis depth dose
  - Corrected to infinite SSD
  - Bremsstrahlung dose, is subtracted (assumed constant at all depths less than Rp

$$g(z) = \frac{D_{\text{meas,e}^-}(0,0,z)}{\operatorname{erf}\left[\frac{A(1+z/\text{SSD})}{\sqrt{2}\sigma_{\text{med}}(z)}\right]\operatorname{erf}\left[\frac{B(1+z/\text{SSD})}{\sqrt{2}\sigma_{\text{med}}(z)}\right]}$$

From Handbook of Radiotherapy Physics
Ed Mayles, Nahum and Rosenwald

Further additions

- The SSD dependence have to be added
- The dose due to bremsstrahlung was originally subtracted from the measured depth–dose curve.
  - This must now be added back to the electron dose, after putting back the inverse square law dependence.
  - It is assumed that the dose beyond the depth of the practical range is entirely due to photons.

The widening of the pencil is limited

- The pencil-beam width (σ_{MCS}) as a function of depth agrees well with experiment at small and moderate depths.
- Then it continues to increase, whereas in reality it goes through a maximum and finally decreases.
- This is managed by the $g(x)$ function or has to managed in
- This is due to the reduction of the number of electrons in the beam at large depths due to range straggling

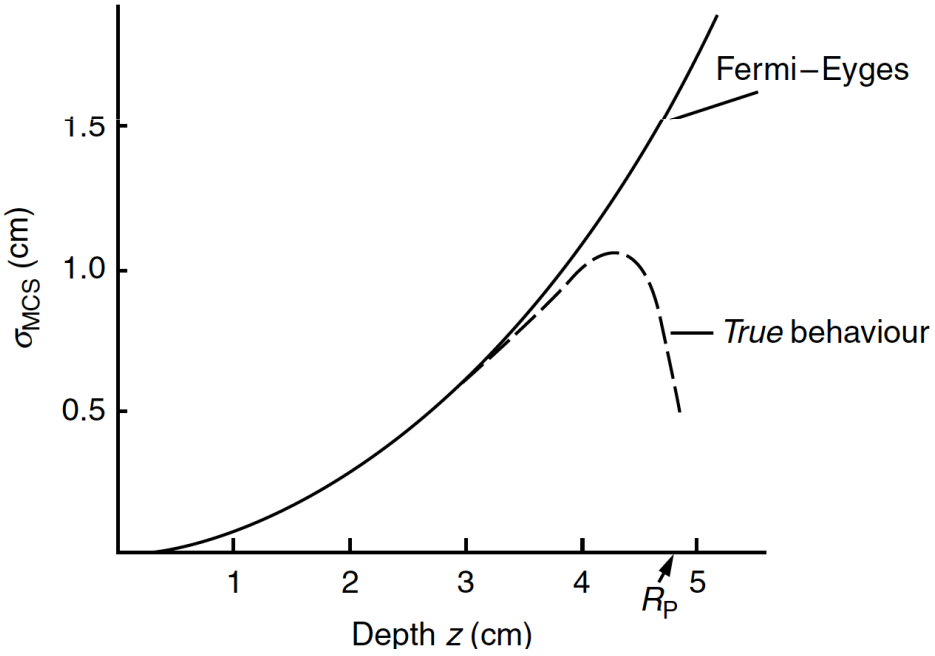

From Handbook of Radiotherapy Physics
Ed Mayles, Nahum and Rosenwald

Beam model plus dose engine (pencil beam)

Starting point

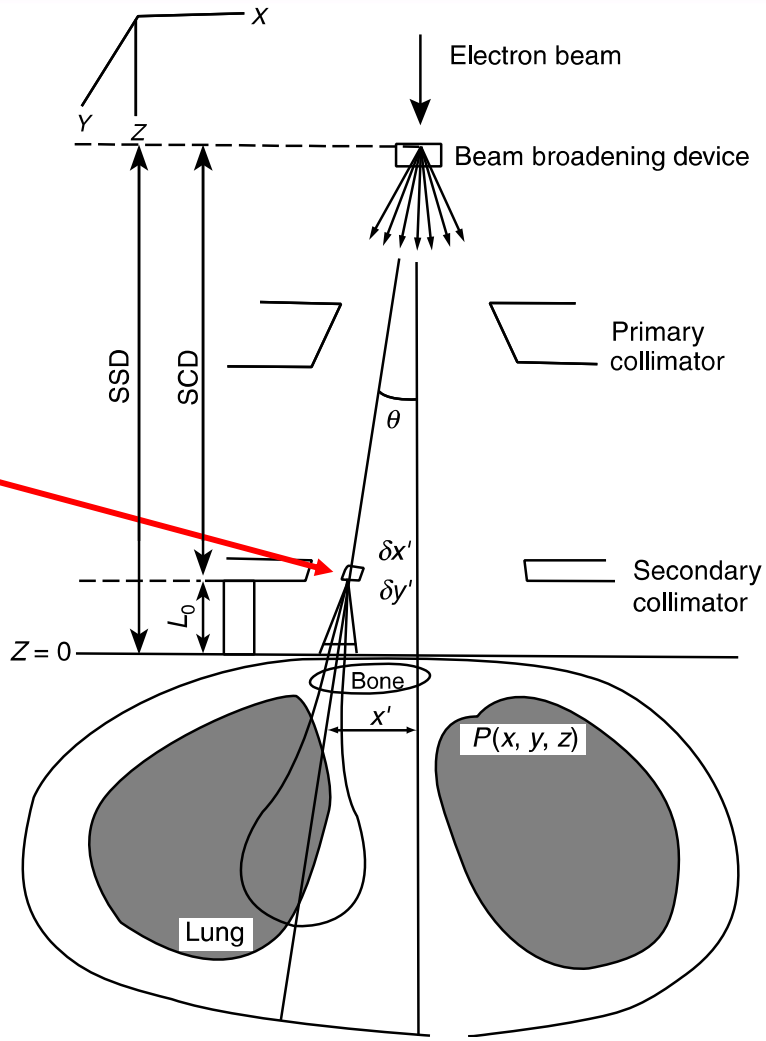

Hogstrom et al., Phys. Med. Biol., 26, 445–459, 1981.

ESTRO School

The semi-infinite slab approximation in tissue

The pencil beams are propagated through tissue as if it was made of a stack of slabs, each with the local heterogeneities along each ray extended laterally into homogeneous slabs.

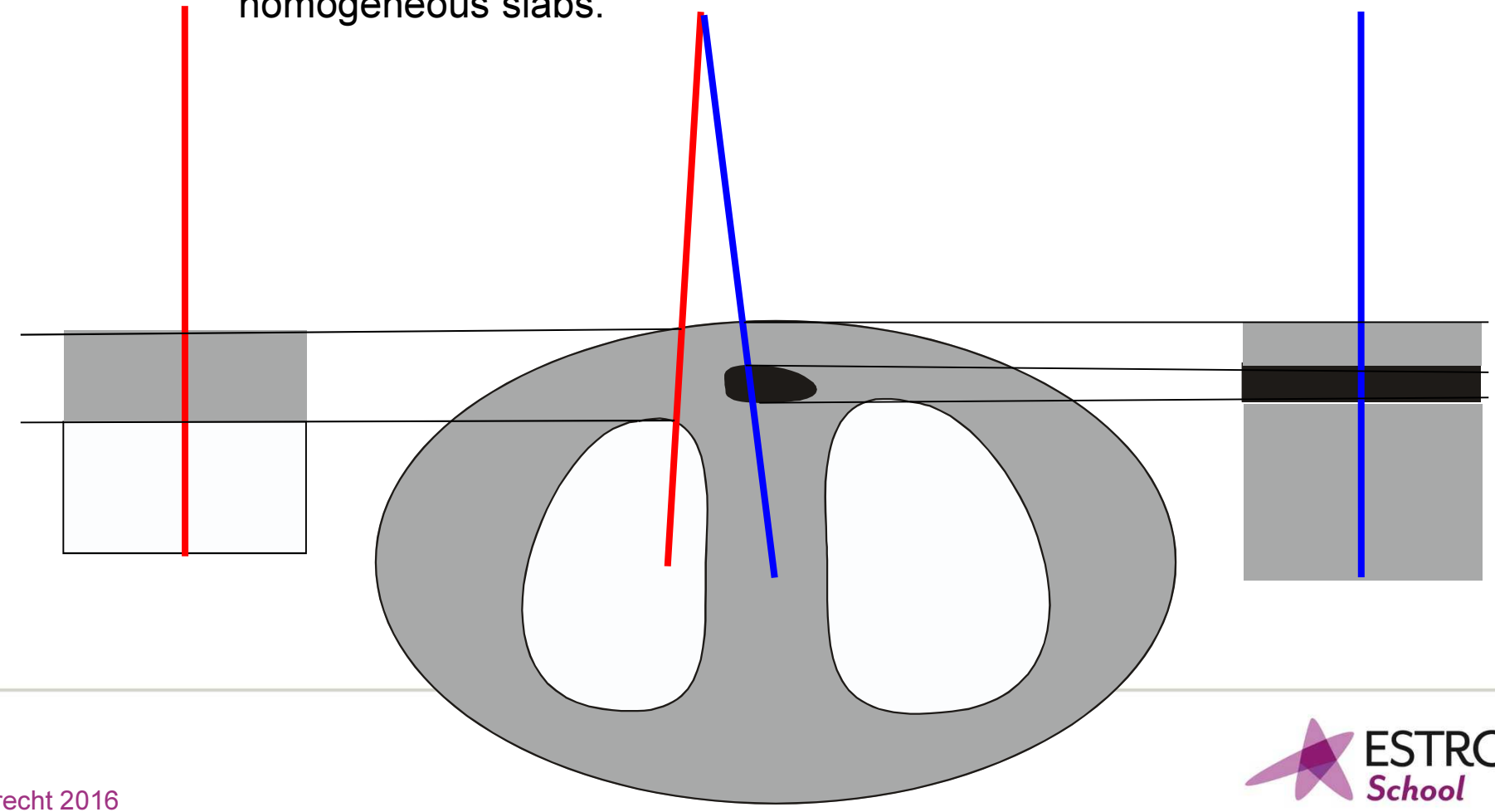

Pencil Beam example, penumbra modeling

At calculation points well inside field limits, PB width set to zero at patient level not to wash out effects from heterogeneities

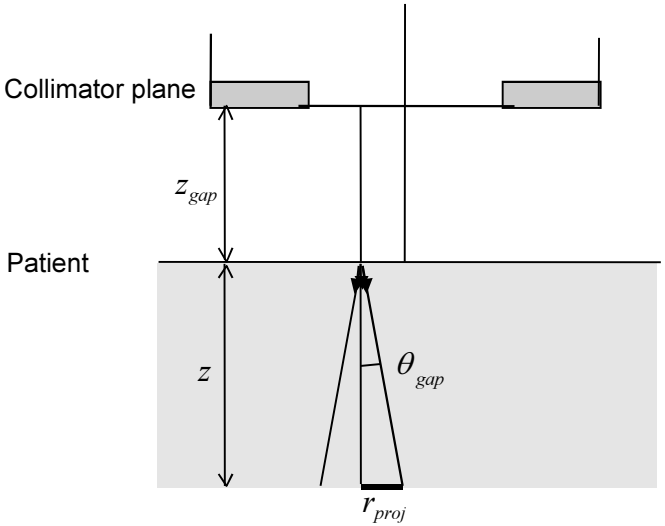

At calculation points in penumbra region, PB width set to zero at collimator level to correctly model penumbra width including effects of in air scattering

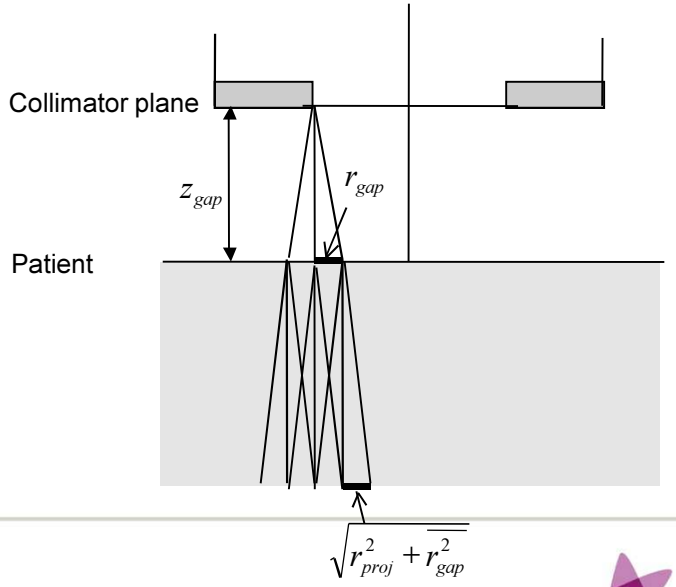

Hot and cold spots

In between regions of much scattered pencils and less scattered pencils, hot and cold spots will occur due to varying degree of lateral equilibrium.

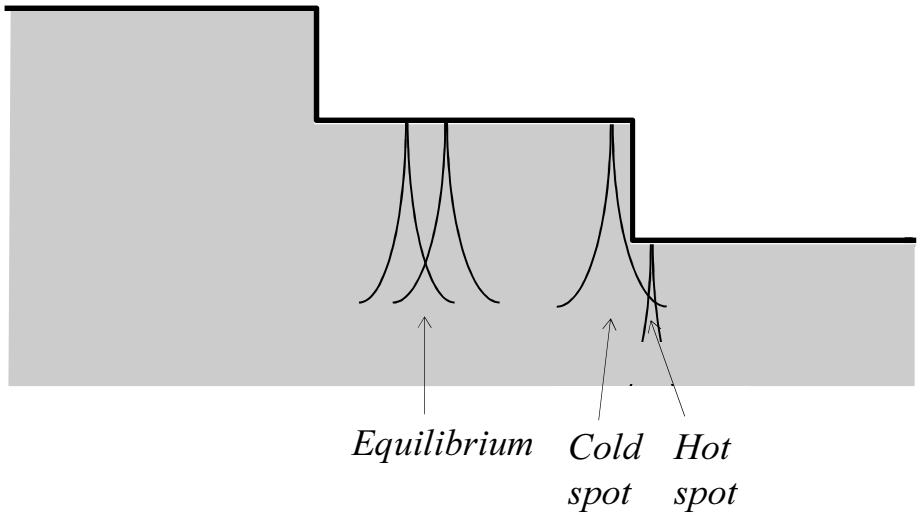

Unresolved issues with electron pencil beam models

Beam modeling:

PB methods assume Gaussian characteristics of the incident beam. Hence, influence from “non Gaussian” features (collimator scattering, etc) yield profile errors and make output factors hard to calculate (has to be table lookup driven).

Penumbra modeling through manipulation of incident pencil width may wash out effects of heterogeneities.

Heterogeneities:

Heterogeneities are well modeled at the first part of the depth range (since voxels are larger than the FE pencil width).

At the end of the electron range, effects of localized heterogeneities (smaller than the FE pencil width using semi-infinite slab approximation) get washed out PB by models. “Redefinition” and “phase space evolution” models fix that, to the cost of CPU&memory…

MONTE CARLO METHODS

Rationale for Monte Carlo dose calculation for electron beams

Slide from Cygler

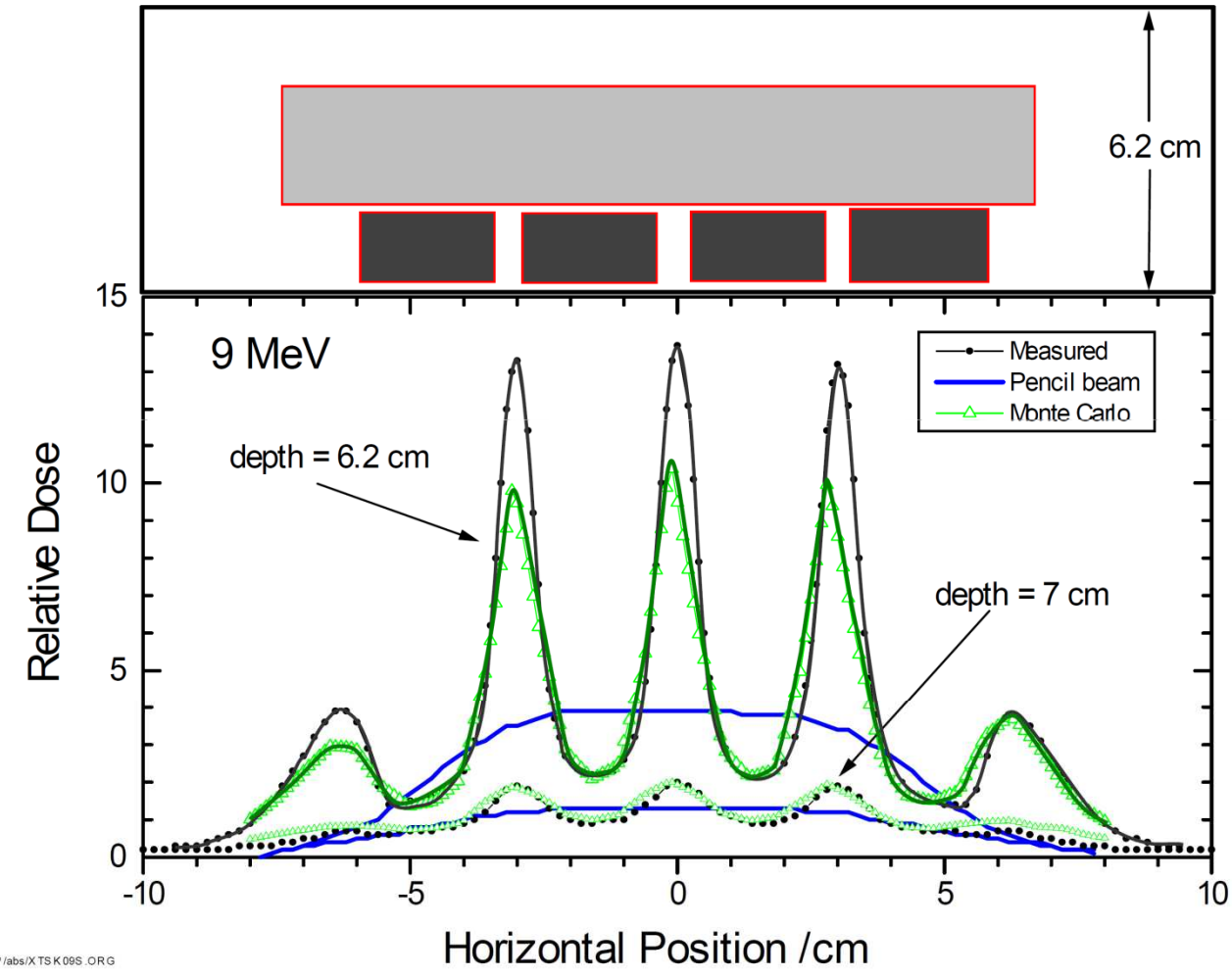

Ding, G. X., et al, Int. J. Rad. Onc. Biol Phys. (2005) 63:622-633

Monte Carlo in commercial TPS

- MDS Nordion 2001 i.e. Oncentra MasterPlan - **Elekta MONACO**
  - First commercial Monte Carlo treatment planning for electron beams
  - Implementation of Kawrakow's VMC++ Monte Carlo dose calculation algorithm (2000)
  - Handles electron beams from all clinical linacs

- Varian Eclipse eMC 2004
  - Based on Neuenschwander's MMC dose calculation algorithm (1992)
  - Handles electron beams from Varian linacs only

- CMS XiO eMC – **Elekta MONACO**
  - VMC++
  - Handles all linacs (only Elekta verification has been published)

PATIENT DOSE ENGINES

VMC++

- VMC was developed by I. Kawrakow, M. Fippel and K. Friedrich with K. Ulm at the U of Leipzig, 1996
  - VMC originally only for electrons
  - Extended later by M.Fippel to photons - xVMC
  - Re-implemented in C++ by I. Kawrakow at NRC - VMC++
- Recent work implements a series of additional VRTs for photons
  - Exact MS theory developed at NRC
  - Boundary crossing algorithm (BCA) allowing multi-voxel CH steps
  - Optimization of sampling algorithms
  - STOPS
  - Quasi-random sequences
    - Generated with emphasis on filling the multidimensional space of interest in as uniform a way as possible
- Used in Elekta/Nucletron Oncentra MasterPlan and Elekta/CMS XiO eMC

VMC++ accuracy and speed

- Sub-percent agreement with EGSnrc
- Is about 100 times faster than BEAMnrc for linac head simulations
- Is 50-150 times faster than EGS4/PRESTA for electron and photon beam simulations in the patient geometry for comparable accuracy.
- CPU times for in-patient simulations (10x10 beam, 5 mm voxels, 2% statistical uncertainty):
  - ~30 seconds for electrons

Electron beam calculations (e.g. Oncentra Monte Carlo electrons)

Beam characterization

- Measure fluence profiles in air with removed applicator, field settings varied with the photon collimators
- Optimize source phase space parameters to fit measured profiles
- Generate source phase space electrons and propagate them with the photon collimators at preset values and the applicator mounted (no insert) to the exit phase space
- Parameterize the exit phase space

Run time calculations

- Generate exit phase space electrons, discard those who stem from areas blocked by the insert
- Add collimator scatter electrons and treatment head photons
- Propagate the generated particles into the patient

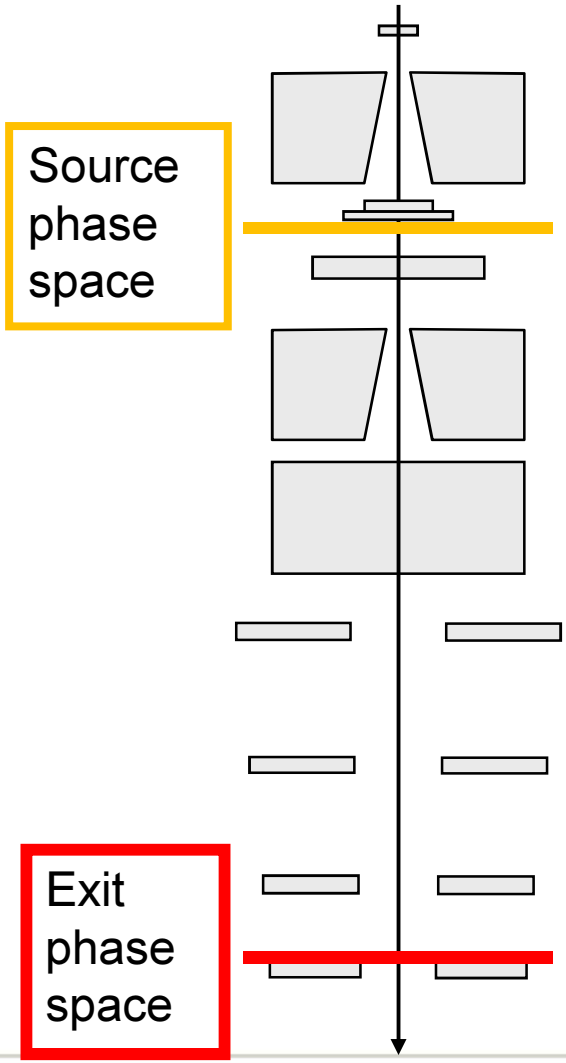

Local to global Monte Carlo

Full MC with many local steps

Global MC with very few steps

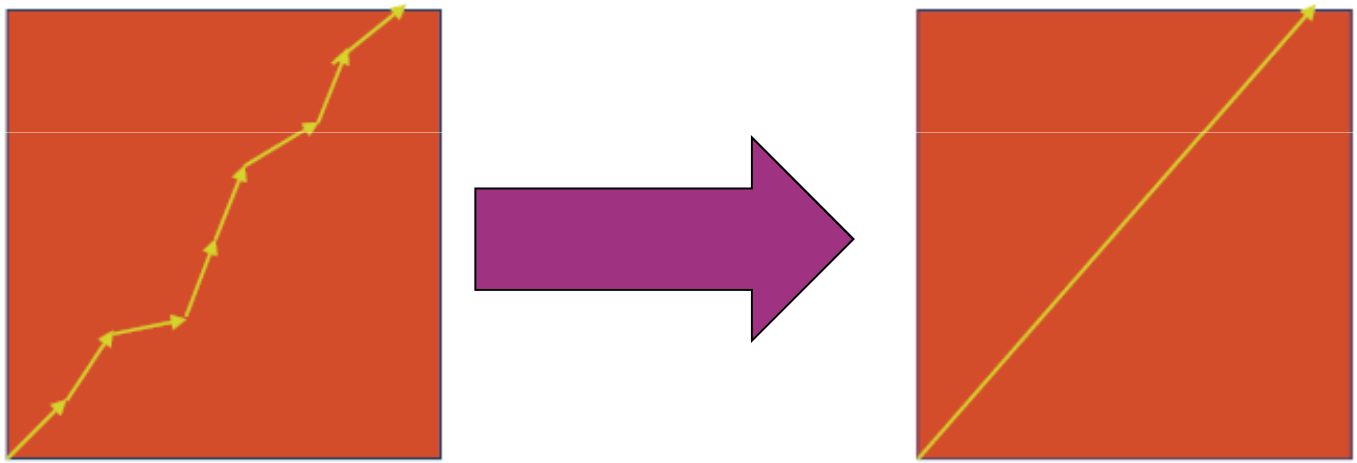

eMC Global MC input

- Local geometries are spheres of various sizes, material compositions and incident electron energies:
  - 5 materials: air, lung, water, lucite and solid bone
  - 5 sphere radii: 0.5, 1.0, 1.5, 2.0 and 3.0 mm
  - 30 incident energy values, between 0.2 and 25 MeV
- 200 000 electrons per sphere were simulated using Monte Carlo with EGSnrc Code System
- Results from simulations were collected to probability distribution functions (PDFs):
  - Exit point and direction of primary electron
  - Energy of primary electron
  - Secondary particles (e- & γ) and their energies

Macro Monte Carlo transport model in Eclipse

- An implementation of Local-to-Global (LTG) Monte Carlo:
- Local: Conventional MC simulations of electron transport performed in well defined local geometries ("kugels" or spheres).
  - Monte Carlo with EGSnrc Code System - PDF for "kugels"
  - 5 sphere sizes (0.5-3.0 mm)
  - 5 materials (air, lung, water, Lucite and solid bone)
  - 30 incident energy values (0.2-25 MeV)
  - PDF table look-up for "kugels"
  - This step is performed off-line.
- Global: Particle transport through patient modeled as a series of macroscopic steps, each consisting of one local geometry ("kugel")

A “kugel”

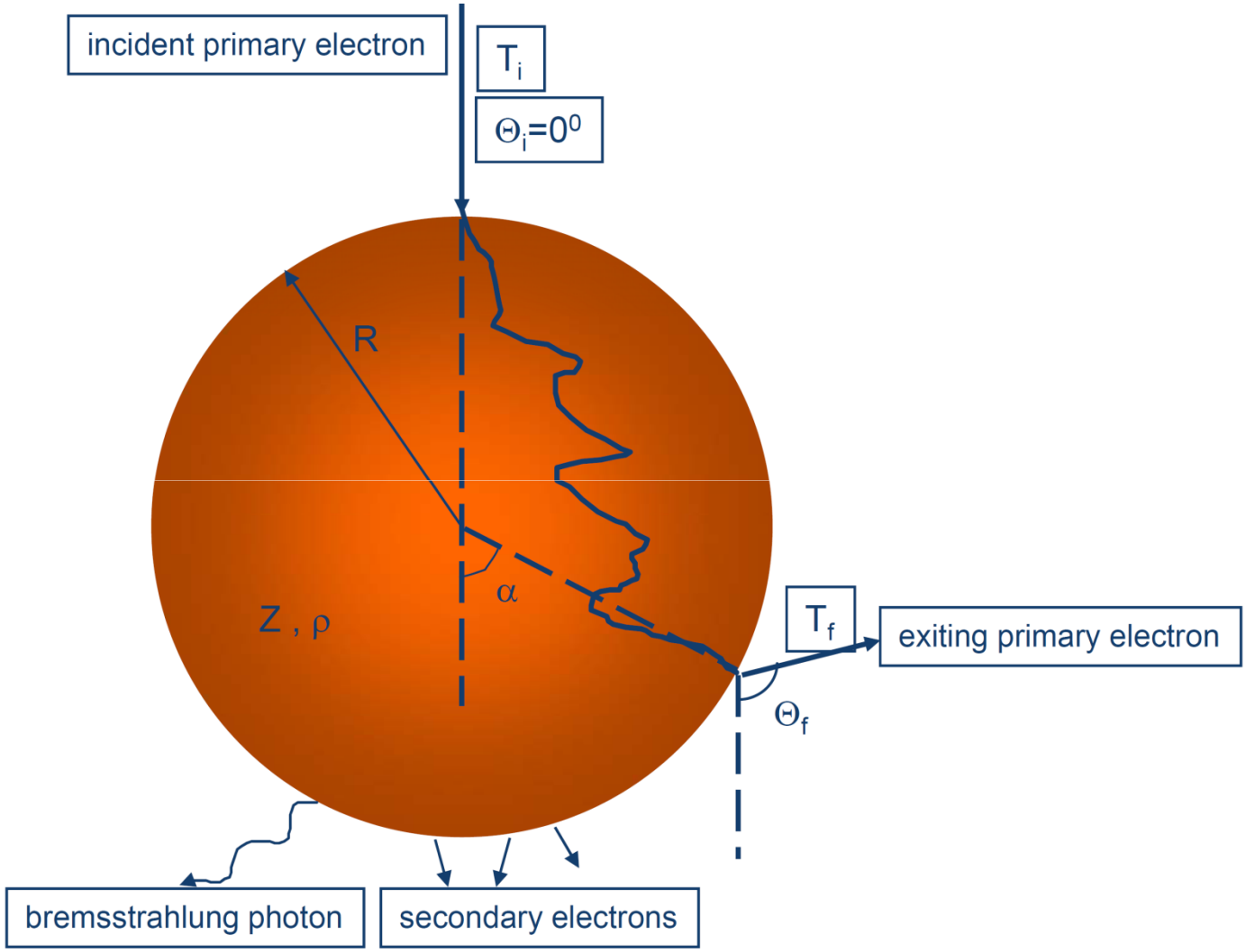

Kugel = sphere

MMC by Neuenschwander et al 1995

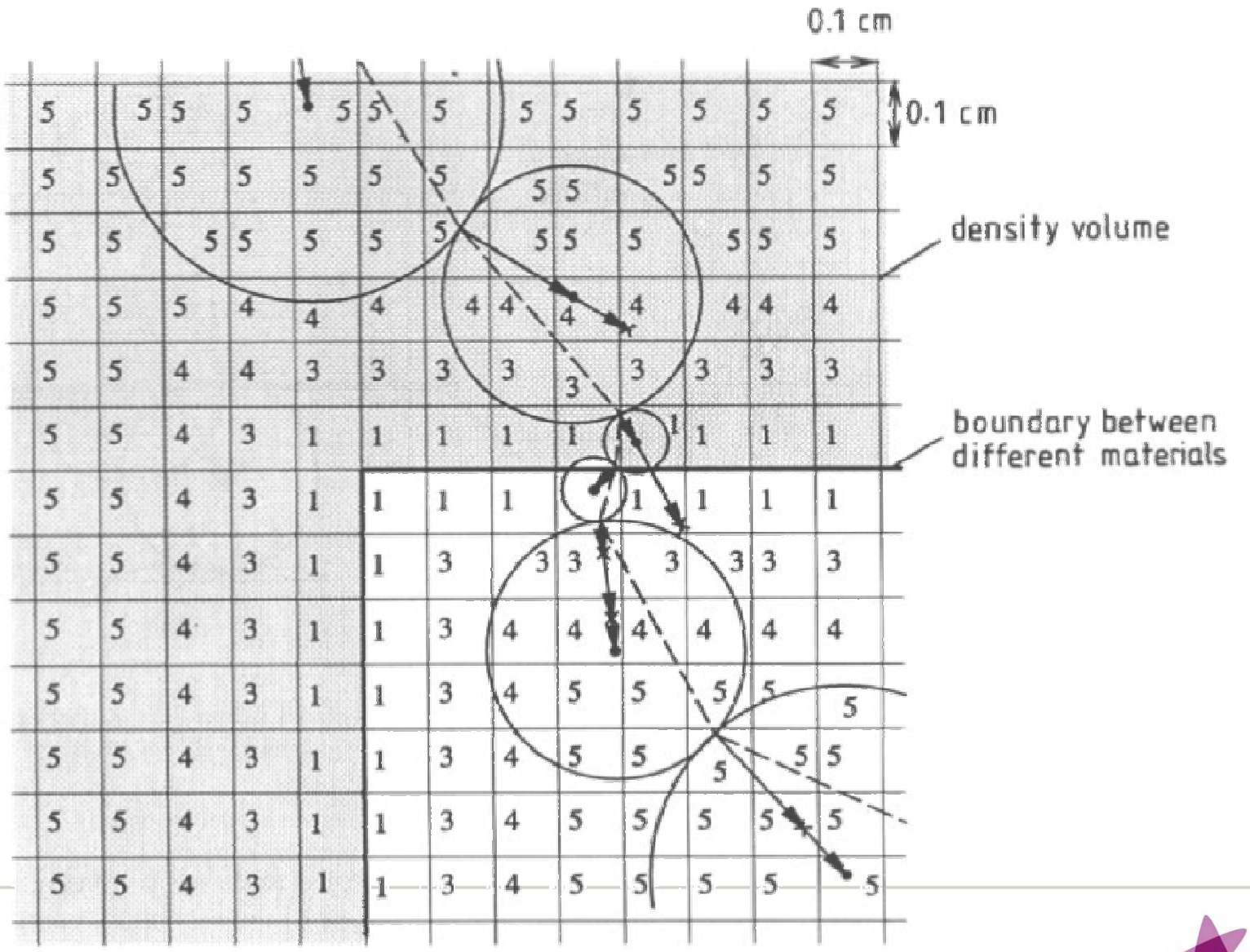

ESTRO School

MMC or kugel transport

- Global geometry calculations
  - CT images are pre-processed to user defined calculation grid
  - HU in CT image are converted to mass density
  - The maximum sphere radius and material at the center of each voxel is determined
- Homogenous areas
  - large spheres
- In/near heterogeneous areas
  - small spheres

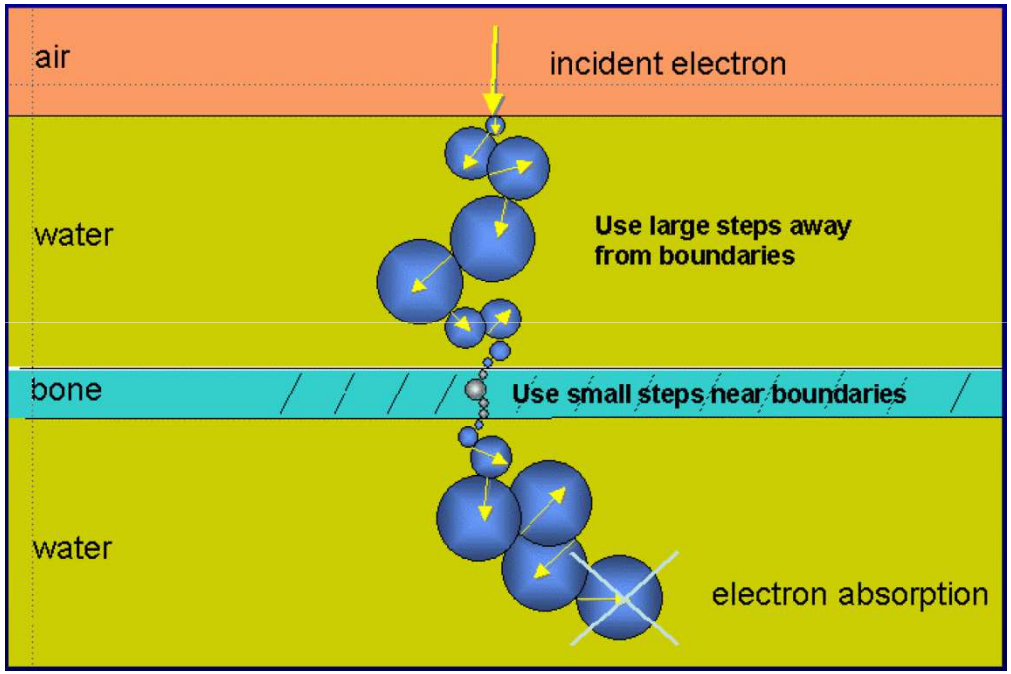

Adopted from DeMarco and Cygler

COMPARISONS

OMP MC vs EGSnrc

12 MeV – 14x14 cm^2 applicator

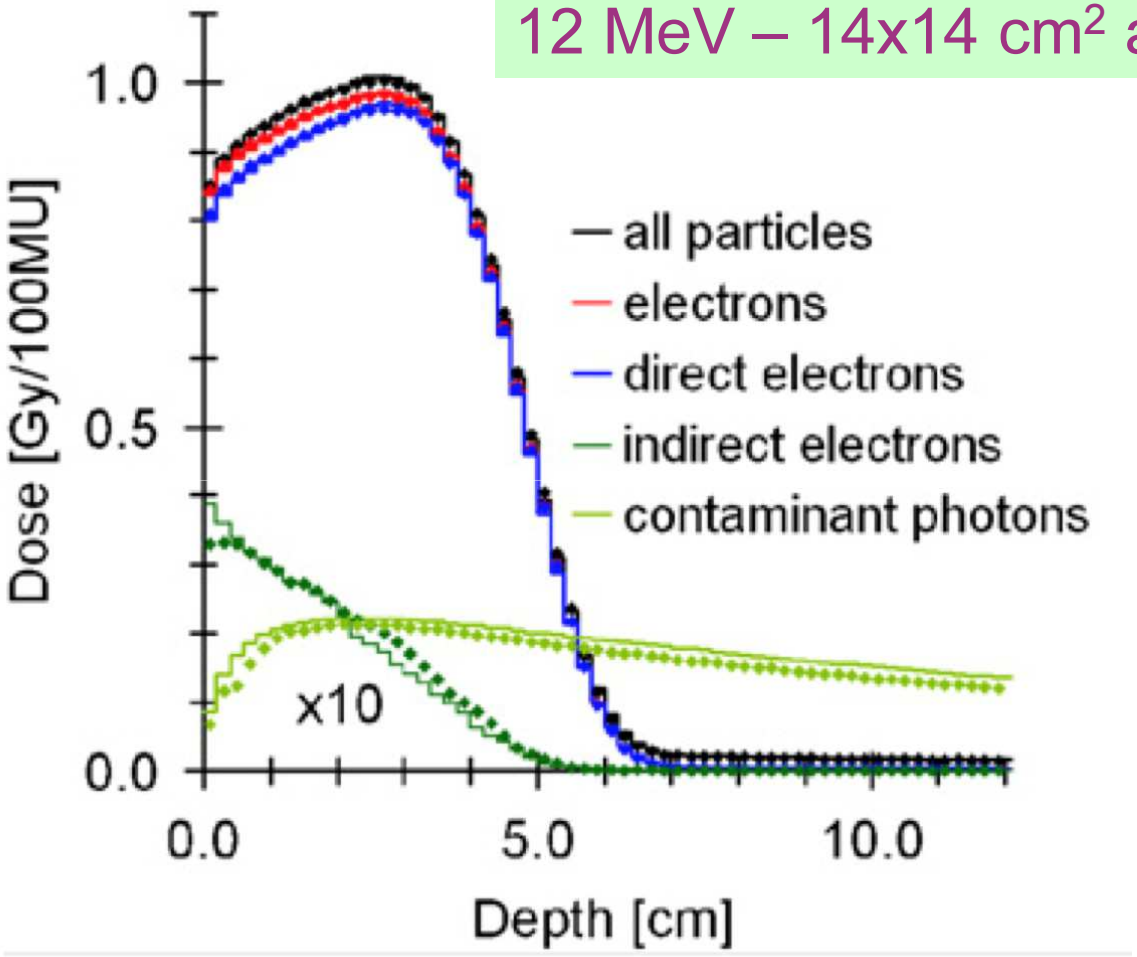

The possibility to separate different dose components for detailed performance QA

Wieslander and Knöös, PMB, 2006

ESTRO School

OMP MC vs EGSnrc

Wieslander and Knöös, PMB, 2006

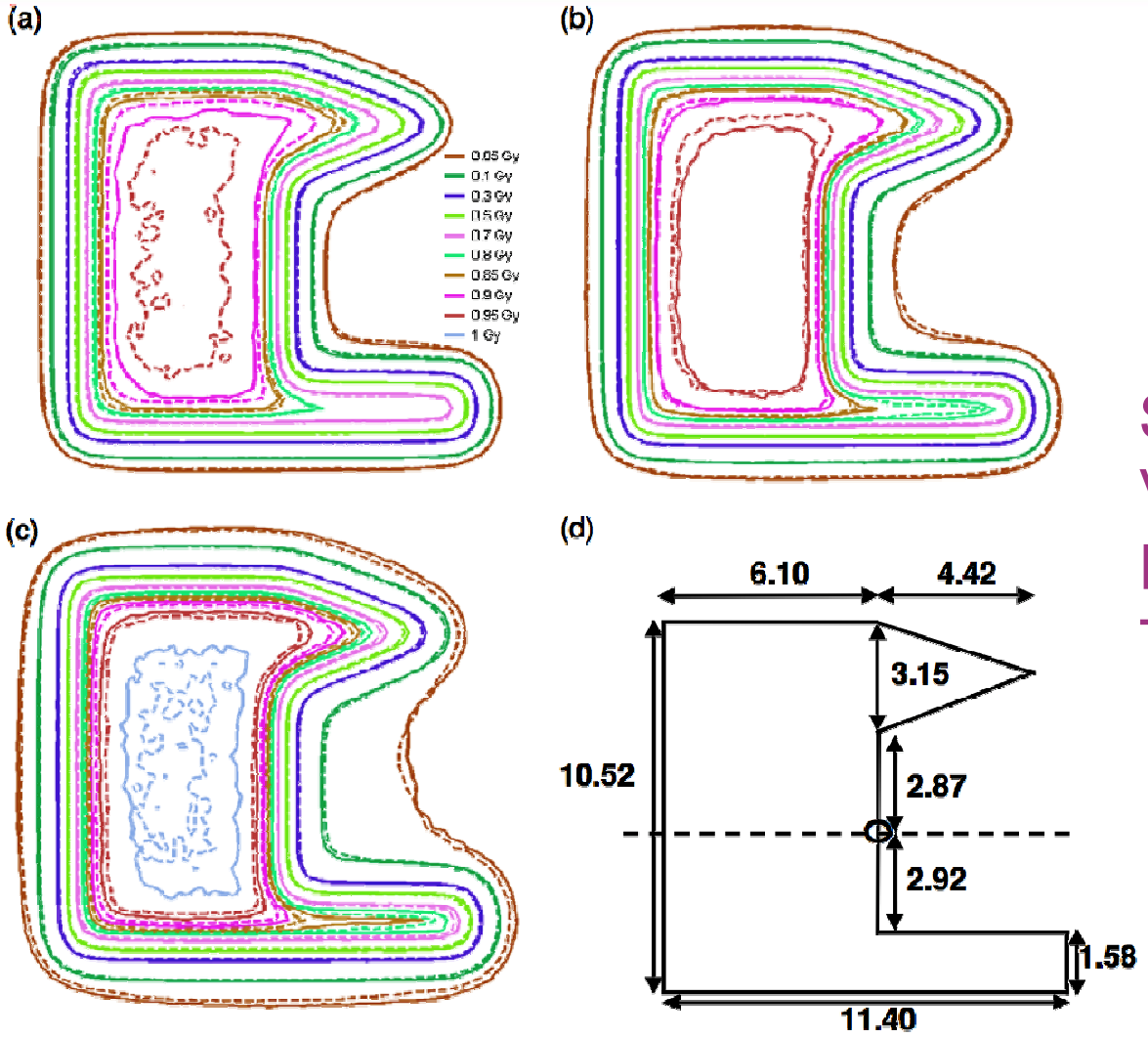

Solid lines
VA (EGSnrc)
Dashed lines
TPS (MC)

Figure 6. 2D isodose distributions in Gy/100 MU for the house field at 1.0, 2.0 and 3.0 cm for 6 (a), 12 (b) and 18 MeV (c), respectively. Solid lines represent the virtual accelerator and dashed lines the TPS. In panel (d), the design of the house field with dimensions given at SSD 100 cm is shown. The circle represents the centre of the 14 × 14 applicator.

ESTRO School

OMP MC vs EGSnrc

VMC++ vs EGSnrc (solid)

PB vs EGSnrc (solid)

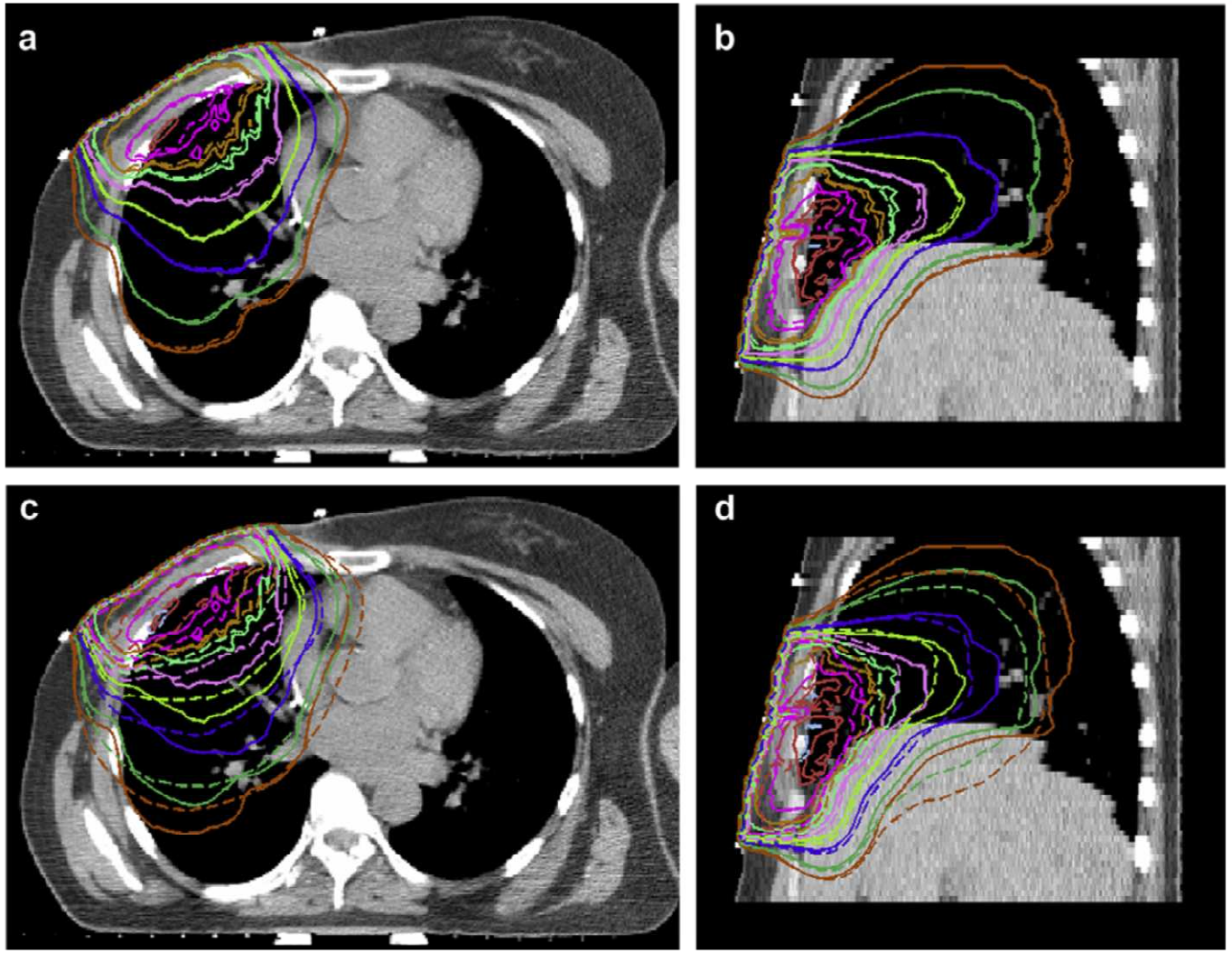

12 MeV electron, 100 MU
Isodose levels 0.05, 0.10, 0.30, 0.50, 0.70, 0.80, 0.85, 0.90, 0.95 and 1.00 Gy.

Wieslander and Knöös, RO 2007

ESTRO School

OMP MC vs EGSnrc

VMC++ vs EGSnrc (solid)

PB vs EGSnrc (solid)

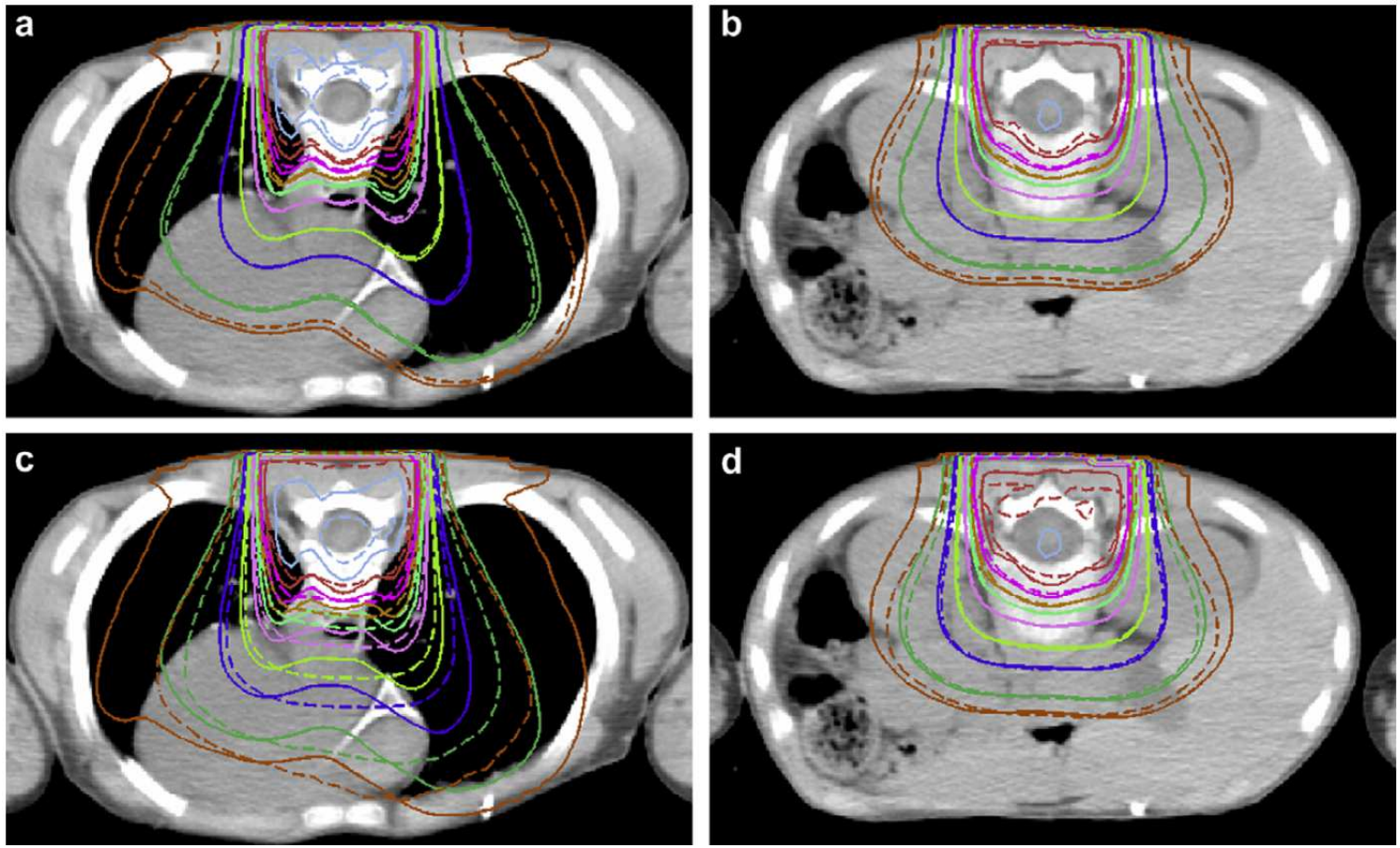

18 MeV electron, 100 MU
Isodose levels 0.05, 0.10, 0.30, 0.50, 0.70, 0.80, 0.85, 0.90, 0.95 and 1.00 Gy.

Wieslander and Knöös, RO 2007

ESTRO School

Electrons in CMS eMC 9 MeV

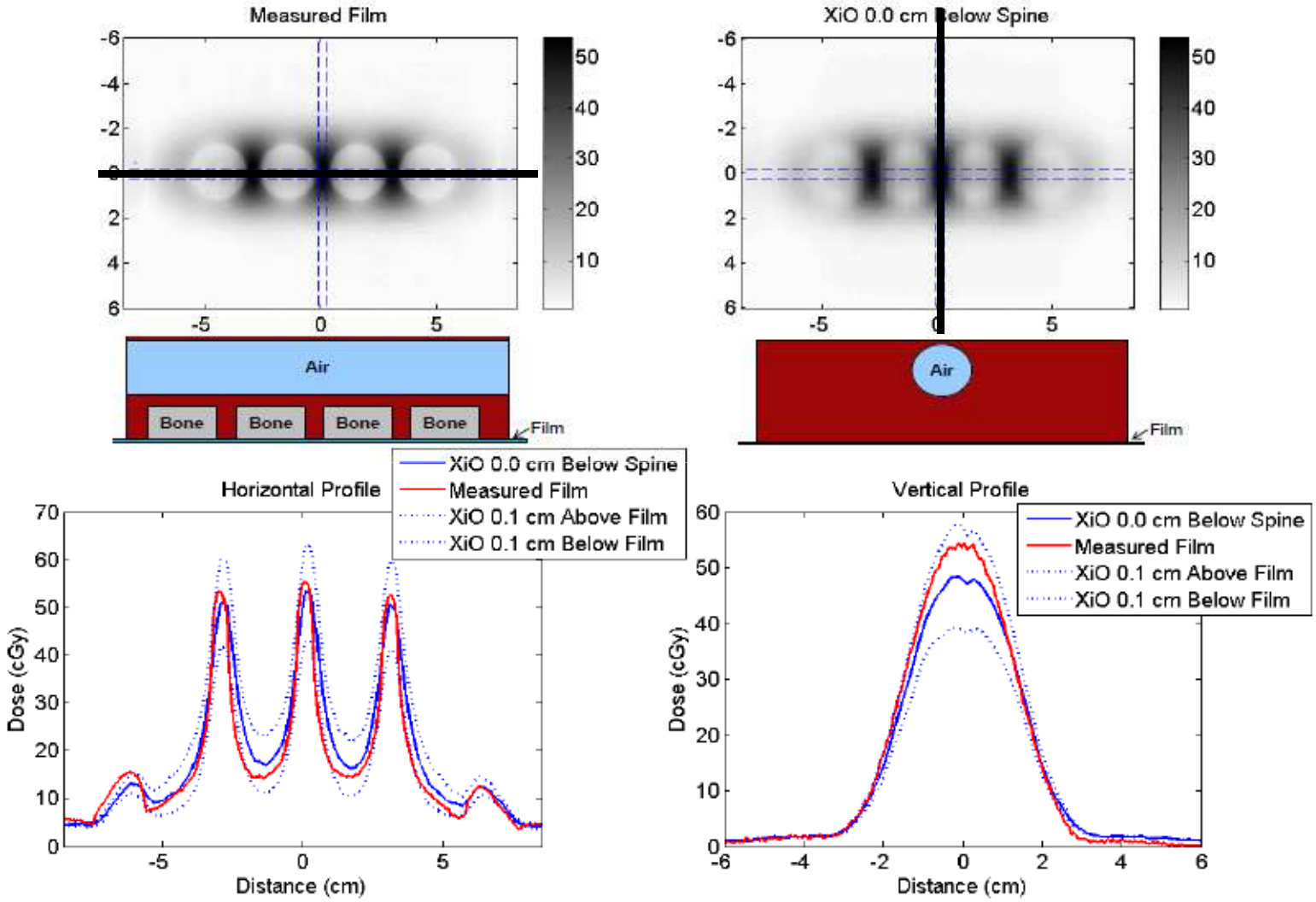

Vandervoort and Cygler, COMP 56th Annual Scientific Meeting, Ottawa June 2010

ESTRO School

Electron In Eclipse I

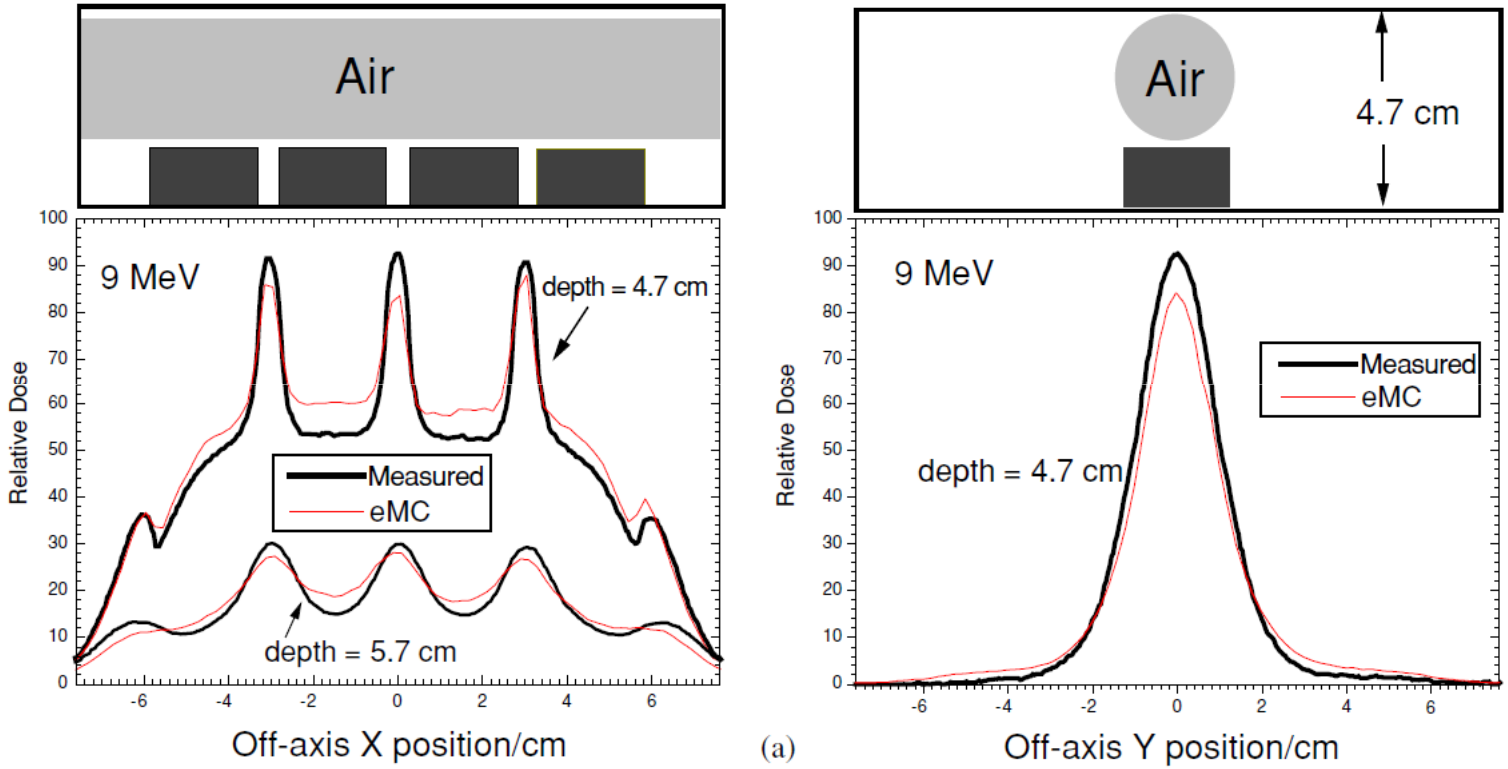

Ding et al PMB 2006

ESTRO School

Electron In Eclipse II

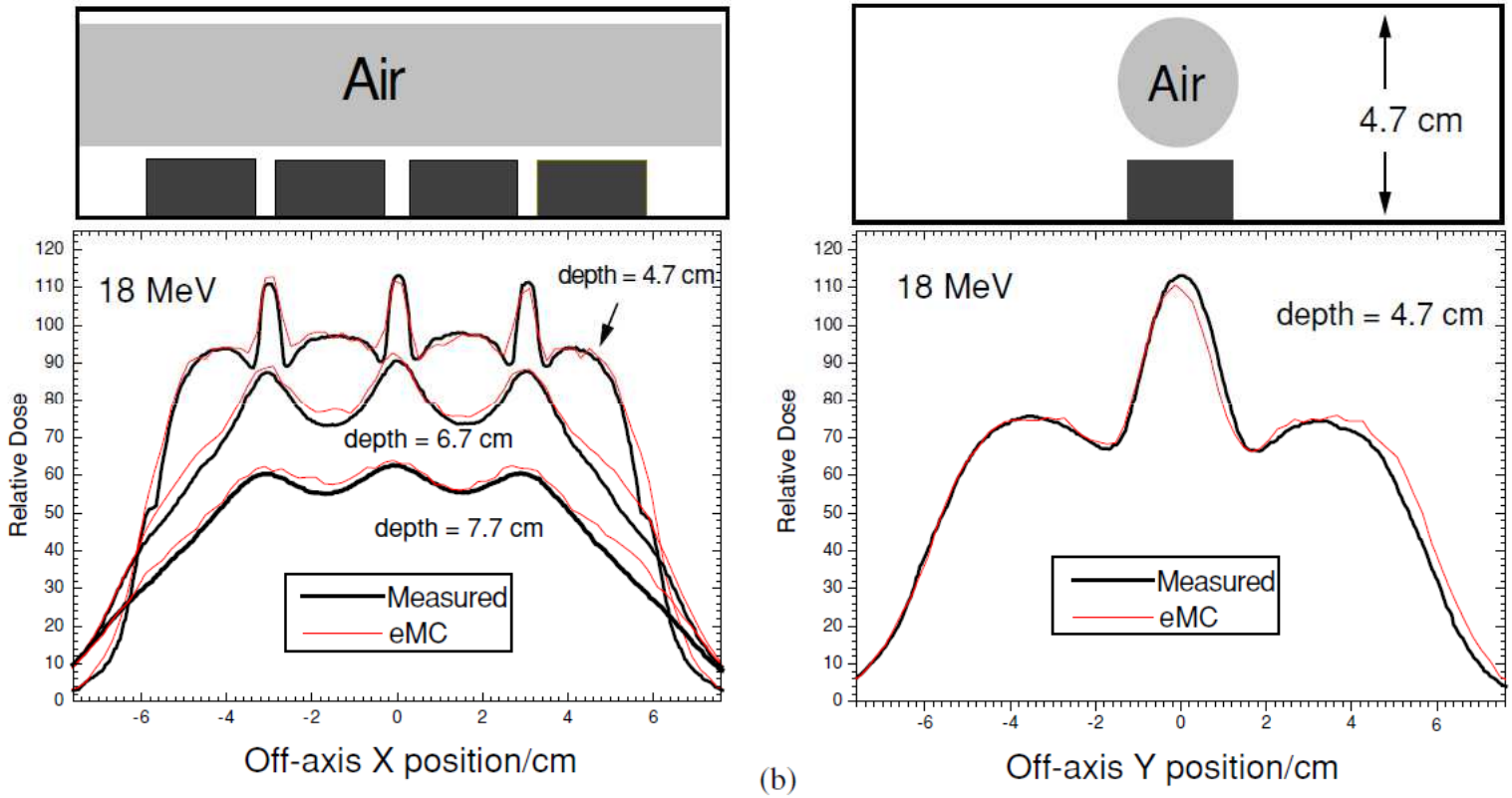

Ding et al PMB 2006

ESTRO School

Conclusions

- Commercial MC based TP system are available
  - easy to implement and use
  - MC specific testing required
- Fast and accurate 3-D dose calculations
- Single virtual machine for all SSDs
- Large impact on clinical practice
  - Accuracy improved
  - More attention to technical issues needed
  - Dose-to-medium calculated
  - MU based on real patient anatomy (including contour irregularities and tissue heterogeneities)
- Requirement for well educated physics staff

From Popple and Cygler at AAPM 2009

Selected suggested reading

- IAEA TRS 380 (2000): Absorbed Dose Determination in External Beam Radiotherapy: An International Code of Practice for Dosimetry based on Standards of Absorbed Dose to Water- International Atomic Energy Agency, Vienna.
- IPEM Code of practice for electron dosimetry,(2003), Phys Med Biol, 48:2929
- IAEA TRS 381 (1997): The use of plane parallel chambers in high energy electron and photon beams - International Atomic Energy Agency, Vienna
- AAPM Task Group 25 (1991) : Clinical electron-beam dosimetry - Med. Phys. 18(1),pp 73-109.
- AAPM Task Group 70 (2009)Recommendations for clinical electron beam dosimetry: Supplement to the recommendations of Task Group 25 -Med. Phys. 36(7), 3240-3269.
- ICRU report 35 (1984): Electron beams with energies between 1 and 50 MeV- International Commission on Radiation Units and Measurements, Bethesda, Maryland.
- Green D and Williams PC (1985), Linear Accelerators for Radiation Therapy, IOP Publishing, ISBN 07503 0476 6
- Gibbons J P (2000), Monitor Unit Calculations for External Photon and Electron Beams, Advanced Medical Physics Publishing Inc, ISBN: 1-883526-08-6
- Khan F.M. (2003): The Physics of Radiation Therapy- Williams and Wilkins, Baltimore, Maryland.
- Klevenhagen S.C.(1993): Physics and Dosimetry of Therapy Electron Beams- Medical Physics Publishing, Madison, Wisconsin.
- Klevenhagen S.C.(1985): Physics of Electron Beam Therapy, Medical Physics Handbooks 13, Adam Hilger Ltd, ISBN 0-85274-781-0
- Klevenhagen S. C (1979) High Energy Electrons in Radiotherapy (Eindhoven: Philips).
- Hogstrom KR (1991) Treatment planning in electron beam therapy. Front Radiat Ther Oncol 25, 30-52+61-63.
- Hogstrom KR and Almond PR (2006). Review of electron beam therapy physics. Phys.Med. Biol. 51 (R544-R489).

Thanks to the faculty who have contributed to these slides

Point kernel based models

Anders Ahnesjö
Uppsala University
Sweden

ESTRO

UPPSALA
UNIVERSITY

Learning objectives

1. Understand the basic principles of the point kernel superposition/convolution/collapse cone family of dose engine models

2. Understand the expected performance of point kernel models versus MC, pencil kernel and grid based models in terms of speed versus accuracy for different clinical situations

3. Contribute to the understanding of the different roles in modern TPS of dose engines versus fluence engines

Physical processes in MV photon beams

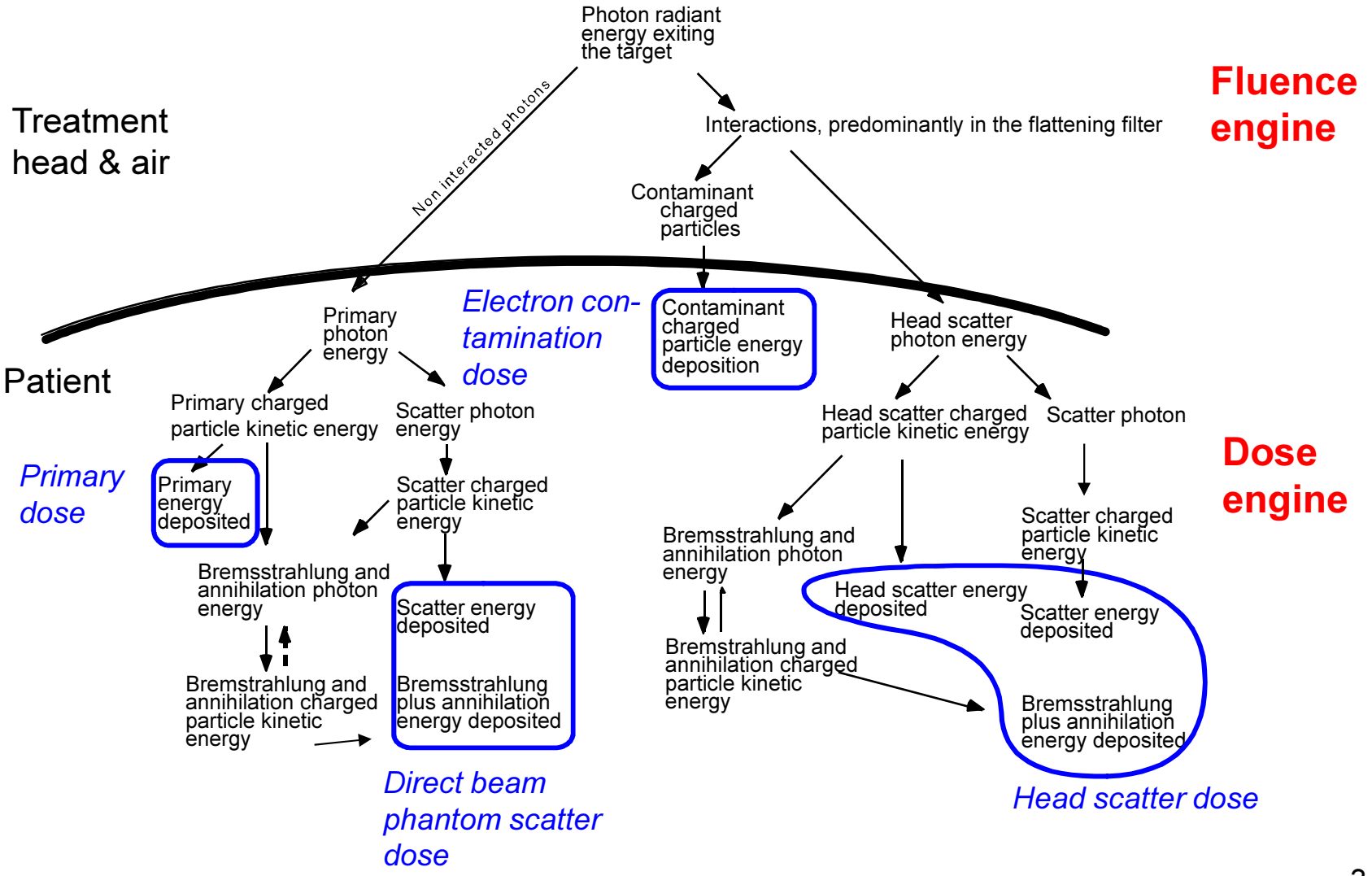

Ahnesjö and Aspradakis, PMB 44 (1999), R99-155

Dose deposition physics:

- Dose is deposited through electrons set in motion by the photon interactions
- Mean free path between electron interaction sites is nanometers (biomolecule size) - but the complete electron path length can be up to 10 cm in lung, less in other tissues
- For fields smaller than the actual electron range, the dose varies strongly with local density variations and field size
- For fields larger than the actual electron range, the dose varies less and is simpler to calculate

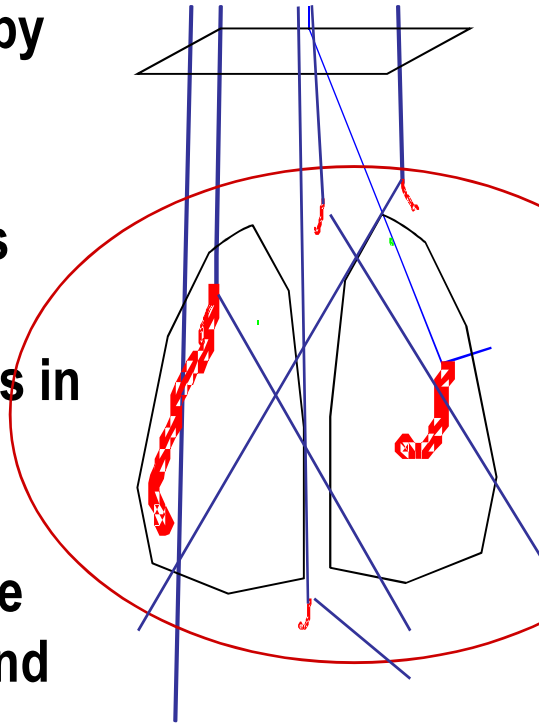

Photon dose calculation methods
Dose engines

”Model based”

“Factor based”

	Method characteristics	*Remarks*
Monte Carlo	Explicit particle transport simulation + Accurate - Noisy dose distributions	Standard research tool, clinical use under development
Analytic solvers	Solves numerically transport equtations + Accurate - Discretization effects	Standard tool in nuclear engineering, less common in medical physics
Point kernel methods ***“Convolution/superposition”*** ***“Collapsed Cone”***	Implicit particle transport + Accurate - Minor systematic errors	Current workhorse for accurate calculations in lung.
Pencil kernel methods	Heterogeneity impact through corrections	The workhorse for many applications, in particular IMRT optimization.
Scatter dose estimations	”Semi” pencil kernel metods	Often used for factorbased calculation schemes
1D heterogeneity corrections	Models what happen along the incident beam direction only	Can be used to correct dose calculated with any method for a homogeneous case

Hybrids possible

”Convolution/superposition”

Point kernel methods

”Collapsed Cone”

Primary Photon beam energy balance

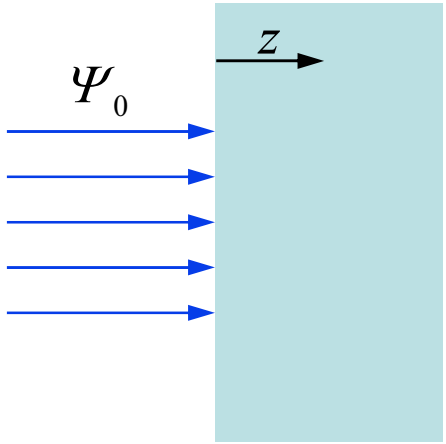

$\Psi_0 = E \cdot \Phi_0$ Incident energy fluence

$\Psi_0 e^{-\mu z}$ Attenuated energy fluence at depth *z*

$\frac{\mu}{\rho}\Psi_0 e^{-\mu z}$ Energy ”taken away” from the direct beam, TERMA, at depth *z*

$\frac{\mu_{en}}{\rho}\Psi_0 e^{-\mu z}$ Energy transfered into collision KERMA at *z*, it is appr. **Primary Dose**

$\frac{\mu - \mu_{en}}{\rho}\Psi_0 e^{-\mu z}$ Energy transfered into photon scatter, SCERMA, at depth *z*

TERMA, Total Energy Released per MAss
KERMA, Kinetic Energy Released per MAss
SCERMA, photon Scatter Energy Released per MAss
Collision KERMA+SCERMA=TERMA

Point Kernel methods:

- Analytical solution of primary particle transport in the phantom
- Use pre-calculated point kernels from Monte Carlo to describe the dose deposition around a primary photon interaction site
- Calculate dose by superposition of all contributions
- Fast superposition methods by use of the Collapsed Cone approximation (any media) or Fast Fourier Transforms (homogeneous media only).

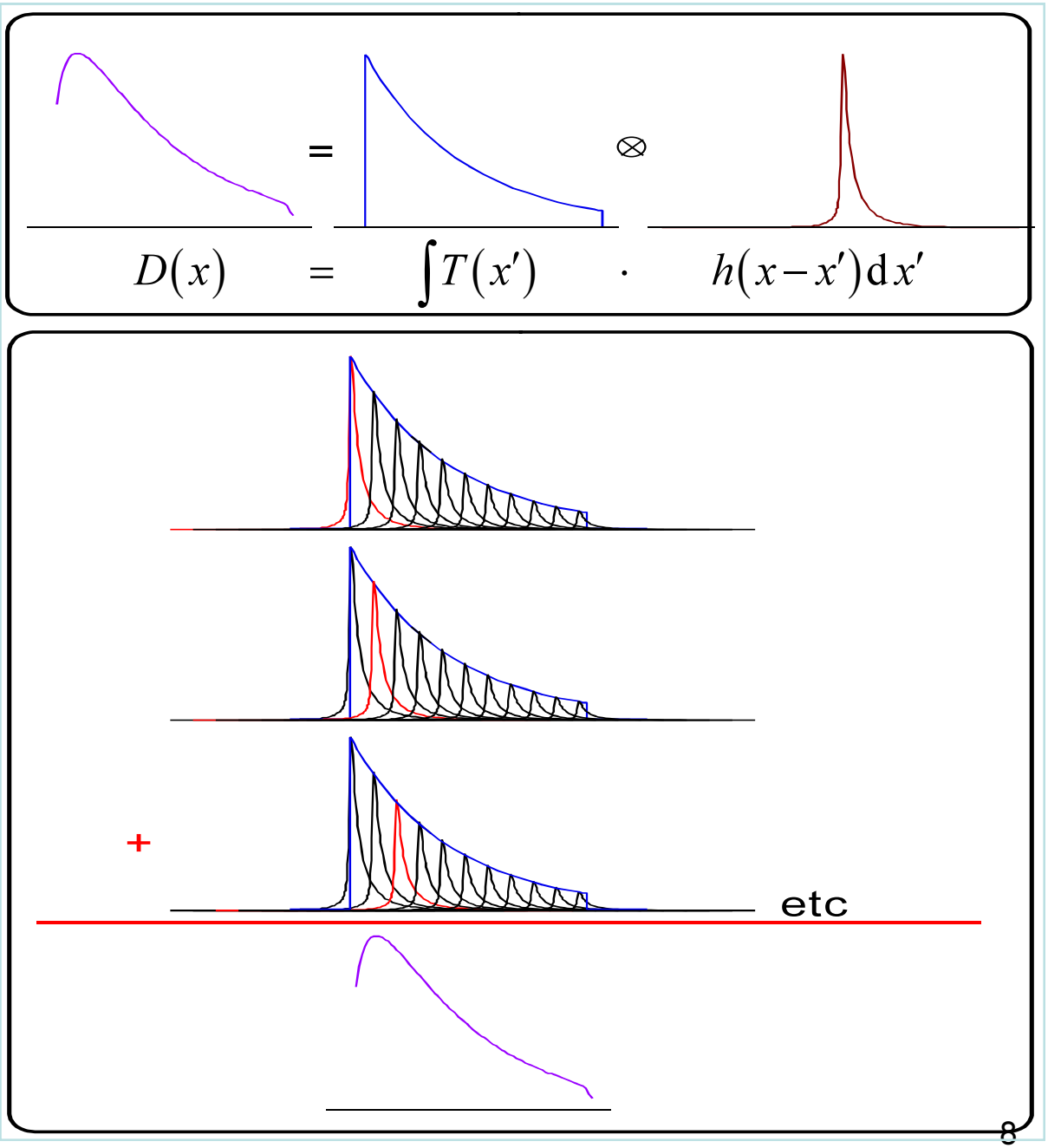

Point Kernel methods consist of two steps:

1. Trace the primary beam through the patient and calculate **how much, and where, the beam have "lost" energy** in the patient

2. **Redistribute ("blur")** that energy into patient absorbed dose **by means of point kernels** that describes the transport and energy absorption of the secondary particles set into motion via primary photon interactions

Tracing the primary beam to release energy (for later transport by point kernels)

Energy fluence

$$\Psi_E(\mathbf{r}) = \underbrace{\Psi_E(\mathbf{r}_0)}_{\substack{\text{Incident modulated and collimated energy fluence}}} \underbrace{\left(\frac{\mathbf{r}_0}{\mathbf{r}}\right)^2}_{\text{Inverse square}} \mathrm{e}^{\overbrace{-\int_{l_{\mathbf{r}_0}}^{l_{\mathbf{r}}} \mu(l)\,\mathrm{d}l}^{\substack{\text{Raytrace integral through CT-matrix}}}}$$

Collision KERMA (*the released energy to become primary dose*)

$$P(\mathbf{r}) = \int_E \frac{\mu_{\text{en}}}{\rho}(E,\mathbf{r}) \quad \Psi_E(\mathbf{r})\,\mathrm{d}E$$

SCERMA (*the released energy to become <u>sc</u>atter dose*)

$$S(\mathbf{r}) = \int_E \frac{\mu-\mu_{\text{en}}}{\rho}(E,\mathbf{r}) \quad \Psi_E(\mathbf{r})\,\mathrm{d}E$$

TERMA=collision KERMA+SCERMA

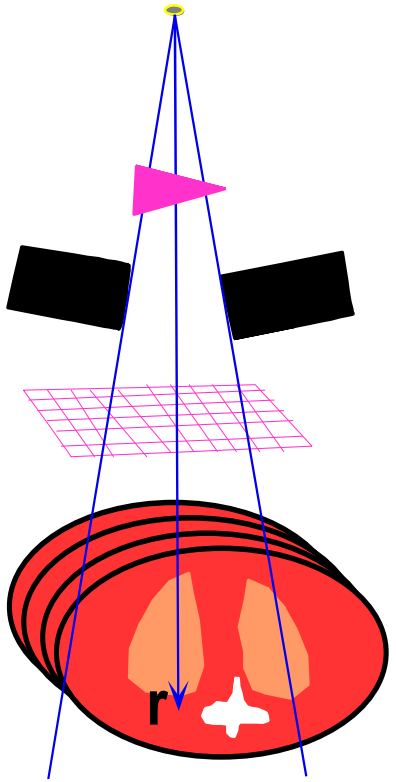

The result for each ray is weigthed by the value of the energy fluence bixel it passes!

Handling the beam spectrum – depth changes

Instead of integrating over energy, the collision kerma and scerma distributions can be calculated directly by raytracing with parameterized exponentials. Effect of spectral changing with depth, i.e. ***depth hardening*** is described by means of the hardening coefficients κ_P and κ_S

e.g. Pinnacle, Raystation

$$\frac{P(z)}{\Psi_0} = \sum_{i=1}^{n} \frac{\Psi_{E_i}}{\Psi_0} \mu_{\text{en}}(E_i) \mathrm{e}^{-\mu(E_i) z}$$

$$\frac{S(z)}{\Psi_0} = \sum_{i=1}^{n} \frac{\Psi_{E_i}}{\Psi_0} \left(\mu(E_i) - \mu_{\text{en}}(E_i)\right) \mathrm{e}^{-\mu(E_i) z}$$

e.g. Oncentra

$$\overset{\text{parameterization}}{=} \frac{P_0}{\Psi_0} \mathrm{e}^{-\mu_{\text{P}}(1-\kappa_{\text{P}} \cdot z) z}$$

$$\overset{\text{parametrization}}{=} \frac{S_0}{\Psi_0} \mathrm{e}^{-\mu_{\text{S}}(1-\kappa_{\text{S}} \cdot z) z}$$

parameters

$$\frac{P_0}{\Psi_0}, \mu_{\text{P}}, \kappa_{\text{P}}$$

$$\frac{S_0}{\Psi_0}, \mu_{\text{S}}, \kappa_{\text{S}}$$

The parameters derived using a (depth dose effective) spectrum. Only μ_{P} and κ_{P} are directly measurable quantities.

Heterogeneities considered by using different sets of parameters for each tissue type, mapped by using lookup tables from the Hounsfield numbers!

Handling the beam spectrum – offaxis changes

Effect of spectral changing with lateral position can be modelled by lateral variation of the energy release parameters. The offaxis variation of μ_P is experimentally accessible, variation of the other raytracing parameters can be correlated to μ_P, see MedPhys, Vol32, pp1722-37.

$$\left(\frac{HVL(0)}{HVL(\delta)} = \frac{\mu_P(\delta)}{\mu_P(0)}\right):$$

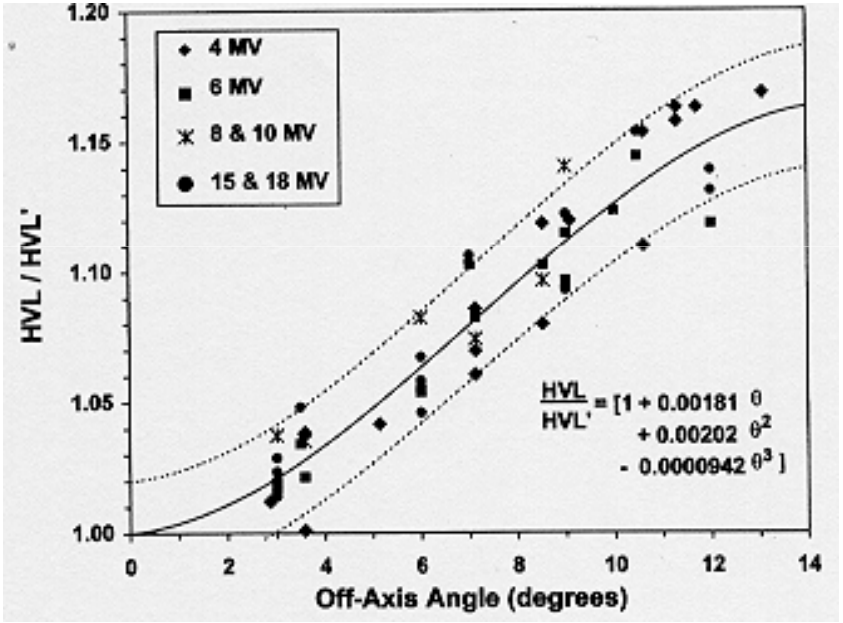

Tailor, R.C., *et al.* Medical Physics, 1998. **25**(5): p. 662-667

Heterogeneities considered by using different sets of parameters for each tissue type, mapped by using tissue lookup tables from the Hounsfield numbers!

Tissue and Phantom Material Characterization

-as used in Oncentra MP-

Composition	$\frac{\rho_{mass}}{\rho_{mass,H_2O}}$	$\frac{\rho_{elec}}{\rho_{elec,H_2O}}$	*HN*
Air (outside patient)	0.00121	0.00109	-992
Air (inside patient)	0.00121	0.00109	-976
Lung (ICRU 44)	0.50	0.50	-480
Adipose (ICRU 44)	0.95	0.95	-96
Muscle (ICRU 44)	1.05	1.04	48
Cartilage (ICRP 23)	1.10	1.08	128
2/3 Cartilage, 1/3 Bone	1.35	1.29	528
1/3 Cartilage, 2/3 Bone	1.60	1.52	976
Bone (ICRP 23)	1.85	1.72	1488
Bone (ICRP 23)	2.10	1.95	1824
½ Bone, ½ Aluminum	2.40	2.15	2224
Aluminum	2.70	2.34	2640
Aluminum	2.83	2.46	2832
Iron	7.87	6.60	>2832
Water	1.00	1.00	-

Note: *Water is not part of an anatomical scale!*

The scale will interpret a water CT-image as a mixture of adipose and muscle!

Tissue and Phantom Material interpolation

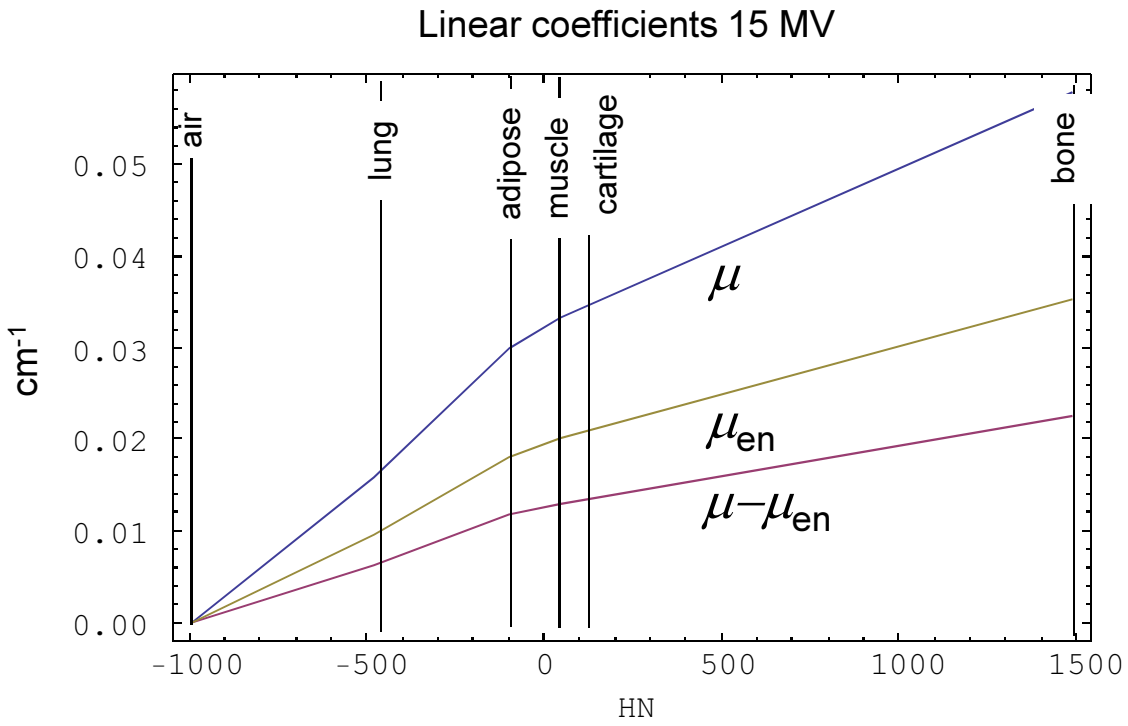

Dose Properties of Point Kernels

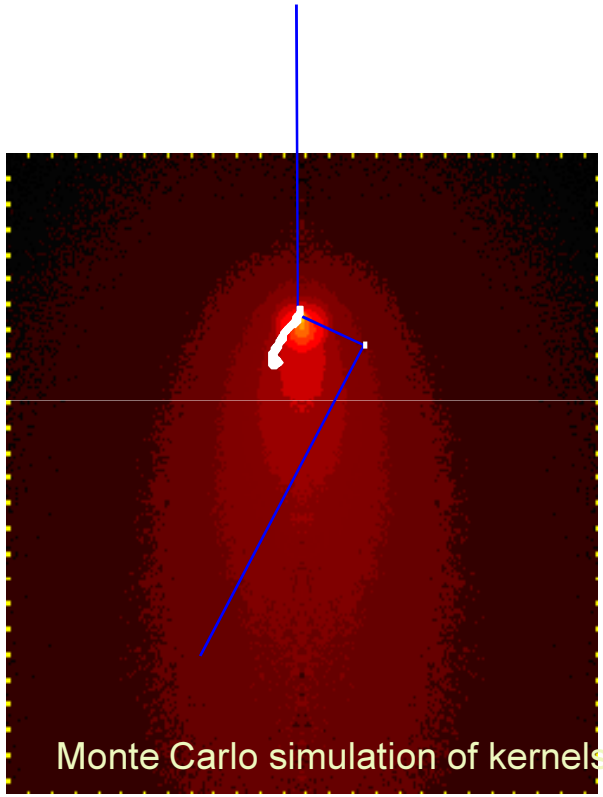

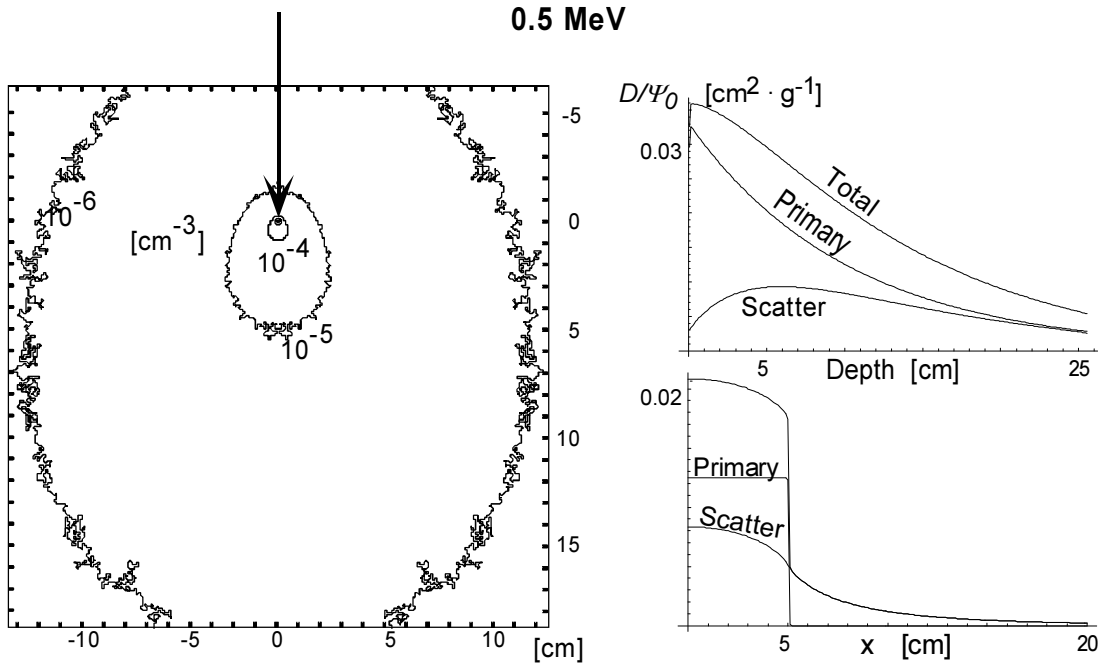

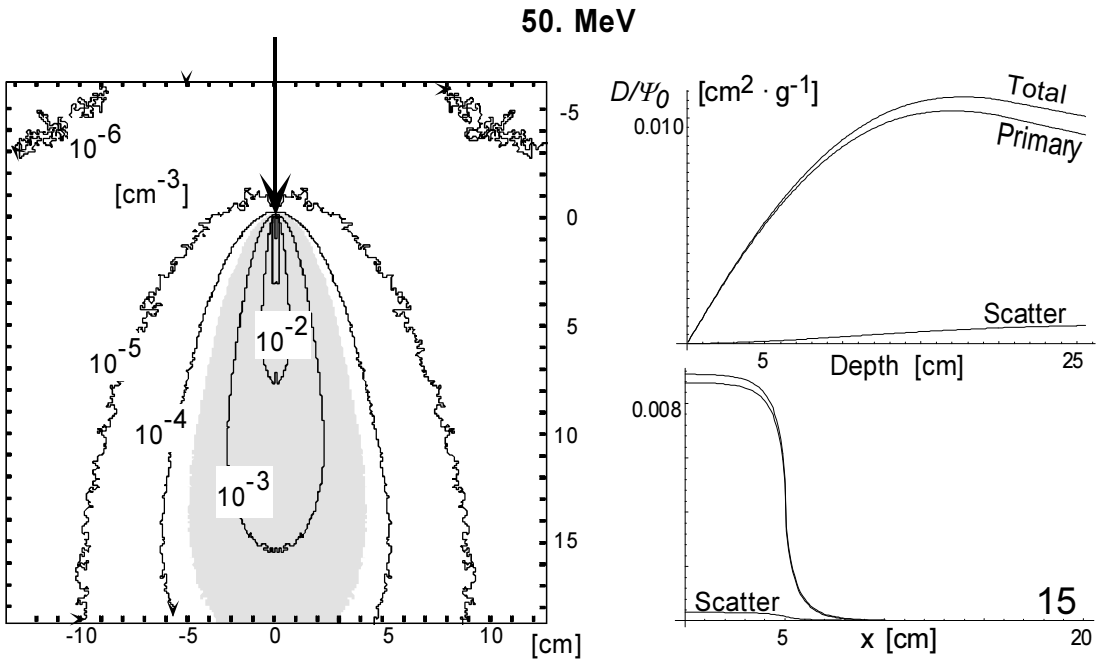

Dose properties for point kernels cont.:

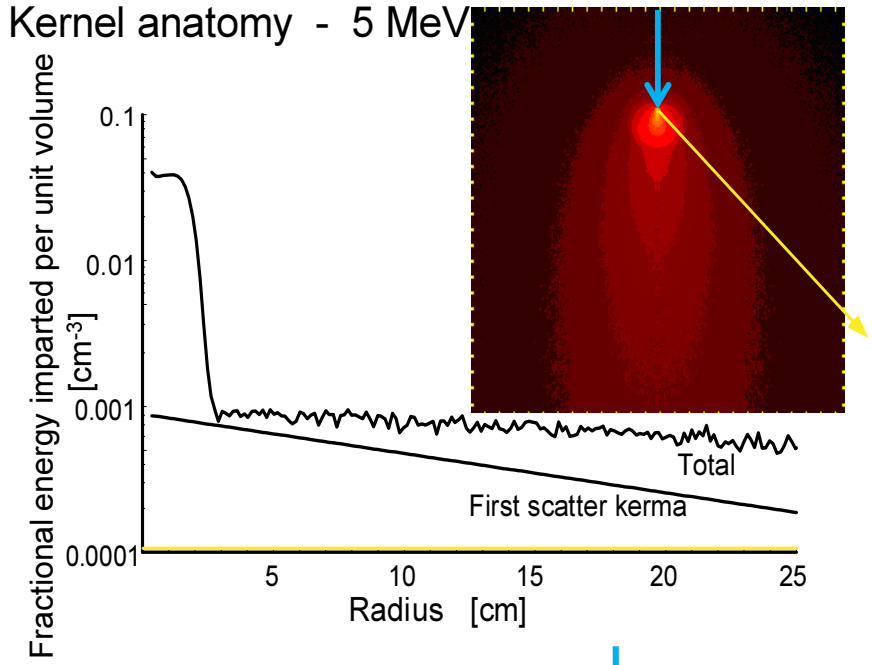

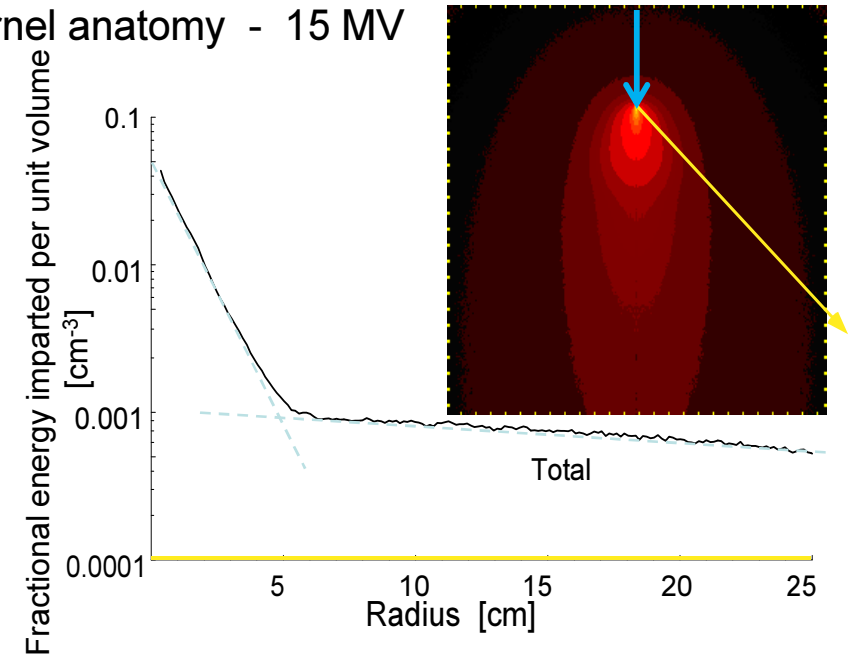

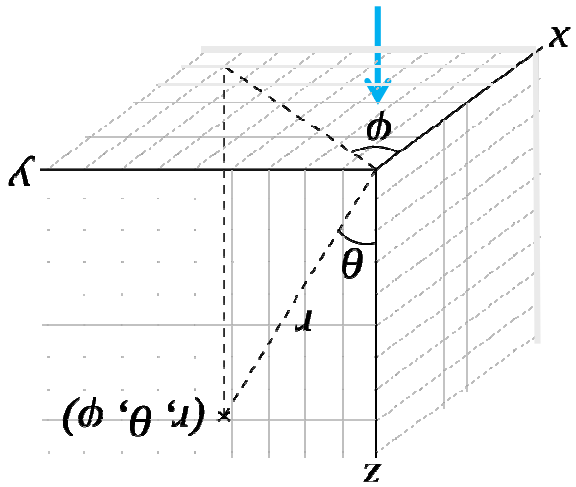

Suitable parameterization of polyenergetic point kernels

$$h(r,\theta) = \frac{A_\theta \, \mathrm{e}^{-a_\theta r} + B_\theta \, \mathrm{e}^{-b_\theta r}}{r^2}$$

Ahnesjö, *A. Med. Phys.* **16** 577–92

Discretizing the angular part of the point kernels: the collapsed cone approximation for superposition of point kernels

Discretization:

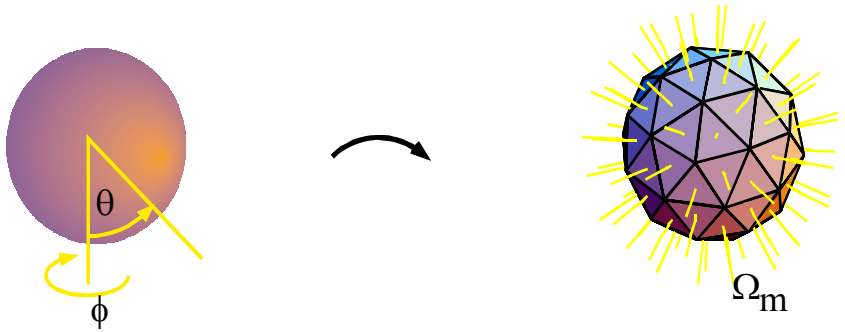

Consequence – displacement of energy deposition location that increase with distance from interaction point

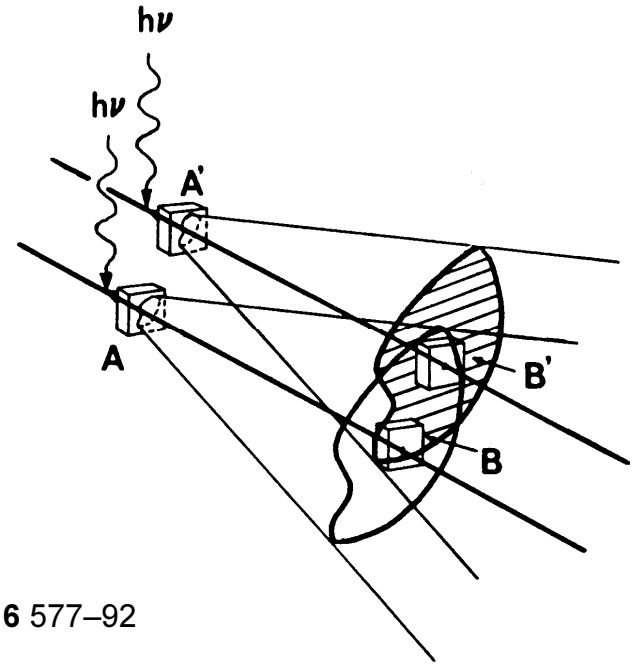

Ahnesjö, *A. Med. Phys.* **16** 577–92

Discretization and parameterization:

Most energy is transported in the forward direction, hence it make sense to have smaller bins in the forward direction.

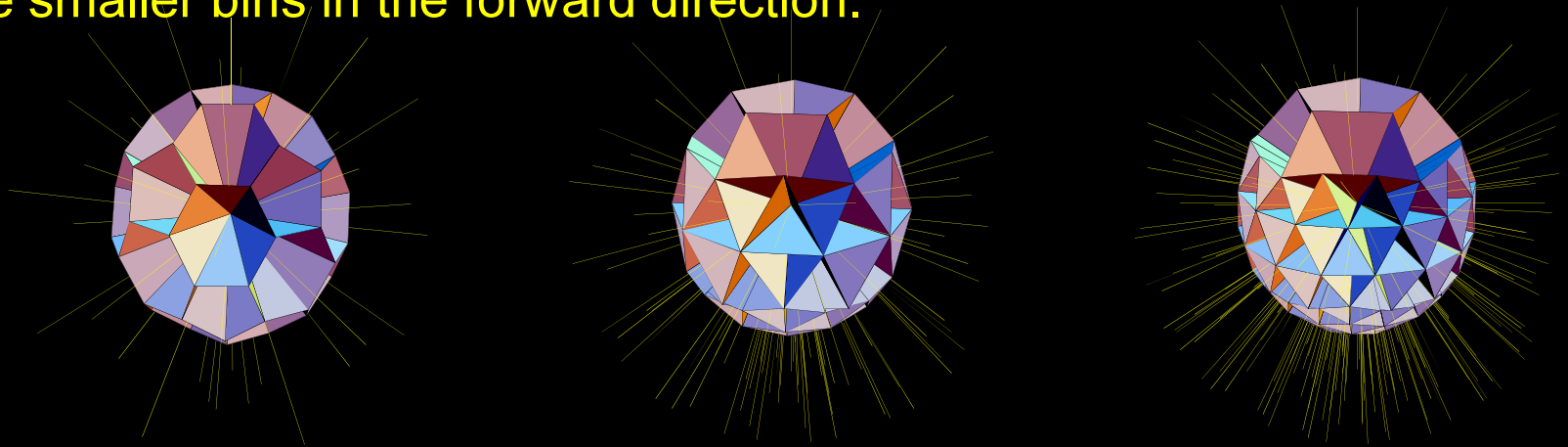

36 bins **106 bins (default in Oncentra, Monaco)** **201 bins**

Discretization into angular bins causes $1/r^2$ dependence in parameterization to vanish

$$h_m(r,\theta) = \iint_{\theta,\phi\in\Omega_m} \frac{A_\theta\, \mathrm{e}^{-a_\theta r} + B_\theta\, \mathrm{e}^{-b_\theta r}}{r^2} \cdot r^2 \sin\theta\, \mathrm{d}\theta\, \mathrm{d}\phi =$$

$$= \Omega_m \left(A_{\Omega_m}\, \mathrm{e}^{-a_{\Omega_m} r} + B_{\Omega_m}\, \mathrm{e}^{-b_{\Omega_m} r} \right)$$

Collapsed Cone transport scheme

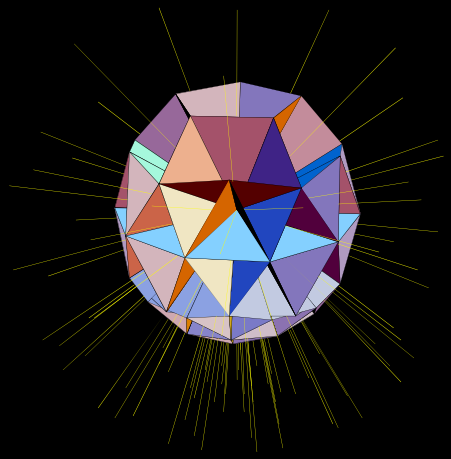

Cone axis

Transport lines

Incident beam

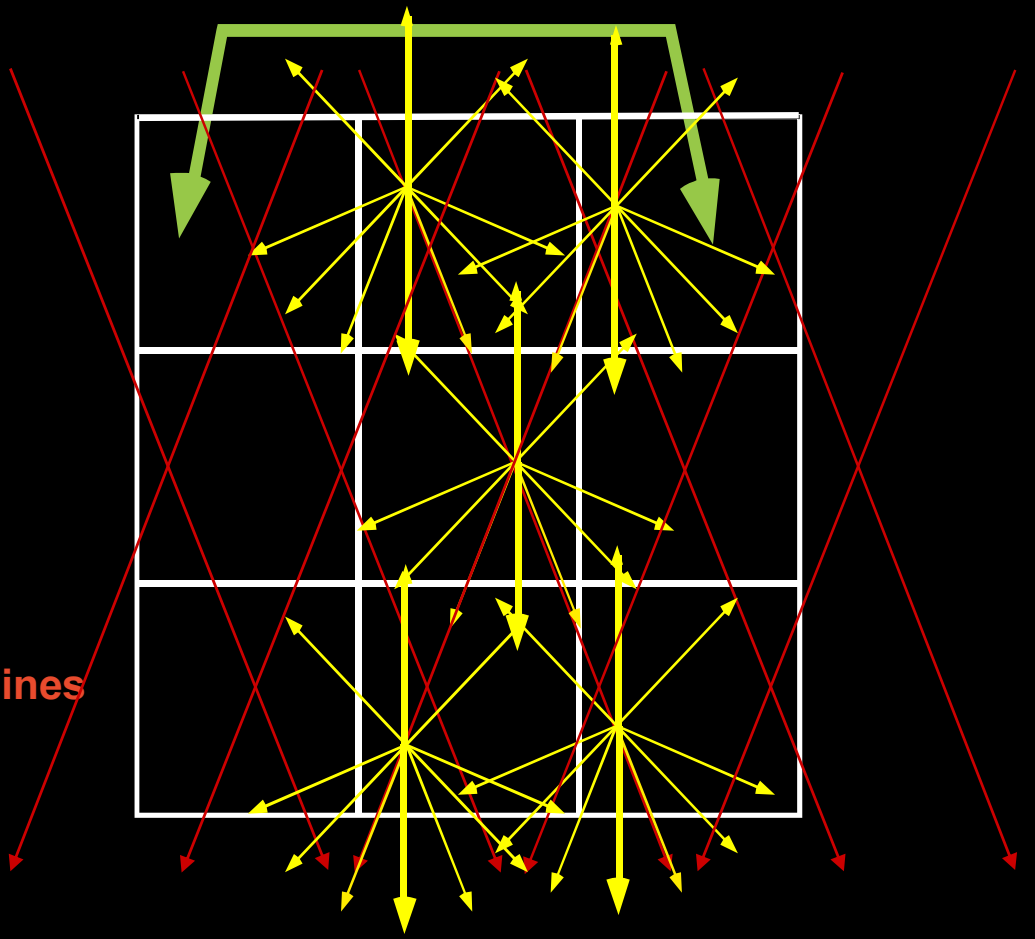

Radiant energy transport along a transport line

Analytical raytrace of kernel exponential through a voxel constitutes a transport step of the radiant energy:

$$R_{\text{out}}(\ell) = R_{\text{in}} \cdot \mathrm{e}^{-a\ell} + \frac{k}{a}\left(1 - \mathrm{e}^{-a\ell}\right)$$

attenuation of incoming energy

radiant energy contribution from the voxel considering intravoxel attenuation

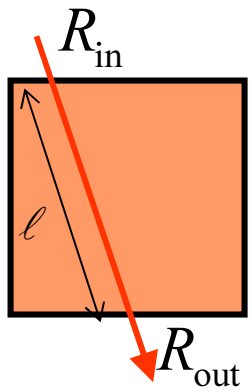

Energy deposited inside the voxel (appr. $a \cdot R$) becomes *the deposited dose*

- Parameter a from kernel parameterization and is scaled to represent the voxel medium, k stems from incident beam energy release (coll KERMA and SCERMA) and medium
- Performed separately for primary and scatter dose

More about transport along a line…

Factorization of attenuation:

$$L = \sum_i \ell_i$$

$$\mathrm{e}^{-aL} = \mathrm{e}^{-a\sum_i \ell_i} = \mathrm{e}^{-a\ell_1}\,\mathrm{e}^{-a\ell_2}\,\mathrm{e}^{-a\ell_3}\ldots = \prod_i \mathrm{e}^{-a\ell_i}$$

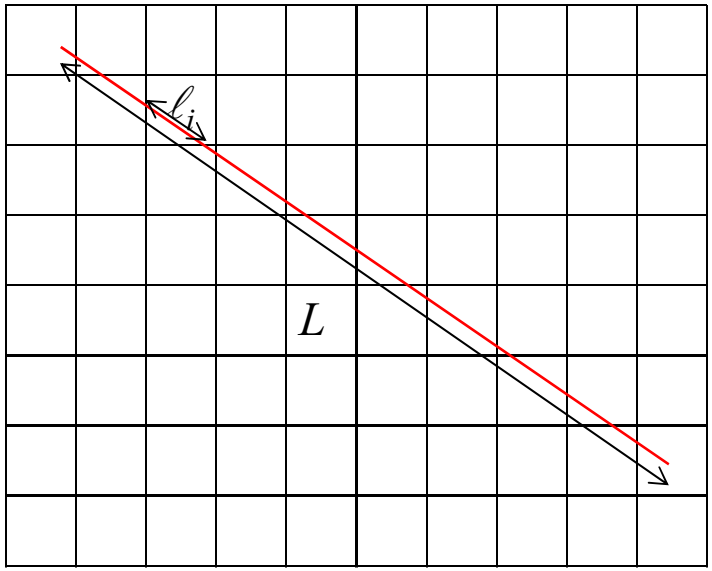

Transport of radiant energy along line:

$$R_i = R_{i-1}\,\mathrm{e}^{-a\cdot\ell_i} + \Delta R_i$$

Net energy release from a step ℓ_i ("collapsed" solid angle $\Delta\Omega$, kernel=$A\mathrm{e}^{-a\ell}$:

$$\Delta R_i = \int_0^{\ell_i} \underbrace{T_i \cdot \rho_i \cdot \Delta\Omega \cdot \frac{A}{a}}_{\text{energy release per length}} \underbrace{\mathrm{e}^{-a\cdot(\ell_i-\ell')}}_{\substack{\text{attenuation from point of release } \ell' \\ \text{to exit at } \ell_i}} \mathrm{d}\ell' = T_i \cdot \rho_i \cdot \Delta\Omega \cdot \frac{A}{a^2}\left(1-\mathrm{e}^{-a\cdot\ell_i}\right)$$

Local dose absorption: $$D_i \approx a\,\frac{R_{i-1}+R_i}{2}$$

Kernel tilting

Consider a point kernel and a transport direction defined for one of the axes. In diverging beams, the kernel transport angle θ varies with location:

- Kernel $h(r) = \dfrac{A_\theta e^{-a_\theta r}}{r^2}$
- Define $\theta' = \theta + \delta$
- Approximate

$$A_{\theta'} = A_\theta + c_1\delta + c_1\delta^2$$

$$a_{\theta'} = a_\theta + d_1\delta + d_1\delta^2$$

- Parameters c_i and d_i determined from Monte Carlo data

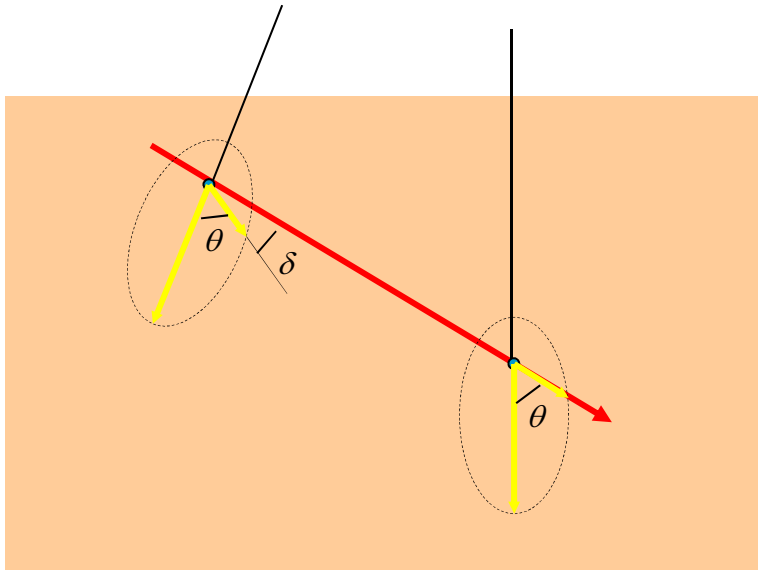

Tilting cont...

Effects increase with

- tilting angle, i.e.
  - shorter SSD
  - larger fields (and off axis segments)
- longer particle range, i.e.
  - low density regions (lung)
  - higher energies

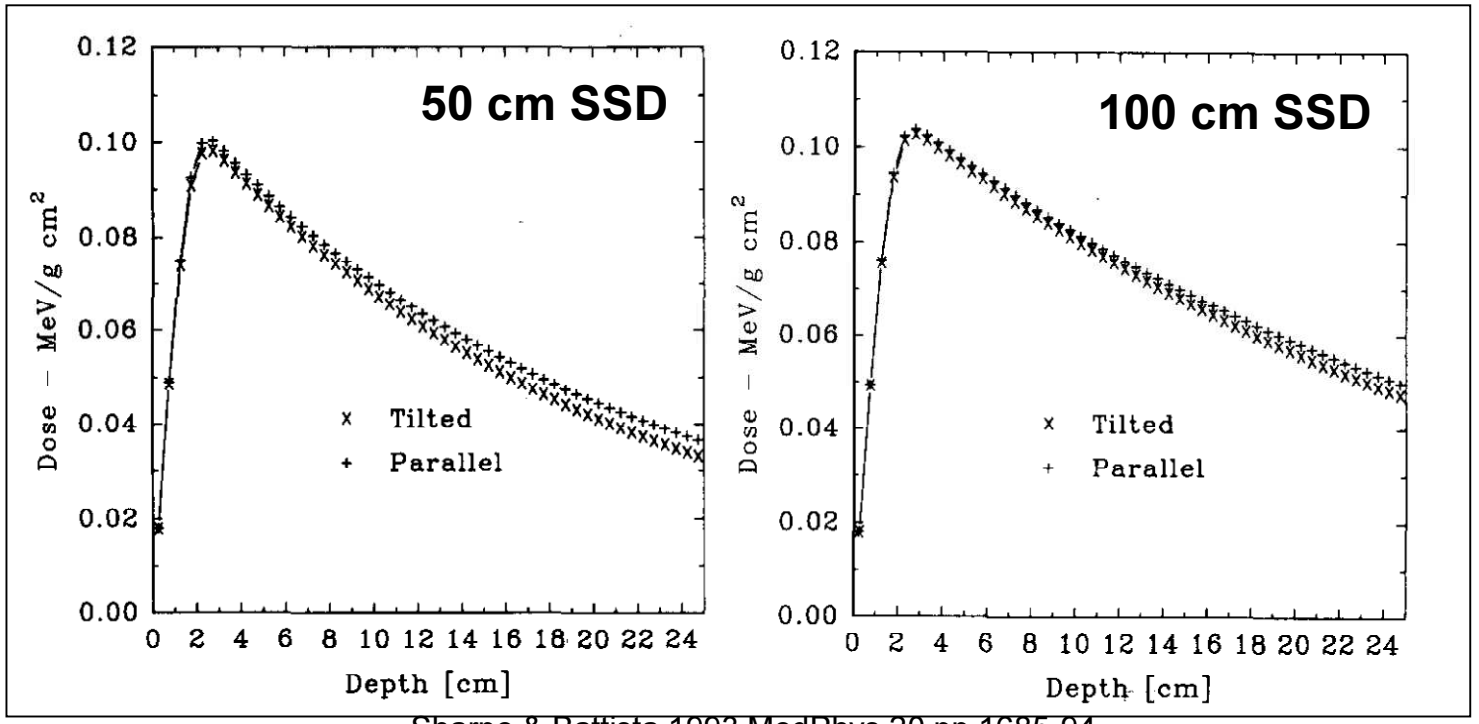

Sharpe & Battista 1993 MedPhys 20 pp 1685-94

18 MV on lung phantom

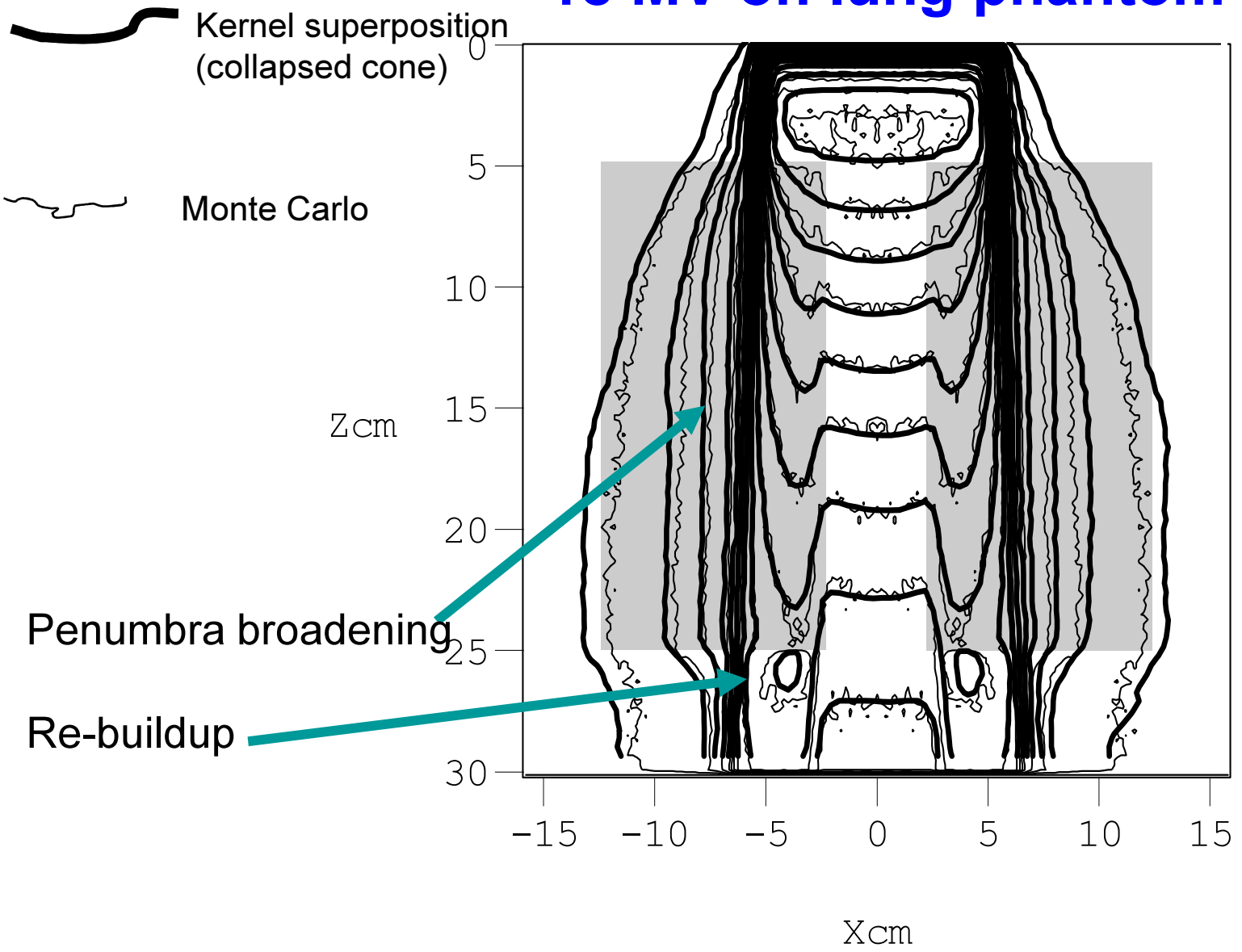

Modelling charged particle contamination

Has to be added as a separate model of the pencil kernel type:

Ahnesjö and Andreo [4]

$$\frac{p_{c_\pm}}{\rho}(r,z) = \alpha e^{-\beta z} e^{-\gamma r^2}$$

The parameters α, β, and γ can be determined through fitting to the difference between measurements and calculated photon dose.

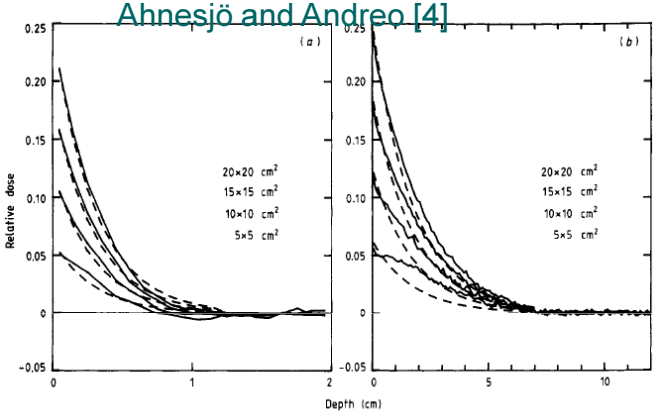

Figure 3. Contaminant dose distributions, expressed in fractions of the maximum total dose, for various field sizes of 4 MV (*a*) and 24 MV (*b*) photon beams. The dashed curves denote the simulated distributions (equation (9)) and the full curves the mean reconstructed distributions.

$$\frac{D_{c_\pm}(z,f)}{\psi} = \alpha e^{-\beta z} \int_{-f/2}^{f/2} \int_{-f/2}^{f/2} e^{-\gamma(x^2+y^2)} dx\, dy$$

$$= \alpha e^{-\beta z} \frac{\pi}{\gamma} \operatorname{erf}^2\left(\sqrt{\gamma}\frac{f}{2}\right),$$

where the error function is defined as

$$\operatorname{erf}(x) = \frac{2}{\sqrt{\pi}} \int_0^x e^{-t^2} dt.$$

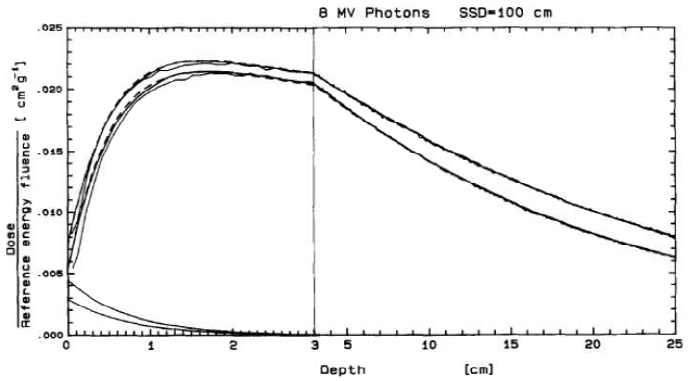

Ahnesjö *et al* Med Phys 19, 263-73

Summary of Point Kernel model properties

- Heterogeneities are considered through scaling of the rectilinear transport along all lines, hence it models:
  - loss of CPE for small fields and in lung
  - penumbra broadening in lung
  - rebuildup after low density media
- Major limitations:
  - rectilinear scaling coarse approximation for multiple scattering
  - angular discretization effects
- Use of media specific μ_{en} in primary raytrace yield dose to medium in medium (not water in medium) but is implementation dependent!
- The dose calculation time for N^3 voxels is with the Collapsed Cone approach reduced from being proportional to N^7 operations to to $M \cdot N^3$ where M is the number of transport directions
- Core calculation loops only a few hundred lines of code, much less complex than a multisource beam modelling code

What about calculation time and accuracy?

Several papers compare CC, PK, MC and measurements

Calculation times CC

(old data, so absolute timing obsolete...)

Calculation time is direct proportional to # voxels times # kernel directions:

Example: # voxels=128x128x128 (appr. $2 \cdot 10^6$), # directions=106

Configuration	**Time (s)**
Masterplan 3.0 Pentium 4 2.8 GHz	210
*Pentium 4 2.8 GHz, improved coding	114
*8 core Xeon 1.86 GHz (1 thread)	95
*8 core Xeon 1.86 GHz (8 threads)	13
*GPU GeForce 8800 GTX	2

The calculations for the parallel transport lines used in the CC approach are extremely suitable for implementation on parallel hardware!

*Kloppenborg B and Loos R 2007 "Parallel collapsed cone dose calculations using a Graphics Processing Unit", Bachelor Thesis, Saxion Hogeschool (Enschede, Netherlands)

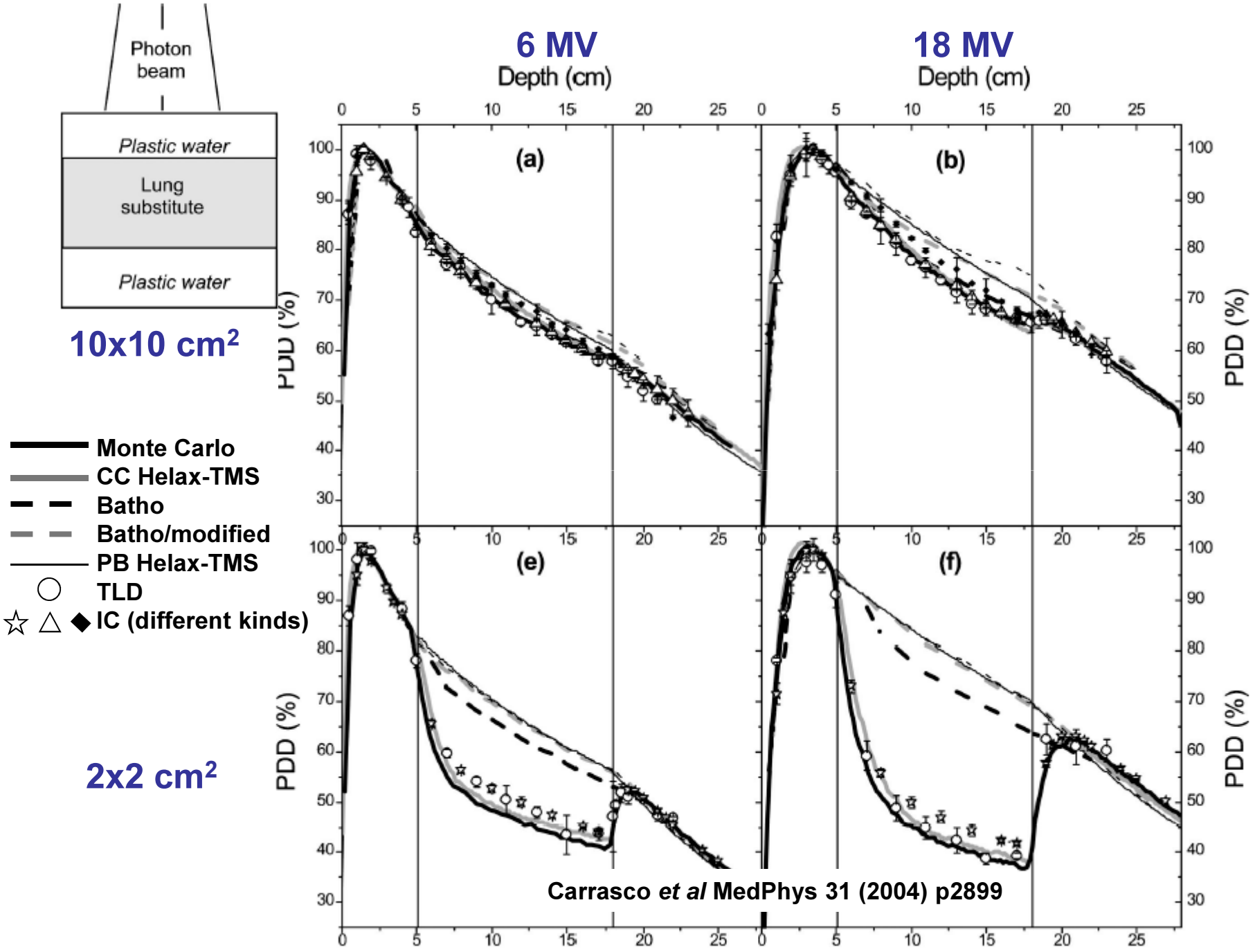
Photon beam
Plastic water
Lung substitute
Plastic water
10x10 cm²
2x2 cm²
Monte Carlo
CC Helax-TMS
Batho
Batho/modified
PB Helax-TMS
TLD
IC (different kinds)
6 MV
18 MV
Depth (cm)
PDD (%)
(a)
(b)
(e)
(f)
Carrasco et al MedPhys 31 (2004) p2899

6 MV

Haedinger *et al* IJROBP 61 (2005) p239

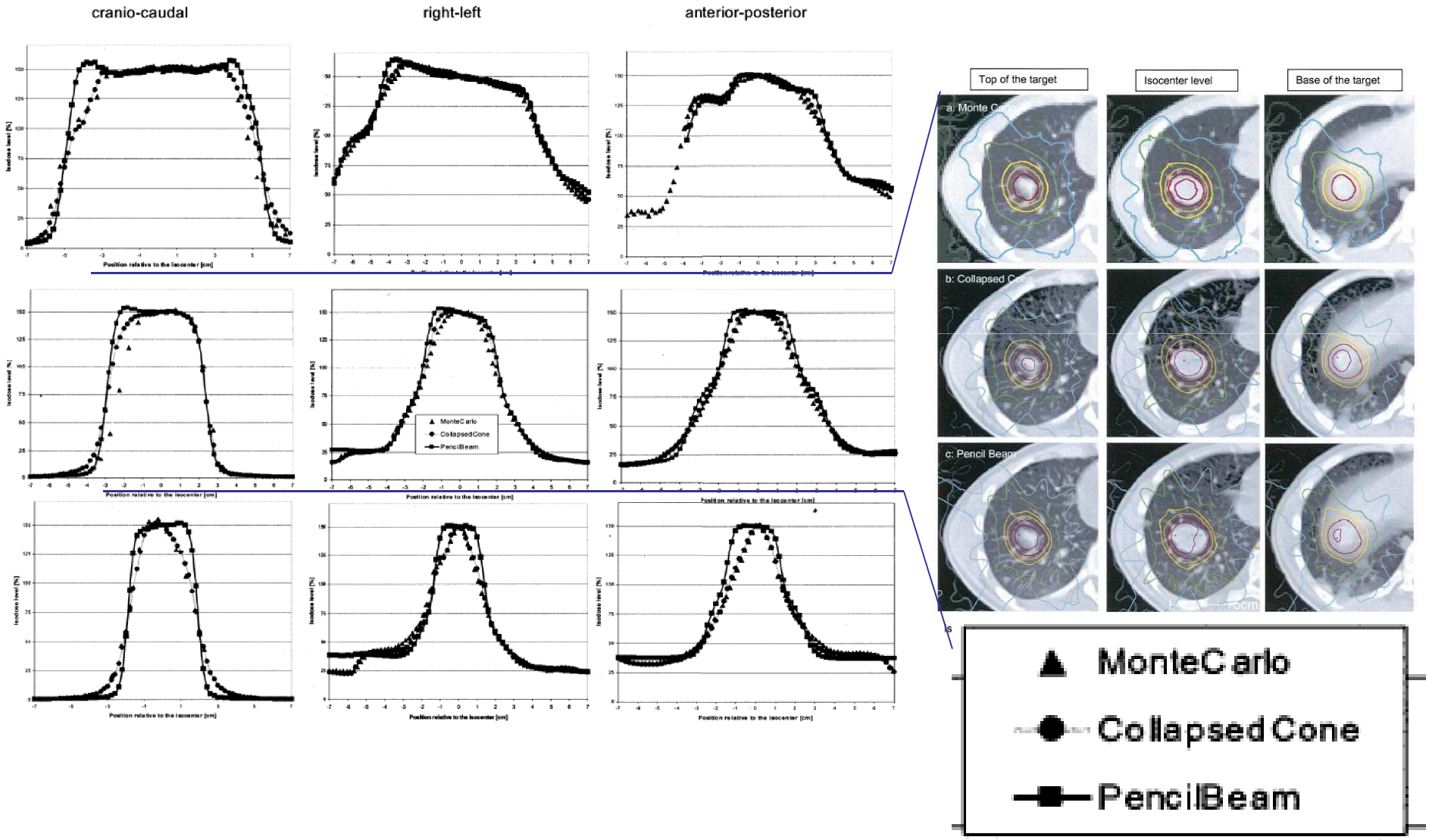

Krieger&Sauer PMB 50 (2005) p859
TMS

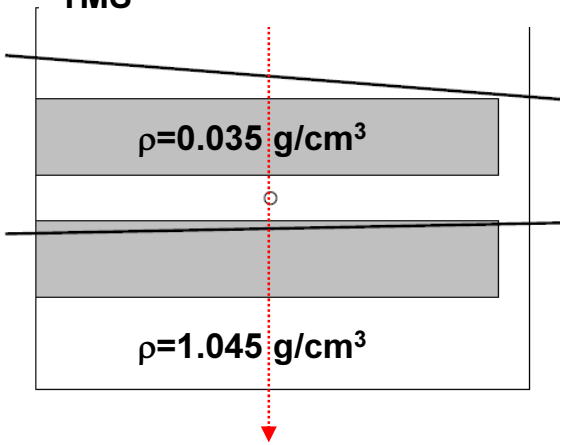

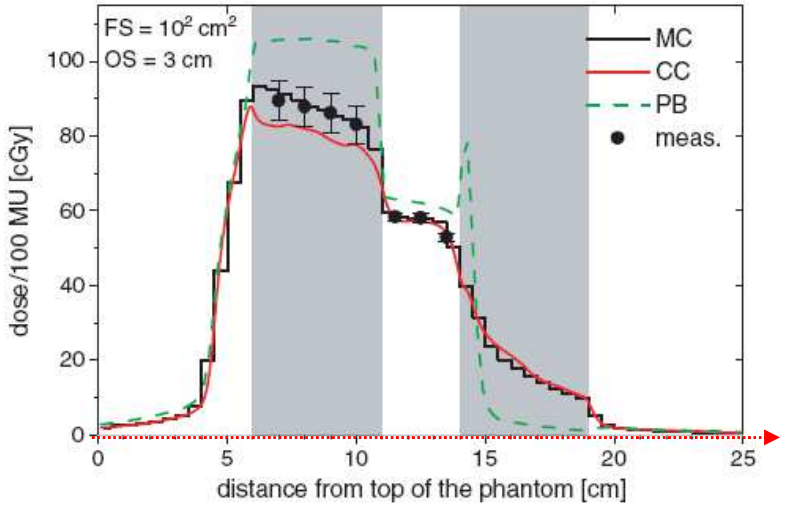

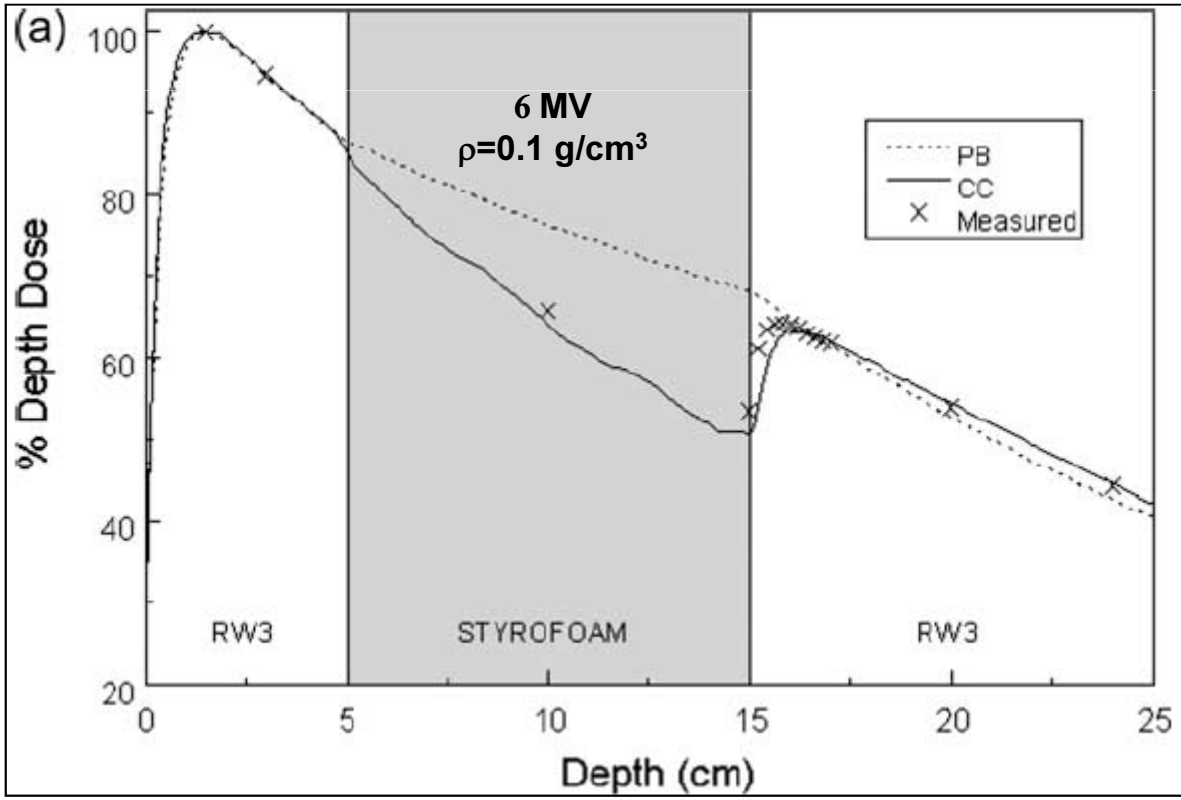

Nisbet *et al* RadOnc 73 (2004) p79
TMS

Dose rebuild-up behind a cylinder cavity

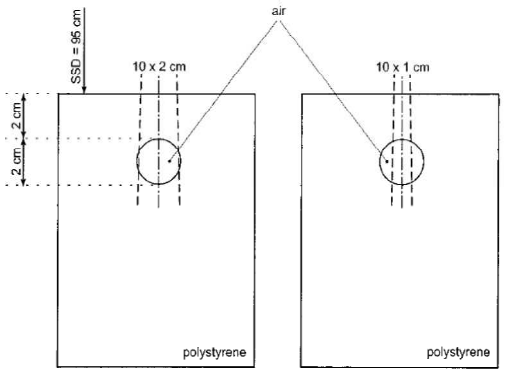

Martens *et al* MedPhys 29 (2002) p1528

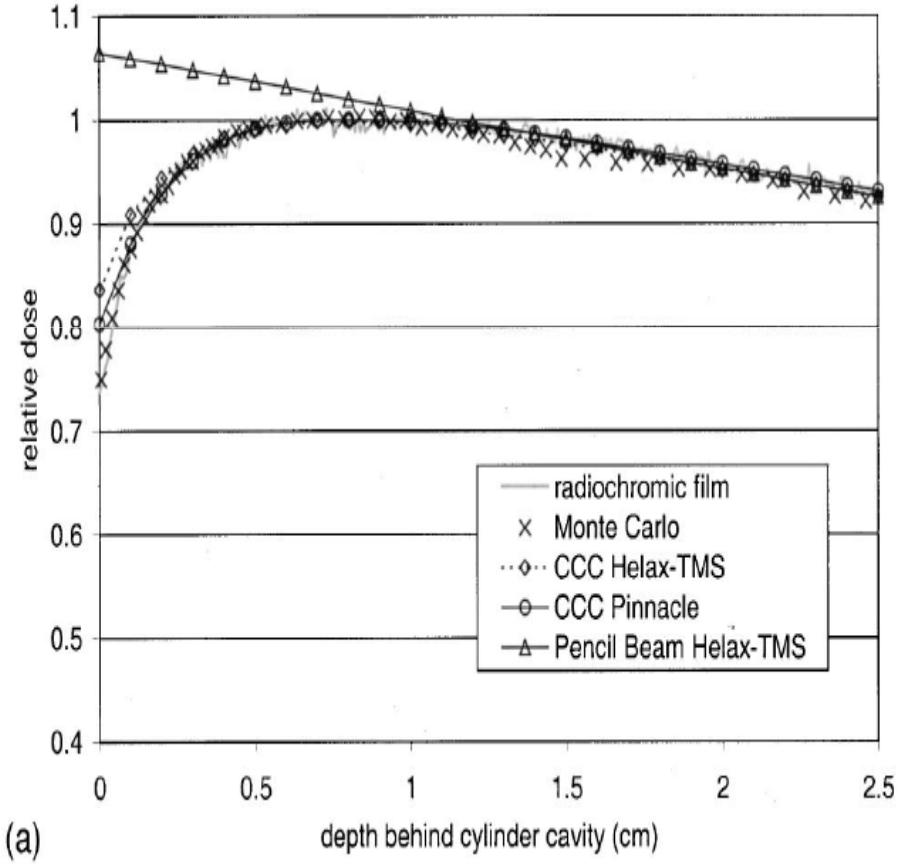

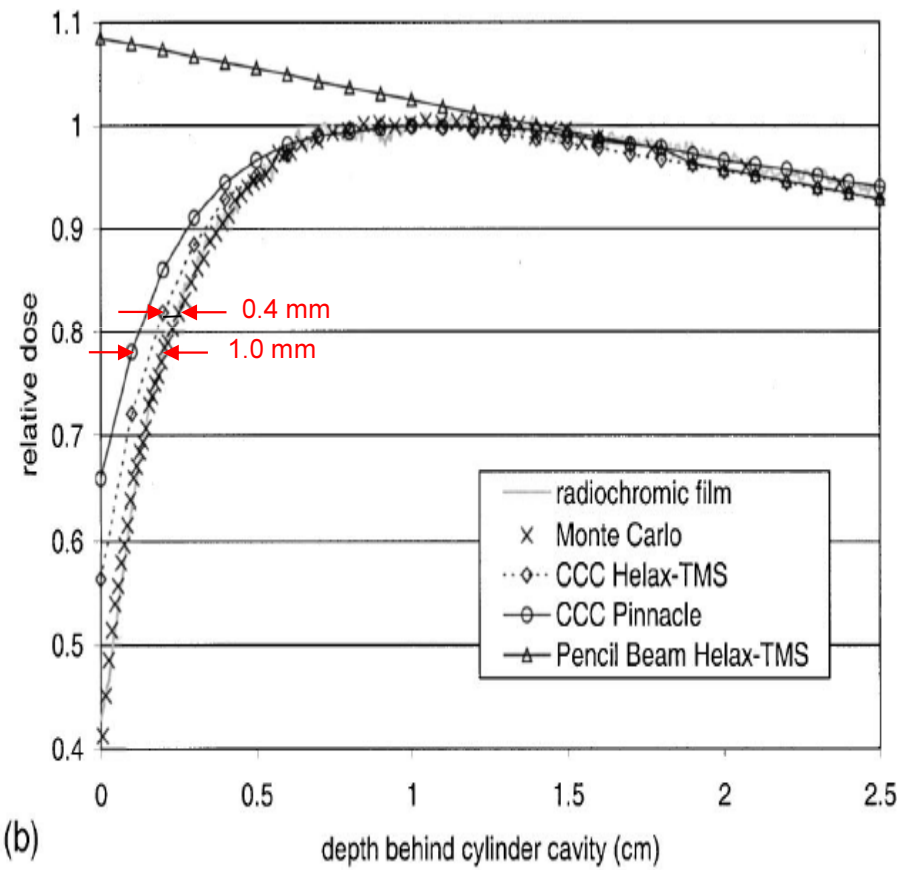

Monte Carlo simulations, PB calculations, CCC calculations and radiochromic film measurements (film strips along the beam axis) for a 10x2 cm^2 **(a)** and a 10x1 cm^2 **(b)** field.

Fogliata *et al* PMB 52 (2007) p1363-85

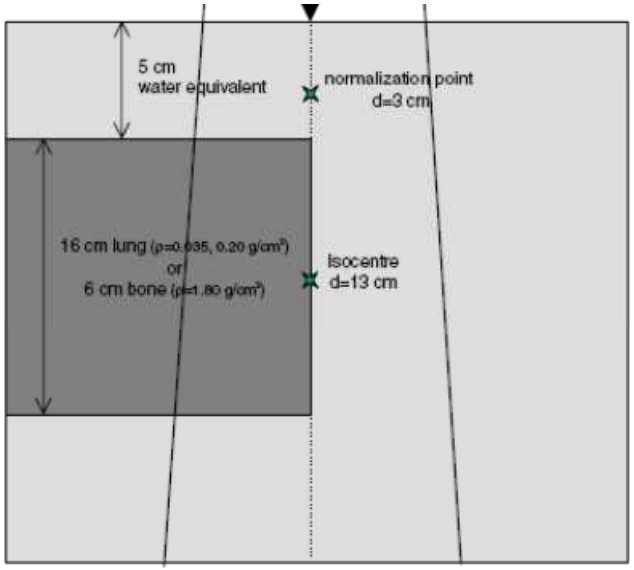

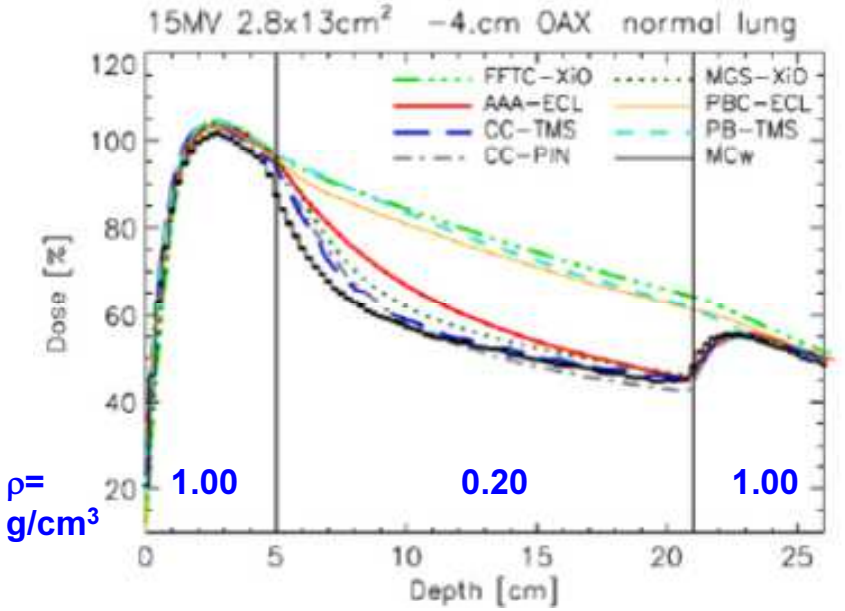

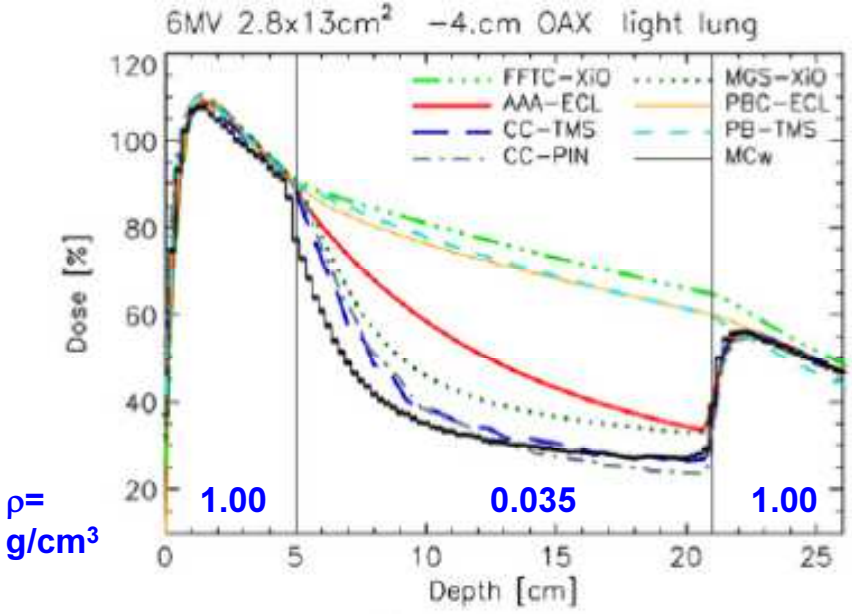

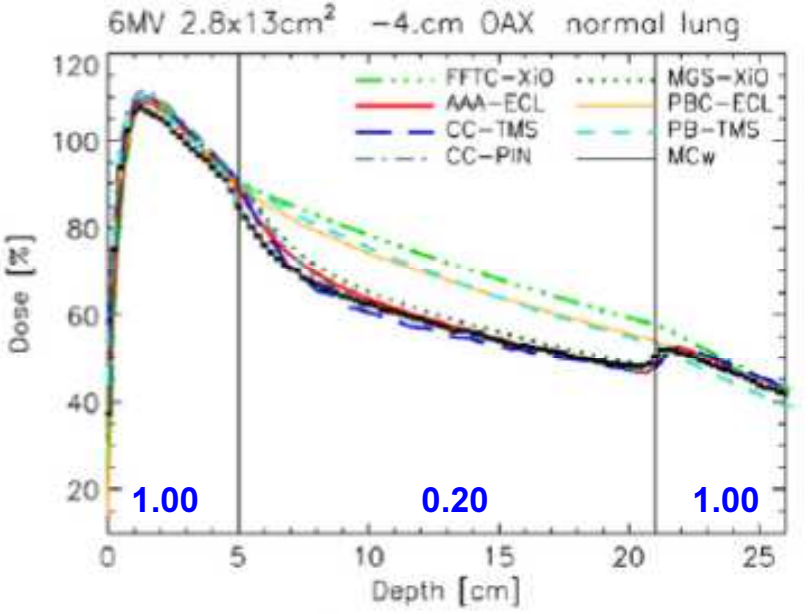

Irvine *et al* ClinOnc 16 (2004) p148

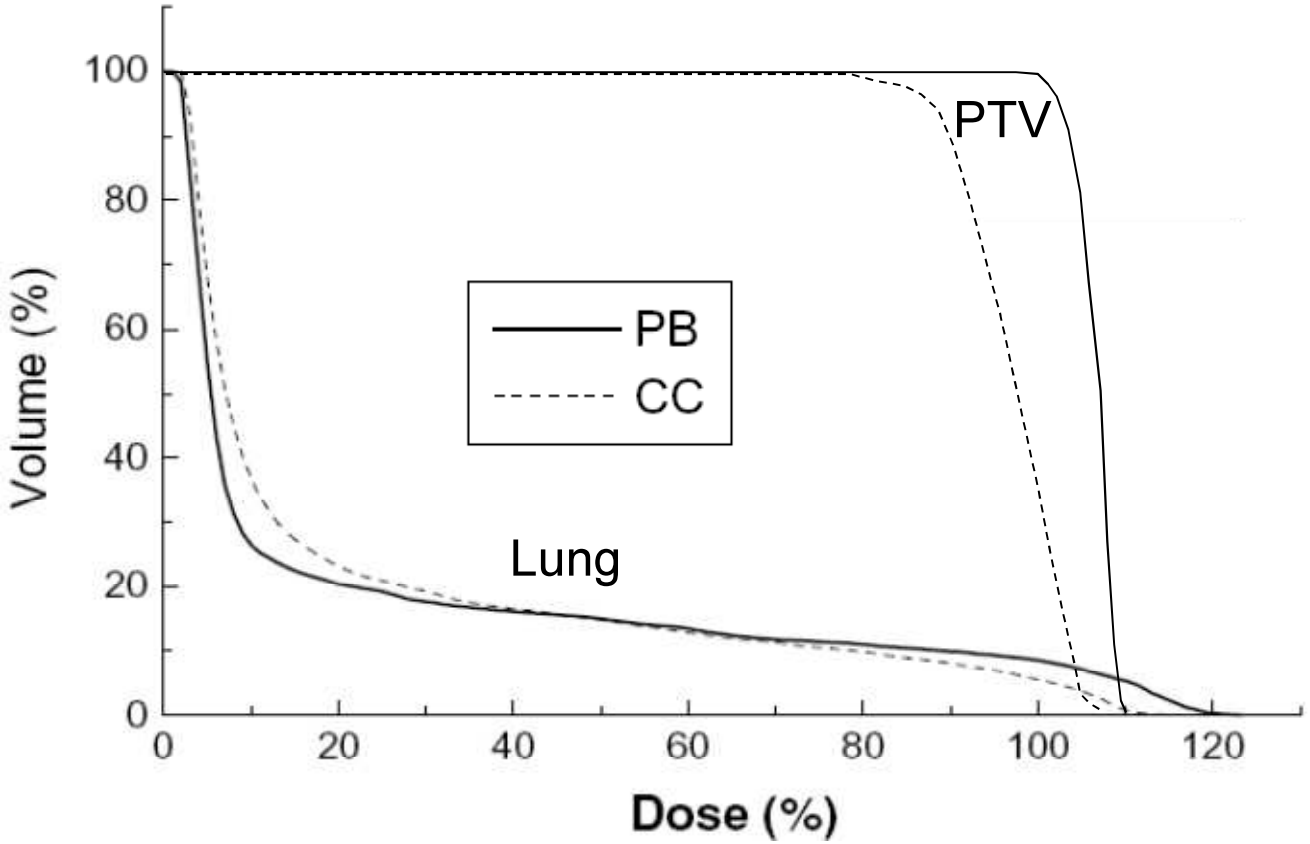

Target mean dose easy to compensate.
PTV is hard to make homogenous

Retrospective lung calculation study, Uppsala Akademiska Sjukhus

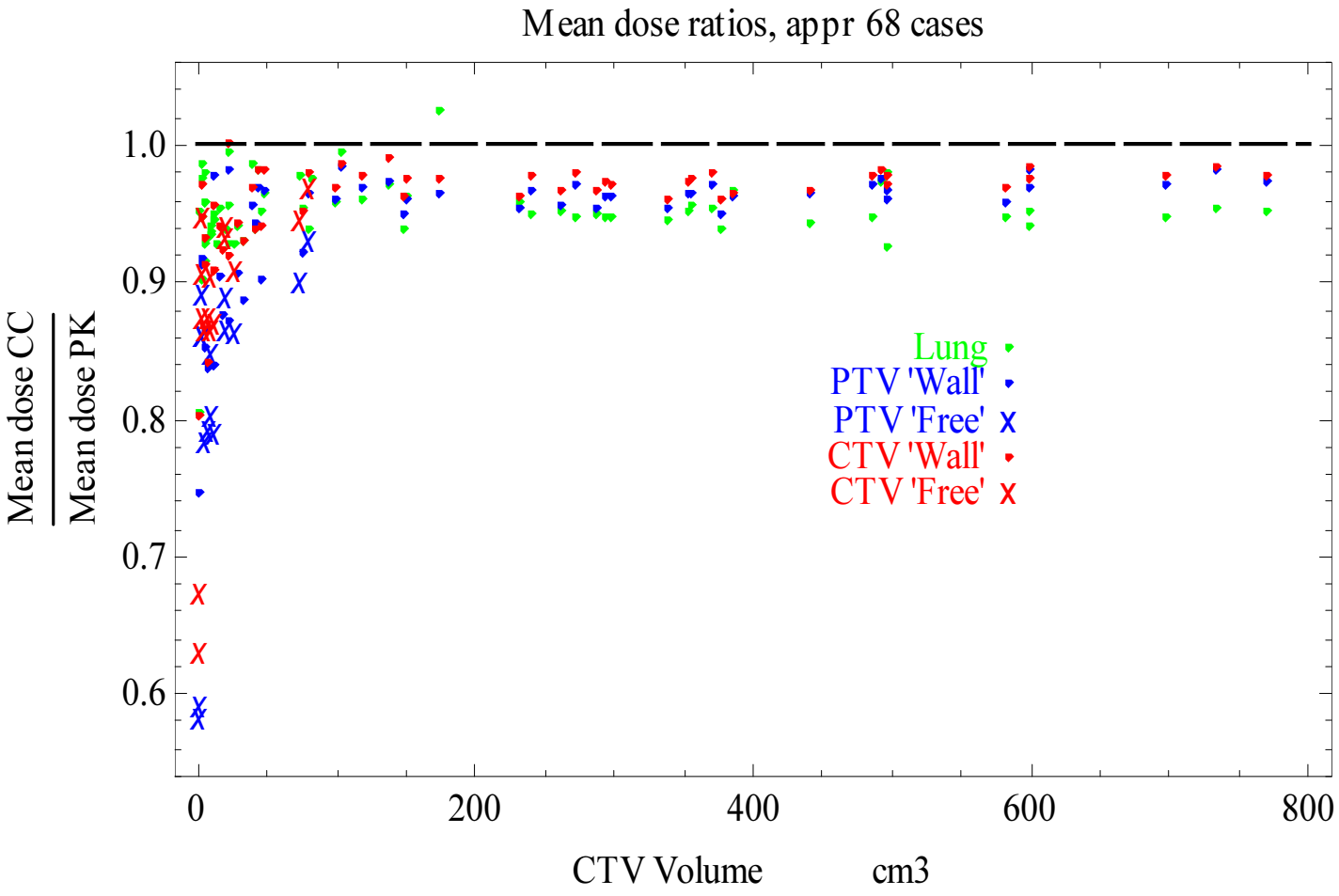

one dot – one patient

- is it the PTV or the CTV/GTV that matters for DVH optimization?

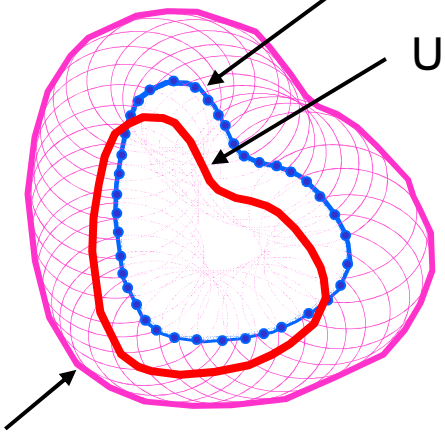

PTV formed from snapshot **CTV** using a translational margin ellipsoid to cover most possible positions of **CTV**

<u>Re-buildup dose makeup</u>: With sufficient beam margins, re-buildup will make DVH of the different CTV instances insensitive of where it is in a homogeneous PTV ”fluence bath” (of heterogeneous dose), cf ”flash” margins for tangential breast!

Simulation results of using multiple instances (~4000) of the same patient with ”moving target” for a 3-fraction treatment

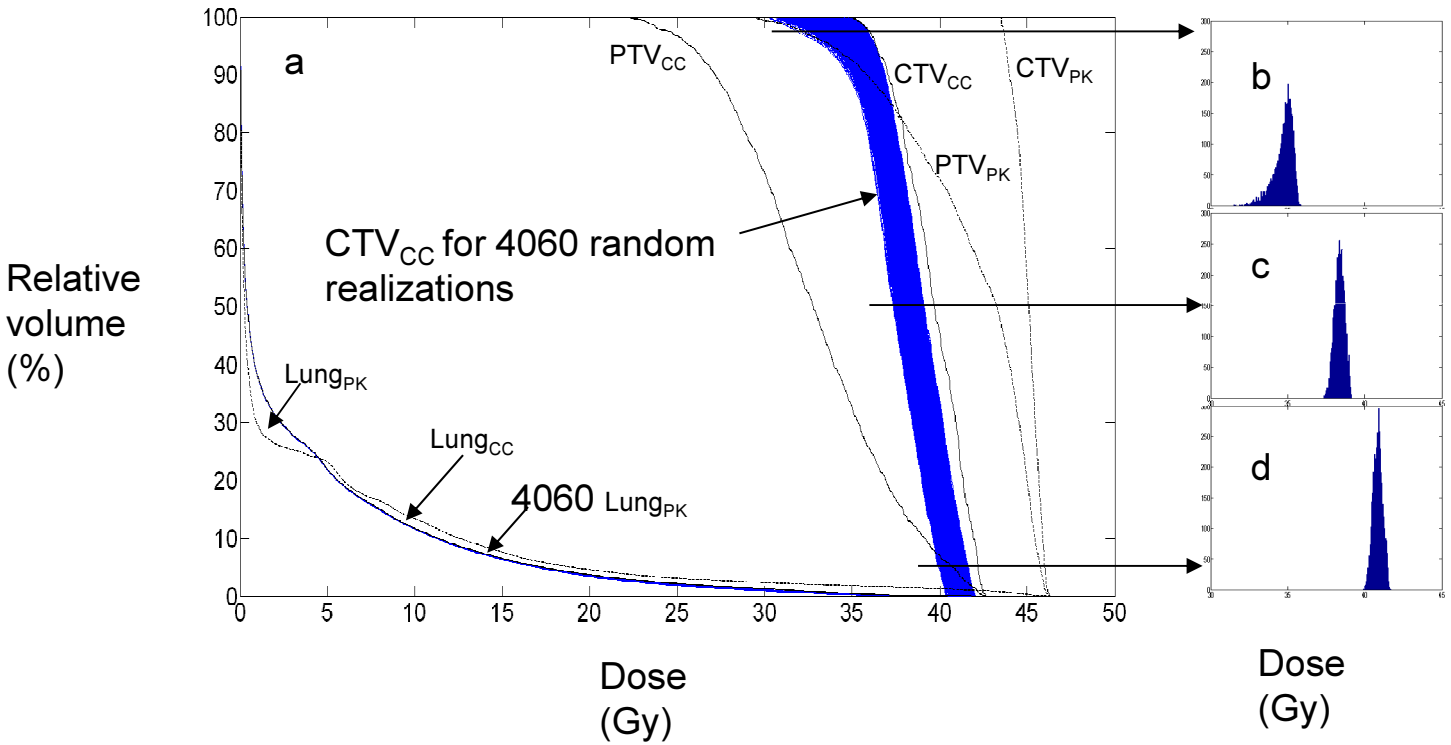

CT images defines the radiation transport arena

- **Imaging sequence must be relevant for the irradiation technique (breath hold, gating etc)**
- **Movements may yield large artifacts, and hence their calculated dose**

In lung, the dose to a small dense object (tumor) covered by large enough field margins is more determined by its size&chape than its position!

Wrong shape – wrong dose!

Wrong place – likely correct dose!

Summary

- Point Kernel algorithms show small deviations versus Monte Carlo for clinical cases, much more accurate than Pencil Kernel models
- Collapsed Cone inherent paralellism can efficiently use Graphical Processor Units for dose calculations literally in seconds
- Accuracy (and speed...) implemention dependent, depending on the approximations used
- Pencil kernel algorithms frequently used instead of point kernels, particularly in applications with optimizations, but will give errors particularly for lung cases

Spectrum corrections of raytraced collision kerma and scerma for attenuated beams (wedges)

Multiply cKERMA by $$k_{PQ}(depth, thickness) = \frac{\frac{(1-g)\mathrm{KERMA}}{\Psi}(\mathrm{mod})}{\frac{(1-g)\mathrm{KERMA}}{\Psi}(\mathrm{open})}$$

Multiply SCERMA by $$k_{SQ}(depth, thickness) = \frac{\frac{\mathrm{SCERMA}}{\Psi}(\mathrm{mod})}{\frac{\mathrm{SCERMA}}{\Psi}(\mathrm{open})}$$

i. e.

$$\frac{P}{\Psi_0}(\mathrm{mod}) = k_{PQ} \cdot \hat{\eta} \cdot \frac{P}{\Psi_0}(open)$$

$$\frac{S}{\Psi_0}(\mathrm{mod}) = k_{SQ} \cdot \hat{\eta} \cdot \frac{S}{\Psi_0}(open)$$

Where $\hat{\eta}$ is the modulation.

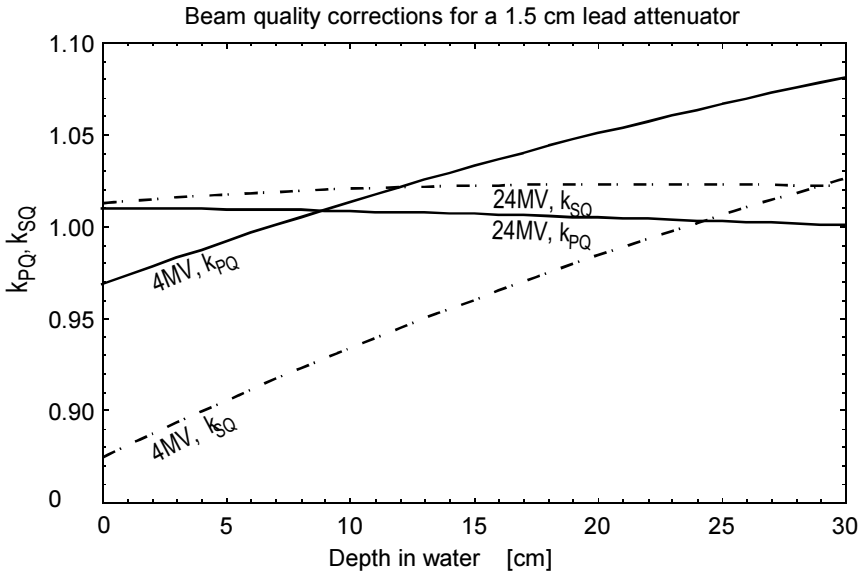

Calculation time comparisons PK,CC and MC

PK - research version of the Oncentra MasterPlan TPS (using FFT and depth interpolation)
CC - research version of the Oncentra MasterPlan TPS
MC - VMC++
All above use single thread on a 1.88 GHz dual core P4 processor
CC GPU - CC implemented using CUDA on a GeForce 8800 GTX graphics card

		Calculation time (seconds) 6 MV photons onto 30^3 cm3 water phantom Multisource treatment head modelling not included									
Voxel size mm^3	Number of voxels	10 x 10 cm^2 field					7 isocentric 10 x 10 cm^2 fields				
		PK	MC 1%	MC 2%	CC	CC GPU	PK	MC 1%	MC 2%	CC	CC GPU
1	27M	205	9934	2301	1970	35	1434	18776	4414	13790	242
2	3.4M	27	1101	299	248	4.3	190	2193	504	1736	30
3	**1.0M**	**7.8**	**319**	**88**	**73**	**1.3**	**55**	**708**	**181**	**511**	**9.1**
4	0.42M	4.3	145	42	31	0.5	31	333	84	217	5.6

Deterministic, grid based transport equations in photon dose calculations

Anders Ahnesjö
Uppsala University
Sweden

ESTRO

UPPSALA
UNIVERSITY

Learning objectives

1. Understand the basic principles of numerical Boltzmann equation solvers as dose engines

2. Understand the expected performance of such models versus MC, point kernel and pencil kernel models in terms of speed versus accuracy for different clinical situations

3. Contribute to the understanding of the different roles in modern TPS of dose engines versus fluence engines

Outline

- Setup of basic equations (continues phase space)
- Sketch of solution path
  - approximations
  - known and unknown quantities
  - discretizations
- Results

Equations setup, recall that…

…the net number of particles streaming through a surface equals the sum of fluence changes inside the volume (divergence theorem):

$$\mathrm{d}N_{\text{in-out}} = \int_S \vec{\Omega}\,\Phi_{E,\Omega}\;\mathrm{d}\vec{A}\,\mathrm{d}\Omega\mathrm{d}E = \left[\begin{array}{c}\text{divergence theorem}\\ \text{(Gauss, Stokes...)}\end{array}\right] = \int_V \vec{\Omega}\;\nabla\Phi_{E,\Omega}\;\mathrm{d}V\mathrm{d}\Omega\mathrm{d}E$$

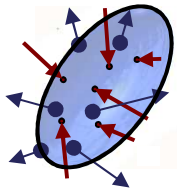

Boltzmann linear transport equations

for photon field radiation transport

Particle conservation book keeping:

$$\underbrace{\mathrm{d}N_{\mathrm{j}}}_{\equiv 0} = \mathrm{d}\Omega \mathrm{d}E \int_{\mathrm{d}V} \Bigg(\underbrace{-\vec{\Omega}\cdot\nabla\Phi_{j,E,\Omega}}_{\substack{\text{net number}\\ \text{through surface}\\ \text{"Gauss divergence theorem"}}} \underbrace{- {}^{\mathrm{att}}\sigma_j\,\Phi_{j,E,\Omega}}_{\text{attenuation}} + \underbrace{\int_{\Omega}\int_{E}\sum_{j'=1}^{3}\sigma_{j'\to j}\,\Phi_{j',E',\Omega'}\,\mathrm{d}E'\mathrm{d}\Omega'}_{\text{secondary particle production}} + \underbrace{Q_j}_{\text{source term}} \Bigg)_{\equiv 0} \mathrm{d}V$$

j=1 photons
j=2 electrons
j=3 positrons

$$\begin{aligned}
\vec{\Omega}\cdot\nabla\Phi_{1,E,\Omega} + {}^{\mathrm{att}}\sigma_{1,E,\Omega}\,\Phi_{1,E,\Omega} &= \int_{\Omega}\int_{E}\sum_{j'=1}^{3}\sigma_{j'\to 1}\,\Phi_{j',E',\Omega'}\,\mathrm{d}E'\mathrm{d}\Omega' + Q_1 \\
\vec{\Omega}\cdot\nabla\Phi_{2,E,\Omega} + {}^{\mathrm{att}}\sigma_{2,E,\Omega}\,\Phi_{2,E,\Omega} &= \int_{\Omega}\int_{E}\sum_{j'=1}^{3}\sigma_{j'\to 2}\,\Phi_{j',E',\Omega'}\,\mathrm{d}E'\mathrm{d}\Omega' + Q_2 \\
\vec{\Omega}\cdot\nabla\Phi_{3,E,\Omega} + {}^{\mathrm{att}}\sigma_{3,E,\Omega}\,\Phi_{3,E,\Omega} &= \int_{\Omega}\int_{E}\sum_{j'=1}^{3}\sigma_{j'\to 3}\,\Phi_{j',E',\Omega'}\,\mathrm{d}E'\mathrm{d}\Omega' + Q_3
\end{aligned}$$

$$\vec{\Omega}\cdot\nabla\Phi_{1,E,\Omega}+{}^{\text{att}}\sigma_{1,E,\Omega}\,\Phi_{1,E,\Omega}=\int_{\Omega}\int_{E}\sum_{j'=1}^{3}\sigma_{j'\to 1}\,\Phi_{j',E',\Omega'}\,\mathrm{d}E'\mathrm{d}\Omega'+Q_1$$

$$\vec{\Omega}\cdot\nabla\Phi_{2,E,\Omega}+{}^{\text{att}}\sigma_{2,E,\Omega}\,\Phi_{2,E,\Omega}=\int_{\Omega}\int_{E}\sum_{j'=1}^{3}\sigma_{j'\to 2}\,\Phi_{j',E',\Omega'}\,\mathrm{d}E'\mathrm{d}\Omega'+Q_2$$

$$\vec{\Omega}\cdot\nabla\Phi_{3,E,\Omega}+{}^{\text{att}}\sigma_{3,E,\Omega}\,\Phi_{3,E,\Omega}=\int_{\Omega}\int_{E}\sum_{j'=1}^{3}\sigma_{j'\to 3}\,\Phi_{j',E',\Omega'}\,\mathrm{d}E'\mathrm{d}\Omega'+Q_3$$

Common simplifications:

- Neglect bremsstrahlung
- Treat positrons as electrons
- Split photons into primary and scatter

$$\vec{\Omega}\cdot\nabla\left(\Phi_{\text{prim ph},E,\Omega}+\Phi_{\text{scat ph},E,\Omega}\right)+{}^{\text{att}}\sigma_{\text{phot}}\left(\Phi_{\text{prim ph},E,\Omega}+\Phi_{\text{scat ph},E,\Omega}\right)=\int_{\Omega}\int_{E}\left(\sigma_{\substack{\text{ph}\to\text{ph},\\E'\to E,\Omega'\to\Omega}}\left(\Phi_{\text{prim ph},E',\Omega'}+\Phi_{\text{scat ph},E',\Omega'}\right)\right)\mathrm{d}E'\mathrm{d}\Omega'$$

$$\vec{\Omega}\cdot\nabla\Phi_{\text{el},E,\Omega}+\left({}^{\text{att}}\sigma_{\text{el}}-\frac{\partial}{\partial E}S\right)\Phi_{\substack{\text{el},\\E,\Omega}}=\int_{\Omega}\int_{E}\left(\sigma_{\substack{\text{ph}\to\text{el},\\E'\to E,\Omega'\to\Omega}}\left(\Phi_{\text{prim ph},E',\Omega'}+\Phi_{\text{scat ph},E',\Omega'}\right)+\sigma_{\substack{\text{el}\to\text{el},\\E'\to E,\Omega'\to\Omega}}\cdot\Phi_{\text{el},E',\Omega'}\right)\mathrm{d}E'\mathrm{d}\Omega'$$

Known, unknowns and wanted

$$\vec{\Omega}\cdot\nabla\left(\Phi_{\text{prim ph},E,\Omega}+\Phi_{\text{scat ph},E,\Omega}\right)+{}^{\text{att}}\sigma_{\text{phot}}\cdot\left(\Phi_{\text{prim ph},E,\Omega}+\Phi_{\text{scat ph},E,\Omega}\right)=\int_{\Omega}\int_{E}\left(\sigma_{\substack{\text{ph}\to\text{ph},\\E'\to E,\Omega'\to\Omega}}\cdot\left(\Phi_{\text{prim ph},E',\Omega'}+\Phi_{\text{scat ph},E',\Omega'}\right)\right)\mathrm{d}E'\mathrm{d}\Omega'$$

$$\vec{\Omega}\cdot\nabla\Phi_{\text{el},E,\Omega}+\left({}^{\text{att}}\sigma_{\text{el}}-\frac{\partial}{\partial E}S\right)\Phi_{\substack{\text{el},\\E,\Omega}}=\int_{\Omega}\int_{E}\left(\sigma_{\substack{\text{ph}\to\text{el},\\E'\to E,\Omega'\to\Omega}}\cdot\left(\Phi_{\text{prim ph},E',\Omega'}+\Phi_{\text{scat ph},E',\Omega'}\right)+\sigma_{\substack{\text{el}\to\text{el},\\E'\to E,\Omega'\to\Omega}}\cdot\Phi_{\text{el},E',\Omega'}\right)\mathrm{d}E'\mathrm{d}\Omega'$$

$\Phi_{\text{prim ph},E,\Omega}$ the primary photon fluence raytraced analytically based on a beam source model

$\Phi_{\text{scat ph},E,\Omega}$, $\Phi_{\text{el},E,\Omega}$ } unknown

Wanted: the dose - calculated from the electron fluence

$$D=\int_{E}S\cdot\int_{\Omega}\Phi_{\text{el},E,\Omega}\mathrm{d}\Omega\,\mathrm{d}E$$

${}^{\text{att}}\sigma_{\text{phot}}$, ${}^{\text{att}}\sigma_{\text{el}}$, $\sigma_{\substack{\text{ph}\to\text{ph},\\E'\to E,\Omega'\to\Omega}}$, $\sigma_{\substack{\text{ph}\to\text{el},\\E'\to E,\Omega'\to\Omega}}$, $\sigma_{\substack{\text{el}\to\text{el},\\E'\to E,\Omega'\to\Omega}}$, $\frac{\partial}{\partial E}S$ } known from interactions physics

Setting up equations:

Making the $\int\int\ldots \mathrm{d}E'\,\mathrm{d}\Omega'$ integrals practical

$$\vec{\Omega}\cdot\nabla\left(\Phi_{\text{prim ph},E,\Omega}+\Phi_{\text{scat ph},E,\Omega}\right)+{}^{\text{att}}\sigma_{\text{ph}}\left(\Phi_{\text{prim ph},E,\Omega}+\Phi_{\text{scat ph},E,\Omega}\right)=\int_{\Omega}\int_{E}\left(\sigma_{\substack{\text{ph}\to\text{ph},\\ E'\to E,\Omega'\to\Omega}}\left(\Phi_{\text{prim ph},E',\Omega'}+\Phi_{\text{scat ph},E',\Omega'}\right)\right)\mathrm{d}E'\mathrm{d}\Omega'$$

$$\vec{\Omega}\cdot\nabla\Phi_{\substack{\text{el},\\ E,\Omega}}+\left({}^{\text{att}}\sigma_{\text{el}}-\frac{\partial}{\partial E}S\right)\Phi_{\substack{\text{el},\\ E,\Omega}}=\int_{\Omega}\int_{E}\left(\sigma_{\substack{\text{ph}\to\text{el},\\ E'\to E,\Omega'\to\Omega}}\left(\Phi_{\text{prim ph},E',\Omega'}+\Phi_{\text{scat ph},E',\Omega'}\right)+\sigma_{\substack{\text{el}\to\text{el},\\ E'\to E,\Omega'\to\Omega}}\cdot\Phi_{\text{el},E',\Omega'}\right)\mathrm{d}E'\mathrm{d}\Omega'$$

Angular part expanded into Legendre polynomials (cross sections) and spherical harmonics (fluence):

$$\sigma_{a\to b}\left(E,E',\Omega\cdot\Omega'\right)\to\sum_{l=0}^{\infty}\frac{2l+1}{4\pi}\sigma_{a\to b,l}\left(E,E'\right)P_l\left(\Omega\cdot\Omega'\right)$$

$$\Phi_{E',\Omega'}\to\sum_{l=0}^{\infty}\sum_{m=-l}^{l}\phi_l^m\left(E'\right)Y_l^m\left(\Omega'\right)$$

where

$$\sigma_{a\to b,l}\left(E,E'\right)=\frac{1}{2}\int_{-1}^{1}\sigma_{a\to b}\left(E,E',\mu\right)P_l\left(\mu\right)\mathrm{d}\mu$$

$$\phi_l^m\left(E'\right)=\int_{\Omega}Y_l^m\left(\Omega'\right)\cdot\Phi_{E',\Omega'}\,\mathrm{d}\Omega'$$

Energy part discretized into energy bins (“groups”).

Combined, the integrals can be rewritten as series with a limited number of terms:

$$\int_{E}\int_{\Omega}\sigma_{a\to b}\left(E',\Omega\cdot\Omega'\right)\Phi\left(E',\Omega'\right)\mathrm{d}\Omega'\,\mathrm{d}E'\approx\sum_{\Delta E_i'}\int_{\Omega}\left(\sum_{l=0}^{\infty}\frac{2l+1}{4\pi}\sigma_{a\to b,l}\left(E_i'\right)P_l\left(\Omega\cdot\Omega'\right)\right)\cdot\left(\sum_{l=0}^{\infty}\sum_{m=-l}^{l}\phi_l^m\left(E_i'\right)Y_l^m\left(\Omega'\right)\right)\mathrm{d}\Omega'\Delta E_i'$$

$$=\sum_{\Delta E_i'}\sum_{l=0}^{\infty}\sum_{m=-l}^{l}\sigma_{a\to b,l}\left(E_i'\right)\phi_l^m\left(E_i'\right)Y_l^m\left(\Omega'\right)\Delta E_i'$$

Acuros: $\infty\approx 7$, # energy bins ≈ 25 (photons); 49 (electrons)

Failla *etal Acuros XB advanced dose calculation for the Eclipse treatment planning system.* Varian white paper

Setting up equations:

Making the $\int_{\Omega}\int_{E}\ldots \mathrm{d}E'\,\mathrm{d}\Omega'$ integrals practical, summary

$$\vec{\Omega}\cdot\nabla\left(\Phi_{\text{prim ph},E,\Omega}+\Phi_{\text{scat ph},E,\Omega}\right)+{}^{\text{att}}\sigma_{\text{ph}}\cdot\left(\Phi_{\text{prim ph},E,\Omega}+\Phi_{\text{scat ph},E,\Omega}\right)=\int_{\Omega}\int_{E}\left(\sigma_{\substack{\text{ph}\to\text{ph},\\ E'\to E,\Omega'\to\Omega}}\left(\Phi_{\text{prim ph},E',\Omega'}+\Phi_{\text{scat ph},E',\Omega'}\right)\right)\mathrm{d}E'\mathrm{d}\Omega'$$

$$\vec{\Omega}\cdot\nabla\Phi_{\text{el},E,\Omega}+\left({}^{\text{att}}\sigma_{\text{el}}-\frac{\partial}{\partial E}S\right)\Phi_{\substack{\text{el},\\ E,\Omega}}=\int_{\Omega}\int_{E}\left(\sigma_{\substack{\text{ph}\to\text{el},\\ E'\to E,\Omega'\to\Omega}}\left(\Phi_{\text{prim ph},E',\Omega'}+\Phi_{\text{scat ph},E',\Omega'}\right)+\sigma_{\substack{\text{el}\to\text{el},\\ E'\to E,\Omega'\to\Omega}}\Phi_{\text{el},E',\Omega'}\right)\mathrm{d}E'\mathrm{d}\Omega'$$

$$\vec{\Omega}\cdot\nabla\left(\sum_{l=0}^{N}\sum_{m=-l}^{l}\left(\phi_{\text{prim ph},l}^{\ m}\left(E_i\right)+\phi_{\text{scat ph},l}^{\ m}\left(E_i\right)\right)Y_l^m\left(\Omega\right)\right)+{}^{\text{att}}\sigma_{\text{phot}}\left(\sum_{l=0}^{N}\sum_{m=-l}^{l}\left(\phi_{\text{prim ph},l}^{\ m}\left(E_i\right)+\phi_{\text{scat ph},l}^{\ m}\left(E_i\right)\right)Y_l^m\left(\Omega\right)\right)=$$

$$=\sum_{\Delta E_i'}\sum_{l=0}^{N}\sum_{m=-l}^{l}\sigma_{\text{ph}\to\text{ph},l}\left(E_i'\right)\left(\phi_{\text{prim ph},l}^{\ m}\left(E_i'\right)+\phi_{\text{scat ph},l}^{\ m}\left(E_i'\right)\right)Y_l^m\left(\Omega'\right)\Delta E_i'$$

....and similar for the electron equation

Setting up equations:

Discretize directions ("discrete ordinates") and locations

$$\vec{\Omega}\cdot\nabla\left(\sum_{l=0}^{N}\sum_{m=-l}^{l}\left(\phi_{\text{prim ph},l}^{\ m}(E_i)+\phi_{\text{scat ph},l}^{\ m}(E_i)\right)Y_l^m(\Omega)\right)+{}^{\text{att}}\sigma_{\text{phot}}\cdot\left(\sum_{l=0}^{N}\sum_{m=-l}^{l}\left(\phi_{\text{prim ph},l}^{\ m}(E_i)+\phi_{\text{scat ph},l}^{\ m}(E_i)\right)Y_l^m(\Omega)\right)=$$

$$=\sum_{\Delta E_i'}\sum_{l=0}^{N}\sum_{m=-l}^{l}\sigma_{\text{ph}\to\text{ph},l}(E_i')\left(\phi_{\text{prim ph},l}^{\ m}(E_i')+\phi_{\text{scat ph},l}^{\ m}(E_i')\right)Y_l^m(\Omega')\Delta E_i'$$

....and similar for the electron equation

The fluence moments $\phi\ldots,_l^m$ contains an integral of the unknown fluence – approximate it by a quadrature summation over a set of angles Ω_n:

$$\phi\ldots,_l^m=\int_{\Omega}Y_l^m(\Omega')\cdot\Phi_{\ldots,\Omega'}\,d\Omega'\approx\sum_n w_n\cdot Y_l^m(\Omega_n')\cdot\Phi_{\ldots,\Omega_n'}$$

Finally, discretize also the locations (Finite Elements), to yield a large, sparse system of linear equations which can be solved iteratively.

Gifford etal, PMB 51, 2253-65

Equations solved:

Method summary

- set up the primary beam (based on a beam model of your choice) and calculate the primary fluence field in the patient
- set up transport equations, discretize (and massage…) them to get a linear equation system (large but sparse matrices…) for a grid of points representing the patient
- solve for the secondary particle fluencies, in particular the electron fluence
- use the electron fluence and calculate dose (multiply by stopping power)

Converges to the true solution (except for neglected interactions) with finer discretizations

One commercial implementation (Acuros™ in Varian Eclipse, EB and brachy versions)*

* Failla *etal Acuros XB advanced dose calculation for the Eclipse treatment planning system.* Varian white paper
* Gifford *etal*, 2006. Phys Med Biol. 51(9):2253-65.
* Gifford *etal*, 2008. Med Phys. 35(6):2279-85.

Equations solved:

Observations

Primary beam photon fluence explicitly raytraced through the patient

- imply the same dependence on
  - — multisource beam model
  - — patient data (HU lookup)

  as pencil kernel, point kernel ("superposition") and Monte Carlo approaches
- used to delimit strike dose artefacts from angular discretization
- secondary particle transport decoupled and can be done in common for all field segments to reduce computation time for (many field…) rotational therapy

Converges to the true solution (except for neglected interactions) with finer discretizations

One commercial implementation (Acuros™ in Varian Eclipse, EB and brachy versions)*

* Failla *etal Acuros XB advanced dose calculation for the Eclipse treatment planning system.* Varian white paper
* Gifford *etal*, 2006. Phys Med Biol. 51(9):2253-65.
* Gifford *etal*, 2008. Med Phys. 35(6):2279-85.

Equations solved:

Some results

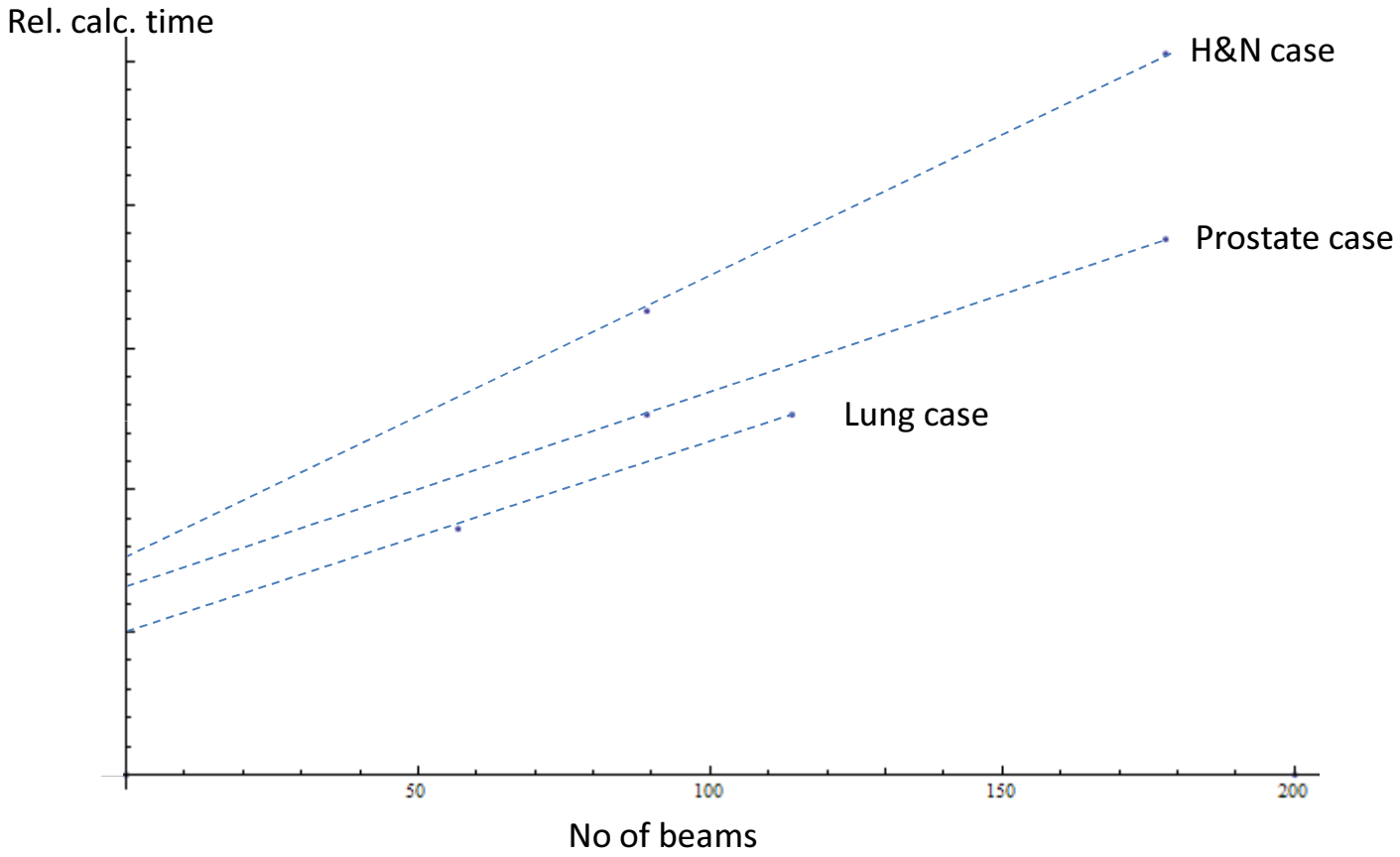

Failla *etal Acuros XB advanced dose calculation for the Eclipse treatment planning system.* Varian white paper

Small differences between models in homogenoeus media

Correct beam modeling essential

Fogliata *etal* 2011. *Dosimetric validation of the Acuros XB .... in water.* Phys Med Biol. **56**(6):1879-904

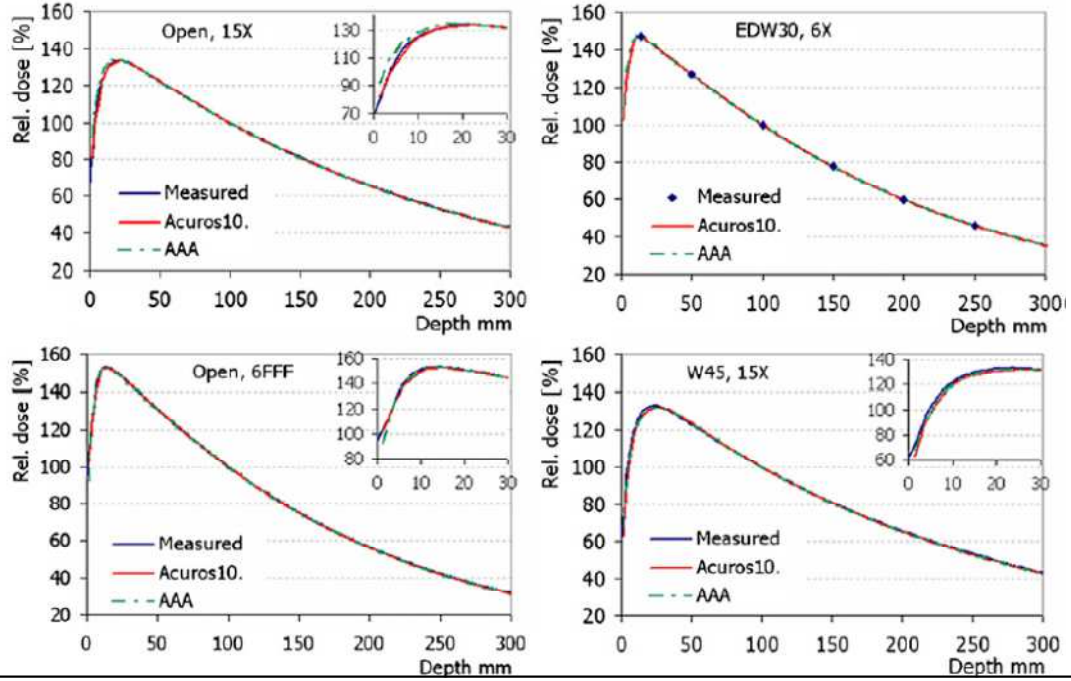

Fogliata *etal* 2011. *Accuracy of Acuros XB and AAA dose calculation for small fields...* Med Phys. **38**(11):6228-37.

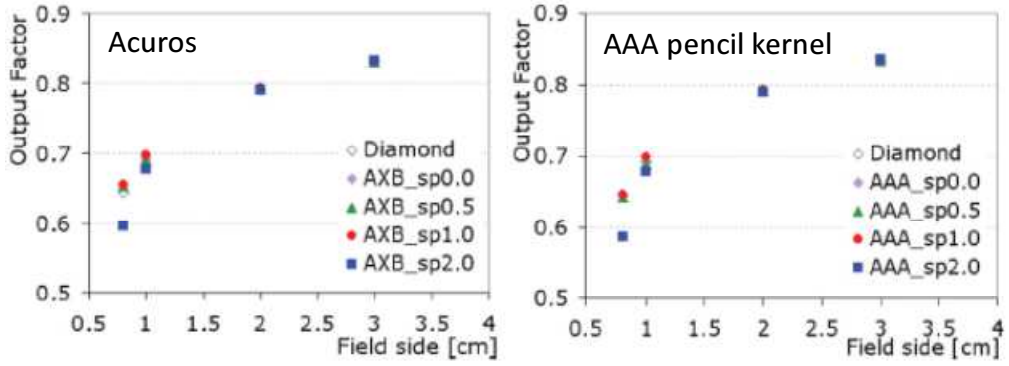

High accuracy for heterogeneous media

6 MV

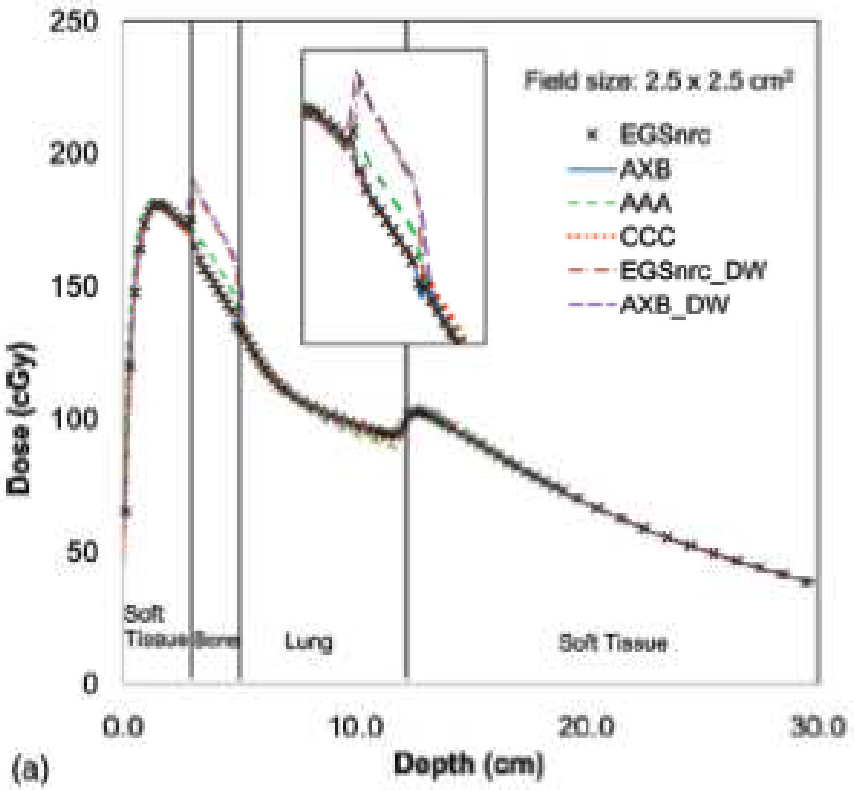

18 MV

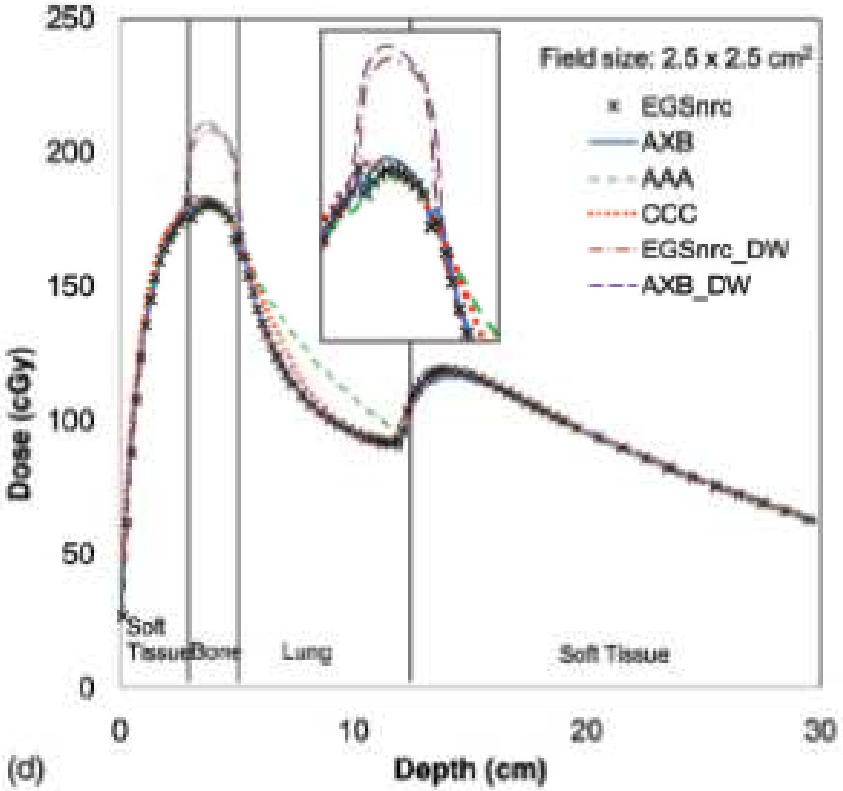

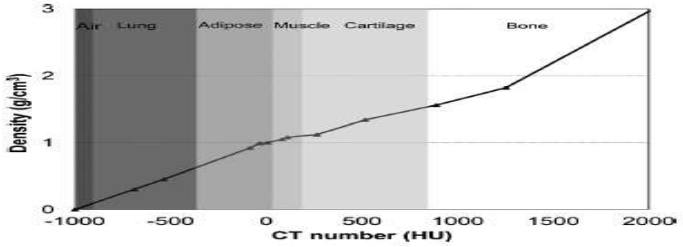

FIG. 1. Graph of CT number and material assignment versus density that was used in Eclipse TPS for AXB algorithm.

Han *etal,* 2011. *Dosimetric comparison of Acuros XB deterministic radiation transport method with Monte Carlo and model-based convolution methods in heterogeneous media.* Med Phys. **38**(5):2651-64.

…heterogeneous media

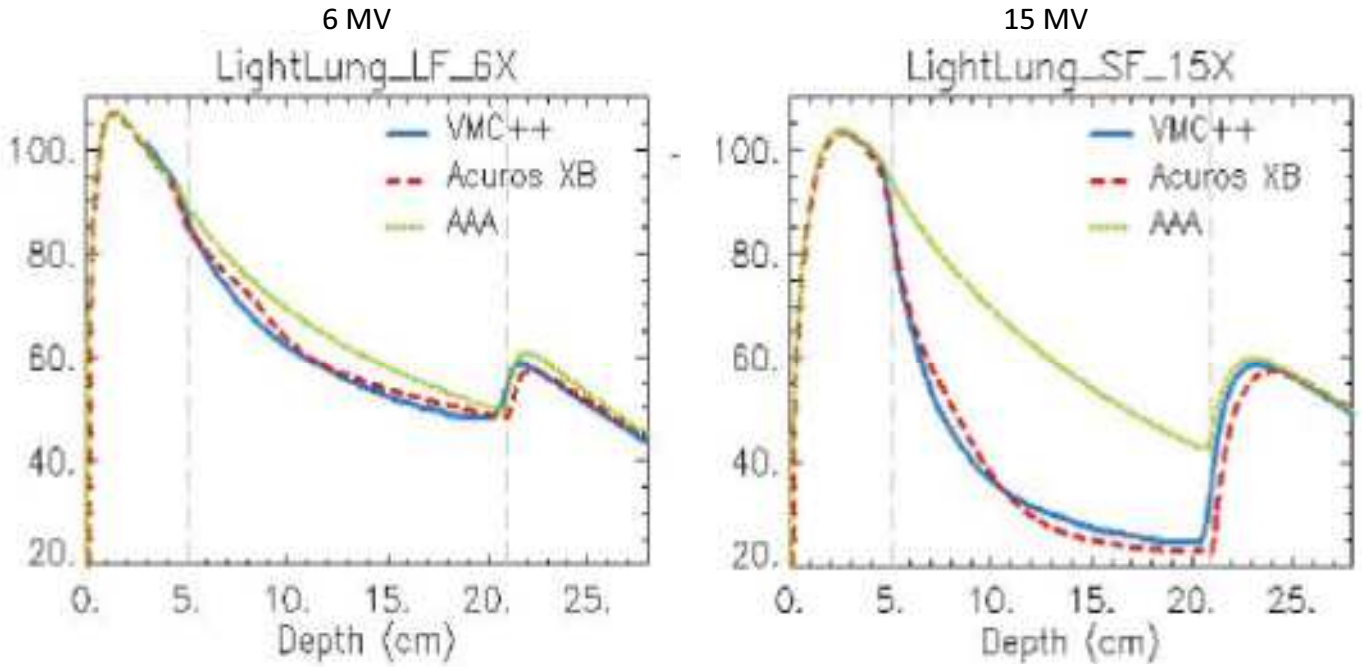

Fogliata *etal* 2011. *Dosimetric evaluation of Acuros XB Advanced Dose Calculation algorithm in heterogeneous media.* Radiat Oncol. **6**:82

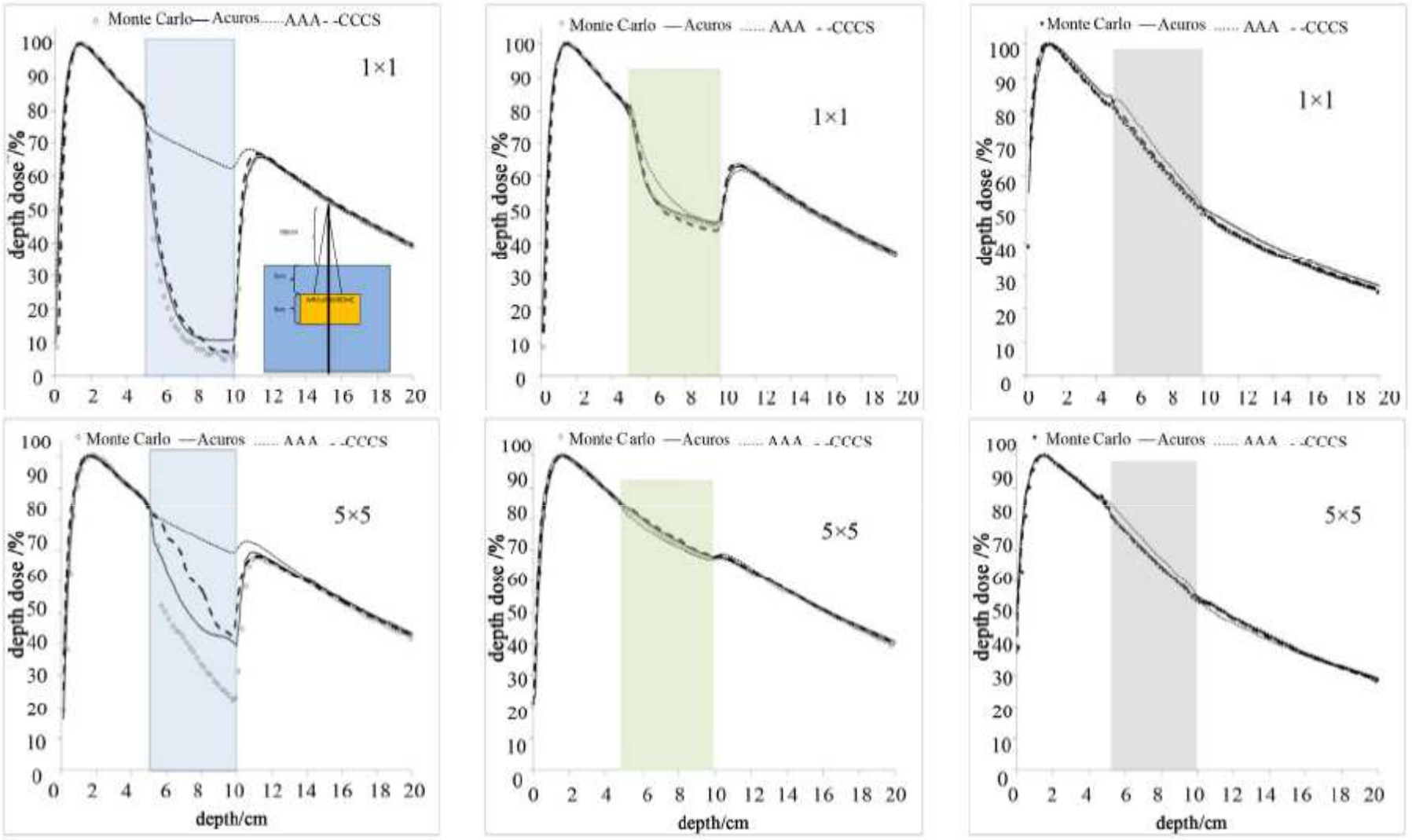

(a) (b) (c)

PDD curves for 3 different inhomogeneities. Column (a): air, Column (b): lung, and Column (c): bone for various small field sizes.

Equations solved:

Take home message

- Beam commissioning, including the multisource beam modeling, is as important for grid based equations solvers as for any other model.
- Once the irradiation conditions are set correctly, residual model limitations are expected to be small and insignificant.
- Artefacts from discretizations can occur

References

Gifford, K.A., M.J. Price, J.L. Horton, Jr., T.A. Wareing, and F. Mourtada, 2008. *Optimization of deterministic transport parameters for the calculation of the dose distribution around a high dose-rate 192Ir brachytherapy source.* Med Phys. **35**(6):2279-85.

Gifford, K.A., J.L. Horton, T.A. Wareing, G. Failla, and F. Mourtada, 2006. *Comparison of a finite-element multigroup discrete-ordinates code with Monte Carlo for radiotherapy calculations.* Phys Med Biol. **51**(9):2253-65.

Boman, E., 2007., *Radiotherapy Forward and Inverse Problem Applying Boltzmann Transport Equation* PhD thesis, Kuopio University, Finland

Vassiliev, O.N., T.A. Wareing, J. McGhee, G. Failla, M.R. Salehpour, and F. Mourtada, 2010. *Validation of a new grid-based Boltzmann equation solver for dose calculation in radiotherapy with photon beams.* Phys Med Biol. **55**(3):581-98.

Failla, G.A., Wareing, T., Archambault, Y., Thompson, S. *Acuros XB advanced dose calculation for the Eclipse treatment planning system.* Varian white paper

Hoffmann, L., M.B. Jorgensen, L.P. Muren, and J.B. Petersen, 2011. *Clinical validation of the Acuros XB photon dose calculation algorithm, a grid-based Boltzmann equation solver.* Acta Oncol.

Fogliata, A., G. Nicolini, A. Clivio, E. Vanetti, and L. Cozzi, 2011. *Accuracy of Acuros XB and AAA dose calculation for small fields with reference to RapidArc((R)) stereotactic treatments.* Med Phys. **38**(11):6228-37.

Han, T., J.K. Mikell, M. Salehpour, and F. Mourtada, 2011. *Dosimetric comparison of Acuros XB deterministic radiation transport method with Monte Carlo and model-based convolution methods in heterogeneous media.* Med Phys. **38**(5):2651-64.

Fogliata, A., G. Nicolini, A. Clivio, E. Vanetti, and L. Cozzi, 2011. *Dosimetric evaluation of Acuros XB Advanced Dose Calculation algorithm in heterogeneous media.* Radiat Oncol. **6**:82.

Bush, K., I.M. Gagne, S. Zavgorodni, W. Ansbacher, and W. Beckham, 2011. *Dosimetric validation of Acuros XB with Monte Carlo methods for photon dose calculations.* Med Phys. **38**(4):2208-21.

Fogliata, A., G. Nicolini, A. Clivio, E. Vanetti, P. Mancosu, and L. Cozzi, 2011. *Dosimetric validation of the Acuros XB Advanced Dose Calculation algorithm: fundamental characterization in water.* Phys Med Biol. **56**(6):1879-904.

Stathakis *etal*,International Journal of Medical Physics, Clinical Engineering and Radiation Oncology, 2012, 1, 78-87

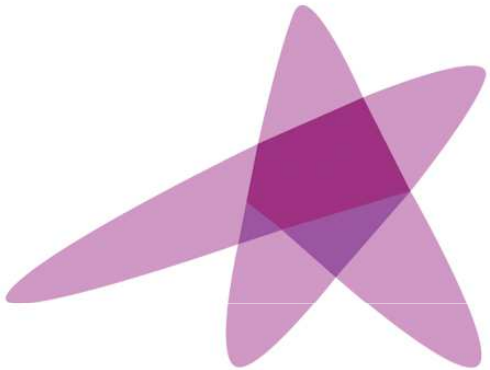

ESTRO School

WWW.ESTRO.ORG/SCHOOL

Small fields

Part I: Measurement

Mania Aspradakis
Maria.Aspradakis@luks.ch

Learning objectives

- Small MV photon field conditions and small field characteristics
- Present status for the determination of dose in small fields:
  - ❖ Reference dosimetry
  - ❖ Relative dosimetry

Learning objectives – 1

Small MV photon field conditions

and

small field characteristics

Lateral electron disequilibrium (lack of lateral CPE)

Lateral charged particle loss

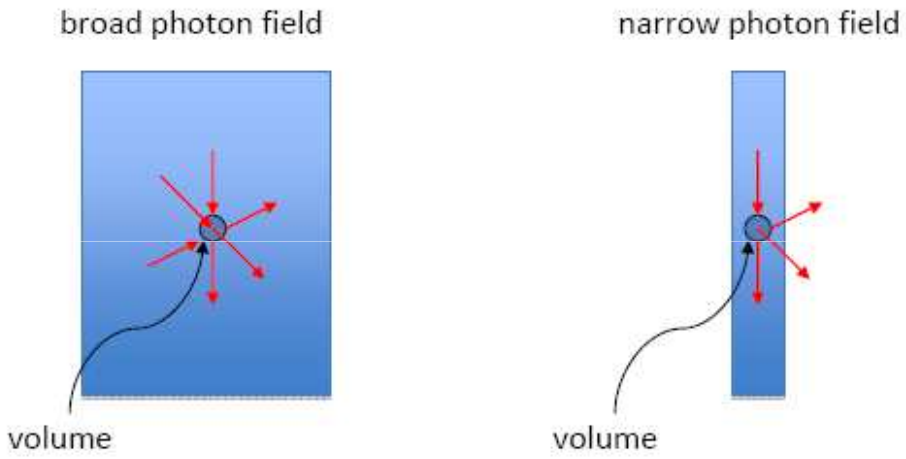

A small field can be defined as a field with a size smaller than the "lateral range" of charged particles

$\frac{D}{K_{coll}}$ *is a measure of the degree of equilibrium or transient equilibrium*

ESTRO School

Lateral electron disequilibarium (lack of lateral CPE)

Minimum field radius required for lateral electron equilibrium (r_{LEE})

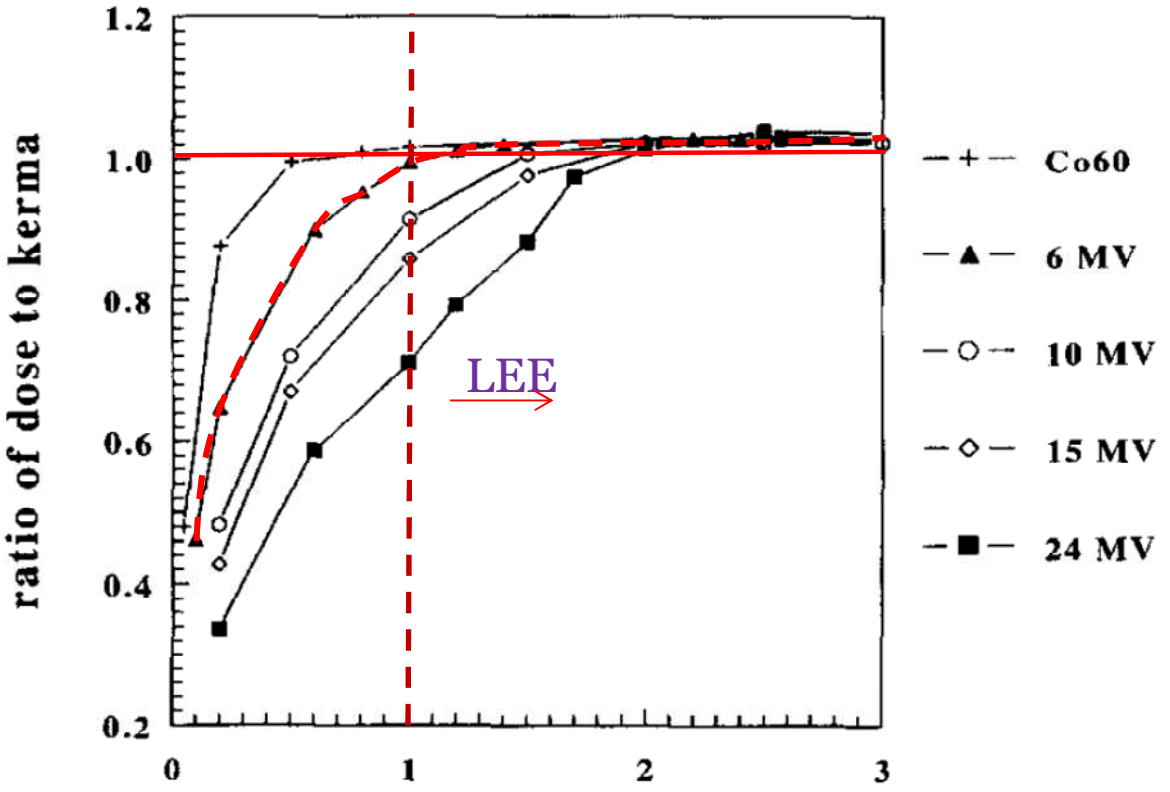

$$r_{LEE}\left[g/cm^2\right] = 5.973 \times TPR_{10}^{20} - 2.688$$

Li et al MedPhys **22**, 1995, 1167-1170

ESTRO School

Occlusion of the primary source

In broad fields:

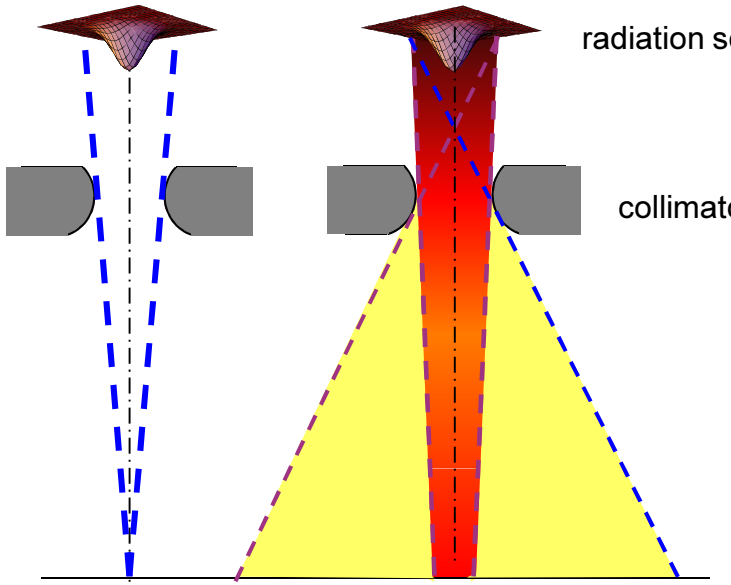

Full view of extended direct beam source from the point of measurement

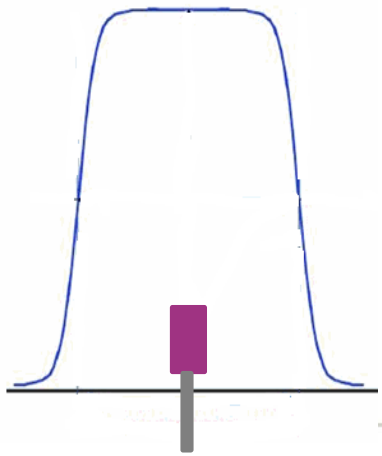

Dose variation across a broad field ('dose profile')

Radiation detector measures in region of uniform dose

ESTRO School

Occlusion of the primary source

In narrow fields:

Occlusion of the beam
focal spot
with decreasing collimator
setting

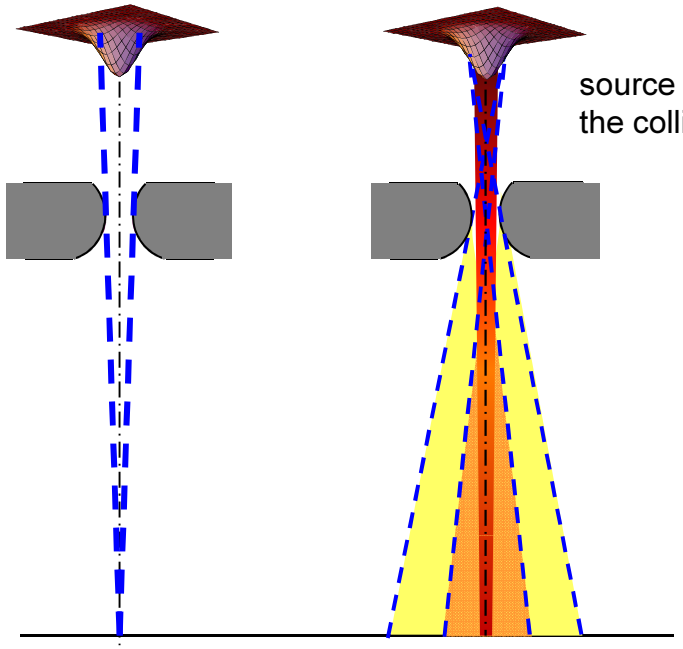

source occlusion by
the collimators

Partial view of
extended direct
beam source from
the point of
measurement

Very narrow dose profile

Radiation detector
measures in non-uniform
dose region

ESTRO School

Occlusion of the primary source

Overlapping penumbras

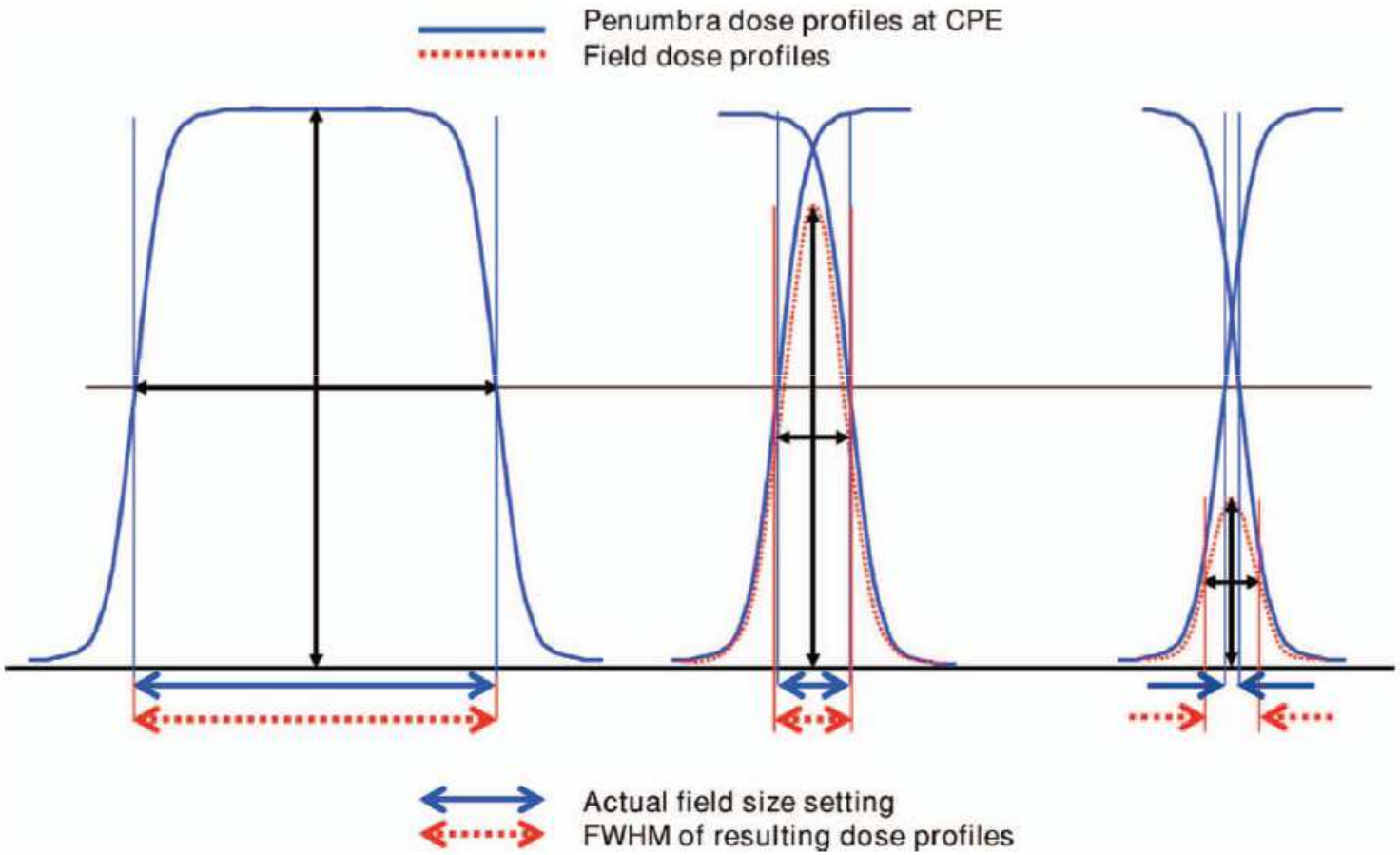

Definition of field size?

ESTRO School

Detector size and construction

- Volume averaging
- Energy dependence (of stopping power and energy absorption coefficient ratios)
- Perturbation effects

Volume averaging

Volume averaging is defined as the ratio of the absorbed dose to water at the reference point in the water phantom in the absence of the detector and the mean absorbed dose to water over the sensitive volume of the detector (still in the absence of the detector).

Sensitive volume of detector, V

Point of dose determination

$D(x_o, y_o, z_o)$

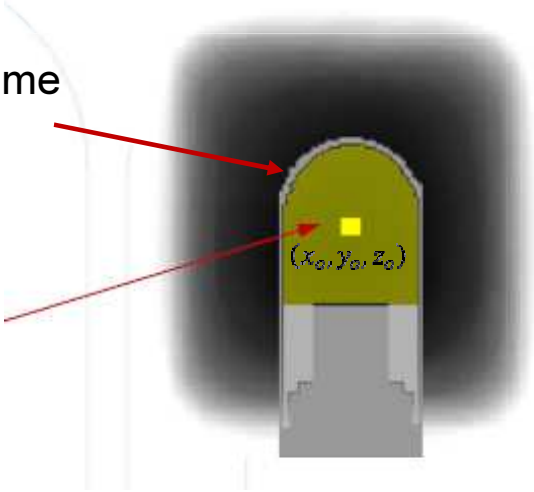

$$k_{vol} = \frac{D(x_o, y_o, z_o)}{D_V}$$

$$D_V = \frac{1}{V} \iiint_V D(x, y, z) dV$$

Georg *et al*, 2nd ESTRO Forum, Pre-meeting workshop 2013

Detector size and construction

Volume averaging

The detector produces a signal that is proportional to the mean absorbed dose over its sensitive volume and this signal is affected by the homogeneitv of the absorbed dose over the detection volume

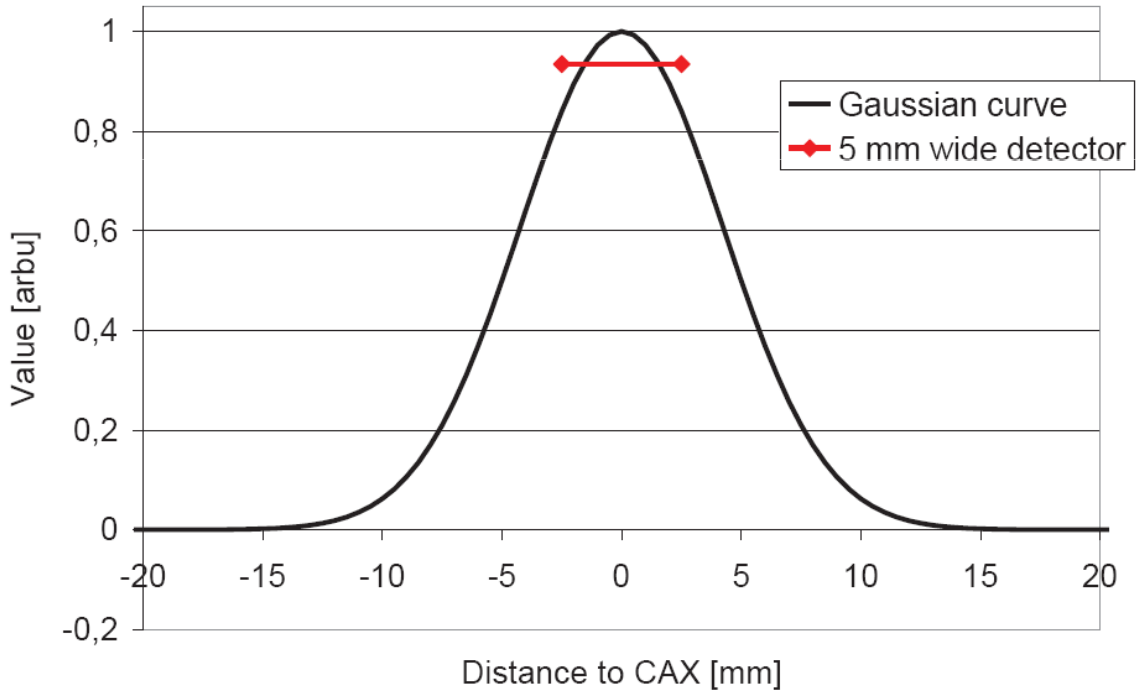

Wuerfel, J. U., Medical Physics International Journal, vol 1, no 1, 2013

ESTRO School

Detector size and construction

Volume averaging

The detector produces a signal that is proportional to the mean absorbed dose over its sensitive volume and this signal is affected by the homogeneity of the absorbed dose over the detection volume

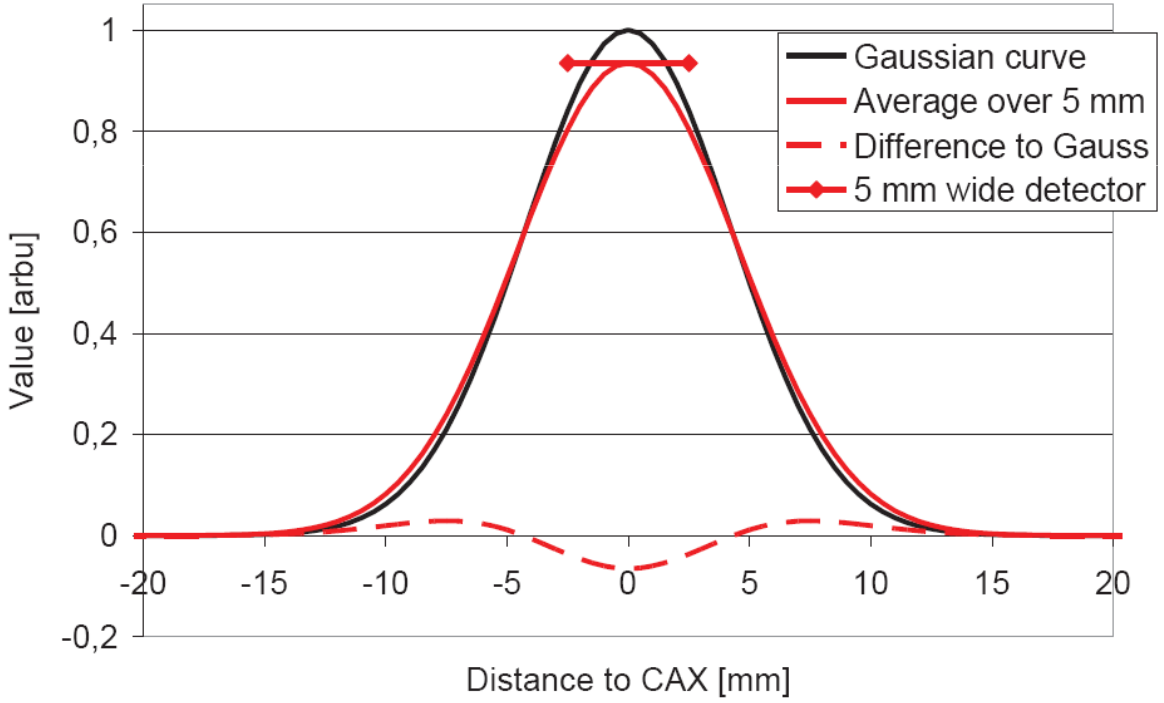

Wuerfel, J. U., Medical Physics International Journal, vol 1, no 1, 2013

ESTRO School

Detector size - the effect of volume averaging

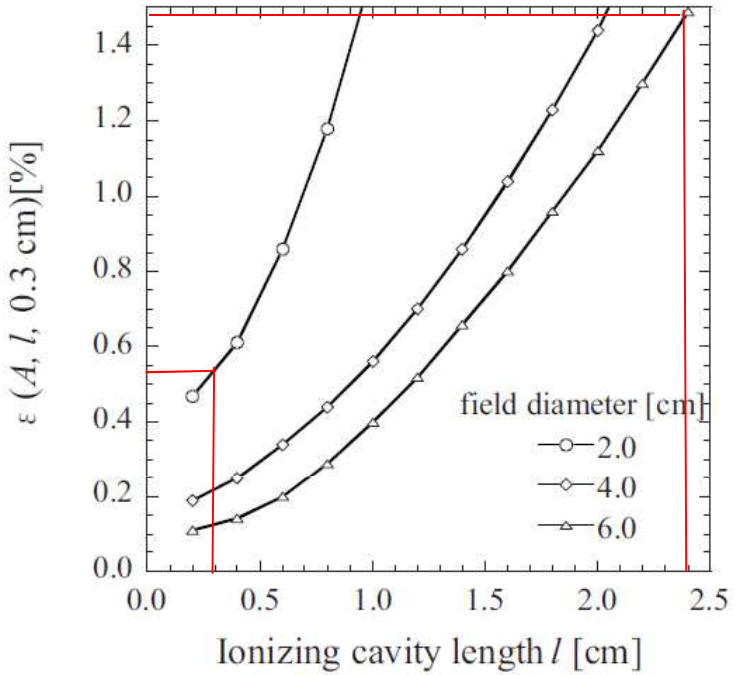

FIG. 2. The error of dosimeter reading $\varepsilon(A, l, 0.3\text{ cm})$ (%) as a function of cavity length l of ionization chamber and field A. The cavity radius r is calculated in 0.3 cm, and these values are for a SCD of 80 cm at a depth of 10 cm in water.

$$\varepsilon(A,l,r) = \frac{100\int_{-l/2}^{l/2}\int_{-r}^{r}|\mathrm{OAR}(A,x,y)-1|\mathrm{d}x\mathrm{d}y}{\int_{-l/2}^{l/2}\int_{-r}^{r}\mathrm{d}r\mathrm{d}y}$$

OAR(x,y) is the off axis distribution of field A in orthogonal directions x and y

- A chamber of cavity length of 24mm underestimates dose by 1.5% in the 6cm field
- A chamber of cavity length of 3mm underestimates dose by 0.5% in the 2cm field

Kawachi *el al* (2008), Med Phys 35 (10)

ESTRO School

Detector size - the effect of volume averaging

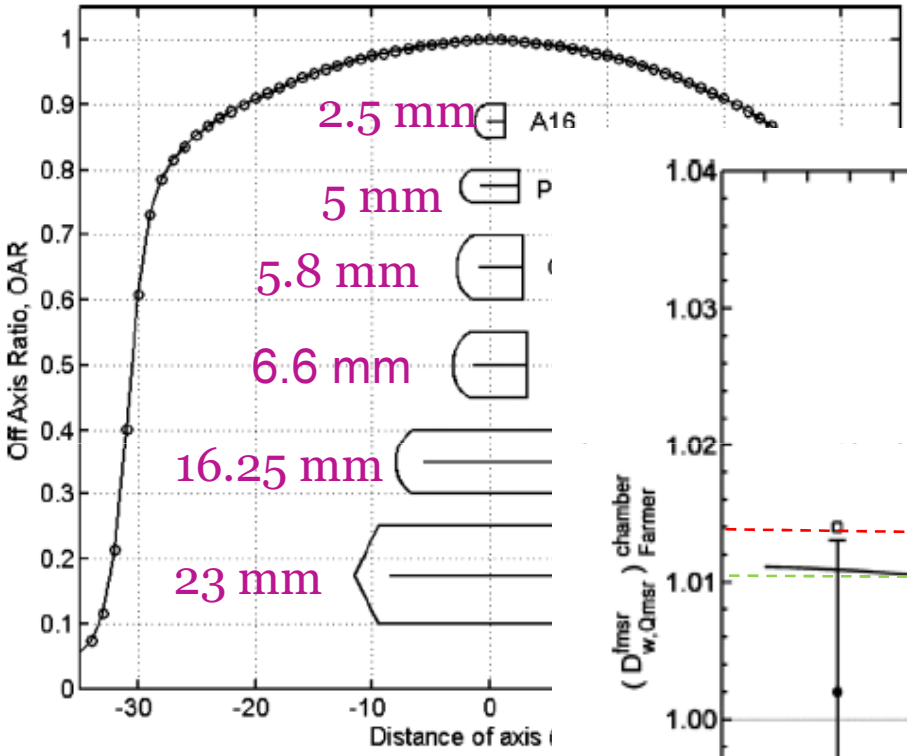

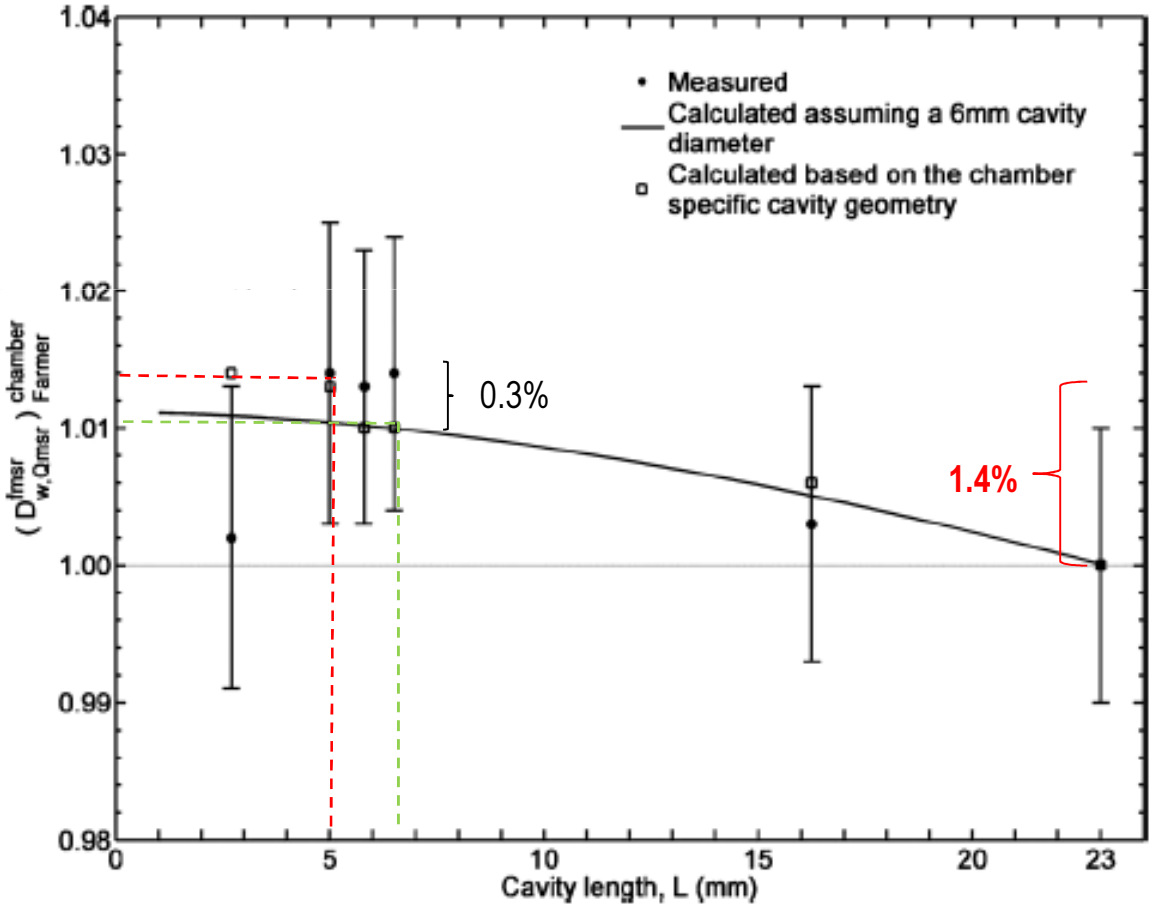

Pantelis *el al* (2010), Med Phys 37 (5)

Detector construction

Energy dependence

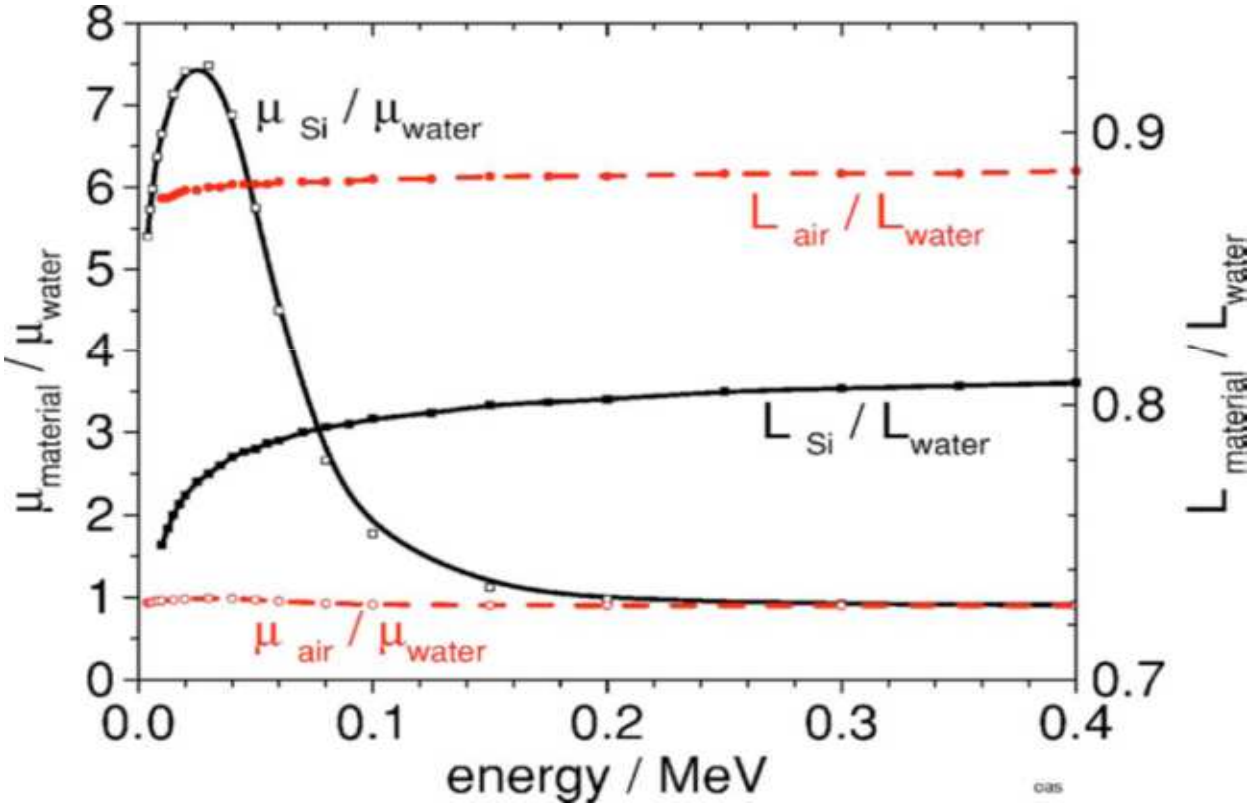

Sauer & Wilbert MP **34**, 2007, 1983-1988

ESTRO School

Detector size and construction

Perturbations due to construction

Ionization chambers

wall, central electrode, air cavity

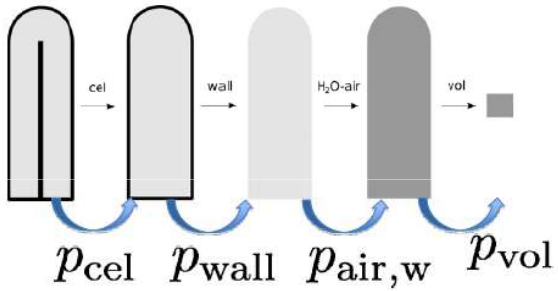

Crop *el al* (2009), PMB,54(9), 2951-2969, 2009

Diodes

housing, shielding, sensitive volume

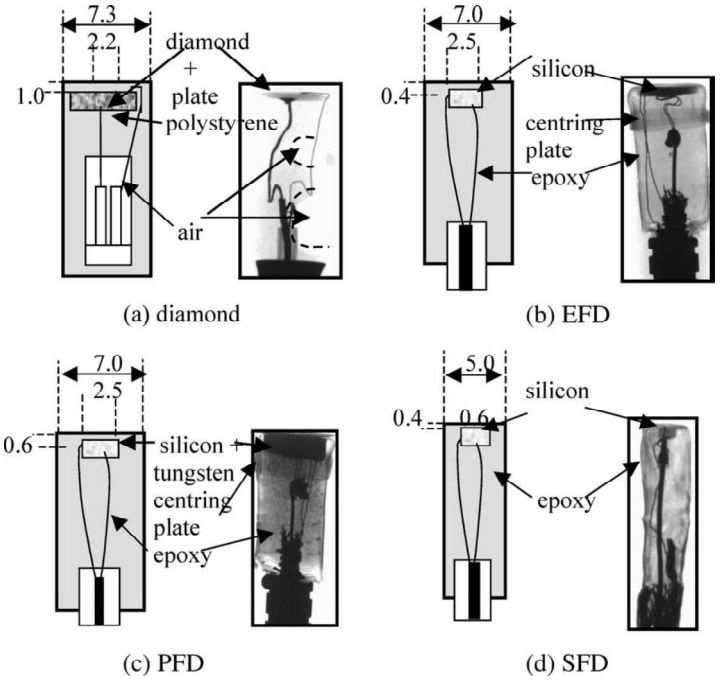

C. McKerracher, D.I. Thwaites /
Radiotherapy and Oncology 79 (2006) 348–351

Perturbations dependent on field size!

ESTRO School

Detector perturbation
the influence of detector density at small field sizes

$$\frac{D_{\text{water-voxel in water}}}{D_{\text{detector-voxel in water}}}$$

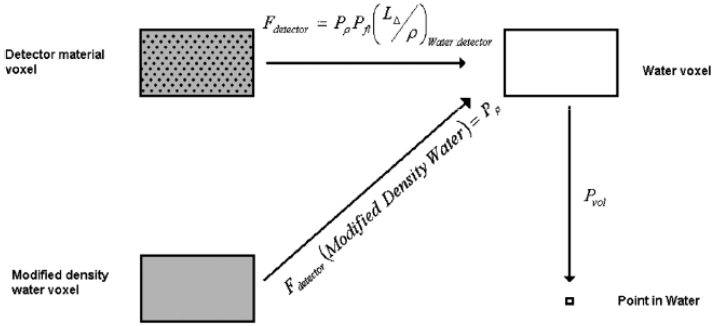

$$\frac{D_{\text{water in water}}}{D_{\text{water-voxel with detector density in water}}}$$

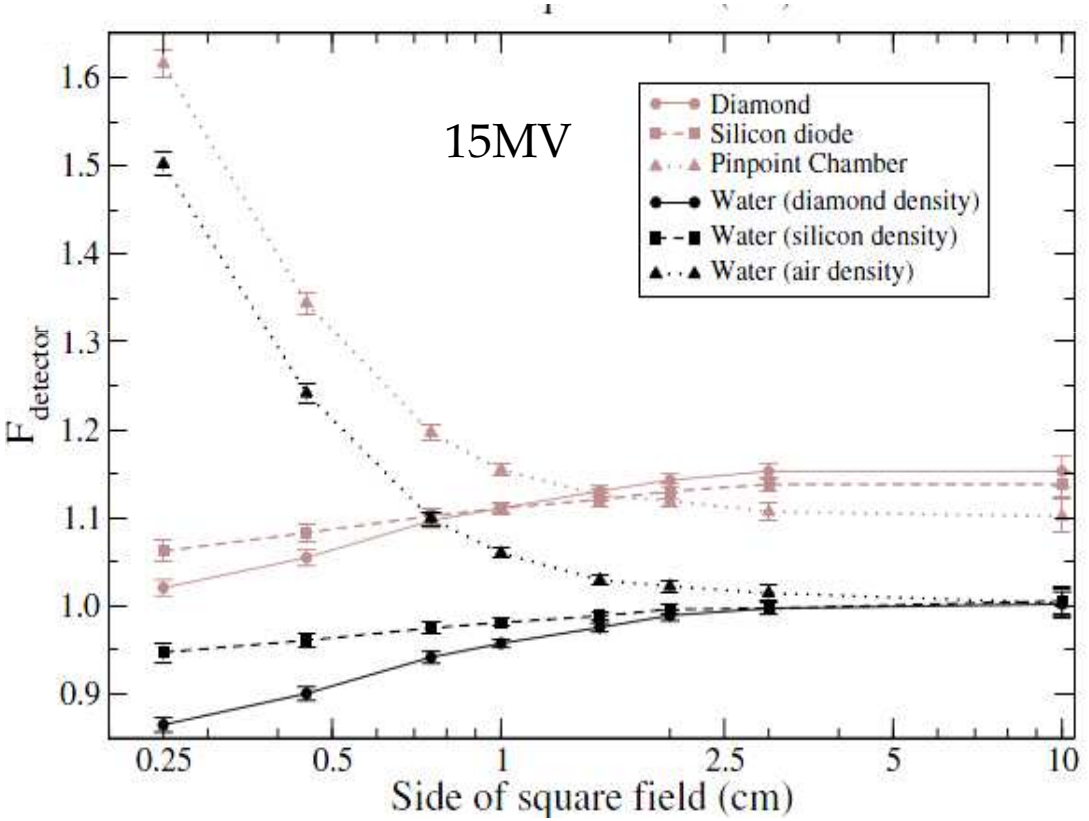

Scott et al PMB, 57 (2012) 4461-4476

ESTRO School

Small MV photon field conditions

- For the selected energy and medium, the field size is not large enough to ensure lateral CPE (lack of LEE).
- The entire source is not in the detector's-eye-view (source occlusion).
- The detector is not small enough and perturbs fluence *significantly* (detector issues)

Small MV photon fields: characteristics

- changes in beam spectra with collimating method, accelerating potential, field size and depth
- dose profiles: overlapping penumbra & apparent widening of field
- drop in beam output

Photon energy fluence spectra in water

variation with field size and depth in water

6MV

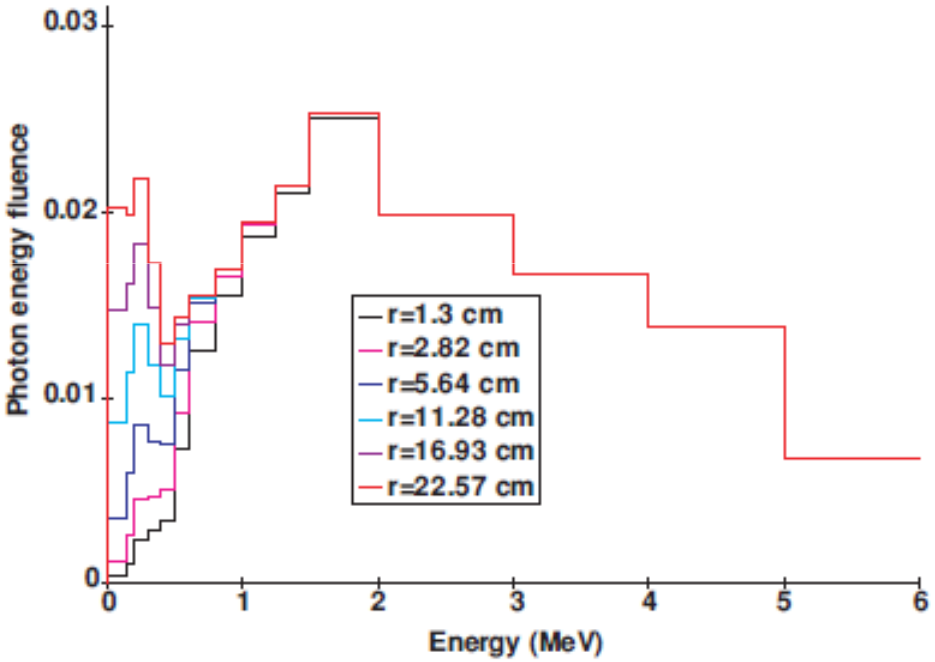

at depth of maximum build-up

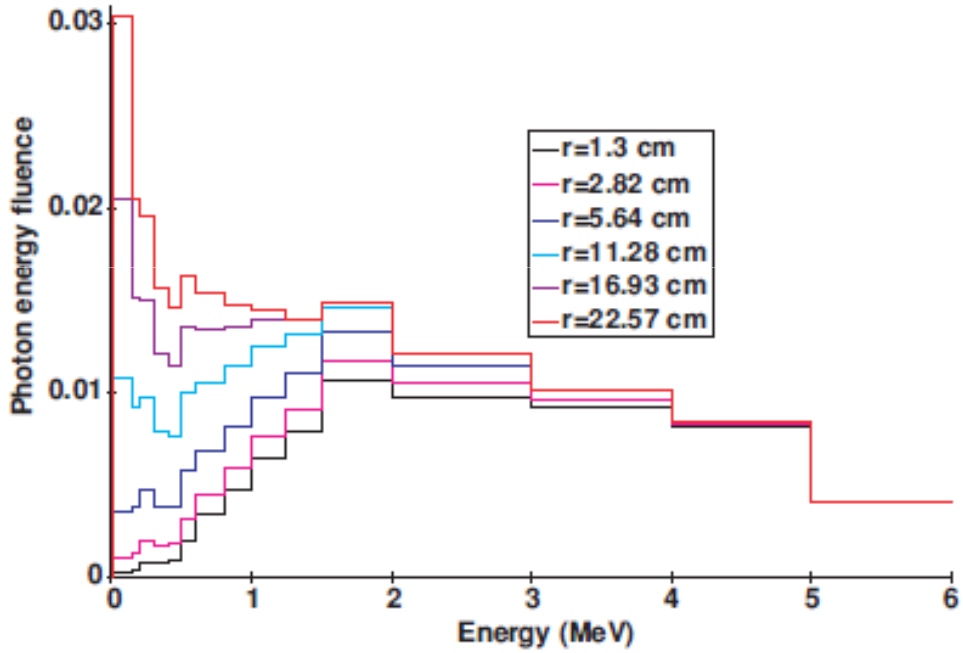

at 150mm depth

Yin et al Phys Med Biol 49(16) (2004)

ESTRO School

Particle fluence spectra in water
variation with field size, 6MV 50mm depth

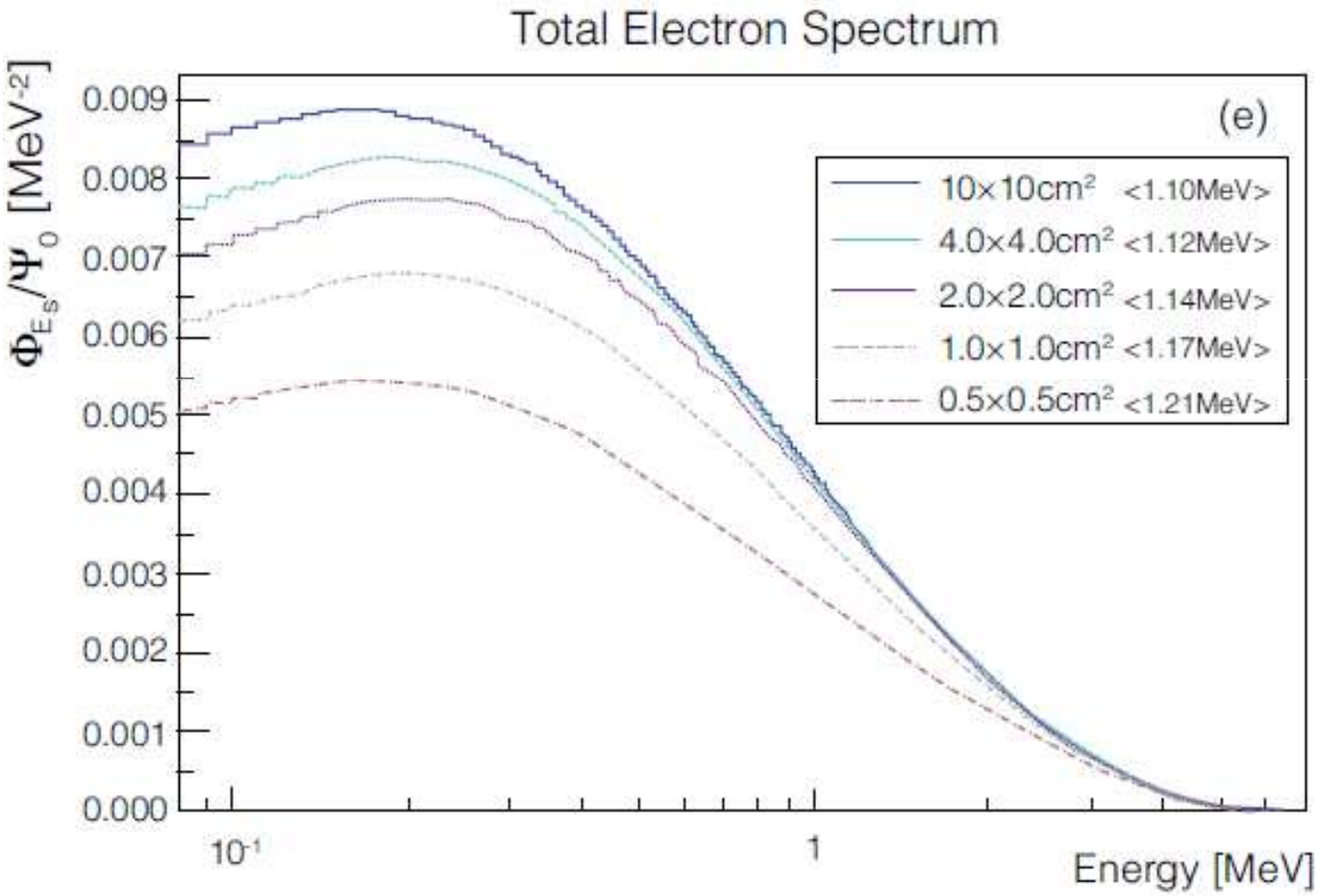

Eklund and Ahnesjö, PMB 53(16) 2008

ESTRO School

Overlapping penumbra, source occlusion → drop in output

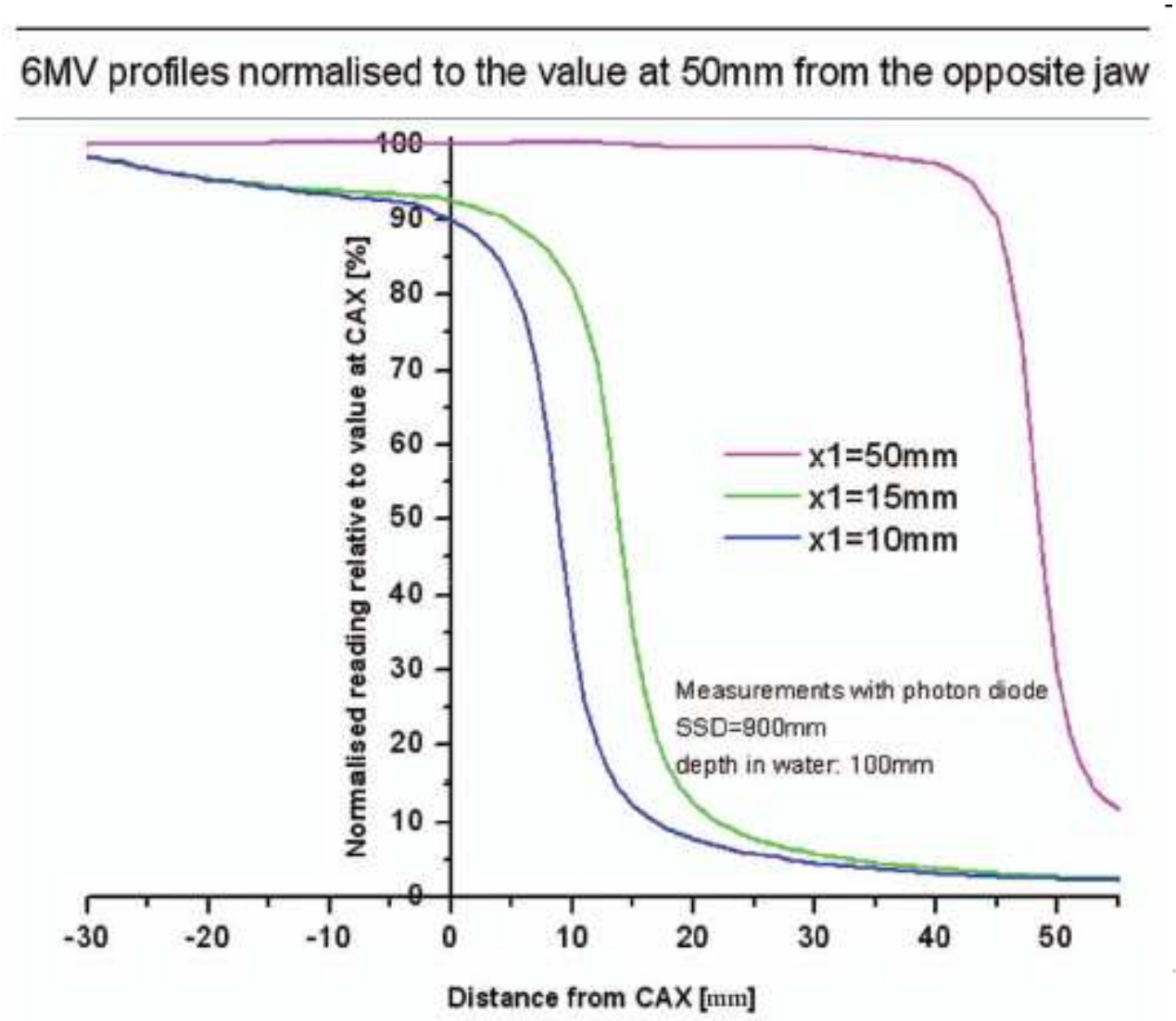

IPEM report 103, 2010

ESTRO School

Drop in output: detector dependence

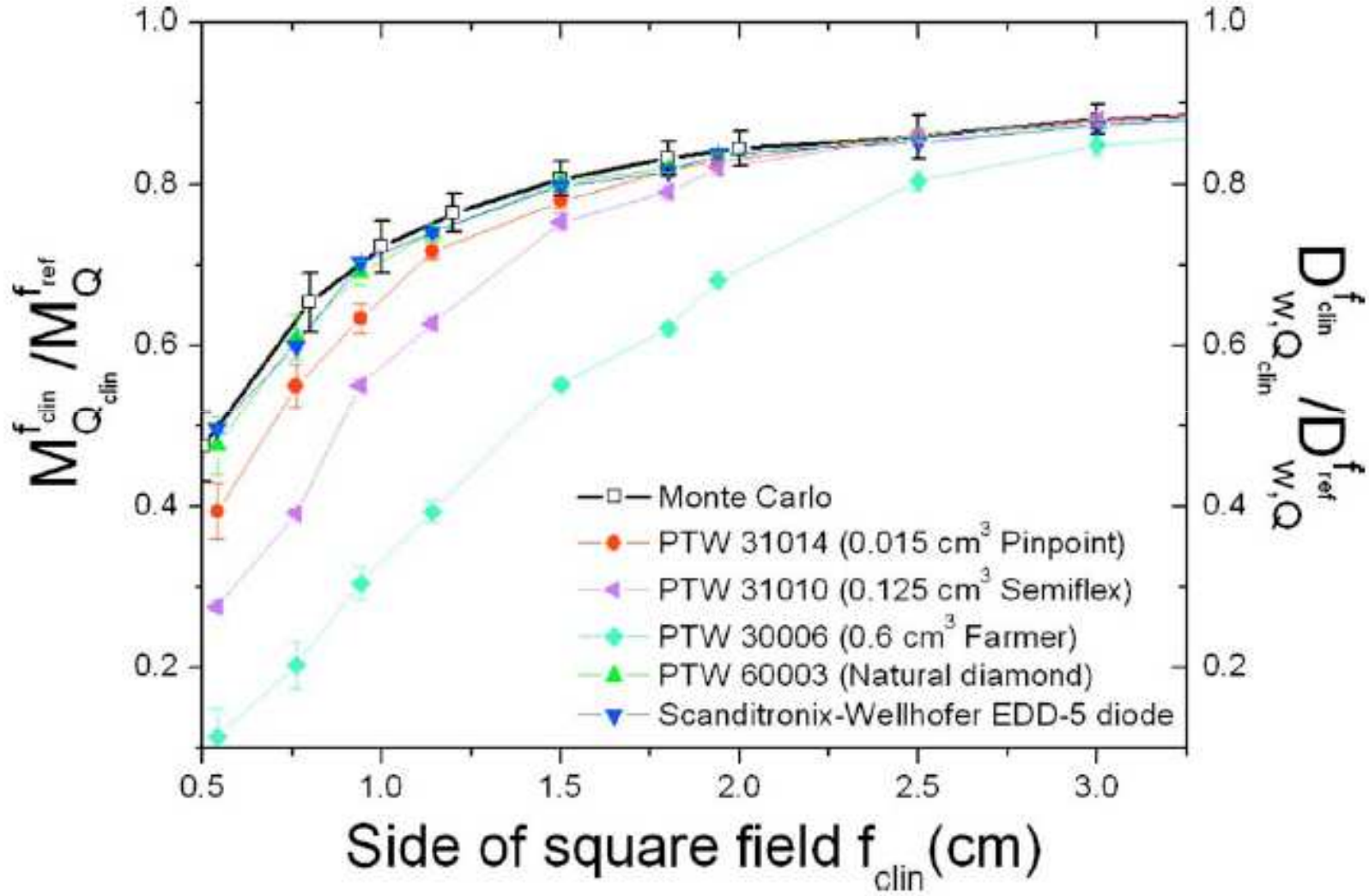

Sanchez-Doblado et al , Physica Medica, 23, 58-66, 2007

ESTRO School

Learning objectives – 2

Current practice and developments on the determination of dose in small fields

Determination of dose in small fields

Careful experimental setup: alignment with beam's CAX

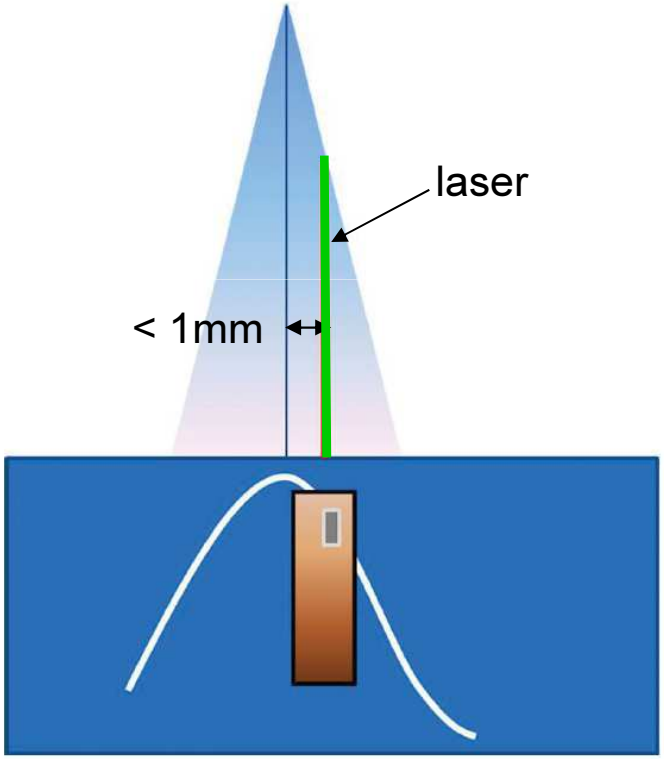

Dietrich & Sherouse Med Phys 38(7), 2011

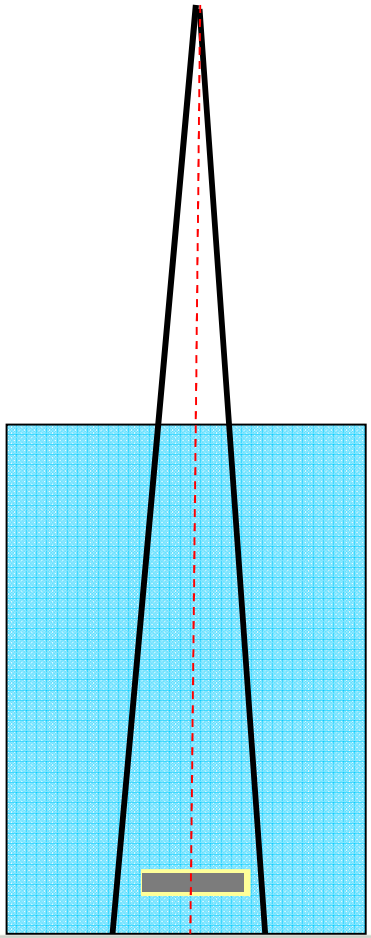

ESTRO School

Determination of dose in small fields

Choice of detector & knowing its dependencies

- Energy dependence of detector response
- Perturbation effects
  - Volume averaging
  - Ionization chambers: wall, central electrode, air cavity different from water
  - Solid state detectors (e.g. diodes): housing, shielding, coating of silicon chip

Relative dose - profiles

- To determine the penumbra correctly use a small detector (consider directional dependence)
- Check the detector response outside the geometrical field

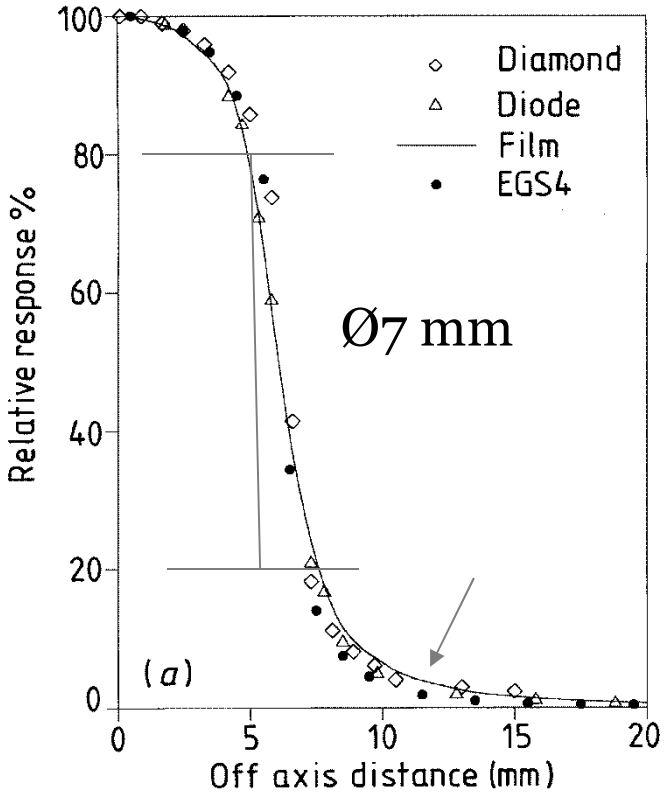

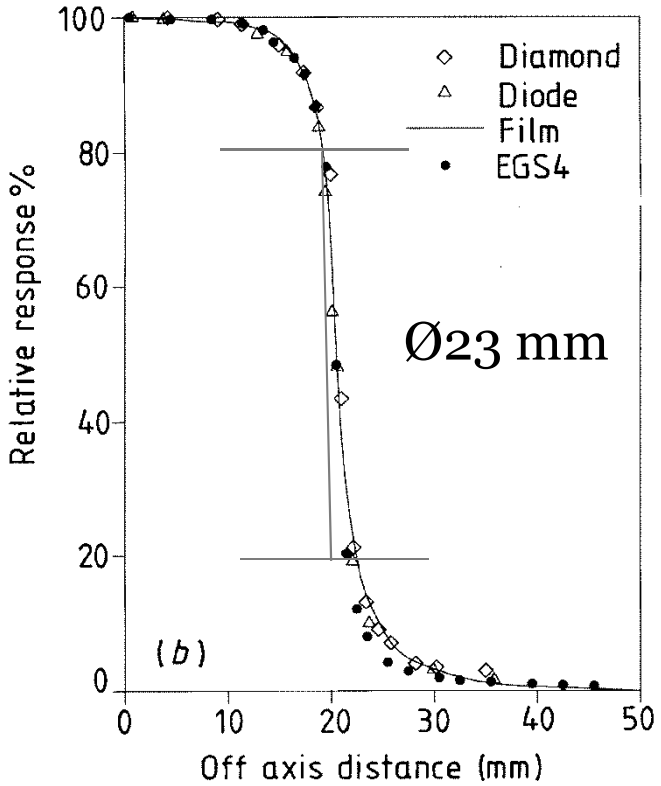

Heydarian et al PMB 41 (1996) 93–110

ESTRO School

Determination of dose in small fields

Relative dose: output factors (field size factor), S_{cp}

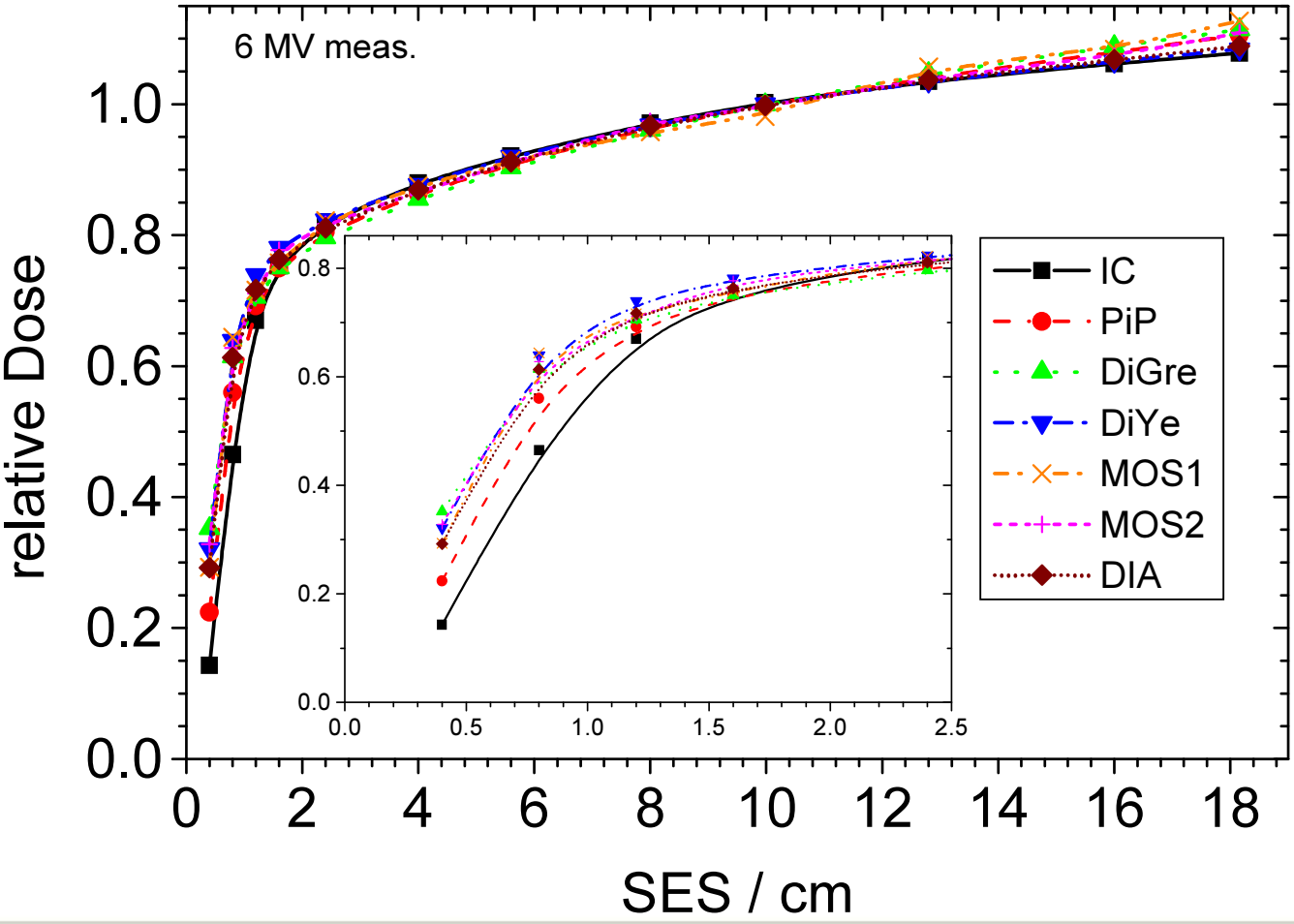

Sauer & Wilbert MP **34**, 2007, 1983-1988

ESTRO School

Determination of dose in small fields

Characterise the sensitivity of the diode

Normalised response ratios

$$\frac{\text{Dose to det}}{\text{Dose to water}} =$$

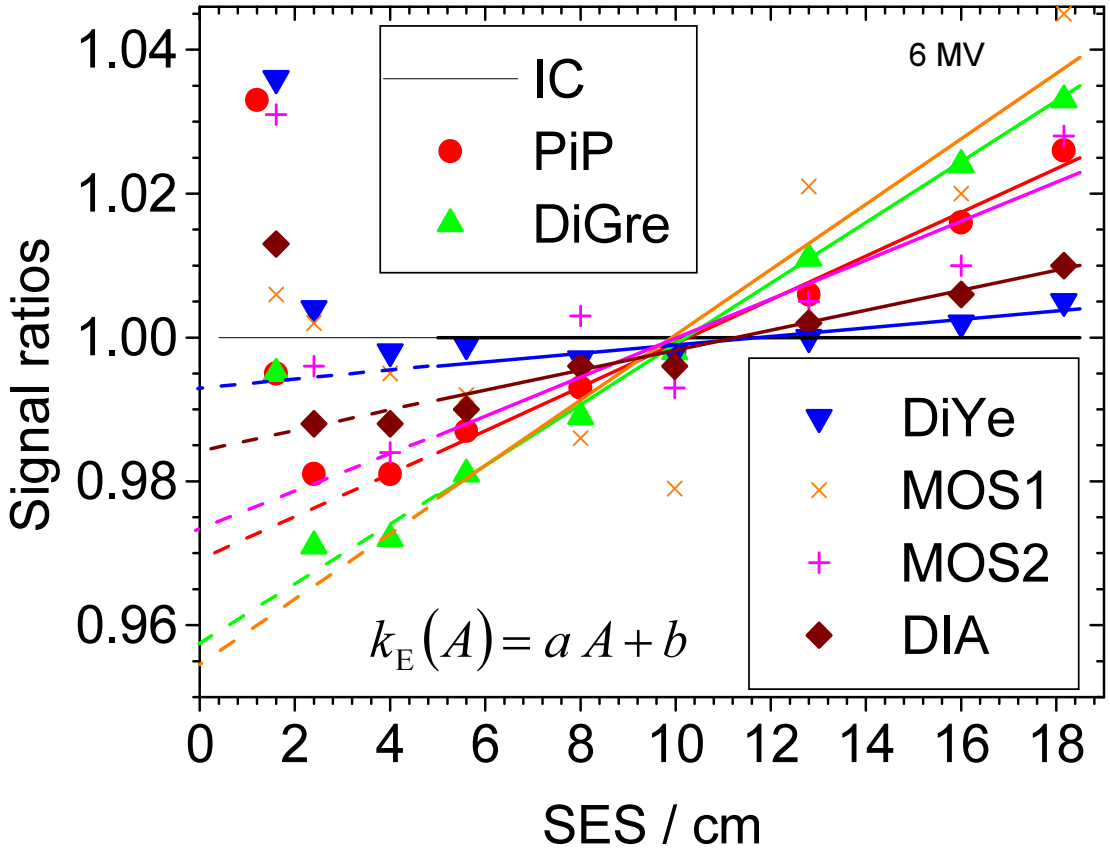

Sauer & Wilbert MP **34**, 2007, 1983-1988

Unshielded diodes under-respond at small fields?

ESTRO School

Relative dose: output factors (field size factor), S_{cp}

$$S_{cp}(A) = \frac{D_w(A, z_{ref})}{D_w(A_{ref}, z_{ref})} = \frac{M(A, z_{ref})}{M(A_{ref}, z_{ref})} \left[\left(\frac{\bar{S}}{\rho}\right)_{air}^{w}\right]_{A_{ref}}^{A} [p_{det}]_{A_{ref}}^{A}$$

A: field size (aperture)

z_{ref}: reference depth

$$D_{water} = M\left[\left(\frac{\bar{W}_{air}}{e}\right)\frac{1}{m_{air}}\right]\left[\left(\frac{\bar{S}}{\rho}\right)_{air}^{water} p_{det}\right]$$

Challenges in the determination of S_{cp}

- volume effect
- energy dependence
- perturbation

ESTRO School

Determination of dose in small fields

Reference dose with air-filled ionisation chambers

$$D_{w,Q}^{f_{ref}} = M_Q^{f_{ref}} \cdot N_{D,w,Q_o} \cdot k_{Q,Q_o}$$

IAEA, TRS-398 (2000)

$$k_{Q,Q_o} = \frac{\left(\frac{\overline{W}_{air}}{e}\right)_Q \left[\left(\frac{\overline{S}}{\rho}\right)_{air}^{water}\right]_Q p_Q}{\left(\frac{\overline{W}_{air}}{e}\right)_{Q_0} \left[\left(\frac{\overline{S}}{\rho}\right)_{air}^{water}\right]_{Q_0} p_{Q_0}} \approx \frac{\left[\left(\frac{\overline{S}}{\rho}\right)_{air}^{water}\right]_Q p_Q}{\left[\left(\frac{\overline{S}}{\rho}\right)_{air}^{water}\right]_{Q_0} p_{Q_0}}$$

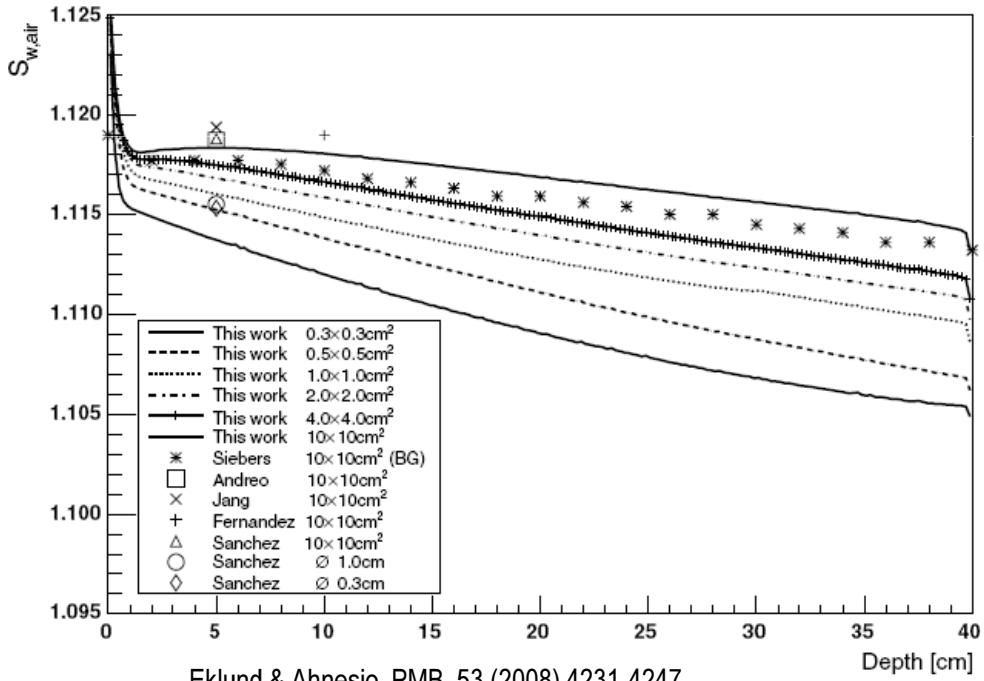

Eklund & Ahnesjo, PMB, 53 (2008) 4231-4247

Note!

There are differences in Sw,air between beams with and without flattening filter (see

Xiong and Rogers , Med Phys 35(5) (2008), p2104)

ESTRO School

Small fields: relative dosimetry - field size factor, S_{cp}

measurement with an ionisation chamber

large perturbation?

$$S_{cp}(A) = \frac{D_w(A, z_{ref})}{D_w(A_{ref}, z_{ref})} = \frac{M(A, z_{ref})}{M(A_{ref}, z_{ref})} \left[\left(\frac{\bar{S}}{\rho} \right)_{air}^{w} \right]_{A_{ref}}^{A} [p_{det}]_{A_{ref}}^{A}$$

Challenge: perturbation factors

A: field size (aperture)

z_{ref}: reference depth

ESTRO School

Small fields: relative dosimetry - field size factor, S_{cp}

measurement with a solid state detector (diode)

large energy dependence

$$S_{cp}^{diode}(A) = \frac{D(A, z_{ref})}{D(A_{ref}, z_{ref})} = \frac{M(A, z_{ref})}{M(A_{ref}, z_{ref})} \left[k_{E,det}\right]_{A_{ref}}^{A} \left[p_{det}\right]_{A_{ref}}^{A}$$

$\left[k_{E,det}\right]_{A_{ref}}^{A}$

Characterise the sensitivity of the detector

$\left[p_{det}\right]_{A_{ref}}^{A}$

≈1 for detector Ø <A (?)

ESTRO School

Small fields: relative dosimetry - field size factor, S_{cp}

Characterise the sensitivity of the diode

MC simulation of normalised response of unshielded diode PTW 60012

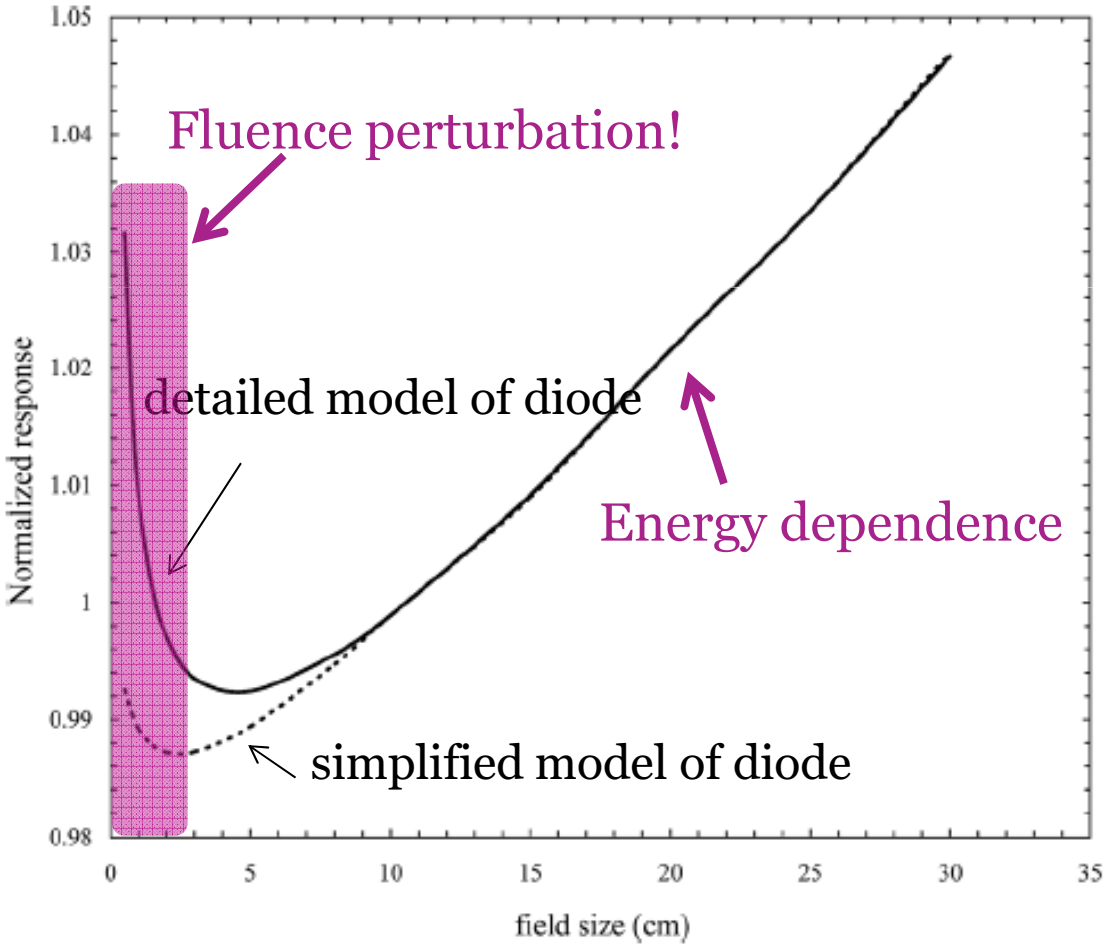

unshielded diode over-responds at small fields

correction to ratio of readings < 1

Franscescon et al MP 38(12), 2011

ESTRO School

Small fields: relative dosimetry - field size factor, S_{cp}

MC simulation of detector response

Correction to ratio of readings

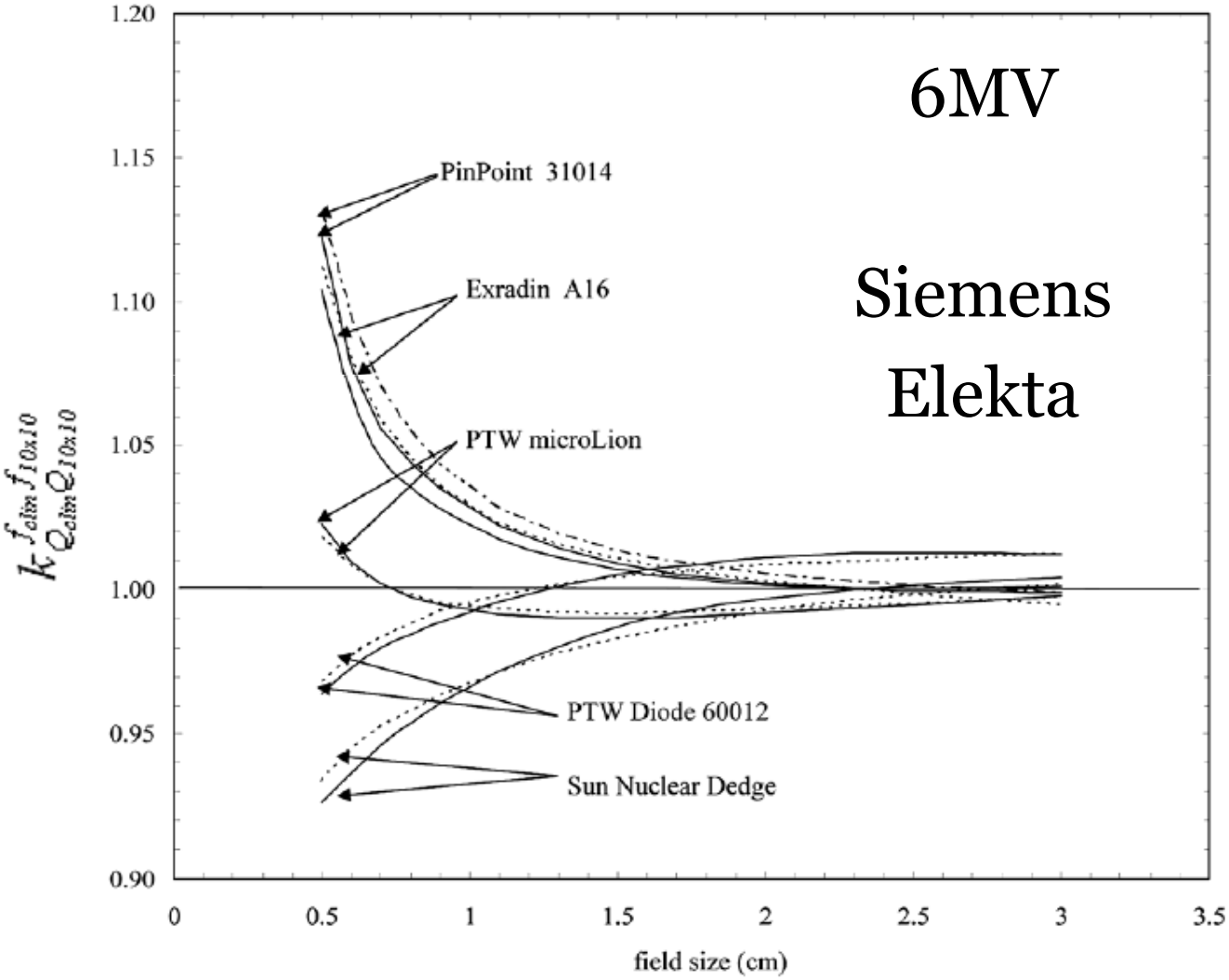

Franscescon et al MP 38(12), 2011

ESTRO School

Challenges in the determination of S_{cp}

- Volume averaging
- Energy dependence
- Fluence perturbation

Correction for volume averaging

Derived from an integration of the 3D dose distribution in the water phantom over the **volume** of the detector.

For example:

Morin et al MP, 40(1), 2013

Defined as the inverse of the detector signal integrated over its **area** and weighted by the off-axis ratio from film measurements (film profiles)

$$F_{\text{average}} = \frac{\int_0^{2\pi} \int_0^{d/2} D(r,\theta)\, r\, dr\, d\theta}{\pi d^2/4}.$$

Here, F_{average} is the average reading of the detector, d is the detector diameter perpendicular to the radiation beam, r and θ represent the position from the center in polar coordinates, and $D(r, \theta)$ is the relative dose value at the position r and θ normalized to the dose at the center of the field. The calcu-

$$k_{vol} = \frac{1}{F_{average}}$$

Small fields: relative dosimetry in practice

Correction for volume averaging

TABLE II. Calculated volume-averaging correction factors [$1/F_{average}$ in Eq. (3)] for each detector.

Detector	5-mm cone diameter	7.5-mm cone diameter	10-mm cone diameter
0.5-mm PSD	1.003	1.001	1.000
1.0-mm PSD	1.011	1.002	1.001
PTW 60008	1.014	1.003	1.001
PTW 60012	1.014	1.003	1.001
MicroLion chamber	1.068	1.016	1.007
SFD diode	1.004	1.001	1.000

Morin et al MP, 40(1), 2013

Detector	Stem orientation	Field size	Volume averaging correction factor
FOD	Perpendicular	4 mm cone, 5 mm MLC	1.009
SFD	Perpendicular	4 mm cone, 5 mm MLC	1.002
SFD	Parallel	4 mm cone, 5 mm MLC	1.003
60012	Perpendicular	4 mm cone, 5 mm MLC	1.004
60012	Parallel	4 mm cone, 5 mm MLC	1.007
EFD, PFD	Perpendicular	4 mm cone, 5 mm MLC	1.018
EFD, PFD	Parallel	4 mm cone, 5 mm MLC	1.037
EFD, PFD	Perpendicular	7.5 mm cone	1.004
EFD, PFD	Parallel	7.5 mm cone	1.007

Ralston et al PMB, 57, 2012

ESTRO School

Minimise energy/field size dependence

An **approximation to account** for the influence of spectral changes between the 10cm × 10cm and a smaller field (e.g. 4cm × 4cm) on detector response would be to *cross-calibrate the small detector against a medium size detector in an intermediate field* (smaller than the reference field of 10cm × 10cm);

This is referred to as '**daisy-chaining'** by Dietrich & Sherouse MedPhys 38(7), 2011

$$S_{cp}(A) \cong \frac{M_{diode}(A)}{M_{diode}(A_{int})} \cdot \frac{M_{IC}(A_{int})}{M_{IC}(A_{ref})}$$

Small fields: relative dosimetry in practice

‘Daisy-chaining’
the normalisation of output factors through an intermediate field

Normalisation to value at 10cm ×10cm

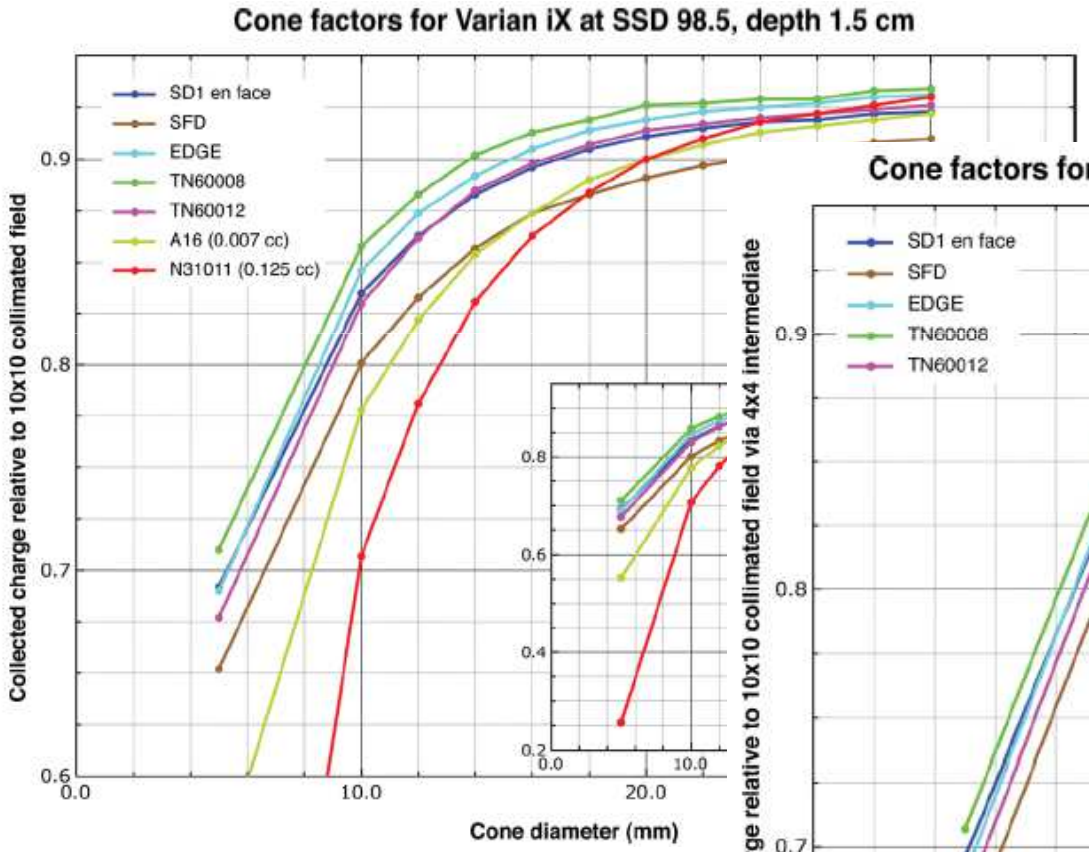

Normalisation to value at 4cm × 4cm

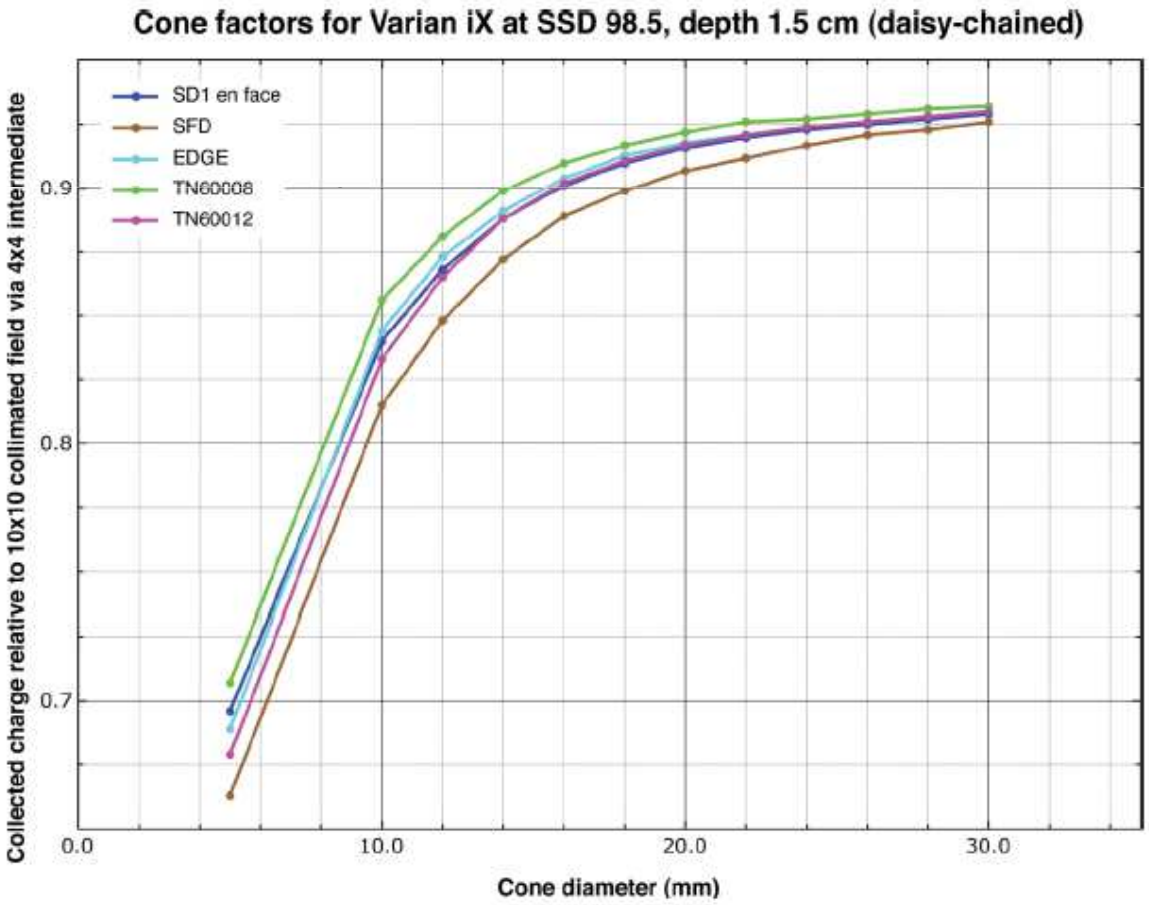

Dietrich & Sherouse Med Phys 38(7), 2011

Small fields: relative dosimetry - field size factor, S_{cp}

$$S_{cp}^{diode}(A) = \frac{D(A, z_{ref})}{D(A_{ref}, z_{ref})} = \frac{M(A, z_{ref})}{M(A_{ref}, z_{ref})} \left[k_{E,det}\right]_{A_{ref}}^{A} \left[p_{det}\right]_{A_{ref}}^{A}$$

On-going research to determine overall correction factors for detectors available in the clinic; based on the IAEA/AAPM formalism of Alfonso *et al* 2008

→ **new CoP**

Small static MV fields: reference dose determination

f_{msr} machine specific reference field

Q_{msr} beam quality of machine specific reference field

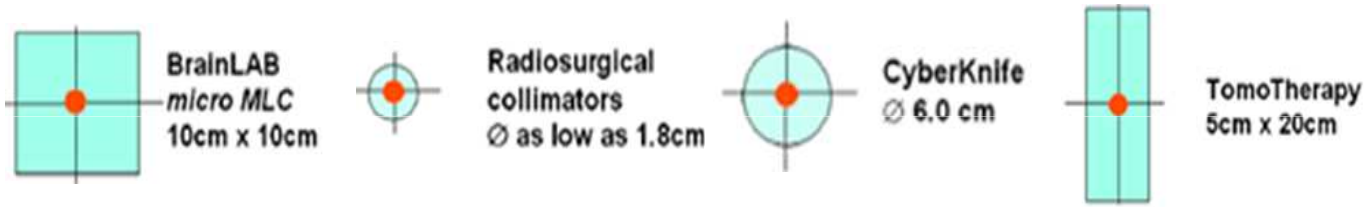

$$D^{f_{msr}}_{w,Q_{msr}} = M^{f_{msr}}_{Q_{msr}} \cdot N_{D,w,Q_o} \cdot k_{Q,Q_o} \cdot k^{f_{msr},f_{ref}}_{Q_{msr},Q}$$

Alfonso el al (2008), Med Phys 35 (11)

IAEA/AAPM formalism for reference dosimetry

field instrument correction factors

$$k_{Q_{msr},Q}^{f_{msr},f_{ref}} = \frac{N_{D,w,Q_{msr}}}{N_{D,w,Q}} = \frac{D_{w,Q_{msr}(pcsr)}^{f_{msr}} \Big/ D_{w,Q}^{f_{ref}}}{M_{Q_{msr}}^{f_{msr}} \Big/ M_{Q}^{f_{ref}}}$$

ref detector

field instrument

Determined through:

- Experiment: by a primary standard
- Experiment: using dosimeters that can measure reference dose traceable to a primary standard and which have sufficiently low uncertainty (alanine, radiochromic film, diamond, liquid ion-chambers ...)
- Calculation: Monte Carlo simulations (MC)

IAEA/AAPM formalism for reference dosimetry

small static MV photon fields

$$k_{Q_{msr},Q}^{f_{msr},f_{ref}}$$

Measurements

Machine	f_{msr}	Reference detector	Field Instrument chamber	$k_{Q_{msr},Q}^{f_{msr},f_{ref}}$	Reference
TomoTherapy	5 × 10 cm²	Alanine	NE2571	1.013(14)	Bailat *et al.* (2009)
			NE2611	0.996(12)	Bailat *et al.* (2009)
				1.000(8)	Duane *et al.* (2006)
			Exradin A1SL	0.984(11)	Bailat *et al.* (2009)
				0.996(8)	Duane *et al.* (2006)
				0.982(19)	Gago-Arias *et al.* (2012)
			PTW 30013	1.016(15)	Pressello *et al.* (2011)
Cyberknife	6 cm ∅	Alanine	PTW 30013	0.999(16)	Pantelis *et al.* (2010)
			PTW 31014	0.987(22)	Gago-Arias *et al.* (2013)
			CC13	0.999(20)	Gago-Arias *et al.* (2013)
Gamma Knife	1.8 cm ∅	MD-55 Film	PTW 233642	0.9967(16)	Somigliana *et al.* (1999)

IAEA/AAPM formalism for reference dosimetry

small static MV photon fields

Reference dosimetry on Cyberknife: chamber factors calculated with MC

$k_{Q_{msr},Q}^{f_{msr},f_{ref}}$

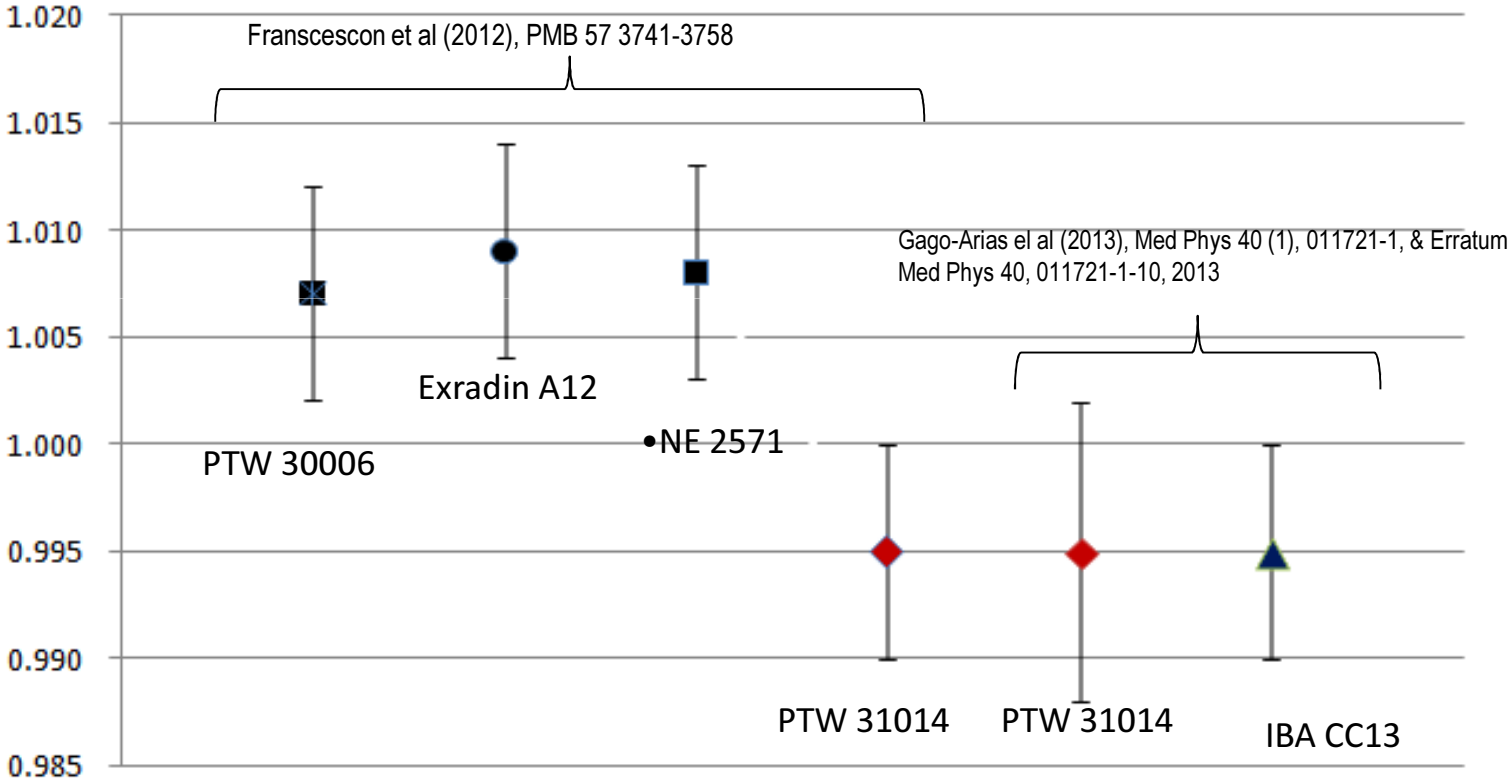

Specification of a reference-class ionisation chamber

Not all micro-chamber designs are considered suitable for reference dosimetry

Characteristic	Limits
Chamber stabilization	0.5% change in reading from beam-on to stabilization (in less than 5min)
Leakage current	Less than 0.1% of reading
Polarity correction	Less than 0.4% in either direction
Ion recombination correction	1. Plot 1/change vs 1/polarising voltage linear 2. Correction linear with dose per pulse 3. 'apparent' initial recombination less than 1.002 at polarising voltage of 300V 4. Difference of 'apparent' initial recombination at opposing polarities less than 0.1%
Thermal expansion of chamber material	Effect of temperature on chamber very small (e.g. 0.04% $^{\circ}C^{-1}$)
Sensitivity to humidity	low
Stable response between calibrations	Change in calibration coefficient less than 0.3%
Long term stability in response	

McEwen , Med Phys 37, 2010, 2179-93

Specification of a reference-class ionisation chamber

Polarity effects in small chambers (affecting recombination correction)

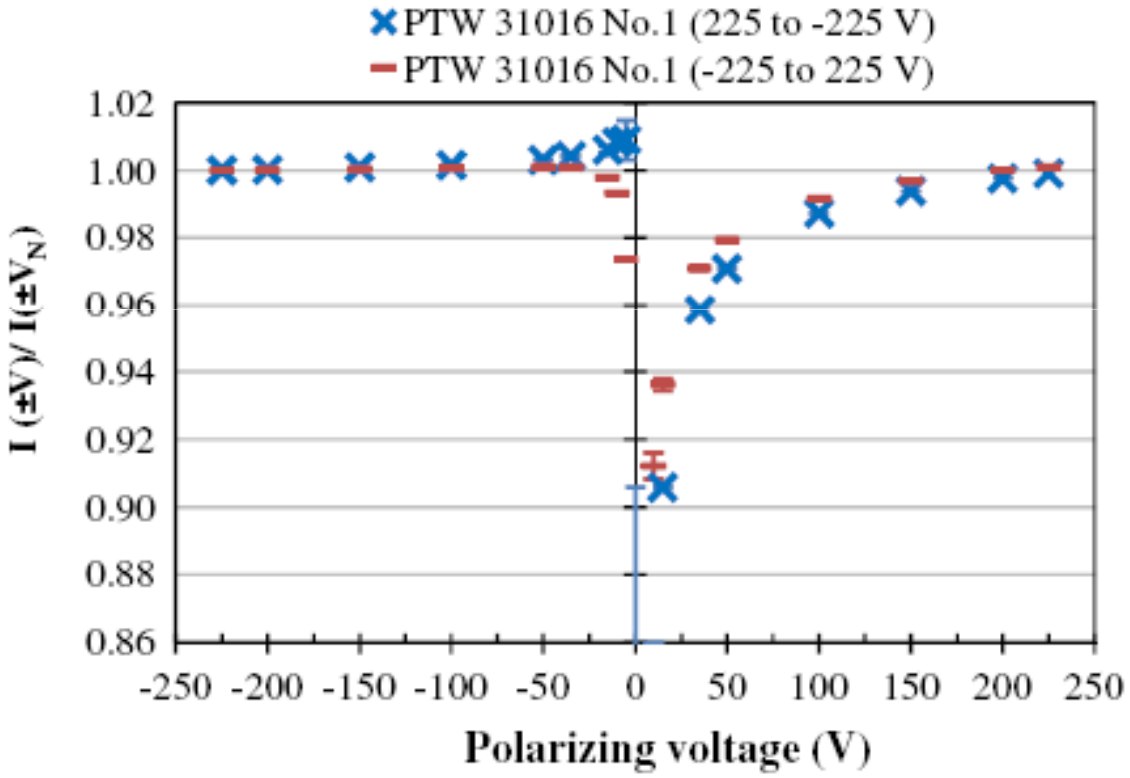

Le Roy (2011), PMB, 56 (2011) 5637-5650

ESTRO School

IAEA/AAPM formalism for reference dosimetry

composite MV photon fields

$$D_{w,Q_{pcsr}}^{f_{pcsr}} = M_{Q_{pcsr}}^{f_{pcsr}} \cdot N_{D,w,Q_o} \cdot k_{Q,Q_o} \cdot k_{Q_{msr},Q}^{f_{msr},f_{ref}} \cdot k_{Q_{pcsr},Q_{msr}}^{f_{pcsr},f_{msr}}$$

$$k_{Q_{pcsr},Q}^{f_{pcsr},f_{ref}}$$

Q_{pcsr} beam quality for the pcsr field

f_{pcsr} represents a class of dynamic or step-and-shoot delivery fields, or a combination of fields, such that full CPE is achieved in a time average sense at the position of the detector

For example, AAPM TG148 recommends:

A field that delivers a uniform 2Gy to a cylinder of 8cm diameter and 10cm length, placed along the axis of a Virtual Water Cclindrical phantom, using 5cm slice thickness and 0.287 pitch and 1.807 modulation factor

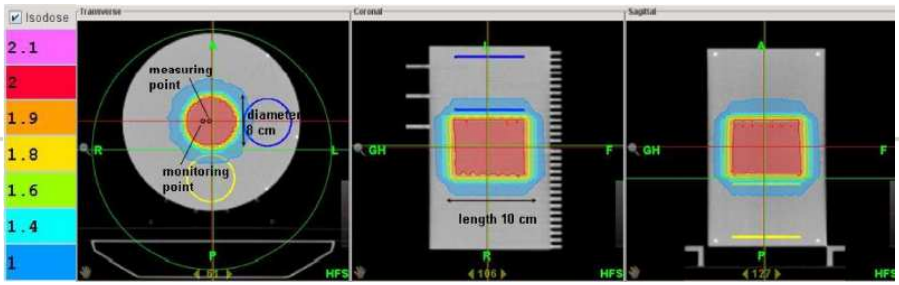

IAEA/AAPM formalism for reference dosimetry

composite MV photon fields

Definition of f_{pcsr}

Alfonso el al (2008), Med Phys 35 (11):
a class of dynamic or step-and-shoot delivery fields, or a combination of fields, such that full CPE is achieved in a time average sense at the position of the detector

Bouchard et al (2012), Med Phys 39 (3)
Formal proof that CPE cannot be practically achieved in a finite volume in external beam RT.

Proposed new definiton of PCSR field:
a field that represents a class of dynamic or step-and-shoot delivery fields, or a combination of fields, such that the absorbed dose distribution is uniform at the position of the detector, as opposed to conventional RT in which a dose gradient is present.

IAEA/AAPM formalism for reference dosimetry

composite MV photon fields

Detector correction factor

$$k_{Q_{pcsr},Q}^{f_{pcsr},f_{ref}} = \frac{D_{w,Q_{pcsr}}^{f_{pcsr}}}{D_{w,Q}^{f_{ref}}} \cdot \frac{M_{Q}^{f_{ref}}}{M_{Q_{pcsr}}^{f_{pcsr}}}$$

Reference field

$$f_{\text{ref}} \begin{cases} \text{conventional } 10\text{cm} \times 10\text{cm} \\ \text{or} \\ f_{\text{msr}} \end{cases}$$

ESTRO School

IAEA/AAPM formalism for reference dosimetry

composite MV photon fields

NE2571

$$k_{Q_{pcsr},Q}^{f_{pcsr},f_{ref}}$$

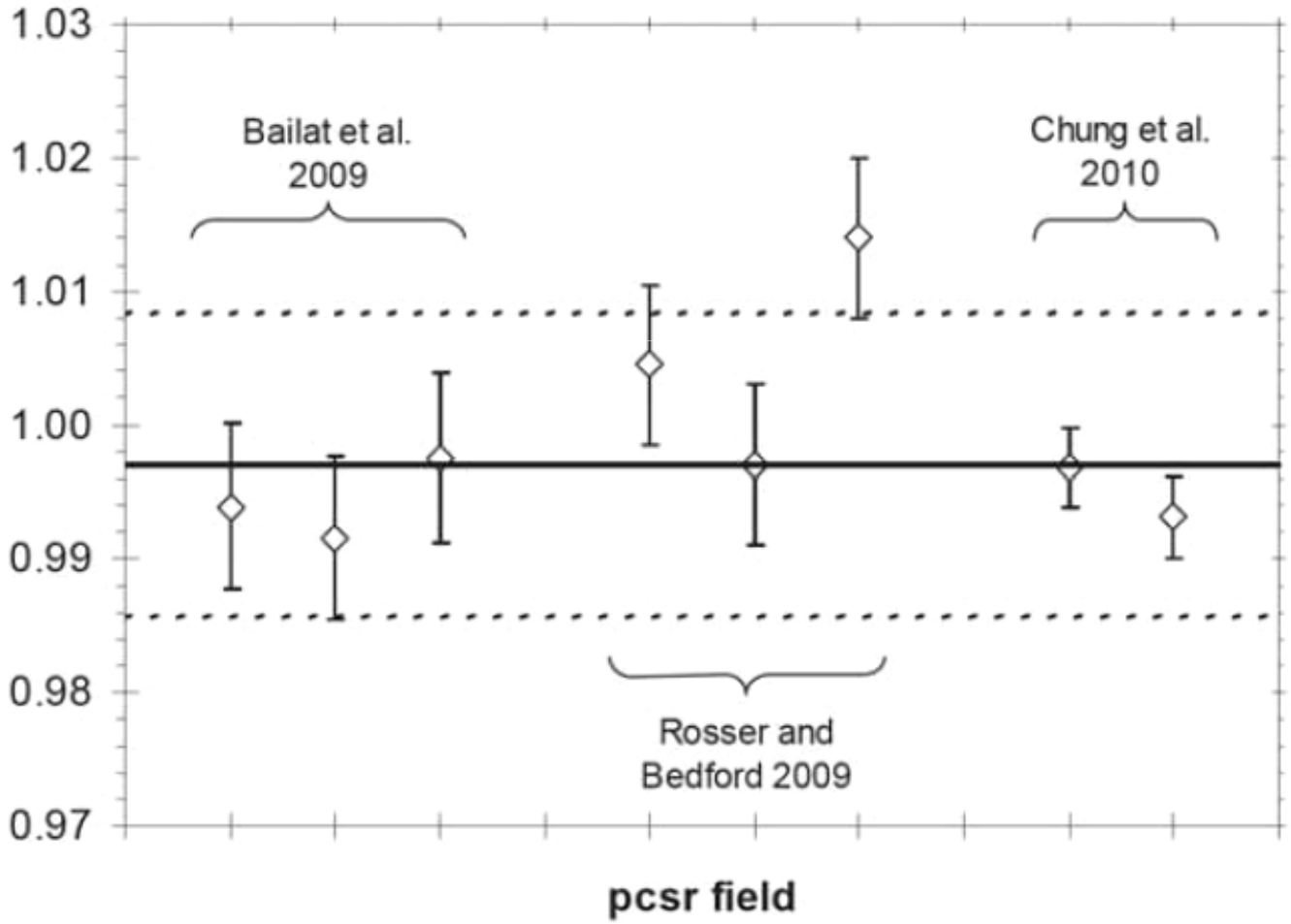

Palmans H 2011 Small and composite field dosimetry: the problems and recent progress *Proc. Int. Symp. on Standards, Applications and Quality Assurance in Medical Radiation Dosimetry IAEA-CN-182/347*

ESTRO School

IAEA/AAPM formalism for reference dosimetry

composite MV photon fields

$k_{Q_{pcsr},Q}^{f_{pcsr},f_{ref}}$

Cago-Arias et al, MP 39(4), 2012

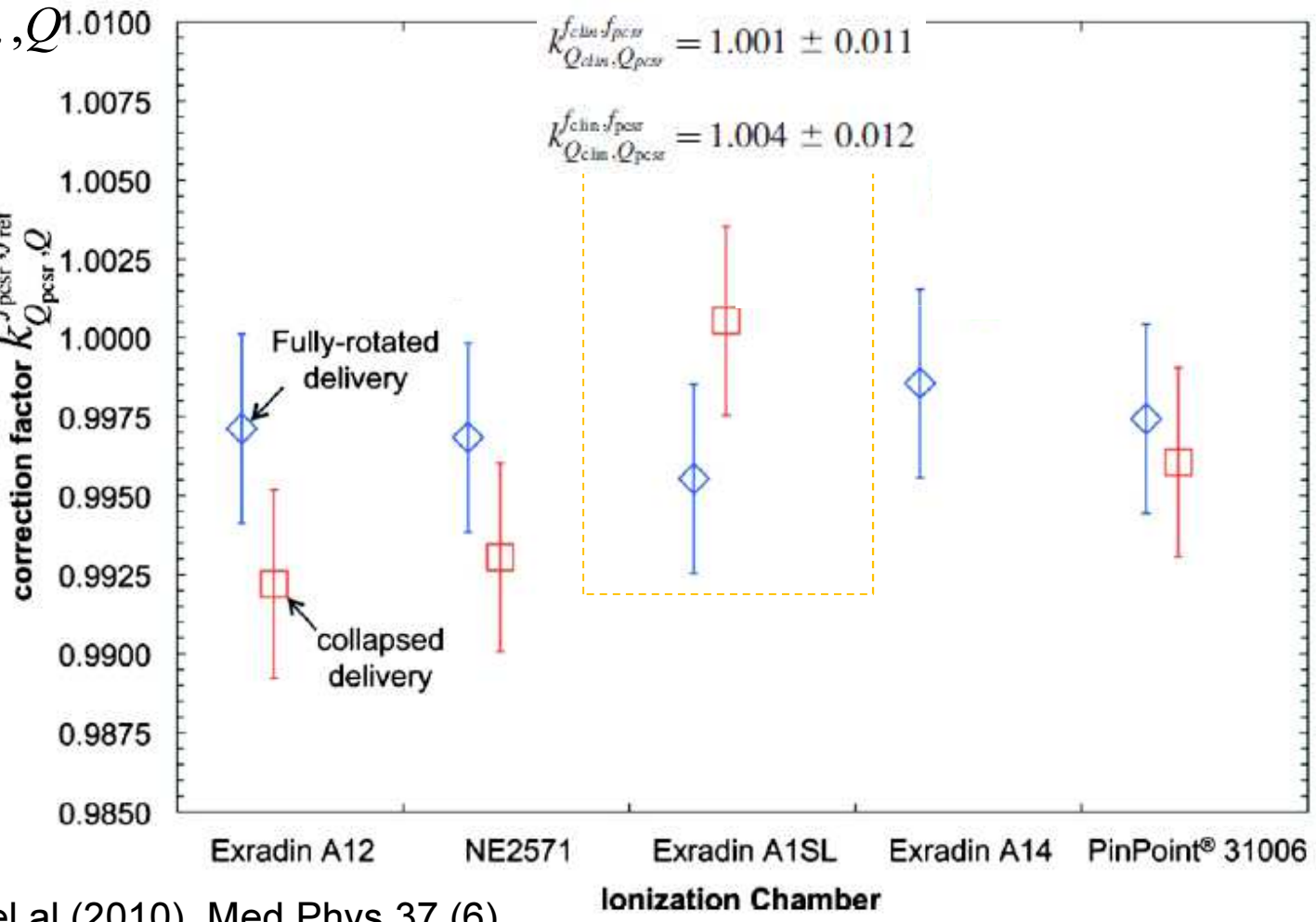

Chung el al (2010), Med Phys 37 (6)

ESTRO School

IAEA/AAPM formalism for reference dosimetry

composite MV photon fields

Standarisation of f_{pcsr}

Chung el al (2012), Med Phys 39 (1)
Proposal that these are to be fields with homogeneity index < 5% and modulation factor < 1.93

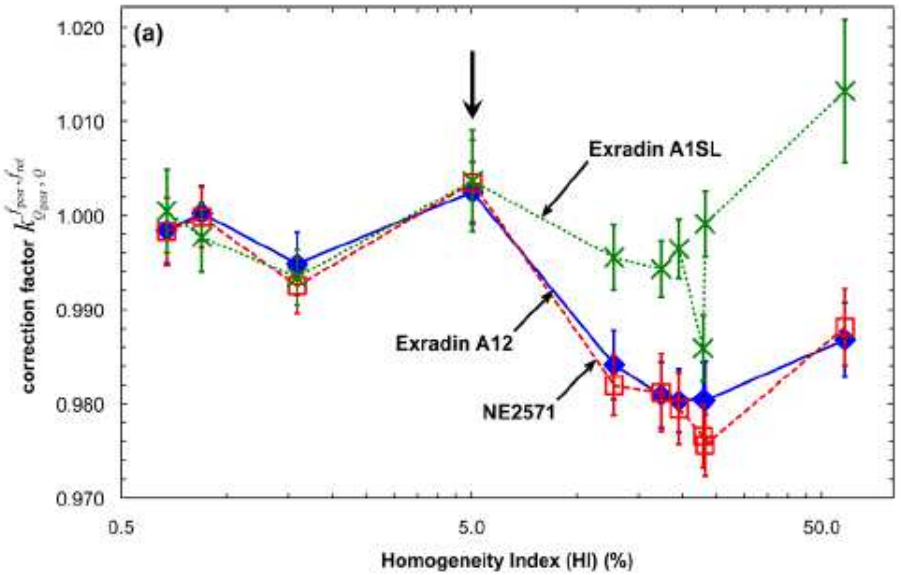

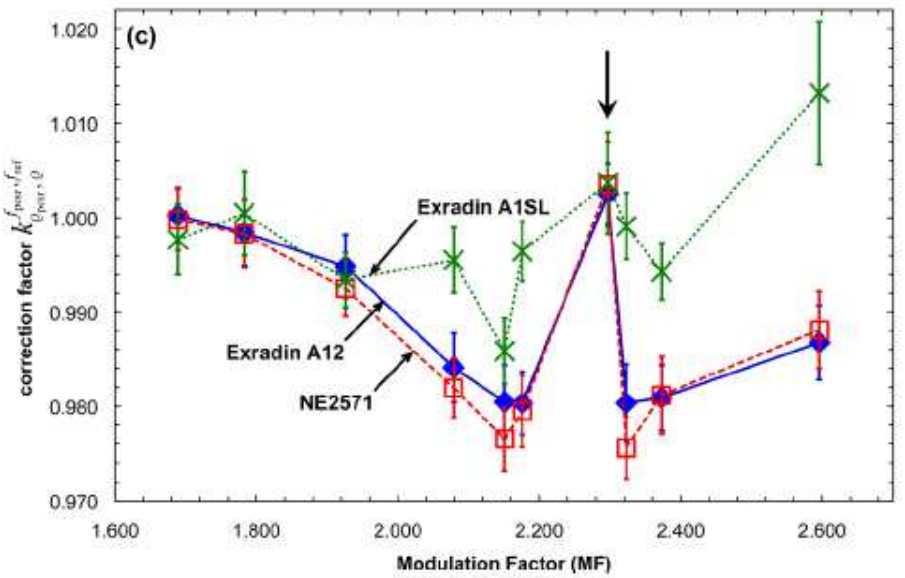

ESTRO School

IAEA/AAPM formalism for relative dosimetry

output factor determination in small static fields

$$D_{w,Q_{clin}}^{f_{clin}} = D_{w,Q_{msr}}^{f_{msr}} \Omega_{Q_{clin},Q_{msr}}^{f_{clin},f_{msr}}$$

Small field detector-specific correction factor

Alfonso el al (2008), Med Phys 35 (11), **new CoP: IAEA TECDOC###**

ESTRO School

IAEA/AAPM formalism for relative dosimetry

output factor determination in small static fields

$$\frac{D_{w,Q_{clin}}^{f_{clin}}}{D_{w,Q_{msr}}^{f_{msr}}} = \Omega_{Q_{clin},Q_{msr}}^{f_{clin},f_{msr}}$$

$$= \frac{M_{Q_{clin}}^{f_{clin}}}{M_{Q_{msr}}^{f_{msr}}} \left[\frac{D_{w,Q_{clin}}^{f_{clin}} \Big/ M_{Q_{clin}}^{f_{clin}}}{D_{w,Q_{msr}}^{f_{msr}} \Big/ M_{Q_{msr}}^{f_{clin}}} \right]$$

$$= \frac{M_{Q_{clin}}^{f_{clin}}}{M_{Q_{msr}}^{f_{msr}}} k_{Q_{clin},Q_{msr}}^{f_{clin},f_{msr}}$$

Small field detector-specific correction factor

Alfonso el al (2008), Med Phys 35 (11), **new CoP: IAEA TECDOC###**

ESTRO School

Small field detector correction factors

Account for three main detector perturbation effects:

$$k_{Q_{\text{clin}},Q_{\text{msr}}}^{f_{\text{clin}},f_{\text{msr}}} \approx \left[p_{vol}\right]_{Q_{\text{msr}}}^{Q_{\text{clin}}} \left[p_{fluence}\right]_{Q_{\text{msr}}}^{Q_{\text{clin}}} \left[p_{spectrum}\right]_{Q_{\text{msr}}}^{Q_{\text{clin}}}$$

Ratio of volume averaging correction factors

Ratio of charged particle fluence perturbation correction factors

Ratio of correction factors to account for the spectral dependence of photon energy absorption in the detector medium

Small field detector correction factors

Only different degree in CPE & spectral effects considered

$$\left[p_{fluence}\right]_{Q_{msr}}^{Q_{clin}} \quad \left[p_{spectrum}\right]_{Q_{msr}}^{Q_{clin}}$$

FS [cm]	0.6	0.9	1.2	1.8	2.4	3.0	4.2	10.0
TLD chips	1.000	…	1.003	1.008	1.004	1.000	1.005	1.010
TLD micro-cubes	0.998				9	1.000	1.001	1.007
IBA SFD diode	0.995				6	1.000	0.990	0.969
IBA PFD diode	0.936				9	1.000	1.000	1.001
IBA EFD diode	0.961				2	1.000	0.997	0.989
PTW 60003Diamond (Sensitive area ~ 15 mm^2)	0.995	…	0.983	0.992	1.002	1.000	0.996	0.995
PTW 60019 microDiamond	0.961	…	0.980	0.990				
RPLD (GDM-302M)	…	…	…	0.993				
Al_2O_3:C	0.980	0.982	0.985	0.991				
Scintillator 1	1.022	1.009	1.000	0.996				
Scintillator 2	1.028	1.015	1.006	1.000				
PTW 31018microLion	0.970	…	0.980	0.990				
IBA CC01	1.000	…	0.993	0.993				
IBA CC04	1.096	…	1.007	0.998				
IBA CC13[b]	…	…	1.033	1.008				
Wellhöfer IC10[b]			0	1.005	1.005	1.000	0.996	0.996
PTW 31014 PinPoint			7	1.002	1.000	1.000	0.998	1.002
PTW 31016 PinPoint 3D			3	1.000	1.001	1.000	0.998	0.999
PTW 31010 Semiflex[b]	…	…	1.027	1.002	1.004	1.000	0.996	0.997
PTW 31013 Semiflex[a,b]	…	…	…	…	1.013	1.000	0.992	0.993

These result confirm previous conclusions that unshielded diodes a better choice of detector than shielded diodes.

active volume > 0.1 cm^3
corrections of 20%-30% !

The corrections for mini-ionization chambers used in this study (active volume between 0.015 cm^3 and 0.05 cm^3) were generally lower than **10%**
and
for micro-chambers (active volume<0.015 cm^3) lower than **3%**.

[a]This chamber was included in the table for completeness but it is not recommended to use for small field dosimetry in fields smaller than 2.0 × 2.0 cm^2 because the volume averaging effect is unacceptably high.

[b]For these ionization chambers, corrections for the smallest field were unacceptably high (>20%) for field sizes smaller than 1 × 1 cm^2 and therefore were excluded from Table V.

Azangwe et al Med. Phys. 41 (7), 2014

ESTRO School

IAEA/AAPM formalism for relative dosimetry

Small field detector correction factors

$$k_{Q_{\text{clin}},Q_{\text{msr}}}^{f_{\text{clin}},f_{\text{msr}}}$$

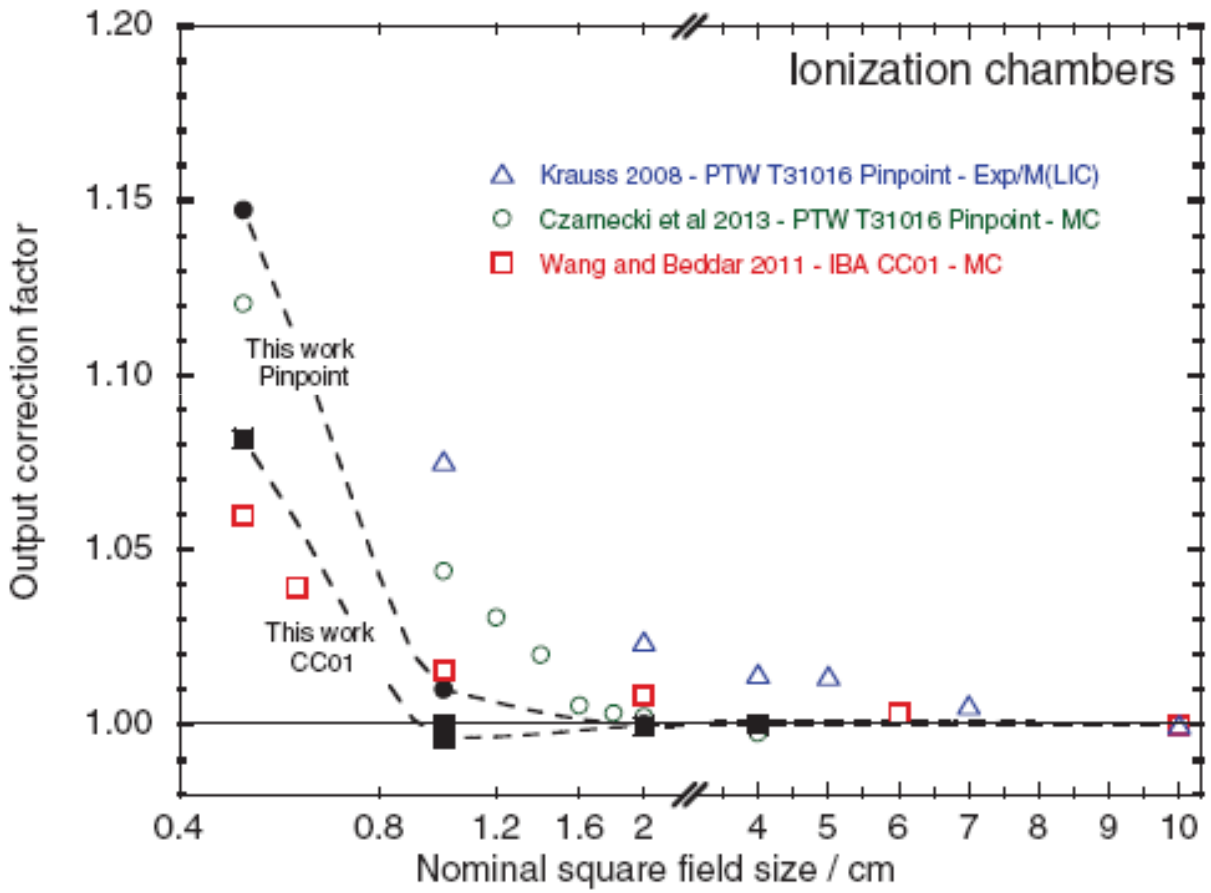

Benmakhlouf et al Med. Phys. 41 (4), 2014

ESTRO School

IAEA/AAPM formalism for relative dosimetry

Small field detector correction factors

$$k_{Q_{\text{clin}},Q_{\text{msr}}}^{f_{\text{clin}},f_{\text{msr}}}$$

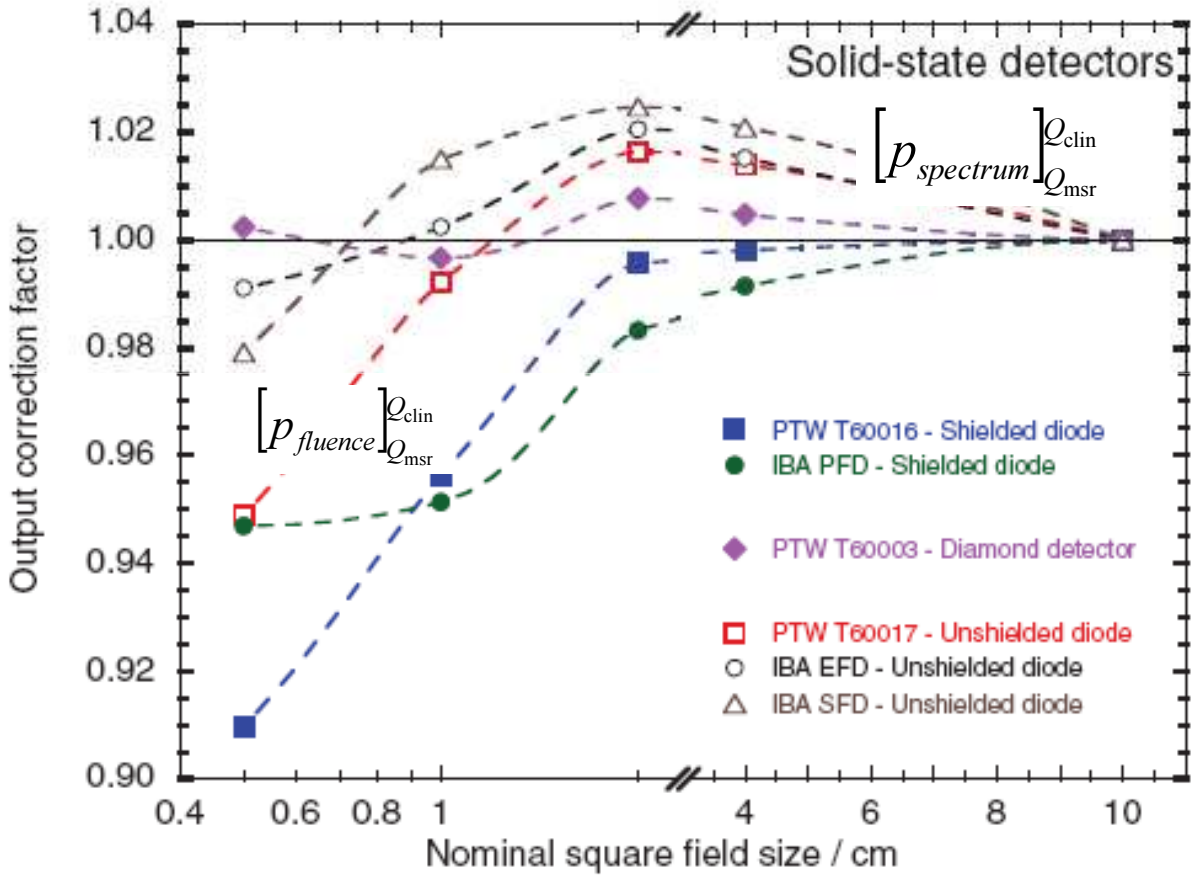

Benmakhlouf et al Med. Phys. 41 (4), 2014

ESTRO School

Note on the determination and compilation of consistent set of small field detector correction factors

$$k_{Q_{\text{clin}},Q_{\text{msr}}}^{f_{\text{clin}},f_{\text{msr}}}$$

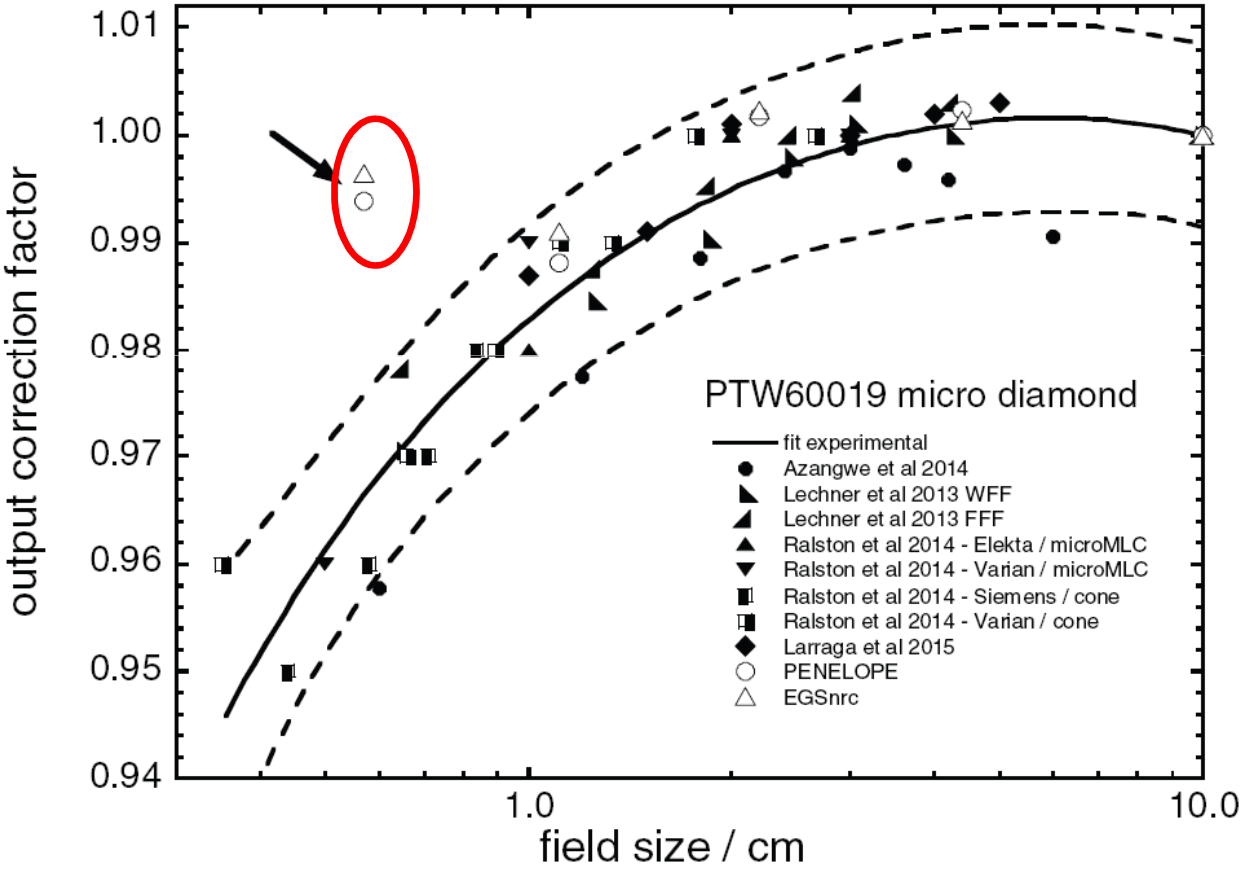

Andreo et al PMB 61 (2016) L1 – L10

ESTRO School

Note on the determination and compilation of consistent set of small field detector correction factors

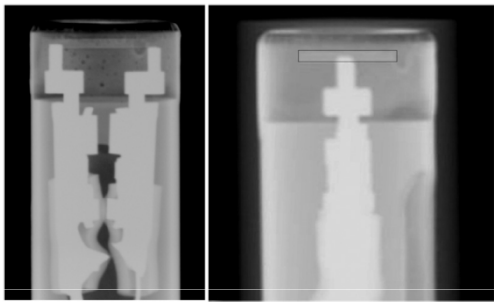

$$k_{Q_{clin},Q_{ms}}^{f_{clin},f_{msr}}$$

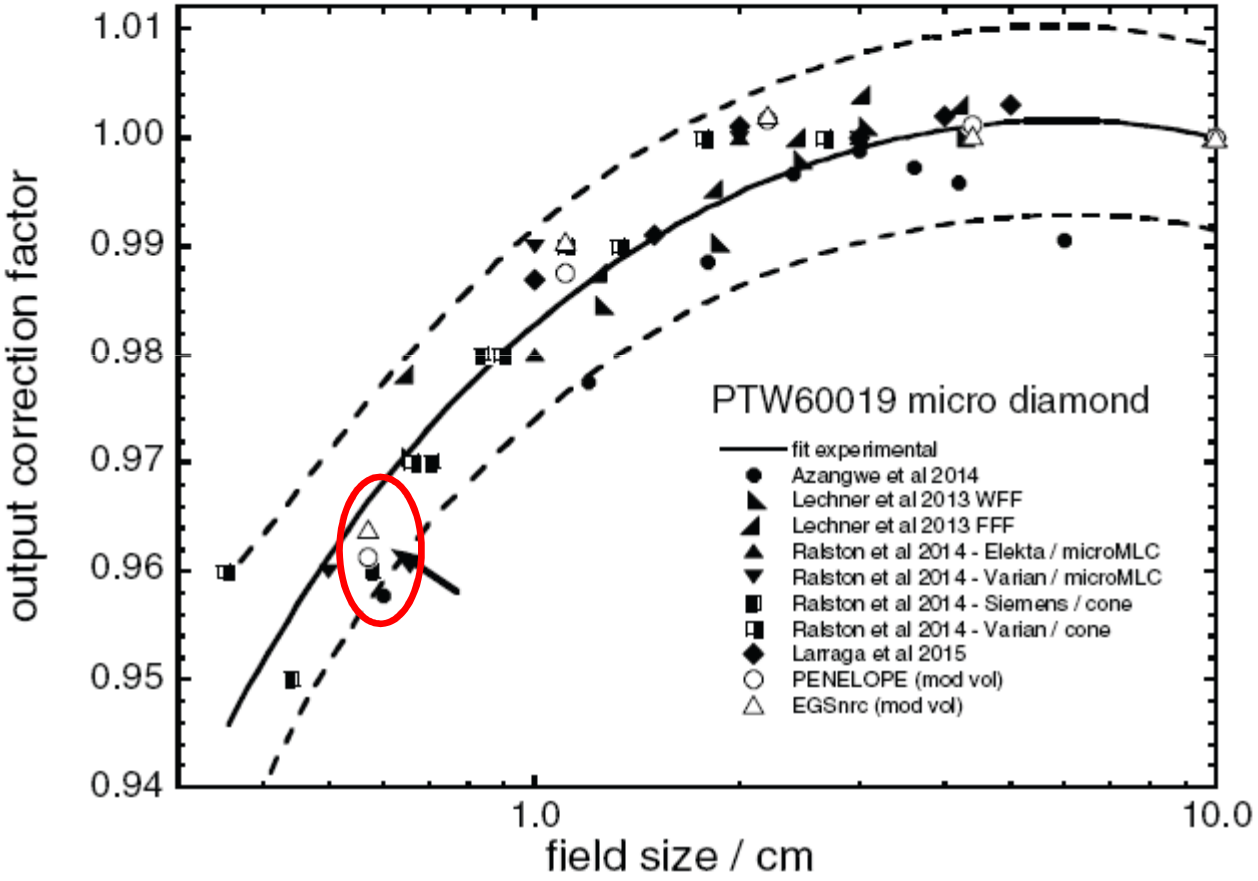

Andreo et al PMB 61 (2016) L1 – L10

ESTRO School

Summary: measurements in small static fields

- Consensus so far on current good practice for reference and relative dosimetry in static small MV photon fields:
  - ✓ Careful experimental setup
  - ✓ Choice of suitably small detector which is known to minimally perturb fluence
  - ✓ Approximately correct for volume averaging and energy dependence of detector
  - ✓ Corroboration of data

Summary: measurements in small static fields

- Consensus so far on current good practice for reference and relative dosimetry in static small MV photon fields:
  - ✓ Careful experimental setup
  - ✓ Choice of suitably small detector which is known to minimally perturb fluence
  - ✓ Approximately correct for volume averaging and energy dependence of detector
  - ✓ Corroboration of data
- Current research efforts in small field dosimetry focus on the determination of detector specific output correction factors.
- Detectors requiring output corrections greater that 5% are not recommended for dose determination in small fields.
- The IAEA TECDOC will include a consistent set of such data and will be an international code of practice for small static field dosimetry.

Background and early reviews on small field dosimetry

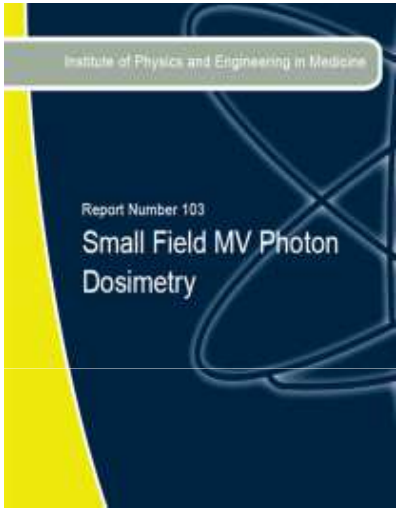

- IPEM Report 103, 2010
- R. Alfonso, P. Andreo, R. Capote, M. S. Huq, W. Kilby, P. Kjäll, T. R. Mackie, H. Palmans, K. Rosser, J. Seuntjens, W. Ullrich, and S. Vatnitsky, "A new formalism for reference dosimetry of small and nonstandard fields," *Med. Phys.* **35**, 5179–5187 (2008).
- I. J. Das, G. X. Ding, and A. Ahnesjö, "Small fields: Nonequilibrium radiation dosimetry," Med. Phys. 35, 206–215 (2008).
- H Palmans (2011) CN-182-INV006, Small and composite field dosimetry: the problems and recent progress. IDOS Conference, Vienna.

Note: There has been an explosion in the literature since 2008 on the topic of small field dosimetry!

ESTRO School

In depth reading on the physics of small MV photon fields

- Bouchard H, Seuntjens, J., Palmans H., 'On charge particle equilibrium violation in external photon fields', Med. Phys. 39 (3), 1473-1480, Mar 2012

- Bouchard H, Seuntjens, J., Duane, S., Kamio, Y., Palmans H., 'Detector dose response in megavoltage small photon beams. I Theroretical concepts', Med. Phys. 42 (10), 6033-47, Oct 2015

- Bouchard H, Kamio, Y., Palmans H., Seuntjens, J., Duane, S., 'Detector dose response in megavoltage small photon beams. II Pencil beams perturbation effects', Med. Phys. 42 (10), 6048-61, Oct 2015

ESTRO School

WWW.ESTRO.ORG/SCHOOL

Dose per Monitor Unit (MU) formalisms
Factor-based approaches

Maria Mania Aspradakis
Maria.Aspradakis@luks.ch

Acknowledgement: Profs. Anders Ahnesjö & Dietmar Georg

ESTRO School

Learning Objectives

I. Dose per Monitor Unit (MU) formalism for first-principles (or model-based) photon dose calculations (how is the calculated dose related to MU)?

II. Dose per Monitor Unit (MU) formalism for factor-based dose calculations
   I. understand the main factors involved
   II. learn how these factors are determined
   III. appreciate how such factors relate to each other
   IV. the AAPM TG-71 / NCS12 / ESTRO factor-based dose per MU formalisms

III. Reflect on the purpose and usefulness of factor-based models in modern radiotherapy physics

Acknowledgement: Profs. Anders Ahnesjö & Dietmar Georg

Beam calibration: Dose per Monitor Unit

Beam output given as the absorbed dose [Gy] per Monitor Unit [MU] in water under calibration conditions

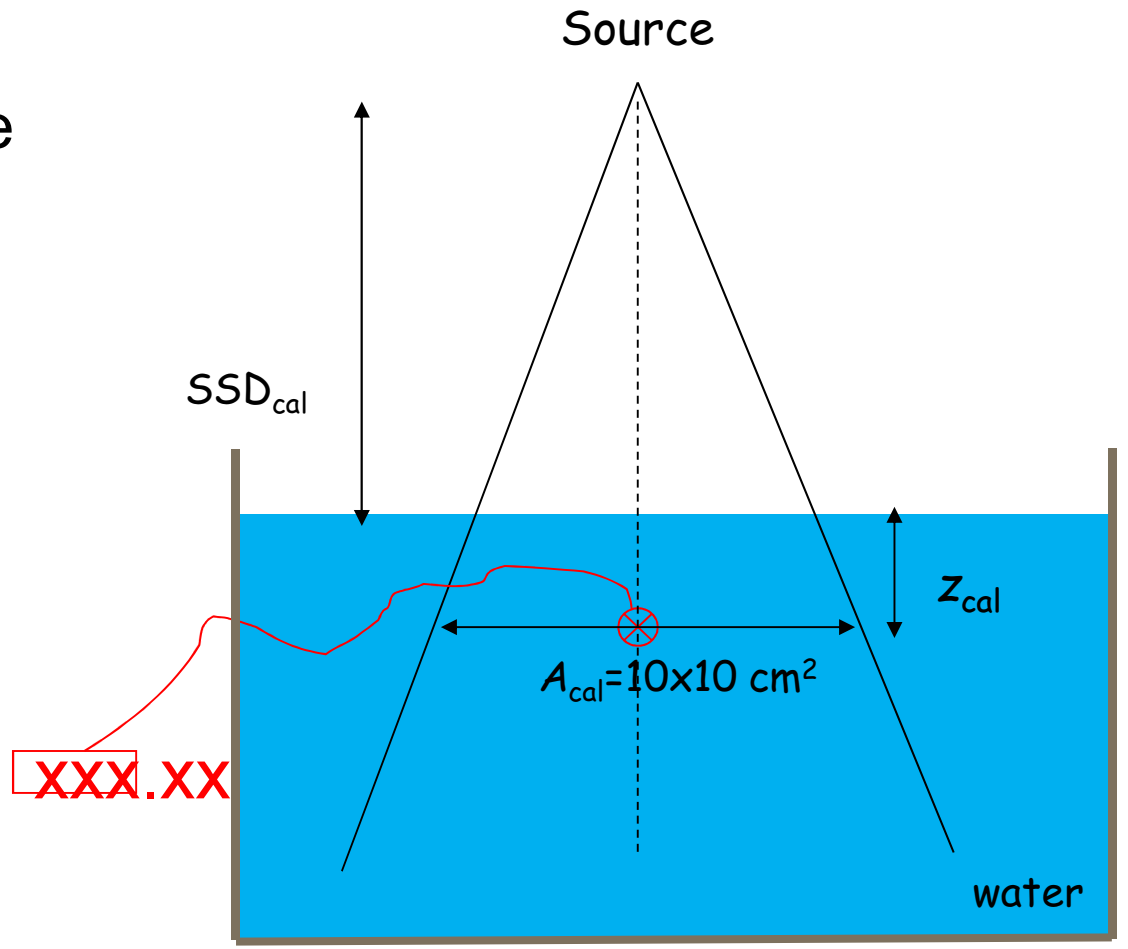

$$\left[D\left(A_{\text{cal}}; x_{\text{cal}}, y_{\text{cal}}, z_{\text{cal}} \right) / M \right]_{\text{Measured}}$$

Dose per MU formalisms: model-based dose calculations

$$\frac{D_{\text{calc}}(A;x,y,z)}{M} = \frac{D_{calc}(A;x,y,z)}{amount\ of\ \ radiation} \cdot F_{\text{calibration}}$$

The amount of radiation incident of the patient is either in terms of:

Particle (*beam phase space*) – e.g **Monte Carlo**

((type, energy, location, direction)$_{\text{particle 1}}$,
(type, energy, location, direction)$_{\text{particle 2}}$,
"
"
"
type, energy, location, direction)$_{\text{particle } N}$)

N of order 10^7

or

Energy fluence (*direct*, *head scatter*) – **kernel-based models**

$$\Psi(x,y) = \frac{\#\,\text{photons@(x , y)} \cdot \text{their energy}}{\text{beam cross section}}$$

ESTRO School

Calculation of monitor units per field for treatment

per field *i*:

$$M_{\mathrm{i}} = \frac{D_{\mathrm{presc}} \cdot w_{\mathrm{i}}}{D_{calc,i}\left(s_{\mathrm{d}}, d; SSD\right) / M}$$

with

$$w_{\mathrm{i}} = \frac{D_i\left(s_{\mathrm{d}}, d; SSD\right)}{\sum_{\mathrm{i=1}}^{\mathrm{all\ fields}} D_{calc,i}\left(s_{\mathrm{d}}, d; SSD\right)}$$

ESTRO School

Dose per MU formalisms

model-based dose calculations

Dose per MU formalisms: model-based dose calculations

$$\frac{D(A;x,y,z)}{M} = \frac{D(A;x,y,z)}{\Psi_o} \cdot \frac{\Psi_o}{M}$$

Energy fluence of **direct photons** at isocentre in air

Calibration factor

relates the MU to the incident direct energy fluence under *reference calibration conditions*

$$\left.\begin{array}{l} \dfrac{D_{\text{ref,meas}}}{M} \\[2ex] \dfrac{D_{\text{ref,calc}}}{\Psi_o} \end{array}\right\} \quad \frac{\Psi_o}{M} = \frac{\left[D(A_{\text{ref}};x_{\text{ref}},y_{\text{ref}},z_{\text{ref}})/M\right]_{\text{meas}}}{\left[D(A_{\text{ref}};x_{\text{ref}},y_{\text{ref}},z_{\text{ref}})/\Psi_o\right]_{\text{calc}}}$$

No monitor backscatter accounted for!

ESTRO School

Dose per MU formalisms: model-based dose calculations

- The signal from the monitor chamber has a component that originates from particles which have backscattered from the upper part of the jaws into the chamber.
- The fraction of this signal depends on the aperture defined by the upper jaws and increases as this decreases.

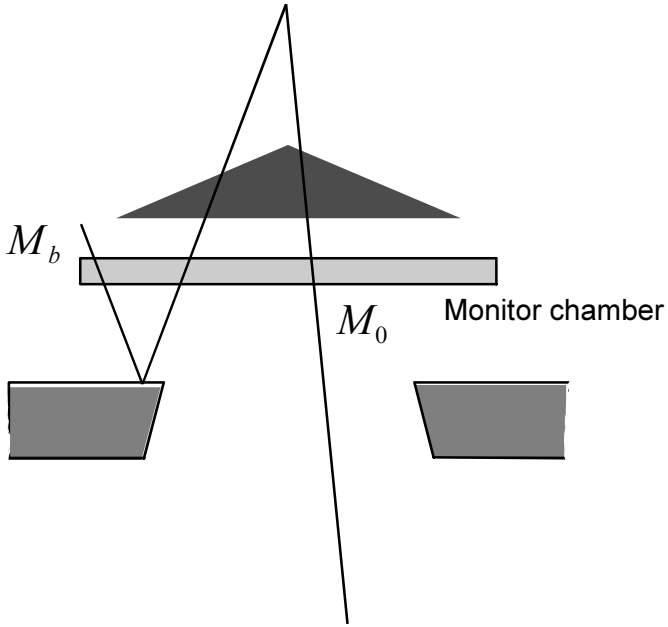

Fraction of the total of the monitor chamber which is attributed to particles that have backscattered into the monitor chamber

$$M = M_0 + M_b(A) = \left(1 + b\left(A\right)\right) M_0$$

or

$$\frac{M_0}{M} = \left(1 + b(A)\right)^{-1}$$

ESTRO School

Dose per MU formalisms: model-based dose calculations

Including monitor signal M_b caused by backscatter as a function of collimator aperture, the formalism is:

$$\frac{D(A;x,y;z)}{M} = \frac{D(A;x,y;z)}{\Psi_0} \frac{\Psi_0}{M_0} \cdot (1+b(A))^{-1}$$

calibration factor

$$\frac{\Psi_o}{M_o} = \frac{\left[D(A_{ref};x_{ref},y_{ref},z_{ref})/M\right]_{meas}}{\left[D(A_{ref};x_{ref},y_{ref},z_{ref})/\Psi_o \cdot (1+b(A_{ref}))^{-1}\right]_{calc}}$$

Note: Different implementations in common TPSs described in the next lecture)

ESTRO School

Dose per MU formalisms

factor-based dose (or MU) calculations

Dose per MU formalisms: factor-based dose calculations

$$\frac{D(A;x,y,z)}{M} = \frac{D(A;x,y,z)}{\Psi_o} \cdot \frac{\Psi_o}{M}$$

Basic factorisation:

$$\frac{D(\text{cond. a})}{M} \equiv \underbrace{D(\text{calibration})/M}_{calibration\ value} \cdot \underbrace{\frac{D(\text{cond. a})/M}{D(\text{calibration})/M}}_{factor\ a}$$

More general…:

$$\frac{D(\text{cond. a})}{M} \equiv \underbrace{D(\text{calibration})/M}_{calibration\ value} \cdot \underbrace{\frac{D(\text{cond. n})/M}{D(\text{calibration})/M}}_{factor\ n} \cdots \underbrace{\frac{D(\text{cond. b})/M}{D(\text{cond. c})/M}}_{factor\ b} \cdot \underbrace{\frac{D(\text{cond. a})/M}{D(\text{cond. b})/M}}_{factor\ a}$$

ESTRO School

Dose per MU formalisms: factor-based dose calculations

Nomenclature used in this presentation (in analogy, but not identical, to that in AAPM Task group report 71)

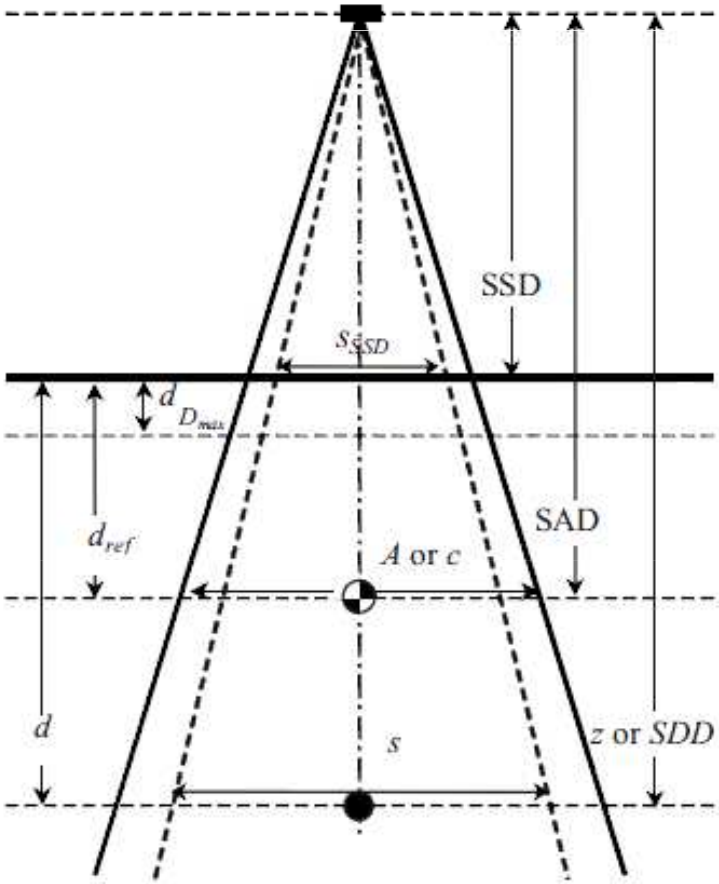

d_{ref} reference depth

$c_{\text{ref}} \equiv r_{\text{ref}}$ reference field size/collimator setting

c_{eqsq} collimator setting (equivalent square)

$s_{\text{d,eqsq}}$ field size at depth (equivalent square)

Calculation point at isocentre:

$$s_{\text{d, eqsq}} = c_{\text{eqsq}}$$

ESTRO School

Dose per MU formalisms: factor-based dose calculations

Reference normalisation conditions

Isocentric

- c_{ref} = 10 x 10 cm²

  Field Size at isocenter

- d_{ref} = 10 cm
- SSD = SAD - d_{ref}

Tissue phantom ratio

TPR(c,d)

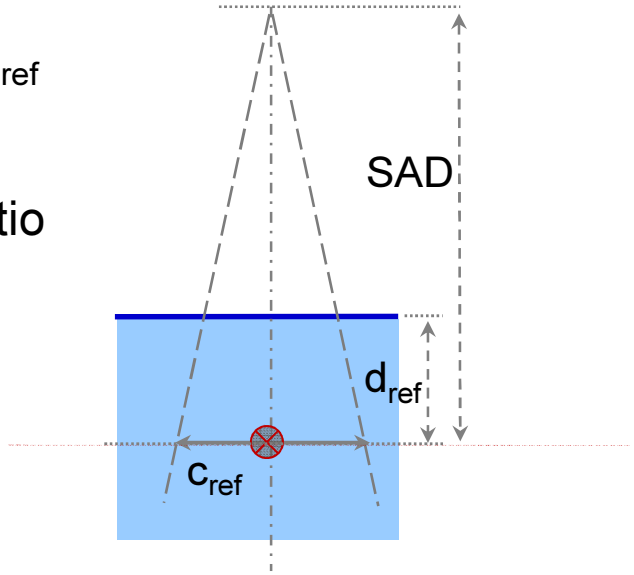

$$\frac{D(c_{ref}, d_{ref}; \mathrm{SAD})}{M} [cGy/MU]$$

Dose per MU formalisms: factor-based dose calculations

Reference normalisation conditions

Isocentric

- c_{ref} = 10 x 10 cm²

  Field size at isocenter
- d_{ref} = 10 cm
- SSD = SAD - d_{ref}

Tissue phantom ratio

TPR(c,d)

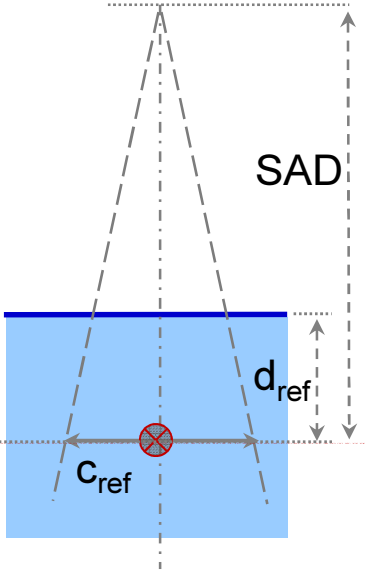

$$\frac{D(c_{ref}, d_{ref}; \mathrm{SAD})}{M}[cGy/MU]$$

Fixed SSD

c_{ref} = 10 x 10 cm²

Field size at surface

d_{ref} = 10 cm

SSD = SAD

Relative depth dose

RDD(s,d)

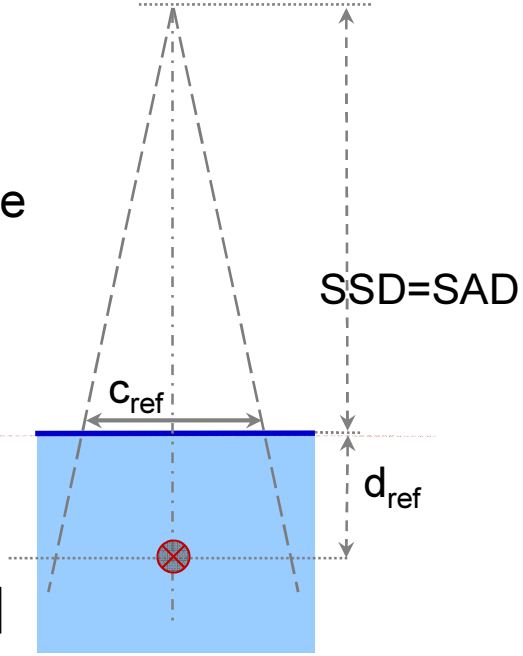

$$\frac{D(c_{ref}, d_{ref}; \mathrm{SSD})}{M}[cGy/MU]$$

ESTRO School

Dose per MU formalisms: factor-based dose calculations

Reference normalisation conditions: choice of reference depth d_{ref}

Reference depth in water of 10 cm recommended irrespective of beam quality index

- Previous recommendations where 5 cm for BQI < 0.70 and 10 cm for BQI > 0.70

Avoids unpredictable influence of contaminating electrons as far as possible

- Rule of thumb: depth of influence ~ $2 \cdot d_{Dmax}$ or MV/3

∴

10cm depth chosen for consistency in reference depth for beam calibration and MU calculation

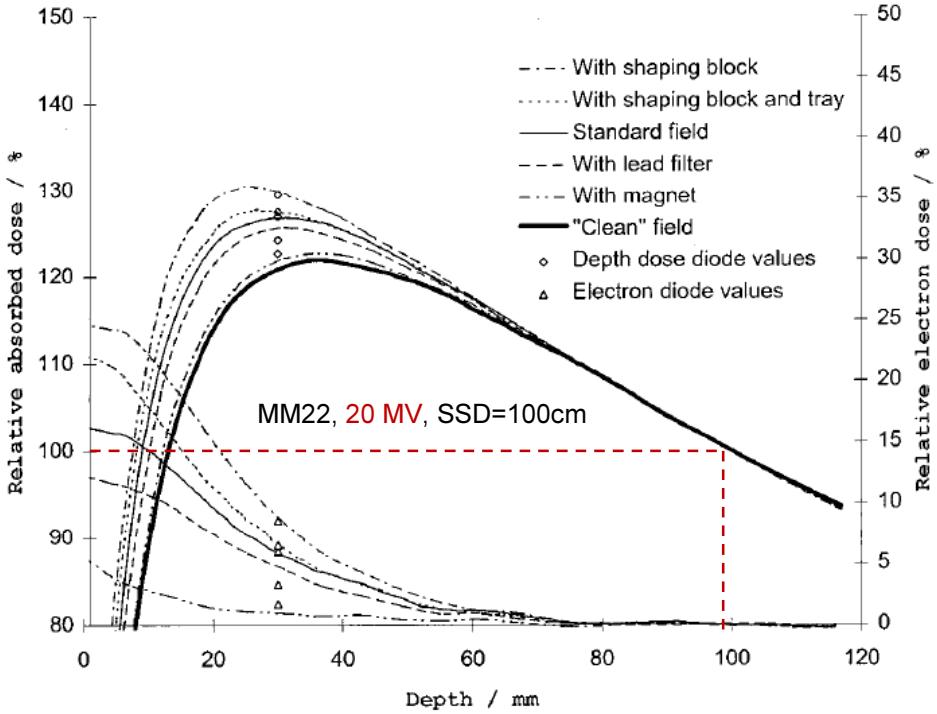

Sjögren and Karlsson, Med, Phys, 25(6), p916, 1998

ESTRO School

Dose per MU formalisms: factor-based dose calculations

$$\frac{D(s_d, d; SSD + d)}{M} = \frac{D_{ref}(c_{ref}, d_{ref}; SSD_{ref})}{M} \cdot [factor(s)]$$

dosimetric quantities to account for all differences from
the reference irradiation geometry in terms of:

- distance from source (~ inverse square law)
- field size and depth (~ scatter dose in medium)
- modulation (~ beam intensity)
- attenuators in the beam path
- position off axis
- heterogeneities

Dose per MU formalisms: factor-based dose calculations

Reference normalisation geometry

reference normalisation geometry could differ from linac calibration geometry (but for simplicity in this lecture we take the two to be the same)

$$\frac{D_{ref}(c_{ref}, d_{ref}; SSD_{ref})}{M}$$

Arbitrary treatment geometry

$$\frac{D(c, s_d, d; SSD)}{M}$$

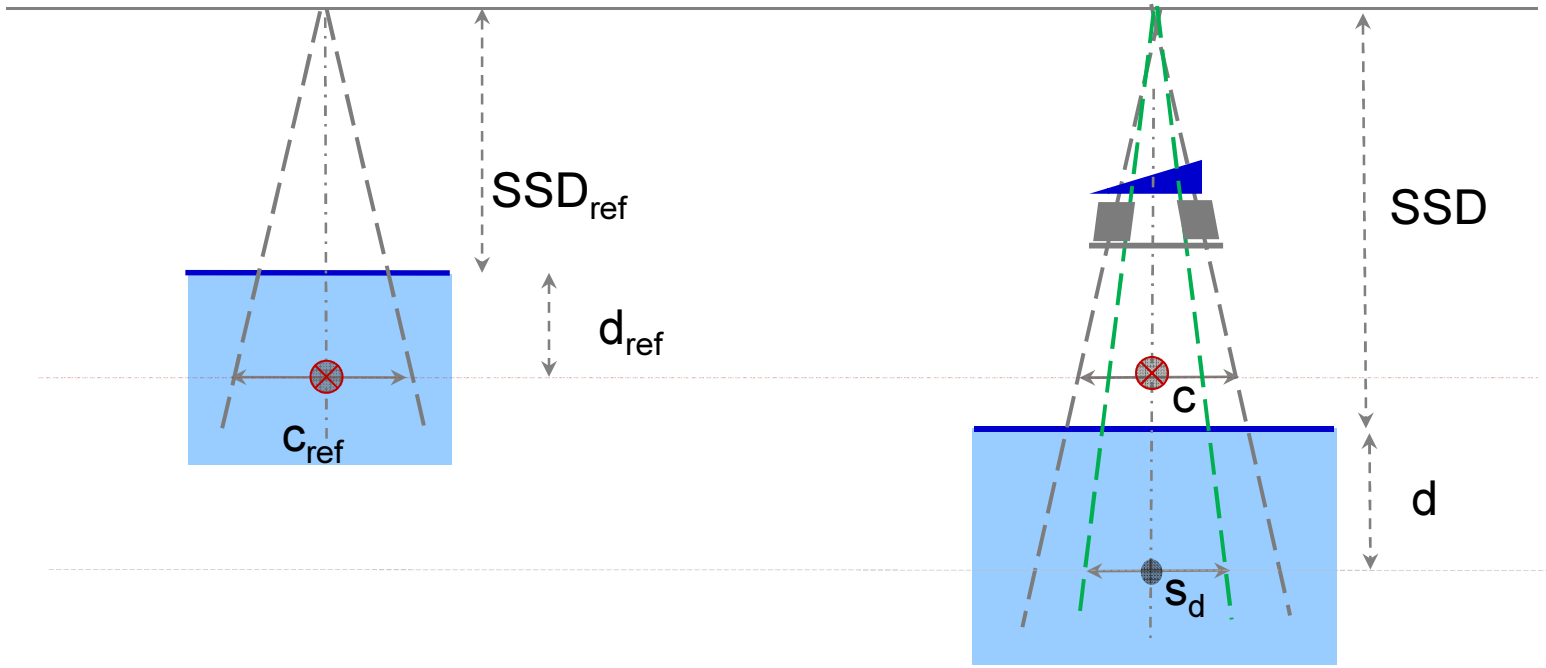

ESTRO School

Dose per MU formalisms: factor-based dose calculations

basic scenario

Isocentric reference normalisation geometry

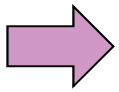

Isocentric treatment geometry: Open beam & calculation point at isocentre and on CAX

$$\frac{D_{ref}(c_{ref}, d_{ref}; SSD_{ref})}{M}$$

$$\frac{D(c, s_d, d; SAD)}{M}$$

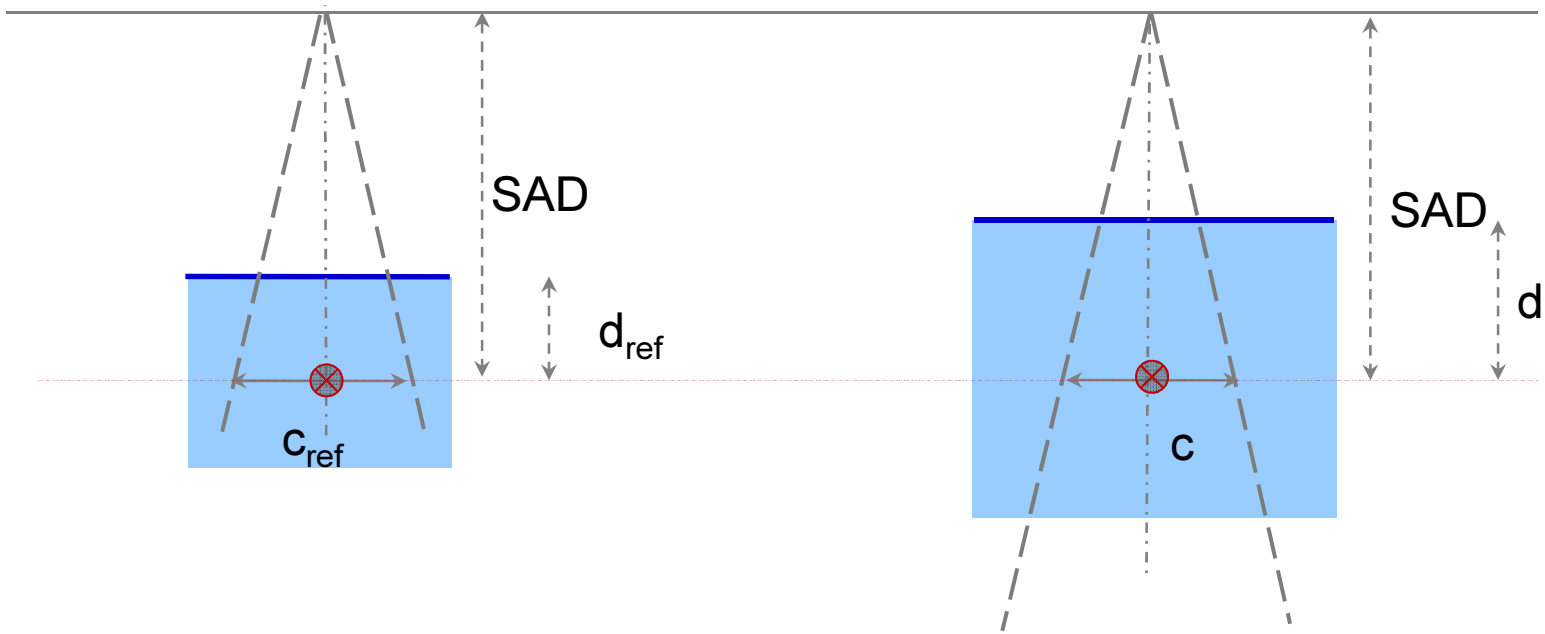

ESTRO School

Dose per MU formalisms: factor-based dose calculations

Isocentric linac reference normalisation geometry

- **Step 1:** account for differences in dose at the calculation point due to changes in energy fluence from the different scatter conditions in the head of the linac
- Step 2:
- Step 3:

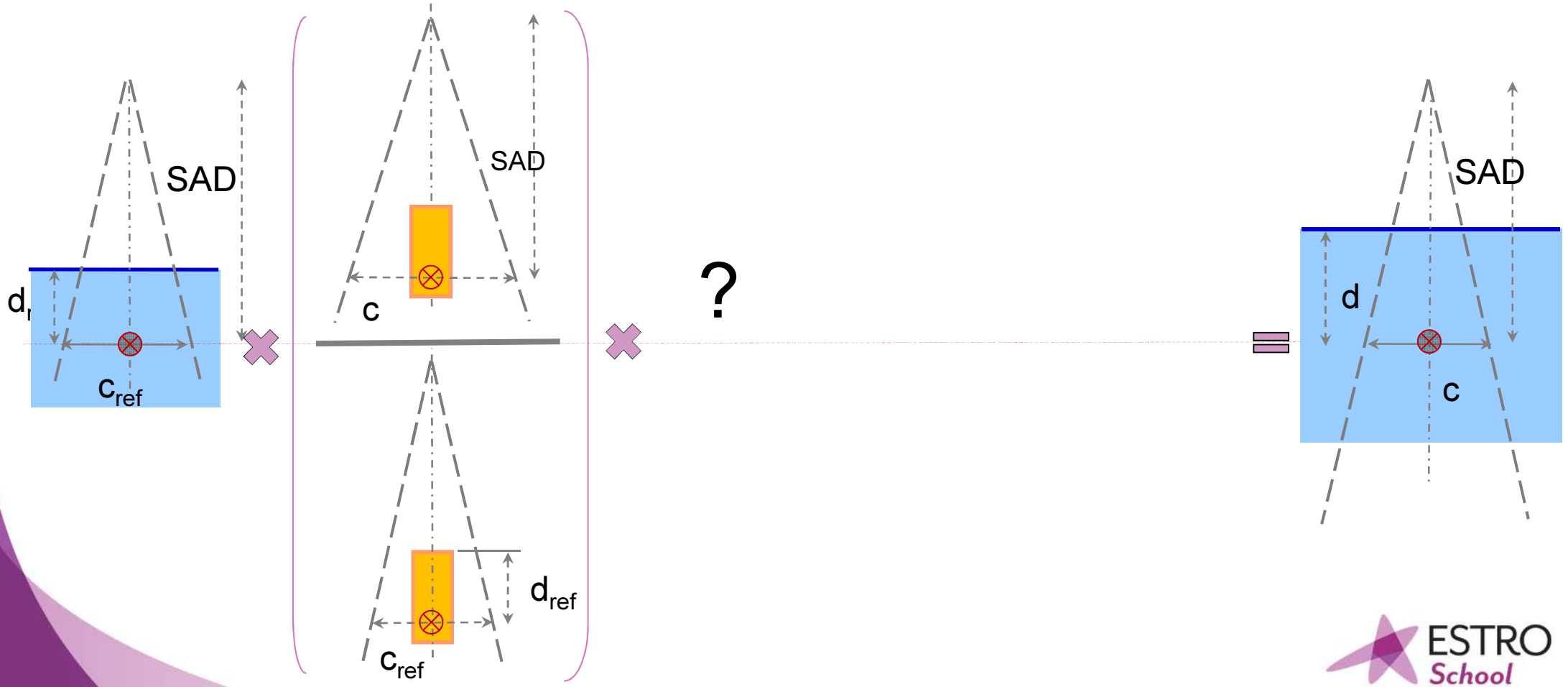

ESTRO School

Dose per MU formalisms: factor-based dose calculations

Isocentric linac reference normalisation geometry

- Step 1: account for differences in dose at the calculation point due to changes in scatter conditions in the head of the linac
- **Step 2**: account for differences in phantom scatter due to the change in field size (amount of phantom irradiated)
- Step 3:

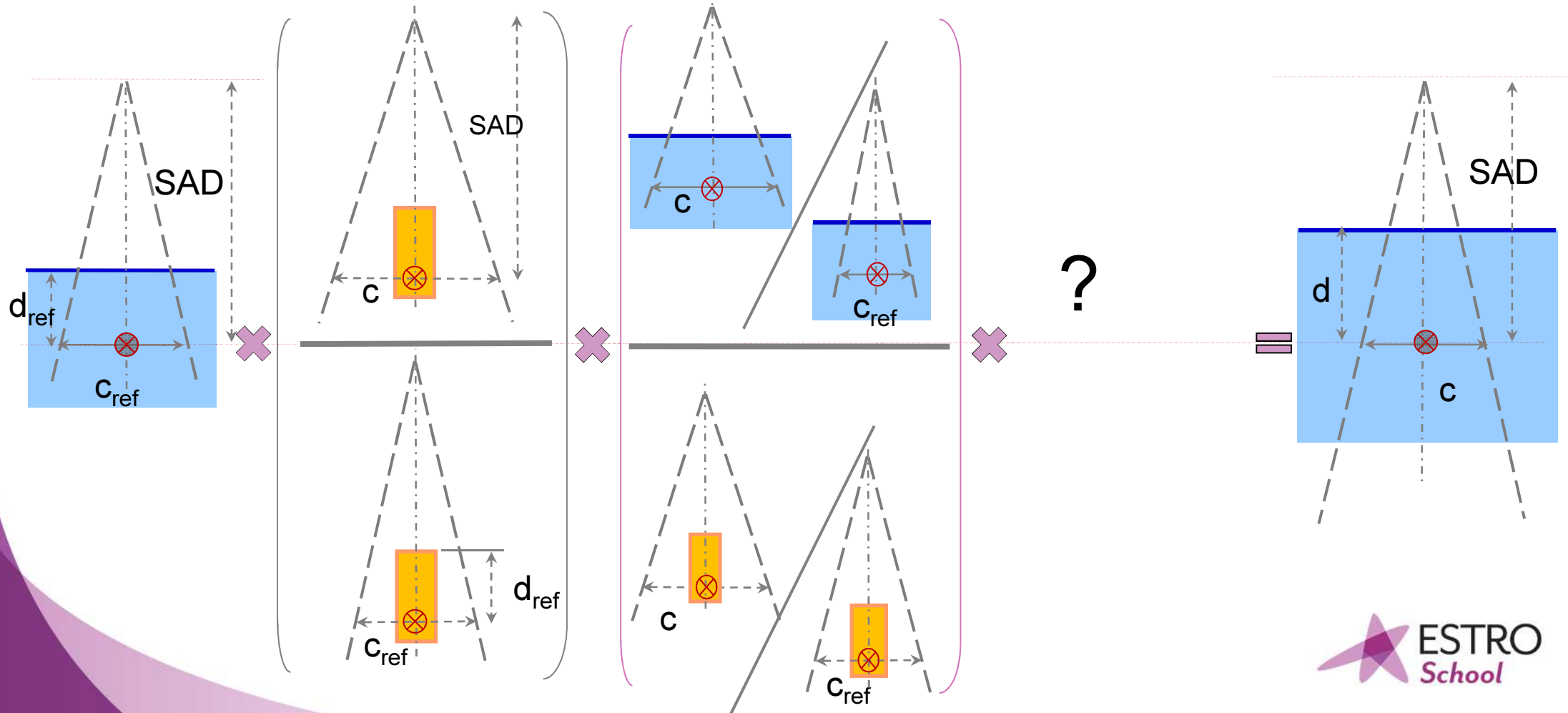

ESTRO School

Dose per MU formalisms: factor-based dose calculations

Isocentric linac reference normalisation geometry

- Step 1: account for differences in dose at the calculation point due to changes in scatter conditions in the head of the linac
- Step 2: account for differences in phantom scatter due to the change in field size (amount of phantom irradiated)
- **Step 3**: account for differences in phantom scatter due to the change of depth

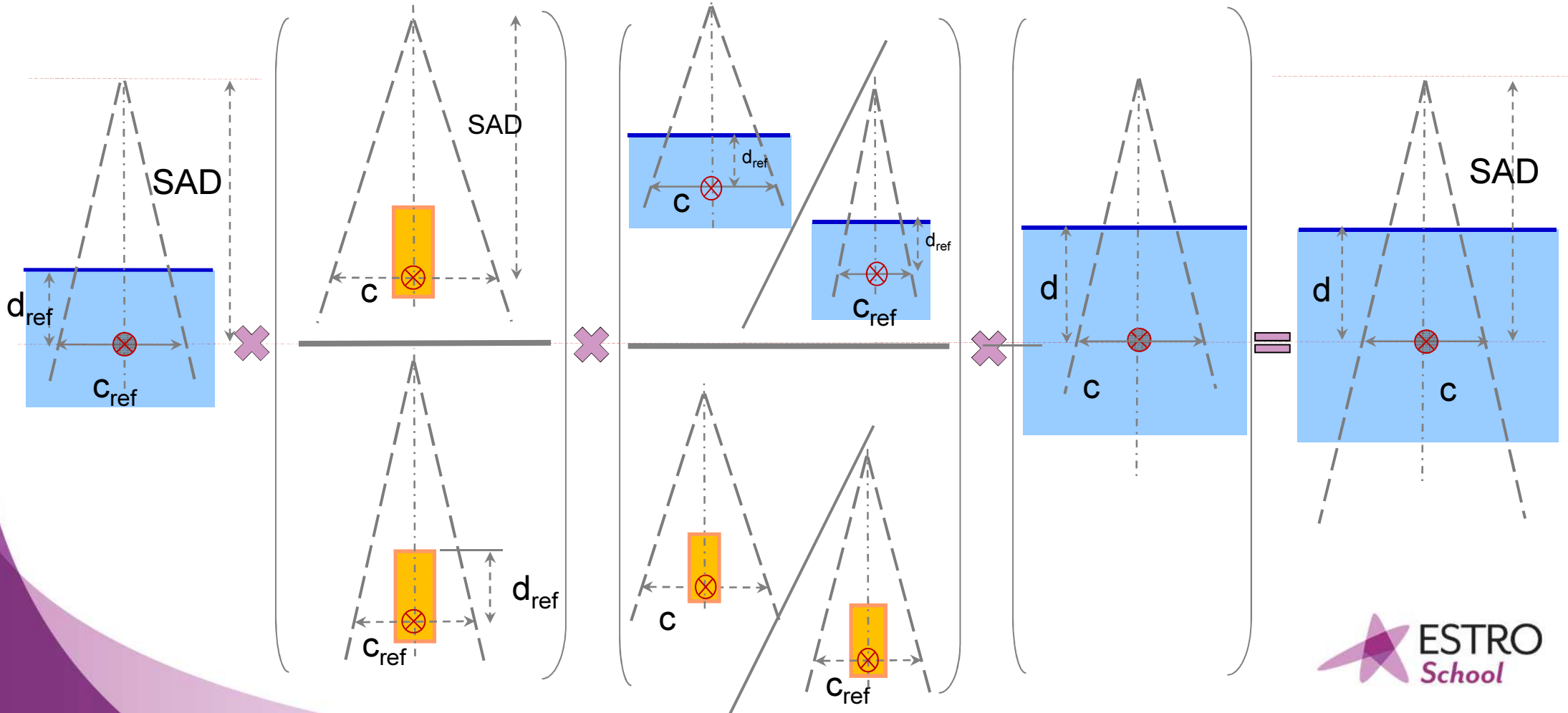

ESTRO School

Factor-based dose calculations

basic dosimetric quantities

In-air output ratio or output factor in air, Sc

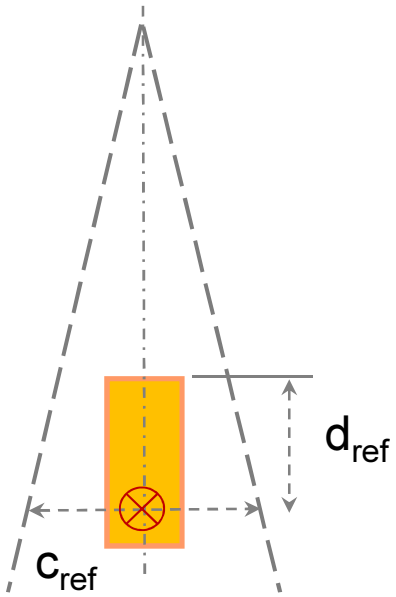

Report pf AAPM TG106: Accelerator beam data commissioning, Med Phys, 35(9), 2008
AAPM TG 74 report, Med Phys 36 (11), 2009

ESTRO School

Factor-based dose calculations: basic dosimetric quantities

In-air output ratio or output factor in air, Sc

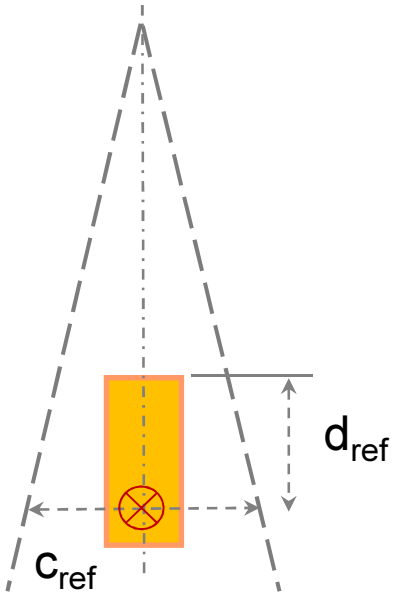

Is the ratio of **primary collision water kerma in free-space K_p** per monitor unit (MU) between an arbitrary collimator setting c and the reference collimator setting c_{ref} at the same location on the beam's central axis:

$$S_c(c) = \frac{K_p(c; d_{ref})/M}{K_p(c_{ref}; d_{ref})/M}$$

Also known as:

Mini-phantom output ratio

Collimator scatter factor

Head scatter factor

Sc quantifies fluence variations with collimator settings that can be used in beam modelling and dose calculations.

Usually d_{ref} = 10cm and c_{ref}=10cm

$$K_p = \int_{\text{primary spectrum}} \Psi_E \frac{\mu_{en}}{\rho} dE$$

Report pf AAPM TG106: Accelerator beam data commissioning, Med Phys, 35(9), 2008
AAPM TG 74 report, Med Phys 36 (11), 2009

ESTRO School

Factor-based dose calculations: basic dosimetric quantities

Determination of S_c in a miniphantom

$$S_c(c) = \frac{K_p(c; d_{ref})/M}{K_p(c_{ref}; d_{ref})/M}$$

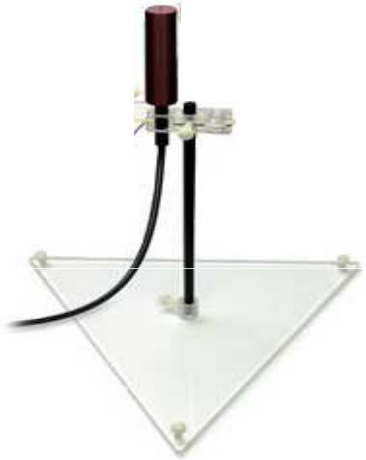

$$\frac{K_p(c)}{K_p(c_{ref})} = \frac{\int_{\text{Primary spectrum of beam } c} \frac{\mu_{en}(E)}{\rho} \cdot e^{-\mu(E)\cdot d} \cdot (\Psi_E(c; z_{ref})/MU) \cdot SF_K(\text{miniphantom}) \cdot dE}{\int_{\text{Primary spectrum of beam } c_{ref}} \frac{\mu_{en}(E)}{\rho} \cdot e^{-\mu(E)\cdot d} \cdot (\Psi_E(c_{ref}; z_{ref})/MU) \cdot SF_K(\text{miniphantom}) \cdot dE}$$

If the photon beam spectrum is identical in both situations, then it follows that S_c effectively measures the **energy fluence output ratio.**

However, in situations when the beam quality in c is different from c_{ref}, it has to be noticed that the measured signal ratio is only *an estimator* of the energy fluence ratio, biased by the mini-phantom and spectrum specific variations of collision kerma and attenuation.

AAPM TG 74 report, Med Phys 36 (11), 2009

Factor-based dose calculations: basic dosimetric quantities

S_c : mini-phantom/buildup cap design – lateral considerations

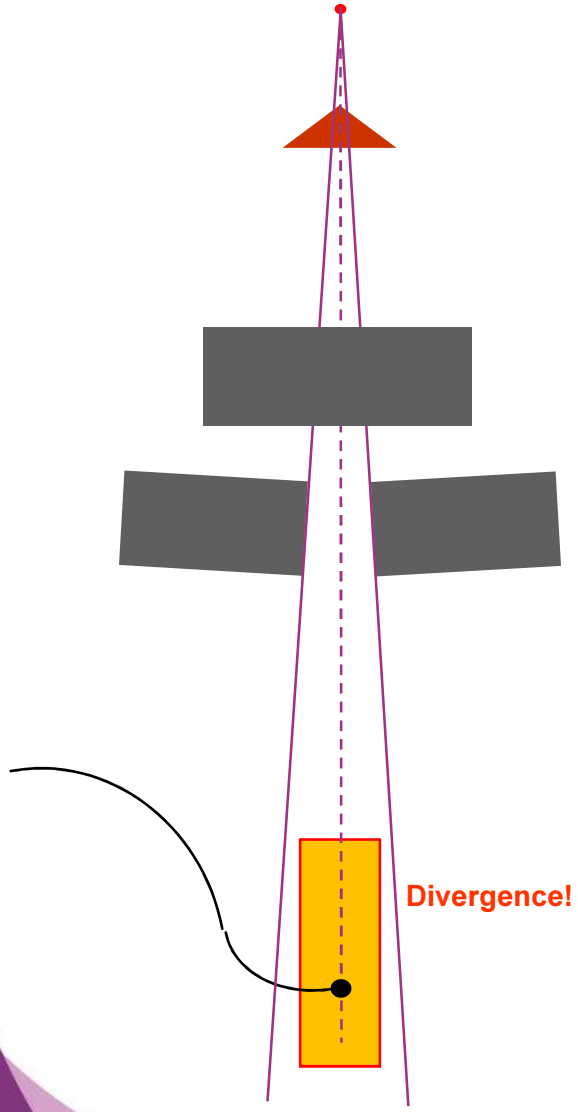

1. The entire mini-phantom/build-up cap should always be enclosed by the radiation field (incl. margin for penumbra).
2. The mp/bc should provide lateral CPE;
   $r_{CPE} \approx 5.973 \cdot TPR_{20,10} - 2.688$ [g/cm^2]
   Experimental investigations suggest that a wall thickness ≥ 1 g/cm^2 is sufficient.

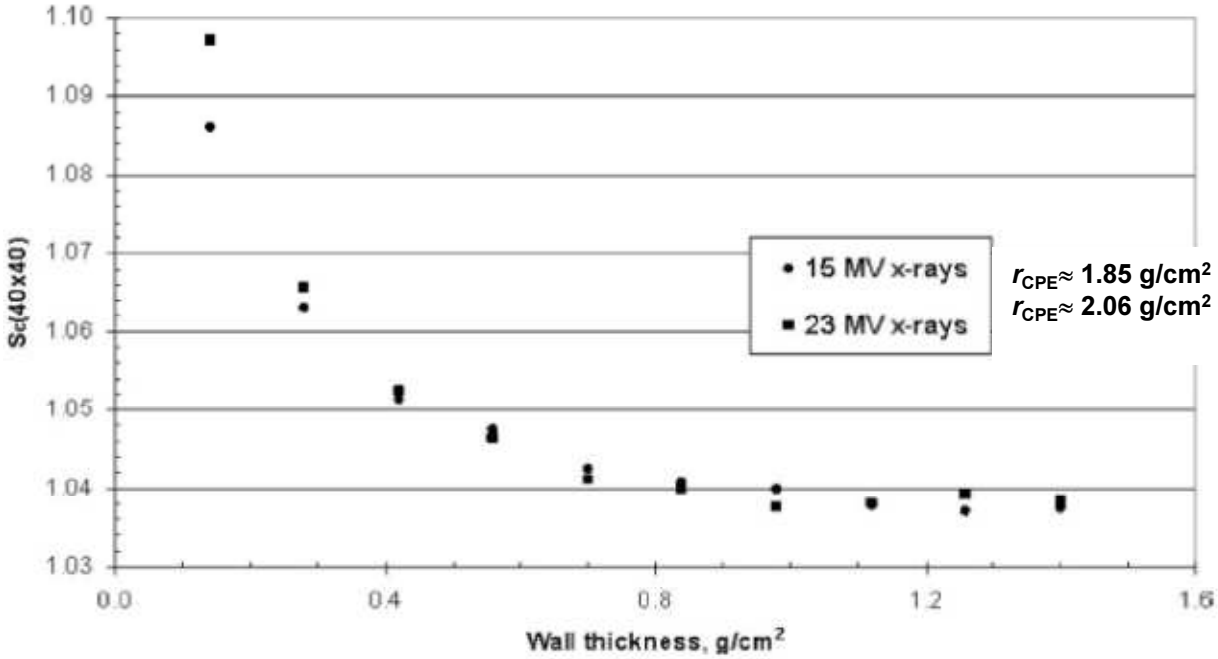

Jursinic PA (2006) , Med Phys 33, 1720-8,
Li et al MedPhys **22**, 1995, 1167-1170

ESTRO School

Factor-based dose calculations: basic dosimetric quantities

S_c : mini-phantom/buildup cap design – depth considerations

The effective measurement depth in the mini-phantom/build-up cap must be large enough to stop contaminating electrons.

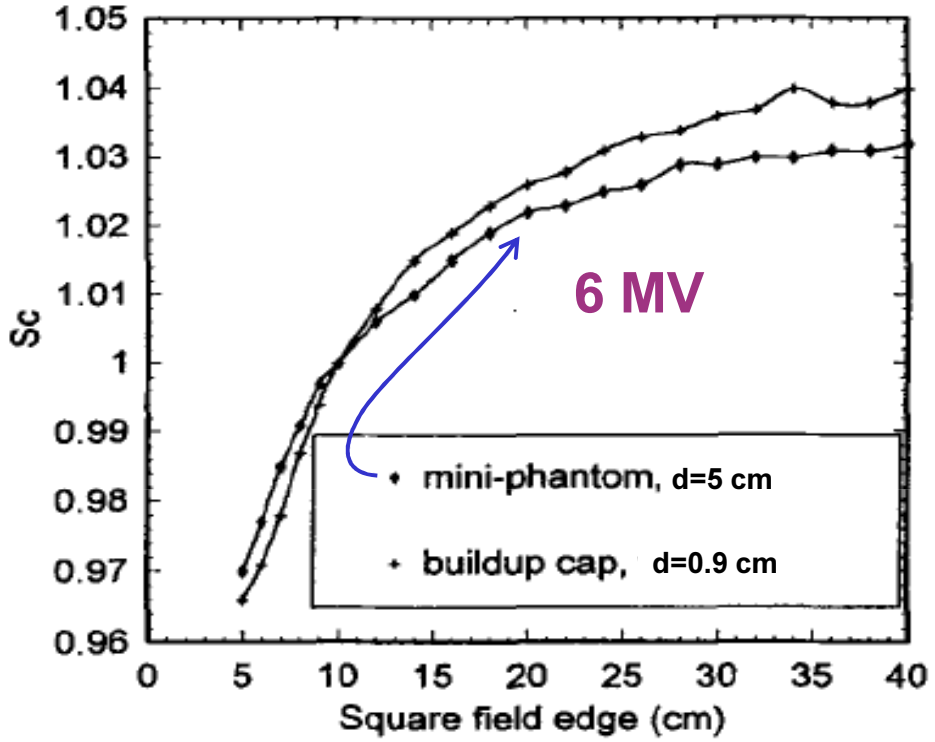

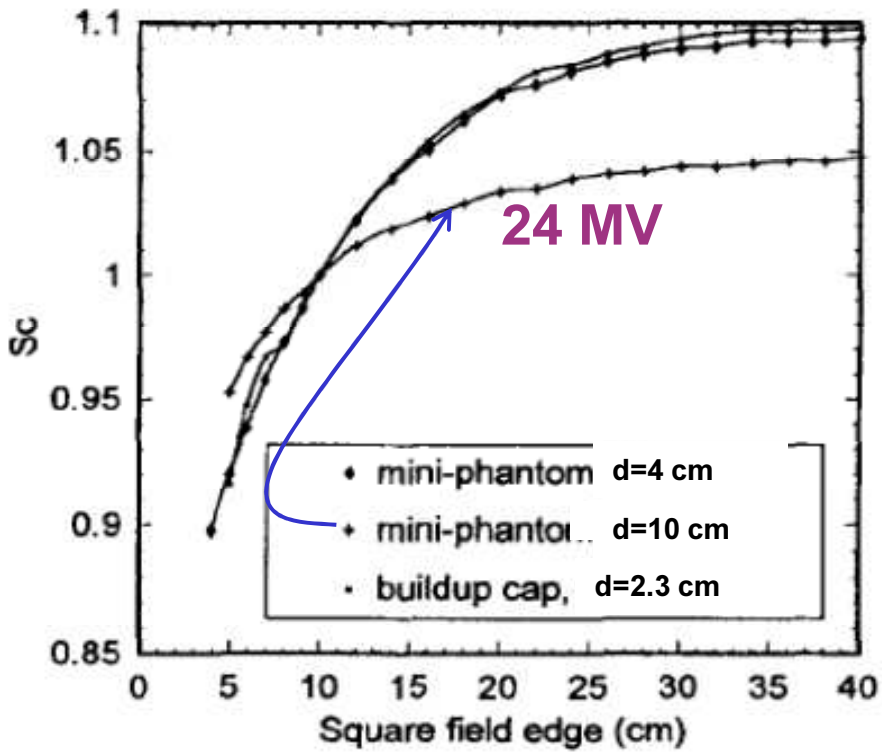

Frye DM, et al (1995) Med Phys 22, 249-53

Two rules of thumb used to eliminate e⁻ contamination:

$$d \geq 2 \cdot d_{max}$$

$$d \geq \mathrm{MV}/3 \ [\mathrm{cm}]$$

Factor-based dose calculations: basic dosimetric quantities

S_c : mini-phantom/buildup cap design – material considerations

- Water-equivalent material (solid water, acrylic (PMMA), graphite)
- For collimator settings < 5cm: miniphantom made of high Z material
- Using a high-*Z* material build-up cap should not introduce any deviations as long as the beam quality is constant...

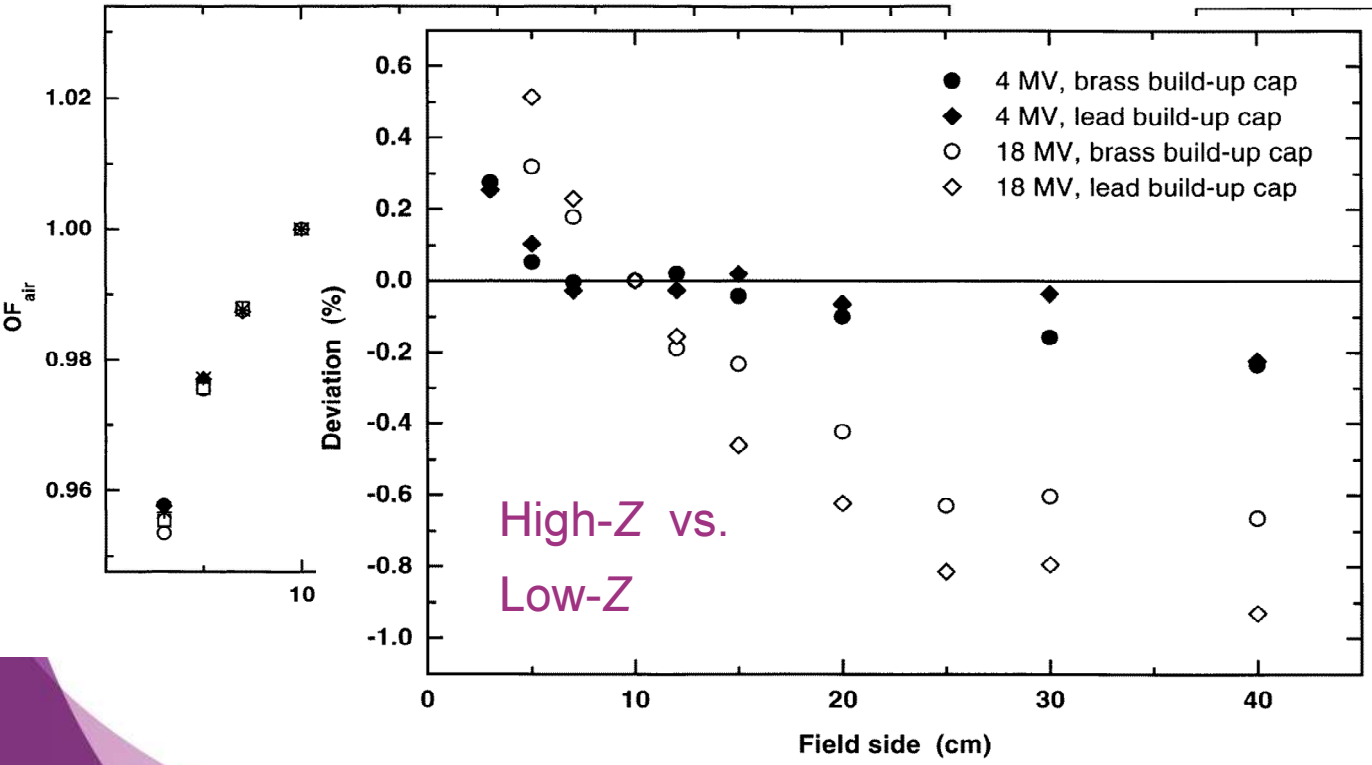

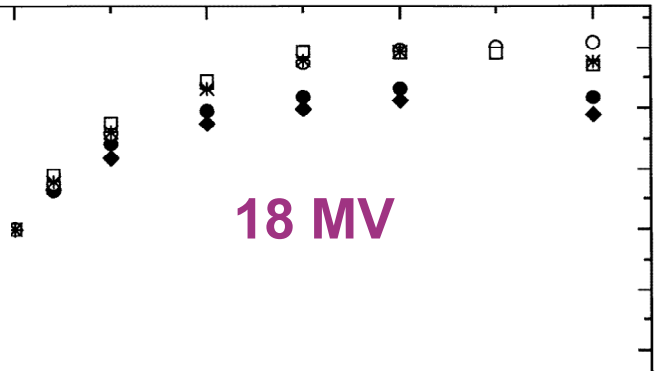

Recommendation: Only use high-*Z* buildup caps for very small fields and normalize these measurements to those in low-*Z* caps in the smallest possible overlapping field size (roughly 4x4 cm^2).

Weber L, Nilsson P, Ahnesjö A (1997) Phys Med Biol 42, 1875-86

ESTRO School

Factor-based dose calculations: basic dosimetric quantities

S_c : mini-phantom/buildup cap design

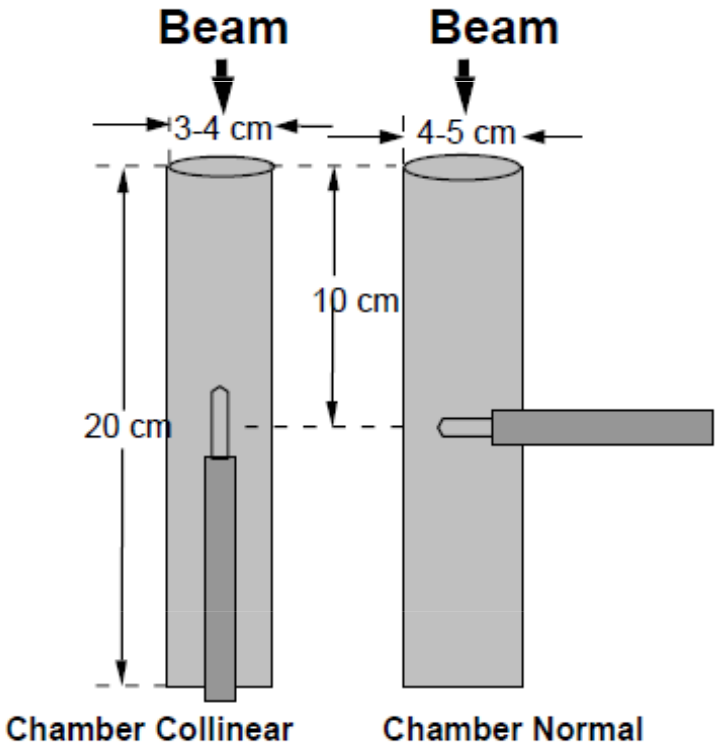

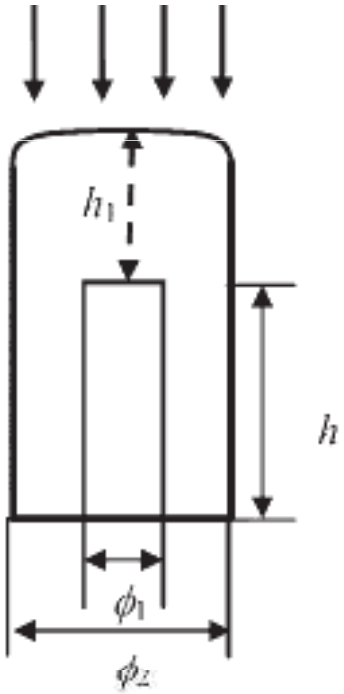

Figure 8.3 Brass mini-phantom design for square fields down to 15 mm × 15 mm and photon energies less than 25 MV recommended by Zhu et al. (2009): Thickness $h_1 \geq 12$ mm (or 10 g/cm², mass density $\rho = 8.4 - 8.7$ g/cm³) and inner diameter ϕ_1 equal to the outer diameter of the detector. Height h is sufficient to cover the detector sensitive volume. The outer diameter ϕ_2 of the mini-phantom can be such that its wall is thinner than the thickness required for CPE but not less than 12 mm for energies up to 18 MV. The total lateral dimension above the chamber should ensure lateral CPE for the photon energy (from Zhu et al. (2009) with permission)

Zhu et al, AAPM Report TG74: 'In-air output ratio Sc for megavoltage photon', *Med Phys 36 (11), 2009*

ESTRO School

Factor-based dose calculations: basic dosimetric quantities

S_c : example data

ESTRO Booklet #6, Figure 4.2, page 254

Side of square field (cm)	*MDS Nordion Theratron 780 ^{60}Co*	*Varian Clinac 600C 4 MV*	*Siemens Primus 6 MV*	*GE-CGR Saturne 41 10 MV*	*EOS SL20 18 MV*
4		0.947	0.937	0.931	0.962
5	0.955		0.957	0.945	
6	0.977	0.976	0.971	0.956	0.978
8	0.989	0.992	0.988	0.978	0.991
10	1.000	1.000	1.000	1.000	1.000
15	1.023	1.016	1.017	1.033	1.016
20	1.038	1.025	1.024	1.046	1.027
25	1.044	1.034	1.028	1.057	1.031
30	1.051	1.039	1.030	1.063	1.035
35	1.042		1.032	1.069	
40		1.047	1.032	1.065	1.035
ratio	1.062	1.050	1.055	1.094	1.050

Factor-based dose calculations: basic dosimetric quantities

Linac head design influences S_c values

Varian Clinac 600C (MLC) - 4 MV

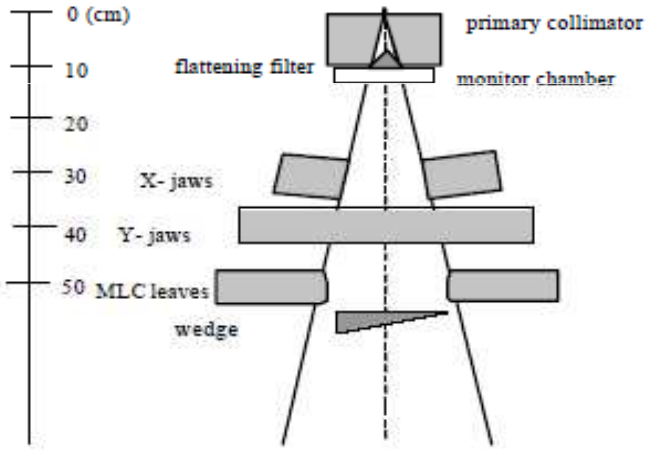

Siemens Primus (MLC) - 6 MV

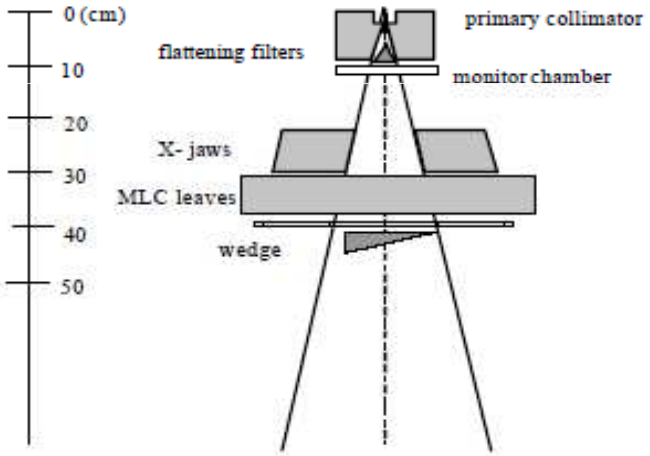

GE-CGR Saturne 41 (MLC) - 10 MV

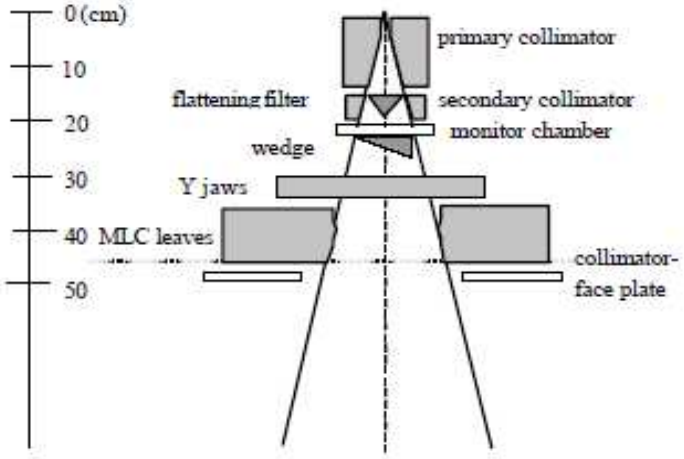

EOS SL20 (MLC) - 18 MV

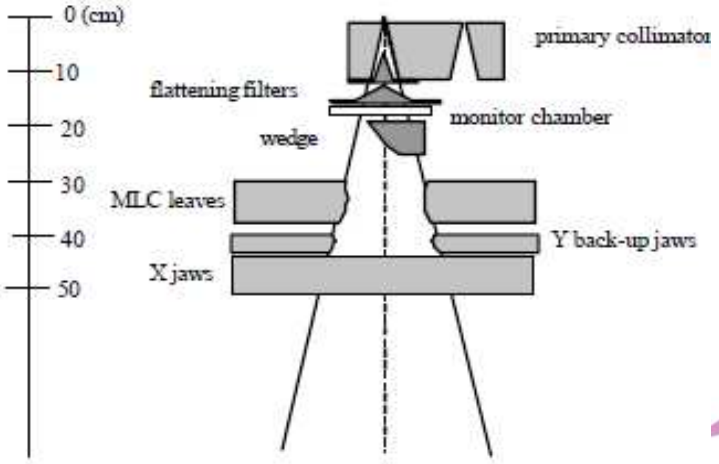

ESTRO School

Summary: in-air output ratio, Sc
isocentric conditions

- To quantify variations in energy fluence incident on the patient
- Function of the collimator setting
- Depends on the photon beam quality and on treatment head design
- Depends on the field orientation for rectangular beams (CEE)
- Almost independent of the source-detector distance
- Does not depend on depth if z > R contam. electrons

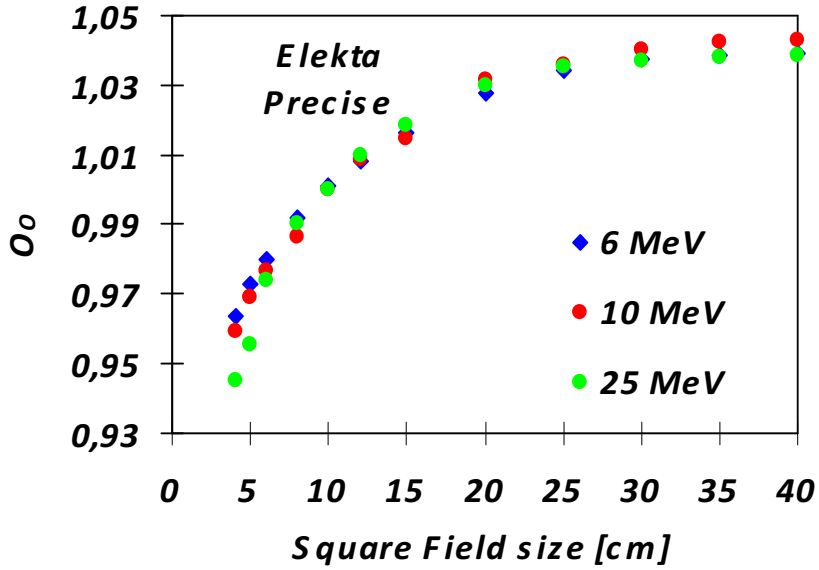

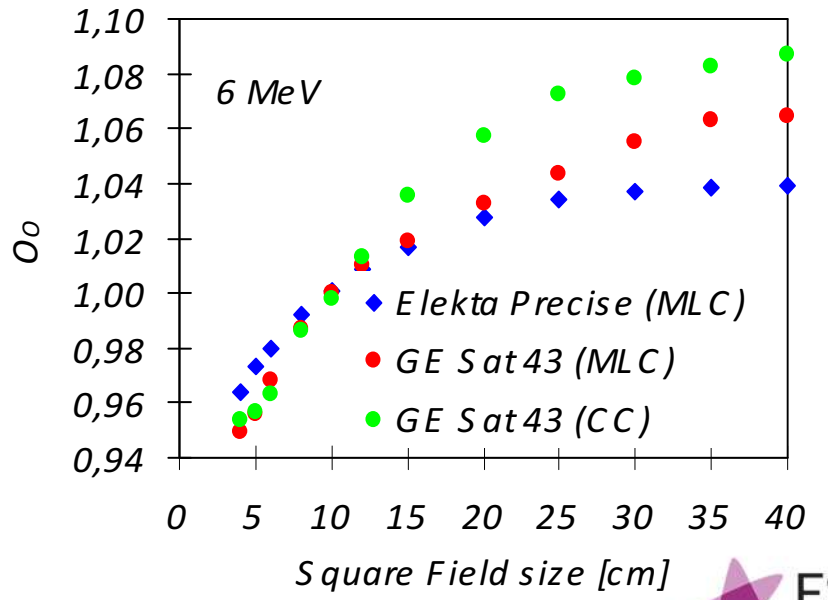

ESTRO School

Summary: in-air output ratio, Sc
isocentric conditions

- Function of the collimator setting
- Depends on the photon beam quality and on treatment head design
- Depends on the field orientation for rectangular beams (CEE)
- Almost independent of the source-detector distance
- Does <u>not</u> depend on depth if z > R contaminant electrons

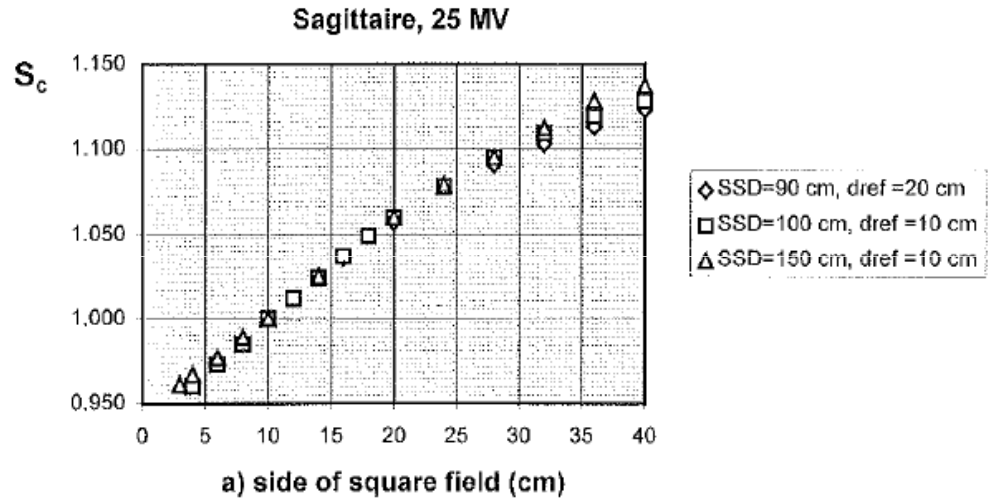

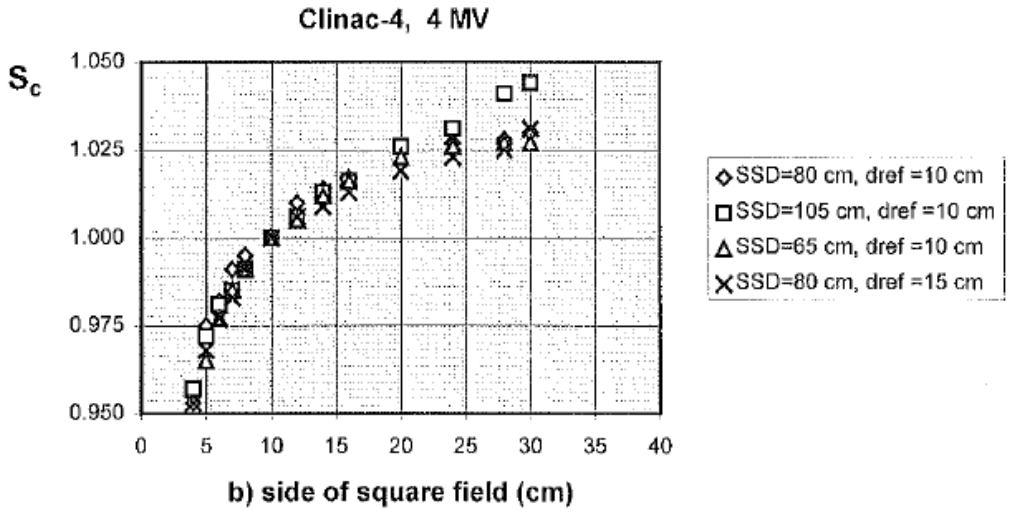

NCS report 12, 1998

ESTRO School

Dose per MU formalisms: factor-based dose calculations

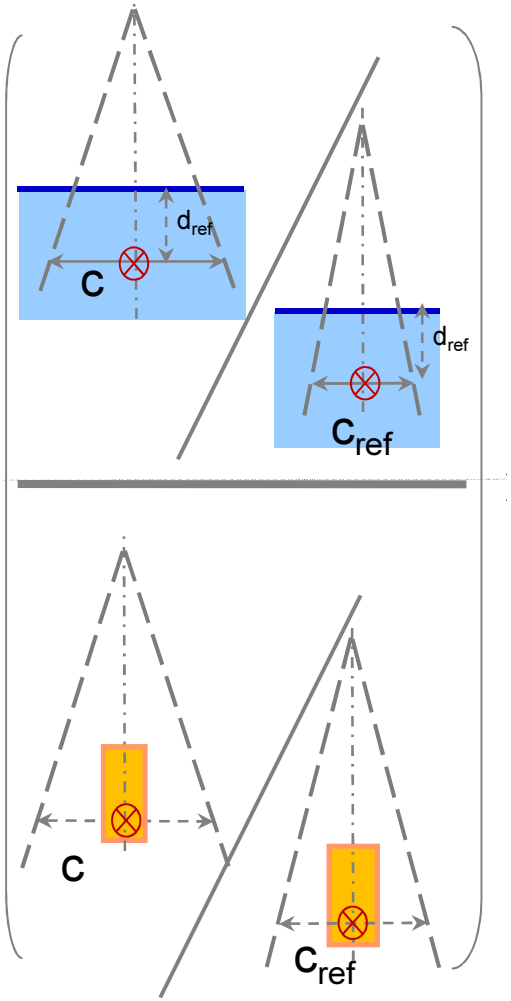

Factor-based dose calculations basic dosimetric quantities

Phantom **scatter factor**

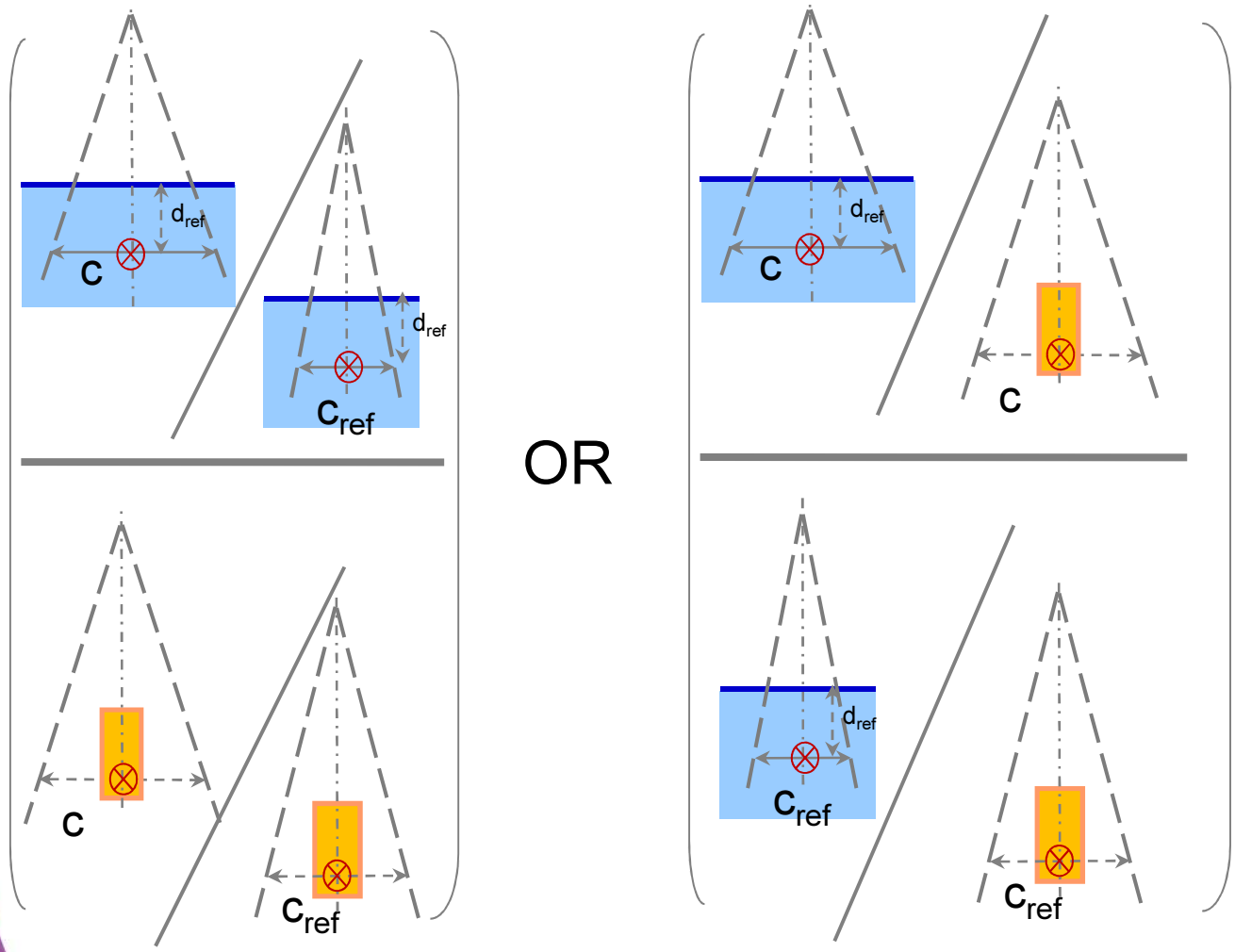

AAPM TG 74 report, Med Phys 36 (11), 2009

ESTRO School

Scatter Factor (SF)
The concept of buildup or (scatter) factor

$$B = \frac{\text{quantity due to primary + scattered radiation}}{\text{quantity due to primary radiation alone}}$$

In narrow beam geometry (only primary radiation): B=1

In broad beam geometry: B>1

$$B \approx \frac{\Psi_{total}}{\Psi_o e^{-\mu z}}$$

Total energy fluence at point of measurement

depth

Narrow beam attenuation coefficient

Unattenuated primary energy fluence

Attix (1986)

ESTRO School

Scatter Factors (total vs primary)

TAR(A,z), SAR(A,z), PSF(A), NPSF(A)

'Primary dose in water is obtained 'in-air' using a buildup cap on the detector (dose to small mass of medium): this is not really 'primary' as it includes scattered radiation from the buildup cap. *Further arguments by Burns J E in Appendix F of* ***BJR Supp 25 (1996)***

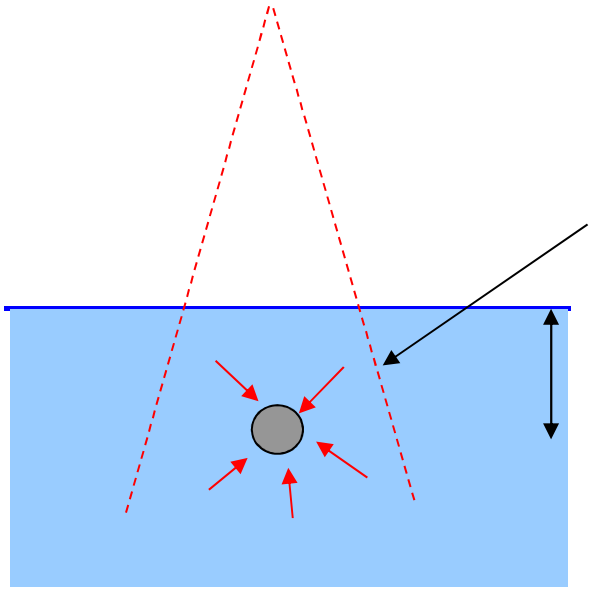

$$D_{total} = D_{Primary} + D_{Scatter}$$

$$= D_{Primary} \times PSF$$

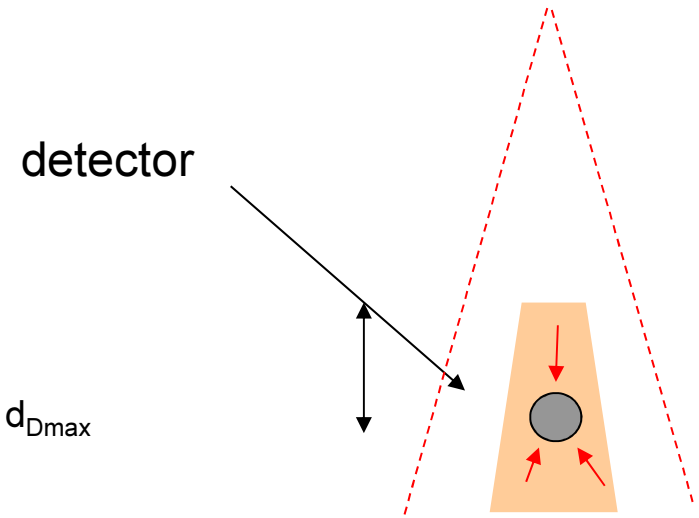

$$D_{total}^{buildup-cap} = D_{Primary}^{buildup-cap} + B' \cdot D_{Primary}^{buildup-cap}$$

$$D_{Primary} \neq D_{total}^{buildup-cap}$$

Factor-based dose calculations basic dosimetric quantities

Phantom scatter factor, S_p

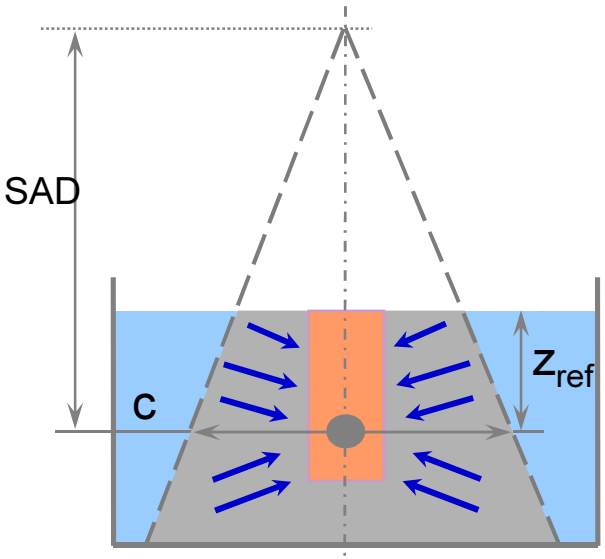

$$S_p(c) = \frac{D_{total}(c;d_{ref}) \,/\, D_{primary}(c;d_{ref})}{D_{total}(c_{ref};z_{ref}) \,/\, D_{primary}(c_{ref};d_{ref})}$$

S_p is the ratio of scatter factors between the actual field size c in the phantom and that of the reference field size c_{ref} , both at the reference depth d_{ref}:

S_p describes the effects of photon scattering in the phantom only

AAPM TG 74 report, Med Phys 36 (11), 2009

ESTRO School

Factor-based dose calculations basic dosimetric quantities

Phantom scatter factor, S_p

$$S_p(s) = \frac{D_{total}(s; z_{ref}) / D_{primary}(s; z_{ref})}{D_{total}(s_{ref}; z_{ref}) / D_{primary}(s_{ref}; z_{ref})}$$

$$D_{primary}(s) = K_p(s)\beta_p(s)$$

s: field size

if s = collimator setting c at the plane of the isocentre

$$S_p(c) = S_{cp} \Big/ \left(\frac{K_p(c)}{K_p(c_{ref})} \frac{\beta_p(c)}{\beta_p(c_{ref})} \right) = \frac{S_{cp}}{S_c\left(\frac{\beta_p(c)}{\beta_p(c_{ref})} \right)} \cong \frac{S_{cp}(c)}{S_c(c)}$$

Total scatter factor
Mainly known as
Output factor

dose to collision kerma ratio

≅ 1 under lateral CPE

AAPM TG 74 report, Med Phys 36 (11), 2009

ESTRO School

Factor-based dose calculations basic dosimetric quantities

Phantom scatter factor, S_p

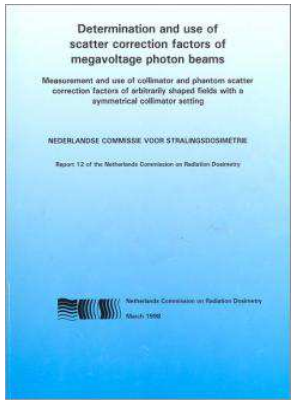

NCS report 12

field size (cm)	Quality index .600	.620	.640	.660	.680	.700	.720	.740	.760	.780	.800
4.0	0.859	0.877	0.892	0.904	0.914	0.921	0.926	0.931	0.931	0.932	0.931
5.0	0.888	0.902	0.913	0.923	0.930	0.937	0.942	0.946	0.948	0.950	0.952
6.0	0.916	0.926	0.934	0.941	0.947	0.952	0.957	0.961	0.963	0.966	0.968
7.0	0.940	0.947	0.953	0.959	0.963	0.967	0.970	0.973	0.975	0.977	0.979
8.0	0.962	0.967	0.970	0.974	0.976	0.978	0.981	0.983	0.985	0.987	0.989
9.0	0.983	0.985	0.986	0.987	0.988	0.989	0.990	0.992	0.993	0.994	0.995
10.0	1.000	1.000	1.000	1.000	1.000	1.000	1.000	1.000	1.000	1.000	1.000
12.0	1.029	1.026	1.024	1.022	1.019	1.017	1.015	1.013	1.011	1.010	1.010
14.0	1.053	1.049	1.044	1.039	1.035	1.030	1.027	1.024	1.021	1.018	1.017
16.0	1.072	1.065	1.059	1.054	1.048	1.043	1.037	1.033	1.029	1.026	1.023
18.0	1.085	1.078	1.072	1.066	1.060	1.054	1.047	1.042	1.037	1.032	1.027
20.0	1.097	1.090	1.084	1.077	1.070	1.063	1.056	1.050	1.043	1.036	1.030
22.0	1.115	1.106	1.097	1.089	1.079	1.071	1.063	1.056	1.048	1.041	1.034
24.0	1.124	1.114	1.106	1.097	1.087	1.079	1.070	1.062	1.053	1.044	1.037
26.0	1.130	1.122	1.114	1.105	1.094	1.086	1.077	1.068	1.058	1.049	1.040
28.0	1.136	1.128	1.120	1.111	1.101	1.092	1.082	1.072	1.062	1.052	1.042
30.0	1.142	1.134	1.126	1.117	1.107	1.097	1.087	1.076	1.066	1.055	1.045
32.0	1.148	1.140	1.132	1.123	1.112	1.102	1.091	1.080	1.069	1.057	1.047
34.0	1.154	1.146	1.137	1.128	1.116	1.106	1.095	1.084	1.072	1.060	1.049
36.0	1.160	1.152	1.142	1.132	1.121	1.110	1.098	1.087	1.075	1.063	1.051
38.0	1.167	1.157	1.147	1.137	1.124	1.113	1.101	1.089	1.077	1.065	1.053
40.0	1.175	1.163	1.153	1.140	1.128	1.116	1.104	1.091	1.079	1.067	1.055

Factor-based dose calculations basic dosimetric quantities

Phantom scatter factor, S_p

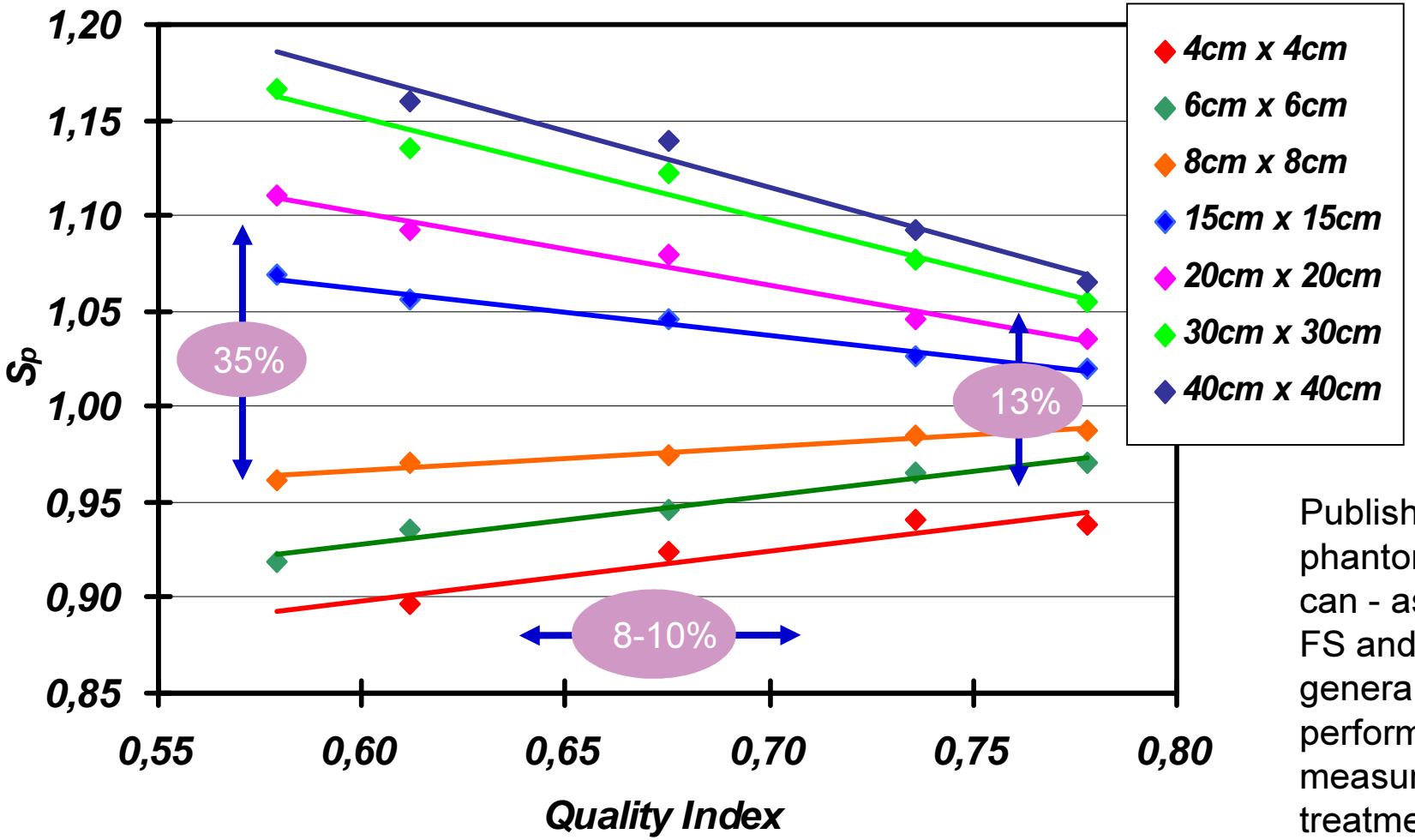

Published data on phantom scatter factors can - as a function of FS and QI - be in general used instead of performing measurements for each treatment unit individually

Georg et al 1999, PMB 44, 2987-3007; Sätherberg et al 1996, PMB 41, 2687-2694)

ESTRO School

Factor-based dose calculations basic dosimetric quantities

Phantom scatter factor, S_p

Square field size	*Co-60*	*4 MV*	*6 MV*	*10 MV*	*18 MV*
(cm)	*QI = 0.579*	*QI = 0.612*	*QI = 0.675*	*QI = 0.736*	*QI = 0.778*
	meas.	*meas.*	*meas.*	*meas.*	*Meas.*
4		0.897	0.924	0.941	0.938
5	0.898		0.933	0.953	
6	0.918	0.937	0.947	0.966	0.970
8	0.961	0.970	0.975	0.985	0.988
10	1.000	1.000	1.000	1.000	1.000
15	1.069	1.056	1.046	1.026	1.021
20	1.110	1.092	1.080	1.047	1.036
25	1.150	1.116	1.104	1.061	1.047
30	1.166	1.135	1.122	1.076	1.055
35	1.186		1.131	1.087	
40		1.159	1.139	1.092	1.066
ratio	1.209	1.165	1.140	1.084	1.068

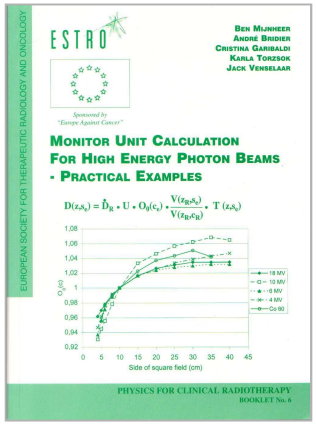

ESTRO Booklet #6

ESTRO School

Dose per MU formalisms: factor-based dose calculations

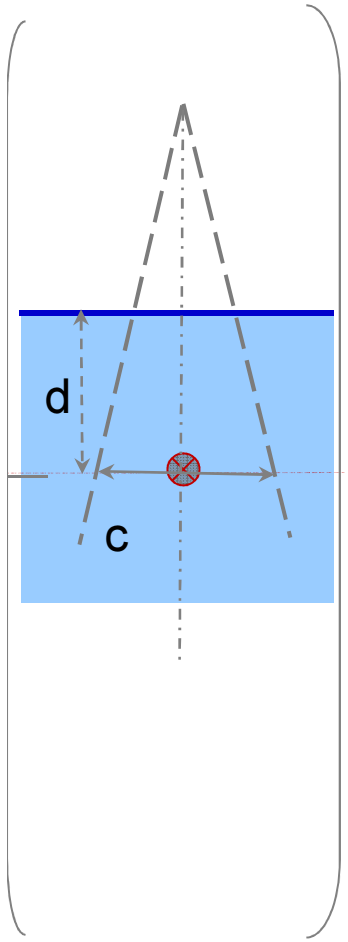

Factor-based dose calculations basic dosimetric quantities

Tissue Phantom Ratio, TPR for isocentric setup

$$T(s,d) = \frac{D(s,d,SAD)}{D(s,d_{\text{ref}},SAD)}$$

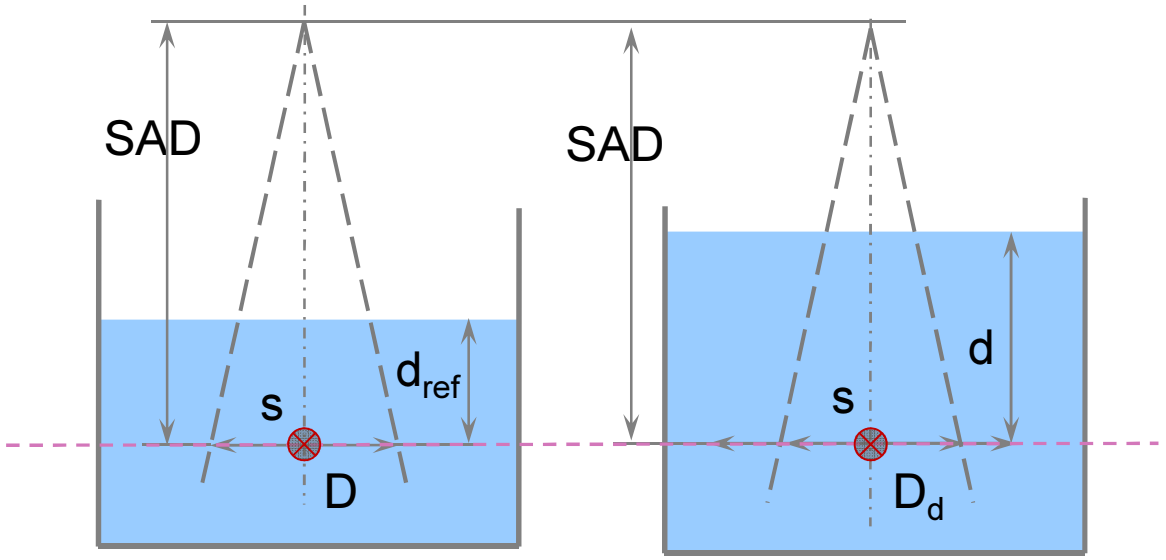

ESTRO School

Tissue-phantom ratios for a 10 x 10 cm² field obtained from BJR Suppl. 25 and from measurements on linacs used in ESTRO booklet nr. 6

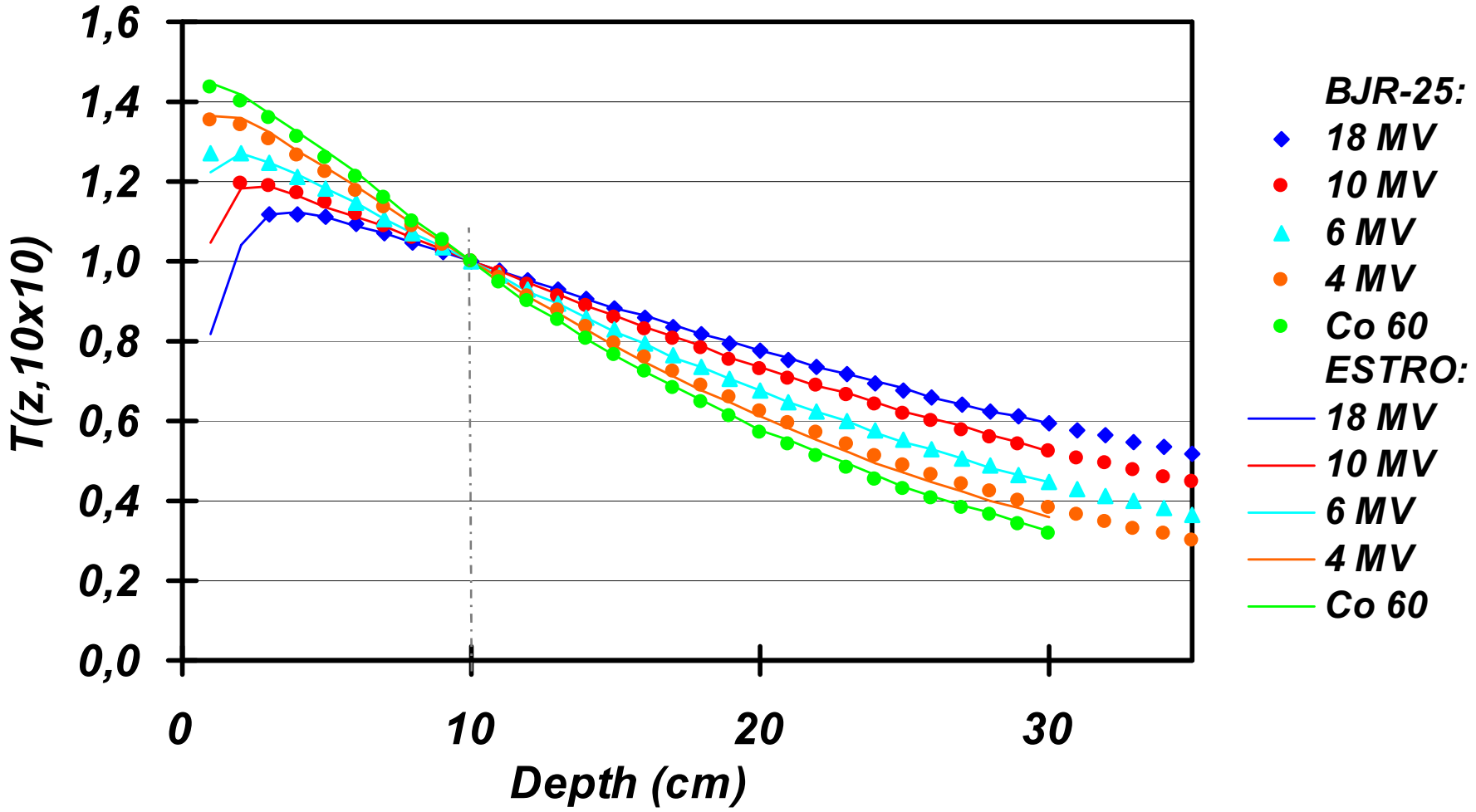

NORMALIZATION DEPTH: 10 cm in water

ESTRO School

Factor-based dose calculations basic dosimetric quantities

Relative depth dose (RDD, or PDD) at an SSD=SAD setup

$SSD_{ref} = SAD$

Relative depth dose, RDD

$$RDD_{\text{ref}}(s,d,SSD_{\text{ref}}) = \frac{D(s,d,SSD_{\text{ref}})}{D(s,d_{\text{ref}},SSD_{\text{ref}})}$$

or

Percentage depth dose, PDD

$$PDD(s,d,SSD_{\text{ref}}) = \frac{D(s,d,SSD_{\text{ref}})}{D(s,d_{\text{ref}},SSD_{\text{ref}})} \cdot 100$$

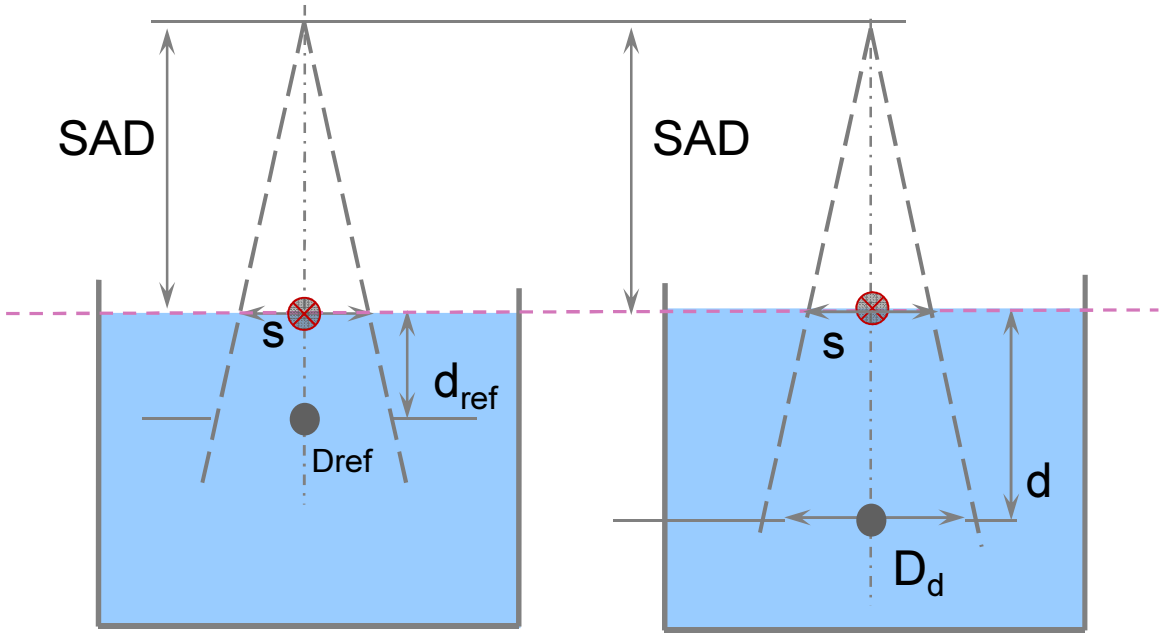

Dose per MU formalisms: factor-based dose calculations

Isocentric formalism: dose per meterset at isocentre (at SAD and on CAX)

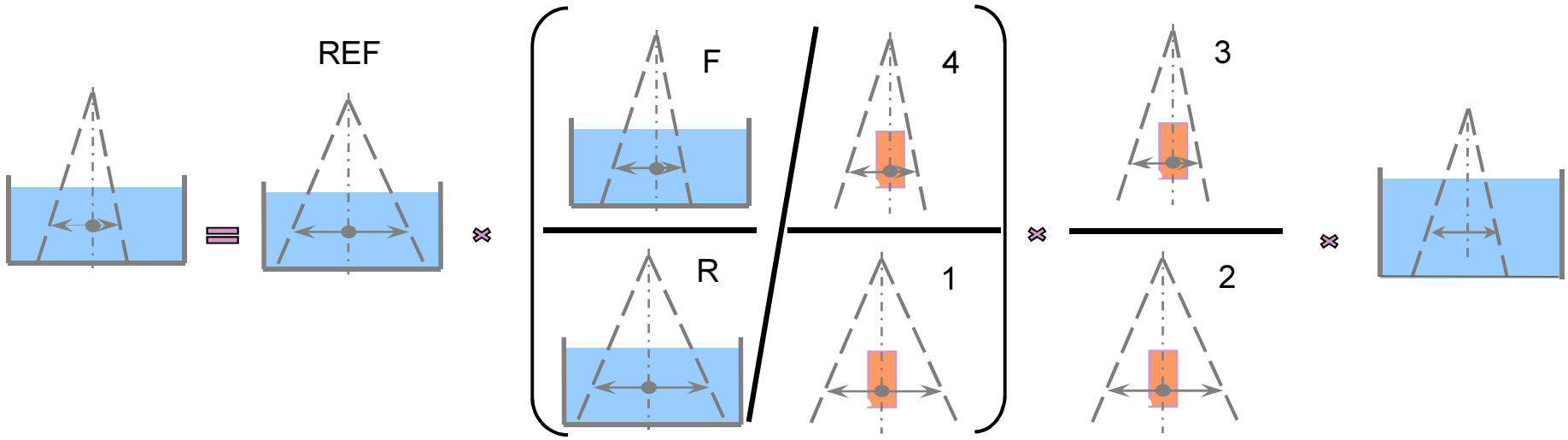

$$\frac{D(c_{\mathrm{d}},d;SAD)}{M}=\frac{D(c_{\mathrm{ref}},d_{\mathrm{ref}})}{M}\cdot S_{\mathrm{p}}(c_{\mathrm{eqsq}})\cdot S_{\mathrm{c}}(c_{\mathrm{eqsq}})\cdot TPR(c_{\mathrm{eqsq}},d)$$

The formalism above applies when the reference normalization conditions are isocentric (SSD_{ref}=90cm and d_{ref}=10cm) and scatter factors are determined isocentrically.

ESTRO School

Dose per MU formalisms: factor-based dose calculations

Isocentric formalism: dose per meterset NOT at isocentre (on CAX)

Scaling energy fluence from that at isocentre to that at the calculation point not at SAD

$$\frac{D(s_{\mathrm{d}}, d; SSD)}{M} = \frac{D(c_{\mathrm{ref}}, d_{\mathrm{ref}})}{M} \cdot S_{\mathrm{c}}(c_{\mathrm{eqsq}}) \cdot S_{\mathrm{p}}(s_{d,\mathrm{eqsq}}) \cdot TPR(s_{\mathrm{d,eqsq}}, d) \cdot \left(\frac{SAD}{SSD + d}\right)^2$$

On the assumption that phantom scatter ratios are independent of SSD

The field size used is that at the calculation point

ESTRO School

Factor-based dose calculations basic dosimetric quantities

Conversion from RDD→TPR (or from TPR→ RDD)

- Its easier to measure PDDs than TPRs in the water tank
- S_c can be measured isocentrically in a mini-phantom
- S_{cp} can be measured isocentrically in water

How can one determine TPRs?

Relationships between quantities

TPR from data measured isocentrically

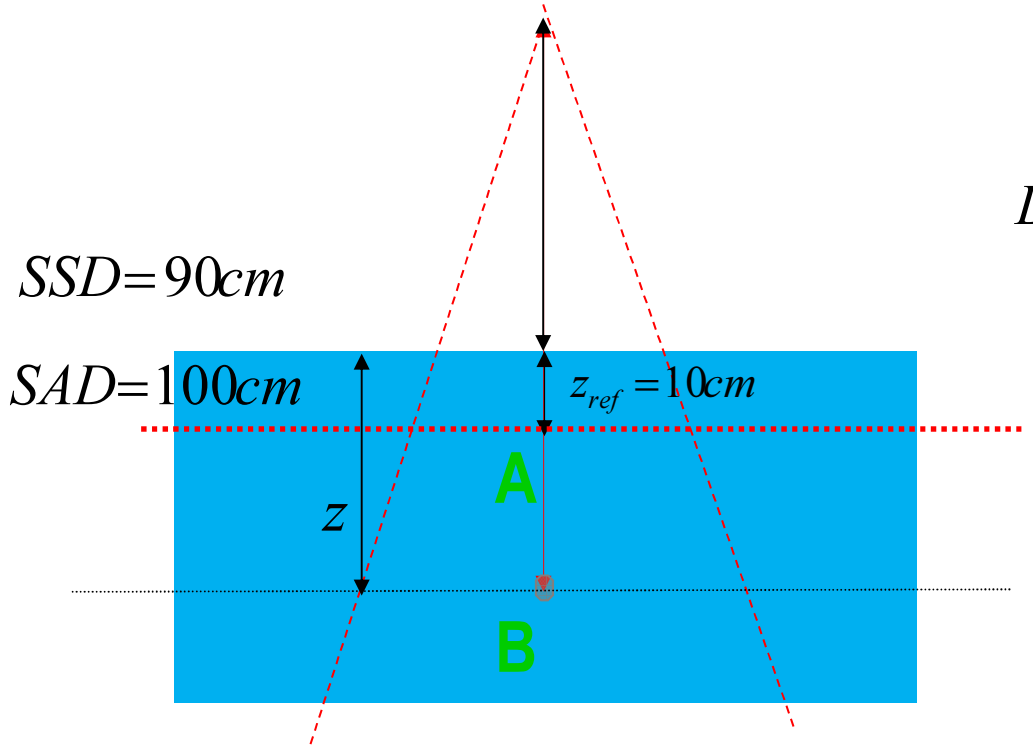

$$D\left(A^{c}_{SAD}, A^{p}_{SAD}, SDD; z\right)$$

$$90cm + z_{ref} = 100cm$$

$$SDD \neq SAD$$

$$S^{iso}_{c}\left(A^{c}_{SAD}\right)$$

$$D_{A} = D_{ref}\left(A^{c}_{SAD,ref}, A^{p}_{SAD,ref}, 90cm + z_{ref}; z_{ref}\right)$$

$$S^{iso}_{p}\left(A^{p}_{SAD}\right) \quad \left(where\ A^{p}_{SAD} = A^{EqSq}_{SAD}\right)$$

$$PDD_{90,10}\left(A^{p}_{SAD}; z\right) = \frac{D_{B}}{D_{A}} = \frac{D_{B}\left(A^{c}_{SAD}, A^{p}_{SAD}, 90cm + z; z\right)}{D_{A}\left(A^{c}_{SAD}, A^{p}_{SAD}, 100cm; 10cm\right)}$$

ESTRO School

Relationships between quantities

TPR from RDD measured isocentrically

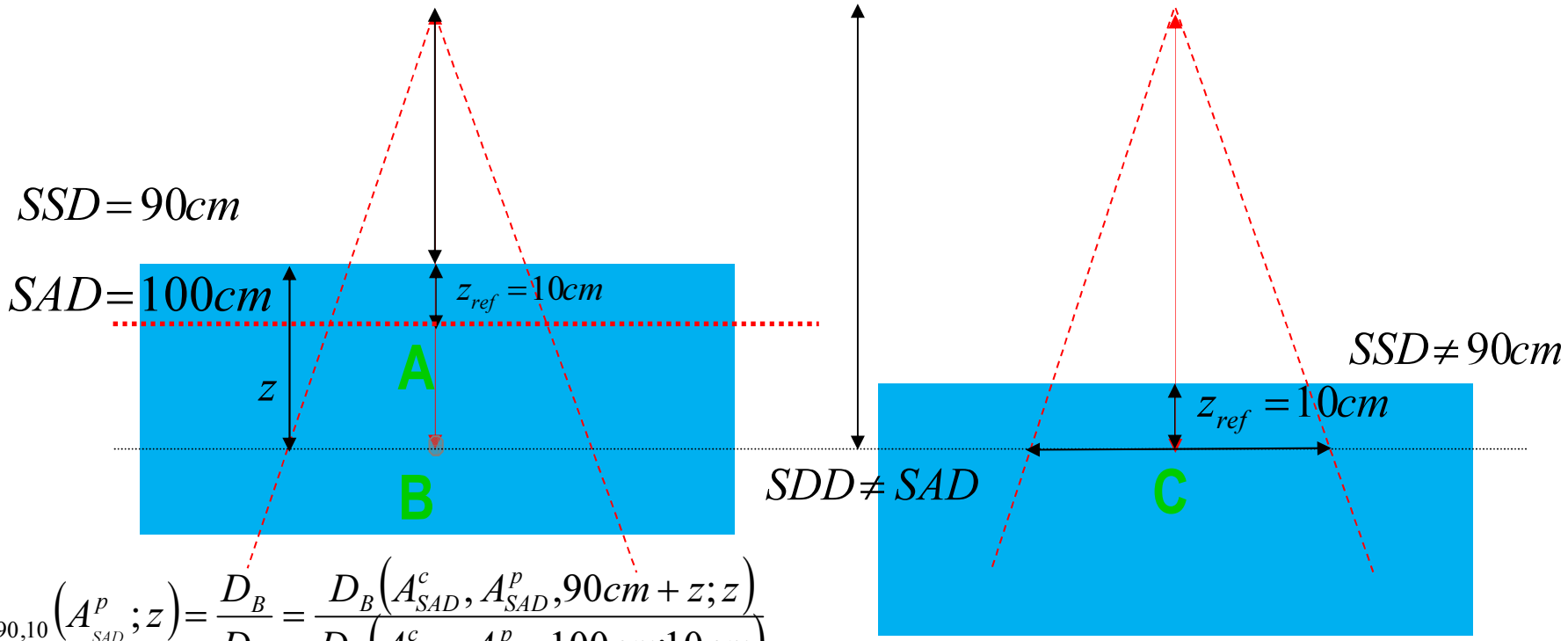

$$PDD_{90,10}\left(A^{p}_{SAD};z\right)=\frac{D_B}{D_A}=\frac{D_B\left(A^{c}_{SAD},A^{p}_{SAD},90cm+z;z\right)}{D_A\left(A^{c}_{SAD},A^{p}_{SAD},100cm;10cm\right)}$$

$$TPR\left(A^{p}_{SAD};z\right)=\frac{D_B}{D_C}=\frac{D_B\left(A^{c}_{SAD},A^{p}_{SAD},90cm+z;z\right)}{D_C\left(A^{c}_{SAD},A^{p}_{SAD},90cm+z;10cm\right)}$$

→Need to relate D_C to D_A

Relationships between quantities

TPR from RDD measured isocentrically

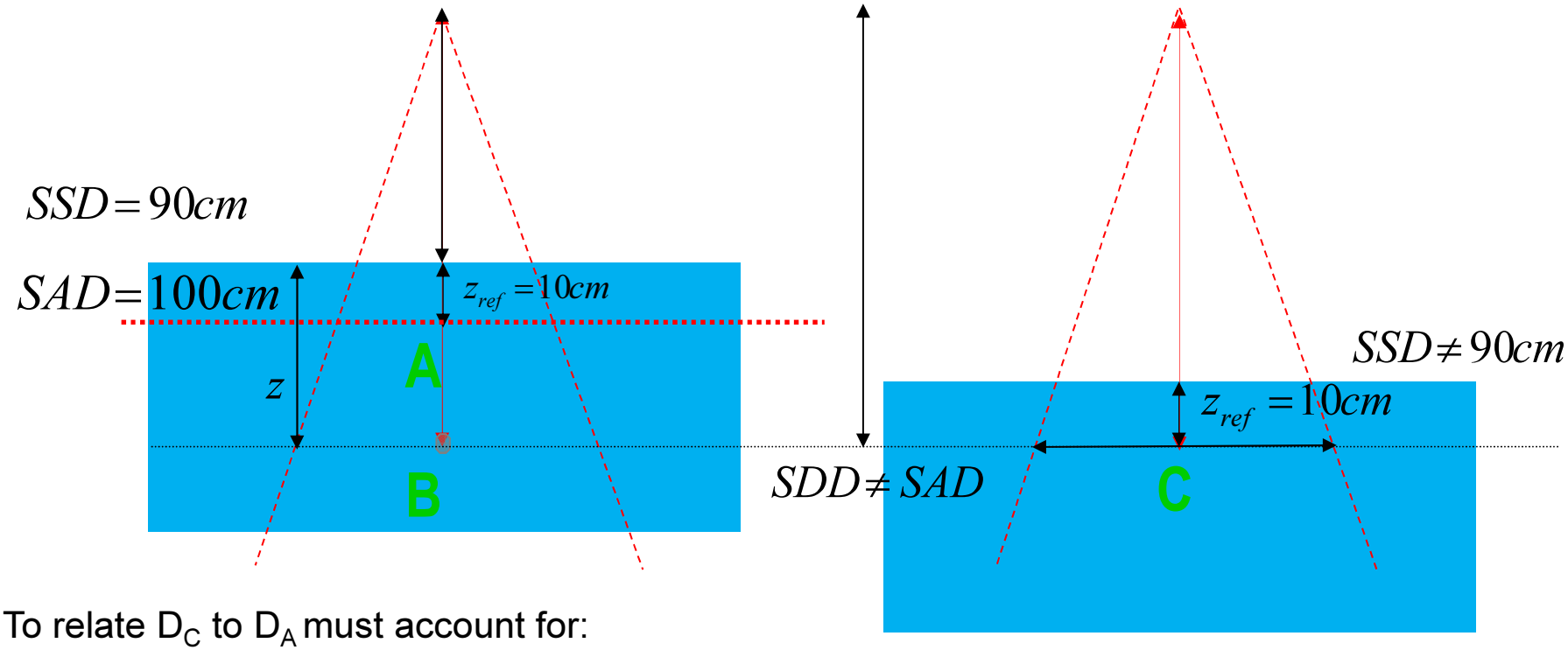

To relate D_C to D_A must account for:

- change in fluence according to inverse square law
- correction in phantom scatter due to the differences in field size at position A and C

$$D_C = D_A \times \left[\frac{(90cm + z_{ref})}{(90cm + z)}\right]^2 \times \frac{S_p^{iso}\left(A_{SAD}^p\left(\frac{90cm + z}{90cm + z_{ref}}\right)\right)}{S_p^{iso}\left(A_{SAD}^p\right)}$$

ESTRO School

Relationships between quantities

TPR from data measured isocentrically

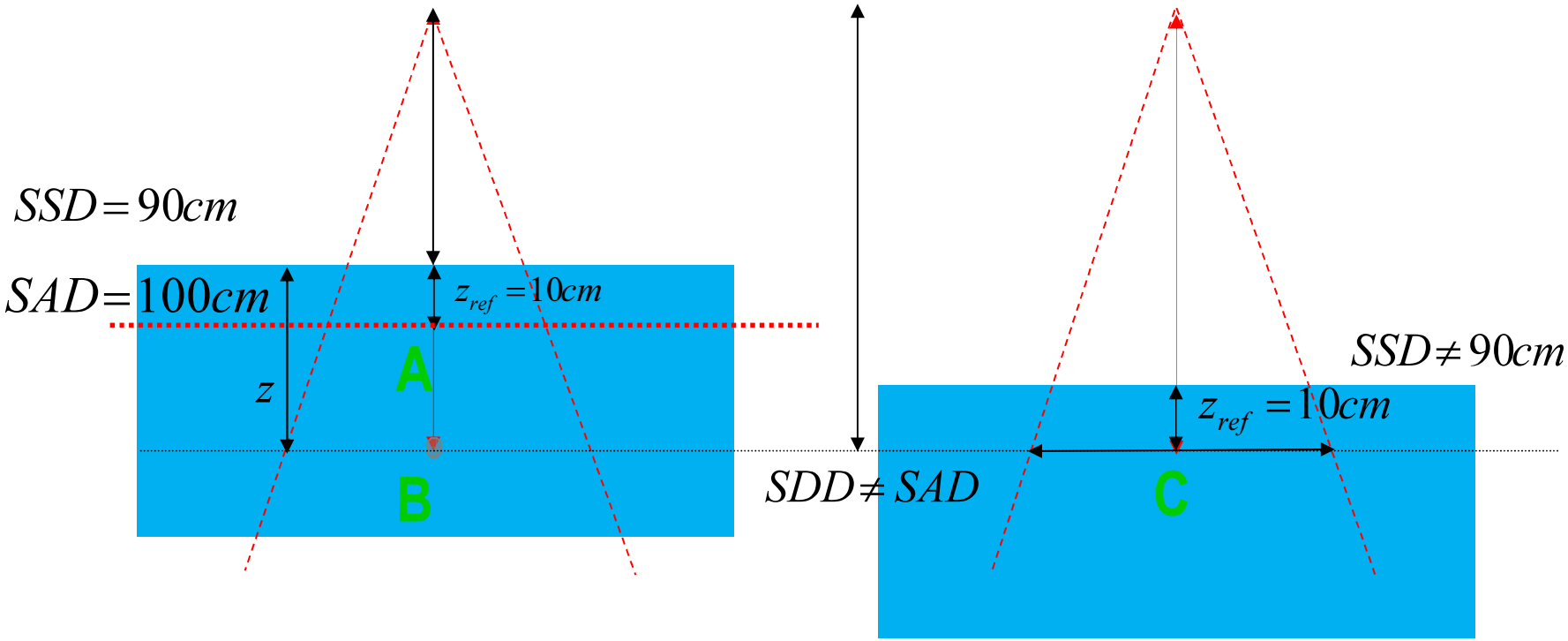

$$TPR\left(A_{SAD}^{EqSq};z\right)=\frac{PDD_{90cm,10cm}\left(A_{SAD}^{EqSq};z\right)}{100}\times\left(\frac{90cm+z}{100cm}\right)^{2}\times\frac{S_{p}^{iso}\left(A_{SAD}^{EqSq}\right)}{S_{p}^{iso}\left(A_{SAD}^{EqSq}\times\frac{90cm+z}{100cm}\right)}$$

A_{SAD}^{EqSq} Is the equivalent square field at SAD for the determination of phantom scatter

PDD normalised at reference depth to 100

ESTRO School

Dose per MU formalisms: factor-based dose calculations

How do factor-based formalisms deal with:

- non-square collimator settings
- fields shaped with blocks or MLCs
- modulation with hard wedges
- modulation with soft (dynamic/virtual) wedges
- other modulations (IMRT fields)
- Inhomogeneities
- points off axis

?

$$\frac{D(c, s_d, d; SSD)}{M}$$

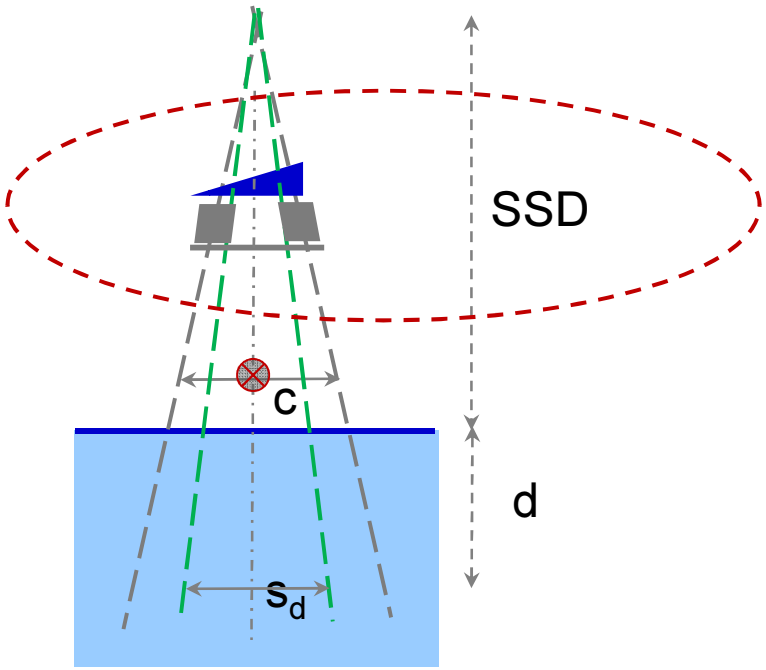

ESTRO School

Dose per MU formalisms: factor-based dose calculations

Isocentric formalism: dose per meterset at isocentre (at SAD and on CAX)

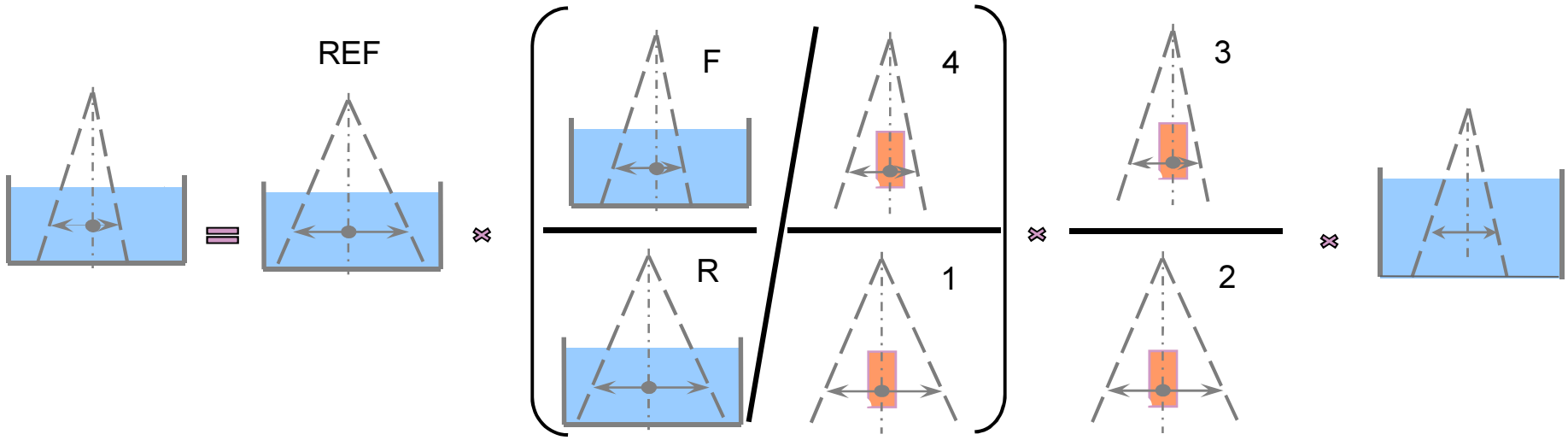

$$\frac{D(c_{\mathrm{d}}, d; SAD)}{M} = \frac{D(c_{\mathrm{ref}}, d_{\mathrm{ref}})}{M} \cdot S_{\mathrm{p}}(s_{\mathrm{eqsq}}) \cdot S_{\mathrm{c}}(c_{\mathrm{eqsq}}) \cdot TPR(s_{\mathrm{eqsq}}, d)$$

The formalism above applies when the reference normalization conditions are isocentric (SSD_{ref}=90cm and d_{ref}=10cm) and scatter factors are determined isocentrically.

ESTRO School

Equivalence between square and rectangular, circular or irregular fields

How this equivalency is defined and determined depends on the dosimetric quantity involved:

a. Dosimetric quantities relating to changes in scattered radiation in the phantom; TPR, S_p, S_{cp}
b. Dosimetric quantities relating to changes in energy fluence from the linac head reaching the phantom; S_c

a. The concept of equivalent square for quantities describing phantom scatter

Equivalent field is defined as 'the standard' (i.e. circular or square) field that has the same central axis depth dose characteristics as the given non-standard field *(Day and Aird 1996, BJR25, 138).*

The equivalency between standard and non-standard fields is determined by the requirement that the contribution to the dose along CAX from scattered photons for the two fields be equal. Namely, that the quantity describing phantom scatter (e.g *scatter factor*) in the standard and non-standard field at the point of calculation is equal.

Phantom scatter: equivalent square of a circular field

The equivalence between a square field and a circular field has be shown to be:

Bjärngard and Siddon Med Phys 9(2), (1982)

$$r = 0.5611\,S$$

This equation can be implemented in sector integration algorithms to calculate the equivalent square of irregularly shaped fields

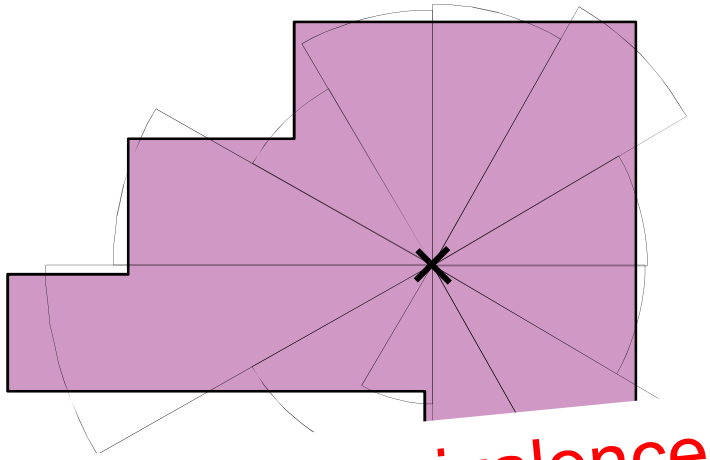

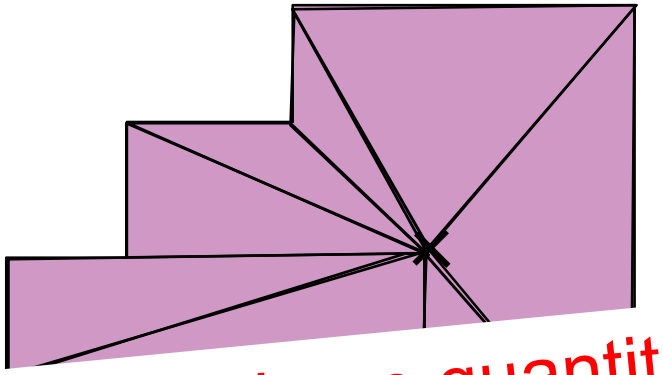

This concept of equivalence is applicable to those quantities where changes in phantom scatter need to be considered

Triangular decomposition
Siddon *et al* (1985), Med Phys 12(2)

ESTRO School

The derivation of the equivalent circular field radius using pencil beam convolution

Simplify the expression known to well model a scatter dose pencil kernel:

$$\frac{p_s}{\rho}(r) \approx \frac{B\,e^{-br}}{r} = \frac{B}{r} + O(r)^0$$

Integrate to get scatter dose per incident energy fluence for a circular field of radius *R*

$$D_{\text{circular field radius R}} \approx \int_0^{2\pi}\int_0^{R} \frac{B}{r}\cdot r\,dr\,d\theta = B2\pi R$$

Integrate also to get scatter dose for a square field of side *S* (a square is composed of 8 triangles 45 degree each)

$$D_{\text{Square field side S}} \approx 8\int_0^{\pi/4}\int_0^{S/2} \frac{B}{r}\cdot\frac{r}{\cos\theta}\,dr\,d\theta = B4S\int_0^{\pi/4}\frac{1}{\cos\theta}\,d\theta = B4S\ln\left(1+\sqrt{2}\right)$$

Set the dose results equal (equivalent field size!) :

$$B2\pi R = B4S\ln\left(1+\sqrt{2}\right)$$

and solve for *R* as function of *S* resulting in

$$R = \frac{2\ln\left(1+\sqrt{2}\right)}{\pi}S = 0.5611S$$

ESTRO School

Phantom scatter: equivalent square of a rectangular field

Area over perimeter method

(Sterling et al 1964 BJR 37, 544; Patomaki 1968, BJR 41,381 etc)

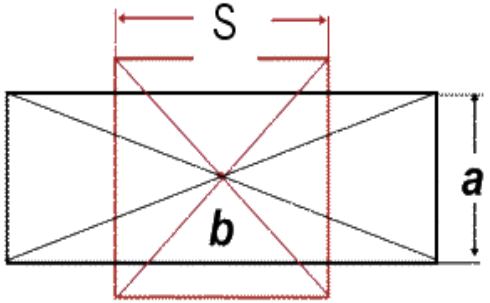

$$S = \frac{Area}{Perimeter}$$

or

"$4A/P$"

$$\frac{S^2}{4S} = \frac{a \cdot b}{2(a+b)}$$

$$S = 2\frac{a \cdot b}{a+b}$$

Method not based on sound physical principles, BUT used for years, with surprisingy accurate results (<1%) for rectangular fields of length <20cm and length/width<4 *(Day and Aird 1996 BJR25, 138,McDermott, MedPhys 25(11), 2215, 1998).*

ESTRO School

Phantom scatter: equivalent square of a circular field

Tabulated data

BJR25 in Appendix A (Day and Aird 1996): Derived from a fitting a linear scatter function to central axis depth dose data as a function of radius

$$S/\delta = 0.891 + 0.00046\,\delta \qquad or \qquad S/\delta = 0.90 \quad or \quad r = 0.555\,S$$

Side of square field — diameter of circular field

Which *accidently* approximates to:

$$S^2 = \pi\, r_{eq}^2 = \pi \left(\frac{\delta_{eq}}{2}\right)^2 \Rightarrow \frac{Sr}{\delta_{eq}} = 0.886 \approx 0.9 \Rightarrow S \approx 1.8r$$

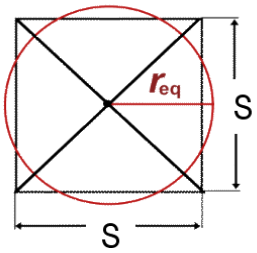

- Depth and beam quality dependence is ignored
- Shown to give of an accuracy within 5% for scatter dose and 2% for total dose for points on CAX

Note: equivalence between square and circular fields, if one were to apply the area over perimeter method...:

$$S = \frac{Area}{Perimeter} \rightarrow \frac{S^2}{4S} = \frac{\pi\, r^2}{2\,\pi\, r} \Rightarrow \ldots \Rightarrow S = 2\,r$$

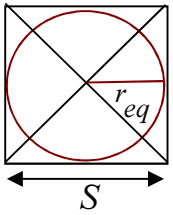

10% over-estimation!

ESTRO School

Phantom scatter: equivalent square of a circular field

Tabulated data

BJR25 in Appendix A (Day and Aird 1996): Derived from a fitting a linear scatter function to central axis depth dose data as a function of radius

$$S/\delta = 0.891 + 0.00046\,\delta \qquad or \qquad S/\delta = 0.90 \quad or \quad r = 0.555\,S$$

Side of square field — diameter of circular field

or:

$$S \approx 1.8r$$

- Depth and beam quality dependence is ignored
- Shown to give of an accuracy within 5% for scatter dose and 2% for total dose for points on CAX

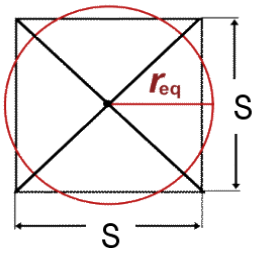

Note: equivalence between square and circular fields, if one were to apply the area over perimeter method...:

$$S = \frac{Area}{Perimeter} \rightarrow \frac{S^2}{4S} = \frac{\pi r^2}{2\pi r} \Rightarrow \ldots \Rightarrow S = 2r$$

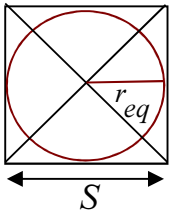

10% over-estimation!

ESTRO School

Phantom scatter: equivalent square of a rectangular field

Tabulated data

NCS Report 12, Appendix 8.6 (1998): Tables constructed by averaging 4 energy specific tales for ^{60}Co, 6, 10, 25 MV photon beams(Venselaar et al, Phys Med Biol, 42: 2369-2381, 1997)

The equivalent square field, to be used for the determination of the phantom scatter factor and phantom scatter related quantities, is defined here as the square field which has the same phantom scatter contribution at the reference point in the beam: at 10 cm depth on the central axis, as the arbitrarily shaped field under consideration.

of QI of 0.573 to 0.783 (^{60}Co to 25 MV). It was shown that the use of the energy-specific tables could eventually lead to a difference of 0.5 - 1.0% in the value of S_p, compared to the use of the BJR-table, in which the use of the BJR-table systematically leads to a lower value of S_p. The relatively small differences

s1 \ s2	2.0	4.0	6.0	8.0	10.0	12.0	14.0	16.0	18.0	20.0	22.0	24.0	26.0	28.0	30.0	32.0	34.0	36.0	38.0	40.0
2.0	2.0																			
4.0	2.8	4.0																		
6.0	3.3	4.9	6.0																	
8.0	3.6	5.4	6.9	8.0																
10.0	3.7	5.7	7.4	8.8	10.0															
12.0	3.8	5.9	7.7	9.4	10.9	12.0														
14.0	3.9	6.0	7.9	9.9	11.6	12.9	14.0													
16.0	4.0	6.1	8.1	10.3	12.2	13.8	15.0	16.0												
18.0	4.0	6.2	8.3	10.6	12.7	14.5	15.9	17.1	18.0											
20.0	4.0	6.2	8.5	10.9	13.2	15.1	16.6	18.0	19.1	20.0										
22.0	4.0	6.3	8.6	11.2	13.7	15.7	17.3	18.7	20.0	21.1	22.0									
24.0	4.1	6.4	8.7	11.5	14.1	16.1	17.9	19.4	20.7	22.0	23.1	24.0								
26.0	4.1	6.4	8.8	11.7	14.4	16.6	18.4	19.9	21.4	22.7	24.0	25.1	26.0							
28.0	4.1	6.4	8.9	11.9	14.7	16.9	18.8	20.4	22.0	23.4	24.7	26.0	27.1	28.0						
30.0	4.1	6.5	9.0	12.0	14.9	17.2	19.1	20.9	22.5	24.0	25.4	26.7	28.0	29.1	30.0					
32.0	4.1	6.5	9.1	12.2	15.1	17.5	19.4	21.2	22.8	24.4	25.9	27.3	28.7	29.9	31.0	32.0				
34.0	4.1	6.5	9.1	12.3	15.3	17.7	19.7	21.5	23.2	24.8	26.4	27.9	29.3	30.6	31.9	33.0	34.0			
36.0	4.1	6.5	9.1	12.4	15.4	17.8	19.9	21.7	23.4	25.1	26.7	28.3	29.8	31.2	32.6	33.8	35.0	36.0		
38.0	4.1	6.5	9.2	12.5	15.5	17.9	20.0	21.9	23.7	25.3	27.0	28.7	30.2	31.7	33.2	34.6	35.8	36.9	38.0	
40.0	4.1	6.5	9.2	12.5	15.6	18.1	20.1	22.0	23.8	25.6	27.3	28.9	30.5	32.1	33.6	35.1	36.5	37.8	39.0	40.0

ESTRO School

b. The concept of equivalent square for quantities describing head scatter

Output in air, Sc: depends upon the orientation of the rectangular fields (on CEE)

Collimator Exchange Effect (CEE): is mainly caused by a difference in extra-focal scattered radiation that can reach the point of interest for the same collimator setting of the upper and lower jaw

- CEE is of the order of 1% to 2.5 % for (most) modern linacs
- for older type of linacs (e.g. Saturne) the difference in output in air with X-Y vs. Y-X setting can amount to 6%

Points Eye View of the extended source

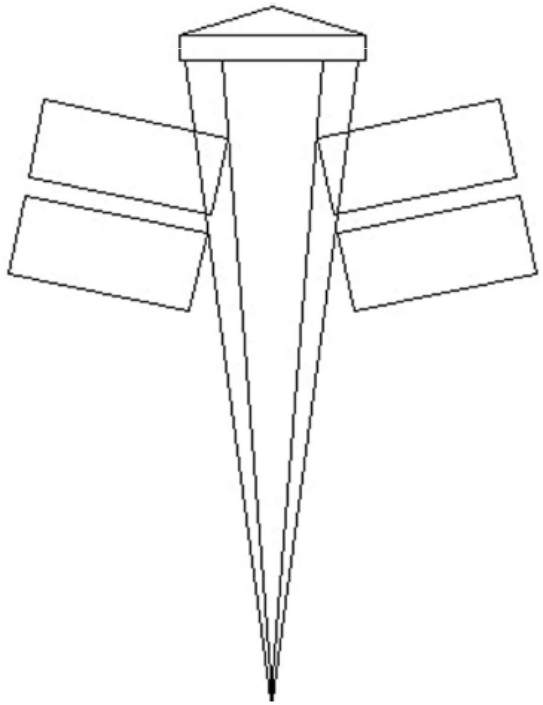

FIG. 12. Points eye view of upper and lower jaws. Schematic diagram of the treatment head showing flattening filter, monitor chamber, and upper and lower jaws. The lower jaws have been rotated by 90° for clarity.

AAPM TG 71 report, Med Phys 41 031501, 2014

ESTRO School

Head scatter: equivalent square of a rectangular field

Empirical approach to account for different influence of collimator layers

$$c_e(x,y) = \frac{(G+1)\cdot x \cdot y}{G\cdot x + y}$$

x ➔ lower jaw

y ➔ upper jaw

G **weighting factor**

depends on:

- treatment head design
- beam energy
- beam modifiers

Linac head

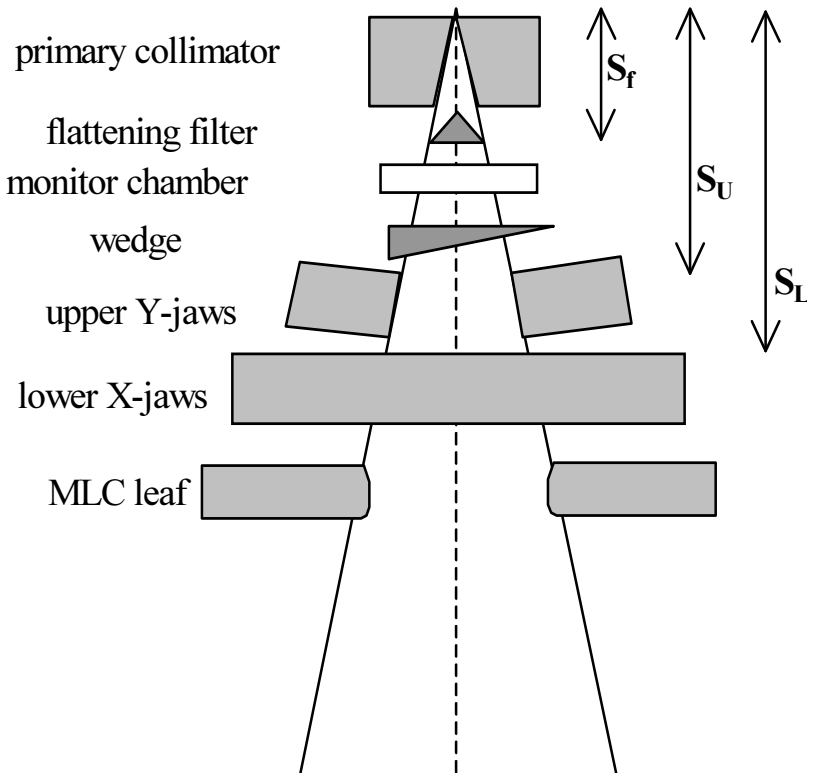

Vadash P and Bjärngard B E (1993) Med. Phys. 20, 733-734.

ESTRO School

Head scatter: equivalent square of a rectangular field

Determination of weighting factor G:

a. Experimentally: set of Sc values measured for square and rectangular fields (e.g. keeping one collimator setting fixed and varying the other one)

b. From treatment head geometry: relative weight (**G**) depends on distance from the X-ray source

$$G = (S_L / S_U)^2$$

Yu and Sloboda (1995)

$$G = (S_L / S_{LI}) (S_{UI} / S_U)$$

Kim et al (1997)

Typical values: 1.4 – 2.0

(See page 30 in ESTRO no. 6)

Linac head

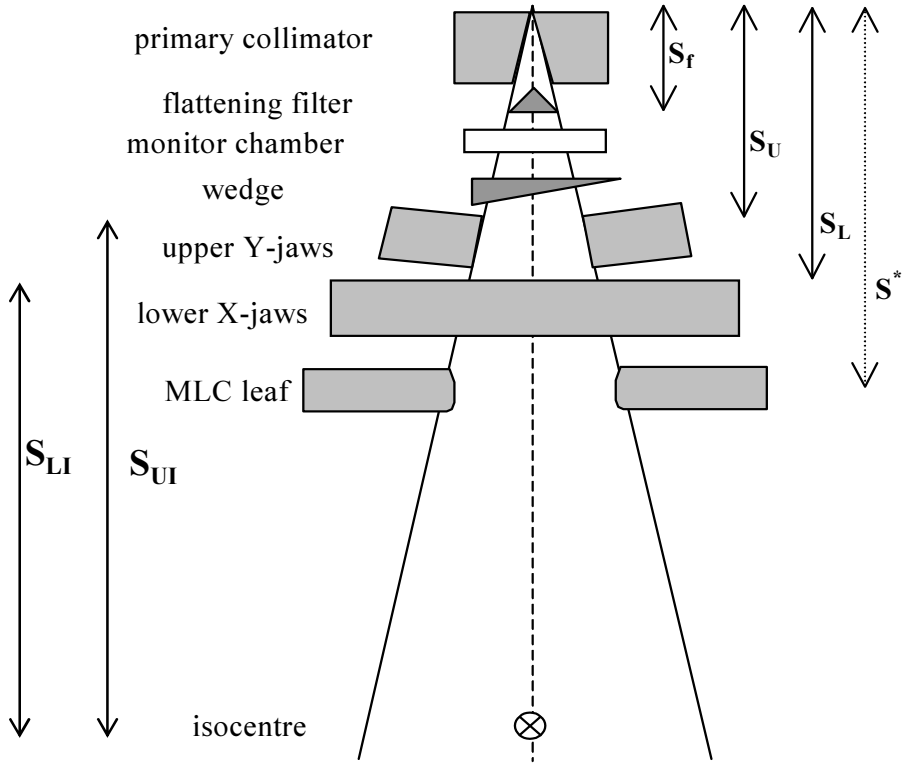

Head scatter: equivalent square of a rectangular field

example of data

ELEKTA, Precise 6 MV

x	y	$Sc_{Meas.}$	c_e	$Sc_{Calc.}$	% diff
30	40	1.043	35.3	1.038	0.4%
5	40	0.999	10.6	1.003	0.3%
10	40	1.020	18.,3	1.026	0.6%
20	40	1.036	28.7	1.036	0.0%
5	30	0.998	10.1	1.000	0.2%
10	30	1.017	16.7	1.022	0.5%
10	20	1.012	14.3	1.016	0.4%

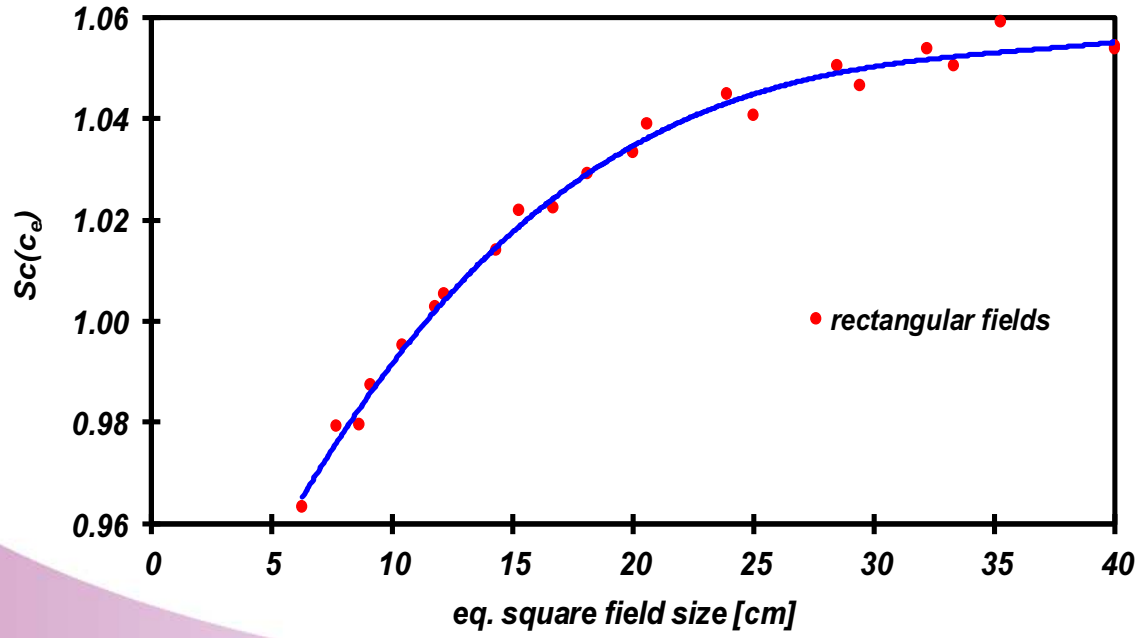

GE Saturne 43, 25 MV

ESTRO School

Summary: equivalence between square, rectangular, circular or irregular fields

- Output in air ratio, S_c, in air is not symmetric in X and Y
  - Equivalent squares with individual weighting of collimator elements can lead to sufficiently accurate approximation
  - For elongated fields less accurate
- Phantom (volume) scatter factor, S_p, is symmetric in X and Y
  - Traditional equivalent square formula lead to sufficiently accurate approximation for S_p, TPR, RDD, PDD
  - For elongated fields less accurate
- Irregular blocked or MLC shaped fields require more sophisticated models

Dose per MU formalisms: factor-based dose calculations

How do factor-based formalisms deal with:

- non-square collimator settings
- fields shaped with blocks or MLCs
- points off axis
- modulation with hard wedges
- modulation with wedges
- other modulations (IMRT fields)
- Inhomogeneities

?

$$\frac{D(c, s_d, d; SSD)}{M}$$

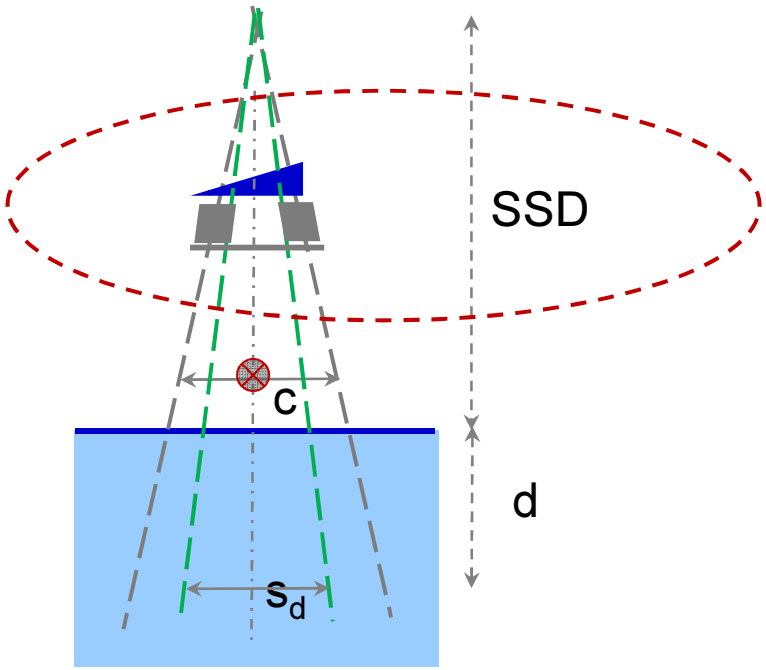

ESTRO School

Dose per MU formalisms: factor-based dose calculations

Irregular fields shaped with MLCs

- MLC design and position in linac head
  - Lower jaw replacement
  - Upper jaw replacement
  - Add-on (3rd level) configuration

- Depending of the MLC design, its influence on Sc and Sp needs to be considered separately:
  - Upper or lower jaw replacement MLC (e.g. Elekta, Siemens linacs)
    - ➢ The equivalent square from a sector intergration of the MLC aperture is used for both Sc and Sp
  - Add-on (3rd level) configuration (eg Varian linacs)
    - ➢ Sc ⇐ eq. Sq. of secondary jaws
    - ➢ Sp ⇐ eq. Sq. from MLC aperture

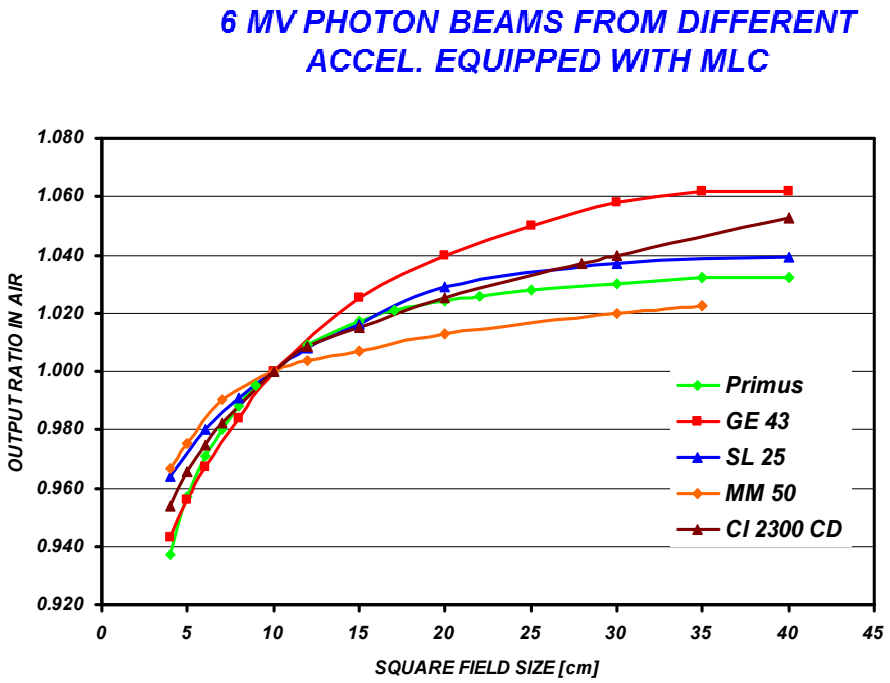

Palta et al 1995 MP
Das et al 1999 MP
Georg et al 1999 PMB

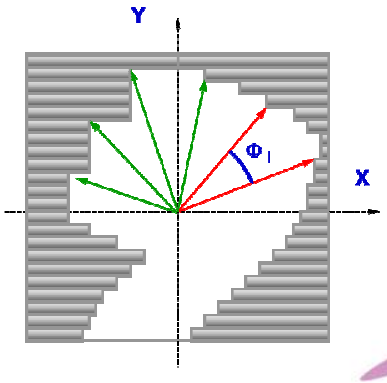

Klein et al 1995 IJROBP
Boyer 1992 MP

ESTRO School

Dose per MU formalisms: factor-based dose calculations

Calculations at points off-axis (asymmetric fields)

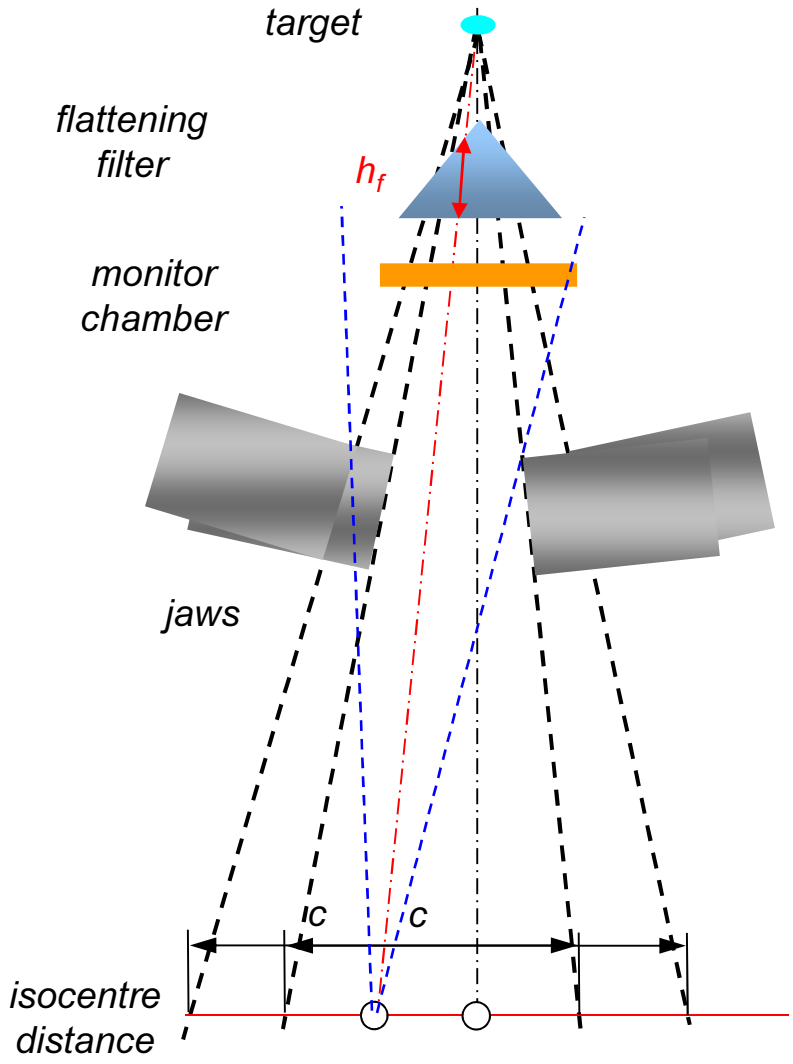

ESTRO School

Dose per MU formalisms: factor-based dose calculations

Calculations at points off-axis (asymmetric fields)

$$\frac{D(s_d, d, x; SSD)}{M} = \frac{D(c_{ref}, d_{ref})}{M} \cdot S_c(c_{eqsq}) \cdot S_p(s_{d,eqsq}) \cdot TPR(s_{d,eqsq}, d) \cdot OAR(d, x) \cdot \left(\frac{SAD}{SSD + d}\right)^2$$

For off-axis positions up to 5cm
no significant variation from the values CAX
On-axis data used

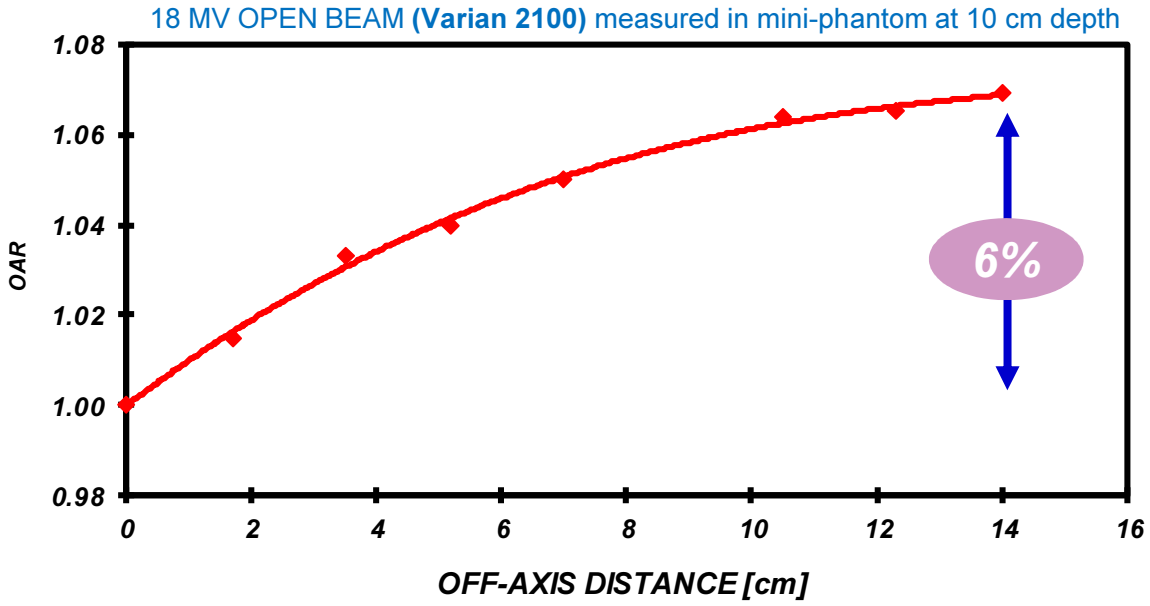

Off-Axis Ratio: representing off-axis variations of primary fluence; different approaches to determine this experimentally

ESTRO School

Dose per MU formalisms: factor-based dose calculations

Modulation with physical wedges

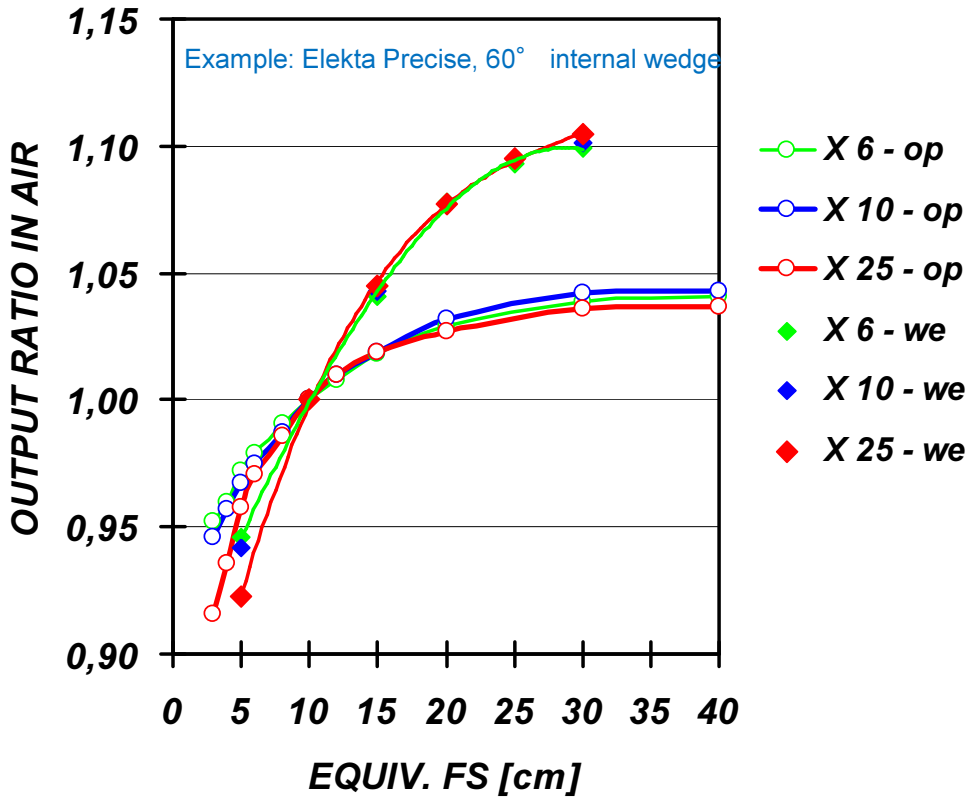

Variation open vs wedged fields:

- With FS
  - ➔ ~ 10% open
  - ➔ ~ 20% wedge
- Wedge angle
- Energy
- Linac specific

- Physical wedges introduce changes in the beam spectrum, which are dependent on wedge material and influence dosimetric parameters that vary with depth (TPR, RDD) as well as phantom scatter, Sp
- The position of the wedge, whether internal (motorised) or external (manually inserted) affects Sc
- Dosimetric parameters for wedged beams should not be confused with open beam data
- Irregular wedged beams need some special considerations for MU calculation / verification

⇒ Additional correction factors needed in the dose per MU formalism

ESTRO School

Dose per MU formalisms: factor-based dose calculations

Modulation with physical wedges

Example of a correction factor that can be determined from a model

Wedge Factor Calculation

$$WF_W = e^{\mu W}$$

where,

e - base of the natural log

μ = linear attenuation coefficient, $= \frac{\ln(WF_{CAX})}{W_{CAX}}$

W = thickness at the point of interest

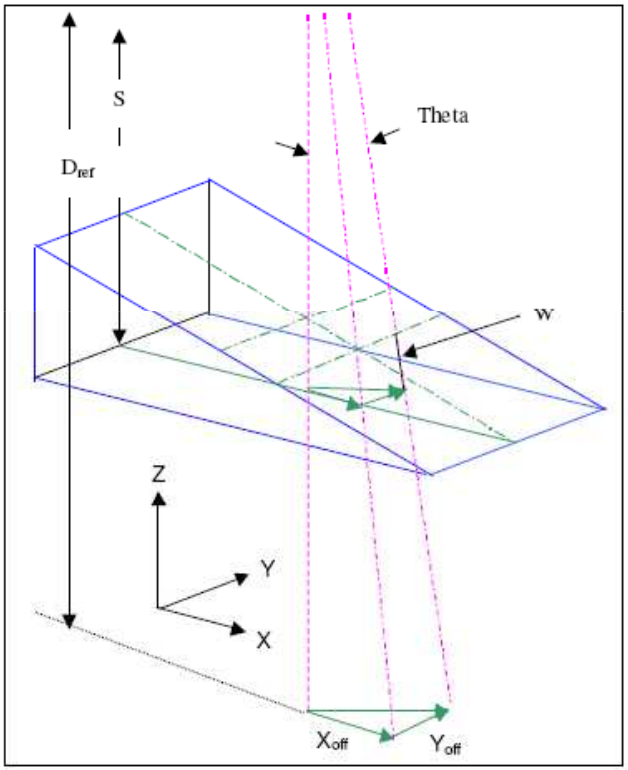

Off Axis Wedge Ratio using the physical dimensions

$$OAWR = \left(\frac{WF_W}{WF_{CAX}(d,f)} \right)$$

where,

WF_W = calculated wedge factor from thickness W

$WF_{CAX}(d,f)$ = interpolated central axis wedge factor at depth d, field size f from entered table

Off axis calculations with OAWR calculated from physical wedge dimensions:

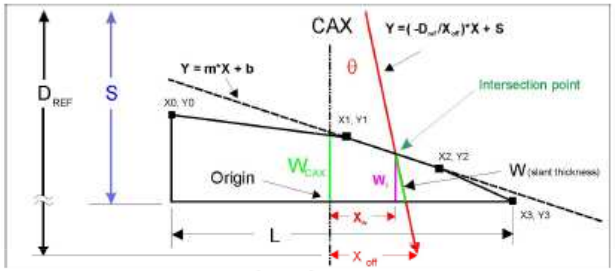

Wedge Diagram 1

For the interval $X_1 < X_w < X_2$, where $X_w = X_{off} * S/D_{ref}$,

$$W = \frac{1}{Cos(\theta)} \left[m \left[X_{off} \left(\frac{S}{D_{ref}} \right) - x_1 \right] + y_1 \right]$$

where,

W = thickness at the point of interest

S = source to wedge distance

$m = \frac{(y_2 - y_1)}{(x_2 - x_1)}$ = slope of the wedge at the point of interest

D_{ref} = reference distance

X_{off} = distance off axis along the sloping side of the wedge at D_{ref}

$$\theta = Tan^{-1} \left(\frac{X_{off}}{D_{ref}} \right)$$

From the manual of: Diamond: Dose Calculation Management s/w, version 2010

ESTRO School

Dose per MU formalisms: factor-based dose calculations

Modulation with physical wedges

Accounting for the presence of physical wedge in dose calculations is not trivial

Let us have a debate!

Is there a role for physical wedges in modern radiotherapy?

Should we continue to commission these for treatment planning?

POINT/COUNTERPOINT Medical Physics
The International Journal of Medical Physics Research and Practice

OA **Radiotherapy using hard wedges is no longer appropriate and should be discontinued**

Christopher F. Njeh, Tae Suk Suh and Colin G. Orton

Med. Phys. **43**, 1031 (2016); http://dx.doi.org/10.1118/1.4939262

ESTRO School

Dose per MU formalisms: factor-based dose calculations

Modulation with non-physical wedges

Non-physical wedges are delivered with one of the Y-jaws moving in or out during beam at variable dose rate and at variable speed.
Wedge factors:

- do not depend on depth (no beam hardening)
- vary with beam energy and off axis position

Varian EDW

- Y-jaw motion into field (0.5 cm from opposing) jaw; in variable speed and dose rate
- Jaw positions per MU: stored lookup (GSTT) tables; one per beam energy
- 7 wedge angles in total (as combination of 60° wedged and open fields)
- WF depends on energy, wedge angle, field size and off-axis position (along Y direction; asymmetric fields)
- WF ≈ 0.4 - 1

Siemens VW

- Y-jaw motion out of field, starting from 1 cm of opposing jaw
- Jaw positions per MU: calculated using a mathematical algorithm with energy dependent parameters.
- Multiple wedge angles between 10° and 60°
- WF depends on energy, wedge angle, field size and off-axis position (along Y direction; asymmetric fields)
- WF ≈ 1 from calculation points on CAX

In MU formalisms WF for non-physical wedges are either derived from measurements or are calculated (from GSTT date or using the algorithm of creating the wedge

Dose per MU formalisms: factor-based dose calculations

Inhomogeneities

Methods to account for inhomogeneities in factor-based dose/MU calculations :

Either scale dosimetric parameters appropriately

Or

Determine a correction factor as a function of scaled dosimetric quantities

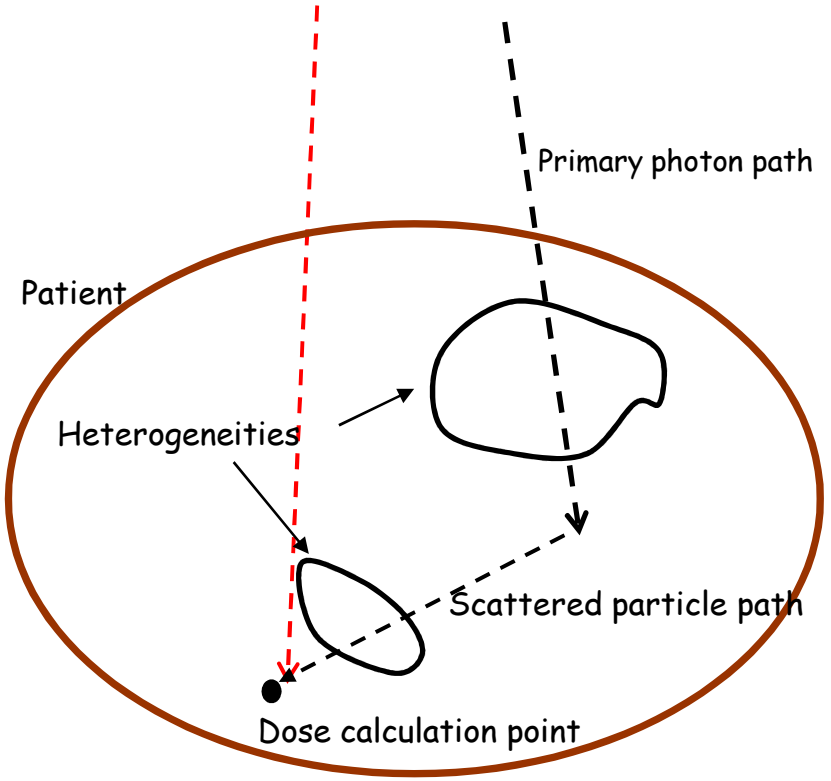

$$\left[\frac{D}{MU}(\ldots)\right]_{\text{heterogeneous}} = CF(\ldots)\left[\frac{D}{MU}(\ldots)\right]_{\text{homogeneous}}$$

ESTRO School

Dose per MU formalisms: factor-based dose calculations

Inhomogeneities

Effective depth to a calculation point is the thickness of water equivalent tissue that would attenuate the radiation by the same amount as the actual tissue along a fan-line between the calculation point and the surface

If the radiation passes through *n* different tissues each if thickness d_i and density ρ_i

$$d_{\text{eff}} = \sum_{i=1}^{n} \rho_i d_i$$

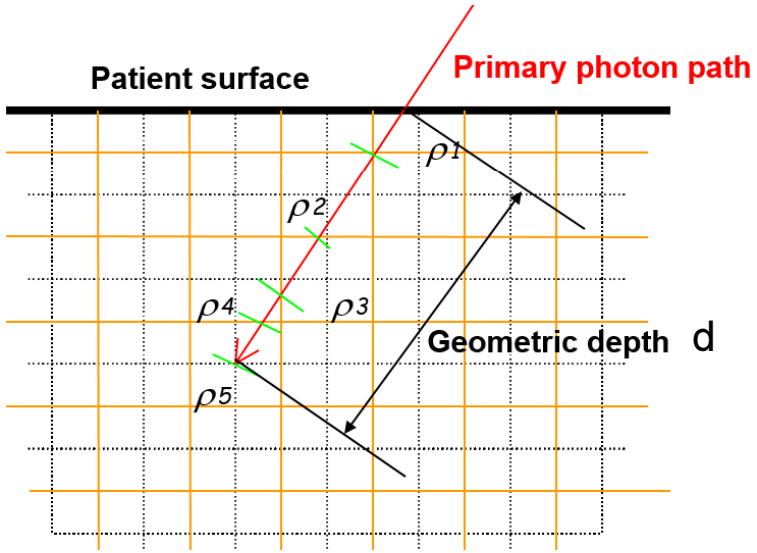

Note:
TPSs usually report an effective depth for a calculation point, but how exactly this is derived is not always apparent

ESTRO School

Dose per MU formalisms: factor-based dose calculations

Intensity modulated fields (IMRT)

Implementations vary based on delivery technique

For IMRT techniques (Segmental-MLC or Dynamic-MLC), the *general approach* for the calculation of dose per MU from a modulated field is:

1. Split the modulated field into K segments
2. Sub-divide each segment into a number of beamlets, M
3. Calculate the dose per MU for each beamlet as an open field based on the factor-based formalism
4. Sum up the doses from each beamlet, with a weight proportional to the contribution of the segment to total dose, and accounting for the effect of MLC leakage and transmission.

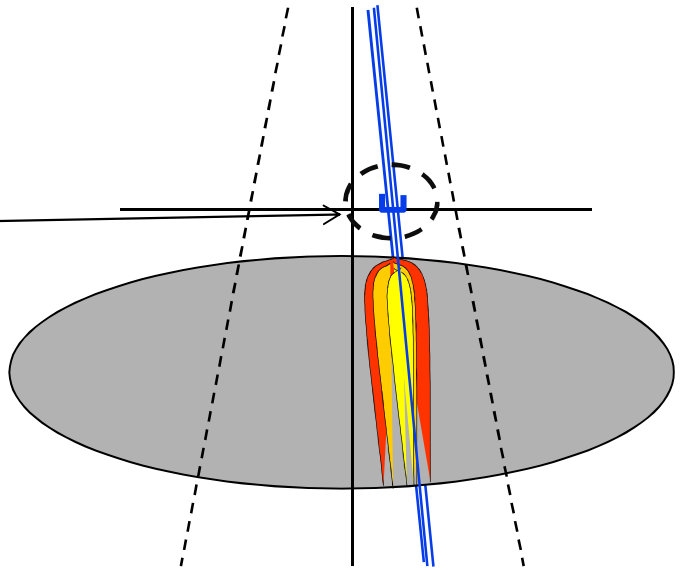

$$\frac{D}{M} = \sum_{m}^{M} C_m d_m^{open}$$

open field (beamlet) dose derived from the dose per MU factor-based formalism

Beamlet weight depending on how it contributes to the dose from the segment. This weight is also adjusted dosimetric properties of the MLC (leakage and transmission)

ESTRO School

In conclusion:

I. Now you understand the general formalism to calculation MU on TPSs using model-based dose engines

BUT, how does a commercial TPS (the TPS in your hospital?) calculate MU?

Stay tuned on the next lecture!

ESTRO School

In conclusion:

II. Now you are familiar with the ‘basic ingredients’ of factor-based dose per MU formalisms (AAPM TG-71 / NCS12 / ESTRO etc) and could relate dosimetric quantities to each other

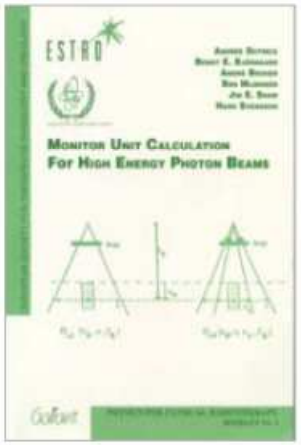

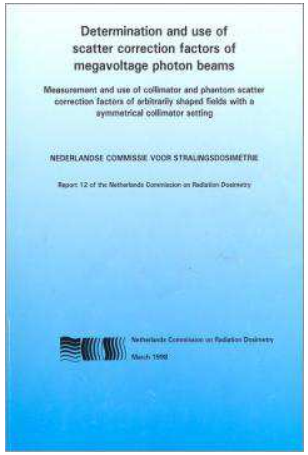

Monitor unit calculations for external photon and electron beams: Report of the AAPM Therapy Physics Committee Task Group No. 71

John P. Gibbons, John A. Antolak, David S. Followill, M. Saiful Huq, Eric E. Klein, Kwok L. Lam, Jatinder R. Palta , Donald M. Roback, Mark Reid, and Faiz M. Khan

Citation: Medical Physics **41**, 031501 (2014); doi: 10.1118/1.4864244
View online: http://dx.doi.org/10.1118/1.4864244
View Table of Contents: http://scitation.aip.org/content/aapm/journal/medphys/41/3?ver=pdfcov
Published by the American Association of Physicists in Medicine

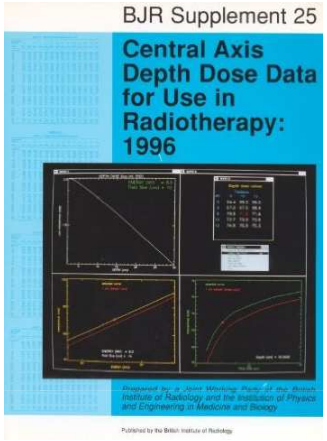

Report of AAPM Therapy Physics Committee Task Group 74: In-air output ratio, S_c, for megavoltage photon beams

Timothy C. Zhu[a)]
University of Pennsylvania, Philadelphia, Pennsylvania 19104
Anders Ahnesjö
Uppsala University, 751 85 Uppsala, Sweden and Nucletron AB, Box 1704, 751 47 Uppsala, Sweden
Kwok Leung Lam
University of Michigan, Ann Arbor, Michigan 48109
X. Allen Li
Medical College of Wisconsin, Milwaukee, Wisconsin 53226
Chang-Ming Charlie Ma
Fox Chase Cancer Center, Philadelphia, Pennsylvania 19111
Jatinder R. Palta
University of Florida, Gainesville, Florida 32610
Michael B. Sharpe
Princess Margaret Hospital, Toronto, ON M5G 2M9, Canada
Bruce Thomadsen
University of Wisconsin, Madison, Wisconsin 53705
Ramesh C. Tailor
RPC, UT MD Anderson Cancer Center, Houston, Texas 77030

Verification of monitor unit calculations for non-IMRT clinical radiotherapy: Report of AAPM Task Group 114

Robin L. Stern[a)]
Department of Radiation Oncology, University of California, Davis, Sacramento, California 95817
Robert Heaton
Radiation Medicine Program, Princess Margaret Hospital, 610 University Avenue, Toronto, Ontario M5G 2M9, Canada and Department of Radiation Oncology, University of Toronto, Toronto, Ontario M5G 2M9, Canada
Martin W. Fraser
Department of Radiation Oncology, Tufts Medical Center, 750 Washington Street #246, Boston, Massachusetts 02111
S. Murty Goddu
Radiation Oncology, Mallinckrodt Institute of Radiology, Washington University, 4921 Parkview Place Campus, Box 8224, St. Louis, Missouri 63110
Thomas H. Kirby
Global Physics Solutions, 5015 Larchmont NE, Albuquerque, New Mexico 87111
Kwok Leung Lam
Department of Radiation Oncology, University of Michigan Medical Center, Ann Arbor, Michigan 48109
Andrea Molineu
Radiological Physics Center, University of Texas MD Anderson Cancer Center, Houston, Texas 77030
Timothy C. Zhu
Department of Radiation Oncology, University of Pennsylvania, 2 Donner, 3400 Spruce Street, Philadelphia, Pennsylvania 19104-4283

ESTRO School

In conclusion:

III. Remember: in the factor-based formalisms, factors should cancel out!

$$\frac{D(\text{cond. a})}{M} \equiv \underbrace{D(\text{calibration})/M}_{\text{calibration value}} \cdot \underbrace{\frac{D(\text{cond. d})/M}{D(\text{calibration})/M}}_{\text{factor d}} \cdot \underbrace{\frac{D(\text{cond. c})/M}{D(\text{cond. d})/M}}_{\text{factor c}} \cdot \underbrace{\frac{D(\text{cond. b})/M}{D(\text{cond. c})/M}}_{\text{factor b}} \cdot \underbrace{\frac{D(\text{cond. a})/M}{D(\text{cond. b})/M}}_{\text{factor a}}$$

IV. The error in factor-based models is proportional to the number of factors:

$$\frac{D}{M} \equiv f_a \cdot f_b \cdots f_n \cdot D(calibration)/M \quad \Longrightarrow \quad \frac{\Delta D}{D} \leq \left|\frac{\Delta f_a}{f_a}\right| + \left|\frac{\Delta f_b}{f_b}\right| + \ldots$$

V. The number of measurements can be reduced by modelling some of the factors (e.g non physical wedge factor)

ESTRO School

In conclusion:

VI. Can you answer the following questions?

- What are the calibration conditions of the linacs in your hospital?
- What formalism do you use in your hospital to calculate MU? Isocentric or fixed-SSD?
- What are the normalisation conditions in the MU formalism you use?

In conclusion:

- What is purpose and usefulness of factor-based models in modern radiotherapy physics?
- Is the check of dose at a point a sufficient, adequate check of a complex radiotherapy plan?
- What are the errors we aim to avoid? (at what level of tolerance we wish to work at?)

Prepare thoughts and/or questions for the MU workshop session later today

Let us have a discussion!

ESTRO School

WWW.ESTRO.ORG/SCHOOL

Dose Modelling and Verification for External Beam Radiotherapy
6th – 10th March 2016, Utrecht

How TPSs calculate Monitor Units (MU)

Maria Mania Aspradakis
Maria.Aspradakis@luks.ch

luzerner kantonsspital
LUZERN SURSEE WOLHUSEN

Anders Ahnejsö
Anders.Ahnesjo@igp.uu.se

UPPSALA UNIVERSITET

ESTRO School

Learning Objective

Understand the different implementations of the dose per meterset formalism on commercial TPSs using model-based dose calculations for MV photon beams

In the interest of time, only 4 TPSs, as representatives of commercial systems widely used, will be discussed:

- Philips Pinnacle v9.10
- Elekta Oncentra Masterplan
- Varian Eclipse v13.6
- Raysearch Raystation v4.7

Dose per MU formalisms: model-based dose calculations

$$\frac{D(A;x,y,z)}{M} = \frac{D(A;x,y,z)}{\Psi_0} \cdot \frac{\Psi_0}{M}$$

Energy fluence of **direct photons** at isocentre in air

Dose engine calibration factor

relates the MU to the direct energy fluence, commonly determined under ***ref****erence* *cal**ibration conditions*

$$\frac{D_{\text{ref,meas}}}{M}$$

$$\frac{D_{\text{ref,calc}}}{\Psi_0} =$$

$$\frac{\Psi_0}{M} = \frac{\left[D(A_{\text{ref}};x_{\text{ref}},y_{\text{ref}},z_{\text{ref}})/M\right]_{\text{meas}}}{\left[D(A_{\text{ref}};x_{\text{ref}},y_{\text{ref}},z_{\text{ref}})/\Psi_0\right]_{\text{calc}}}$$

No monitor backscatter accounted for!
How monitor backscatter is handled varies in different TPSs

ESTRO School

Backscatter into the monitor chamber

- The signal from the monitor chamber can be affected from particles which have backscattered from the upper part of the jaws into the chamber (dependent on linac head and monitor chamber design,)
- At narrower collimations there is more backscatter than in larger fields ⇒ monitor chamber reaches faster its pre-set value ⇒ linac relative output decreases with decreasing field size

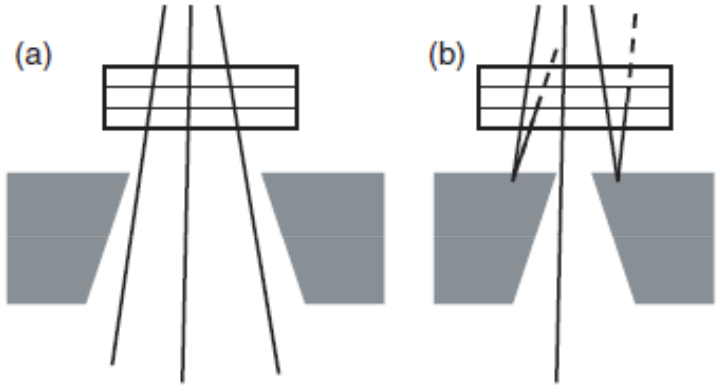

Figure 4. Schematic representation of backscatter to the monitor ion chamber from collimating jaws for different positions field sizes. When going from a large field (a) to a smaller one (b), the backscatter fraction increases.

Verhaegen & Seuntjens, Phys. Med. Biol, 48 (2003) R107-R164

Backscatter into the monitor chamber

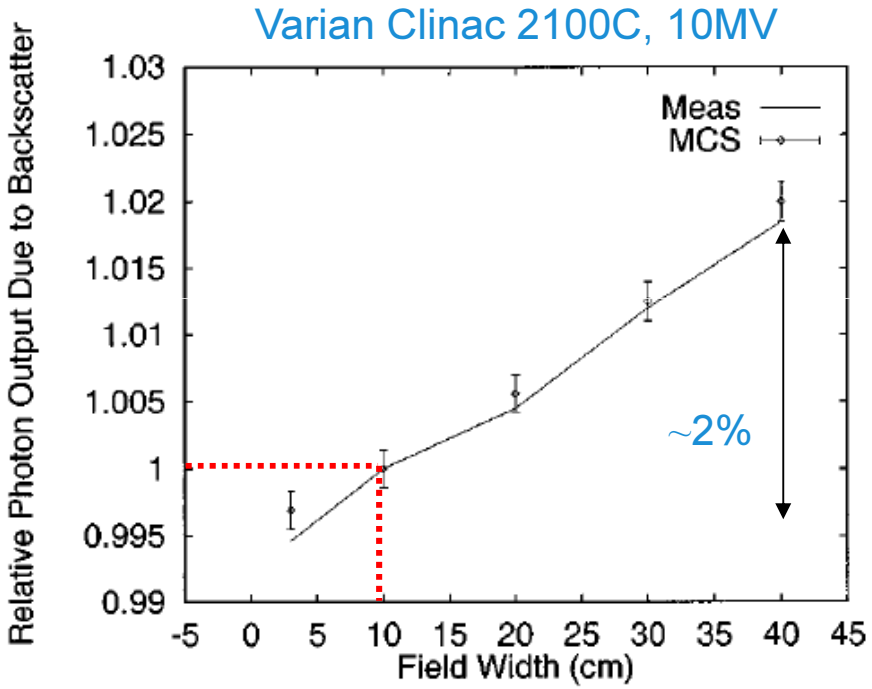

Liu et al Med, Phys. 27(4), 2009

FIG. 9. Relative photon output due to the backscatter, S_{cb}, of symmetric and square fields. The straight line (''meas'') shows data from measurement of electron target pulses. The discrete points (''MCS'') are from the Monte Carlo simulation. The one standard errors of the data are shown by the error bars.

- The effect is included in the measured output factors (S_{cp}, S_c), and thus in factor-based dose per MU formalisms. But needs to be accounted for separately in model-based dose per MU formalisms.

Dose per MU formalisms

1. The monitor signal caused by backscatter as a function of collimator aperture, can be modelled as an additional fraction b of the direct signal. The formalism would be:

$$\frac{D(A;x,y;z)}{M} = \frac{D(A;x,y;z)}{\Psi_0} \frac{\Psi_0}{M_0(1+b(A))}$$

$$\frac{\Psi_0}{M_0} = \frac{\left[D(A_{ref};x_{ref},y_{ref},z_{ref})/M\right]_{Measured}}{\left[\left(D(A_{ref};x_{ref},y_{ref},z_{ref})/\Psi_0\right)\right]_{Calculated}}\left(1+b(A_{ref})\right)$$

Explicit as a backscatter correction factor: $\frac{1+b(A_{ref})}{1+b(A)}$

2. Alternatively the effect of the backscatter into the monitor chamber on the calculation of MU can be accounted for indirectly through the use of a correction factor that reflects the change in output due to this backscatter with collimator setting

Dose per MU formalism: Elekta Oncentra MasterPlan

Dose per MU formalism: Elekta Oncentra MasterPlan

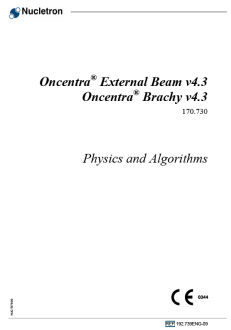
Nucletron

Oncentra® External Beam v4.3
Oncentra® Brachy v4.3
170.730

Physics and Algorithms

Dose engine results are linked to meterset values through:

$$D(\mathbf{r}) = M \frac{1 + b^{\text{calib}}}{1 + b(A)} \frac{(D/M)^{\text{calib}}_{\text{meas}}}{d^{\text{calib}}} d(\mathbf{r}) \qquad \text{(Eq. 5.8)}$$

where $(D/M)^{\text{calib}}_{\text{meas}}$ is the dose at the calibration point and geometry measured per meterset value, d^{calib} is the calculated dose for the same point and b^{calib} is the calculated backscatter signal fraction, all obtained for the same calibration geometry. For Cobalt-60 units the calibration dose rate is corrected for the decay of the source from the calibration date until the date when the dose calculation is performed.

All the internal Oncentra dose calculation engines yield the dose per energy fluence. More specifically, a dose engine d is defined by the relation:

$$d(\mathbf{r}) = \frac{D(\mathbf{r})}{\Psi_0} \qquad \text{(Eq. 5.5)}$$

where $D(\mathbf{r})$ is the absolute dose at position $\mathbf{r}$, including effects from head scatter etc. Thus dose engine calculates the dose scaled to absolute dose considering beam setup parameters, patient, etc.

ESTRO School

Including monitor signal M_b caused by backscatter depending on collimator setting

$$\frac{D(A;x,y;z)}{M} = \frac{D(A;x,y;z)}{\Psi_0}\frac{\Psi_0}{M_0}\cdot\left(1+b(A)\right)^{-1}$$

$$\frac{\Psi_0}{M_0} = \frac{\left[D\left(A_{\text{ref}};x_{\text{ref}},y_{\text{ref}},z_{\text{ref}}\right)/M\right]_{\text{Meas}}}{\left[\left(D\left(A_{\text{ref}};x_{\text{ref}},y_{\text{ref}},z_{\text{ref}}\right)/\Psi_0\right)\cdot\left(1+b\left(A_{\text{ref}}\right)\right)^{-1}\right]_{\text{Calc}}}$$

Includes head scatter and phantom scatter

$$M = M_0 + M_b(A) = \left(1+b\left(A\right)\right)M_0$$

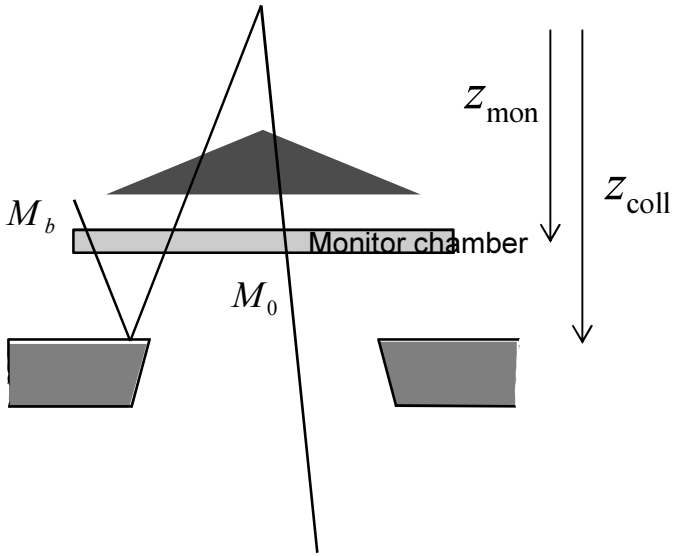

Plan with dose weighted fields and prescribed dose D_{pres}:

$$w_i = \frac{D\left(A_i;\text{prescription conditions}\right)}{\sum_{i=1}^{\text{all fields}} D\left(A_i;\text{prescription conditions}\right)}$$

$$M_i = \frac{D_{\text{presc}}\cdot w_i}{\frac{D\left(A_i;\text{at prescription point/conditions from field } i\right)}{M}}$$

Empirical factor from S_c measurements

$$b(A) = k_{\text{back}}\, F\, \frac{z_{\text{mon}}^2}{z_{\text{coll}}^2}$$

$$F = \iint_{\substack{\text{Irradiated}\\ \text{collimator}\\ \text{area}}} \frac{\cos^3\theta}{\pi\left(z_{\text{coll}}-z_{\text{mon}}\right)^2}\,\mathrm{d}A$$

ESTRO School

Output factor normalizition, <u>the</u> norm for comparison of calculations and measurements:

$$\frac{\left[D(A;x,y,z)/M\right]_{\text{Measured}}}{\left[D(A_{\text{ref}};x_{\text{ref}},y_{\text{ref}},z_{\text{ref}})/M\right]_{\text{Measured}}} \longleftrightarrow \frac{\left[D(A;x,y,z)/M\right]_{\text{Calculated}}}{\left[D(A_{\text{ref}};x_{\text{ref}},y_{\text{ref}},z_{\text{ref}})/M\right]_{\text{Calculated}}}$$

Global norm for deviations:

$$\frac{\left[D(A;x,y,z)/M\right]_{\text{Calculated}} - \left[D(A;x,y,z)/M\right]_{\text{Measured}}}{\left[D(A_{\text{ref}};x_{\text{ref}},y_{\text{ref}},z_{\text{ref}})/M\right]_{\text{Measured}}}$$

Local norm for deviations:

$$\frac{\left[D(A;x,y,z)/M\right]_{\text{Calculated}} - \left[D(A;x,y,z)/M\right]_{\text{Measured}}}{\left[D(A;x,y,z)/M\right]_{\text{Measured}}}$$

Dose per MU formalism: Varian Eclipse v13.6 TPS

Dose per MU formalisms: Varian Eclipse v13.6 TPS

Overview of Eclipse TPS (29. Feb 2016)

Multi-source beam model that describes:

- primary photon source
- extra-focal photon source
- electron contamination source
- (hard) wedge scatter source

Dose engines

- Pencil Beam Convolution (PBC v10.0.28)
- Anisotropic Analytical Algorithm for photons (AAA v13.6.23)
- Acuros External Beam for photons (Acuros XB v13.6.23)
- Cone Dose Calculation for photons (CDC v13.6.23)
- Generalised Gaussian Pencil Beam for electrons (GGPB v10.0.28)
- Electron Monte Carlo Algoritm (eMC v13.6.23)
- Proton Convolution Superposition (PCS v13.6.23)

Dose Optimisation algorithms for IMRT/VMAT planning

- Photon Optimiser (PO v13.6.23)
- Dose Volume Optimiser (DVO v13.6.23)
- Plan Geometry Optimiser algorithm (PGO V13.6.23)
- Progressive Resolution Optimiser (PRO v13.6.23)
- Nonlinear Universal proton Optimiser v13.6.23

Intermediate dose calculation using: Multi-Resolution Dose Calculation Algorithm (MRDC v13.6.23)

Fluence Delivery modelling algorithms for IMRT planning

- Algorithms that correct optimal fluence maps to deliverable fluence maps based on constraints imposed by the MLC (Leaf Motion Calculator, LMC)

} Depending on MLC motion (static or dynamic), the total MU of a beam are adjusted appropriately

Portal Dose Image Prediction (PDIP v13.6.23)

ESTRO School

Dose per MU formalism: Varian Eclipse v13.6 TPS

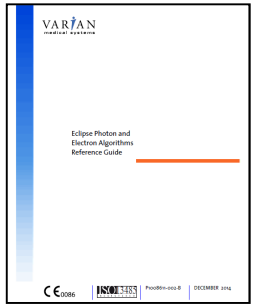

Relevant pages in the Manual: Eclipse Photon & Electron Reference Guide, Dec2014

The final MU are calculated from the prescribed dose, plan normalization, field weight, field normalization and a normalization factor determined by the dose calculation algorithm. The normalization factor determined by the AAA and Acuros XB is the MU value for 1 Gy to 100% of the current field. AAA and Acuros XB calculate the monitor units at the normalization point MUnorm for open field, hard wedge, Enhanced Dynamic Wedges and physical compensators as in the equation:

Equation 2

$$MU_{norm} = CBSF(X,Y) \times \left(\frac{MU_{calib}}{D_{calib}}\right) \times \left(\frac{D_{ref}}{D_{norm}(X,Y)}\right) \times \frac{1}{WCF(X,Y)}$$

where

CBSF(X,Y) = Collimator backscatter factor for an open field with same collimator settings (more information: Equation 1 on page 23).

In case of treatment units where MLC defines the field size (for example Elekta), the collimator backscatter factor is calculated based on the effective field size in X and Y direction instead of the collimator jaw settings (X, Y).

MU_{calib} = User-defined value of parameter Reference Dose In MU at Calibration Depth. (For hard wedges, this parameter is read from the wedge parameters. More information: Hard Wedge Parameters on page 65.)

D_{calib} = User-defined value of parameter Reference Dose In Gy at Calibration Depth. (For hard wedges, this parameter is read from the wedge parameters. More information: Hard Wedge Parameters on page 65.)

D_{ref} = Dose calculated by the AAA or Acuros XB for the reference conditions (more information: Output Factor Geometry on page 84) at the calibration depth, which is the value of the Absolute Dose Scaling Factor parameter. (For hard wedges, this parameter is read from the wedge parameters.)

$D_{norm}(X,Y)$ = Dose calculated by the AAA or Acuros XB at the field normalization point, based on the selected field normalization method.

WCF(X,Y) = Wedge correction factor for hard wedge field with the collimator jaw settings (X,Y).

In case the field contains a block or an MLC, the wedge correction factor is calculated based on the effective field size in X and Y direction instead of the collimator jaw settings (X, Y).

The calculation of MU is based on output factor measurements performed for different field sizes in a certain reference geometry (more information: Output Factor Geometry on page 84), and calibration calculations made for the reference field size.

The change in the output factor as a function of field size is caused by changes in phantom scatter, head scatter and collimator backscatter into the monitor chamber. The phantom and head scatter effects are accounted for by the photon beam source model and the volumetric dose calculation algorithm (AAA or Acuros XB). The remaining change in the output factors is assumed to be caused by collimator backscatter. It is estimated from the measured output factor table as shown in the equation.

Equation 1

$$CBSF(X,Y) = \frac{OF_{ref}}{OF(X,Y)} \times \frac{D'(X,Y)}{D'_{ref}}$$

where

X,Y = Collimator settings ($X = X_2 - X_1$, $Y = Y_2 - Y_1$)

CBSF(X,Y) = Collimator backscatter factor for an open field with same collimator settings.

OF_{ref} = Output factor table value for reference field size. The value is normally 1.0. The reference field size is given by the parameter Absolute dose reference field size, defined in the AAA and Acuros XB Parameters (more information: Table 12 on page 59).

OF(X,Y) = Output factor table value for field size X,Y.

D'(X,Y) = Dose at the reference point calculated by the AAA or Acuros XB for the field size X,Y and the reference geometry when ignoring the effect of collimator back scatter.

D'_{ref} = Dose calculated by the AAA or Acuros XB for the reference conditions in the reference geometry (more information: Output Factor Geometry on page 84) when ignoring the effect of collimator back scatter.

The reference field geometry used in the measurement of the output factor table is indicated by the Source-Phantom Distance parameter defined in the output factor table in Beam Configuration (more information: Table 5 on page 48). The reference point depth from the surface of the phantom is given by the Detector depth from phantom surface parameter, also defined in the output factor table.

STRO School

Dose per MU formalism: Varian Eclipse v13.6 TPS

$$CBSF(A) = \frac{D_{\text{calc}}(A)/\Psi_o}{D_{\text{calc}}(A_{\text{ref}})/\Psi_o} \cdot \frac{S_{\text{cp,meas}}(A_{\text{ref}})}{S_{\text{cp,meas}}(A)} = \frac{S_{\text{cp,calc}}(A)}{S_{\text{cp,meas}}(A)}$$

$$S_{\text{cp,calc}}(A)$$

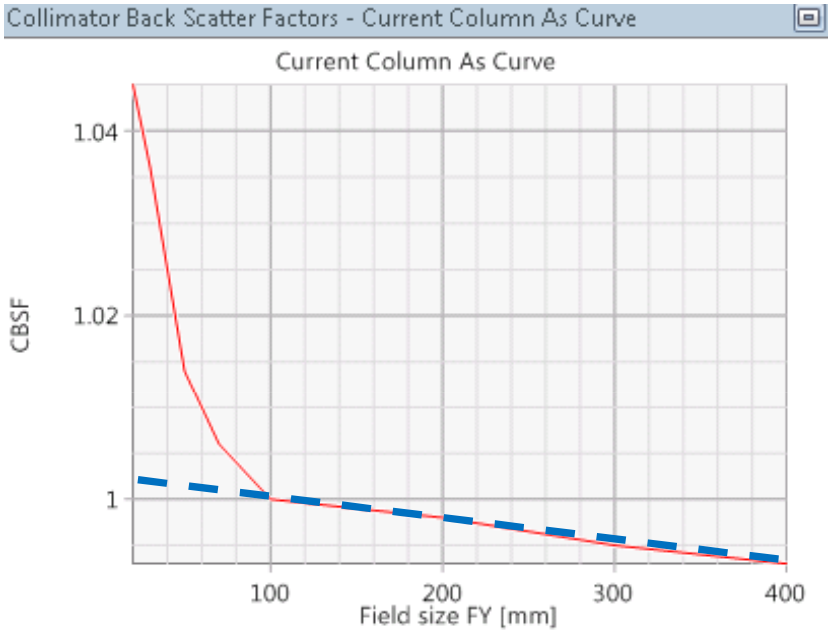

As a result of the beam configuration process, a table of CBSC(X,Y) factors for symmetric rectangular fields is generated and stored for each MV beam (input for this are the measured S_{cp} data)

Korhonen, Doctoral Dossertation, Helsinky University of Technology, 2009

ESTRO School

Dose per MU formalism: Varian Eclipse v13.6 TPS

Open beams

1. The dose engine calculates the ratio of dose per energy fluence in the treatment field and under reference conditions.
2. This ratio of doses is corrected by a factor interpolated from the CBSC table for the equivalent square of the beam aperture, as defined by the upper collimator or by the MLC (if the MLC is the upper jaw, as is the case on an Elekta linac).

The MUs to deliver the prescribed dose at a point in an arbitrary field are thus given by:

$$M = \frac{D_{\text{presc}}[Gy]}{\left[\frac{D_{\text{calc}}(A)/\Psi_o[Gy/\#]}{D_{\text{calc}}(A_{\text{ref}})/\Psi_o\,[Gy/\#]}\right] \cdot \frac{D_{meas}(A_{\text{ref}})}{M}\left[\frac{Gy}{MU}\right] \cdot \frac{1}{CBSF(A)}}$$

ESTRO School

Dose per MU formalism: Philips Pinnacle TPS

Dose per MU formalism: Philips Pinnacle TPS

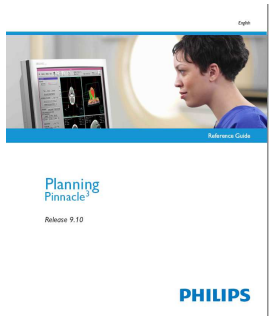

Convolution algorithm monitor unit calculations

Because the convolution algorithm can accurately compute phantom scatter (S_p), we can use the following equation to compute dose:

$$MU = \frac{D_{presc}}{ND \cdot OF_c \cdot TTF \cdot (D/MU)_{cal}}$$

ref

where:

D_{presc} is the prescription dose per fraction at the prescription point, in units of cGy.

ND is the Normalized Dose at the reference point.

OF_c is the computed correction factor determined during commissioning.

TTF is the total transmission factor.

$(D/MU)_{cal}$ is the dose per Monitor Unit at the calibration point.

Normalized dose is the ratio of dose per unit energy fluence at the prescription point to dose per unit energy fluence at the reference point for the calibration field (the point at which $(D/MU)_{cal}$ was measured) as determined by the convolution superposition calculation for the treatment geometry.

Philips Medical Systems

The convolution/superposition algorithm uses a head scatter model when computing the incident energy fluence. This head scatter model is intended to predict the increased output of the accelerator due to scatter in the head. During the computation of OF_p and OF_c the head scatter is included in the OF_p. Therefore, the OF_c represents the residual effects of head scatter not included in the model. Similarly, the effects of the wedge are also included in OF_p.

Pinnacle³ uses output factors generated using the following equation (which resembles S_c, S_p formalism):

$$OF_c = OF/OF_p$$

where

OF is the user-measured overall output factor.

OF_p is the computed phantom output factor, which includes the head scatter model and wedge effects.

OF_c is an internal normalization factor that will not match measured S_c values. OF_c is tabulated by equivalent square. The value used for a given field is interpolated linearly from the output factor table based on the equivalent square of the unblocked field. OF_c is also tabulated by wedge. If the beam has a wedge, an output factor for that wedge must be available.

ESTRO School

Dose per MU formalism: Philips Pinnacle TPS

The formalism in Pinnacle uses in essence the same approach as that in Eclipse. Unfortunately the manual does not explicitly describe what is accounted for by the *internal correction factor* correcting for *residual head scatter effects…*

$$MU = \frac{D_{presc}}{ND \cdot OF_c \cdot TTF \cdot (D/MU)_{cal}}$$

Pinnacle[3] uses output factors generated using the following equation (which resembles S_c, S_p formalism):

$$OF_c = OF/OF_p$$

$$CF_{\text{residual}}(A) = \frac{S_{\text{cp,meas}}(A)}{S_{\text{cp,calc}}(A)}$$

where

OF is the user-measured overall output factor.

OF_p is the computed phantom output factor, which includes the head scatter model and wedge effects.

OF_c is an internal normalization factor that will not match measured S_c values. OF_c is tabulated by equivalent square. The value used for a given

or

$$CF_{\text{residual}}(A) \cong \frac{1}{CBSF(A)}$$

ESTRO School

Dose per MU formalism: Raysearch Raystation

Dose per MU formalism: Raysearch Raystation

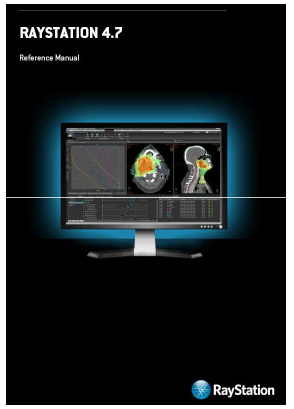

Output factor corrections – used in energy fluence computations

Part of the output factor increase with field size is caused by increased secondary scattering of energy from the sides into the center of the field (phantom scatter); this effect is part of the radiation transport in the collapsed cone dose calculation (*section 3.3 Collapsed cone dose computation on page 42*). A smaller part (for Varian, Elekta and Siemens LINACs) of the field size dependence is caused by the projection of extended sources through the collimators (head scatter). The phantom scatter and head scatter is generally not sufficient to completely describe the output factor variation. The remaining field size dependence, the output factor correction, is introduced into the energy fluence and dose computation to account for effects such as backscattering from collimators into the beam monitor. The output factor correction can be normalized to 1.0 for the reference field size; it generally increases slightly with field size. The output factor corrections can be fitted to the output factors in the auto-modeling or selected by the user to give a best fit to dose curves and output factor measurements. When computing the fluence for a segment the output factor corrections are computed using the field measure (*Field measure on page 33*).

Same as Pinnacle

Field measure

The field measure is calculated from the jaw or MLC openings, $I_{x\text{-jaw/MLC}}$ and $I_{y\text{-jaw/MLC}}$, using an equivalent square formula.

ESTRO School

In conclusion

- Similarities in physics background
- Large differences in the “explanation” in the manuals
- Advice to vendor: Make more effort in using present day standard physics terms
- Advice to users: make an effort to understand and review beam modelling results

Detectors for measurement; best detector for different jobs

Part III: 2D/3D detectors

Núria Jornet

Servei de Radiofísica
Hospital Sant Pau, Barcelona

Introduction

With the advent of intensity modulated treatment techniques, soft wedges and stereotactic radiosurgery 2D/3D dosimetry gained importance.

Film was/is often the dosimeter of choice

Trend towards 'filmless' RT departments

Commercially available 2D detectors

Based on different physical phenomena

2D detectors 3D dose reconstruction.

3D detectors

Development of methods to compare 2D / 3D information

Learning objectives

To have an overview of the 2D-3D dosimetry systems commercially available.

To know the strengths and limitations of each system.

To be able to chose the dosimetry system better suited for the type of measurements that have to be performed.

Ideal properties of a 2D detector

- Linearity response-dose (<1%)
- Non dependence response with dose rate (<1%)
- Non angular dependence (<1%)
- Non energy dependence
- Non beam modality dependence
- Repetability (<0.5%) and reproductibility of response
- No dependence on atmospheric conditions
- High sensitivity
- Water-tissue equivalent
- **Uniformity in X and Y direction**
- **High spatial resolution**
- Small sensitive volume (volume effects)
- Stability of the response with time (fading)
- No variation of the response with accumulated dose
- On line reading vs permanent record of dose distribution

2D/3D detectors

- Films:

Silver-halide films (seldom used nowadays)

Radiochromic films

- EPIDs
- Point detector 2D arrays
- Transmission chambers

2D detectors

- Gels [3D detector]

3D detectors

Film dosimetry

Principle of measurement:

Radiation is the catalizer of a chemical reaction in the film emulsion
The film opaqueness is related with radiation dose.
Film opaqueness is quantified through the light transmission factor (T)
T is measured by the optical density (OD)

$$OD = -\log_{10}(T) = -\log_{10}(I_0/I)$$

ADVANTAGES

- High spatial resolution [1 to 5 um]
- Low cost (silver-halide)
- Wide accessibility
- Can be placed inside different phantoms without perturbing charged particle equilibrium
- Two-dimensional nature
- Integrating dosimeter

REAL PROPERTIES OF FILM

$OD = f(D, D_R, E, Q, d, FS, \varphi, pc)$

D……dose
D_R….dose rate
E……energy
Q……radiation type
d……depth
FS….field size
φ……orientation
pc……processor conditions

Film dosimetry-Silver Halide films

1

2

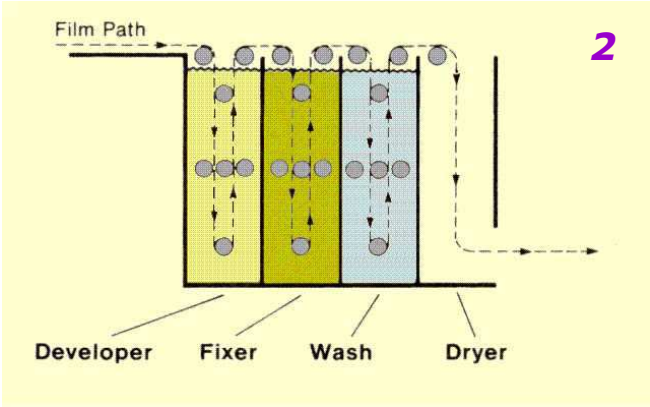

3

DISADVANTAGES

- No on-line response [developing+reading]
- No water equivalence
- Energy dependence
- Saturation high doses
- Needs developing [QA of the developer needed for accurate results]
- Time consuming
- Sensible to light

Film dosimetry-Silver Halide films

1

2

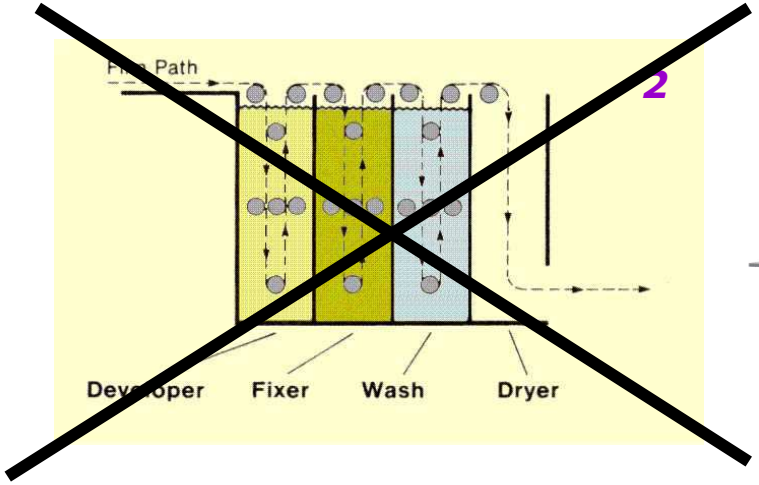

3

DISADVANTAGES

- No on-line response [developing+reading]
- **No water equivalence**
- **Energy dependence**
- Saturation high doses
- Needs developing [**QA of the developer needed for accurate results**]
- Time consuming
- Sensible to light

Film dosimetry - Radiochromic films

Silver halide films

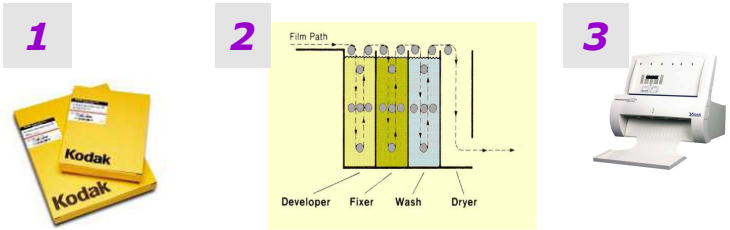

- No on-line response
- No water equivalence
- Energy dependence
- High spatial resolution
- Saturation high doses
- Needs developing
- Time consuming

Radiochromic films

- No on-line response
- Water equivalence
- No (little) energy dependence
- High spatial resolution
- No dose-rate dependence
- Insensitive to visible light
- No need of processing-"Real time" development, stability reached in ~ 2 h
- Can be evaluated with flatbed scanner (transmission mode-fluorescent light source and a linear CCD array detector) –need of corrections

Energy response of different detectors

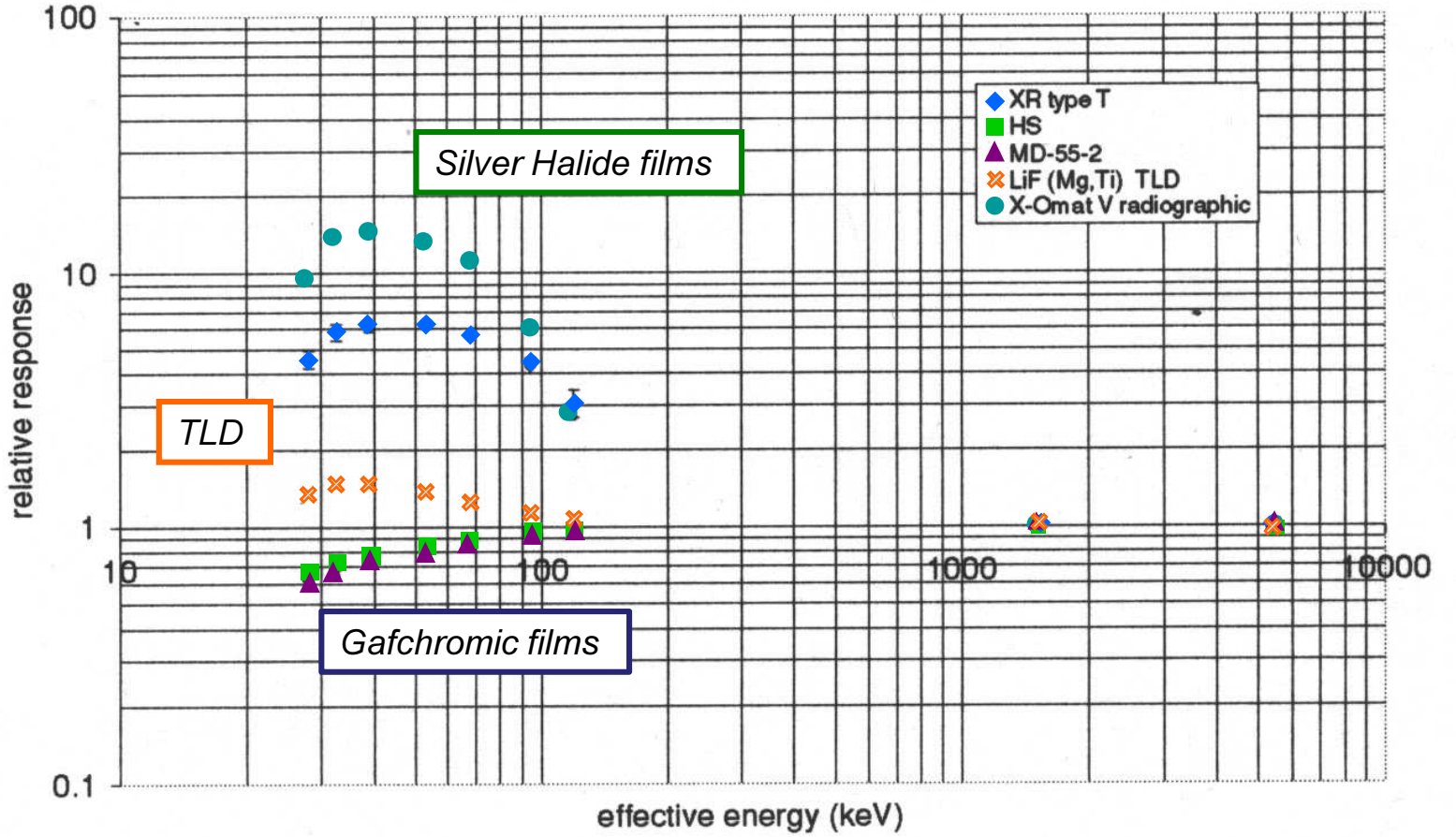

Cheung et al 2004, PMB 49

Radiochromic films

- Film emulsion is a radiation sensitive monomer. The coloration process is based on radiation-induced polymerization. The polymer is blue in color and film absorbs light in the red part of visible spectrum.

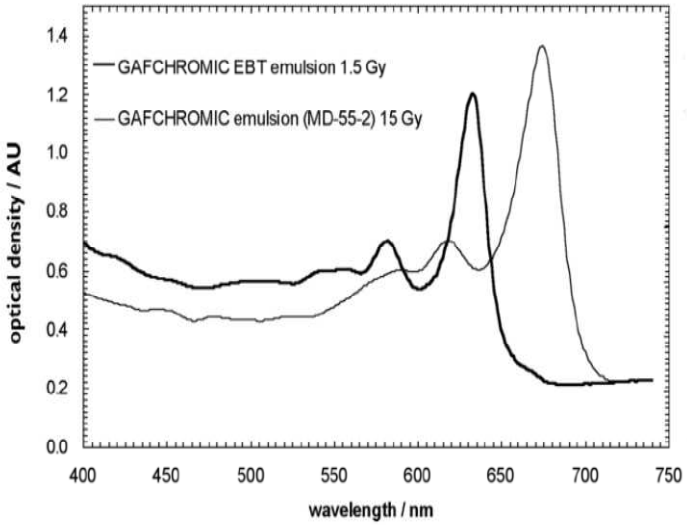

Soares et al. chapter 23 AAPM Summer School, 2009

Radiochromic films

PRIOR EBT GAFCHROMIC FILMS

[HD-810; MD-55-2; HS]

- Low sensitivity
- Small size
- Inherent optical density non-uniformity in one sheet (15%)
- [Need of double-exposure]
- High price

Table 23-3. Radiochromic Film Characteristics for Readout at 633 nm

Film Model	Emulsion thickness (μm)	Sensitivity (mAU/Gy)	Useful range (Gy)
HD-810	6.5	3	10–1000
MD-55-2	32	20	1–100
HS	38	35	0.5–50
EBT	34	400 to 800[a]	0.05–10
XR-RV2	17		0.01–5
XR-QA	50	0.001–0.2	

[a] For a dose of 1 Gy, depending on film orientation.

POST EBT GAFCHROMIC FILMS (2004)

[EBT;EBT2;EBT3;EBT XD]

- Dose range 2cGy – 8 Gy
- Saturation ~ 10Gy (15Gy)
- Different sizes available
- Z_{eff} ~ 7.05 (chlorine addition)
- Significant better homogeneity
- [no need of double-exposure techniques]
- Lower price
- Replaced by EBT2 (2009): addition of a yellow marker dye [allows corrections of non thickness uniformity of the active layer when using flat bed scanners]
- EBT3 (2011) symmetrical construction and anti-Newton rings.
- Use of laser densitometers creates interference patterns. NOT RECOMMENDED

Film dosimetry -dosimetric dependences (EBT)

Energy dependence

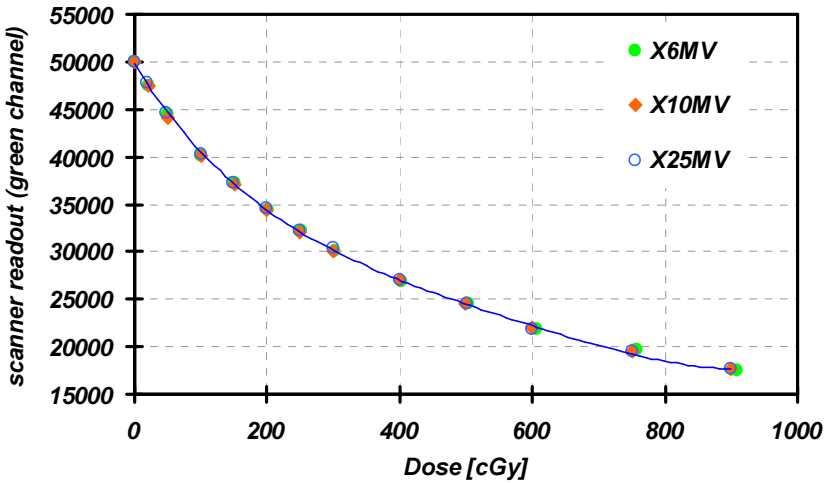

CALIBRATION

SSD = 95cm
z = 5cm
FS = 5x5cm²

Mean difference=0.6%
Maximum difference =1.3%

Depth dependence

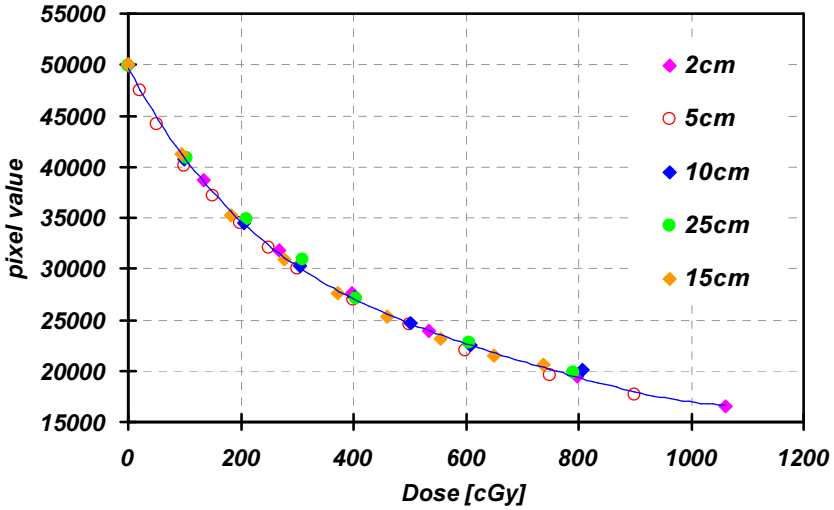

max deviation from fit curve:
4.4% around 8Gy

Fuß M, MSc thesis 2007

Film dosimetry -dosimetric dependences (EBT)

Field size dependence

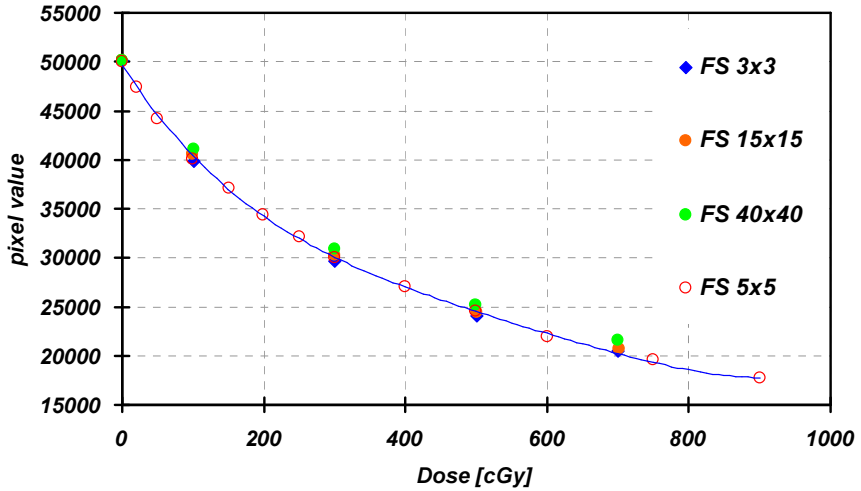

CALIBRATION

SSD = 95cm
z = 5cm
FS = 5x5cm²

Difference between 3x3cm² and 40x40cm² fields < 5%

Fuß M, MSc thesis 2007

Dose response of EBT2 films depending on Beam modality and energy

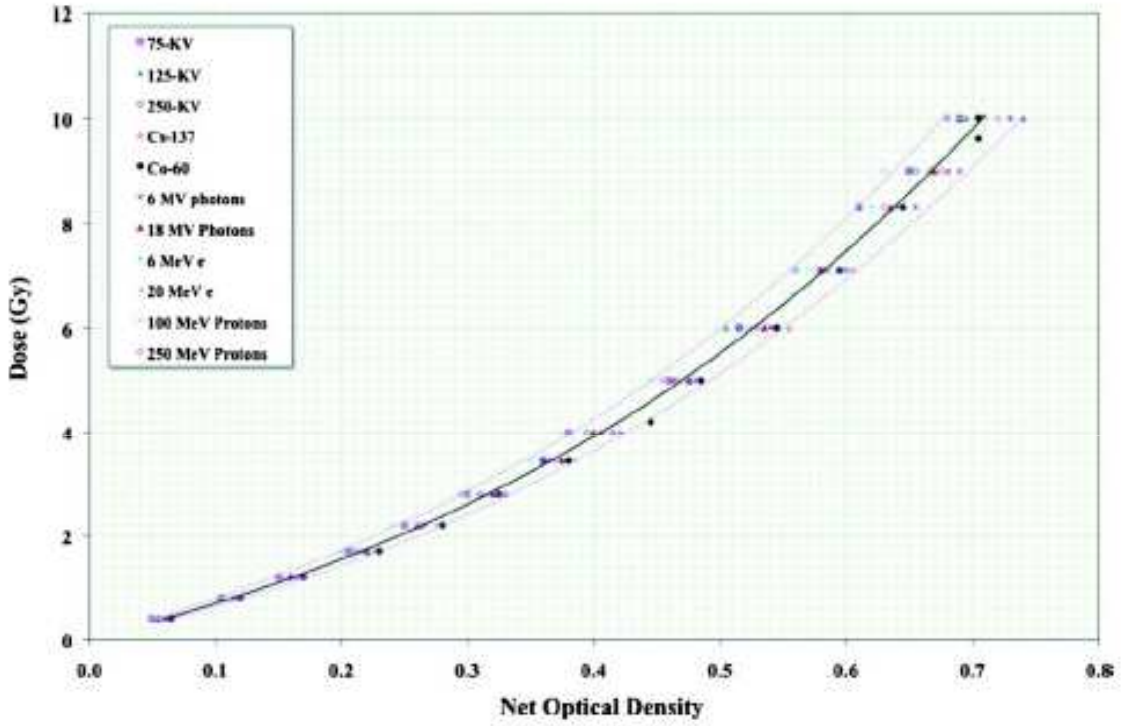

FIG. 3. Dose responses of EBT2 films for a range of beam energies from different radiation sources. The region between the two extreme curves represents the trend of all the data collectively and encompasses more than 95% of the data. The variation in data in this the region between the 3 and 10 Gy doses corresponds to $1\sigma = \pm 4.5\%$.

Variation within ±4.5% 1SD

RX from 75kV to 18MV
Protons 100-250 MeV
Electrons 6-20 MeV

Arjomandy *et al.*
Medical Physics, Vol. 37, No. 5, May 2010

Remember that radiochromic film dosimetry is a two step process

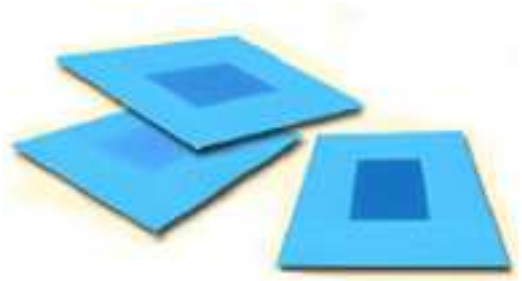

FILM CHARACTERISTICS:

Composition of the dye
Homogeneity
Batch uniformity

SCANNING SYSTEM AND PROTOCOL

SCANNER REQUIREMENTS

EBT dosimetry

- Epson Expression 10000XL or V700
- Color depth: **48 bit (16 bits per color channel-red).**

  [8 bit per chanel-256 grey levels

  -1grey level-0.5%]
- Scanner table: A4 / letter or A3
- Resolution: up to 3200 dpi (75 dpi enough)
- Disable all color correction options. Need of raw data

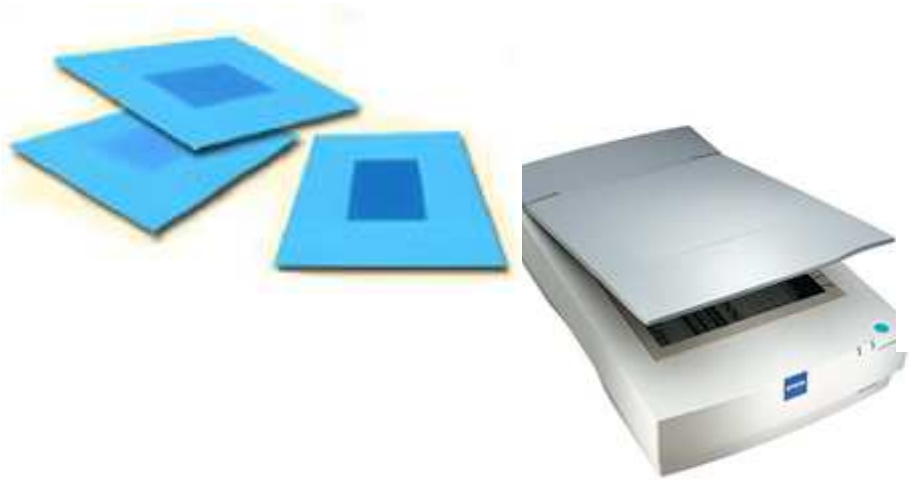

Wilcox et al MP (34 (2007), Paelinck et al PMB 52 (2007)

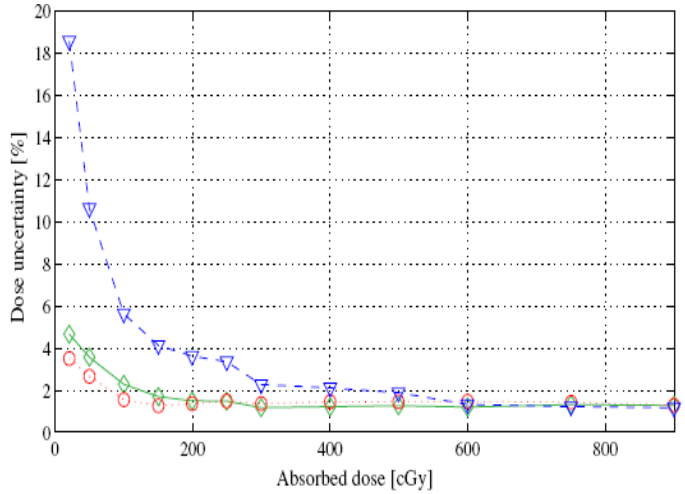

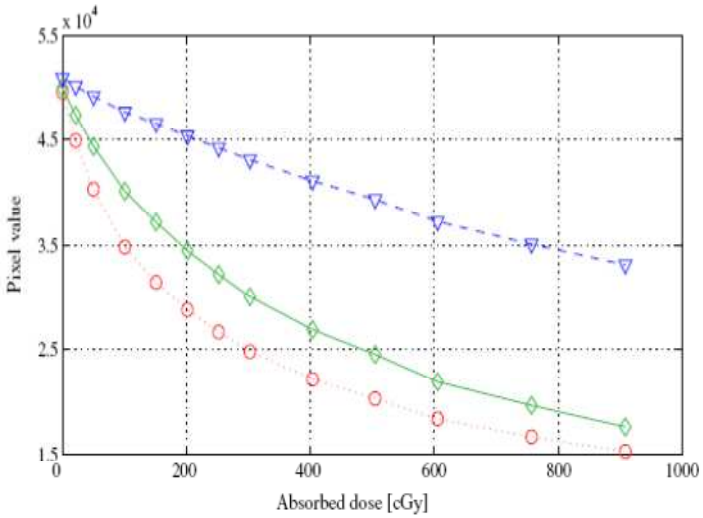

Fuß et al, PMB 52 (2007),

Film dosimetry-Readout (densitomer/scanner)

1. Confocal point-source scanners

- Translation of a point source focused to a detector over the film.
- Point by point measurements
- Spatial resolution: 0.25-0.8 mm in diameter.

Important. BEFORE USE

1. Check response, spatial integrity, susceptibility to image artifacts and time needed to reach steady-state operation conditions

2. Higher dimensional scanners

- Translation of a line source focused to a line or area detector array, over the film.
- Spatial resolution: 0.34-0.042 mm in diameter.

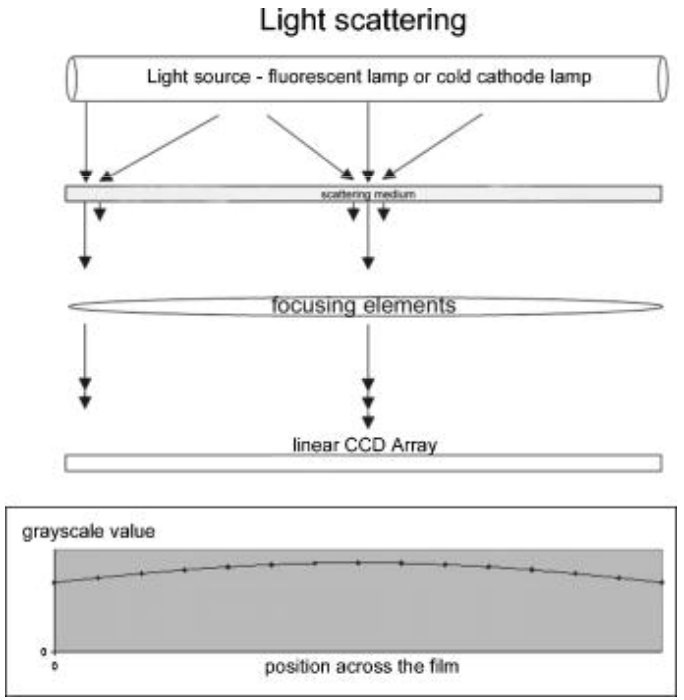

Fiandra et al. Med. Phys. ***33****, 4314 (2006)*

Densitometer-scanner

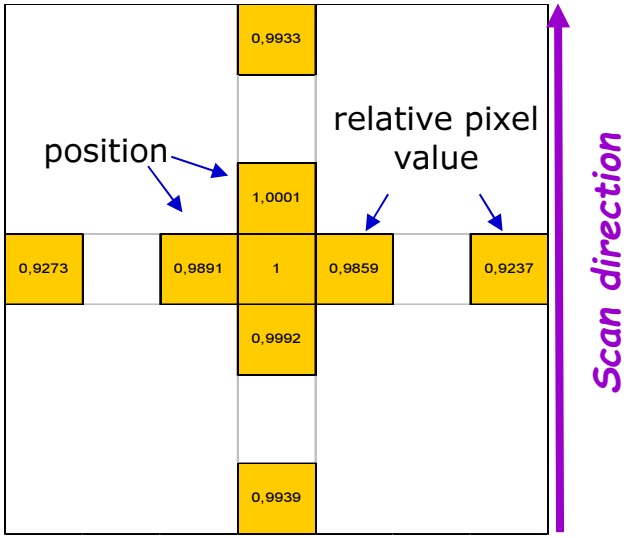

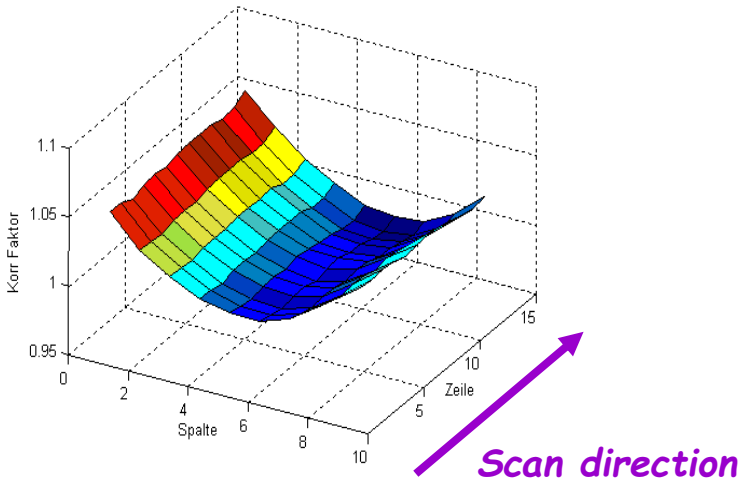

Scanner homogeneity

- pixel value varies with position on the scanner plate
  - small effects (<1%) when moving films vertically
  - up to 8% variation when moving films horizontally, dose dependent
  - Effect of light source + scattering
- 2D correction for “full” films
  - Dose dependent
  - Scanner dependent

Densitometer-scanner

- Optical density is a function of the wavelength of the light source
- Flat-bed color photo-document scanner use broad band fluorescent visible light sources
- OD it will also depend on the sensitivity of CCD array

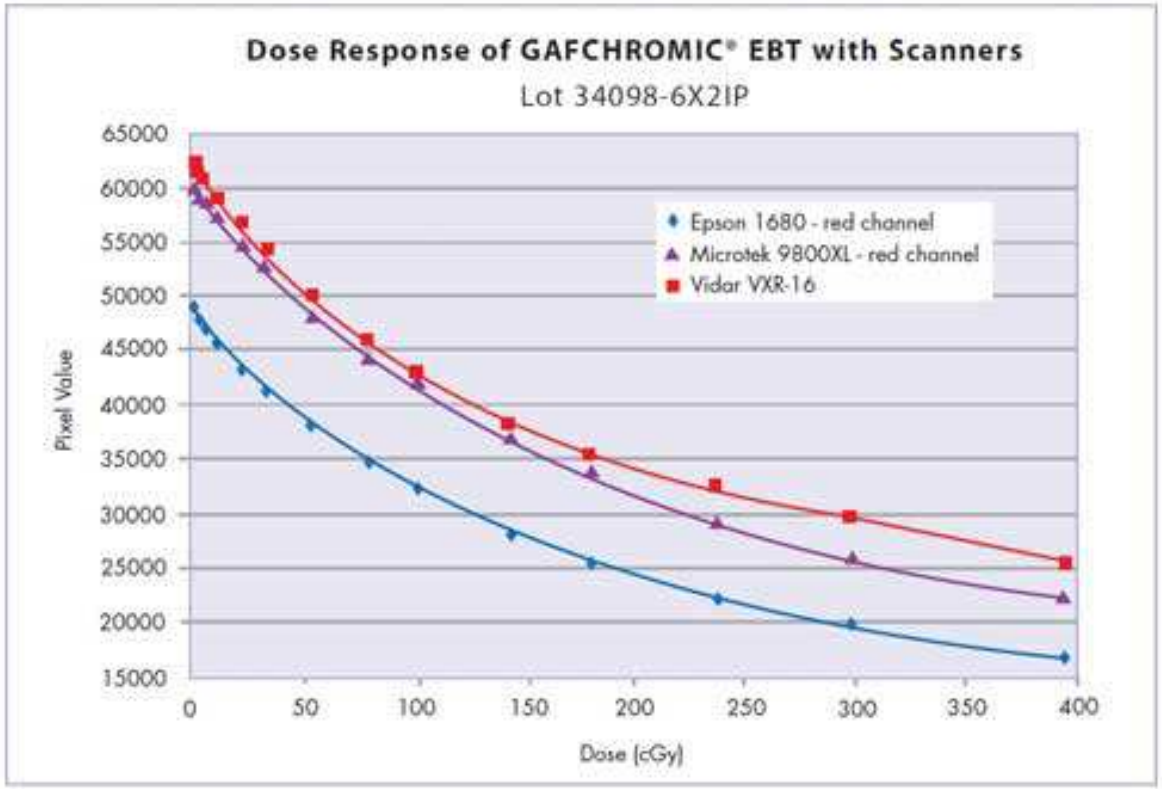

Issues with EBT2

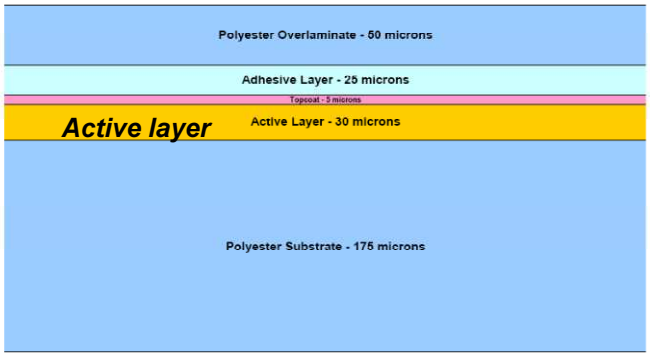

Marker dye in the active layer-yellow color

- Make the response independent of small thickness differences of the active layer.
- Less sensitive to UV light, less permeable to water
- Nearly energy independent response [50kV-MV]

Homogeneity of EBT2 (Early batches 2009-2010)

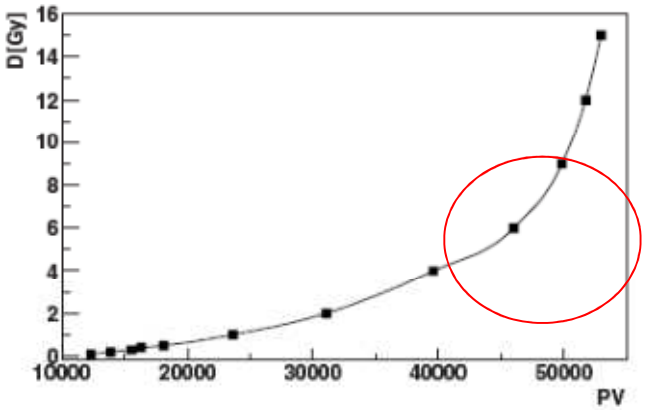

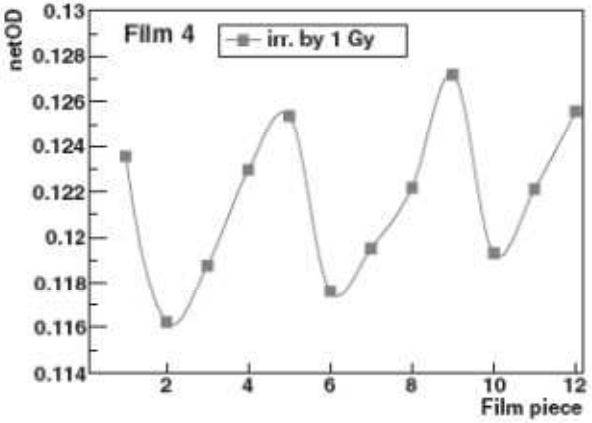

Bernadette Hartman et al. Med.Phys. 37 (2010)

Issues with EBT2- multichannel film dosimetry (film QA pro-software)

Rational

- Use of the three colour channels.
- Different response in the three channels enables discrimination between dose related and non-dose related signals

Advantages

- Compensation for nonhomogeneity of dye thickness
- Increases signal to noise level
- Mitigates lateral dose dependency of flat bed scanners
- Extends the dose range to 10cGy-100 Gy
- Nearly energy independent response [50kV-MV]

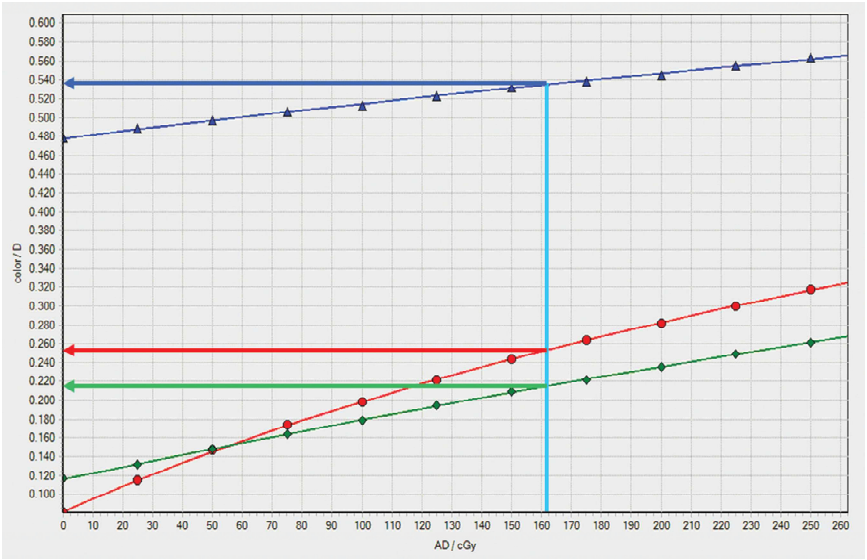

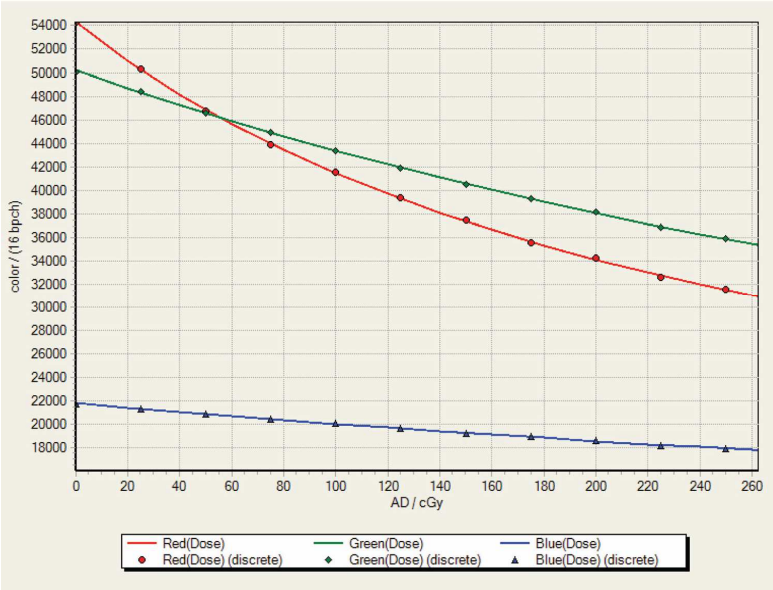

Remember that for 16 bits depth:

d=-log (PV/65535)

Where d is density and PV refers to pixel value

Micke et al. Med.Phys. 38 (2011)
Mendez et al. Med. Phys. 41 (2014)
Mendez, Med. Phys. 40(2013)

Dosimetry process using gafchromic films

- Film exposure to radiation

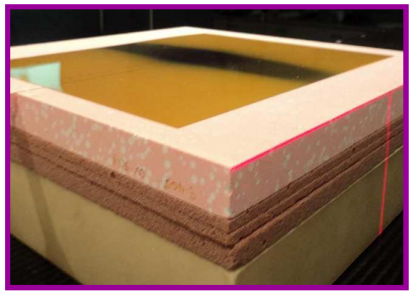

Free application (I. Méndez et al.)
https://radiochromic.com/

- Scanning the film to determine the OD over one or more spectral bands.

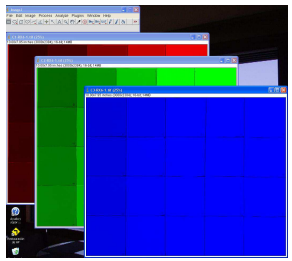

- Use dose-optical density response information of each color channel to convert the scanned image in to its dose equivalent (dose mapping)

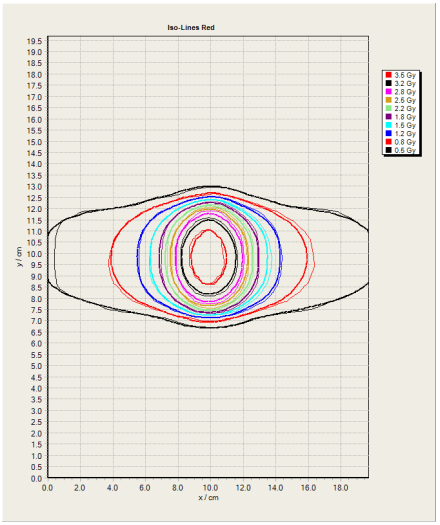

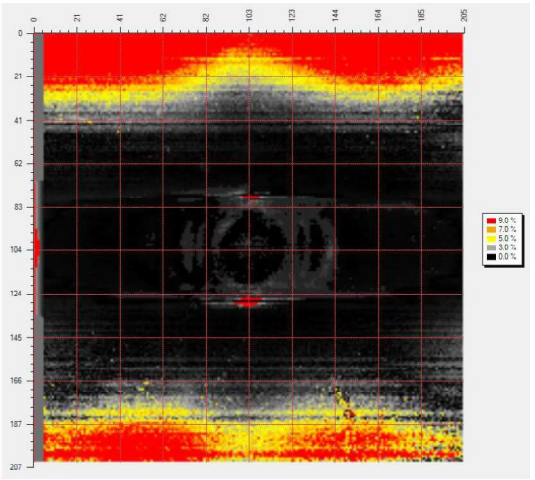

Gamma evaluation
2%-3mm

Film handling tips

- **Not handle films with bare hands**
- Control temperature during irradiation, storage and readout. Use the same conditions to films used for calibration
- Do not expose films to **ultraviolet** or **sun light** for hours.
- Although can be used in water, prolonged immersions will cause water to seep into the emulsion at the cut edges.
- **If small square pieces are used for calibration keep track of the initial sheet orientation (coating direction).**

Film handling tips

- **The range of dose levels used for calibration must cover the measurement range.**
- **6 films per point dose recommended for calibration**
- Films should be assigned doses in a random pattern (avoid trending to inhomogeneities)
- **Use the same scanning protocol** for calibration and for measuring
  - Need to be scanned in the same orientation [orientation of "needle like mictro-crystals (EBT)]
  - For best results, scan one day following irradiation (min. two hours)
- Take into account **corrections for the scanner**. Linearity and non homogeneity.

Dose uncertainties EBT

TABLE II. Dose uncertainties for various sources of deviations at $D=2.0$ Gy. "Observed variation" column shows uncertainty values in case of a single film, no lateral correction, irrespective of film batch. "Reduced variation" columns show uncertainty values when the recommendations mentioned in the text are followed, such as applying two or three films, film of the same batch, lateral correction, and an optimized scan mode.

EBT GafChromic film	Observed variations (1 SD) Single film	Recommendations/Improvements	Reduced variations (1 SD) Two films	Reduced variations (1 SD) Three films
Scanner	0.3%	Scanner	0.3%	0.3%
Lateral correction (position)	Up to 1.0% systematic	Limited scan area (OD and position)	0.5%	0.5%
Scan mode	Up to 10% systematic	Scan mode	...	...
Fit accuracy (OD→Dose)	0.5%	Fit accuracy (OD→Dose)	0.5%	0.5%
Intra batch variations	0.5%	Intra batch variations	0.5%	0.5%
Inter batch variations	0.2%	Use a single batch/box	...	...
Background (single batch)	0.5%	Background	0.5%	0.5%
Energy dependence	0.5%	Energy dependence	0.5%	0.5%
Angular dependence	0.5%	Angular dependence	0.5%	0.5%
Intrinsic film inhomogeneity	1.1%	Film inhomogeneity after averaging films	0.7%	0.6%

Van Battum et al Med. Phys 35; 2008

Overall uncertainy:

- Using central part of the scanner
- One film : 1.8% (1SD)
- Two films : 1.3% (1SD)

Application example; Dynamic MLC Gravity test

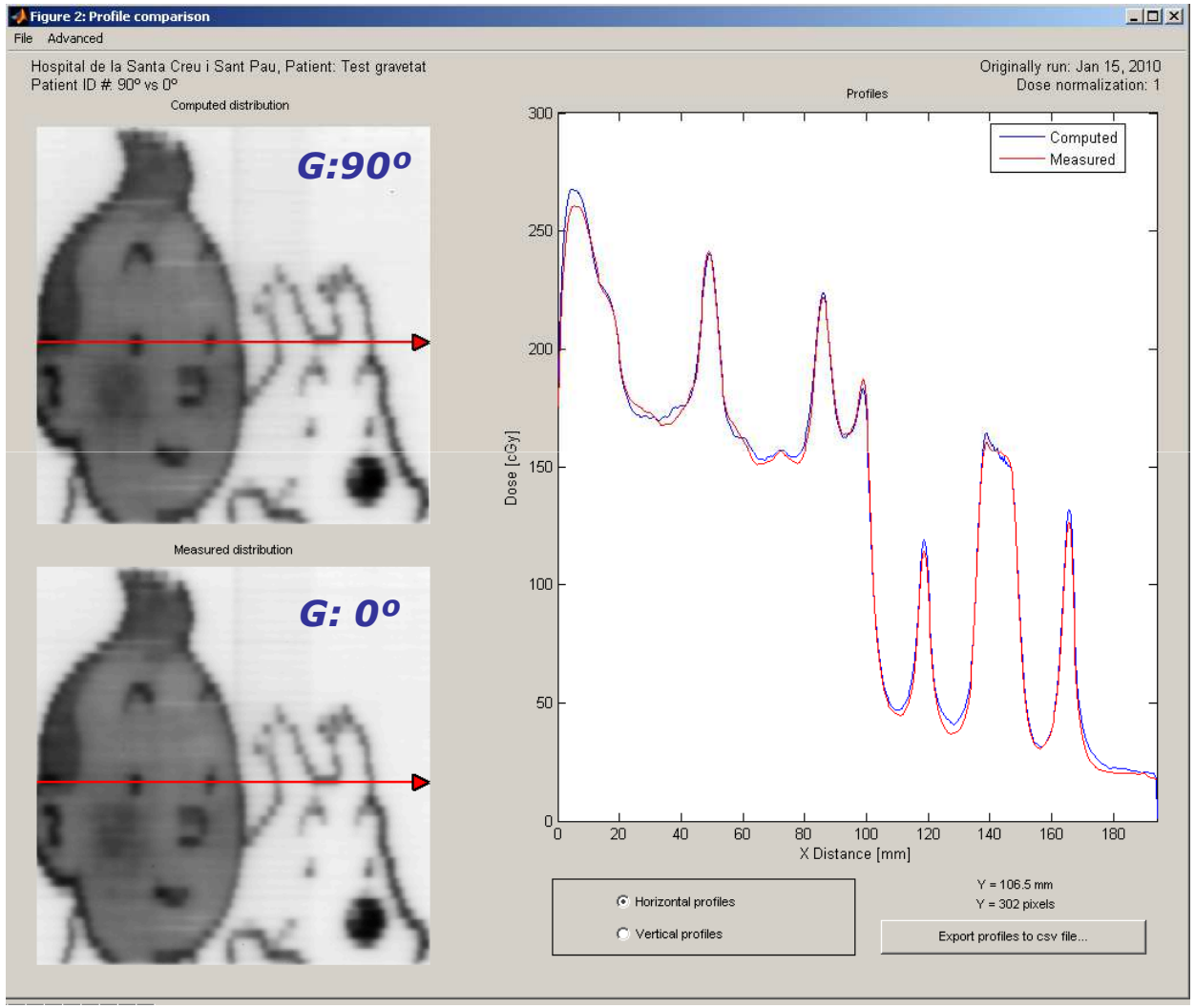

EBT- DoseLab (one channel)

2 D - DETECTOR ARRAYS

- Trends towards so called “digital hospitals”
  - ➔ No access to film processing machine
  - ➔ Film dosimetry limited to radiochromic films
- Wish to implement fast real-time procedures for measurements
- **2D detector arrays are an option**
  - No necessity to downscale MUs to the sensitive range (not for EBT- XT)
  - Potential for absolute dose measurements
  - Results available immediately after irradiation
  - Mostly limited to single beam verification

2 D - DETECTOR ARRAYS

- **Use different physical principles**
  - IC, diodes, fluorescence screen, ….

- **Limited spatial resolution (>7 mm)**
  - Impact on gamma-evaluation

- **Differences in build-up and backscatter (!)**

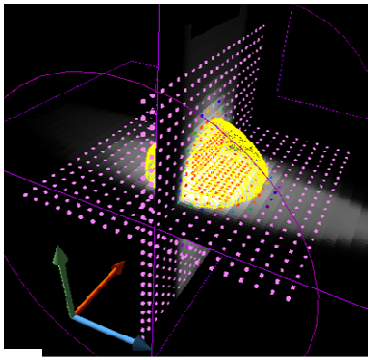

- **Software** (import of dose distributions, evaluation, etc)

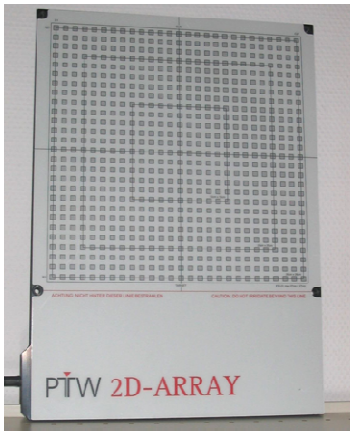

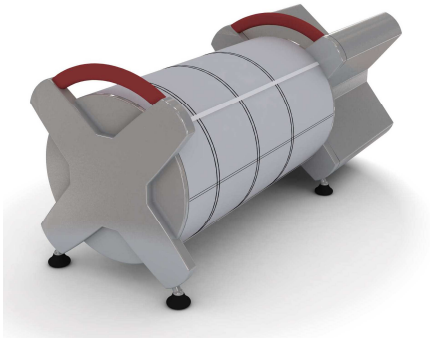

2 D - DETECTOR ARRAYS

MatriXX (IBA)

1020 i.c.
0.080 cm^3
24x24 cm^2

Seven29 (PTW)

729 i.c.
0.125 cm^3
27x27 cm^2

Mapcheck2 (Sun Nuclear)

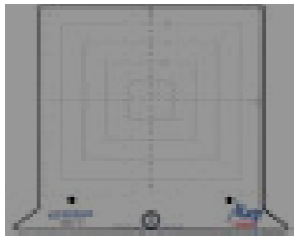

1527 diodes
0.000019 cm^3.
32x26cm^2
Build up 2cm –Backscatter 2.3cm

Limited spatial resolution.

Diodes : energy-dose-rate dependence, need recalibration (6 months)

i.c.: volume averaging effects

		Manufacturer	Sun Nuclear	IBA	PTW
		Product	MapCHECK	MatriXX	729
Advantage	1	Active Dimension (mm)	0.8 x 0.8	4.5 (diameter)	5.0 x 5.0
		Active Area (mm^2)	0.64	15.90	25.00
	2	Active Thickness (mm) Active Volume (cm^3)	0.03 0.000019	5.0 0.08	5.0 0.125
	3	Sensitivity (nC/Gy)	32.0	2.4	3.3

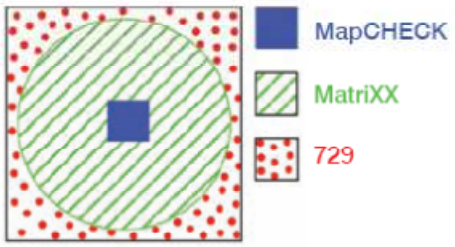

2 D - DETECTOR ARRAYS- Mapcheck2

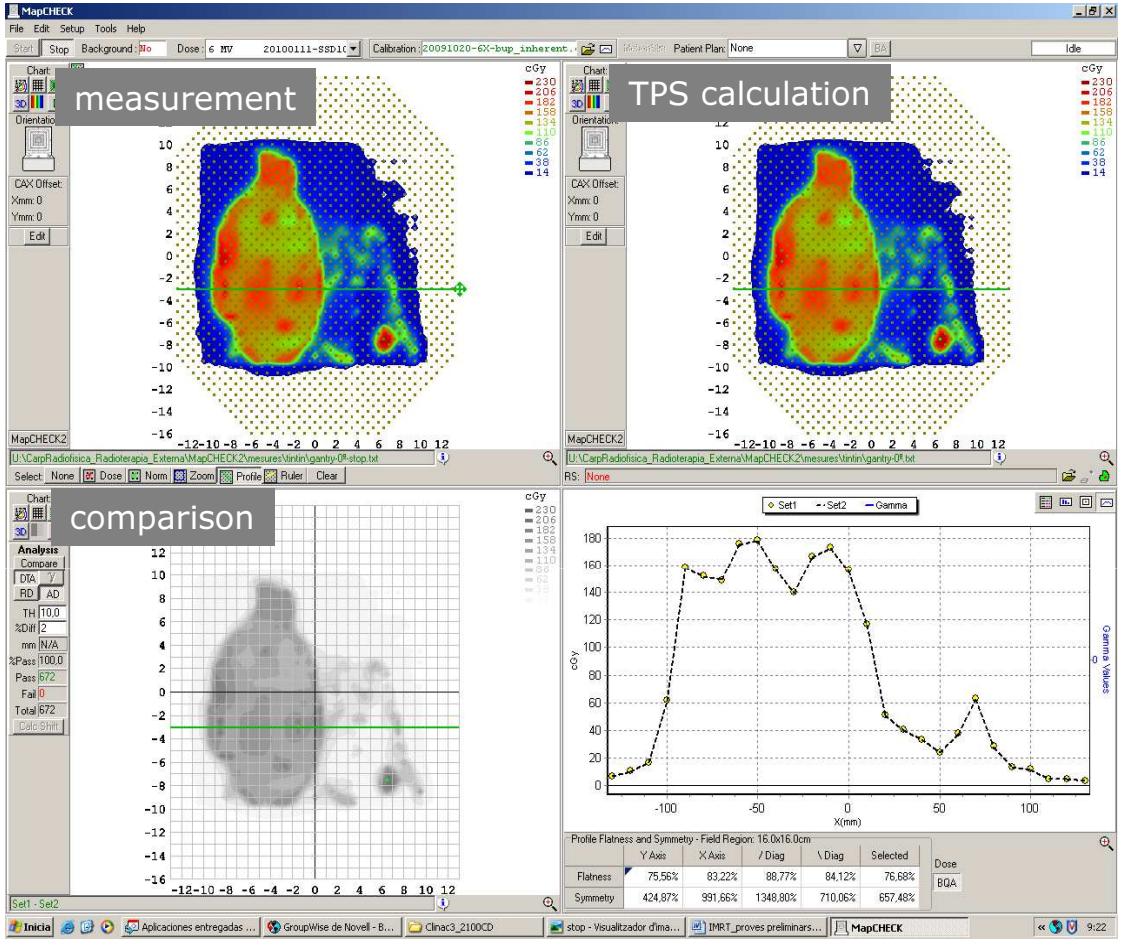

MapCHECK 2

1527 díodes
Resolution: 7.07 mm
Surface: 26 cm x 32 cm

MapPHAN (*virtual water*) + Plastic Water

SDD = 100 cm
z = 10 g/cm2

Detector array handling tips

- Determine the effective point of measurement. Water equivalent depth
- Calibrate the array following the manufacturer methodology
  (calibration coefficient +homogeneity factor)
- Check linearity with dose, dose rate dependence, angular dependence.
- Compare your results with literature

EPID as 2D DETECTOR

- Trends towards so called "digital hospitals"
  - No access to film processing machine
  - Film dosimetry limited to radiochromic films
- Wish to implement fast real-time procedures for measurements

- EPID are an option
- No necessity to downscale MUs to the sensitive range
  - Potential for absolute dose measurements
  - Results available "immediately" after irradiation
  - Mostly limited to single beam verification
  - **Good spatial resolution**
  - Need of corrections to convert the resulting signal into fluence or dose in detector

EPID as 2D DETECTOR

- Standard equipment on new linacs
- Suitable for dosimetry
- Potential for a variety of applications

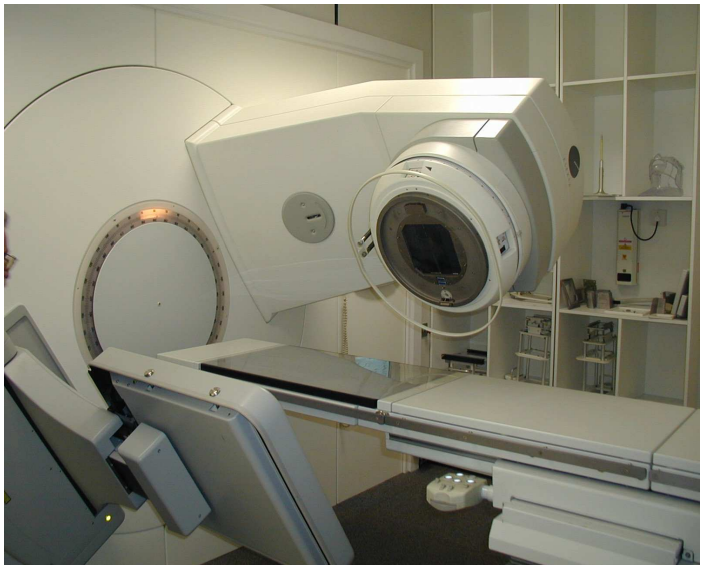

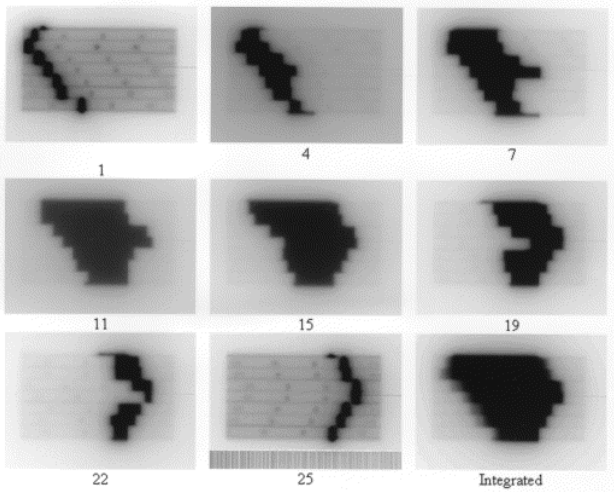

FLUOROGRAFIC SCREEN+VIDEO CAMERA

LIQUID FILLED IONISATION CHAMBER

AMORPHOUS SILICON

Amorphous silicon (a-Si) type of EPID – principles of operation

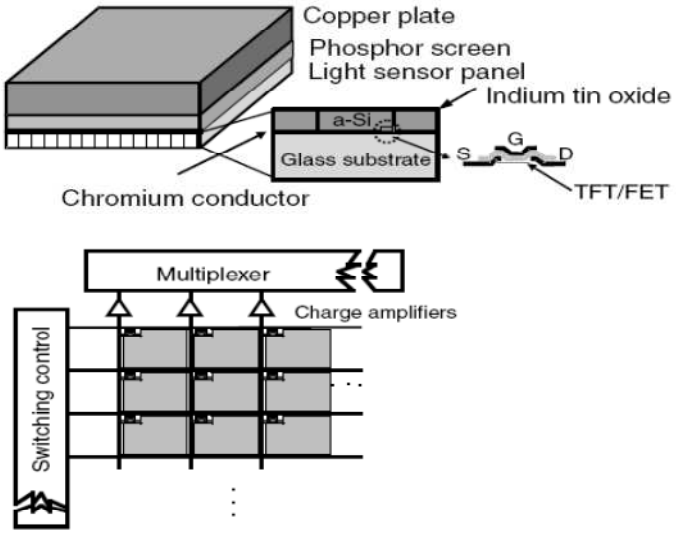

A. Nahum, Mayles, Rosenwald, *Handbook of radiotherapy*

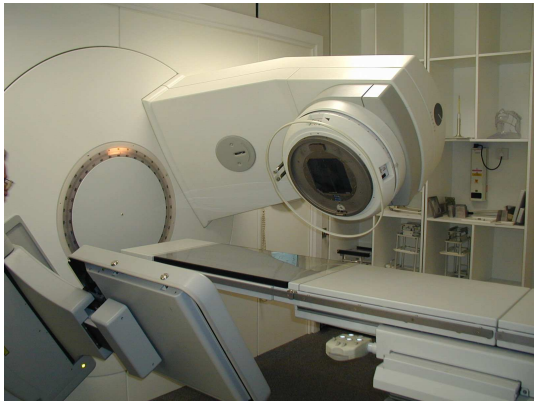

- Compton electrons produced in the copper plate
- Electrons produce light photons in the phosphor material
- The light sensor detector pixels are photodiodes and TFT transistors connected to readout and scanning electronics.

Amorphous silicon (a-Si) type of EPID – principles of operation

Parameters of the Varian and Elekta Amorphous Silicon Imager Panels

Model/Supplier	Portal Vision aS500/Varian[a]	iViewGT/Elekta[b]
Detector area	40.14 cm×30.11 cm	40.96 cm×40.96 cm
Pixel format	512×384	512×512
Pixel pitch	0.784 mm	0.80 mm
Maximum image acquisition rate	15 fps	3 fps
Image display and storage rate	2 s per image	~0.3 s per image
Pixel depth	14 bits	16 bits
Metal plate thickness	1mm Cu	1mm Cu
Scintillator	Gd_2O_2S:Tb	Gd_2O_2S:Tb
f_{50}	0.45 lp/mm	0.46 lp/mm
Software tools	Comprehensive	Comprehensive

Nahum, Mayles, Rosenwald, Handbook of radiotherapy

CALIBRATION OF EPID

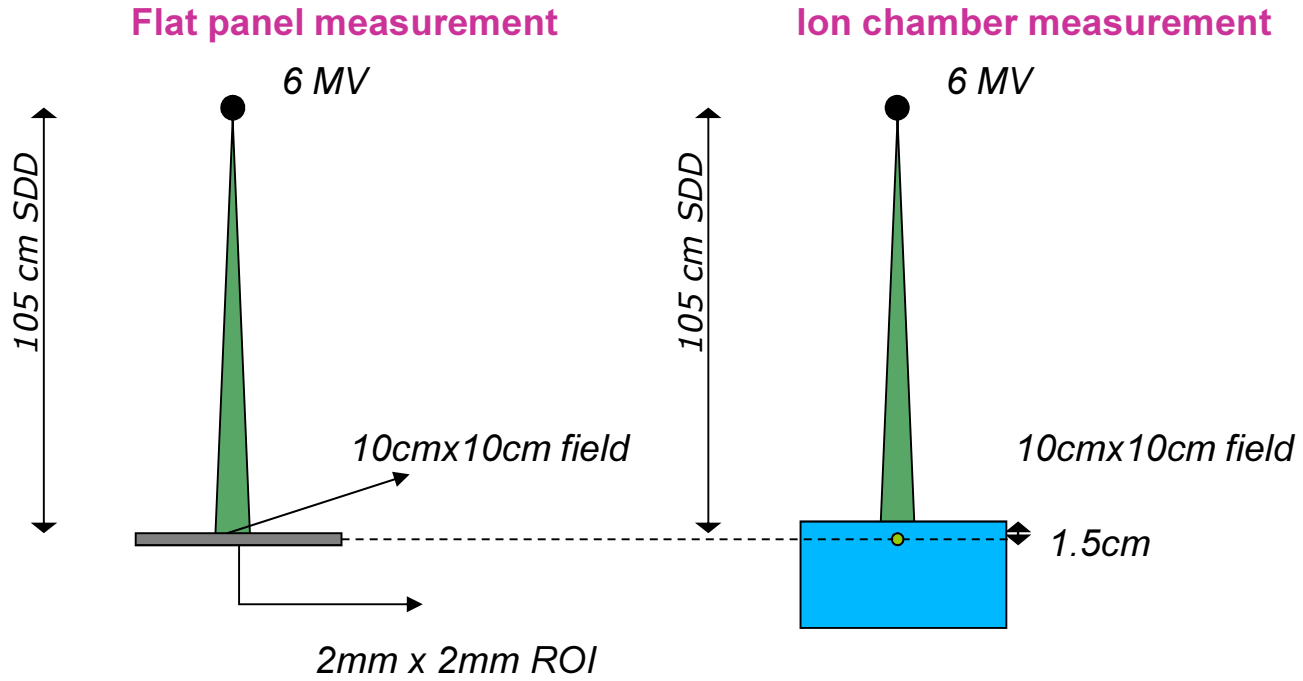

FLUOROGRAFIC SCREEN+VIDEO CAMERA: linear in response up to certain dose

LIQUID FILLED IONISATION CHAMBER: $I = a D^{1/2} + bD$ D is Dose rate.

AMORPHOUS SILICON: linear with dose, need of selecting adquisition parameters to avoid saturation

CALIBRATION OF EPID
correction factors

THE INTENSITY AT EACH POINT IN THE IMAGE MUST BE CALIBRATED IN A QUANTITATIVE SENSE

- The dose response of each pixel point must be known
- The effects of scattered radiation in the detector must be understood
- The temporal stability of the detector must be known.

DEPENDING ON THE DETECTOR: DIFFERENT CORRECTION FACTORS CAN BE EXPECTED

- Field size
- Air gap between the phantom/patient exit surface and the detector (transmission measurements)
- Other parameters

CALIBRATION OF EPID
correction factors

Variation in off-axis sensitivity of a-Si EPIDs

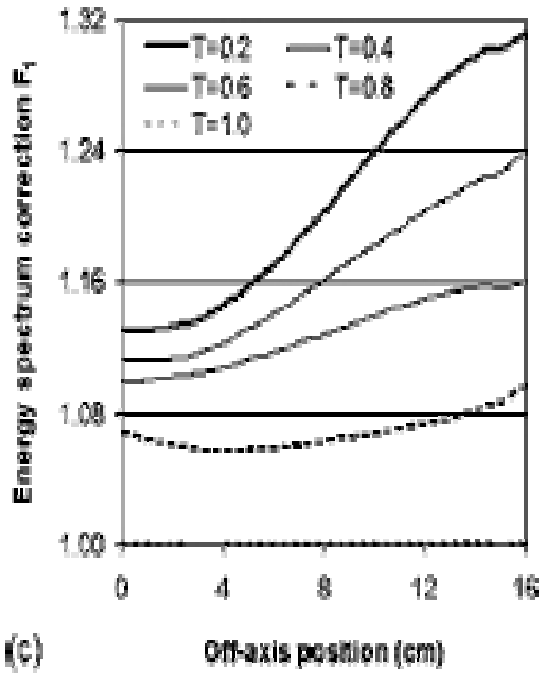

6 MV

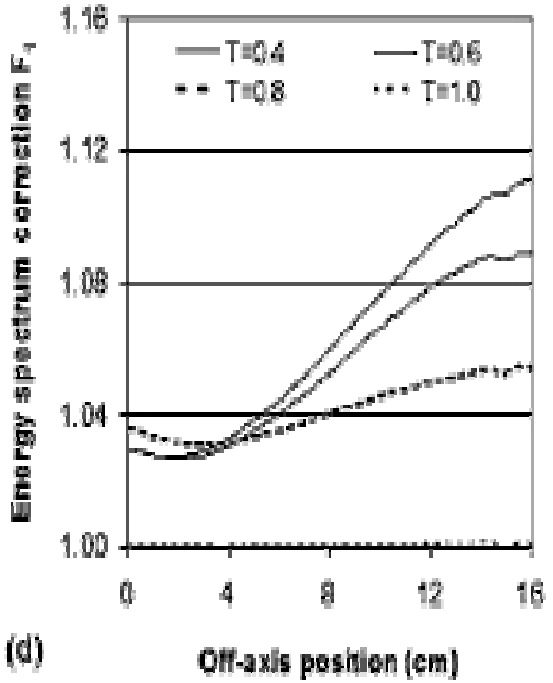

10 MV

B. Nijsten et al., Med Phys. 34, 3872-3884, 2007

Application example; Dynamic MLC test

Comparison of a line profile extracted from a dosimetric EPID image to:

(a) a film scan (open symbols)

(b) ion chamber measurements in a water phantom (closed symbols).

All measurements have been normalised to the data point on the beam-axis.

(Van Esch et al. Radiother Oncol 60: 181-190, 2001)

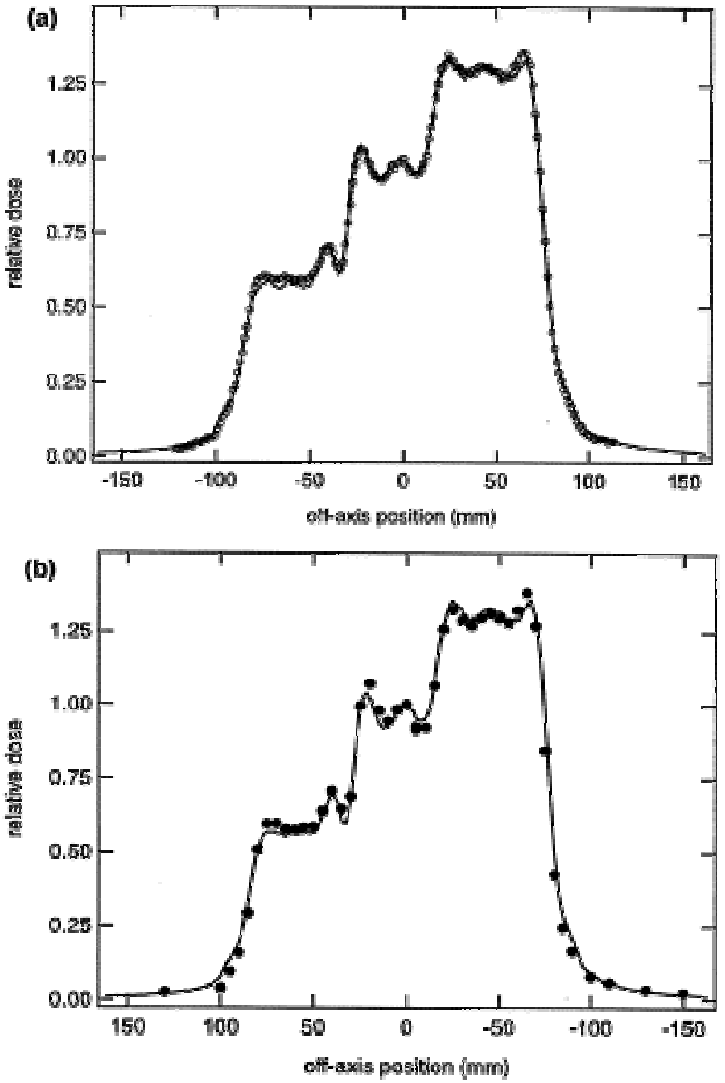

Application example; Portal imaging (Varian)

Amophous silicon (aSi1000): 1024 × 768 píxels

Resolution: 0.4 mm

Surface: 40 cm x 30 cm

SDD = 105 cm

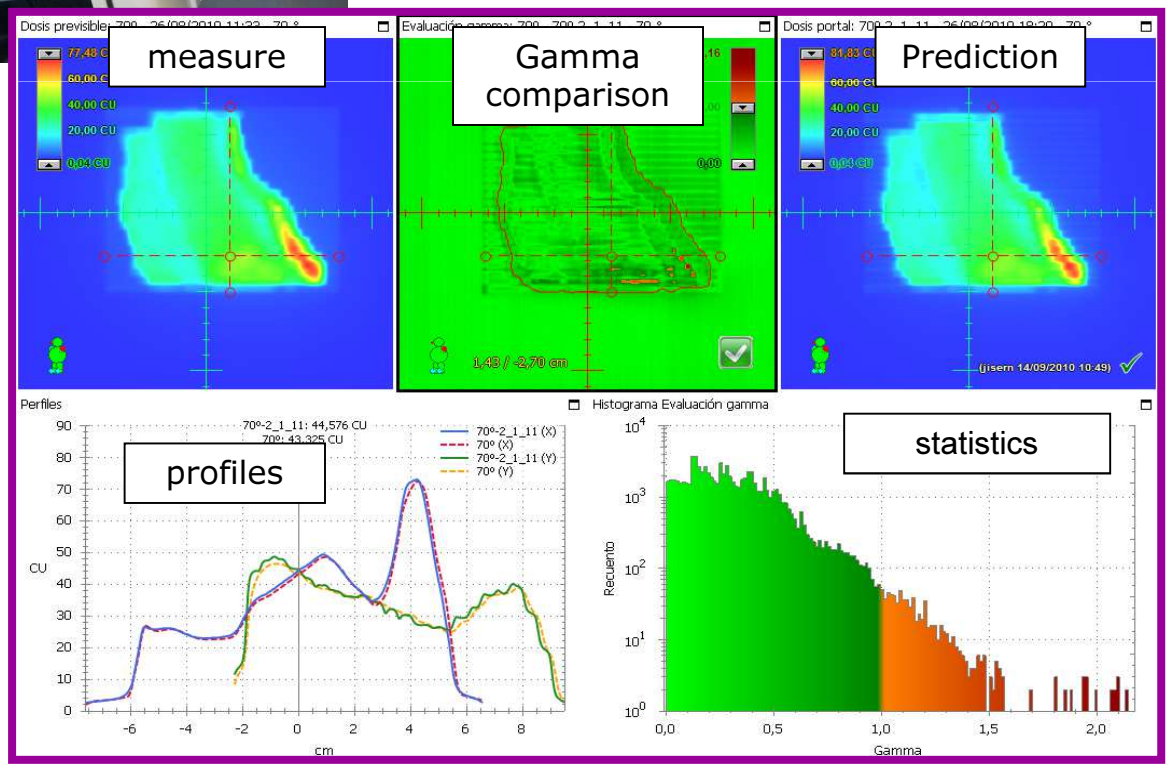

2D detector's comparison: spatial-dose resolution

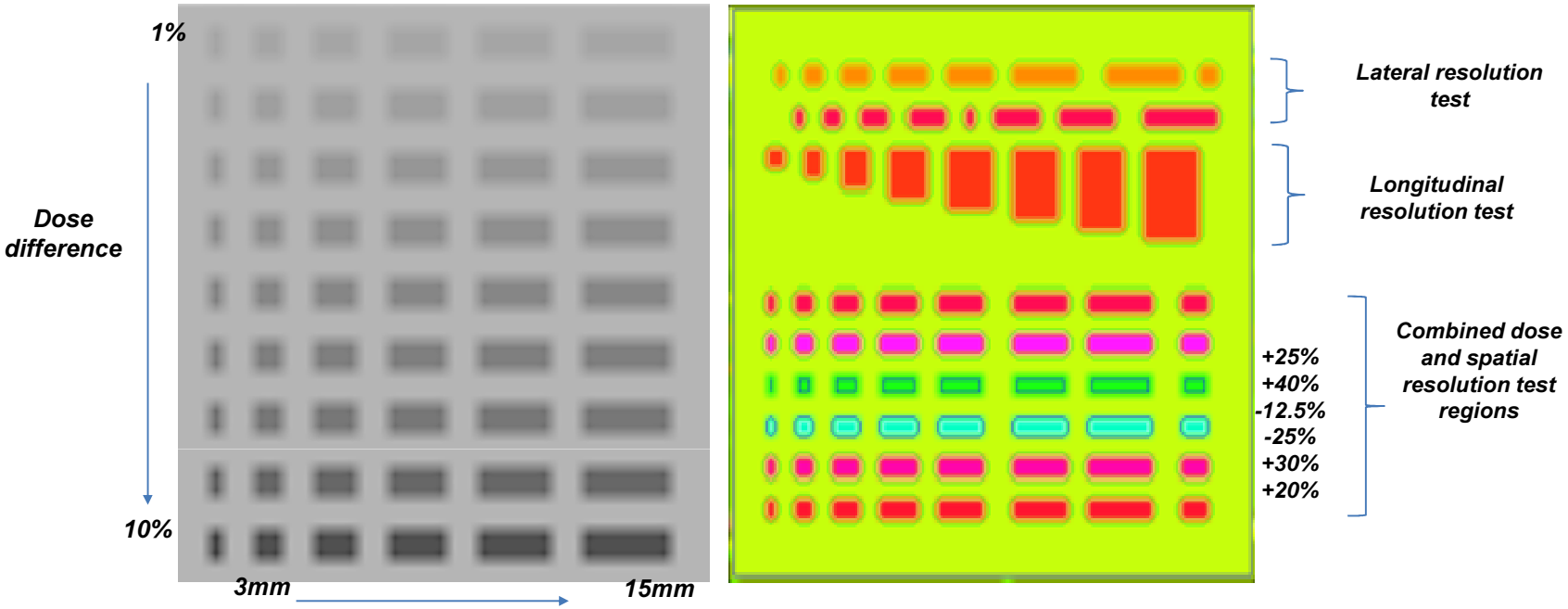

Single gantry test fields for resolution and sensitivity assessment. (left) the sensitivity test, and (right) the resolution test. In the resolution test the values in the lower half represent difference in % dose between the regions and the background (lime green) area.

2D detector's comparison: spatial-dose resolution

Gafchromic film | 2D array | 2D array | EPID

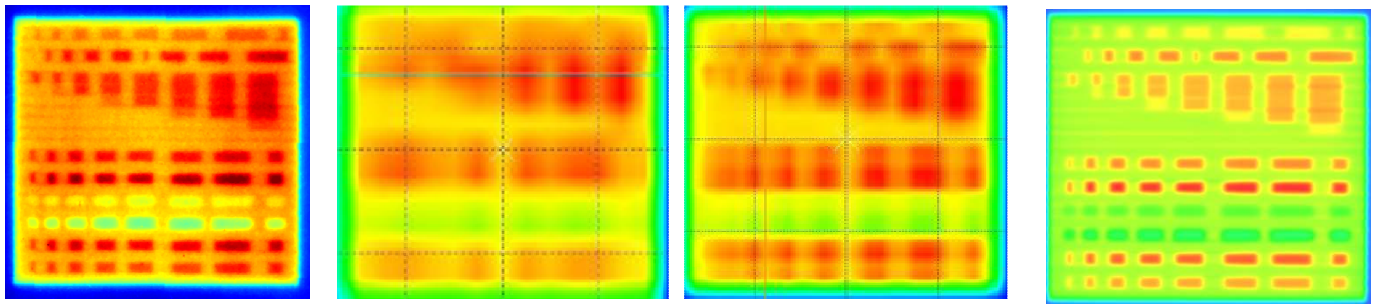

Single acquisition | Double acquisition

From Andrew Nisbet, ESTRO premetting Geneve 2013

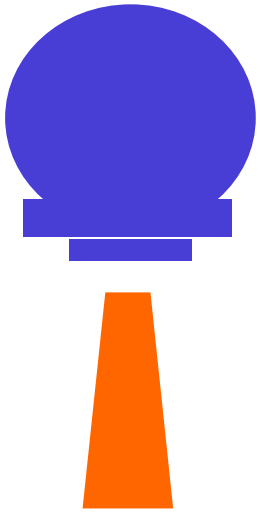

2D ARRAYS, EPID

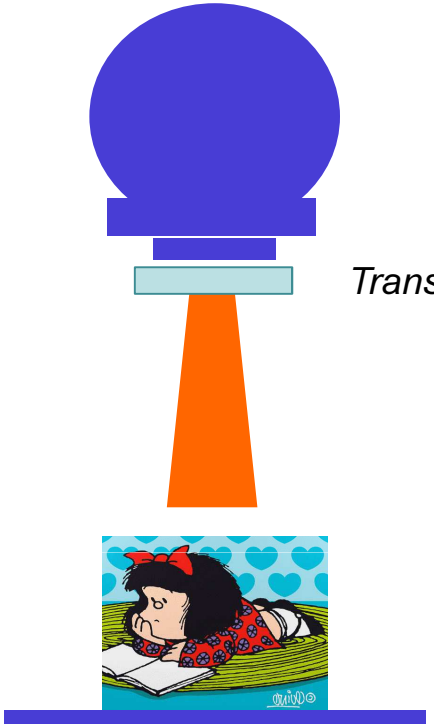

Transmission chamber

Periodic QC Dynamic wedges
Beam symetry and flatness

Pre-treatment verification IMRT
VMAT

WE CHECK DELIVERY

How can we know that the delivery is as planned when treating the patient?

Transmission chambers

"Dolphin"
(IBA)

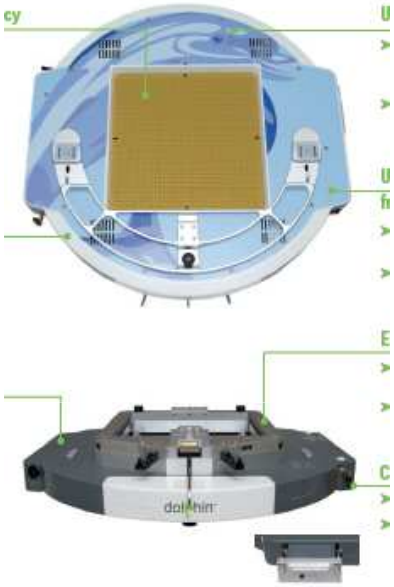

pp i.c. matrix
1513 i.c.
0.02 cm^{3-} 5mm center to center
Attenuation 1% (6MV)
Measures dose fluence
MC modelling of detector reponse

David
(PTW)

Multiwire i.c.
nº of wires = nº leaf pairs

Attenuation 5% (6MV)
Measures dose-length product

Delta 4 TD
(Scandidos)

diode matrix
4040 diodes
1mm (disc shaped)
2.5 x 5 mm spacing
Attenuation 1% (6MV)
Sensitivity decrease:
0.04% per kGy

Dose measurement
accuracy 1.5%

MLC position accuracy
1mm

LIMITED SPATIAL RESOLUTION
NEED TO REMOVE ELECTRON
CONTAMINATION FROM THE HEAD

"3D" detector matrix

Delta4
(Scandidos)

2 ortogonal planes
2D diode matrix
3D dose reconstruction

*James L Bedford et al Phys. Med. Biol. **54** (2009)*

ArcCHECK
(Sun Nuclear)

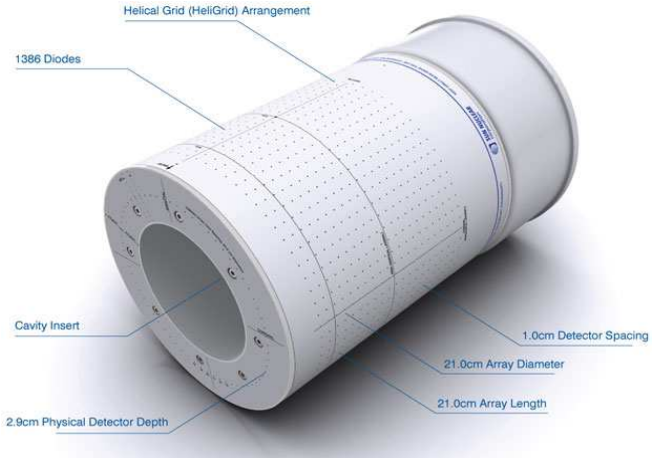

Cylindrical disposition
diode matrix
3D dose reconstruction

Daniel Létourneau et al. Med.Phys. 36 (2009)

3D dosimetry systems

- **Films, 2D arrays, EPIDs: partial sampling of a 3D dose distribution**

- 3D dosimetry materials:

  - Polymer gels: Polyacrylamide gels (PAG)
  - Fricke gels
  - Radiochromic plastics

- Reading systems:

  - Magnetic resonance (MR) imaging
  - Optical- Computed Tomography (optical CT)

GEL DOSIMETRY SYSTEMS

- Gel dosimetry systems are true 3-D dosimeters.
- The gel dosimeter is a phantom that can measure absorbed dose distribution in a full 3-D geometry.
- Gels are nearly tissue equivalent and can be molded to any desired shape or form.

GEL DOSIMETRY SYSTEMS

Polymer gels

- In polymer gel, monomers such as acrylamid are dispersed in a gelatin or agarose matrix.
- Upon radiation, monomers undergo a polymerization reaction, resulting in a 3-D polymer gel matrix. This reaction is a function of absorbed dose.
- The dose signal can be evaluated using MR imaging, X-ray computed tomography (CT), optical tomography, vibrational spectroscopy or ultrasound.

GEL DOSIMETRY SYSTEMS

Advantages

- A number of polymer gel formulations are **commercially available**.
- There is a **semi-linear** relationship between the NMR relaxation rate and the absorbed dose at a point in the gel dosimeter.
- Due to the large proportion of water, polymer gels are nearly **water equivalent** and no energy corrections are required for photon and electron beams used in radiotherapy.
- Polymer gels are well suited for use in **high dose gradient regions**, (e.g., stereotactic radiosurgery).

GEL DOSIMETRY SYSTEMS

Disadvantages

- Method usually needs access to an MRI machine.
- Post-irradiation effects can lead to image distortion.
- Possible post-irradiation effects:
  - Continual polymerization.
  - Gelation and strengthening of the gel matrix.

http://www.ecnurad.ugent.be/QMRI/en/research.html

3D RADIATION DOSIMETRY USING monomer / polymer gels

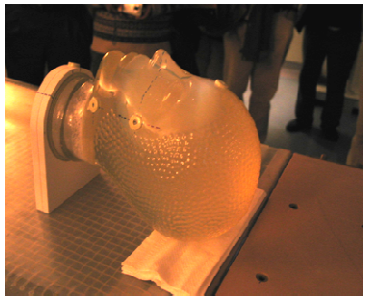

IRRADIATION (TREATMENT)

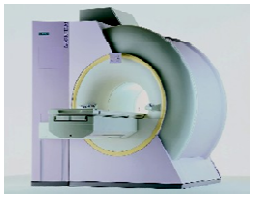

qMRI

$$R2 = \frac{1}{T2}$$

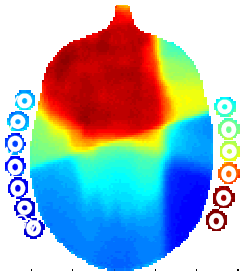

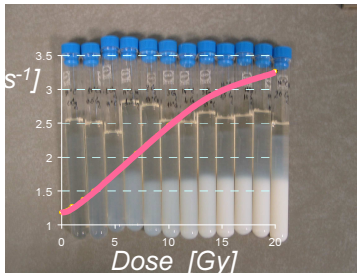

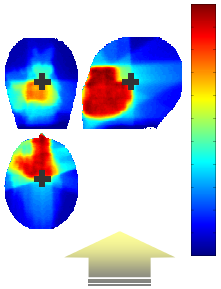

GEL FABRICATION

From Yves De Deene – Univ Ghent

GEL DOSIMETRY SYSTEMS

Prostate IMRT verification

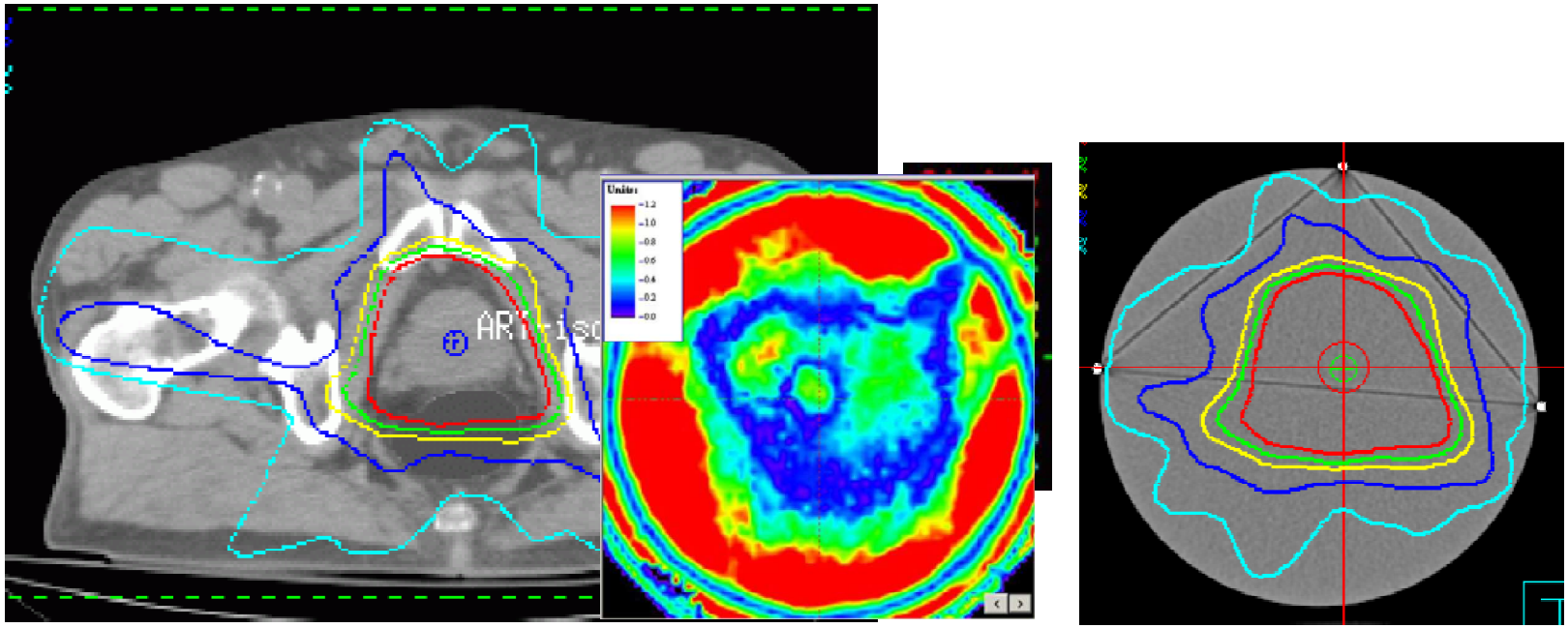

(a) (b)

Figure 2. Pinnacle isodose distributions through a common slice from (a) the original prostate patient treatment plan (consisting of a 5 field IMRT Tx), and (b) recomputed isodoses of the same plan, with identical beam orientations and segments etc, for the 17 cm diameter gel dosimeter. The prescription (total MU's) was scaled in the latter so the dose matched the dynamic range of the gel and scanner.

From Oldham et al 2004, 3rd DOSGEL meeting, Journal of Physics: Conference Series 3 (2004) 293–296

SUMMARY

How to choose the 2D dosimetry system

Its use:

Comissioning treatment units
Data adquisition for TPS
Comissioning TPS
QA treatment unit: Periodic QC.
Pretreatment QA
In vivo dosimetry

Dosimetric requirements:

Accuracy
Spatial resolution
Absolute vs relative dose measurements

Logistics:

Available phantoms
Time slots for QA in Treatment units
Time needed to calibrate the dosimetry system
Post processing time/complexity


Questions?

RECOMMENDED READING

►**General:**

►Clinical dosimetry measurements in radiotherapy. AAPM monograph nº34 (2009)

►**Film dosimetry:**

►AAPM TG69. Radiographic film for megavoltage beam dosimetry.Med.Phys. 34(6); 2006

►AAPM Report nº 63. Radiochromic film dosimetry. Med. Phys. 25(11); 1998

►Devic S., Seuntjens J. et al. Dosimetric properties of improved GafChromic films for seven different digitizers. Med. Phys. 31(9); 2004

►Devic S., Seuntjens J. et al. Precise radiochromic film dosimetry using a flat-bed document scanner. Med. Phys. 32(7); 2005

►Zeidan O.A., Stephenson S.A.L. et al. Characterisaton and use of EBT radiochromic film for IMRT verification. Med.Phys. 33(11); 2006

►Fuss M., Sturtewagen E. Dosimetric characterisation of GafChromic EBT film and its implication on film dosimetry quality assurance. Phys. Med. Biol. 52; 2007

►Bouchard H., Lacroix F. On the characterization and uncertainty analysis of radiochromic film dosimetry. Med. Phys. 36(6); 2009

►Devic. Radiochromic film dosimetry: Past, present and future. Phys. Medica 27 (2011)

►Méndez et al. On multichannel film dosimetry with channel-independent perturbations. Med. Phys. 41(1);2014

►Micke et al. Multichannel film dosimetry with nonuniformity correction. Med. Phys. 38 (2011)

RECOMMENDED READING

►**Arrays:**

►Spezi E. et al. Characterisation of a 2D ion chamber array for the verification of radiotherapy treatments. Phys. Med. Biol. 50; 2005 [Seven29™ (PTW)]

►Herzen J. et al. Dosimetric evaluation of a 2D pixel ionization chamber for implementation in clinical routine. Phys. Med. Biol 52; 2007 [MatriXX (IBA)]

►Létorneau D. et al. Evaluation of a 2D diode arrray for IMRT quality assurence. Radiother. Oncol.70(2); 2004

►Létorneau D., Publicover J. et al. Novel dosimetric phantom for quality assurance of volumetric modulated arc therapy. Med.Phys. 36(5);2009

James L Bedford et al. Evaluation of the Delta4 phantom for IMRT and VMAT verification. Phys. Med. Biol. 54 ;2009

EPID:

W. Van Elmpt, L. McDermott et al. A literature review of electronic portal imaging for radiotherapy dosimetry. Radiother Oncol. 88(3);2008

Gel Dosimetry:

Oldham et al. High resolution gel-dosimetry by optical-CT and MR scanning. Med. Phys. 28(7);2001

Methods for comparison

Tommy Knöös

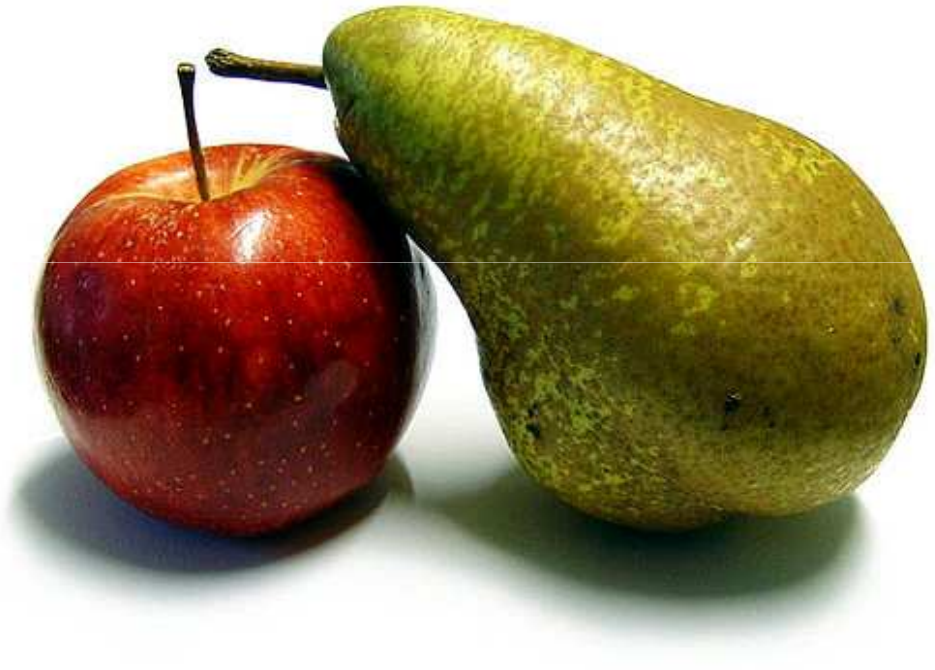

Learning objectives

- Comparisons
- Evaluation
- Dose difference
- Distance to agreement
- Gamma evaluation

Contents

- Point by point
- Distributions
- Examples

Comparisons between measurement and calculations

- Look at differences: do we use a substraction, a division (or ratio), in gray or in %?
  - Then, in % of what?
    - in % of max of beam dose or other “global” point/dose?
    - in % of “local” dose?
- What are the data that we have?
  - point dose values? How many?
  - Curves or measurement along a liner i.e. PDD, profiles…
  - 2D distributions e.g. from film or 2D-array system
  - 3D distributions?
- What are the criteria that we should use?
- Should we reject all, if only a few points exceed the criterion in a specified case?
- Is it OK with the same criteria for the whole distribution?
- Is it reasonable to have the same criteria in simple and in very complex cases?

How to express deviations?

Calculated and measured dose distributions can be compared according to

1) to the **local dose** value

$$d(i,B) = D_{calc}(i,B) / D_{meas}(i,B)$$
$$d\%(i,B) = 100 \cdot \left(D_{calc}(i,B) - D_{meas}(i,B)\right) / D_{meas}(i,B)$$

2) to the dose at a **specific point inside the beam** under consideration

$$d(i,B) = D_{calc}(i,B) / D_{meas}(ref,B)$$
$$d\%(i,B) = 100 \cdot \left(D_{calc}(i,B) - D_{meas}(ref,B)\right) / D_{meas}(ref,B)$$

this is proposed in the IAEA TRS-1583

3) to the **dose in a reference field**

$$d(i,B) = D_{calc}(i,B) / D_{meas}(ref,R)$$
$$d\%(i,B) = 100 \cdot \left(D_{calc}(i,B) - D_{meas}(ref,R)\right) / D_{meas}(ref,R)$$

B – present beam, R – Ref beam

Suggestion

- Absorbed dose is given per monitor unit[1]

- Dose is normalised to a reference field (output normalised)

$$d(i) = \frac{\left[\dfrac{D_c(i)/M_c}{D_c(ref)/M_c}\right]}{\left[\dfrac{D_m(i)/M_m}{D_m(ref)/M_m}\right]} \qquad d\%(i) = 100 \cdot \left[d(i) - 1\right]$$

Booklet nº7

- Gives that monitor units are implicitly checked too
- Get rid of any fluctuation in the treatment output.

1) Equiv. to dose rate c.f. ^{60}Co - Gy/min

Criteria depending on position in photon beam

Points along the central axis of the beam beyond the depth of dose maximum: **low dose gradient area**.

Points on and off the central axis in the build-up and penumbra region. This region includes also points in the proximity of interfaces: **high dose gradient area**.

Points **inside** the beam (*e.g.*, inside 80% of the geometrical beam) but off the central axis: **low dose gradient area**.

Points **outside** the geometrical beam or below shielding blocks, jaws, MLC, *etc*… where the dose is lower than, for instance, 7% of the central axis dose at the same depth: **low dose gradient area**.

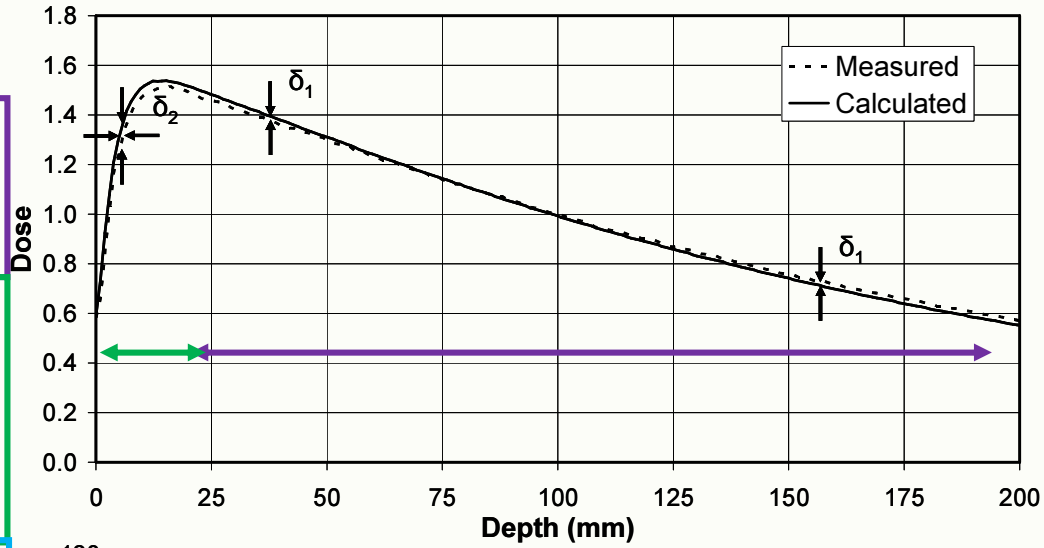

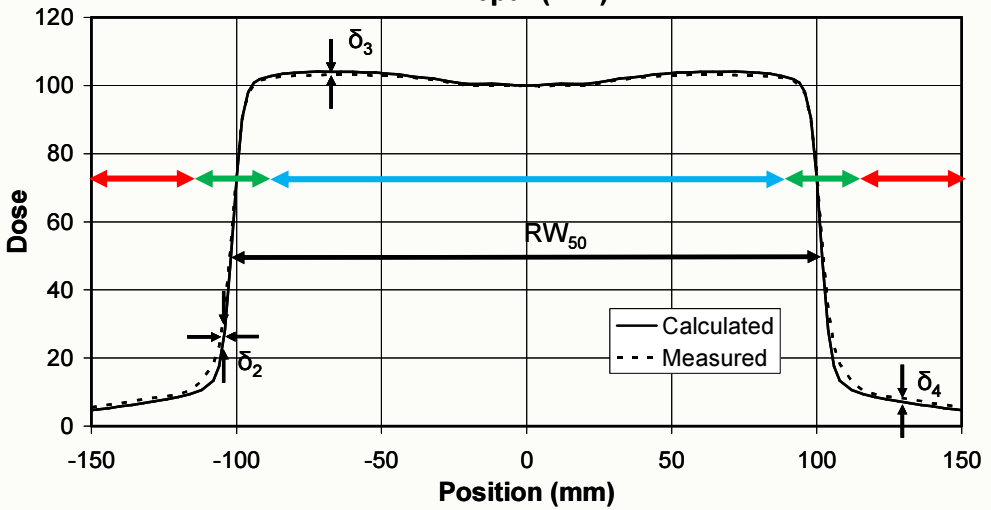

Adopted from Venselaar, 2001

Tolerances δ for the local dose deviation *d%(i)*

	Region	Homogenous, simple geometry	Complex geometry (wedge, inhomogeneity, asymmetry, blocks / MLC)	More complex geometries****
δ_1	*Central beam axis data* – high dose, low dose gradient	2%	3%	4%
δ_2*	*Build-up region of central axis beam, penumbra region of the profiles* - high dose, high dose gradient	2 mm or 10%	3 mm or 15%	3 mm or 15%
δ_3	*Outside central beam axis region* - high dose, low dose gradient	3%	3%	4%
δ_4**	*Outside beam edges* – low dose, low dose gradient	30% (3%)	40% (4%)	50% (5%)
RW_{50} ***	***Radiological width* – high dose, high dose gradient.**	2 mm or 1%	2 mm or 1%	2 mm or 1%
δ_{50-90}	***Beam fringe* – high dose, high dose gradient**	2 mm	3 mm	3 mm

(normalized at central axis same depth)

Adopted from Venselaar, 2001

Confidence limit

Statistical approach

The confidence limit is based on the determination of the mean deviation between calculation and measurement for a number of data points for comparable situations, and the standard deviation (1 SD) of the deviation, and is defined as:

$$\Delta = |\text{mean deviation}| + k * SD$$

k=1.5 - In later publications it was suggested to use a factor of 2, instead of the value of 1.5

(Venselaar *et al.*, Radiother. Oncol. 60, 191–201, 2001)

Tolerances δ, confidence limit, for the local dose deviation *d%(i)*

Region		Homogenous, simple geometry	Complex geometry (wedge, inhomogeneity, asymmetry, blocks / MLC)	More complex geometries****
δ_1	*Central beam axis data* – high	2%	3%	4%
δ_2*				m
δ_3				
δ_4**				(5%)
RW_{50} ***	**dose, high dose gradient.**			m or 1%
$\delta_{50\text{-}90}$	***Beam fringe*** **– high dose, high dose gradient**	2 mm	3 mm	3 mm

The tolerances, if applied to the confidence limit, can be exceeded in two ways; either because the mean deviation of all points is too large
or because a few data points show extreme deviations and therefore the SD is too large.

(normalized at central axis same depth)

Adopted from Venselaar, 2001

EXAMPLES – POINT AND LINE MEASUREMENTS (N=1)

Open field depth doses 6 MV

Depth dose curves normalized to the output at 10 cm depth of the 10cm x 10cm field.

Ratio, $d(i)$, between calculated and measured dose per monitor unit values

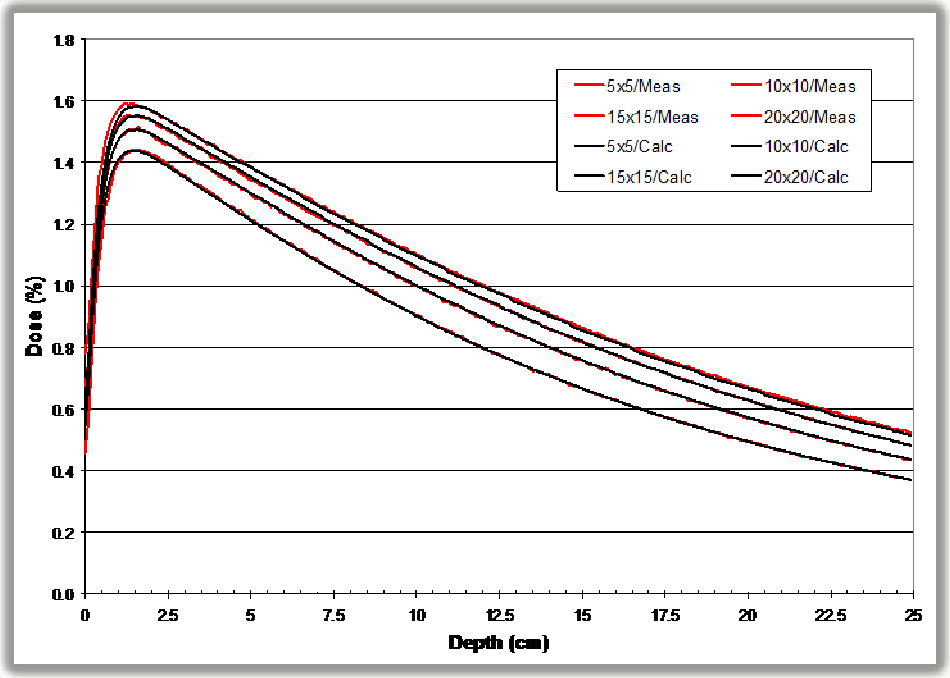

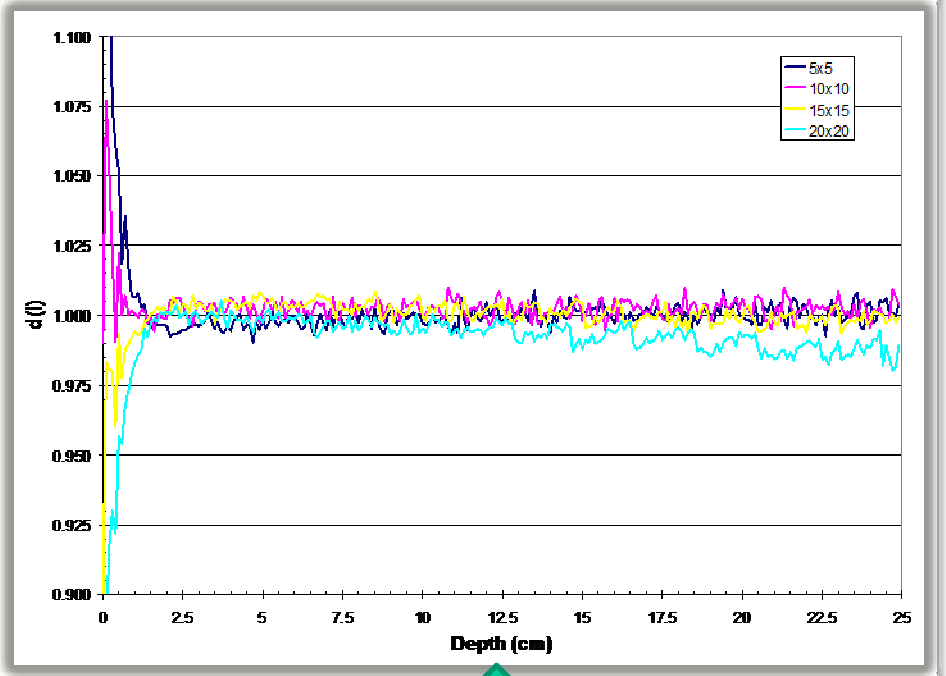

$$d(i) = \frac{\frac{D_c(i)/M_c}{D_c(ref)/M_c}}{\frac{D_m(i)/M_m}{D_m(ref)/M_m}}$$

Evaluation of PDDs

Build-up region (0-2 cm)	**Field size**	**Field size**	**Field size**	**Field size**
Tol. 10 %	5x5 cm^2	10x10 cm^2	15x15 cm^2	20x20 cm^2
Average deviation (%)	3.7	0.7	- 1.3	- 3.7
Standard deviation (%)	6.2	2.1	2.4	5.1
Confidence limit (%)	**13.0**	3.9	5.0	**11.3**
Remaining curve (2-25 cm)				
Tol. 2 %	5x5 cm^2	10x10 cm^2	15x15 cm^2	20x20 cm^2
Average deviation (%)	- 0.1	0.2	0.1	- 0.6
Standard deviation (%)	0.3	0.3	0.3	0.5
Confidence limit (%)	0.5	0.7	0.6	1.4

Statistical evaluation of the deviations between calculated and measured data of the four 6 MV depth dose curves. Note that the confidence limits for the 5x5 cm^2 and 20x20 cm^2 do not fulfill the recommended 10% accuracy requirement of dose calculations of a TPS in the build-up region.

Dose and monitor unit calculation

Data from point measurements using an ionization chamber positioned at 20 cm depth along the central beam axis in a large water phantom, source-skin distance 90 cm, irradiated with a beam of 18 MV x-rays.

		Measured			Calculated			
	Type	Dose (Gy)	MU	(Dose/MU) meas	Dose	MU	(Dose/ MU) calc	*d(i) /d%(i)*
5x5	Open	0.557	100	0.00557	1.00	184.78	0.00541	0.971 / -2.9%
	60º Wedge	0.152	100	0.00152	1.00	677.73	0.00148	0.969 / -3.1%
10x10	Open	0.614	100	0.00614	1.00	165.46	0.00604	0.984 / -1.6%
	60º Wedge	0.173	100	0.00173	1.00	579.46	0.00173	1.000 / 0.0%
20x20	Open	0.673	100	0.00673	1.00	149.80	0.00668	0.993 / -0.7%
	60º Wedge	0.197	100	0.00197	1.00	527.66	0.00189	0.964 / -3.6%
30x30	Open	0.694	100	0.00694	1.00	145.35	0.00688	0.991 / -0.9%
	60º Wedge	0.206	100	0.00206	1.00	509.46	0.00196	0.951 / -4.9%
5x20	Open	0.597	100	0.00597	1.00	168.16	0.00595	0.997 / -0.3%
	60º Wedge	0.167	100	0.00167	1.00	593.02	0.00169	1.010 / +1.0%
20x5	Open	0.589	100	0.00589	1.00	172.77	0.00579	0.983 / -1.7%
	60º Wedge	0.164	100	0.00164	1.00	622.97	0.00162	0.979 / -2.1%

Dose and monitor unit calculation

Data from point measurements using an ionization chamber positioned at 20 cm depth along the central beam axis in a large water phantom, source-skin distance 90 cm, irradiated with a beam of 18 MV x-rays.

		Measured			Calculated			
	Type	Dose (Gy)	MU	(Dose/MU) meas	Dose	MU	(Dose/ calc	MU) %(i)
5x5	Open	0.557	100	0.00557	1.00	184.78		%
	60º Wedge	0.152	100	0.00152	1.00	677.7		3.1%
10x10	Open	0.614	100	0.00614				0.984 / -1.6%
	60º Wedge	0.173	100	0.00173			173	1.000 / 0.0%
20x20	Open	0.673	100			.80	0.00668	0.993 / -0.7%
	60º Wedge	0.197	10			527.66	0.00189	0.964 / -3.6%
30x30	Open	0.6			1.00	145.35	0.00688	0.991 / -0.9%
	60º Wed			0206	1.00	509.46	0.00196	0.951 / -4.9%
5x20			100	0.00597	1.00	168.16	0.00595	0.997 / -0.3%
			100	0.00167	1.00	593.02	0.00169	1.010 / +1.0%
20x5		0.589	100	0.00589	1.00	172.77	0.00579	0.983 / -1.7%
	60º Wedge	0.164	100	0.00164	1.00	622.97	0.00162	0.979 / -2.1%

Obtaining the dose/MU either by fixed MU at measurents or fixed dose at calculation!

DISTRIBUTIONS (N>1)

Methods for dose distribution comparison

- Dose distribution overlays - requires that the user interpret the differences themselves
- Dose-difference distributions - has the limitation that very large dose differences can be caused by relatively small spatial discrepancies in steep dose gradient regions
- Distance-to-agreement - has the limitation of large distances in homogeneous areas
- Quantitative comparison tools
  - Composite tool
  - Gamma and similar tools - useful when a large amount of dose data needs to be reviewed quickly, such as for routine patient QA. When discrepancies are identified, the clinical impact of those discrepancies can e.g. be determined using the dose difference tool.
- No single dose comparison tool provides all of the information necessary to quantitatively evaluate or compare dose distributions.

Inspired by Low et al 2011, Med Phys

An early attemp at WUSTL

The dose-difference, $\delta(\mathbf{r}_m)$, at position $\mathbf{r}_m$ (on the measured distribution) is equal to

$$\delta(\mathbf{r}_m,\mathbf{r}_c)\equiv D_m(\mathbf{r}_m)-D_c(\mathbf{r}_c)$$

← Dose difference

The DTA, $d(\mathbf{r}_m)$, is given by

$$d(\mathbf{r}_m)=\min\{r_0(\mathbf{r}_m,\mathbf{r}_c)\}\in\{\mathbf{r}_c\},$$

← The distance between the two nearest points with the same dose

where

$$r_0(\mathbf{r}_m,\mathbf{r}_c)=\{r(\mathbf{r}_m,\mathbf{r}_c)\}\Rightarrow\delta(\mathbf{r}_m,\mathbf{r}_c)=0$$

zero between calculated and measured dose

Binary composite model

C=0 if both criteria fulfilled

C=1 if one or both fail

$$c(\mathbf{r}_m)=\delta_f(\mathbf{r}_m)\times d_f(\mathbf{r}_m),$$

where

$$\delta_f(\mathbf{r}_m)=\begin{cases}0 & |\delta(\mathbf{r}_m)|\leq\Delta D_M\\ 1 & |\delta(\mathbf{r}_m)|>\Delta D_M\end{cases}$$

and

$$d_f(\mathbf{r}_m)=\begin{cases}0 & |d(\mathbf{r}_m)|\leq\Delta d_M\\ 1 & |d(\mathbf{r}_m)|>\Delta d_M\end{cases}$$

Harms et al Med Phys 1998

Example

Harms et al Med Phys 1998

3% / 3 mm

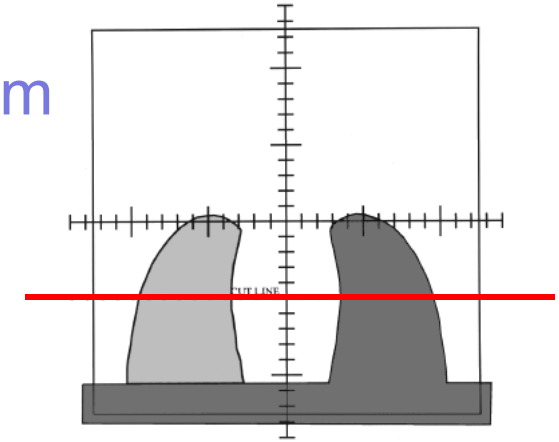

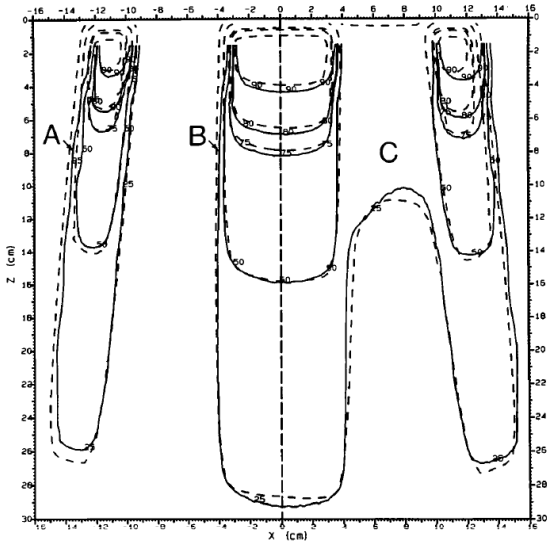

Dose diffence

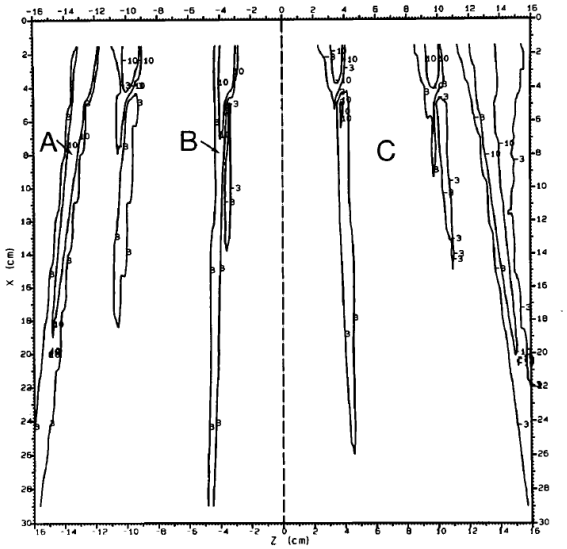

Distance to agreement

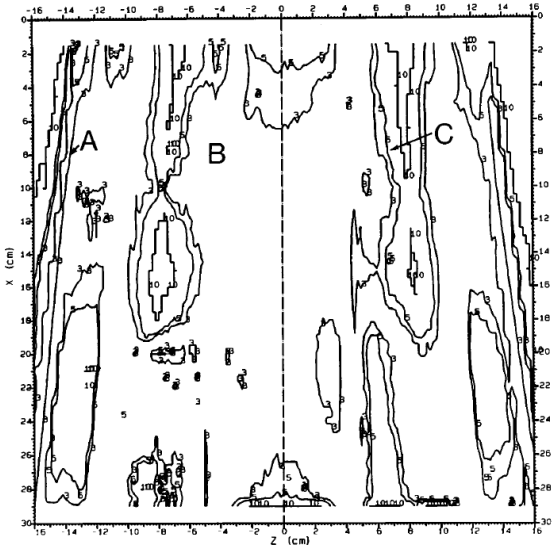

Composite

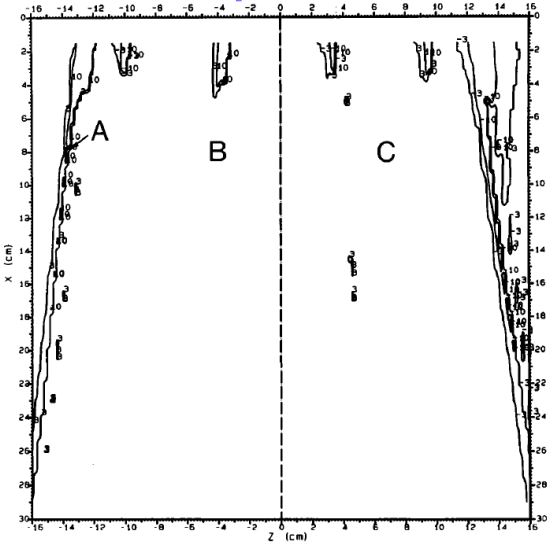

Gamma evaluation (also at WUSTL)

- A more quantative measure
- Combining
  - Dose difference
  - Distance to agreement (DTA)
- Instead of binary composite function, use

$$\gamma(\mathbf{r}_m) = \min\{\Gamma(\mathbf{r}_m, \mathbf{r}_c)\} \forall \{\mathbf{r}_c\},$$

where

$$\Gamma(\mathbf{r}_m, \mathbf{r}_c) = \sqrt{\frac{r^2(\mathbf{r}_m, \mathbf{r}_c)}{\Delta d_M^2} + \frac{\delta^2(\mathbf{r}_m, \mathbf{r}_c)}{\Delta D_M^2}},$$

Low et al Med Phys 1998

Gamma function

- Same DTA and dose difference but normalised to the tolerance (as in the Harms et al paper)
- Square-root summed together
- For eached ”measured” point - gamma can be calculated
- Even for a single point compared to a calculated dose matrix
- 2D or 3D!!! Usually only in 2D

Gamma analysis

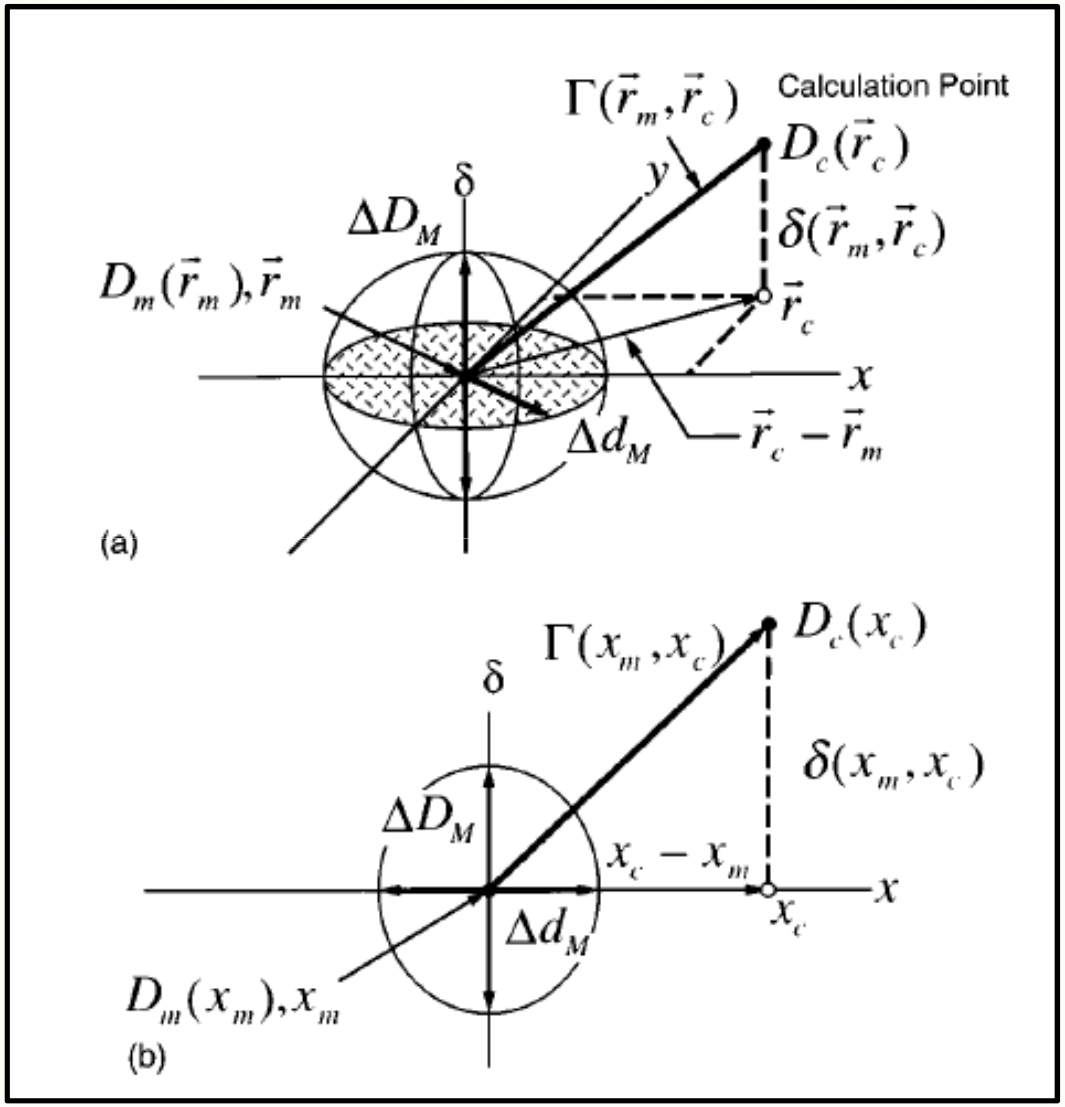

Two dimensional e.g. films or detector arrays

One dimensional e.g. Profiles and depth doses

Gamma (γ) analysis in 2D

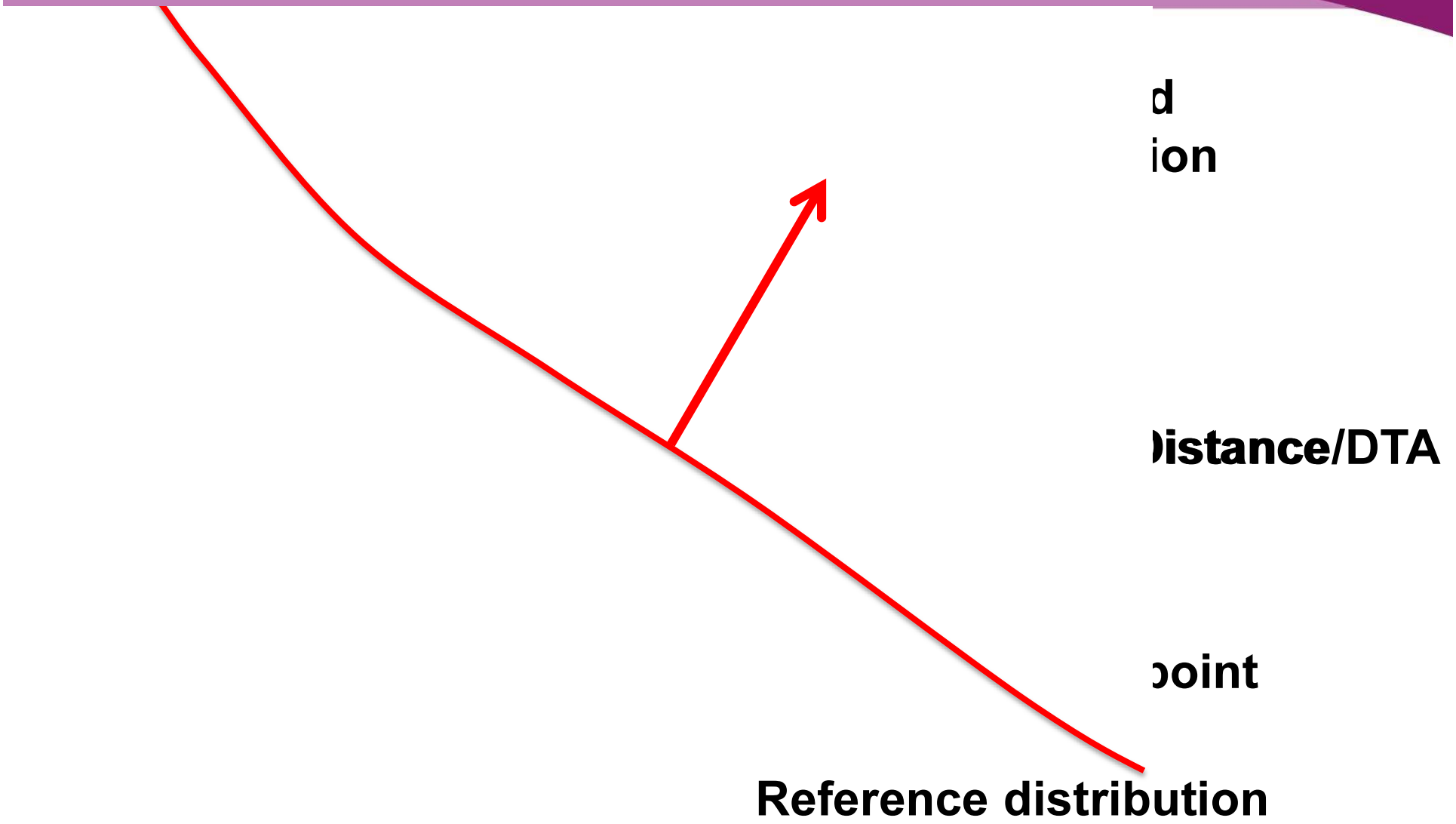

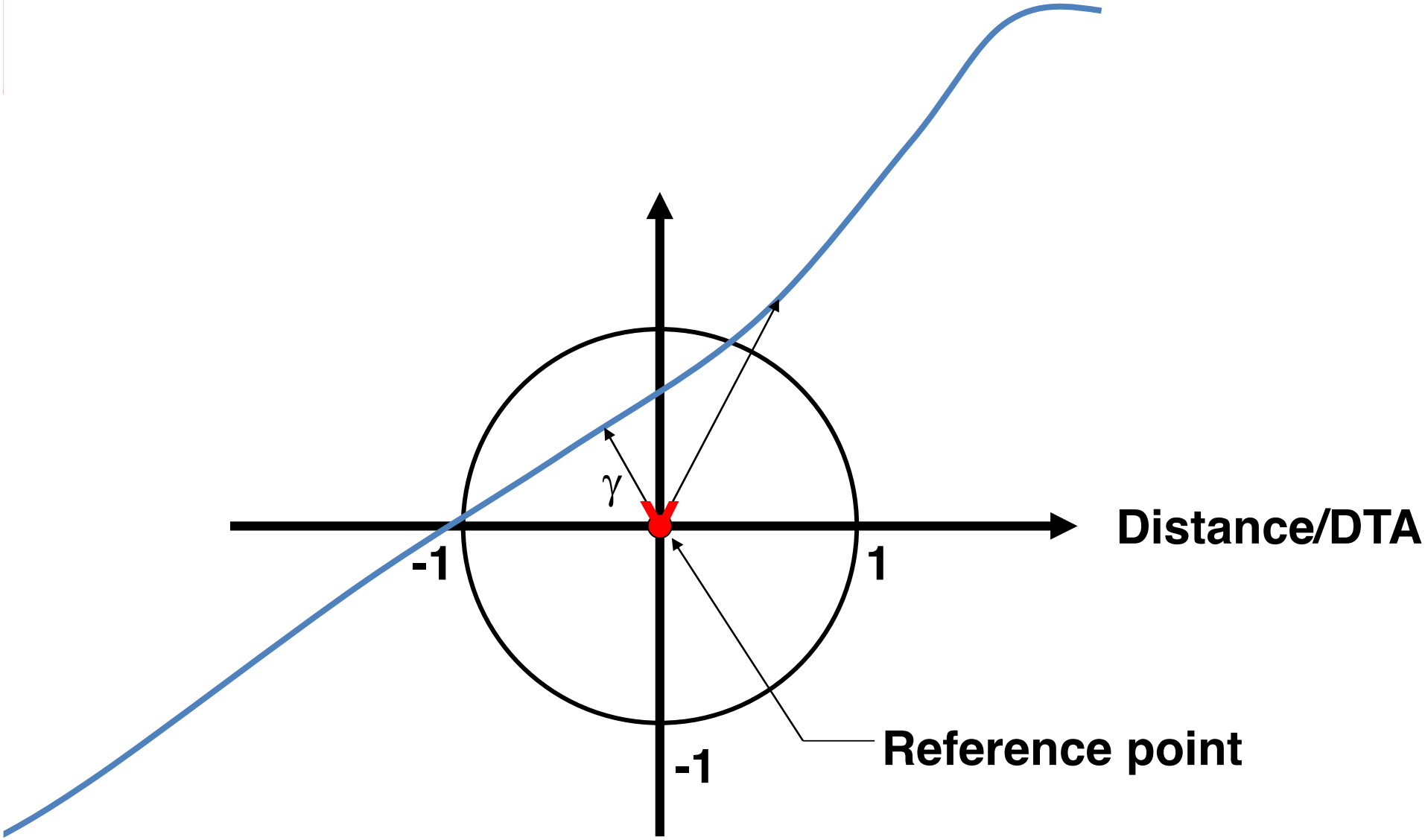
γ
-1
1
-1
Distance/DTA
Reference point

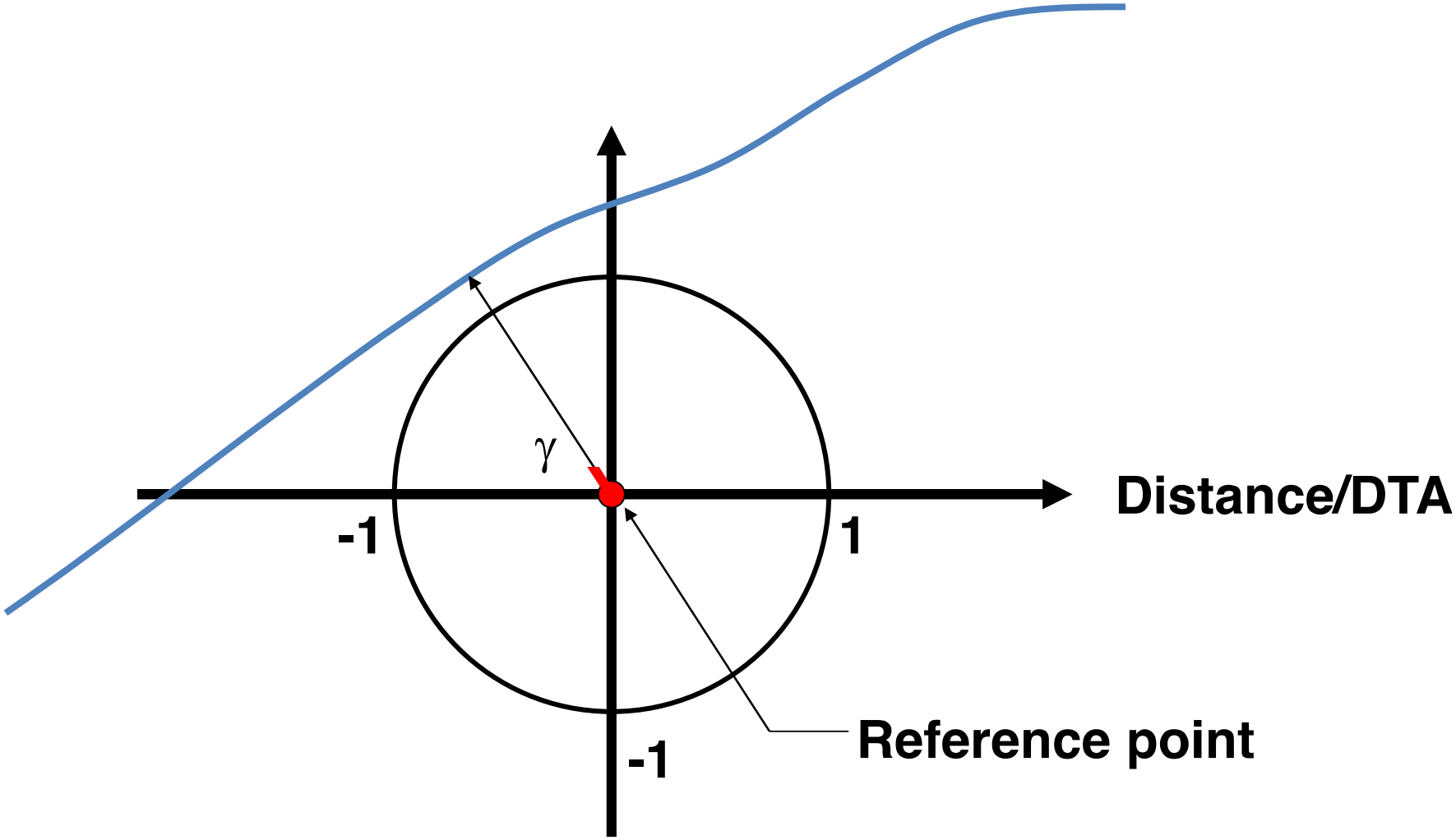
γ
Distance/DTA
-1
1
-1
Reference point

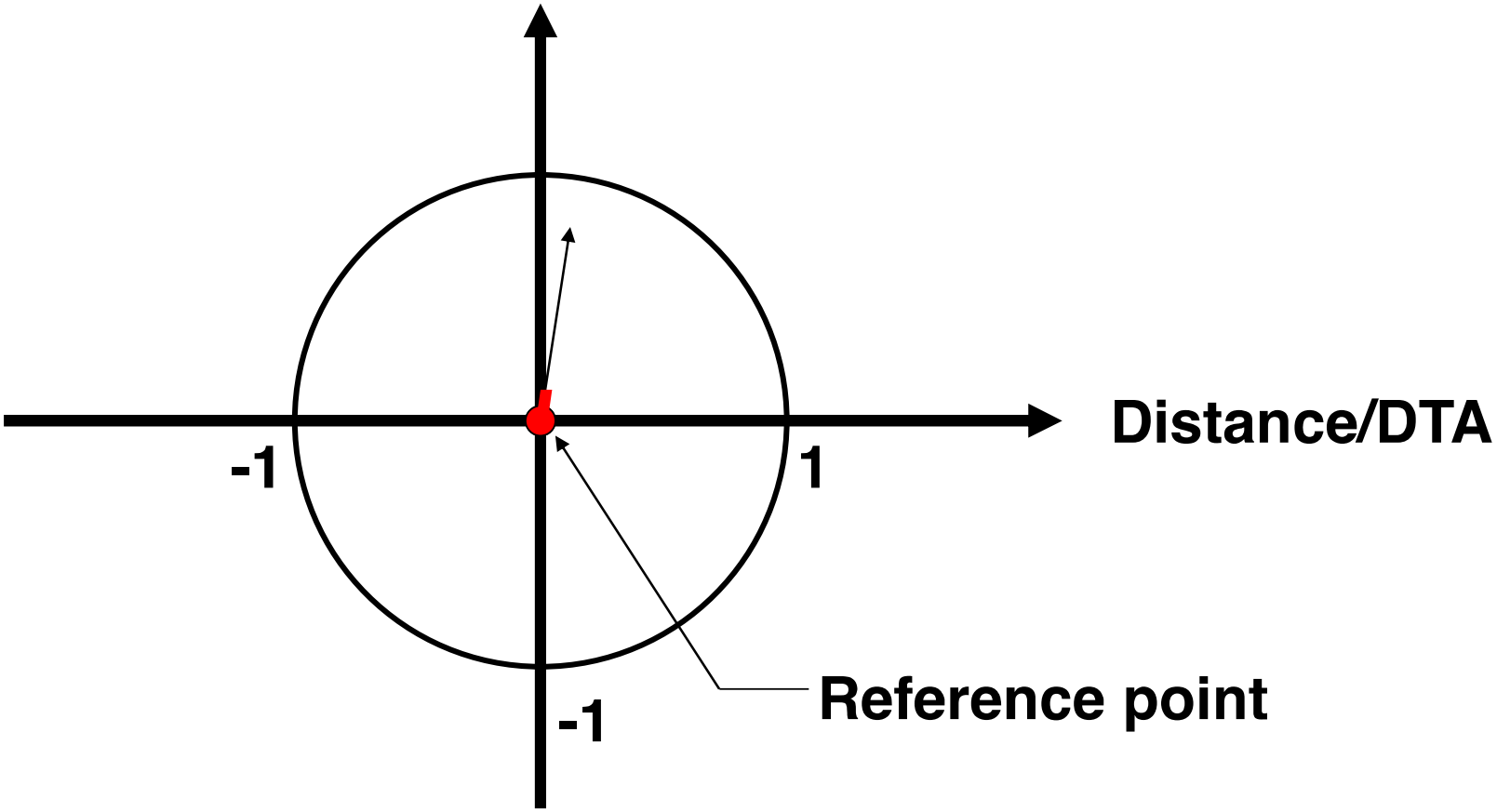
Distance/DTA
-1
1
-1
Reference point

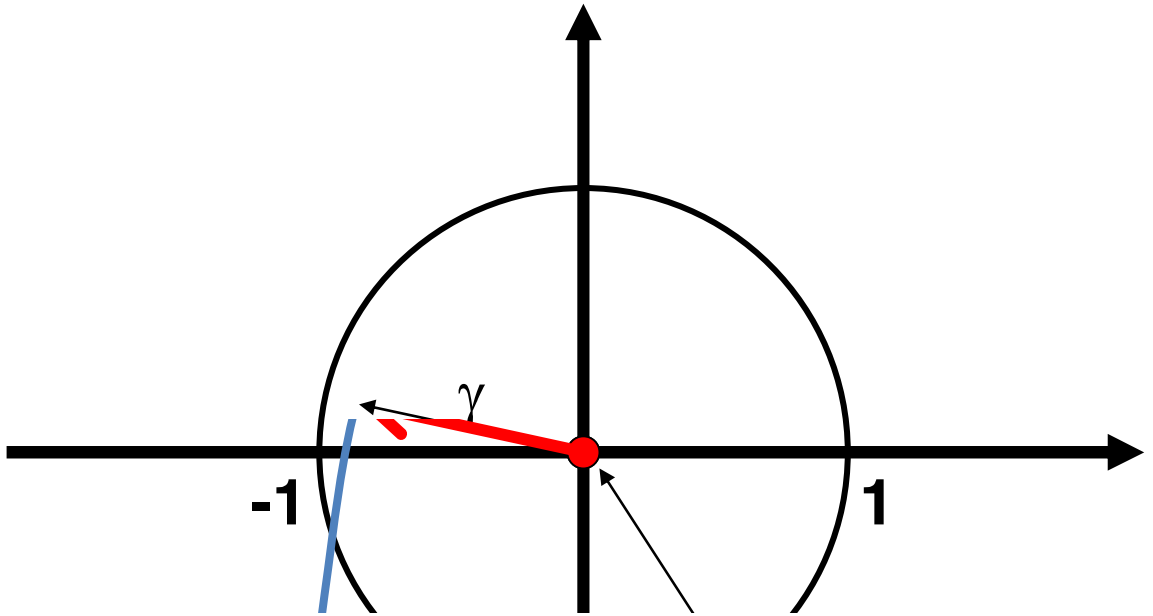

γ defaults to dose-difference and DTA in shallow and steep dose gradients, respectively

point

Gamma evaluation – value and angle

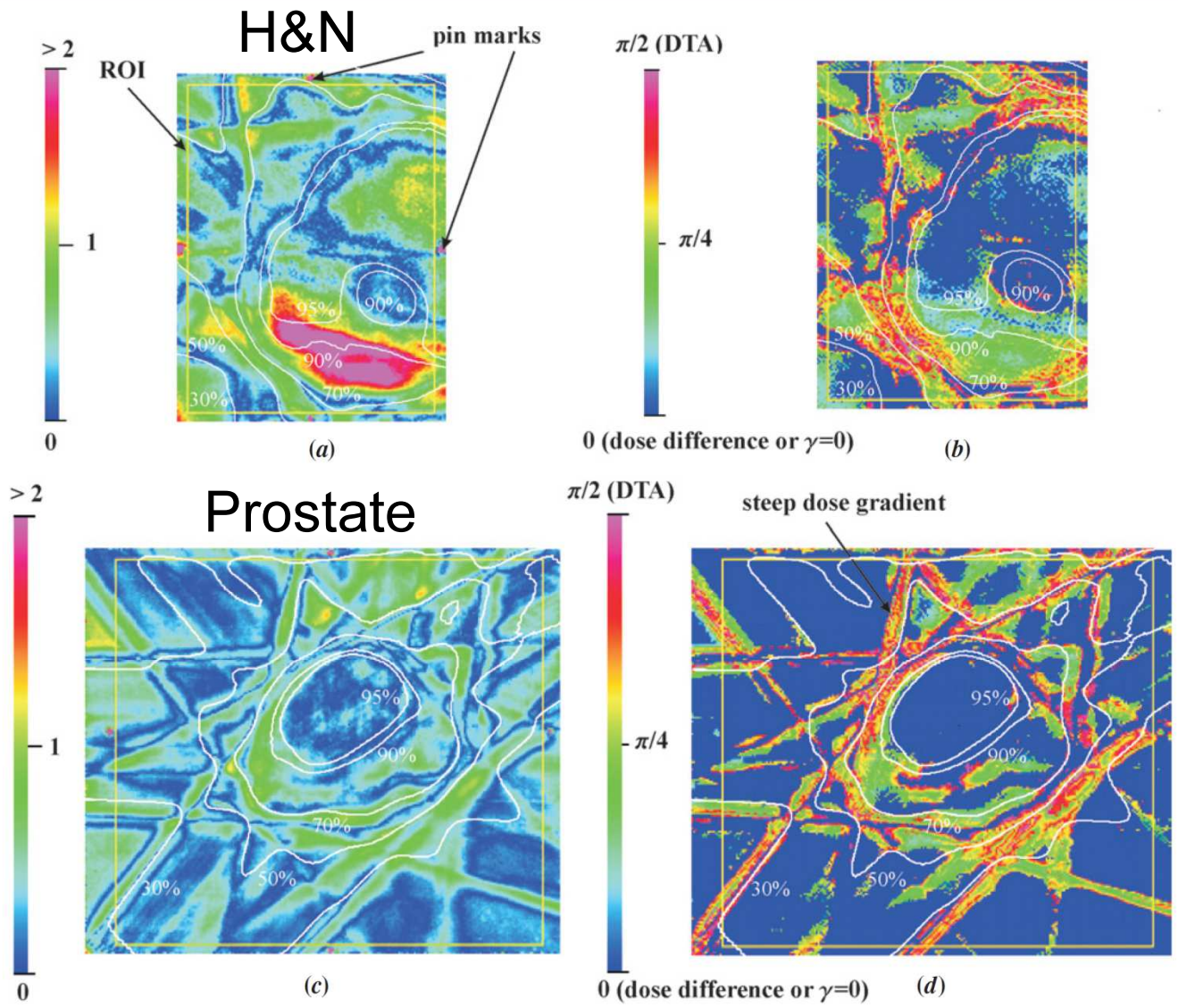

With the angle added one can easily judge if it is DTA or dose that contributes to the deviation

White lines represent isodoses (30%, 50%, 70%, 90% and 95%) calculated with the TPS

3%/3mm

Stock et al PMB 2005

ESTRO School

EXAMPLES

Example on evaluation

Reference

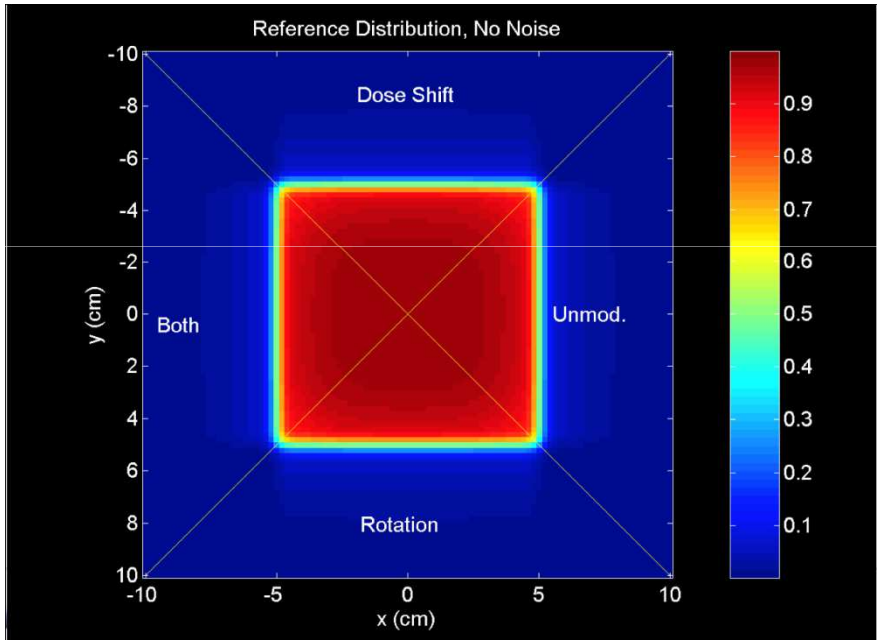

Evaluation

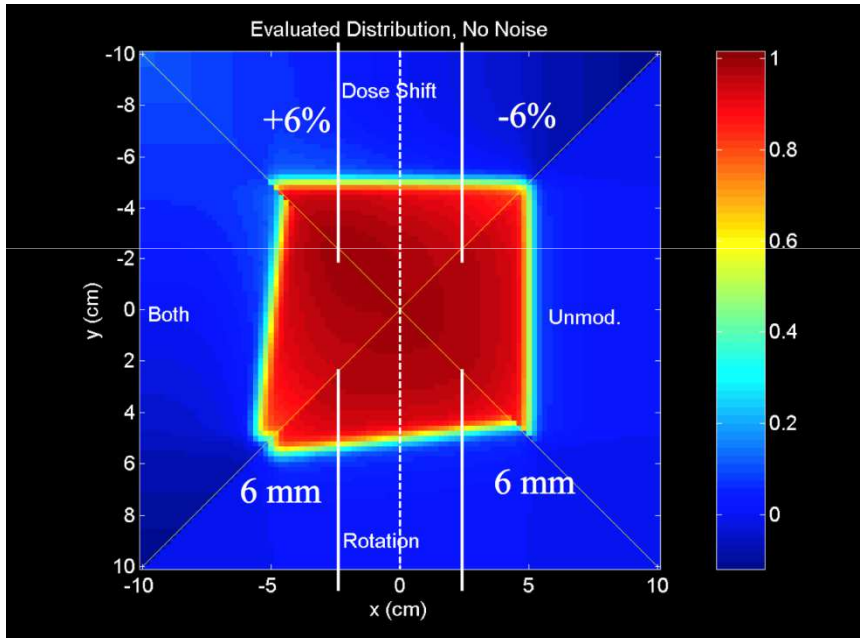

Low and Dempsey, Med Phys, 2003

ESTRO School

Analysis – Dose difference and DTA

Dose difference

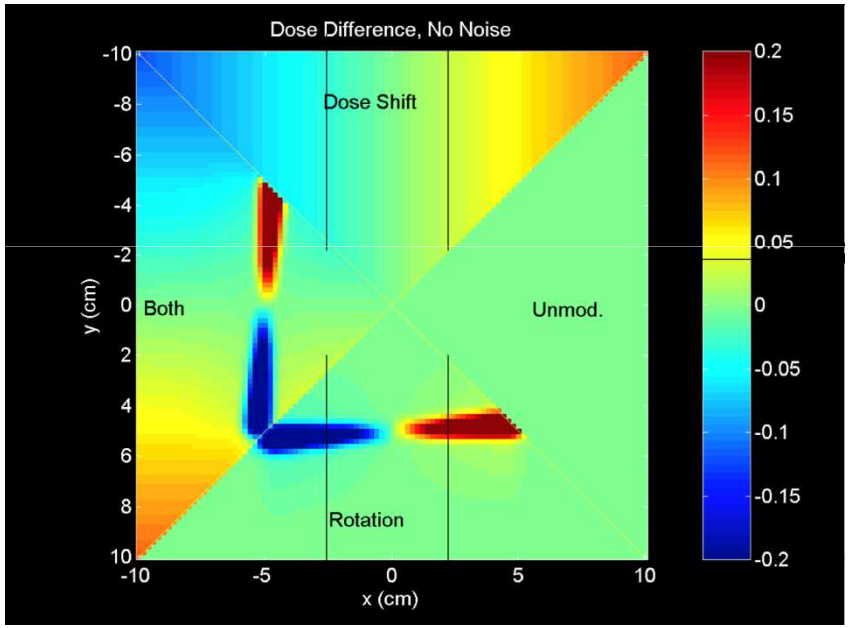

Distance to agreement

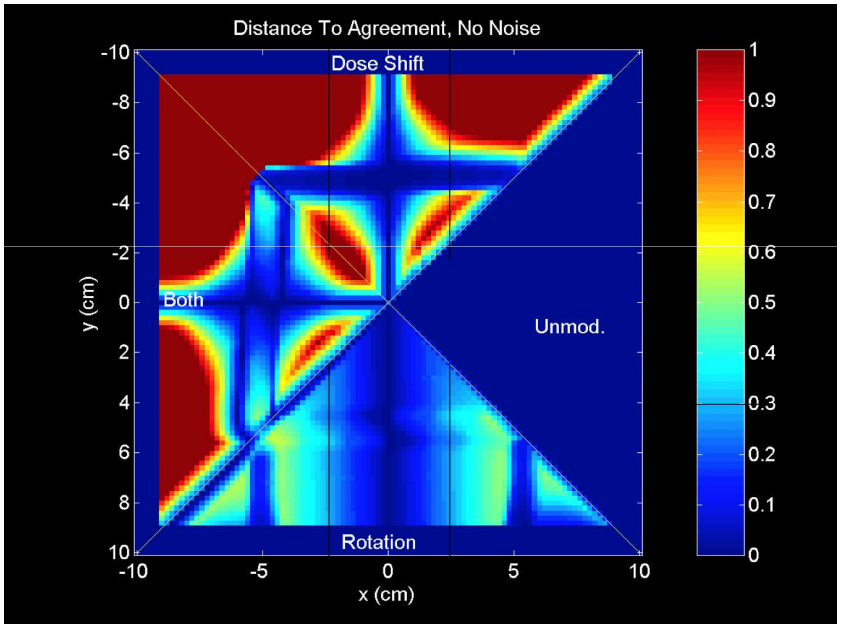

Low and Dempsey, Med Phys, 2003

ESTRO School

Analysis – Composite and Gamma

Composite

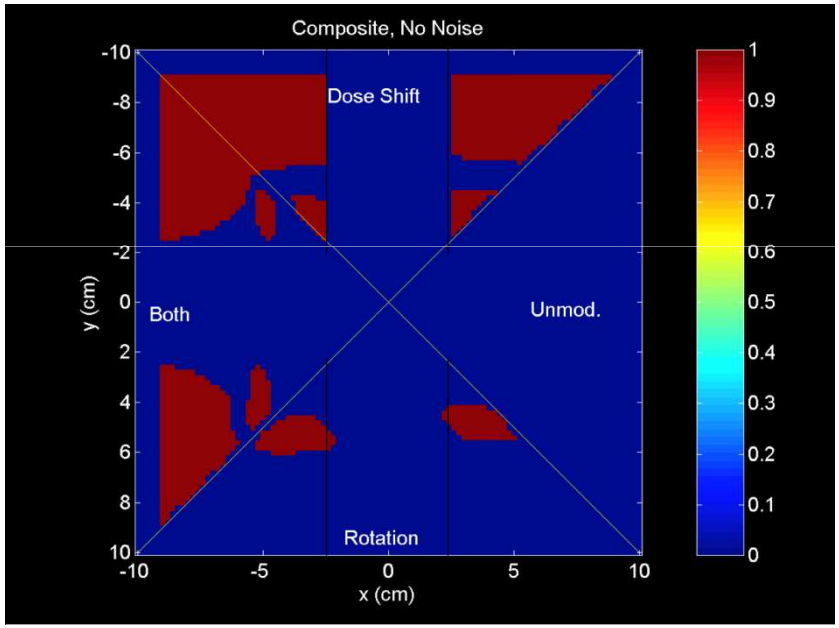

Gamma

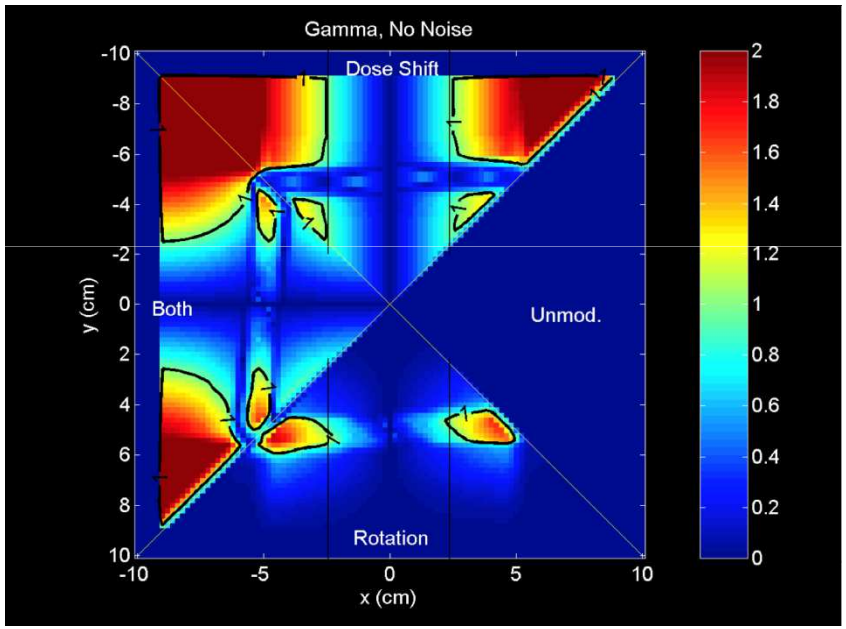

Low and Dempsey, Med Phys, 2003

ESTRO School

Course evaluation grid – interpolation

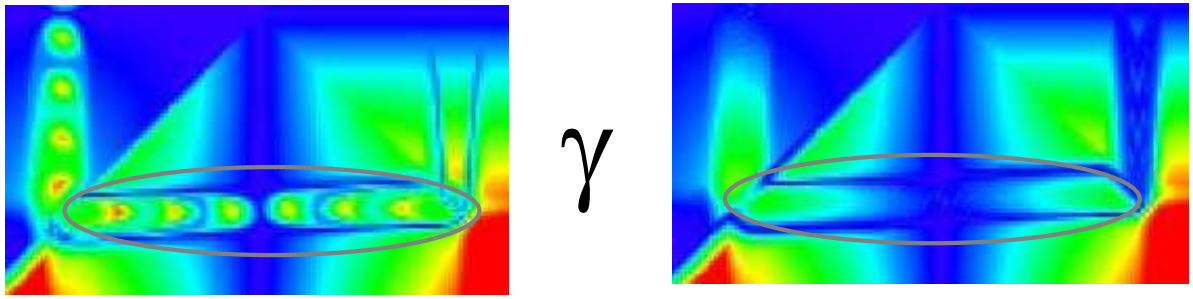

Uninterpolated

Interpolated voxels 8x

Further reading - Ju et al. Med. Phys. 35, 879-887 (2008)

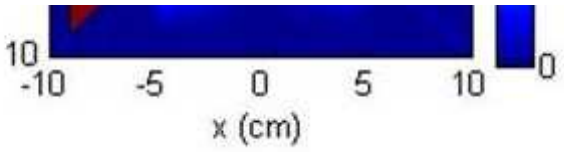

No Noise

3% Noise Evaluation

3% Noise Reference

Underestimation

Low and Dempsey, Med Phys, 2003

Don’t loose the details

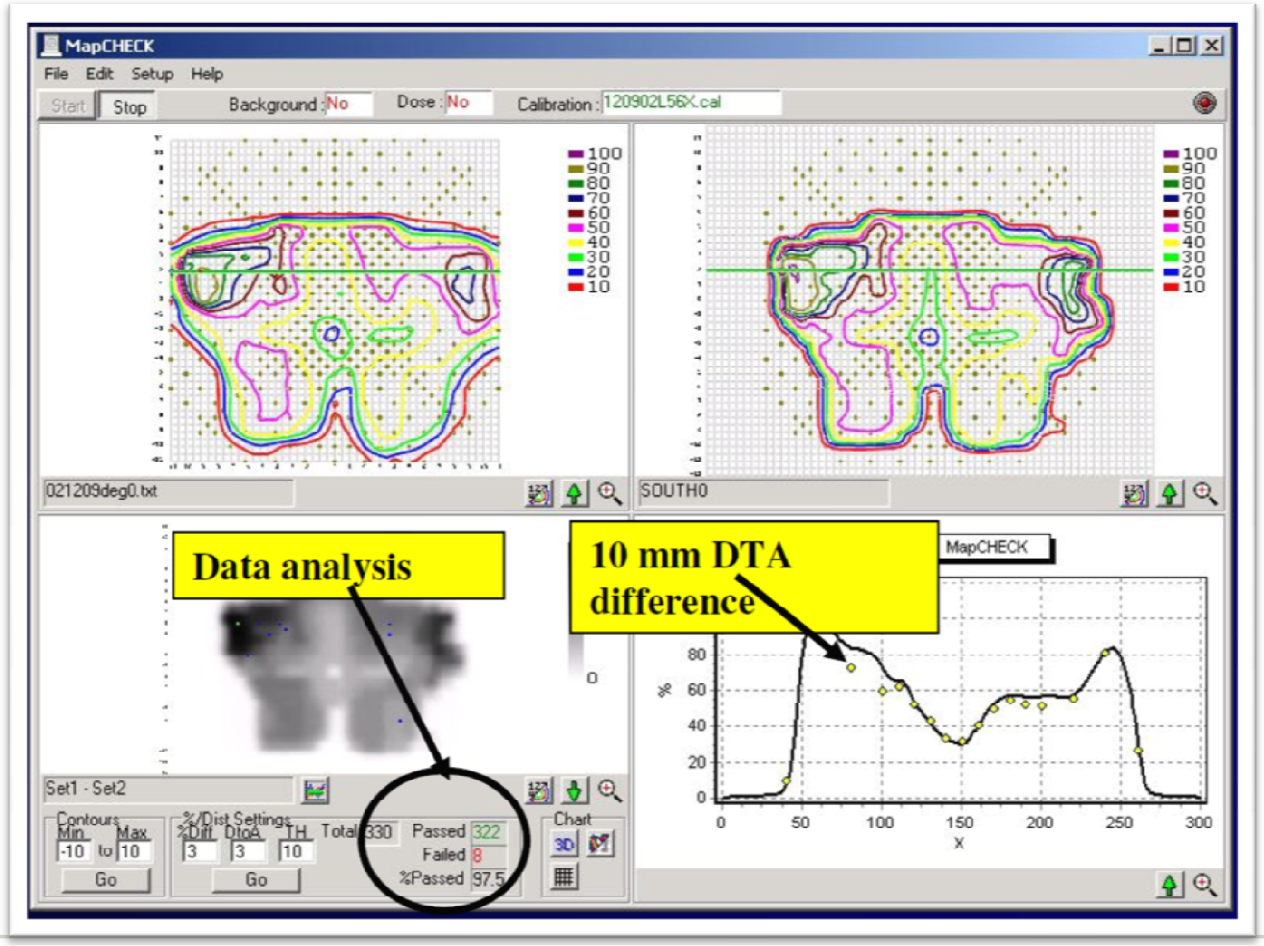

Comparison of a measured and calculated cross-plot (at 5 cm depth) of an intensity modulated field incident on a flat phantom. A diode-array (MapCheck; Sun Nuclear Corp.) was used for this comparison, which shows that 97.5% of the points meet 3% criteria even though DTA (distance to agreement) for a few points is 10 mm.

Can be crucial for organs at risk.

From J Palta AAPM 2005

ESTRO School

Choice of reference point - important

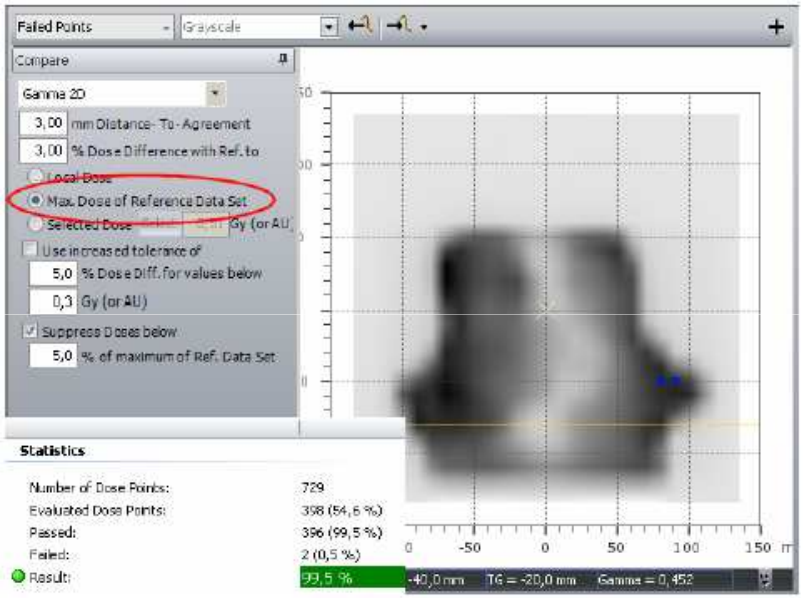

Figure 1: Comparison with a global dose point as reference

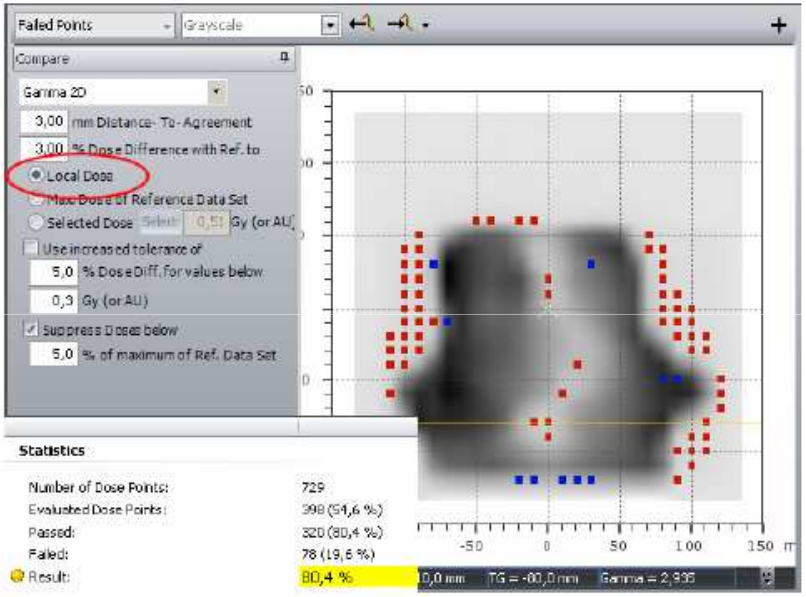

Figure 2: Comparison with local dose points as reference

ESTRO School

Different methods

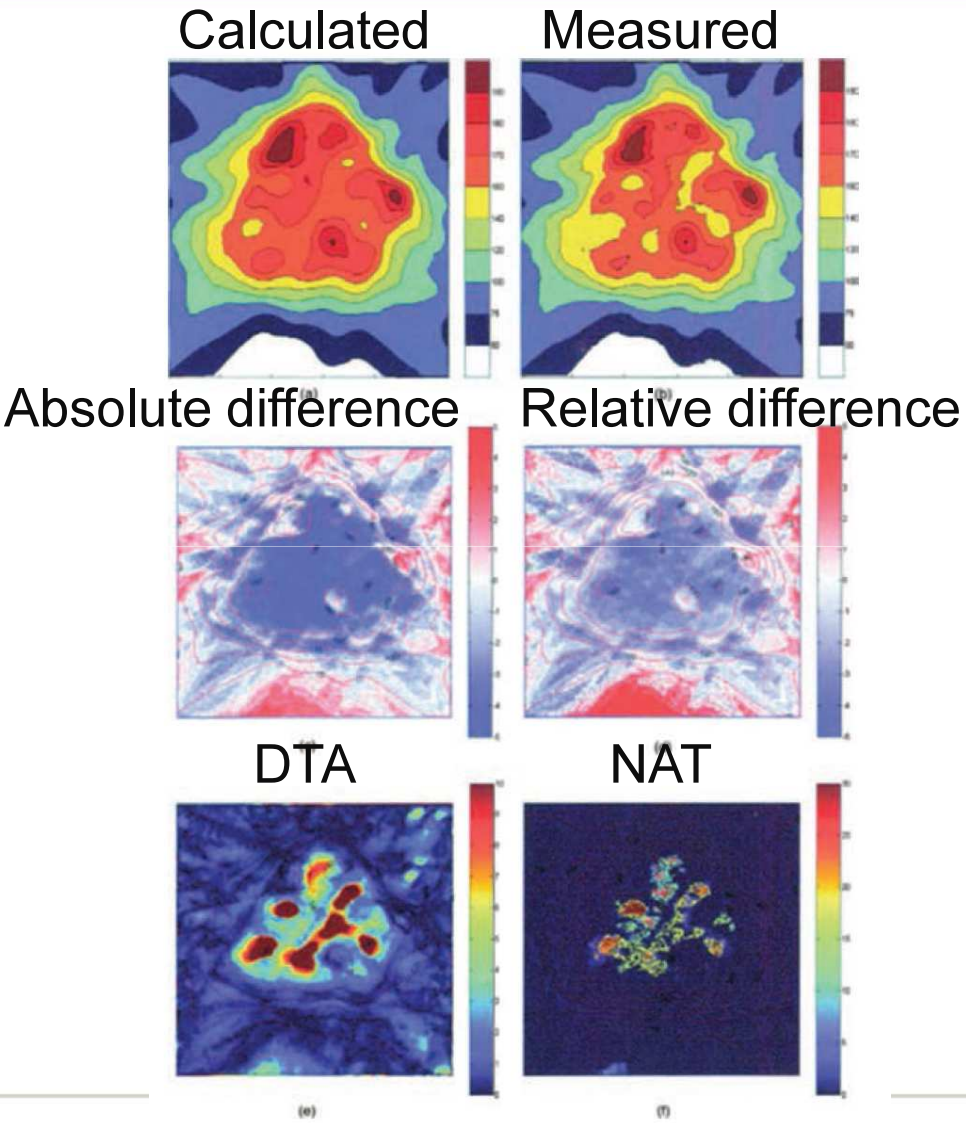

The NAT calculation is similar to gamma, but is zero where the doses agree within acceptable tolerances, so the comparison values are displayed only in the regions that fail the comparison and are greater than 75% of the prescription dose.

This allows the user to focus on the regions that failed and not be distracted by the regions that passed the comparison tests.

N. L. Childress and I. I. Rosen, Int. J. Radiat. Oncol., Biol., Phys. 56, 1464–1479 2003
Low et al Med Phys 38(3) 2011..

Should IMRT patient QC be done field-by-field or for the composite plan?

- Assume a 5 field plan each beam contributes with 1/5 to the target

- Each beam are delivered within 3 % of calculation
- Except for one that is 15% off.
- This **plan** will not pass field-by-field QC
- For a composite plan you **will not** detect this, the plan is within 3%!!!

John Schreiner's Commandments

1. "know and understand your dosimetry system completely, including its limitations, before applying it to a particular validation task"

2. "engage in the clinical exchange of ideas and knowledge through publication in scientific journals, and, perhaps more importantly, through regular communication, meetings and workshops with colleagues locally, nationally and internationally"

Schreiner L J in J Med Phys 2011;36:189-91

Gamma Analysis 3%G/3mm

Example #1

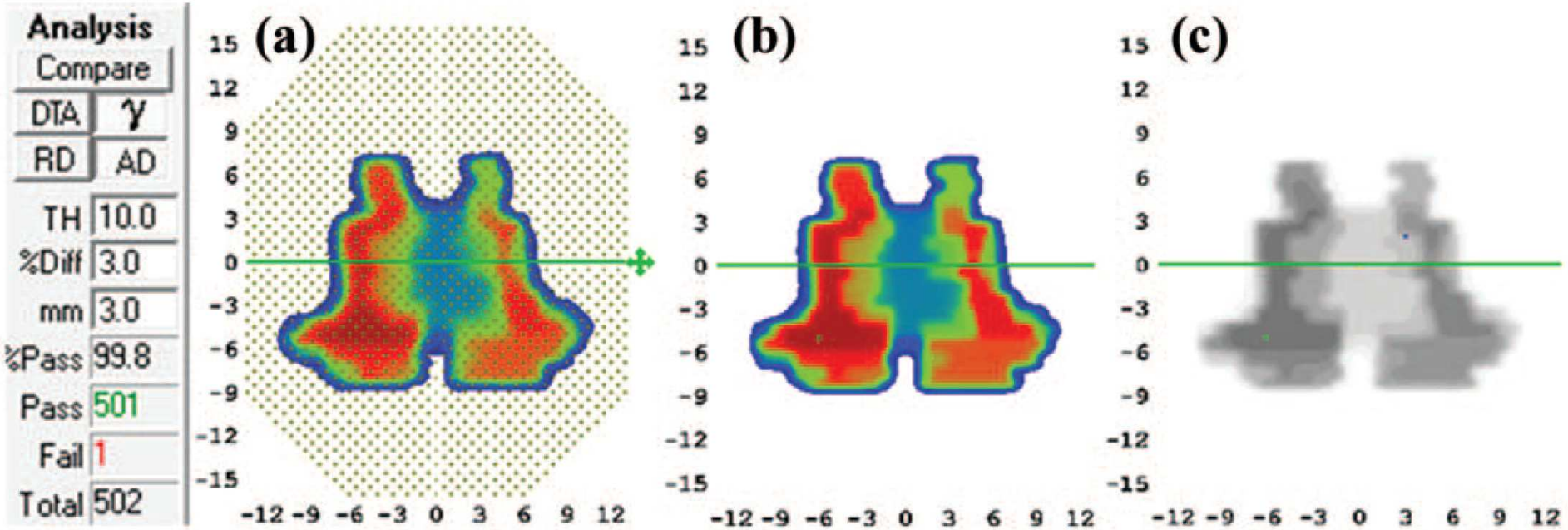

Med Phys 2013 – Nelms et al

ESTRO School

Line or Profile Analysis

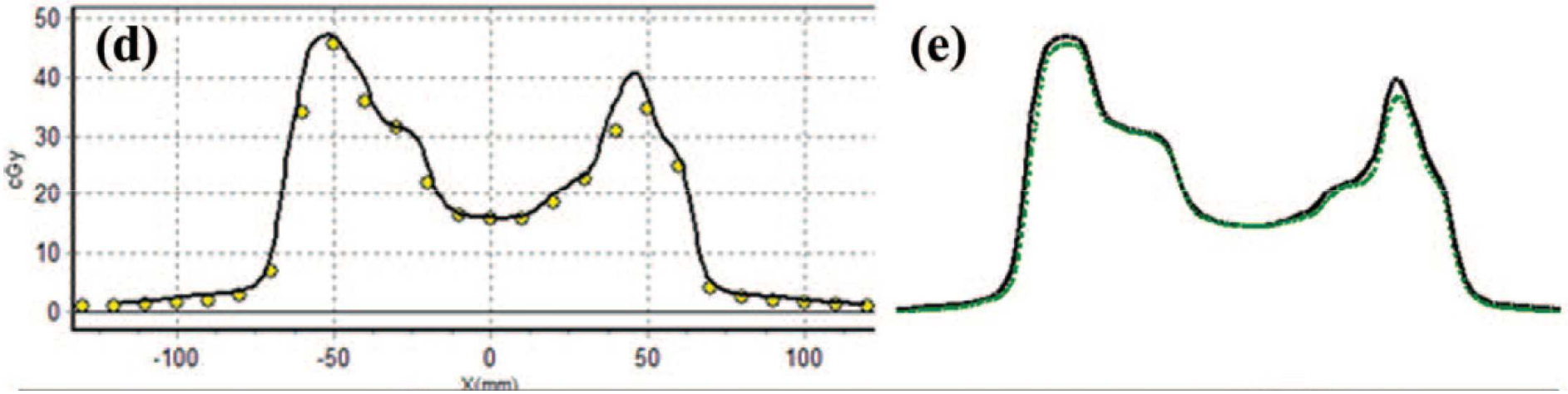

Measurements consistently lower

Med Phys 2013 – Nelms et al

ESTRO School

Measurement Based 3D Calculation

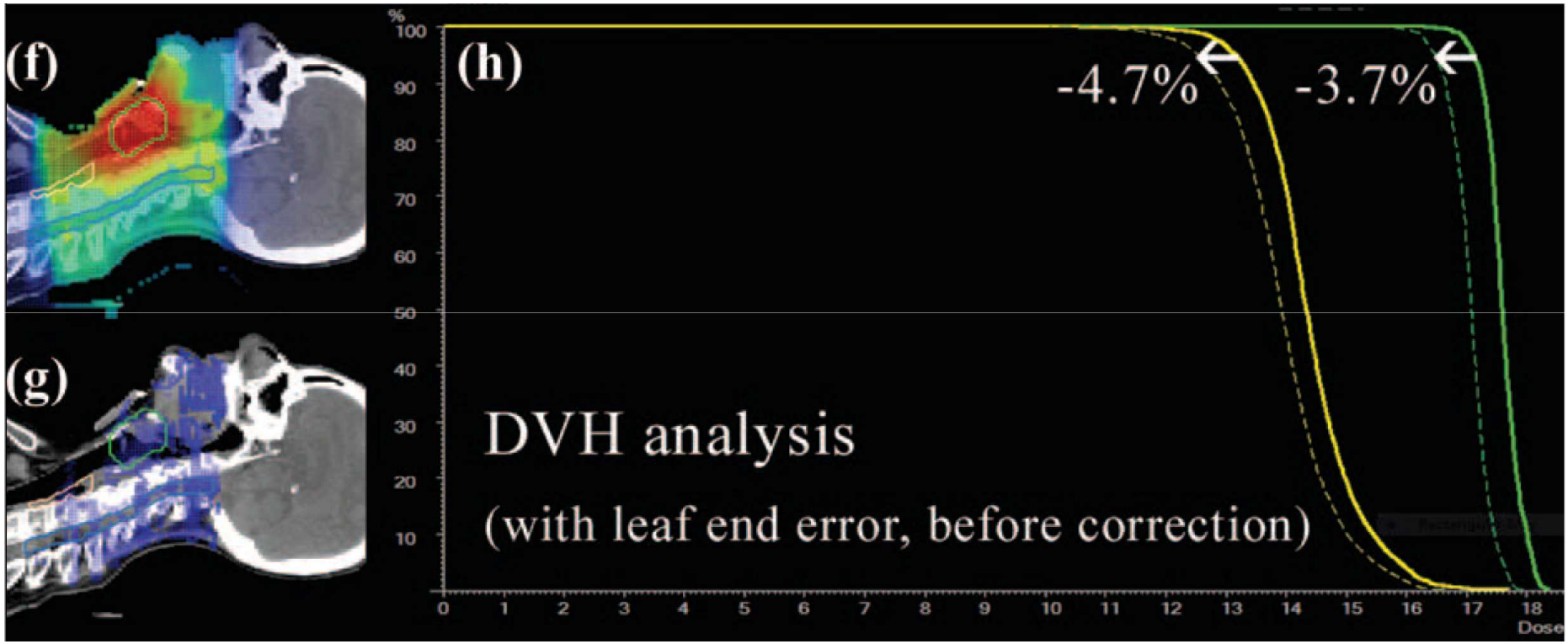

"Measured" dose in both target volumes are about 4% too low

Med Phys 2013 – Nelms et al

ESTRO School

3%G/3mm Fails but 2%L/2mm Detects T/G Errors

Example #2

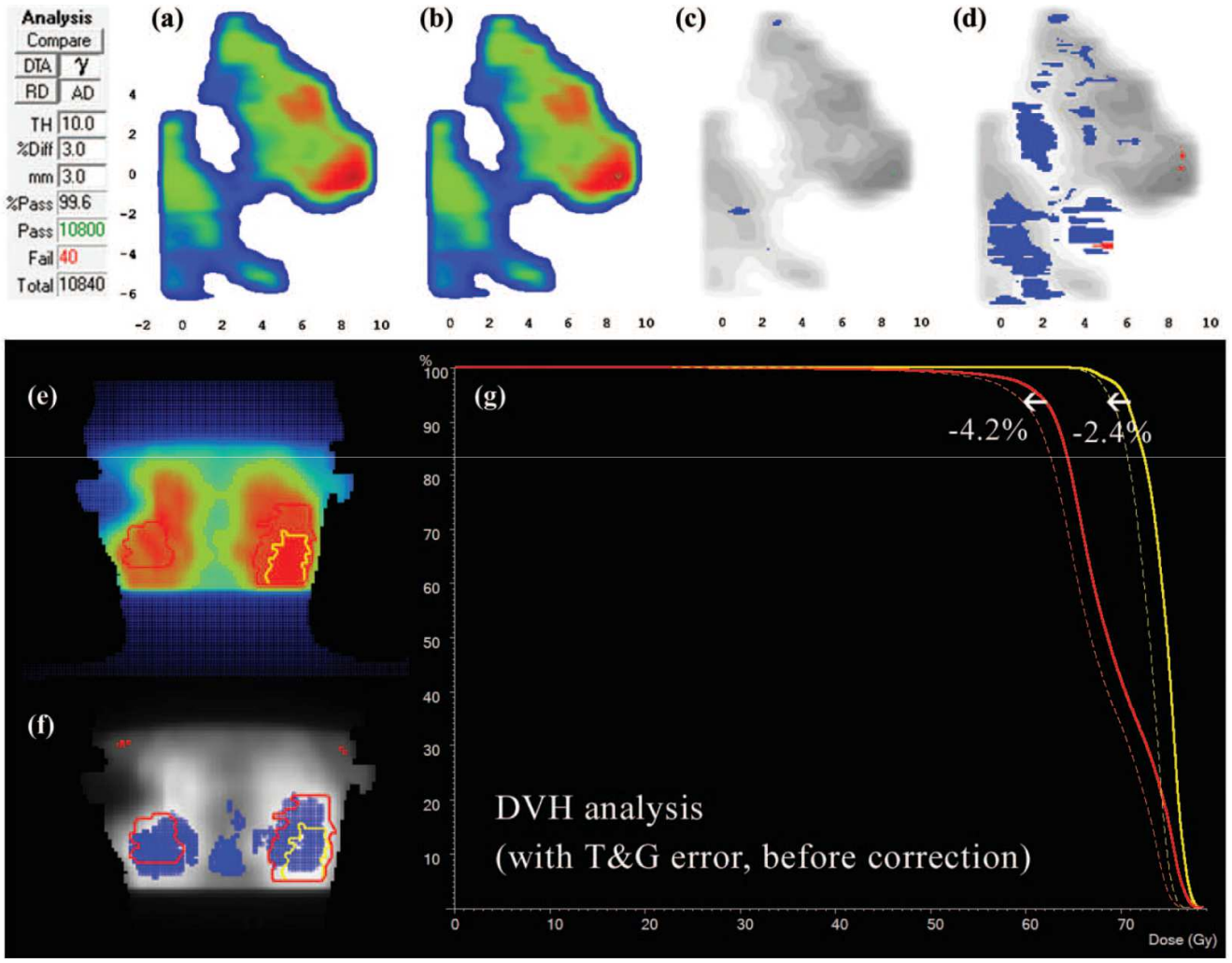

Med Phys 2013 – Nelms et al

1st Commandment Explained

- Metric for γ-analysis
  - "Overreliance on the insensitive metric is counterproductive to quality improvement and can lead to the sense of complacency among the clinical physicists."
  - "IMRT and VMAT commissioning, along with product validation, would benefit from the retirement of the 3%/3 mm passing rates as a primary metric of performance, and the adoption instead of tighter tolerances, more diligent diagnostics, and more thorough analysis."

Med Phys 2013 – Nelms et al

Delta4 and EPID (Portal Dosimetry)

Delta^4-phantom

- 2 diode matrices 3D-phantom
- PMMA
- TPS algorithm

EPID

Electronic Portal Imaging Device

- 2D-detector
- aSi (amorphous silicone)
- Portal Dosimetry Image Prediction (PDIP) algorithm

Courtesy A Karlsson Hauer

Delta^4 vs EPID

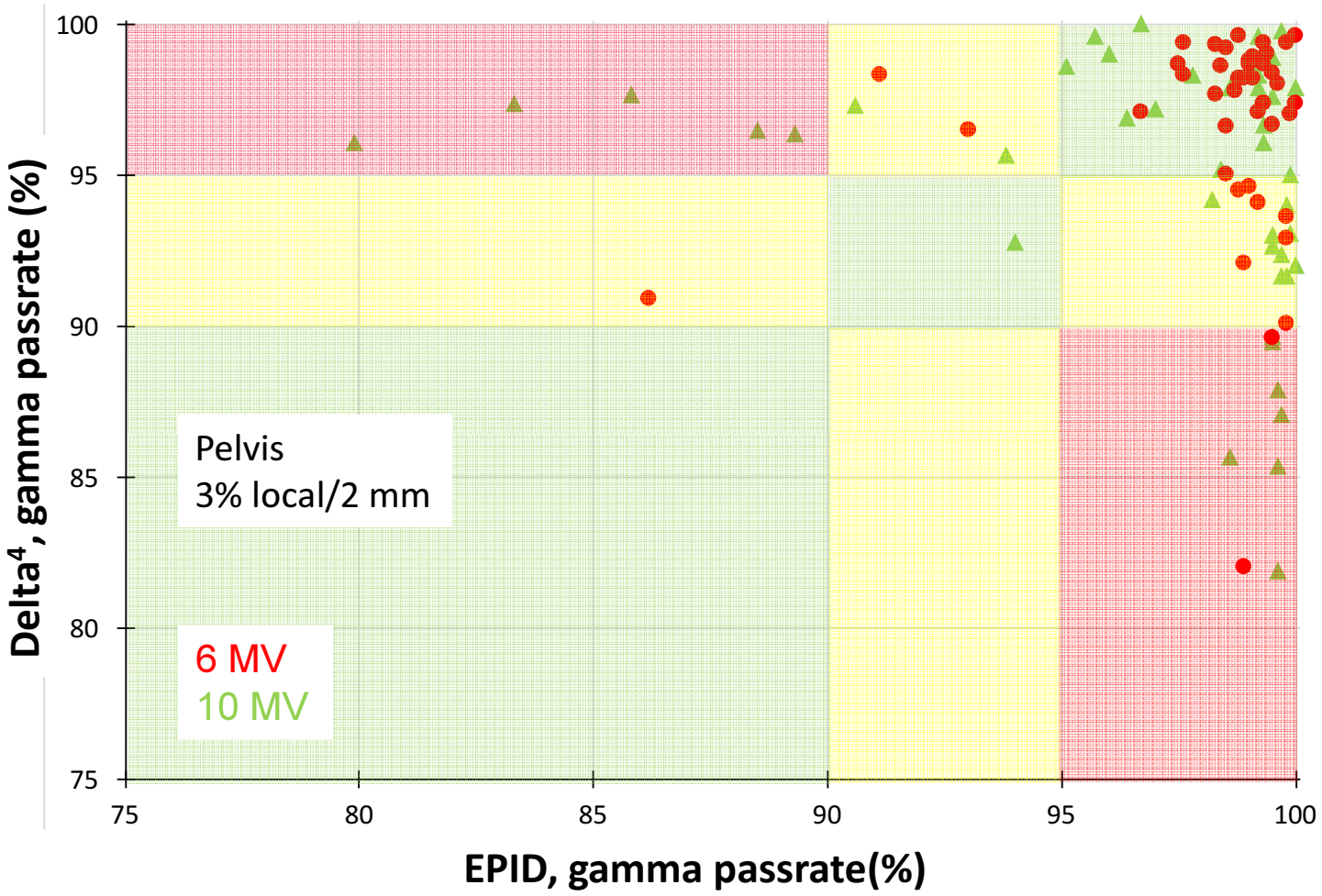

Courtesy A Karlsson Hauer

Criticism of the 3%/3 mm γ metric

- The ubiquitous 3%/3 mm γ analysis metric is **not sensitive enough** to provide optimal results in IMRT/VMAT commissioning.
- Overreliance on the insensitive metric is **counterproductive** to quality improvement and can lead to the sense of complacency among the clinical physicists.
- Use of this metric also enables manufacturers to release products that may not be validated with sufficient rigor, hindering them from designing error out of the system before commercial release.
- "adoption of more sensitive metrics/tighter tolerances enables continual improvement of the accuracy of radiation therapy dose delivery"
- Adoption of sensitive metrics and tighter tolerances fit the larger goal to better standardize the methods and processes of commissioning and product validation, with the ultimate goal to increase quality…

Nelms et al, Med Phys 2013.

Taking patient specific QA further…

- "none of the approaches tested to verify IMRT plans by means of gamma analysis using 3%/3 mm or 2%/2 mm criteria solve the problem of evaluating treatment plans. Neither is it clear whether global 3D gamma analysis is superior to local 3D gamma analysis." - Carrasco et al 2012
- "a suitable alternative for evaluating and reporting the measured planar differences is to transfer their impact to the plan DVH and then to compare the resulting DVHs with the clinical tolerances of the PTV and OAR." - Carrasco et al 2012
- "the essence of patient-specific IMRT QA is to ensure that the dose distribution that is going to be delivered to the patient is of the same comparable quality as the approved plan, and such quality is evaluated by patient dose statistics and DVH curves." - Zhen – et al 2011
- "The evolution from gamma passing rates to DVH based metrics is natural in this way." – Zhen –et al 2011

Crowe et al 2016

"This study suggests that it is possible, and advisable, to select γ- criteria that specifically prioritize the property (**either dose difference or distance to agreement**) of greatest **clinical importance** for each treatment modality or anatomical site while also identifying action levels that **maintain acceptable QA pass rates**"

"the adoption of more sensitive γ-criteria, specifically 2%/2 mm, 2%/3 mm, or 3%/2 mm could be beneficial"

Med Phys 2016

Conclusions

Measurements and calculations – output normalised

Compile data – but do not forget the details

Uncertainty budget

Good understanding of the tools used

Delta^4

Semi – Measured data

TPS data

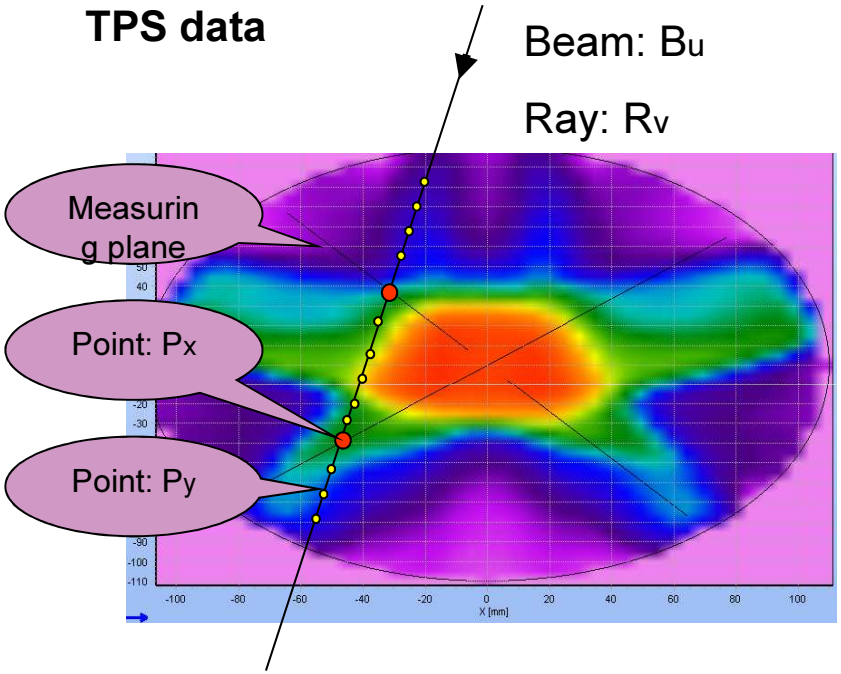

Measurement and Semi-measurement data

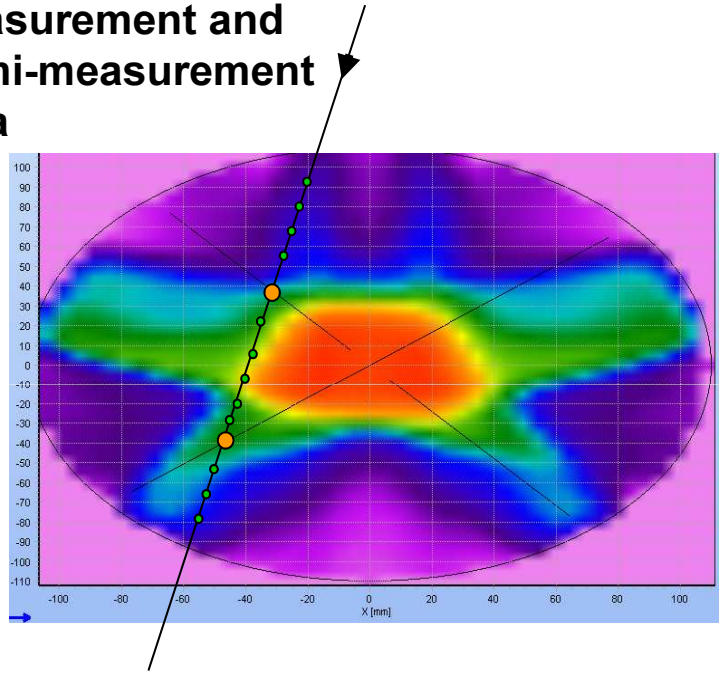

- TPS data in any point along the ray; except the measuring plane
- TPS data along the ray, in the measuring plane
- Measured data along the ray, in the measuring plane
- Semi-measured data along the ray, except the measuring plane.

$$D_{(Bu, Rv, Py)} = D_{(Bu, Rv, Px)} * D_{(Bu, Rv, Py)} / D_{(Bu, Rv, Px)}$$

ESTRO
ScandiDos

Delta^4

patient structure use in phantom

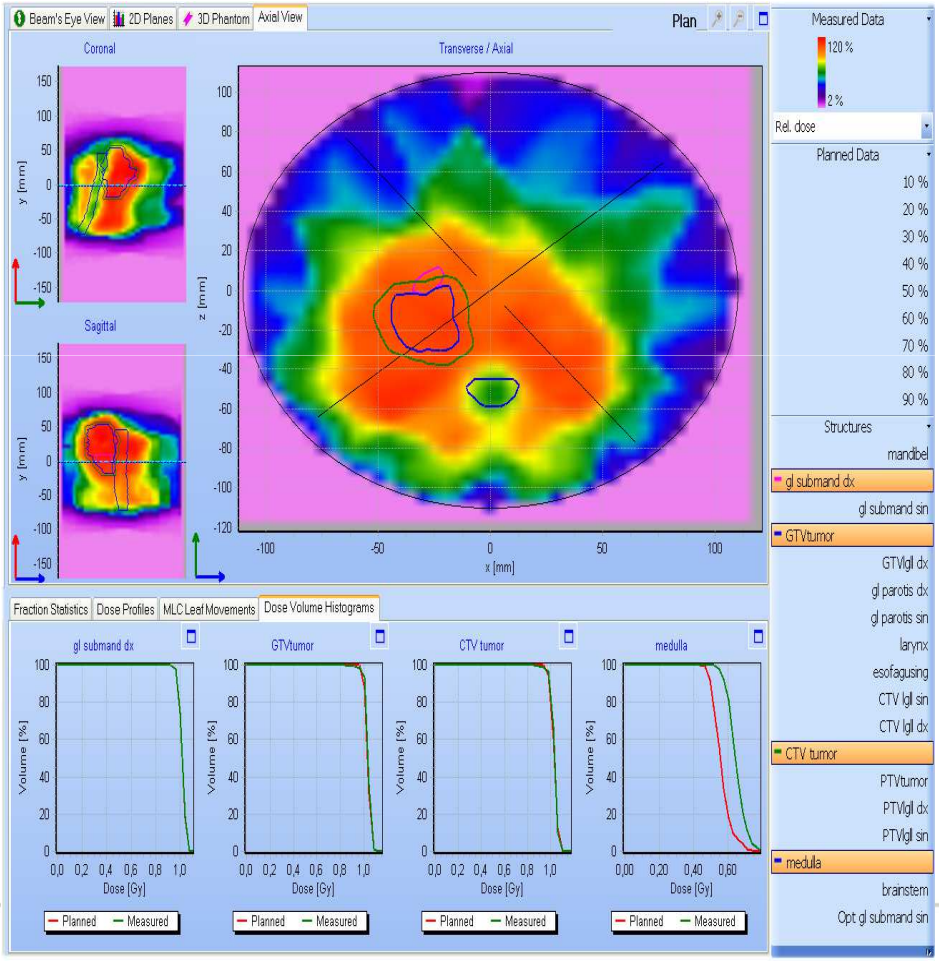

- **DVH – TPS data in phantom**
- **DVH – Semi- measured data in phantom**
- **DVH – compare**

ScandiDos

Thank You

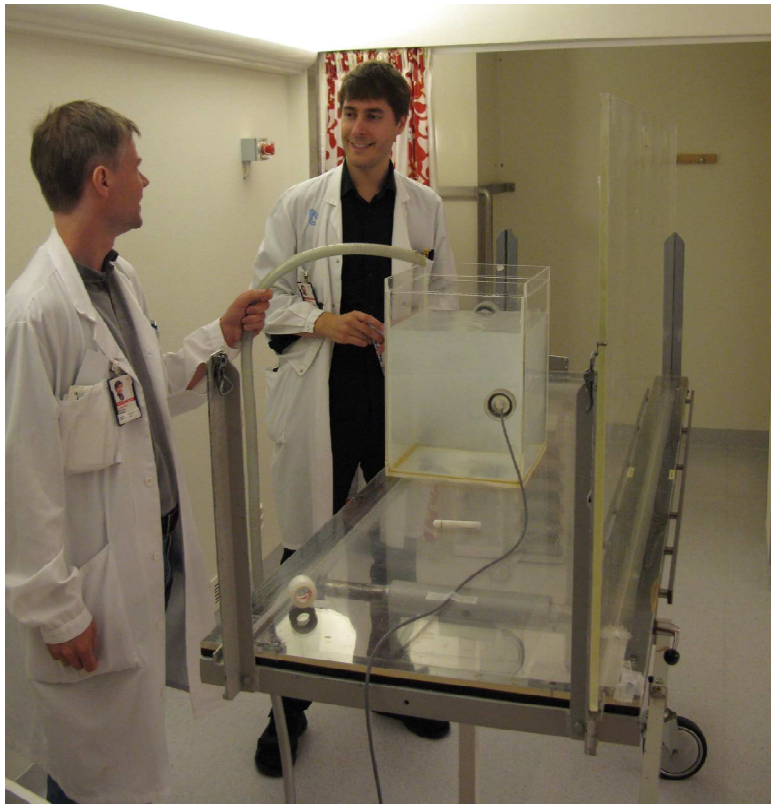

Quality Assurance of Treatment Planning Systems

Núria Jornet, Hospital Sant Pau, Barcelona
Brendan McClean, Saint Luke's Hospital, Dublin

ESTRO School

Learning Objectives

- Understand what is meant by QA for TPS
- Identification of some documentation available
- Review responsibility for
  - Vendor
  - User
- Define the nature of the information we want to know about our black boxes
- Commissioning and performance testing examples
- To be able to design specific tests to know how accurate is the TPS for the clinical conditions in which will be used.

Quality Assurance-historical background

"The physicist in charge needs a standarised set of tests and test conditions to control the reliability of the output"

Dahlin 1983

Quality Assessment; how do we know that we are performing well?

ESTRO School

Quality Assessment; how do we know that we are performing well?

- A quality programme assures that the **quality standards** are fullfilled
- Need that the **quality standards** are well defined
- We need **quality indicators** that we can measure and compare with **quality standards**
- Tolerances have to be set with “clinical” criteria

The results are as good as the quality standards

Quality assessment; how do we know that we are performing well?

Quality standards

Quality standards are a group of criteria to which we will compare the results of our tests.

In other words:

Without quality standards, quality cannot be demonstrated.

What is "good"?

TPS-QA

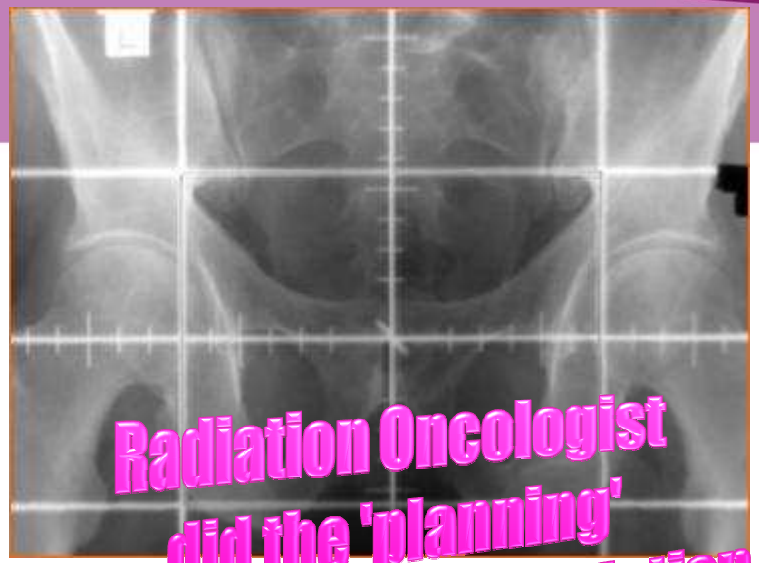

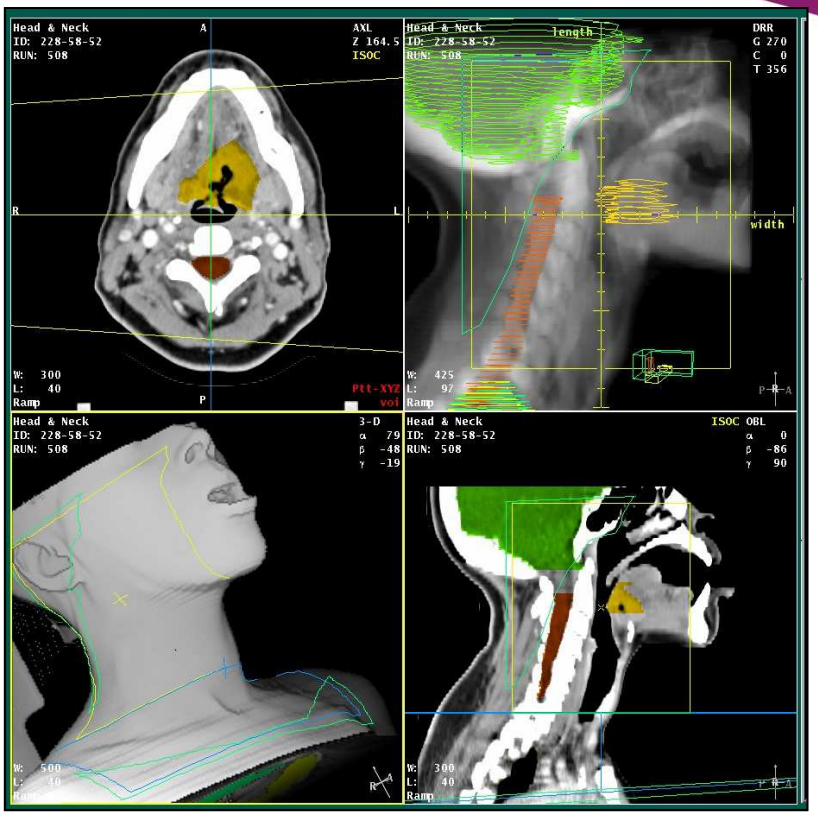

Now in 3D many more areas for QA
Including non-dosimetric factors
(Image geometry, orientation, fusion etc)

ESTRO School

Computer planning system – 'Hub' of RT

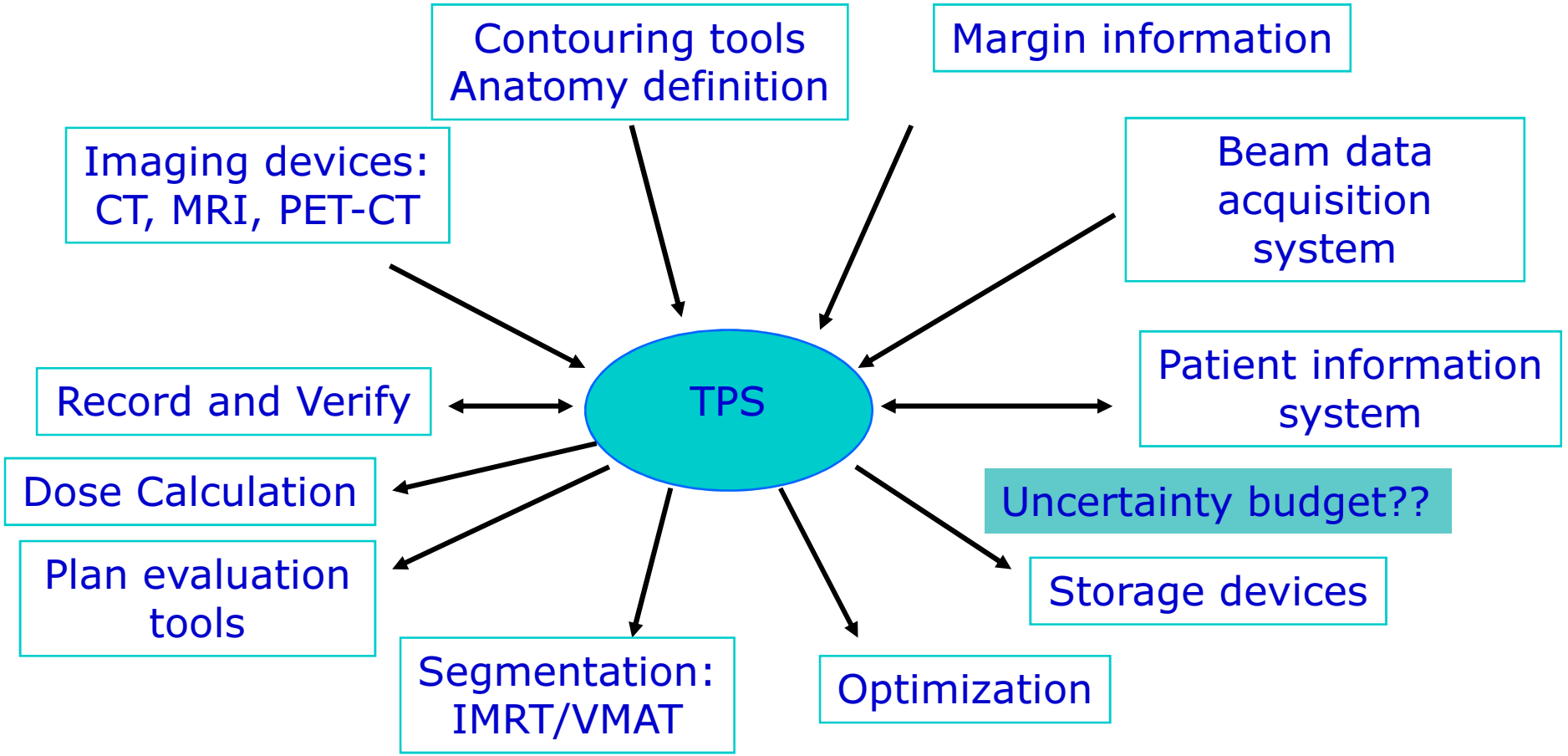

Computer planning system – 'Hub' of RT

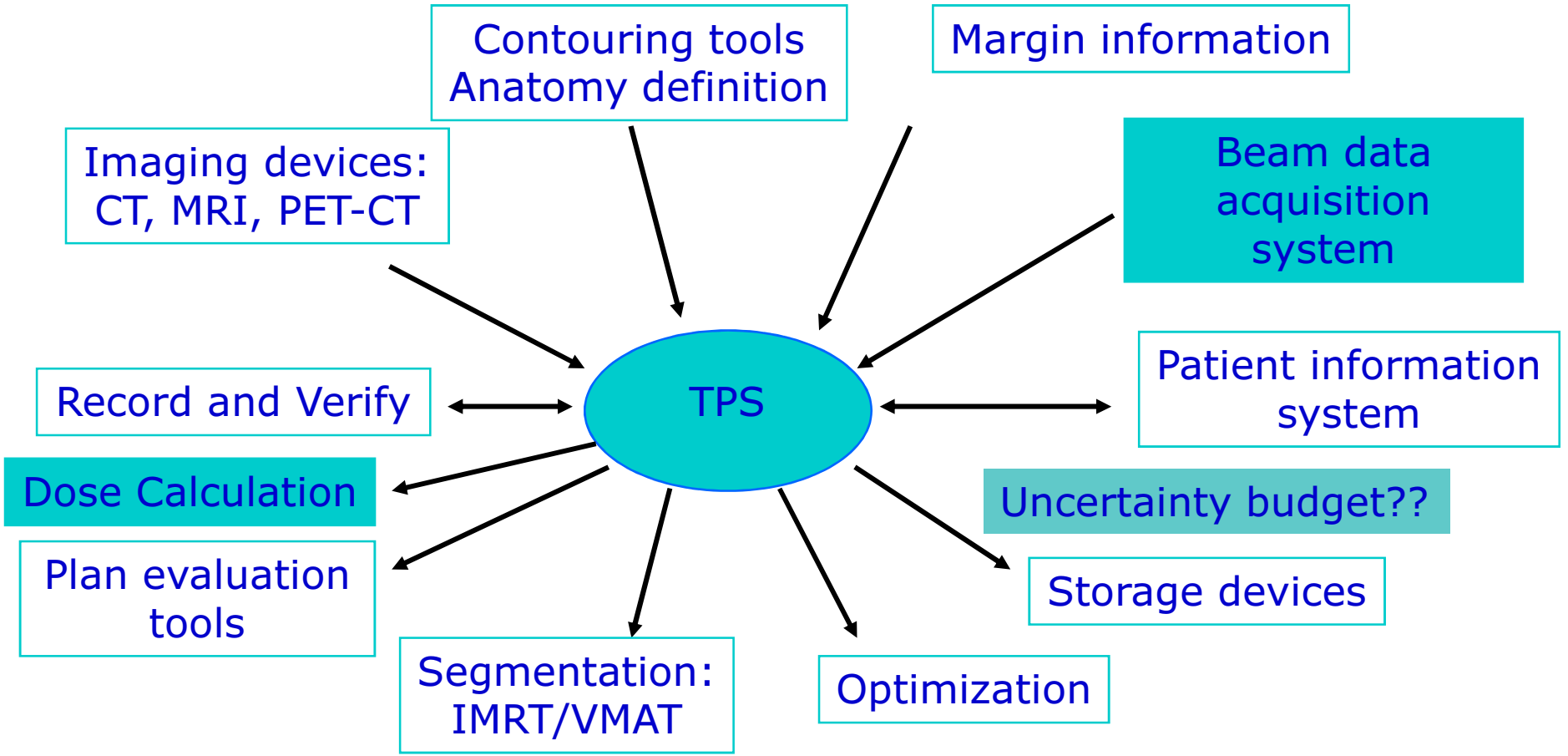

"Dose algorithms are the most unique, critical and complex software in a TPS" (Van Dyk)

Responsabilities:

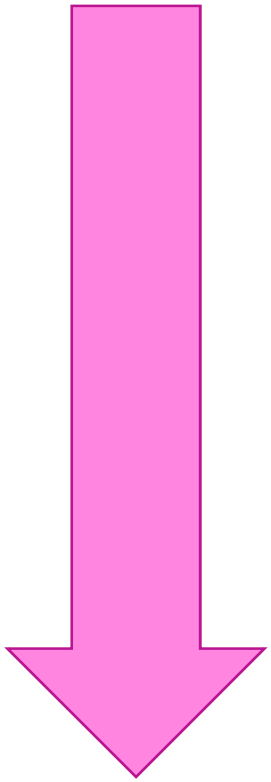

1) Generic performance — Vendor

2) Generic performance in users environment — Vendor/user

3) Specific performance in users environment — User

Responsibility: The Vendor

- Provide as much accurate data as possible.
- Accurate specification of system.
- Summary of published literature.
- Detailed system documentation: Design, algorithm capabilities, user guides, dose normalisation, etc.
- User training
- Clear communication regarding bugs and fixes
- Technical support
- **Dose Calculation:**
  - **Description of all factors**
  - **Equations for basis of calculations**
  - **Limits of all variables used**

Beam and source modeling
Multisegment techniques
Energy Deposition
Heterogeneity correction
Dose normalisation
….etc

Typical questions to ask in TRS430

Responsibility: The Vendor

TABLE 11. EXTERNAL BEAM DOSE CALCULATION ALGORITHM: DOSE IN WATER-LIKE MEDIUM WITHOUT A BEAM MODIFIER

	Question
General principle of relative dose calculation	From interpolation in tables? From analytical functions? By addition of primary and scatter components? By superposition of pencil beam kernels? By superposition of point dose kernels? By Monte Carlo calculation? From a combination of the above possibilities?
If an integration (or superposition or convolution) algorithm takes place	What are the shape and dimensions of the volume elements? What are the limits of the integration volume? Is it applied differently for each of the dose components (i.e. primary, scatter, etc.)? Is there any correction for spectral modifications with depth?
Influence of flattening filter	Is there a correction for intensity and quality variation across the beam (horns)? Is there a correction for scatter radiation from the head and flattening filter (extrafocal)?
Influence of main collimator (photons) and/or applicator (electrons)	What is the model used to describe the profile in the penumbra region? How is it adjusted to match the actual measurements? Is there a difference between the *x* and *y* collimator pairs?
Dose in the buildup region	Is there any specific model to describe the dose in the buildup region? Is it sensitive to patient surface obliquity? How? Is it sensitive to beam modifiers, including block trays? How?

Typical questions to ask in TRS430

ESTRO School

Responsibility – The user

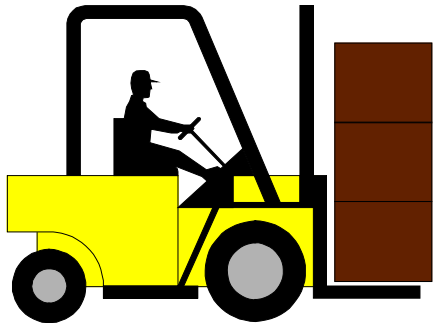

Delivery of product

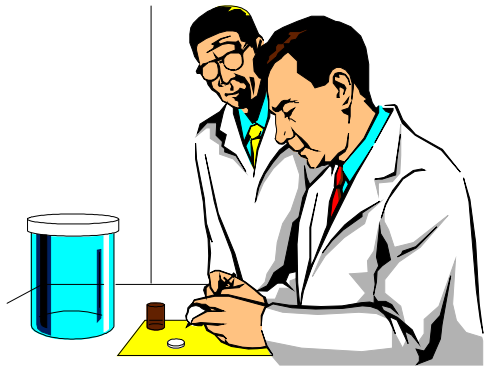

Physicists @ acceptance

- Defines treatment capabilities to be used
- Provides input data
  - GIGO!!
  - Eg choice of correct detector
- Learn general principles of model
- Know parameters and input that affect accuracy
- Provide acceptance, commissioning and QA process
- Detailed record keeping
- User training
- Etc.

Responsibility – The user

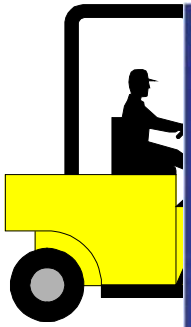

Delivery

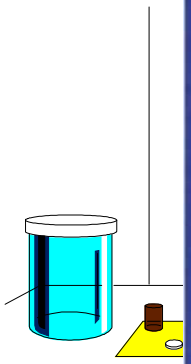

Physicists @ acceptance

The New York Times

RADIATION BILLS RAISE QUESTION OF SUPERVISION

By WALT BOGDANICH and REBECCA R. RUIZ

Published: February 25, 2010

Dose in 76 patients exceeded prescription by 50%

Beam measurement error by physicist

Ion chamber

Detector too large – blurs measured dose profile for small beams

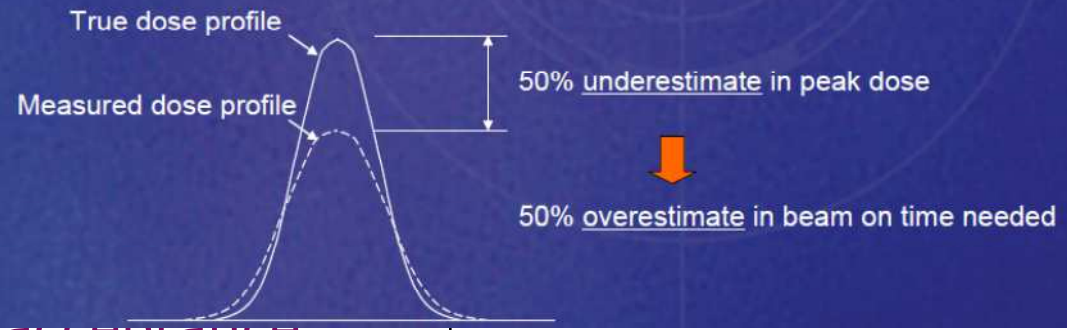

abilities to be

detector

s of model

input that

mmissioning

g

Commissioning

Basic checks [homogeneous phantoms] :

- Dose distributions
  - Calculated profiles and PDD for different field sizes defined by secondary jaws, MLC. Wedged fields… in homogeneous phantoms
- Monitor Unit calculation
  - Calculated profiles and PDD for different field sizes defined by secondary jaws, MLC. Wedged fields… in homogeneous phantoms

Vendor-user

Performance testing:

- Compare dose distributions and MU calculations for clinical situations.

Dose administration QA

From Anders A	Testing link by link			Chain testing
Test object:	**CT**	**TPS**	**Treatment**	**CT TPS Treat**
Test objective:	**Anatomy mapping**	**Dose calculated in well specified geometries**	**Dose delivery**	**Dose/MU Positioning**
Standards:	**Phantom replication**	**Dose measured in well specified geometries**	**Reproducibility**	**Measured dose**
	Dose deviations traceable to TPS/measurements			***Cause of dose deviations may not be obvious***

Peer Review during/after commissioning
Plan of work, methods and results all critically reviewed
- Confidence!

Performance testing

Any specific treatment

Treatment technique not covered by the vendor

User's interest to

- search for limitations
- Understand limitations and put in place processes to prevent non-verified use

PERFORMANCE TESTING

A user doing special measurements

Remember…

- Testing all components of a treatment-planning process can be a formidable task.

- Physicist must ascertain extent and complexity of treatment-planning needs of clinic

- Based on this information, physicist must establish elements of acceptance, commissioning, and QA of the TP S.


You're
Hopelessly
Lost...
Sorry

Not really… We can go through documents…

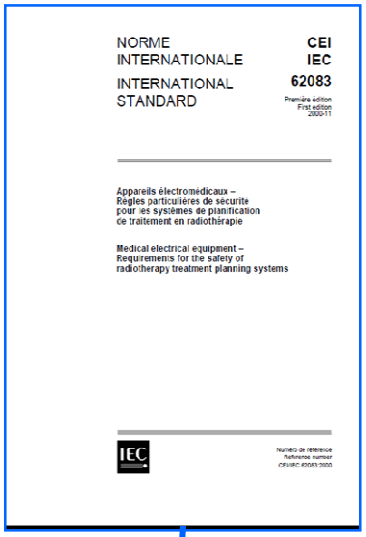

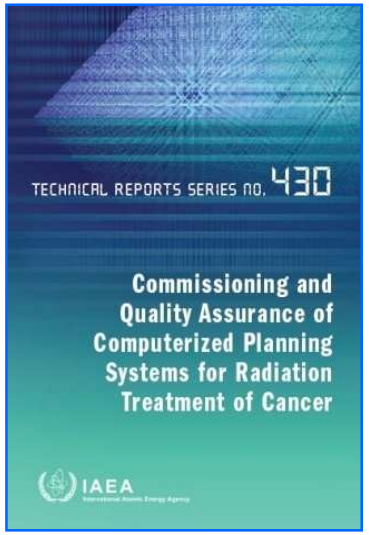

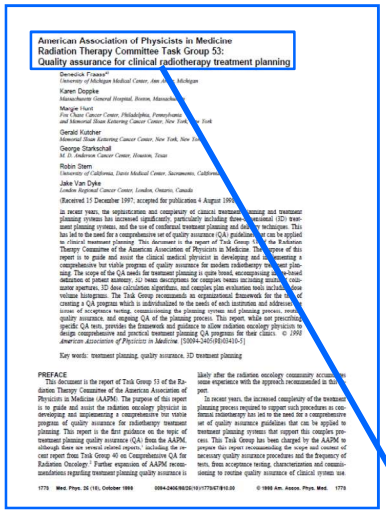

Medical electrical equipment – Requirements for the safety of radiotherapy treatment planning systems

American Association of Physicists in Medicine Radiation Therapy Committee Task Group 53: Quality assurance for clinical radiotherapy treatment planning

ESTRO School

Literature

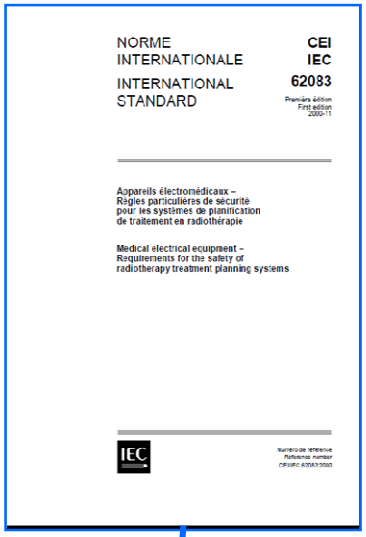

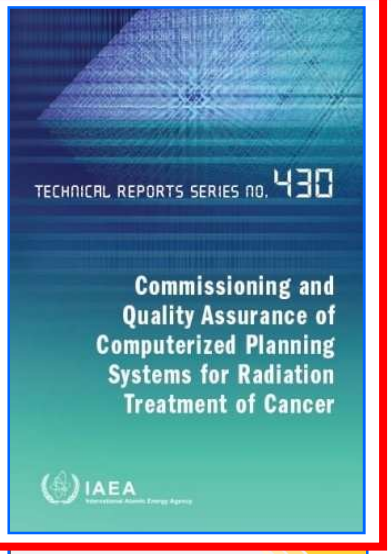

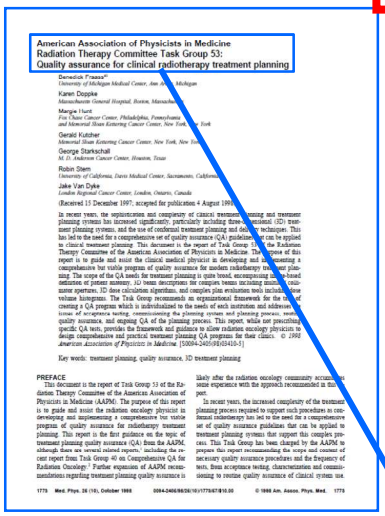

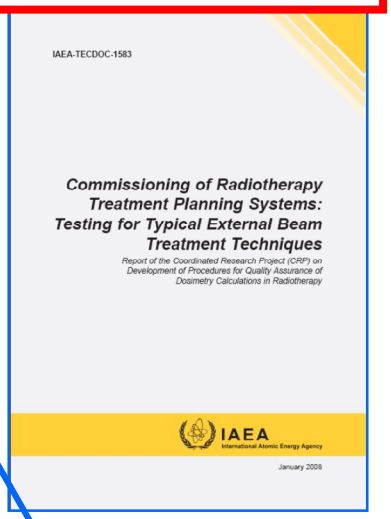

Medical electrical equipment – Requirements for the safety of radiotherapy treatment planning systems

American Association of Physicists in Medicine Radiation Therapy Committee Task Group 53: Quality assurance for clinical radiotherapy treatment planning

ESTRO School

Literature

American Association of Physicists in Medicine
Radiation Therapy Committee Task Group 53:
Quality assurance for clinical radiotherapy treatment planning

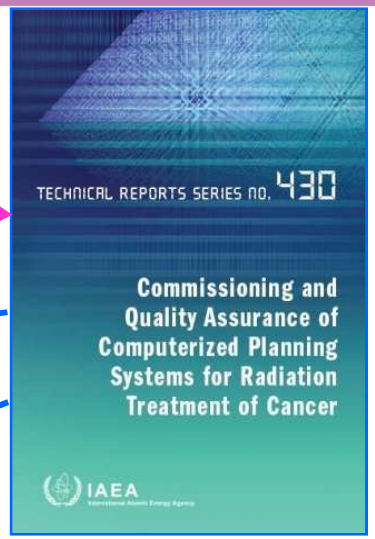

Framework
Large number tests
Many for system vs
Individual user

Extension with emphasis on practical tests

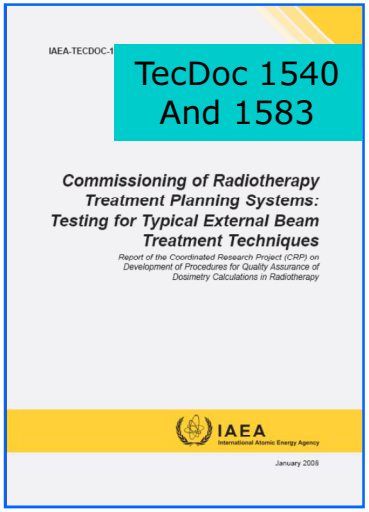

TecDoc 1540
And 1583

Quality assurance of 3-D treatment planning systems for external photon and electron beams

Practical guidelines for initial verification and periodic quality control of radiation therapy treatment planning systems

NEDERLANDSE COMMISSIE VOOR STRALINGSDOSIMETRIE

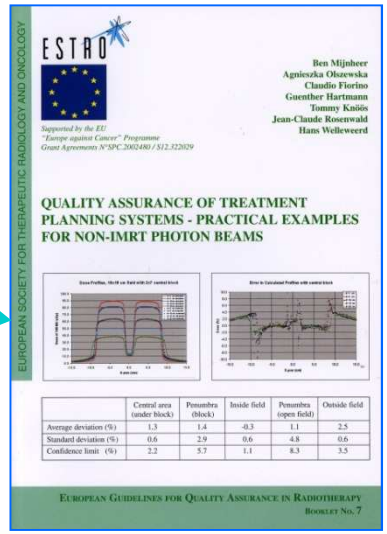

QUASIMODO
Booklets 7 and 9

ESTRO School

We can take tests from these documents and adapt to our own necessities.

American Association of Physicists in Medicine
Radiation Therapy Committee Task Group 53:
Quality assurance for clinical radiotherapy treatment planning

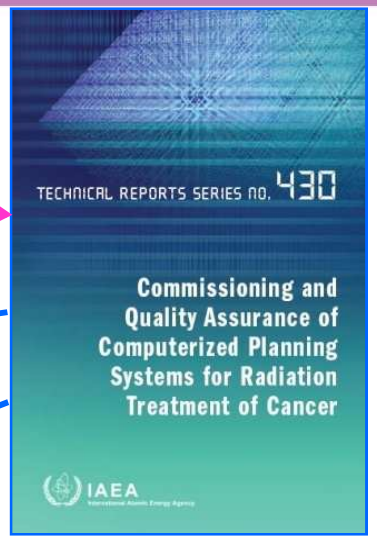

Framework
Large number tests
Many for system vs
Individual user

Extension with emphasis on practical tests

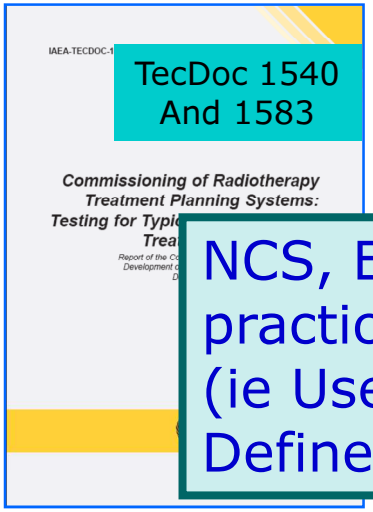

TecDoc 1540
And 1583

NCS, ESTRO, TecDocs focus on
practical approach and **how** to do tests
(ie User focused)
Defines minimum set of tests

QUASIMODO
Booklets 7 and 9

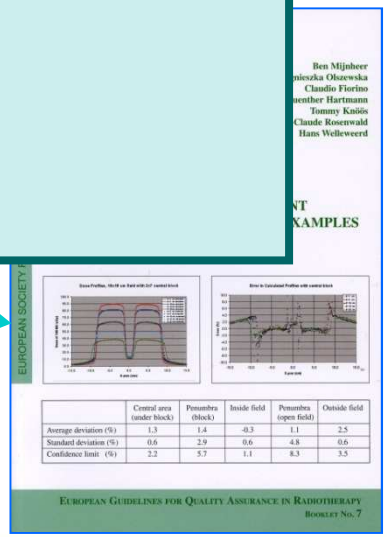

ESTRO School

Commissioning tests do not only deal with dose calculation

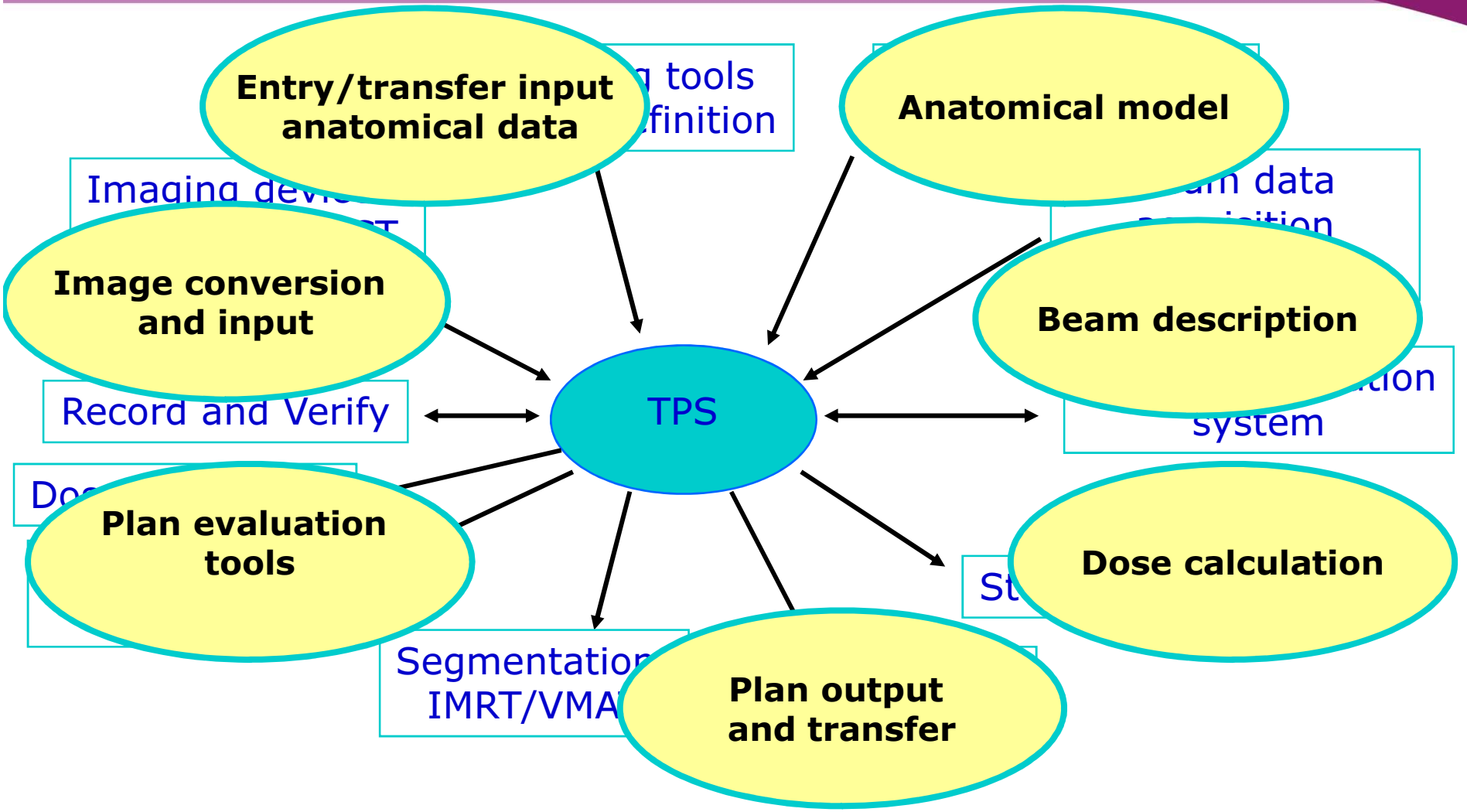

ESTRO School

We will focus on the QA of dose calcualtion

- Basic Patient entry
- Image conversion and input
- Anatomical structures
- Beam description
- **Dose Calculation**
  - **Close co-operation with vendor**
  - **Use eg Booklet 7, 9 or NCS as a start but modify to own needs**
  - **Essential to verify dose over whole volume!**
- Plan output

Commissioning – Dose Calculation Engine

Create work plan	• Identify the algorithm type and special issues • Define an efficient plan for data collection, dose distribution comparisons and analysis of results
Perform measurements	• Plan and Measure • Transfer • Analyse and Prepare data for TPS
Check and configure	• Verify input data • Confirm machine/beam configuration • Determine beam modelling fitting parameters
Perform Calculation Checks	• Compare beam specific calculations with measured data • Beam, algorithm and clinical specific calculations
Comparison and Analysis	• Verify that the calculations perform as expected in the user's hands • Verify behaviour over the range of expected clinical usage and at the limits set for clinical use • Verify calculation techniques and plan comparison tools

Beam modeling

Plan Comparison tools

Standards

Performance testing

Typical Peer Review process:

- Physicist in charge sets out a work plan and schedule
  - Includes literature review, manufacturers data
- Preliminary meeting (critical audience!)
  - Background theory if appropriate
  - Risk analysis (databases?)
  - Tests to be undertaken
  - Detectors and techniques used
  - Final plan
- Regular updates
- Final Peer Review
  - Results, analysis and comparison with existing data
  - Training and implementation plan
  - Ongoing QC
- Documentation
  - QART signoff
- Presentation to clinicians and other interested parties

Slab Inhomogeneity	10x10 cm^2 field 2cm air slab, 2 cm slab of high density material. CAX PDD & off axis points at 2 depths.	15x15 cm^2 field. 1cm air slab, 1 cm bone slab.	Yes : e diode	Yes: e diode & Mapcheck 2D absolute dose measurement.	Dmax, R80, R50 (approx)	9, 12, 15 MeV
Cylinder inhomogeneity	10x10 cm^2 field with 2cm diameter air & high density cylinders. CAX PDD & off axis points at 2 depths.	10x10 cm^2 field. 2.5cm diameter bone cylinder. 6cm diameter air cylinder.	Yes : e diode	Yes: e diode & Mapcheck 2D absolute dose measurement.	Dmax, R80, R50 (approx)	9, 12, 15 MeV
Abutting fields	Electrons to electrons, cax 10cm apart. Electrons to photons. CAX PDD & off axis points at 3 depths.	10x10cm^2 fields. 2 electron field. Photon and electron field.	No	Yes: Mapcheck 2D absolute dose measurement.	Dmax, R80	12, 15 MeV
Slab bolus	Test not included on list.	TPS check only	No	No	B re	
Complex surface shapes	Test not included on list. IAEA document.	Curved surface, 20x20cm^2 & 5x5cm^2 off axis.	No	Attempted PTW 729 ion chamber array.	dmax	9, 15 MeV
Build up region	Test not included on list. IAEA document.	10x10cm^2 field.	Yes: E diode	PTW 729 ion chamber array.	Build up region	9, 12, 15 MeV
Bulk density	Test not included on list. IAEA document.	TPS check	No	Could not be done.	-	-

Blue = NCS document

Green = IAEA document

Plus cutouts, grid size, Linac matching etc

Performance testing-methods

Need to have a setting of realistic performance conditions.

In performance testing, it is often crucial (and often difficult to arrange) for the test conditions to be similar to the expected actual use.

Performance testing-methods

Design of a QC test:

1. Definition of a **specification**: *(Capability of calcualting DVH)*
2. The measurement of **performance** associated to that specification
3. The comparison of the measurement with the **standard**
4. The possible action steps if the perfomance fails out of the **tolerance**

- ❑ Need to know what is an acceptable deviation from a known standard

Performance testing

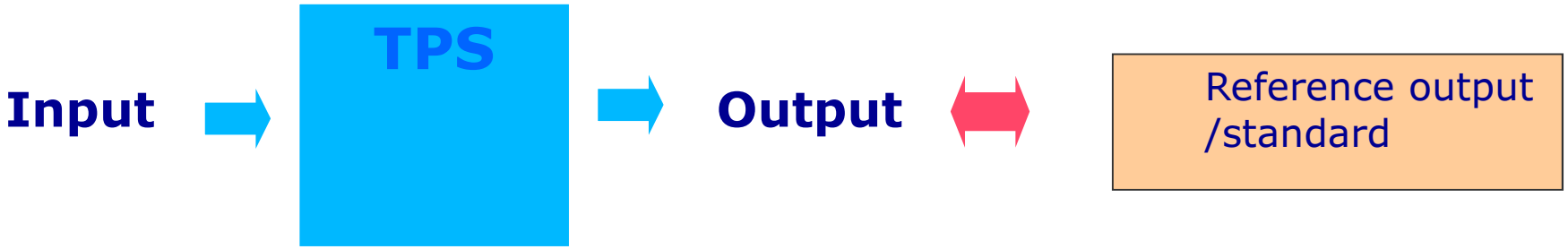

If Δ[output-standard]<tolerance*s*

The TPS performs well

Performance testing – dose calculations

If Δ[output-standard]<tolerances

The TPS performs well

How to design tests cases

- Design your own test cases addressing your typical clinical situations.
- Use test cases proposed in international recommandations. Ex. TG53, IAEA...

IAEA set of test-cases

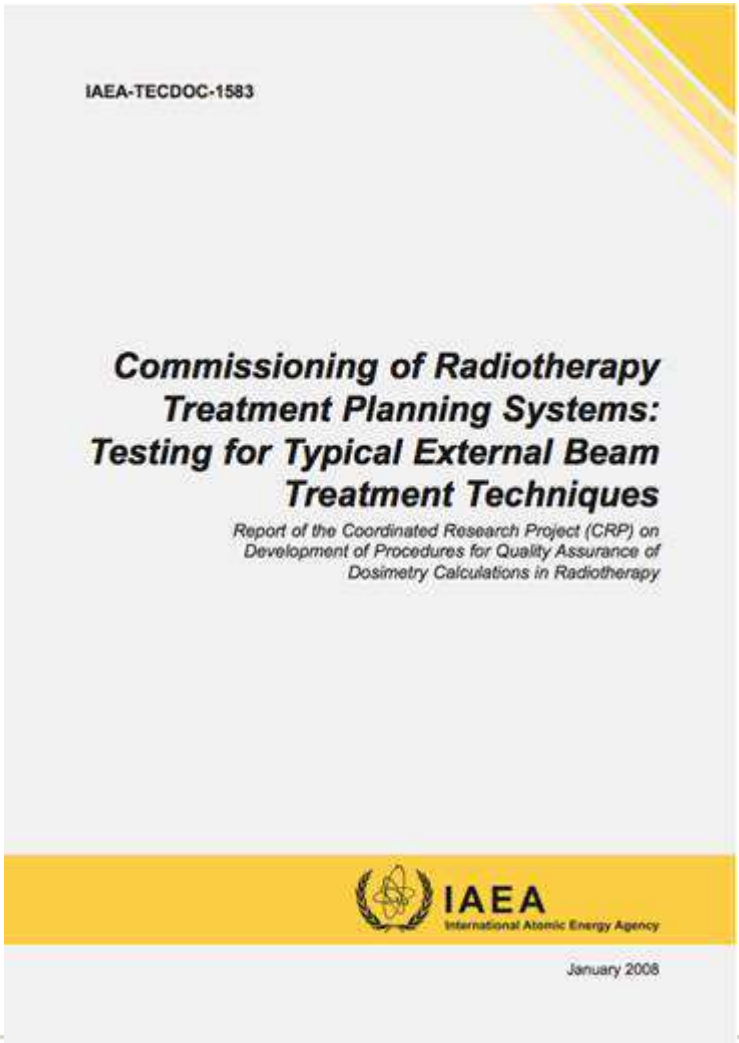

- Practical guidance for the implementation of TRS 430
- Create a set of acceptance and commissioning tests for dosimetry calculations in RT.
- Covers only standard techniques.
- Includes clinical commissioning tests. Based on the use of a specific phantom.

Test cases (TRS-430)

- **Non dosimetric tests**:
  - Verification of digitized contours
  - Verification of the CT number-electron density conversion
- **Dosimetric tests**:
  - Testing for reference conditions on CT data
  - Oblique incidence, lack of scattering, tangential fields
  - Significant blocking on field corners
  - Four field box
  - Automatic expansion and customized blocking
  - Oblique incidence with irregular fields and beam center blocked
  - Three fields, two wedge paired, asymmetric collimation
  - Non coplanar fields, collimator and couch rotation

Material-Phantoms (TRS-430)

- **CT phantom:**
  - Check of CT number to relative electron density conversion
  - Beam geometry assessments
  - DRR generation
  - Multiplanar reconstruction

- **Slab geometry phantom:**
  - Water/tissue equivalent material
  - Possibility for film dosimetry
  - Checks of corrections for inhomogeneous geometries

- **Anthropomorphic phantom**
  - Dosimetric measurements of typical or special treatment techniques.

Test cases (TRS-430)-identify test environment

Case 1: Testing for reference conditions based on CT data

The purpose of this test is to verify the calculation for the reference field. A 10 cm x 10 cm field with a gantry angle of 0° and collimator angle of 0° is used to confirm the basic beam data. The measurement points are defined in the middle of holes 1, 3, 5, 9 and 10: see Figure A.3 and Table A.2.

Table A.2 Geometry for case 1

Case	Number of beams	Set-up	Reference point	Measurement point	Field Size [cm] L x W	Gantry angle	Collimator angle	Beam modifiers
1	1	SSD=SAD 100 cm (linac) 80 cm (Co-60)	3	1 3 5 9 10	10x10	0	0	none

Test cases (TRS-430)-test

Instructions for Case 1:

(1) Perform the treatment plan with the RTPS according to Table A.2 and document it.
(2) Calculate with RTPS MU/time needed to deliver 2 Gy to the reference point #3.
(3) Report the computed dose at points 1, 5, 9 and 10.
(4) Perform manual MU/time calculation and compare result with RTPS MU/time calculated values.
(5) Set up the phantom on the couch of the treatment machine with Head first supine towards gantry.
(6) Align the phantom with lasers intersection at the centre of hole #5.
(7) Set gantry angle to 0°.
(8) Set SSD=100 cm (80 cm for C0-60 or nominal SSD).
(9) Set collimator rotation to 0°.
(10) Set field size: Length (Y) = 10 cm Width (X) = 10 cm

(11) Insert ionisation chamber into the tissue plug and place it into hole #3.
(12) Irradiate the phantom with the RTPS calculated MU/time.
(13) Register the value of the measured doses. Repeat irradiation at least three times and determine average value.
(14) Change the position of the ionisation chamber to the next hole #5.
(15) Repeat steps 12 and 13 after changing the position of the chamber.
(16) Change the position of the ionisation chamber to the next hole #1.
(17) Repeat steps 12 and 13 after changing the position of the chamber.
(18) Insert ionisation chamber into the bone-equivalent plug and place it into hole #10.
(19) Repeat steps 12 and 13 after changing the position of the chamber.
(20) Insert ionisation chamber into the lung-equivalent plug and place it into hole #9.
(21) Repeat steps 12 and 13 after changing the position of the chamber.
(22) Fill in Table A.3 with calculated and measured data and compare results.

Test cases (TRS-430)

Table A.3. Comparison of measured and calculated data for case 1

Case	Location of measuring point	Calculated dose [Gy]	Measured dose [Gy]	Deviation [%]	Agreement criterion [%]
1	1				2
	3				2
	5				2
	9				4
	10				3

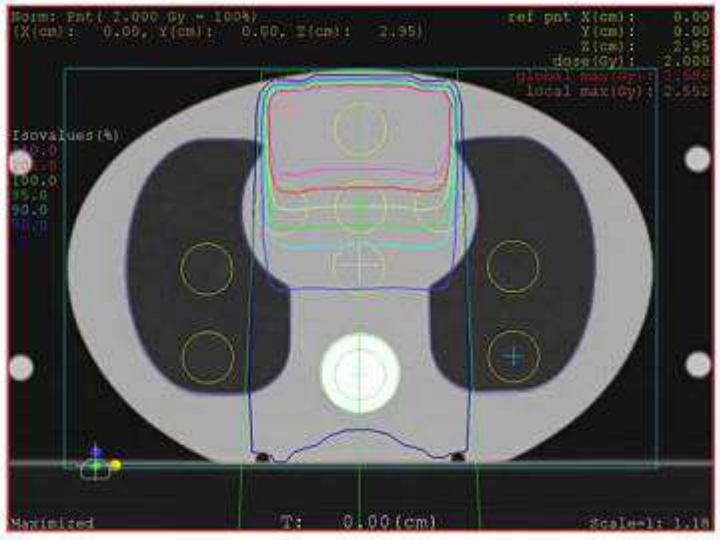

Figure A.5. A sample dose distribution in central plane for case 1.

Performance testing – references

If Δ[output-standard]<tolerances

The TPS performs well

Performance testing – references

MEASUREMENTS: Algorithm input data (usually specified by the vendor)

Try to use a different measurement system from the one used to get the data for beam configuration

Performed in the department with their own measuring equipment/phantoms.

Audit (i.e. mailed phantom+TLD+Films)

Benchmark data (published)

CALCULATIONS: Other TPS/calculation algorithm, version, MonteCarlo

Performance testing – tolerances

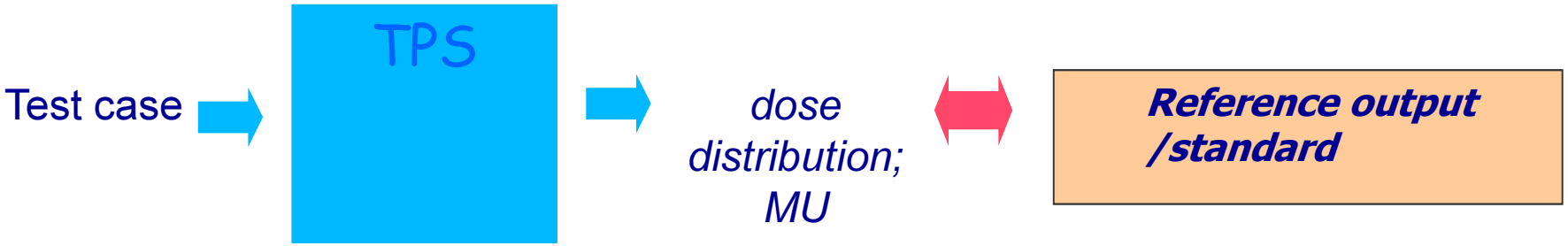

If Δ[output-standard]<tolerances

The TPS performs well

ESTRO School

Verify the accuracy of the algorithm

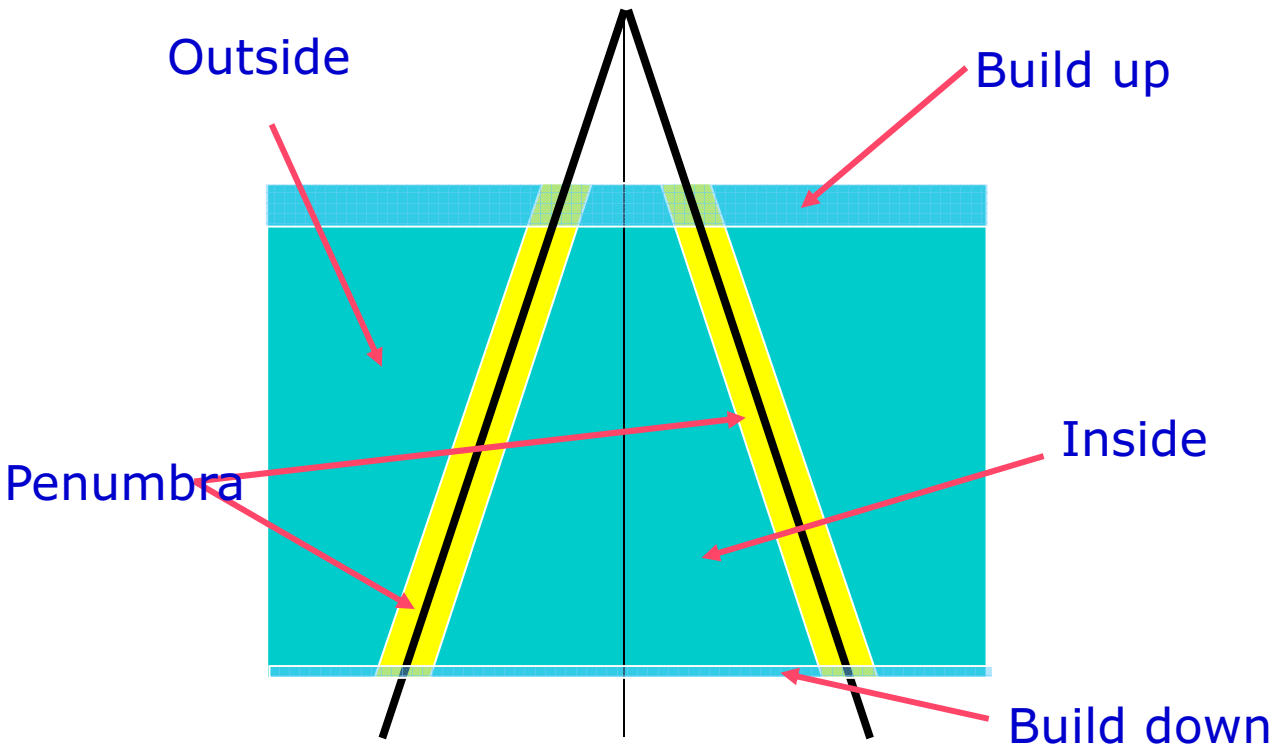

- **Establish limits of dose algorithm**
- **Quantify or interpret in different regions**
- **Agree criteria of acceptance**

How define the tolerances

The final criteria should reflect both what is achievable in clinical practice with up-to-date equipment, and the radiobiological requirements for accuracy [dose delivery in the patient, one should strive for an overall accuracy of 3.5% (1 SD) in the value of the dose delivered to the ICRU reference point]

- Different methods for comparison of dose distribution: Tommy Knöös
- How to fix tolerances: Núria

Performance testing – dose calculations

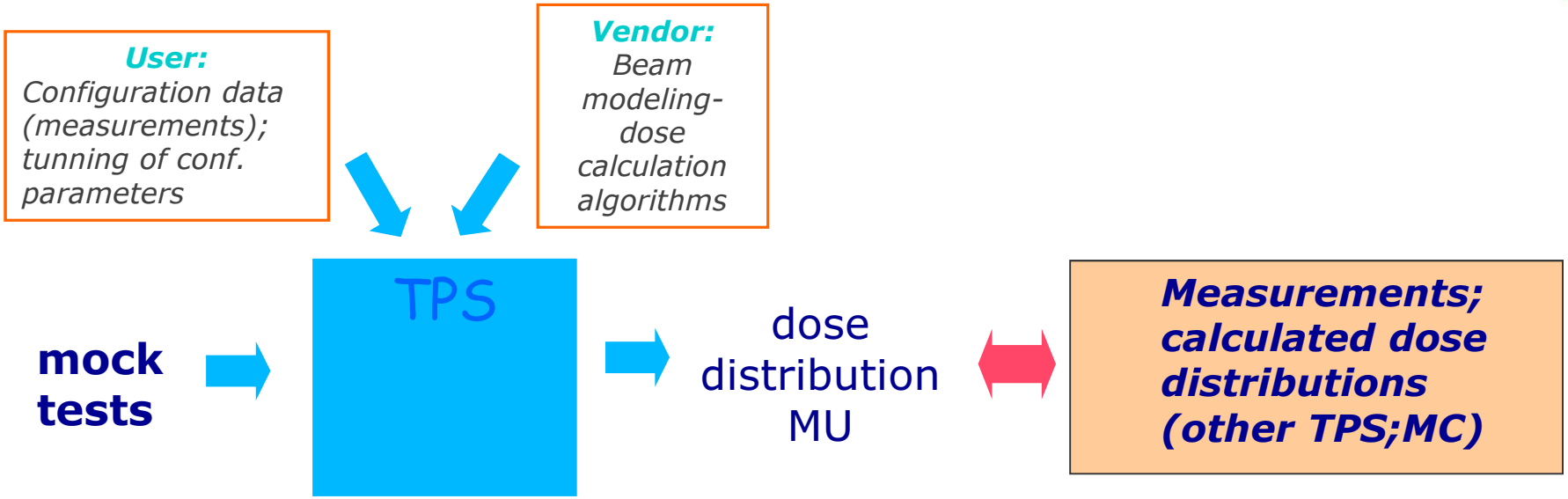

If Δ[output-standard]<tolerances

The TPS performs well

Performance testing – dose calculations

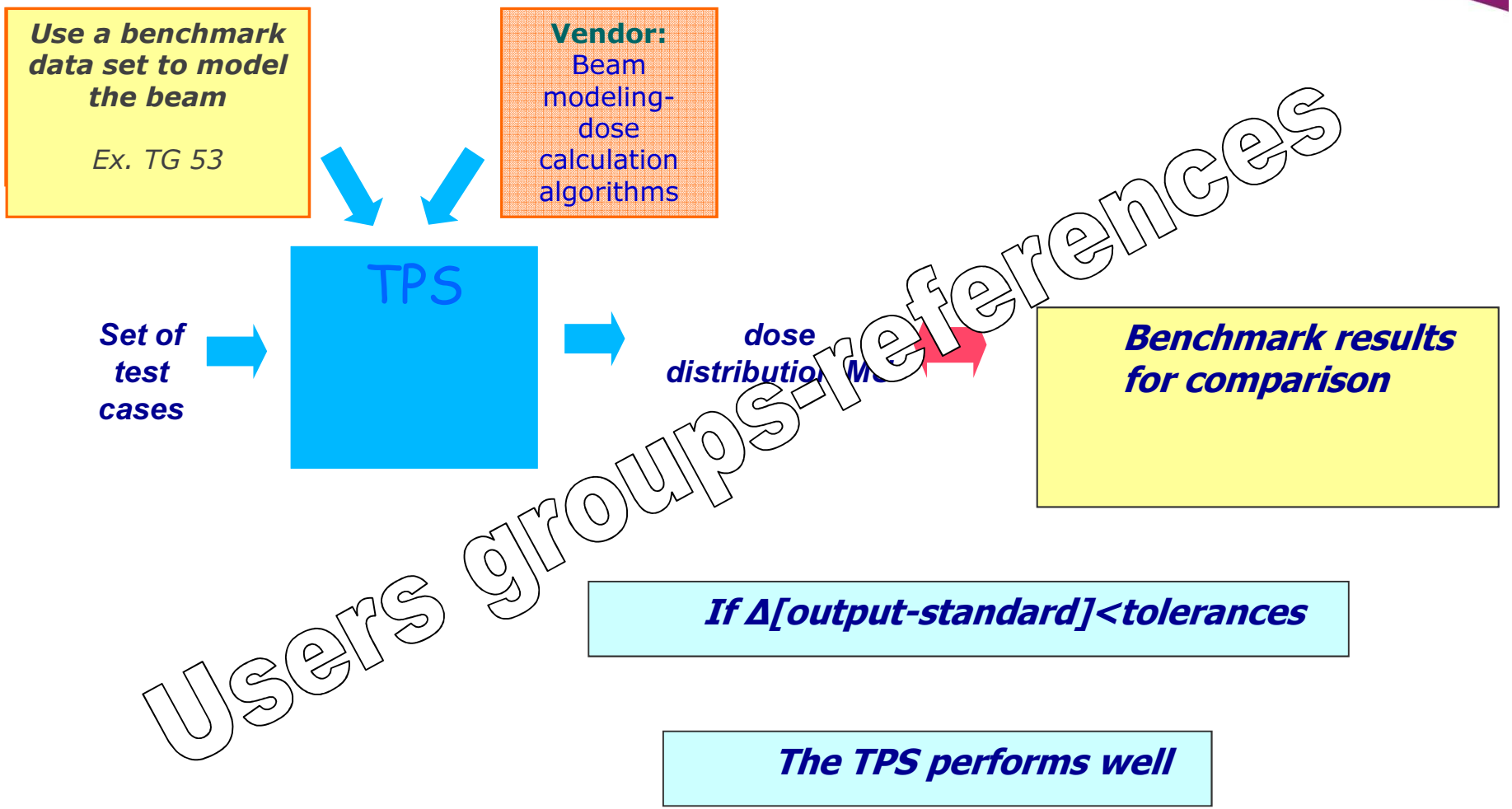

Performance testing – test packages

AAPM TG23 (1994): Beam data from two beams/13 test cases

3D test cases not included

wedge field case: 45º and normal incidence

asymmetric collimation not covered

absolute dose determination not included

AAPM TG53 (1998): Data set reviewed and upgraded

More tests are prepared i.e. 3D test included

NCS Beam Data set from two modern Elekta linacs (3 energies)

Possibility to adapt data set with latest technical developments.

Specific demands of basic beam data could be realized

New tests prepared

AAPM TG67 (to be published): update of beam data and test cases

TG 67 [Radiation Therapy Committee]

AAPM Radiation Therapy Committee Task Group 67 Benchmark Datasets for Photon Beams

CAX %dd, open fields	Open and wedge field profiles, in air	Output factors (Sc,p) at dmax
CAX %dd, wedge fields	Open field profiles, 2 SSD's	Output factors measured at 10 cm depth
CAX %dd, 90 cm SSD, open and wedged	Off axis HVL	Collimator factors (Sc)
Diagonal profile for max collimator setting, in phantom	MLC penumbra profiles	Phantom scatter factors (Sp) (either published data or values derived from Sc,p and Sc values)
Diagonal profile for max collimator setting, in air	MLC/Collimator jaw transmission	Collimator transmission
Diagonal profile for max square field	MLC setting and radiation field offset	Wedge transmission factors
Star profiles for max field size, open and wedge	Wedge profiles, nominal SSD	Tray transmission factors
Open field profiles, nominal SSD	Physical wedge dimensions	Absolute dose reference condition and value
Open field profiles, 90 cm SSD	Block edge profiles	Absolute dose for 100cm SSD

Performance testing – Test package example

Application of a test package in an intercomparison of the photon dose calculation performance of treatment planning systems used in a clinical setting

Jack Venselaar[a,*], Hans Welleweerd[b]

[a]Department of Radiotherapy, Dr B. Verbeeten Institute, P.O. Box 90120, 5000 LA Tilburg, The Netherlands
[b]Department of Radiotherapy, University Medical Center, P.O. Box 8500, 3508 GA Utrecht, The Netherlands

Received 26 May 2000; received in revised form 12 December 2000; accepted 9 January 2001

- Use of a common data set as input for 7 commercial planning systems
- Test package
- Comparison: Percentage deviations of the local dose except points ourside the penumbra or under blocs where the deviation was expressed relatively to the dose on the central axis of the open beam.
- Confidence límit:

$$\Delta = |\text{average deviation}| + 1.5 \times SD$$

- Tolerance: depending on the region

Performance testing – example

Values of the criterion for the confidence limit for the different types of test geometries[a]

Description	Tolerance
	in % of local dose
1 Homogeneous, simple geometry	
Output factors	1
Central axis data of square fields	2
Off-axis data	3
2 Complex geometry (wedged fields, inhomogeneities, irregular fields, asymmetrical collimator setting)	
Central and off-axis data	3
3 More complex geometries, i.e. combinations of #2	
Central and off-axis data	4
	In % relative to the dose at the same depth, but at the central axis of the open beam
4 Outside beam edges	
In simple geometry	3
In complex geometry (see #2)	4
In more complex geometry (combinations of #2)	5

Performance testing – drawnbacks of this approach

Advantages:

- The results only depend on beam modeling and the calculation algorithms as implemented in the TPS.
- Ideal for TPS comparison as avoids uncertainties due to different set of measurements performed at different sites at different times.

Disadvantages

- Different planning systems need different data
- Some of them require tunning of parameters
- Need of modeling a “new beam” with no clinical application
- Difficult to have a good data set for beam configuration that can be used in all planning systems.

Performance testing – dose calculations

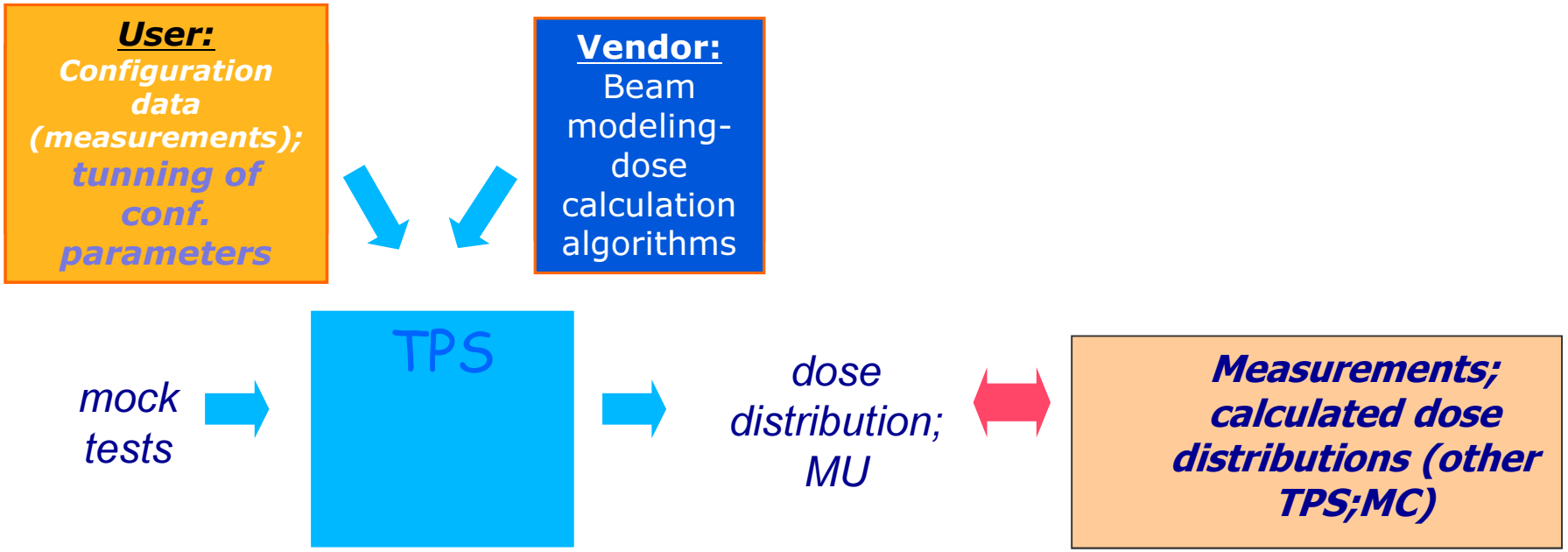

If Δ[output-standard]<tolerances

The TPS performs well

Performance testing – ex. Feed back configuration parameters

Automated beam model optimization

Daniel Létourneau[a] and Michael B. Sharpe
Radiation Medicine Program, Princess Margaret Hospital, Toronto, Ontario, Canada
and Department of Radiation Oncology, University of Toronto, Toronto, Ontario M5G 2M9, Canada

Amir Owrangi
Radiation Medicine Program, Princess Margaret Hospital, Toronto, Ontario M5G 2M9, Canada

David A. Jaffray
Radiation Medicine Program, Princess Margaret Hospital, Toronto, Ontario M5G 2M9, Canada;
Department of Radiation Oncology, University of Toronto, Toronto, Ontario M5S 2E3, Canada;
and Department of Medical Biophysics, University of Toronto, Toronto, Ontario M5G 2M9, Canada

(Received 23 November 2009; revised 26 January 2010; accepted for publication 8 March 2010; published 22 April 2010)

Performance testing – ex. Feed back configuration parameters

Automated beam model optimization

Med Phys 37 (2010)

Background

- Beam model accuracy for IMRT calculation (calculation performance depends on the tunning by the user of multiple parameters
- Pinnacle (Philips Medical Systems)
- IMRT and SBRT requirement of measurement data for TPS commissioning and beam model accuracy have increased.

Aim

- Development and validation of an automated beam model optimisation system (ABMOS)

Performance testing – ex. Feed back configuration parameters

User:
Configuration data (measurements); tunning of conf. parameters

Vendor: Beam modeling- dose calculation algorithms

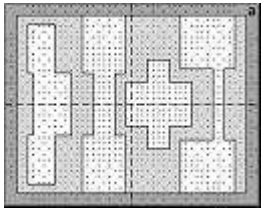

TPS

Planar fluence prediction

High resolution 2D array measurements

MapCheck (Sun Nuclear) sampling 0.2 mm

Configuration parameters

Jaw and MLC transmission
Radiation source size
Extrafocal radiation contribution
MLC rounded lef-end transmission

Cost function= 1-Gamma evaluation pass rate

2%-1mm Th 10% Tolerance 85% points

Performance testing – ex. Feed back configuration parameters

Automated beam model optimization

Med Phys 37 (2010)

Results

TABLE II. Comparison of beam model parameter values for the initial and the optimized beam model for the Synergy S treatment unit.

Beam model parameters		Initial beam model	Optimized beam model
MLC transmission:	$\%T_{MLC}$ (%)	0.400	0.175
Jaw transmission:	$\%T_{X\text{-jaws}}$ (%)	0.400	1.590
	$\%T_{Y\text{-jaws}}$ (%)	0.400	1.590
MLC interleaf leakage:	L_{height} (%)	2.000	2.208
	L_{width} (cm)	0.150	0.071
Orthogonal source size:	S_X (cm)	0.035	0.066
	S_Y (cm)	0.035	0.042
Extrafocal scatter source:	G_{height} (%)	8.500	8.500
	G_{width} (cm)	1.850	1.850
Second degree polynomial:	a	-1.140×10^{-3}	-1.630×10^{-3}
(Pos(z)=az^2+bz+c)	b	-1.530×10^{-5}	-1.530×10^{-5}
(Rounded leaf-end correction)	c	6.996×10^{-2}	6.235×10^{-2}

IMRT beam pattern

46.1% to 87.3%

Pretreatment results

(3%-2mm Th 10%)

Prostate: 91.4% to 98.2%
Paraspinal: 77.1% to 96.4%

Performance testing – ex. Accuracy of configuration data- volume averaging

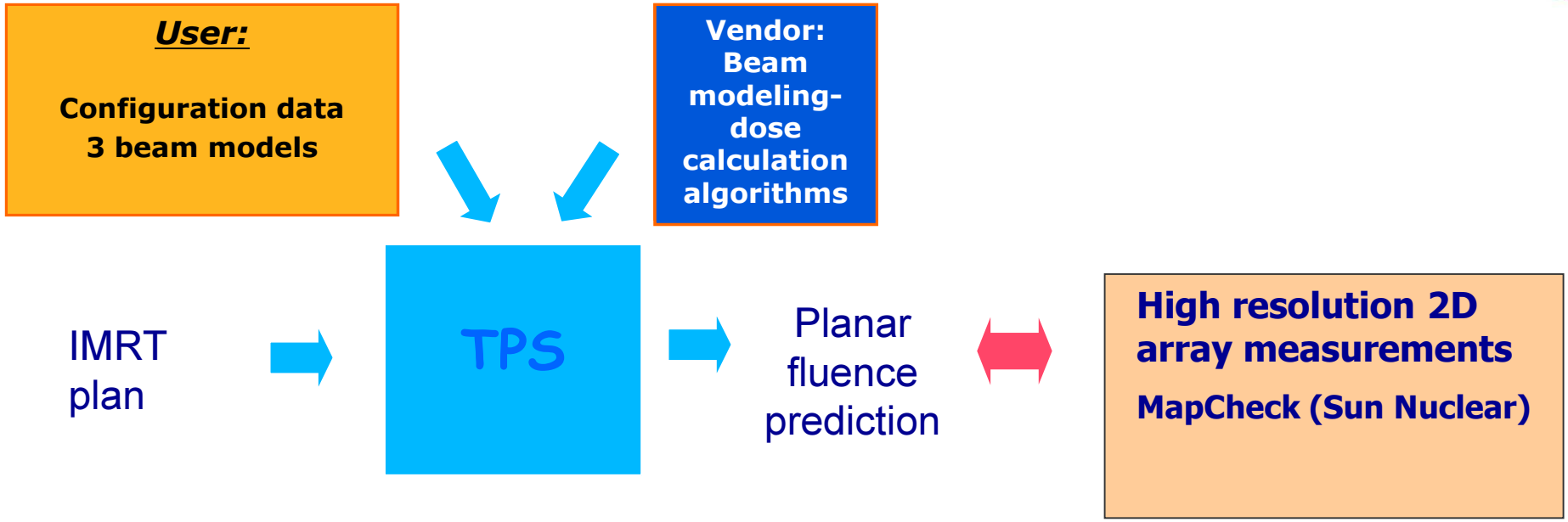

Three beam models (profiles)

- 6mm diameter ion chamber
- 4mm diameter ion chamber
- True profiles (analytic fitting/deconvolution)

Gamma analysis (3%-3mm)

Guanghya Yan et al. Med Phys 35(8) 2008

ESTRO School

Performance testing – ex. Feed back configuration parameters

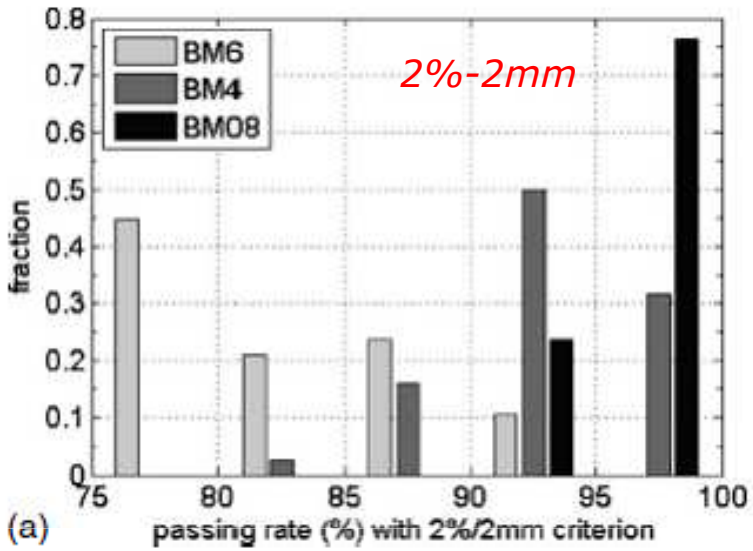

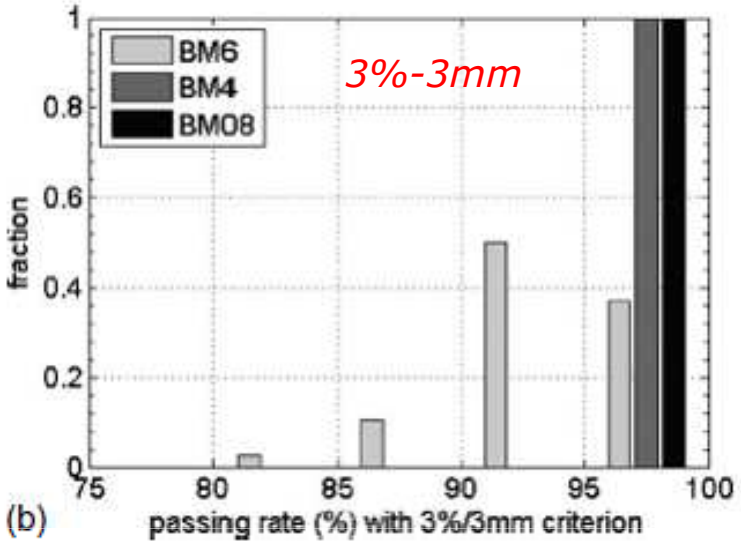

Gamma analysis (2%-2mm; 3%-3mm)

Three beam models (profiles)

- 6mm diameter ion chamber (BM6)
- 4mm diameter ion chamber (BM4)
- True profiles (analytic fitting/deconvolution)(BM08)

The use of the appropiate detector has a direct impact in the results of gamma evaluation; agreement between planning and delivery

Guanghya Yan et al. Med Phys 35(8) 2008

ESTRO School

Performance testing
Small field dose calculation accuracy for general purpose TPS

General purpose TPS are not necessarily designed to be used in small fields

Performance testing
Small field dose calculation accuracy for general purpose TPS

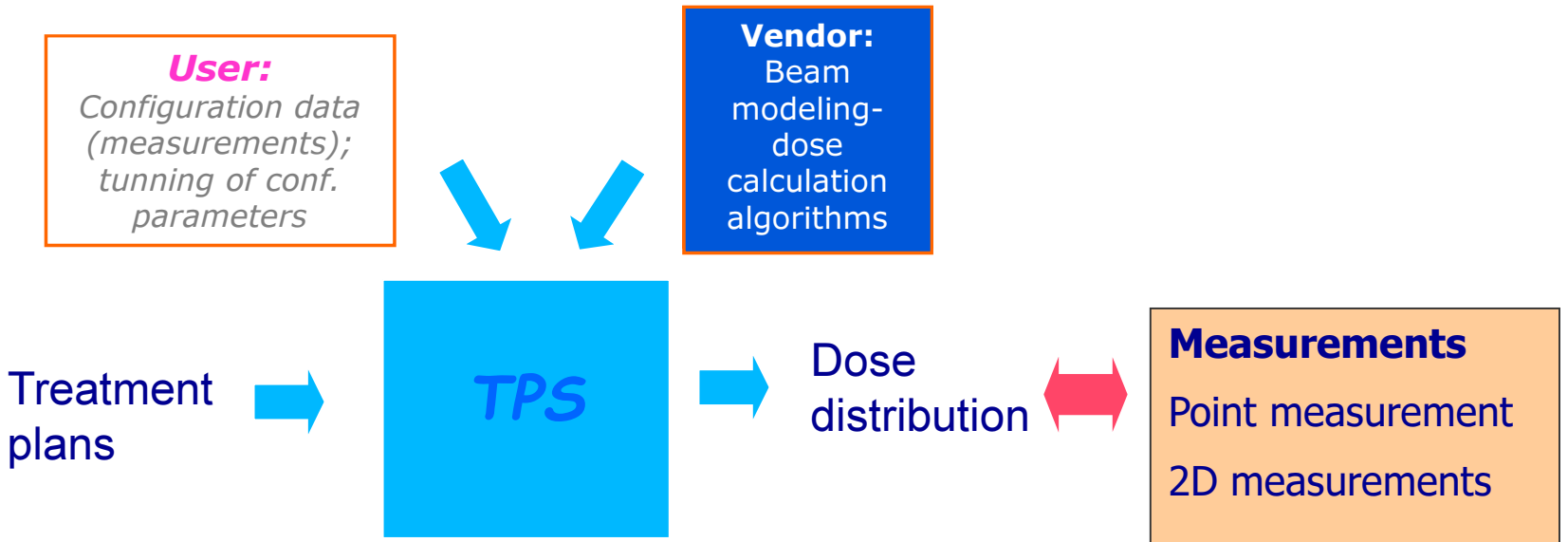

Dose differences and Gamma analysis (3%-2mm)

Flogliata et al. Med Phys 35(8) 2008

Performance test example: Small fields

General purpose TPS are not designed to be used in small fields

Design performance tests to check the capability of the calculation algorithms for small fields

- **Define the conditions for the test**:
  - simple/baseline conditions
  - treatment plans
- **Select the data against which the TPS calculation will be compared** (reference data)
  - Measurements: detector/phantom
  - Calculation: other TPS/algorithm; MC...
- **Compare TPS calculation with the reference data;**
  - Tolerance levels.

Performance test example: Small fields

Accuracy of Acuros XB and AAA dose calculation for small fields with reference to RapidArc® stereotactic treatments

Antonella Fogliata,[a)] Giorgia Nicolini, Alessandro Clivio, Eugenio Vanetti, and Luca Cozzi
Oncology Institute of Southern Switzerland, Medical Physics Unit, CH-6500 Bellinzona, Switzerland

(Received 5 July 2011, revised 25 August 2011; accepted for publication 4 October 2011, published 27 October 2011)

- **Define the conditions for the test**:

  simple/baseline conditions

  treatment plans

- **Select the data against which the TPS calculation will be compared** (reference data)

  Measurements: detector/phantom

  Calculation: other TPS/algorithm; MC...

- **Compare TPS calculation with the reference data;**

  Tolerance levels. *3%-2mm*

ESTRO School

Performance testing
Small field dose calculation accuracy for general purpose TPS

User:
Configuration data (measurements); tunning of conf. parameters

Vendor:
Beam modeling- dose calculation algorithms

TPS

Dose distribution

Measurements
Point measurement
2D measurements

Patient cases

Rapid Arc IMRT Eclipse
PTV (0.3-7 cm^3)
Single partial arc (110º-250º)
2Gy at isocenter
Maximum dose rate:600MU/min

Dose differences and Gamma analysis (3%-2mm)

<u>Optimisation and dose calculation using different:</u>

DLG (dosimetric leaf gap)
LT (leaf transmission)
Spot size parameter (0, 0.5, 1, 2 mm)
Acuros XB and AAA.

Measurements

Point measurements: PTW-Octavius phantom-
Diamond detector at the isocenter

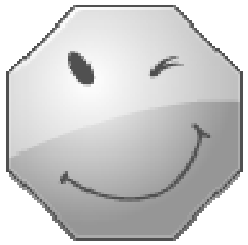

2D dose distributions: EPID+GLAaS algorith***m***

Results evaluation

3. Compare TPS calculation with the reference data; tolerance levels:

Point measurements:

Measurement compared to the mean dose in a circular structure of 4mm diameter (simulation of the detector sensitive area)

2D measurements:

2D gamma analysis (2mm;3% of the maximum dose; evaluation inside the jaw setting, no low dose threshold).

Results

The DLG has a higher impact on discrepancies

The best results are obtained for DLG 2mm and TL 1.4%

This applies for the two algorithms

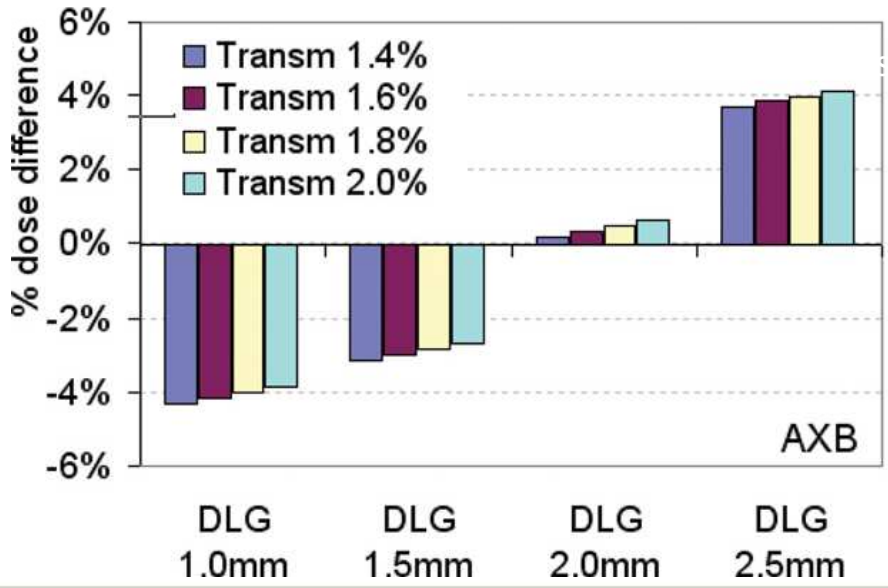

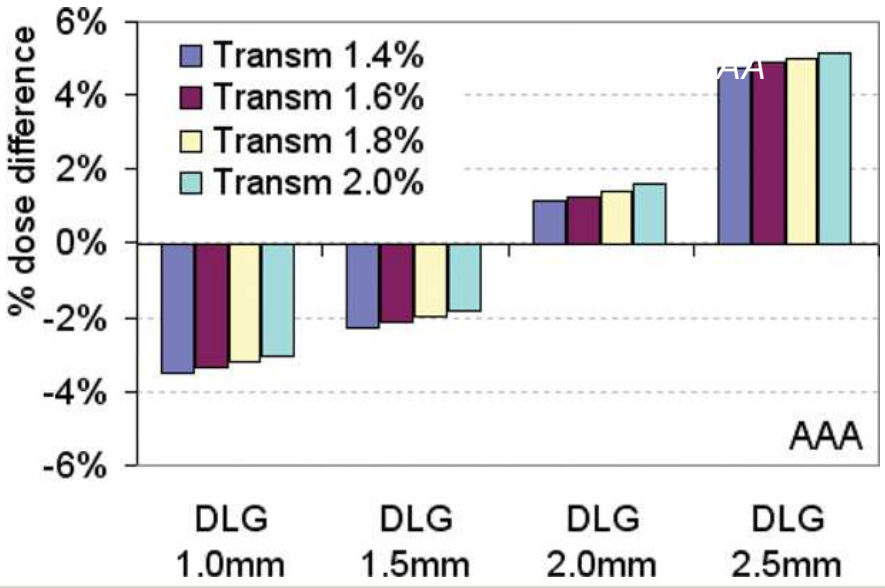

ESTRO School

Results

:

Spot size

AAA: 0-2 mm
Acuros XB: 0.5-1mm-2 mm

Default values in red

Stereotactic specific configuration including OF for small fields (MU calculation).

Modify the Spot size to a value between 0.5-1 mm.

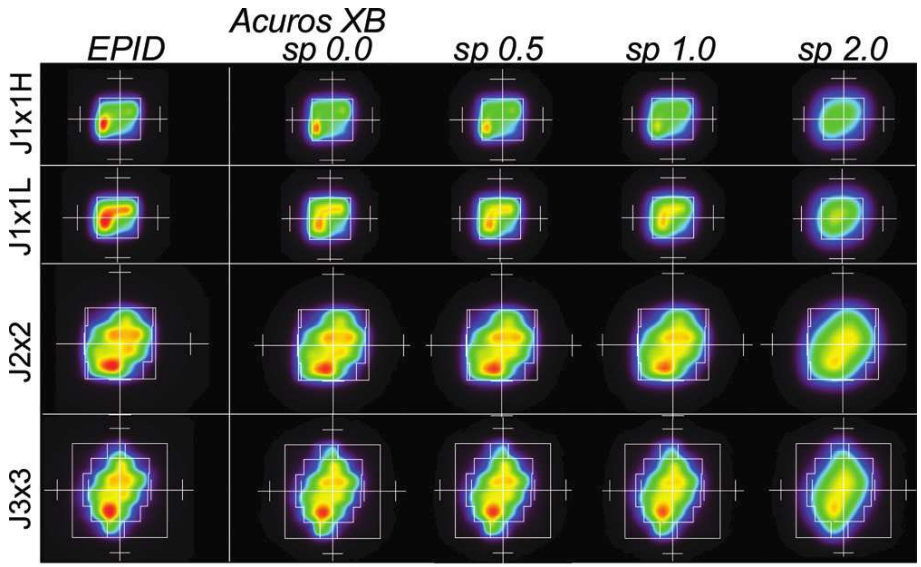

Acuros

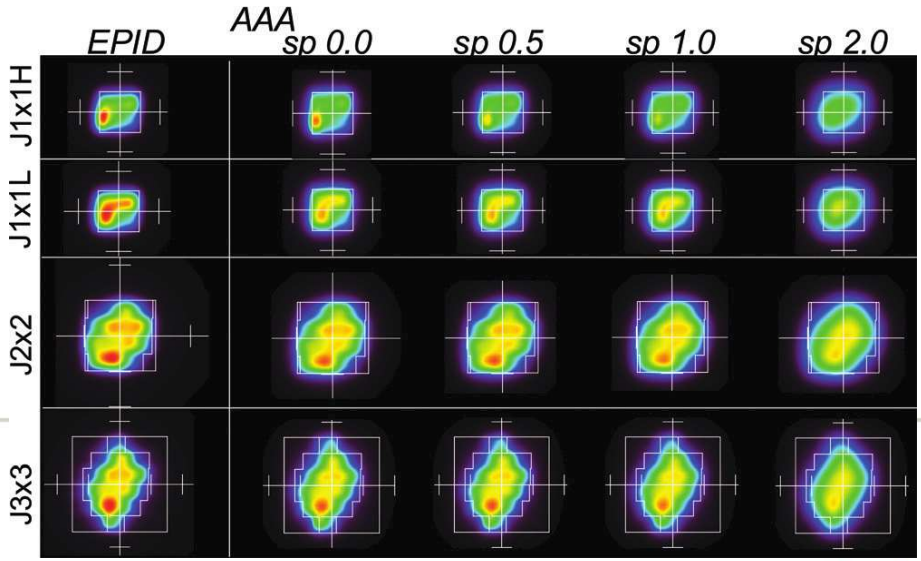

AAA

Performance testing new TPS version-upgrade or periodic tests

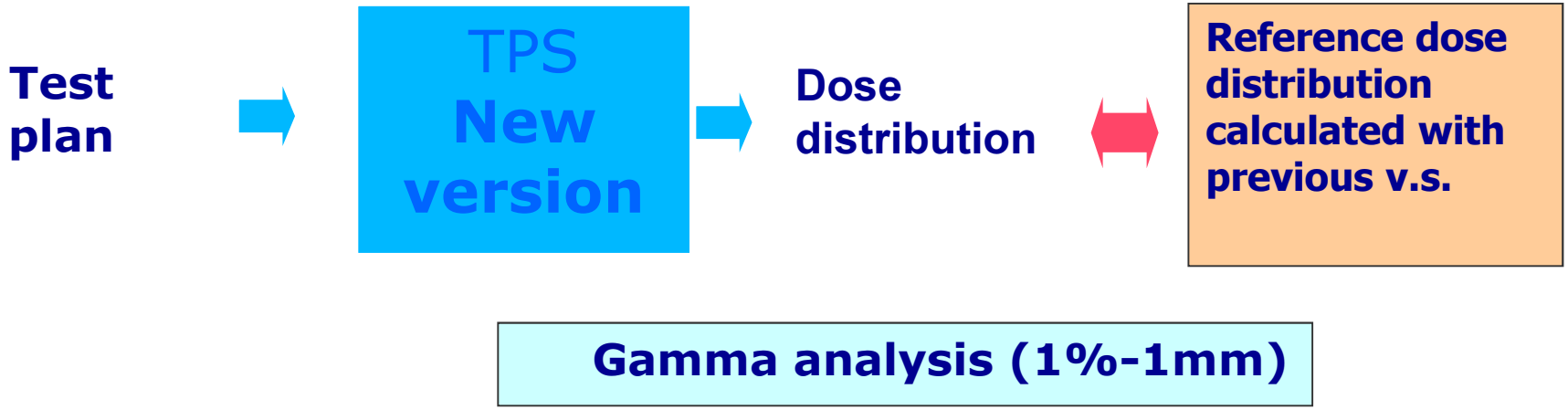

Change of vs: Example Eclipse

6 MV X-rays

$$I_1 = \sqrt{\frac{1}{4N}\sum_{i=1}^{N}\left\{\left(\frac{\Delta z_{\max}}{1\text{mm}}\right)^2 + \left(\frac{\Delta z_{50}}{1\text{mm}}\right)^2 + \left(\frac{\Delta D_{10}}{1\%}\right)^2 + \left(\frac{\Delta D_{20}}{1\%}\right)^2\right\}_i}$$

$$I_2 = \sqrt{\frac{1}{6N}\sum_{i=1}^{N}\left\{\Delta d_{20}^2 + \Delta d_{50}^2 + \Delta d_{80}^2 + \Delta d'^2_{20} + \Delta d'^2_{50} + \Delta d'^2_{80}\right\}_i}$$

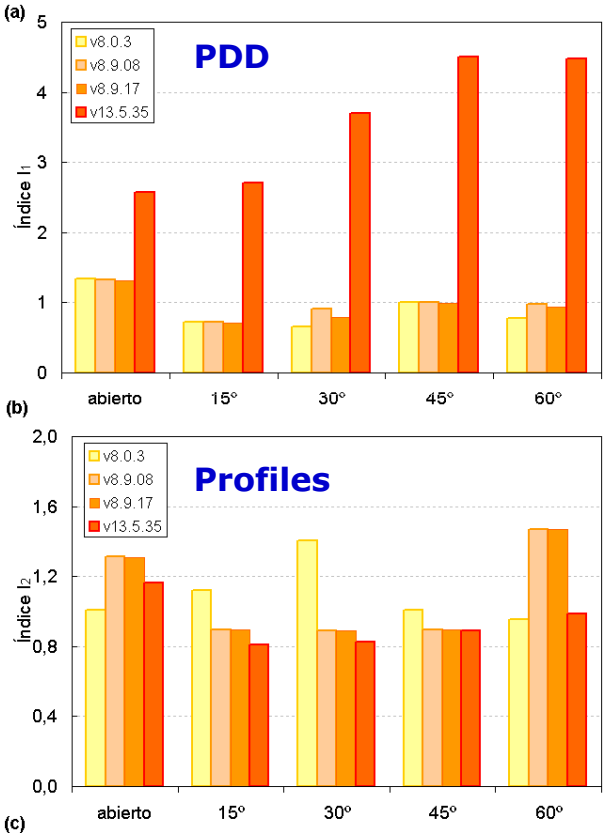

$$I_3 = \sqrt{\frac{1}{N}\sum_{i=1}^{N}\Delta D_{\text{abs}}^2}$$

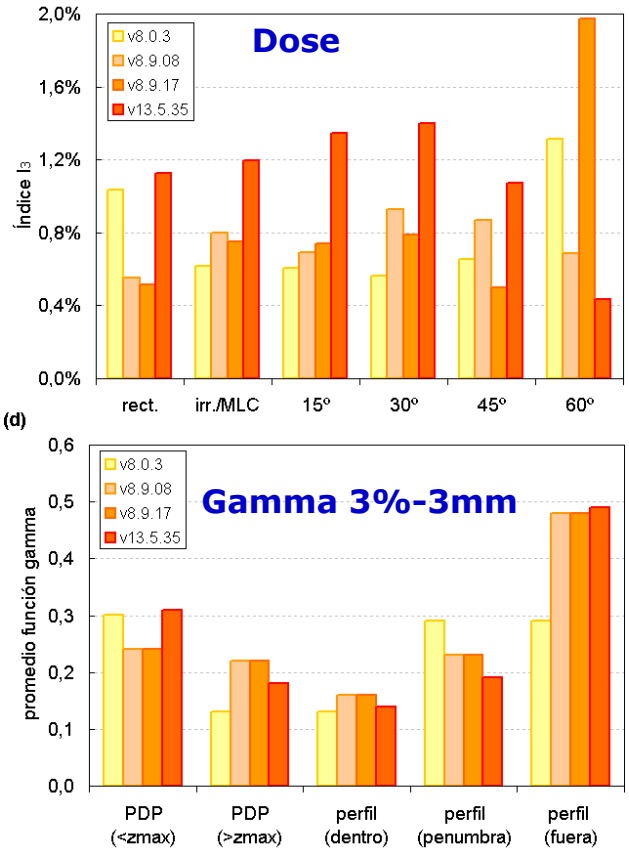

PDD differences up to 8mm and 3%.

MU differences up to 2%

Vs 13.5 uses a calculated spectra while the previous vs use a theoretical spectra.

Thanks to Artur Latorre-Mussoll Servei de Radiofisica Hospital Sant Pau

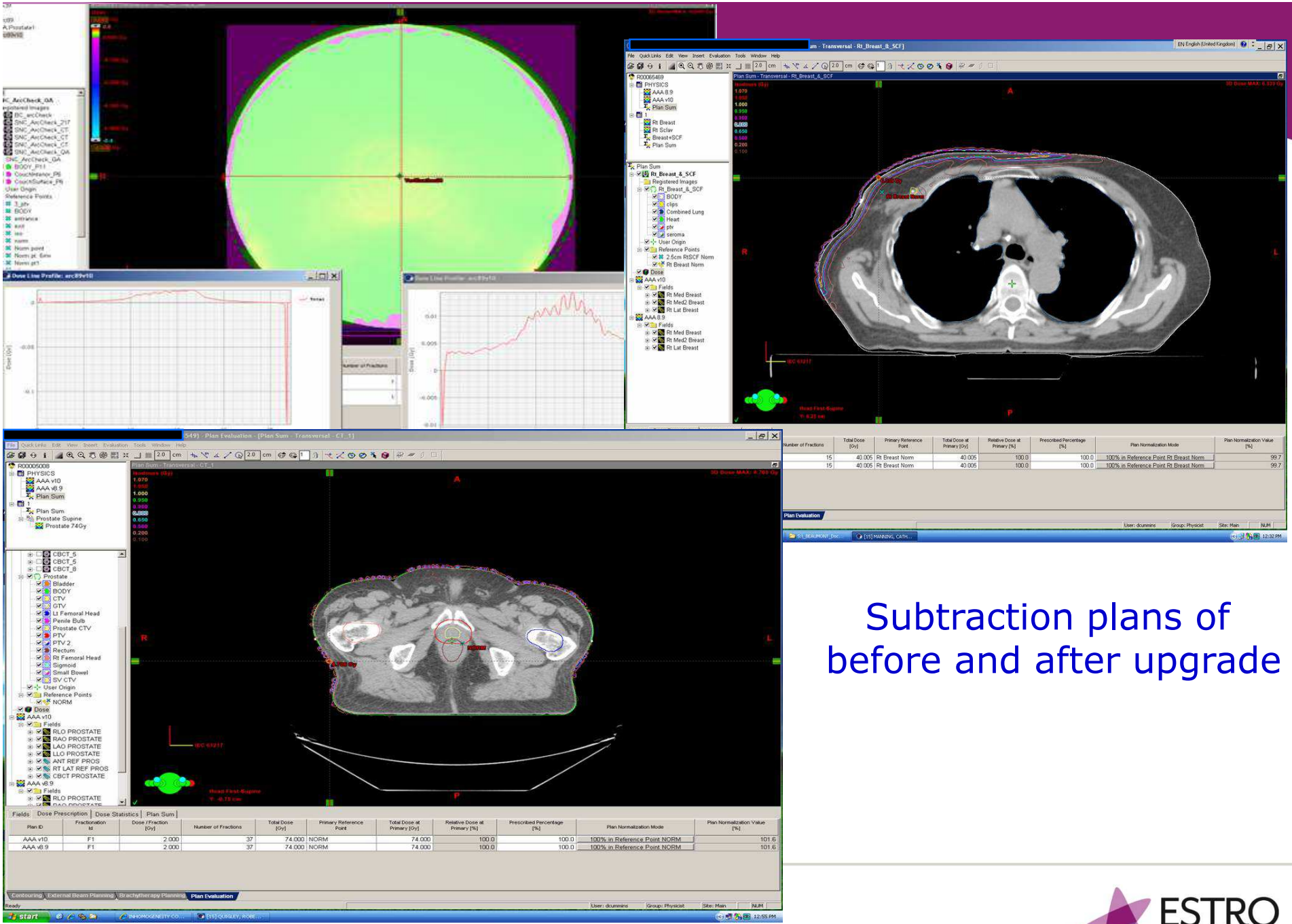

Subtraction plans of before and after upgrade

ESTRO School

Ongoing QC – when?

Regular intervals:
eg checksum, RANDO pre-plans

When significant software upgrades
Eg Eclipse v8.9 to v10

Significant Information Upgrades
Eg Mosaiq

New clinical uses/requests

Of course, ongoing IMRT QA
In-vivo dosimetry
MU checks etc!!

Summary-Recap

- TPS has a direct effect on patient outcome so a high quality QA process is essential
- Enormous number of parameters involving physics – getting the answers to these questions???
- Role of the QMP is critical
  - Understand models and limitations
  - Ensure TPS is used consistent with linac commissioning data
  - Ensure high quality input data
  - Awareness of changes anywhere in the RT Chain
  - Design QA process *for your clinic*
  - Training at start and on -going essential
- Establish periodic QC programme
- External audits

Summary-recap

- Think on the clinical situation for which the TPS will be used
- Design tests that mimic these clinical situations
- Think carefully on which data/measurements will you use as reference for comparison and on the method for comparison.
- Clearly define tolerances to confirm that your TPS **perfoms well.**

DVH and Dose based metrics

Brendan McClean

Feidhmeannacht na Seirbhíse Sláinte
Health Service Executive

Saint Luke's
Radiation Oncology
Network

Utrecht 2016

ESTRO School

Learning Objectives

- Identify the need for accurate DVH construction
- Investigate the limitations and assumptions of DVH calculation
- Examine QC requirements for DVH use

Dose Volume Histograms

- Graphical representation that relates dose received by a patient and the volume of tissue receiving each dose

- *Differential* DVH
- *Cumulative* DVH

$$DVH_{RelCum}(D) = 1 - \frac{1}{V}\int_{0}^{D_{max}} \frac{dV(D)}{dD}\, dD$$

Max dose in structure

Volume of structure

Differential DVH

The ideal DVH

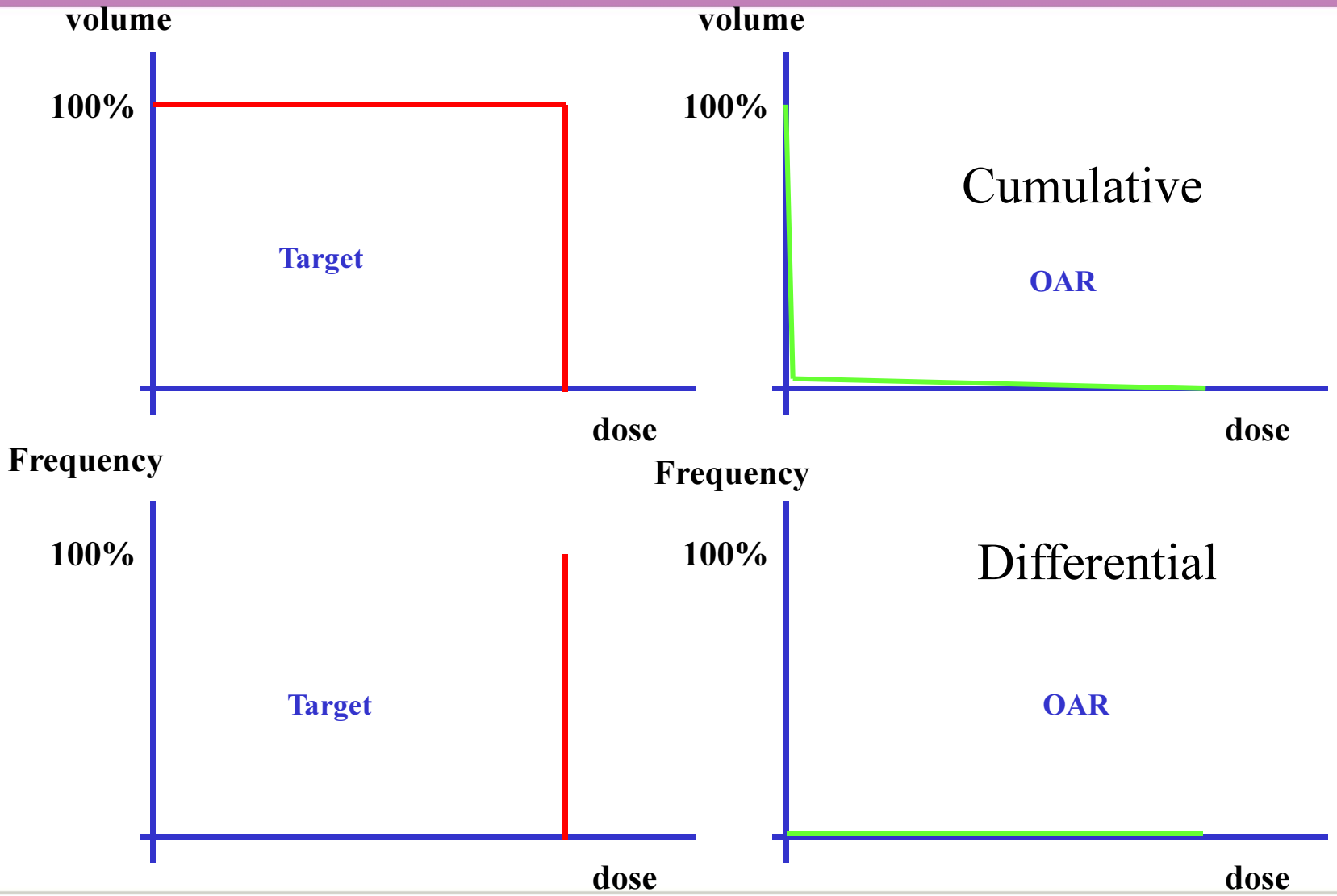

ESTRO School

The Reductionist View

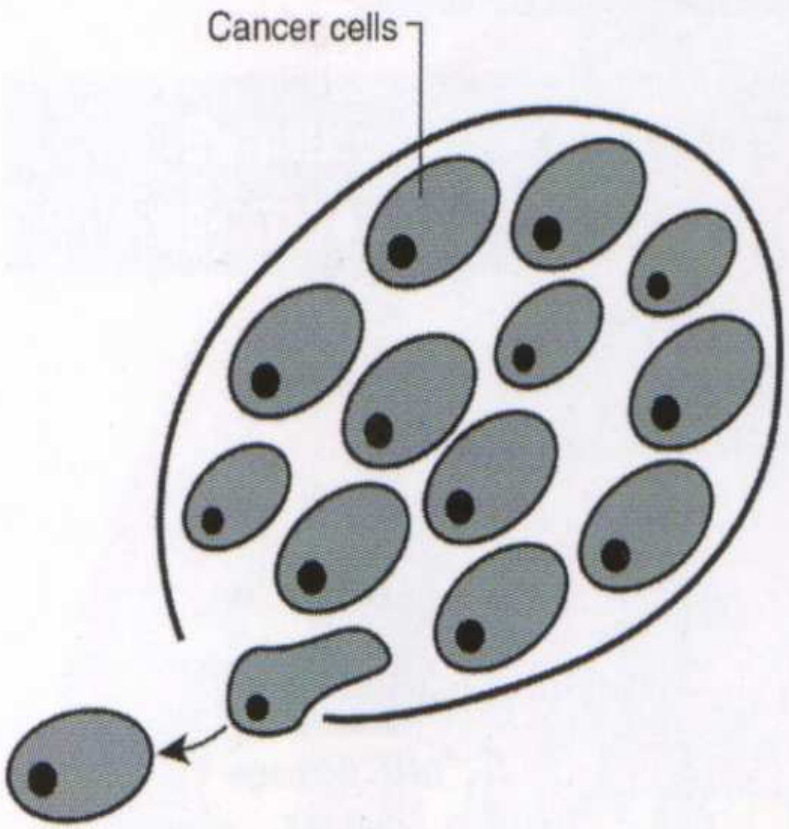

A Heterotypic Cell Biology

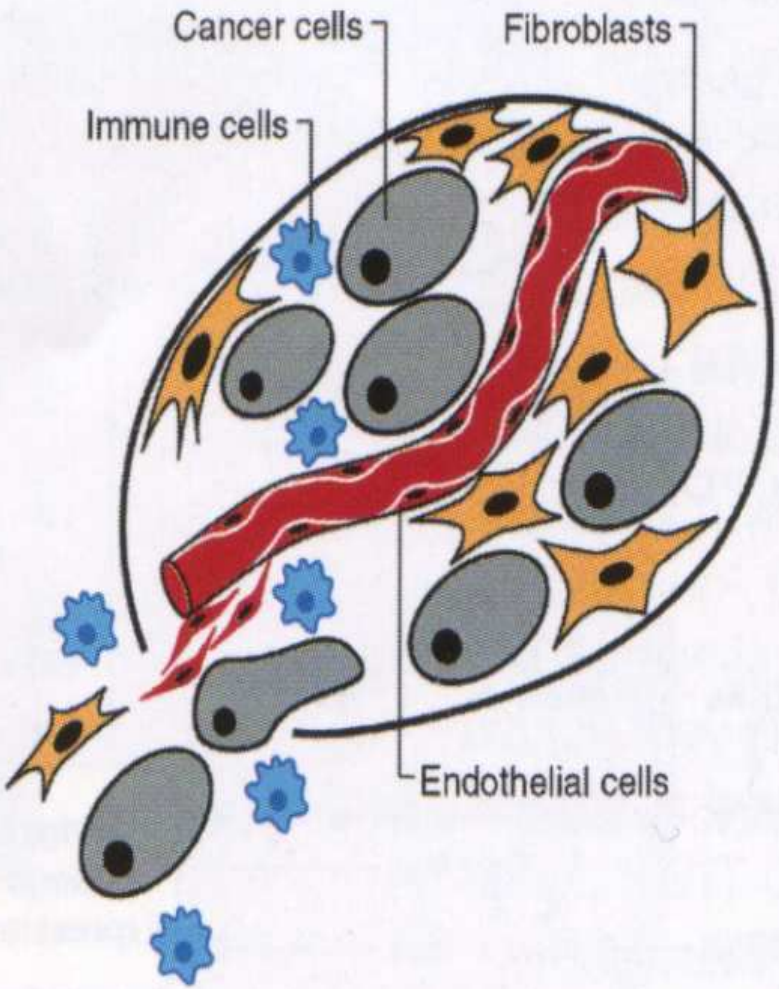

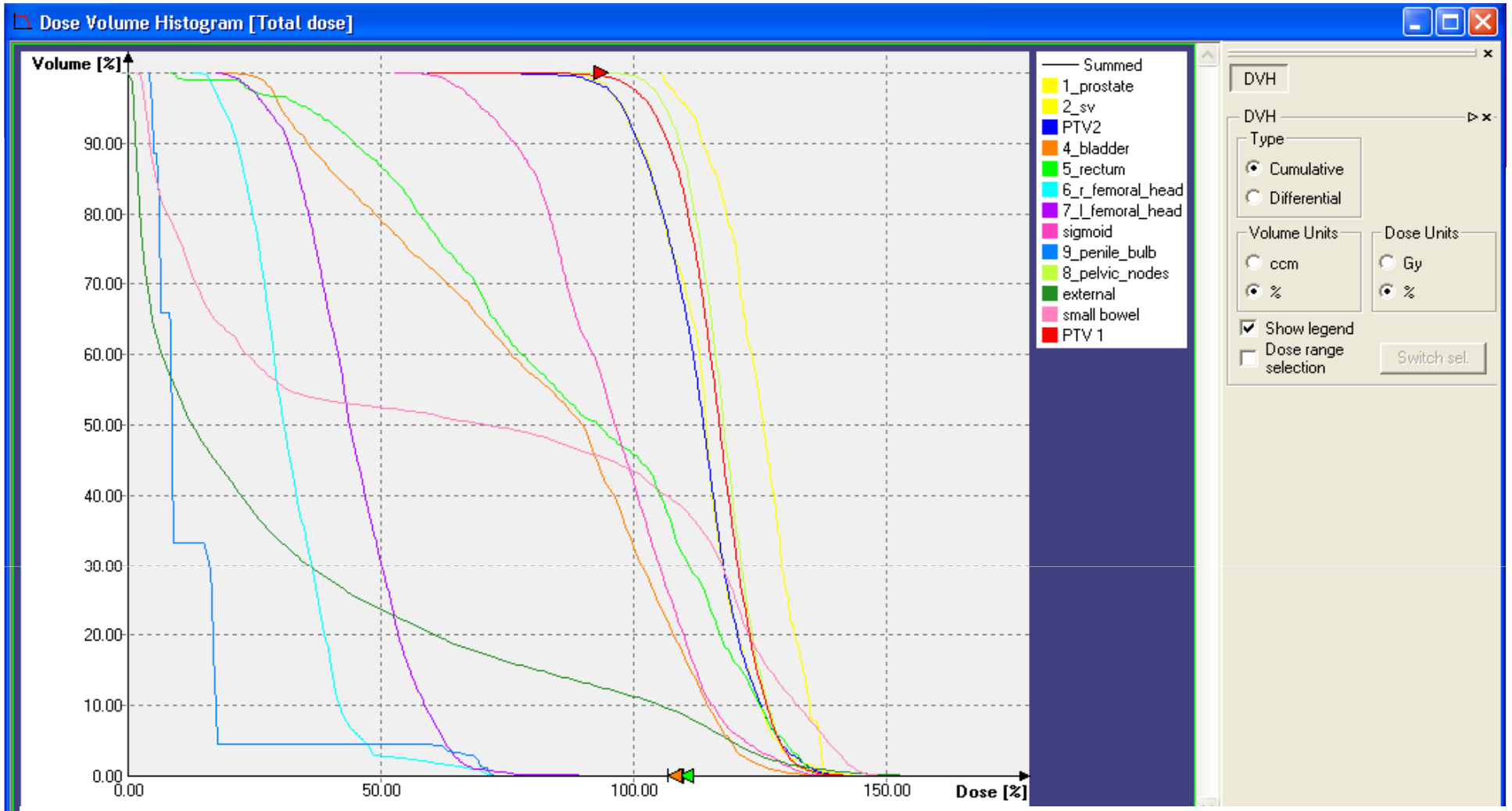

OAR	DVC	Recommended
Rectum	Dmax	<=78 Gy
	V75	<5%
	V70	<30%
	V50	<50%
	EUD	<63

James Balter
Randall K. Ten Haken
Marc L. Kessler

Limitations – No spatial Information

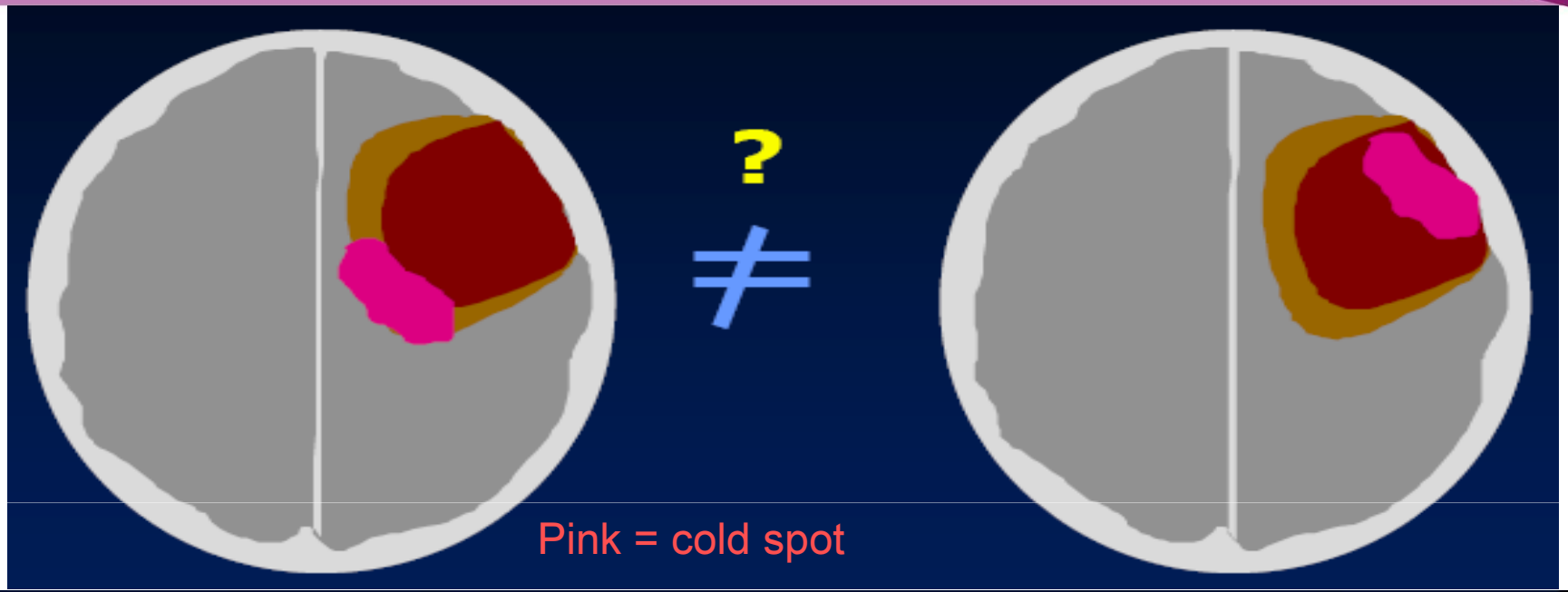

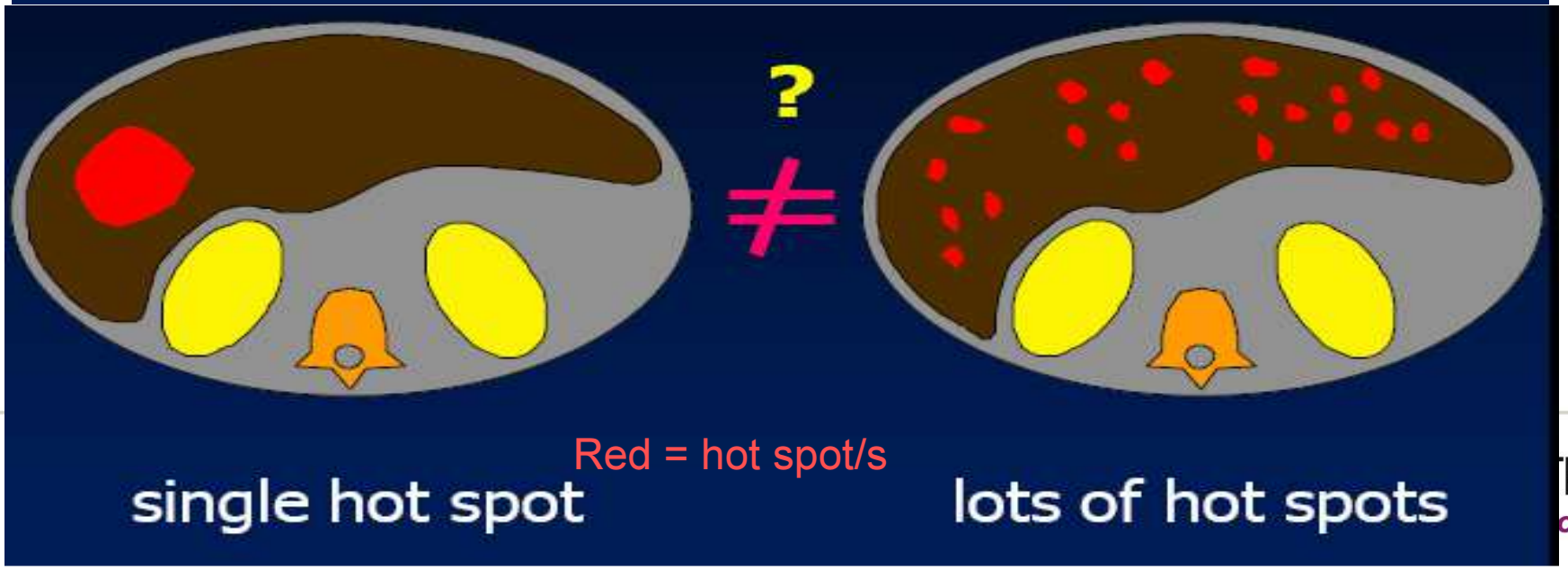

Need Accurate DVH's…..

- Various metrics calculated from DVH
  - *Calculation of biological indices*
- Used to correlate local control
  - *Clinical Trial outcome analysis*
- Used to report dose homogeneity
- IMRT Optimisation (Dose Volume Constraints)
- Used to correlate with morbidity for OAR's
  - *Clinical decisions are based on these*
- Used to develop dose constraints for prospective treatment planning
- Move from passing rates to DVH based QA metrics?

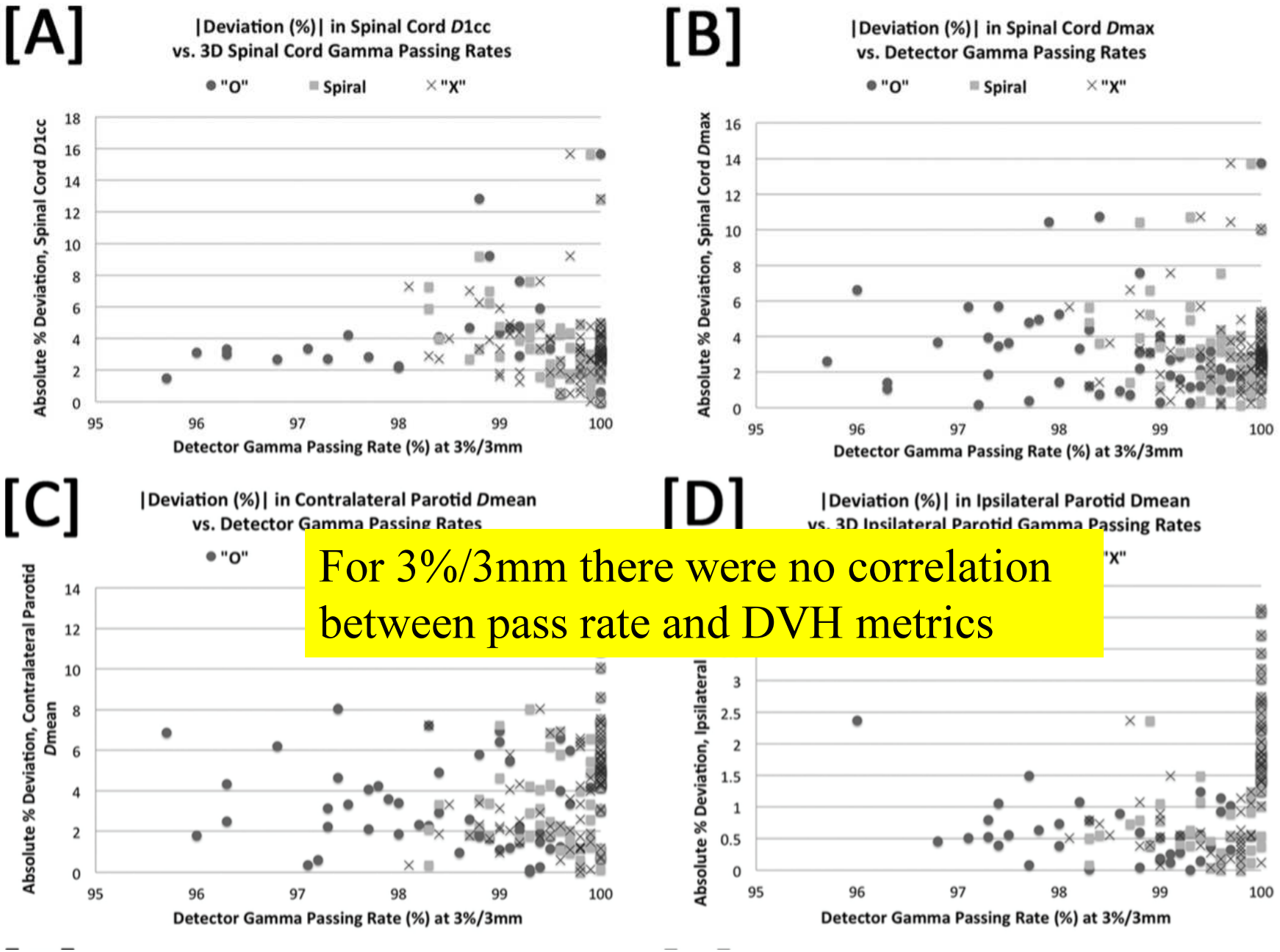

For 3%/3mm there were no correlation between pass rate and DVH metrics

Need Accurate DVH's…..

- Various metrics calculated from DVH
  - *Calculation of biological indices*
- Used to correlate local control
  - *Clinical Trial outcome analysis*
- Used to report dose homogeneity
- IMRT Optimisation (Dose Volume Constraints)
- Used to correlate with morbidity for OAR's
  - *Clinical decisions are based on these*
- Used to develop dose constraints for prospective treatment planning
- Move from passing rates to DVH based QA metrics?
- ***Accuracy in DVH construction essential***
  - Need dose calculation to compute dose in small fields, inhomogeneous tissue, non-equilibrium regions
  - **'Use of dose volume reporting is dependent on accurate dose calculation algorithms' (ICRU83)**

Inside/Outside VOI

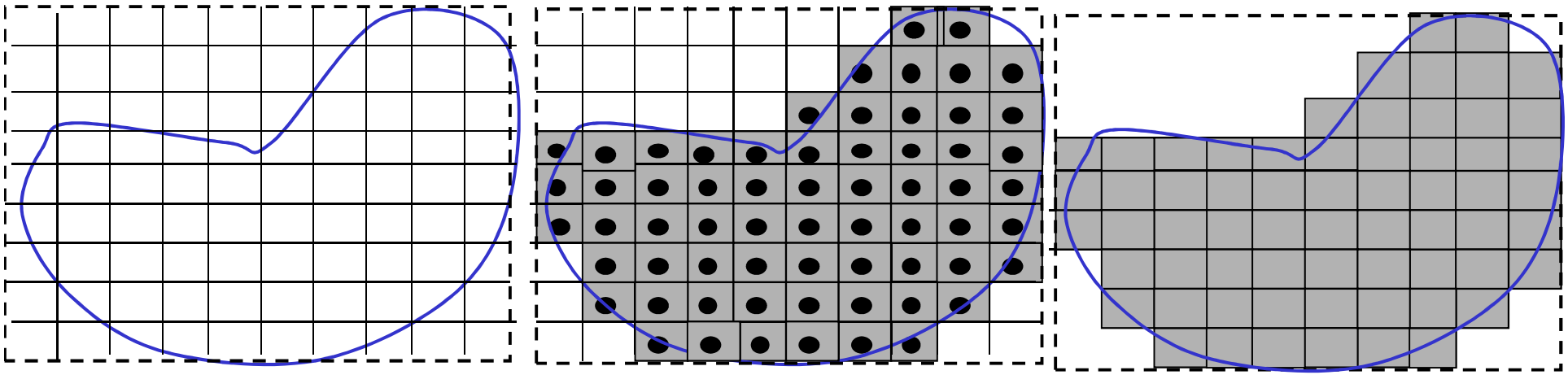

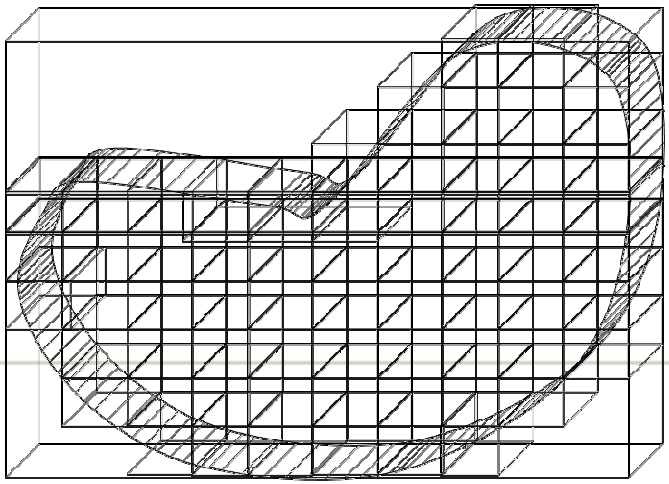

Partial/fractional voxels?
Consistency with TPS's?

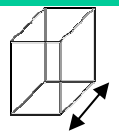

Slice Thickness

Sampling

Grid Sampling

- The true volume can be approximated by the ratio of number of points falling inside relative to outside

$$\frac{V}{V_0} = \frac{N}{N_0} \qquad V = V_0 \cdot \frac{N}{N_0}$$

Random Sampling

- **DVH can be constructed from set of randomly distributed dose points in the VOI**
- **Sample fewer voxels to get equivalent accuracy**

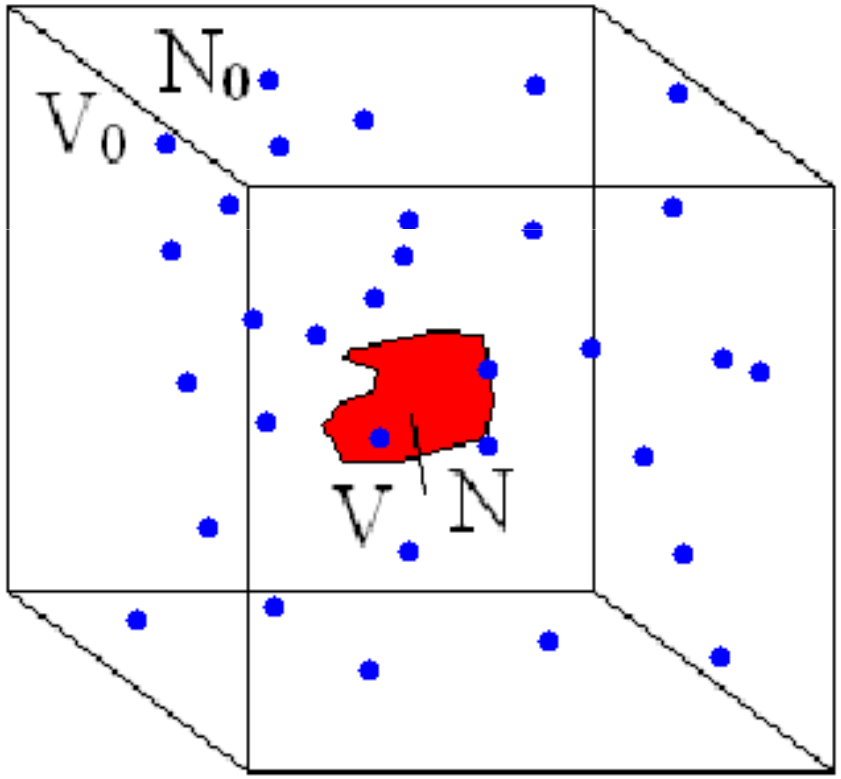

Andrzej Niemierko and Michael Goitein
Med Phys 1990

OMP – all dose voxels sampled
Eclipse – Grid and interpolation
ERGO++ - random sampling

ESTRO School

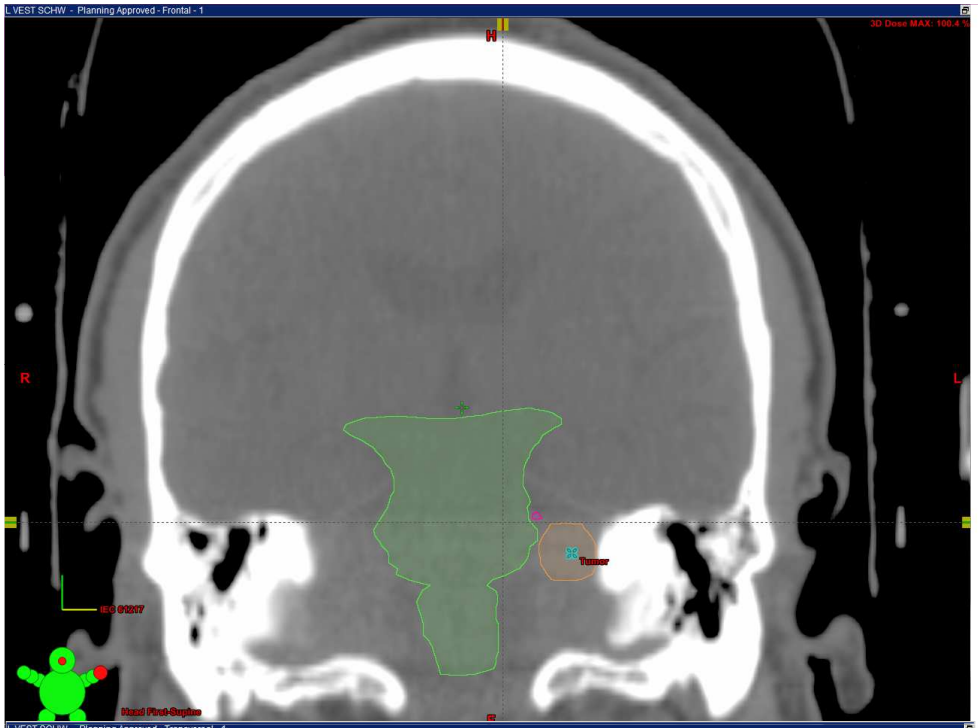
L VEST SCHW - Planning Approved - Frontal - 1
3D Dose MAX: 100.4 %
H
R
L
Tumor
IEC 61217
Head First-Supine

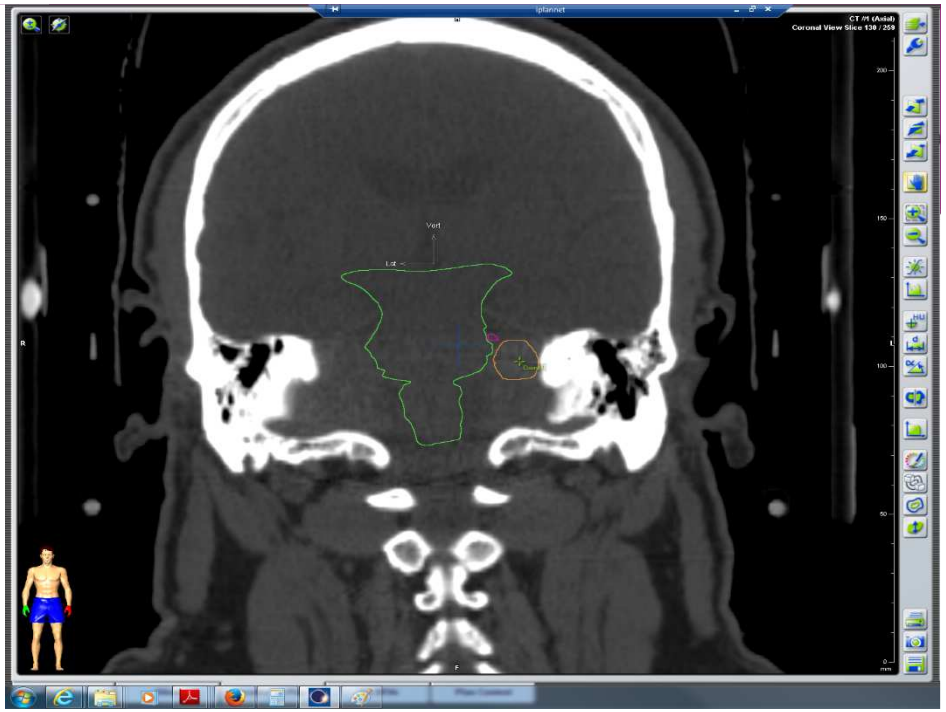
iplannet
CT #1 (Axial)
Coronal View Slice 138 / 259
Vert
Lat
R
L

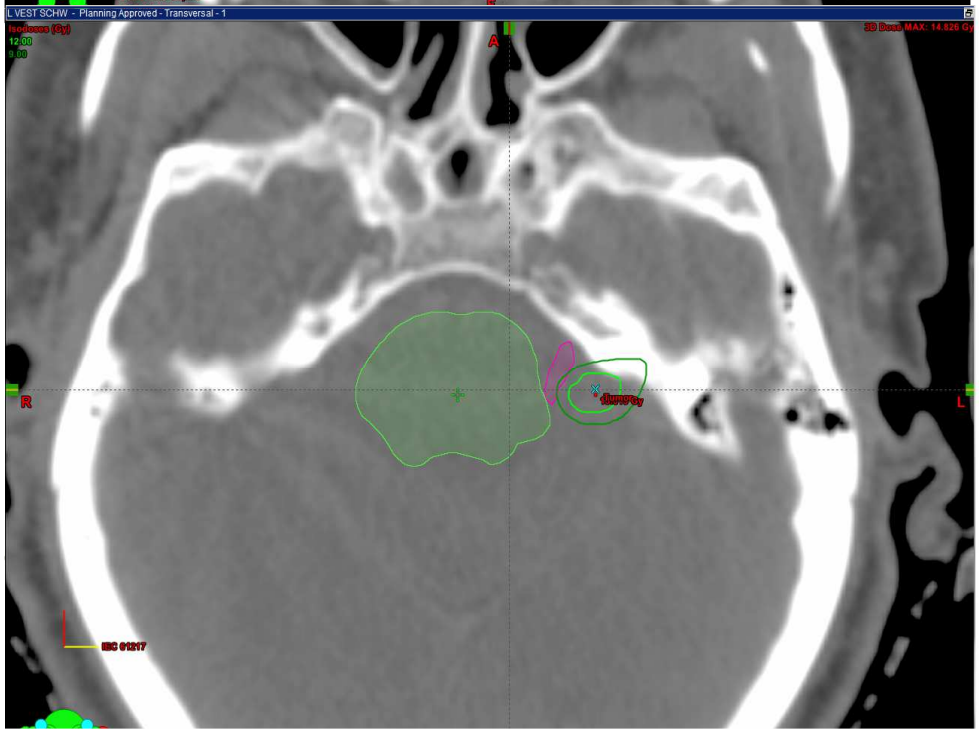
L VEST SCHW - Planning Approved - Transversal - 1
Isodoses (Gy)
12.00
9.00
3D Dose MAX: 14.826 Gy
A
R
L
IEC 61217

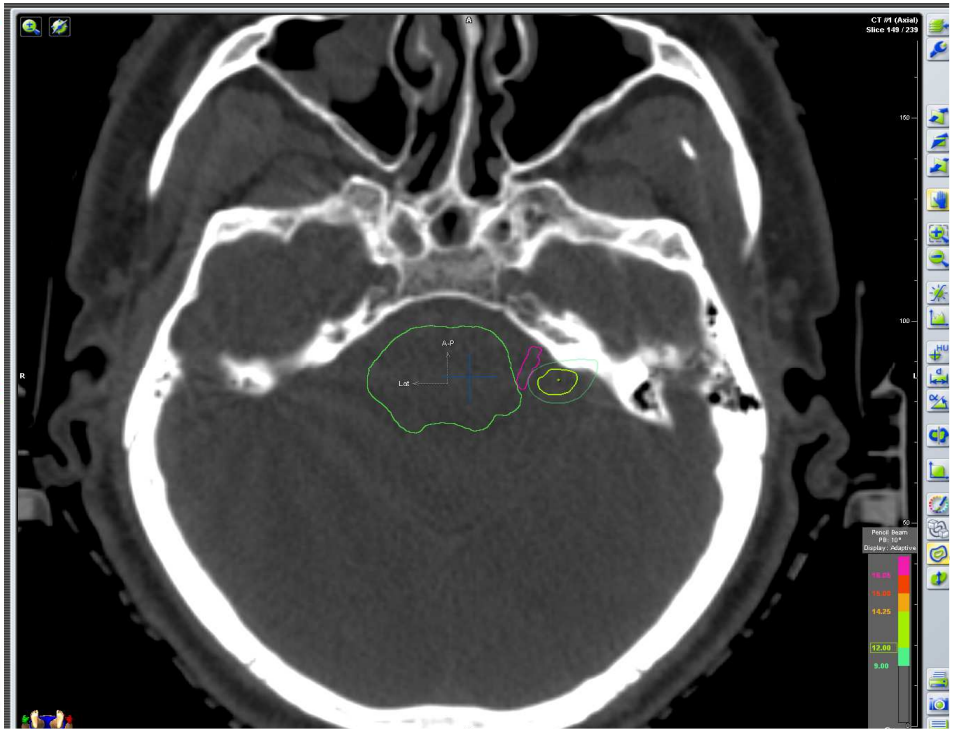
CT #1 (Axial)
Slice 149 / 239
A-P
Lat
R
L
14.25
12.00
9.00

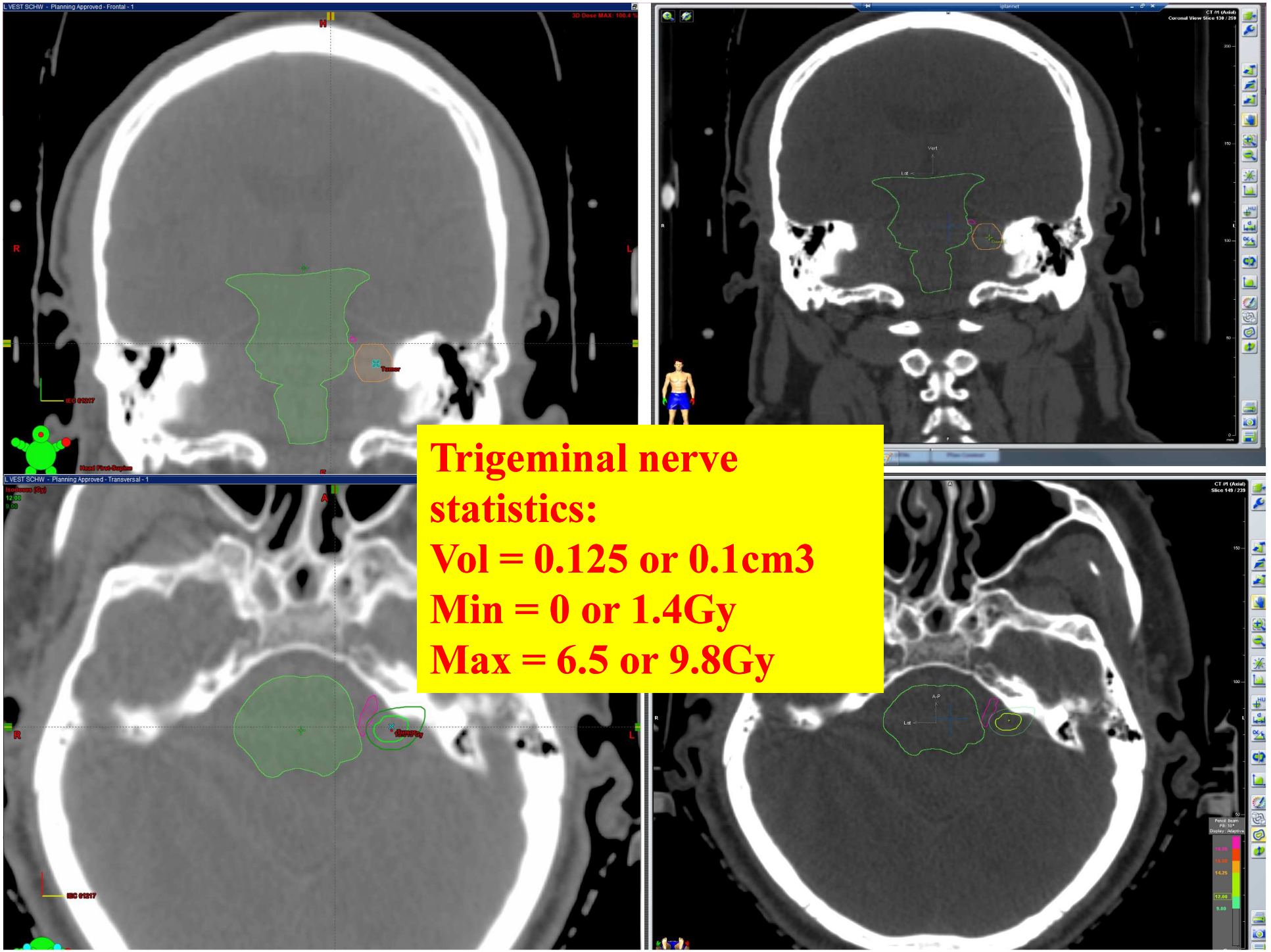
Trigeminal nerve
statistics:
Vol = 0.125 or 0.1cm3
Min = 0 or 1.4Gy
Max = 6.5 or 9.8Gy

(some) Dose metrics from DVH's

ICRU 83

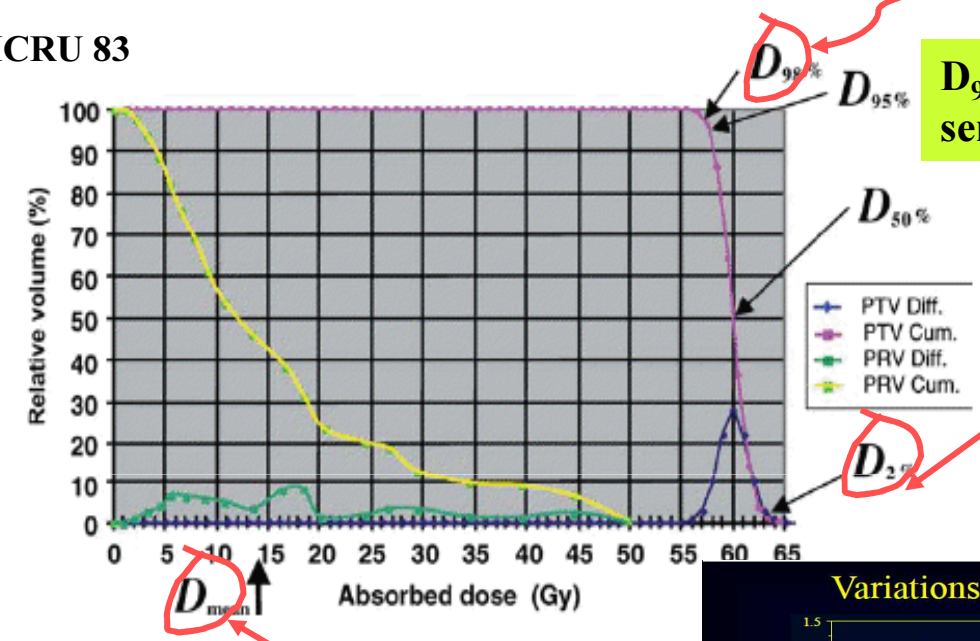

$D_{98\%}$ 'near minimum' since $D_{100\%}$ is highly sensitive to calculation and accuracy of CTV

$D_{2\%}$ 'near maximum' rather than previous maximum absorbed dose

$$HI = \frac{D_{2\%} - D_{98\%}}{D_{50\%}}$$

$$D_{mean} = \frac{1}{V}\int_0^{D_{max}} D\frac{dV(D)}{dD}\,dD$$

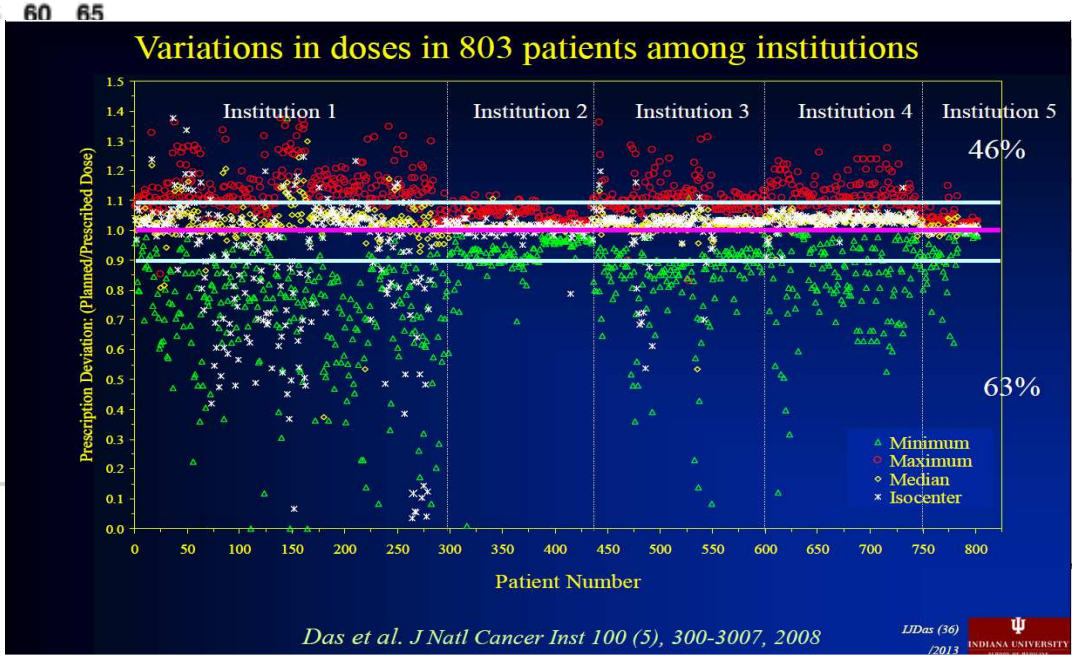

D_{median} is dose received by 50% of volume
If differential DVH is symmetric and unimodal for PTV then median and mean doses are nearly the same

Utrecht 2016

Dose Distribution Index (DDI)

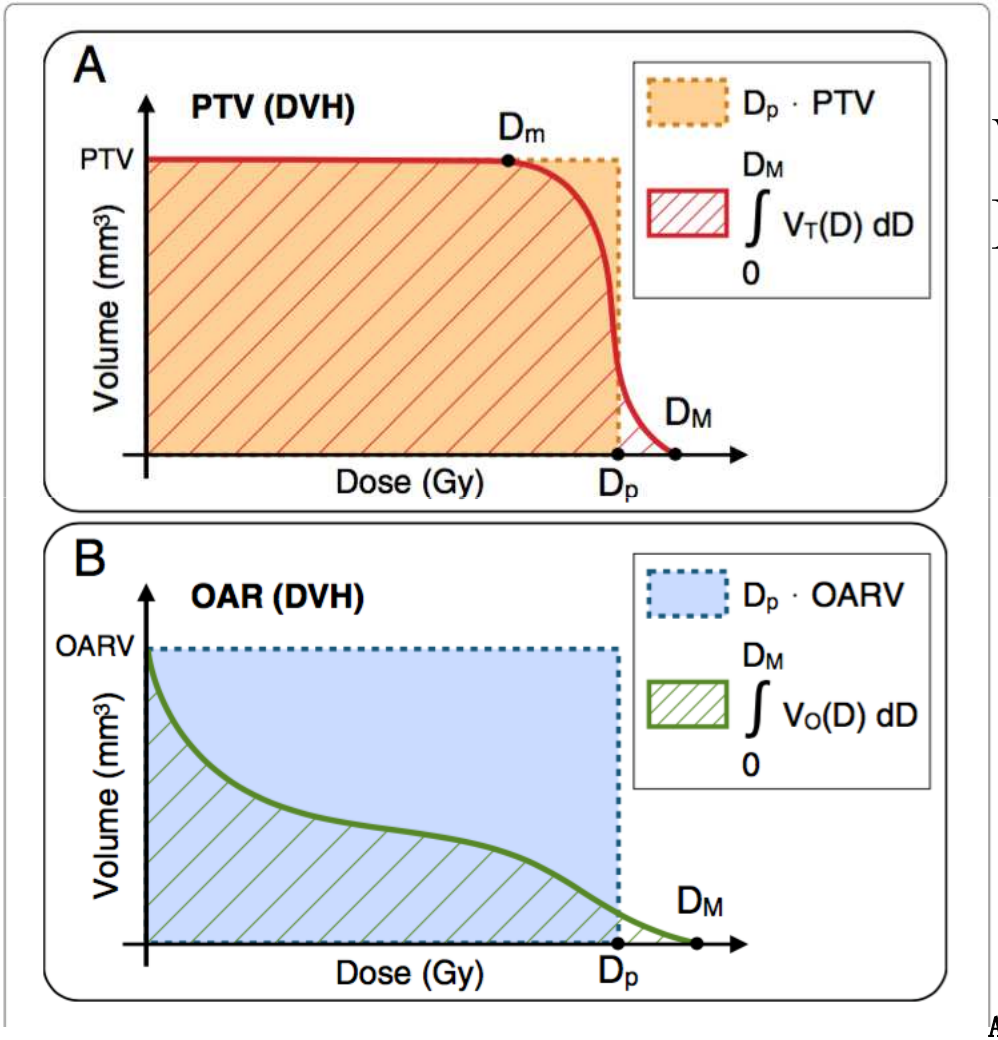

Weighted sum of 3 components:

DDI=

$1/3(\omega_T I_T + \omega_o I_o + \omega_R I_R)$

Alfonso *et al. Radiation Oncology* (2015)

Plan Evaluation: DVH Summary

- Ideal: Summarize DVH into a Single Index
- How do we summarize a DVH?
  - Mean Dose?
  - Median Dose? not useful in all cases!
- Reduce DVH (Power Law gives a relationship between Dose and fractional volume for a given NTCP)
  - Effective Volume Method [Converting bin volumes into volumes for a particular reference dose] (V_{eff})
  - Effective Dose Method [Converting bin doses to an equivalent dose to the whole organ] (D_{eff})
  - Then: Substitute V_{eff} or D_{eff} into Lyman Equations to get NTCP as dose is now uniform to organ
- Statistical Indices that describe complication and cure rates: NTCP, TCP and EUD

$$EUD = \left[\sum_i \Delta V_i (D_i)^a\right]^{\frac{1}{a}}$$

Accuracy and limitations

- **Factors affecting DVH accuracy:**
  - Accuracy to which VOI is delineated (Main contribution)
  - Dose bin size
  - Distance Map voxel size
  - Sampling method and sampling resolution
  - Shape of VOI
  - Dose Calculation Algorithm (difference in modelling heterogenities, penumbra…)
  - Dose voxel size

Accuracy and limitations

- **Factors affecting DVH accuracy:**
  - Accuracy to which VOI is delineated (Main contribution)
  - Dose bin size
  - Distance Map voxel size
  - Sampling method and sampling resolution
  - Shape of VOI
  - Dose Calculation Algorithm (difference in modelling heterogenities, penumbra…)
  - Dose voxel size

Accuracy – Contour Definition

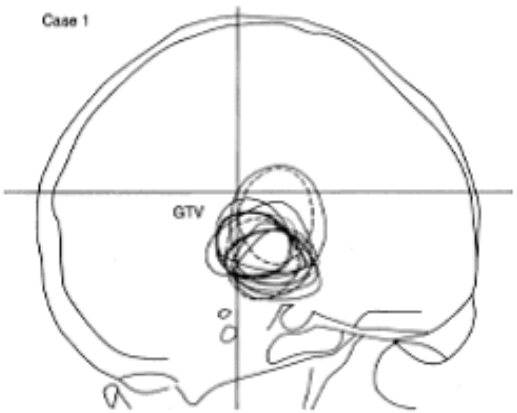

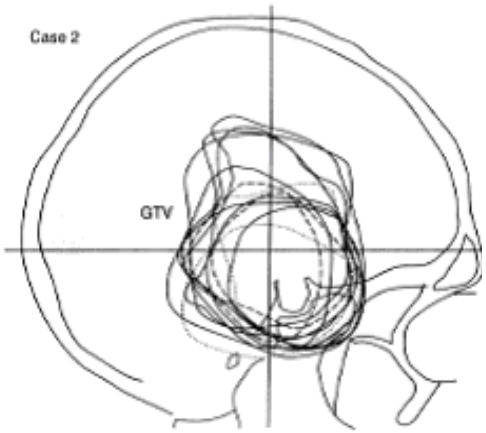

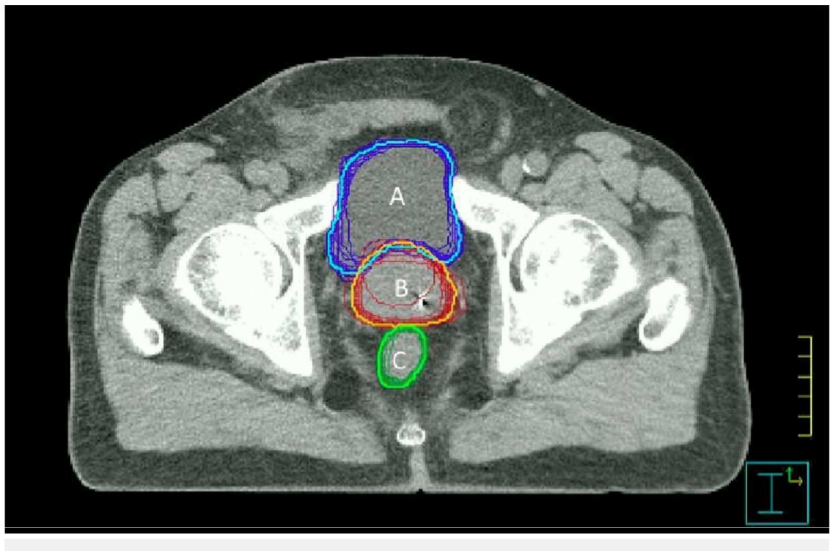

Barghi et al 2013

- Taken from ICRU Rpt. 50
- Also: Inter-observer variation(1SD) 13% small cylinder, 5% large cylinder, 3% cone shape (Kirisits et al RO 2007)

Complete OAR's often not scanned or delineated – though DVC's applied for full organ

Inter- and Intra-Planner Variation

- One TPS system (Eclipse/Helios)
- Identical Machine (6 MV, Varian)
- Five institutions
  - Sewel, NJ
  - Orlando, Florida
  - Buffalo, NY
  - Worcester, Massachusetts
  - Waterbury, CT
- Identical constraints
- Independent planning of each site 3 times

LIDas (33) /2013

INDIANA UNIVERSITY

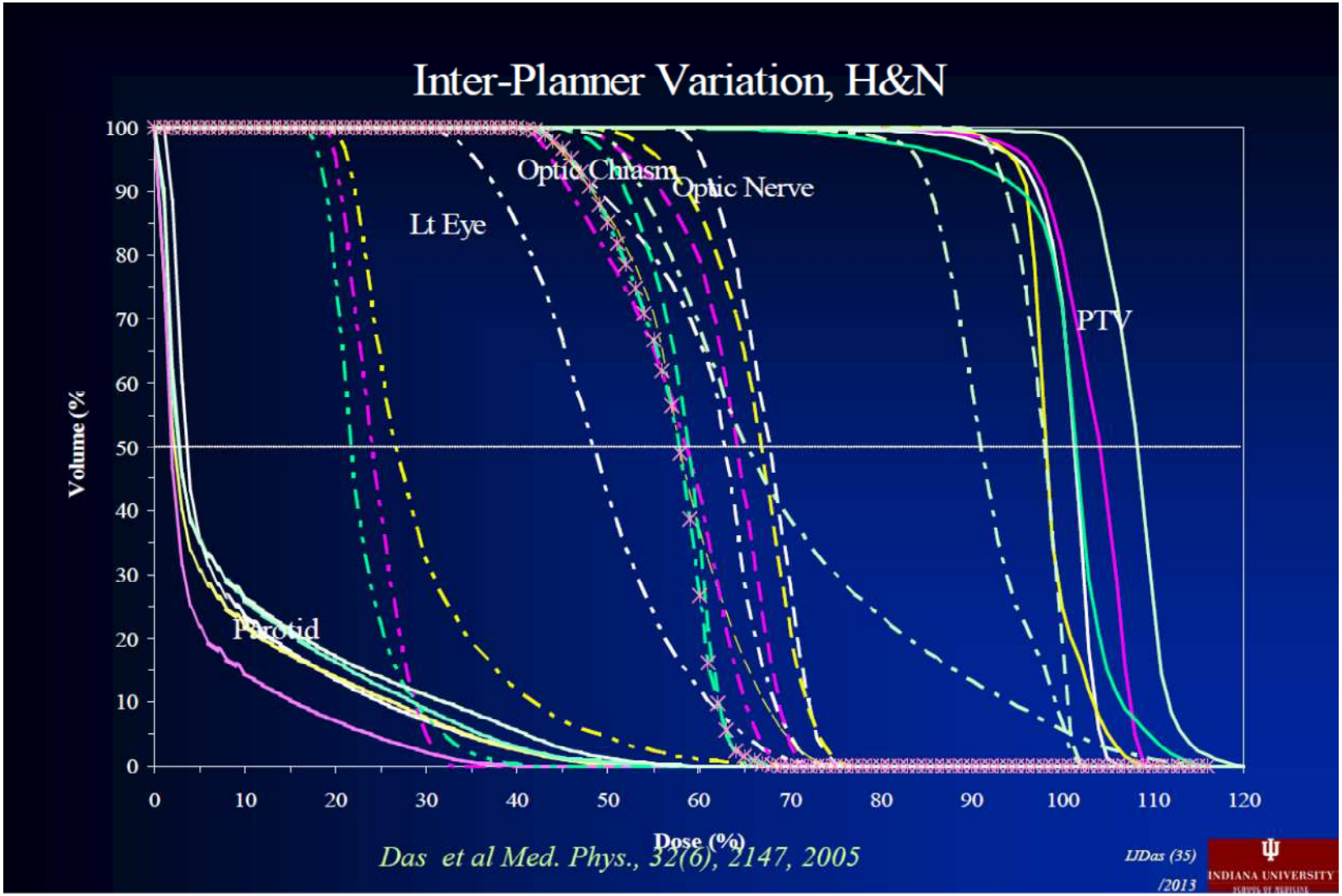
Inter-Planner Variation, H&N
Volume (%
Dose (%)
Optic Chiasm
Optic Nerve
Lt Eye
PTV
Parotid
Das et al Med. Phys., 32(6), 2147, 2005
LJDas (35)
/2013
INDIANA UNIVERSITY

Accuracy and limitations

- **Factors affecting DVH accuracy:**
  - Accuracy to which VOI is delineated (Main contribution)
  - Dose bin size
  - Distance Map voxel size
  - Sampling method and sampling resolution
  - Shape of VOI
  - Dose Calculation Algorithm (difference in modelling heterogenities, penumbra…)
  - Dose voxel size

Dose Bin Size

- For Nucletrons Oncentra Masterplan TPS (used at St. Lukes): the default setting is 200 bins
- This can have an effect on the DVH appearance (and DVH accuracy!)

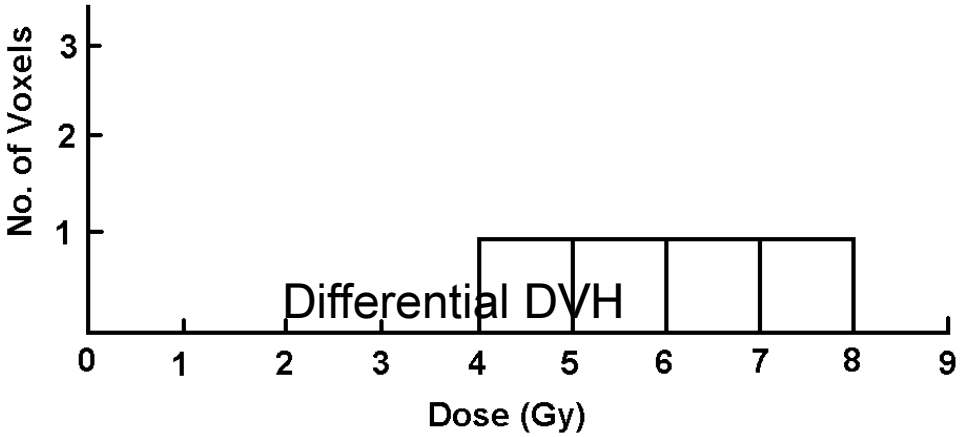

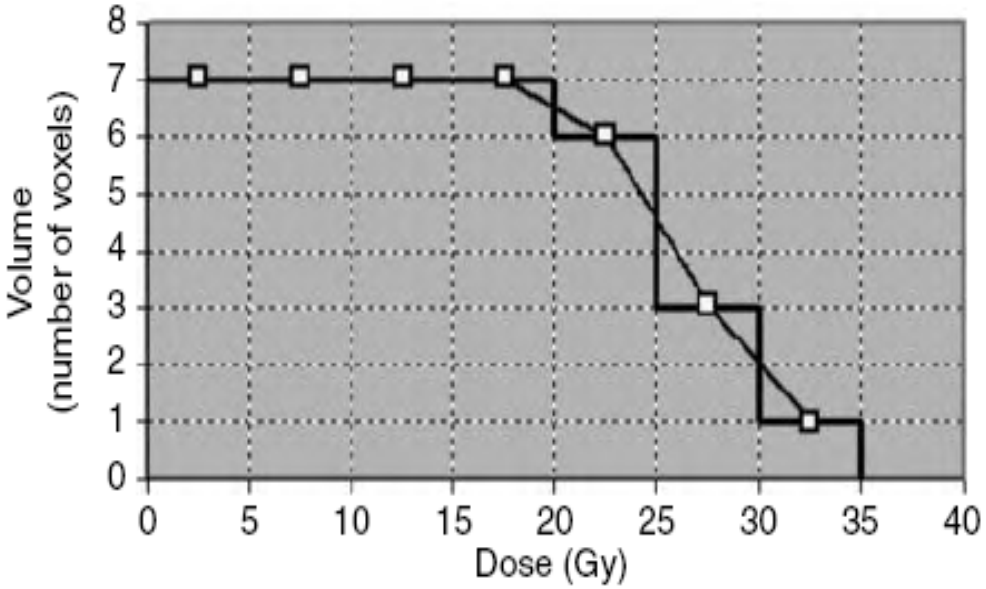

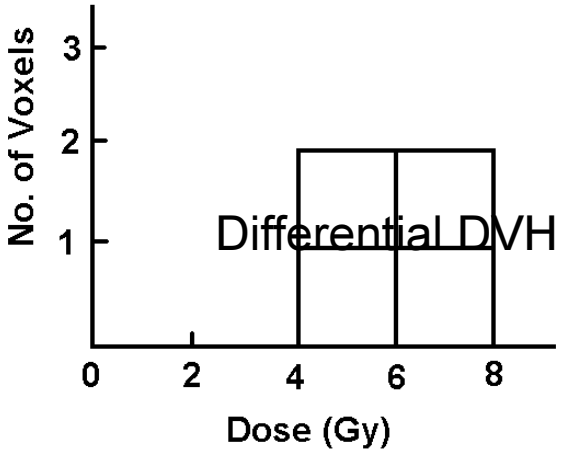

Accuracy and limitations

- **Factors affecting DVH accuracy:**
  - Accuracy to which VOI is delineated (Main contribution)
  - Dose bin size
  - Distance Map voxel size
  - Sampling method and sampling resolution
  - Shape of VOI
  - Dose Calculation Algorithm (difference in modelling heterogenities, penumbra…)
  - Dose voxel size

Accuracy: Distance Map Voxel Size

- Predefined (usually for each VOI type i.e. target or OAR etc.)
- Automatic Voxel Size to achieve both reasonable accuracy and speed
- This can have an affect on the volume accuracy of the DVH

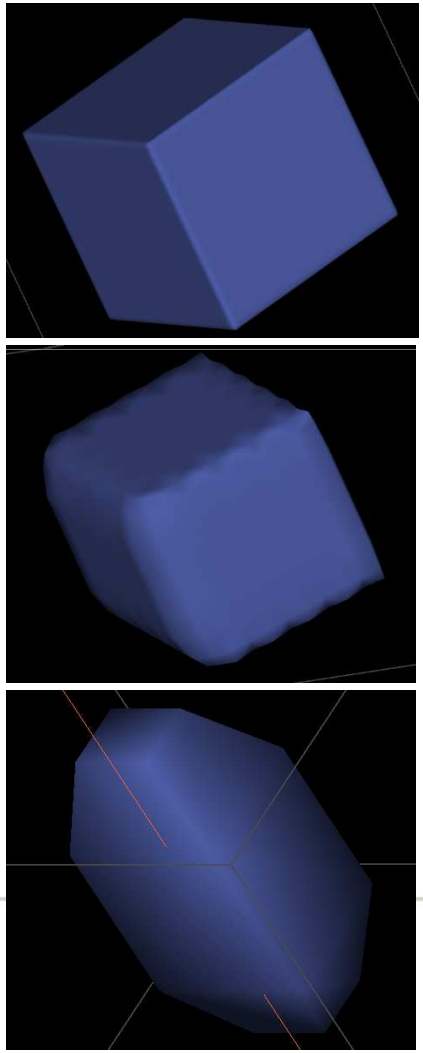

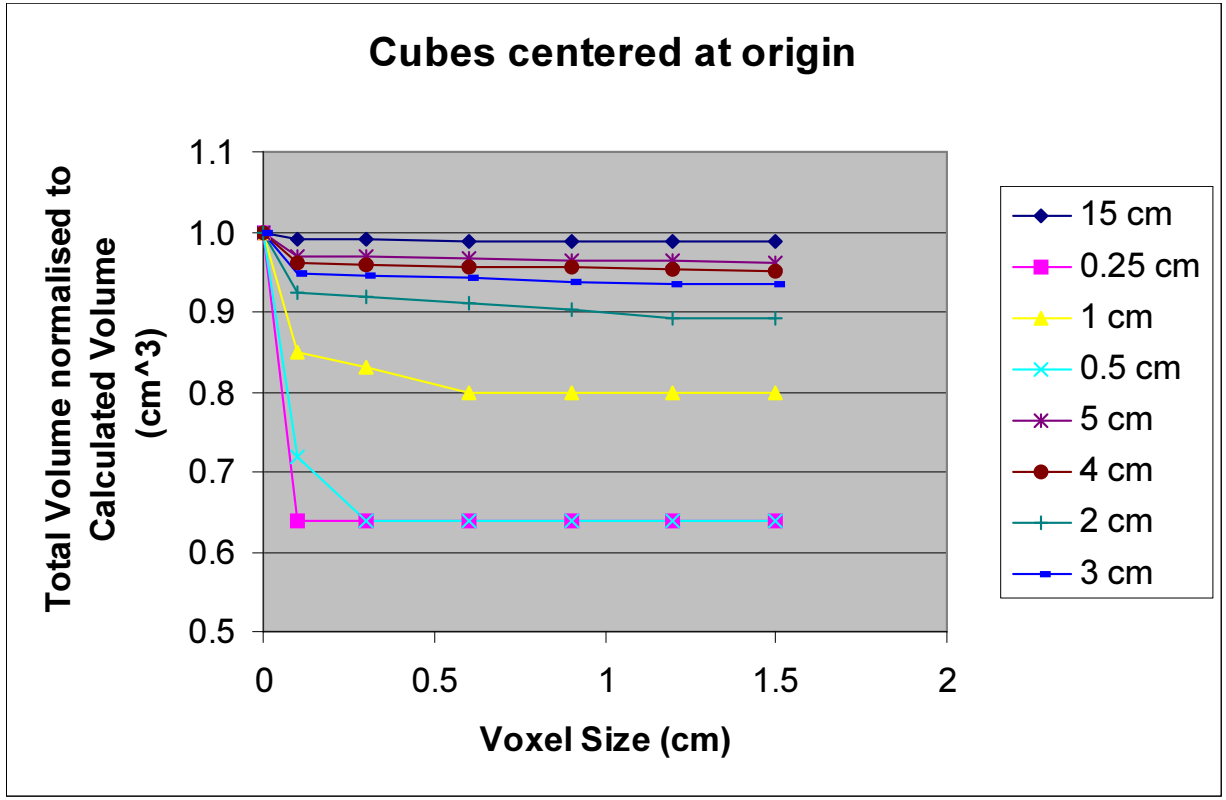

ESTRO School

Accuracy: Distance Map Voxel Size

Voxel Size: 0.1 cm

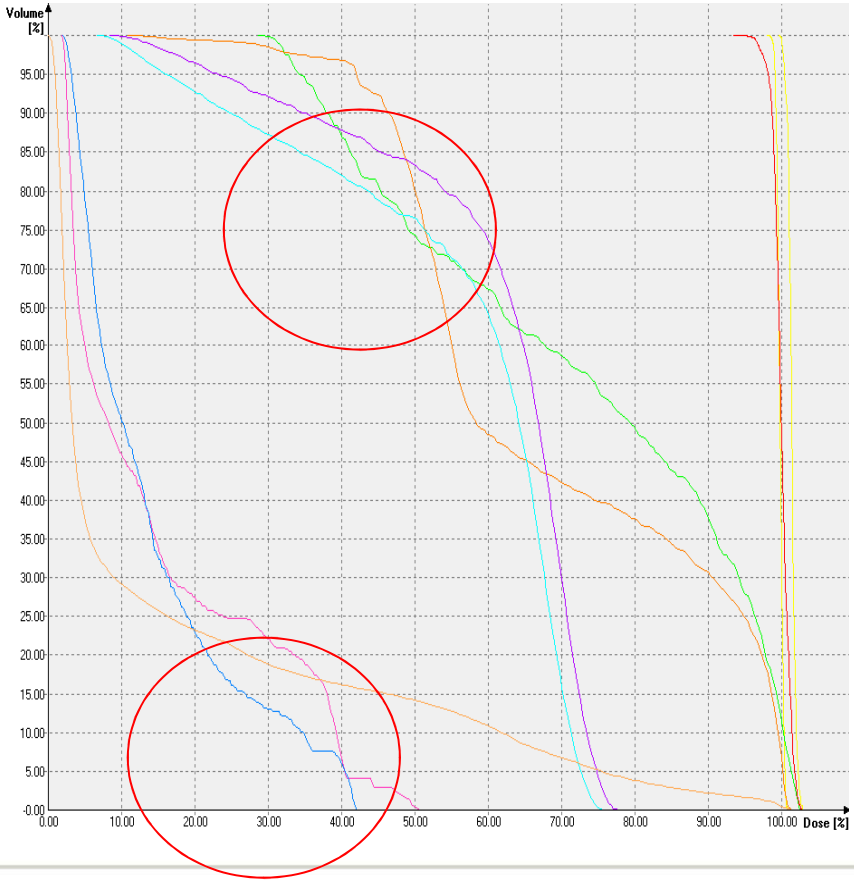

Voxel Size: 1.5 cm

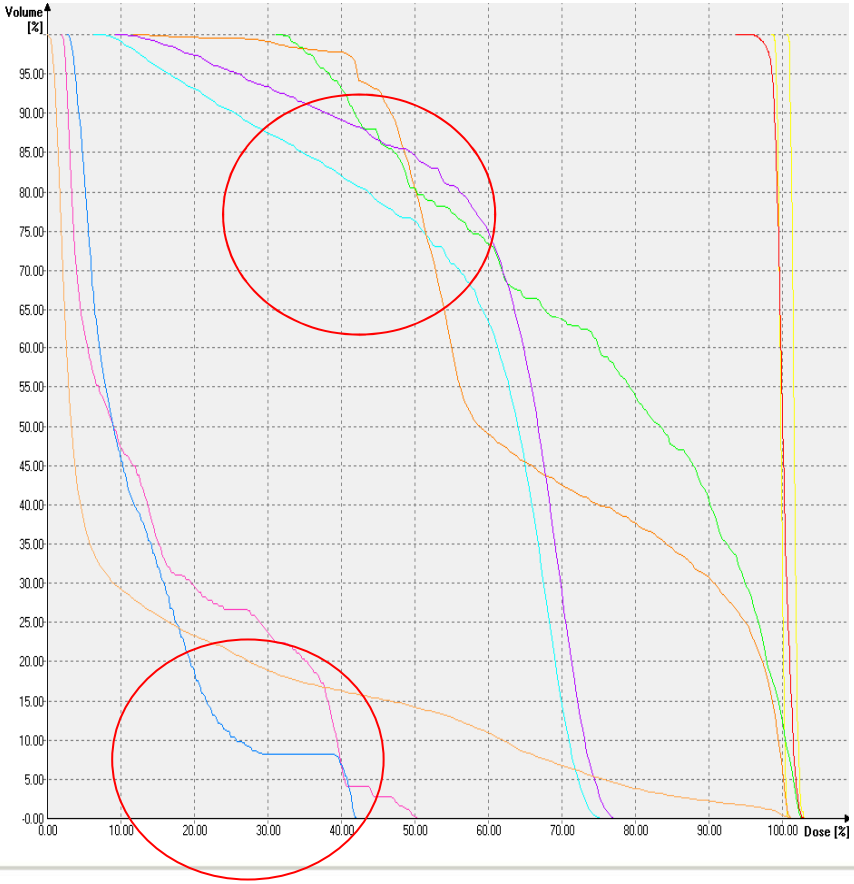

ESTRO School

Accuracy and limitations

- **Factors affecting DVH accuracy:**
  - Accuracy to which VOI is delineated (Main contribution)
  - Dose bin size
  - Distance Map voxel size
  - Sampling method and sampling resolution
  - Shape of VOI
  - Dose Calculation Algorithm (difference in modelling heterogenities, penumbra…)
  - Dose Voxel Size

Dose deposition approximations (patient)

15 MV photons

(Dose contr. normalization)

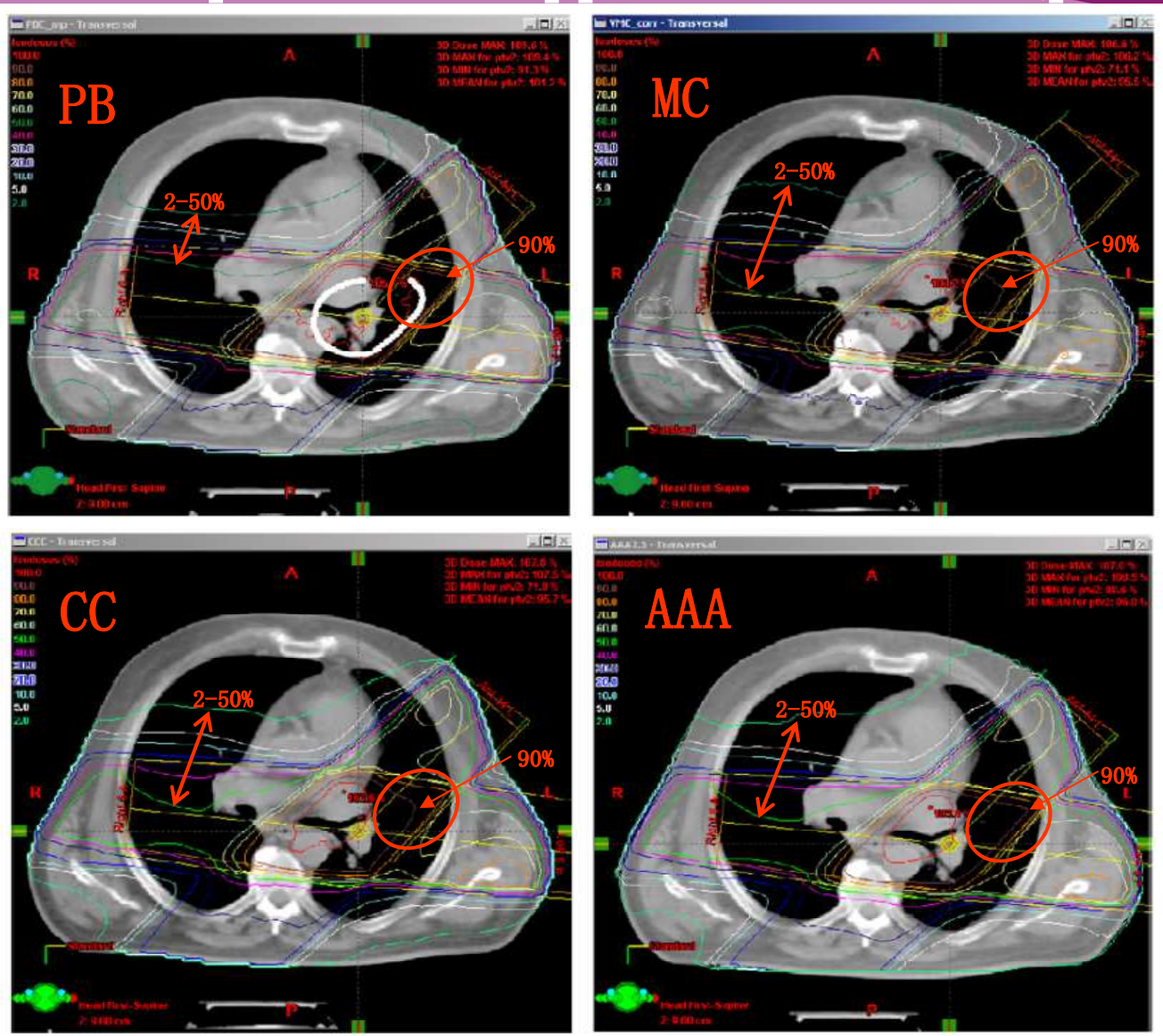

Hasenbalg *et al* [17]

Dose deposition approximations (patient)

Cumulative DVH for PTV and left lung (case from previous page).

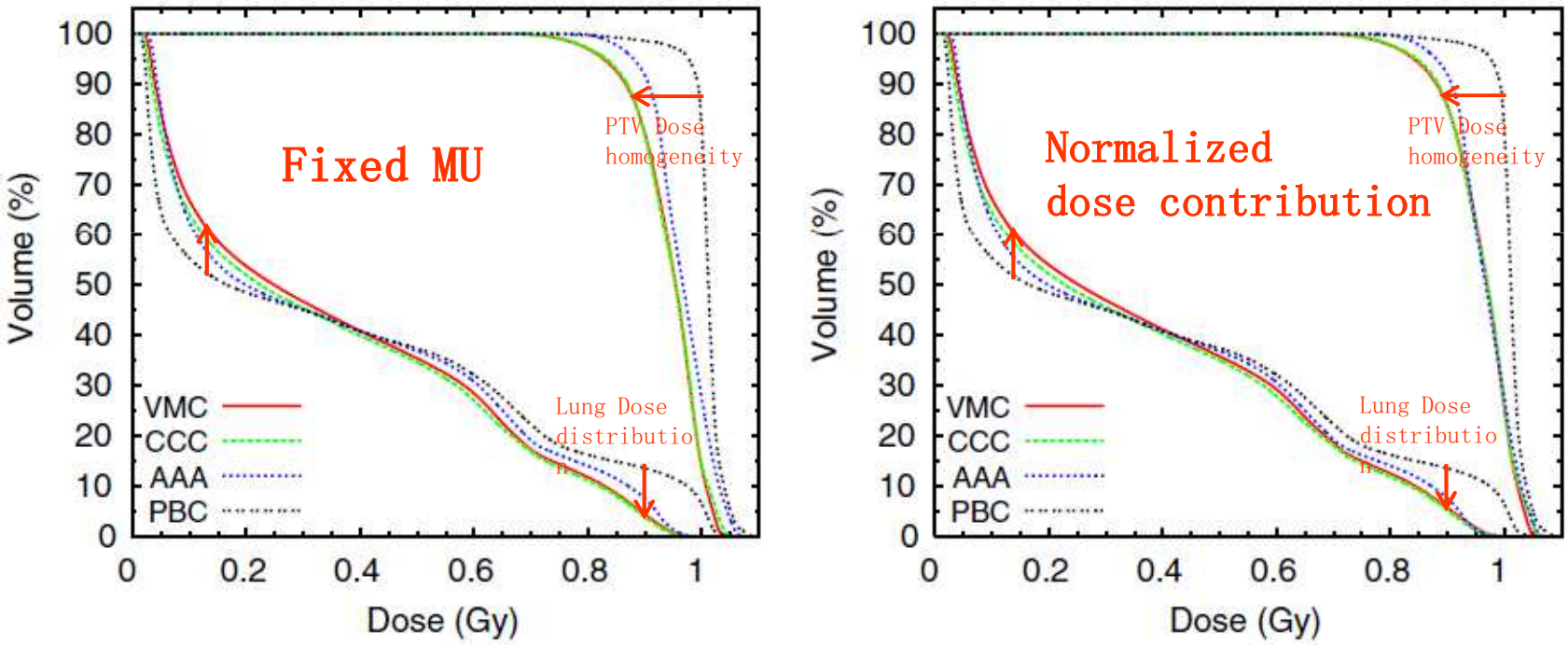

Hasenbalg *et al* [17]

Including dose calculation uncertainty in DVH construction

- Uncertainty in a dose point has both type A and type B uncertainty components
  - (both for measured data)
- A probability density function can be used to model uncertainty:

- Used Rectangular, Gaussian and Triangular distributions

$$f_i(\delta_i) = f\left(\frac{\delta_i - D(z_i)}{\sigma_i}\right)$$

Henriquez and Caastrillon MP 2010

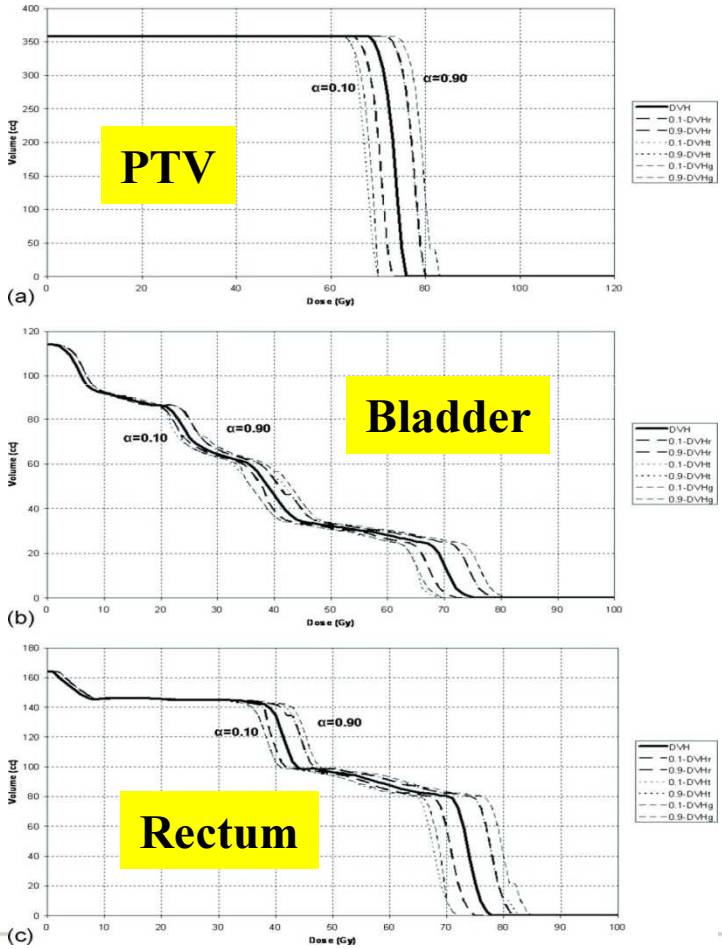

Prostate

ESTRO School

Including dose calculation uncertainty in DVH construction

- Uncertainty in a dose point has both type A and type B uncertainty components
  - (both for measured data)
- A probability density function can be used to model uncertainty:

- Used Rectangular, Gaussian and Triangular distributions

$$f_i(\delta_i) = f\left(\frac{\delta_i - D(z_i)}{\sigma_i}\right)$$

Henriquez and Caastrillon MP 2010

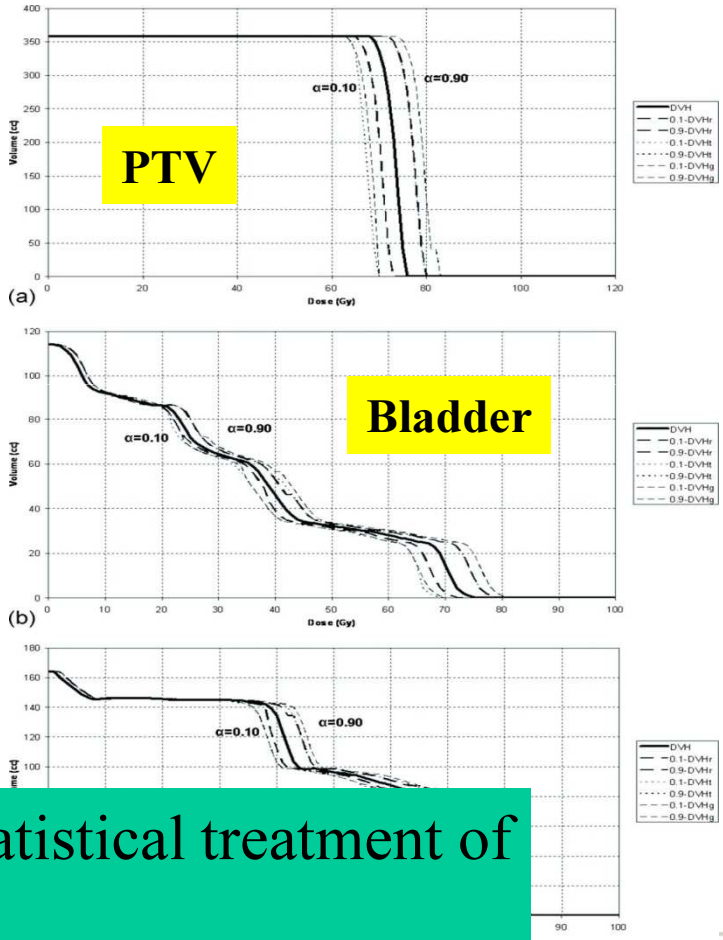

Report uncertainty in DVH to enhance statistical treatment of Clinical trial results?

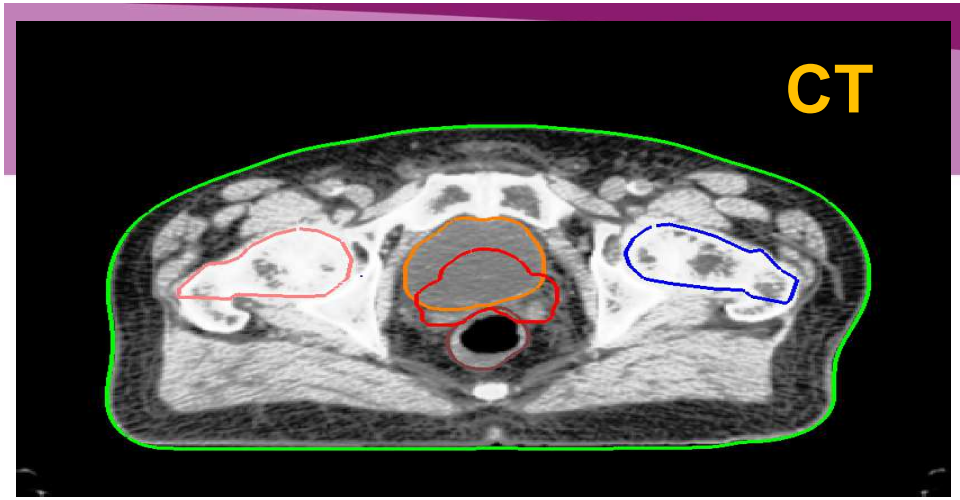
CT

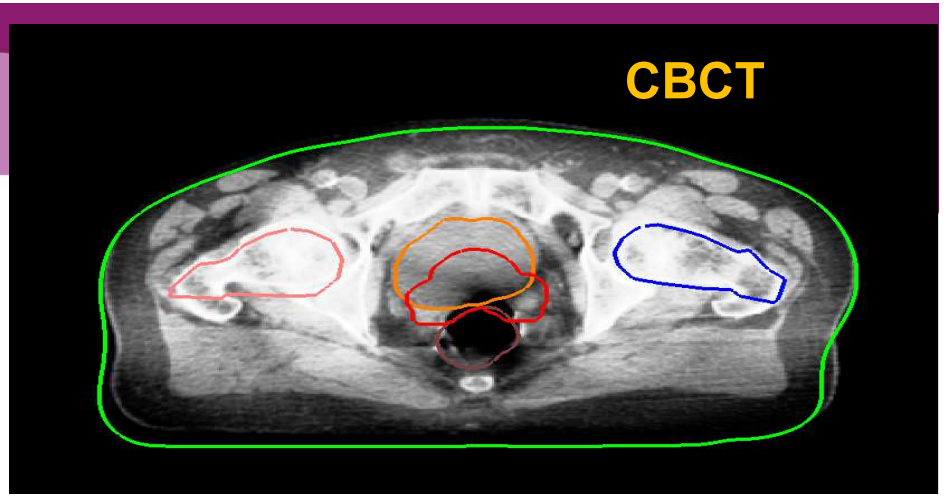
CBCT

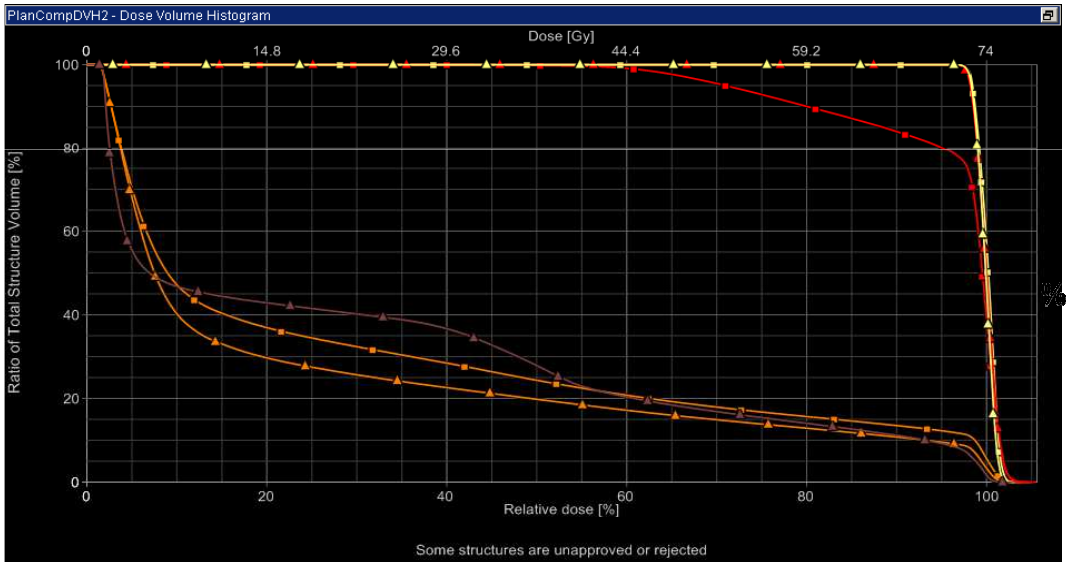
PlanCompDVH2 - Dose Volume Histogram
Dose [Gy]
0
14.8
29.6
44.4
59.2
74
Ratio of Total Structure Volume [%]
100
80
60
40
20
0
0
20
40
60
80
100
Relative dose [%]
Some structures are unapproved or rejected

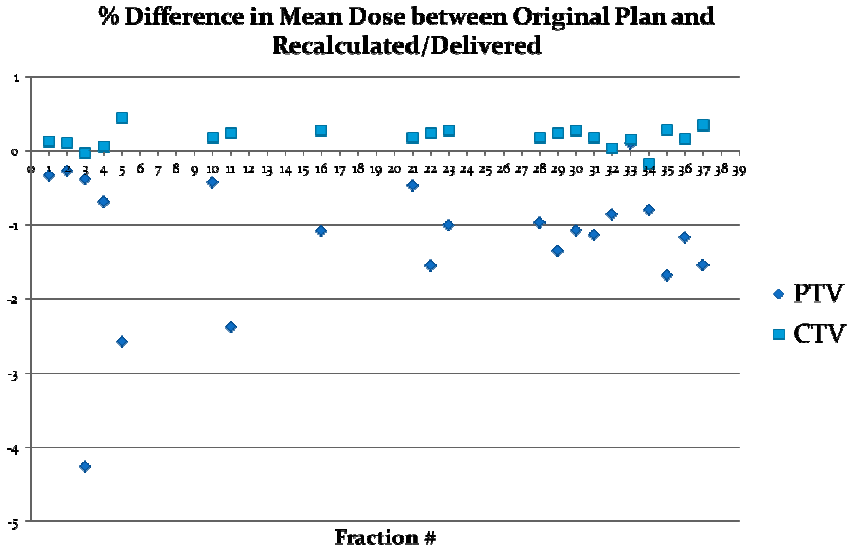
% Difference in Mean Dose between Original Plan and Recalculated/Delivered
1
0
-1
-2
-3
-4
-5
0 1 2 3 4 5 6 7 8 9 10 11 12 13 14 15 16 17 18 19 20 21 22 23 24 25 26 27 28 29 30 31 32 33 34 35 36 37 38 39
Fraction #
PTV
CTV

Including uncertainties

- Current practice not include patient specific uncertainty analysis (Setup, intra/inter fraction motion, structure delineation
- Probabilistic TP (PTP) does away with PTV
- Dose to an element of tissue considered as a random variable
  - Organs and tumour moving through dose cloud
- Need to define probability density function of anticipated uncertainties
  - Define dose coverage to CTV not PTV
  - Use the multiple image data sets acquired during treatment initial fractions

Including uncertainties

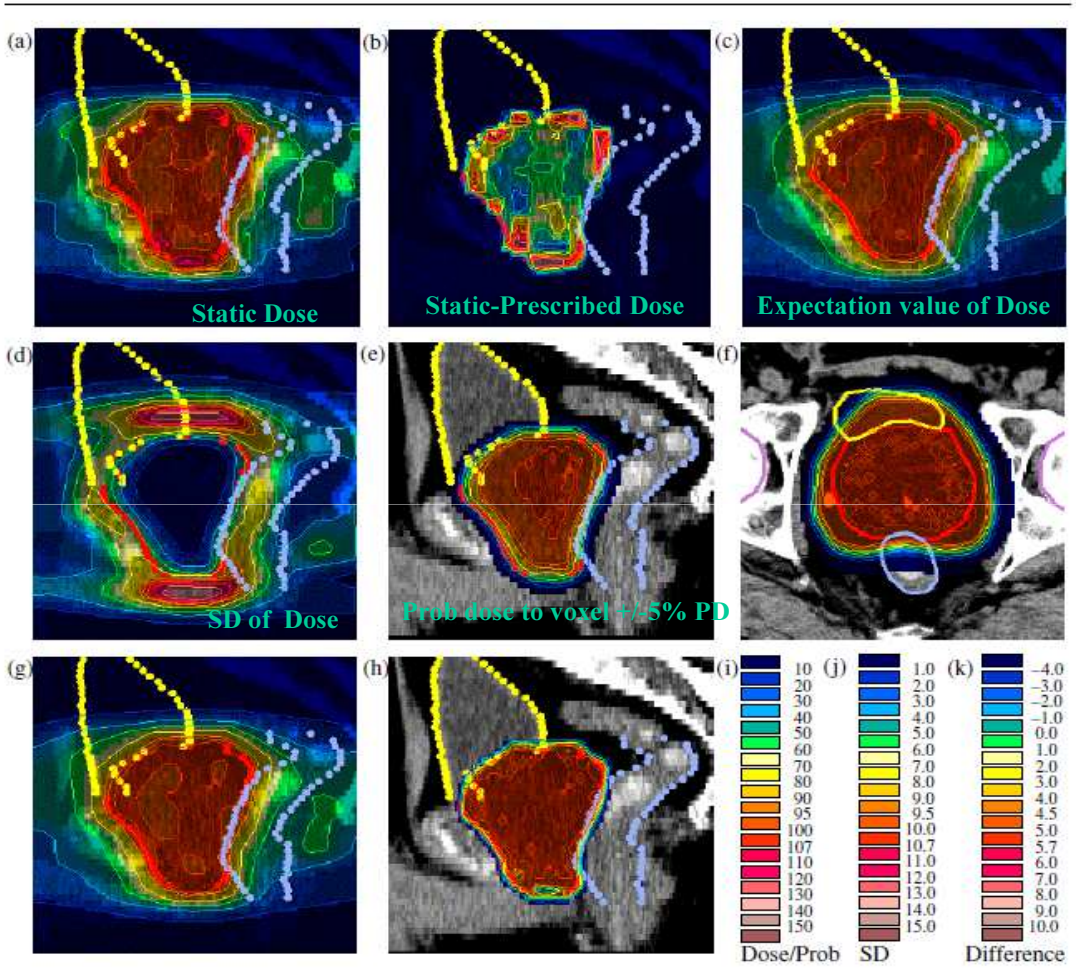

Malcike, Unkelback, Oeflke
PMB 512006

Included uncertainties in the optimisation

Large number of ways of presenting dose distribution for patient

Which ones are useful??

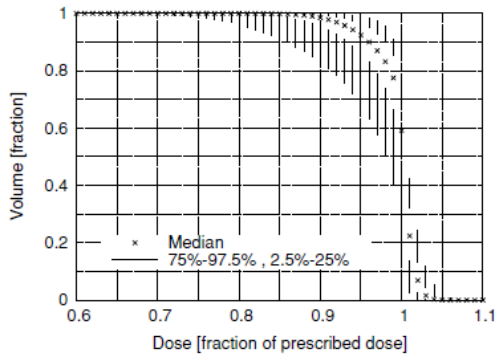

ESTRO School

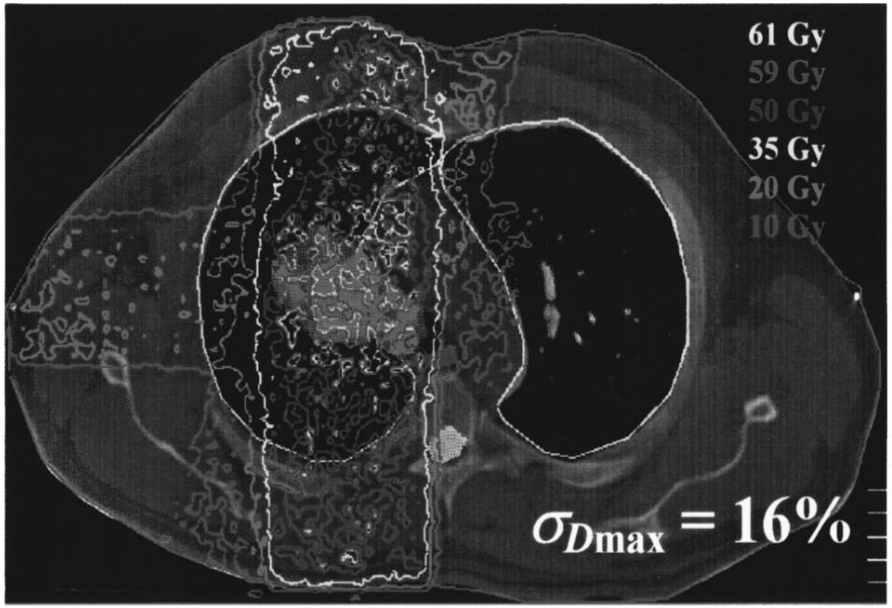

(e)

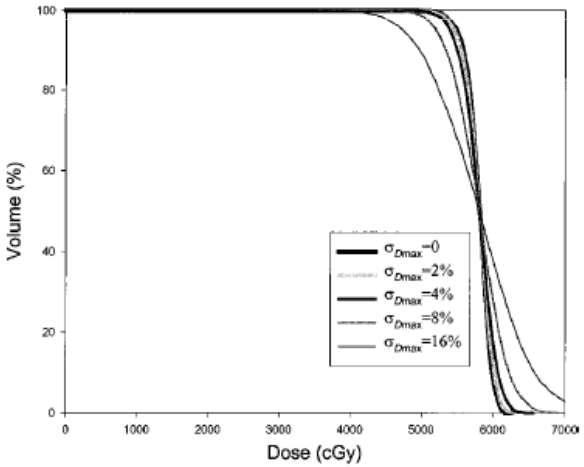

FIG. 4. Target dose volume histograms for various statistical uncertainty levels.

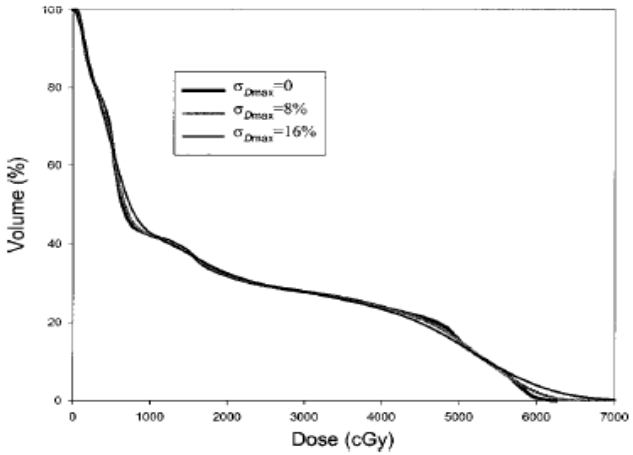

FIG. 5. Lung dose volume histograms for various statistical uncertainty levels.

MC uncertainty of 2% not affect DVH
Greater uncertainty, greater 'smoothing'

Effect of statistical uncertainty much less on OAR

Keall et al MP 2000

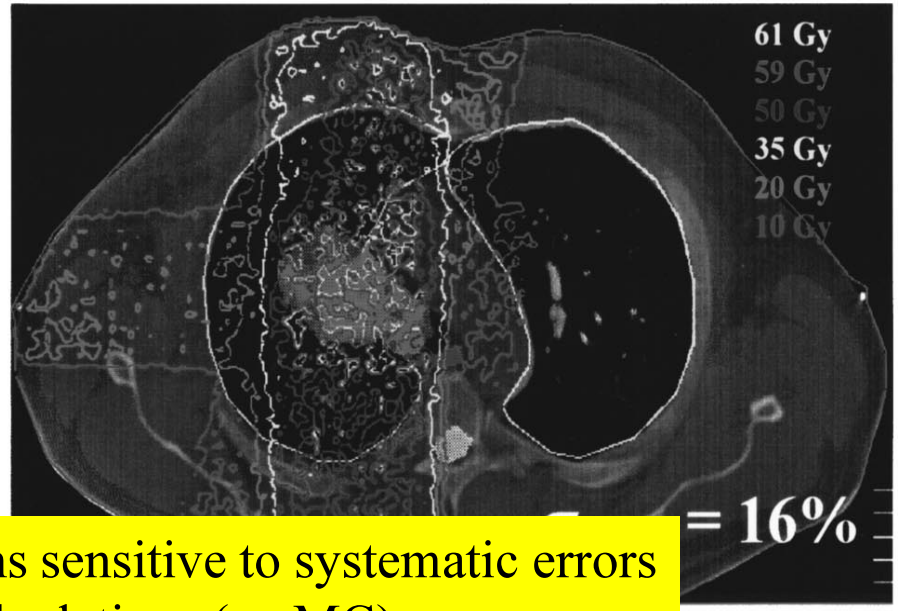

Conclude: TCP/NTCP calculations sensitive to systematic errors
Important to use accurate dose calculations (eg MC)

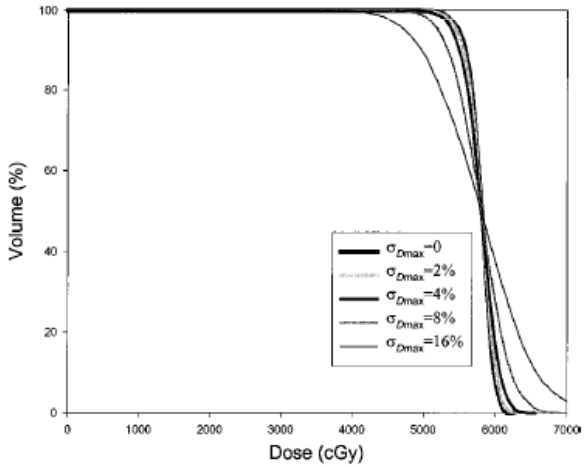

FIG. 4. Target dose volume histograms for various statistical uncertainty levels.

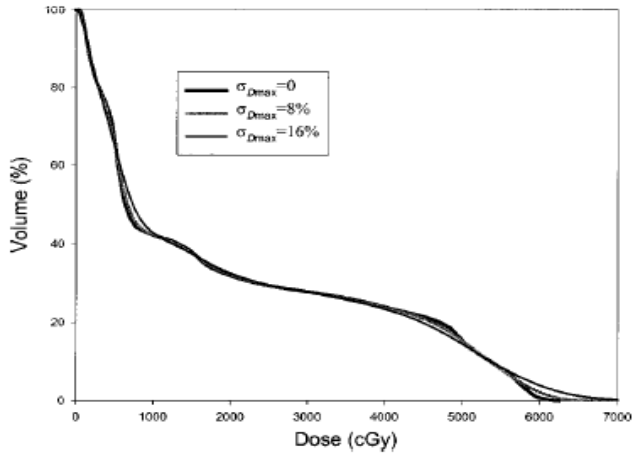

FIG. 5. Lung dose volume histograms for various statistical uncertainty levels.

MC uncertainty of 2% not affect DVH
Greater uncertainty, greater 'smoothing'

Effect of statistical uncertainty much less on OAR

Keall et al MP 2000

Invariant and Variant Dose Distributions Cho et al MP 2002

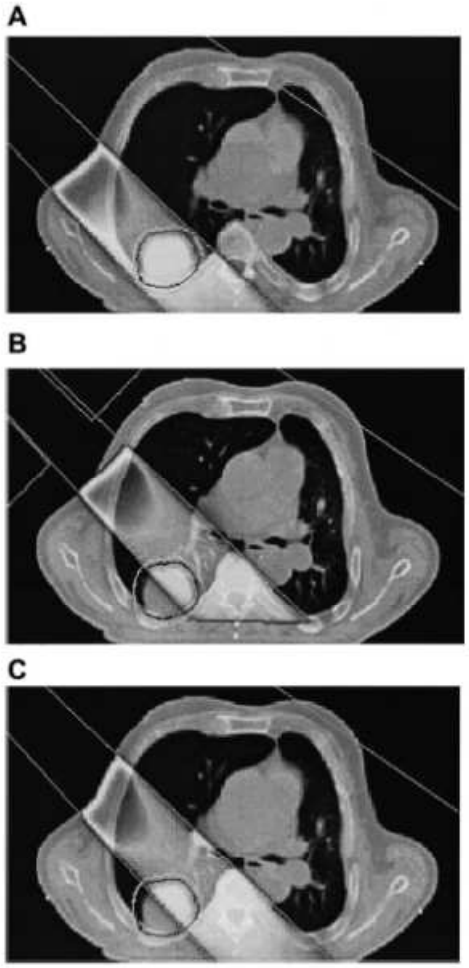

- Invariant (main effect on DVH):
  - Negligible dosimetric effect from contour or tissue inhomogeneity effects as function of displacement
- Variant (secondary effect):
  - Due to tissue inhomogeneity and contour effects as well
- Conclude:
  - Differences in relative volume and relative dose depending on displacement
  - Variant effects of contour changes, inhomogeneities and set up are negligible on EUD

Note: Worst case!

Accuracy and limitations

- **Factors affecting DVH accuracy:**
  - Accuracy to which VOI is delineated (Main contribution)
  - Dose bin size
  - Distance Map voxel size
  - Sampling method and sampling resolution
  - Shape of VOI
  - Dose Calculation Algorithm (difference in modelling heterogenities, penumbra…)
  - Dose Voxel Size

Accuracy: Dose Voxel Size

- Predefined
  - eg 0.25 cm dose voxel size used clinically
- This can have an effect on the DVH appearance (and DVH accuracy)

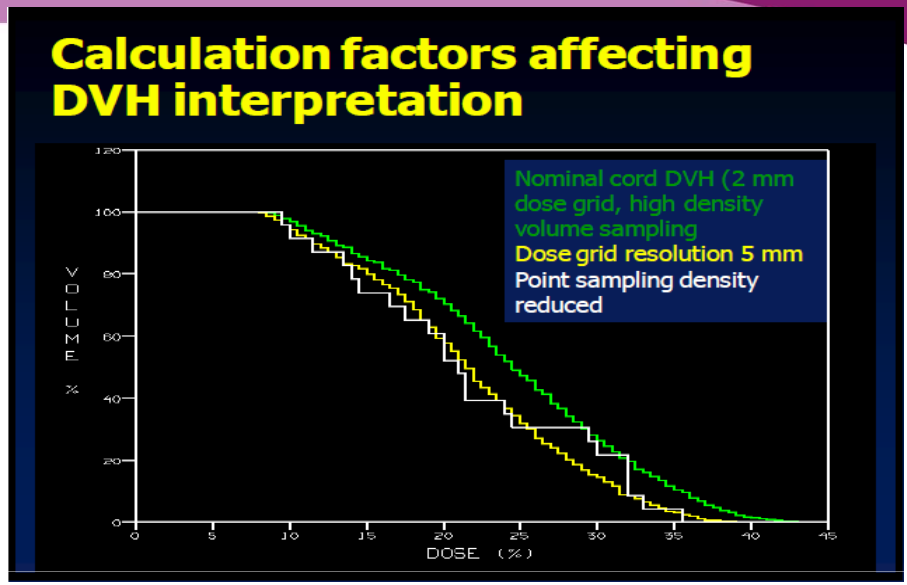

"QA of DVHs" AAPM Poster by Cheng 2009

Ten Haken and Kessler

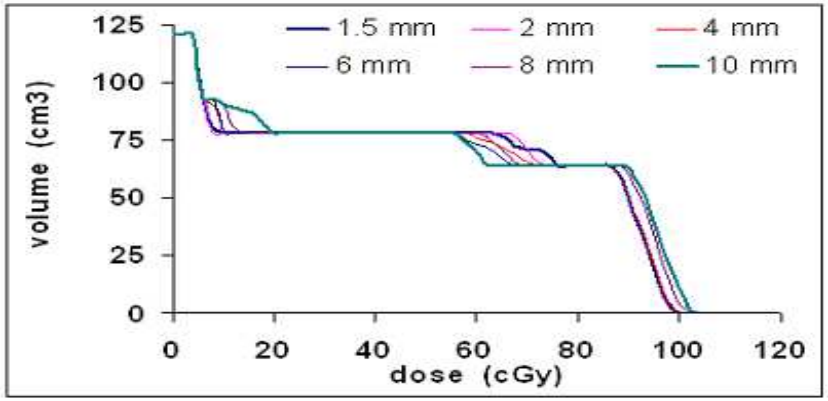

DVH of a cylinder for different dose grid sizes

Quality Assurance/Commissioning

- For example IAEA TRS430, AAPM TG 53 and others make recommendations of how test DVH performance
- Should test *volume* and *dose binning* accuracy

Volume Tests

Depends on approach To shape 'ends'

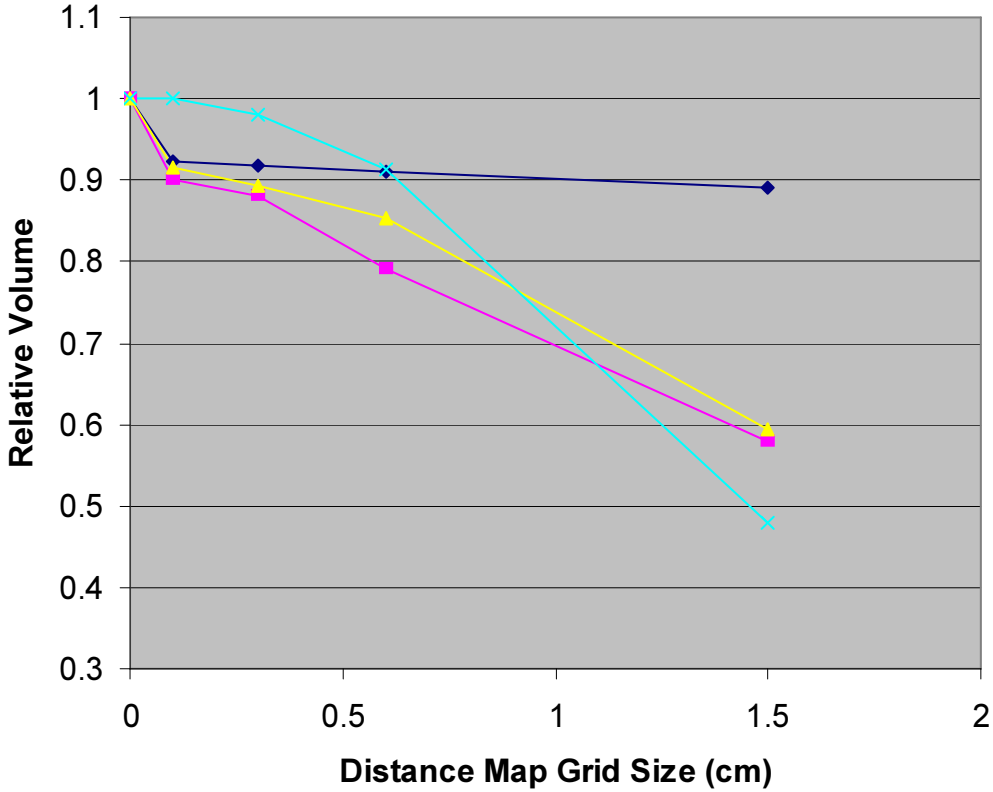

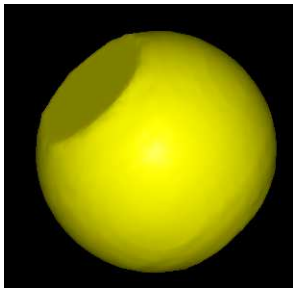

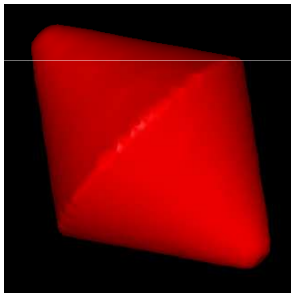

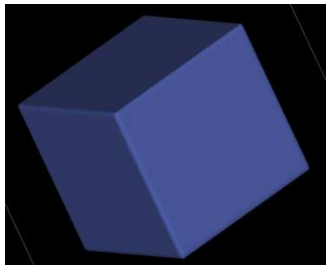

From Paul Kinsella St Luke's

ESTRO School

Volume Tests

From Kirisits et al MP 2007

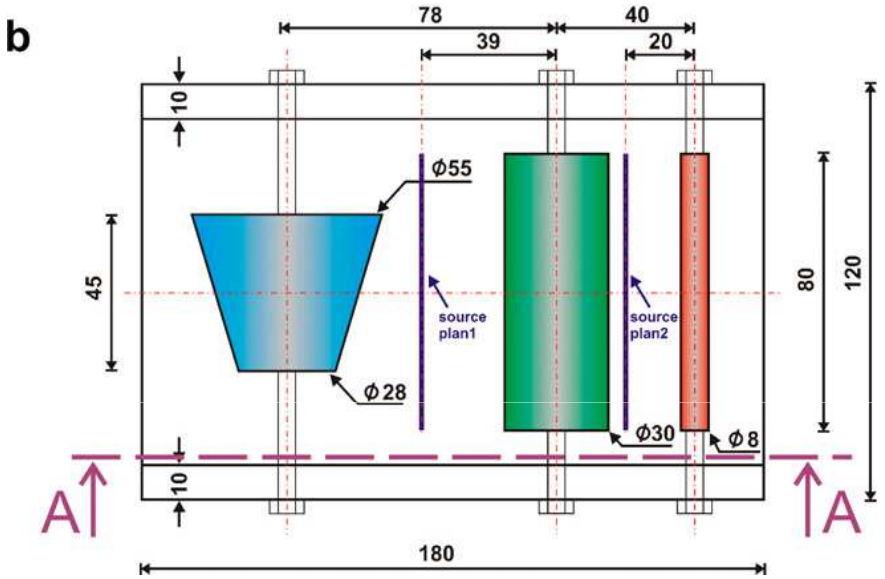

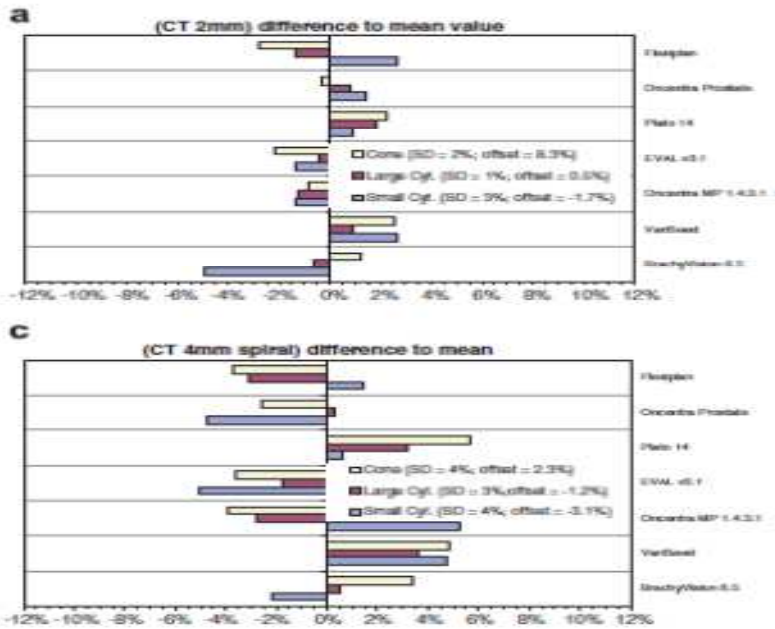

Note: Similar magnitude of errors for inter-system and inter-observer

Table 2
Deviations of DVH parameters for the two different treatment plans and for the 4 mm slice thickness CT image set

	Inter-system variation		Inter-observer variation	
	Large cylinder	Cone	Large cylinder	Cone
Treatment plan 1				
$D_{0.1cc}$				
1 SD (%)	3	3	5	4
Maximum (%)	8	6	11	11
D_{1cc}				
1 SD (%)	1	5	1	2
Maximum (%)	2	11	1	5
D_{2cc}				
1 SD (%)	1	5	1	3
Maximum (%)	3	12	3	7

ESTRO School

Dose Binning Tests

- Isodose lines Method

Panista et al PMB 1998

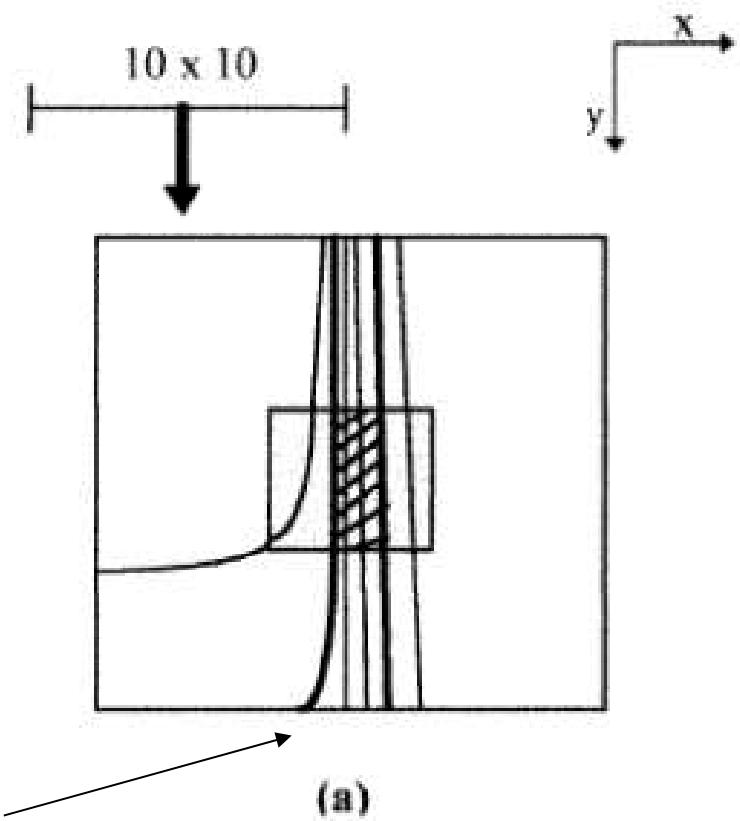

Isodose Lines

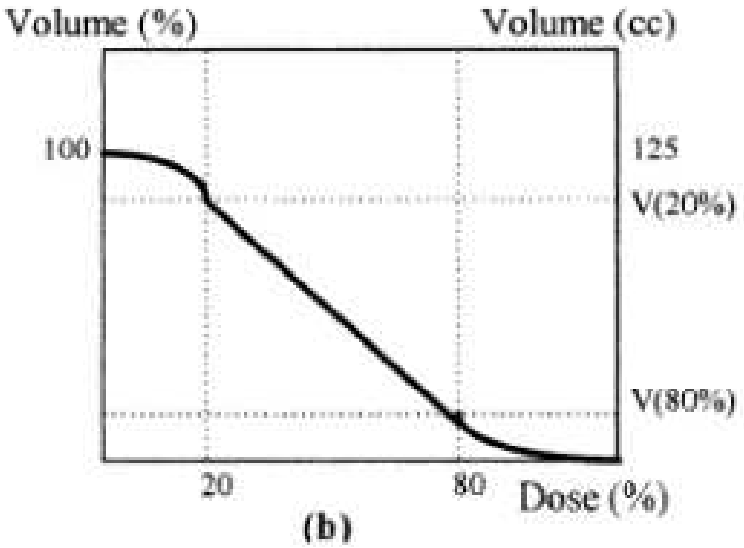

ESTRO School

Summary

- Important to ensure DVH calculation is accurate as it is central to clinical decisions
- Physicists should be familiar with the influence of different parameters on DVH construction
- DVH construction should be tested (QC)
- Clinical trials:
  - recording contouring practice?
  - DVH metric calculation methods? Predictive power?
  - DVH uncertainties?
  - Consistency among vendors?

ESTRO School

WWW.ESTRO.ORG/SCHOOL

Uncertainties, Tolerance and Action limits

Núria Jornet

Servei de Radiofísica
Hospital Sant Pau, Barcelona

Learning objectives

- to understand the need to report on the quality of a measurement result in addition to the result itself
- to understand the conceptual difference between the error and the uncertainty of a result
- to know the document **"Guide to the expression of uncertainty in measurement" (abbreviated as GUM)**
- to understand how to set action limits taking into account clinical tolerance limits and uncertainties.

Outline of part 1

i. Introduction: How to communicate the quality of a measurement result?

ii. The "Guide to the expression of uncertainty in measurement" (GUM)

iii. Error and /or uncertainty?

Accurate measurements and **associated scientific communication** are indispensable in the quality control of almost any product or service starting from development ending with the final product

Example of scientific communication

When measuring we aim at high accuracy

In fact, also the world of medical physics is full of measurements which require an **accuracy as high as possible.**

An important example is the dose determination in reference dosimetry

$$D_w = M\ [C] \cdot N_{D,w}\,[Gy/C] \cdot k_Q$$

We need to know the accuracy of such a measurement

Everybody feels to have an idea of what accuracy means. We can express this "feeling" by the expression:

$$\text{measured}(D_w) \approx \text{true}(D_w)$$

A better formulation could be this expression:

$$\text{true}(D_w) = \text{measured}(D_w) \pm \text{uncertainty interval}$$

Note: This is not a mathematical equation!

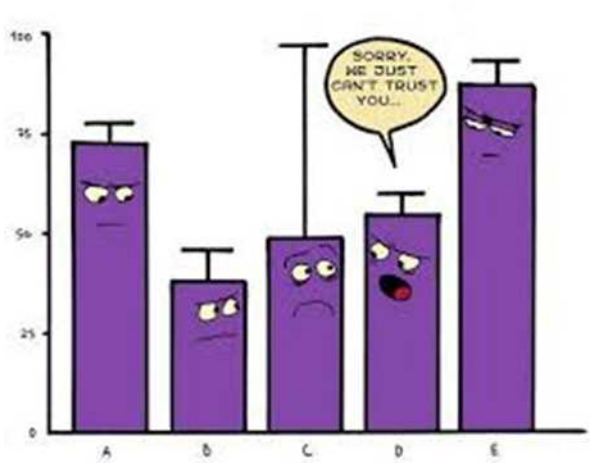

This statement:

$$\text{true}(D_w) = \text{measured}(D_w) \pm \text{uncertainty interval}$$

abbreviated as: $D_{w,true} = D_{w,m} \pm u$

could be interpreted as:

$D_{w,true}$ probably lies somewhere in the interval (2*u) around the measured value:

$$\{D_{w,m} - u,\ D_{w,m} + u\}$$

Illustration that $D_{w,true}$ probably lies somewhere in the interval around the measured value: $2 \cdot u$

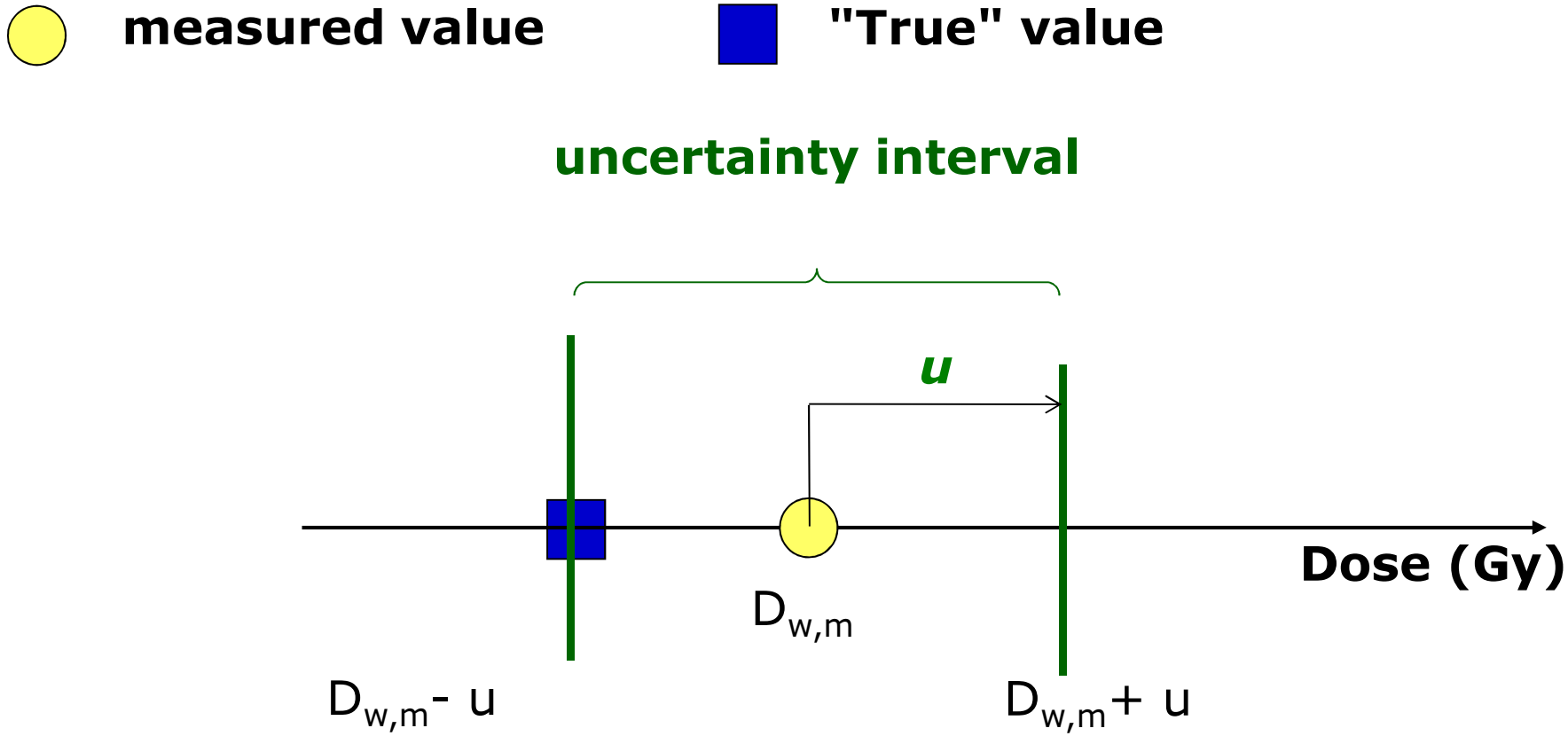

However this information is still incomplete, because we need a clear understanding what the word "**probably**" means.

Example:

A dose is measured and found to be 100 cGy.

However, even assuming an identical uncertainty of measurement, this result might be reported either as:

(100 ± 0.1) cGy ⟸ with 99% confidence limits

or:

(100 ± 0.07) cGy, ⟸ with 95% confidence limits

There are obviously different ways to report the same measurement and the same associated accuracy!

The lesson of this example that even an additional information on uncertainty can be ambiguous unless the level of confidence is also given.

Very frequently, one standard deviation is used as the quoted range meaning that the true value lies within the quoted range of uncertainty with a probability of 67%.

By convention, in this case the uncertainty is reported as

standard uncertainty

1st RECAP:

(1) When reporting the result of a measurement, it is obligatory that a **quantitative information of the quality of the result** must be given.

Otherwise the receiver of this information cannot really asses its **reliability**.

(2) This information could be an information on the interval of the probable range of the correct value associated by the confidence limit that this range really includes the correct value.

Need of a standarized meathod to report uncertainty

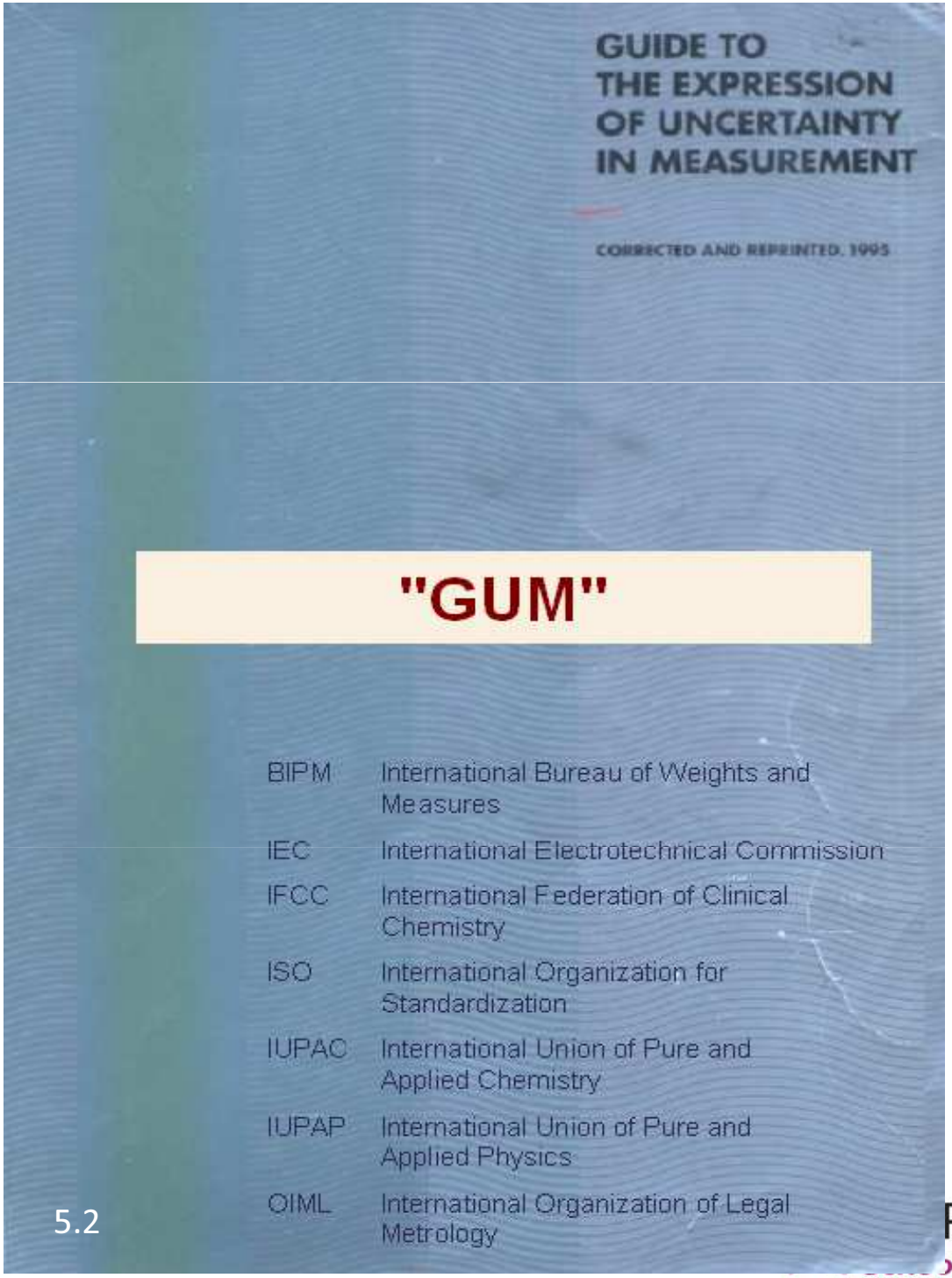

… this is the standard:

the so-called GUM

In 1995, the International Organization for Standardization (ISO) has published the corrected version of the

"Guide to the expression of uncertainty in measurement"

in order to ensure that the method for evaluating and expressing uncertainty is uniform **all over the world**.

It presents a consensus between seven "highest level" metrological organizations:

BIPM, IEC, IFCC, ISO, IUPAC, IUPAP, OIML

on how the uncertainty in measurement should be dealt with.

GUM aims to:

1. Promote adequate use of the expressions **"true"** value, **"error"** and **"uncertainty"**
2. Treat "random " and "systematic " influence factors an overall uncertainty in the same way, namely in **mathematical methods of statistics**
3. Introduce a realistic (not a safe) expression of the uncertainty

The terms **accuracy** and **precision** are frequently used to describe the quality of a measurement:

Accuracy — specifies the **proximity** of the mean value of a measurement to the **true value**.

Precision — specifies the **degree of reproducibility** of a measurement.

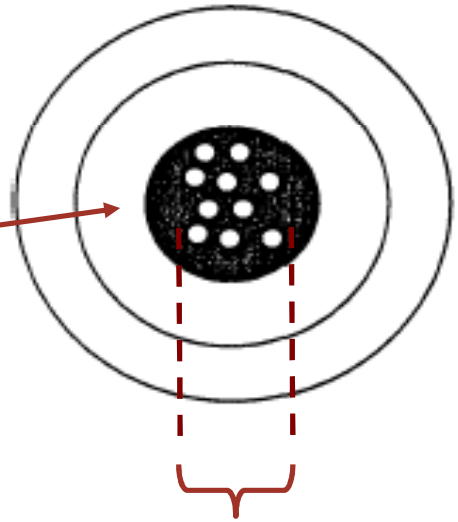

Note:
High precision

is equivalent to

a small standard deviation σ

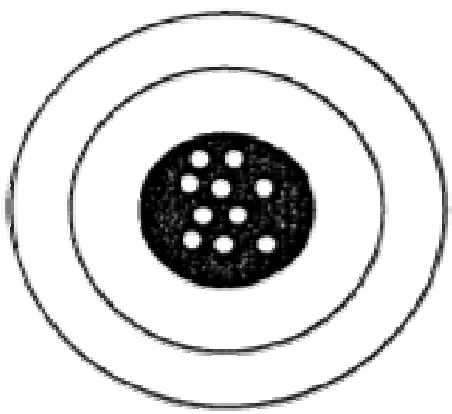

High precision
&
High accuracy

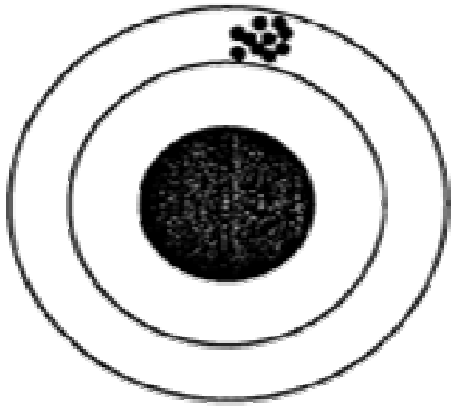

High precision
&
Low accuracy

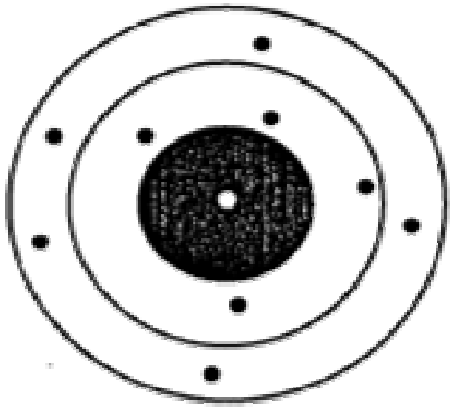

Low precision
&
High accuracy

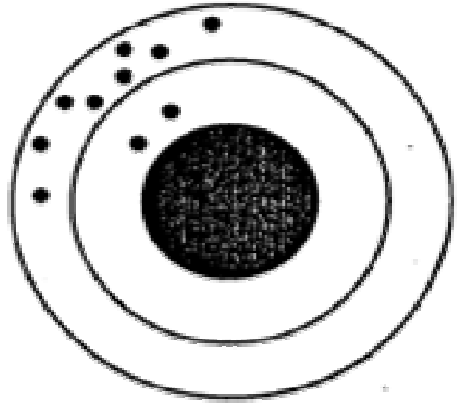

Low precision
&
Low accuracy

Note: Each of these characterizations refer to the known target point which is the center of the target.
This point could be named the **true value**

An error or the accuracy can be quantitatively determined only if we know the true value

Without the knowledge of the true value, the terms accuracy would be meaningless.

Now the question arises: How to find out the true value??

How to know the “true value”?

Answer: Obviously one must define more exactly the influence factors for the quantity to be measured !

Question: Can we fix all measuring conditions?

Answer: In principle, the quantity to be measured **cannot be completely** described without an **infinite** amount of information.

If it is impossible to define **all conditions,** the "true value" must ultimately remain unknown

Consequence:

If the true value remains unknown, the value of an "**error**" and even worse, also that of "**accuracy**" can not be exactly evaluated and therefore also must remain unknown.

GUM recommends:

The term "**error**" should be generally avoided and substituted by the term "**uncertainty**" of a result (except in such cases where indeed a real error is involved in the measurement)

2nd RECAP

(1) When reporting the result of a measurement, it is obligatory that a **quantitative information of the quality of the result** must be given. It is recommended to use the uncertainty of a measurement for that.

(2) The International Organization for Standardization (ISO) has published a **"Guide to the expression of uncertainty in measurement"** in order to ensure that the method for evaluating and **expressing uncertainty is uniform all over the world**.

(3) According to this guide, **the term "error** of a measurement" **should be generally avoided** and substituted by the term "uncertainty of a measurement" of a result.

Uncertainties

Weight = 58 ±1 Kg

Tolerance and action limits

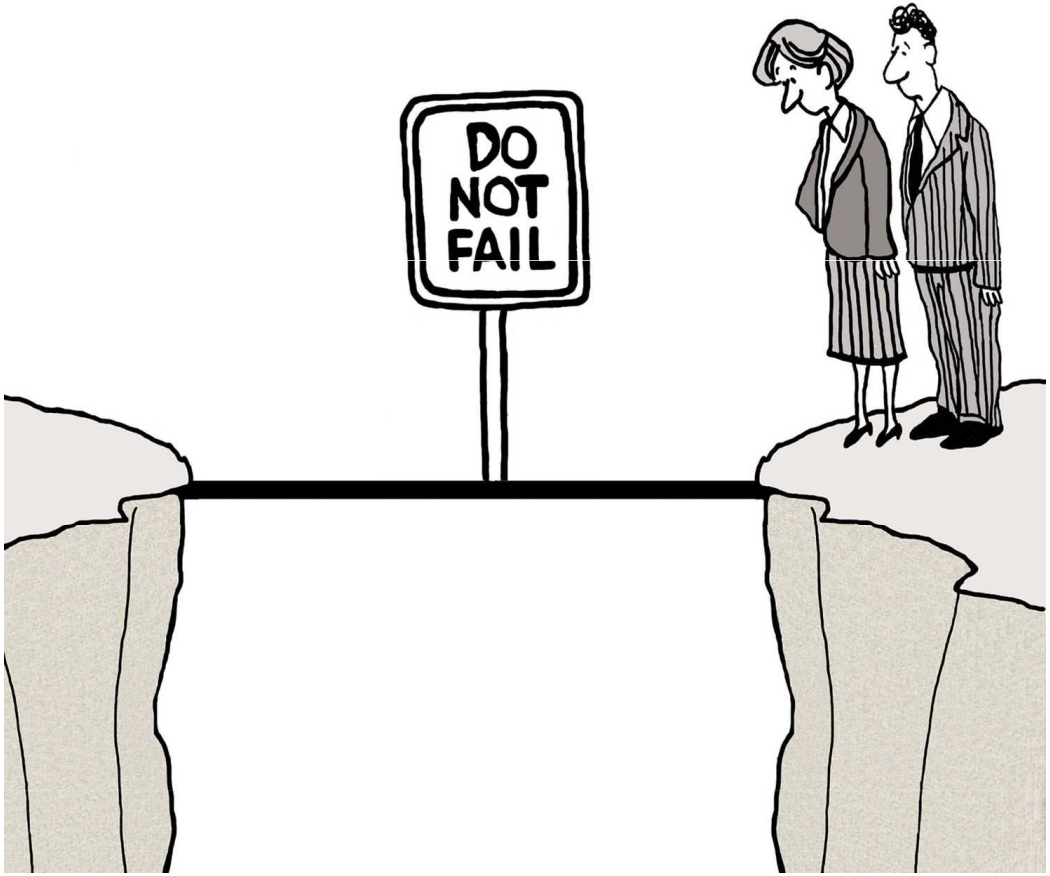

Weigth limit = 60 Kg
Tolerance = 2 Kg

ESTRO School

Uncertainties

We know how to calculate and report uncertainty

σ = 1 Kg

Tolerance and action limits

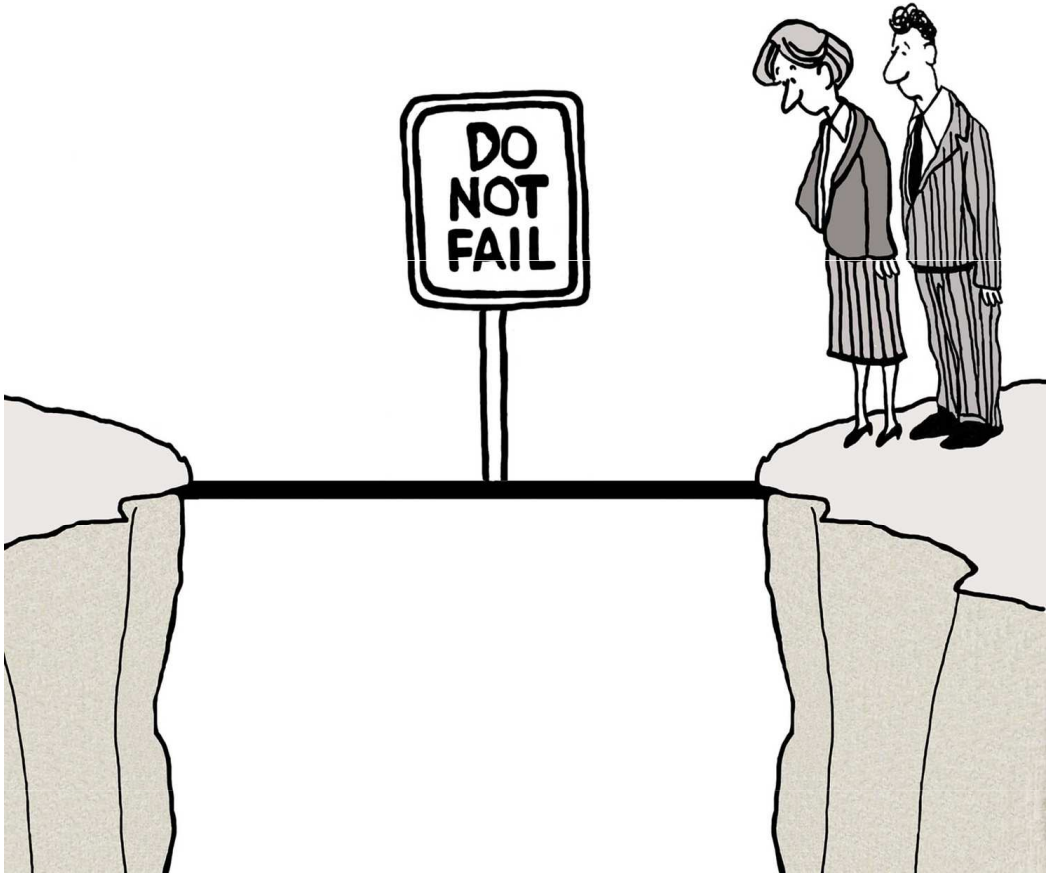

Weigth limit = 60 Kg
Tolerance = 2 Kg

ESTRO School

Uncertainties

σ = 1 Kg

Tolerance and action limits

Weigth limit = 60 Kg
Tolerance = 2 Kg

ESTRO School

Outline of part 2

- Tolerance and action limits and its relation with the uncertainty of measurements

Friday afternoon at the medical physics department…

Dose measurement

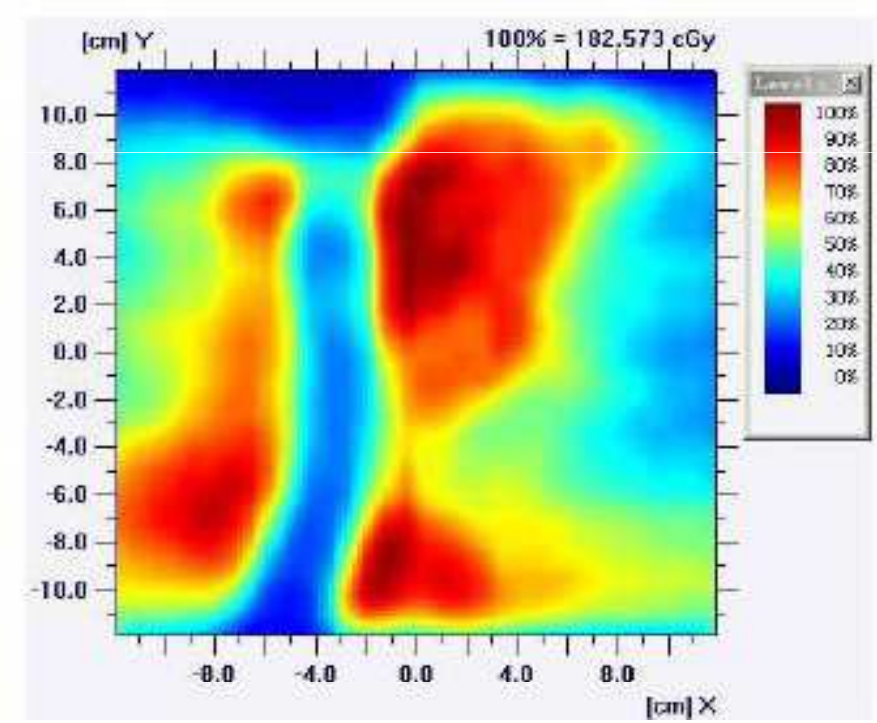

TPS dose calculation

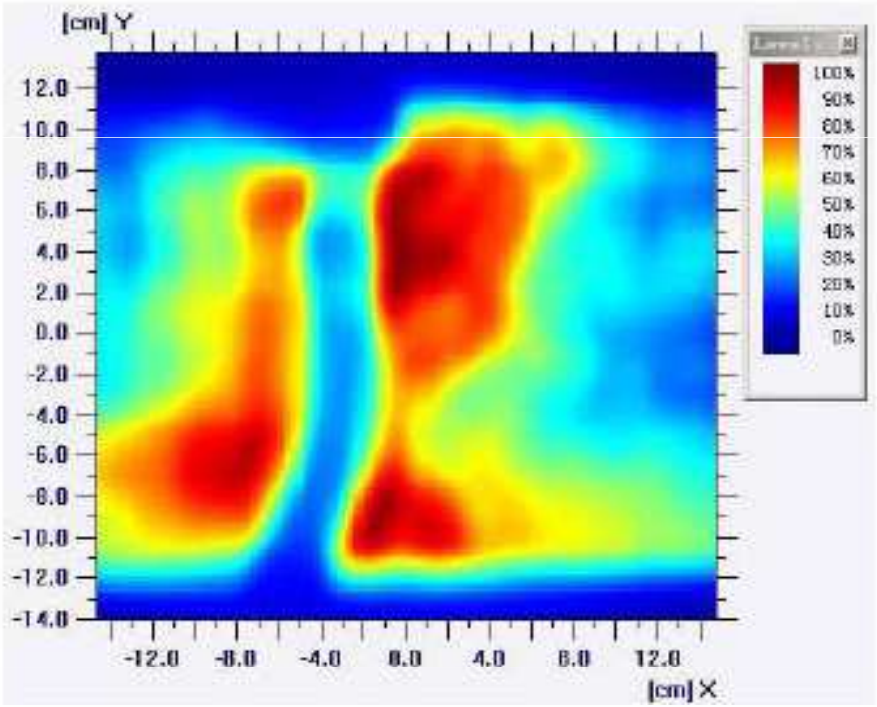

Not OK for treatment?

We need limits to make objective decisions!

From Jörgen Olofsson (Dose Modeling and dose verification ESTRO COURSE)

ESTRO School

How are those limits set?

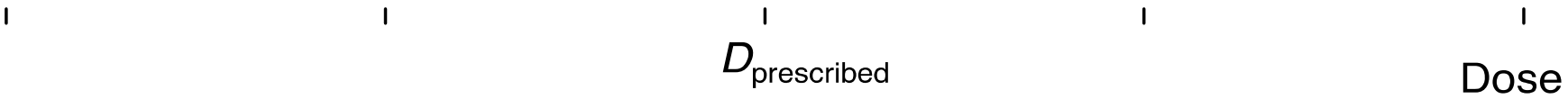

A reasonable (?) tolerance limit: ± 2σ

A reasonable (?) action limit: ± 4σ (= 2 × tolerance limit)

From Jörgen Olofsson (Dose Modeling and dose verification ESTRO COURSE)

Action limits - Traditional philosophy

- Prescribed dose (=TPS dose)
- Independent dose calculation/measurement

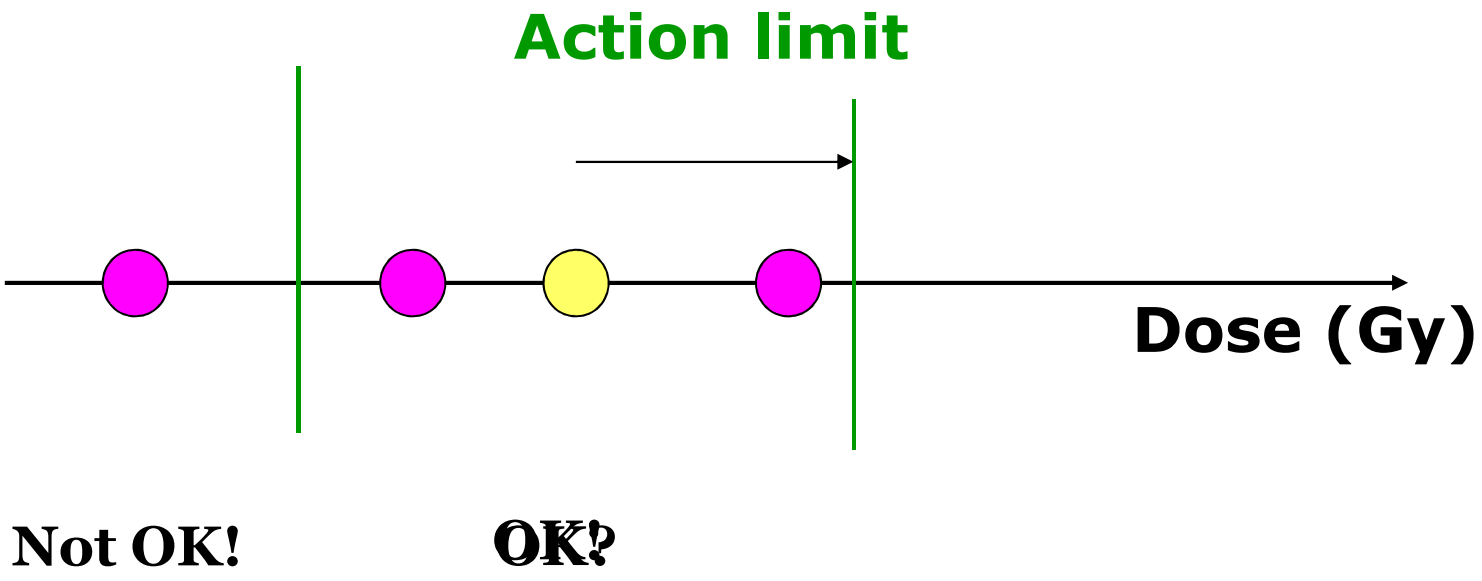

From Jörgen Olofsson (Dose Modeling and dose verification ESTRO COURSE)

Reality

Prescribed dose (=TPS dose)

True dose (=Actually delivered dose)

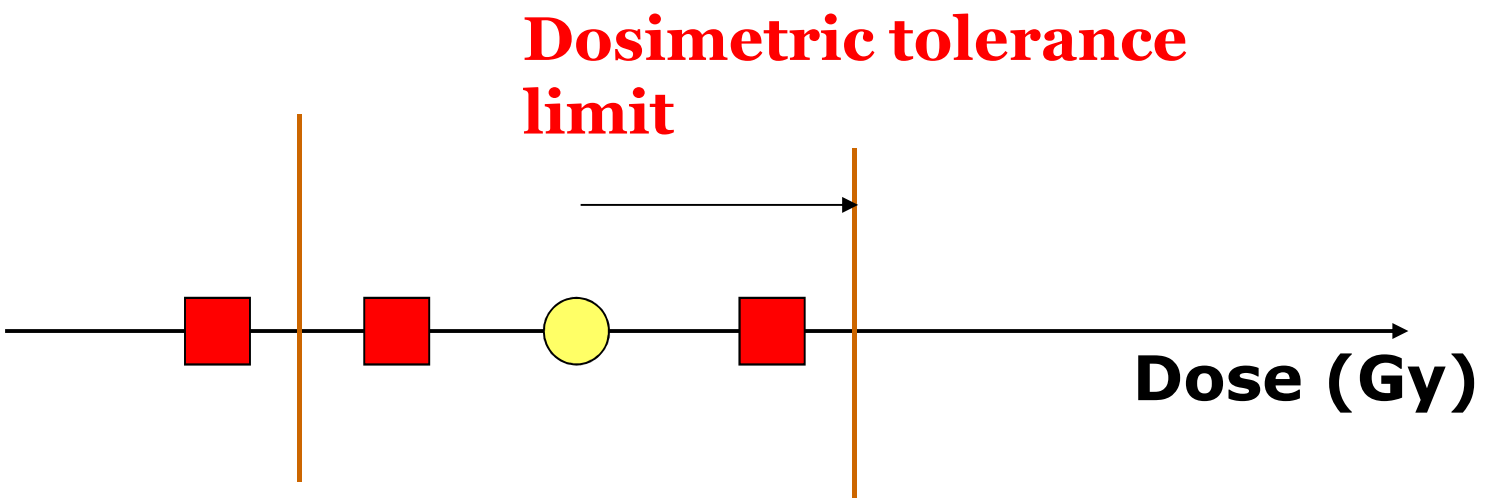

Not OK! **OK?** **Do we know the True dose?**

From Jörgen Olofsson (Dose Modeling and dose verification ESTRO COURSE)

ESTRO School

Action limits - Proposed philosophy

Prescribed dose

True dose

Independent dose calc/meas

Probability distribution for the true dose

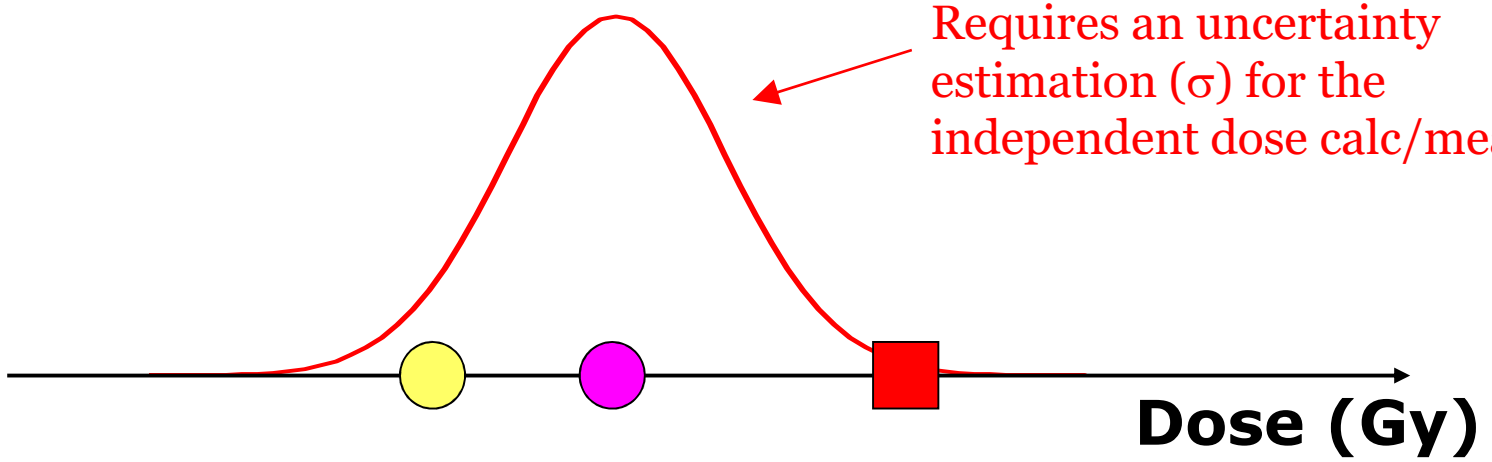

OK?

Not OK?

What is the Clinical tolerance limit?

From Jörgen Olofsson (Dose Modeling and dose verification ESTRO COURSE)

ESTRO School

- Clinical tolerance limits or specifications should be based on clinical experience.
- Clinical experience can be summarized through statistical analysis of the outcome of a particular treatment for a particular tumor disease.
- Examples:
  - Local tumor control as a function of dose.
  - Fraction of survivors after five years as a function of dose.
- At the same time, normal tissue complications must be taken into account.

From Jörgen Olofsson (Dose Modeling and dose verification ESTRO COURSE)

Minimum acceptable cure rate

Maximum acceptable complication rate

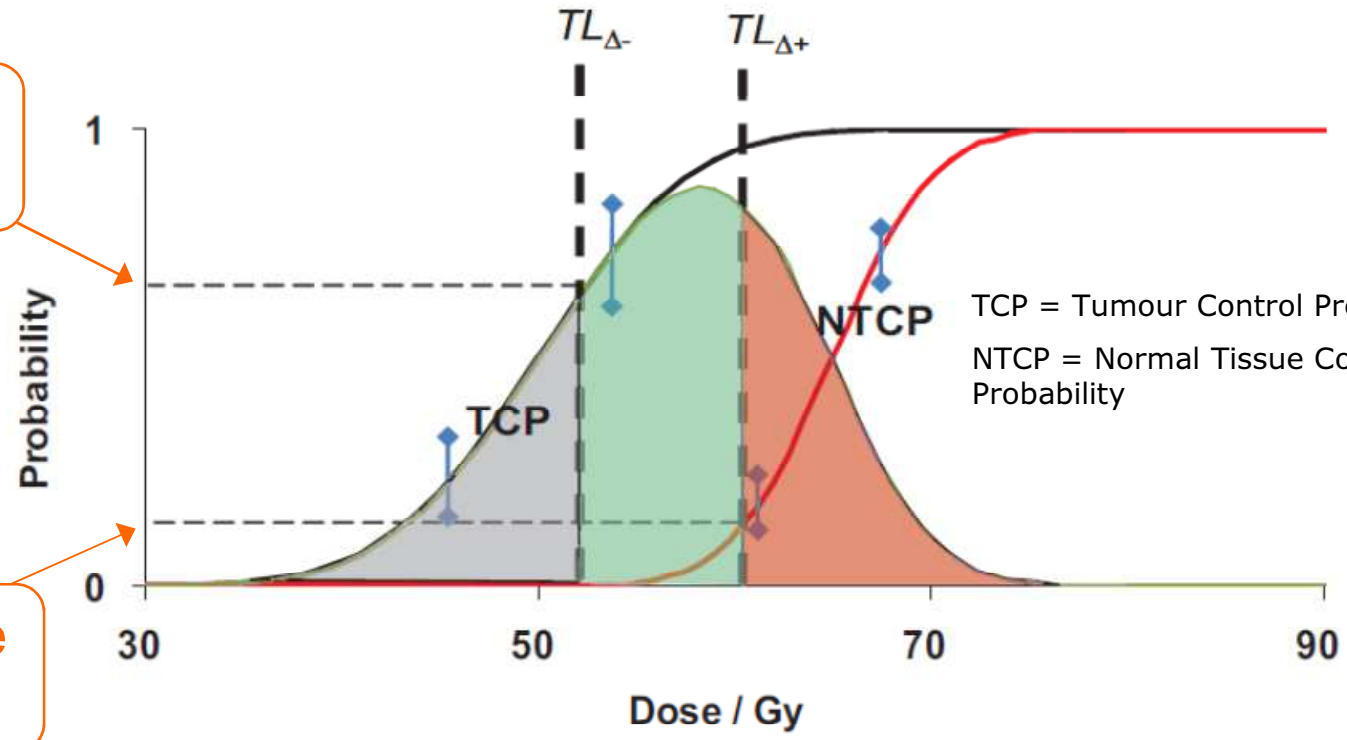

Figure 3.2 Illustration of the procedure to obtain dosimetric tolerance limits from TCP and NTCP data. $TL_{\Delta-}$ is set to a minimum acceptable cure rate and $TL_{\Delta+}$ to a maximum acceptable complication rate.

ESTRO Physics Booklet #10 [2]

ESTRO School

Action limits - Proposed philosophy

Step 1: Determine the uncertainty (σ) for the dose measurement, yielding the probability distribution for the true dose.

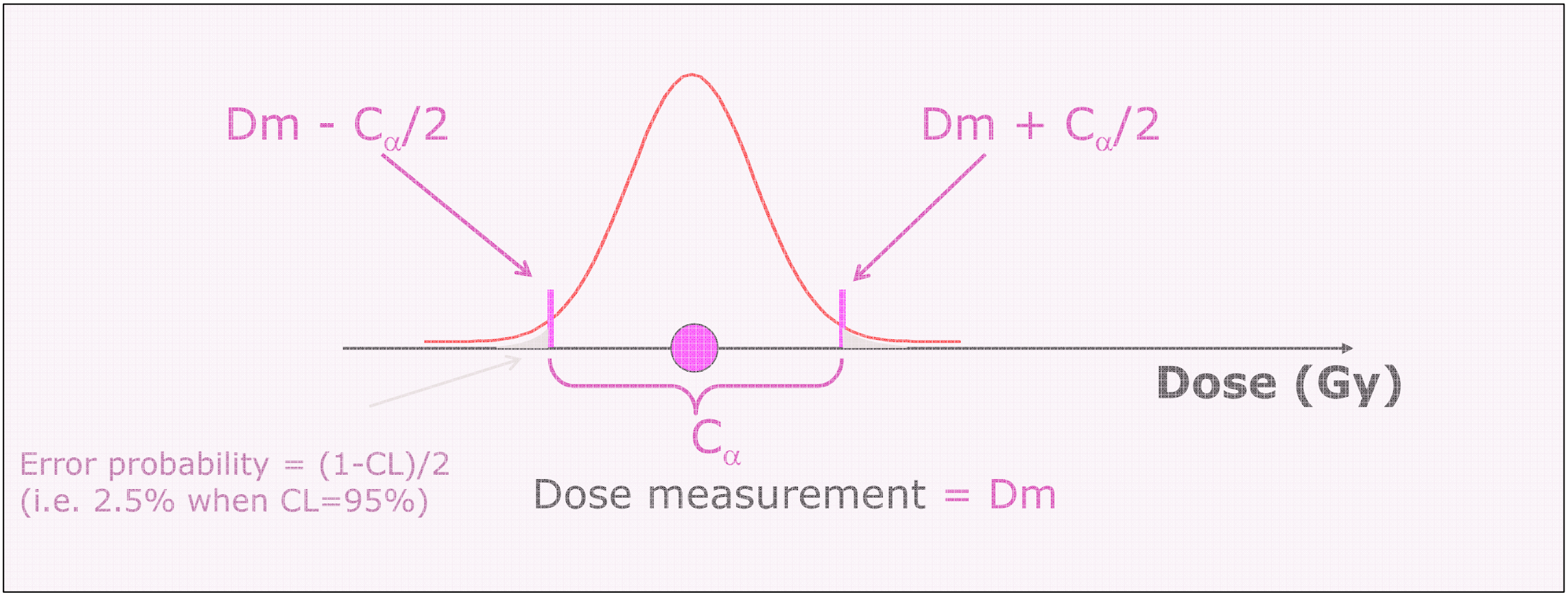

Step 2: Set a confidence level CL for the true dose, e.g. CL =95%, and determine the corresponding dose interval C_α.

From Jörgen Olofsson (Dose Modeling and dose verification ESTRO COURSE)

ESTRO School

Action limits - Proposed philosophy

Step 3: Adjust the true dose probability distribution such that the dose limits IDC-$C_\alpha/2$ and IDC+$C_\alpha/2$ coincide with the clinical tolerance limits.

Prescribed dose

Probability distribution for the true dose

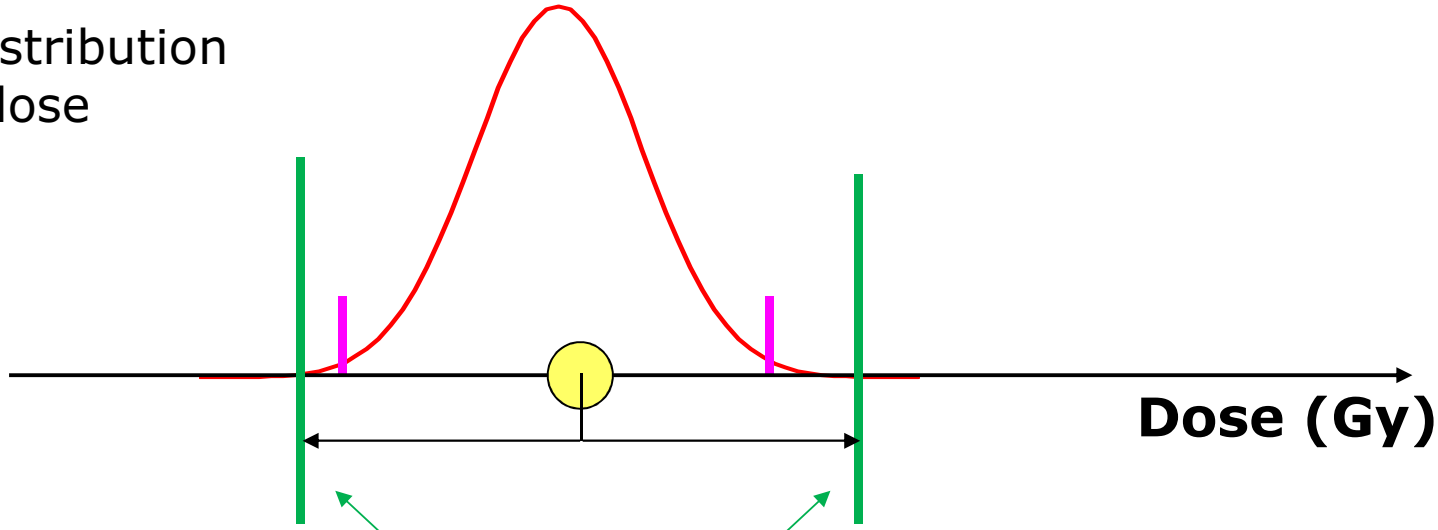

is set to a minimum acceptable cure rate

$TL_{\Delta-}$

$TL_{\Delta+}$

is set to a maximum acceptable complication rate

Clinical tolerance limits

From Jörgen Olofsson (Dose Modeling and dose verification ESTRO COURSE)

ESTRO School

Action limits - Proposed philosophy

Step 4: Define the center of the true dose probability distribution as the lower and upper **action limit**, respectively.

Prescribed dose

Probability distribution for the true dose

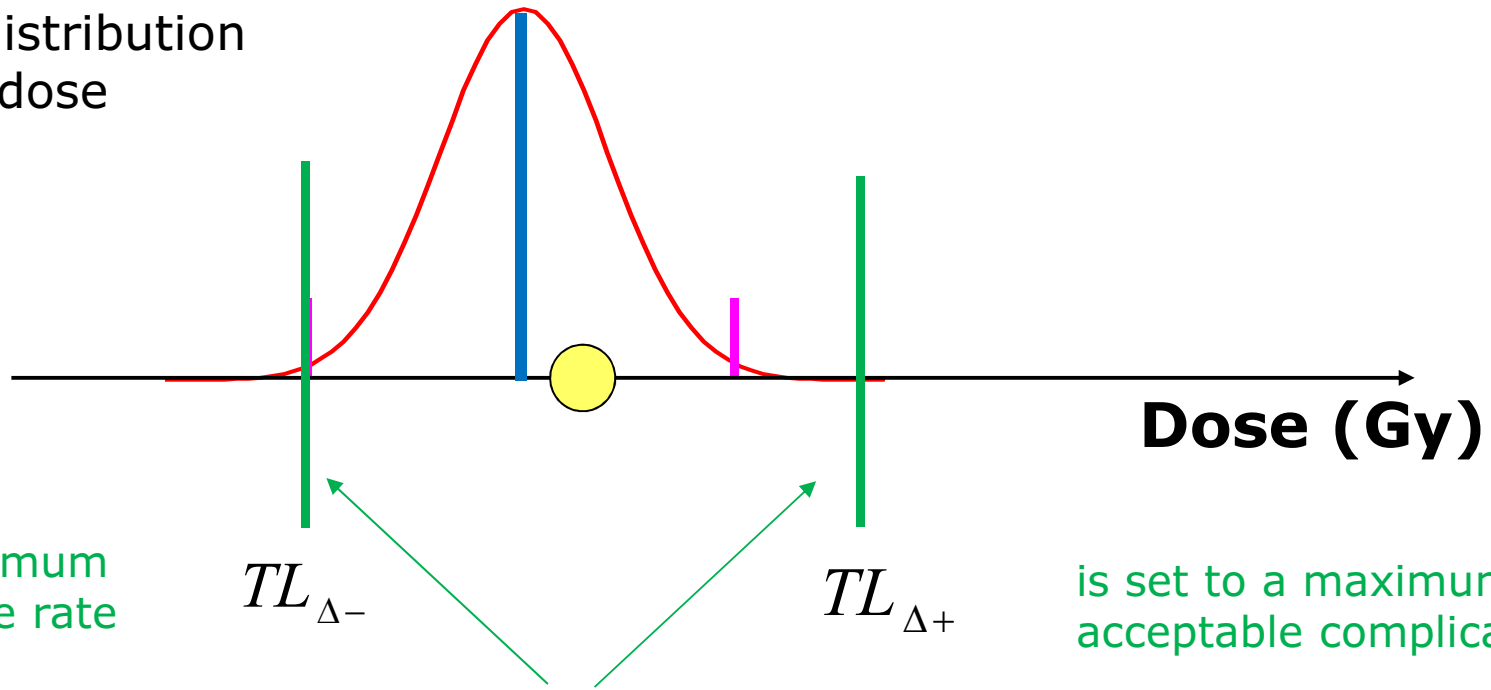

is set to a minimum acceptable cure rate

is set to a maximum acceptable complication rate

Clinical tolerance limits

From Jörgen Olofsson (Dose Modeling and dose verification ESTRO COURSE)

ESTRO School

Action limits - Proposed philosophy

Step 3: Adjust the true dose probability distribution such that the dose limits IDC-$C_\alpha/2$ and IDC+$C_\alpha/2$ coincide with the clinical tolerance limits.

Prescribed dose

Probability distribution for the true dose

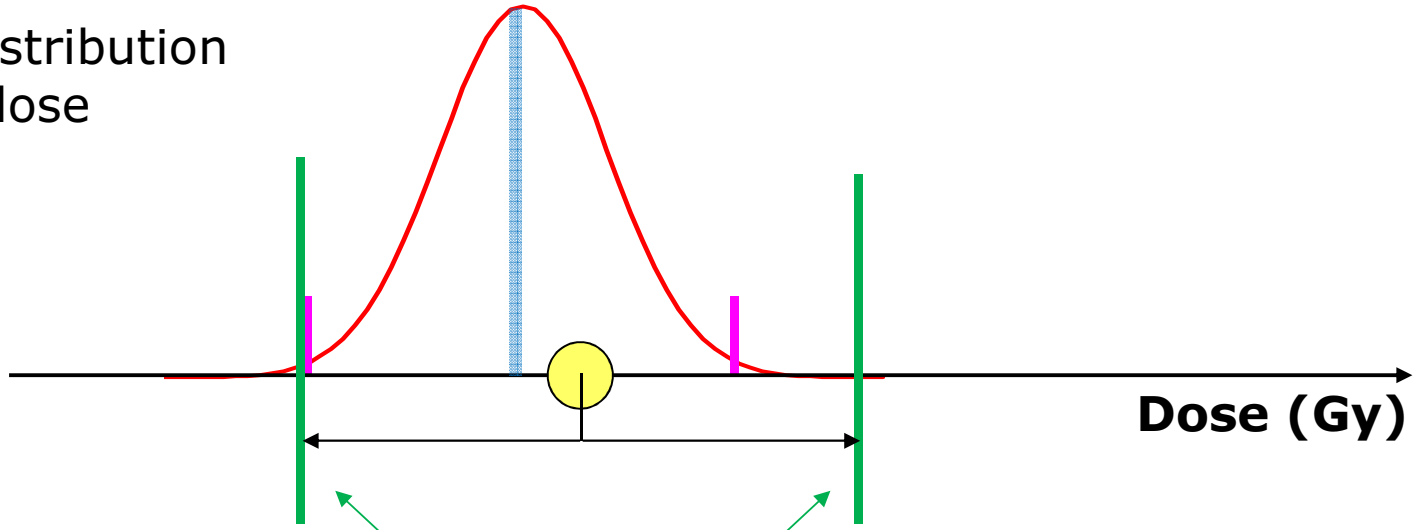

is set to a minimum acceptable cure rate

$TL_{\Delta-}$

$TL_{\Delta+}$

is set to a maximum acceptable complication rate

Clinical tolerance limits

T. From JörgenOlofsson (Dose Modeling and dose verification ESTRO COURSE)

Action limits - Proposed philosophy

Step 4: Define the center of the true dose probability distribution as the lower and upper **action limit**, respectively.

Prescribed dose

Probability distribution for the true dose

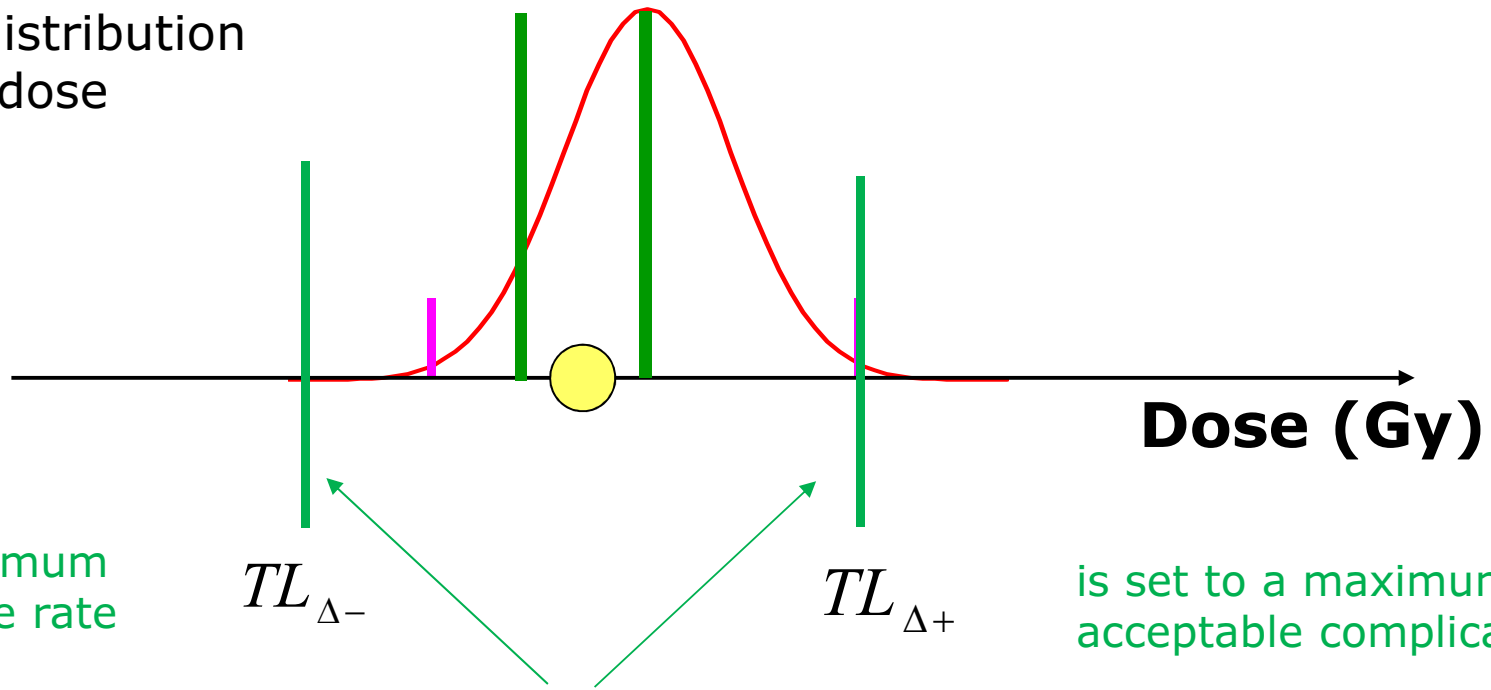

is set to a minimum acceptable cure rate

is set to a maximum acceptable complication rate

Clinical tolerance limits

From Jörgen Olofsson (Dose Modeling and dose verification ESTRO COURSE)

ESTRO School

Action limits - Proposed philosophy

Hence, the action limits should be calculated as

Clinical tolerance=specification

Measurement uncertainty

$$\Delta L_{\pm} = TL_{\pm} \pm \frac{C_{\alpha}}{2}$$

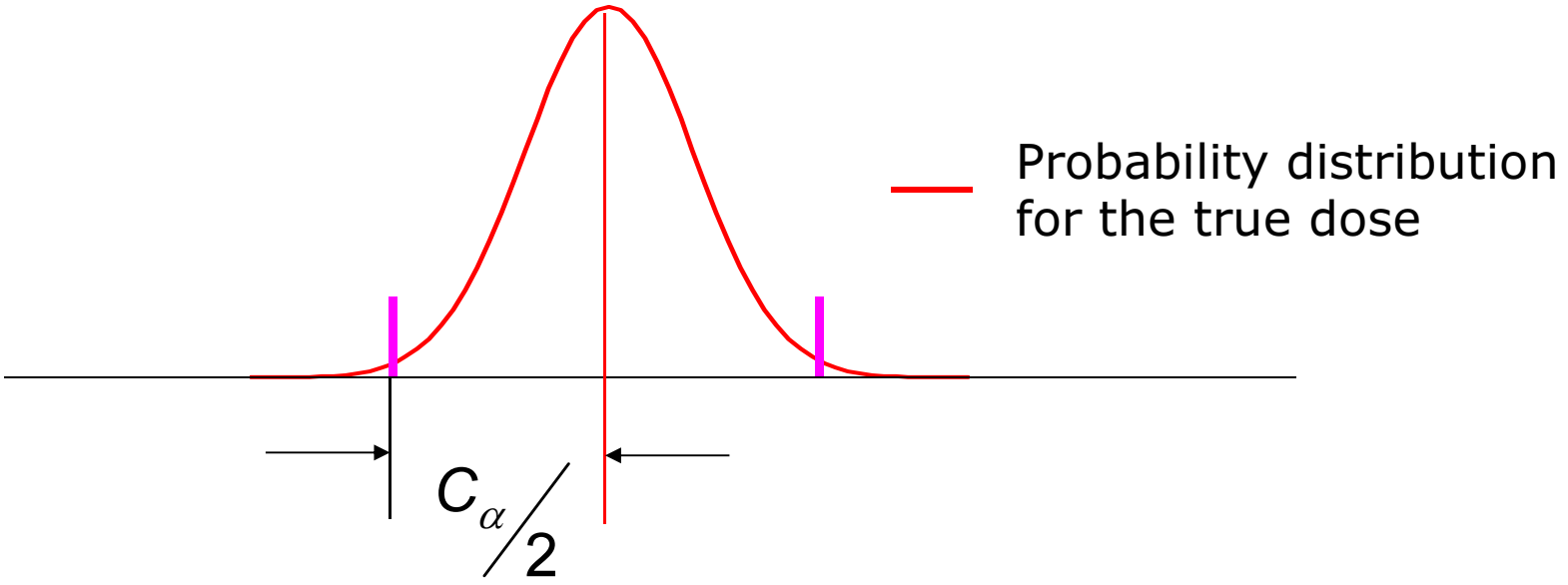

From Jörgen Olofsson (Dose Modeling and dose verification ESTRO COURSE)

ESTRO School

Example with small uncertainty:

Prescribed dose

Probability distribution for the true dose

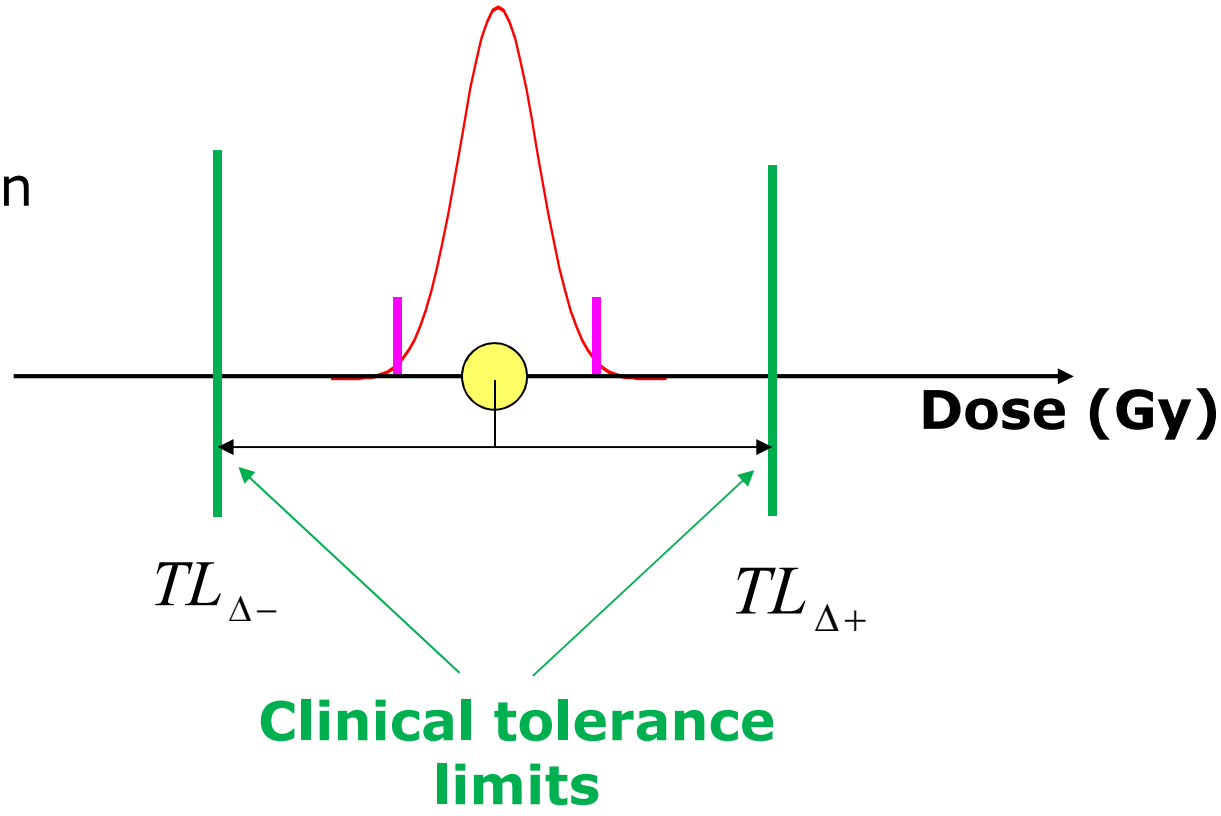

From Jörgen Olofsson (Dose Modeling and dose verification ESTRO COURSE)

Example with small uncertainty:

Prescribed dose

Probability distribution for the true dose

Action limits smaller than tolerance limits

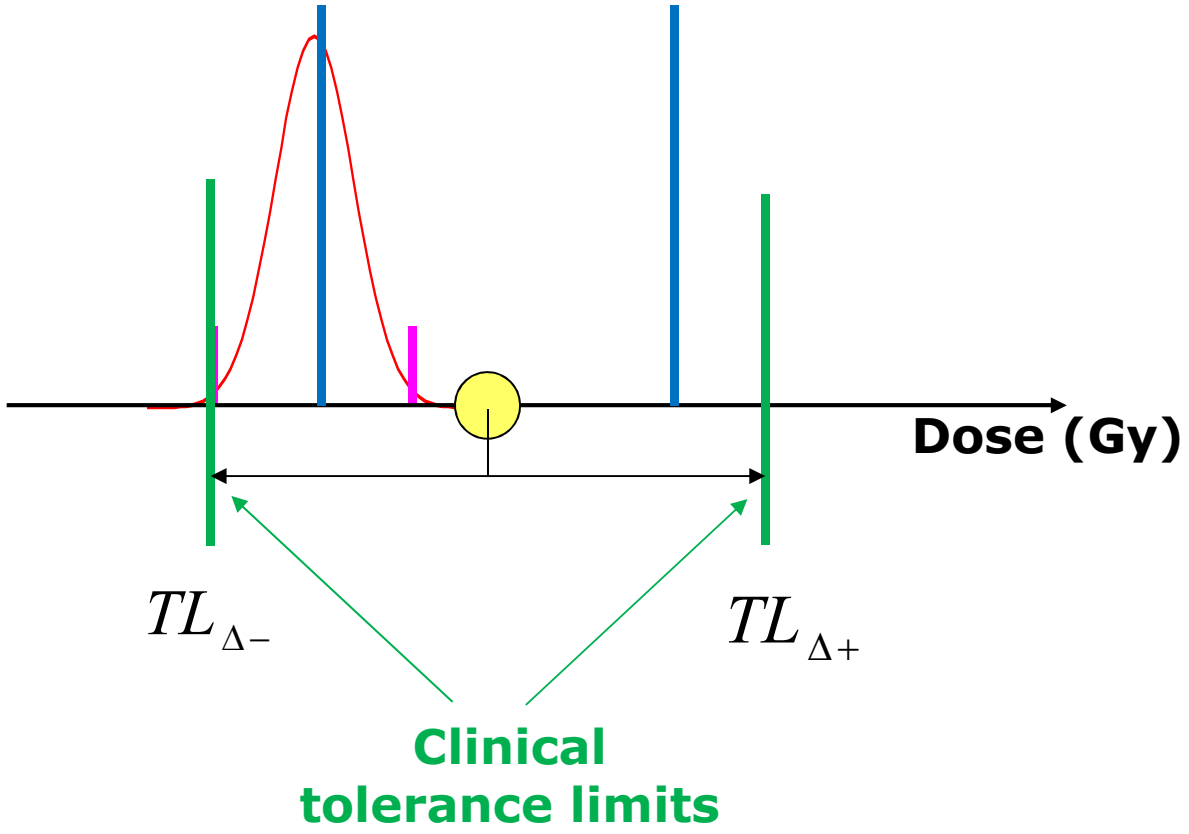

Example with large uncertainty:

Prescribed dose

Probability distribution for the true dose

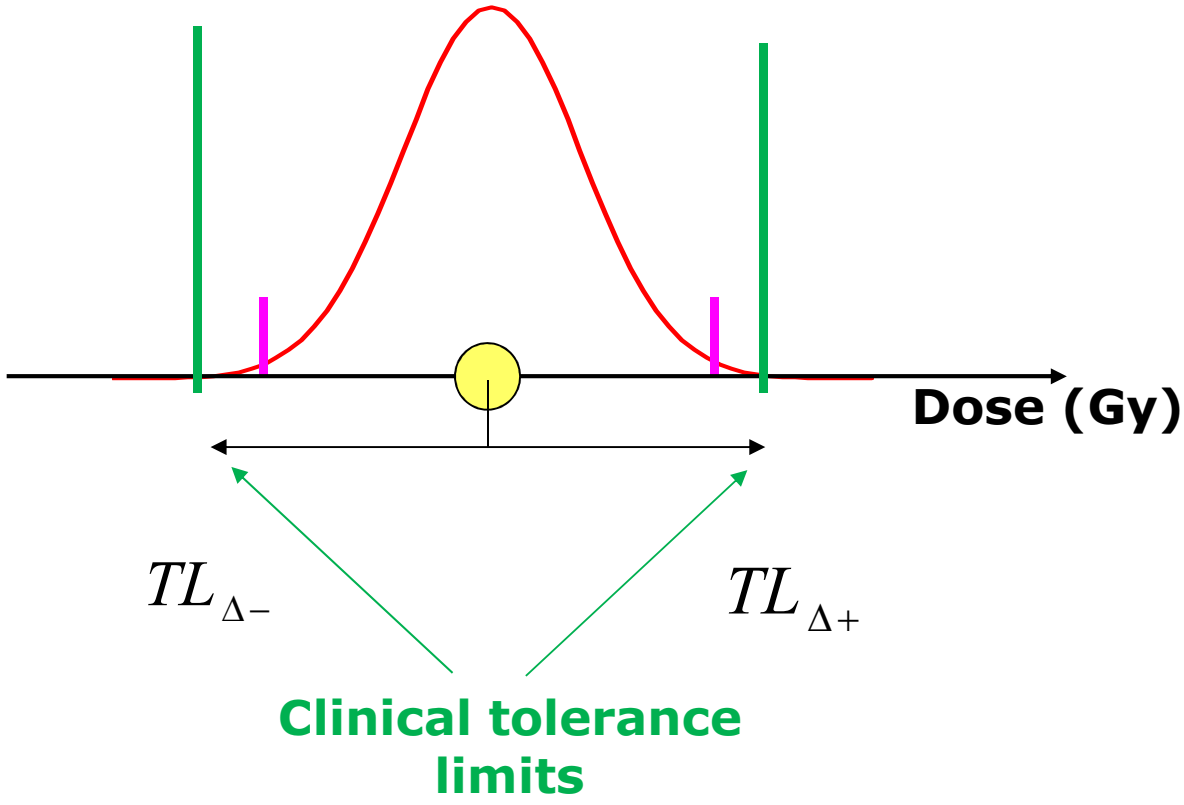

T. From JörgenOlofsson (Dose Modeling and dose verification ESTRO COURSE)

Example with large uncertainty:

Prescribed dose

Probability distribution for the true dose

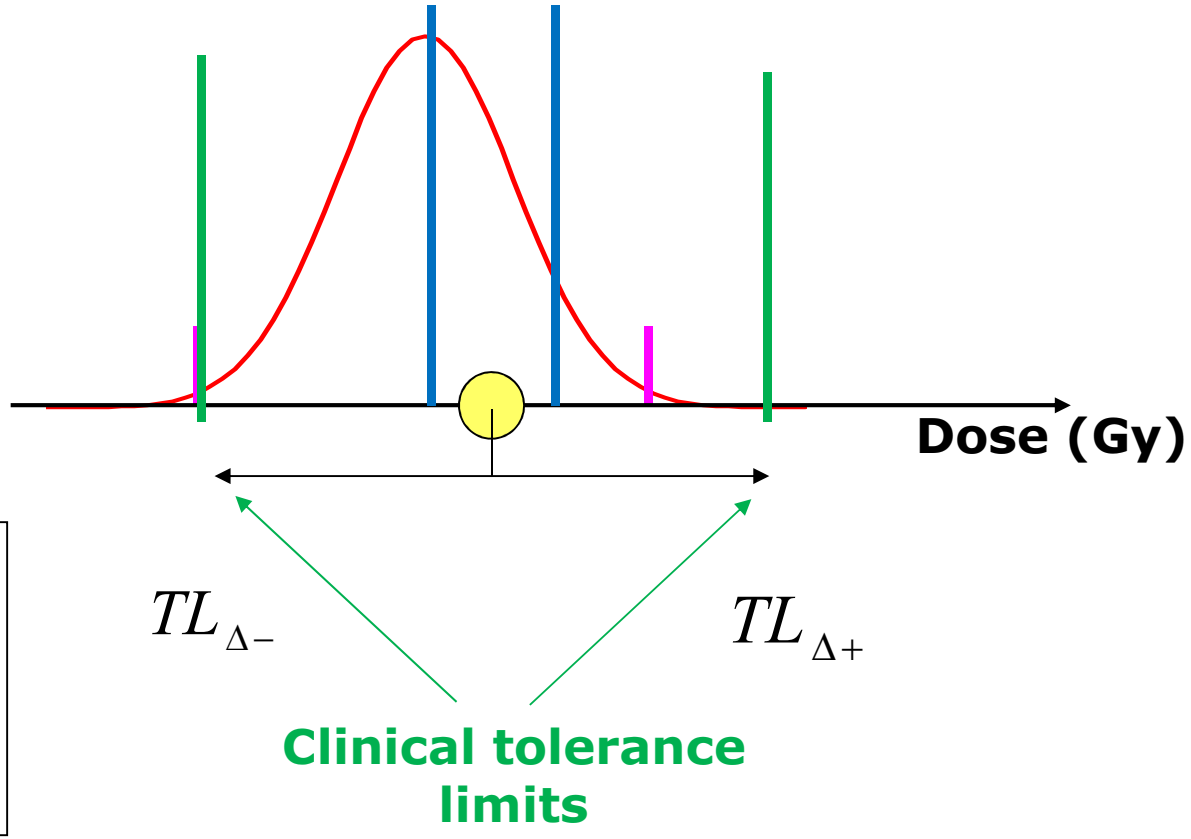

Action limits go to zero when dose measurement uncertainty increases

From Jörgen Olofsson (Dose Modeling and dose verification ESTRO COURSE)

ESTRO School

Relations between TL_{Δ}, AL_{Δ}, σ and α

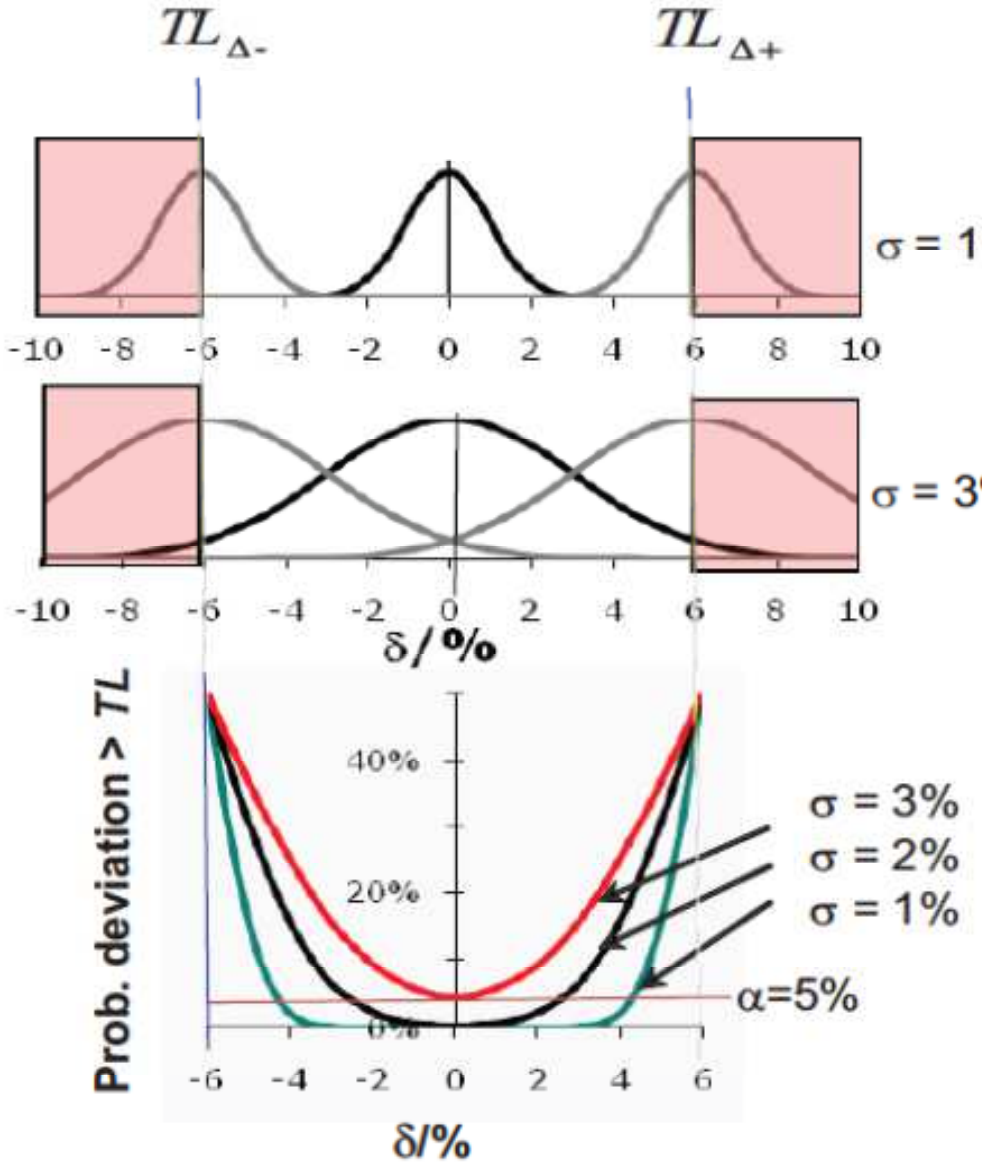

AL_+ = 6-1=5

AL_+ = 6-6=0

$$\Delta L_{\pm} = TL_{\pm} \pm \frac{C_{\alpha}}{2}$$

Dosimetric tolerance set to ± 6%

Different measurements standard deviations (σ)

What is the Action level (δ) if I set the confidence level in 95% (α=5%)?

Relations between TL_Δ, AL_Δ, σ and α

In relation to the uncertainty (σ):

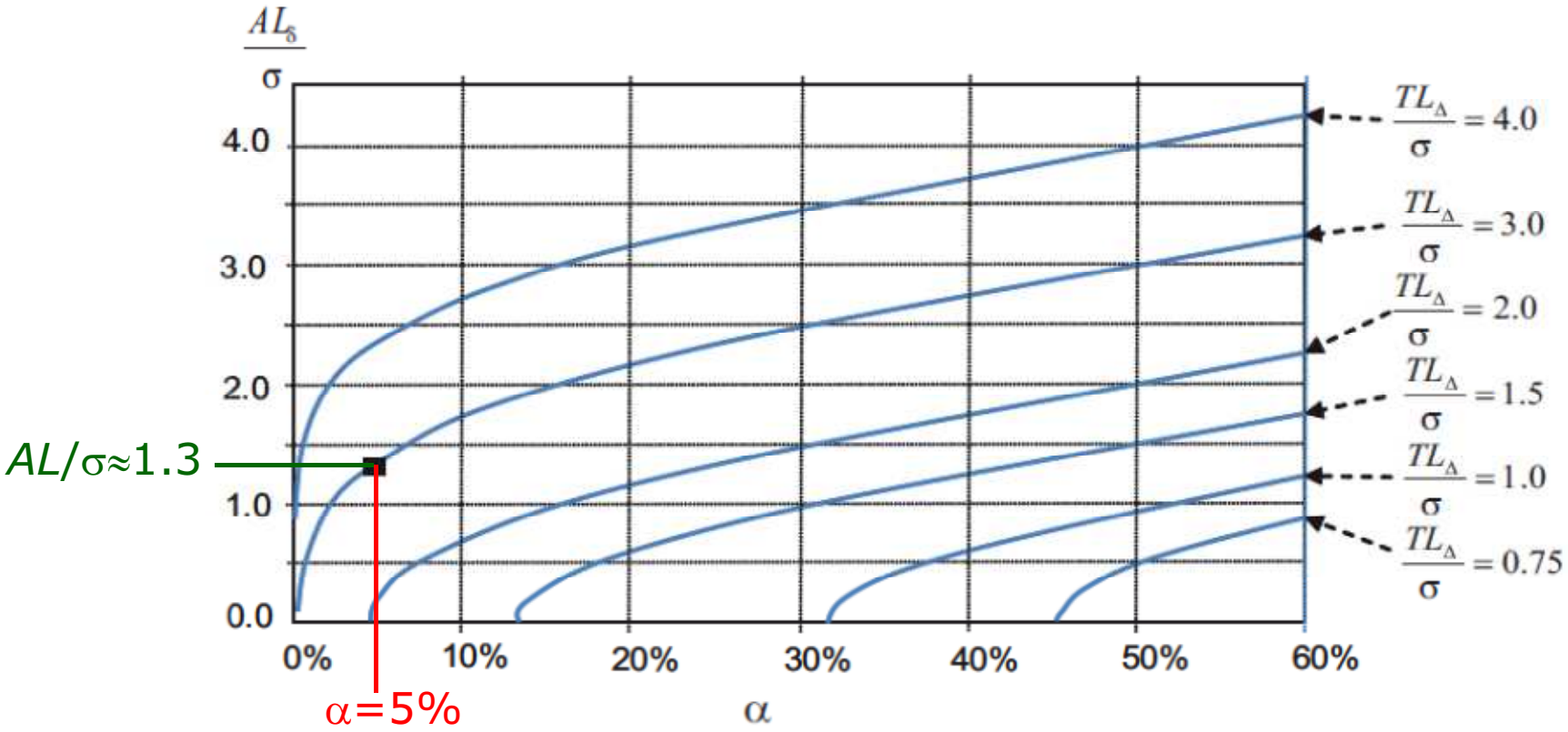

Figure 3.5 The vertical axis shows the action limit normalized to the estimated standard deviation σ_{total} for the independent dose calculation, IDC. The horizontal axis represents α. The six curves represent varying relations between the dosimetric tolerance limit TL_Δ and σ_{total}.

ESTRO Physics Booklet #10

ESTRO School

Friday afternoon at the medical physics department…

Dose measurement

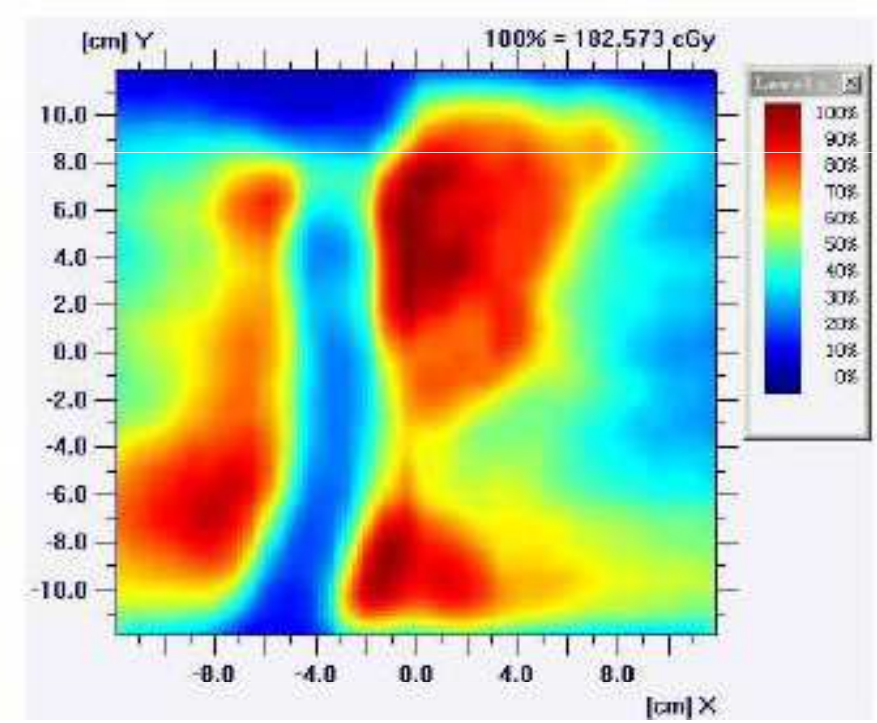

TPS dose calculation

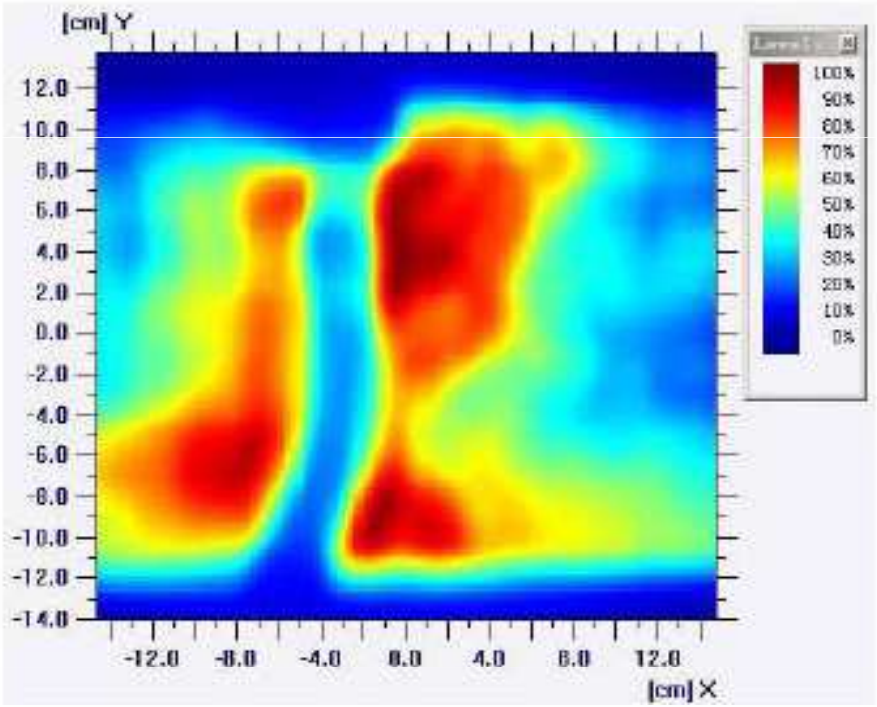

Not OK for treatment?

We need limits to make objective decisions!

From Jörgen Olofsson (Dose Modeling and dose verification ESTRO COURSE)

ESTRO School

IMRT; Does it make sense to have different action limits for different sites?

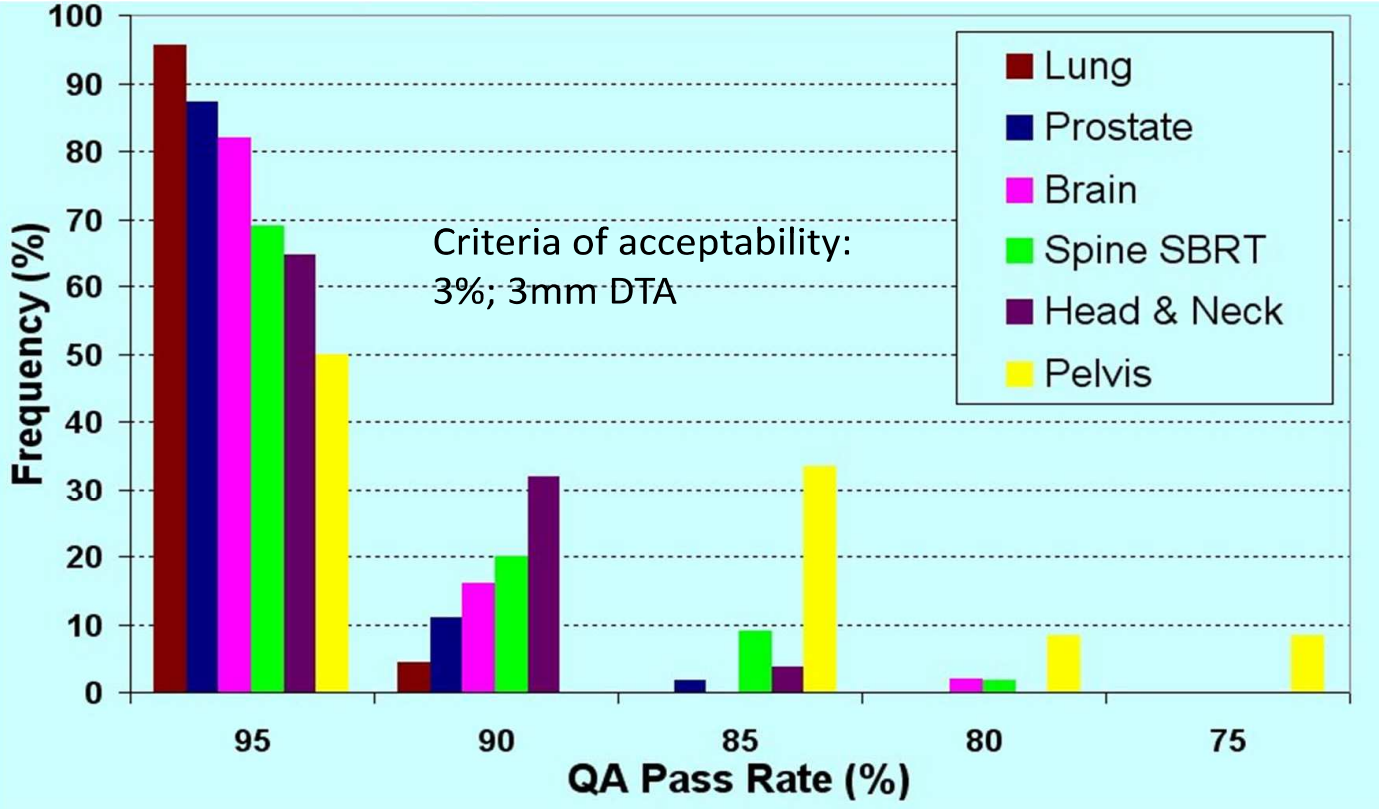

Higher failure rates for more complex delivery

Data from Florida University

IMRT; Does it make sense to have different action limits for different sites?

The uncertainty in the measurement: The same

1. If clinical tolerance limits the same : YES
2. If clinical tolerance limits depend on the site : YES

The action levels should be the SAME

Same gamma settings (3%-3mm)

ESTRO School

IMRT; Does it make sense to have different action limits for different treatment units?

The uncertainty in the measurement: The same

The clinical tolerance limits: The same

1. YES
2. NO

The action levels should be the SAME

Same gamma settings (3%-3mm)

Conclusion

Be critical when setting value driven tolerance and action limits

The action limit must be set according to clinical tolerances and measurement uncertainty

If your measuring equipment has large uncertainties it may not be suitable for QC

Uncertainties

Maximum weight= 60 Kg

σ = 1 Kg

Tolerance and action limits

Weigth limit = 60 Kg
Tolerance = 2 Kg

ESTRO School

Uncertainties

59 Kg
σ = 1 Kg

Probability 0.3%

Tolerance and action limits

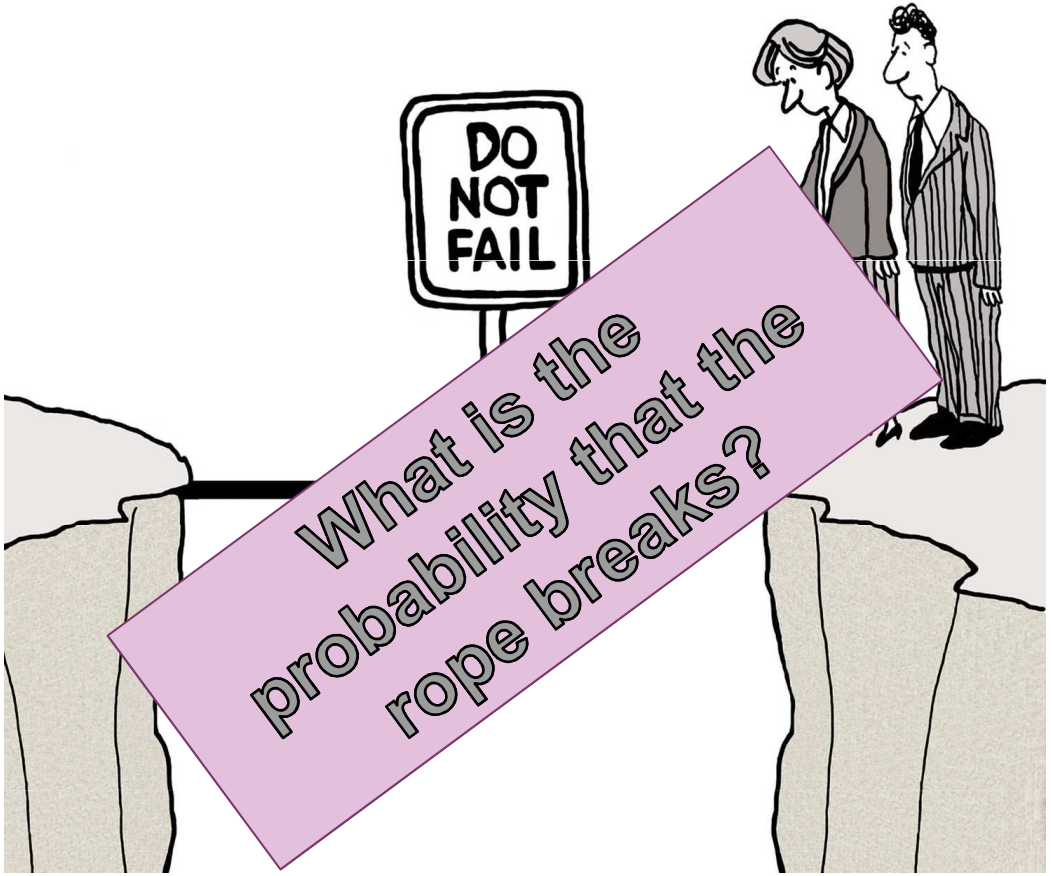

Weigth limit = 60 Kg
Tolerance = 2 Kg

ESTRO School

“Medicine is a science of uncertainty and an art of probability”

Sir William Osler (1849-1919)
A Canadian Physician,
The Father of Modern Medicine

ESTRO School

References

International Organization for Standardization:
Guide to the Expression of Uncertainty in Measurement, ISO (1993), ISBN 92-67-10188-9

May be obtained also via:

http://www.bipm.org/en/publications/guides/gum.html

H. Jin, J. Palta, T Suh and S. Kim. A generalized *a priori* dose uncertainty model of IMRT delivery. Med. Phys. 35, 982 (2008)

M. Karlsson et al. ESTRO booklet nº10. Independent dose calculations concepts and methods. (2010).

M. Goitein, Calculation of the uncertainty in the dose delivered during radiation therapy. Med. Phys. 12(5) (1985)

Lujan et al. A method for incorporating organ motion due to breathing into 3D dose calculations. Med. Phys. 26 (5) (1999)

G.K Svensson et al. AAPM Report 13. Physical aspects of Quality Assurance in Radiotherapy. (1994)

Extra-material

Uncertainty calculation fundamentals

i. Measurements: A statistical view on the outcome of a measurement
ii. Some essentials on statistics
iii. Value and uncertainty of a measurand
iv. Combined uncertainty
v. Type A and B evaluation of uncertainty
vi. Expanded uncertainty and coverage factor

Learning objectives

- to know what a measurand is and that it is subjected to a probability distribution
- to know the difference between an expectation value and the corresponding estimate in statistics
- to know how GUM defines uncertainty
- to be familiar with the formalism of combined uncertainties
- to know the difference between type A and type B evaluation of uncertainties

The concept of a measurand

Some words on the situation of a measurement:

The objective of a **measurement** is, of course, to determine the **value of the particular quantity** to be measured.

In the following this quantity
- a well defined physical quantity -
will be abbreviated by the term
measurand.

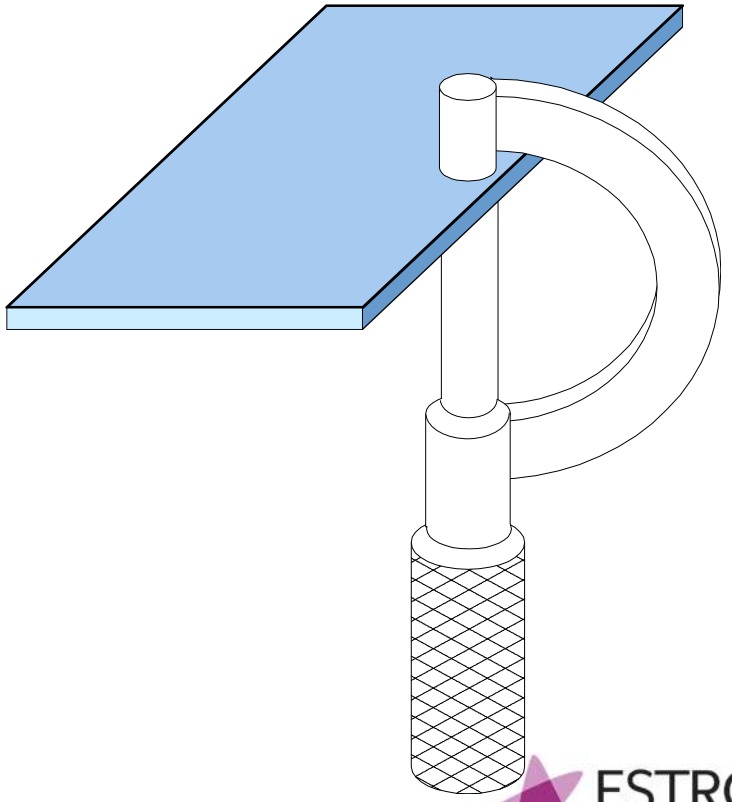

A measurement generally begins with:

1) an appropriate **specification** of the measurand,
2) the **method** of measurement,
3) and the **measurement procedure.**

The concept of a measurand

It is understood that the **result of the measurement** including all required corrections is the **best estimate** of the value of the measurand.

However, since the measurand cannot be completely specified without an **infinite** amount of information, the result of a measurement is only an **approximation** or **estimate** of the value of the measurand.

It means: All possible outcomes of a measurement are subjected to a **probability distribution**.

Thus the estimate of the value of the measurand is **complete only** when it is accompanied by a statement of the **uncertainty of that estimate**.

With this statistical view, the term "**result**" is used to denote a **single random value** out of all values that could reasonably be attributed to the value of the measurand.

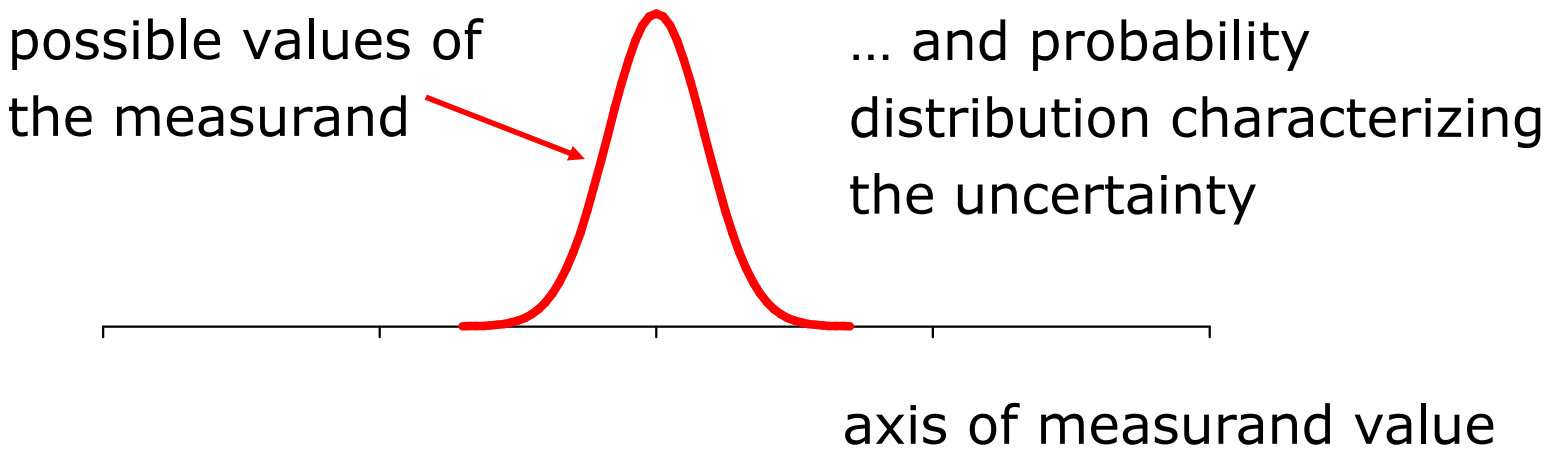

The value of the measurand is a stochastic quantity!!!

Four statistical essentials

A short excursion of how to treat a **stochastic quantity X** is summarized in the **five** following essentials:

① A one dimensional **stochastic quantity X** is entirely described by its **probability density f(x)** such that

$$\int_{-\infty}^{\infty} f(x)\,dx = 1$$

and that the probability w that $a < X \leq b$

is given by the integral

$$w = \int_{a}^{b} f(x)\,dx$$

② A stochastic quantity X can characterized by so-called **expectation values** of variables or functions of x.

The expectation value of an arbitrary function g(X) denoted as **E(g(X))**

is generally obtained from the probability density f(x) by the following integral:

$$E\left(g(X)\right) = \int_{-\infty}^{\infty} g(x) \cdot f(x)\, dx$$

③ There are **two** most important expectation values:

a) The expectation value E(X) of the stochastic quantity **X itself**

$$E(X) = \xi = \int_{-\infty}^{\infty} x \cdot f(x)\, dx$$

b) The expectation value of the function **g(X) = (X- ξ)²** , expressed as E((X- ξ)²) which is called the **variance**

$$E\left((X-\xi)^2\right) = \sigma^2 = \int_{-\infty}^{\infty} (x-\xi)^2 \cdot f(x)\, dx$$

④ Frequently, the probability density f(x) of the stochastic quantity X is not exactly known.

The only information which may be available is a sample of N **random realizations** of X, namely X_1, X_2, X_3, …. X_N.

In this case, the value of the two most important expectation values can only be **estimated** based on the random sample:

a) estimate for ξ: $\overline{X} = \frac{1}{N}\sum_{i=1}^{N} X_i$, i.e. the mean value;

b) estimate for σ^2 : $s^2 = \frac{1}{N-1}\sum_{i=1}^{N}\left(X_i - \overline{X}\right)^2$

⑤ It is extremely important to carefully differentiate between:

Estimate of the variance of the stochastic quantity X:

$$s(X)^2 = \frac{1}{N-1}\sum_{i=1}^{N}\left(X_i - \overline{X}\right)^2$$

Estimate of the variance of the estimate of the expectation value of the stochastic quantity X:

$$s(\overline{X})^2 = \frac{s^2}{N} = \frac{1}{N\cdot(N-1)}\sum_{i=1}^{N}\left(X_i - \overline{X}\right)^2$$

How uncertainty is determined

Coming back to the situation of a measurement, we now introduce - according to GUM - the two definitions:

1) The **best estimate** of the **value of the measurand** is determined from its **expectation value** with respect to its associated probability density distribution.

   If this distribution is not known, it can be **estimated as the mean value** from a random sample obtained from repeated measurements.

2) The **standard uncertainty** u of the value of the measurand is determined as the **positive root of the variance** with respect to its associated probability density distribution.

   If this distribution is not known, the **estimate of the variance of the mean value** can be used instead.

This is exemplified assuming that the probability density of the measurand is known and that it has a Gaussian shape.

1) The best estimate of the value of the measurand:

2) The standard uncertainty of the value of the measurand:

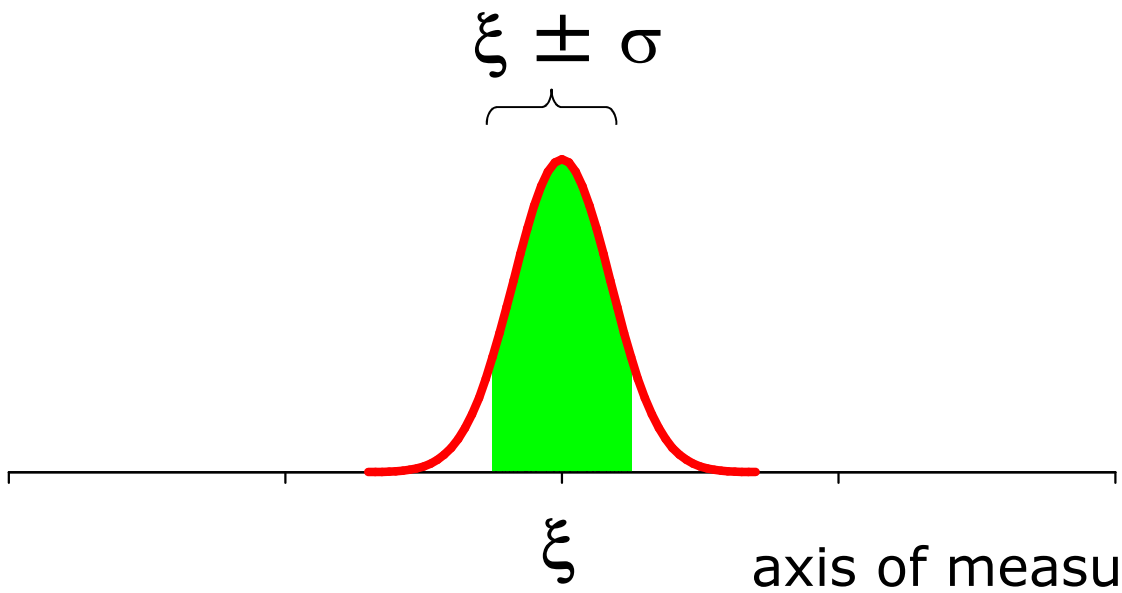

A simple example of uncertainty evaluation with unknown distribution:

In a dosimetric measurement a charge (the measurand) is measured 20 times, yielding C_1 to C_{20}.

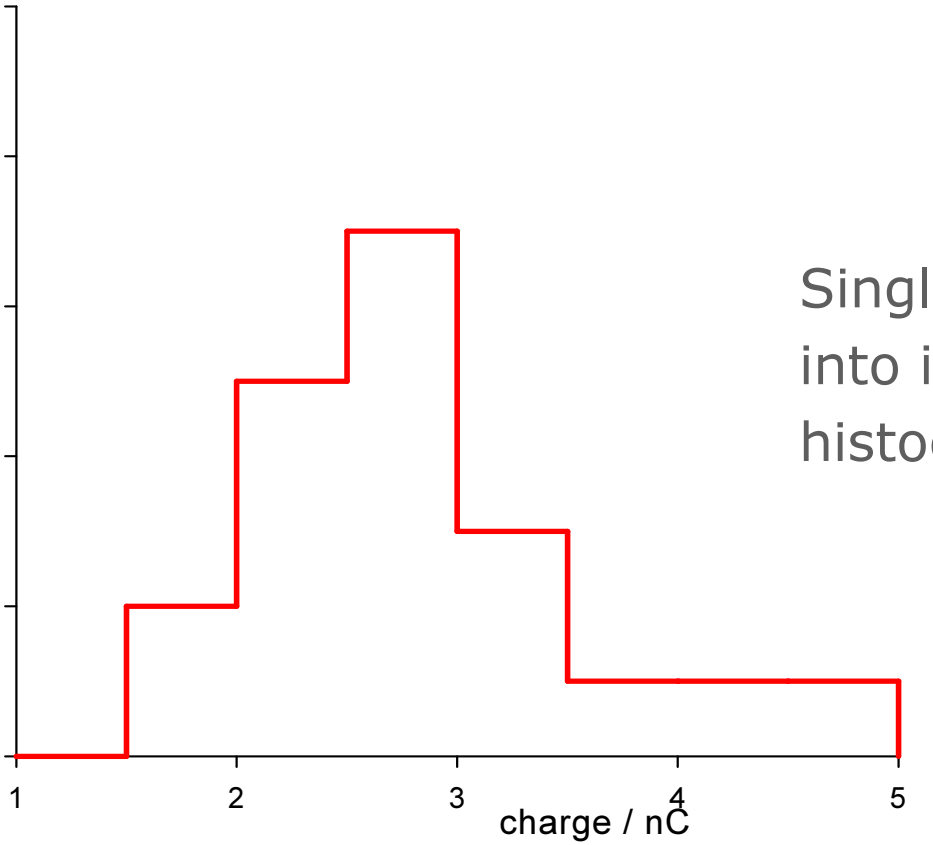

Single values have been grouped into intervals and are shown as a histogram.

The best estimate for the correct charge is obtained as the mean value $\overline{C}$ of the single values C_1 to C_{20}:

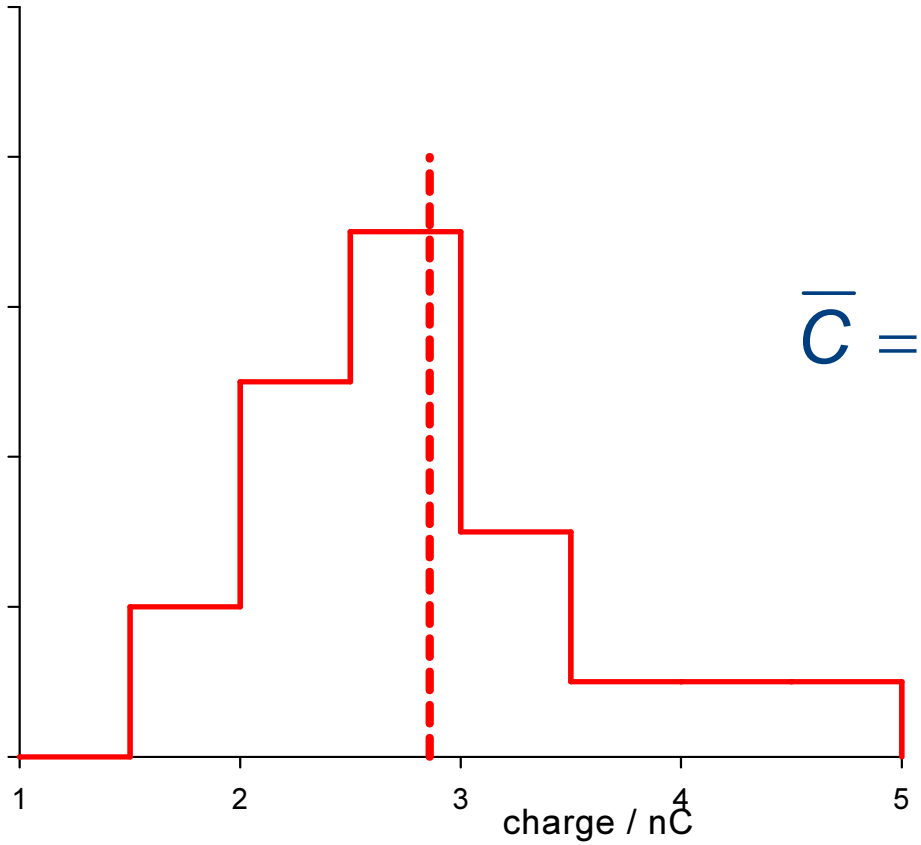

$$\overline{C} = \frac{1}{N}\sum_{i=1}^{N} C_i$$

The **uncertainty u** for the charge is obtained from the **estimate** of the standard deviation of the **mean value** of C.

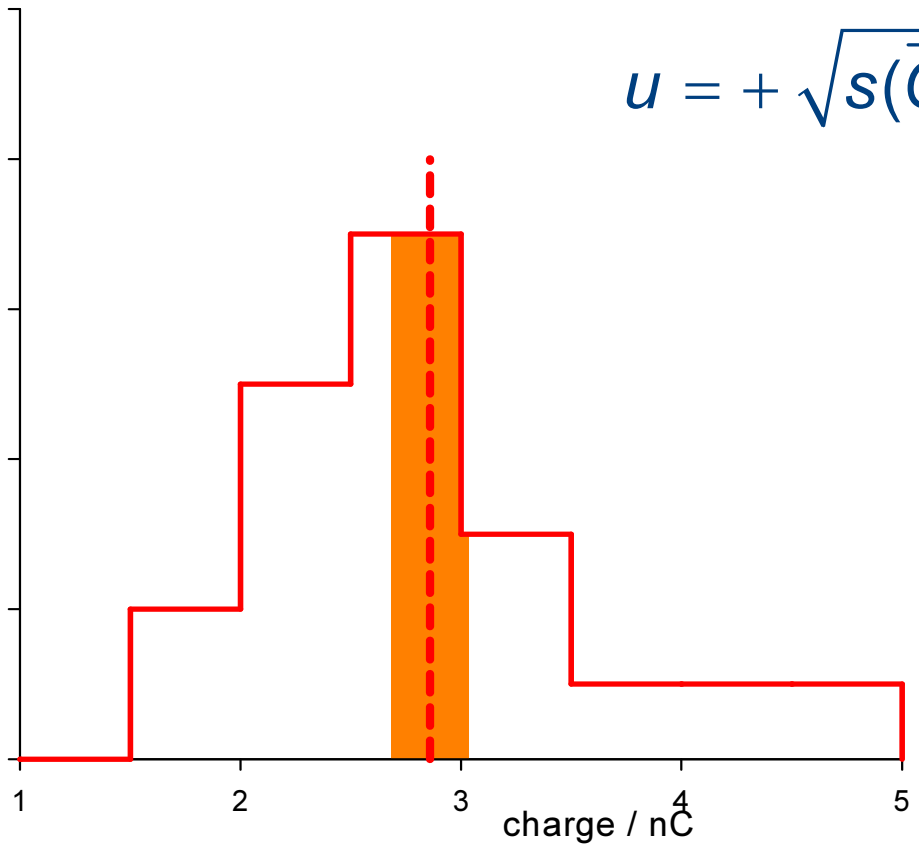

$$u = +\sqrt{s(\overline{C})^2} = \sqrt{\frac{1}{20 \cdot (20-1)} \sum_{i=1}^{N} \left(C_i - \overline{C}\right)^2}$$

Combined uncertainty

In most cases a measurand, now called Y, is not measured directly, but is determined from ***N*** other input quantities
$\boldsymbol{X_1}$, $\boldsymbol{X_2}$, **….**, $\boldsymbol{X_N}$, through a functional relationship ***f***:

$$Y = f(X_1, X_2, ...X_N)$$

The functional relationship ***f*** is also referred to as the model equation for the measurand.

The set of input quantities X_1, X_2, ..., X_N may be differentiated into two following categories:

① Input quantities whose values **and uncertainties** are directly determined in **the current measurement**.

These values and uncertainties may be obtained from:

- a single observation

- repeated observations

- judgment based on experience.

Input values may also involve the determination of corrections to instrument readings and corrections for influence quantities, such as ambient temperature, barometric pressure, and humidity.

② Input quantities whose values **and uncertainties** are brought into the measurement **from external sources**, such as:

- quantities associated with calibrated measurement standards

- certified reference materials

- reference data obtained from handbooks.

The values of input quantities are – of course – also subjected to probability distribution.

Therefore, an **estimate** of the measurand Y, denoted by y, is obtained using **input estimates** x_1, x_2, ..., x_N for the values of the N input quantities X_1, X_2, ..., X_N.

Thus the **output estimate** y, which is the result of the measurement, is given by:

$$y = f(x_1, x_2, ...x_N)$$

estimates

A combined (standard) uncertainty is then obtained as the positive square root of the **sum of variances** weighted according to how the result is influenced by varying different influence components (if not correlated).

$$u_c = + \sqrt{\sum_{i=1}^{N} \left(\frac{\partial f}{\partial x_i} \right)^2 \cdot u^2(x_i)}$$

$\frac{\partial f}{\partial x_i}$ = sensitivity factor

Combined uncertainty

It remains to determine:

- the estimates: x_1, x_2, ..., x_N
  for the N input quantities X_1, X_2, ..., X_N

- the corresponding uncertainties
  $u(x_1)$, $u(x_2)$, ….. ,$u(x_N)$,

Combined uncertainty

We start with the determination of the input estimates x_1, ..., x_N

Each input estimate x_i *is* obtained from a **distribution** of possible values of the input quantity X_i .

This probability distribution may be:

a) **frequency based**, that is, based on a series of N observations $X_{i,k}$ of X_i;

$$x_i = \frac{1}{N}\sum_{k=1}^{N} x_{i,k}$$

b) or it may be an **a priori distribution $p_i(x)$;**

$$x_i = \int_{-\infty}^{+\infty} x \cdot p_i(x) \cdot dx$$

Type A and B evaluation

Next we have to determine the estimates for the corresponding uncertainties $u(x_i)$.

GUM says: The uncertainties are grouped into **two different categories** according to the method **how the uncertainty is being evaluated**:

Type A evaluation:

refers to those input quantities which are evaluated by statistical analysis of series of observations

Type B evaluation :

refers to those input quantities which are evaluated by other means

Type A evaluation:

Step 1: Determine the **mean value** from a series of observations:

$$x_i = \frac{1}{N}\sum_{k=1}^{N} x_{i,k}$$

Step 2: Determine the **positive root of the estimate of the variance** of the mean value

$$u = +\sqrt{s(\overline{x}_i)^2} = \sqrt{\frac{1}{N \cdot (N-1)}\sum_{k=1}^{N}(x_{i,k} - \overline{x})^2}$$

Type B evaluation:

The uncertainty cannot be evaluated by repeating the measurement.

The corresponding distribution must be evaluated as a **a-priory distribution** based on **any other available information** such as:

- previous measurement
- experience
- general knowledge
- manufacturer's specification

Type B evaluation:

Typical examples for an **a-priory probability distribution** are:

1) Gaussian probability distribution

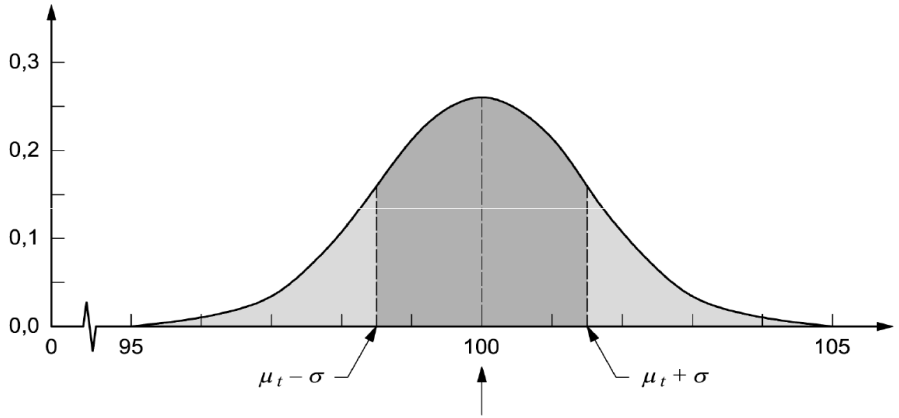

2) Rectangular probability distribution

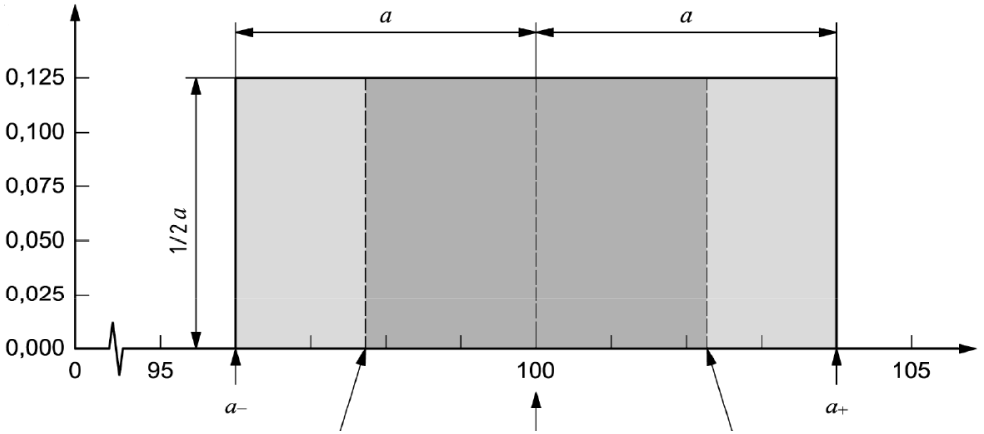

3) Triangle probability distribution

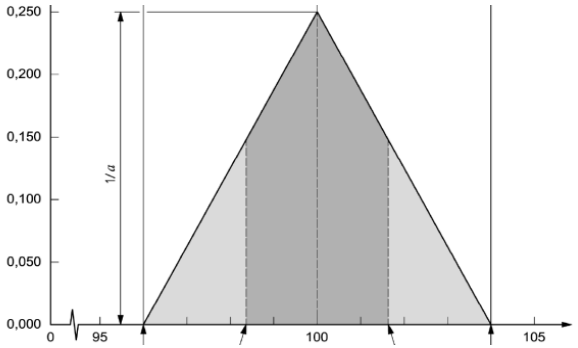

Type B evaluation:

Example for a type B evaluation:

One of the input quantities in the dose determination is the correction factor for the air temperature and pressure

$$k_\rho = \frac{(273.2 + T)}{(273.2 + T_0)} \frac{P_0}{P}$$

Temperature measurement with a Thermometre

T = 293.25 K =20ºC

The thermometer has a traceable calibration.

However this only says that the measured value is correct within an interval of ± 0.2° C. What is the underlying distribution??

All one can do is to **suppose** that there is a symmetric lower and upper bound of the interval {T-Δ, T+Δ}, and that any value between this interval has an **equal probability**.

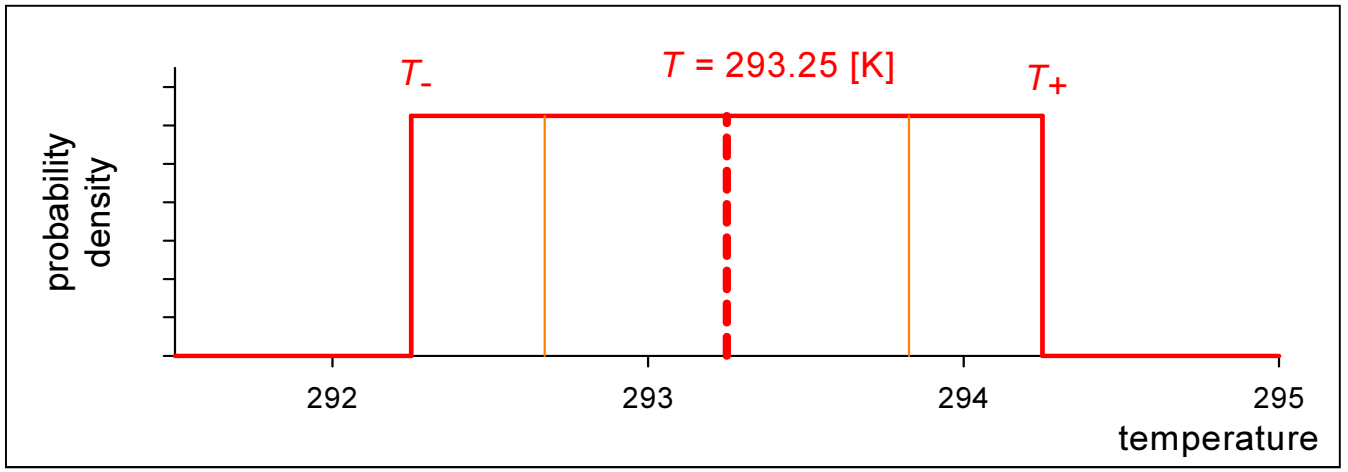

Step 1: Construct the **a priority** probability density $p(x)$ for the temperature distribution:

$$p(x) = C \quad \text{for} \quad \mathrm{T} - \Delta \le \mathrm{x} \le \mathrm{T} + \Delta$$
$$p(x) = 0 \quad \text{otherwise}$$

The integral $\int_{-\infty}^{\infty} p(x)\,dx$ must be unity.

$$\int_{-\infty}^{\infty} p(x)dx = C \cdot x\Big|_{T-\Delta}^{T+\Delta} = C \cdot 2\Delta \qquad C = \frac{1}{2\Delta}$$

$$p(x) = \frac{1}{2\Delta} \quad \text{for} \quad T - \Delta \le x \le T + \Delta$$
$$p(x) = 0 \quad \text{otherwise}$$

Step 2: Calculate the **expectation value** ξ and the **variance** σ^2 of the temperature using that probability density $p(T)$

Expectation value:

$$\xi = \int_{-\infty}^{+\infty} x \cdot p(x)\,dx = \frac{1}{2\Delta}\int_{T-\Delta}^{T+\Delta} x\,dx = T$$

Variance:

$$\sigma^2 = \int_{-\infty}^{+\infty} (x-\xi)^2\, p(x)\,dx = \frac{1}{2\Delta}\int_{T-\Delta}^{T+\Delta} (x-T)^2\,dx = \frac{1}{3}\Delta^2$$

Standard uncertainty:

$$u_B = \sqrt{\sigma^2} = \frac{\Delta}{\sqrt{3}}$$

Corresponding standard uncertainty:

$$u_B = \frac{0.2\ °C}{\sqrt{3}}$$

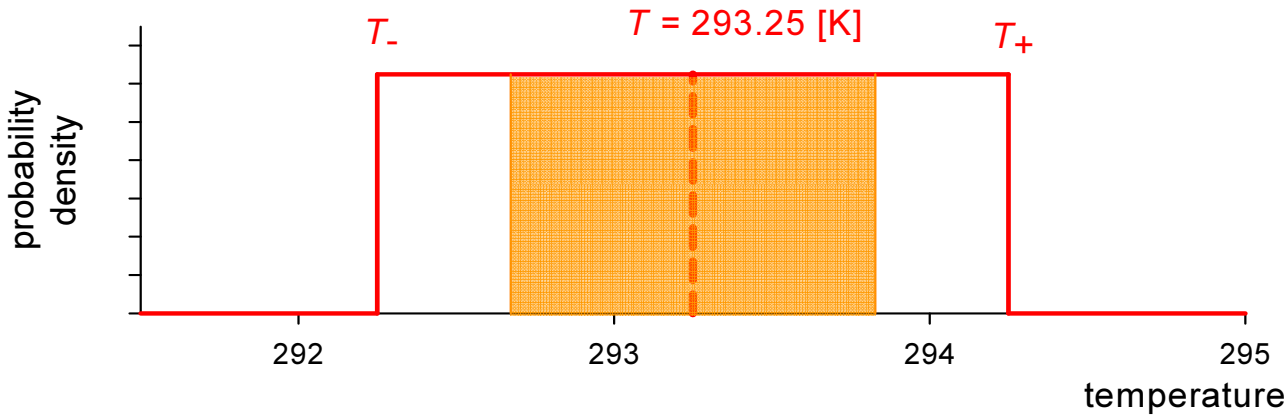

The coverage factor and expanded uncertainty

A last remark on the probability range of uncertainty:

We know: The combined (standard) uncertainty is the positive square root of the sum of variances weighted according to how the result is influenced by varying different influence components (if not correlated).

$$u_c = + \sqrt{\sum_{i=1}^{N} \left(\frac{\partial f}{\partial x_i} \right)^2 \cdot u^2(x_i)}$$

If this standard uncertainty is used as the quoted range, then the measurand lies within $\xi \pm \sigma$ with a probability of 67%.

The coverage factor and expanded uncertainty

If one wishes to report a result and its uncertainty with a higher probability than 67%, one can say:

$$y = \xi + U = \xi + 2 \cdot u_c$$ with 97%

or: $$y = \xi + U = \xi + 3 \cdot u_c$$ with 99%

where the "2" or the "3" is called the **"coverage factor"** and the product between coverage factor and standard uncertainty is termed the **expanded uncertainty U**.

The coverage factor and expanded uncertainty

Example for a coverage factor and expanded uncertainty in a Calibration Certificate

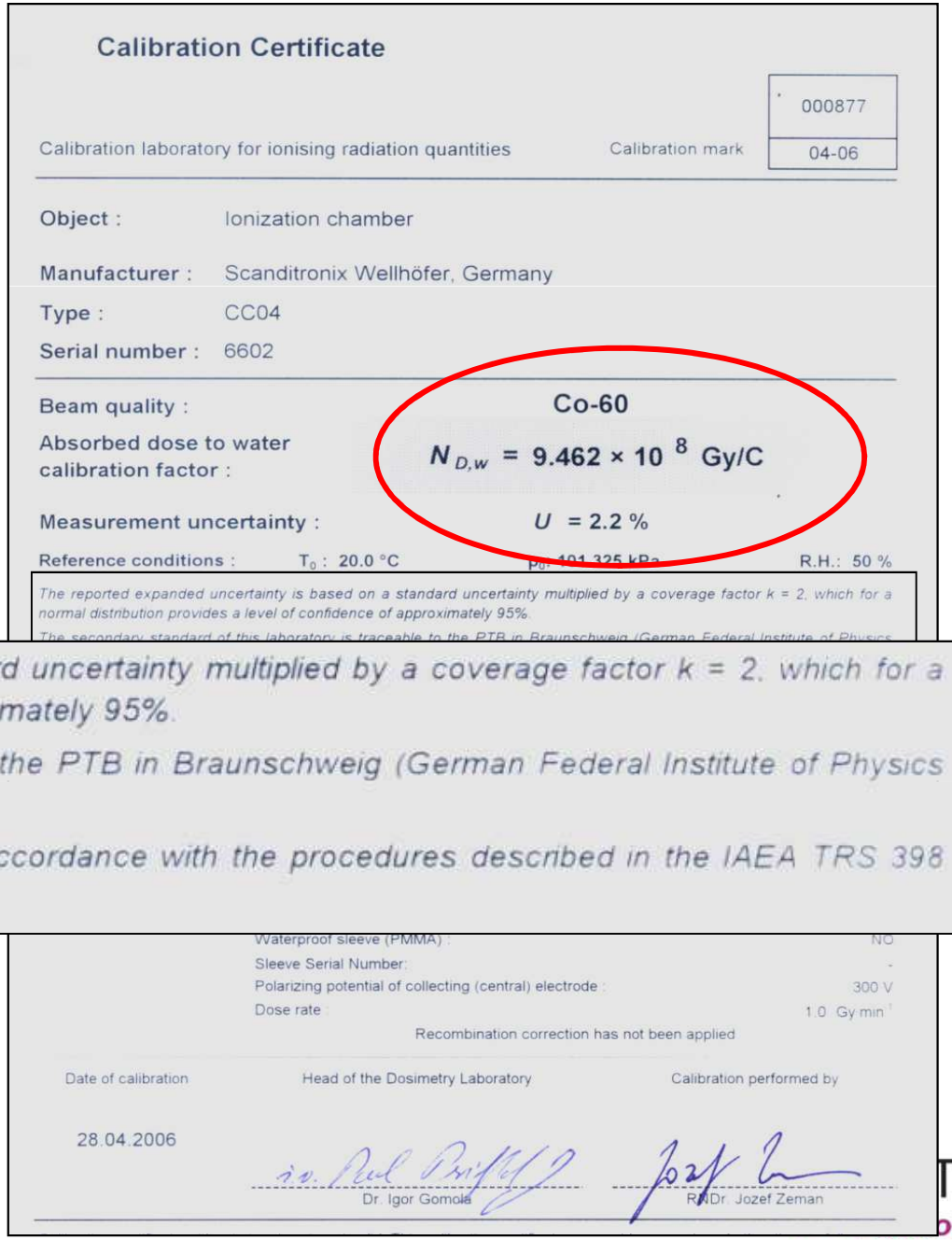

Calibration Certificate

000877

Calibration laboratory for ionising radiation quantities — Calibration mark: 04-06

Object : Ionization chamber

Manufacturer : Scanditronix Wellhöfer, Germany

Type : CC04

Serial number : 6602

Beam quality : Co-60

Absorbed dose to water calibration factor : $N_{D,w} = 9.462 \times 10^{8}$ Gy/C

Measurement uncertainty : $U = 2.2\ \%$

Reference conditions : T_0 : 20.0 °C — p_0: 101.325 kPa — R.H.: 50 %

The reported expanded uncertainty is based on a standard uncertainty multiplied by a coverage factor k = 2, which for a normal distribution provides a level of confidence of approximately 95%.

The secondary standard of this laboratory is traceable to the PTB in Braunschweig (German Federal Institute of Physics and Metrology).

Calibration reported in this certificate was carried out in accordance with the procedures described in the IAEA TRS 398 Code of Practice.

Waterproof sleeve (PMMA) : NO

Sleeve Serial Number : -

Polarizing potential of collecting (central) electrode : 300 V

Dose rate : 1.0 Gy min^{-1}

Recombination correction has not been applied

Date of calibration	Head of the Dosimetry Laboratory	Calibration performed by
28.04.2006	Dr. Igor Gomola	RNDr. Jozef Zeman

RECAP

(1) The term **measurand** denotes a well defined physical quantity to be measured.

(2) The value of a measurand is a **stochastic quantity** subjected to a **probability distribution**.

(3) If this probability distribution is known, then the best estimate of the measurand is the expectation value of the measurand.

(4) The corresponding standard uncertainty is the positive square root of the variance of the probability distribution.

(5) If this probability distribution is not known and the only available information is a sample of **random realizations,** then the best estimate of the measurand is **the mean value** of the random realizations.

(6) The corresponding standard uncertainty is the positive square root of the **estimate** of the variance of the **mean value**.

(7) The combined uncertainty is given by the following formula:

$$u_c = + \sqrt{\sum_{i=1}^{N} \left(\frac{\partial f}{\partial x_i} \right)^2 \cdot u^2(x_i)}$$

(8) The **expanded uncertainty** is the product of the **coverage factor** and standard uncertainty.

Margins in dose calculations

Anders Ahnesjö
Uppsala University
Sweden

ESTRO

UPPSALA
UNIVERSITY

Learning objectives

To understand

1. the link between dose calculations and the probabilistic concepts of the CTV, ITV and PTV

2. how the probabilistic approaches are used in margin recipe design

3. the major limitations in common margin recipes

4. Some hints about probabilistic planning

Clinical implementation of ICRU report 83 and its forerunners reports 62 and 50 established the GTV->CRT->ITV->PTV concepts

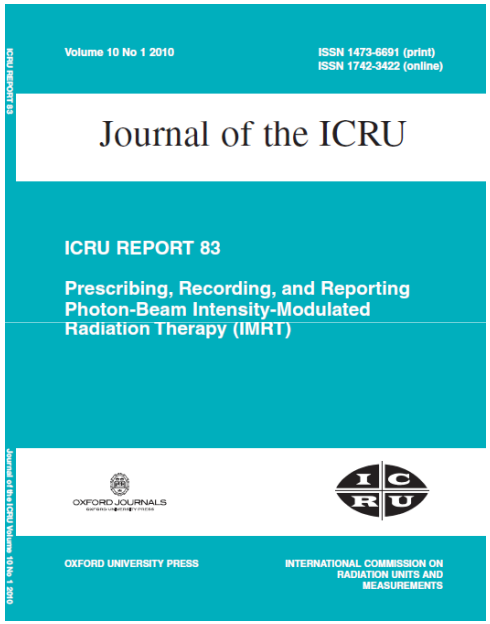

***To be discussed**:*

Probabilistic background of CRT->PTV margin recipes.

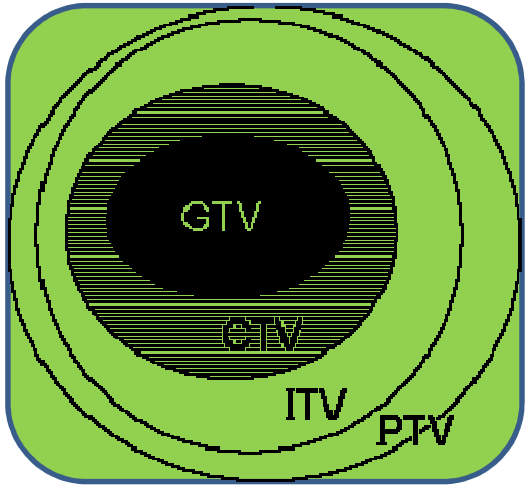

- GTV, Gross Tumor Volume
- CTV, Clinical Target Volume
- ITV, Internal Target Volume
- PTV, Planning Target Volume

- OAR, Organ At Risk
- PRV, Planning organ-at-Risk Volume

- TV, Treated Volume

GTV, CTV, and OAR are purely oncological/anatomical concepts which delineation is independent of treatment technique.

ITV, PTV, and PRV are treatment planning (margin) dependent concepts

TV is treatment dependent concept

Type of deviations

Systematic deviations Σ

- Treatment **preparation** errors, *random* between “patients”, *systematic* per “patient” (“patient”=planning image set)
- Remains equal for all fractions based on the planning image set
- Sources:
  - CTV delineated from a snapshot (movements)
  - Delineation errors
  - Systematic positioning/alignment errors of devices

Random errors σ

- Treatment **execution** errors
- Different and uncorrelated between fractions
- Sources:
  - Positioning deviations
  - Field uncertainties

Algorithms for CTV2PTV margin recipes

Outline

- Some useful math of normal distributions (Gaussians)!
- Derivation of van Herk margin formula (vHMF), approximations and extensions

The normal distribution (Gauss) in 1D

Probability Density Function, PDF

$$\Pr\left(X \in [x, x+\mathrm{d}x], \mu, \sigma\right) =$$

$$= \mathrm{PDF} \cdot \mathrm{d}x = \frac{\mathrm{e}^{-\frac{(x-\mu)^2}{2\sigma^2}}}{\sqrt{2\pi}\sigma}\,\mathrm{d}x$$

Cumulative Density Function, CDF

$$\Pr\left(X \le x_0, \mu, \sigma\right) = \int_{-\infty}^{x_0} \frac{\mathrm{e}^{-\frac{(x-\mu)^2}{2\sigma^2}}}{\sqrt{2\pi}\sigma}\,\mathrm{d}x =$$

$$= \mathrm{CDF} = \frac{1}{2}\left(1 + \mathrm{Erf}\left(\frac{x_0 - \mu}{\sqrt{2}\sigma}\right)\right)$$

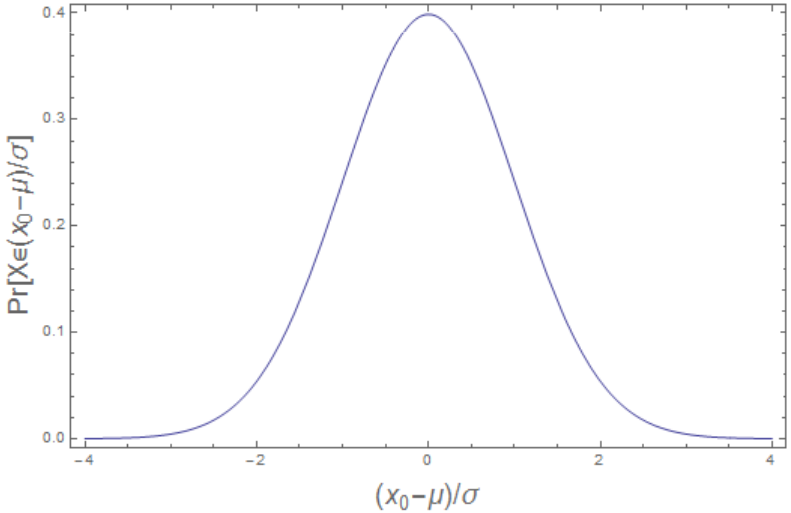

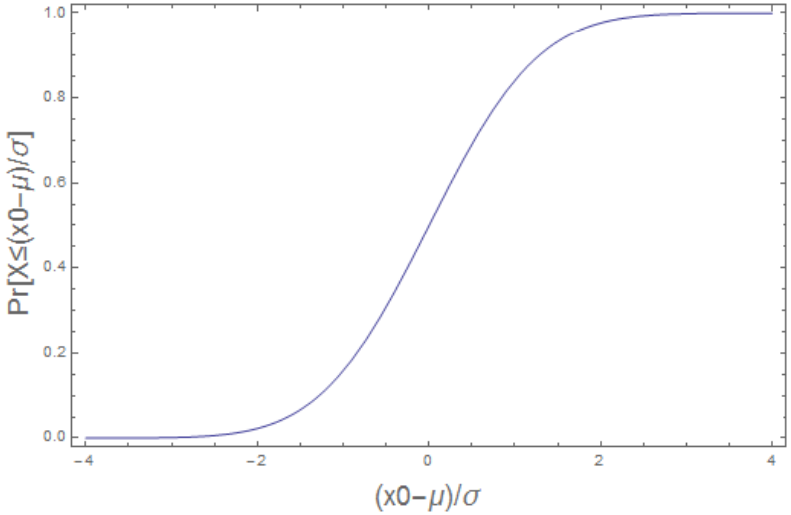

Normalization requirements:

$$\int_{-\infty}^{\infty} \mathrm{PDF}(x) \cdot \mathrm{d}x \equiv 1$$

$$\mathrm{CDF}(\infty) \equiv 1$$

Static dose surrogate in 3D; convolve over a box function

$$"D(x,0,0)" = \int_{-\infty}^{\infty}\int_{-\infty}^{\infty}\int_{-\infty}^{\infty} "\Psi(x',y',z')"\cdot k(x-x',y-y',z-z')\,dx\,dy\,dz = \underbrace{1\cdot 1}_{\text{if } f_y, f_z >> \sigma_p} \cdot \frac{1}{2}\left(\text{Erf}\left(\frac{x+f_x}{\sqrt{2}\cdot\sigma_p}\right) - \text{Erf}\left(\frac{x-f_x}{\sqrt{2}\cdot\sigma_p}\right)\right)$$

where

$$"\Psi(x,y,z)" = \begin{cases} 1 & \begin{cases} -f_x \le x \le f_x \\ -f_y \le y \le f_y \\ -f_z \le z \le f_z \end{cases} \\ 0 & (x,y,z) \in \text{elsewhere} \end{cases}$$

and a 3D Gaussian ”kernel”:

$$k(x-x',y-y',z-z') = \frac{e^{-\frac{(x-x')^2}{2\sigma_p^2}} e^{-\frac{(y-y')^2}{2\sigma_p^2}} e^{-\frac{(z-z')^2}{2\sigma_p^2}}}{2\sqrt{2}\pi^{3/2}\sigma_p^3}$$

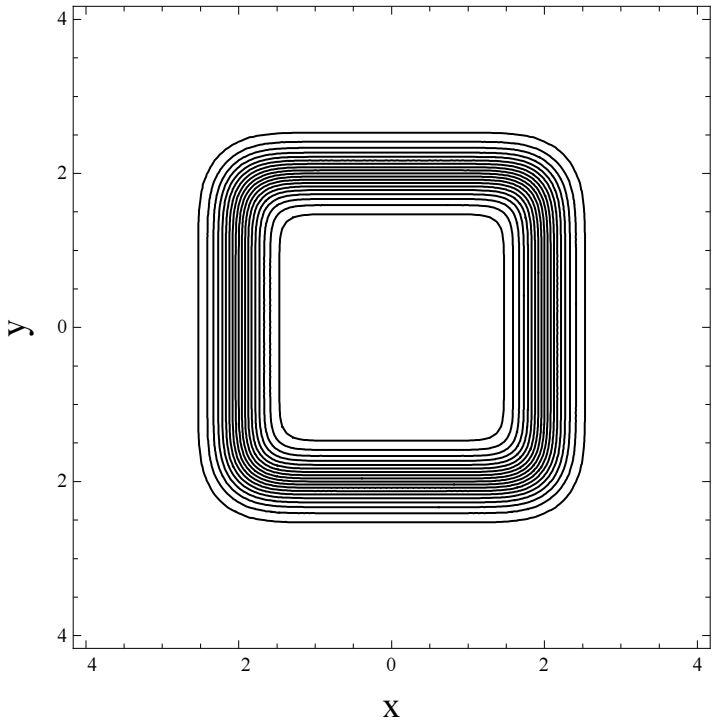

Same result along ”main” axes as for a 1D Gaussian (same σ_p)!

In margin recipes common to assume dose profile as ”straight out of a large target”. Convolution model assumes infinite number of fractions, where $\sigma_p \to \sqrt{\sigma_p^2 + \sigma^2}$

Rotational symmetrical 3D Gauss – we can substitute for radius

$$\mathrm{PDF}(x,y,z,\Sigma) = \frac{e^{-\frac{x^2}{2\Sigma^2}}}{\sqrt{2\pi}\Sigma} \cdot \frac{e^{-\frac{y^2}{2\Sigma^2}}}{\sqrt{2\pi}\Sigma} \cdot \frac{e^{-\frac{z^2}{2\Sigma^2}}}{\sqrt{2\pi}\Sigma}$$

$$x^2 + y^2 + z^2 \to r^2$$

$$\mathrm{PDF}(r,\Sigma) = \frac{e^{-\frac{r^2}{2\Sigma^2}}}{(2\pi)^{\frac{3}{2}}\Sigma^3}$$

Probability that we find something in a spherical shell [*r*,*r*+d*r*]:

$$\Pr(r \in [r, r+\mathrm{d}r]) = \underbrace{\frac{e^{-\frac{r^2}{2\Sigma^2}}}{(2\pi)^{\frac{3}{2}}\Sigma^3}}_{\mathrm{PDF}(r)} \cdot \underbrace{4\pi r^2 \mathrm{d}r}_{\text{shell volume at } r}$$

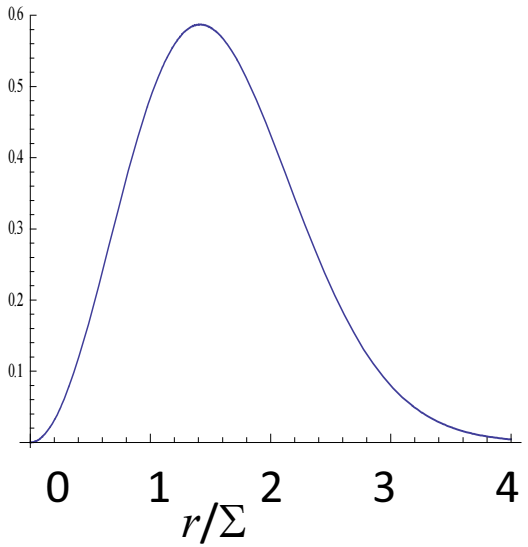

Rotational symmetrical 3D Gauss – cumulative function

Probability that we find something within a sphere of radius *R*:

$$\Pr\left(r \le R, \Sigma\right) = \int_0^R \frac{\mathrm{e}^{-\frac{r^2}{2\Sigma^2}}}{\left(2\pi\right)^{\frac{3}{2}}\,\Sigma^3} \cdot 4\pi r^2 \mathrm{d}r = \left[\ldots\right] = \mathrm{Erf}\left(\frac{R/\Sigma}{\sqrt{2}}\right) - \mathrm{e}^{-\frac{R^2/\Sigma^2}{2}} \cdot \sqrt{\frac{2}{\pi}} \cdot R/\Sigma$$

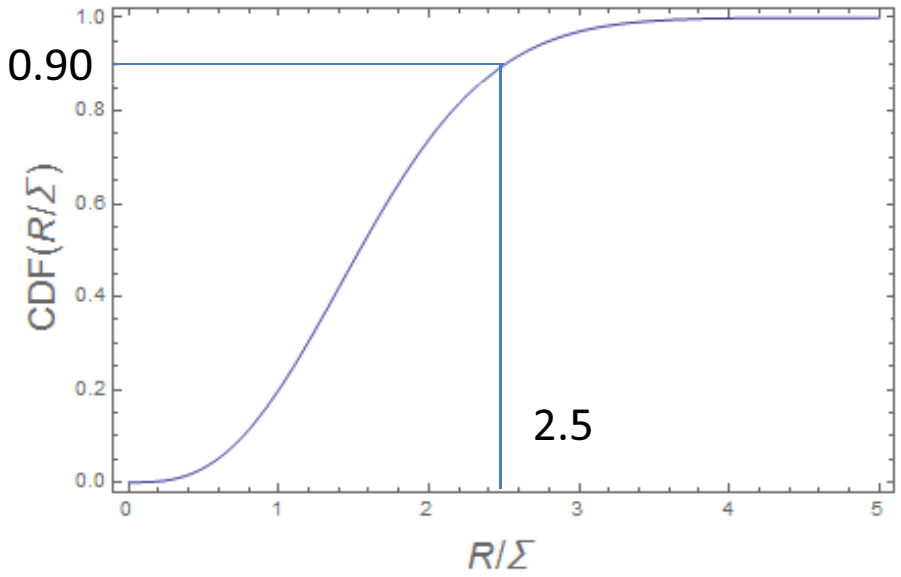

Note:

$$\Pr\left(r \le R, \Sigma\right) = 0.90 \quad \Rightarrow \quad R = 2.5001 \cdot \Sigma$$

The probability that a sphere of radius R is completely contained within R+2.5·Σ is 90%!

CTV2PTV margin algorithm design concepts

Van Herk *etal*, IJROBP, 2000 pp. 1121–1135:

"*The PTV is the volume, defined in* ***treatment room coordinates****, to which the* ***prescribed dose[a] must be delivered*** *in order to obtain a clinically acceptable and specified probability that the prescribed dose is actually received by the CTV, which has an uncertain location[b]* "

[a] 95% **delivered** dose, including delivery (**random** per patient&fraction) uncertainties $\sigma^2=\sigma^2_{pos}+\sigma^2_{mov}$… and dose profile "penumbra" σ_p

[b] considering CTV preparation uncertainties $\Sigma^2=\Sigma^2_{CTpos}+\Sigma^2_{delineation}$… (random but for each patient **systematic**) so that for 90% of the patients the entire CTV is inside the ITV

Margin: $$M = 2.5 \cdot \Sigma + f\left(\sigma, \sigma_p\right)$$

"considering CTV preparation uncertainties so that for 90% of the patients the entire CTV is inside the ITV"

True, unknown CTV
inside the true, unknown ITV

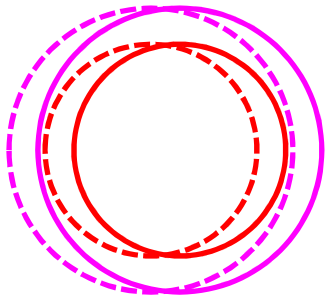

Captured CTV
inside the captured ITV

Due to symmetry, the probability of the true, but unknown CTV being inside the captured ITV is equal to the probability of the captured CTV being inside the true, unknown ITV

"considering CTV preparation uncertainties so that for 10% of the patients some CTV is outside the ITV"

How much is some?

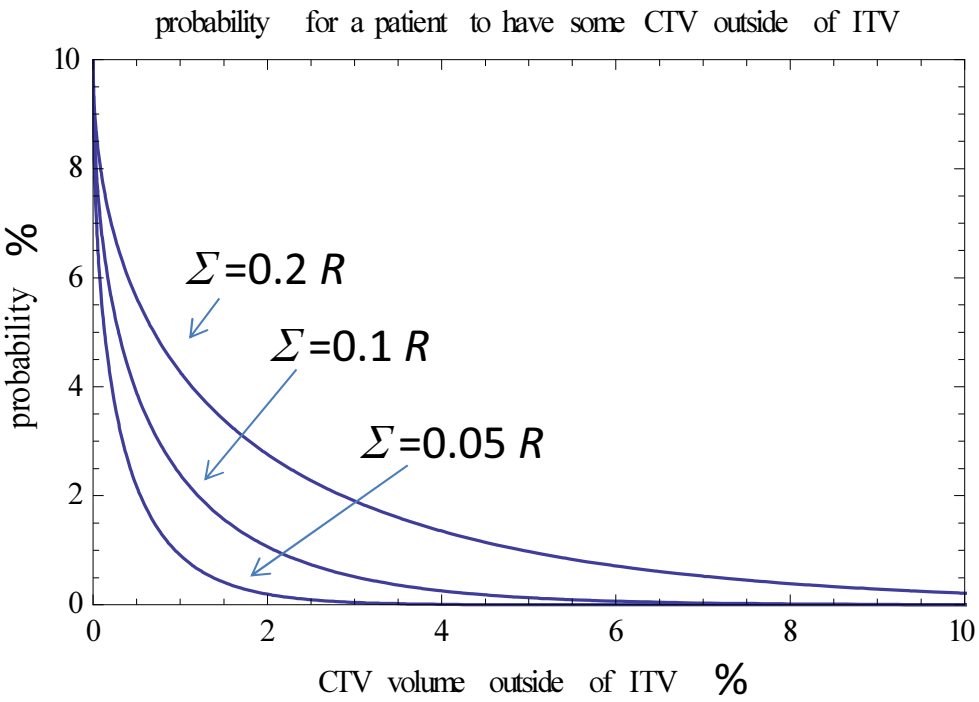

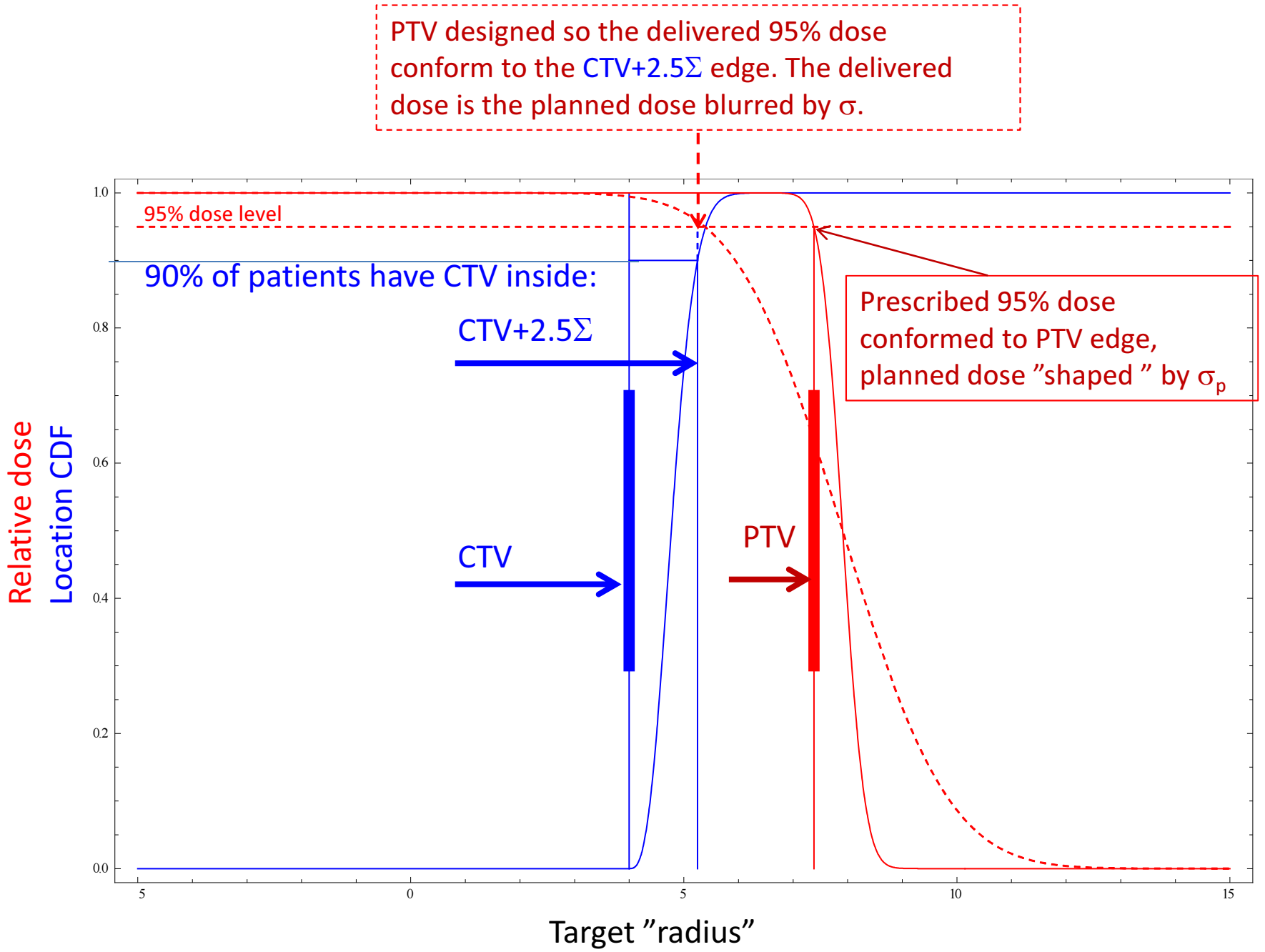
PTV designed so the delivered 95% dose conform to the CTV+2.5Σ edge. The delivered dose is the planned dose blurred by σ.
95% dose level
90% of patients have CTV inside:
CTV+2.5Σ
CTV
PTV
Prescribed 95% dose conformed to PTV edge, planned dose ”shaped ” by σp
Relative dose
Location CDF
Target ”radius”
1.0
0.8
0.6
0.4
0.2
0.0
5
0
5
10
15

”Exact” version of vHMF for 90% CDF(CTV) and 95% dose

$$M = 2.5 \cdot \Sigma + 1.645 \cdot \left(\sqrt{\sigma^2 + \sigma_{\mathrm{p}}^2} - \sigma_{\mathrm{p}} \right)$$

Most common version

$$M = 2.5 \cdot \Sigma + 0.7 \cdot \sigma \quad \mathrm{cm}$$

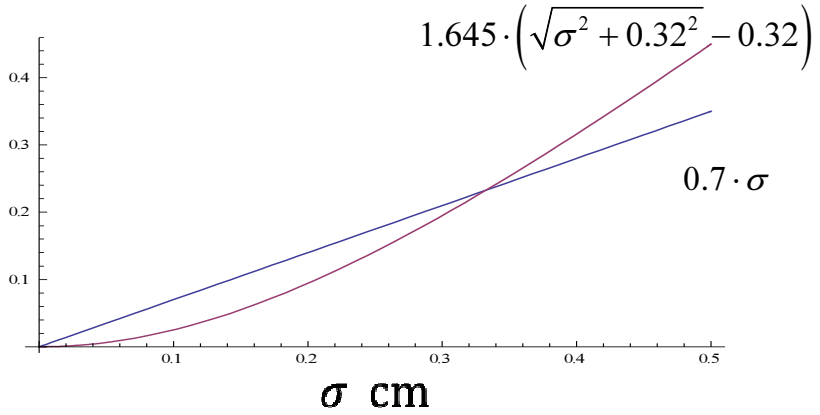

Limitations?

- large box shaped PTV for the dose profile (analytical convolution)
- spherical shape of the CDF for the CTV (analytical CDF)
- infinite number of fractions (convolution)

Limitations - tissue heterogeneties
NOT included in ”dose modell”

In margin recipe:
homogeneous assumption

dense tumor
low density lung

dense tumor
low density lung

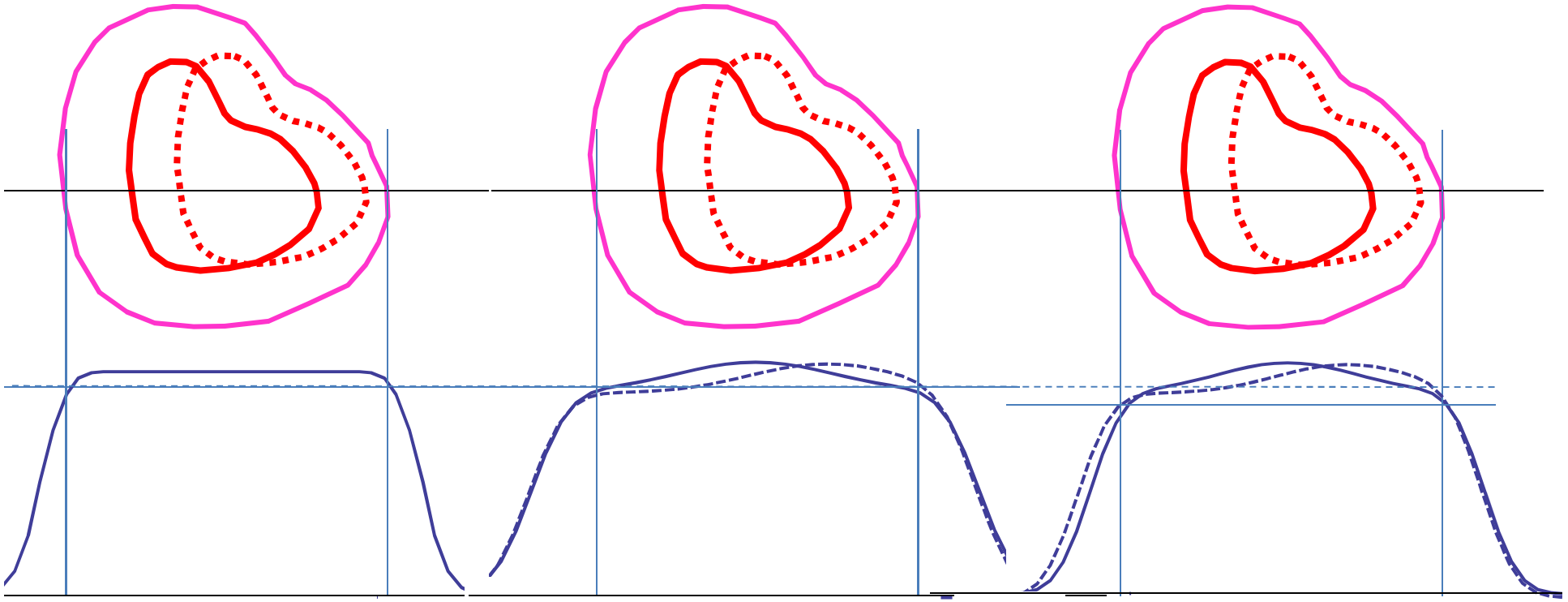

standard PTV criteria
results in large fields
and high lung dose

relaxed PTV criteria saves
lung and still provide CTV
dose (dense CTV raise
CPE level)

”Nominal” CTV_{CC} gives the maximum CTV DVH,
other ”CTV positions” gives similar (but slightly lower) DVH

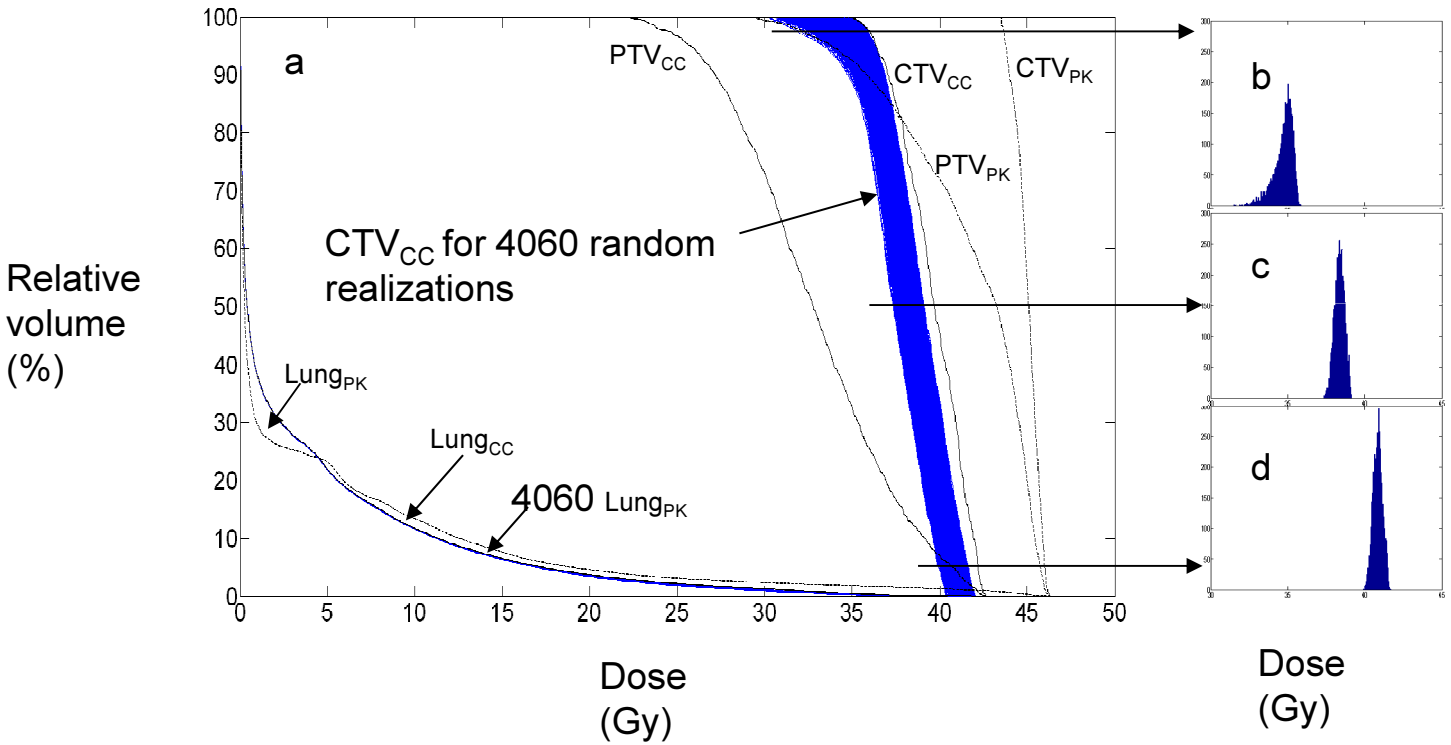

Limited number of fractions

Gordon & Siebers 2006, PMB, pp 1967-1990

$E(r)$, conservative estimate of dose for one fractions along profile
$F(r)$, estimate of average dose for all but one fractions along profile
$G(r)$ weighted average of E and F: $G(r)=(E(r)+(N\text{-}1)\ *F(r)\ )/N$

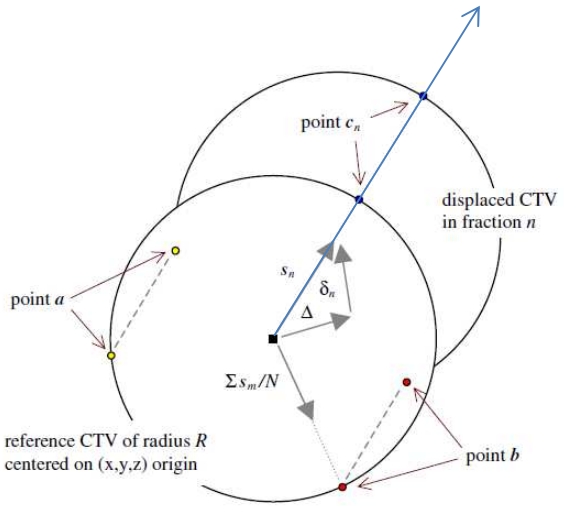

Figure 1. CTV displacements and dose calculation points.

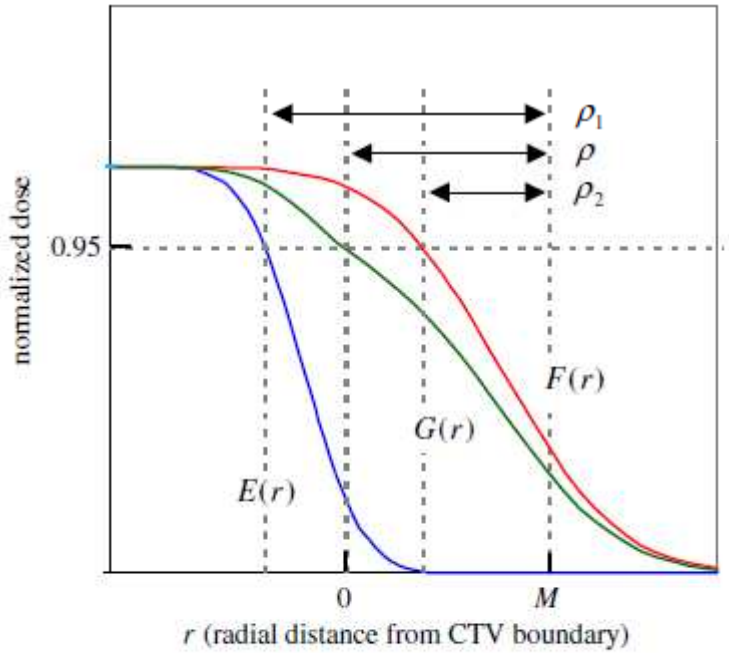

Figure 3. Radial dose profiles $E(r)$, $F(r)$ and $G(r)$.

Probabilistic planning

Limitations in van Herks margin recipes for current CTV-to-PTV planning paradigm:

- the underlying statistics is build on the assumption on infinite number of fractions
- combines math assumptions of spherical target shape (for location uncertainty) and box shaped target (for isodose shape analysis)
- no utilization of patient specific geometry for margin reduction

Is there an alternative approach?

Probabilistic planning

PTV based planning

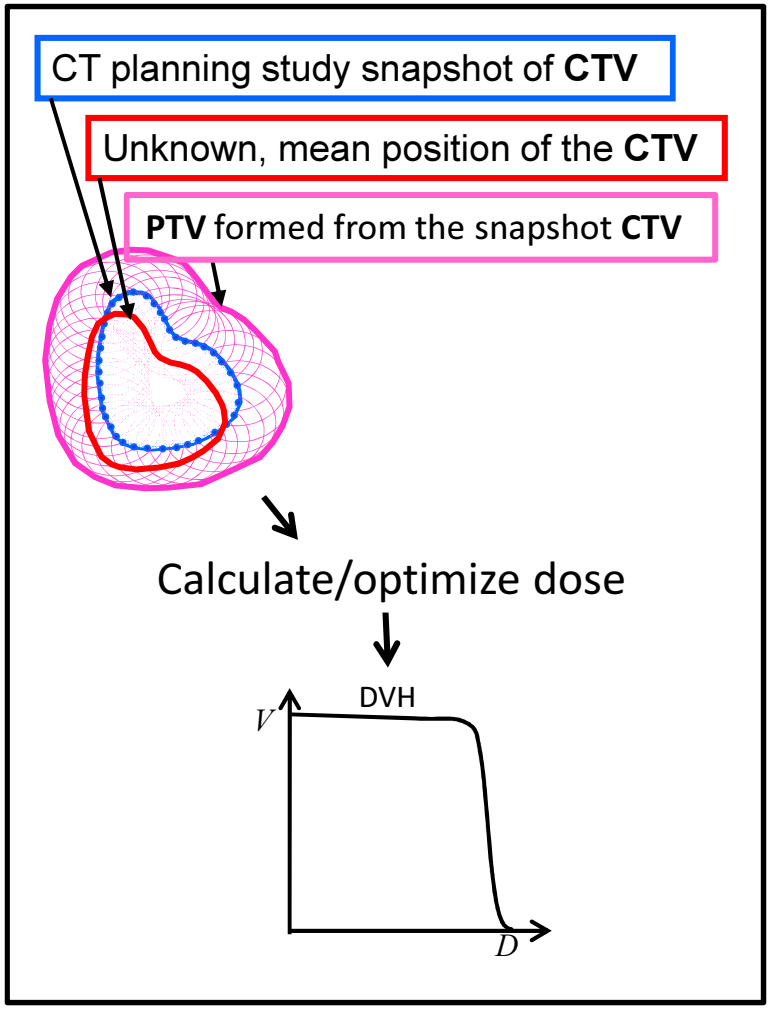

CTV based planning

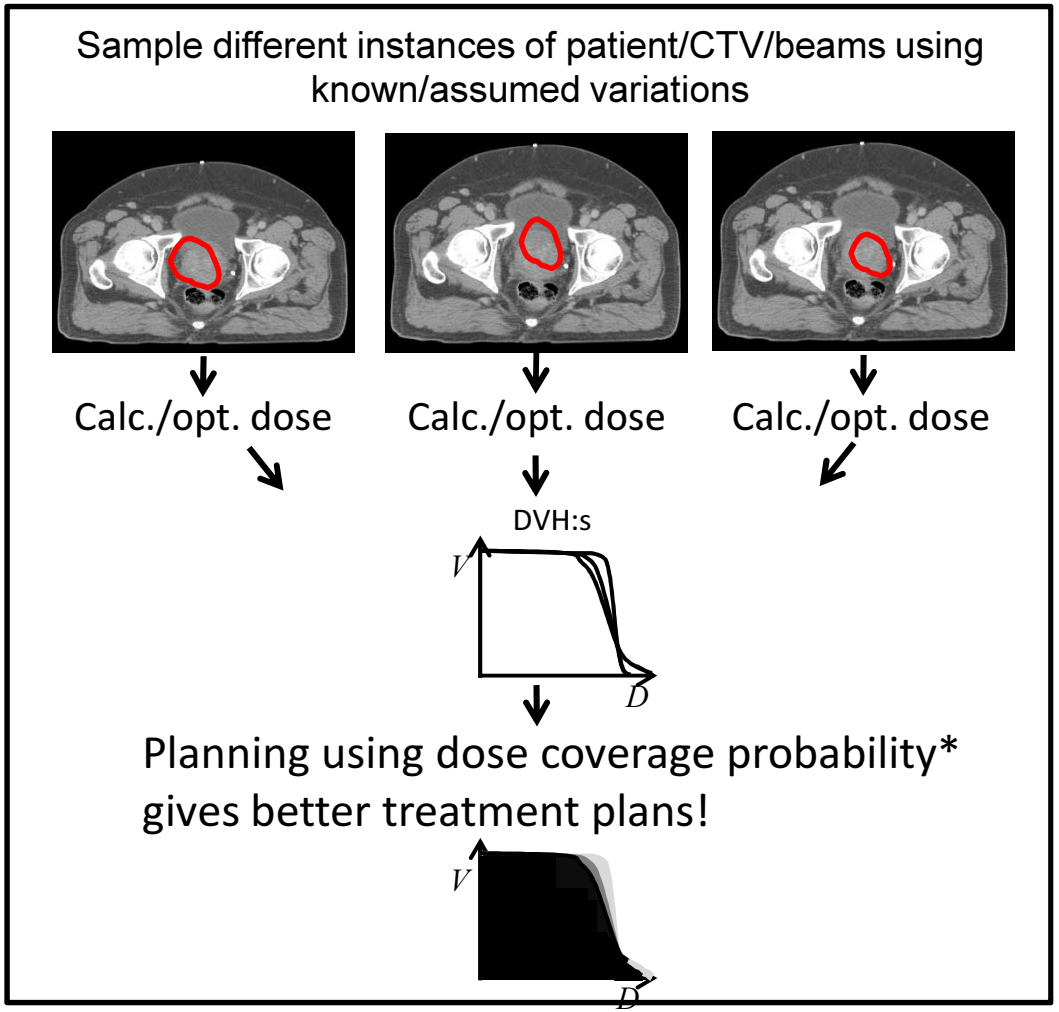

* e.g. Gordon etal, MedPhys 2010 37 p550-63

Probabilistic planning

With many instances of the patient simulated, we get distributions of DVH lines

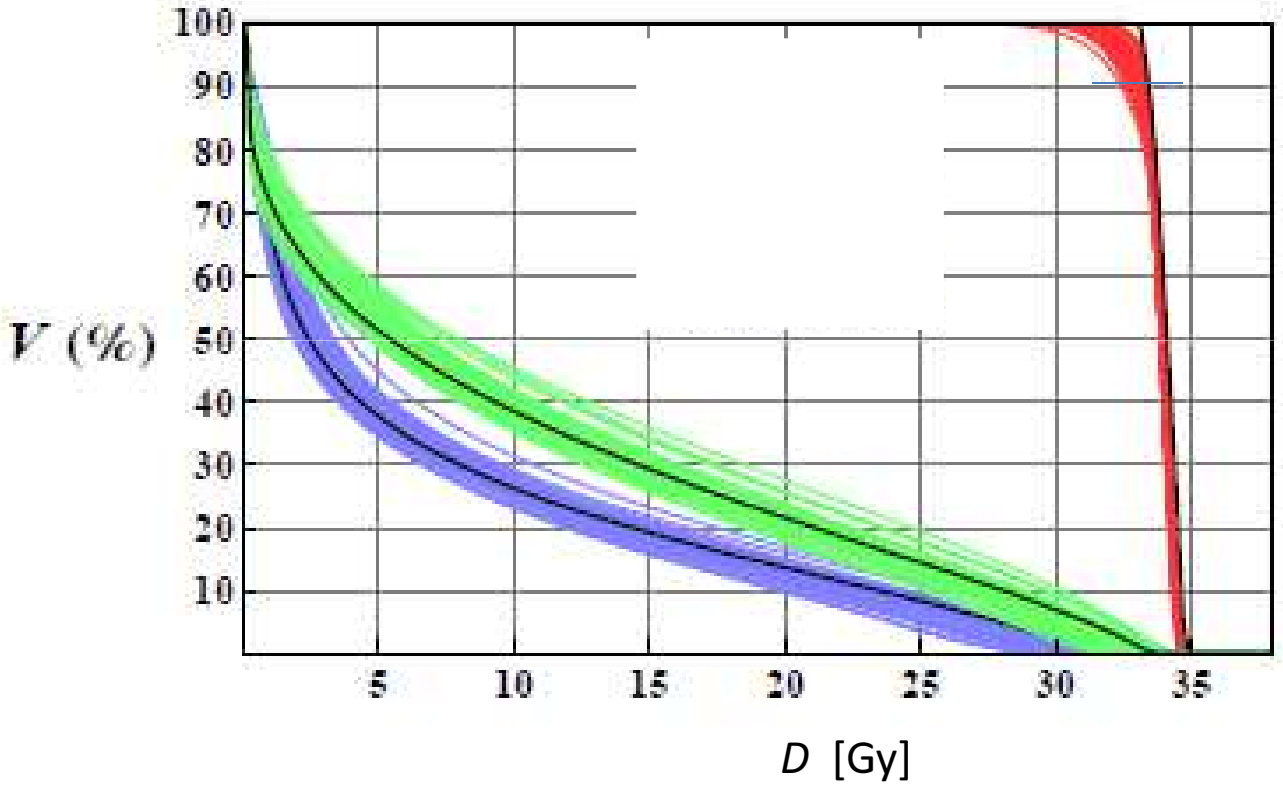

Probabilistic planning

Dose Volume Coverage Map - DVCM

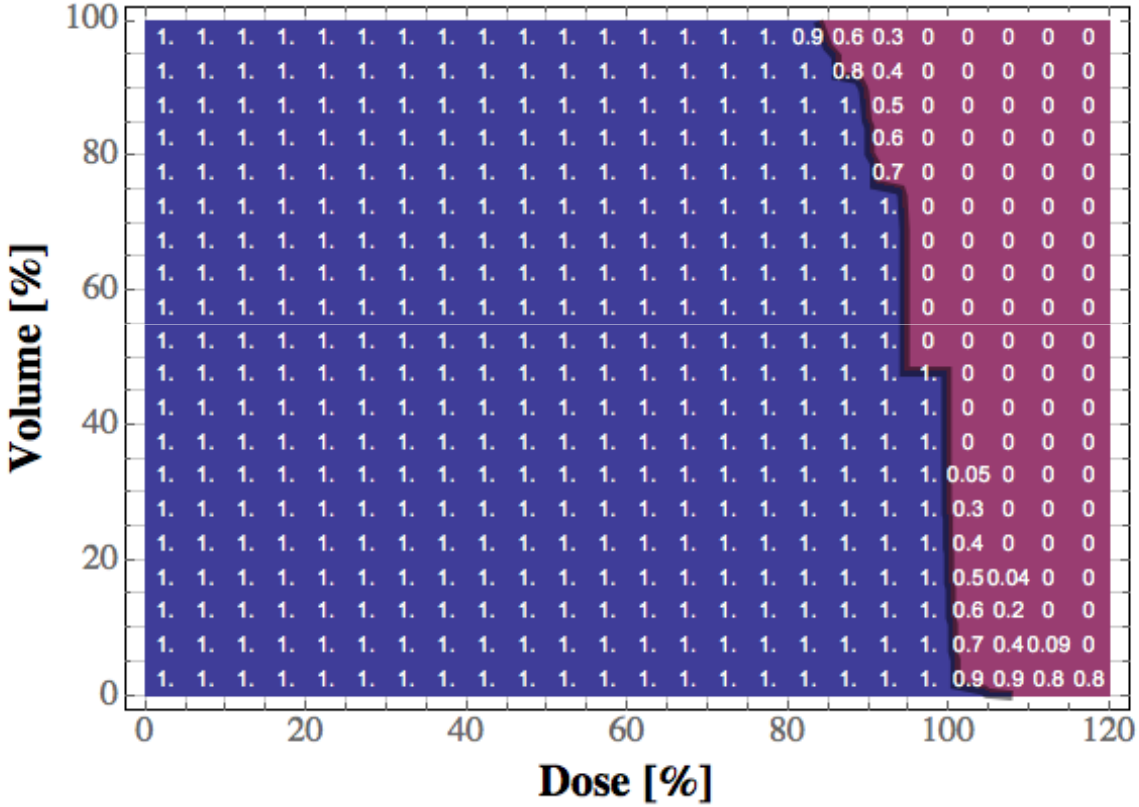

Gordon J J, Sayah N, Weiss E and Siebers J V 2010 Coverage optimized planning: probabilistic treatment planning based on dose coverage histogram criteria. *Med. Phys.* **37** 550–63

Probabilistic dose modeling

the need for speed

Planning paradigm	**Number of recalculations**
CRT forward	1
PTV based IMRT	100
Probabilistic planning	100000

Most publications on probabilistic planning demonstrates proof-of-principle utilize (over)-simplified dose calculation:

- translation of a single distribution neglecting attenuation variations
- convolving lateral uncertainty distributions with output fluence
  - applicable only for a large number (>40) of dose fractions

Fast dose algorithms and smart sampling strategies needed!

Probabilistic dose modeling

development of fast algorithms – work in progress

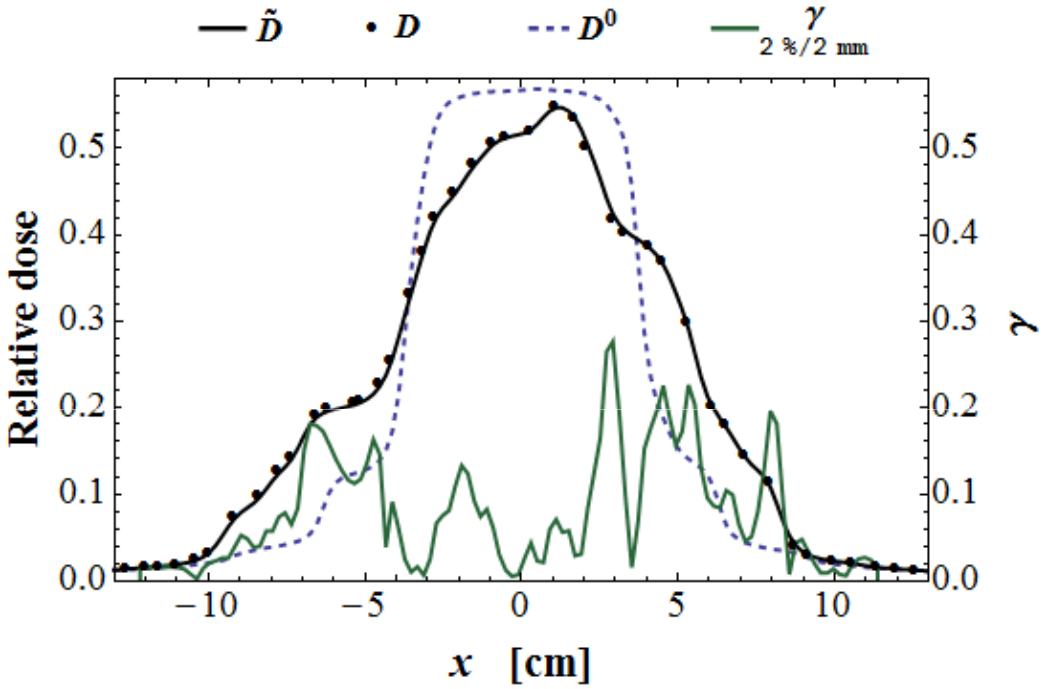

Dose profile (parallel to the leaf direction) for a single treatment scenario where a modulated IMRT beam was subject **to randomly sampled setup-errors during 5 fractions**. The dose is normalized to dose under calibration conditions. Results for the perturbation algorithm, $\tilde{D}$, (solid black) are shown with full dose calculation, D, (dots black) and compared using the 3D gamma comparison (solid green). The static dose profiles without setup error, D^0, (dashed blue) is shown for comparison.

Tilly, Ahnesjö Phys. Med. Biol. 60 (2015) 5439–5454


-Thank you-

Limited number of fractions

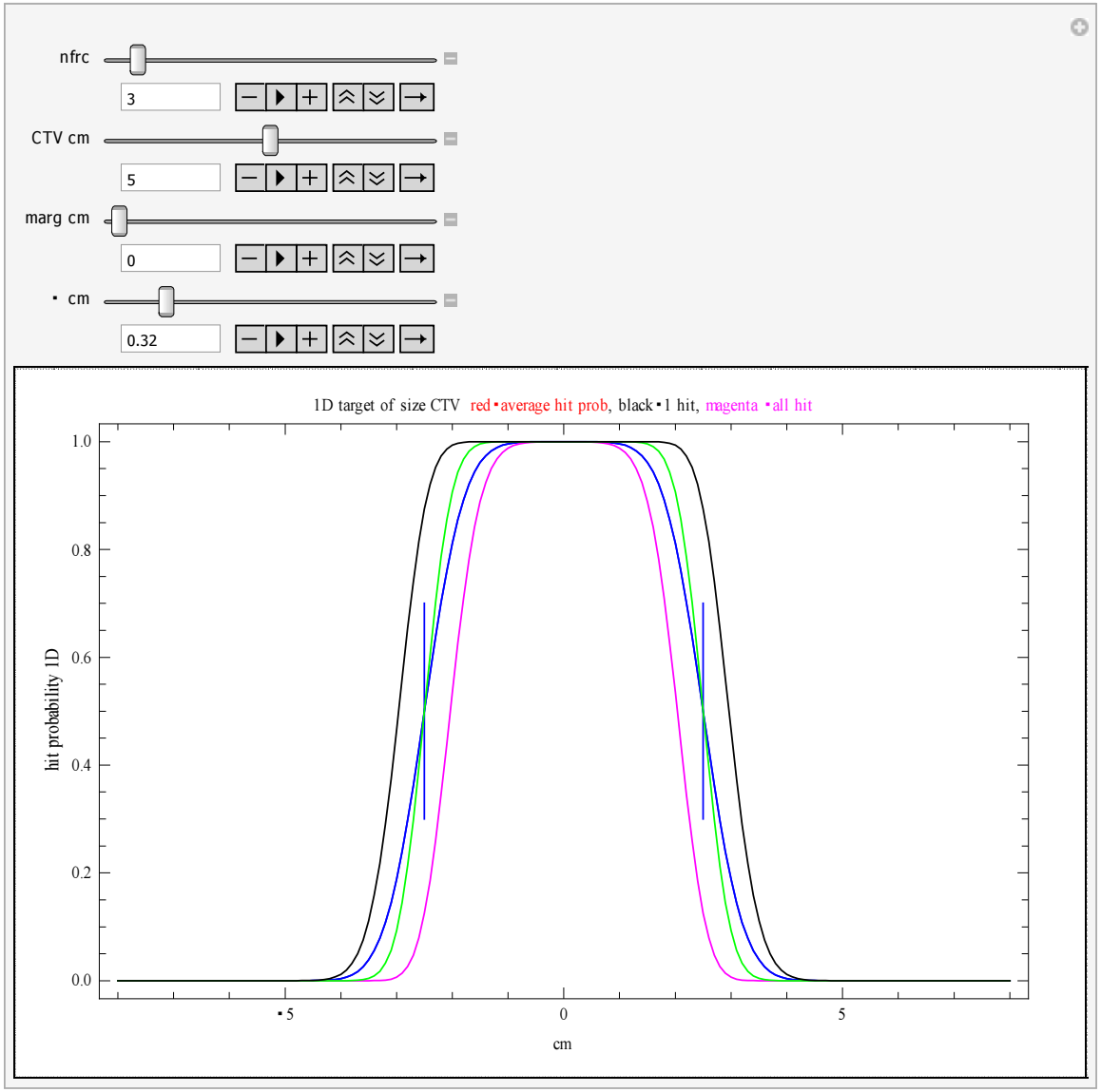

Margin calculator

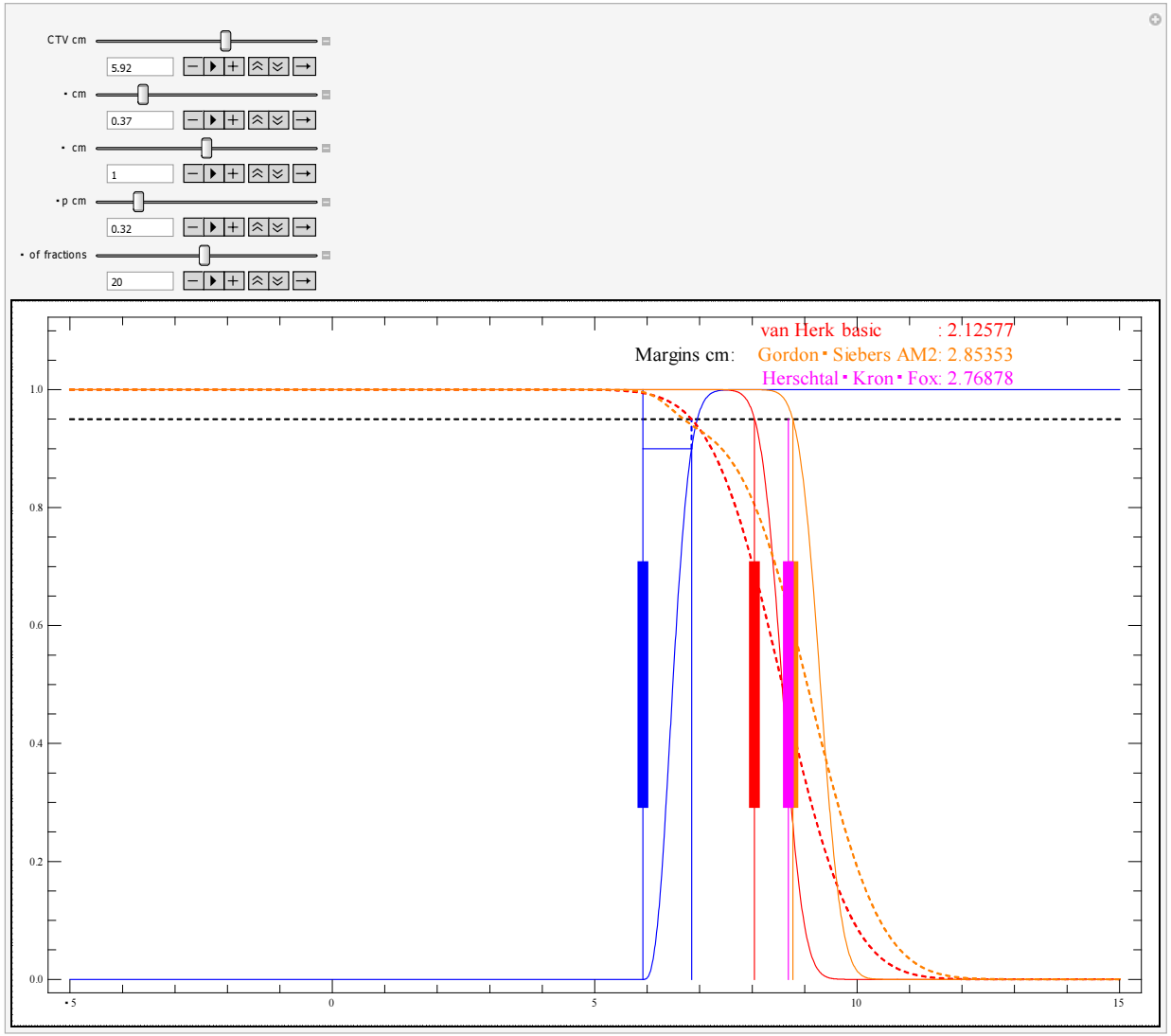

Probabilistic planning

With many instances of the patient simulated, the DVH line "thickness" become distributions, and optimization criteria set accordingly

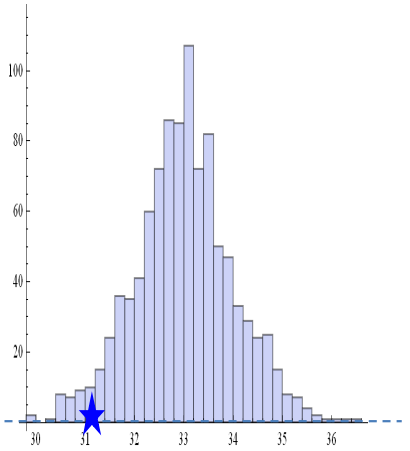

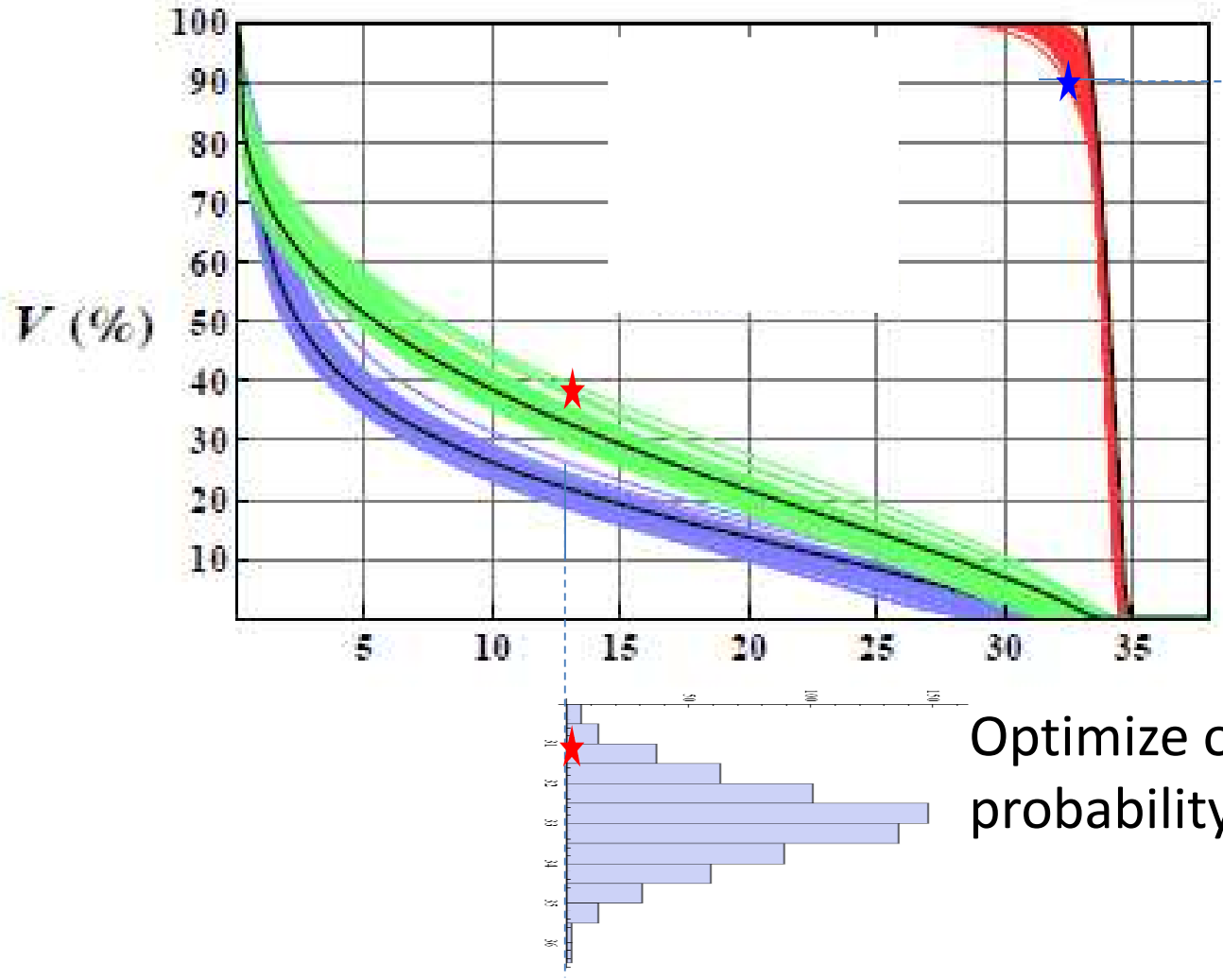

Optimize of dose-volume probability criteria: ★ ★